



# Abstract Volume 20th Swiss Geoscience Meeting

18–20 November 2022 · Lausanne

## ABOUT THIS PUBLICATION

### PUBLISHER AND CONTACT

Swiss Academy of Sciences (SCNAT) • Platform Geosciences  
House of Academies • Laupenstrasse 7 • P.O. Box • 3001 Bern • Switzerland  
+41 31 306 93 25 • info@geosciences.scnat.ch • geo.scnat.ch  @SwissGeoMeeting

### ORGANISATION SGM 2022

University of Lausanne, Faculty of Geosciences and Environment (FGSE)  
Musée Cantonal de Géologie de Lausanne (MCGL)

### PATRONNAGE

Swiss Academy of Sciences (SCNAT) • Platform Geosciences

### LOCAL ORGANISING COMMITTEE

Thierry Adatte, ISTE (Co-president) • Virginia Ruiz-Villanueva, IDYST (Co-President) •  
Gilles Borel, MCGL • Anne-Marie Chagros, ISTE • Rémy Freymond, FGSE • Samuel Jaccard, ISTE •  
Javier del Hoyo Gibaja, IDYST • Georgina King, IDYST • Christophe Lambiel, IDYST & CIRM •  
Johanna Marin-Carbonne, ISTE • Martin Müller, IGD • Benita Putlitz, ISTE • Céline Rozenblat, IGD •  
Marie Violay, EPFL • Sven Daniel Wolfe, IGD

### COORDINATION

Pierre Dèzes, SCNAT

### PARTICIPATING SOCIETIES AND ORGANISATIONS

Commission for the Swiss Journal of Palaeontology  
Commission on Atmospheric Chemistry and Physics ACP  
Swiss Association for Geography (ASG)  
Swiss Commission for Phenology and Seasonality (CPS)  
Swiss Commission on Remote Sensing  
Swiss Committee for Stratigraphy (SKS/CSS)  
Swiss Geocomputing Centre  
Swiss Geodetic Commission  
Swiss Geological Society  
Swiss Geological Survey – swisstopo  
Swiss Geomorphological Society (SGmS)  
Swiss Geophysical Commission  
Swiss Hydrogeological Society SGH  
Swiss Hydrological Commission CHy  
Swiss Palaeontological Society (SPG/SPS)  
Swiss Snow, Ice and Permafrost Society  
Swiss Society for Hydrology and Limnology SGHL  
Swiss Society for Quaternary Research (CH-QUAT)  
Swiss Society of Mineralogy and Petrology  
Swiss Soil Science Society  
Swiss Tectonics Studies Group

### COVER PHOTO

Les vignobles en terrasses du Lavaux, patrimoine mondial de l'UNESCO. Credits: P.Dèzes

## Table of contents

1	Structural Geology, Tectonics and Geodynamics.....	2
2	Mineralogy, Petrology and Geochemistry .....	62
3	Stable and radiogenic isotope geochemistry .....	116
4	Environmental Biogeochemistry of Trace Elements .....	144
5	Palaeontology .....	172
6	Stratigraphy and Sedimentology: processes and deposits through time.....	208
7	Seismic Hazard and Risk in Switzerland: From Science to Mitigation.....	240
8	Deep geothermal energy, CO <sub>2</sub> -storage and energy-related exploration of the subsurface. ....	266
9	Scientific Drilling Through Time and Space: On Land and Under the Sea .....	306
10	Quaternary environments: landscapes, climate, ecosystems and human activity during the past 2.6 million years .....	316
11	Geomorphology .....	340
12	Soil: Formation, Processes, and Conservation.....	362
13	Hydrology and Hydrogeology.....	388
14	Limnology in Switzerland .....	440
15	Cryospheric Sciences.....	458
16	Atmospheric Composition and Biosphere-Atmosphere Interactions .....	490
17	Climatology.....	490
18	Tackling the Climate Crisis: Interdisciplinary Perspectives on Climate Change Education and Communication .....	490
19	Earth Observation and Remote Sensing .....	514
20	Geoscience and Geoinformation – From data acquisition to modelling & visualisation.....	546
21	Spatial data science: extracting knowledge from geo-environmental data.....	566
22	Virtual Representation of Forests: Methods and Applications.....	568
23	Alpine Hazards: Early Detection, Monitoring, Warning, Modelling, Mitigation .....	590
24	Human Geographies: Materials, Natures, Politics .....	628
25	Human Geographies: Bodies, Cultures, Societies .....	640
26	Human Geographies: Cities, Regions, Economies.....	646
27	Global change and sustainability issues in mountain areas .....	658

# 1 Structural Geology, Tectonics and Geodynamics

Sandra Borderie, Paul Tackley, Jonas Ruh, Vénice Akker

*Swiss Tectonics Studies Group of the Swiss Geological Society*

TALKS:

- 1.1 Andjić G., Zhou R., Jonell T.N., Aitchison J.C.: Volcaniclastic records from the Indus Suture Zone support a single Dras-Kohistan-Ladakh Arc
- 1.2 Attia I., Moustafa A.R.: Geometry of normal faults in the Gulf of Suez rift basin
- 1.3 Balazs A., Gerya T., Tari G., May D.: Continental slivers in oceanic transform faults controlled by tectonic inheritance
- 1.4 Ceccato A., Behr W.M., Zappone A.S.: Structural evolution of the Rotondo granite (val Bedretto, Gotthard massif): implications for alpine tectonics and shear zone evolution in the External Crystalline Massifs
- 1.5 Frings K.A., von Hagke C., Kukla P., Landgraf A., Madritsch H.: Using low temperature thermochronometry to estimate long-term exhumation rates of sites for radioactive waste disposal
- 1.6 Gunatilake T., Miller A.S.: 3D model reveals thermal decomposition as a primary driver of Apennines seismicity
- 1.7 Hufford L., Tokle L., Behr W., Madonna M.: Experimental Investigation of Glaucomphane Deformation and Rheology Through General Shear Experiments
- 1.8 Iten G., Nibourel L., Looser N., Guillong M., Tavazzani L., Bernasconi S.M., Heuberger S.: Age and temperature conditions of folding and thrusting in the Säntis Nappe and the adjacent Subalpine Molasse from calcite U-Pb dating and clumped isotope thermometry
- 1.9 Juchler L., Nibourel L., Morgenthaler J., Coray M., Schläfli S., Baland P., Ruh J., Galfetti T., Heuberger S.: Stratigraphic thickness variations of the Helvetic Kieselkalk in central Switzerland: new automatically extracted thickness data from mapped bedrock exposures and field orientation measurements
- 1.10 Looser N., Madritsch H., Aschwanden L., Wohlwend S., Guillong M., Traber D., Bernasconi S.M.: Temperature and fluid evolution in the Mesozoic formations of central northern Switzerland over the last 200 Ma: insights from coupled carbonate clumped isotopes and U-Pb dating
- 1.11 Lupi M., De Gori P., Valoroso L., Baccheschi P., Minetto R., Mazzini A.: Arc progression capitalises on low-angle thrust faults in East Java, Indonesia.
- 1.12 Mannini S., Ruch J., Hollingsworth J., Swanson D.A., Johanson I.: Gravitational volcano flank motion imaged by historical air photo correlation during the M7.7 Kalapana earthquake (1975), Big Island, Hawaii
- 1.13 Mosar J., Borderie S., Hauvette L., Jordan P., Marro A., Schori M., Sommaruga A., Ursprung A.: Jura Fold-and-Thrust Belt: on basement, thrusting and timing
- 1.14 Moscariello A., Erutuya O.E., Clerc N., Mondino F., Guglielmetti L.: Shortening tectonic style in the Western Alpine foreland: Example from the Geneva Basin (Switzerland) and implications for subsurface geo-fluid circulation.
- 1.15 Muñoz-Montecinos J., Behr W.: Permeability and Fluid Flow in the deep Slow Slip and Tremor Source: Insights From the Cycladic Blueschists (Greece)

- 1.16 Panza E., Ruch J.: It's the rift turn: Faults, obliquity, and magma propagation in the Icelandic North Volcanic Zone using UAV-based structural data
- 1.17 Schenker F.L., Maino M., Tagliaferri A., Perozzo M., Castelletti C., Giacomazzi D., Vandelli A., Wennubst R., Gouffon Y., Ambrosi C.: 3D reconstruction of the sole shear zone of the Adula nappe and its repercussion on the Alpine regional geology
- 1.18 Schmalholz S.M., Vaughan Hammon J., Candioti L.: The tectono-metamorphic evolution of the Western Alps: new insights from the comparison of model predictions and observations
- 1.19 Schmid S.M., Handy M., Paffrath M.: Imaging crust and mantle structure of the Western Alps by geophysical methods: controversies regarding the geological interpretation of the deep structure of the Western Alps
- 1.20 Schmid T., Schreurs G., Adam J., Zwaan F.: Lower crustal flow during continental rifting: Considerations for 3D deformation and insights from analogue modelling experiments
- 1.21 Schwichtenberg B., Fusseis F., Butler I.B., Andò E.: Beyond the grain scale – What 4D microtomography tells us about diffusive transport during dissolution precipitation creep
- 1.22 Talebkéikhah M., Momeni S., Lu G., Lecampion B.: Experimental investigation of fracture behavior after ceasing injection in a permeable and porous medium
- 1.23 Zwaan F., Schreurs G., Madritsch H., Herwegh M.: Rheologically weak layers affecting fault architecture in the Northern Alpine Foreland Basin: Insights from analogue models

## POSTERS:

- P 1.1 Akker I.V., Behr W.M., Rast M., Hufford L.J., Braden Z.: How sediments control deformation along a subduction margin – the Chugach accretionary prism, Alaska (USA)
- P 1.2 Andjić G., Zhou R., Buchs D.M., Aitchison J.C., Zhao J.: Determining the age and tectonic evolution of Paleozoic oceanic islands using calcite U-Pb geochronology and biostratigraphy
- P 1.3 Verard C., Baud A., Bucher H., Edward O.: Tracking back Permian–Triassic sections from Oman over the Mesozoic –Cenozoic: Geodynamic and paleogeographic implications
- P 1.4 Champion A., Metral L., Lupi M., Muñoz Burbano F., Got JL., Ruch J.: Natural seismicity assessment of the Vuache fault
- P 1.5 Gray T., Tackley P., Gerya T.: Free surface methods applied to global scale numerical geodynamic models
- P 1.6 Halter W.R., Kulakov R., Duretz T., Schmalholz S.M.: Viscous strain localization by anisotropy development: Numerical models and benchmarks
- P 1.7 Jossevel C., Epard J-L.: Stratigraphic contact in the Mattmark area implying a reexamination of the nappe stack in the Saas valley
- P 1.8 Lee T., Diehl T., Kissling E., Wiemer S.: New insights into the Rhône-Simplon fault system (Swiss Alps) from a consistent earthquake catalogue covering thirty-five years
- P 1.9 Liu M., Gerya T., Chen L., Connolly J.: The effect of grain size reduction for the origin of the mid-lithosphere discontinuity
- P 1.10 Macherel E., Podladchikov Y., Räss L., Schmalholz S.M.: Analytical estimates for velocities of diapirs rising in deforming power-law viscous rock: tests with GPU-based 3-D numerical solutions
- P 1.11 Madritsch H., Looser N., Decker K., Schneeberger R., Gegg L., Guillong M., Schöpfer K. & Schnellmann M.: Strain partitioning at the eastern tip of the arcuate Jura Belt: new absolute deformation ages and insights on the role of precursor structures
- P 1.12 Nevskaia N., Zhan W., Berger A., Stünitz H., Herwegh M.: Mass transport in experimentally deformed granitoid ultramylonites
- P 1.13 Pantet A., Epard J.-L.: Structure and stratigraphy of continent-derived metasediments units (Cimes Blanches and Frilihorn) intercalated within the ophiolites around Zermatt: Relations with the Mischabel backfold, Alphubel basement and Mont Fort nappe (Pennine Alps, SW Switzerland and NW Italy)
- P 1.14 Rast M., Madonna C., Selvadurai P.A., Wenning Q., Ruh J.B., Salazar Vásquez A.: Can the build-up of swelling stress in clay-rich rocks induce slip along faults?
- P 1.15 Rime V., Foubert A., Atnafu B., Kidane T.: New kinematic model and paleogeological maps give new insight on the evolution of the Afar Region
- P 1.16 Rogger J., Mills B.J.W., Gerya T., Pellissier L.: Thermal adaptation evolution of the biosphere regulates Earth's long-term climate
- P 1.17 Rostami M., Manijou M., Moritz R., Shole A.: Geodynamic evolution of the Iranian plate during the formation of the Neotethys ocean
- P 1.18 Ruh J.B.: Grain size reduction undermines the importance of viscous shear heating in lithospheric mantle shear zones
- P 1.19 Decker K., Schneeberger R., Madritsch H.: Paleo-strain reconstruction from drill core mapping and their relevance for northern Switzerland
- P 1.20 Tagliaferri A., Schenker F.L., Schmalholz S.M., Ulianov A.: Geological mapping and U-Pb dating of detrital and magmatic zircon crystals in the Lepontine dome (Central European Alps)

- P 1.21 Tokle L., Behr W.M., Braden Z., Cisneros M.: Structural Mapping of the Eclogite Zone, Tauern Window: Implications for the rheology of the subduction zone interface
- P 1.22 Verard C.: On the reliability of the PANALESIS (v.0) paleogeographic maps
- P 1.23 Zhan W., Nevskaya N., Niemeijer A., Berger A., Spiers C., Herwegh M.: Effect of Phyllosilicate Content and Composition on Fault Gouge Friction under Hydrothermal Conditions
- P 1.24 Zwaan F., Schreurs G.: Rotational rifting and the evolution of the East African Rift System: Insights from analogue models

## 1.1

# Volcaniclastic records from the Indus Suture Zone support a single Dras-Kohistan-Ladakh Arc

Goran Andjić<sup>1</sup>, Renjie Zhou<sup>2</sup>, Tara N.Jonell<sup>3</sup>, Jonathan C. Aitchison<sup>2</sup>

<sup>1</sup> Institut des Sciences de la Terre, Université de Lausanne, Bâtiment Géopolis, CH-1015 Lausanne ([goran.andjic@unil.ch](mailto:goran.andjic@unil.ch))

<sup>2</sup> School of Earth and Environmental Sciences, The University of Queensland, 4072 St Lucia, Australia

<sup>3</sup> School of Geographical & Earth Sciences, University of Glasgow, United Kingdom

The Himalayan orogen is the result of the collision between India and Eurasia and the closure of the intervening Neotethys Ocean. The suture zone between India and Eurasia (Figure 1) hosts an incomplete and complex archive of the paleogeography that once existed between them prior to continent-continent collision. Investigating suture zone rocks may therefore provide valuable information on the building blocks of the orogen and the overall history of the India-Eurasia convergent system.

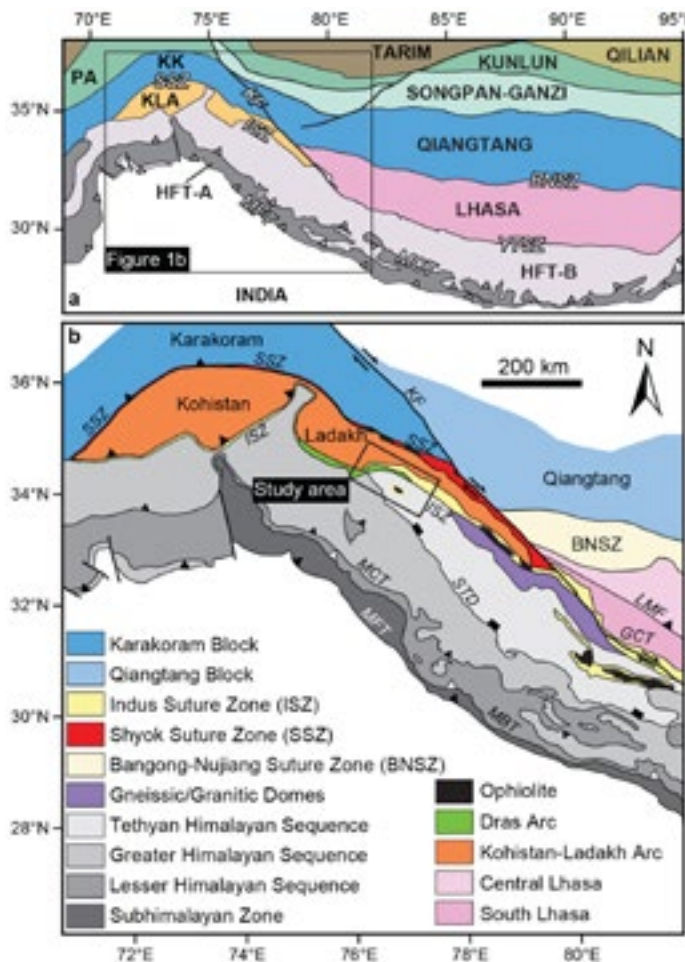


Figure 1. (a) Terrane map of major crustal blocks and tectonic boundaries of the Himalayan orogen. (b) Simplified geological map of the western Himalayan orogen. Blocks: HFT-A = Himalaya Fold-and-Thrust Belt, Sequence A; HFT-B = Himalaya Fold-and-Thrust Belt, Sequence B; KK = Karakoram; KLA = Kohistan-Ladakh; PA = Pamir. Tectonic structures: BNSZ = Bangong-Nujiang Suture Zone; GCT = Great Counter Thrust; ISZ = Indus Suture Zone; KF = Karakoram Fault; LMF = Luobadui-Milashan Fault; MCT = Main Central Thrust; MFT = Main Frontal Thrust; SSZ = Shyok Suture Zone; STD = South Tibetan Detachment; YTSZ = Yarlung Tsangpo Suture Zone. (a) and (b) from Andjić et al. (2022).

Tectonic interpretations of arc remnants in the Himalayan orogen remain uncertain, despite their important implications for the overall convergence history between India and Eurasia. Provenance results from deep-water volcaniclastic rocks of the Indus Suture Zone in Ladakh (Figure 1b) provide new constraints on the Mesozoic tectonic evolution of the Dras and Kohistan-Ladakh arcs. Detrital zircon (DZ) U-Pb ages and whole-rock geochemistry of the fault-bounded Upper Cretaceous Nindam and Paleocene Jurutze formations present age patterns and compositions that are consistent with those of the Dras and Kohistan-Ladakh arcs, respectively. The combination of DZs of the Nindam and Jurutze formations with the igneous zircons of the Dras and Kohistan-Ladakh arcs shows similar age distributions that support a Late Jurassic to Paleocene tectonic connection between all these units. We argue that the secular trends in geochemical composition of DZs and volcaniclastic material are consistent with the magmatic evolution of one convergent margin, which shifted from a primitive to a mature stage during the Late Cretaceous.

The recognition of a single Dras-Kohistan-Ladakh arc sets the stage for reevaluating competing scenarios of the Mesozoic evolution of the India–Eurasia convergent system. We find that the most likely scenario is that of a Jurassic arc formed above a south-dipping intraoceanic subduction zone and accreted to Eurasia during the Early Cretaceous, after which it evolved above a north-dipping subduction zone. This solution is the most compatible with the commonly proposed models for Mesozoic evolution of arc-related units exposed in Tibet.

## REFERENCES

- Andjić, G., Zhou, R., Jonell, T.N., & Aitchison, J.C. 2022: A single Dras-Kohistan-Ladakh arc revealed by volcaniclastic records. *Geochemistry, Geophysics, Geosystems*, 23, e2021GC010042.

## 1.2

# Geometry of normal faults in the Gulf of Suez rift basin

Ibrahim Attia <sup>1</sup>, Adel R. Moustafa <sup>2</sup>

*Sipetrol International S.A., Cairo, Egypt (iattia@sipetrol-eg.com)*

*Department of Geology, Ain Shams University, Cairo 11566, Egypt*

The Gulf of Suez basin is one of the world's most complicated rift basins. Hydrocarbon exploration of this basin is hampered by the effect of Miocene evaporites on the seismic imaging of potential hydrocarbon reservoirs, especially the pre-rift fault-controlled traps. Mapping fault geometry at these pre-rift levels is based mainly on inadequate seismic reflection data as well as borehole data, but one of the main problems is the fault dip angle(s).

Textbook-quoted 60° dip angle of normal faults is not always matching the borehole data. Integration of the excellent surface (outcrop) data from both sides of the rift as well as borehole data (including dipmeter and image-log data) help solve this problem to accurately map the 3D geometry of tilted fault blocks and make good estimates of the hydrocarbon reserves.

The data used in this study is based on the integration of outcrop (faults, formation contacts, ... etc.) and subsurface (well and seismic) data to build a comprehensive model for the Gulf of Suez rift basin. We reached a good estimate of the initial fault dip angle (before block rotation) to range from 68° to 72° (Figure 1).

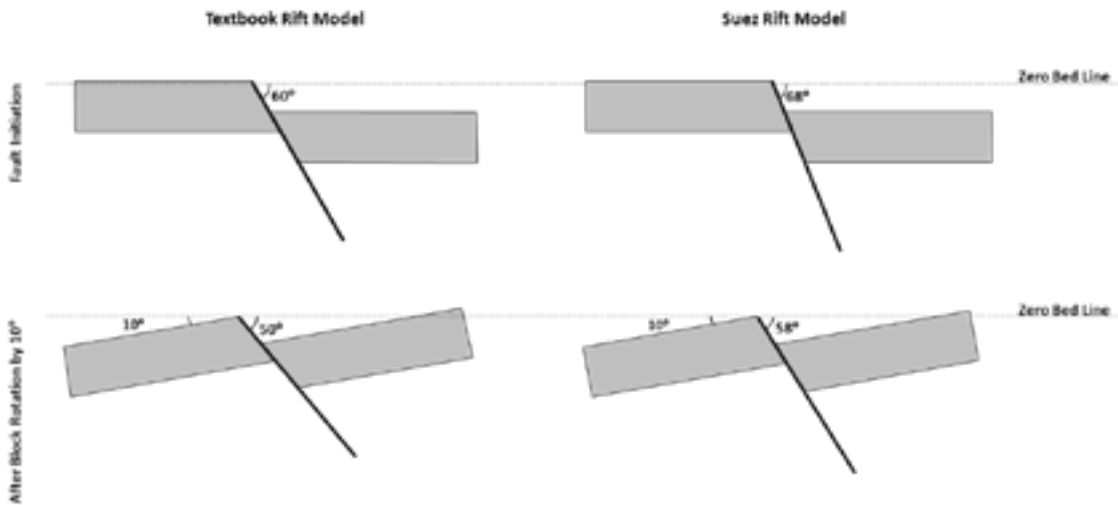


Figure 1. Schematic model for the textbook rift model on the left-hand side comparison with our observation for the Suez rift model on the right-hand side.

## 1.3

# Continental slivers in oceanic transform faults controlled by tectonic inheritance

Attila Balazs<sup>1</sup>, Taras Gerya<sup>1</sup>, Gabor Tari<sup>2</sup>, Dave May<sup>3</sup>

<sup>1</sup> ETH Zurich, Geophysical Fluid Dynamics Group, Zurich, Switzerland ([attila.balazs@ersw.ethz.ch](mailto:attila.balazs@ersw.ethz.ch))

<sup>2</sup> OMV Upstream, Vienna, Austria

<sup>3</sup> University of California San Diego, Scripps Institution of Oceanography, La Jolla, USA

The ocean floor shows variable morphological features, transtensional and transpressional structures, magmatic and amagmatic domains. Surprisingly, continental blocks separated from the continental margins from 100s or 1000s km distance have been occasionally reported, however, their origin remains controversial (e.g. Palmiotto et al. 2016). We conducted 3D magmatic-thermo-mechanical numerical experiments with the code I3ELVIS (Gerya et al. 2013; Balazs et al. 2022) to simulate the dynamics of continental rifting, continental transform fault zone formation and persistent oceanic transform faults. Numerical modelling results allow to explain the first order observations from passive and transform margins, such as diachronous incipient rifting, strain localization into individual oblique rift basins and the opening of structurally separate oceanic basins. Our models also show the evolution of continental blocks between oceanic spreading ridges bounded by strike-slip fault zones inherited from the preceding continental rifting stage. The formation of such continental slivers is controlled by the relative timing between the onset of oceanic spreading and the strike-slip fault zones formation. This is connected to the rheology of the plates and linked to different thermal gradients, divergence velocities and surface processes. Our model results are compared with observational data from the Romanche transform of the Equatorial Atlantic, the East Greenland Ridge of the Northern Atlantic and the Zabargad Islands in the Red Sea.

## REFERENCES

- Balazs A., Gerya T., MAy D., Tari G. 2022. Contrasting transform and passive margin subsidence history and heat flowevolution: insights from 3D thermo-mechanical modelling. London, Special Publications, 524.
- Gerya T.V. 2013. Initiation of transform faults at rifted continental margins: 3D petrologicalthermomechanical modeling and comparison to the Woodlark Basin. *Petrology*, 21, 550–560.
- Palmiotto C., Corda L., Bonatti E. 2016. Oceanic tectonic islands. *Terra Nova*, 29, 1-12.

## 1.4

# Structural evolution of the Rotondo granite (val Bedretto, Gotthard massif): implications for alpine tectonics and shear zone evolution in the External Crystalline Massifs.

Alberto Ceccato, Whitney M. Behr, Alba S. Zappone

*Department of Earth Sciences, ETH Zurich, Sonneggstrasse 5, 8092 Zurich, Switzerland (aceccato@erdw.ethz.ch)*

The analysis of Alpine deformation structures of the External Crystalline Massifs (ECMs) can improve our understanding of Alpine tectonics and strain localization processes during continental collision. Here we present field (and tunnel) structural analyses on the Rotondo granite (Val Bedretto, Gotthard massif), aimed at unraveling its tectonic evolution during Alpine continental collision. We also compare and discuss the models of strain localization and development of Alpine ductile shear zones inferred from structural analyses of other granitoid ECMs units (Grimsel – Aar; Fibbia – Gotthard; Mont Blanc).

Field structural analyses reveal a sequence of deformation structures for the Rotondo granite, including, from oldest to the youngest: (i) biotite-bearing shear fractures and cataclasites; (ii) NE-SW-striking, top-to-SE reverse ductile shear zones developed at amphibolite to upper-greenschist facies conditions that exploit various precursory structures and synkinematic veins and breccias; (iii) strike-slip reactivation of SE-verging shear zones with mainly dextral kinematics at greenschist facies conditions; (iv) NW-SE- and N-S-striking conjugate sets of oblique-slip faults, along with extensional chlorite + quartz veins; (v) NW-SE-striking normal faults; (vi) zeolite- and gouge-bearing strike-slip faults. These deformation structures reflect the main sequence of backthrusting, strike-slip tectonics and following activity of the Simplon-Rhone fault system during Miocene exhumation and cooling of the southwestern Gotthard massif.

Field and microstructural observations from the ductile shear zones cropping out in the Rotondo granite provide new insight into models of strain localization and tectonic evolution of Alpine ductile shear zones previously inferred from the other granitoid ECMs:

- Pre-Alpine and Alpine metamorphic reactions differently affecting plagioclase in the different granitoid facies of the massif may have controlled the development of distributed vs. localized deformation at amphibolite conditions (possibly in addition to the solely mica content as proposed by Wehrens et al., 2016).
- Alpine shear zones in the equigranular granite exploit precursor structural and compositional heterogeneities (biotite-bearing shear fractures, quartz veins, and mafic and aplitic dykes), commonly preserving their (complex) geometry at the small scale. Thicker shear zones commonly incorporate thick quartz and/or calcite layers, clearly generated as shear-plane-parallel veins or hydraulic breccias. Therefore, the finite geometry and composition of Alpine ductile shear zones might have been acquired through several, distinct and discontinuous stages of fluid injection, veining and following ductile shearing, rather than through a continuous, diffusion-controlled widening process (Oliot et al., 2014).
- Biotite-bearing shear fractures and cataclasites are observed all over the granitoid units of ECMs (Guermani & Pennacchioni, 1998; Rolland et al., 2009; Wehrens et al., 2016). They seem to either pre-date or to be contemporaneous with co-planar mafic dykes, and they are too misoriented to be related to Alpine tectonics (Herwegh et al., 2017). There is no striking evidence for frictional-viscous cyclicity on these structures (Wehrens et al., 2016). Thus, biotite-bearing shear fractures and cataclasites seem to be inherited structural features from Pre-Alpine tectonics of regional significance, common to many other ECMs.

## REFERENCES

- Guermani, A. & Pennacchioni, G., 1998: Brittle precursors of plastic deformation in a granite: An example from the Mont Blanc massif (Helvetic, western Alps). *Journal of Structural Geology*, 20, 135–148.
- Herwegh, M., Berger, A., Baumberger, R., Wehrens, P., & Kissling, E., 2017: Large-Scale Crustal-Block-Extrusion During Late Alpine Collision. *Scientific Reports*, 7, 1–10, <https://doi.org/10.1038/s41598-017-00440-0>, 2017.
- Oliot, E., Goncalves, P., Schulmann, K., Marquer, D., & Lexa, O., 2014: Mid-crustal shear zone formation in granitic rocks: Constraints from quantitative textural and crystallographic preferred orientations analyses. *Tectonophysics*, 612–613, 63–80.
- Rolland, Y., Cox, S. F., & Corsini, M.: Constraining deformation stages in brittle-ductile shear zones from combined field mapping and  $^{40}\text{Ar}/^{39}\text{Ar}$  dating: The structural evolution of the Grimsel Pass area (Aar Massif, Swiss Alps). *Journal of Structural Geology*, 31, 1377–1394.
- Wehrens, P., Berger, A., Peters, M., Spillmann, T., & Herwegh, M., 2016: Deformation at the frictional-viscous transition: Evidence for cycles of fluid-assisted embrittlement and ductile deformation in the granitoid crust. *Tectonophysics*, 693, 66–84.

## 1.5

# Using low temperature thermochronometry to estimate long-term exhumation rates in the Molasse Basin of central northern Switzerland

Kevin A. Frings<sup>1,2</sup>, Christoph von Hagke<sup>2</sup>, Peter Kukla<sup>3</sup>, Angela Landgraf<sup>4</sup>, Herfried Madritsch<sup>4</sup>

<sup>1</sup> Institute for Tectonics and Geodynamics, RWTH Aachen University, Lochnerstraße 4-20, D-52064 Aachen  
(frings@geol.rwth-aachen.de)

<sup>2</sup> Department of Geology, Salzburg University PLUS, Hellbrunnerstr. 34, 5020 Salzburg

<sup>3</sup> Geological Institute, RWTH Aachen University, Wüllnerstrasse 2, D-52080 Aachen

<sup>4</sup> Nagra, Hardstrasse 73, CH-5430 Wettingen, Switzerland

Previous studies on landscape evolution of the Alpine foreland in northern Switzerland agree that exhumation occurred in the area since the late Miocene (e.g.; Mazurek et al., 2006; Cederbom et al., 2011). However, estimates of exhumation magnitudes range between few hundreds of meters to < 3 km. Similarly, exact timing of exhumation, as well as the underlying driving mechanism(s) remain elusive. Three main processes responsible for exhumation have been proposed: plate convergence (e.g.; Persaud & Pfiffner, 2004), climate-driven erosion (e.g.; Cederbom et al., 2004; Champagnac et al., 2009), and deep-seated, mantle related processes (e.g.; Cederbom et al., 2011; von Hagke et al., 2012). However, the relative contribution of the individual drivers is not yet well known.

In this study, we present an extensive apatite (U-Th-Sm)/He thermochronological data set, which helps constraining cooling and exhumation of the uppermost 2-3 km of the crust. We focus on the deep borehole in Bülach (ZH), drilled by Nagra, centrally located in the area of interest, namely the Molasse Basin north of the Jura Mountain. By dating multiple grains along the entire well section, we are able to perform statistical analysis of the single grain age data to derive time temperature paths that enable us to reconcile previous seemingly contradicting studies.

Our results show an expected spread in single grain ages for detrital studies in the Molasse sediments, with a general trend towards younging ages at depth. Based on these data it is possible to determine a reset of the ages at a depth of about 600 meters. However, samples from the Triassic Dinkelberg Fm. ("Bundsandstein") and the Permian Weitenau Formation ("Rotliegend"), show no reset of single grain ages. Instead, an even larger spread of single grain ages can be observed, begging the question to its cause. Using 1-D thermal models we can show that this can mostly be explained by provenance age of the single grains. Overall, we can determine a consistent t-T history based on our data set. Best fits show, that about 1100 meters of erosion occurred since about 13 Ma, starting slowly and accelerating after 9 Ma. Based on modeling results we suggest that the majority of this signal is the result of large-scale mantle-related processes.

In summary, we show that our approach reconciles previous studies and significantly reduces the errors of the amount and timing of exhumation. It is thus a promising way forward to constrain exhumation histories and past landscape evolution.

## REFERENCES

- Cederbom, C.E., Sinclair, H.D., Schlunegger, F., Rahn, M.K., 2004: Climate-induced rebound and exhumation of the European Alps, *Geol.*, 32, 709.
- Cederbom, C.E., van der Beek, P., Schlunegger, F., Sinclair, H.D., Oncken, O., 2011: Rapid extensive erosion of the North Alpine foreland basin at 5-4 Ma, *Basin Research* 23, 528–550.
- Champagnac, J.-D., Schlunegger, F., Norton, K., Blanckenburg, F. von, Abbühl, L.M., Schwab, M., 2009: Erosion-driven uplift of the modern Central Alps, *Tectonophysics*, 474, 236–249.
- Mazurek, M., Hurford, A.J., Leu, W., 2006: Unravelling the multi-stage burial history of the Swiss Molasse Basin: integration of apatite fission track, vitrinite reflectance and biomarker isomerisation analysis, *Basin Research*, 18, 27–50.
- Persaud, M., Pfiffner, O., 2004: Active deformation in the eastern Swiss Alps: post-glacial faults, seismicity and surface uplift, *Tectonophysics*, 385, 59–84.
- von Hagke, C., Cederbom, C.E., Oncken, O., Stöckli, D.F., Rahn, M.K., Schlunegger, F., 2012: Linking the northern Alps with their foreland: The latest exhumation history resolved by low-temperature thermochronology, *Tectonics*, 31, TC5010.

## 1.6

# 3D model reveals thermal decomposition as a primary driver of Apennines seismicity

Thanushika Gunatilake<sup>1,2</sup>, Stephen A. Miller<sup>1</sup>

<sup>1</sup> Centre for Hydrogeology and Geothermics, University of Neuchâtel, Emile-Argand 11, CH-2000 Neuchâtel  
(thanushika.gunatilake@unine.ch)

<sup>2</sup> Swiss Seismological Service, ETH Zürich, Sonneggstrasse 5, CH-8092-Zürich

Earthquakes in the Central Apennines generate extensive and robust aftershock sequences, with high-pressure CO<sub>2</sub> often implicated as an important contributor to seismogenesis. Diffusion of mantle-derived CO<sub>2</sub> trapped in reservoirs at depth is assumed to drive these sequences, yet evidence of diffusion fronts remains elusive. The thermal decomposition of CO<sub>2</sub> imposes numerous additional and isolated sources providing substantial quantities of internally derived high-pressure fluids driving the aftershock sequences. In this work, we analyze a 3-dimensional numerical model of non-linear diffusion with a source term that mimics the generation of additional fluid by thermal decomposition. Model results show strong correlations between the spatial distribution of 50,000 observed hypocenters and calculated fluid pressure fields from the 2009 L'Aquila (Mw 6.3) and the 2016 Amatrice-Visso-Norcia (Mw 6.5) earthquakes. We also show strong correlations with observed temporal aftershock rates, and identify the onset of thermal decomposition correlating with Mw > 4, suggesting a minimum magnitude for generating significant aftershock sequences. The implications of thermal decomposition in seismogenesis are far-reaching because our results suggest this mechanism applies to all carbonate systems, and also in systems containing extensive hydrous minerals, such as within subduction zones.

## 1.7

# Experimental Investigation of Glaucomphane Deformation and Rheology Through General Shear Experiments

Lonnie Hufford<sup>1</sup>, Leif Tokle<sup>1</sup>, Whitney Behr<sup>1</sup> and Claudio Madonna<sup>1</sup>

<sup>1</sup> Structural Geology and Tectonics Group, Geological Institute, Department of Earth Sciences, ETH Zurich, Sonneggstrasse 5, 8092, Zürich, Switzerland ([lonnie.hufford@erdw.ethz.ch](mailto:lonnie.hufford@erdw.ethz.ch))

Glaucomphane is a primary strain-accommodating mineral in subducted oceanic crust at blueschist facies conditions. Despite this, the flow law parameters and range of deformation mechanisms in glaucomphane aggregates have not been characterized experimentally. Here we present a suite of constant-rate, general shear, deformation experiments in a Griggs apparatus to investigate the mechanical properties, microstructures and deformation mechanisms in glaucomphane aggregates. The starting material consists of glaucomphane powder separated from natural MORB-affinity blueschists from Syros Island, Greece, with sieved grain size populations from 75-90 µm and 63-355 µm. Our experimental suite thus far includes temperatures ranging from 650° to 750°C, pressures of 1.0 GPa, and a shear strain rate of ~3x10<sup>-6</sup>/s. The 700°C constant-rate experiment with a starting grain size range of 75-90 µm (LH060) exhibits evidence for frictional deformation by fracturing observed with microstructural analysis while the mechanical data is consistent with a mechanical steady-state flow. The 700°C constant-rate experiment with a starting grain size population of 63-355 µm (LH049) has microstructures consistent with frictional deformation by fracturing and viscous deformation via dislocation glide. This experiment produced a similar steady-state flow stress to LH060; however, the smaller grain size population reached a lower peak stress. The 725°C experiment displays both frictional and viscous deformation by fracturing and dislocation glide. In the constant-rate experiment conducted at 750°C, we observed exsolution microstructures suggesting we reached the chemical stability field for glaucomphane. To better characterise glaucomphane deformation, further experiments will be conducted to investigate the evolution of deformation.

## 1.8

# Age and temperature conditions of folding and thrusting in the Säntis Nappe and the adjacent Subalpine Molasse from calcite U-Pb dating and clumped isotope thermometry

Gillian Iten<sup>1</sup>, Lukas Nibourel<sup>1</sup>, Nathan Looser<sup>2</sup>, Marcel Guillong<sup>2</sup>, Lorenzo Tavazzani<sup>2</sup>, Stefano M. Bernasconi<sup>2</sup>, Stefan Heuberger<sup>1</sup>

<sup>1</sup> Georesources Switzerland Group, Department of Earth Sciences, ETH Zurich, Sonneggstrasse 5, 8092 Zürich, Switzerland  
(giten@student.ethz.ch)

<sup>2</sup> Climate Geology Group, Department of Earth Sciences, ETH Zurich, Sonneggstrasse 5, 8092 Zürich, Switzerland.

We present new absolute estimates of the timing and fluid temperature conditions of folding and thrusting in the Säntis Nappe and the adjacent Subalpine Molasse (Fig. 1) by applying calcite U-Pb dating and clumped isotope thermometry on syntectonic calcite mineralisations. In the Säntis Nappe, we focused on the Sax-Schwende Fault (SSF), a N-S striking transfer fault which cross-cuts the dominantly WSW-ENE striking folds and on thrusts of the Säntis Nappe such as the Rotsteinpass Thrust (RST), the most continuous thrust in the study area which is accompanied by several thrust imbricates (Fig. 2). The oldest ages obtained from the RST show that compressional deformation in the Säntis Nappe initiated ca. 41 Ma ago or earlier. These ages are in agreement with the kilometre-scale refolding of the RST and with the refolding of the main foliation and associated calcite veins along this thrust system at the outcrop scale. Fluid temperatures of 120–130 °C were associated with this early thrusting (Fig. 1). These temperatures are lower than the maximum temperatures of 150 °C reached between 35 and 25 Ma, suggesting that thrusting and folding along the RST initiated under prograde metamorphic conditions during net burial in the footwall to the Austroalpine and Penninic nappes (grey line in Fig. 2). Along the SSF, the ages range between 35 and 10 Ma. These ages are in line with structural observations suggesting continued activity of the SSF during folding and thrusting in the Säntis nappe. The youngest ages are 10 Ma old and associated temperatures of 100 °C highlight continued deformation along the SSF and the Säntis Thrust during exhumation of the area related to the northward progradation of deformation to the Subalpine Molasse. Our field observations reveal secondary faults and flexures in the Subalpine Molasse in front of the SSF. This indicates that this fault was not restricted to the Säntis Nappe but also affected tectonically lower levels.

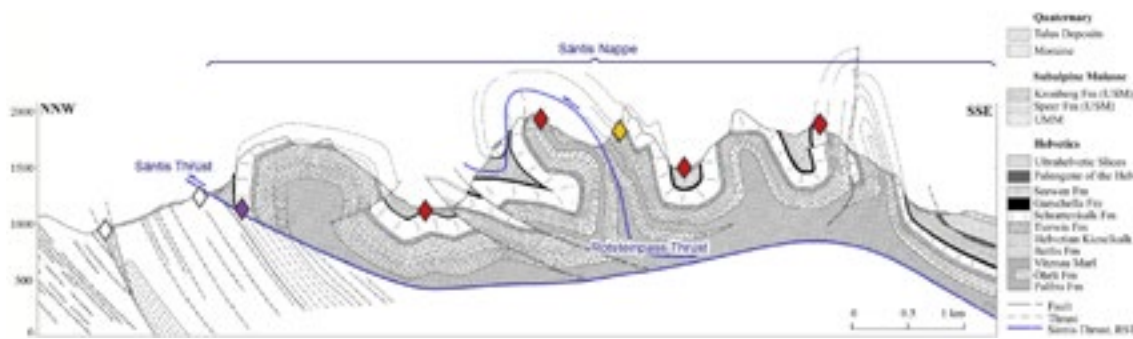


Figure 1. Cross section of the study area (modified after Funk et al., 2000) showing the most important tectonic features of the Säntis Nappe and the adjacent Subalpine Molasse. Colored diamonds highlight sampling localities (legend as in Fig. 2).

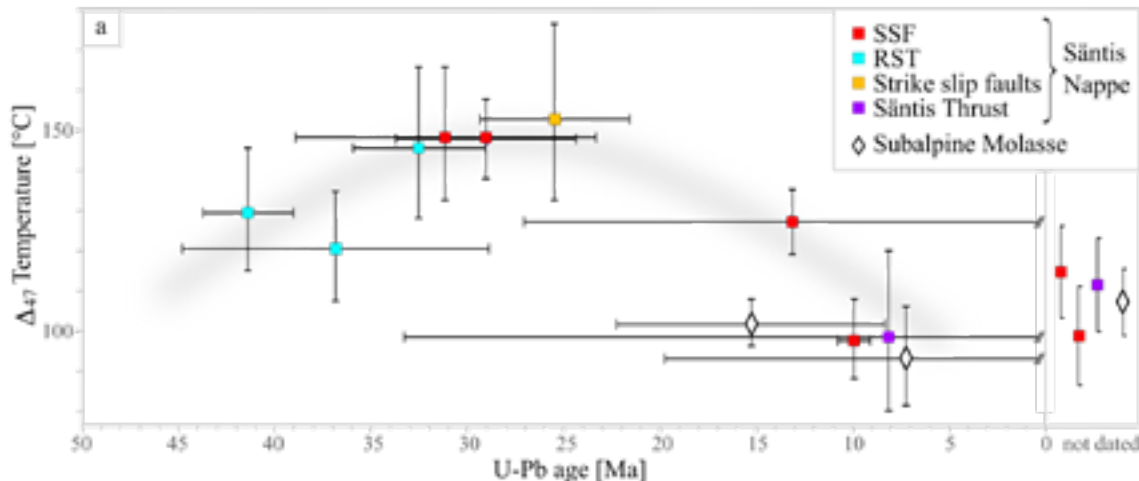


Figure 2. Results from U-Pb dating and clumped isotope thermometry from the Säntis Nappe (colored data points) and the adjacent Subalpine Molasse (white data points). The approximate temperature-time trend estimated for the Säntis Nappe is schematically shown as a grey line. SSF – Sax-Schwende Fault, RST – Rotsteinpass Thrust (see also Fig. 1).

## REFERENCES

- Funk, H., K. Habicht, R. Hantke, and A. Pfiffner, 2000: Blatt 1115 Säntis.-Geologischer Atlas der Schweiz 1: 25 000, Erläuterungen 78. Bundesamt für Wasser und Geologie Bern, Switzerland.

## 1.9

# Stratigraphic thickness variations of the Helvetian Kieselkalk in central Switzerland: new automatically extracted thickness data from mapped bedrock exposures and field orientation measurements

Lorena Juchler<sup>1</sup>, Lukas Nibourel<sup>1</sup>, Joël Morgenthaler<sup>1</sup>, Maira Coray<sup>1</sup>, Salome Schläfli<sup>2</sup>, Pauline Baland<sup>2</sup>, Jonas Ruh<sup>3</sup>, Thomas Galfetti<sup>2</sup>, Stefan Heuberger<sup>1</sup>

<sup>1</sup> Georesources Switzerland Group, Department of Earth Sciences, ETH Zurich, Sonneggstrasse 5, 8092 Zürich, Switzerland ([lorena.juchler@sunrise.ch](mailto:lorena.juchler@sunrise.ch))

<sup>2</sup> Swiss Geological Survey, Swiss Federal Office of Topography swisstopo, Seftigenstrasse 264, 3084 Wabern Switzerland.

<sup>3</sup> Geological Institute, Department of Earth Sciences, ETH Zurich, Sonneggstrasse 5, 8092 Zürich, Switzerland.

Hard rock aggregates are essential for the Swiss road and railway infrastructure. To secure the access to this raw material, the Georesources Switzerland Group is mandated to develop an inventory of potential hard rock deposits. One key parameter for the evaluation of potential occurrences is the stratigraphic thickness of a given target lithostratigraphic unit.

In the Swiss Alps, potential target units are affected by strong sedimentary and tectonic thickness variations. This can make the determination of thickness through cross-sections or 3D models time-consuming. Here, we present a new Matlab-based approach which automatically extracts the stratigraphic thickness of a target unit, using orientation field measurements and mapped bedrock exposures from the 1:25'000 harmonised Swiss geological vector data set GeoCover.

The aim of the approach is to scan large-scale areas for the stratigraphic thickness in a short amount of time. To test the approach we analyse the Helvetian Kieselkalk on nine 1:25'000 geological map sheets covering central Switzerland, which is the key area for the extraction of this unit. We propose different numeric filtering parameters to detect unreliable model outputs. Thickness data from literature are used to independently validate the quality of the model output.

Our results highlight strong thickness variations and discrete thickness jumps across major nappe boundaries of central Switzerland (see Fig. 1 and 2). The highest thickness values of more than 1000 m are estimated for the southernmost Wildhorn Nappe, which is in agreement with the literature data. In the Helvetic border chain, the model detects minor but systematic along-strike variation between ca. 100 and 340 m. In areas with precisely mapped geological contacts and accurate orientation measurements, the model output is in good agreement with the literature data, even at the presence of folds and faults (Figs. 1 and 2). Inconsistencies between model and literature mostly occur near fold hinges (Fig. 1) or in areas with poor exposure of the base or the top contacts (Fig. 2). The overall good agreement between model and literature data, the rapidity, the possibility to assess the reliability of the automatically extracted thickness data highlight the potential of the approach, which enables an early identification of promising areas for potential raw material extraction.

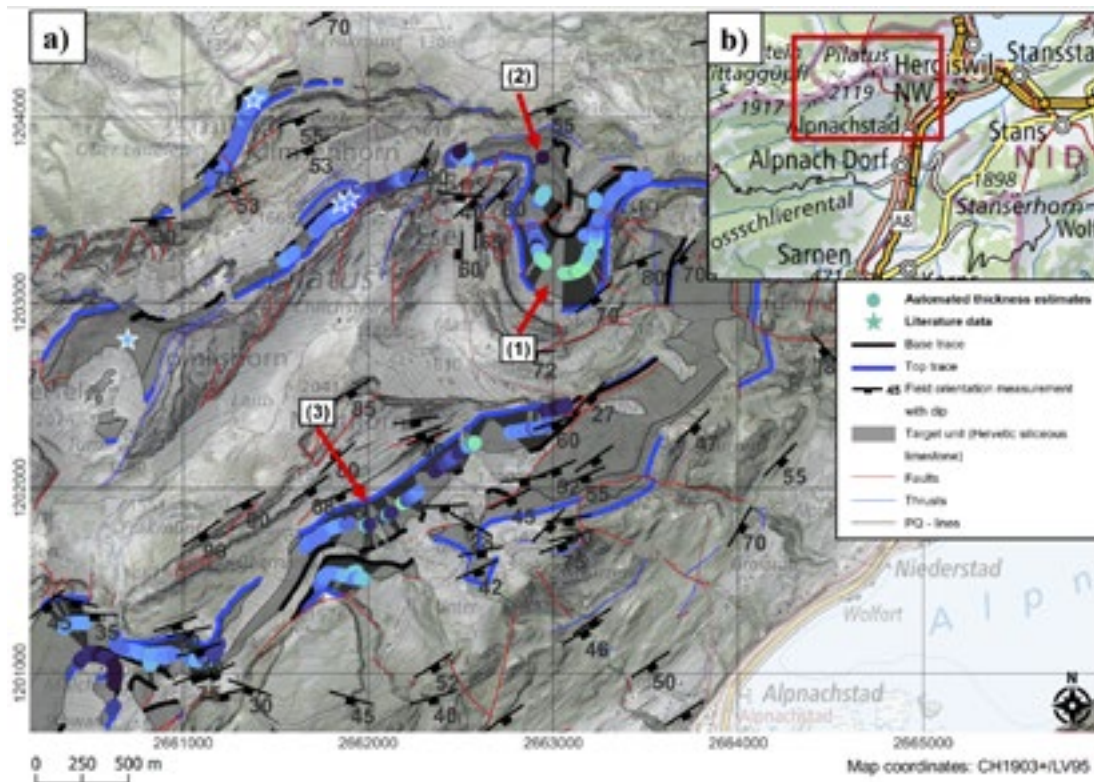


Figure 1. Overall good agreement between model output (colored dots) and literature thickness data (stars) in the Pilatus area with good exposure and with densely spaced orientation field measurements. Arrows (1), (2) and (3) highlight outliers due to orientation measurements which are not in agreement with the mapped contacts (most likely due to folding).

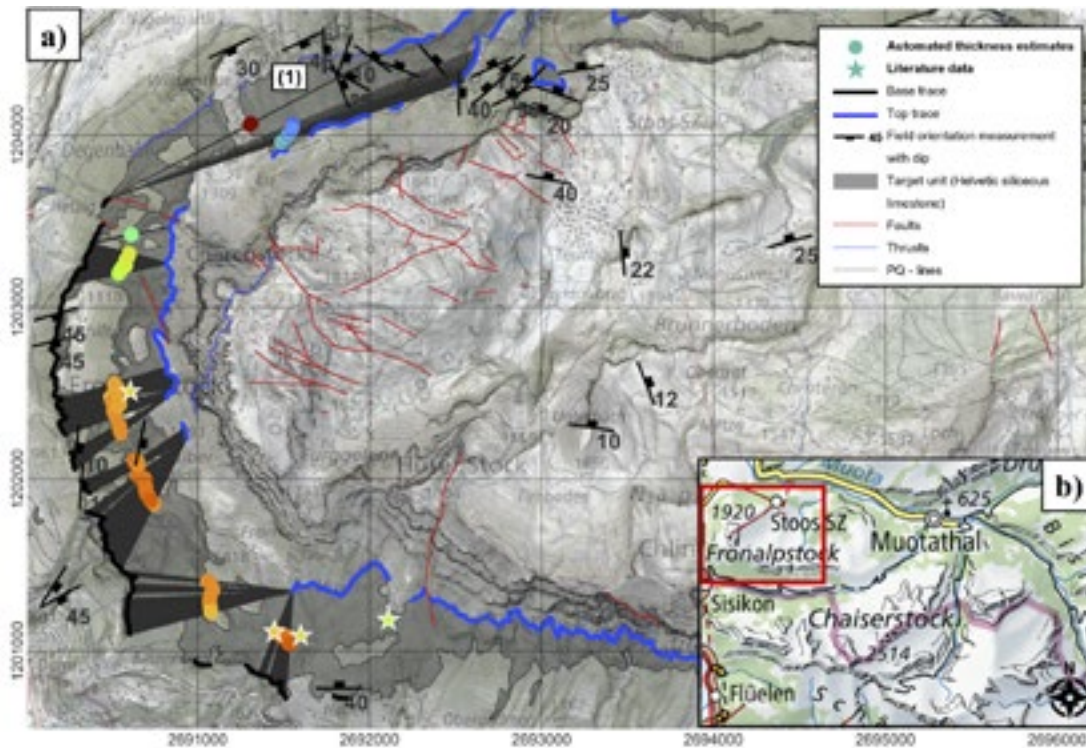


Figure 2. Extract from map sheet Muotathal with overall good agreement between model output (colored dots) and literature thickness data (stars). The (1) highlights unreliable thickness estimates due to the poor exposure of the base contact in the area.

## 1.10

# Temperature and fluid evolution in the Mesozoic formations of central northern Switzerland over the last 200 Ma: insights from coupled carbonate clumped isotopes and U-Pb dating

Nathan Looser<sup>1</sup>, Herfried Madritsch<sup>2,3</sup>, Lukas Aschwanden<sup>4</sup>, Stephan Wohlwend<sup>1</sup>, Marcel Guillong<sup>1</sup>, Daniel Traber<sup>2</sup> & Stefano M. Bernasconi<sup>1</sup>

<sup>1</sup> Department of Earth Sciences, ETH Zürich, Sonneggstrasse 5, 8050, Zürich ([nathan.looser@erdw.ethz.ch](mailto:nathan.looser@erdw.ethz.ch))

<sup>2</sup> Nagra, Hardstrasse 73, CH-5630 Wettingen

<sup>3</sup> Swisstopo, Seftigenstrasse 264, CH-3084 Wabern

<sup>4</sup> Institute of Geological Sciences, University of Bern, Baltzerstrasse 1+3, 3012 Bern

Secondary carbonates form in a wide range of diagenetic environments during different stages in the history of sedimentary basins. Besides the timing of mineralization, the isotopic composition of such carbonates records the temperature and isotopic composition of the precipitating fluid. If preserved and datable, they allow to define absolute time frames for the evolution of temperature and sources of the precipitating fluids during burial.

In this study, we combine carbonate clumped isotopes and in-situ laser ablation-inductively coupled plasma-mass spectrometry (LA-ICP-MS) U-Pb dating of secondary carbonates to reconstruct the multi-stage burial history of the Mesozoic formations in central northern Switzerland over the last 200 Ma. Our extensive dataset of > 100 samples collected from deep exploration boreholes of Nagra as well as from key outcrops comprises early to late diagenetic cements covering the entire Middle-Triassic to Upper Jurassic sedimentary record.

We constrain burial temperatures and fluid sources for four different geodynamic intervals since the Early Jurassic: 1) Unexpectedly high temperatures of up to 120 °C despite shallow burial depths and oxygen isotopic compositions of the precipitating fluids ( $\delta^{18}\text{O}_{\text{fluid}}$ ) well below equilibrium with the host rocks during Middle Jurassic to Early Cretaceous, which coincide with high subsidence rates and which we relate to high basal heat flow due to major crustal extension. 2) Cooling to 30-50 °C together with a shift towards a meteoric fluid source during Eocene to Oligocene resulting from forebulge-related Late Cretaceous (?) to Eocene uplift and erosion. 3) Increase in burial temperatures to 50-100 °C resulting from a second cycle of basin evolution with burial under Molasse deposits and persisting during the formation of the Jura fold-and-thrust belt while the fluids remained of meteoric origin. 4) Cooling to present-day conditions related to large-scale erosion of the Molasse Basin at its northern margin during Pliocene.

## 1.11

### Arc progression capitalises on low-angle thrust faults in East Java, Indonesia.

Lupi, M1., De Gori, P2., Valoroso, L2. , Baccheschi, P2. , Minetto, R. 3, Mazzini, A. 4

*1 Department of Earth Sciences, Universtiy of Geneva, Geneva, Switzerland.*

*2 Instituto Nazionale di Geofisica e Vulcanologia, Roma, Italy.*

*3 University Grenoble Alpes, ISTerre, Grenoble, France.*

*4 Center for Earth Evolution and Dynamics, University of Oslo, Oslo, Norway.*

East Java features a smooth transition from magmatic to sedimentary volcanism. The spatial distribution of the eruptive centers is affected by the local tectonics. Fluids migrate from the upper crust below the volcanic arc and capitalize on low-angle thrust faults to feed the eruptive systems occurring in the back arc. In 2006 a large sediment hosted geothermal system named Lusi, pierced the Kendeng basin in East Java and since then it continues erupting relentless. We deployed a temporary seismic network to investigate the velocity structure of this region. Specifically, we study the spatial and structural relationships between the volcanic arc and the back-arc domains, by performing a local earthquake tomography. By combining geochemical, geological and geophysical data we propose a conceptual model suggesting that magmas and hydrothermal fluids may migrate from the middle to the upper crust into the sedimentary basins capitalising on existing thrust faults. In this model, Lusi is located at the intersection of low-angle thrust faults and steep-dip strike slip faults, in region where the hydraulic transmissivity of the upper crust is enhanced.

## 1.12

# Gravitational volcano flank motion imaged by historical air photo correlation during the M7.7 Kalapana earthquake (1975), Big Island, Hawaii

Stefano Mannini<sup>1</sup>, Joël Ruch<sup>1</sup>, James Hollingsworth<sup>2</sup>, Donald A. Swanson<sup>3</sup>, Ingrid Johanson<sup>3</sup>

<sup>1</sup> Department of Earth Sciences, University of Geneva, Rue des Maraîchers 13, 1205, Geneva, Switzerland

<sup>2</sup> ISTerre Université Grenoble Alpes, UMR 5275 CNRS, 1381 Rue de la Piscine, 38610 Gières, France

<sup>3</sup> U.S. Geological Survey - Hawaiian Volcano Observatory, 1266 Kamehameha Ave., Hilo, HI 96720, United States of America

Volcanic islands are often subject to flank instability, resulting from a combination of magma intrusions along rift zones, gravitational spreading and extensional faulting observed at the surface. The Kilauea is one of the most active volcanoes on Earth and its south flank show recurrent flank acceleration related to large earthquakes and magmatic intrusions. Despite several studies on the flank instability, it is still not clear how the basal detachment connects to the fault systems located along the south flank.

Here we focus on the M 7.7 Kalapana earthquake that occurred on 29 November 1975. It triggered ground displacement of several meters all over the south flank of the Kilauea volcano. The identification and quantification of the co-seismic rupture aim to better understand the overall flank motion and its connection to key structural components, such as between the southwest and east rift zones and the deep basal detachment where large earthquakes episodically nucleate.

Using optical imagery correlation technique, we analyzed the displacement that occurred during the 1975 earthquake. We used 26 and 22 historical air photos as pre-event (October 1974 and July 1975, respectively) and 7 and 44 for the post-event time period (December 1976 and March 1977, respectively). The resulting displacement maps show metrical horizontal (north-south direction) and vertical displacement along a 25 km long East-West sector of the Kilauea south flank. We show that the ground rupture is continuous with most portions of faults that have been reactivated. Locally, the displacement values we found are in good agreement with punctual EDM and levelling measurements. Several fault segments have been activated close to the shore and their extension were previously unnoticed. Interestingly, we observe along the Hilihina Pali fault a constant increase of the offset away from the epicenter in the West direction, from a few meters up to ~12 meters, west of the Hilihina Pali road, in good agreement with long-term fault motion evidenced by the westward increase of the fault scarp height. The deformation turns out to be higher where the faults are oriented NE-SW (western sector) compared to E-W oriented structures. This suggests that the flank is likely strongly influenced by gravitational effect, typical from large landslide processes. This observation provides additional information to better understand the connection between the Hilihina fault system and the basal detachment. Episodic flank motions on volcanic islands are rare events and this work contributes to the overall comprehension of volcano flank instability elsewhere.

## 1.13

### Jura Fold-and-Thrust Belt: on basement, thrusting and timing

Jon Mosar<sup>1</sup>, Sandra Borderie<sup>1</sup>, Louis Hauvette<sup>1,4</sup>, Peter Jordan<sup>2</sup>, Adeline Marro<sup>1</sup>, Marc Schori<sup>3</sup>, Anna Sommaruga<sup>1</sup>, Anina Ursprung<sup>1</sup>

<sup>1</sup> Department of Geosciences, University of Fribourg, Chemin du Musée 6, CH-1700-Fribourg ([jon.mosar@unifr.ch](mailto:jon.mosar@unifr.ch))

<sup>2</sup> Gruner Böhringer AG, Mühlegasse 10, CH-4104 Oberwil

<sup>3</sup> GEOTEST AG, Bernstrasse 165, CH-3052 Zollikofen

<sup>4</sup> Hydro-Geo-Environnement, Chemin Fief-de-Chapitre 7, CH-1213 Petit-Lancy, Genève

The Jura Mountains, in France and Switzerland, form a classic thin-skinned fold-and-thrust belt (FTB), and are part of the Alpine foreland, together with the Western Alpine Molasse Basin. The Molasse Basin initiated as a flexural basin and evolved into a wedge-top basin following the initiation of the main foreland decollement level. The Jura FTB enjoyed a transport of some 30km towards the foreland along a main decollement in the mechanically weak Triassic salt-rich evaporites. It behaves as a mechanical wedge in hydrostatic conditions propagating towards the Alpine foreland. Changes in the surface topography, the basal decollement inclination and in the basal friction, lead to wedge-internal accommodations, which are operated by oscillating forward and backward stepping sequences of thrusting and related fold development. Recent and current works about the Jura FTB lead to an update of our knowledge of this area.

- A new basement map of the Alpine foreland, including the Jura FTB allows us to assess the importance and relevance of inherited paleotopography and fault reactivation for the cover deformation. Analogue modelling has helped show that oblique steps in the basement topography lead to the formation of normal and reverse faulting and oblique fold structures in the cover. A retrodeformation of the whole Jura further makes it possible to identify new basement structures in the hinterland.
- Distinct tectonic nappes are identified through a re-assessment of the tectonics and kinematics. These nappes, define structural domains where lateral coherence ensures kinematic consistency across the whole FTB range. They are bound by major strike-slip faults (acting as inherited, rigid boundaries), progressive en-echelon relay zones and major thrusts, some of which may exhibit 15 km long ramps and flats.
- A new relative chronology of thrusting and deformation is proposed thanks to kinematic reconstructions. Combined with published absolute ages and ages from the sedimentary record, it possible to assess oscillating and repeated thrust and fault activity. Deformation in the Jura FTB is partitioned and distributed along discrete faults that clearly operate in a forward and backward oscillating manner.
- The current state of stress of the Jura FTB is explored by numerical modelling of local and regional profiles. The models notably confirm the importance of changes of basement topography (changes in dip or offsets up or down) on stress and deformation distributions, and stress magnitudes. Distance to criticality can thus be compared with wedge mechanics approaches. Moreover, modeling of retrodeformed sections will characterize the importance of topography versus décollement properties (i.e. friction and angle of dip).
- Finally, the new basement and tectonic maps, the renewed kinematic understanding and timing, allow us to link of different types of faults observed in the field, such as normal faults, inverted inherited faults, thrust faults and strike-slip faults, to major tectonic processes such as flexural bending, rifting, faulting due to steps in basement topography, and thrusting inside a mechanical wedge.

## 1.14

# Shortening tectonic style in the Western Alpine foreland: Example from the Geneva Basin (Switzerland) and implications for subsurface geo-fluid circulation.

Andrea Moscariello<sup>1</sup>, Ovie Emmanuel Eruteya<sup>1</sup>, Nicolas Clerc<sup>2</sup>, Fiammetta Mondino<sup>3</sup>, Luca Guglielmetti<sup>1</sup>

<sup>1</sup>*Geo-Energy Reservoir Geology and Sedimentary Basin Analysis, Université de Genève, Rue des Maraîchers 13, 1205, Geneva, Switzerland (Andrea.Moscariello@unige.ch)*

<sup>2</sup>*GESDEC Service de Géologie, Sol et Déchets, Canton of Geneva, Quai du Rhône 12, 1205 Genève, Switzerland*

<sup>3</sup>*Geneva Earth Resources SA, Rue Jean Jaquet 10, 1201 Geneva*

The Western Swiss Alpine foreland, located between the Alpine front and the folded Jura chain is described as generally undisturbed plateau where the shortening related to the Alpine compression is accommodated mostly by deeply rooted sliding of the thick Mesozoic series over the Triassic evaporites. In addition to the basal sliding, attesting for the thin-skin tectonic character of the regional deformation, a series of several-km long N-S and NW-SE regional strike slip faults were thought to be formed in order to accommodate the regional shortening resulting in the lateral compartmentalization of the undeformed thick succession of Mesozoic and Cenozoic sediments (Moscariello, 2019). Recent seismic interpretation has however highlighted a higher level of complexity in the structural framework which most likely consist of more discontinuous and variably oriented and vertically extended fault segments (Clerc and Moscariello, 2020).

The role of high-angle faults deeply rooted in the underlying Hercynian basement in the deformation of the Swiss Plateau is still under debate. However, evidence of a relationship between the occurrence of buttress of Hercynian basement and the development of salt-cored anticlinal structures in the overlying Mesozoic, targeted in the past by hydrocarbon exploration, indicate the importance of these Paleozoic structures in explaining the present-day deformation style of the Swiss Plateau subsurface, such as the Mount Salève, whose location likely corresponds to a the NW boundary of a NE-SE oriented Permo-Carboniferous graben formed during upper Paleozoic time and infilled by sin-tectonic sediments. Seismic interpretation suggest that in correspondence of deeply buried Permo-Carboniferous depocenter during Triassic time anomalous thickness of evaporites formed which later were deformed during the Alpine compression forming the core of reliefs formed during the Cenozoic tectonic. 2D seismic observations are also supported by gravity data which highlight the occurrence of depo centers and lateral changes in density fields corresponding to lateral variations of preserved sedimentary sequences vs. basement rocks (Guglielmetti and Moscariello, 2021).

In addition to the key role played by deeply rooted fault systems, this study highlights the presence of several structural discontinuities confined within specific stratigraphic intervals both within the Cenozoic and Mesozoic succession. These deformation consist of low-angle inverse faults/thrusts which root generally in correspondence with shale and marly intervals, i.e. ductile/plastic lithologies occurring within the Oligocene clastics, Lower Cretaceous and Lower Jurassic series. In places fault and dense fracture network associated with these deformations cross the entire thickness of the Mesozoic sequence above the Triassic anhydrites showing a listric character rooted in the Lower Jurassic shale intervals (e.g. Toarcian). Thrust anticlines formed in the low-angle hanging wall have also been observed. These compressional features have an axis generally oriented parallel to the main deformation of the Jura chain, which display a progressive rotation from NE-SW to N-S direction. Specifically, the continued deformation of the area during the Alpine orogenesis led to the formation of small anticlines ridges such as the NE-SW oriented hills of Bernex and Dardagny-Satigny, and the development of transpressive strike slip such as the Vuache Mountain.

These observations indicate a higher structurally complexity than previously thought. It reflects a complex history of deformation indicating that shortening is accommodated by small low-angle inverse faults and thrusts displaying tens to few hundreds of meters of lateral displacement with little vertical offset.

The outcome of this ongoing study has key implications for the understanding the structural controls on the subsurface circulations of both hydrocarbon and geothermal fluids.

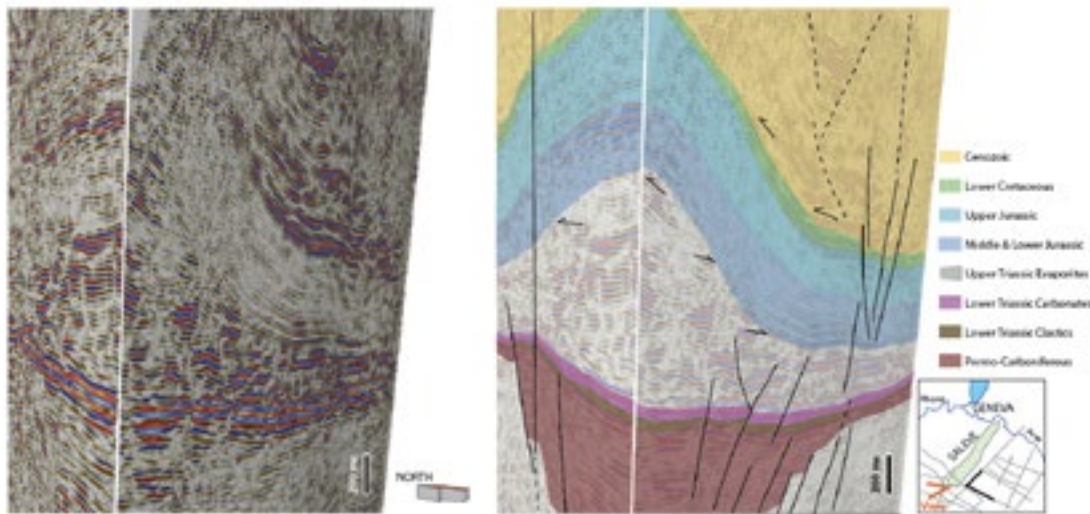


Fig. 1. Seismic interpretation of the south-eastern sector of the Salève Mountain. The length of the composite seismic profile is about 10.5 km.

## REFERENCES

- Clerc N. and Moscariello A., 2020. A revised structural framework for the Geneva Basin and the neighboring France region as revealed from 2D seismic data: implications for geothermal exploration, *Swiss Bull. angew. Geol.*, 25/1+2, 2020, 109-131.
- Guglielmetti L. and Moscariello A. 2021. On the use of gravity data in delineating geologic features of interest for geothermal exploration in the Geneva Basin (Switzerland): prospects and limitations. *Swiss J. of Geosci.*, 114(15).
- Moscariello A. 2019. Exploring for geo-energy resources in the Geneva Basin (Western Switzerland): opportunities and challenges. *Swiss Bull. angew. Geol.*, 24/2, 105-124.

## 1.15

# Permeability and Fluid Flow in the deep Slow Slip and Tremor Source: Insights From the Cycladic Blueschists (Greece)

Jesús Muñoz-Montecinos<sup>1</sup>, Whitney Behr<sup>1</sup>

<sup>1</sup> Structural Geology and Tectonics Group, Geological Institute, Department of Earth Sciences, ETH Zürich, Sonneggstrasse 5, 8092, Zürich, Switzerland (jmunoz@erdw.ethz.ch)

The base of the forearc, in particular along the deep subduction environment, is commonly regarded as a region where high pore fluid pressures might lead to the generation of transient seismic and aseismic events. Thus, explaining various aspects of Slow Slip and Tremor (SST). The fluids occurring therein are thought to migrate episodically across and up-dip along the subduction interface. This implies, therefore, that permeability is dynamic at temporal and spatial scales (Gosselin et al., 2020). For this region, permeability estimates are derived from Vp/Vs ratios and laboratory experiments, but exhumed metamorphic rocks may provide valuable observations. We herein use an exposure of blueschist-greenschist-facies rocks that underwent metamorphic P-T conditions comparable to the active Cascadia subduction margin. Thus, by comparing an exhumed complex to seismological observations, we shed a light into the hydrological (e.g., porosity, permeability and velocity of fluid flow) and seismic-wave, elastic petrophysical properties of the deep subduction environment where SST occur.

We selected the Megas Gialos locality in the Syros Island (Greece) as it preserves a fabric that is overprinted by abundant, late syn- to post-kinematic metamorphic veins. These features likely record deformation during prograde burial and underplating, followed by fluid injection and hydrofracturing into, and brittle-viscous deformation of, the underplated lithologies in the forearc. Oxygen ( $\delta^{18}\text{O}$ ) and carbon ( $\delta^{13}\text{C}$ ) isotopic ratios from the carbonate-bearing veins are consistent with a mafic contribution, suggesting that the fluids were injected from a deep-seated source. In addition, we applied a multi-scale investigation through drone mapping and micro-scale observations on quartz, calcite and epidote-bearing vein networks. Along-dip fluid pathways are recorded by chlorite-epidote-rich metasomatic reaction zones or selvages and extensional quartz veins oriented parallel to the main fabric, while across-dip fluid conduits correspond to dilatational (mode 1) and dilatational-shear (mode 2) veins that crosscut the main foliation. Our observations reveal that episodic hydrofracturing –evidenced in the form of crack-seal (healing) textures– occurred in a very episodic manner. Thus allowing to estimate upper and lower boundaries of across-foliation porosities during transient fluid injection in the range of 0.008 to 0.08. Individual fracturing events caused dilation in the 10-1000 ums range. Furthermore, by using Darcy's law along with a physical formulation (Walder and Nur, 1984), we estimate transient permeabilities associated with hydrofracturing and fluid flow in the order of  $10^{-16}$  to  $10^{-12} \text{ m}^2$ . These values are several orders of magnitude higher than would be expected for pristine rocks at these conditions, but compatible with geophysical observations of transient fluid flow in the SST region (e.g., Cruz-Atienza et al., 2018; Dal Zilio and Gerya 2022). Our results allow estimating the rates of porosity reduction necessary to seal the porosity created at the time scale of SST processes, as well as determining seismic velocity profiles derived from rock textural analysis (EBSD data) that incorporate the effects of fluids. Thus, this investigation will help to calibrate further numerical simulation and serve as a reference for seismological investigations aimed at illuminating the physical mechanisms governing the deep SST source.

## REFERENCES

- Cruz-Atienza, V. M., Villafruente, C., & Bhat, H. S. 2018: Rapid tremor migration and pore-pressure waves in subduction zones. *Nature communications*, 9(1), 1-13.
- Dal Zilio, L., & Gerya, T. 2022: Subduction earthquake cycles controlled by episodic fluid pressure cycling. *Lithos*, 426, 106800.
- Gosselin, J. M., Audet, P., Estève, C., McLellan, M., Mosher, S. G., & Schaeffer, A. J. 2020: Seismic evidence for megathrust fault-valve behavior during episodic tremor and slip. *Science Advances*, 6(4), eaay5174.
- Walder, J., & Nur, A. 1984: Porosity reduction and crustal pore pressure development. *Journal of Geophysical Research: Solid Earth*, 89(B13), 11539-11548.

## 1.16

# It's the rift turn: Faults, obliquity, and magma propagation in the Icelandic North Volcanic Zone using UAV-based structural data

Elisabetta Panza<sup>1</sup>, Joël Ruch<sup>1</sup>

<sup>1</sup> Department of Earth Sciences, University of Geneva, Rue des Maraîchers 13, 1205 Genève ([elisabetta.panza@unige.ch](mailto:elisabetta.panza@unige.ch))

Volcano-tectonic systems involve a relation between magma propagation and faulting that is fundamental in volcanology research. Earth's upper crust is often modelled as homogeneous and elastic. However, rifting events and tectonic motion systematically reactivate inherited structures that play a key role in volcano-tectonic processes and exert a fundamental influence on eruptions locations.

This study aims at investigating inherited structures' role on magma propagation in extensional settings, subject to different degrees of opening obliquity.

Being a portion of a mid-ocean ridge on a magma plume, Iceland is home of several volcano-tectonic events, which release over days or weeks the tectonic strain deficit accumulated over centuries. Despite a steady ~2cm/yr average extension rate in the far-field given by geodetic data, metrical stepwise opening is often recorded after each event in the near-field, suggesting a cyclic nature of strain loading and release.

We performed an extensive structural mapping based on UAV imagery and field observations in the North Volcanic Zone. We studied four selected rift zones within the Askja and Bardarbunga volcanic systems. The chosen rifts display different obliquity degrees, progressively bending from an almost N-S orientation in the North to a rather NE-SW to the South, while the strain field orientation of the rift shows a constant extension vector's azimuth of ~104°.

The results stem from a detailed morphological and structural analysis of the processed imagery (~3 cm/px DEMs and ~2 cm/px orthomosaics) and analysed fracture orientations, sense of opening and the effect of topography on the rift segments. The strength of the obliquity signal increases going from North (where no clear obliquity dominance is observed) to South (where Holuhraun shows distinct obliquity in a left-lateral sense), following the curvature of the overall rift segments. The processed imagery revealed typical structures related to volcano-tectonic processes, such as monoclines, open fractures, nested grabens with fault scarps that suggest reactivation, and intrusions oblique to the graben shoulders.

Our observations help constraining the strain configuration and its evolution during intrusions during the Holocene time and tempt to unveil the processes that govern magma propagation in a fractured crust at divergent plate boundaries.

## 1.17

### 3D reconstruction of the sole shear zone of the Adula nappe and its repercussion on the Alpine regional geology

Filippo Luca Schenker<sup>1</sup>, Matteo Maino<sup>2</sup>, Alessia Tagliaferri<sup>1,3</sup>, Michele Peruzzo<sup>2</sup>, Claudio Castelletti<sup>4</sup>, Daphné Giacomazzi<sup>1</sup>, Alessia Vandelli<sup>5</sup>, Rocco Wennubst<sup>1</sup>, Yves Gouffon<sup>6</sup>, Christian Ambrosi<sup>1</sup>

<sup>1</sup> University of Applied Sciences and Arts of Southern Switzerland (SUPSI), Institute of Earth Sciences, Dipartimento ambiente costruzioni e design, CH-6850 Mendrisio (filippo.schenker@supsi.ch)

<sup>2</sup> Department of Earth and Environmental Sciences, University of Pavia, via Ferrata 1, 27100 Pavia, Italy

<sup>3</sup> University of Lausanne (UNIL), Institute of Earth Sciences (ISTE), Bâtiment Géopolis, Quartier UNIL-Mouline, CH-1015 Lausanne

<sup>4</sup> CSD Ingegneri SA, Via P.Lucchini 12, CH-6900 Lugano

<sup>5</sup> Geosfera, Via Cresperone 9A, CH-6932 Breganzona

<sup>6</sup> Swiss Geological Survey, Federal Office of Topography swisstopo, Seftigenstrasse 264, CH-3084 Wabern

Intense shearing stretches and elongates deformable bodies within a viscous matrix preferentially along the shear direction. Hence, constrictional structures are typical and sometimes diagnostic of crustal shear zones within a non-coaxial deformation. In such a geodynamic scenario, the deformational evolution leads to the loss of the lateral continuity of the more competent lithological units, challenging the large-scale geological mapping, potentially resulting in misleading regional interpretations.

Here we present detailed geological maps and profiles (scale 1:10'000) along the crustal shear zone at the base of the Adula nappe, the largest high-pressure unit of the Central Alps. Overall, geological data show that the lithological contacts are horizontal or dip gently E-SE, parallel to the penetrative foliation developed at amphibolite metamorphic facies conditions. On the foliation plane, the mineral and stretching lineation is oriented from NNW-SSE to N-S independently on the orientation of the schistosity. However, within this general trend, up to several km-long gneissic bodies (mostly ortogneisses) deflect the foliation steeply to the E or to the W depicting large-scale prolate ellipsoids, elongated parallel to the mineral and stretching lineation. Around these deflections, folds with axes parallel to this prolate bodies show, on the plane sub-orthogonal to the lineation, concentric- or  $\Omega$ -shapes typical of sheath folds. In addition, large-scale  $\Omega$ -folds have been mapped over 30 km along the shear zone building large-scale structures such as tectonic windows. We conclude that the most complete explanation for these complex structural patterns is the progressive constrictional shear regime during the emplacement of the Adula nappe in the Eocene-Oligocene, without invoking a regional polyphase deformation. The crustal shear zone was active at upper amphibolitic Barrovian metamorphic condition, during the vanishing stage of the exhumation of the nappe, entailing fast exhumation rates with significant heat advection and/or shear heating along the nappe boundaries.

## 1.18

# The tectono-metamorphic evolution of the Western Alps: new insights from the comparison of model predictions and observations

Stefan Schmalholz<sup>1</sup>, Joshua Vaughan Hammon<sup>1</sup>, Lorenzo Candiotti<sup>1</sup>

<sup>1</sup> Institute of Earth Sciences, University of Lausanne, Géopolis, CH-1015 Lausanne ([stefan.schmalholz@unil.ch](mailto:stefan.schmalholz@unil.ch))

The Alps are presumably one of the best studied orogens worldwide, but arguably also one of the most disputed ones. Despite more than 150 years of research, several of the main geodynamic processes remain contentious, such as (i) the mechanism of (U)HP rock exhumation, for example exhumation during plate divergence or syn-convergent exhumation or (ii) the mechanism of subduction initiation, for example spontaneous initiation due to gravitational sinking of old and cold oceanic lithosphere or induced initiation due to far-field convergence of the African and European plates. Also important for the Alpine orogeny is the pre-convergence configuration of the Alpine Tethys, for which also two end-member scenarios are commonly proposed: (i) a “mature oceanic” scenario, involving a significant amount of mature oceanic crust (typically 6 km thick) which was generated at a spreading ridge or (ii) an “embryonic oceanic” scenario, involving hyper-extended continental European and Adriatic margins bounding an embryonic ocean basin mainly consisting of exhumed, partially serpentinized mantle, crustal allochrons as well as basalts and gabbros which resulted from decompression melting during oceanic core complex formation.

Here, we summarize the results of two recently finished PhD theses and present new results of 2D petrological-thermomechanical numerical models which we conducted to investigate the physical feasibility of some of the disputed mechanisms and scenarios mentioned above, namely an “embryonic ocean” scenario, induced subduction initiation and syn-convergent exhumation. The main feature of our models is that they simulate the entire Mesozoic evolution involving rifting, ocean basin formation, subduction initiation, subduction of continental crust and its subsequent exhumation. The models simulate a duration of ca. 150 Myr and were calibrated so that they reproduce observed profiles of temperature, densities and effective viscosities across the lithosphere-upper mantle system down to a depth of 660 km. To test the applicability of our models to the Alps, we calculate, amongst others, the peak pressures and temperatures throughout the modelled orogenic wedge and compare these modelled peak metamorphic conditions with a wealth of available metamorphic data. A main feature of the Western Alps is the so-called HP, or eclogite, belt including the internal crystalline massifs of Monte Rosa, Gran Paradiso and Dora Maira. Common peak pressures range between 14 and 24 kbar and peak temperatures between 450 and 600 °C. Typical vertical exhumation velocities range between 0.5 and 1 cm/yr.

We present a simulation which predicts these peak metamorphic conditions and exhumation velocities as well as the first order present-day distribution of metamorphic facies observed across the Western Alps. We further present a series of new simulations to investigate the impact of mechanical heterogeneities in the continental crust as well as of geometrical and material weakening mechanisms in the crust on the burial and exhumation dynamics.

## 1.19

# Imaging crust and mantle structure of the Western Alps by geophysical methods: controversies regarding the geological interpretation of the deep structure of the Western Alps

Schmid S.M., Handy, M., Paffrath, M.

While various authors claimed and still claim slab detachment to have occurred in the Western Alps based on mantle tomography data (e.g. Handy et al., 2021), others (e.g. Malusa et al., 2021) recently proposed that no such slab detachment occurred, seemingly based on p-wave mantle tomography data (Zhao et al., 2016). However, it can be shown that, contrary to the interpretation of their own data by Malusa et al. (2021), the tomography data by Zhao et al. (2016) clearly indicate that such slab detachment occurred if these data are properly analysed in the context of geological data regarding the formation of the arc of the Western Alps. There is in fact no major difference between the mantle tomography data of Zhao et al. (2016) and those of Paffrath al. (2021). Slab detachment in the Western Alps allows for SE-directed influx of asthenospheric mantle present below the European plate below the Adriatic lithosphere. This accommodates NE-directed roll back of the Apennines. Substantial counterclockwise rotation of western Adria and oroclinal bending is facilitated by a thin orogenic lithosphere (only crust?) present in the southern Western Alps due to slab detachment. A recently constructed large-scale crustal profile across the Western Alps across the Cottian Alps and the southern Dora Maira massif (Michard et al., in press) based on field evidence reveals massive back thrusting and folding that so far was grossly underestimated. On a lithospheric scale such back-thrusting is supported by mantle tomography indicating that the entire Alpine crust underlying the Dora Maira massif (i.e. half of the internal Western Alps) being part of the European plate is underlain by the Ivrea geophysical anomaly that is part of the Southern Alpine (Adriatic) domain.

## REFERENCES:

- Handy, M.R., Schmid, S.M., Paffrath, M., Friederich, W. & AlpArrayWorking Group 2021. Orogenic lithosphere and slabs in the greater Alpine area – interpretations based on teleseismic P-wave tomography. *Solid Earth*, 12, 2633–2669.
- Malusa, M.G., Guillot, S., Zhao, L., Paul, A., Solarino, S., Dumont, T., et al. 2021. The deep structure of the Alps based on the CIFALPS seismic experiment: A synthesis. *Geochemistry, Geophysics, Geosystems*, 22, e2020GC009466.
- Michard, A., Schmid, S.M., Lahfid, A., Ballèvre, M., Manzotti, P., Chopin, C., Iaccarino, S. & Dana, D. accepted. The Maira-Sampeyre and Val Grana Allochthons (south Western Alps): review and new data on the tectonometamorphic evolution of the Briançonnais distal margin. *Swiss Journal of Geosciences* 115, 2022.
- Paffrath, M., Friederich, W., Schmid, S.M., Handy, M.R. & the AlpArray and AlpArray-Swath-D Working Groups 2021. Imaging structure and geometry of slabs in the greater Alpine area – a P-wave travel-time tomography using AlpArray Seismic Network data. *Solid Earth*, 12, 2671–2702.
- Zhao, L., Paul, A., Malusa, M. G., Xu, X., Zheng, T., Solarino, S., et al. 2016. Continuity of the Alpine slab unraveled by high-resolution P wave tomography. *J. Geophys. Res. Solid Earth*, 121, 8720–8737.

## 1.20

# Lower crustal flow during continental rifting: Considerations for 3D deformation and insights from analogue modelling experiments

Timothy Schmid<sup>1</sup>, Guido Schreurs<sup>1</sup>, Jürgen Adam<sup>2</sup>, Frank Zwaan<sup>1,3</sup>

<sup>1</sup> Institute of Geological Sciences, University of Bern, Baltzerstrasse 1 + 3, CH 3012 Bern ([timothy.schmid@geo.unibe.ch](mailto:timothy.schmid@geo.unibe.ch))

<sup>2</sup> Department of Earth Sciences, Royal Holloway University of London, Egham, United Kingdom

<sup>3</sup> Helmholtz Centre Potsdam – GFZ German Research Centre for Geosciences, Germany

In continental rift settings, faulting and the interaction of fault segments in the upper brittle crust is often accompanied by material flow in lower crustal parts. If the crust is thick enough, lower parts of the crust can flow and deform in a ductile fashion to accommodate thinning of the upper brittle crust. Such ductile flow has been suggested to be a viable mechanism for removal of lower crustal material perpendicular to the divergence direction and may explain discrepancies between estimated amounts of extension in the upper and lower crust (i.e., Clift, 2015).

Here, we investigate lower crustal deformation in continental rift settings by means of crustal-scale analogue models. To this end, we use experimental set-ups that simulate either orthogonal or rotational divergence. Our models consist of a simplified two-layer setup with an upper sand layer and a lower viscous mixture to simulate the upper brittle and lower ductile crust, respectively. All used analogue materials are properly scaled to crustal rheologies and applied boundary conditions scale to geological deformation rates. By the use of Digital Image Correlation and Digital Volume Correlation techniques (DIC and DVC) we gain quantitative insights on brittle faulting and coeval internal model deformation and demonstrate the importance of material flow perpendicular to the divergence direction. Especially experiments with an underlying divergence gradient (i.e., rotational divergence) show enhanced rift-axis parallel flow (towards areas with higher extension) in the lower crust that compensates for greater thinning of the upper crust. As a consequence, mass is not conserved in 2D plane-strain cross sections, a fact, which should be considered when estimating the amount of crustal extension from two dimensional cross sections.

## REFERENCES

- Clift, P., D., 2015: Coupled onshore erosion and offshore sediment loading as causes of lower crust flow on the margins of South China Sea, *Geoscience Letters*, 2, 1-1.

## 1.21

# Beyond the grain scale - What 4D microtomography tells us about diffusive transport during dissolution precipitation creep

Berit Schwichtenberg<sup>1,2</sup>, Florian Fusseis<sup>2</sup>, Ian B. Butler<sup>2</sup>, Edward Andò<sup>3</sup>

<sup>1</sup> Institute for Geology, University of Bern, Baltzerstrasse 1+3, CH-3012 Bern (berit.schwichtenberg@outlook.com)

<sup>2</sup> School of Geosciences, University of Edinburgh, James Hutton Road, GB-EH9 3FE Edinburgh

<sup>3</sup> EPFL AVP CP IMAGING-GE, École Polytechnique Fédérale de Lausanne, BM 4142 (Bâtiment BM) Station 17, CH-1015 Lausanne

Chemical compaction by dissolution-precipitation creep has a crucial influence on the dynamic evolution of the hydraulic rock properties relevant to geological repositories and reservoirs. To fully comprehend how chemical, mechanical and hydraulic processes are linked we first have to understand the spatial and temporal scales of feedbacks emerging during dissolution-precipitation creep.

In order to analyse slow chemical compaction processes on the grain scale and determine the effects of chemical and mechanical feedbacks, we conducted oedometric compaction experiments on layered NaCl-biotite samples. In addition to that, time-resolved (4-D) microtomography allowed us to capture the dynamic evolution of the microstructure and the porosity over time scales of up to 2000 hours of compaction.

While percolation analysis in combination with advanced digital volume correlation techniques showed that porosity reduction was promoted in the vicinity of biotite grains, we did not observe the classically attributed reinforcing effect of phyllosilicates upon dissolution-precipitation creep. Instead, our results suggest that the porosity reduction was not achieved by pore collapse but rather by the precipitation of dissolved NaCl sourced outside the biotite-bearing layer.

According to the classical theory of dissolution-precipitation creep, length scale of diffusive transport in closed systems without advection do not exceed the grain scale and dissolution sites are locally connected to precipitation sites (e.g. Gratier et al., 2013). However, we propose that, in our experiments, the diffusive transport processes invoked in the classical models are complemented by chemo-mechanical feedbacks that emerge on longer length scales (Fig. 1) and were first postulated by Merino et al. (1983). These feedbacks cause the redistribution of NaCl by driving NaCl diffusion from marginal pure NaCl layers into the biotite-bearing layer over distances of several hundred micrometres and several grain diameters.

Our observations invite a renewed discussion of the effect of phyllosilicates on dissolution-precipitation creep as well as the length scales of the diffusive material transport therein.

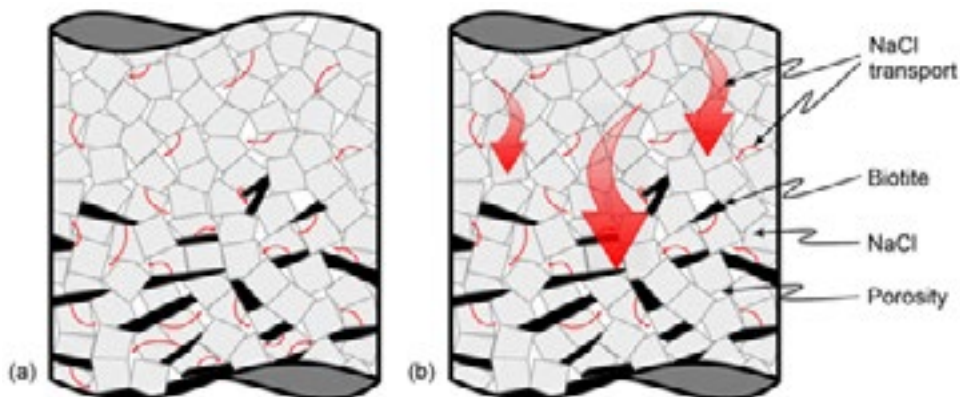


Figure 1. Possible transport length scales during dissolution-precipitation creep. In (a), diffusion occurs only on the grain scale as described in the classical literature. In (b), we added diffusive transport on longer length scales as described in Merino et al. (1983). However, diffusive transport on the grain scale is considered to be active as well.

## REFERENCES

- Gratier, J.-P., Dysthe, D. K., and Renard, F.: The role of pressure solution creep in the ductility of the Earth's upper crust, in: Advances in Geophysics, vol. 54, pp. 47–179, Elsevier, Amsterdam, Netherlands, 2013.  
 Merino, E., Ortoleva, P., and Strickholm, P.: Generation of evenly-spaced pressure-solution seams during (late) diagenesis: A kinetic theory, Contrib. Mineral. Petr., 82, 360–370, 1983.

## 1.22

# Experimental investigation of fracture behavior after ceasing injection in a permeable and porous medium

Mohsen Talebkeikhah<sup>1</sup>, Seyyedmaalek Momeni<sup>1</sup>, Guanyi Lu<sup>1</sup>, Brice Lecampion<sup>1</sup>

<sup>1</sup> Geo-Energy Laboratory - Gaznat Chair on Geo-Energy, Ecole Polytechnique Fédérale de Lausanne, Switzerland  
(mohsen.talebkeikhah@epfl.ch)

Hydraulic fracturing is most commonly used in oil and gas reservoirs to increase well productivity by injecting a fluid into the geomaterial to create fracture channels that increase the permeability of the reservoir. This process involves a variety of complicated processes. One of the most well-known phenomena that occur during this process is that all crack channels close after fluid injection is ceased, especially in permeable and porous media, which is due to fluid loss into the poroelastic medium. Depending on the type of crack propagation regime, the closure of the crack may occur exactly after injection is stopped, when toughness dominates, or the crack propagates due to the energy stored in the fluid, when viscosity dominates (Peirce 2022). However, fluid losses in poroelastic media stop crack propagation and the crack closes until it is completely collapsed. This closure of the crack channel reduces the permeability and efficiency of hydraulic fracturing. Recently, a few numerical solutions have been developed to model and simulate this process and to derive multiscale asymptotes for this recession phenomenon. However, there is no experimental study to validate the results of these solutions. In this study, for the first time, an experiment was conducted on a sandstone block to practically simulate these phenomena.

## REFERENCES

- A. Peirce. The arrest and recession dynamics of a deflating radial hydraulic fracture in a permeable elastic medium. *Journal of the Mechanics and Physics of Solids*, page 104926, 2022.

## 1.23

# Rheologically weak layers affecting fault architecture in the Northern Alpine Foreland Basin: Insights from analogue models

Frank Zwaan<sup>1,2</sup>, Guido Schreurs<sup>1</sup>, Herfried Madritsch<sup>3</sup>, Marco Herwegen<sup>1</sup>

<sup>1</sup> University of Bern, Institute of Geological Sciences, Baltzerstrasse 1+3, 3012 Bern, Switzerland

(frank.zwaan@geo.unibe.ch)

<sup>2</sup> Helmholtz Centre Potsdam - GFZ German Research Centre for Geosciences, Telegrafenberg, Potsdam, 14473, Germany

<sup>3</sup> National Cooperative for the Disposal of Radioactive Waste (Nagra), Hardstrasse 73, 5430 Wettingen, Switzerland

We present a series of analogue models inspired by the geology of the Zürcher Weinland region in the Northern Alpine Foreland Basin of Switzerland (Roche et al. 2020) to explore the influence of rheological weak layers on the 3D evolution of tectonic deformation.

Our model series test the impact of varying weak layer thickness and rheology, as well as different kinematics of an underlying "basal fault" (normal dip- to strike-slip, and slip rate variations). Model analysis focuses on deformation in the weak layer's overburden and, uniquely, within the weak layer itself. We find that for low to moderate basal fault displacements, the above-mentioned parameters strongly influence the degree of coupling between the basal fault and the weak layer overburden. Coupling between the basal fault and overburden decreases by reducing the strength of the weak layer, or by increasing the weak layer's thickness. As a result, basal fault deformation is less readily transferred through the weak layer, leading to a different structural style in the overburden (Fig 1). By contrast, increasing the amount (or rate) of basal fault slip enhances coupling and leads to a more similar structural style between basal fault and weak layer overburden. Moreover, basal fault normal dip-slip motion has a stronger impact on faulting in the overburden compared to basal fault strike-slip motion.

Our model results compare fairly well to natural examples in the Northern Alpine Foreland Basin, explaining various structural features. These comparisons suggest that rheological weak layers such as the Jurassic Opalinus Clay have exerted a stronger control on fault zone architecture than is commonly inferred, potentially resulting in vertical fault segmentation and variations in structural style (Roche et al. 2020). Furthermore, the novel addition of internal marker intervals to the weak layer in our models reveals how complex viscous flow within these layers can accommodate basal fault slip. Our model results demonstrate the complex links between fault kinematics, mechanics and 3D geometries, and can be used for interpreting structures in the Alpine Foreland, as well as in other settings where similar mechanical weak layers are present.

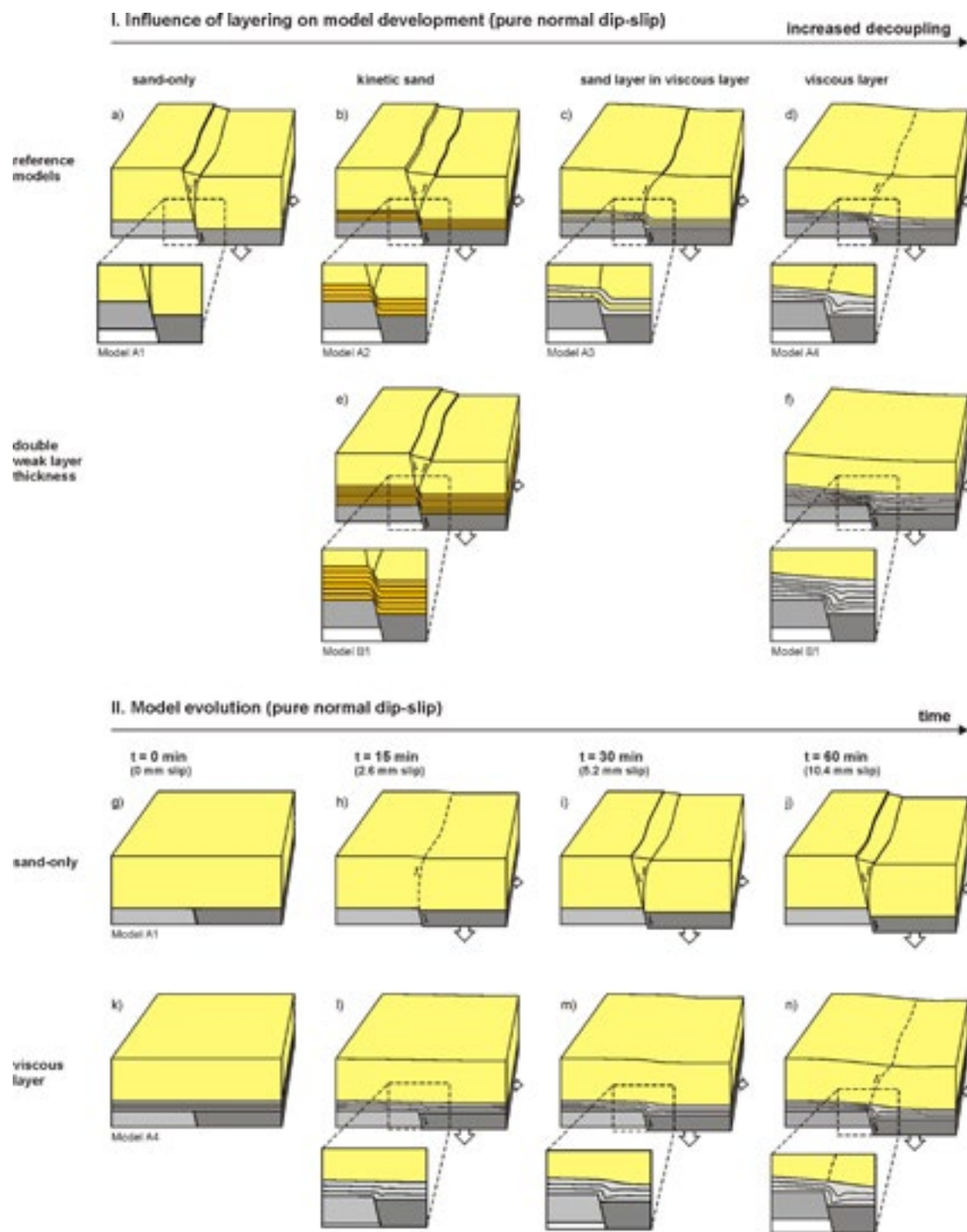


Figure 1. Schematic overview of the influence of viscous layer properties on model development (in pure normal dip-slip models, final state).

## REFERENCES

- Roche, V., Childs, C., Madritsch, H., & Camanni, G. 2020: Layering and structural inheritance controls on fault zone structure in three dimensions: a case study from the northern Molasse Basin, Switzerland, Journal of the Geological Society, 177, 493-508. <https://doi.org/10.1111/jgs2019-052>

## P 1.1

# How sediments control deformation along a subduction margin – the Chugach accretionary prism, Alaska (USA)

Akker I.V.<sup>1</sup>, Behr W.M.<sup>1</sup>, Rast M.<sup>1</sup>, Hufford L.J.<sup>1</sup> and Braden Z.<sup>1</sup>

<sup>1</sup>Structural Geology and Tectonics Group, Geological Institute, ETH Zürich, Sonneggstrasse 5, CH-8092 Zürich  
([vakker@erdw.ethz.ch](mailto:vakker@erdw.ethz.ch))

Along subduction plate interfaces a variety of deformation styles, mechanisms, as well as seismic activity is reported. These variations arise from differences in pressure-temperature conditions, fluid composition, fluid pressure conditions and compositional variations in the materials entering the subduction zone. Here, we study the Jurassic-Cretaceous Chugach accretionary complex along the Kenai Peninsula in southern Alaska. This exhumed complex recorded megathrust deformation at low-grade conditions (prehnite-pumpellyite). The complex comprises different underplated slices of both oceanic and sedimentary material. In the west, the slices comprise oceanic crustal basalts and pelagic sediments. Towards the east, an increasing trench sediment input is observed. In this work we examine deformational styles, from outcrop to micron scale in two sections of the Chugach that preserve several megathrust fault splays: one basalt-dominated and one sediment-dominated. With the use of drone images, we establish 3D models, that give insights in the dimensions, shapes and orientations of the shear zones and other structures. Microstructural observations are ongoing and will be used to document the microphysical mechanisms of deformation within these two contrasting shear zones. Ultimately, comparing these two sites provides new insights in the role of sediments in the structural control of the plate interface and will ultimately contribute to the understanding of slow vs. fast deformation processes.

## P 1.2

# Determining the age and tectonic evolution of Paleozoic oceanic islands using calcite U-Pb geochronology and biostratigraphy

Goran Andjić<sup>1</sup>, Renjie Zhou<sup>2</sup>, David M. Buchs<sup>3</sup>, Jonathan C. Aitchison<sup>2</sup>, Jianxin Zhao<sup>2</sup>

<sup>1</sup> Institut des Sciences de la Terre, Université de Lausanne, Bâtiment Géopolis, CH-1015 Lausanne ([goran.andjic@unil.ch](mailto:goran.andjic@unil.ch))

<sup>2</sup> School of Earth and Environmental Sciences, The University of Queensland, 4072 St Lucia, Australia

<sup>3</sup> School of Earth and Environmental Sciences, Cardiff University, United Kingdom

Active accretionary wedges result from the convergence between a downgoing oceanic plate and an overriding plate. There, loose sediment and rock material sourced from both plates is stacked into fault-bounded, deformed packages that are incorporated into the overriding plate. In modern settings, both accretionary complexes and downgoing plates lay far below sea level, making methods of getting first-hand observations complex and costly (such as drilling/dredging/seismic reflection). In contrast, exhumed ancient accretionary complexes provide a more accessible way to study the tectonic evolution of subduction zones and oceanic plates partly or completely lost to subduction.

Documenting the history of ancient oceanic plates from accretionary complexes is faced with the challenge of dealing with dismembered pieces of oceanic crust, whereby the original succession of lithologies—called ocean plate stratigraphy (OPS)—was partly or entirely lost. Establishing the timing of formation and subduction of oceanic plates hence implies determining the age of meter- to kilometer-sized blocks of oceanic crust and the sedimentary matrix in which they are embedded. Dating OPS in accretionary complexes has classically relied on paleontology rather than on geochronology because processing and identifying fossils, such as radiolarians, are well practiced by the community. In contrast, mafic igneous rocks from the oceanic crust generally lack minerals commonly used in geochronological studies (such as zircon), and are often subject to strong alteration. Therefore, if a block of mafic igneous rock is not in stratigraphic contact with a datable sedimentary rock, its age is very likely to remain unknown.

We studied the accretionary complex represented by the Carboniferous Texas Beds in the southern segment of the New England Orogen, which is the youngest belt of a collage of Paleozoic subduction-related orogens occupying the eastern third of the Australian continent. Altered ocean island basalt (OIB)-like rocks, cherts and shallow-marine carbonates are embedded throughout the complex. Although these rock associations were considered to represent remnants of oceanic islands based on existing biostratigraphic, geochemical and lithological data, their original relationship was obscured by tectonic dismemberment, possibly during accretion and/or gravitational collapse of islands arriving at the subduction zone. Their exact timing of formation and accretion, which is critical to reconstruct the origin and evolution of the dismembered OPS, was not known before.

Two distinct types of calcite were formed in the studied OIB-like volcanic rocks. One calcite type precipitated in amygdules (voids representing former gas bubbles in a molten lava), whereas the other type precipitated in orthogonal fractures which are also visible among all the lithologies in the accretionary complex. Besides distinct morphologies, these calcites have distinct U-Pb geochronological ages and geochemical signatures. Calcite precipitation from low-temperature hydrothermal fluids in amygdules occurred at around 378–354 million years ago (Ma), whereas calcite precipitation from seawater in fractures occurred at around 331–279 Ma.

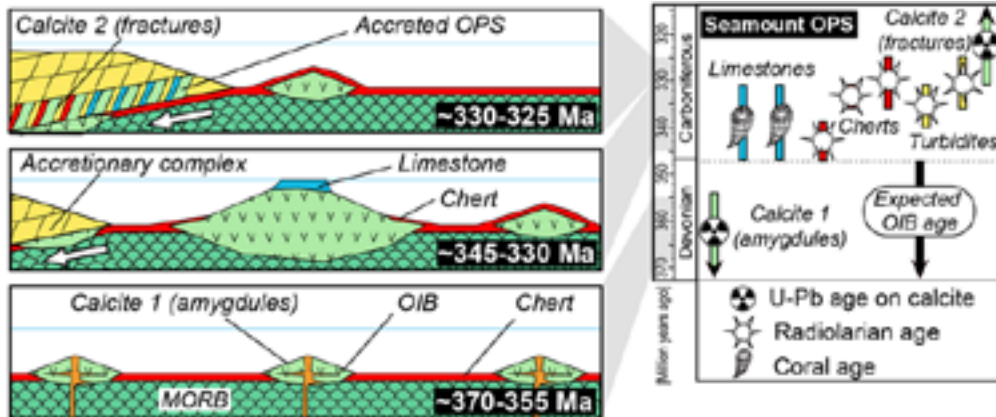


Figure 1. Summary of the age constraints used to establish the timing of formation and accretion of Paleozoic intraplate volcanoes. Modified from Andjić et al. (2022). OPS = Ocean Plate Stratigraphy; OIB = Oceanic Island Basalt; MORB = Mid-Ocean Ridge Basalt.

Taken at face value, the timing of precipitation of the two generations of calcite does not translate into clear geological implications. It is only when combined with new and existing fossil age data that the significance of the geochronological ages becomes meaningful. When integrating data from all the lithologies making up the accretionary complex, it is possible to reconstruct the following sequence of events (Figure 1):

- > no later than 354 Ma = intraplate volcanic eruptions;
- > 347–330 Ma = deep to shallow marine sedimentation on intraplate volcanoes;
- > 330–325 Ma = accretion of intraplate volcanoes to Gondwana;
- > no earlier than 330 Ma = brittle deformation of intraplate volcanoes within the accretionary complex.

The main conclusion of our work is that a minimum age of formation of altered and weathered, mafic volcanic rocks can be obtained using calcite U-Pb geochronology. In the context of accreted OPS, the broader geological implications of the minimum age of formation of volcanic rocks have to be determined in conjunction with fossil, structural, and geochemical data.

## REFERENCES

- Andjić, G., Zhou, R., Buchs, D.M., Aitchison, J.C., & Zhao, J. 2022: Paleozoic ocean plate stratigraphy unraveled by calcite U-Pb dating of basalt and biostratigraphy. *Communications Earth & Environment*, 3, 113.

## P 1.3

# Tracking back Permian–Triassic sections from Oman over the Mesozoic–Cenozoic: Geodynamic and paleogeographic implications

Christian Vérard<sup>1</sup>, Aymon Baud<sup>\*2</sup>, Hugo Bucher<sup>3</sup>, Oluwaseun Edward<sup>2</sup>

<sup>1</sup> Earth and Environmental Sciences, University of Geneva, Rue des Maraîchers 13, CH-1205, Geneva.

<sup>2</sup> Faculty of Geoscience and Environment, University of Lausanne, Quartier UNIL-Mouline, Géopolis, CH-1015, Lausanne.

<sup>3</sup> Paläontologisches Institut und Museum, Universität Zürich, Karl-Schmid-Strasse 4, CH-8006 Zürich.

\* aymon.baud@unil.ch

Three sections from Oman — Wadi Musjah, Jebel Rabat A, and Jebel Aweri — spanning the Changhsingian (Upper Permian) to Olenekian (Lower Triassic) are studied in detail to investigate changes in seawater chemistry during this interval (see other abstract – poster by Edward et al.). Together with other sections described in Baud (2022 and references therein), we here define their palaeo-location and palaeogeography through time using the Panalesis plate tectonic model (Vérard, 2019). We propose that the sections of Wadi Musjah and Jebel Rabat A were part of seamounts sitting on very distal margin tilted blocks located at some 100 -200 km relative to where they are found now. The seamount(s) was (were) caught in the subduction prism of the Hawasina nappes and transported towards the Omani margin, before the Semail plate obduction brought them onto the passive margin where they are currently located (see scenario after Vérard & Stampfli, 2022 and references therein). The third section — Jebel Aweri — has a different history. As part of the Batain Hills, the section is proposed to belong to the Masirah tectonic element, a zone along the eastern Oman and Yemen margin (Schreurs & Immenhauser, 1999), which underwent a transpressive motion, in particular in the Late Cretaceous – Palaeogene when the India tectonic plate rotated relative to the Africa plate, triggering a ‘scissor effect’ with up to 250 km shortening and thrusting onto the Oman – Yemen passive margin. We infer that the “Eastern Ophiolite Belt” from the Masirah Island and metamorphism in the Batain are associated with this event.

## REFERENCES

- Baud, A., 2022- *preprint*. La transition permo-triasique sur la marge omanaise, 32 pages. In Société Géologique de France (ed.) : Destination Oman. Géochronique, Volume spécial.
- Schreurs, G., Immenhauser, A., 1999. West-northwest directed obduction of the Batain Group on the eastern Oman continental margin at the Cretaceous-Tertiary boundary. *Tectonics*, 18 (1), 148-160.
- Vérard, C., 2019. Panalesis: Towards global synthetic palaeogeographies using integration and coupling of manifold models. *Geological Magazine*, 156 (2), 320-330; doi:10.1017/S0016756817001030.
- Vérard, C., Stampfli, G. M., 2022-*submitted*. From the UniL to the Panalesis model: Development of concepts, tools and scenarios for a comprehensive global modelling of the Neoproterozoic and Phanerozoic Earth. *Earth- Science Reviews*, special publications, 34 pages.

## P 1.4

# Natural seismicity assessment of the Vuache fault – Structural Geology, Tectonics and Geodynamics

Amaury Champion\*, Matteo Lupi\*, Francisco Muñoz Burbano\*, Joël Ruch\*, Jean-Luc Got\*\*, Laurent Metra\*\*

\* UNIGE, University de Genève section des sciences de la terre et de l'environnement, rue des Maraîchers 13, 1205 Genève

\*\* ISTerre, Institut des sciences de la terre, 1381 Rue de la Piscine, 38610 Gières, France

The Vuache fault is a major active fault that may cause moderate magnitude earthquakes. Recently it caused the M5.3 earthquake in 1996 next to Annecy, France. The structural formation of the fault belongs to the genesis of the Alps and has a complex tectonic history. The movement of the fault changed drastically through time. The current kinematics show strike-slip motion linking Annecy's Lake to the Jura Haute Chaîne. The main fault plane, oriented NW-SE is crossing thick carbonates rocks, which are well known for their capability to host fluids. To monitor the seismic activity of the fault, we deployed a seismic network composed of 12 short period stations (Lennartz 1Hz, equipped with datacube digitizers). This temporary network implements the one of the ISTerre who deployed stations in the southern segment of the fault. The aim of this work is to constrain the natural seismic activity of the area. Preliminary results indicate a weak seismicity that has been shown to be characterized by strike-slip focal mechanisms. Yet, seismicity is at crustal depths suggesting that the fault is a major structure that has been accommodating the Alpine orogenesis.

## P 1.5

# Free surface methods applied to global scale numerical geodynamic models

Timothy Gray, Taras Gerya, Paul Tackley

*Department of Earth Sciences, ETH Zurich, Switzerland (timothy.gray@erdw.ethz.ch)*

The study of coupled Earth systems, and in particular the coupled interactions between the lithosphere, atmosphere, and biosphere, have received greater attention in recent years (Gerya et al. 2020). Interactions between these systems occur primarily at the surface, and are driven on the large scale by topographic and bathymetric evolution controlled by deep mantle processes. However, due to the large difference in length scales between the mantle and the surface, it is difficult to capture topographic evolution to a high degree of accuracy in existing global mantle convection models including a free surface boundary condition.

Global mantle convection models incorporating a free surface often employ a marker-in-cell technique with a layer of “sticky air” (i.e. material with the density of the air and sufficiently low viscosity, which is still much higher than that of real air) to characterise the surface. However, accurate topographic evolution using this method requires a high density of markers near the surface. This need for additional computational resources motivates alternative methods of tracking the interface between the air and rock layers, as is done frequently in existing multiphase fluid flow codes. Such interface tracking methods include the use of a Lagrangian surface marker chain with an appropriate remeshing procedure (van Keken, 1997), the use of a level-set function defined by the distance to the surface (Hieber & Koumoutsakos, 2005), or the introduction of a volume of fluid method with piecewise-linear interface reconstruction and a geometric advection routine (Katopodes, 2019).

We demonstrate toy models and benchmarks of these methods implemented in the Julia programming language within a framework suitable for inclusion within existing geodynamic models. Future work will involve the implementation of these methods within the existing code StagYY (Tackley, 2008) and benchmarking of results. Models of global scale topography and evolution produced using StagYY may then be used as a tool for further studies on the coupling of mantle dynamics with modelling of the landscape, and the evolution of the atmosphere and biosphere.

## REFERENCES

- Gerya, T., Stern, R., Pellissier, L., & Stemmler, D. (2020). Bio-geodynamics of the Earth: State of the art and future directions. EGU2020, EGU2020-10657.
- van Keken, P. E., King, S. D., Schmeling, H., Christensen, U. R., Neumeister, D., & Doin, M.-P. (1997). A comparison of methods for the modeling of thermochemical convection. *Journal of Geophysical Research: Solid Earth*, 102(B10), 22477–22495. <https://doi.org/10.1029/97JB01353>
- Hieber, S. E., & Koumoutsakos, P. (2005). A Lagrangian particle level set method. *Journal of Computational Physics*, 210(1), 342–367. <https://doi.org/10.1016/j.jcp.2005.04.013>
- Katopodes, N. D. (2019). Chapter 12—Volume of Fluid Method. In N. D. Katopodes (Ed.), *Free-Surface Flow* (pp. 766–802). Butterworth-Heinemann. <https://doi.org/10.1016/B978-0-12-815485-4.00018-8>
- Tackley, P. J. (2008). Modelling compressible mantle convection with large viscosity contrasts in a three-dimensional spherical shell using the yin-yang grid. *Physics of the Earth and Planetary Interiors*, 171(1), 7–18. <https://doi.org/10.1016/j.pepi.2008.08.005>

**P 1.6**

## **Viscous strain localization by anisotropy development: Numerical models and benchmarks**

William R. Halter<sup>1</sup>, Roman Kulakov<sup>2</sup>, Thibault Duretz<sup>1,2</sup>, Stefan M. Schmalholz<sup>1</sup>

<sup>1</sup> ISTE, Université de Lausanne, Géopolis, CH-1015 Lausanne ([william.halter@unil.ch](mailto:william.halter@unil.ch))

<sup>2</sup> Institut für Geowissenschaften, Goethe-Universität Frankfurt, DE-60438 Frankfurt a. M.

Viscous strain localization and associated softening mechanisms in a deforming lithosphere are important for subduction initiation or the generation of tectonic nappes. Many strain localization and softening mechanisms have been proposed as being important during the viscous, creeping, deformation of the lithosphere, such as thermal softening, grain size reduction, reaction-induced softening or anisotropy development. However, which localization mechanism is the controlling one and under which deformation conditions is still contentious. In this contribution, we focus on strain localization in viscous rock due to the generation of anisotropy, for example due to the development of a foliation. We numerically model the generation and evolution of anisotropy during two-dimensional viscous simple shear to quantify the impact of anisotropy development on strain localization and on the effective softening. We calculate the finite strain ellipse during viscous deformation. The aspect ratio of the finite strain ellipse serves as proxy for the magnitude and evolution of anisotropy, which determines the ratio of normal to tangential viscosity. To track the orientation of the anisotropy during deformation we apply a director method.

We benchmark two independently developed numerical finite difference algorithms modelling anisotropic viscous deformation. The code MDOODZ (Duretz et al., 2021), written in C, employs a direct solver and the second code, written in Julia, is a pseudo-transient iterative solver. We compare both codes for two nature-inspired scenarios: A) a fixed, pre-existing anisotropy with a given initial orientation that changes with progressive shearing; B) an initially isotropic material developing a viscous anisotropy with progressive shearing as function of local finite strain. Scenario A) represents the viscous deformation of a geologic unit with an inherited layering, e.g., a sequence of flysch or a foliated paragneiss which is re-deformed during an orogeny. Scenario B) represents the viscous deformation of an initially, more or less isotropic rock, e.g., an undeformed granite. In both scenarios, the anisotropy evolution leads to strain localization. We will present the results of our numerical simulations and discuss their application to natural shear zones.

**REFERENCES**

Duretz T., R. de Borst and P. Yamato (2021), Modeling Lithospheric Deformation Using a Compressible Visco-Elasto-Viscoplastic Rheology and the Effective Viscosity Approach, *Geochemistry, Geophysics, Geosystems*, Vol. 22 (8), e2021GC009675

## P 1.7

# Stratigraphic contact in the Mattmark area implying a reexamination of the nappe stack in the Saas valley

Christophe Jossevel<sup>1</sup>, Jean-Luc Epard<sup>1</sup>

<sup>1</sup> Institut des Sciences de la Terre, Université de Lausanne, Géopolis, CH-1015 Lausanne (christophe.jossevel@unil.ch)

The Pennine Alps in the Matter and Saas Valleys exhibit tectonic units corresponding to an ocean and to a continental margin. Despite their complexity due to strong deformation, they are key areas to study the structure of distal domains and propose paleogeographic reconstruction. The Monte Rosa and the Zermatt-Saas nappes are the two main tectonic units in the area. They are separated by only a few hundred meters, but many tectonic units are sandwiched between them. These units consist of cover and basement. Their relations with the neighboring units and their origin have been the subject of several interpretations because of their complex structure due to the strong shearing they have undergone. Some authors were already discussing several hypotheses in the middle of the XX<sup>th</sup> century (Bearth 1939). However, the retreat of the glaciers has produced new outcrops that provide more complete and continuous information on these units. This is the case for the Gornergrat nappe formed of Mesozoic sediments whose attribution remains unclear and debated. Recent outcrops near the Britannia hut, at the base of the Allalinhorn, provide new data on the nature of the rocks and the structural relationships between the different tectonic units outcropping in this region. Mapping, lithostratigraphic studies, structural analysis and geochronology allow to better constrain the origin of the Gornergrat nappe and its position in the stacking of the Pennine nappes in the Saas Valley.

## REFERENCES

Bearth P. (1939): Über den Zusammenhang von Monte Rosa- und Bernhard-Decke. Eclogae Geol. Helvetia 32, 101-111.

## P 1.8

# New insights into the Rhône-Simplon fault system (Swiss Alps) from a consistent earthquake catalogue covering thirty-five years

Timothy Lee<sup>1</sup>, Tobias Diehl<sup>1</sup>, Edi Kissling<sup>2</sup>, Stefan Wiemer<sup>1</sup>

<sup>1</sup> Swiss Seismological Service, ETH Zurich, 8092, Switzerland (timothy.lee@sed.ethz.ch)

<sup>2</sup> Institute of Geophysics, ETH Zurich, 8092, Switzerland

Seismotectonic interpretations in regions characterized by low to moderate seismicity require consistent earthquake catalogues covering periods of several decades. Inevitable changes in network configuration and analysing procedures, however, introduce significant bias to the hypocentre parameters and uncertainty estimates reported in such catalogues. To overcome these limitations, we developed a procedure using coupled hypocentre-velocity inversions to compute consistent hypocentre locations covering time periods of several decades while accounting for changes in network geometry. We apply these procedures to thirty-five years of instrumentally recorded seismicity along the Rhône-Simplon fault system in southwest Switzerland, which is located in the transition between the Central and Western Alps. The entire catalogue is relocated using a probabilistic location algorithm in combination with the derived minimum 1-D velocity models. A combination of location parameters is used to define consistent location-quality classes allowing for reliable interpretation of epicentres and focal depths. The relocated catalogue is interpreted together with a recent 3-D P-wave tomographic model and available 2-D reflection seismic profiles. The relocated hypocentres indicate that the major band of seismicity north of the Rhône valley is associated with a 30-40 km long, steeply north-dipping shear zone, which roots in the crystalline basement of the Aar Massif and extends to the shallowest levels of the sedimentary cover of the Helvetic nappes in the Rawil Depression. Seismicity towards the southwest indicates the existence of a similar shear zone within the Aiguille Rouge Massif. This zone possibly extends to the northeast and joins the Rawil Fault zone. To the south of the Rhône valley, seismicity is scattered within the Penninic nappes, but limited to the hanging wall of the Pennine Basal Thrust (PBT). The Penninic nappes are characterized by a relatively higher  $V_p$  of about 5% compared to the Aar Massif, indicating differences in composition or metamorphic grade across the PBT.

## P 1.9

# The effect of grain size reduction for the origin of the mid-lithosphere discontinuity

Mingqi Liu<sup>1</sup>, Taras Gerya<sup>1</sup>, Ling Chen<sup>2</sup>, James Connolly<sup>1</sup>

<sup>1</sup> Department of Earth Sciences, ETH Zurich, Sonneggstrasse 5, CH-8092 Zurich ([mingqi.liu@erdw.ethz.ch](mailto:mingqi.liu@erdw.ethz.ch))

<sup>2</sup> Institute of Geology and Geophysics, Chinese Academy of Sciences, Beijing 100029, China

In the last decades, the high heterogeneity of lithospheric mantle in term of its physical properties and chemical compositions is widely documented by geophysical, petrological, and geochemical studies. A sharp discontinuity in seismic velocity (~2-10% reduction over no more than 30-40 km) is detected at 60 – 160 km depth in the continental lithosphere and at an average depth of 70 km in the oceanic lithosphere. Several models have been proposed for the genesis of this mid-lithosphere discontinuity (MLD) that include (1) presence of partial melts or fluids, (2) layered anisotropy, (3) layered composition, and (4) elastically accommodated grain boundary sliding. However, all of these models have some limitations and cannot explain all the characteristics of the MLD. Here we propose a new model for the genesis of the MLD and explore its mechanism through thermomechanical numerical modeling at subduction zones. In the model, the deforming lithospheric mantle is affected by grain size reduction and growth processes. Numerical results show that the lithospheric deformation induced by subduction causes the grain size to sharply decrease within the 10-20 km thick brittle/ductile transition zone over significant regions inside the lithosphere. The depth depends mainly on the age of oceanic lithosphere and the thickness of continental lithosphere and is consistent with the observations. In addition, based on the previous study of dislocation slip-system and related olivine fabrics in the mantle, grain size reduction plays an important role in fluid pumping and phase nucleation through grain boundaries. This may in turn produce an increased intra-lithospheric water content resulting in high electrical conductivities and large seismic velocity drops at the MLD depths.

## P 1.10

# Analytical estimates for velocities of diapirs rising in deforming power-law viscous rock: tests with GPU-based 3-D numerical solutions

Emilie Macherel<sup>1</sup>, Yuri Podladchikov<sup>1</sup>, Ludovic Räss<sup>2,3</sup>, Stefan M. Schmalholz<sup>1</sup>

<sup>1</sup> University of Lausanne, ISTE, Lausanne, Switzerland ([emilie.macherel@unil.ch](mailto:emilie.macherel@unil.ch))

<sup>2</sup> Laboratory of Hydraulics, Hydrology and Glaciology (VAW), ETH Zurich, Switzerland

<sup>3</sup> Swiss Federal Institute for Forest, Snow and Landscape Research (WSL), Birmensdorf, Switzerland

Diapirism is an important mechanism of mass transport. It often occurs in deforming rock units, for example during strike-slip deformation, and the deformation behaviour of the rocks is mostly described by a power-law flow law. The effective viscosity depends on the deviatoric stresses and may reduce significantly where stresses are high. We investigate here how the rising velocity of a diapir is impacted by two types of stress regimes: (i) regional stress due to the far-field deformation, e.g. strike-slip, and (ii) local stress variation around the rising diapir. There exist analytical estimates for the rising velocity, which are based on several simplifications. Here, we test the accuracy of these velocity estimates with full 3-D numerical calculations.

We developed a fast 3-D numerical algorithm based on the pseudo-transient finite-difference (PTFD) method. This method enables efficient simulations of high resolution 3-D viscous flow by implementing an iterative implicit solution strategy. The main challenges are to guarantee convergence, minimize the iteration count and ensure optimal execution time per iteration. We implemented the PTFD algorithm using the Julia language ([julialang.org](https://julialang.org)) and the ParallelStencil.jl and the ImplicitGlobalGrid.jl packages, which enable optimal parallel execution on CPUs and GPUs and ideal scalability up to thousands of GPUs, respectively. We present PTFD simulations of mechanically heterogeneous (less dense and less viscous spherical inclusion), incompressible 3-D power-law viscous flow under gravity in cartesian, cylindrical and spherical coordinates.

The rising velocity of the diapir depends on two dimensionless numbers: (i)  $\tau_b/\tau_{xy}^{\infty}$  ( $\tau_{xy}^{\infty}$  being the far-field stress and  $\tau_b$  the reference stress that marks the transition between linear and power-law viscous deformation) which represents the far-field stress impact, and (ii)  $\Delta p g r / \tau_{xy}^{\infty}$  ( $\Delta p$  being the density-difference between the inclusion and the surrounding medium,  $g$  is the gravitational acceleration and  $r$  is the inclusion radius) which represents the impact of the buoyancy stress. We perform systematic simulations by varying these two dimensionless numbers and compare the analytical estimates with the numerically calculated velocities. We find that analytical and numerical results agree well. Moreover, we are able to provide an improved analytical estimate by adapting a “shape factor”. The improved analytical estimate is useful to test the impact of various parameters on the diapir’s velocity using the two dimensionless numbers.

## P 1.11

# Strain partitioning at the eastern tip of the arcuate Jura Belt: new absolute deformation ages and insights on the role of precursor structures

Herfried Madritsch<sup>1,2</sup>, Nathan Looser<sup>3</sup>, Kurt Decker<sup>4</sup>, Raphael Schneeberger<sup>1</sup>, Lukas Gegg<sup>5</sup>, Marcel Guillong<sup>3</sup>, Katerina Schöpf<sup>4</sup> & Michael Schnellmann<sup>1</sup>

<sup>1</sup> Nagra, Hardstrasse 73, CH-5630 Wettingen

<sup>2</sup> Swisstopo, Seftigenstrasse 264, 3084 Wabern

<sup>3</sup> Geologisches Institut, ETH Zürich, Sonneggstrasse 5, 8050, Zürich

<sup>4</sup> Institut für Geologie, University of Vienna, Josef Holaubek-Platz 2, AT-1090 Vienna,

<sup>5</sup> Institute of Geological Sciences, University of Bern, Baltzerstrasse 1-3, CH-3012 Bern (now at Geologisches Institute University of Freiburg)

Over the last 15 years, the region of central northern Switzerland has been intensively explored on behalf of Nagra for the characterization of potential sites for a national radioactive waste disposal. Based on geological field work, seismic surveying, and structural geological insights from deep boreholes we present an update of the region's tectonic map and key findings regarding its Late Miocene evolution, in particular the formation of the easternmost tip of the Jura Mountains. New constraints on formation timing of regional structures are provided by U-Pb dating of calcite slickenfibres from key outcrops that sustain our tectono-kinematic model.

The newly available seismic data confirm the previously noted the importance of Late Paleozoic structures acting as precursors for the Late Cenozoic fault zones that define the region's present-day tectonic zonation (Laubscher 1986, Diebold & Noack 1997). This particularly accounts for so-called "Hercynian Faults", e.g. NW-SE to WNW-ESE striking structures as exposed in the Black Forest Massif further to the north. In the lower Aare Valley, a transfer structure of this strike was localized that is separating the mildly deformed Mesozoic sequence north of the Jura Main Thrust (the so-called "Vorfallenzone"; Nagra 2008) in an eastern and a western part. The variable deformation style of Late Cenozoic contractional structures found in these two areas also appears to be strongly influenced by the structural configuration of the underlying basement (namely the polarity of the underlying Permocarboniferous grabens). Formation ages of anticlines related to Alpine shortening provided by U-Pb dating of calcite slickenfibres reveal that they were active contemporaneously with the bounding normal faults of the eastward adjacent Hegau-Lake Constance graben. This suggests that at the eastern tip of the Jura, deformation between basement and cover was actually kinematically linked and not decoupled as suggested for the central part of the range already in Late Miocene times (~ 7 Ma). This interpretation is corroborated by the structural analysis of drillcore's from the thrust belt's presumed basal décollement in Mid- to Upper Triassic evaporites. While indication for horizontal shear zones can be found within these rocks, the accommodated strain appears to be small.

We conclude, that at the eastern tip of the Jura Mountains, basement faults did not only passively control the localization of Late Miocene contractional faults but were actively involved in this deformation phase. Thereby, the kinematics of these precursor structures (reverse, strike-slip and extension) varied depending on their orientation with respect to Late Miocene Alpine foreland stress field.

## REFERENCES

- Diebold, P., & Noack, T. 1997: Late Paleozoic troughs and tertiary structures in the eastern Folded Jura. In O. A. Pfiffner, et al. (Eds.), Results of NRP 20 (p. 59–63). Basel: Birkhäuser.  
 Laubscher, H. 1986: The eastern Jura - Relations between thin-skinned and basement tectonics, local and regional. Geologische Rundschau, 75(3), 535–553.  
 Nagra 2008: Vorschlag geologischer Standortgebiete für das SMA und das HAA-Lager. Geologische Grundlagen (Nagra Tech. Ber. NTB 08–04). Wettingen: Nagra.

**P 1.12****Mass transport in experimentally deformed granitoid ultramylonites**

Natalia Nevskaya<sup>1</sup>, Weijia Zhan<sup>1</sup>, Alfons Berger<sup>1</sup>, Holger Stünitz<sup>2,3</sup>, Marco Herwegh<sup>1</sup>

<sup>1</sup> Institut für Geologie, University of Bern, Baltzerstrasse 1+3, CH-3012 Bern (natalia.nevskaya@geo.unibe.ch)

<sup>2</sup> Department of Geology, Tromsø University, Dramsveien 201, 9037 Tromsø, Norway

<sup>3</sup> Institut des Sciences de la Terre d'Orléans (ISTO), Université d'Orléans, 1A rue de la Férollerie, 45100 Orléans, France

The rheology of viscously deformed granitoids with their mixed phases is not yet understood, although these rocks are abundant in Earth's crust. In our on-going study, we show that at temperatures of the brittle to viscous transition these fine-grained, polymineralic rocks are mechanically weaker than monomineralic, coarser ones. For a better understanding of this effect, we performed deformation experiments on a Griggs type apparatus (at 1.2 GPa confining pressure, 650°C and displacement rates of  $10^{-5}$  m/s<sup>-1</sup>), and observed strong strain localization and extreme grain size reduction (from  $\mu\text{m}$  down to nm) in our cylindrical samples. This localization inside the mylonitic starting material allows us to investigate the microstructural evolution of the shear zones as well as the role of chemical mass transfer processes towards and along the shear zone. This is done by defining microstructural domains in the experimentally deformed samples, which are in the following analyzed by an EDX analyzer (TEAMS®) on a ZEISS EVO50 SEM. Resulting local bulk chemistry ( $\sim$ 200 - 2000  $\mu\text{m}^2$  per analysis) demonstrates a clear relationship between chemical changes and characteristic microstructures. Using the Grant (1986) mass calculations on the isocon diagrams in combination with the known volume of the shear zone segments, we will estimate the mass transport. The main effect is the decrease of SiO<sub>2</sub> and increase of FeO content within the shear zones in comparison to the adjacent starting material. In addition to the chemical measurements, we observe the precipitation of new biotite grains, which is consistent with the conclusions from bulk chemistry data. The identified new biotites are often located inside or close to pores. These pores occur inside the highly strained shear zone and have characteristics of so-called "creep- cavities" (e.g. Fusseis et al. 2009, Gilgannon et al. 2017, 2021). Moreover, newly formed biotites have higher  $X_{\text{Mg}}$  values, which further support the transport of Fe. This means that even on the short experimental timescale (i.e. 3-4 days) there is sufficient time to activate dissolution, nucleation and precipitation processes. Whereas the solution kinetics are enhanced by the small grain sizes (e.g., <100 nm), the role of nucleation and growth must be directly related to local stress variations and resulting oversaturation of the fluid at low stress sites or progressively forming creep-cavities. These findings provide new insights in the often observed faster reaction kinetics in deformed rocks compared to static metamorphic reactions.

The observed mass transfer inside an experiment (= "pseudo-closed system") provides the opportunity to quantify amount and rates of mass transfer processes during the deformation process including solution/precipitation and grain boundary sliding.

**REFERENCES:**

- Grant, J. A. 1986: The Isocon Diagram – A Simple Solution to Gresens' Equation for Metasomatic Alteration, *Economic Geology*, 81, 1976-1982
- Fusseis, F., Regenauer-Lieb, K., Liu, J., Hough, R. M. & De Carlo, F. 2009: Creep cavitation can establish a dynamic granular fluid pump in ductile shear zones, *Nature*, 459, 974-977
- Gilgannon, J., Fusseis, F., Menegon, L., Regenauer-Lieb, K., Buckman, J. 2018: Hierarchical creep cavity formation in an ultramylonite and implications for phase mixing, *Solid Earth*, 8, 1193–1209
- Gilgannon, J., Waldvogel, M., Poulet, T., Fusseis, F., Berger, A., Barnhoorn, A. & Herwegh, M. 2021: Experimental evidence that viscous shear zones generate periodic pore sheets, *Solid Earth*, 12, 405–420

## P 1.13

# Structure and stratigraphy of continent-derived metasediments units (Cimes Blanches and Frilihorn) intercalated within the ophiolites around Zermatt: Relations with the Mischabel backfold, Alphubel basement and Mont Fort nappe (Pennine Alps, SW Switzerland and NW Italy)

Adrien Pantet<sup>1</sup> and Jean-Luc Epard<sup>1</sup>

<sup>1</sup> Institute of Earth Sciences, University of Lausanne (adrien.pantet@unil.ch)

The nature of the mechanisms leading to the imbrication of continental- and oceanic-derived units in collision zones is a long standing and, in several cases, still debated subject in geology. The studied area around Zermatt (SW Switzerland and NW Italy) exhibits some classic examples of such imbrications. In particular, the units called *Cimes Blanches* and *Frilihorn* (e.g. Escher et al. 1993) or *Faisceau Vermiculaire* (Argand 1916), consist of a set of thin but widely-extending bands of continent-derived metasediments intercalated at different levels in the thick complex of ophiolites and oceanic metasediments exposed over this region. Despite the very wide variety of mechanisms that have been invoked to explain such intercalations and the complex tectonic architecture of this area, no real consensus has been reached within the geological community concerning these questions.

We present new data concerning the structure and stratigraphy of the different bands constituting the *Faisceau Vermiculaire* in the area surrounding Zermatt and, in particular, in the Täschalpen sector, where the *Faisceau Vermiculaire* is locally in contact with Paleozoic basement units forming the Mischabel backfold and the Alphubel anticline.

Our lithological and stratigraphic observations allow: (i) to confirm the presence in the *Faisceau Vermiculaire* of widespread breccias, for the most part of probable Lower to Upper Jurassic age, that are intensely stretched and therefore locally difficult to recognize; (ii) to confirm the interpretation of the first authors (e.g. Güller 1947; Bearth 1976) suggesting the stratigraphic nature of the contacts between the *Faisceau Vermiculaire* and the overlying non-ophiolitic, p.p. Upper Cretaceous, calcschists (*Série Rousse*), which constitute the lower part of the Schistes Lustrés of the Combin zone; (iii) to confirm the existence of a strong contrast in the Jurassic to Cretaceous/Paleogene stratigraphic sequences between the autochthonous cover of the Siviez-Mischabel nappe (Barrhorn Series, Briançonnais s.str.) and the series formed by the *Faisceau Vermiculaire* and *Série Rousse*, which is characteristic of a sedimentation in a deeper basin (Prepiedmont basin) with an important clastic and detritic input (Staub 1942; Sartori 1987); (iv) to interpret the contact of the *Faisceau Vermiculaire* and the *Série Rousse* with the basement forming the Alphubel anticline east of Zermatt, as a stratigraphic contact; the locally discordant character of this contact is interpreted as the result of the activity of synsedimentary Jurassic normal paleofaults; (v) to confirm the widely accepted interpretation concerning the tectonic nature of the contact separating the *Faisceau Vermiculaire* and the *Série Rousse* from the basement forming the hinge of the Mischabel backfold; this basement is separated from the one forming the Alphubel anticline by a deep early syncline, involving ophiolites of the Tsaté nappe, the eastward prolongation of this syncline in the Mischabel massif is potentially important but hidden by the moraines and glaciers.

We propose a new tectonic scheme for the structure of the *Faisceau Vermiculaire* and adjacent units. It involves an early northward folding of the *Faisceau Vermiculaire* together with the *Série Rousse* and ophiolitic Schistes Lustrés of the Tsaté nappe, followed by major backfolding responsible for the southward emplacement of these units above the HP Zermatt-Saas and Monte Rosa nappes. With respect to the Siviez-Mischabel and Tsaté nappes, our tectonic study at regional scale shows that the ensemble formed by the Alphubel basement, the *Faisceau Vermiculaire* and the *Série Rousse* share an identical tectonic position with the Mont Fort nappe outcropping north and west of the Dent Blanche klippe. Based on tectonic and stratigraphic arguments, we propose that the Alphubel basement, the *Faisceau Vermiculaire* and the *Série Rousse* form together the eastern prolongation of the Mont Fort nappe, in the lower limb of the Mischabel backfold.

## REFERENCES

- Argand, E. (1916). Sur l'arc des Alpes occidentales. Eclogae Geologicae Helvetiae, 14, 145–191.
- Bearth, P. (1976). Zur Gliederung der Bündnerschiefer in der Region von Zermatt. Eclogae Geologicae Helvetiae, 69(1), 149–161. doi:10.5169/SEALS-164499
- Escher, A., Masson, H., & Steck, A. (1993). Nappe geometry in the Western Swiss Alps. Journal of Structural Geology, 15(3–5), 501–509. doi:10.1016/0191-8141(93)90144-Y
- Güller, A. (1947). Zur Geologie der südlichen Mischabel- und der Monte Rosa-Gruppe: mit Einschluss des Zmutt-Tales westlich Zermatt. Eclogae Geologicae Helvetiae, 40(1), 39–164. doi:10.5169/SEALS-160900
- Sartori, M. (1987). Structure de la zone du Combin entre les Diablons et Zermatt (Valais). Eclogae Geologicae Helvetiae, 80(3), 789. doi:10/gfhzz3
- Staub, R. (1942). Gedanken zum Bau der Westalpen zwischen Bernina und Mittelmeer. Mitteilungen aus dem Geologischen Institut der Eidg. Technischen Hochschule und der Universität Zürich, (B) 7, 138 pp.

## P 1.14

# Can the build-up of swelling stress in clay-rich rocks induce slip along faults?

Markus Rast<sup>1</sup>, Claudio Madonna<sup>1</sup>, Paul A. Selvadurai<sup>2</sup>, Quinn Wenning<sup>3</sup>, Jonas B. Ruh<sup>1</sup>, Antonio Salazar Vásquez<sup>3,4</sup>

<sup>1</sup> Geological Institute, ETH Zürich, Zürich, Switzerland (markus.rast@erdw.ethz.ch)

<sup>2</sup> Swiss Seismological Service, ETH Zürich, Zürich, Switzerland

<sup>3</sup> Institute of Geophysics, ETH Zürich, Zürich, Switzerland

<sup>4</sup> Eastern Switzerland University of Applied Sciences, Rapperswil, Switzerland

Clay-rich rocks occur in a wide range of tectonic settings and are of particular interest for the mechanical properties of shallow subduction zone interfaces, since clay minerals are relatively abundant in sediments entering the subduction zone (Underwood, 2007) and begin to control the frictional behavior at concentrations of about 20 % (e.g., Crawford et al., 2008). In contact with a polar fluid, clay minerals are able to swell or, under confined conditions, to build-up swelling stress, the extent in both cases will depend on the clay mineralogy and the pore water chemistry (Wagner, 2013). Many studies have focused on the closing of cracks in clay-rich sedimentary rocks by swelling ('self-sealing'), as it is of high interest in relation to using such rocks as natural barriers in nuclear waste deposits or as subsurface caprocks for the storage of CO<sub>2</sub> (e.g., Wenning et al., 2021). However, less is known about the effect of swelling on the stress state of clay-rich rocks and the ability to induce slip along pre-existing faults, which is addressed in the present study.

Triaxial shear experiments are performed using oblique saw-cut cylindrical samples, where the top half consists of a clay-rich rock (Opalinus clay) and the bottom half of a permeable sandstone (Berea sandstone) (Fig. 1). To estimate the frictional properties of the interface between Opalinus clay and Berea sandstone, dry experiments are performed at 10 to 25 MPa confining pressure and constant axial displacement of 0.1 mm/min. Fluid injection experiments, where fluids are injected through the permeable footwall sandstone, are performed at 10 MPa confining pressure, constant axial displacement, and an initial differential stress of about 70 % of the expected yield stress. The effect of swelling stress is estimated by comparing the fluid pressures required to initiate slip when a non-polar fluid is injected (no swelling is expected) and when a polar fluid is injected (swelling stress will develop). In order to distinguish the (poro)elastic deformation of the matrix and the deformation due to slip along the saw cut, the sample assemblage is equipped with fiber optics strain sensors glued to the surface of the sample in some experiments (Vásquez et al., 2022).

For fluid injection experiments with a non-polar fluid (decane), the mechanical data indicate that slip along the saw cut occurs at fluid pressures close to what is expected from Mohr-Coulomb theory, i.e., the Mohr circle touches the failure envelope defined by the dry experiments. Preliminary results of a polar fluid injection experiment (using deionized water) indicate that slip is induced at fluid pressures corresponding to stress conditions under which no failure is expected based on the dry experiments. This suggests that the polar fluid either alters the frictional properties of the interface (i.e., reduces its frictional strength) or that the stress state is not fully described by confining pressure, axial stress, and fluid pressure, since swelling stress comes into play. This may have implications for (1) subduction zones where changing fluid compositions and transient fluid flow could change the stress state due to swelling stress build-up, (2) the interpretation of wet friction tests of clay minerals and clay-rich rocks where swelling stress is usually not considered, or (3) the consideration of clay-rich rocks as natural barriers in nuclear waste deposits where swelling is considered to primarily close cracks rather than induce slip.

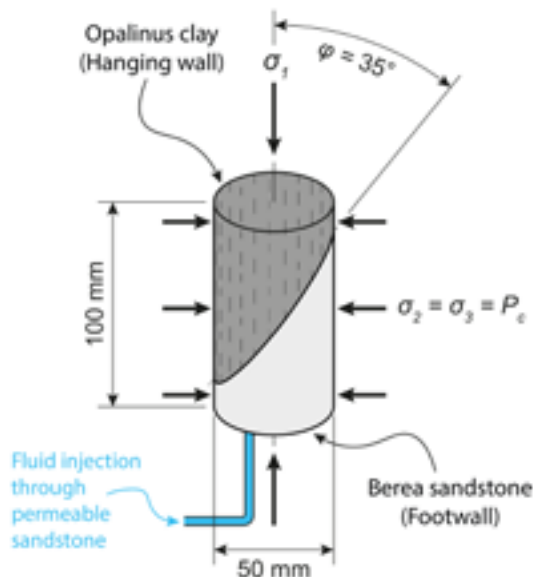


Figure 1. Experimental setup of the present study. Axial stress  $\sigma_1$ , confining pressure  $P_c$  (equal to intermediate and smallest principal stress  $\sigma_2$  and  $\sigma_3$ , respectively), and fluid pressure  $P_f$  are applied in a triaxial deformation apparatus.

## REFERENCES

- Crawford, B. R., Faulkner, D. R., and Rutter, E. H. (2008). Strength, porosity, and permeability development during hydrostatic and shear loading of synthetic quartz-clay fault gouge. *Journal of Geophysical Research: Solid Earth*, 113(3).
- Underwood, M. B. (2007). Sediment Inputs to Subduction Zones: Why Lithostratigraphy and Clay Mineralogy Matter. In Dixon, T. H. and Moore, C., editors, *The Seismogenic Zone of Subduction Thrust Faults*, pages 42–85. Columbia University Press, New York Chichester, West Sussex.
- Vásquez, A. S., Rabaiotti, C., Germanovich, L. N., and Puzrin, A. M. (2022). Distributed fiber optics measurements of rock deformation and failure in triaxial tests. *Journal of Geophysical Research: Solid Earth*, 127.
- Wagner, J.-F. (2013). Mechanical Properties of Clays and Clay Minerals. In Bergaya, F. and Lagaly, G., editors, *Developments in Clay Science*, volume 5, pages 347–381. Elsevier.
- Wenning, Q. C., Madonna, C., Kurotori, T., Petrini, C., Hwang, J., Zappone, A., Wiemer, S., Giardini, D., and Pini, R. (2021). Chemo-Mechanical Coupling in Fractured Shale With Water and Hydrocarbon Flow. *Geophysical Research Letters*, 48(5).

## P 1.15

# New kinematic model and paleogeological maps give new insight on the evolution of the Afar Region

Valentin Rime<sup>1</sup>, Anneleen Foubert<sup>1</sup>, Balemwal Atnafu<sup>2</sup>, Tesfaye Kidane<sup>3</sup>

<sup>1</sup> Department of Geosciences, University of Fribourg, Ch. Du Musée 6, 1700 Fribourg ([valentin.rime@unifr.ch](mailto:valentin.rime@unifr.ch))

<sup>2</sup> School of Earth Sciences, Addis Ababa University, Addis Ababa, Ethiopia

<sup>3</sup> School of Agricultural, Earth and Environmental Sciences, University of KwaZulu-Natal, Westville Campus, Durban, South Africa

The Afar Region encompasses the Afar Depression, the Danakil block, the southernmost Red Sea, the westernmost Gulf of Aden, as well as the surrounding Ethiopian, Somalian and Yemenite Plateaux. It is situated at the junction between the Gulf of Aden, the Red Sea and the East African Rift System and thus forms a key region of the Afro-Arabian Rift System. The Afar Region experienced important magmatic activity since approx. 30 Ma with the eruption of flood basalts, followed by rifting and continental breakup.

By combining newly compiled and integrative geological maps as well as a comprehensive review of the geological history of the region, we propose a new plate kinematic model for the Afar Region. New paleogeological maps unveil the full evolution of a triple junction from pre-rift to oceanic spreading. They show that magmatic, sedimentary and tectonic events are strongly diachronous throughout the region. It also highlights the importance of the Afar hotspot on the rift evolution.

## P 1.16

# Thermal adaptation evolution of the biosphere regulates Earth's long-term climate

J. Rogger<sup>1,2</sup>, B.J.W. Mills<sup>3</sup>, T.V. Gerya<sup>1</sup>, L. Pellissier<sup>2,4</sup>

<sup>1</sup> Swiss Federal Institute of Technology Zurich, Department of Earth Sciences, Zurich, Switzerland

<sup>2</sup> Swiss Federal Institute of Technology Zurich, Department of Environmental Systems Science, Zurich, Switzerland

<sup>3</sup> University of Leeds, School of Earth and Environment, Leeds, United Kingdom

<sup>4</sup> Swiss Federal Institute for Forest, Snow and Landscape Research, Birmensdorf, Switzerland

Sustained habitable conditions and the evolution of complex life on Earth depend on efficient climate regulation mechanisms that keep carbon fluxes between geologic reservoirs and the atmosphere-ocean system in balance. The terrestrial biosphere plays an important role in regulating the long-term climate by controlling burial rates of photosynthetically fixed CO<sub>2</sub> as well as by mediating CO<sub>2</sub> consumption through silicate mineral weathering during plant nutrient acquisition, balancing out carbon inputs to the atmosphere-ocean system by volcanism or metamorphism. Current biogeochemical models of the Phanerozoic Earth neglect that the strength of the impact of the terrestrial biosphere on global carbon fluxes is subject to evolutionary dynamics and that it depends on how well the biosphere is adapted to prevailing environmental conditions [1]. Here, we develop a theoretical model to reconstruct million-yearly global organic and inorganic carbon fluxes over the last 400 Myrs. We show that the speed of evolutionary adaptation of the terrestrial biosphere to climatic shifts strongly affects the long-term atmosphere-ocean carbon mass balance. When considering a slow rate of thermal adaptation of the biosphere, resulting in reduced organic carbon burial and especially, strongly reduced silicate weathering rates following temperature shifts, a closer balance of reconstructed Phanerozoic carbon inputs and outputs to and from the atmosphere-ocean system is obtained. Such a balance is a prerequisite to maintain habitable conditions on Earth's surface on a multi-million-year timescale. We argue that the climate evolution of the Phanerozoic Earth is strongly defined by biological and evolutionary processes. Understanding these biological dynamics and how they shape the interactions between Earth's biosphere, geosphere and the climate system may help to understand large shifts in Phanerozoic temperatures and the development of the atmospheric composition of the planet.

[1] Mills, B.J. et al. Modelling the long-term carbon cycle, atmospheric CO<sub>2</sub>, and Earth surface temperature from the late Neoproterozoic to present day. *Gondwana Research* 67, 172-186. DOI: 10.1016/j.gr.2018.12.001

**P 1.17****Geodynamic evolution of the Iranian plate during the formation of the Neotethys ocean**

MAHIN ROSSTAMI<sup>1</sup>, MOHAMMAD MZANIJOU<sup>1</sup>, ROBERT MORITZ<sup>2</sup>, ALI SHOLEH<sup>3</sup>

<sup>1</sup> Department of Geology, Faculty of Science, Bu-Ali Sina University, Hamedan, Iran

<sup>2</sup> Department of Earth Science, Geneva University, Switzerland

<sup>3</sup> Department of Geology, Faculty of Basic Sciences, Tarbiat Modares University, Tehran, Iran ([Rostami.m99@gmail.com](mailto:Rostami.m99@gmail.com))

Collisional orogenies are suitable sites for the occurrence of porphyry and epithermal deposits, and most Cenozoic porphyry deposits in the Tethyan Orogeny were formed in a back-arc, post-subduction, or collisional setting (Richards 2014). As part of the African-Arabian collision zone, the Iranian plateau is located in the central part of the 12,000 km Tethyan belt (Richards 2014), and hosts hundreds of porphyry and epithermal deposits. The occurrence of mineralization in Iran is affected by the opening and closing of large and small oceanic basins, such as the Neo-Tethys Ocean, which was formed in the early Permian-Triassic by the separation of the Cimmerian continental fragments from Gondwana. As the subcontinents moved northward, the Neo-Tethys oceanic basin experienced its maximum extension in the Jurassic (Stampili 2000). The collision of these subcontinents with the southern margin of Eurasia followed the decline of the Paleo-Tethys ocean. In the continuation of the fragmentation of Gondwana, other parts were separated from it in the form of African-Arabian continents, India and Australia. The collision of these subcontinents with Eurasia during the Late Cretaceous-Present (Alavi 1994), or Eocene (Ghasemi & Talbot, 2006), Oligocene (Karagharan Bafghi et al. 2012), or Miocene (Hassanzadeh 1993) ended the life of the Neo-Tethys ocean and the Alpine-Zagros-Himalaya orogenic belt was formed.

The geotectonic development of the Zagros Orogeny is directly related to the evolution of the Neo-Tethys Ocean, followed by continent-continent collision in the Tertiary (Zarasundi et al. 2020). The Zagros orogeny, as the central part of the Alpine-Himalayan orogeny, extends for 2000 km from the northwest to the south of Iran (Babazadeh et al. 2018). The Zagros fold-and-thrust belt consists of three parallel belts (Alavi 1994): 1- Urmia-Dokhtar magmatic arc (UDMA), 2- Sanandaj-Sirjan metamorphic zone (SaSZ), and 3- Zagros folded belt.

Urmia-Dokhtar magmatic arc or UDMA has a width of 2000 km (Ghorbani et al. 2014), and as a narrow strip of 50 to 80 km (Alavi 2007) extend from the Little Caucasus mountain range (Moritz and et al. 2019) and Anatolia (Omidi, 1984) in the northwest to Gulf of Oman (Falcon, 1969) in the southeast. Magmatic activity in the UDMA, which continued from the Eocene to the Quaternary (Ayati 2012), reached its maximum during the Eocene (Alavi 1994, 2007). Based on Raeisi et al. (2021), the change of magma composition from calc-alkaline during the Eocene to adakitic in the early Miocene caused an increase in the fertility of the productive magma and the formation of porphyry systems deposits. Shafei et al. (2009) suggested that the change in magma composition is caused by the change from the subduction stage to the collision stage. A similar change in the composition of magmatism in another part of the metallogenic belt in the Lesser Caucasus was also reported by Moritz et al. (2013, 2015). Based on the age of mineralization, the UDMA metallogenic belt can be divided into three parts: the northwest, the middle, and finally the southeast. The first part, which is known as the Arasbaran zone, hosts world-class deposits, including the copper-molybdenum porphyry Songun (Aghazadeh et al. 2015), the Sary Gunay epithermal gold deposit (Richards et al. 2006), the Carlin-Zarshouran type gold deposit (Mehrabi et al. 1999, Asadi et al. 1999) and Agdarreh carbonate-hosted gold deposit (Daliran 2008). Metallogenesis in this zone has lasted for about 9 million years, and the earlier Miocene is considered as the peak of porphyry mineralization in this zone (Aghazadeh et al. 2014). The central part of UDMA hosts Kahang porphyry copper deposit (Raeisi et al. 2021), Dali porphyry copper-gold deposit (Zarasvandi et al. 2015), and Darreh-Zereshk and Aliabad porphyry copper deposits (Zarasvandi et al. 2005). In the southeastern part of UDMA, which is known as the Kerman porphyry copper belt, mineralization occurred in the late Oligocene and Miocene, and the most important porphyry deposits of Sarcheshmeh and Meiduk were formed in the middle Miocene period (Aghazadeh et al. 2014).

The Sanandaj-Sirjan zone (SaSZ) joined Eurasia as a part of the Cimmerian continental fragments in the Late Triassic (Sheikholeslami et al. 2016). This zone with a width of 150 to 200 km is formed parallel to the Zagros thrust-fold belt and extends from the northwest (Sanandaj) to the southeast (Sirjan) (Ghazi & Moazzen 2015). This zone is mainly composed of metamorphic rocks such as metacarbonates, schists, gneisses and amphibolites (Ghazi & Moazzen 2015) and is intruded by gabbroic to granitic intrusive rocks (Dilek et al. 2010). The metamorphism attributed to northeastward subduction of Neo-Tethys oceanic crust under the SaSZ (Agard et al. 2006, Moritz et al. 2006). Azizi & Stern (2019) suggested that the mafic melt produced from the lithospheric mantle is injected into the continental crust and caused metamorphism in the continental crust. Igneous activity in the SaSZ mainly occurred in the Mesozoic (Richards 2015). Unlike stock-like intrusions in UDMA, granitoid masses in SaSZ were mainly formed as batholiths in the Jurassic time. The Cenozoic magmatism in UDMA was more oxidized/hydrous in nature than the Mesozoic magmatism in the SaSZ (Zarasvandi et al. 2020). This factor, along with factors such as sufficient water content (Richards 2011b) and rich magma source (Richards 2011a), has caused magmatism in UDMA to be associated with extensive mineralization of the porphyry system, while this is not the case in the Sanandaj-Sirjan zone (Zarasvandi et al. 2020).

**REFERENCES:**

- Azizi, H., and Stern, R.J., 2019, Jurassic igneous rocks of the central Sanandaj–Sirjan zone (Iran) mark a propagating continental rift, not a magmatic arc: *Terra Nova*, 31, 415–423. doi:10.1111/ter.12404.
- Richards, J.P., 2011a, Magmatic to hydrothermal metal fluxes in convergent and collided margins: *Ore Geology Reviews*, 40, 1–26. doi:10.1016/j.oregeorev.2011.05.006.
- Moritz, R., Ghazban, F. & Singer, B. 2006: Eocene Gold Ore Formation at Muteh, Sanandaj-Sirjan Tectonic Zone, Western Iran: A Result of Late-Stage Extension and Exhumation of Metamorphic Basement Rocks within the Zagros Orogen. *Economic Geology* 101, 1–28.

**P 1.18****Grain size reduction undermines the importance of viscous shear heating in lithospheric mantle shear zones**

Jonas B. Ruh<sup>1</sup>

<sup>1</sup> *Structural Geology and Tectonics Group, Geological Institute, Department of Earth Sciences, ETH Zürich, Sonneggstrasse 5, 8092 Zürich (jonas.ruh@erdw.ethz.ch)*

Active plate tectonics require weak boundaries that accommodate large strain over long time periods. Many studies argue that shear heating converted from dissipated mechanical energy may be responsible for the necessary weakening in the mantle lithosphere to initiate and sustain weak plate boundaries. Here, I present simple numerical simulations of pure olivine systems with a composite diffusion-dislocation creep rheology coupled to a self-consistent grain size evolution model to investigate the effect of grain size reduction on shear heating. Results demonstrate that the weakening related to grain size reduction and the activation of grain-size-sensitive diffusion creep undermines the importance of shear heating in mantle shear zones. Depending on shear zone width, shear velocity and apparent stresses, estimations on ideal shear zone widths and viscosities are presented.

## P 1.19

# Paleo-strain reconstruction from drill core mapping and their relevance for northern Switzerland

Kurt Decker<sup>1</sup>, Raphael Schneeberger<sup>2</sup>, Herfried Madritsch<sup>2</sup>,

<sup>1</sup> Institut für Geologie, University of Vienna, Vienna, Austria

<sup>2</sup> Nagra, Wettingen, Switzerland (raphael.schneeberger@nagra.ch),

Within the frame of the siting process in Switzerland, the national cooperative for the disposal of radioactive waste (Nagra) conducted a deep drilling campaign. In total eight vertical and one deviated borehole were drilled from the surface, mostly into the basement across the entire mesozoic stratigraphic sequence. The boreholes were cored over large intervals resulting in a total of about 6.1 km mostly oriented cores available for numerous subsequent analyses. The primary interest of Nagra lays on the formation called Opalinus Clay, as it was selected as potential host rock for a deep geological repository.

In the process of host rock characterisation, the tectonic overprint of the potential future host rock plays an important role. Therefore, all cores were carefully mapped according to a pre-defined manual (Ebert and Decker, 2019). Structural logging aimed for little interpretation to decrease cognitive bias. During the quality control of the mapping, key structures along each borehole were investigated and discussed. Based on those key structures and observed cross-cutting relationships we identified:

- (1) a NNW-extension, which could uniquely be dated to start in Early Jurassic based on the observation of a neptunian dyke filled with Liassic sediments and other extensional structures in Jurassic sediments deformed by sediment compaction.
- (2) a local NE-SW extension observed in four boreholes more in the eastern part of the study area.
- (3) a NNE-shortening and finally
- (4) a NNW-shortening. Shortening is associated with about E-W-extension. The cross-cutting relationships indicate that the two shortenings and the associated extensions occurred coevally. Absolute age dating of veins is in progress with however no successful age dating for the samples taken within the Opalinus Clay.

Within this presentation, we introduce the aforementioned tectonic characterisation of the drill cores as well as the paleo-strain reconstructions and their meaning for a regional understanding of the tectonic evolution of northern Switzerland. Where, the younger shortening events are compatible on a larger regional scale with the folding of the Jura Mountains and the Miocene reactivation of the Hegau zone (Schori 2021, Egli et al. 2016). The NNW-shortening is further aligned with the currently measurement principle horizontal stress axis. The two shortening directions could result from re-activation of pre-existing basement structures and related stress deflections from a similar general stress regime.

## REFERENCES

- Ebert A., Decker K. (2019): Structural analysis manual. Nagra Arbeitsbericht. NAB 19-012.
- Egli, D., Mosar, J., Ibele, T. et al. The role of precursory structures on Tertiary deformation in the Black Forest—Hegau region. Int J Earth Sci (Geol Rundsch) 106, 2297–2318 (2017). <https://doi.org/10.1007/s00531-016-1427-8>
- Schori, M. (2021). The development of the Jura fold-and-thrust belt: pre-existing basement structures and the formation of ramps. PhD Thesis University of Fribourg, Switzerland.

## P 1.20

# Geological mapping and U-Pb dating of detrital and magmatic zircon crystals in the Lepontine dome (Central European Alps)

Alessia Tagliaferri<sup>1,2</sup>, Filippo Luca Schenker<sup>1</sup>, Stefan Markus Schmalholz<sup>2</sup>, Alexey Ulianov<sup>2</sup>

<sup>1</sup> Institute of Earth Sciences, University of Applied Sciences and Arts of Southern Switzerland (SUPSI), CH-6850 Mendrisio, Ticino, Switzerland ([alessia.tagliaferri@supsi.ch](mailto:alessia.tagliaferri@supsi.ch))

<sup>2</sup> Institute of Earth Sciences, University of Lausanne (UNIL), CH-1015 Lausanne, Vaud, Switzerland  
([alessia.tagliaferri@unil.ch](mailto:alessia.tagliaferri@unil.ch))

The Barrovian metamorphism of the Lepontine dome (Central European Alps) is manifested by isogrades that cross-cut tectonic nappe contacts, which is commonly interpreted as a metamorphism that occurred after nappe emplacement. However, the pervasive mineral and stretching lineation in amphibolite facies, associated to top-to-foreland shearing, suggests that peak Barrovian conditions are coeval to thrusting. Here, we combined extensive fieldwork and U-Pb zircon dating on gneisses and post-foliation dikes to better constrain the relation between metamorphism and nappe emplacement.

Metamorphic zircon rims show two groups of ages, at 33-31 Ma and 24-22 Ma. The younger group is observed in post-tectonic dikes and related metasomatic overprint in the country rock. The older group occurs in syn-kinematic migmatites along a crustal-scale shear zone. On its footwall, magmatic and detrital zircon cores suggest that the Cima Lunga unit, previously interpreted as a mélange with Mesozoic fragments, was a pre-Variscan metasedimentary sequence intruded by Permian granitic sills, now orthogneisses. This unit was tectonically reworked within the Simano nappe during the overthrusting of a major Alpine high-pressure nappe, here defined as the Maggia-Adula nappe, imprinting the regional lineation and peak-temperature metamorphism until ca. 31 Ma. Péclet (1-10) and Brinkman (0.002-1.8) numbers, computed for estimated values on the newly-defined Maggia-Adula shear zone system, suggest an advection-dominated heat transfer with significant diffusion during and after nappe emplacement, generating Barrovian isogrades discordant to the thrust. Shear heating played a not-negligible role if effective viscosities were  $>10^{21}$  Pa·s. The local advection of magma/fluids cutting the nappe contact at 24-22 Ma sourced from deeper migmatites exhuming along the Alpine backstop.

In this contribution, we focus on the field relationships between the Cima Lunga unit and the Simano nappe as well as on the pre-Variscan detrital and Permian magmatic U-Pb zircon ages. Our results have consequences on the definition of the nappe structure of the Lepontine dome, suggesting that the Cima Lunga unit has a pre-Variscan origin and was already part of the Simano nappe during the formation of the Alps.

## P 1.21

# Structural Mapping of the Eclogite Zone, Tauern Window: Implications for the rheology of the subduction zone interface

Tokle, L.<sup>1</sup>, Behr, W.M.<sup>1</sup>, Braden, Z.<sup>1,2</sup>, and Cisneros, M.<sup>1,3</sup>

<sup>1</sup>*Structural Geology and Tectonics Group, Geological Institute, Department of Earth Sciences, ETH Zurich, Sonneggstrasse 5, 8092, Zürich, Switzerland*

<sup>2</sup>*School of Public Policy and Global Affairs, University of British Columbia*

<sup>3</sup>*Lawrence Livermore National Laboratory, Livermore, CA (leif.tokle@erdw.ethz.ch)*

The subduction zone interface is a shear zone of varying thickness that defines the boundary between the subducting slab and overriding plate. The rheology of this shear zone controls several important aspects of subduction dynamics, but accurately estimating its rheology can be complex due to the wide range of subduction materials and their varying rheological properties. Of particular importance is the relative strengths of metasedimentary and metabasic rocks at various temperature and pressure conditions. To better understand these rheological contrasts in naturally deformed rocks, we are conducting field and microstructural work in the Eclogite Zone in the Tauern Window, Austria. The eclogite zone preserves intercalated metamafic (metabasalt and metagabbro) and metasedimentary (quartzite, garnet mica schist, marble and calc-schist) rocks that were subducted and exhumed to the surface as a single structural unit. Graphite thermometry and quartz-in-garnet inclusion barometry from mica schists indicate T and P of 500+/-40°C and 1.9+/-0.2 GPa, consistent with previous estimates from conventional thermobarometry. Using high resolution drone imaging, 2D structural mapping, and 3D structural modeling, we have documented the map-scale relationships between metamafic and metasedimentary rocks in the Eissee region near Matrei. Our mapping demonstrates that the mafic eclogites consistently define slabs, lenses and boudins of up to 2 km in along-strike length and 0.2 km in thickness, embedded within the metasedimentary units, all of which are relatively uniformly deformed to very high strain. This suggests that eclogitized metamafic rocks persist as rheological heterogeneities within the subduction channel through both the subduction and exhumation paths. This length scale of heterogeneity on the deep interface could potentially contribute to unique seismic signatures (e.g. slow slip and tremor) and may also affect the large-scale geodynamics of subduction through influencing the bulk viscosity of the interface.

**P 1.22****On the reliability of the PANALESIS (v.0) paleogeographic maps**

Christian VERARD<sup>1</sup>

<sup>1</sup> Department of Earth Sciences, University of Geneva, Rue des Maraîchers 13, CH-1205 Geneva ([christian.verard@unige.ch](mailto:christian.verard@unige.ch))

Paleogeography is the definition of the geography of the Earth in the geological past. However, geography depends on the relief (or topography, on land and under the sea) and the sea level which defines the coastline. Relief is a multifactorial resultant whose heart is the geodynamic context that created it (Verard, 2019). In other words, there are no paleogeographic reconstructions if there is no plate tectonic model underlying them.

The paleogeographic maps presented here are derived from the PANALESIS model (preliminary version or v.0), corresponding to paleo-digital elevation models (paleo-DEM) that cover the entire Phanerozoic on a global scale associated with sea level variations from Haq et al. (1987, 2008, 2018).

The results show two main facts. First, the main shortcomings of the method for converting a plate tectonic map to a paleogeographic map (Verard et al., 2015) are relatively well understood and should be able to be improved with new versions of the plate tectonic model (Verard, 2021) and conversion code. Secondly, lithofacies databases (fossils and paleo-environments) on a global scale are needed to identify areas that are outside the “standard mode” defined by synthetic topography and to understand the reasons for this discrepancy. Conversely, variations (global to regional) in lithofacies can only be understood if a quantified topographic model is proposed as a reference, which PANALESIS is, to date, the only one to offer.

Work is under progress to propose a website where the 42 paleogeographic maps of PANALESIS will be available for everyone.

**REFERENCES**

- Verard, C., 2019. PANALESIS: Towards global synthetic palaeogeographies using integration and coupling of manifold models. *Geological Magazine*, 156 (2), 320-330.
- Haq, B. U., Hardenbol, J., Vail, P. R., 1987. Chronology of fluctuating sea levels since the Triassic. *Science*, 235 (4793), 1156-1167.
- Haq, B. U., Schutter, S. R., 2008. A chronology of Paleozoic sea-level changes. *Science*, 322 (5898), 64-68.
- Haq, B. U., 2018. Triassic eustatic variations reexamined. *The Geological Society of America (GSA Today)*, 28, 6 pages.
- Verard, C., Hochard, C., Baumgartner, P. O., Stampfli, G. M., 2015. 3D palaeogeographic reconstructions of the Phanerozoic versus sea-level and Sr-ratio variations. *Journal of Palaeogeography*, 4 (2), 167-188.
- Verard, C., 2021. 888 – 444 Ma global plate tectonic reconstruction with emphasis on the formation of Gondwana. *Frontiers in Earth Science*, 9 (666153), 28 pages.

## P 1.23

# Effect of Phyllosilicate Content and Composition on Fault Gouge Friction under Hydrothermal Conditions

Weijia Zhan<sup>1</sup>, Natalia Nevkaya<sup>1</sup>, André Niemeijer<sup>2</sup>, Alfons Berger<sup>1</sup>, Chris Spiers<sup>2</sup>, Marco Herwegen<sup>1</sup>

<sup>1</sup> Institute of Geological Sciences, University of Bern, Baltzerstrasse 1+3, CH-3012 Bern (weijia.zhan@geo.unibe.ch)

<sup>2</sup> Faculty of Geosciences, HPT Laboratory, Utrecht University, Princetonlaan 4, 3584 CB Utrecht, Netherlands

Phyllosilicates are abundant in mature fault zones found in both subduction megathrust and continental fault systems. These sheet silicates often exhibit low frictional strength and tend to be frictionally stable. In earthquake mechanics, measurements of these frictional properties are crucial for understanding earthquake nucleation. Many previous studies have focused on characterizing the frictional behavior of phyllosilicate-quartz mixtures at room temperature and room humidity. Although increasing temperature and pressure have been proven to alter phyllosilicate structure and composition, only a few studies have addressed changes in phyllosilicate frictional response under hydrothermal conditions similar to those at seismogenic depths.

To explore such effects further, we conducted frictional sliding experiments on three types of fault “gouge” material under hydrothermal conditions, using a ring shear deformation apparatus. The gouge mixtures used were derived from crushed granitoid ultramylonite, muscovite-rich fault gouge and phlogopite-rich gouge, respectively. The mineralogy of our samples is given in Table 1. The experiments were run at elevated temperatures up to 650°C and a constant effective normal stress of 100MPa (100MPa pore fluid pressure and 200MPa normal stress). Velocity steps of 1-3-0-30-100μm/s were applied to measure the velocity dependence of friction as an indicator of frictional stability.

Our experiments showed pronounced changes in steady state strength and its velocity dependence as a function of phyllosilicate mineralogy and content. At temperatures from 20 to 350°C, the granitoid gouges were consistently stronger ( $\mu=0.62-0.71$ ) than muscovite-rich gouges ( $\mu=0.43-0.53$ ) and phlogopite-rich gouges ( $\mu=0.36-0.46$ ). The frictional strength of muscovite-rich gouges and phlogopite-rich gouges increased with increasing temperature while the frictional strength of granitoid gouges remained relatively constant. All samples showed transitions in velocity dependence with increasing temperatures, from velocity-strengthening to velocity-weakening and back to velocity-strengthening. The velocity-weakening behavior of granitoid gouges occurs in a lower temperature window ( $T=150-450^\circ\text{C}$ ) than muscovite-rich gouges ( $T=300-600^\circ\text{C}$ ) and phlogopite-rich gouges ( $T=350-600^\circ\text{C}$ ). We suggest that the observed differences in velocity-weakening regime are related to differences in the thermally activated, rate-dependent deformation mechanisms operating in the involved minerals at higher temperatures.

**Table 1.** List of Samples Used in This Study and Their Mineralogy According to Quantitative XRD.

Sample	Composition (wt%)
Granitoid ultramylonite	55% feldspar, 36% quartz, 6% biotite, 3% epidote
Muscovite-rich natural fault gouge	38% quartz, 38% muscovite, 16% poorly recrystallized mica, 5% feldspar, 4% chlorite
Phlogopite-rich natural fault gouge	36% quartz, 22% phlogopite, 19% muscovite, 17% poorly recrystallized mica, 4% feldspar, 2% swelling clays

## P 1.24

# Rotational rifting and the evolution of the East African Rift System: Insights from analogue models

Frank Zwaan<sup>1,2</sup>, Guido Schreurs<sup>1</sup>

<sup>1</sup> University of Bern, Institute of Geological Sciences, Baltzerstrasse 1+3, 3012 Bern, Switzerland  
(frank.zwaan@geo.unibe.ch)

<sup>2</sup> Helmholtz Centre Potsdam - GFZ German Research Centre for Geosciences, Telegrafenberg, Potsdam, 14473, Germany

The East African Rift System (EARS) represents a major tectonic feature splitting the African continent in two main plates with the Nubian Plate situated to the west, and the Somalian Plate to the east (Fig. 1a). From its northern end in the Afar triangle, the EARS stretches some 5000 km southward, comprising various rift segments and two microplates (the Victoria and Rovuma plates). The EARS is a key location for studying rift evolution as it contains rift basins in various stages of development. Researchers have proposed various scenarios for the evolution of the EARS, but the role of regional rotational rifting, caused by the rotation of the Somalian Plate, has received only limited attention. In this study we present analogue models that are specifically tailored to explore the dynamic evolution of the EARS within the broader rotational rifting framework. We apply a rotational rifting set-up and include different geometries of inherited weaknesses that mimic the complex structural grain of the EARS (Fig. 1b-d).

Our model results show that rotational rifting leads to rift propagation. Yet we need to distinguish between the propagation of distributed deformation, which can move very rapidly towards the rotation axis, and localized deformation, which can significantly lag behind. The various structural weakness arrangements in our models lead to a variety of different structures. Laterally overlapping weaknesses are required for localizing parallel rift basins to create rift pass structures, possibly leading to the segregation of micro-plates (Fig. 1c). These plates start rotating if the rift basins on both sides are sufficiently developed and become laterally dominant, as is the case for the Victoria Plate in the EARS, and likely also for the Rovuma Plate.

Additional model observations involve the development of early pairs of rift-bounding faults flanking the rift basins, followed by the localization of deformation along the axes of the most developed rift basins. Such a shift of deformation to the basin centre has been observed along the Main Ethiopian Rift, and is associated with incipient continental break-up. We also observe how the orientation of rift segments with respect to the regional (rotational) plate divergence affect deformation along these segments: oblique rift segments are less wide and show a strike-slip deformation component (Fig. 1c-d).

Overall, our model results provide a good fit with the large-scale features of the EARS, and provide constraints on the timing of general rift development, and the segregation and rotation of the Victoria plate within the broader rotational rifting framework of the EARS.

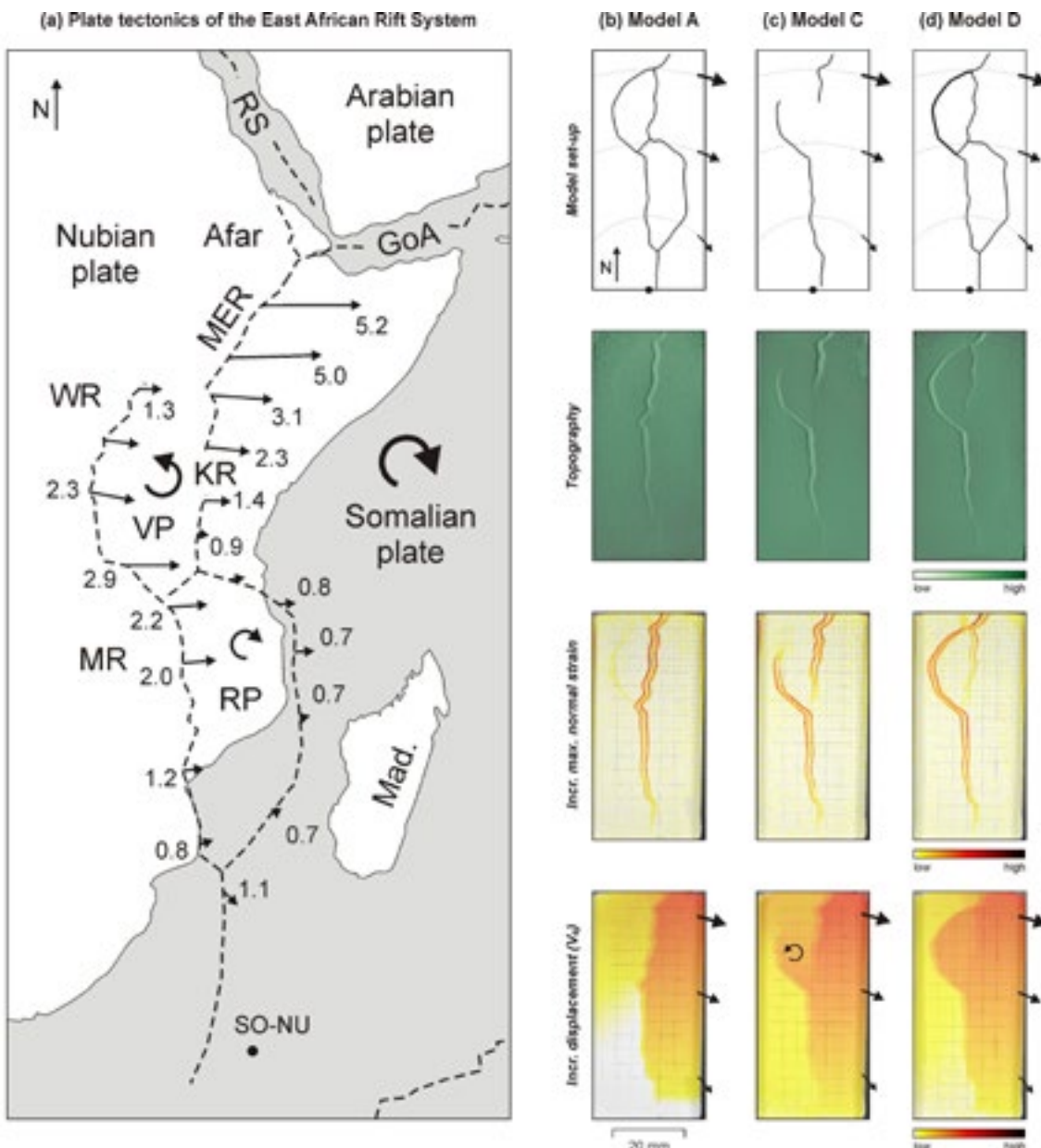


Figure 1. Comparison of the East African Rift System (EARS) with model results. (a) Tectonic setting of the EARS. GoA: Gulf of Aden, MER: Main Ethiopian Rift, MR: Malawi Rift, RP: Rovuma Plate, RS: Red Sea, SO-NU: Somalia-Nubia rotation pole, VP: Victoria Plate, WR: Western Rift. Plate boundaries and motions after Saria et al. (2014). (c-d) Final stage ( $t = 150$  min) model results. Top row: General model set-up showing seed (inherited weakness) geometries following different segments of the East African Rift System shown in (a), and model kinematics. Second row: Final model topography. Third row: Incremental maximum normal strain showing active extension. Bottom row: Incremental eastward displacement ( $V_e$ ). Increments used for DIC analysis: 10 min.

## REFERENCES

- Saria, E., Calais, E., Stamps, D.S., Delvaux, D., & Hartnady, C.J.H., 2014: Present-day kinematics of the East African Rift, Journal Geophysical Research: Solid Earth, 119, 3584-3600. <https://doi.org/10.1002/2013JB010901>

## 2 Mineralogy, Petrology and Geochemistry

Francesca Piccoli, Julien Allaz, Florence Bégué

*Swiss Society of Mineralogy and Petrology*

TALKS:

- 2.1 Alleon J., Pasquier V., Marin-Carbonne J.: Organic-pyritic-rich laminae in the 3.4-Ga Buck Reef Chert record hydrothermal processes
- 2.2 Forshaw J.B. Pattison D.R.M.: What is an average pelite?
- 2.3 Jordan M., Pilet S., Brenna M.: Melt Channelling and Lithospheric Metasomatism along Mid-ocean Ridges – A Case Study from Iceland
- 2.4 Jorgenson C., Caricchi L., Stuckleberger M., Fevola G., Weber G., Giordano G., Lubbers J.: A myriad of melt inclusions: a 3D view into the different types of melt inclusions and what they tell us about eruptions
- 2.5 Keller T.: Numerical modelling of thermo-chemical-mechanical magma chamber evolution
- 2.6 Kitoga L.S., Moyen J.F., Marin-Carbonne J., Boyet M.: The evolution of Si-K-CO<sub>2</sub> metasomatism in cherts and silicified lava of the Barberton Greenstone belt
- 2.7 Klein B.Z., Muntener O.: Mn/Mg Ratios of arc lavas show that early garnet fractionation occurs near the Moho of thick continental arcs
- 2.8 Lueder M., Hermann J.: Coupled hydrogen and trace element exchange in rutile: Implications for trace element valance states
- 2.9 Markmann T.A., Lanari P., Piccoli F., Tamblyn R., Lüder M.: Quantitative compositional mapping via LA-ICP-MS: an implementation for multi-phase application
- 2.10 Miranda M., Zajacz Z.: Development of new methods to track magma degassing and fluid fluxing in complex magmatic systems: The study of heavy halogens
- 2.11 Musu A., Corsaro R.A., Higgins O., Jorgenson C., Petrelli M., Caricchi L.: Volcanic crystals record the temporal evolution of magmatic processes: insights from the February-March 2021 lava fountain sequence of Mt. Etna (Italy)
- 2.12 Pastore C., Jorgenson C., Dominguez L., Biassse S., Higgins O., Musu A., Caricchi L., Bonadonna C.: Tracing the evolution of the architecture of the plumbing system during the 2021- Cumbre Vieja eruption (Spain)
- 2.13 Paul A.N., Chew D., Spikings R.A.: Discriminating metamorphic and thermally activated, volume diffusion processes – implications for apatite U-Pb thermochronology using ID-TIMS-TEA
- 2.14 Roodpeyma T., Driesner T.: Experimental Data of AlkaliChloride Thermodynamics in Reaction with Alkali-Feldspars under Supercritical Condition
- 2.15 Saintilan N.J., Vitale Brovarone A., Spangenberg J.E., Schönbächler M.: Preservation of osmium isotopic signatures recording sub-seafloor to trench hydrothermal alteration during forearc metamorphism of subducting oceanic lithosphere
- 2.16 Sönmez Ş.U., Moritz R., Lavoie J., Ulianov A., Popkhadze N., Natsvlishvili M., Spangenberg J.: Late Cretaceous Magmatic and Metallogenic Evolution of the Northern Lesser Caucasus, Tethyan Orogenic Belt: New Zircon U-Pb Age Constraints from the Beqtaqari Epithermal Deposits, Bolnisi District, Georgia

- 2.17 Spiekermann G., Näpflin A., Murakami M.: Positive thermal Raman shifts in silicates
- 2.18 Tamblyn R., Hermann J., Hasterok D., Sossi P., Pettke T., Chatterjee S.: Serpentinites as a source of water for continental crust formation in the Archean
- 2.19 Troch J., Huber C., Bachmann O., Fonseca Teixeira L.M., Ackerson M.: From Niggli's gas mineralisators to extraction from crystal mushes: Linking pegmatites with their host granites
- 2.20 Turlin F., Moritz R., Keskin S., Utku Ş. Sönmez Ulyanov A.: Variscan granitoids from Eastern Pontides, NE Turkey: A record of a 2.0 Ga-long of this Gondwana-derived terrane

## POSTERS:

- P 2.1 Allaz J., Guillong M., Tavazzani L., Zehnder L.: A new albite microanalytical reference material ( $\mu$ RM) from Piz Beverin (Graubünden, Switzerland) and evaluation of potential K-feldspar minerals  $\mu$ RM
- P 2.2 Antoine C., Spikings R.A., Paul A.N., Erde Bilir M., Bégué F., Schaltegger U.: Diffusion vs fluids: Ar distribution, chemical composition, oxygen isotopes and  $^{40}\text{Ar}/^{39}\text{Ar}$  geochronology of muscovite crystals from Ecuador and Colombia.
- P 2.3 Dominguez H., Lanari P., Riel N.: Numerical advection schemes for an accurate and efficient modelling of magma ascent
- P 2.4 Esteves M; Sena A.A; Alves A.: Geochemistry of melt inclusions from Paraná-Etendeka Magmatic Province, Brazil
- P 2.5 Fonseca Teixeira L.M., Laurent O., Troch J., Siddoway C.S., Bachmann O.: Tracking volcanic, plutonic, and pegmatitic environments in sediments: A case study from the Pikes Peak batholith, Colorado
- P 2.6 Gies N., Hermann J., Lanari P.: SpecXY – Presenting a tool for working with spatially resolved spectroscopic data
- P 2.7 Giordano G., Caricchi L.: Determining the state of activity of volcanoes
- P 2.8 Grocolas T., Reubi O., Toussaint A., Müntener O.: Apatite as a tool to quantify the evolution of crystal–melt–fluid systems
- P 2.9 Hänggi P., Franz L., Krzemnicki M.S.: Examination of the microstructure and composition of jadeite jade – a combination of X-ray microtomography and petrographic methods
- P 2.10 Jost C., Higgins O., Caricchi L., Ulyanov A.: Using magmatism to trace onset and migration of a subduction: Insights from Saint Martin (Lesser Antilles)
- P 2.11 Keller F., Popa R.-G., Allaz J., Geshi N., Bachmann O.: Variations in water saturation state during the build up to the Aso-4 super-eruption
- P 2.12 Moore J., Gillespie J., Evans K., Baumgartner L.P.: Melt mixing and transport across the Whale Head Rock contact aureole of the Albany-Fraser Orogen, Western Australia
- P 2.13 Noebel K.M., Ellis B.S., Bachmann O.: Zircon against all odds: High temperature rhyolites from the Snake River Plain, USA
- P 2.14 Pacchiega L., Cesare B., Bartoli O., Marschall H.: Petrological study of metapelitic granulites from Serre lower crust, Calabria, Italy
- P 2.15 Piccoli F., Rubatto D., Millonig L.J.: Chronology of dehydration/hydration reaction in the subducted oceanic lithosphere recorded by chlorite-schists
- P 2.16 Pilet S., Reymond J., Rochat L., Corsaro R.A., Chiaradia M., Caricchi L., Müntener O.: Mt Etna as Melts from the Low Velocity Zone
- P 2.17 Reynes J., Hermann J., Lanari P.: Attenuated Total Reflectance Fourier Transform Infrared Spectroscopy (ATR-FTIR) for a quick characterization of garnet
- P 2.18 Schmalholz S.M., Moulas E., Räss L., Müntener O.: Shear-driven formation of olivine veins by dehydration of ductile serpentinite: a numerical study with implications for transient weakening
- P 2.19 Sfalcin J., Braize D., Lupi M., Kouzmanov K., Dini A.: Deep Electrical Resistivity Tomography as an exploration tool to decipher the architecture of the Calamita distal Fe-skarn deposit, Elba Island (Italy)
- P 2.20 Stotsky V., Di Lorenzo F., do Sameiro Marques Fernandes M., Krack M., Scheinost A., Lanson M., Lanson B., Churakov S.V.: Molecular scale understanding of cation adsorption on swelling clay minerals
- P 2.21 Toussaint A., Grocolas T., Müntener O.: Crystal growth versus diffusional re-equilibration in k-feldspar

- P 2.22 Ulrich M., Rubatto D., Hermann J., Piccoli F.: Tracking fluid flow in subducted serpentinites of the Zermatt-Saas Unit
- P 2.23 Vesin C., Rubatto D., Pettke T., Deloule E., Bouvier A-S.: Insights into multistage oceanic serpentinization from in situ trace elements and oxygen isotope analysis
- P 2.24 Vieira Duarte J.F. , PettkeT., Hermann J., Marin-Carbonne J., Piccoli F., Bouvier A.-S.: Sulfide geochemistry and sulfur isotope study in subducted hydrous ultramafic rocks
- P 2.25 Zappatini A., Hofmann B., Eggenberger U., Gnos E., Al-Ghafri H., Almuati M.: 20\_0129: a new lunar meteorite from Oman

## 2.1

### Organic-pyritic-rich laminae in the 3.4-Ga Buck Reef Chert record hydrothermal processes

Julien Alleon<sup>1\*</sup>, Virgil Pasquier<sup>1</sup>, Johanna Marin-Carbonne<sup>1</sup>

<sup>1</sup> ISTE, University of Lausanne, CH-1015 Lausanne (\*julien.alleon@unil.ch)

Organic-rich laminae of the 3.4 Ga Buck Reef Chert have been interpreted as fossilized microbial mats. The presence of anoxygenic photosynthetizers was inferred from their carbon isotopic composition, their restriction to shallow water marine paleoenvironments, the presence of siderite and the absence of iron oxides. Here, combining mineralogical data, molecular compositions of the organic-rich laminae, and sulfur isotopic compositions of the associated pyrite crystals, we investigate the geological history of these laminae and their paleoenvironmental significance. Altogether, our data indicate that hydrothermal inputs were significant during the formation of the organic-pyritic-rich laminae and their host sediments.

## 2.2

### What is an average pelite?

Jacob B. Forshaw<sup>1,2</sup> and David R. M. Pattison<sup>2</sup>

<sup>1</sup> Institute of Geological Sciences, University of Bern, Baltzerstrasse 1+3, Bern 3012, Switzerland

(jacob.forshaw@geo.unibe.ch)

<sup>2</sup> Department of Geoscience, University of Calgary, 2500 University Drive, Calgary, T2N 1NV, Canada

Pelites (shales and mudstones) are arguably the most important rock type for interpreting metamorphism. Their significance derives from their widespread occurrence and the range of mineral assemblages they develop at different conditions of pressure and temperature. Here we have compiled a database of 5729 major element whole rock analyses of pelites from different metamorphic grades (shales to granulite facies paragneisses) to 1) determine an average composition, 2) examine the range and variability in their composition, and 3) assess if there is evidence for grade-related geochemical changes. Table 1 shows the median worldwide pelite composition and median compositions from eleven different regions/orogens. Median values are given instead of average values to eliminate the effect of extremes. The median  $X_{Mg} = MgO/(MgO+FeO^{total})$  in moles is 0.39 (Table 1). The median  $X_{Fe3+} = 2\times Fe_2O_3/(2\times Fe_2O_3+FeO)$  in moles was measured in 1964 samples and is 0.23. On an AFM diagram, the median worldwide pelite plots within a strong clustering of analyses between  $X_{Mg}^{proj} = \text{molar } MgO/(MgO+FeO^{total}) = 0.30 - 0.55$  (median = 0.42) and

$A^{Ms} = \text{molar } (Al_2O_3 - 3 \times K_2O)/(Al_2O_3 - 3 \times K_2O + FeO^{total} + MgO) = 0.0 - 0.4$  (median = 0.19). Pelites show a continuous decrease in volatile content with increasing metamorphic grade and a decrease in  $X_{Fe3+}$  from diagenetic to biotite zone. Lower median  $SiO_2$  values and higher median  $Al_2O_3$  and  $A^{Ms}$  values in the porphyroblast and subsolidus sillimanite-or-K-feldspar zones, as well as higher median  $MnO$  values in the garnet zone, may reflect sampling bias or metasomatism.

Table 1. Median pelite compositions

	n	SiO <sub>2</sub>	TiO <sub>2</sub>	Al <sub>2</sub> O <sub>3</sub>	FeO	MnO	MgO	CaO	Na <sub>2</sub> O	K <sub>2</sub> O	X <sub>Mg</sub>	X <sub>Fe3+</sub>	X <sub>Mg</sub> <sup>*</sup>	A <sup>Ms</sup>	X <sub>Mg</sub> <sup>proj</sup>
(wt%)															
Worldwide	5729 (1964)	64.13	0.91	19.63	6.85	0.08	2.41	0.65	1.38	3.95	0.39	0.23	0.46	0.19	0.42
Acadian	403 (56)	62.93	1.05	20.22	7.26	0.11	2.47	0.53	1.31	4.11	0.38	0.18	0.42	0.21	0.41
Alpine	134 (69)	61.41	1.00	21.41	7.72	0.11	2.32	0.79	1.28	3.97	0.35	0.32	0.43	0.24	0.38
Buller	137 (0)	65.29	0.76	18.44	6.15	0.05	3.37	0.37	1.16	4.41	0.50	N.A.	N.A.	0.09	0.52
Bushveld	132 (0)	63.56	0.79	19.14	7.71	0.06	3.22	0.62	1.05	3.85	0.43	N.A.	N.A.	0.18	0.45
Central Asian Belt	119 (69)	63.06	0.99	20.49	7.68	0.11	2.06	0.83	1.26	3.52	0.32	0.21	0.42	0.28	0.35
Cordilleran	329 (127)	63.73	0.95	20.20	6.99	0.08	2.41	0.68	1.09	3.85	0.38	0.19	0.45	0.26	0.41
Dalradian	862 (605)	60.47	1.08	21.28	7.84	0.10	2.78	0.72	1.73	4.00	0.39	0.22	0.45	0.21	0.42
Himalaya	192 (86)	66.56	0.71	18.41	6.15	0.07	2.03	0.53	1.20	4.34	0.37	0.25	0.45	0.10	0.40
Moine	102 (24)	61.24	1.01	19.20	7.32	0.12	2.40	2.30	2.52	3.89	0.37	0.17	0.42	-0.07	0.40
Sanbagawa	148 (6)	70.60	0.60	15.87	4.61	0.15	1.89	0.67	2.24	3.38	0.42	0.18	0.48	0.03	0.45
Trans-Hudson	128 (25)	64.42	0.76	18.87	7.29	0.07	2.54	0.73	1.52	3.80	0.38	0.17	0.48	0.16	0.41

Note: All iron as FeO total with volatiles (LOI, H<sub>2</sub>O, CO<sub>2</sub>, and SO<sub>3</sub>) removed and values renormalised to 100%

$X_{Mg}$ ,  $X_{Fe3+}$ ,  $X_{Mg}^{*}$ ,  $A^{Ms}$ , and  $X_{Mg}^{proj}$  defined in text. n = Number of analyses. () = Number of analyses with measured FeO and Fe<sub>2</sub>O<sub>3</sub>

This project has received funding from the European Research Council (ERC) under the European Union's Horizon 2020 research and innovation programme (grant agreement No 850530).

## 2.3

# Melt Channelling and Lithospheric Metasomatism along Mid-ocean Ridges - A Case Study from Iceland

Maud Jordan<sup>1</sup>, Sébastien Pilet<sup>1</sup>, Marco Brenna<sup>2</sup>

<sup>1</sup> Institute of Earth Sciences, University of Lausanne, 1015 Lausanne, Switzerland

<sup>2</sup> Department of Geology, University of Otago, 9016 Dunedin, New Zealand

Magmatism in Iceland is classically explained by the interaction of the mid-Atlantic ridge with the Iceland plume. Holocene volcanism (0–11.5 ka) is not restricted to the rift zone (RZ) but also occurs off-axis, specifically in the western Snæfellsnes Volcanic Belt (SVB) and in the Southern Flank Zone (SFZ).

While the volcanic activity of the SFZ seems correlated with the actual location of the Iceland plume, the plume relation to the SVB is uncertain. The distribution of volcanic activity between the RZ and the SVB is not continuous as there is a gap of 60–80 km where no Holocene volcanoes are observed. The lavas in the SVB are characterized by transitional to alkaline compositions, with elevated incompatible trace element content. In contrast, the RZ volcanic rocks have tholeiitic compositions with trace element signatures slightly more enriched than MORB. Rift and off-rift Iceland lavas are all characterized by positive Ba and Nb anomalies, particularly in alkaline rocks.

Geochemical modelling indicates that Iceland rift and off-rift magmas can be produced from a peridotitic mantle source if lithospheric processes are involved. We demonstrate that recycled crust in the form of pyroxenite is not required to generate SVB alkaline lavas. Alternatively, based on numerical simulations of melt extraction at mid-ocean ridges (Hebert & Montési, 2010; Keller et al., 2017; Sim et al., 2020; Turner et al., 2017), we suggest that the SVB alkaline lavas are the result of channelized low-degree melts produced on the periphery of the melting column at distances > 65 km from the ridge axis. These melts accumulate and percolate into the lithosphere producing amphibole ± phlogopite-bearing hydrous cumulates. Incongruent melting of these cumulates via renewed magmatic activity and melt-peridotite reaction can reproduce the alkaline compositions observed in the SVB, including the Ba and Nb anomalies. In contrast, the same melt extraction models suggest that low-degree melts produced at distances < 65 km from the central ridge axis rise vertically to the base of the lithosphere and are then focussed towards the ridge axis in decompression channels (Hebert & Montési, 2010; Keller et al., 2017; Sim et al., 2020; Turner et al., 2017). We propose that these melts interact with hydrous cumulates previously formed during the development of decompression channels at the lithosphere-asthenosphere boundary and acquire specific Ba and Nb anomalies. The mixing of these distal enriched melts with more depleted melts extracted from the central part of the melting regime explains the composition of the RZ lavas.

Our results highlight the importance of mantle dynamics below mid-ocean ridges and lithospheric interaction to produce off-axis magmatism with enriched alkaline signatures.

## REFERENCES

- Hebert, L. B., & Montési, L. G. J. (2010). Generation of permeability barriers during melt extraction at mid-ocean ridges. *Geochemistry, Geophysics, Geosystems*, 11(12), 1–17. <https://doi.org/10.1029/2010GC003270>
- Keller, T., Katz, R. F., & Hirschmann, M. M. (2017). Volatiles beneath mid-ocean ridges: Deep melting, channelised transport, focusing, and metasomatism. *Earth and Planetary Science Letters*, 464, 55–68. <https://doi.org/10.1016/j.epsl.2017.02.006>
- Sim, S. J., Spiegelman, M., Stegman, D. R., & Wilson, C. (2020). The influence of spreading rate and permeability on melt focusing beneath mid-ocean ridges. *Physics of the Earth and Planetary Interiors*, 304(July 2019). <https://doi.org/10.1016/j.pepi.2020.106486>
- Turner, A. J., Katz, R. F., Behn, M. D., & Keller, T. (2017). Magmatic Focusing to Mid-Ocean Ridges: The Role of Grain-Size Variability and Non-Newtonian Viscosity. *Geochemistry, Geophysics, Geosystems*, 18(12), 4342–4355. <https://doi.org/10.1002/2017GC007048>

## 2.4

# A myriad of melt inclusions: a 3D view into the different types of melt inclusions and what they tell us about eruptions

Corin Jorgenson<sup>1</sup>, Luca Caricchi<sup>1</sup>, Micheal Stuckleberger<sup>2</sup>, Giovanni Fevola<sup>2</sup>, Gergor Weber<sup>3</sup>, Guido Giordano<sup>4</sup>, Jordan Lubbers<sup>5</sup>

<sup>1</sup> Department of Earth Sciences, University of Geneva, Rue de Maraîchaine 13, CH-1205 Genève, (corin.jorgenson@etu.unige.ch)

<sup>2</sup> German Electron Synchrotron DESY, Notkestraße 85, DE-22607 Hamburg

<sup>3</sup> Department of Earth Sciences, University of Oxford, 3 S Parks Rd UK- OX1 3AN Oxford

<sup>4</sup> Department of Earth Sciences, University of Roma Tre, Via Ostiense, 133B, IT- 00154, Rome

<sup>5</sup> U.S. Geological Survey, 4230 University Dr Suite 100, US-99508, Anchorage

Melt Inclusions (MI) are small features found in igneous minerals. Melt inclusions trap melt in the plumbing system and thus provide a unique view of a magmatic system prior to eruption. Volatiles, such as CO<sub>2</sub> and H<sub>2</sub>O, which are usually degassed prior to eruption can be trapped in these inclusions. The characterisation of vapour bubbles in melt inclusions is an essential step for the determination of the volatile budget of MIs.

Here we present a 3D textural analysis of >2000 melt inclusions covering a variety of shapes, sizes, bubble distributions, and crystallinities. These inclusions are from 79 high-resolution tomographic scans of clinopyroxene and leucite phenocrysts from the Colli Albani Caldera Complex (Italy) acquired at the German Electron Synchrotron (DESY). Colli Albani is a mafic and alkaline volcano that produced seven large volume ignimbrites (up to 59 km<sup>3</sup>), which is atypical for systems erupting magma of this chemistry (Giordano et al., 2010).

We find a single crystal can host a wide range of melt inclusions including microcrystalline inclusions, glassy bubble bearing inclusions, glassy bubble free inclusions, and tube inclusions. Systematically, the smallest melt inclusions are more likely to be bubble free and glassy, whereas the larger melt inclusion often host one or more vapour bubble (up to 159 bubbles) and are sometimes microcrystalline or simply multi-phase. Vapour bubbles in glassy melt inclusions exist either as a single large vapour bubble or as several smaller vapour bubbles distributed along the margin of the melt inclusion. Notably, some of these vapour bubbles are quenched while attempting to coalescence. We suggest that such large bubble number is caused by rapid decompression. The extremely rapid ascent of magma at Colli Albani Volcano could explain the association between low viscosity magma and VEI 6 eruptions.

## REFERENCES

- Giordano, G., & The CARG team. 2010: The Colli Albani Volcano. In R. Funiciello & G. Giordano (Eds.), Special Publications of IAVCEI (Vol. 3). The Geological Society of London on behalf of The International Association of Volcanology and Chemistry of the Earth's Interior. <https://doi.org/10.1144/IAVCEI003>

## 2.5

# Numerical modelling of thermo-chemical-mechanical magma chamber evolution

Tobias Keller<sup>1,2</sup>

<sup>1</sup> Institute for Geochemistry & Petrology, Department of Earth Sciences, ETH Zürich, Clausiusstrasse 25, CH-8092 Zürich (tobias.keller@erdw.ethz.ch).

<sup>2</sup> School of Geographical & Earth Sciences, University of Glasgow, Lilybank Gardens, Glasgow G12 8QQ, Scotland.

Crustal magma chambers are thought of as the locus of magmatic differentiation as well as the source of volcanic eruptions. Magma chamber evolution conceptually comprises a range of processes including fractional crystallisation, wall rock assimilation, mafic recharge, and volatile degassing. Geochemical observations are routinely interpreted as resulting from a combination of these, yet such process-based interpretations remain to be tested by models that predict geochemical signatures based on realistic magma dynamics. The time evolution and eruptability of magma chambers has mostly been studied using 0-D box models [e.g., Degruyter & Huber, 2014] which do not resolve the spatial evolution and complex reaction-transport dynamics of silicate melt and crystals, and volatile fluid bubbles. Some models [Dufek & Bachmann, 2010; Gutierrez & Parada, 2010] have resolved the coupled fluid mechanics and thermo-chemistry of magma chamber dynamics, but their results have not been reproduced, nor their methods further developed or applied in more than a decade.

Here, I introduce a new 2-D numerical model of the three-phase fluid mechanics of crystals and bubbles suspended in melt coupled to simplified chemical thermodynamics including silicates and volatiles based on an idealised, calibrated phase diagram. The model tracks the geochemical evolution of trace elements, stable, and radiogenic isotope systems. The mathematical model is based on a recent theory framework [Keller & Suckale, 2019] and is numerically implemented in Matlab using the finite-difference staggered-grid method [e.g., Gerya, 2009]. The numerical algorithm is benchmarked by the Method of Manufactured Solutions and by confirming conservation of total mass and energy in the domain. The simulation code will be made openly available to the community. First results demonstrate the utility of the model for studying fractional crystallisation, wall rock assimilation, and mafic recharge in shallow magma chambers. Various expressions of stratified convection are observed under a range of conditions, with the presence of an exsolved volatile phase having a major effect on the dynamics. A key advance of the model is that it elucidates relationships between geochemical signatures and underlying magma dynamics, hence providing new avenues for the process-based interpretation of igneous rock chemistry.

## REFERENCES

- Degruyter & Huber, *Earth Planet Sc Lett*, 2014.
- Dufek & Bachmann, *Geology*, 2010.
- Gutiérrez & Parada, *J Petrol*, 2010.
- Keller & Suckale, *Geophys J Int*, 2019.
- Gerya, *Cambridge Univ Press*, 2009.

## 2.6

# The evolution of Si-K-CO<sub>2</sub> metasomatism in cherts and silicified lava of the Barberton Greenstone belt

L.S. Kitoga<sup>1,2</sup>, J-F Moyen<sup>1</sup>, J. Marin-Carbonne<sup>3</sup>, G. Stevens<sup>2</sup>, M. Boyet<sup>1</sup>

<sup>1</sup> Laboratoire Magmas et Volcans, Université Clermont Auvergne, CNRS, IRD, OPGC, F-63000 Clermont-Ferrand, France

<sup>2</sup> Department of Earth Sciences, University of Stellenbosch, Private Bag X1, Matieland 7602, South Africa

<sup>3</sup> Institut des Sciences de la Terre, Université de Lausanne, 1015 Lausanne, Switzerland

Chert layers cap silicified tops of lava flows in Early Archean greenstone belts, and particularly in the uniquely preserved Barberton Greenstone Belt (3.5-3.2 Ga) of South Africa. The Si-, K- and CO<sub>2</sub>- metasomatisms observed in these silica-rich zones have been ascribed to low-temperature (<150°C) seawater-seafloor couplings during the Archean (Hofmann & Harris, 2008). Yet, the silicified zones were subsequently metamorphized and sometimes deformed, such that the signature of seafloor metasomatism may be confused with the potential effects of later-stage metamorphism and deformation. We have investigated the petrography and geochemistry of different sections extending from chert layers through silicified lava tops, in order to understand the evolution metasomatism.

At the Middle Marker and H4 localities, silicification is associated with alkali (K, Rb and Ba) enrichment, and this is consistent with occurrence a muscovite-rich bands towards the top of the section. In contrast, the alkali concentrations decrease towards the top in pillows of H3 and in the massive lava of Msauli locality. Carbonates occur in capping chert layers, but also associated with sulphides and chlorines, and rarely overgrowing older muscovite, in silicified pillows far below the capping cherts. While chlorite thermometry confirms that a greenschist facies metamorphism (<360°C) affected all the investigated localities, only the Middle Marker locality with the highest abundance in muscovite depicts shear deformation.

We argue that, originally, extensive silica deposition near the seafloor during metasomatism was due to near saturation of silica in the early Archean Ocean that lacked silica-fixing micro-organisms. Early stage silicification occurred coevally with alkali uptake to form K-rich clay, which suggests involvement of slightly acid and low-temperature fluids. The fluids must have progressively evolved to alkaline and saline by interacting with the basaltic volcanics, to such an extent that later stage silicification was associated with carbonate, halite or sylvite and sulphide growth at the expense of K-rich clay. After deposition of a ca. 10 Km succession in the Barberton, soft layers resulting from K-metasomatism accommodated shear deformation during the main regional tectono-thermal event of 3.2 Ga. These results are inconsistent with an imbricated and repetitive stratigraphy previously proposed in the Barberton Greenstone belt by M. de Wit and co-workers who interpreted the carbonate-fuchsite-bearing shear zones as overthrusting faults (e.g. de Wit, 1982; Grosch, 2019) or Raman thermometry, both proposing a narrow range in metamorphic conditions of around 320°C regional for the BGB. This study demonstrates that a range of petrological and thermodynamic modelling techniques are required in an integrated approach to unravel the very low- to medium-grade metamorphic conditions preserved in the oldest part of the BGB. The study investigates low-temperature metamorphic processes in the Komati, Hooggenoeg, Kromberg and Mendon formations of the c. 3530-3298 Ma Onverwacht Group. Chlorite thermodynamic modelling indicates metamorphic conditions of between 250 and 445°C, in the c. 3482 Ma Komati Formation, but uncertainties on these conditions are large (c. 80 and 100°C).

## REFERENCES

- de Wit, M. J. E. (1982). Gliding and overthrust nappe tectonics in the Barberton Greenstone Belt. *Journal of Structural Geology*, 4(2), 117–136.
- Grosch, E. G. (2019). Metamorphic processes preserved in early archean supracrustal rocks of the barberton greenstone belt, South Africa. *Geological Society Special Publication*, 478(1), 315–334.
- Hofmann, A., & Harris, C. (2008). Silica alteration zones in the Barberton greenstone belt : A window into subseafloor processes 3.5-3.3 Ga ago. *Chemical Geology*, 257, 224–242.

## 2.7

### Mn/Mg Ratios of arc lavas show that early garnet fractionation occurs near the Moho of thick continental arcs

Benjamin Z. Klein<sup>1</sup>, Othmar Müntener<sup>1</sup>

<sup>1</sup> Institute of Earth Sciences, University of Lausanne, CH-1015 Lausanne ([benjaminzachary.klein@unil.ch](mailto:benjaminzachary.klein@unil.ch))

The fractionation of garnet from arc magmas is hypothesized to play an important role in a wide range of geologic processes including the formation of continental crust, the oxidation of arc magmas and the development of porphyry copper deposits. However, garnet is only stable in mafic to intermediate hydrous arc magmas at pressures of at least 0.8-1 GPa and is extremely rare in erupted arc magmas. It is therefore difficult to directly document and study garnet fractionation in the field. Instead, garnet fractionation is frequently inferred based on trace element proxies such as La/Yb, Dy/Yb and Sr/Y. As garnet stability is strongly pressure sensitive, these ratios are also commonly used as proxies for fractionation pressure and crustal thickness. However, this approach is problematic as these ratios span a wide range of values in primary mantle melts independent of crustal thickness, and can also be modified within the crust by amphibole fractionation and plagioclase accumulation.

We show here that Mn/Mg ratios provide an attractive alternative method for inferring garnet fractionation in erupted lavas. Using a large compilation of experimental data and new high-precision analyses of Mn partitioning in existing garnet-bearing experiments, we show that all common cumulate silicate phases except garnet have Mn/Mg KD values below 0.5, while the garnet KD is greater than 1, and thus garnet fractionation produces derivative magmas with distinctly lower Mn/Mg ratios. Additionally, primary mantle melts have highly restricted Mn/Mg ratios that are consistent with melt in equilibrium with mantle olivine. Therefore, this ratio does not appear to keep a record of subducted slab contributions, unlike most trace element proxies. Using the compiled experimental data, we parameterized an empirical model of Mn partitioning in garnet as a function of pressure and temperature. This model allows for the rigorous investigation of the role of garnet fractionation at both modern and ancient subduction zones. We find clear evidence for garnet fractionation in most arcs with seismically estimated crustal thicknesses greater than ~45 km. This garnet fractionation signature is observable at relatively unevolved melt compositions ( $\leq$ 54 wt. % SiO<sub>2</sub>). At these melt compositions garnet is likely only stable at pressures of at least 1.5 GPa, suggesting that garnet fractionation initiates at or below the Moho.

## 2.8

# Coupled hydrogen and trace element exchange in rutile: Implications for trace element valence states

Mona Lueder<sup>1</sup>, Jörg Hermann<sup>1</sup>

<sup>1</sup> Institut für Geologie, Universität Bern, Baltzerstrasse 3, CH-3012 Bern (mona.lueder@geo.unib.ch)

Rutile is a common accessory high-pressure metamorphic mineral occurring in amphibolite-, blueschist-, eclogite- and granulite facies rocks with various bulk rock compositions. It has an affinity to incorporate a variety of trace elements. So far, most attention has been on Zr, Nb and Ta in rutile, that are used for thermometry and as indicator for magmatic reservoirs and subduction zone processes (e.g. Foley et al., 2000; Zack et al., 2004). Additionally, even though rutile is a nominally anhydrous mineral (NAM), it can incorporate significant amounts of H<sup>+</sup>, which is coupled with di- and trivalent cations through linked substitutions for Ti<sup>4+</sup> (e.g. Johnson et al., 1968). However, H<sup>+</sup> in natural rutile has been rarely studied. Here, we present new results from Fourier Transform (FT) IR spectropscopy and Laser Ablation Inductively Coupled Mass Spectrometry (LA-ICP-MS) on H<sup>+</sup> and trace element contents in rutile, with implications for valence states and coupled exchange of trace elements.

Through application of a new in-situ FTIR method, we were able to identify six trace elements in natural rutile that can be coupled with H<sup>+</sup>. All investigated samples contain H<sup>+</sup> related to Ti<sup>3+</sup> and Fe<sup>3+</sup>. Coupling with Al<sup>3+</sup>, Mg<sup>2+</sup>, Fe<sup>2+</sup> and Cr<sup>2+</sup> is less common. FTIR and LA-ICP-MS data show that the molar abundance of di- and trivalent cations and H<sup>+</sup> exceed the contents of commonly investigated trace elements (e.g. Zr, Nb, Ta, U) in rutile by up to two orders of magnitude. Thus, understanding the incorporation of H<sup>+</sup>, di- and trivalent cations is vital to understand rutile trace element geochemistry. Di- and trivalent cations are incorporated for Ti<sup>4+</sup> through coupled substitutions with either H<sup>+</sup> or pentavalent cations or through the formation of oxygen vacancies (e.g. Meinholt, 2010). Comparison of trace element contents and trace element related H<sup>+</sup> contents show that H<sup>+</sup> incorporation does not suffice for charge balance of di- and trivalent cations, thus coupling with pentavalent cations and oxygen vacancies has to occur. Cr<sup>2+</sup> is preferentially coupled with H<sup>+</sup> while Al<sup>3+</sup> is mostly coupled to pentavalent cations, and Fe<sup>2+</sup> and Fe<sup>3+</sup> have varying preferred coupling in different investigated samples.

OH-band positions in rutile are specific to trace elements in fixed valence states. Thus, valence states of multivalent cations (Ti, Fe, Cr, V) can be inferred from H<sup>+</sup> contents. The Ti<sup>3+</sup>-related H<sup>+</sup> content allows calculation of a minimum proportion of Ti<sup>3+ / ΣTi</sup> of ~0.1 %. Fe and Cr are usually incorporated as trivalent cations, however Cr<sup>2+</sup>- and Fe<sup>2+</sup>-related OH-bands allow the identification of divalent species present, that can be interpreted as evidence for low oxygen fugacity conditions. Evidence for V<sup>3+</sup> was not found, even in low oxygen fugacity samples that contain Fe<sup>2+</sup> and/or Cr<sup>2+</sup>. Thus, V is most likely incorporated as V<sup>4+</sup>, as this has the closest ionic radius to the substituted Ti (Shannon, 1976). However, the presence of pentavalent V cannot be excluded completely in highly oxidised samples. Thus, Ti, Fe, Cr, V and related H<sup>+</sup> are a potentially powerful tool to constrain redox conditions of subduction zone fluids.

## REFERENCES

- Foley, S. F., Barth, M. G., and Jenner, G. A. 2000: Rutile/melt partition coefficients for trace elements and an assessment of the influence of rutile on the trace element characteristics of subduction zone magmas. *Geochim. Cosmochim. Acta*, 64, 933–938.
- Johnson, O. W., Ohlsen, W. D., and Kingsbury, P. I. 1968: Defects in rutile. III. Optical and electrical properties of impurities and charge carriers. *Phys. Rev.*, 175, 1102–1109.
- Meinholt, G. 2010: Rutile and its applications in earth sciences, *Earth-Science Reviews*. 102(1–2), 1–28.
- Shannon, R.D. 1976: Revised effective ionic radii and systematic studies of interatomic distances in halides and chalcogenides. *Acta Crystallogr A*, 32, 751–767.
- Zack, T., Moraes, R., and Kronz, A. 2004: Temperature dependence of Zr in rutile: Empirical calibration of a rutile thermometer. *Contrib. Mineral. Petrol.*, 148, 471–488.

## 2.9

# Quantitative compositional mapping via LA-ICP-MS: an implementation for multi-phase application

Thorsten A. Markmann<sup>1</sup>, Pierre Lanari<sup>1</sup>, Francesca Piccoli<sup>1</sup>, Renée Tamblyn<sup>1</sup>, Mona Lüder<sup>1</sup>

<sup>1</sup>Institute of Geological Sciences, University of Bern, Baltzerstrasse 1+3, CH-3012 Bern ([thorsten.markmann@geo.unibe.ch](mailto:thorsten.markmann@geo.unibe.ch))

Laser ablation inductively coupled plasma mass spectrometry (LA-ICP-MS) is largely used in geosciences for *in-situ* determination of the chemical composition of minerals with a high spatial resolution (< 10 µm). Geological materials can host textures in elemental and isotopic compositions that are otherwise not perceptible to the naked eye. Mapping and imaging of such patterns is a major step helping geoscientist to understand the formation of these geological products. Acquiring two-dimensional, quantitative and meaningful data from LA-ICP-MS mapping experiments is not trivial. It requires an analytical procedure and an adapted data reduction scheme including pixel allocation and multi-phase calibration.

In this work, we present a module integrated in XMapTools that covers data reduction and image generation of multi-element mapping experiments applied to LA-quadrupole-ICP-MS experiments. Instrumental conditions have a direct effect on the image quality and so have the pixel allocation strategies. Rendering to quadratic pixels by interpolation outperforms averaging where one pixel comprises several sweep times. To benchmark the LA-ICP-MS imaging tool a digital sampling model was applied to an annulus of fixed concentration. Depending on the texture size and orientation analysed, the spot size together with the scanning direction can lead to a shift in composition. Still, careful data reduction offers new insights into geological processes from single or multi-phase imaging of trace elements and isotope ratios. Chemical mapping of rutile grains, as an example, revealed inhomogeneity in the Zr distribution and is thereby relevant for the results in thermometry.

*This project has received funding from the European Research Council (ERC) under the European Union's Horizon 2020 research and innovation program (grant agreement No 850530).*

## 2.10

# Development of new methods to track magma degassing and fluid fluxing in complex magmatic systems: The study of heavy halogens

Miranda Mara<sup>1</sup>, and Zajacz Zoltan<sup>1</sup>

<sup>1</sup> Department of Earth Sciences, University of Geneva, Rue des Maraîchers 13, 1205 Genève ([mara.miranda@unige.ch](mailto:mara.miranda@unige.ch))

Magma degassing and fluid fluxing within trans-crustal magma reservoirs play an important role in the transport of volatiles and ore metals. Tracking the migration of magmatic fluids within such systems is challenging, yet important for the understanding of magmatic-hydrothermal ore genesis and volcanic degassing. Previously, the systematics in the concentration of H<sub>2</sub>O and CO<sub>2</sub> in silicate melt inclusions trapped in igneous phenocrysts have been used for this purpose. However, CO<sub>2</sub> is lost in the very early stages of magma degassing and H<sub>2</sub>O is known to diffuse rapidly from the melt inclusion at magmatic temperatures, limiting the range of applicability of this technique.

Here, we aim to develop new geochemical tools to track magma degassing and fluid fluxing, which can be applied over a broad melt/magma composition range. We hypothesize that halogen ratios may be particularly useful for this purpose, because previous studies have found that the fluid/melt partition coefficients (D<sup>f/m</sup>) of halogens increase with increasing halogenide ion radius. However, the data available on bromine and iodine partitioning are rather limited, and therefore, we are studying the D<sup>f/m</sup> of these heavy halogens simultaneously with that of Cl as a function of composition, pressure, and fluid salinity. The new partition coefficient data will allow using halogen concentrations measured in silicate melt inclusions in natural systems to track magma degassing and fluid fluxing.

So far, the experiments were conducted at 785°C and 150 to 300 MPa. We used a peralkaline, metaluminous, and peraluminous haplogranitic starting glass and starting fluids with 7 different salinities. The experiments were performed in externally heated René 41 and Molybdenum-Hafnium Carbide (MHC) pressure vessels.

Halogen concentrations in the run product glasses were determined by Laser Ablation Inductively Coupled Plasma Mass Spectrometry (LA-ICP-MS) at the University of Geneva. The concentration of halogens in the run fluid was then estimated by mass balance calculation allowing us to determine the D<sup>f/m</sup> of Cl, Br and I depending on a function of fluid salinity and confining pressure. On average, the D<sup>f/m</sup> of Br and I are 2 and 5 times higher than that of Cl, respectively. The D<sup>f/m</sup> of all three studied halogens increases by a factor of 4 to 8 with fluid salinity increasing from 0.5 to 32 molal, but the variation in partition coefficient ratios (i.e. exchange coefficients) is limited. The aluminum saturation index of the silicate melt also affects the D<sup>f/m</sup> of halogens, they partition less strongly into the fluid from peralkaline and peraluminous melts than from those with metaluminous composition. Moreover, D<sup>f/m</sup> of halogens shows a clear relation between fluid salinity and increasing pressure. With increasing pressure for low-fluid salinities, all three halogens partition stronger towards the fluid phase but the opposite trend was observed at high-fluid salinities. This difference can be rationalized by taking into account the much lower compressibility of high-salinity fluids. Overall, our results up to date indicate that I/Cl and Br/Cl ratios in the silicate melt will decrease during progressive magma degassing, with the I/Cl ratio being more sensitive and thus more applicable during the early stages of magma degassing, and Br/Cl being well-suited to address crystallization-driven degassing in more crystalline/felsic systems. The I/Cl ratios may serve as a sensitive indicator of fluid fluxing.

## 2.11

# Volcanic crystals record the temporal evolution of magmatic processes: insights from the February-March 2021 lava fountain sequence of Mt. Etna (Italy)

Alessandro Musu<sup>1</sup>, Rosa Anna Corsaro<sup>2</sup>, Oliver Higgins<sup>1</sup>, Corin Jorgenson<sup>1</sup>, Maurizio Petrelli<sup>3</sup>, Luca Caricchi<sup>1</sup>

<sup>1</sup> Department of Earth Sciences, University of Geneva, Rue des Maraîchers 13, CH-1205 Geneva, Switzerland.  
(alessandro.musu@unige.ch)

<sup>2</sup> Istituto Nazionale di Geofisica e Vulcanologia, Osservatorio Etna-Sezione di Catania, Catania, Italy

<sup>3</sup> Department of Physics and Geology, University of Perugia, Piazza dell'Università, 1, 06123 Perugia, Italy.

The South-East Crater (SEC) at Mt. Etna started a long period of lava fountaining activity in December 2020 producing over 66 paroxysms until February 2022. A rather intense phase occurred between February 16th and April 1st, 2021, amounting to a total of 17 paroxysmal events interspersed by a repose time varying between 1 and 7 days. The volcano was extensively monitored during the entire eruptive series, allowing us to relate the chemistry and texture of the erupted products to volcanological parameters and thus to eruptive dynamics. We investigate the temporal evolution of the magmatic system of this phase by quantifying variations in composition and texture of clinopyroxene throughout the sequence. Clinopyroxene major element transects from five representative lava fountains allow us to determine the relative proportions of deep versus shallow-stored magmas that fed these events. The geochemical dataset of clinopyroxene has been studied using the hierarchical clustering (HC) algorithm, an unsupervised machine learning technique, which allowed us to identify clusters of similar chemical-textural zones in minerals and thus to trace the temporal evolution of pre-eruptive conditions during this intense eruptive phase. We apply random forest thermo-barometry to relate each cluster to P-T conditions of formation. Our results provide quantitative relationships between mineral chemistry, texture, monitoring parameters, and eruptive dynamics. This approach contributes to a better characterisation of the past activity of volcanic systems, which is crucial for anticipating their future behaviour.

## 2.12

### Tracing the evolution of the architecture of the plumbing system during the 2021- Cumbre Vieja eruption (Spain)

Camille Pastore<sup>1</sup>, Corin Jorgenson<sup>1</sup>, Lucia Dominguez<sup>1</sup>, Sébastien Biasse<sup>1</sup>, Oliver Higgins<sup>1</sup>, Alessandro Musu<sup>1</sup>, Luca Caricchi<sup>1</sup>, Costanza Bonadonna<sup>1</sup>.

<sup>1</sup> Department of Earth Sciences, University of Geneva, Genève, Switzerland

After a period of quiescence of 50 years, the Cumbre Vieja volcano (La Palma, Spain) started a new eruptive event on the 19<sup>th</sup> of September 2021. This event lasted 85 days (ending on the 13<sup>th</sup> of December 2021) and was characterized by volcanic activity such as lava effusion, strombolian explosions, lava fountaining, ash venting, tephra columns, and gas emissions. This eruption represents the most destructive volcanic event that occurred in the last century in Europe and is the longest event recorded in the history times of the Island. Moreover, the Cumbre Vieja rift is the most active region of the Canary Archipelago, and this region is considered to be the most probable site for future eruptive events in the Canaries. Therefore, studying the 2021 eruption of Cumbre Vieja is of great interest to understand the evolution and the dynamics of this volcano thus contribute to the long-term risk assessment in case of any future eruptive event as it would help to understand the evolution and the mechanics of this volcano.

This study combines the physical and the petrological analysis of tephra deposits to reconstruct the syneruptive evolution of the architecture of the plumbing system during the 2021- Cumbre Vieja eruption. The physical analysis is assessed by studying the stratigraphy and the grainsize of the different eruptive units. The petrological analysis consists in analyzing the minerals and glasses of the pyroclasts. The minerals and glasses will be analyzed for major elements using an Electron Probe Microanalyzer. A machine learning thermobarometry approach will be applied to estimate the pressure and temperature conditions of crystallization of these minerals. From the stratigraphy analysis, three different units were identified; the lower unit, the middle unit and the upper unit. These units are subsequently separated into sub-units delimiting different activity phases. The petrological analysis of the clinopyroxenes show two main compositional groups. These compositional groups are represented by two chemical zonations in the clinopyroxenes. Moreover, these groups have different temperature, pressure, and chemical conditions. The first compositional group is found in the core of the minerals and has a colder (~950°C), deeper (2-3.5 kBar) and more evolved composition (1-2 wt% MgO) than the second compositional group. This second group is found in the rim of the clinopyroxene minerals and is hotter (1050-1100 °C) and less evolved (3.5-4.5 wt% MgO) than the first group.

## 2.13

# Discriminating metamorphic and thermally activated, volume diffusion processes – implications for apatite U-Pb thermochronology using ID-TIMS-TEA

André Navin Paul<sup>1</sup>, David Chew<sup>2</sup>, Richard Alan Spikings<sup>1</sup>

<sup>1</sup> Department of Earth Sciences, Université de Genève, Rue des Maraîchers 13, CH-1205 Geneva, Switzerland  
(Andre.Paul@unige.ch),

<sup>2</sup> Department of Geology, Trinity College Dublin, Dublin 2, Ireland

The application of apatite (and other minerals) U-Pb thermochronology hinges on the assumption that Pb-in-apatite diffusion is controlled by thermally-activated volume diffusion. If the grains have resided within the Pb-partial-retention-zone (PbPRZ) for some time and all diffusion parameters are equivalent for all grains, thermally-activated volume diffusion predicts a positive correlation between diffusion radius and U-Pb date. Previous studies have proven the viability of this assumption and successfully extracted time-Temperature histories using either bulk grain vs diffusion length scale correlation, or *in-situ* analysis of core-to-rim profiles (Cochrane et al., 2014; Paul et al., 2019), that are in good agreement with expected thermal histories. However, the scatter in the extracted U-Pb data and thermal histories can exceed predictions from volume diffusion, warranting concerns on the accuracy of the t-T paths modelled. While effects such as parent isotope zonation and grain boundary conditions (Paul et al., 2019; Popov and Spikings, 2021) have been identified, there are cases where extreme gradients in parent isotope zonation and partition coefficients at grain boundaries are required to justify measured data. Hence, we will focus our attention on subtle to significant metamorphic alteration in this contribution.

Processes such as secondary/metamorphic growth or fluid assisted dissolution/reprecipitation may be difficult to assess qualitatively and quantitatively prior to bulk grain ID-TIMS U-Pb analyses. Recent advances in the geochemical discrimination of primary vs secondary/ altered apatite (O'Sullivan et al., 2020) suggest that the use of Sr/Y vs LREE can be beneficial to the interpretation of complicated relationships in U-Pb vs diffusion length scale space. In apatites which may relate to low-grade metamorphic conditions, higher Sr/Y and lower LREE contents are expected. Data presented include ID-TIMS U-Pb single grains, for which the trace elements were determined by ID-TIMS-TEA. We will utilize examples from the active margin of Ecuador, where geochemically primary apatite is preserved in some cases, and variable development of metamorphic overgrowths, recrystallisation and fluid interaction is present (Paul et al., 2019, 2018). Additionally, we will showcase an example from the Freetown Layered Complex, Sierra Leone (Callegaro et al., 2017), where primary apatite seemingly relates to predictions from thermally activated volume diffusion and exhibits seemingly pristine geochemical composition. We then demonstrate a combined U-Pb vs Sr/Y diagram, to suggest a tool for the identification of samples suitable for use in apatite U-Pb thermochronology studies.

## REFERENCES

- Callegaro, S., Marzoli, A., Bertrand, H., Blichert-Toft, J., Reisberg, L., Cavazzini, G., Jourdan, F., Davies, J.H.F.L., Parisio, L., Bouchet, R., Paul, A., Schaltegger, U., Chiaradia, M., 2017. Geochemical Constraints Provided by the Freetown Layered Complex (Sierra Leone) on the Origin of High-Ti Tholeiitic CAMP Magmas. *J. Petrol.* 58, 1811–1840. <https://doi.org/10.1093/petrology/egx073>
- Cochrane, R., Spikings, R.A., Chew, D., Wotzlaw, J.F., Chiaradia, M., Tyrrell, S., Schaltegger, U., Van der Lelij, R., 2014. High temperature (>350°C) thermochronology and mechanisms of Pb loss in apatite. *Geochim. Cosmochim. Acta* 127, 39–56. <https://doi.org/10.1016/j.gca.2013.11.028>
- O'Sullivan, G., Chew, D., Kenny, G., Henrichs, I., Mulligan, D., 2020. The trace element composition of apatite and its application to detrital provenance studies. *Earth-Science Rev.* 201, 103044. <https://doi.org/10.1016/J.EARSCIREV.2019.103044>
- Paul, A.N., Spikings, R.A., Chew, D., Daly, J.S., 2019. The effect of intra-crystal uranium zonation on apatite U-Pb thermochronology: A combined ID-TIMS and LA-MC-ICP-MS study. *Geochim. Cosmochim. Acta* 251, 15–35. <https://doi.org/10.1016/j.gca.2019.02.013>
- Paul, A.N., Spikings, R.A., Ulianov, A., Ovtcharova, M., 2018. High temperature (<350°C) thermal histories of the long lived (>500Ma) active margin of Ecuador and Colombia: apatite, titanite and rutile U-Pb thermochronology. *Geochim. Cosmochim. Acta*. <https://doi.org/10.1016/J.GCA.2018.02.033>
- Popov, D. V., Spikings, R.A., 2021. Numerical modelling of radiogenic ingrowth and diffusion of pb in apatite inclusions with variable shape and U-Th zonation. *Minerals* 11, 364. <https://doi.org/10.3390/MIN11040364/S1>

## 2.14

# Experimental Data of AlkaliChloride Thermodynamics in Reaction with Alkali-Feldspars under Supercritical Condition

Taraneh Roodpeyma<sup>1</sup>, Thomas Driesner<sup>1</sup>

<sup>1</sup> *Geochemistry and Petrology Institut, Department of Earth Sciences, Swiss Federal Institute of Technology Zürich, Sonneggstrasse 5, 8092 Zürich (taraneh.roodpeyma@erdw.ethz.ch)*

Understanding thermodynamics of electrolytes under hydrothermally related supercritical condition requires more relevant experimental data points. Such dataset needs to be obtained in very low concentrated regions of solution so that the value of activity coefficient, which is not known for higher concentrations, is regarded as unity. In order to study the correct equilibrium constant which is not available in previous experimental studies, we have conducted fluid-rock equilibrium experiments under conditions close to critical point of pure water. These values will be presented and compared with the existing knowledge that is being applied in chemical modelings (Lagache & Weisbrod 1977). In addition, using the new database, we can track the behavior of the activity coefficient ratio of the electrolytes from very low (0.1 mmolal) to very high concentrations (13 molal) of solution.

## REFERENCES

- Lagache, M., & Weisbrod, A. 1977: The System: Two Alkali Feldspars-KCl-NaCl-H<sub>2</sub>O at Moderate to High Temperatures and Low Pressures, *Contrib. Mineral. Petrol.* 62, 77-101.

## 2.15

# Preservation of osmium isotopic signatures recording sub-seafloor to trench hydrothermal alteration during forearc metamorphism of subducting oceanic lithosphere

Nicolas J. Saintilan<sup>1</sup>, Alberto Vitale Brovarone<sup>2,3,4</sup>, Jorge E. Spangenberg<sup>5</sup>, Maria Schönbächler<sup>1</sup>

<sup>1</sup> Institute of Geochemistry and Petrology, Department of Earth Sciences, Clausiusstrasse 25, 8092, Zürich, Switzerland

<sup>2</sup> Dipartimento di Scienze Biologiche, Geologiche e Ambientali, Alma Mater Studiorum Università di Porto San Donato, 40126 Bologna, Italy

<sup>3</sup> Sorbonne Université, Muséum National d'Histoire Naturelle, UMR CNRS 7590, IRD, Institut de Minéralogie, de Physique des Matériaux et de Cosmochimie, IMPMC, 75005 Paris, France

<sup>4</sup> Institute of Geosciences and Earth Resources, National Research Council of Italy, via G. Moruzzi 1, 56124 Pisa, Italy

<sup>5</sup> Institute of Earth Surface Dynamics, University of Lausanne, Building Geopolis, 1015 Lausanne, Switzerland

Hydrated and oxidized altered oceanic crust (AOC) undergoes sulfur-iron redox reactions during subduction of the oceanic lithosphere [Gerrits et al., 2019]. These reactions produce oxidized fluids that may, in turn, oxidize the arc-mantle system [Walters et al., 2020]. Here, we address whether the redox sensitive and chalcophile metal osmium (Os) is mobile in the presence of oxidized, sulfate-bearing fluids in AOC on the metamorphic forearc path of subducting oceanic lithosphere. To this end, we applied mineral-specific rhenium-osmium (Re-Os) geochronology, coupled with bulk sulfur ( $d^{34}\text{S}$  V-CDT) analyses of individual sulfide species and supported by petrographic observations to lawsonite-bearing, blueschist- and eclogite-facies lithologies ( $T = 520 \pm 20^\circ\text{C}$  and  $P = 2.3 \pm 0.1 \text{ GPa} \sim \text{ca. } 70 \text{ km depth}$ ) in the subducted AOC of Alpine Corsica [Vitale Brovarone et al., 2011]. Lawsonite-eclogites (Law-Ecl) and lawsonite-blueschists (Law-Bs) in Alpine Corsica were interpreted as metamorphic products that experienced the same P-T conditions as portions of hydrothermally altered oceanic crust with slightly different chemistry (e.g., CaO concentrations) and water contents [Vitale Brovarone et al., 2011].

The Re-Os systematics of pyrite (4.9–18.0 ng g<sup>-1</sup> Re, 29.5–52.0 pg g<sup>-1</sup> Os) in Law-Ecl of pillow basalt protolith are preserved and define a robust isochron with a date of  $185.9 \pm 4.4$  million years ago (Ma) and an initial  $^{187}\text{Os}/^{188}\text{Os}$  ratio (Os<sub>i</sub>) of  $0.19 \pm 0.47$ . Pyrite ( $d^{34}\text{S}_{\text{pyrite-Law-Ecl}} = +7.7$  to  $+8.3\text{\textperthousand}$ ), which results from the hydrothermal alteration of oceanic crust driven by seawater ( $d^{34}\text{S}_{\text{seawater Lower Jurassic}} = \sim +18.0\text{\textperthousand}$ ; Kampfschulte & Strauss, 2004) in sub-seafloor setting, may be related to early Jurassic ocean–continent transition of the slow-spreading Alpine Tethys ( $186 \pm 2$  Ma) [Tribuzio et al., 2016]. The Os<sub>i-pyrite-Law-Ecl</sub> ( $0.19 \pm 0.47$ ) is compatible with the  $^{187}\text{Os}/^{188}\text{Os}$  seawater value ( $\sim 0.25$ ) for the Lower Jurassic (Pliensbachian; Toma et al., 2020). It contains contributions of radiogenic  $^{187}\text{Os}^*$  from erosion and weathering of the continental crust into the hyper-extended margin of the Alpine Tethys.

Conversely, the Re-Os systematics of pyrite (11.2–12.0 ng g<sup>-1</sup> Re, 18.3–19.3 pg g<sup>-1</sup> Os) in Law-Bs of pillow basalt protolith have been reset. All pyrite aliquots yield consistent, preliminary model ages younger than 112 Ma but older than ca. 81 Ma for a set of realistic Os<sub>i</sub> values for the primitive upper mantle (0.12) and the upper continental crust (0.8 to 5) in the context of the Alpine Tethys. Pyrite, which has etched and dissolution features predates schistosity in Law-Bs. Considering the significantly heavier  $d^{34}\text{S}_{\text{pyrite-Law-Bs}}$  ( $+14.6$  to  $+14.8\text{\textperthousand}$ ), we hypothesize that a Re-Os date at ca. 81 Ma reflects the release of oxidized, sulfate-bearing aqueous fluids, which mobilized Os and light  $^{32}\text{S}$  from pre-existing pyrite in Law-Bs prior to prograde subduction metamorphism at ca. 37 to 34 Ma [Vitale Brovarone and Herwartz, 2013]. This hydrothermal event possibly took place during the bending of the oceanic lithosphere in a trench setting.

At the present state, the following conclusions can be drawn:

- (1) Pyrite in Law-Ecl preserves its Re-Os signatures through eclogite-facies peak metamorphism ( $\sim 520^\circ\text{C}$  and  $2.3 \text{ GPa}$ ) and provides information on the pyrite formation during hydrothermal alteration of the oceanic protolith. Our study confirms earlier findings that pyrite preserves its Re-Os systematics through low-T, high-P metamorphism (e.g., Tianshan eclogite,  $\sim 570^\circ\text{C}$  and  $2.1 \text{ GPa}$ ; van Acken et al., 2014);
- (2) Pyrite in Law-Bs might hold an Os<sub>i</sub> recording the suite of hydrothermal events in the AOC from sub-seafloor to trench settings;
- (3) Given Re-Os systematics in pyrite that record hydrothermal events prior to prograde path and peak metamorphism, we suggest that Os is not lost from pyrite neither in eclogite-facies rocks nor blueschist-facies rocks that underwent prograde path and peak metamorphism down to ca. 70 km depth.

## REFERENCES

- Gerrits, A.R., Inglis, E., Dragovic, B., Starr, P.G., Baxter, E.F., & Burton, K., 2019: Tracing the source of oxidizing fluids in subduction zones using iron isotopes in garnet, *Nature Geoscience*, 12, 1029–1033.

- Kampfschulte, A., & Strauss, H., 2004: The sulfur isotopic evolution of Phanerozoic seawater based on the analysis of structurally substituted sulfate in carbonates, *Chemical Geology*, 204, 255-286.
- Toma, J., Creaser, R.A., & Panā, D.I., 2020: High-precision Re-Os dating of Lower Jurassic shale packages from the Western Canadian Sedimentary Basin, *Palaeogeography, Palaeoclimatology, Palaeoecology*, 560, 110010.
- Tribuzio, R., Garzetti, F., Corfu, F., Tiepolo, M., & Renna, M.R., 2016: U-Pb zircon geochronology of the Ligurian ophiolites (Northern Apennine, Italy): Implications for continental break-up to slow seafloor spreading, *Tectonophysics*, 666, 220-243.
- Van Acken, D., Su, W., Gao, J., & Creaser, R.A., 2014: Preservation of Re-Os isotope signatures in pyrite throughout low-T, high-P eclogite facies metamorphism, *Terra Nova*, 26, 402-407.
- Vitale Brovarone, A., & Herwartz, D., 2013: Timing of HP metamorphism in the Schistes Lustrés of Alpine Corsica: New Lu-Hf garnet and lawsonite ages, *Lithos*, 172-173, 175-191.
- Vitale Brovarone, A., Groppo, C., Hetényi, G., Compagnoni, R., & Malavieille, J., 2011: Coexistence of lawsonite-bearing eclogite and blueschist: phase equilibria modelling of Alpine Corsica metabasalts and petrological evolution of subducting slabs, *Journal of Metamorphic Geology*, 29, 583-600.
- Walters, J.B., Cruz-Uribe, A.M., Marschall, H.R., 2020: Sulfur loss from subducted altered oceanic crust and implications for mantle oxidation, *Geochemical Perspective Letters*, 13, 36-41.

## 2.16

# Late Cretaceous Magmatic and Metallogenic Evolution of the Northern Lesser Caucasus, Tethyan Orogenic Belt: New Zircon U-Pb Age Constraints from the Beqtakari Epithermal Deposits, Bolnisi District, Georgia

Şafak Utku Sönmez<sup>1</sup>, Robert Moritz<sup>1</sup>, Jonathan Lavoie<sup>1</sup>, Alexey Ulianov<sup>2</sup>, Nino Popkhadze<sup>3</sup>, Malkhaz Natsvlishvili<sup>4</sup>, Jorge Spangenberg<sup>2</sup>

<sup>1</sup>Department of Earth Sciences, University of Geneva, Rue des Maraîchers 13, 1205 Geneva, Switzerland; (safak.soenmez@unige.ch)

<sup>2</sup>Institute of Earth Sciences, University of Lausanne, 1015 Lausanne, Switzerland

<sup>3</sup>Al. Janelidze Institute of Geology, Iv.Javakhishvili Tbilisi State University, Georgia

<sup>4</sup>Rich Metals Group, Tbilisi, Georgia

The Bolnisi District is one of the major ore zones in the Lesser Caucasus, which was formed during Late Cretaceous magmatism, and which was linked to northeast-verging subduction of the Neothethys ocean along the Eurasian margin. The Mashavera and Gasandami suites of the Bolnisi District host different epithermal gold and base metal deposits.

This study focuses on the Beqtakari Deposit (9.4Mt @ 2.93g/t Au, 33.23g/t Ag, 1.44% Zn, and 0.66% Pb) for a better understanding of the absolute age of magmatic and alteration events, the composition of magmatic host rocks, and the three-dimensional distribution of the hydrothermal alteration zones in the Bolnisi District. The volcanic and volcanioclastic rocks in Beqtakari have mainly rhyolitic to rhyodacitic, and subsidiary intermediate to mafic compositions, which have been attributed to the Gasandami Suite. New uranium-lead dating indicates that the felsic host rocks have been emplaced between  $85.32 \pm 0.19$  and  $84.68 \pm 0.18$  Ma. Barren volcanioclastic rocks of the Upper Gasandami unit overlie the felsic host rocks of the Beqtakari Deposit and have been dated at  $84.44 \pm 0.28$  Ma. These new results enable us to bracket the duration of the mineralization event between  $84.68 \pm 0.18$  and  $84.44 \pm 0.28$  Ma

The predominant alteration minerals at Beqtakari include chlorite, epidote, sericite (K-illite-muscovite±phengite) and kaolinite group minerals (kaolinite-halloysite-nacrite). These alteration minerals are accompanied by carbonates (calcite-dolomite-ankerite). Barite and gypsum are also observed in the deposit area. Polymetallic mineralization is hosted by silicified and brecciated rhyodacite dated at  $84.68 \pm 0.18$  Ma. It consists of quartz-barite±calcite veins with pyrite-sphalerite-galena-chalcopyrite and subsidiary late cross-cutting tennantite-tetrahedrite. Smithsonite is associated with late-stage veins. One first fluid inclusion assemblage in Beqtakari, Fia (I), is hosted by sphalerite and is interpreted as primary in origin. It yielded homogenization temperatures ranging between 268 to 229°C (mean of  $232 \pm 18$  °C) and salinities from 3.9 to 3.1 wt% NaCl (mean of  $3.6 \pm 0.4$  wt% NaCl). Another fluid inclusion assemblage also hosted by sphalerite, Fia (I) sub-type, yielded slightly higher homogenization temperatures ranging between 294 and 261°C (mean of  $271.8 \pm 13.3$  °C), and a similar range of salinities from 3.9 to 3.4 wt% NaCl (mean of  $3.6 \pm 0.1$  wt% NaCl).

The sulfur isotopic compositions ( $\delta^{34}\text{S}$  values) of sulfide minerals from Beqtakari exhibit a narrow range between -1.7 and +4.0 ‰ VCDT and suggest a deep/magmatic sulfur origin. The  $\delta^{34}\text{S}$  values of gypsum and barite samples partly overlap with the sulfur isotopic composition of Late Cretaceous seawater sulfate.

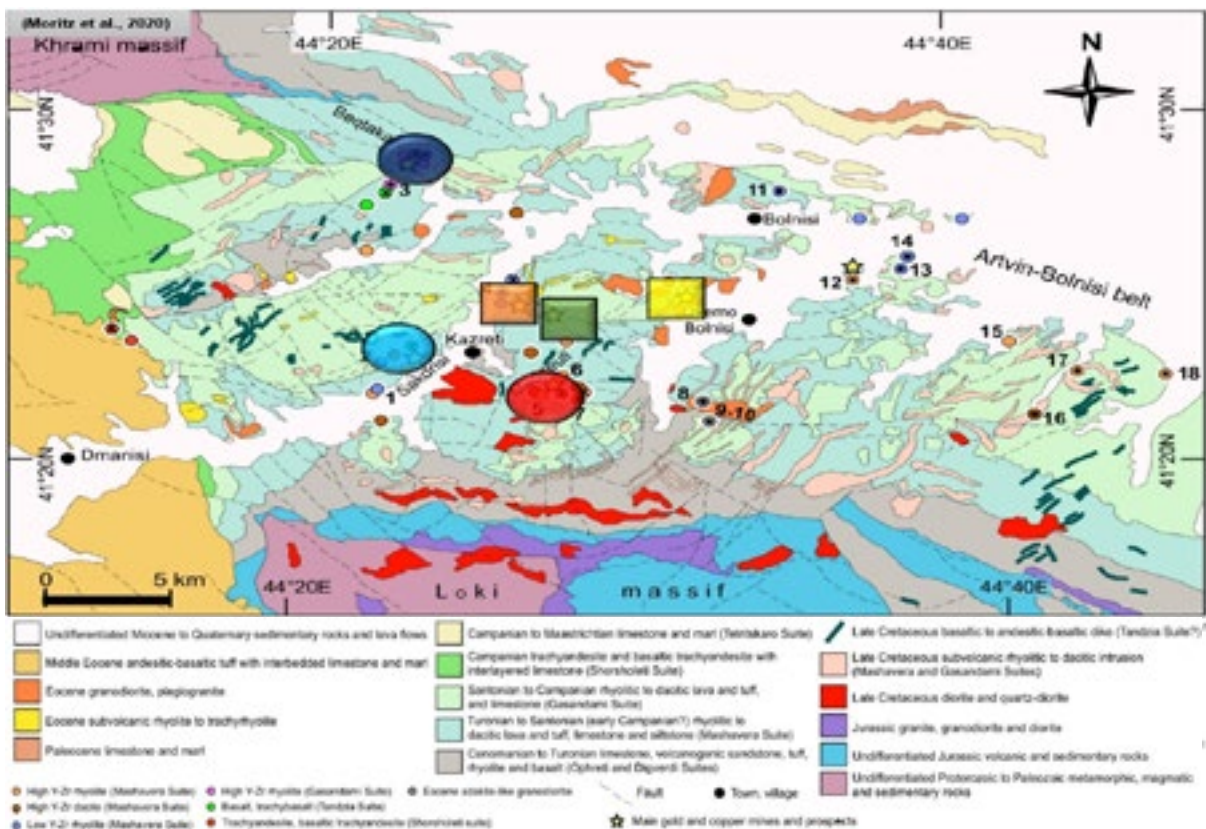


Figure 1. Regional Geology of the Bolnisi District.

## 2.17

### Positive thermal Raman shifts in silicates

Georg Spiekermann<sup>1</sup>, Alissa Näpflin<sup>1</sup>, Motohiko Murakami<sup>1</sup>

<sup>1</sup>*Institut für Geochemie und Petrologie, ETH Zürich, Clausiusstrasse 25, 8092 Zürich (gspiekerm@ethz.ch)*

In real crystals, increased temperature normally has a lowering effect on the frequencies of Raman-active vibrational modes. Here we show positive thermal Raman shifts in a variety of silicate minerals, and discuss how this property can be used for a fruitful shake-hands between mineralogy and materials science.

## 2.18

# Serpentinites as a source of water for continental crust formation in the Archean

Renée Tamblyn<sup>1</sup>, Jörg Hermann<sup>1</sup>, Derrick Hasterok<sup>2</sup>, Paolo Sossi<sup>3</sup>, Thomas Pettke<sup>1</sup>, Sukalpa Chatterjee<sup>1</sup>

<sup>1</sup> Institut für Geologie, Universität Bern, Bern, Switzerland

<sup>2</sup> Department of Earth Sciences, University of Adelaide, Adelaide, Australia

<sup>3</sup> Institut für Geochemie und Petrologie, ETH Zurich, Zurich, Switzerland

Water plays a critical role in the formation of continental crust on Earth today. Subducted mafic-ultramafic rocks trap and transport water from the oceanic floor and release this water via dehydration reactions during subduction-related metamorphism, to ultimately form arc magmas and create the andesite-dacite-dominated continental crust (Jagoutz and Kelemen, 2015). In contrast, the preserved Archean continental crust is dominantly comprised of tonalite-trondhjemite-granodiorite (TTG) suites associated with less abundant low-grade greenstone belts. The exact processes that form TTGs, as well as the source rock they are derived from, are difficult to constrain from the sparse Archean geological record. However, studies show that the water-present partial melting of metamorphosed basalt at temperatures of 750–950 °C with at least 5 weight % free water is required to produce large volumes of partial melt with TTG compositions (e.g. Xiong et al., 2009; Pourteau et al., 2020). Therefore, a source of free water at high temperatures during basalt genesis is needed. We suggest that serpentinised ultramafic rocks (komatiites), a constituent of Archean greenstone belts, may hold the key.

Using petrology, mineral chemistry and phase equilibria modelling of representative komatiite samples, combined with analysis of a global geochemical dataset of komatiites and basaltic komatiites, we show that during metamorphism serpentinised komatiites can release at least 6 weight % mineral-bound water. Up to 5 weight % of this water is released by breakdown of chlorite and tremolite at temperatures between 680 and 800 °C, regardless of the P–T path (i.e., tectonic scenario) experienced by these serpentinised komatiitic rocks. As the temperatures of chlorite and tremolite dehydration are above the wet basalt solidus, the released water can trigger voluminous partial melting of basalt to ultimately create TTG batholiths. This extreme hydration potential of hydrated komatiites is due to their high XMg (XMg = molar Mg/[Mg+Fe]), which stabilises hydrous minerals during oceanic alteration on the seafloor, but also extends the stability of Mg-rich chlorite to high temperatures. During prograde metamorphism, the XMg, CaO and Al<sub>2</sub>O<sub>3</sub> content of the reactive rock composition determines the proportion of chlorite vs amphibole, and therefore the volume of water which can be transported to temperatures of > 750 °C. Similar to serpentinites today, komatiites may have played a vital role in the deep water cycle and the formation of continental crust in the Archean.

## REFERENCES

- Jagoutz, O. and Kelemen, P.B., 2015: Role of arc processes in the formation of continental crust. *Annual Review of Earth and Planetary Sciences*, 43, pp.363-404.
- Pourteau, Amaury, Luc S. Doucet, Eleanore R. Blereau, Silvia Volante, Tim E. Johnson, William J. Collins, Zheng-Xiang Li, and David C. Champion. 2020: TTG Generation by Fluid-Fluxed Crustal Melting: Direct Evidence from the Proterozoic Georgetown Inlier, NE Australia. *Earth and Planetary Science Letters* 550:116548.
- Xiong, Xiaolin, Hans Keppler, Andreas Audétat, Gudmundur Gudfinnsson, Weidong Sun, Maoshuang Song, Wansheng Xiao, and Li Yuan. 2009: Experimental Constraints on Rutile Saturation during Partial Melting of Metabasalt at the Amphibolite to Eclogite Transition, with Applications to TTG Genesis. *American Mineralogist* 94(8–9):1175–86. doi: 10.2138/am.2009.3158.

## 2.19

# From Niggli's gas mineralisators to extraction from crystal mushes: Linking pegmatites with their host granites

Juliana Troch<sup>1,2</sup>, Chris Huber<sup>3</sup>, Olivier Bachmann<sup>4</sup>, Ludmila Maria Fonseca Teixeira<sup>4</sup>, Mike Ackerson<sup>2</sup>

<sup>1</sup> Division of Earth Sciences and Geography, RWTH Aachen University, Bunsenstrasse 8, 52072 Aachen, Germany

<sup>2</sup> Department of Mineral Sciences, Smithsonian National Museum of Natural History, 10<sup>th</sup> St & Constitution Avenue, Washington DC 20560, USA (trochj@si.edu)

<sup>3</sup> Department of Earth, Environmental and Planetary Sciences, Brown University, 324 Brook Street, Providence RI 02912, USA

<sup>4</sup> Institute of Geochemistry and Petrology, ETH Zurich, Clausiusstrasse 25, 8092 Zurich, Switzerland

With their extreme grain sizes and occurrence of a wide variety of rare minerals, including gem minerals, granitic pegmatites have long fascinated geoscientists. Their common spatial association with granitic plutons suggests a close genetic relationship; however, with growing recognition of these granites as dominantly mushy, near-solidus systems that may source explosive volcanic eruptions, our understanding of silicic magmatic systems has changed considerably over the last decades. Here, we explore some examples of how early observations by outstanding Swiss mineralogist and pegmatite connaisseur Paul Niggli (1888–1953) have shaped our understanding of pegmatite formation and how they can be applied to modern explanations of pegmatite extraction mechanisms from near-solidus silicic magmatic systems.

1. *Transitional character between magmatic and hydrothermal realm.* Niggli describes this as the key feature of pegmatites. This continuum is facilitated by “gas mineralisators”, easily-volatile elements that increase similarity between fluid and melt. Indeed, alkali elements and F have been experimentally confirmed to reduce the miscibility gap between silicate melt and aqueous fluid and reduce the solidus temperature, allowing for pegmatite crystallization at lower temperatures than the traditionally inferred solidus for granitic melts. Observation of a parallel evolution of quartz crystallization temperatures in pegmatites and their host granites suggests significant (<20%) crystallization below the traditionally inferred solidus can also occur in granitic systems.
2. *Overpressurization and rapid crystallization.* Niggli argues that internal overpressurization during continuous crystallization forces pegmatite intrusion into neighboring rock, and that the resulting drop in pressure and temperature drives rapid crystallization. Such overpressurization is predicted in thermomechanical models of silicic magmatic systems at near-solidus temperatures, when the system is dominated by an exsolved magmatic volatile phase. Rapid cooling of the low-viscosity liquid drives rapid crystallization and extensive crystal growth, as illustrated by disequilibrium textures in undercooling experiments.
3. *Common trace element flavors.* Pegmatites commonly share trace element and isotopic signatures of other magmas in the same province, even when field relationships do not indicate a clear source granite. The contribution of “gas mineralisators” within this trace element budget and the concentration of water in the parental melt exert important control on the relative timing of fluid saturation and rare element enrichment in the source granitic system, potentially leading to the observed variety in pegmatites types and their correlation with tectonic settings.

Overall, many of Niggli's ideas have been proven true by additional experimental and analytical studies, underlining the clear-sighted and revolutionary nature of his work. As such, Niggli's prescient ideas in many aspects form the basis of our modern concept of integrated silicic magmatic systems containing plutonic, volcanic, pegmatitic and hydrothermal environments.

## 2.20

# Variscan granitoids from Eastern Pontides, NE Turkey: A record of a 2.0 Ga-long of this Gondwana-derived terrane

François Turlin<sup>1</sup>, Robert Moritz<sup>1</sup>, Serdar Keskin<sup>2</sup>, Şafak Utku Sönmez<sup>1</sup>, Alexey Ulyanov<sup>3</sup>

<sup>1</sup> Department of Earth Sciences, University of Geneva, Rue des Maraîchers 13, 1205 Geneva, Switzerland;  
(francois.turlin@unige.ch)

<sup>2</sup> General Directorate of Mineral Research and Exploration (MTA), Eastern Black Sea District Office, TR-61010 Trabzon, Turkey

<sup>3</sup> Institute of Earth Sciences, University of Lausanne, 1015 Lausanne, Switzerland

The Eastern Pontides constitutes an Alpine segment in NE Turkey. They consist in a Gondwana-derived terrane that has been accreted to the Eurasian margin and that was subsequently reworked during successive orogenic events associated with the closure of Paleotethys and Neotethys oceans. There is only little evidence of this long history, which has been preserved in the rock record within the Eastern Pontides. The oldest relics of the pre-Alpine evolution are Carboniferous granitoids (~309-323 Ma, this study and unpublished U-Pb zircon ages) that crop out within the central part of the Eastern Pontides as a belt parallel array of Variscan granitoid plutons. The Artvin granitoid is one of the best exposed and preserved examples. While its northwestern and southeastern margins are obliterated by normal faults that probably also facilitated its exhumation during successive thermal relaxation/orogenic collapses of the belt, it is bordered in the northeast and southwest by concordant Jurassic detrital sedimentary sequences of the Berta Formation.

The Artvin granitoid is composed of several Al-rich granitic phases crosscut by several generations of mafic magmas. In this study, we report new LA-ICP-MS U-Pb zircon ages for the different events of granitic rocks. The first event corresponds to a  $324.4 \pm 0.6$  Ma leucogranite, the zircon cores of which yielded inherited ages as old as ca. 2.4 Ga. It was followed by a  $323.7 \pm 0.8$  Ma leucogranite with abundant zircon inheritance as old as ca. 1.9 Ga and that hosts xenoliths of partially molten micaschist and felsic intrusive rocks. The main volume of the Artvin granitoid consists of a  $320.6 \pm 0.6$  Ma leucogranite crosscut by mafic dykes and sills, and by  $315.4 \pm 0.7$  Ma micro-leucogranite dykes.

These geochronological data, along with the chemical composition of the granitic phases indicate that the Artvin granitoid is a syn-tectonic pluton emplaced during the Variscan Orogeny. Along with its inherited zircon grains, it represents a perfect natural laboratory to investigate the pre-Variscan evolution of the Eastern Pontides. Ongoing work will collect Hf isotopic compositions and trace elements in zircon that will be combined with the available U-Pb dates. These data will allow us to reconstruct the evolution of a Gondwana crustal segment of the Eastern Pontides since the Early-Paleoproterozoic.

## P 2.1

# A new albite microanalytical reference material ( $\mu$ RM) from Piz Beverin (Graubünden, Switzerland) and evaluation of potential K-feldspar minerals $\mu$ RM

Julien Allaz<sup>1</sup>, Marcel Guillong<sup>1</sup>, Lorenzo Tavazzani<sup>1</sup> and Lydia Zehnder<sup>1</sup>

<sup>1</sup> ETH Zürich, Inst. of Geochemistry & Petrology, Dept. of Earth Sciences, Switzerland

As analytical instruments become more stable and reliable, and measurements even more precise, the community deserves better microanalytical reference materials ( $\mu$ RM) for calibration of major and minor elements or as secondary  $\mu$ RM to ensure accuracy. Such material must be homogeneous, available in large quantity, well characterised, stable, and with a reference elemental composition confirmed by various analytical techniques and laboratories (e.g., FIGMAS; Bullock et al., 2021). A major problem is the availability and reliability of those  $\mu$ RM, notably for common EPMA and SEM-EDS analyses (e.g., silicate, oxide, carbonate), and especially for Na and K. Many cations can be synthesised in high-purity simple or complex oxides  $\mu$ RM ( $A_xO_y$  or  $A_xB_zO_y$ ). However, for matrix-matched  $\mu$ RM, the community still relies mostly on natural samples. The challenge is therefore to find and to certify the homogeneity of a significant source of such natural material, so it can be used in many labs and last for the foreseeable future.

We propose an albite  $Ab_{99.6(2)}$  as a new  $\mu$ RM for Na and Si analysis. It originates from an open fracture in the Bündnerschiefer of the Tomül nappe, NE of Piz Beverin (Switzerland). This mineral sample was analysed by EPMA, LA-ICP-MS, and XRF, and proved to be very homogeneous at both the micron-scale and at the gram-scale, with very rare micro-impurities in fractures (e.g., carbonate [calcite  $\pm$ Sr], framboidal pyrite, apatite, chlorite, graphite), and only minor variation of Ca, K, and Sr at the  $\sim$ 100 ppm level in sealed fractures.

In parallel, five distinct K-feldspar mineral samples were evaluated: an adular, an orthoclase, and three individual batches of yellow ferric “orthoclase” (actually sanidine; Simmons and Falster, 2002). The adular and orthoclase samples are of unknown origin (although likely from Switzerland). They are the perfect example of a possibly “bad”  $\mu$ RM with local yet significant heterogeneities, making them unsuitable as good  $\mu$ RM. On the contrary, the three batches of yellow sanidine are more promising. They all come from the Itrongay pegmatite field in Madagascar. Each individual batch is homogeneous at the centimetre to micrometre-scale, but they each have a unique Fe-Al content.

*Acknowledgments:* Many thanks to Drs. Peter Brack and Andrea Galli (ETH mineral collection curators, past and present) for donating the Piz Beverin albite, and to Drs. Eric Reusser and Adolf Peretti for the K-feldspar minerals.

## REFERENCES

- Simmons, W. B. & Falster, A. U. (2002). Yellow orthoclase (sanidine) from South Betroka, Madagascar. *Mineralogical Record* 79.
- Bullock, E., Nachlas, W., Neill, O., Allaz, J. & Handt, A. von der (2021). The FIGMAS Online Database of Standards and Reference Materials – an Update. *Microscopy and Microanalysis* 27, 1572–1573.

## P 2.2

# Diffusion vs fluids: Ar distribution, chemical composition, oxygen isotopes and $^{40}\text{Ar}/^{39}\text{Ar}$ geochronology of muscovite crystals from Ecuador and Colombia.

Clémentine Antoine<sup>1</sup>, Richard Alan Spikings<sup>1</sup>, André Navin Paul<sup>1</sup>, Mustafa Erde Bilir<sup>1</sup>, Florence Bégué<sup>1</sup>, Urs Schaltegger<sup>1</sup>

<sup>1</sup> Département des Sciences de la Terre et de l'Environnement, Université de Genève, rue des Maraischers 13, CH-1205 Genève.

The thermochronologic study of the accretion of the Calima and Pallatanga-Pinon terranes with the South American plate in the Andean Cordillera highlighted strong thermal fluctuations throughout the Triassic to the Early Cretaceous (Spikings et al., 2015). Between ~ 209 and ~ 114 Ma (late Triassic to early Cretaceous), the subduction of the Pacific plate caused a progressive trenchward migration of the magmatic arc (e.g. Cochrane et al., 2014b; Spikings et al., 2015). The study of different mineral phases (apatite, rutile, muscovite, and biotite) evidenced a gradient of decreasing ages towards 75 Ma during the collision of an oceanic plateau with north-western South America (Paul et al., 2018, 2019, Vallejo et al., 2006; Spikings et al., 2010; Villagomez and Spikings, 2013). Apatite U-Pb dates ( $63.3 \pm 9.3$  to  $128.5 \pm 0.6$  Ma) and  $^{40}\text{Ar}/^{39}\text{Ar}$  dates ( $70.60 \pm 0.5$  from muscovite, to  $76.23 \pm 0.41$  Ma from biotite) from the Sabanilla Migmatite correlate well with the records of low-temperature thermochronometers, attributed to the collision of the Caribbean Large Igneous Province with the continental margin at ca. 75 Ma (Spikings et al., 2015; Paul et al., 2018, 2019). U-Pb and  $^{40}\text{Ar}/^{39}\text{Ar}$  thermochronometers of central to northern Ecuador Triassic lithologies and the Tres Lagunas Granite, record dates ranging from  $66.4 \pm 3.0$  to  $228.9 \pm 8.9$  Ma (apatite U-Pb) and  $164.79 \pm 0.86$  to  $169.51 \pm 6.26$  Ma (disturbed  $^{40}\text{Ar}/^{39}\text{Ar}$  muscovite plateau dates). These dates were interpreted to reflect thermally activated volume diffusion, based on the systematics of apatite U-Pb *in-situ* analyses, caused by variable degrees of post-formation burial in an extensional and later again compressive arc setting (Paul et al., 2018, 2019). However, new geochemical data using quantitative and qualitative EPMA maps of single muscovite crystals and *in-situ* SIMS Oxygen isotopes may challenge the hypothesis of thermally activated volume diffusion for  $^{40}\text{Ar}/^{39}\text{Ar}$  in muscovite. The North-South, trench parallel, sample set ranges from the Cajamarca Complex (Colombia), the Tres Lagunas Granite (Central Ecuador), and the Sabanilla Migmatite (South Ecuador). The new geochemical and isotope data result in a revised hypothesis for the mobilisation of argon isotopes within these muscovite crystals. Fluid assisted Ar mobilisation and muscovite recrystallization may be the dominant mechanisms controlling  $^{40}\text{Ar}/^{39}\text{Ar}$  geochronological dates derived from those muscovite crystals, contrary to the previous interpretation made from apatite U-Pb systematics.

## REFERENCES

- Cochrane, R., Spikings, R., Gerdés, A., Winkler, W., Ulianov, A., Mora, A., & Chiaradia, M. (2014). Distinguishing between *in-situ* and accretionary growth of continents along active margins. *Lithos*, 202, 382-394.
- Paul, A. N., Spikings, R. A., Ulianov, A., & Ovtcharova, M. (2018). High temperature (> 350 C) thermal histories of the long lived (> 500 Ma) active margin of Ecuador and Colombia: Apatite, titanite and rutile U-Pb thermochronology. *Geochimica et cosmochimica acta*, 228, 275-300.
- Paul, A. N., Spikings, R. A., Chew, D., & Daly, J. S. (2019). The effect of intra-crystal uranium zonation on apatite U-Pb thermochronology: A combined ID-TIMS and LA-MC-ICP-MS study. *Geochimica et Cosmochimica Acta*, 251, 15-35.
- Spikings, R. A., Crowhurst, P. V., Winkler, W., & Villagomez, D. (2010). Syn-and post-accretionary cooling history of the Ecuadorian Andes constrained by their *in-situ* and detrital thermochronometric record. *Journal of South American Earth Sciences*, 30(3-4), 121-133.
- Spikings, R., Cochrane, R., Villagomez, D., Van der Lelij, R., Vallejo, C., Winkler, W., & Beate, B. (2015). The geological history of northwestern South America: from Pangaea to the early collision of the Caribbean Large Igneous Province (290–75 Ma). *Gondwana Research*, 27(1), 95-139.
- Vallejo, C., Spikings, R. A., Luzieux, L., Winkler, W., Chew, D., & Page, L. (2006). The early interaction between the Caribbean Plateau and the NW South American Plate. *Terra Nova*, 18(4), 264-269.
- Villagómez, D., & Spikings, R. (2013). Thermochronology and tectonics of the Central and Western Cordilleras of Colombia: Early Cretaceous–Tertiary evolution of the northern Andes. *Lithos*, 160, 228-249.

## P 2.3

# Numerical advection schemes for an accurate and efficient modelling of magma ascent

Hugo Dominguez<sup>1</sup>, Pierre Lanari<sup>1</sup>, Nicolas Riel<sup>2</sup>

<sup>1</sup> Institute of Geological Sciences, University of Bern, 3012 Bern, Switzerland

<sup>2</sup> Institute of Geosciences, Johannes Gutenberg University Mainz, J.-J.-Becher-Weg 21, D-55128, Mainz, Germany

Modeling magma ascent in the crust involves combining different numerical techniques to solve a complex coupled system. These methods need to be both accurate and efficient to mitigate the propagation of numerical errors and to have a satisfying computational run-time. Solving numerically the advection of the physical properties (e.g. chemical composition) is one of the most challenging part. The reason is not because of its physical complexity, but due to the fact that it is difficult to solve numerically the transport on an Eulerian mesh especially because geological applications present usually sharp gradients. Advection is commonly done by using a marker-in-cell technique which is always stable and has low numerical diffusion. Nevertheless, this technique can still present major drawbacks, like accumulation of markers on long time simulation or with sharp discrepancy in the velocity field.

In this study, we present two alternative strategies based on high-order numerical techniques: a Weighted Essentially Non-Oscillatory scheme (WENO) and a Quasi-Monotone Semi-Lagrangian scheme (QMSL). These two schemes were implemented to compare their advantages and drawbacks. They were applied to a realistic case study involving a flow of magma in a porous matrix in 2D. The results show that these 2 schemes have low diffusion, preserve the monotonicity, and can be good alternatives to the classical marker-in-cell technique.

## FUNDING

This project has received funding from the European Research Council (ERC) under the European Union's Horizon 2020 research and innovation programme (grant agreement No 850530).

**P 2.4****Geochemistry of melt inclusions from Paraná-Etendeka Magmatic Province, Brazil**

Melina Esteves<sup>1</sup>, Ana Sena<sup>1</sup>, Adriana Alves<sup>1</sup>

<sup>1</sup> Geoscience Institute, University of São Paulo, Rua do Lago, 562, São Paulo 05508080 Brazil. ([melina.cbe@usp.br](mailto:melina.cbe@usp.br))

The link between Continental Flood Basalts, extinctions, and environmental changes is mainly attributed to the effects of volcanic emissions, where the expelled volatile species have an important effect on atmospheric composition. It is highly probable that magmatic degassing is an insufficient killer mechanism, and an important additional volatile flux should be provided by alternative sources, as outgassing associated with contact metamorphism. Despite access to the volatiles released via interaction of magmas and sedimentary bedrocks is crucial, recognizing the original magmatic gases is the first step. Estimates on the volatile content of magmas erupted in the past commonly come from melt inclusions (MI), since most volatiles have low solubilities in magmas at atmospheric pressure, and therefore virtually all erupted lavas are degassed. Brazil hosts one of the world's most expressive CFB associated with the breakup of Gondwana Supercontinent and the opening of the Atlantic Ocean, the Paraná-Etendeka Magmatic Province. Some uncertainties prevent the concrete identification of volcanic activity as a trigger of environmental changes. In this context, this work contributes by investigating MI of the province aiming to explore the potential of using partially crystallized MI and their shrinkage bubbles to establish magmatic volatile content. MI of three silicic rocks samples (AS-350G, AS-367 and AS-622) were submitted to petrography, scanning electron microscope, microprobe, Raman spectroscopy. The results show that MI present in pyroxene and plagioclase megacrystals are rounded to oval (10 to 20 $\mu$ m), composed of a glassy matrix with dispersed nanocrystals, mostly clinopyroxene, and, frequently, apatite crystals, whose origin is interpreted as prior to the inclusion. Analysis reveals high values for Cl and S. MI also shows the presence of several shrinkage bubbles carrying volatiles (e.g. CO<sub>2</sub>, SO<sub>4</sub>). Samples define liquid lines descent indicating that the crystal has mostly trapped evolved liquids. Calculations of apatite saturation temperature provided temperatures of 1269°C (AS-350G) and 865°C (AS-367) and fO<sub>2</sub>=ΔQFM +0.1 +0.4 and fO<sub>2</sub>=ΔQFM +0.6, respectively (Miles et al., 2014). Most of the inclusions underwent degassing of sulfur and the silicic volcanic rocks from Paraná-Etendeka Province may have released ~6.6Gt S considering a degassing effectiveness of 43%.

**REFERENCES**

- Miles, A.J., Grahama, C.M., Hawkesworthb, C.J., Gillespiec, M.R., Hintona, R.W., Bromiley, G.D. 2014: Apatite: A new redox proxy for silicic magmas?, *Geochimica et Cosmochimica Acta*, 132, 101-119.

## P 2.5

# Tracking volcanic, plutonic, and pegmatitic environments in sediments: A case study from the Pikes Peak batholith, Colorado

L. M. Fonseca Teixeira<sup>1</sup>, O. Laurent<sup>2</sup>, J. Troch<sup>3</sup>, C. S. Siddoway<sup>4</sup>, and O. Bachmann<sup>1</sup>

<sup>1</sup> Institute of Geochemistry and Petrology, ETH Zürich, Zürich, Switzerland ([ludmila.fonseca@erdw.ethz.ch](mailto:ludmila.fonseca@erdw.ethz.ch))

<sup>2</sup> CNRS, Observatoire Midi-Pyrénées, Géosciences Environnement Toulouse, Toulouse, France

<sup>3</sup> Department of Mineral Sciences, Smithsonian National Museum of Natural History, Washington DC, USA

<sup>4</sup> Colorado College, Colorado Springs, CO, USA

Understanding magmatic processes in the early Earth's history is a major geological challenge, as erosion, metamorphism, and weathering may destroy most of the original rock record. Old sedimentary layers may be the only record available on Earth's surface that can allow for identification of lithologies that were completely altered or consumed and could provide key insights into Earth's early magmatic evolution, such as the volcanic:plutonic ratio and the role of volatiles in magmas.

We compared crystallisation temperatures obtained in quartz and zircons from magmatic samples and sedimentary dikes from the Pikes Peak batholith (Colorado, USA). The magmatic examples included the 1.1 Ga A-type Pikes Peak granite, its many pegmatite bodies, and the associated subvolcanic rhyodacitic Keeton Porphyry. The sedimentary crystals were retrieved from the Cryogenian Tava sandstone, which occurs in intra-granite sedimentary dikes at the Keeton Porphyry location and represents the oldest terrestrial sediments in the Front Ranges of Colorado.

Grayscale blue cathodoluminescence images of hundreds of sedimentary quartz grains were calibrated with selected Ti contents analysed by LA-ICPMS, allowing for fast and statistically meaningful identification of ranges in crystallization temperatures. By comparing these to Ti-in-quartz and in-zircon temperature data from the different lithologies in the Pikes Peak area and additional data from other settings worldwide, we can estimate the proportions of volcanic, plutonic and pegmatitic quartz in these sediments. Preliminary results suggest that low-temperature quartz derived from the pegmatites provides the most contribution to the Tava sedimentary dikes. A small portion of high-Ti quartz, consistent with the Keeton Porphyry range, hints at a possible volcanic source. Comparison of Ti-in-zircon temperatures from Tava sandstone and the Pikes Peak batholith results on statistically higher temperatures for the sedimentary zircons of age compatible with the Pikes Peak batholith also suggests a potential volcanic contribution. The applied techniques can be useful to identify lithologies that are no longer available on the Earth's surface, providing significant information on how different magmatic environments are represented in the sedimentary record and on the magmatic history of old terrains that may not be obtained elsewhere.

## P 2.6

# SpecXY - Presenting a tool for working with spatially resolved spectroscopic data

Nils B. Gies 1, Jörg Hermann 1, Pierre Lanari 1

1 Institut für Geologie, Baltzerstrasse 1+3, 3012 Bern, Switzerland

Spectroscopic data are an essential component of modern geosciences. In recent years there has been a shift in petrology and crystallography from using single-spot analyses to 2-dimensional mapping. Maps help revealing patterns in a sample, which would otherwise not be detected with single point measurements. Often in single spot analyses mixed signals of the mineral of interest and (micro-)inclusions e.g., melt-, or fluid-inclusion, mineral exsolutions or mineral inclusions are obtained. Filtering and extracting signal information from multiple combined pixels can help to improve the signal to noise ratio and thus the quality of the data. In this way, compositional maps can be generated of the mineral of interest, providing information on growth conditions as well as potential modifications afterwards.

We present the software solution SpecXY for preparing, editing, extracting, and comparing spatially resolved spectral datasets. The software can handle XY resolved spectra with special focus on spatially resolved data. Spatially resolved numerical data such as e.g., EPMA or LA-ICP-MS major- and trace element maps can be imported, referenced and possible correlations can be investigated. In this contribution we present an example based on Fourier Transform Infrared Spectroscopy (FTIR) data, imaging the distribution of trace amounts of H<sub>2</sub>O in clinopyroxene.

An example compiled of seven FTIR-FPA maps with different sizes of an oriented CPX single crystal with amphibole lamellae inclusions from Varallo, (Italy) demonstrates the semi-automatic classification and extraction of the resulting filtered mean spectra. The maps contain a total number of 170000 spectra with a resolution of 5.5 micron/pixel. In addition, we discuss the complications and possible errors in the deconvolution of the obtained spectra and present a Monte Carlo Simulation-based workflow to address these errors. Further, we show the difference in calculated water content of overestimated single-point FTIR-MCT measurements and extracted filtered inclusion free mean spectra from high-resolution FTIR-FPA maps reducing the resulting water content from 300 ppm to 30 ppm. Our results show the importance of a detailed investigation of possible inclusions and mixed spectra which for inclusion rich samples is only possible in a high-resolution mapping and filtering approach.

## P 2.7

### Determining the state of activity of volcanoes

Guido Giordano, Luca Caricchi

The definition of active volcano remains qualitative, which makes the assessment and communication of volcanic hazard at long-dormant volcano extremely challenging. The state of activity of a volcanic system has been defined based on the recent eruptive history of a volcano. However, field, petrographic, and geochemical evidence, together with thermal modelling suggest that thermal structure and behavior of volcanic system changes in time. Additionally, volcanic plumbing systems can develop to occupy a significant portion of the Earth's crust, and absence of magma at shallow depths, where its detection by geophysical methods is comparatively simpler, does not imply the absence of magma at depth.

We review literature and use existing data for emblematic volcanic systems to identify the essential data required to define the state of activity of volcanoes and their plumbing systems. We explore global eruptive records, in combination with heat flux and other geological and geophysical datasets to determine the evolutionary stage of volcanic plumbing systems. We define a "Volcanic Activity Index" (VAI), which considers the entire eruptive history of a volcanic system, and it is applicable to any volcano. VAI provides an estimate of the potential of a system to feed eruptions in the future, which is especially important for long quiescent volcanoes. Most importantly, our analysis can serve to drive the efficient collection of the basic data required for the rapid estimation of the state of activity of poorly studied volcanoes.

**P 2.8****Apatite as a tool to quantify the evolution of crystal–melt–fluid systems**

Thomas Grocolas<sup>1</sup>, Olivier Reubi<sup>1</sup>, Aurore Toussaint<sup>1</sup>, Othmar Müntener<sup>1</sup>

<sup>1</sup> Institute of Earth Sciences, University of Lausanne, Quartier Mouline, CH-1015 Lausanne ([thomas.grocolas@unil.ch](mailto:thomas.grocolas@unil.ch))

Volatile elements play a key role in the differentiation of magmas by controlling their chemical and physical properties. Indeed, volatile saturation and exsolution is directly impacting the eruptive style of volcanoes at the surface. Volatile concentrations within the melt are commonly inferred from glass inclusions which, however, may have experienced post-entrapment modification, or may not be present in the studied rocks. Alternatively, volatile-bearing minerals such as biotite, amphibole or apatite represent an invaluable tool to reconstruct the volatile history of their parental melt. Volatile-bearing minerals can also be used to identify an exsolved fluid, track its composition, and determine its source. Here we investigate the volatile evolution of differentiating magmas from emplacement to interstitial melt extraction within the plutonic bodies of the Western Adamello tonalite (WAT) and the Listino Ring complex (LRC), both located in the Adamello batholith, Italy. The WAT (37.8–36.4 Myr, Floess, 2013) is a tonalitic body displaying *in situ* crystal (trondhjemite, hornblende-gabbro)–melt (granite) segregations. The LRC (41.7–41.2 Myr, Verberne, 2013) exhibits a concentric structure mainly composed of tonalite, granodiorite, and granitic dikes. Apatite, biotite, amphibole, and plagioclase are ubiquitous in these lithologies and, by using existing partition coefficients for apatite, amphibole, and biotite, geothermometers, and the plagioclase hygrometer, we determined the volatile compositions of the evolving melts.

We find that the calculated melts from both locations have the same range of F (200–400 ppm), Cl (50–1100 ppm), and H<sub>2</sub>O (4.8–5.2 wt.%) concentrations. In detail, the calculated melts from the WAT tonalite, trondhjemite, and hornblende-gabbro have the same composition, in good agreement with a crystal–melt segregation model. With differentiation, the Cl/F ratio and Cl concentration decrease, the OH/Cl ratio increases, and the H<sub>2</sub>O and F concentrations remain similar. We interpret this evolution as the result of the incorporation of Cl into an exsolving fluid starting at least at the onset of apatite crystallisation at 900–920 °C, and most likely upon emplacement. On the other hand, F is only moderately compatible ( $D_{\text{melt-fluid}} \approx 1$ ) in the fluid phase (e.g., Iveson et al., 2018) and, given its stationary behaviour along the liquid lines of descent, is evenly distributed between crystals (apatite and biotite) and melt ( $D_{\text{melt-crystal}} \approx 1$ ). After determining the initial F, Cl, and H<sub>2</sub>O concentrations upon emplacement and using known distribution coefficients, we quantitatively modelled the melt volatile evolution and showed that after 85 % crystallisation, ~15–35 wt.% of the total chlorine and ~10–20 wt.% of the total fluorine have been incorporated into the fluid phase. Measuring apatite allows the reconstruction of the volatile evolution in the crystal–melt–fluid system which can be critical to better understand how volatile elements behave through differentiation and eventually lead to magmatic–hydrothermal mineralisation.

**REFERENCES**

- Floess, D. 2013: Contact metamorphism and emplacement of the Western Adamello tonalite. PhD thesis, University of Lausanne.
- Iveson, A. A., Webster, J. D., Rowe, M. C., & Neill, O. K. 2018: Major element and halogen (F, Cl) mineral–melt–fluid partitioning in hydrous rhyodacitic melts at shallow crustal conditions, *Journal of Petrology*, 58, 2465–2492.
- Verberne, R. 2013: The role of magma rheology during emplacement of the Listino Suite, Adamello Massif, Italy. PhD thesis, University of Lausanne

**P 2.9****Examination of the microstructure and composition of jadeite jade – a combination of X-ray microtomography and petrographic methods**

Philipp Hänggi\*, Leander Franz\* and Michael S. Krzemnicki\*\*

\*Department of Environmental Sciences, Mineralogy and Petrology, University of Basel, Switzerland

(phil.haenggi@stud.unibas.ch)

\*\*Swiss Gemmological Institute SSEF, Aeschengraben 26, 4051 Basel, Switzerland

High-quality jadeite jade is one of the most valuable gemstone materials in the jewellery trade. In addition to colour and translucency, mineralogical homogeneity and the absence of cracks are crucial for the quality of jadeite jade. The last two characteristics were investigated using a combination of petrographic methods and X-ray microtomography. High-quality jade monominerally consists of jadeite and has a fine, polycrystalline structure. However, such high-quality jade was deliberately avoided for the examinations presented here, as the main aim of this study was the identification of different mineralogical phases by X-ray microtomography and their determination by petrographic methods. The overall goal was to create a database in which each mineralogical phase is assigned a characteristic value corresponding to its attenuation coefficient, in order to use non-destructive X-ray microtomography as a tool for the precise examination of mineralogically inhomogeneous jadeite samples. The attenuation coefficient is a material dependent constant with the unit  $\text{cm}^{-1}$ , which expresses the ability of a mineral phase to attenuate X-rays. With a computer tomography (CT) scan, the values are presented in shades of grey as a tomogram. If the settings remain the same, these values are comparable for measurements on the same device. Comparing the attenuation coefficients of mineral phases to identify their composition is a well-known technique. For this purpose, a program can be used to visualize the minerals present based on their attenuation values (Bam et al. 2020). However, in addition to the density of the material and the energy of the X-rays, the chemical formula of the minerals must be known, which is not the case for unworked jade specimens. In general, the attenuation coefficient decreases with increasing energy of the X-rays, decreasing density of the material and lower atomic numbers of the elements present in the material (Bam et al. 2020).

Investigations for this study were performed on seven jade samples from Myanmar and Italy. The petrographic methods used to determine the mineralogical composition are thin section microscopy and Raman spectroscopy.

The left image of figure 1 shows the surface of a sliced and polished sample from Myanmar. Different minerals are optically well visible and can also easily be distinguished in the CT scan (image in the middle). On the right side, a visualization of the minerals based on their attenuation coefficient values is presented. Albite, which has the lowest value, appears in a faintly greyish colour. Jadeite, which has a higher value, is shown in red and chromian omphacite with the highest value is shown in blue.

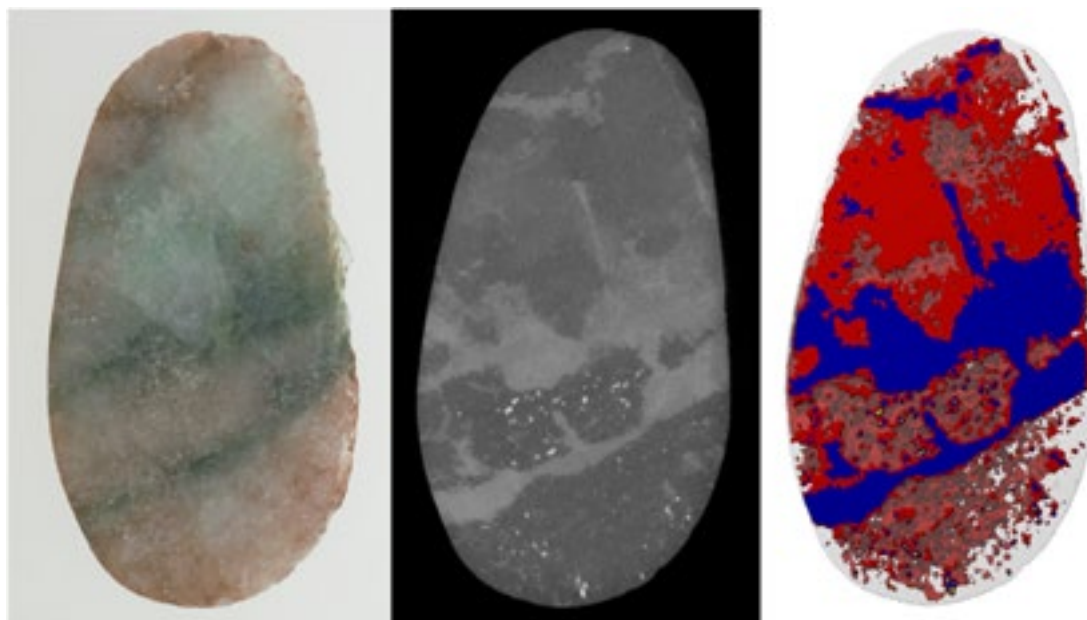


Figure 1. The left image shows the surface of a sliced and polished jadeite sample from Myanmar; the central image presents a tomogram of its surface; the right image shows a visualization of the sample based on the attenuation coefficient values of the minerals with slightly greyish albite, red jadeite and blue chromian omphacite. Length of the sample: 2 cm.

Attenuation coefficients were determined for seven different mineral phases. Jadeite could be assigned the same value ( $3.5 \text{ cm}^{-1}$ ) for the attenuation coefficient in three different samples and can thus be distinguished from other minerals. The remaining four samples either contained no jadeite or contained chromium jadeite which was assigned a value of  $3.8 \text{ cm}^{-1}$  in one sample. Since there is a scatter in relation to the attenuation coefficient within each mineral phase, the modal value was always chosen for the creation of the database. This approach is sufficient to distinguish between the phases mentioned in Figure 1, since the phases have quite different values (albite:  $2.9 \text{ cm}^{-1}$ , jadeite:  $3.5 \text{ cm}^{-1}$ , chrome-omphacite  $4.3 \text{ cm}^{-1}$ ). Therefore, variations of the attenuation coefficient within the same mineral phase should be investigated more thoroughly in the future.

In summary, the biggest advantage of the X-ray microtomography method is that 3D recordings of the sample are created, giving a quick overview of the mineral composition of the rock. Also, fractures in the rock that are invisible to the eye are thus easily detected.

## REFERENCES

- Bam, L., Miller, J. & Becker, M. 2020: A Mineral X-Ray Linear Attenuation Coefficient Tool (MXLAC) to Assess Mineralogical Differentiation for X-Ray Computed Tomography Scanning. *Minerals*, 10, 441.

**P 2.10****Using magmatism to trace onset and migration of a subduction: Insights from Saint Martin (Lesser Antilles)**

Clothilde Jost<sup>1</sup>; Oliver Higgins<sup>1</sup>; Luca Caricchi<sup>1</sup>; Alexey Ulyanov<sup>2</sup>

<sup>1</sup> Department of Earth Sciences, University of Geneva, Genève, Switzerland

<sup>2</sup> Institute of Earth Sciences, University of Lausanne, UNIL-Mouline, 1015-CH Lausanne, Switzerland

Volcanism can provide insights on geodynamic processes such as the onset and migration of subduction (Arculus et al., 2019). Located in the eastern Caribbean, Saint Martin Island was formed through arc volcanism due to the westward subduction of the Atlantic plate under the Caribbean plate (Davidson et al., 1993). Saint Martin is a part of the extinct northern part of the Lesser Antilles arc (Allen et al., 2019). This branch of the arc, named the Limestone Caribbees, was active during the Oligocene, before the arc migrated west until it reached its current position (Aitken et al., 2011). Contrary to the other islands in the Limestone Caribbees, Saint Martin features a range of outcropping volcanic and magmatic units. The older clastic units could provide insights on the onset of magmatism on this convergent margin and the younger lithologies could have been emplaced during intra-oceanic arc migration. We will focus on the evolution of magma through time, using zircons from the different lithologies found on the island. Old studies from Saint Martin contain K-Ar rock ages ranging from 26 to 37 Ma (Briden et al., 1978; Nagle et al., 1976) and  $^{40}\text{Ar}/^{39}\text{Ar}$  ages centering around 26 Ma (Davidson et al., 1993). Recent studies report zircon ages of  $\approx 30$  Ma and apatite fission track ages of  $\approx 20$  Ma (Noury et al., 2021) geo-thermochronology, chronostratigraphic, and structural analyses highlights the tectono-thermal evolution of the St. Martin granodiorite from its emplacement to its surface exposure. The described vertical motions in this part of the upper plate of the Lesser Antilles subduction zone since 30 Myrs are linked to the migration of the Lesser Antilles volcanic arc toward the plate interior. Results suggest that the St. Martin granodioritic pluton emplaced at 4–5 km depth and underwent a four-step history: (a. Our newly acquired data complement and significantly extend this dataset. Using Laser Ablation Inductively Coupled Plasma Mass Spectrometry, we have dated and analysed trace elements in zircons from 6 key samples and obtained ages from  $\approx 51.3$  to 23.2 Ma, giving us an unprecedented 30 Ma of magmatic history to work with. Using the results, we will try to understand how magmatism evolved through the Oligocene in the Lesser Antilles, as well as during the migration of an intra-oceanic arc. We will also try to link this magmatic history to the tectonic processes that may have taken place during Oligocene in the Lesser Antilles.

**REFERENCES**

- Arculus, R., Gurnis, M., Ishizuka, O., Reagan, M., Pearce, J., & Sutherland, R. (2019). How to Create New Subduction Zones : A Global Perspective. *Oceanography*, 32(1), 160-174. <https://doi.org/10.5670/oceanog.2019.140>
- Briden, J. C., Rex, D. C., Faller, A. M., & Tomblin, J. F. (1978). K-Ar Geochronology and Palaeomagnetism of volcanic rocks in the Lesser Antilles Island Arc. *Philosophical Transactions of the Royal Society of London. Series A, Mathematical and Physical Sciences*.
- Davidson, J. P., Boghossian, N. D., & Wilson, M. (1993). The Geochemistry of the Igneous Rock Suite of St Martin Northern Lesser Antilles. *Journal of Petrology*, 34, 839-S66.
- Nagle, F., Stipp, J. J., & Fisher, D. E. (1976). K-Ar geochronology of the Limestone Caribbees and Martinique, Lesser Antilles, West Indies. *Earth and Planetary Science Letters*, 29(2), 401-412. [https://doi.org/10.1016/0012-821X\(76\)90145-X](https://doi.org/10.1016/0012-821X(76)90145-X)
- Noury, M., Philippon, M., Cornée, J., Bernet, M., Bruguier, O., Montheil, L., Legendre, L., Dugamin, E., Bonno, M., & Münch, P. (2021). Evolution of a Shallow Volcanic Arc Pluton During Arc Migration : A Tectono-Thermal Integrated Study of the St. Martin Granodiorites (Northern Lesser Antilles). *Geochemistry, Geophysics, Geosystems*, 22(12). <https://doi.org/10.1029/2020GC009627>

## P 2.11

# Variations in water saturation state during the build up to the Aso-4 super-eruption

Franziska Keller<sup>1</sup>, Răzvan-Gabriel Popa<sup>1</sup>, Julien Allaz<sup>1</sup>, Nobuo Geshi<sup>2</sup>, Olivier Bachmann<sup>1</sup>

<sup>1</sup> Institute of Geochemistry and Petrology, ETH Zürich, Clausiusstrasse 25, 8092 Zürich ([franziska.keller@erdw.ethz.ch](mailto:franziska.keller@erdw.ethz.ch))

<sup>2</sup> Geological Survey of Japan, AIST, 1-1-1 Higashi, Tsukuba, Ibaraki 305-8567, Japan

Volatile exsolution in upper crustal magma reservoirs plays a key role in the growth of magmatic reservoirs, and can also strongly influence eruptive styles. Using the partitioning behavior of volatile elements between silicic melts, apatite, and an exsolved water-rich volatile phase, we evaluate the pre-eruptive physical state of magmas from pre-Aso-4 explosive eruptions and the subsequent Aso-4 caldera-forming event of the Aso volcanic system (Kyushu, Japan). Apatite is a common accessory mineral in many arc magmas, incorporating most of the major magmatic volatiles (OH, C, F, Cl, and S) in its crystal structure. Previous studies revealed that the measurement of halogens in apatite crystals are a powerful petrological tool to estimate the physical state of water in the magma chamber, complementary to measuring volatiles in melt inclusions, due to (1) the presence of halogens as major structural constituents in apatite along with other minor key elements (e.g., Mg, S, REE) and (2) the strong partitioning of Cl over F in apatite upon exsolution of a water-rich volatile phase.

The implementation of MgO and Ce<sub>2</sub>O<sub>3</sub> contents in apatite as a differentiation index allowed the new interpretation of the F-Cl-OH record in apatite from the Aso-4 and pre-Aso-4 eruptions, indicating water-saturated storage conditions in Aso-4 magmas, as opposed to water undersaturated conditions in the pre-Aso-4 explosive eruptions. Similarly, the volatile contents of melt inclusions and matrix glasses give evidence for volatile outgassing during magma storage in the Aso-4 reservoir, strengthening the hypothesis of volatile exsolution in the magma reservoir prior to the Aso-4 event. Hence, we suggest that the physical state of volatiles in the upper crustal reservoir of the Aso-4 system changed prior to the catastrophic caldera-forming event, recording a transition from water-undersaturated to water-saturated conditions from pre-Aso-4 to Aso-4 magmas, helping the magma chamber to grow to a gigantic size.

## P 2.12

### Melt mixing and transport across the Whale Head Rock contact aureole of the Albany-Fraser Orogen, Western Australia

Moore, J<sup>1</sup>, Gillespie, J<sup>2</sup>, Evans, K<sup>2</sup>, Baumgartner, L. P.<sup>1</sup>

<sup>1</sup> Institute of Earth Sciences, University of Lausanne, UNIL-Mouline, CH-1015 Lausanne, Switzerland

<sup>2</sup> The Institute for Geoscience Research (TIGeR), School of Earth and Planetary Sciences, Curtin University, Perth, WA 6845, Australia

The processes that facilitate the production of granitoids are elucidated by the study of exposed lower crustal sections. The focus of this study is an exposure of the lower crustal portion of Albany-Fraser-Orogen (AFO) of Western Australia. This outcrop, located at Whale Head Rock in the western AFO, preserves the interface between an intrusive body and migmatised sedimentary rocks. Detailed mapping, petrography and thermodynamic modelling are combined to characterize the sources and distribution of melt generations in the aureole. U-Pb dating of zircon indicates that the tonalite crystallisation and a second generation of migmatization of the metapelitic units were coeval at ca. 1.3 Ga. While thermodynamic modelling yields peak conditions of ca. 850°C and 0.5 GPa, in metapelites throughout the area. Metapelites within the contact aureole are retrogressed at upper amphibolite-facies conditions. The contact zone evolves from igneous dominated textures to migmatitic sediments, dominated by concordant, internally derived leucosomes. The distribution of mineral assemblages and mineral chemistry across this section indicates that the mixing between intrusive and internally generated melt is structurally constrained. The back reaction with late stage, more evolved, melts within this mixing zone indicates that it acts as a pathway for continued melt removal and transport. This study represents an outcrop scale model for the complex processes that are involved in the production of granitoids at high temperature, medium pressure conditions. Giving further insight into the generation and extrapolation of melt from thinned crustal settings

## P 2.13

# Growing zircon against all odds – High temperature rhyolites from the Snake River Plain, USA

Kristina M. Noebel<sup>1</sup>, Ben S. Ellis<sup>1</sup>, Olivier Bachmann<sup>1</sup>

<sup>1</sup> Institute for Geochemistry and Petrology, ETH Zurich, Clausiusstrasse 25, 8092 Zurich, Switzerland  
 (kristina.noebel@erdw.ethz.ch)

Despite its occurrence as an accessory phase, zircon contains age, compositional and isotopic information that is commonly used to inform petrologists about magmatic systems. The ignimbrites from the Snake River Plain (SRP), USA, present a rather hostile growth environment for zircon, yet, it is an ubiquitous accessory mineral phase throughout the region. These rocks are characterized by high magmatic temperatures of ~ 900 - 1050°C, zircon saturation temperatures, however, are 100 – 200°C beneath that, rendering the crystallization of zircon in these magmas difficult. Storage temperature and melt composition are considered to be the most important factors influencing zircon saturation, whereas the melt composition parameter is to be divided into the zirconium (Zr) concentration of the melt and the silicate melt polymerization. The latter describes the balance between network-modifying cations (e.g. Na, K, Ca, Mg, Fe<sup>2+</sup>) and silicate melt network formers (Si, Al), usually expressed as a simplified single compound parameter,  $M$  being the classical one (Watson and Harrison, 1983). For two systems with the same temperature, the one with the lower  $M$  also requires a lower Zr content to reach zircon saturation and vice versa (Szymanowski et al., 2020). Different studies optimized the melt parameter, and focus on a potential local Zr-saturated layer around growing phenocrysts, which offers an environment for zircon to crystallize. This applies if the growth rate of a low  $Kd^{Zr}$  mineral is < 0.2 and faster than the diffusion rate of the rejected  $Zr^{4+}$ . Additionally, the melt movement has to be weak enough to not destroy these fragile Zr-enriched zones, which is more likely, the higher the crystallinity of the magma is (Bacon, 1989; Bea et al., 2022).

Bea et al., (2022) showed via numerical modelling that zircon crystallization in Zr-saturated boundary layers is quite possible in Mid Atlantic Ridge Basalts. Here, we try to apply the hypothesis and investigate potential local saturation zones in high silica (~ 75 wt.% SiO<sub>2</sub>) and high temperature ignimbrites.

With its low abundance in most magmatic rocks, zircon is typically concentrated via crushing and heavy liquid separation. While this efficiently produces a zircon separate, it acts to remove all petrographic evidence on the crystallization environment. To obtain the petrographic context of the zircons, we chose one of the largest and youngest eruptions of the SRP, the Castleford Crossing Ignimbrite (zircon U/Pb laser age of 8.409 ± 0.13 Ma, prepared by traditional mineral separation), to conduct element maps of thin sections applying WDS mapping tools of an electron microprobe. This unit is, for this region, highly crystalline (20 – 25 %) and analyses of several Zr maps show an average of 70 zircon crystals of various sizes (15 µm – 150 µm) per thin section. Out of these, approximately 70 % grow attached to or as inclusions in phenocrysts, which are typically oxides or plagioclase. This is in good agreement with the suggested process of a local saturation interface created around growing phenocrysts. Zircons and their adjacent/host mineral will be analysed for their trace elements and in-situ ages and the zircon saturation model from Crisp and Berry (2022) will be applied, to test this hypothesis and determine the extent of potential boundary zones.

## REFERENCES

- Bacon, C.R., 1989. Crystallization of accessory phases in magmas by local saturation adjacent to phenocrysts. *Geochimica et Cosmochimica Acta*, 53(5): 1055-1066
- Bea, F. et al., 2022. Zircon crystallization in low-Zr mafic magmas: Possible or impossible? *Chemical Geology*, 602:120898.
- Crisp, L.J., Berry, A.J., 2022. A new model for zircon saturation in silicate melts. *Contributions to Mineralogy and Petrology*, 177(7): 1-24.
- Watson, E.B., and Harrison, T.M., 1983. Zircon saturation revisited: Temperature and composition effects in a variety of crustal magma types: *Earth and Planetary Science Letters*, 64(2), 295-304.
- Szymanowski, D., Forni, F., Wolff, J. A., & Ellis, B.S., 2020. Modulation of zircon solubility by crystal-melt dynamics. *Geology*, 48(8), 798-802.

**P 2.14****Petrological study of metapelitic granulites from Serre lower crust, Calabria, Italy**

Luca Pacchiega<sup>1</sup>, Bernardo Cesare<sup>2</sup>, Omar Bartoli<sup>2</sup>, Horst Marschall<sup>3</sup>

<sup>1</sup> Institut of Geological Sciences, University of Bern, Baltzelstrasse 1-3, CH-3012 Bern, Switzerland

(luca.pacchiega@geo.unibe.ch)

<sup>2</sup> Dipartimento di Geoscienze, Università degli Studi di Padova, Via G. Gradenigo 6, 35131, Padova, Italy

<sup>3</sup> Institut für Geowissenschaften, Goethe Universität, Altenhöferallee 1, 60438, Frankfurt am Main, Germany

This study investigates residual metapelitic granulites belonging to the lower crustal section exposed in the Serre Massif (Calabria, Italy). The aim is to unveil their metamorphic evolution during the Variscan orogeny, when this crustal section underwent widespread anatexis and melt extraction (Schenk 1984). This research reports the first application of the Zr-in-rutile thermometer for this lower crustal terrane. The rutiles included in garnet cores record prograde temperatures from 630 to 780 °C, linked to anatexis of the rock. The rutiles included in garnet rims record temperatures of ~850 °C, corresponding to the metamorphic peak. The rutiles in the rock matrix, which were affected by Zr diffusional resetting during cooling, record temperatures of ~700-800 °C. Additionally, the trace element composition of rutile has been characterized by EPMA and LA-ICPMS. Nanogranitoids (NG), i.e., droplets of anatexic silicate melt trapped during incongruent melting (Cesare et al. 2015), and multiphase inclusions (MI, Carvalho et al. 2020) have been found in peritectic garnets. Both types of inclusions have been microstructurally and chemically characterized. They are of primary origin and they were simultaneously trapped during partial melting within garnet. MI contain a fluid with variable proportions of CO<sub>2</sub>, CH<sub>4</sub> and N<sub>2</sub>. The coexistence of NG and MI attests for carbonic fluid-present anatexis of the Serre lower crust. EPMA compositional maps of garnet grains (Figure 1) revealed further details about the mode of entrapment of the inclusions at the onset of partial melting.

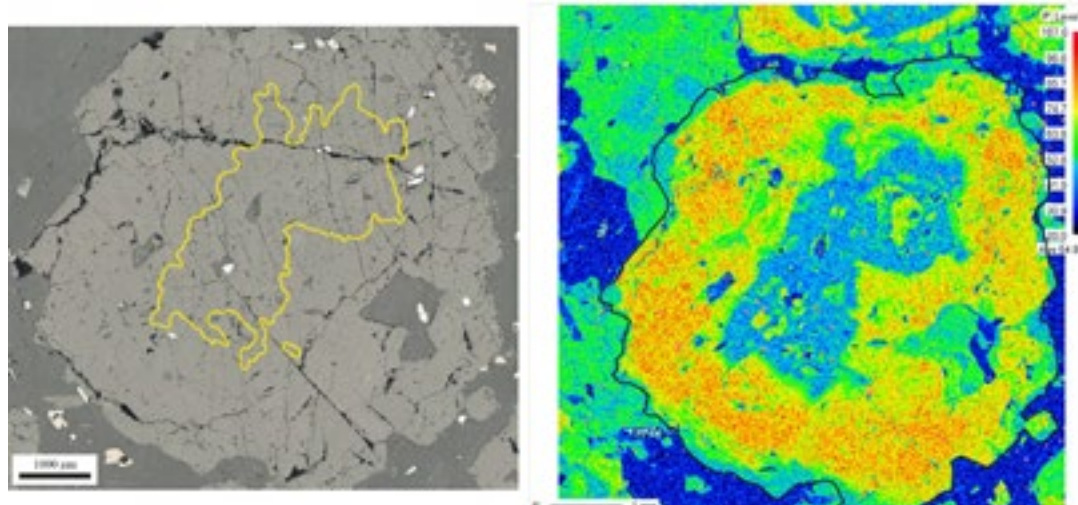


Figure 1. Left: reflected light photomicrograph of a garnet crystal. The yellow line marks the perimeter of the inclusion-rich core. Right: Phosphorous chemical map of the same garnet.

**REFERENCES**

- Carvalho B.B., Bartoli O., Cesare B., Tacchetto T., Gianola O., Ferri F., Aradi L.E. & Szabó C. 2020: Primary CO<sub>2</sub>-bearing fluid inclusions in granulitic garnet usually do not survive. *Earth Planet Sci. Lett.* 536, 116-170.
- Cesare, B., Acosta-Vigil, A., Bartoli, O. & Ferrero, S. 2015: What can we learn from melt inclusions in migmatites and granulites? *Lithos*, 239, 186-216.
- Schenk, V. 1984: Petrology of felsic granulites, metapelites, metabasics, ultramafics, and metacarbonates from Southern Calabria (Italy): Prograde metamorphism, uplift and cooling of a former Lower Crust. *J. Petrol.* 25, 255-298.

## P 2.15

# Chronology of dehydration/hydration reaction in the subducted oceanic lithosphere recorded by chlorite-schists

Francesca Piccoli<sup>1</sup>, Daniela Rubatto<sup>1</sup>, Leo J. Millonig<sup>2</sup>

<sup>1</sup> Institut für Geologie, University of Bern, Baltzerstrasse 3, CH-3012 Bern (francesca.piccoli@geo.unibe.ch)

<sup>2</sup> Departement of Geology, Goethe-University Frankfurt, Altenhöferallee 1, 60438 Frankfurt am Main, Germany

Tracking in time fluid pulses liberated from subducting serpentinites is a challenging task. Two main challenges are finding suitable mineral for geochronology and determining the spatial relations between fluid source, i.e. serpentinites, and metasomatic rocks. Moreover, dehydration can be diachronous within a unit. Hence, the knowledge of the timing of dehydration within large oceanic units can shed light on their  $P-T-t$  evolution and on potential differences of subduction rates and/or thermal regimes. In this study, we investigate several geochronometers in metasomatic rocks, i.e. chloritized rodingites and mafic dykes, that are embedded within dehydrating serpentinites from the Zermatt-Saas unit (Unter Theodulgletscher unit and Pfwulve pass). We make use of petrological, geochemical and geochronological data on garnet, titanite, rutile and zircon in chloriteschists to constrain the timing of dehydration/hydration reaction and the characteristics of serpentinite derived fluids at the source. In the investigated samples from the Unter Theodulgletscher unit, a first generation of garnet is consumed during chloritization, while a second garnet generation grows in textural equilibrium with chlorite and titanite. U-Pb dating of garnet core and rim, returned overlapping ages between 44 and 46 Ma. Garnet veinlets cutting across the foliation of the blackwall are instead resolvably younger and yield an age of ca. 38-39 Ma. Titanite formation is petrographically linked to the chloritization reaction and consumption of garnet cores, which are Ti-rich andradites. Titanite from this lithology yields an age of ca. 45 Ma, which indicates that fluid release and chloritization occurred at peak conditions. Zircon in chlorite-schists from Pfwulve displays a preserved magmatic core and a recrystallized metamorphic rim. In situ U-Pb analyses returned a Jurassic age for the zircon cores and an Alpine age for the rims of ca. 47 Ma. Rutile yields a younger age of ca. 34 Ma, probably linked to re-setting during exhumation. The consistency of our multi-mineral geochronological data indicates that petrochronology of chloriteschists is a robust way to track in time fluid pulses in the subducted slab and that in the case of the Zermatt-Saas unit, serpentinite dehydration and metasomatism was coeval at the km-scale.

## P 2.16

### Mt Etna as Melts from the Low Velocity Zone

Sebastien Pilet<sup>1</sup>, Jules Reymond<sup>1</sup>, Laetitia Rochat<sup>1</sup>, Rosa Anna Corsaro<sup>2</sup>, Massimo Chiaradia<sup>3</sup>, Luca Caricchi<sup>3</sup>, Othmar Müntener<sup>1</sup>

<sup>1</sup> Institute of Earth Sciences, University of Lausanne, Switzerland

<sup>2</sup> Istituto Nazionale di Geofisica e Vulcanologia (INGV-OF), Catania, Italy

<sup>3</sup> Department of Earth Sciences, University of Geneva, Switzerland

Mt Etna is one of the most active volcanoes on Earth, but Mt Etna differs from other giant active volcanoes in subduction zones or oceanic islands by the eruption of large volumes of alkaline lavas. Volcanism at Mt Etna has been associated with a slab window caused by the roll back of the Ionian slab producing mantle upwelling and melting. However, the opening of a slab window does not explain how large volumes of highly enriched alkaline magmas are generated, neither why Mt Etna activity starts by the emission of small volume of tholeiitic lavas. Here, we show that the formation of Mt Etna is the result of focusing and extraction of pre-existing low-degree melts from the base of the subducting plate. The presence of low degree melt at the base of the lithosphere is supported by various geophysical studies to explain the seismic and electric properties of this critical zone which decouple rigid lithospheric plate from the weak asthenosphere. We use geochemical data and modelling to show that extraction of such low degree melts coupled with melt-peridotite reaction during the transport of melt within the lithospheric mantle satisfies the temporal, compositional, volatile and volumetric constraints of lavas from Mt Etna. This hypothesis provides a self-consistent mechanism to link Mt Etna with the formation of Hyblean plateau lavas on the northern margin of the African plate. Mt Etna maybe a unique place where melts from the seismic Low Velocity Zone are extracted to the surface.

## P 2.17

# Attenuated Total Reflectance Fourier Transform Infrared Spectroscopy (ATR-FTIR) for a quick characterization of garnet

Julien Reynes<sup>1,2</sup>, Jörg Hermann<sup>2</sup> and Pierre Lanari<sup>2</sup>

<sup>1</sup> Institute of Earth Sciences, University of Lausanne, Geopolis building, CH-1015 Lausanne

<sup>2</sup> Institute of Geological Sciences, University of Bern, Baltzerstrasse 1+3, CH-3012 Bern

Garnet is a very common rock-forming mineral on Earth with various solid solutions that occurs in metamorphic and mantle rocks with rare occurrences in igneous rocks and even in sediments as detrital fragments. This semi-precious mineral has an economic interest as abrasive material for the industry and is widely used in jewelry. Its price mainly varies according to its optical and physical properties and colours, which are strongly bound to its composition. Quick chemical identification of material is usually achieved using vibrational spectroscopy. If Raman spectroscopy is usually privileged for minerals, ATR-FTIR can also be well suited for a quick characterization of minerals.

ATR-FTIR spectroscopy is an internal reflection-based method. The sample is placed in contact to an ATR sensor (diamond or germanium crystal with a flat tip) that has an index of refraction that is significantly higher than the one of the sample. The sensor acts as a waveguide, internally reflecting the light multiple times at the sample surface. This reflectance causes an evanescent wave that extends beyond the sample surface and penetrate the sample with a depth of 0.5-5 µm. IR radiation absorbed by the sample will cause the wave to be attenuated, and an IR absorbance spectrum is recorded. The method is now widely used in the industry for the chemical analysis of liquids and solids, but its potential applications to mineralogy are still underdeveloped.

In this study, a set of more than 60+ gem-quality garnets of various composition (including near endmember composition) have been measured using ATR-FTIR and electron probe micro-analyser (EPMA). The suite of measured spectra was compared to quantitative analyses from EPMA in order to evaluate the chemical information recorded in the IR spectrum. Up to 9 characteristic bands (B9-B1) are identified in the mid infrared region (1000-360 cm<sup>-1</sup>). The band positions are shifted systematically from high wavenumbers to low wave numbers in the order pyrope-almandine-spessartine-grossular-andradite. The shift of the highest band B9 (960-877 cm<sup>-1</sup>) is linearly correlated with the unit cell parameter, giving a good proxy on the garnet composition. Additional information is recorded by the low wavenumbers bands.

Position of B1 (470-427 cm<sup>-1</sup>) and B2 and (420-360 cm<sup>-1</sup>) are linearly shifting with grossular and andradite molar endmember proportions (for calcium-rich garnets). Similarly, position of B6 (650-580 cm<sup>-1</sup>) is linearly shifting with pyrope, almandine and spessartine endmember proportions (for pyrope-almandine-spessartine garnets). Therefore, the composition of garnet can be quickly evaluated from the position of the bands in the ATR-FTIR spectrum.

ATR-FTIR spectroscopy provides a good proxy for the garnet composition, and a fast and non-destructive identification of garnet gems with low-cost equipment and minimal sample preparation.

**P 2.18****Shear-driven formation of olivine veins by dehydration of ductile serpentinite: a numerical study with implications for transient weakening**

Stefan M. Schmalholz<sup>1</sup>, Evangelos Moulas<sup>2</sup>, Ludovic Raess<sup>3,4</sup>, Othmar Muenter<sup>1</sup>

<sup>1</sup> Institute of Earth Sciences, University of Lausanne, 1015 Lausanne, Switzerland (stefan.schmalholz@unil.ch)

<sup>2</sup> Institut of Geosciences and Mainz Institute of Multiscale Modeling (M3ODEL), Johannes Gutenberg University of Mainz, Germany

<sup>3</sup> Laboratory of Hydraulics, Hydrology and Glaciology (VAW), ETH Zurich, Zurich, Switzerland

<sup>4</sup> Swiss Federal Institute for Forest, Snow and Landscape Research (WSL), Birmensdorf, Switzerland

Serpentinite subduction and the associated formation of dehydration veins is important for subduction zone dynamics and water cycling. Field observations suggest that en-echelon olivine veins in serpentinite mylonites formed by dehydration during simultaneous shearing of ductile serpentinite. Here, we test a hypothesis of shear-driven formation of dehydration veins with a two-dimensional hydro-mechanical-chemical numerical model. We consider the reaction antigorite + brucite = forsterite + water. Shearing is viscous and the shear viscosity decreases exponentially with porosity. The total and fluid pressures are initially homogeneous and in the antigorite stability field. Initial perturbations in porosity, and hence viscosity, cause fluid pressure perturbations. Dehydration nucleates where the fluid pressure decreases locally below the thermodynamic pressure defining the reaction boundary. Dehydration veins grow during progressive simple-shearing in a direction parallel to the maximum principal stress, without involving fracturing. The porosity evolution associated with dehydration reactions is controlled to approximately equal parts by three mechanisms: volumetric deformation, solid density variation and reactive mass transfer. The temporal evolution of dehydration veins is controlled by three characteristic time scales for shearing, mineral-reaction kinetics and fluid-pressure diffusion. The modelled vein formation is self-limiting and slows down due to fluid flow decreasing fluid pressure gradients. Mineral-reaction kinetics must be significantly faster than fluid-pressure diffusion to generate forsterite during vein formation. The self-limiting feature can explain the natural observation of many, small olivine veins and the absence of few, large veins. We further discuss implications for transient weakening during metamorphism and episodic tremor and slow-slip in subduction zones.

## P 2.19

# Deep Electrical Resistivity Tomography as an exploration tool to decipher the architecture of the Calamita distal Fe-skarn deposit, Elba Island (Italy)

Braize Damian<sup>1</sup>, Sfalcin Julien<sup>1</sup>, Lupi Matteo<sup>1</sup>, Kouzmanov Kalin<sup>1</sup>, Dini Andrea<sup>2</sup>

<sup>1</sup> Department of Earth Sciences, University of Geneva, Rue des Maraîchers 13, CH-1205, Genève  
(damian.braize@etu.unige.ch; julien.sfalcin@etu.unige.ch)

<sup>2</sup> Istituto di Geoscienze e Georisorse, CNR, 56124 Pisa, Italy

The deposit of Calamita, on the south-eastern coast of Elba Island, Italy, is a distal Fe-skarn containing massive magnetite-hematite ore bodies hosted in marbles and micaschists from the Tuscan Units. Skarn and ore formation at Calamita matches with the waning stage of the Miocene magmatism on Elba and shares peculiarities with several other Fe-skarn deposits on the island, formed during the post-collisional extension of the Apennine orogenic belt. To date, no genetic or spatial link between the Calamita deposit and a potential causative intrusion has been established.

In this project, a DERT (Deep Electrical Resistivity Tomography) 2D survey has been carried out to study the subsurface geology of the deposit based on a resistivity and IP modelling. 37 injections were performed on 25 cableless IRIS Fullwavers over a 4-kilometers linear profile, using an hybrid dipole-dipole configuration. Geophysical data are combined with a high-resolution 3D Digital Elevation Model acquired by standard and thermal drone imagery. In parallel, we conducted geological surveying in the region, identifying major faults and lithologies.

The resistivity profile correlates well with the surface geology, based on the electrical conductivities of the rocks. Chargeability model fits with the outcropping ore bodies and indicates the presence of hidden mineralization. The model is reliable until 200 meters depth and progressively loses resolution until 500 m depth.

The obtained model allows us to draw several conclusions: (1) The main ore body is constrained in depth by sharp lithological transitions; (2) The results are the first encouraging example of DERT applied to ore deposits carried on with such an innovative technology. We are planning a further full-3D DERT acquisition at the Calamita deposit to calculate ore body volumes and to establish the possible usage of the Fullwaver technology as a new exploration tool for mineral resources.

## REFERENCES

- Gance, J., Leite, O., Texier, B., Bernard, J., Truffert, C., & Instruments, I. 2018: The Fullwaver systems : Distributed network of autonomous devices for deep 3D electrical resistivity and induced polarization survey. *EGU General Assembly Conference Abstracts*, 20, 12569.
- Tanelli, G., Benvenuti, M., Costagliola, P., Dini, A., Lattanzi, P., Mainieri, C., Mascaro, I., & Ruggieri, G. (2001). The iron mineral deposits of Elba island : State of the art. *Ofioliti*, 26(2a), 239-247.

## P 2.20

# Molecular scale understanding of cation adsorption on swelling clay minerals

Vasyl Stotskyi<sup>1,2</sup>, Fulvio Di Lorenzo<sup>1</sup>, Maria Marques Fernandes<sup>1</sup>, Matthias Krack<sup>1</sup>, Andreas Scheinost<sup>3</sup>, Martine Lanson<sup>4</sup>, Bruno Lanson<sup>4</sup> and Sergey V. Churakov<sup>1,2</sup>

<sup>1</sup>Paul Scherrer Institut (PSI), Laboratory for Waste Management, CH-5232 Villigen PSI, Switzerland, vasyl.stotskyi@psi.ch

<sup>2</sup>Institute of Geology (IfG), University of Bern, Baltzerstrasse 3, CH-3012 Bern, Switzerland

<sup>3</sup>Helmholtz-Zentrum Dresden-Rosendorf, Institute of Resource Ecology D-01328 Dresden, Germany

<sup>4</sup>Univ. Grenoble Alpes, Univ. Savoie Mont Blanc, CNRS, IRD, Univ. Gustave Eiffel, ISTerre, F-38000 Grenoble, France

In nature, clay minerals act as a chemical sink for dissolved micronutrients and pollutants thanks to their high sorption capacity and low permeability. Therefore, they are commonly used in the construction of engineered disposal facilities for hazardous materials, such as radioactive waste. The assessment of risks associated with the mobilization of metal contaminants in argillaceous environments relies on a detailed understanding of their retention mechanisms on natural minerals (Bradbury & Baeyens 1997; Dähn et al. 2011; Churakov & Dähn 2012). This knowledge is essential to developing reliable and robust predictive transport models. Despite decades of research on metal adsorption onto clay minerals, there are still substantial knowledge gaps in understanding the mechanism of ion uptake on specific adsorption sites.

The 2SPNE SC/CE model from Bradbury & Baeyens (1997) postulates the existence of two types of surface complexation sites on 2:1 clay minerals (such as illite and montmorillonite) for divalent and trivalent metals. So-called "strong" sites have a high affinity, but low capacity, while "weak" sites have a high capacity, but low affinity. The existence of both sites on edge surfaces of montmorillonite was confirmed first by Dähn et al. (2011) using X-ray absorption spectroscopy (XAS), and later by Churakov & Dähn (2012) through the linear fitting of reference spectra generated by ab initio MD simulations.

Our project aims to improve the understanding of sorption mechanisms of common di- and trivalent elements ( $Zn^{2+}$ ,  $Ni^{2+}$ ,  $Lu^{3+}$ ) on clay mineral surfaces and, hence, improve thermodynamic sorption models by using advanced atomistic simulations and X-ray absorption spectroscopy for quantitative description of sorption processes. To improve the understanding of retention processes we use synthetic saponite, it has almost zero impurities and, if necessary, we can easily modify its structural composition. Compare to other smectites, saponite has a talc-like structure, where Al partially substitutes Si in tetrahedral positions, while octahedral positions are fully occupied by Mg.

Adsorption behavior of  $Ni^{2+}$  and  $Lu^{3+}$  on saponite resembles the adsorption of these elements on montmorillonite (Marques Fernandes & Baeyens 2020) (non-linear shape of the isotherms), suggesting the existence of at least two different sorption sites (or mechanisms). Based on this, samples with strong and weak sites prevailing were prepared and measured using XAS. The recorded spectra confirm the existence of two structurally different sorption sites on saponite for Lu (see Fig.1). In the case of  $Ni^{2+}$  sorption, we observed the formation of a new Ni-LDH-like phase on the surface at moderate Ni loadings (40 mmol/kg).

It was reported by Fink et al. (2015) that lanthanides and actinides can be incorporated into hectorite structure in course of recrystallization. Since sorption occurs at the surface-water interface, the reference spectra of doped saponite will help us to distinguish different sorption sites due to their stronger or weaker bonding strength. Therefore, we tried to synthesize saponite with the incorporation of small quantities of Ni and Lu. Our XAS measurements show, that Ni can be incorporated, while Lu cannot (see Fig.1).

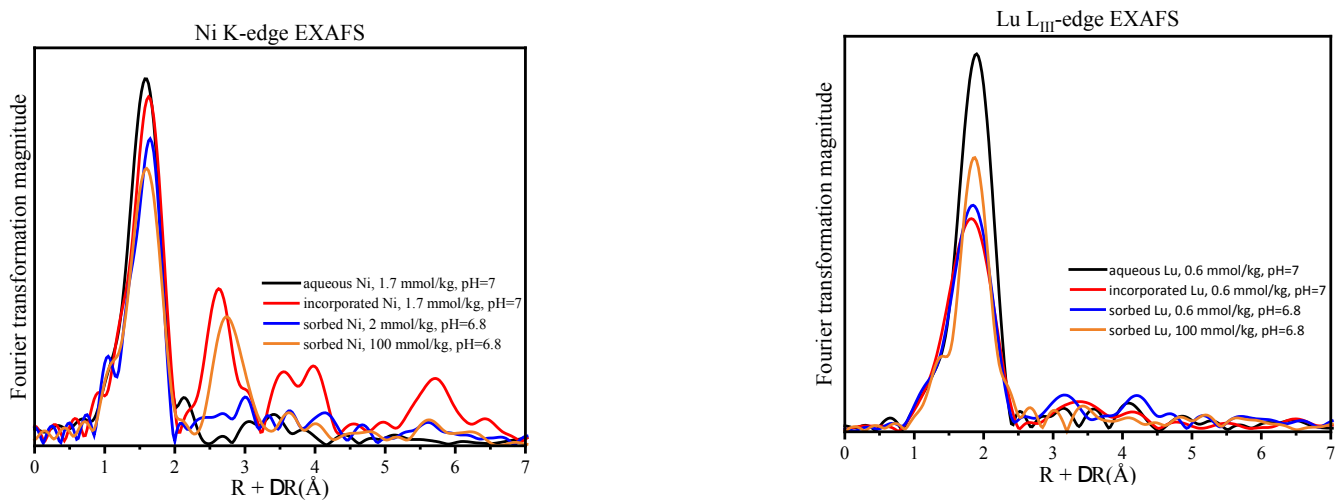


Figure 1. Measured EXAFS spectra for Ni (left) and Lu (right) samples.

The most stable surfaces and their geometries were determined using geometry optimization. Further, edge surface-water interfaces were constructed for the most stable surfaces to simulate cation adsorption.

To justify the accuracy of the model, Zn-Ni cation exchange reactions between weak and strong sites on (100) and (130) edges of saponite were simulated and free energies were obtained (it was shown that sorption of divalent elements on smectites is a fully competitive reaction (Marques Fernandes & Baeyens 2020) and, hence, follows trends calculated using thermodynamic sorption model). Since experimental values are being currently investigated, we used results obtained for montmorillonite as a trustworthy proxy. Theoretical values obtained for Zn-Ni exchange on saponite are equal to 14.6 and 5.8 kJ/mol for (100) and (130) surfaces, respectively. The experimental value obtained for the same reaction on montmorillonite is 9.1 kJ/mol. Considering good agreement between two systems, this suggests a stronger affinity of Zn to strong sites than Ni, i.e. in case Ni is adsorbed on strong sites, Zn is capable to substitute all Ni atoms.

## REFERENCES

- Bradbury M.H. and Baeyens B. 1997: A mechanistic description of Ni and Zn sorption on Na- montmorillonite Part II: modelling. *J. Contam. Hydrology* 27, 223-248.
- Dähn R., Baeyens B., and Bradbury M.H. 2011: Investigation of the different binding edge sites for Zn on montmorillonite using P-EXAFS – The strong/weak site concept in the 2SPNE SC/CE sorption model. *Geochimica et Cosmochimica Acta* 75, 5154-5168.
- Churakov S.V. and Dähn R. 2012: Zinc adsorption on clays inferred from atomistic simulations and EXAFS spectroscopy. *Environ. Sci. & Technol.* 46, 5713-5719.
- Marques Fernandes M. and Baeyens B. 2020: Competitive adsorption on illite and montmorillonite: Experimental and modelling investigations. Nagra Technical Report 19-05.
- Finck N., Dardenne K., and Geckeis H. 2015: Am(III) coprecipitation with and adsorption on the smectite hectorite. *Chemical Geology* 409, 12-19.

## P 2.21

### Crystal growth versus diffusional re-equilibration in k-feldspar

Aurore Toussaint, Thomas Grocolas, and Othmar Müntener

*Institute of Earth Sciences, University of Lausanne, 1015 Lausanne, Switzerland (aurore.toussaint@unil.ch)*

Diffusion and crystal growth are key processes to understand magma dynamics, and thus the evolution of igneous systems to extract crucial information on residence times, crystal growth timescales or cooling rates (e.g., Costa et al., 2020, Costa 2021). As k-feldspar is a major mineral in felsic plutonic rocks and sometimes exceeds 30 vol%, investigating k-feldspar provides valuable information on magma dynamics. K-feldspar has been used to determine timescales of crystal growth or residence times for volcanic and plutonic systems, although to a lesser extent for the latter (e.g., Moore & Sisson 2008, Rout et al., 2021).

As chemical zoning (e.g., Ba zoning) is commonly observed in k-feldspar megacrysts, this makes them ideal targets for studying and developing methods to distinguish crystal growth from diffusional re-equilibration. Therefore, our study focuses on the investigation of trace element chemistry and zoning patterns (EPMA, LA-ICP-MS analyses and high-resolution imaging) of k-feldspar megacrysts using samples from Sierra Nevada (United States), Bergell (Italy/Switzerland), and Sardinia (Italy) to unravel coupled growth and/or diffusion patterns. The preliminary results on k-feldspar zoning from the different samples show Ba zoning preserved despite perthite exsolutions (Sierra Nevada, Bergell), with an average of 7 to 10 zones of random spacing and thickness (80 to 700 $\mu$ m) per crystal. Petrography and EPMA data highlight three different features. (1) Sawtooth chemical profiles encompassing textural growth patterns combined with Ba zoning and a more evolved composition towards the borders (more K-rich zones, as commonly observed with fractional crystallization) correlated with the zones of higher Ba composition (Sierra Nevada, Bergell). (2) Sawtooth and relaxed step-function profiles (potentially related to diffusion) when megacrysts display textural growth patterns associated to Ba zoning essentially (Sierra Nevada, Bergell). (3) No obvious zoning on high-resolution maps but relaxed step-function profiles within single crystals (Sardinia). (1) and (2) could be observed within a single rock sample. In addition to Ba zoning, there are various mineral inclusions related to Ba zoning (zoned plagioclase, biotite – Sierra Nevada, Bergell – amphibole and titanite – Sierra Nevada) that are located on and parallel to the growth planes, correlated to Ba-rich zones. On the contrary, inclusions (mostly zoned plagioclase and biotite) are  $\pm$ randomly distributed within k-feldspar from Sardinia. Ultimately, we aim to quantify k-feldspar growth times by coupled-growth and diffusion and comparing the results to absolute growth times derived from U-Pb dating of zircons (e.g., Barboni and Schoene 2014).

## REFERENCES

- Barboni, M., & Schoene, B. (2014). Short eruption window revealed by absolute crystal growth rates in a granitic magma. *Nature Geoscience*, 7(7), 524-528.
- Costa, F. (2021). Clocks in magmatic rocks. *Annual Review of Earth and Planetary Sciences*, 49, 231-252.
- Costa, F., Shea, T., & Ubide, T. (2020). Diffusion chronometry and the timescales of magmatic processes. *Nature Reviews Earth & Environment*, 1(4), 201-214.
- Moore, J. G., & Sisson, T. W. (2008). Igneous phenocrystic origin of K-feldspar megacrysts in granitic rocks from the Sierra Nevada batholith. *Geosphere*, 4(2), 387-400.
- Rout, S. S., Blum-Oeste, M., & Wörner, G. (2021). Long-term temperature cycling in a shallow magma reservoir: insights from sanidine megacrysts at Taápaca volcano, Central Andes. *Journal of Petrology*, 62(9), egab010.

## P 2.22

# Tracking fluid flow in subducted serpentinites of the Zermatt-Saas Unit

Michelle Ulrich<sup>1</sup>, Daniela Rubatto<sup>1,2</sup>, Jörg Hermann<sup>1</sup>, Francesca Piccoli<sup>1</sup>

<sup>1</sup> Institut für Geologie, University of Bern, Baltzerstrasse 1+3, CH-3012 Bern ([michelle.ulrich@geo.unibe.ch](mailto:michelle.ulrich@geo.unibe.ch))

<sup>2</sup> Institut Des Sciences de La Terre, University of Lausanne, Quartier Mouline, CH-1015 Lausanne

The chemical and isotopic complexities acquired by serpentinites during oceanic hydration can lead to variability in the fluid released upon subduction metamorphism. We investigated serpentinite samples that underwent the dehydration reaction of brucite + antigorite to produce metamorphic olivine and aqueous fluid. The scope of the study is to determine whether antigorite and olivine reached geochemical and/or isotopic equilibrium, and how this is affected by fluid flow and deformation. Olivine-bearing serpentinites were collected from a continuous, km-scale outcrop between the Upper- and Lower Theodulgletscher (Zermatt-Saas Unit), where dehydration occurred at ca. 2.5 GPa and 550–600 °C (Kempf et al., 2020). Metamorphic olivine textures (static, shear bands and veins) that represent different stages from in-situ fluid production to fluid-related transport and precipitation were analysed in situ for trace elements and oxygen isotopes.

The immobile trace elements Mn and Ni show equilibrium partitioning between olivine and antigorite for all samples. The fluid-mobile element B shows geochemical equilibrium only in more deformed samples from the Upper Theodulgletscher. In the Lower Theodulgletscher samples, increasing deformation and fluid-flux define a trend towards B equilibrium partitioning. Equilibrium in more deformed samples is also recorded by the oxygen isotopic composition of antigorite and olivine. Olivine has homogenous  $\delta^{18}\text{O}$  across the km-scale with low values of 1.2 to 2.3 ‰. However, antigorite shows two distinct isotopic values of  $\delta^{18}\text{O}$  3.9–4.3 ‰ and 5.6–7.3 ‰ for Upper - and Lower Theodulgletscher, respectively. It follows that, at the T of the brucite-out reaction, isotopic equilibrium between antigorite and olivine was mainly recorded by samples from the Upper Theodulgletscher, which generally have stronger mylonitic deformation. In the least deformed portions, the B and O disequilibrium suggests that the precipitation of olivine was induced by external fluids with low  $\delta^{18}\text{O}$ . The homogenous  $\delta^{18}\text{O}$  of the olivine suggests that the fluid released by the dehydration reaction that produced olivine was inter-connected across the studied area.

## REFERENCES

- Kempf, E. et al., 2020: The role of the antigorite + brucite to olivine reaction in subducted serpentinites (Zermatt, Switzerland). Swiss J Geosci, 113, 16.

## P 2.23

# Insights into multistage oceanic serpentinization from *in situ* trace elements and oxygen isotope analysis

Coralie Vesin<sup>1</sup>, Daniela Rubatto<sup>1,2</sup>, Thomas Pettke<sup>1</sup>, Etienne Deloule<sup>3</sup>, Anne-Sophie Bouvier<sup>2</sup>

<sup>1</sup> Institute of Geological Sciences, University of Bern, Bern CH-3012, Switzerland ([coralie.vesin@geo.unibe.ch](mailto:coralie.vesin@geo.unibe.ch))

<sup>2</sup> Institut des Sciences de la Terre, University of Lausanne, Lausanne CH-1015, Switzerland

<sup>3</sup> Centre de Recherches Pétrographiques et Géochimiques (CRPG), CNRS, Université de Lorraine, 54501 Vandoeuvre-lès-Nancy, France

Serpentinization is the major reaction leading to water incorporation into ultramafic rocks of the oceanic lithosphere. The main loci of abyssal serpentinization are mid-ocean ridges (MOR) and extended passive margins (PaMa), where mantle peridotite interacts with seawater. Serpentine forms after olivine in a mesh texture and as bastite after orthopyroxene, and its chemical composition gives insights about the conditions of serpentinization.

To reconstruct the conditions of the multistage serpentinization process, we combined *in situ* trace element and oxygen isotope analyses of serpentine on 13 samples from drill cores: Mid-Atlantic Ridges (Sites 1272A & 1274A), Hess Deep (Sites 895D & 895E) and the conjugate passive margin Newfoundland-Iberia (Sites 1070A & 1277A).

The concentration of transition metals in serpentine tracks the chemical exchange between the different textural sites (i.e. mesh rim, mesh centre, bastite). In the Newfoundland samples, the element redistribution between the mesh and the bastite sites suggests a coeval serpentinization of olivine and orthopyroxene. On the other hand, samples from MOR and the Iberia passive margin likely underwent episodic serpentinization that preserved distinct transition metal concentrations in mesh and bastite, characteristic of their precursor olivine and orthopyroxene.

The fluid-mobile elements Cl and B are taken as proxy for the salinity of the serpentinizing fluid. The fluid composition was likely highly saline for MOR settings serpentinization with Cl/B from 25 to 200, while serpentine in PaMa samples shows Cl/B below 25, independent of textural site. The lowest Cl/B ratio in serpentine is taken to represent interaction with the least evolved hydration fluid composition, thus allowing to calculate the serpentinization temperature with a fair assumption of  $\delta^{18}\text{O}_{\text{fluid}} = 0 \text{ ‰}$ . O isotope composition of MOR samples are comparable between samples, but show within sample variations of up to 6 ‰. The calculated temperatures are 150–290°C. In one PaMa sample,  $\delta^{18}\text{O}$  variations of ~10 ‰ between the textural sites allow reconstructing a cooling history of the sample from 190 to 75°C.

This study illustrates the power of *in situ* analysis to distinguish coeval from episodic serpentinization stages, to characterize aspects of the hydration fluid chemistry (e.g., salinity), and to better quantify the temperature of the reaction. It also shows that the serpentinization process varies significantly, even within a single setting and at the scales of 100 µm.

## P 2.24

# Sulfide geochemistry and sulfur isotope study in subducted hydrous ultramafic rocks

Joana F. Vieira Duarte<sup>1</sup>, Thomas Pettke<sup>1</sup>, Jörg Hermann<sup>1</sup>, Johanna Marin-Carbonne<sup>2</sup>, Francesca Piccoli<sup>1</sup>, Anne-Sophie Bouvier<sup>2</sup>

<sup>1</sup> Institute of Geological Sciences, University of Bern, Baltzerstrasse 3, CH-3012 Bern (joana.vieira@geo.unibe.ch)

<sup>2</sup> Institute of Earth Sciences, University of Lausanne, Géopolis, CH-1015 Lausanne

Oxide and sulfide minerals contained in ultramafic rocks are useful tools to assess the redox conditions of the rock and fluids liberated upon progressive serpentinite dehydration during subduction, as these minerals contain two relevant redox sensitive elements, iron and sulfur. Sulfur is of great importance as it can occur in eight valence states ( $S^{2-}$  to  $S^{6+}$ ), offering an effective way to transfer redox budget from the rock to the serpentinite dehydration fluids.

In this study, we investigate the sulfide mineral assemblages present in ultramafic rocks which underwent an oceanic serpentinitization stage followed by subduction metamorphism to different peak pressure and temperature conditions (650-840°C and 1.6-3.2 GPa). By combining trace element geochemistry obtained by LA-ICP-MS and in-situ sulfur isotope signatures of sulfide minerals measured at the SwissSIMS laboratory we explore the origin and redox conditions of sulfide crystallization.

Results show that despite being an accessory phase (< 0.20 vol.%), sulfides are present in all our samples, suggesting limited S loss during antigorite-dehydration reaction. Pentlandite ± pyrrhotite + magnetite (or chromite) along with peak metamorphic silicate minerals is the stable paragenesis across the different lithologies. Selenium contents in sulfides are used as a tracer for their origin in a given sample; high Se concentrations of ~140 ppm are indicative of a dominant mantle sulfide signature, while lower Se concentrations of ~4-15 ppm reveal significant sulfur addition via abiotic and possibly biotic sulfate reduction upon oceanic hydration. Such variable sulfur sources are consistent with variable in situ sulfide  $\delta^{34}S$  data, ranging between a mantle inherited signature of -3.25 to -1.28 ‰ and an oceanic hydration signature of up to +8.70 ‰. Combined sulfur concentration and isotope ratio results further suggest that sulfides in chlorite-peridotites ( $\delta^{34}S$  values of 1.45 to 5.32 ‰) preserve the signatures of serpentinite protoliths, thus implying small fluid - mineral isotopic fractionation, indicative of prevalence of  $H_2S$  in the escaping dehydration fluids.

## P 2.25

### 20\_0129: a new lunar meteorite from Oman

Anna Zappatini<sup>1</sup>, Beda Hofmann<sup>1,2</sup>, Urs Eggenberger<sup>1</sup>, Edwin Gnos<sup>3</sup>,  
Hussain Al-Ghafri<sup>4</sup>, Muati Almuati<sup>4</sup>

<sup>1</sup> Institute of Geology, University of Bern, Baltzerstrasse 3, CH-3012 Bern ([anna.zappatini@geo.unibe.ch](mailto:anna.zappatini@geo.unibe.ch))

<sup>2</sup> Naturhistorisches Museum Bern, Bernastrasse 15, CH-3005 Bern

<sup>3</sup> Muséum d'histoire naturelle, Route de Malagnou 1, CH-1208 Genève

<sup>4</sup> Ministry of Heritage and Tourism, Al Khuwair, Muscat, Oman

With only 554 out of 77666 recognized meteorites, lunar meteorites make up a small fraction of the meteorites found on Earth (Meteoritical Bulletin Database, 2022). As lunar meteorites have a lower sampling bias than the samples obtained through the Apollo missions, each new lunar meteorite helps to better understand the history of the moon (Gross et al., 2014).

Sample 20\_0129 is a 59.9 g lunar meteorite found during the 2020 Omani-Swiss meteorite search campaign in the Rub' al Khali desert, Dhofar province, Oman. The specimen partially retains a rounded surface formed by ablation during atmospheric entry. It partly shows a fractured surface indicating the existence of additional specimens. A lunar origin was suspected in the field based on bulk Fe/Mn measured with a portable XRF device.

20\_0129 is a fine-grained crystalline impact melt breccia dominated by pyroxene and plagioclase with small amounts of clasts and mineral fragments. Its bright matrix is crosscut by brownish melt veins. The melt veins crosscut shocked plagioclase crystals, indicating multiple shock events. A small external part of the sample contains spherules with radial pyroxene-plagioclase in a dark clastic matrix, probably representing attached lunar regolith. The sample consists of poikilitic plagioclase (60%, 20% thereof transformed to maskelynite), pyroxene (30%), olivine (5%) plus metal and sulfides (5%). Zr-, P- and Al-rich accessory phases were found in a preliminary SEM-EDX examination. The bulk chemistry is consistent with an origin in the feldspathic lunar highlands.

The lunar origin of 20\_0129 is confirmed by the low bulk K/U ratio of 1400 and the intermediate Mn/Fe ratio of 67 (Korotev, 2005), based on LA-ICP-MS analyses. The mineral chemistry is quantified by electron microprobe analyses, while noble gas analyses will provide information on the exposure history and pairing. Dating of Zr minerals using U-Pb geochronology and <sup>40</sup>Ar/<sup>39</sup>Ar dating of plagioclase will help to infer the timing of the impacts observed in the sample.

## REFERENCES

- Gross, J., Treiman, A. H., & Mercer, C. N. 2014: Lunar feldspathic meteorites: Constraints on the geology of the lunar highlands, and the origin of the lunar crust. *Earth and Planetary Science Letters*, 388, 318–328.  
Korotev, R. L. 2005: Lunar geochemistry as told by lunar meteorites. *Geochemistry*, 65, 297–346.



### 3 Stable and radiogenic isotope geochemistry

Nicolas David Greber, Afifé El Korrh, Andres Rüggeberg, Johanna Marin-Carbonne

*Swiss Society of Mineralogy and Petrology (SSMP)*

#### TALKS:

- 3.1 Ahmad Q., Wille M., König S., Rosca C., Pettke T., Hermann J.: Barium recycling at the Tongan subduction zone revisited
- 3.2 Brown A., Roebbert Y., Sato A., Abe M., Weyer S., Bernier-Latmani R.: Fractionation of U isotopes during bacterial reduction
- 3.3 Carrasco H., Spikings R.: Geochronological, geochemical and isotopic characterisation of the Mesozoic (160 – 110 Ma) Andean margin within Ecuador
- 3.4 Chatterjee S., Ravindran A., Ahmad Q., Wille M., Mezger K., Prakash Pandey O.: Dykes trace sediment subduction in the Archean
- 3.5 Clavijo-Arcos R.E., Clarkson M.O., Vance D., Bernasconi S., Guillong M., Sial A.N., Müller M.N., Correia O., Shalev N.: Ancient microbially-influenced dolomites as chronologic archives of global geologic records? – Insights using LA-ICP-MS U-Pb geochronology from a post-Sturtian cap dolomite, Brazil
- 3.6 de Carvalho C.F.M., Lehmann M.F., Pati S.: Uncovering the drivers for the variability in isotope fractionation of O<sub>2</sub> during enzymatic reactions
- 3.7 Decraene M-N., Marin-Carbonne J., Thomazo C., Brayard A., Bouvier A-S., Bomou B., Adatte T., Olivier N.: Pyrite iron isotope compositions track local sedimentation conditions through the Smithian-Spathian transition (Early Triassic, Utah, USA)
- 3.8 Dupeyron J., Decraene M.-N., Marin-Carbonne J., Busigny V.: Ferric iron was the dominant source of sedimentary pyrite from Archean to Paleoproterozoic: insights from in situ Fe isotope compositions
- 3.9 Gillespie J., Kinny P.D., Cavosie A.J., Kirkland C.L., Martin L., Roberts M.P., Aleshin M., Fougerouse D., Quadir Z., Nemchin A.A.: Crustal growth and reworking in the early Archean Narryer Terrane: new evidence from strontium isotopes in apatite inclusions
- 3.10 Kirichenko Y., Rickli J.D., Bontognali T.R.R., Shalev N.: Understanding stable Sr isotope fractionation associated with gypsum precipitation
- 3.11 Kruttsch P.M., Anand A., Storck J.-C., Greber N., Mezger K.: The accretion history of the ureilite parent body: Constraints from Cr and Ti isotope anomalies
- 3.12 Schaltegger U., Gaynor S.P., Ruiz M.: Complex single-zircon, high-precision U-Pb dates – what is the accurate scientific interpretation?
- 3.13 Zakharov D., Zozulya D., Colón D., Daniela Rubatto D.: Neoarchean surface conditions recorded in the 2.67 Ga low-δ<sup>18</sup>O magmatic-hydrothermal system from the Kola Peninsula

## POSTERS:

- P 3.1 Baconnais I., Holmden C.: Transport of anomalously fractionated chromium isotopes from shelf to basin in the Canadian Arctic Ocean
- P 3.2 Bovay T., Marin-Carbonne J., Bouvier A-S., Kouzmanov K. , Greber ND., Saitoh M., Marger K., Berger A.: Development of sphalerite as a standard for sulfur isotope analysis by SIMS
- P 3.3 Edward O., Leu M., Dudit L., Le Houedec S., Bucher H., Baud A., Vérard C., Vennemann T.: Latest Permian to Early Triassic (Spathian) integrated carbon, strontium and neodymium isotope chemostratigraphy from Oman exotic blocks
- P 3.4 Gilliard D., Janssen D.J., Schuback N., Jaccard S.L.: Variability in seawater Cr concentration and stable isotope composition along Atlantic Meridional Transect 29 (AMT29)
- P 3.5 Müller I.A., Messori F., Guillong M., Peyrotty G., Samankassou E., Linnemann U., Hofmann M., Zieger J., Martignier A., Bouvier A.-S., Venneman T., Kouzmanov K., Ovtcharova M.: The negative carbon isotope excursion at the onset of the Ediacaran Nama Group in Namibia
- P 3.6 Senger M.H., Greber N.D.; Davies J.F.H.L., Schaltegger U.: Molybdenum isotopes in the ~2.48 Ga-old Kuruman Formation, South Africa
- P 3.7 Kramer J., Vennemann T.: Hydrology of the Blausee – Mitholz area drainage basin and its sensitivity to potential sources of pollution: constraints from chemical and isotopic compositions of sediments and waters
- P 3.8 Luz Z., Leu M., Edward O., Baud A., Bucher H., Vennemann T.: Climate cooling event in the Early Triassic subtropics
- P 3.9 Mazzoli A., Piantoni C.T., Paulus T.J., Callbeck C.M., Zopfi J., Frey C., Lehmann M.F.: Have we been calculating benthic nitrogen fluxes wrong? A comparison of porewater sampling methods in two Swiss lakes
- P 3.10 Paulus T.J. , Mazzoli A., Frey C., Zopfi J., Callbeck C., Lehmann M.F.: Isotope effect of benthic N removal in two Swiss lakes
- P 3.11 Yining L., Wenhui L., Netta S.: Magnesium isotope signature of Middle Ordovician dolomites from the Ordos Basin, China3.

### 3.1

## Barium recycling at the Tongan subduction zone revisited

Qasid Ahmad<sup>1</sup>, Martin Wille<sup>1</sup>, Stephan König<sup>2</sup>, Carolina Rosca<sup>3</sup>, Thomas Pettke<sup>1</sup>, Jörg Hermann<sup>1</sup>

<sup>1</sup> Institute of Geological Sciences, University of Bern, Baltzerstrasse 1+3, 3012 Bern (qasid.ahmad@geo.unibe.ch)

<sup>2</sup> Instituto Andaluz de Ciencias de la Tierra (IACT), CSIC & UGR, Avenida las Palmeras 4, Armilla, 18100 Granada, Spain

<sup>3</sup> Isotope Geochemistry Group, Department of Geosciences, University of Tübingen, Schnarrenbergstrasse 94-96, 72076 Tübingen

Subduction zones are characterized by the highest mass fluxes between crust and mantle, where slab-derived aqueous fluids and hydrous melts facilitate element transfer into the mantle wedge. Despite their significance, the debate remains regarding the specific mechanisms of element recycling to arc magmatism. Barium (Ba) plays a key role to trace this recycling as generally more than 90% of the Ba in arc lavas derives from the subducted slab. Recently, the isotopic composition of Ba ( $\delta^{138/134}\text{Ba}$ ) has been introduced as a new tool to investigate this slab-mantle wedge transport and ultimately the incorporation of this element into arc lavas. Significant stable Ba isotope fractionation occurs during Earth's surface processes leading to distinct Ba concentrations and Ba isotopic ratios in different marine lithologies. Characterizing the Ba-isotope composition of marine sediments and altered oceanic crust (AOC) is therefore a necessary step to applying this novel isotope system for the investigation of Ba cycling in the ocean system and ultimately its recycling at subduction zones.

Here we report Ba isotopic data of pelagic sediment and AOC samples from the DSDP site 595/596 on the subducting SW-Pacific plate to complement previously published Ba isotope data of Tongan arc lavas. Our data shows that subducting sediments are isotopically heavier than previously assumed and can account for isotopically heavy Ba reported for Tongan arc lavas. There are downhole trends towards higher  $\delta^{138/134}\text{Ba}$ , which allow differentiating between diagenetic and primary Ba fractionation processes in the sediment pile. The new data permits to estimate the isotopic signature of mobilized sedimentary Ba and further evaluate the importance of AOC-derived Ba, which was previously established as a major Ba source for heavy Ba measured in Tongan arc lavas (Wu et al., 2020). Our results show that sedimentary Ba is an important contributor to the Tongan arc lavas, which is potentially released during the early stages of subduction.

### REFERENCES

- Wu, F., Turner, S., Schaefer, B.F., 2020. Mélange versus fluid and melt enrichment of subarc mantle: A novel test using barium isotopes in the Tonga-Kermadec arc. *Geology* 48, 1053–1057. <https://doi.org/10.1130/G47549.1>

## 3.2

### Fractionation of U isotopes during bacterial reduction

Ashley Brown<sup>1</sup>, Yvonne Roebbert<sup>2</sup>, Ataru Sato<sup>3</sup>, Minori Abe<sup>3,4</sup>, Stefan Weyer<sup>2</sup>, Rizlan Bernier-Latmani<sup>1</sup>

<sup>1</sup> Environmental Microbiology Laboratory, EPFL, CH-1015 Lausanne (ashley.brown@epfl.ch)

<sup>2</sup> Institut für Mineralogie, Leibniz Universität Hannover, Germany

<sup>3</sup> Department of Chemistry, Tokyo Metropolitan University, Japan

<sup>4</sup> Hiroshima University, Japan

Microbial reduction of U(VI) is widespread in the environment, both in pristine and engineered environments. Several studies have shown that such enzymatic redox transformations are accompanied by mass-independent isotope fractionation, with enrichment of the heavy U-238 in the U(IV) products, in accordance with nuclear field shift theory. This has led to the emergence of U isotope signatures as a paleo-redox proxy.

However, fundamental mechanistic information is lacking on the factors that affect the direction and magnitude of the U isotope signature. Recent research has implicated reaction rate as a primary determinant of U isotope fractionation, however, the reasons for this are not well established.

To explore this question, reaction kinetics and associated isotope fractionation during U(VI)-citrate reduction by *S. oneidensis* were assessed. U isotope analyses with MC-ICP-MS reveal relatively constant isotope fractionation factors of  $\sim 0.5\text{‰}$ , irrespective of reaction rates imposed by biomass concentrations. This is far from equilibrium isotope fractionation of  $\sim 2\text{‰}$ , as determined both experimentally and theoretically, using *ab initio* calculations.

Second, we followed the reduction of U(VI) in systems in which reaction rates are limited by electron flow from the donor, lactate. Here, isotope signatures were dependent on lactate concentrations, giving rise to fractionation factors as high as  $0.8\text{‰}$  under low lactate regimes. These data suggest that electron flux from bacterial metabolism may be an important determinant of fractionation.

Finally, using a mathematical framework first established for microbial sulfur fractionation, we invoke the redox state of the U(VI)-reducing proteins as a key controller of back-reaction, and subsequently, fractionation.

Collectively, these findings suggest that U isotope signatures in nature may be complicated by factors other than the local redox conditions; for example, by spatio-temporal changes in supply of organic matter, as an electron donor for microbial metabolism.

### 3.3

## Geochronological, geochemical and isotopic characterisation of the Mesozoic (160 – 110 Ma) Andean margin within Ecuador

Hugo Carrasco<sup>1</sup>, Richard Spikings<sup>1</sup>

<sup>1</sup> Department of Earth Sciences, University of Geneva, Rue des Maraîchers 13, 1205, Geneva, Switzerland  
 (hugo.carrasco@unige.ch)

Volcanic rocks of the Alao Arc are exposed in the western flank of the Eastern Cordillera of Ecuador. The dominantly mafic character of this volcanic units has precluded accurate geochronology, because they do not host zircons, and has hindered tectonic models for the Andes of Ecuador and Colombia. New whole rock geochemistry, isotopic tracing (Sr, Nd and Pb), and  $^{40}\text{Ar}/^{39}\text{Ar}$  geochronology is evaluated to better constrain the tectonic origin and crystallization age of the Alao Arc, and how the northwestern South American margin evolved during the Cretaceous.

Major and trace elements from the Alao Arc show two different volcanic suites that comprise typical arc-like volcanic rocks and E-MORB-like basalts. E-MORB-like signatures suggest that the melts formed by melting depleted mantle above thinning crust characteristic of an extensional tectonic setting. Likewise, trace elements and Sr-Nd-Pb isotopic compositions reveal crustal contamination which suggest a continental arc development. This is consistent with detrital zircons and dense minerals studies on the associated sedimentary rocks of the Alao Arc that indicate derivation from Gondwanan continental crust.

$^{40}\text{Ar}/^{39}\text{Ar}$  groundmass dates from this study do not record the crystallization age of the Alao Arc. However, plateau and weighted mean  $^{40}\text{Ar}/^{39}\text{Ar}$  date populations are around ~75 Ma and ~40 Ma and coincide with later major tectonic events in the region. An age between ~140-110 Ma for the Alao Arc is proposed, based on: maximum depositional ages in sedimentary rocks, tectonic correlation with the Quebradagrande Arc of Colombia, the mode of pervasive deformation within the Eastern Cordillera of Ecuador, and a systematic oceanward younging and more isotopically juvenile igneous rocks caused by the extension of the continental margin.

The overall data supports that the Alao Arc were develop in-situ as a continental arc on highly attenuated continental crust in an extensional tectonic setting during Early Cretaceous times (Spikings et al., 2015, 2019). And also new crust was formed in the Early Cretaceous by extension and hyperextension of the continental margin.

### REFERENCES

- Spikings, R., Cochrane, R., Villagomez, D., Van der Lelij, R., Vallejo, C., Winkler, W., & Beate, B. 2015. The geological history of northwestern South America: from Pangaea to the early collision of the Caribbean Large Igneous Province (290–75 Ma). *Gondwana Research*, 27, 95-139.
- Spikings, R. A., Cochrane, R., Vallejo, C., Villagomez, D., Van der Lelij, R., Paul, A., & Winkler, W. 2019. Latest Triassic to Early Cretaceous tectonics of the Northern Andes: Geochronology, geochemistry, isotopic tracing, and thermochronology.

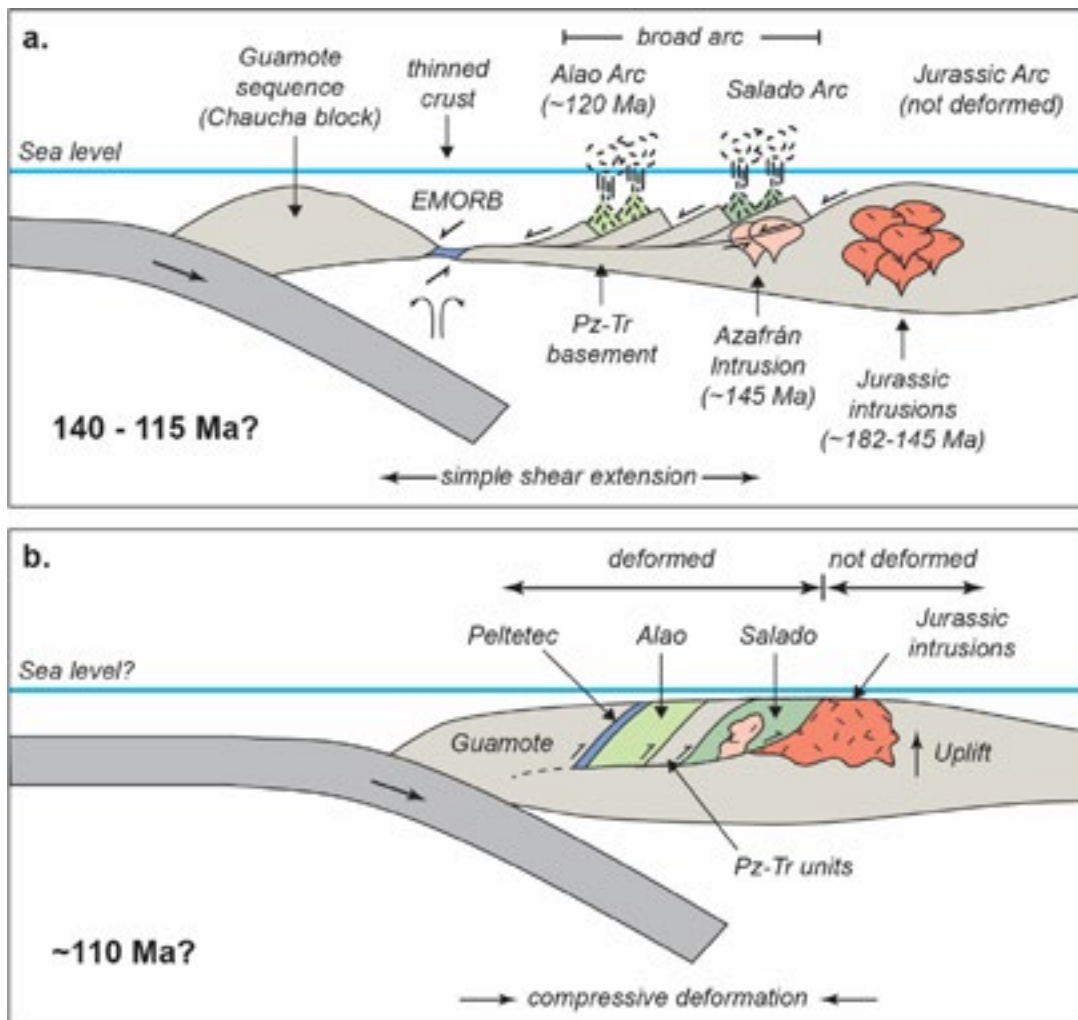


Figure 1. Schematic model for the tectonic evolution of the northwestern South American margin in Ecuador during the Early Cretaceous (140-110 Ma). Modified from Spikins et al. (2015)

### 3.4

## Dykes trace sediment subduction in the Archean

Sukalpa Chatterjee<sup>1</sup>, Arathy Ravindran<sup>2</sup>, Qasid Ahmad<sup>1</sup>, Martin Wille<sup>1</sup>, Klaus Mezger<sup>1</sup>, Om Prakash Pandey<sup>3</sup>

<sup>1</sup> Institut für Geologie, Balzzerstrasse 1+3, 3012, Bern, Switzerland

<sup>2</sup> Institut für Geochemie und Petrologie, ETH-Z, Clausiusstrasse 25, CH-8092 Zürich, Switzerland

<sup>3</sup> Department of Earth Sciences and Engineering, King Abdullah University of Science and Technology (KAUST), Thuwal 23955, Saudi Arabia

In the current plate tectonic regime of Earth, subduction zones are the primary manifestation of mantle convection and the location where crustal materials get recycled back into the Earth's mantle. This large scale mass transfer from crust to mantle via subduction and the dehydration, remelting of subducted material that interact with mantle melts drive the elemental cycles and chemical evolution of the hydrosphere, atmosphere and lithosphere. There is significant understanding of how present day subduction driven plate tectonic mechanisms works and drive continental crust formation. However, whether similar crustal and elemental recycling mechanisms were prevalent in the Archean is not well known. Cratonic scale dykes are mostly feeder systems to flood basalt eruptions (Muirhead et al., 2014). Studies of these dyke swarms emplaced into different Archean cratons have been shown to effectively track the secular evolution of metasomatized sub-continental lithospheric mantle (SCLM) beneath Archean cratons (Bartels et al., 2015; Pandey & Paul, 2022).

Different mafic dykes emplaced from Archean to Proterozoic time in the Singhbhum Craton (Pandey et al., 2021) show progressively evolved radiogenic isotope compositions pointing to a crustal source component involved in their petrogenesis. This crustal signature can either be the product of source contamination by crustal derived fluids during prior subduction (mantle metasomatism) or due to crustal assimilation during dyke emplacement.

Four dyke swarms belonging to the Newer Dolerite Dykes, emplaced in the Singhbhum Craton between 2.80Ga and 1.76Ga (Pandey et al., 2021) have high concentration of compatible trace elements indicating the parental melts were in equilibrium with a mantle peridotite source and were not modified by crustal assimilation and fractional crystallization during ascent and emplacement. Combined Sr-Nd-Hf isotopes of these dykes show progressively more evolved crustal signatures in their source, along with high intra-swarm variability. Radiogenic isotope data combined with trace element signatures affirm the establishment of a compositionally heterogeneous metasomatized lithospheric mantle before 2.80Ga beneath the Singhbhum Craton. Furthermore, stable Mo isotopes in these dykes show correlation of  $\delta^{98/95}\text{Mo}$  with Sr-Nd-Hf isotopes, indicating Mo isotopes preserve primary mantle source signatures. In addition, covariation of  $\delta^{98/95}\text{Mo}$  with Ba/Th, Th/Nb indicate the metasomatic overprint of the subcontinental-lithosphere of the Singhbhum Craton was facilitated by melts derived from Archean subducted sediments with heavy  $\delta^{98/95}\text{Mo}$  signatures.

### REFERENCES

- Bartels, A., Nielsen, T. F. D., Lee, S. R., & Upton, B. G. J. (2015). Petrological and geochemical characteristics of Mesoproterozoic dyke swarms in the Gardar Province, South Greenland: Evidence for a major sub-continental lithospheric mantle component in the generation of the magmas. *Mineralogical Magazine*, 79(4), 909–939.
- Muirhead, J. D., Aioldi, G., White, J. D., & Rowland, J. V. (2014). Cracking the lid: Sill-fed dikes are the likely feeders of flood basalt eruptions. *Earth and Planetary Science Letters*, 406, 187–197.
- Pandey, O. P., & Paul, D. (2022). Secular evolution of the subcontinental lithospheric mantle beneath Indian cratons: Insights from geochemistry and geochronology of the Precambrian mafic dykes. *Lithos*, 422–423, 106729.
- Pandey, O. P., Mezger, K., Upadhyay, D., Paul, D., Singh, A. K., Söderlund, U., & Gumsley, A. (2021). Major-trace element and Sr-Nd isotope compositions of mafic dykes of the Singhbhum Craton: Insights into evolution of the lithospheric mantle. *Lithos*, 382–383, 105959.

### 3.5

## Ancient microbially-influenced dolomites as chronologic archives of global geologic records? – Insights using LA-ICP-MS U-Pb geochronology from a post-Sturtian cap dolomite, Brazil

Rolando E. Clavijo-Arcos<sup>1\*</sup>, Matthew O. Clarkson<sup>1</sup>, Derek Vance<sup>1</sup>, Stefano Bernasconi<sup>2</sup>, Marcel Guillong<sup>1</sup>, Alcides N. Sial<sup>3</sup>, Marius N. Müller<sup>4</sup>, Osvaldo Correia<sup>5</sup>, and Netta Shalev<sup>1</sup>

<sup>1</sup> Institute of Geochemistry and Petrology, Department of Earth Sciences ETH Zürich, Clausiusstrasse 25, 8092 Zürich, Switzerland (\*correspondence: r.clavijo@erdw.ethz.ch)

<sup>2</sup> Geological Institute, Department of Earth Sciences ETH Zürich

<sup>3</sup> NEG-LABISE, Department of Geology, Federal University of Pernambuco, Recife, Brazil

<sup>4</sup> Department of Oceanography, Federal University of Pernambuco, Recife, Brazil

<sup>5</sup> GEOQUANTT, Department of Geology, Federal University of Pernambuco, Recife, Brazil

Chronologic constraints on Precambrian sedimentary successions, for which a biostratigraphic framework and/or volcanic ash layers are often limited, have been set based on field correlations or dating approaches that either provide maximum/minimum ages (e.g., from U-Pb on detrital zircons from diamictites) or that are sensitive to post-diagenetic alteration, even at shallow burial temperatures (e.g.,  $^{87}\text{Sr}/^{86}\text{Sr}$ ). However, stromatolitic carbonates have emerged as a promising archive for constraining the age of Precambrian carbonate successions using U-Pb dating [e.g., Moorbat et al., 1987; Hohl and Viehmann, 2021]. Here, we report a U-Pb LA-ICP-MS analysis acquired in microbial dolomite phases (coarse rhombic dolomite texture) from the Jacoca Formation cap dolomite unit, overlying the glacially influenced Sturtian Jacarecica Formation diamictite, Sergipano fold-and-thrust belt, Brazil. Laser ablation U-Pb analyses of this dolomite phase yield an isochron in Tera-Wasserburg space, with a lower intercept age of  $659.3 \pm 14.7$  Myr ( $n = 156$ ) and an upper intercept common Pb  $^{207}\text{Pb}/^{206}\text{Pb}$  value of  $0.8737 \pm 0.0010$ . This, therefore, suggests an early meltwater marine dolomitization stage that is consistent with the termination of the Sturtian glaciation based on other geochronologic analyses on multiple paleocontinents, as well as a globally synchronous termination of the Sturtian glaciation at 660 Myr [e.g., Kendall et al., 2006; Fanning and Link, 2008; Rooney et al., 2014; Wang et al., 2019]. Consequently, the direct U-Pb dating tool applied to microbial dolomite phases could have a wide applicability to dating the time of deposition of Precambrian unfossiliferous dolomitized carbonate platforms, and therefore to address the long-standing problem of radiometric calibrations for global stratigraphic correlations and seawater isotope reconstructions through deep time.

### REFERENCES

- Fanning, C. M., & Link, P. K. (2008). Age constraints for the Sturtian glaciation; data from the Adelaide geosyncline, South Australia and Pocatello Formation, Idaho, USA. In *Selwyn Symposium* (Vol. 91, pp. 57-62). Melbourne: Geological Society of Australia Abstracts.
- Hohl, S. V., & Viehmann, S. (2021). Stromatolites as geochemical archives to reconstruct microbial habitats through deep time: Potential and pitfalls of novel radiogenic and stable isotope systems. *Earth-Science Reviews*, 218, 103683.
- Kendall, B., Creaser, R. A., & Selby, D. (2006). Re-Os geochronology of postglacial black shales in Australia: Constraints on the timing of “Sturtian” glaciation. *Geology*, 34(9), 729-732.
- Moorbat, S., Taylor, P. N., Orpen, J. L., Treloar, P., & Wilson, J. F. (1987). First direct radiometric dating of Archaean stromatolitic limestone. *Nature*, 326 (6116), 865-867.
- Rooney, A. D., Macdonald, F. A., Strauss, J. V., Dudás, F. Ö., Hallmann, C., & Selby, D. (2014). Re-Os geochronology and coupled Os-Sr isotope constraints on the Sturtian snowball Earth. *Proceedings of the National Academy of Sciences*, 111(1), 51-56.
- Wang, D., Zhu, X. K., Zhao, N., Yan, B., Li, X. H., Shi, F., & Zhang, F. (2019). Timing of the termination of Sturtian glaciation: SIMS U-Pb zircon dating from South China. *Journal of Asian Earth Sciences*, 177, 287-294.

### 3.6

## Uncovering the drivers for the variability in isotope fractionation of O<sub>2</sub> during enzymatic reactions

Carolina F.M. de Carvalho<sup>1</sup>, Moritz F. Lehmann<sup>1</sup>, Sarah Pati<sup>1</sup>

<sup>1</sup> Department of Environmental Sciences, University of Basel, Bernoullistrasse 32, CH-4056 Basel  
(carolina.carvalho@unibas.ch)

Molecular oxygen (O<sub>2</sub>) is one of the most important electron acceptors for a large variety of biotic and abiotic processes in the environment. A wide range of oxygen isotope enrichment factors associated with biological respiration have been reported in field and laboratory studies ( $\epsilon$  from -29 to -1 ‰). The observed variability in  $\epsilon$  values has mainly been attributed to the different types of respiring organisms. However, what ultimately modulates respiratory isotope fractionation of O<sub>2</sub> remains unclear. All biological O<sub>2</sub> consumption, including respiration, detoxification, and biosynthesis, occurs at the enzyme-level. Only a few isotope enrichment factors have been reported for isolated enzymatic O<sub>2</sub> reduction reactions. These laboratory-scale studies also display a wide range of isotope enrichment factors ( $\epsilon$  from -10 to -33 ‰), without any clear correlation between  $\epsilon$  values and the type of enzyme, substrate, or O<sub>2</sub> reduction mechanism. In this study, we aim at applying O<sub>2</sub> stable isotope analysis to a systematic selection of O<sub>2</sub> consuming enzymes, to improve our molecular understanding of oxygen isotope fractionation of O<sub>2</sub> at the enzyme-level. In a first series of experiments, we have determined kinetic parameters and isotope enrichment factors of O<sub>2</sub> reduction by a series of copper- and flavin-dependent oxidase enzymes. These oxidase enzymes reduce O<sub>2</sub> to water (four-electron reduction), or to hydrogen peroxide (two-electron reduction), independent from substrate oxidation. Thus, the variability in observed O isotope fractionation should only depend on the active-site structure and/or the O<sub>2</sub> reduction mechanism. Our experimental  $\epsilon$  values cover the same range as previously reported for laboratory-scale studies with other enzymes. While we did not find significant differences between the two types of active-site structures,  $\epsilon$  values systematically correlated with a given enzyme's affinity for O<sub>2</sub> in flavin-dependent oxidases. These results represent an important first step towards an improved understanding and generalization of oxygen isotope fractionation at the enzyme- and, ultimately, at the organism-level.

### 3.7

## Pyrite iron isotope compositions track local sedimentation conditions through the Smithian-Spathian transition (Early Triassic, Utah, USA)

Marie-Noëlle Decraene<sup>1</sup>, Johanna Marin-Carbonne<sup>1</sup>, Christophe Thomazo<sup>2</sup>, Arnaud Brayard<sup>2</sup>, Anne-Sophie Bouvier<sup>1</sup>, Brahim Samba Bomou<sup>1</sup>, Thierry Adatte<sup>1</sup> and Nicolas Olivier<sup>3</sup>

<sup>1</sup> ISTE, Université de Lausanne, Switzerland ([marie-noelle.decreaene@unil.ch](mailto:marie-noelle.decreaene@unil.ch))

<sup>2</sup> Biogéosciences, Université de Bourgogne Franche Comté, Dijon, France

<sup>3</sup> LMV, Université Clermont Auvergne, Clermont-Ferrand, France

The Early Triassic is marked by important environmental perturbations such as marine anoxia, acidification and swings of global temperature. Such changes were documented for example through large carbon isotope excursions of organic and carbonate reservoirs during the late Smithian and the Smithian-Spathian boundary (SSB), only ~2 Ma after the end Permian mass extinction event. However, shallow-water environments seem to have preserved favorable conditions for the recovery of some nectopelagic organisms and a few ecosystems. In order to explore redox fluctuations through the SSB, we analyzed iron isotope compositions ( $\delta^{56}\text{Fe}_{\text{SIMS}}$ ) of micrometric pyrites from the Lower Weber Canyon section (Utah, USA) by SIMS (secondary ion mass spectrometer). This section was located on a sedimentary ramp system that evolved from (1) a siliciclastic peritidal inner ramp, to (2) a storm-dominated mid ramp, and finally to (3) a mud-dominated mid to outer ramp. We measured eight samples characteristic of the dominant lithologies (siltstones, bioclastic limestones and silty marls) spanning from the late Smithian to the early Spathian. All samples preserve a wide isotopic range (~7‰), with  $\delta^{56}\text{Fe}$  values from -2.0‰ to +5.4‰. Progressive enrichment for both  $\delta^{56}\text{Fe}_{\text{SIMS}}$  and bulk  $\delta^{34}\text{S}$  are recorded through the SSB, suggesting a concurrent distillation of both sulfate and Fe-oxide reservoirs. In contrast with the above, our results show a decoupling between Fe and S isotope during the late Smithian. We suggest that coupling of the Fe and S reduction, likely microbial, directly reflects porewater-water column disconnection in an environment occasionally affected by storm events. The absence of Fe-S coupling results from redox reactions within microbial mats located in the inner ramp system. This study demonstrates that micropyrites formed through the SSB record local conditions within the sediment and therefore cannot be used to infer the redox state of the overlying water column.

### 3.8

## Ferric iron was the dominant source of sedimentary pyrite from Archean to Paleoproterozoic: insights from *in situ* Fe isotope compositions

Juliette Dupeyron<sup>1,2</sup>, Marie-Noëlle Decraene<sup>1</sup>, Johanna Marin-Carbonne<sup>1</sup>, Vincent Busigny<sup>2</sup>

<sup>1</sup> Institut des Sciences de la Terre, Université de Lausanne, 1015 Switzerland (juliette.dupeyron@unil.ch)

<sup>2</sup> Université Paris Cité, Institut de Physique du Globe de Paris, CNRS, F-75005, Paris, France

Iron isotope compositions (expressed as  $\delta^{56}\text{Fe}$ ) in sedimentary pyrite have been widely used as tracers of redox and chemical evolution of the ocean through geological time. Previous studies mostly built on the chemical extraction of sulfides from bulk rock samples, and focused on visible macroscopic pyrites, which may introduce a sampling bias. *In situ* analyses of micropyrite grains can provide new insights into the processes of pyrite formation and their time evolution. Here, we compile ca. 2000 *in situ* iron isotope compositions of Archean to Paleoproterozoic sedimentary pyrite, from previous literature and unpublished data. Contrasting with bulk analyses, micropyrite displays a large and constant range of  $\delta^{56}\text{Fe}$  values, from -4 to +4 ‰, through time. Micropyrite  $\delta^{56}\text{Fe}$  values are not significantly influenced by metamorphic grade. A bimodal distribution of positive *versus* negative  $\delta^{56}\text{Fe}$  values can be attributed to two different processes of pyrite formation, Fe (oxy)hydroxide sulfidation, *versus* kinetic and possibly microbially mediated pyrite precipitation. These processes are tightly related to rock lithology and thus to sedimentary conditions, and have existed since 3.8 Ga.

### 3.9

## Crustal growth and reworking in the early Archean Narryer Terrane: new evidence from strontium isotopes in apatite inclusions

Jack Gillespie<sup>1</sup>, Pete Kiny<sup>1</sup>, Aaron J Cawosie<sup>1</sup>, Chris L. Kirkland<sup>1</sup>, Laure A.J. Martin<sup>2</sup>, Malcolm P Roberts<sup>2</sup>, Matvei Aleshin<sup>2</sup>, Denis Fougerouse<sup>3</sup>, Zakaria Quadir<sup>1</sup> and Alexander A. Nemchin<sup>1</sup>

<sup>1</sup> TIGeR, Curtin University, Perth, Australia ([jack.gillespie1@gmail.com](mailto:jack.gillespie1@gmail.com))

<sup>2</sup> Centre for Microscopy, Characterisation and Analysis, The University of Western Australia, Perth, Australia

<sup>3</sup> Geoscience Atom Probe, John de Laeter Centre, Curtin University, Perth, Australia

The limited preservation of ancient crustal material poses a challenge for understanding the composition of Earth's early crust. As a result of poor preservation and near-ubiquitous overprinting by later geological events, deciphering the early evolution of our planet often relies on the isotopic composition of resistive minerals, such as zircon. Although the isotopic information recorded by zircon grains has proved an invaluable asset to workers seeking to understand the geological evolution of the Earth, it is limited by the range of elements easily incorporated into the structure of the mineral.

One way to overcome these limitations is by analysing inclusions of other minerals that were trapped within the zircon during crystallisation. Apatite has great potential in this respect, as it is commonly found as inclusions in magmatic zircon and records a variety of useful isotopic information. Here I present an approach for investigating igneous petrogenesis and crustal evolution by combining  $^{87}\text{Sr}/^{86}\text{Sr}$  measurements of apatite inclusions with U–Pb and Hf isotope analysis of their host zircon crystal. The Sr isotope information contained in the apatite can be accessed by applying a novel SIMS technique we developed for this purpose.

A case study applying this new approach to Eoarchean igneous rocks of the Narryer Terrane in the northern Yilgarn Craton of Western Australia demonstrates how this can be used to understand the evolution of this key locality, with implications for both regional geology and the growth of the continental crust.

### 3.10

## Understanding stable Sr isotope fractionation associated with gypsum precipitation

Yana Kirichenko<sup>1</sup>, Jörg D. Rickli<sup>1</sup>, Tomaso R.R. Bontognali<sup>2,3</sup>, Netta Shalev<sup>1</sup>

<sup>1</sup> Institute of Geochemistry and Petrology, Department of Earth Sciences, ETH Zürich, Clausiusstrasse 25, CH-8092 Zürich (ykirichenko@ethz.ch)

<sup>2</sup> Space Exploration Institute, Faubourg de l'Hôpital 68, CH-2000 Neuchâtel

<sup>3</sup> Department of Environmental Sciences, University of Basel, Klingelbergstrasse 27, CH-4056 Basel

The global cycle of strontium (Sr) is controlled by fundamental Earth system processes, such as weathering, alteration of the oceanic crust, and carbonate sedimentation. Importantly, it is closely linked to the long-term cycling of carbon. Therefore, reconstruction of the isotope composition and concentration of Sr in past seawater can give valuable insights into the evolution of Earth's surface throughout geologic history. While the widely used radiogenic strontium isotopes ( $^{87}\text{Sr}/^{86}\text{Sr}$ ) can trace the oceanic Sr input fluxes, the 'non-traditional' stable-Sr isotope system ( $\delta^{88/86}\text{Sr}$ ) is responsive to both oceanic input and output fluxes. However, records of past seawater  $\delta^{88/86}\text{Sr}$  are currently scarce and need validation by new independent archives.

Gypsum ( $\text{CaSO}_4 \cdot 2\text{H}_2\text{O}$ ) is an evaporitic mineral, precipitating directly from concentrated seawater, and is therefore considered to be a good recorder of brine chemistry. Strontium is found in gypsum as a minor element, substituting for Ca in the crystal lattice, with concentrations up to thousands of ppm. Furthermore, gypsum can accumulate in large volumes, and therefore act as a significant source or sink of Sr, presumably capable of changing the isotope composition of seawater. This study focuses on exploring the potential of gypsum as an archive for seawater  $\delta^{88/86}\text{Sr}$  and on investigating the Sr isotope fractionation associated with gypsum precipitation.

A series of seawater evaporation experiments were performed at 30°C to produce gypsum in a laboratory. To evaluate the role of transport controls in the evaporating solutions, both stirred and unstirred precipitation experiments were conducted. Evaporation was interrupted between the onset of gypsum precipitation (DE - degree of evaporation of ~3) and the onset of halite precipitation (DE of ~10), and both solids and solutions were collected and analyzed for their elemental and  $\delta^{88/86}\text{Sr}$  values. Additionally, natural gypsum samples were analyzed: modern gypsum and associated pore water from Dohat Faishakh Sabkha in Qatar and Messinian gypsum from the Lower and Upper Gypsum of Sicily.

All the gypsum samples have higher  $\delta^{88/86}\text{Sr}$  values than the precipitating solutions. This observed  $^{88}\text{Sr}$ -enrichment in gypsum is opposite in direction to the Sr isotope fractionation associated with precipitation of calcium carbonate minerals, which are typically depleted in  $^{88}\text{Sr}$  (e.g., Böhm 2012; Fietzke&Eisenhauer 2006). However, the isotope difference between solids and precipitating solutions varies among the experiments depending on the stirring environment ( $\Delta^{88/86}\text{Sr}_{\text{gyp-sol}}$  of 0.04 – 0.23‰). Similarly, the partition coefficient of Sr into gypsum ( $K_g$ ) is not uniform but ranges from 0.07 to 0.22 and is negatively correlated with the isotope fractionation values. Presumably, the stirred experiments represent a more objective  $\Delta^{88/86}\text{Sr}_{\text{gyp-sol}}$  with an average of  $0.22 \pm 0.02\text{‰}$ . The study also explores multiple mechanisms controlling the variability of Sr partitioning and isotope fractionation.

The measured Messinian gypsum samples have  $\delta^{88/86}\text{Sr}$  close to those expected based on a  $\Delta^{88/86}\text{Sr}_{\text{gyp-sol}}$  of 0.22, deduced from the stirred experiments, and the  $\delta^{88/86}\text{Sr}$  value of Messinian seawater (Paytan et al., 2021).

### REFERENCES

- Böhm, F., Eisenhauer, A., Tang, J., Dietzel, M., Krabbenhöft, A., Kisakürek, B., Horn, C., 2012. Strontium isotope fractionation of planktic foraminifera and inorganic calcite. *Geochimica et Cosmochimica Acta* 93, 300–314.
- Fietzke, J., Eisenhauer, A., 2006. Determination of temperature-dependent stable strontium isotope ( $^{88}\text{Sr}/^{86}\text{Sr}$ ) fractionation via Bracketing Standard MC-ICP-MS. *Geochemistry, Geophysics, Geosystems* 7.
- Paytan, A., Griffith, E.M., Eisenhauer, A., Hain, M.P., Wallmann, K., Ridgwell, A., 2021. A 35-million-year record of seawater stable SR isotopes reveals a fluctuating global carbon cycle. *Science* 371, 1346–1350.

### 3.11

## The accretion history of the ureilite parent body: Constraints from Cr and Ti isotope anomalies

Pascal M. Kruttasch<sup>1</sup>, Aryavart Anand<sup>1</sup>, Julian-Christopher Storck<sup>1</sup>, Nicolas Greber<sup>1,2</sup>, Klaus Mezger<sup>1</sup>

<sup>1</sup> Institut für Geologie, Universität Bern, Baltzerstrasse 1+3, CH-3012 Bern ([pascal.kruttasch@geo.unibe.ch](mailto:pascal.kruttasch@geo.unibe.ch))

<sup>2</sup> Museum d'histoire naturelle de Genève, route de Malagnou 1, 1208 Genève

The dynamics of early solar system materials are pivotal to understand the formation and subsequent evolution of terrestrial planets such as Earth and Mars. The primordial components of these chemically evolved planets remain enigmatic due to equilibration and differentiation of their primary building blocks. Mass-independent isotopic heterogeneities (e.g., O, Mo, Cr, Ti) in meteorites and their constituents have been widely used to constrain isotopic reservoirs in the early Solar System, and to understand mixing between them. In this respect, ureilites are of particular interest because they allow insights into the accretion mechanisms of the planetesimals within the first few million years of the Solar System. They represent the mantle of a carbon-rich planetary embryo with a diameter of ~690 km (Warren 2012) to a Mars-sized body (Nabiee et al. 2018) and exhibit heterogeneities in mass-independent isotopes of O, Mo, Cr and Ti (Clayton and Mayeda 1996; Budde et al. 2019; Zhu et al. 2020; Kruttasch et al. 2022a, b; Williams et al. 2020). The reason for the isotopic heterogeneities in ureilites lacks consensus but may be related to (1) mixing of material from at least two chemically and isotopically distinct reservoirs and/or (2) ureilites may derive from several bodies with a similar formation history. However, the multiple parent body hypothesis is difficult to reconcile with the similar cooling history and the same statistical distribution of Mg# in monomict and polymict ureilites (Downes et al. 2008; Herrin et al. 2010).

To further investigate isotopic heterogeneities in main group ureilites, combined analyses of Cr and Ti isotopes on a suite of whole rock (WR) samples, acid-leachates and chromite-silicate separates were measured by Thermal Ionization Mass Spectrometer (TIMS) and Inductively-Coupled Plasma Mass Spectrometer (MC-ICPMS) at the University of Bern, following a chemical procedure involving sample digestion and Cr-Ti purification by cation-anion exchange chromatography.

The current WR dataset (this study; Williams et al. 2020) of the combined Cr and Ti analyses shows variations in the neutron-rich isotopes  $^{54}\text{Cr}$  of >30 ppm and  $^{50}\text{Ti}$  of >60 ppm. The variations also show a negative correlation in the  $\epsilon^{54}\text{Cr}-\epsilon^{50}\text{Ti}$  diagram, almost perpendicular to the positive correlation of the bulk non-carbonaceous chondrite (NC) bodies (Earth, Mars, Angrite parent body). Moreover, the  $^{54}\text{Cr}$  and  $^{50}\text{Ti}$  abundances in WR ureilites are the lowest determined in any known meteorite group and suggest formation as an end-member in the early Solar System. Chromium isotopic compositions of the acid-leachates and chromite-silicate separates from chromite-bearing ureilites (Kruttasch et al. 2022a, b) are homogeneous within analytical uncertainty, except for chromites in LaPaz Icefield (LAP) 03587. Chromites in LAP 03587 are of secondary origin – (1) abundant as symplectic inclusions with Ca-rich pyroxene, formed by subsolidus exsolution from olivine, and (2) in veins associated with areas of secondary reduction (Goodrich et al. 2013, 2014). Thus, the extreme negative  $\epsilon^{54}\text{Cr}$  signature of chromites in LAP 03587 may carry the isotopic signatures of an impactor component that was not homogenized on the parent body and may have originated from a yet unidentified reservoir. The combined Cr and Ti isotope data of WR and chemical separates from ureilite meteorites demonstrate that the formation of the parent body occurred by mixing constituents from at least two chemically and isotopically distinct reservoirs.

### REFERENCES

- Budde et al., 2019: Molybdenum isotopic evidence for the late accretion of outer Solar System material to Earth, *Nature Astronomy* 3, 736–741.
- Clayton and Mayeda, 1996: Oxygen isotope studies of achondrites, *Geochimica et Cosmochimica Acta* 60(11), 1999–2017.
- Downes et al., 2008: Evidence from polymict ureilite meteorites for a disrupted and re-accreted single ureilite parent asteroid gardened by several distinct impactors, *Geochimica et Cosmochimica Acta* 72, 4825–4844.
- Herrin et al., 2010: Thermal and fragmentation history of ureilitic asteroids: Insights from the Almahata Sitta fall, *Meteoritics & Planetary Science* 45(10–11), 1789–1803.
- Goodrich et al., 2013: Chromium valences in ureilite olivine and implications for ureilite petrogenesis, *Geochimica et Cosmochimica Acta* 122, 280–305.
- Goodrich et al., 2014: Petrology of chromite in ureilites: Deconvolution of primary oxidation states and secondary reduction processes, *Geochimica et Cosmochimica Acta* 135, 126–169.
- Kruttasch et al., 2022a: Chromium isotope systematics of the chromite-bearing ureilites LaPaz Icefield 03587 and Cumulus Hills 04048, LPS LIII, Abstract #2107.
- Kruttasch et al., 2022b: Chromium isotope systematics of main group ureilites and the diamond-bearing achondrite Northwest Africa 12969, MetSoc LXXXV, Abstract #6340.
- Nabiee et al., 2018: A large planetary body inferred from diamond inclusions in a ureilite meteorite, *Nature Communications* 9,

1327.

- Warren, 2012: Parent body depth–pressure–temperature relationships and the style of the ureilite anatexis, Meteoritical and Planetary Science 47(2), 109–227.
- Williams et al., 2020: Chondrules reveal large-scale outward transport of inner Solar System materials in the protoplanetary disk, Proceedings of the National Academy of Sciences, 117(38), 23426–23435.
- Zhu et al., 2020: Chromium isotopic constraints on the origin of the ureilite parent body, The Astrophysical Journal 888, 126.

### 3.12

## Complex single-zircon, high-precision U-Pb dates – what is the accurate scientific interpretation?

Urs Schaltegger<sup>1</sup>, Sean P. Gaynor<sup>1,2</sup>, Mélissa Ruiz<sup>1</sup>

<sup>1</sup> Department of Earth Sciences, University of Geneva, Rue des Maraîchers 13, 1205 Geneva, Switzerland  
(urs.schaltegger@unige.ch)

<sup>2</sup> Department of Geosciences, Princeton University, 219 Guyot Hall, Princeton, NJ 08544, USA  
(sean.gaynor@princeton.edu)

Linear arrays along a “discordia” in the  $^{206}\text{Pb}^*/^{238}\text{U}$  -  $^{207}\text{Pb}^*/^{235}\text{U}$  concordia space are often used in geochronology to interpret a diverse geologic history from complex or disturbed systems in zircon, as well as to identify the main crystallization episode of the mineral. The intercepts between these discordia lines and the concordia curve are then interpreted in terms of age for a primary and secondary growth or thermal event in the history of the dated zircon. Discordant points show a discrepancy between their apparent  $^{206}\text{Pb}/^{238}\text{U}$  and  $^{207}\text{Pb}/^{235}\text{U}$  dates. The ability to resolve discordance of individual points is largely a function of their uncertainty, and therefore, determining the degree of concordance and recognizing linear discordia fits is a function of analytical precision.

We present an example how a mixture of two U-Pb age components yield a linear array in the concordia space, and how this array may possibly be incorrectly interpreted. Thin Alpine metamorphic overgrowths on 335 Ma-old Variscan magmatic zircon from the Aar Massif (Central Alpine basement) yield a discordia array that intersects at an Alpine metamorphic age of 24 Ma (Gaynor et al., 2022). The small degree of discordance can be resolved at extremely high precision. The thin rims cannot be readily identified through cathodo-luminescence imaging. In this specific case, we can circumvent the mixing of these two unrelated age components by introducing a *physical* abrasion step to remove the rims, as has been used successfully in previous studies (e.g., Schaltegger and Corfu, 1992). *Chemical* abrasion of the zircon is inefficient for this, since this pretreatment removes internal parts with more elevated degrees of decay damage and related Pb-loss relative to the Alpine rims that only suffered minimal decay damage. Finally, using modeling data, we build on these concepts to show how scatter of chemically abraded zircon data in the concordia space may erroneously be interpreted as prolonged magmatic zircon growth or residence in case of low data precision.

This study allows us to draw several conclusions: (1) growth of metamorphic rims around Variscan zircon at Alpine upper greenschist conditions seems to be an ubiquitous phenomenon in the Aar massif; (2) future U-Pb single zircon work in the Alpine basement will need to use physical prior to chemical abrasion to yield accurate, high-precision U-Pb dates; (3) analytical precision matters, and the interpretation of complex age spectra must take this into account.

### REFERENCES

- Gaynor S.P., Ruiz M., & Schaltegger U. (2022) The importance of high precision in the evaluation of zircon U-Pb ages. *Chem. Geol.*, 603, 120913
- Schaltegger, U. & Corfu, F. (1992) The age and source for late Hercynian magmatism in the Central Alps: Evidence from precise U-Pb ages and initial Hf isotopes. *Contrib. Mineral. Petrol.* 111, 329-344

### 3.13

## Neoarchean surface conditions recorded in the 2.67 Ga low- $\delta^{18}\text{O}$ magmatic-hydrothermal system from the Kola Peninsula

David Zakharov<sup>1\*</sup>, Dmitry Zozulya<sup>2</sup>, Dylan Colón<sup>3</sup> and Daniela Rubatto<sup>4</sup>

<sup>1</sup> Institute of Earth Sciences, University of Lausanne, Lausanne, CH-1015 Switzerland ([david.zakharov@unil.ch](mailto:david.zakharov@unil.ch))

<sup>2</sup> Geological Institute, Kola Science Centre of the Russian Academy of Sciences, Apatity, 184209 Russia

<sup>3</sup> Department of Earth Sciences, University of Geneva, Geneva, CH-1205 Switzerland

<sup>4</sup> Institute of Geological Sciences, University of Bern, Baltzerstrasse 3, Bern, CH-3012 Switzerland

The surface temperatures of the first ½ of Earth's history remains poorly constrained due to the scarcity of well-preserved environmental proxies. Here we reconstruct the surface conditions at 2.67 Ga using surface water archive derived from hydrothermally altered rocks. The  $\delta^{18}\text{O}$  of meteoric precipitation recorded in these rocks is sensitive to the surface temperatures of the subaerially exposed crust. Due to the high-temperature reactive circulation around cooling plutons, the meteoric water is recorded in high-temperature refractory silicate minerals with  $\delta^{18}\text{O}$  values  $<0\text{\textperthousand}$ . The 3000 km<sup>2</sup> Keivy complex of the Kola craton formed via the intrusion of peralkaline granitic and mafic magmas in the low  $\delta^{18}\text{O}$  hydrothermally altered crust at 2.67 Ga. Using whole rock data, mineral separates, and in situ zircon  $\delta^{18}\text{O}$  measurements, we disentangle the mechanisms of reaction between the shallow magma and local precipitation, which is rarely available for lithologies of such age. Our measurements document direct meteoric water-rock exchange as well as near-contemporaneous igneous assimilation of altered materials. Coupled with U-Pb geochronology, we investigate in detail how low- $\delta^{18}\text{O}$  meteoric water is captured in magmas. Zircon with magmatic ages of 2.67 Ga depict melts with  $\delta^{18}\text{O}$  between 0 and +3‰ that likely formed via assimilation of near-contact hydrothermally altered rocks. The well-preserved zircon were used to constrain magmatic emplacement at  $2673.5 \pm 0.3$  Ma using high-precision U-Pb TIMS geochronology. Hydrothermal alteration produced near-contact altered lithologies with whole rock  $\delta^{18}\text{O}$  values as low as -7‰. The  $\delta^{18}\text{O}-\Delta^{17}\text{O}$  of altered host rocks and assimilated magmas unambiguously fingerprints the surface waters with  $\delta^{18}\text{O} = -18 \pm 6\text{\textperthousand}$ , providing one of the earliest records of continental precipitation. Today such precipitation is found in high-latitude regions with mean annual temperatures below 0 °C. Given existing paleomagnetic data, at 2674 Ma Kola craton was exposed to such precipitation at high latitudes between 60° and 90°, indicating that the climate was likely accompanied by temperatures below freezing. Our newly derived Neoarchean environmental proxy is in accord ca. 2.7 Ga glacial episodes, permitting the existence of cool climate at high latitudes despite an atmosphere presumably rich in CO<sub>2</sub> and CH<sub>4</sub>.

## P 3.1

# Transport of anomalously fractionated chromium isotopes from shelf to basin in the Canadian Arctic Ocean

Isabelle Baconnais<sup>1,2</sup>, Chris E. Holmden<sup>2</sup>

<sup>1</sup> Institute of Earth Sciences, University of Lausanne, Quartier UNIL–Mouline, CH-1015 Lausanne

(isabelle.baconnais@unil.ch)

<sup>2</sup> Department of Geological Sciences, University of Saskatchewan, 114 Science Place, Saskatoon, SK S7N 5E2, Canada

(chris.holmden@usask.ca)

In the Oceans, the cycle of chromium (Cr) and its isotopic system is greatly controlled by the biological pump and the oceanic circulation (Janssen et al., 2020; Janssen et al., 2021). Through these processes, the inter-conversion of the stable Cr(VI) and the isotopically-lighter, particle-reactive Cr(III) between surface waters and deep waters leads to the formation of a strong correlation between the total dissolved concentration of Cr ( $[Cr]_T$ , ng.kg<sup>-1</sup>) and its isotopic ratio ( $\delta^{53}\text{Cr}$ , ‰) on a global scale (Scheiderich et al., 2015). However, measurements of  $[Cr]_T$  and  $\delta^{53}\text{Cr}$  in the Arctic Ocean show that more than 70 % of the dissolved Cr composition plots below the global Cr correlation in a region encompassing the Canada Basin, Canadian Arctic Archipelago, Baffin Bay, and the Labrador Sea.

Using mass balance equations, we demonstrate that the Arctic seawater contains small amounts of excess Cr with anomalously-low  $\delta^{53}\text{Cr}$  values. The lowest values reach  $-2.7 \pm 0.4$  ‰ ( $1\sigma$ ) near the margins of the Canada Basin. These anomalously-low  $\delta^{53}\text{Cr}$  values are attributed to the shelf-export of isotopically-light Cr(III) produced by the reduction of Cr(VI) by ferrous iron (Fe(II)) over the reducing sediments of the Chukchi Shelf. Fe(II) is a potent reducing agent of Cr(VI) with a fractionation factor  $\epsilon$  ( $-4.2$  ‰ to  $-1.5$  ‰; Ellis et al., 2002; Døssing et al., 2011; Kitchen et al., 2012) three to four times larger than the biologically-mediated fractionations that control the slope of the global Cr correlation ( $-0.85$  ‰; Scheiderich et al., 2015). The proposed system works in correlation with the Fe shuttle (e.g. Jensen et al., 2020) and uses the formation of nanoparticulate Fe(III) oxyhydroxides and Mn oxides to drive the scavenging of Cr(III) and its export away from the shelf. Solutions to some caveat in the hypothesis are presented regarding the apparent lack of an isotopically-heavy pool of Cr being created as a response to the production of isotopically-light Cr(III), and alternative hypotheses that include the role of estuarine removal are briefly discussed.

## REFERENCES

- Døssing, L.N., Dideriksen, K., Stipp, S.L.S., Frei, R., 2011. Reduction of hexavalent chromium by ferrous iron: A process of chromium isotope fractionation and its relevance to natural environments. *Chemical Geology*, 285(1): 157-166.
- Ellis, A.S., Johnson, T.M., Bullen, T.D., 2002. Chromium isotopes and the fate of hexavalent chromium in the environment. *Science*, 295(5562): 2060-2062.
- Janssen, D.J. et al., 2021. Release from biogenic particles, benthic fluxes, and deep water circulation control Cr and  $\delta^{53}\text{Cr}$  distributions in the ocean interior. *Earth and Planetary Science Letters*, 574(117163): 1-13.
- Janssen, D.J. et al., 2020. Biological Control of Chromium Redox and Stable Isotope Composition in the Surface Ocean. *Global Biogeochemical Cycles*, 34(1): e2019GB006397.
- Jensen, L.T. et al., 2020. A comparison of marine Fe and Mn cycling: U.S. GEOTRACES GN01 Western Arctic case study. *Geochimica Et Cosmochimica Acta*, 288: 138-160.
- Kitchen, J.W., Johnson, T.M., Bullen, T.D., Zhu, J., Raddatz, A., 2012. Chromium isotope fractionation factors for reduction of Cr(VI) by aqueous Fe(II) and organic molecules. *Geochimica et Cosmochimica Acta*, 89: 190-201.
- Scheiderich, K., Amini, M., Holmden, C., Francois, R., 2015. Global variability of chromium isotopes in seawater demonstrated by Pacific, Atlantic, and Arctic Ocean samples. *Earth and Planetary Science Letters*, 423: 87-97.

## P 3.2

# Development of sphalerite as a standard for sulfur isotope analysis by SIMS

Bovay Thomas<sup>1</sup>, Johanna Marin-Carbonne<sup>1</sup>, Anne-Sophie Bouvier<sup>1</sup>, Kalin Kouzmanov<sup>2</sup>, Nicolas Greber<sup>3</sup>, Masafumi Saitoh<sup>4</sup>, Katharina Marger<sup>5</sup>, Alfons Berger<sup>6</sup>

<sup>1</sup> Institut of Earth Sciences (ISTE), University of Lausanne, Bâtiment Geopolis, CH-1015 Lausanne (thomas.bovay@unil.ch)

<sup>2</sup> Earth Sciences Departement (DST), University of Geneva, Rue de Maraîchers 13, CH-1205 Geneva

<sup>3</sup> Natural History Museum Geneva, route de Malagnou 1, CH-1208 Genève

<sup>4</sup> The University of Tokyo, Hongo 7-3-1, Tokyo 113-0033, Japan

<sup>5</sup> BSL Baustofflabor AG, Postgässli 23a, CH-3661 Uetendorf

<sup>6</sup> Institute of Geological Sciences (IfG), University of Bern, Baltzerstrasse 3, CH-3012 Bern

Secondary Ion mass spectroscopy (SIMS) is a powerful tool used to investigate high resolution in situ isotopic variations. This instrumental analytical method requires inevitably the use of reference standards material to correct for intrumental mass fractionniation (IMF) inherent to the technique. However the availability of matrix-matched reference materials for in situ data aquisition is limited. The understanding of sulfur isotope system is crucial for a variety of geochemical processes, such as tracing the origin of sulfur in ore deposits, or investigating the origin of life on Earth in Archean sediments. Measurement of sulfur isotopes in key sulfide minerals, such as sphalerite, can significantly improve our comprehension of those processes, since it occurs in both of the above geological processes.

This study investigates sphalerite as a potential standards for sulfur isotope analysis by SIMS. Four different sphalerite population from hydrothermal skarns (Rhodopes massif, Bulgaria) were selected. A wide range of chemical compositions with Fe(apfu) 0.01-0.14 was investigated, and matrix effect was not identified as affecting the IMF. There is a heterogeneous  $\delta^{33}\text{S}$  and  $\delta^{34}\text{S}$  signature within grain population (based on 7-8 grains) with standard deviation >1 ‰. In comparision the standard deviation of measurements ( $\delta^{33}\text{S}$  and  $\delta^{34}\text{S}$ ) performed on a single grain is homogeneous, i.e. <0.2 ‰. Inversed pole figures obtained by EBSD measurements using SEM reveal crystal orientation effect. Those are associated to the primary incident beam position and the crystal orientation. The precision can be improved by using a projected beam, which create a flatter and shallower pit compared to typically used gaussian beam, but might not be better than 0.6-1‰ (2sd; e.g. Kozdon).

## REFERENCES

- Kozdon, R., Kita, N. T., Huberty, J. M., Fournelle, J. H., Johnson, C. A., John W. Valley, J. V. 2010: In situ sulfur isotope analysis of sulfide minerals by SIMS: Precision and accuracy, with application to thermometry of ~3.5 Ga Pilbara cherts, Chemical Geology, 275, 243-253

## P 3.3

# Latest Permian to Early Triassic (Spathian) integrated carbon, strontium and neodymium isotope chemostratigraphy from Oman exotic blocks

Oluwaseun Edward<sup>1</sup>, Marc Leu<sup>2</sup>, Louis Dudit<sup>2</sup>, Sandrine Le Houedec<sup>3</sup>, Hugo Bucher<sup>2</sup>, Aymon Baud<sup>4</sup>, Christian Vérard<sup>3</sup>, Torsten Vennemann<sup>1</sup>

<sup>1</sup> Institute of Earth Surface Dynamics, Géopolis, University of Lausanne, CH-1015 Lausanne, Switzerland  
(oluwaseun.edward@unil.ch)

<sup>2</sup> Paläontologisches Institut der Universität Zürich, Karl Schmid-Strasse 4, 8006 Zürich, Switzerland

<sup>3</sup> Department of Earth Sciences, Université de Genève, Rue des Maraîchers 13, CH-1205 Genève

<sup>4</sup> Institute of Earth Sciences, Géopolis, University of Lausanne, CH-1015 Lausanne, Switzerland

The Oman ‘exotic blocks’ – marine pelagic carbonate successions that were rifted and obducted onto the Gondwanan margin – preserve a chemostratigraphic record of late Paleozoic to Mesozoic evolution of the Arabian passive margin of the NeoTethys. Given their offshore marine paleo-environment of deposition, these ‘exotics’ preserve a stratigraphic record of global marine environmental and faunal changes during the Paleozoic to Mesozoic (e.g., Brühwiler et al., 2012). In this study, we test the utility of these carbonate successions as recorders of global seawater chemistry and assess marine environmental evolution in the NeoTethys via carbon (C), strontium (Sr), and Neodymium (Nd) isotope measurements. The ensuing isotopic record spans the Permian-Triassic boundary (PTB) to Spathian (Olenekian) from three exotic blocks – Jebel Aweri, Jebel Rabat and Wadi Musjah, Oman. The carbonate C-isotope record shows that major carbon cycle perturbations spanning the PTB to Olenekian, as first documented from the Indian side of the NeoTethys (Atudorei, 1999), are faithfully recorded in the Oman exotics, but with attenuated magnitude.  $^{87}\text{Sr}/^{86}\text{Sr}$  ratios increase progressively from the PTB to Spathian ( $^{87}\text{Sr}/^{86}\text{Sr} = 0.7072$  to 0.7080) for both bulk carbonates and biogenic apatite, potentially indicating enhanced global continental weathering over the studied interval. The Sr isotope trend is consistent with those previously reported for coeval conodonts and brachiopods from other localities (e.g., Martin&MacDougall, 1995; Korte et al, 2003). The Nd isotope record is characterized by short-term variations superimposed on the secular PTB to Spathian decreasing trend, the most striking of which is a negative excursion coincident with the global negative C-isotope excursion of the middle Smithian. The offshore paleolocation of the sampling sites in the NeoTethys argues against a hypothesis where the negative excursion is related to enhanced riverine input of weathered old continental crust (with less radiogenic Nd isotope compositions). This excursion might, however, be related to upwelling of  $^{13}\text{C}$ -depleted deep waters due to paleo-circulation changes. Furthermore, variation in the range of  $\epsilon_{\text{Nd}}(t)$  values between Jebel Rabat (-9.5 to -5.4), Wadi Musjah (-7.7 to -5.9) and Jebel Aweri (-7.2 to -1.3) suggests significant lateral, vertical and temporal water mass heterogeneity in the NeoTethys during the Early Triassic. Our results are compatible with the Oman ‘exotic blocks’ constituting archives of open-ocean geological conditions for the global carbon cycle, continental weathering fluxes and paleo-circulation patterns from the latest Permian to the Early Triassic.

## REFERENCES

- Atudorei, N.-V., 1999, Constraints on the Upper Permian to Upper Triassic marine carbon isotope curve [PhD Dissertation]: University of Lausanne, Switzerland, 160 p.
- Brühwiler, T., Bucher, H., Goudemand, N., and Galfetti, T., 2012, Smithian (Early Triassic) ammonoid faunas from Exotic Blocks from Oman: taxonomy and biochronology: Palaeontographica. Abteilung A: Palaeozoologie-Stratigraphie, v. 296, no. 1-4, p. 3-107. DOI: 10.5167/uzh-59710.
- Korte, C., Kozur, H. W., Bruckschen, P., and Veizer, J., 2003, Strontium isotope evolution of Late Permian and Triassic seawater: Geochimica Et Cosmochimica Acta, v. 67, no. 1, p. 47-62. DOI: 10.1016/S0016-7037(02)01035-9.
- Martin, E., and Macdougall, J., 1995, Sr and Nd isotopes at the permian/triassic boundary: A record of climate change: Chemical Geology, v. 125, no. 1-2, p. 73-99. DOI: 10.1016/0009-2541(95)00081-V.

## P 3.4

### Variability in seawater Cr concentration and stable isotope composition along Atlantic Meridional Transect 29 (AMT29)

Delphine Gilliard<sup>1</sup>, David J. Janssen<sup>2</sup>, Nina Schuback<sup>3,4</sup>, Samuel L. Jaccard<sup>1</sup>

<sup>1</sup>Faculty of Geosciences and Environment, Institute of Earth Sciences (ISTE), 1015 Lausanne (delphine.gilliard@unil.ch)

<sup>2</sup>Eawag – Swiss Federal Institute of Aquatic Science and Technology, Seestrasse 79, 6047 Kastanienbaum

<sup>3</sup>Swiss Polar Institute, Rue de l'Industrie 17, 1950 Sion, Switzerland

<sup>4</sup>Chelsea Technologies Ltd., West Molesey, KT8 2QZ, UK

Over the last decade, the stable chromium (Cr) isotope composition has emerged as a potentially useful paleo-proxy recording past oxygenation changes in the atmosphere and oceans. Although Cr is a promising paleo-proxy, the modern marine Cr cycle remains poorly understood. Some important oceanic regions, such as large swaths of the Atlantic Ocean, have yet not been thoroughly investigated. Seawater Cr data from the Atlantic Meridional Transect 29 (AMT29) contributes to complete this gap. The AMT 29 samples were collected at 12 oceanographic stations along a meridional transect extending from 47.2°N; -9.2°E to 41.54°S; -35.26°E during October and November 2019. The sampling campaign for Cr focused on shallow waters with maximum depth of 2000 m. Most of the data from previous Cr studies follow a linear relationship between  $\delta^{53}\text{Cr}$  and  $\text{Ln}([\text{Cr}])$ . This strong linear relationship suggests that a limited number of mechanisms are responsible for the isotopic fractionation of Cr in the ocean. 60% of the Cr measurements generated along AMT29 are in line with this global array. The somewhat unexpected behaviour of the remaining 40% of the data is not yet well understood and could relate to specific regional processes. Since AMT29 crosses different biogeographical regions and water masses, several different parameters could affect the biogeochemical cycling of Cr. This complexity of biogeochemical parameters and their interactions may explain the unexpected behaviour at some of the stations. In addition, the study focused on particular environments such as oxygen minimum zones (OMZ) and its potential impact on the cycling of Cr. The data from AMT29 contribute to the global data set of dissolved Cr and further demonstrates its complexity. To better understand Cr and improve its applications, studies on dissolved Cr focussing on pore water, sediments, and particulate Cr are required.

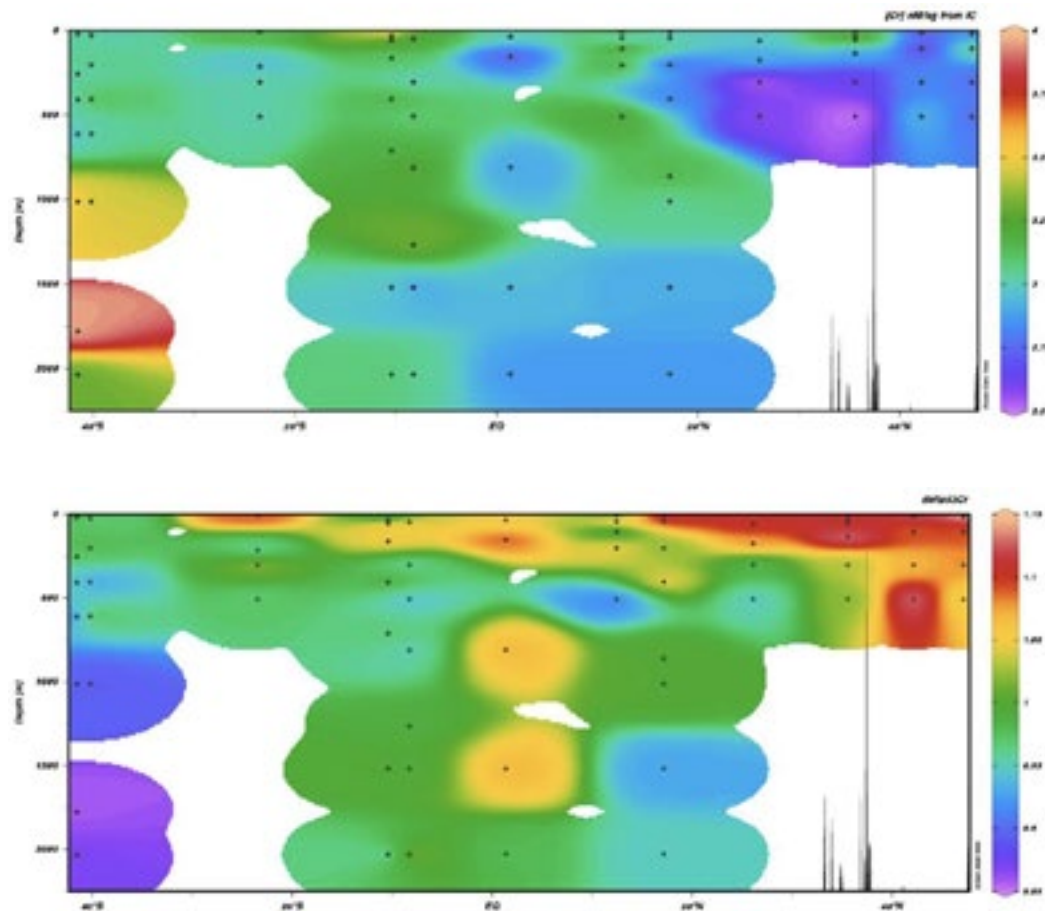


Figure 1. Section of the AMT 29 of  $[\text{Cr}]$  and  $\delta^{53}\text{Cr}$ . Panel A stands for  $[\text{Cr}]$  and panel B for  $\delta^{53}\text{Cr}$ . The black, white and between brackets dots represent sample sites. The white line represents the mixed layer depth (MLD).

## P 3.5

# The negative carbon isotope excursion at the onset of the Ediacaran Nama Group in Namibia

Inigo A. Müller<sup>1\*</sup>, Fabio Messori<sup>1</sup>, Marcel Guillong<sup>2</sup>, Giovan Peyrotty<sup>1</sup>, Elias Samankassou<sup>1</sup>, Ulf Linnemann<sup>3</sup>, Mandy Hofmann<sup>3</sup>, Johannes Zieger<sup>3</sup>, Agathe Martignier<sup>1</sup>, Anne-Sophie Bouvier<sup>4</sup>, Torsten Venneman<sup>4</sup>, Kalin Kouzmanov<sup>1</sup>, Maria Ovtcharova<sup>1</sup>

<sup>1</sup> Department of Earth Sciences, University of Geneva, 1205 Geneva, Switzerland

<sup>2</sup> Department of Earth Sciences, ETH Zurich, 8092 Zurich, Switzerland

<sup>3</sup> Senckenberg Museum of Mineralogy and Geology, 01109 Dresden, Germany

<sup>4</sup> Institute of Earth Surface Dynamics, University of Lausanne, 1015 Lausanne, Switzerland

\*inigo.mueller@unige.ch

The final stage of the Proterozoic, the Ediacaran, shields fascinating insights on the development and dispersal of complex metazoans related to dramatic compositional changes in the atmosphere and hydrosphere. Alternating sequences of siliciclastic and carbonate rocks of the Namibian Nama basin record the final stage of the Ediacaran and contain a vast amount of soft-bodied fauna, as well as some of the first organisms with hard shells (e.g., Cloudina, Namacalathus). However, the sparsity of ash beds at the base of the Nama group, preclude accurate and precise constraints on the onset of the Ediacaran biota in Nama group and correlation with chemo stratigraphic records worldwide.

To circumvent the lack of ash layers we apply U-Pb dating to carbonate rocks from various stratigraphic sections of the Nama Group combining the spatial resolution of LA-ICP-MS and the high-precision ID-TIMS U-Pb dating. The combination with mineralogical and geochemical techniques ( $\delta^{13}\text{C}$ ,  $\delta^{18}\text{O}$ , XRD, SEM, EPMA, clumped isotope thermometry, QEMSCAN, SIMS) enables us to identify different carbonate phases and to relate them to their pristine or diagenetic formation conditions, respectively.

With this study, we improve carbonate U-Pb dating through the distinction of pristine, early and late diagenetic carbonate phases and reduction of the matrix effect from different carbonate compositions. Thus, we contribute to a more robust stratigraphic age model for pre-Cambrian marine carbonates in the Nama Group that allows us to better constrain the early development of the Ediacaran metazoan ecosystems and the relation to changes in environmental conditions.

## P 3.6

# Molybdenum isotopes in the ~2.48 Ga-old Kuruman Formation, South Africa

Senger, M.H.<sup>1</sup>, Greber, N.D.<sup>2</sup>, Davies, J.F.H.L.<sup>3</sup>, Schaltegger, U.<sup>1</sup>

<sup>1</sup> Department of Earth Sciences, University of Geneva, Rue de Maréchais 13, 1205 Geneva

<sup>2</sup> Natural History Museum Geneva, Route de Malagnou 1, 1208, Geneva.

<sup>3</sup> University of Québec, Department of Earth and Atmospheric Sciences/Sciences de la Terre et de l'atmosphère, Avenue du Président-Kennedy 201, Montréal QC H2X 3Y7, Canada

The Great Oxidation Episode represents a long-term major shift in atmospheric and water-column redox conditions. Its onset is marked by the loss of mass-independently fractionated sulfur from the marine sedimentary units and its end coincides with the collapse of the positive carbonate excursion known as the Lomagundi-Jatuli Episode. With such time constraints, it is currently understood as a process that occurred over hundreds of million years, between ~2.4 Ga to ~2.0 Ga. However, other proxies sensitive to global seawater redox condition indicate that short-lived oxygenation events, so called “oxygen oases”, preceded the Great Oxidation Episode. For instance, the molybdenum (Mo) isotopic system is a very instructive proxy because it can trace oxic environments in organically rich mudstones deposited under euxinic conditions. Thus, and to shed light on the understanding of these oxygen oases, we measured the Mo isotopic compositions ( $\delta^{98}\text{Mo}$ ) of shales preserved within the world-class Kuruman banded iron formation. Importantly, the sampled UUBH1 drillcore has an age model recently published by Lantink et al. (2019).

Our results show a continuous general shift from heavy to lighter Mo isotope values throughout the drillcore with minor positive spike within this trend. In fact, the upper part of the drillcore yields the lightest  $\delta^{98}\text{Mo}$  values measured so far in the Neoarchean/Paleoproterozoic sedimentary sequences. As for the Mo contents, the samples show values overlapping with the upper continental crust (average around 1-2 ppm) with the exception of the deepest part of the drillcore that is enriched up to 12 ppm. Such enrichments indicate an euxinic water column, as observed in highly restricted modern basins (e.g., in the Black Sea). This is also consistent with petrographical observations as well as Fe-speciation analyses previously published (Ostrander et al., 2020; 2022). We also observe a positive correlation between  $\delta^{98}\text{Mo}$  and Mo content, which likely indicates that the contemporary  $\delta^{98}\text{Mo}_{\text{seawater}}$  has been captured in our samples.

Although still open to interpretation, we think that the  $\delta^{98}\text{Mo}$  measured in the lower part of the drillcore provides a minimum value for the  $\delta^{98}\text{Mo}_{\text{seawater}}$ . This implies that some transient oxygenation preceded the deposition of the Kleine Naute Shale located at the bottom of the studied section, leaving behind an enriched seawater reservoir. For the upper part of the drillcore, the basin became progressively oxic enough to oxidize various thiomolybdates into molybdates based on the very light  $\delta^{98}\text{Mo}$  values. If our interpretation is correct, then we report the development of an oxygen oasis within the Kuruman Formation that could develop in less than ~10 Ma.

## REFERENCES

- Lantink, M. L., Davies, J. H., Mason, P. R., Schaltegger, U., & Hilgen, F. J. (2019). Climate control on banded iron formations linked to orbital eccentricity. *Nature geoscience*, 12(5), 369-374.
- Ostrander, C. M., Kendall, B., Olson, S. L., Lyons, T. W., Gordon, G. W., Romaniello, S. J., Zhen, W., Reinhard, C.T., Roy, M., & Anbar, A. D. (2020). An expanded shale  $\delta^{98}\text{Mo}$  record permits recurrent shallow marine oxygenation during the Neoarchean. *Chemical Geology*, 532, 119391.
- Ostrander, C. M., Severmann, S., Gordon, G. W., Kendall, B., Lyons, T. W., Zheng, W., Roy, M., & Anbar, A. D. (2022). Significance of 56Fe depletions in late-Archean shales and pyrite. *Geochimica et Cosmochimica Acta*, 316, 87-104.

## P 3.7

# Hydrology of the Blausee – Mitholz area drainage basin and its sensitivity to potential sources of pollution: constraints from chemical and isotopic compositions of sediments and waters

Josephine Kramer<sup>1</sup> and Torsten Vennemann<sup>1</sup>

<sup>1</sup> Faculty of Geosciences and the Environment, University of Lausanne, CH-1002 Chavannes-pres-Renens  
(josephine.kramer@unil.ch)

Both natural causes such as those related to changes in climate as well as human industrial and agricultural activities may have severe consequences on the water quality in rivers and lakes. An increase in temperature and/or decrease in seasonal precipitation, for example, may adversely increase the nutrients in the water and also lead to a decrease in oxygen levels, both of which may have an impact on the biota within rivers and lakes. Such situations may be further aggravated by the release of toxins (pesticides, herbicides, heavy metals, excessive fertilizers) to the surface waters through our human activities (Reichenberger et al., 2007). Many Swiss rivers and lakes are no exceptions to such problems, and this is particularly the case in Alpine drainage systems that are very sensitive to environmental changes and for which a number of important fish-kills have been noted over the past few years.

This study focuses on the hydrology of the Blausee-Mitholz region. The major and trace element composition of select sediments, in addition to the major anions, cations and trace metal content, TOC (Total Organic Carbon) and DIC (Dissolved Inorganic Carbon), as well as the stable isotopic composition of the ground and surface waters are being analysed on a seasonal basis. The aim of the study is to help assess any risk that may be associated with the heavy metal content, organic pollutants, and nutrient inputs, all of which may be influenced by deposited railroad material, an old ammunition depot and intensive agriculture, as well as natural conditions (i.e., heat stress) and its speciation and bioavailability. Different rivers (Kander) and streams (e.g., Stägebach, Rotbach) as well as the Blausee are being analysed also for their stable H-and - O isotope composition as well as the C- isotope composition of the DIC to provide valuable insights into the distribution and mixing proportions of substances and the flow paths of the different rivers and streams within the drainage basin.

Furthermore, physical-chemical parameters show how nature interact with human causes. The strength of these factors also depend on natural characteristics, such as the sub-surface geology and biogeochemical compositions of the soils within the drainage basin and the interplay with the human activities. An improved understanding of the local hydrological conditions of the catchment and communication of the results to the local responsible and affected parties may help alleviate future adverse effects on the biota within the rivers and lakes of this region.

## REFERENCES

- Reichenberger S., Bach M., Skitschak A., Frede H.G., 2007: Mitigation strategies to reduce pesticide inputs into ground-and surface water and their effectiveness; A review, *Science of The Total Environment*, 384, 1-35.

## P 3.8

### Climate cooling event in the Early Triassic subtropics

Zoneibe Luz<sup>1</sup>, Marc Leu<sup>2</sup>, Oluwaseun Edward<sup>1</sup>, Aymon Baud<sup>3</sup>, Hugo Bucher<sup>2</sup>, Torsten Vennemann<sup>1</sup>

<sup>1</sup> Institut des Dynamiques de la Surface Terrestre, Université de Lausanne, Géopolis, CH-1015 Lausanne  
(zoneibe.luz@gmail.com; franziska.blattmann@unil.ch; torsten.vennemann@unil.ch)

<sup>2</sup> Paläontologisches Institut und Museum, Universität Zürich, Karl-Schmid-Strasse 4, CH-8006 Zürich  
(marc.leu@pim.uzh.ch; hugo.fr.bucher@pim.uzh.ch)

<sup>3</sup> Institut des Sciences de la Terre, Université de Lausanne, Géopolis, CH-1015 Lausanne (aymon.baud@unil.ch)

In the aftermath of the largest mass extinction, the Early Triassic comprised major environmental perturbations during which nektonic marine organisms (e.g., ammonoids, conodonts) underwent a series of extinction-origination cycles (Brayard & Bucher 2015; Widmann et al. 2020). Early Triassic palaeotemperatures were not invariably hot and varied along with changes in the carbon cycle (e.g., Goudemand et al. 2019). A major and protracted extinction of nekton within the Early Triassic spanned the late Smithian (600 ky) and peaked around at the Smithian–Spathian boundary (SSB), some 2.7 Ma after the end-Permian extinction event (252 Ma) (MacLeod 2014). Oxygen isotope values – a proxy for relative changes in sea-surface temperature – were analysed from pristine preserved conodont bioapatite (Conodont Alteration Index CAI 1) to gain a better understanding of the role temperature played during the late Smithian extinction. Conodont  $\delta^{18}\text{O}$  values were analysed from two sections in Oman (Hawasina and Batain Nappes) representing pure carbonate settings deposited on offshore seamounts, thus excluding abnormal salinity fluctuations that could influence the oxygen isotope compositions of the seawater. Combined with clumped isotope measurements ( $\delta^{47}\text{O}$ ,  $\Delta_{47}$ ) from associated brachiopods, a  $\delta^{18}\text{O}_{\text{water}}$  value of  $-1.7 \pm 0.8 \text{ ‰}$  can be estimated for contemporary waters. Secondary ion mass spectrometric (SIMS) O-isotope measurements on conodonts provided high-resolution constraints on the evolution of sea-surface temperature changes across the extinction interval. The middle Smithian negative  $\delta^{18}\text{O}$  anomaly extended into the early Late Smithian, where it reached its lowest values. This nadir was followed by a protracted first-order, positive trend representing a cooling by about  $7.5 \text{ °C}$  during the late late Smithian and earliest Spathian. This first-order cooling trend confirms previous trends noted for shelf sections on the northern Indian margin and South China (e.g., Goudemand et al. 2019). Conodont biozonation, calibrated with chronostratigraphy (measured by U-Pb ages), suggests this cooling trend lasted for about 300 ky (average cooling rate of  $1 \text{ °C}$  per 40 ky, Fig. 1). This estimate confirms that the mid-late Smithian to earliest Spathian cooling recorded from the Tethyan realm was much too long to be accounted for by a volcanic winter, and was likely too slow to drive nektonic species directly to extinction. The highly resolved SIMS time series obtained from the expanded Smithian–Spathian boundary Batain section suggests the presence of short-term temperature oscillations superimposed onto the first-order cooling trend. Causes of the Early Triassic climatic upheavals may differ from those associated directly with the Permian-Triassic boundary mass extinction by their typically slower pace rather than their amplitude. It is possible that Early Triassic climate changes and extinctions were driven by mechanisms unrelated to those associated with the PTBME and concurrent SLIP volcanism.

## REFERENCES

- Brayard, A. & Bucher H. 2015: "Permian-Triassic extinctions and rediversifications," in Ammonoid Paleobiology: From Macroevolution to Paleogeography, In: Topics in Geobiology (Eds. C. Klug et al.), Dordrecht: Springer, 44, 465-473.
- Goudemand, N. et al. 2019: Dynamic interplay between climate and marine biodiversity upheavals during the early Triassic Smithian–Spathian biotic crisis, Earth-Science Reviews, 195, 169-178.
- MacLeod, N. 2014: The geological extinction record: History, data, biases, and testing, in Volcanism, Impacts, and Mass Extinctions: Causes and Effects, Geological Society of America Special Papers, 505, 1-28.
- Widmann, P. et al. 2020: Dynamics of the largest carbon isotope excursion during the Early Triassic biotic recovery, Frontiers in Earth Science, 8, 196.

## P 3.9

# Have we been calculating benthic nitrogen fluxes wrong? A comparison of porewater sampling methods in two Swiss lakes

Alessandra Mazzoli<sup>1</sup>, Chiara T. Piantoni<sup>1</sup>, Tim J. Paulus<sup>1</sup>, Cameron M. Callbeck<sup>1</sup>, Jakob Zopfi<sup>1</sup>, Claudia Frey<sup>1</sup>, Moritz F. Lehmann<sup>1</sup>

<sup>1</sup> Biogeochemistry, Department of Environmental Sciences, University of Basel, Bernoullistrasse 30, CH-4056 Basel (alessandra.mazzoli@unibas.ch)

Lake sediments act as important sinks of fixed nitrogen (N) in terrestrial watersheds, due to suboxic N<sub>2</sub> production by denitrification and anammox, as well as N burial. Benthic habitats play a particularly crucial role in the freshwater N cycle, as they are characterized by high N transformation rates and steep dissolved inorganic N (DIN) porewater concentration gradients. These gradients are often used to calculate nutrient fluxes and are thus useful for quantitatively estimating benthic process rates, benthic N loss and lacustrine N budgets.

The lack of a standardized method for porewater sampling, particularly in reactive lake sediments, where the maximum N turnover often occurs within the top 1-2 cm, exacerbates the uncertainties in N budgets. In this study we assessed the distribution of ammonium (NH<sub>4</sub><sup>+</sup>) and nitrate (NO<sub>3</sub><sup>-</sup>) concentrations, as well as their stable N isotope compositions ( $\delta^{15}\text{N}$ ) in sediment porewater, using and evaluating four different porewater sampling techniques (whole-core squeezing, rhizon samplers, sectioning-centrifuging and peepers) in two Swiss lakes of different trophic state, Lakes Baldegg (eutrophic) and Sarnen (oligotrophic).

Preliminary results showed good reproducibility of each method, but significant inter-method differences in the calculated DIN porewater gradients/penetration depths, and thus, in the benthic fluxes. For instance, in Lake Baldegg the nitrate penetration depth was 0.5-0.75 cm when employing the whole-core squeezing or the sectioning-centrifuging methods, but it exceeded 2 cm when rhizons and peepers were used. Moreover, ammonium concentrations obtained with the peepers were consistently 40-50% lower than those in the rhizon samples in Lake Sarnen, with obvious implications for the quantification of ammonium fluxes out of the lake sediments. This deviation was even more pronounced in Lake Baldegg. Based on our results, the latter sampling methods, i.e. the commonly used rhizon approach, as well as the use of peepers, may significantly underestimate fixed-N elimination in lacustrine N budgets.

## P 3.10

### Isotope effect of benthic N removal in two Swiss lakes

Tim J. Paulus<sup>1\*</sup>, Alessandra Mazzoli<sup>1</sup>, Claudia Frey<sup>1</sup>, Jakob Zopfi<sup>1</sup>, Cameron Callbeck<sup>1</sup>, Moritz F. Lehmann<sup>1</sup>

<sup>1</sup> Department of Environmental Sciences, University of Basel, Bernoullistrasse 30, 4056 Basel, Switzerland,  
 \*tim.paulus@unibas.ch

Aquatic sediments play a critical role in moderating the availability of fixed nitrogen (N) in the biosphere. Microbial N cycling processes, such as denitrification and anammox, contribute to fixed nitrogen removal to N<sub>2</sub> gas. N isotopic measurements of dissolved inorganic N (e.g., nitrate (NO<sub>3</sub><sup>-</sup>)) can provide insights into the different sources, sinks, and pathways of N, if the associated N isotope signatures/ effects are constrained. While substantial work has been done to resolve N loss using microbial metagenomicbased approaches and rate measurements, how nitrogenloss processes imprint naturalabundance isotopes of <sup>15</sup>N and <sup>18</sup>O of NO<sub>3</sub><sup>-</sup> remains largely understudied in the context of freshwater lake sediments. Current evidence from the marine environments suggests that denitrification in the water column involves high NO<sub>3</sub><sup>-</sup> isotope effects (>20‰). In contrast, the NO<sub>3</sub><sup>-</sup> isotope effect of sedimentary denitrification in the ocean is suppressed at the level of the sediment-water interface (apparent N or O isotope effect or  $\varepsilon_{app} < 5\text{\textperthousand}$ ). How anammox affects  $\varepsilon_{app}$  in either marine or freshwater systems, is completely unknown. This study aims to achieve a deeper understanding of NO<sub>3</sub><sup>-</sup> N and O isotope fractionation during benthic N transformation and sedimentary N-loss (including anammox), and its ultimate expression in the water column of freshwater lakes. We also investigate how values for  $\varepsilon_{app}$  may vary with environmental conditions (e.g., trophic state) that impact the reactivity and amount of organic matter in the sediments, as well as the balance between benthic N cycle reactions.

Our two study sites are the Swiss lakes Baldegg (eutrophic) and Sarnen (oligotrophic), which were chosen because of their contrasting trophic states. We conducted incubation experiments following three different sampling campaigns to assess the sedimentary  $\varepsilon_{app}$  in these two lakes. More specifically, we carried out whole-core incubations under oxic conditions and examined the change <sup>15</sup>N/<sup>14</sup>N and <sup>18</sup>O/<sup>16</sup>O of NO<sub>3</sub><sup>-</sup> with net NO<sub>3</sub><sup>-</sup> depletion in the overlying water. We integrated naturalabundance N and O isotope measurements with <sup>15</sup>Nlabel based N transformationrate measurements, to understand how the differential combination of the different N transformation pathways may modulate  $\varepsilon_{app}$ . We demonstrate that nitrification, DNRA, denitrification, anammox and organic matter remineralization overlap spatially in the sediments of Lake Sarnen. In contrast, these processes are, in parts, spatially decoupled in Lake Baldegg. Moreover, the relative importance of anammox versus denitrification is significantly greater in Lake Sarnen. Preliminary data indicate that in both lakes the net N isotope effect of sedimentary NO<sub>3</sub><sup>-</sup> consumption is strongly underexpressed at the ecosystem level, with NO<sub>3</sub>-N  $\varepsilon_{app}$  values systematically below 4‰. Yet, systematic differences between the two lakes, both with respect to the nitrateN  $\varepsilon_{app}$ , as well as the dual N vs. O isotope signature in the supernatant NO<sub>3</sub><sup>-</sup> pool, are discernible, and can be partly explained in the context of their different reactivity and N cycle regimes.

## P 3.11

# Magnesium isotope signature of Middle Ordovician dolomites from the Ordos Basin, China

Yining Li<sup>1,2</sup>, Wenhui Liu<sup>1</sup>, Netta Shalev<sup>2</sup>

<sup>1</sup> Department of Geology, Northwest University, Taibai North Road 229, 710069 Xi'an, China ([msmoomin@icloud.com](mailto:msmoomin@icloud.com))

<sup>2</sup> Department of Earth Sciences, ETH Zürich, Clausiusstrasse 25, 8092 Zurich, Switzerland

As a significant sink of seawater magnesium,  $\delta^{26}\text{Mg}$  values of syndepositional marine dolomites can be utilized to reconstruct seawater Mg isotope composition in the past. This, in turn, may serve as a good tracer for the Mg cycle throughout Earth's history. Furthermore,  $\delta^{26}\text{Mg}$  values of ancient dolomites precipitated in different depositional environments may help in reconstructing the paleo-conditions that prevailed in these environments, in particular, the hydrology and restriction conditions of ancient sedimentary basins.

In this study, we collected Middle Ordovician marine dolomite samples from five profiles distributed in the different locations of the Ordos Basin, North China Plate. During the Ordovician, marine carbonates were deposited in the whole area of the Ordos Basin under different sedimentary settings that can be generally divided into open marine settings, a dolomite platform, and a saline gypsum lake. After systematic petrology observation (optic and cathode luminescence microscope), we microdrilled fine-crystallized dolomite to conduct chemistry and Mg isotope analyses. The dolomites from profile #1, which were deposited in an open marine environment, exhibit the lowest  $\delta^{26}\text{Mg}$  values between  $-2.31\text{\textperthousand}$  to  $-2.21\text{\textperthousand}$ . The  $\delta^{26}\text{Mg}$  values of dolomite samples are generally heavier toward the more evaporitic center of the basin. The highest  $\delta^{26}\text{Mg}$  values ( $-1.84\text{\textperthousand}$  to  $-1.70\text{\textperthousand}$ ) were measured in samples from profile #5 located in the saline gypsum lake area.

We suggest that this gradient of  $\delta^{26}\text{Mg}$  values from the outer parts of the basin toward the center is resulting from a prior formation of dolomite in open versus gradually more restricted settings. Dolomite is enriched in the lighter isotope,  $^{24}\text{Mg}$ , relative to its precipitating solution. Thus, under restricted settings, dolomite formation will increase the  $\delta^{26}\text{Mg}$  value of the remaining dissolved Mg in the solution and consequently, also the  $\delta^{26}\text{Mg}$  values of further precipitating dolomites. This further suggests that the Mg isotope composition of dolomite can be used to reconstruct the enclosure degree of ancient evaporitic basins. Together with the observation that  $\delta^{26}\text{Mg}$  values of dolomite samples from profile #1 vary in a narrow range of  $0.10\text{\textperthousand}$  between different formations, this also suggests that profile #1 located in open marine settings can be utilized to reconstruct the Mg isotope signature of seawater during the Middle Ordovician.

## 4 Environmental Biogeochemistry of Trace Elements

Montserrat Filella, Marie Marques, Adrien Mestrot, Andreas Voegelin, Lenny Winkel

### TALKS:

- 4.1 Aeppli M.: Invited talk: Follow the electrons: redox-active minerals in biogeochemical processes
- 4.2 Biswas S., Gerchow J., Janka G., Vogiatzi Stergiani M., Knecht A., Amato A., Filella M., Hofmann B.A., Megatli-Niebel I., Raselli L., Querel E., Remhof A.: Applied physics research with Muon-Induced X-Ray Emission (MIXE) at PSI
- 4.3 Chin N., Liu X., Domeignoz-Horta L., DeAngelis K., Keiluweit M.: Microbial and geochemical drivers of manganese-mediated organic matter oxidation in soils
- 4.4 de Meyer C., Escalera R., Huallpara L., Carpio E., Ormachea M., Mestrot A.: Testing arsenic and manganese removal by natural aeration of contaminated groundwater in rural Amazonia
- 4.5 Förster F., Reynaud S., Omanovic D., Samankassou E., Ferrier-Pages C., Sheldrake T.: Fertilizing effect of volcanic ash on the hermatypic coral *Stylophora pistillata*
- 4.6 Gibaja J., Monbaron L., Vuaridel M., Ruiz-Villanueva V.: What does the chemical composition of cellulose tell us about the provenance of instream wood?
- 4.7 Gindro K.: Invited talk: The unlimited potential of fungi
- 4.8 Morgenthaler U., Worms I., Viacava K., Slaveykova V., Mestrot A.: Insights into colloidal antimony in pore water of contaminated soils analyzed with AF4-ICP-MS and SEC-ICP-MS
- 4.9 Nenonen V., Kaegi R., Hug S.J., Mangold S., Göttlicher J., Winkel L.H.E., Voegelin A.: Effects of dissolved organic compounds on phosphate uptake of Fe(III)-precipitates formed by Fe(II) oxidation.
- 4.10 Qian Y., Scheinost A.C., Grangeon S., Hoving A., Grenche J.M., Marques Fernandes M., Churakov S.: Retention of Tc on Fe-bearing clay minerals
- 4.11 Reusser J.E., Siegenthaler M.B., Winkel L.H.E., Kretzschmar R., Wächter D., Meuli R.G.: Assessing trace element concentrations in surface soils across Switzerland
- 4.12 Tercier-Waeber M.-L., Abdou M., Penezic A., Confalonieri F., Coynel A., Schäfer J.: Estuarine biogeochemical processes influencing the potentially bioavailable fraction of a range of trace metals
- 4.13 Wielinski J., Jimenez-Martinez J., Göttlicher J., Steininger R., Mangold S., Hug S.J., Berg M., Voegelin A.: Spatiotemporal mineral phase evolution and arsenic retention in microfluidic models of zerovalent iron-based water treatment

## POSTERS:

- P 4.1 Blattmann F.R., Ragon C., Vennemann T., Vérard C., Kasparian J., Brunetti M., Adatte T., Bucher H., Magill C.R.: Multidisciplinary perspectives on Early Triassic pyrogenic carbon cycling
- P 4.2 Bosco-Santos A., Ceriotti G., Berg J.: Microbial-Mineral Chips: a closer look at Fe reduction
- P 4.3 Bruggmann S., McManus J., Severmann S.: On the behaviour of W and Re in pore fluids and sediments from a continental margin
- P 4.4 Brito F., Wiggenhauser M.: Isotope fingerprints for deciphering the role of chelating thiols to separate zinc from cadmium in plants (IsoThiolPrint)
- P 4.5 Ni C., Keiluweit M.: “Enzyme or Manganese latch”: Fungal-mediated litter-C turnover coupled to manganese biogeochemistry
- P 4.6 Segovia-Campos I., Kanellakopoulos A., Barrozo I., Fock-Chin-Ming E., Baxarias Fontaine A., Pallada S., Triscone G., Perron K., Filella M., Ariztegui D.: The green microalgae *Tetraselmis chui*, a potential 90Sr bioremediation agent
- P 4.7 Thomas C., Filella M., Ionescu D., Sorieul S., Oehlert A., Zahajská P., Ferreira Sanchez D., Gedulter G., Agnon A., Ariztegui D.: Localized heavy arsenic enrichment in Dead Sea microbial mats
- P 4.8 Viacava K., Morgenthaler U., Dubach D., Mestrot A.: Mobilisation and chemical speciation of antimony upon flooding of shooting range soil
- P 4.9 Vincent J.: Geochemical imprints of volcanic ash leaching in coral skeletons
- P 4.10 Zelano I., Hausalden D., Pena J.: Transformation of plant-derived carbon by Manganese oxides

## 4.1

# Follow the electrons: redox-active minerals in biogeochemical processes

Meret Aeppli<sup>1</sup>

<sup>1</sup> Institut d'ingénierie de l'environnement, EPFL, Rte Cantonale, CH-1015 Lausanne ([meret.aeppli@epfl.ch](mailto:meret.aeppli@epfl.ch))

Redox-active minerals represent important reactants in various subsurface biogeochemical processes. Iron-bearing minerals are of particular importance, given that iron is the most abundant redox-active metal in the Earth's crust. Iron commonly exists in redox states +III and +II and can undergo a myriad of microbially and chemically mediated reactions. As a result, the biogeochemical cycling of iron is tied to the cycling of other main elements, including carbon and sulfur, and has important consequences for the bioavailability, toxicity, and mobility of trace elements. Redox reactions involving iron occur over an unusually large range of environmental conditions, reflecting the large span in redox potentials of different Fe(III)-Fe(II) redox couples. The redox properties of iron minerals are difficult to assess as they are determined by a number of factors, including mineral type and particle size, solid phase Fe(III):Fe(II) ratio, and solution chemistry. However, we need information on these properties across different environmental conditions in order to be able to accurately predict reactions involving iron in the environment.

Here, I present an approach to measure rates and extents of electron transfer to iron minerals and link the measured values to calculations of reaction thermodynamics in order to make findings generally applicable across environmental conditions. In this talk, I highlight three research projects in which I applied this approach: the first project assessed how redox properties differ between iron minerals and evolve during mineral transformations. I studied mineral redox properties in controlled laboratory systems by quantifying the reduction of synthetic iron (oxy)hydroxides under selected thermodynamic conditions in electrochemical cells. The second project aimed at elucidating effects of mineral redox reactivity on rates of anaerobic microbial respiration in a floodplain soil. To this end, I tracked electron transfer to iron in soil incubations and linked electron transfer and mineral redox reactivity to iron mineralogy and carbon dioxide production. The third project focused on microbial iron reduction and its effect on water quality in a heterogeneous aquifer system under groundwater flow. I used an artificial aquifer system consisting of ferrihydrite-coated sand and embedded reduced sediment to study the export of microbial cells and organic carbon substrates from the sediment and resulting microbial iron reduction in the sand. Taken together, these examples illustrate how we can characterize the redox reactivity of minerals and use the obtained information to answer research questions related to various aspects of subsurface biogeochemistry.

## 4.2

# Applied physics research with Muon-Induced X-ray Emission at PSI

Sayani Biswas<sup>1</sup>, Lars Gerchow<sup>1</sup>, Gianluca Janka<sup>1</sup>, Stergiani Marina Vogiatzi<sup>1,2</sup>, Andreas Knecht<sup>1</sup>, Alex Amato<sup>1</sup>, Montserrat Filella<sup>3</sup>, Beda A. Hofmann<sup>4,5</sup>, Isabel Megatli-Niebel<sup>6,7</sup>, Lilian Raselli<sup>7</sup>, Edouard Quérel<sup>8</sup>, and Arndt Remhof<sup>8</sup>

<sup>1</sup> Paul Scherrer Institute, 5232 Villigen PSI, Switzerland ([sayani.biswas@psi.ch](mailto:sayani.biswas@psi.ch))

<sup>2</sup> Institute for Particle Physics and Astrophysics, ETH Zürich, 8093 Zürich, Switzerland

<sup>3</sup> Department F.-A. Forel, University of Geneva, Boulevard Carl-Vogt 66, CH-1205 Geneva, Switzerland

<sup>4</sup> Naturhistorisches Museum Bern, Bernastrasse 15, CH-3005 Bern, Switzerland

<sup>5</sup> Institute of Geological Sciences, University of Bern, Baltzerstrasse 1+3, CH-3012 Bern, Switzerland

<sup>6</sup> University of Cologne, Germany

<sup>7</sup> Augusta Raurica, Augst, Switzerland

<sup>8</sup> Laboratory Materials for Energy Conversion, Empa, Swiss federal Laboratories for Materials Science and Technology, 8600 Dübendorf, Switzerland

One of the non-destructive methods for analysing the elemental composition, which recently gained momentum since its first usage in the 1980's, is the Muon-Induced X-ray Emission technique (MIXE). Its main advantage over the other existing non-destructive techniques, like X-Ray Fluorescence (XRF), is that the elemental composition can be determined deep inside the sample (up to a few mm). Unlike the neutron activation techniques, MIXE does not introduce high activity in the sample, enabling it to be taken back right after the measurement. Moreover, all the elements in the periodic table, except hydrogen, can be identified with this technique.

Due to the above-mentioned advantages, a new Germanium Array for Non-destructive Testing (GIANT) setup (funded by the SNSF Sinergia project "Deepμ", Grant: 193691) was developed at the continuous muon source at Paul Scherrer Institute (PSI) (see Fig. 1). The continuous-wave character of the muon beam at PSI enables the quantitative determination of elemental composition to as low as ~0.5 wt% within ~1 h of data acquisition time.

The isotopic ratios of elements with  $Z > 25$  as well as estimation of different oxidation states of elements are being studied with the present setup. A proof-of-principle experiment showing the usage of MIXE at PSI to perform a depth-dependent elemental determination, using a simple three-layered sandwich sample (Fe, Ti, and Cu) has been recently published (Biswas 2022). We present here a few examples of how this technique is used with the GIANT setup at PSI to determine the elemental/isotopic composition in (i) consumer plastics, plastic litter from Swiss lakes and references provided by the University of Geneva (ii) meteorites from Natural History Museum, Bern, (iii) archaeological artefacts from the Augusta Raurica museum in Basel, and (iv) Li-ion batteries from Empa.

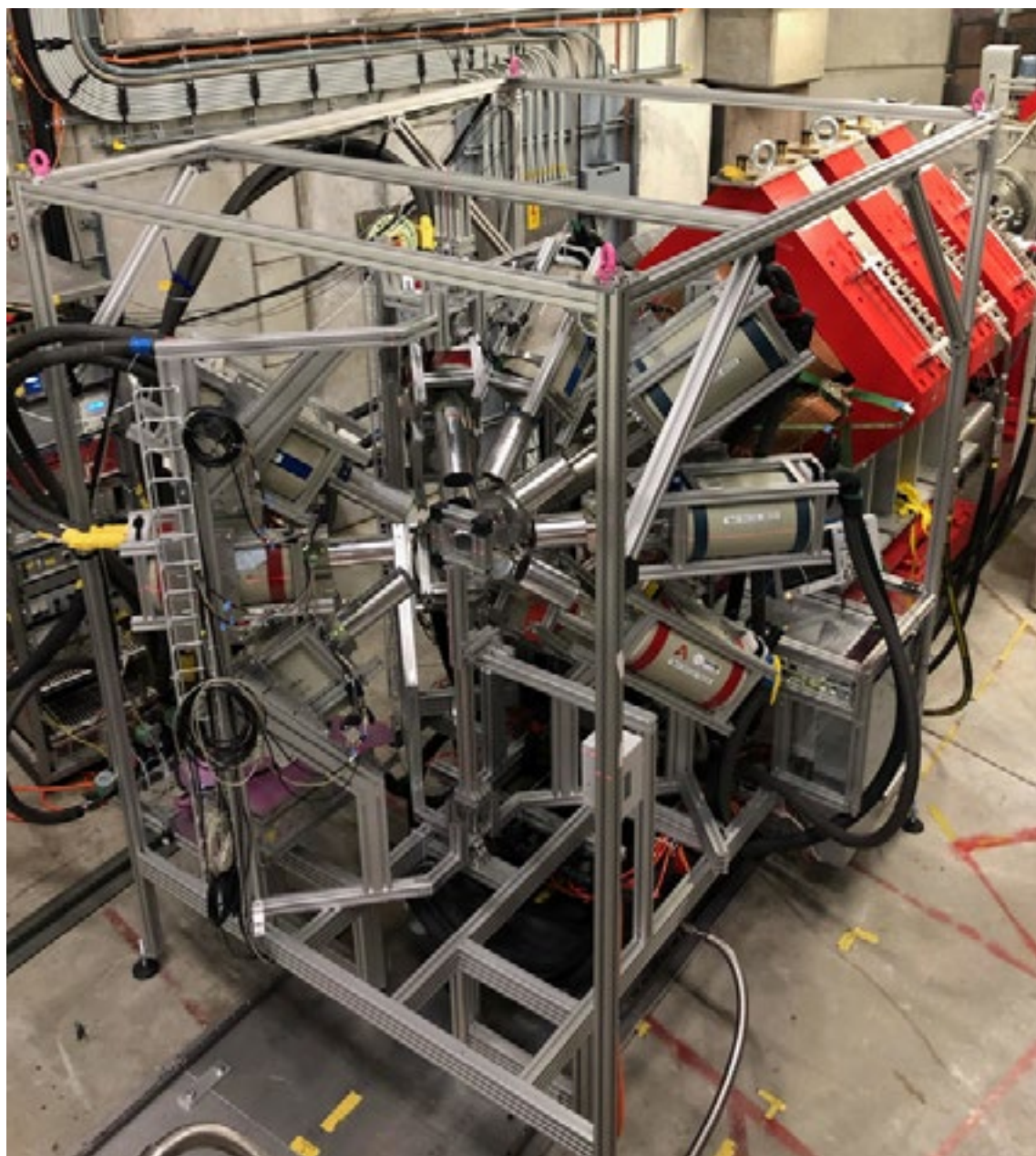


Figure 1. Germanium Array for Non-destructive Testing (GIANT) setup at Paul Scherrer Institute (PSI) used for applied physics research.

## REFERENCES

- Biswas, S. et al. 2022: Characterization of a Continuous Muon Source for the Non-Destructive and Depth-Selective Elemental Composition Analysis by Muon Induced X- and Gamma-rays, *Appl. Sci.*, 12, 2541.

## 4.3

### Microbial and geochemical drivers of manganese-mediated organic matter oxidation in soils

Nathan Chin<sup>1</sup>, Xiao-Jun Allen Liu<sup>1</sup>, Luiz Domeignoz-Horta<sup>2</sup>, Kristen DeAngelis<sup>1</sup>, Marco Keiluweit<sup>1,3</sup>

<sup>1</sup> University of Massachusetts Amherst, Amherst, MA, United States ([nathanchin@umass.edu](mailto:nathanchin@umass.edu))

<sup>2</sup> University of Zurich, Zurich, Switzerland

<sup>3</sup> University of Lausanne, Lausanne, Switzerland

Manganese (Mn) has recently been found to act as an important control on soil organic matter degradation, regulating the balance between greenhouse gas emissions and carbon storage in soils. In particular, reactive Mn(III) is a critical driver of organic matter degradation. However the microbial controls and biogeochemical drivers of Mn(III) formation in soils are largely unknown. Here we show that oxic-anoxic interfaces, which are ubiquitous in soils and sediments, serve as microbial hotspots of Mn(III)-mediated organic matter degradation. To do this, we used soil diffusion reactors with varying Mn availability and quantified changes in microbial dynamics, Mn transformations, and organic matter degradation across redox gradients over a 12-week incubation period. Wet-chemical and X-ray spectroscopic analyses showed that Mn(III) formation was greatest at the interface and increased with Mn availability. Metatranscriptomics revealed enhanced expression of Mn(II)-oxidizing enzymes at the interface, coinciding with increases in fungal-to-bacterial ratios as indicated by qPCR. Spectroscopic measurements, bioassays, and microbial respiration rates show that organic matter degradation increased with enhanced Mn availability and Mn(III) formation at the interface. In sum, our results suggest that the microbial formation of reactive Mn(III) species across oxic-anoxic interfaces is a critical regulator of microbial organic matter degradation in soils. These findings imply a tight yet underappreciated coupling of Mn and C cycles in redox-active soil environments.

## 4.4

### Testing arsenic and manganese removal by natural aeration of contaminated groundwater in rural Amazonia

Caroline de Meyer<sup>1</sup>, Ramiro Escalera Vásquez<sup>2</sup>, Lizangela Hualpara Llully<sup>3</sup>, Edward Carpio Deza<sup>4</sup>, Mauricio Ormachea Muñoz<sup>3</sup>, Adrien Mestrot<sup>1</sup>

<sup>1</sup> Soil Science Unit, Institute of Geography, University of Bern, Bern, Switzerland ([demeyerc.caroline@gmail.com](mailto:demeyerc.caroline@gmail.com))

<sup>2</sup> Research Center for Industrial Processes, Private University of Bolivia, Cochabamba, Bolivia

<sup>3</sup> Institute of Research in Chemistry, Major University of San Andres, La Paz, Bolivia

<sup>4</sup> Center for Development of Advanced Materials and Nanotechnology, Nacional University of Engineering, Lima, Peru

Groundwater in Amazonian floodplains is naturally enriched in arsenic and manganese, thereby forming a potential harm to the health of people relying on this groundwater for consumption. The contaminated groundwater is anoxic, typically rich in dissolved iron and in humics, and is hence in disequilibrium with the environmental conditions upon pumping of the groundwater to the surface. As a result, once at the surface, orange-reddish iron(hydr)oxides quickly form, and an oily film appears at the water surface. Because of these dislikable aspects, it is a common practice by locals to let the water stand for a certain time before use or consumption. Although local customers are not even aware of its presence, this practice could have the beneficial side-effect of capturing toxic trace elements into the formed solid phases.

Here we investigated, through combined field and laboratory studies, what the effect of this practice is on the removal of arsenic and manganese from the water and what internal (e.g. hydrochemistry) and external (e.g. pumping rhythm) factors influence the removal.

## 4.5

# Fertilizing effect of volcanic ash on the hermatypic coral *Stylophora pistillata*

Frank Förster<sup>1</sup>, Stephanie Reynaud<sup>2</sup>, Dario Omanovic<sup>3</sup>, Elias Samankassou<sup>1</sup>, Christine Ferrier-Pages<sup>2</sup>, Tom Sheldrake<sup>1</sup>

<sup>1</sup> Department of Earth Sciences, University of Geneva, Rue des Maraîchers 13, 1205 Genève, Switzerland  
(frank.foerster@unige.ch)

<sup>2</sup> Centre Scientifique de Monaco, Coral Ecophysiology team, 8 Quai Antoine 1er, MC-98000 Monaco

<sup>3</sup> Center for Marine and Environmental Research, Ruđer Bošković Institute, Bijenička cesta 54, HR-10000 Zagreb, Croatia

Volcanic eruptions disturb all ecosystems in their vicinity, with one such example being coral reefs around tropical islands. Volcanic ash and pyroclastic material deposited in the ocean can smother living coral reefs (Vroom & Zglicynski, 2011) or lead to overgrowth of macroalgae and cyanobacteria (Houk, 2011). However, less emphasis has been paid to the effect of ash-leached limited trace metals into the water column and the impact on the coral and its endosymbiotic zooxanthellae. This study presents the first critical examination of the interaction between volcanic ash and corals, performed in laboratory settings. For this, coral microcolonies of *Stylophora pistillata* were equally distributed in control tanks and in tanks regularly exposed to volcanic ash over a period of 6 weeks. The physiological response (photosynthesis-respiration-rate, photosynthetic efficiency, growth rate) of the coral to the volcanic ash was measured throughout the 6 weeks. After the experiment, organic tissue was analysed using mass spectroscopy for leached trace and minor elements in the coral tissue and its symbionts.

Our findings indicate a fertilizing effect of the volcanic ash to the holobiont coral, which results in increased photosynthetic activity of the microcolony. Ash-leaching increases metal and nutrient availability in the seawater, and so consequently both coral tissue and zooxanthellae are enriched in trace metals. The availability of Fe and Mn primarily increases the efficiency of the photosynthetic apparatus of the zooxanthellae. Despite the enrichment in heavy metals in coral tissue (Co59, Cr52, Cu63) and in zooxanthellae (As75, Co59, Cr52, Mo95, Ni60, V51), no toxicologic effect could be observed. The present study introduces a new experimental approach to connect coral biogeochemistry with volcanology and explores for the first time the beneficial role of volcanic ash as important nutrient source for living corals. The implication of this advantageous interaction needs to be tested for the more complex coral reef ecosystem, but yields the potential to counterbalance external stresses such as those induced by climate change.

## REFERENCES

- Vroom, P., & Zglicynski, B. 2011: Effects of volcanic ash deposits on four functional groups of a coral reef, *Coral Reefs*, 30(4), 1025-1032.  
Houk, P. 2011: Volcanic disturbances and coral reefs. In: Hopley, D. (eds) *Encyclopedia of Modern Coral Reefs. Encyclopedia of Earth Sciences Series*. Springer, 1138-1140.

## 4.6

# What does the chemical composition of cellulose tell us about the provenance of instream wood?

Javier del Hoyo<sup>1\*</sup>, Laetitia Monbaron<sup>1</sup>, Marceline Vuaridel<sup>1</sup>, Virginia Ruiz-Villanueva<sup>1</sup>

<sup>1</sup> Institute of Earth Surface Dynamics, University of Lausanne, Quartier Mouline, 1015 Lausanne. \*Javier.delhoyo@unil.ch

Large Wood (LW) in rivers is an essential component of fluvial ecosystems. Its presence has a series of ecological effects, highlighting its influence on fluvial and sediment dynamics, modifying river geomorphology and increasing the availability of ecological habitats and, thus, boosting the associated biodiversity (Wohl, 2017). However, during flood events, the presence of LW is also related to an increased risk on infrastructures and population (De Cicco et al., 2018). Therefore, it is imperative to understand LW dynamics at the catchment scale to properly design management of wood in rivers. Above all, it is of utmost importance to identify the source areas that are supplying most wood along the river network.

To this end, we look for tracers within the wood cellulose that are related to where the tree was growing before becoming instream wood. We explore the chemical composition of the wood, as many of the minor and trace elements present in the soil, and related to the geology and land cover of a particular area, are nutrients that trees need for their development and store in their cellulose (Sandak et al., 2011). Therefore, relative values of these elements can be used to distinguish between different regions and thus different LW source areas within a river catchment.

The study area is the Rhone River catchment (~3000 km<sup>2</sup>) downstream from Lake Léman and down to the Génissiat dam 50 km downstream, where all the incoming wood is retained at the reservoir, particularly after flood events. The LW arriving at the dam comes mainly from the two major tributaries of the Rhone: the 108 km long Arve river (a 1984 km<sup>2</sup> basin) from the Alps and the 47 km long Valseline river (a 370 km<sup>2</sup> basin) from the Jura.

We have taken reference samples from living trees along both rivers, and samples of LW from the Génissiat reservoir, whose origin is unknown. The chemical composition of the samples is being analysed with inductively coupled plasma optical emission spectroscopy (ICP-OES). Results from the reference samples showed significant differences in the concentration of some elements (e.g., Ba, Mg, Mn, Sc, etc.) and between the trees growing in one basin and the other and even between trees from different regions within the same river subcatchment.

We still need to compare the samples obtained from Génissiat with the reference samples, to infer their provenance. The gained knowledge will allow to identify LW source areas after relevant flood events, and thus better manage the wood in rivers and potential related hazards.

*This work is supported by the SNSF Eccellenza project PCEFP2-186963 and the University of Lausanne.*

## REFERENCES

- De Cicco, P. N., Paris, E., Ruiz-Villanueva, V., Solari, L., & Stoffel, M. (2018). In-channel wood-related hazards at bridges: A review. *River Research and Applications*, 34(7), 617–628.
- Sandak, A., Sandak, J., & Negri, M. (2011). Relationship between near-infrared (NIR) spectra and the geographical provenance of timber. *Wood Science and Technology*, 45(1), 35–48.
- Wohl, E. (2017). Bridging the gaps: An overview of wood across time and space in diverse rivers. *Geomorphology*, 279, 3–26

## 4.7

### The unlimited potential of fungi

Katia Gindro

*Agroscope, route de Duiller 50, 1260 Nyon, Switzerland*

Fungi are cosmopolitan and ubiquitous. They can be found in rainwater, air, soil, litter, green and woody plants, in our pharmaceutical and food industry, in all living and dead tissues. They are the main recyclers of organic matter and the most active producers of secondary metabolites. Their enzymatic potential is by far the most diversified, allowing them to continuously adapt to their environment and to degrade any organic matter for their nutritional, developmental and reproductive needs. This gives them, in addition to a continuous adaptive plasticity to their environment, the possibility to develop resistance to the different fungicidal active ingredients used in agronomy and medicine. In the same way, fungi have developed an important potential of remediation by their capacity to immobilize heavy metals or to degrade pollutants such as phytosanitary or pharmaceutical products.

These combined skills allow us to exploit their inestimable potential for the development of very diversified research projects, for example for the discovery of new bioactive compounds for both agronomy and medicine, for the remediation of water polluted by certain persistent phytosanitary products or by copper, or for the discovery of new colorants and flavors. This conference will allow you to discover the fascinating world of fungi and their unlimited potential.

## 4.8

### Insights into colloidal antimony in pore water of contaminated soils analyzed with AF4-ICP-MS and SEC-ICP-MS

Ursina Morgenthaler<sup>1</sup>, Isabelle Worms<sup>2</sup>, Karen Viacava<sup>1</sup>, Vera Slaveykova<sup>2</sup>, Adrien Mestrot<sup>1</sup>

<sup>1</sup> Institut of Geography, University of Bern, Hallerstrasse 12, 3012 Bern, Switzerland ([ursina.morgenthaler@giub.unibe.ch](mailto:ursina.morgenthaler@giub.unibe.ch))

<sup>2</sup> Department F.-A. Forel for environmental and aquatic sciences, School of Earth and Environmental Sciences, University of Geneva, Boulevard Carl-Vogt 66, 1211 Geneva, Switzerland

Elevated concentrations of antimony (Sb) in soils pose a significant risk for Sb mobilization and subsequent migration to the surrounding environment. Despite its toxicity to plants, animals, and humans, the geochemistry of Sb is still poorly understood. Sb has been found to be very mobile, especially under flooded soil conditions. Indeed, Sb concentrations in runoff water from contaminated shooting range soils often exceed those of lead (Pb), even though lead bullets only contain 1-5% of Sb as a hardening agent. One hypothesis for the high mobility of Sb in flooded soils is colloid-facilitated transport, a process that has been found to strongly regulate the mobility of trace elements and other contaminants. Previous studies on colloid-Sb interactions and transport are scarce and inconclusive.

We incubated Sb contaminated soils from three Swiss shooting ranges under flooded conditions. Sb mobility was monitored alongside a series of explanatory variables in soil pore water, which was sampled over the whole incubation time of 3 months. To determine the abundance and nature of Sb-bearing colloids, and their role in Sb mobility, pore water samples taken at the beginning, in the middle, and at the end of the incubation experiment were analyzed with asymmetric flow field-flow fractionation (AF4) and size exclusion chromatography (SEC), both coupled to inductively coupled plasma mass spectroscopy (ICP-MS).

Both chromatography methods yielded distinctive fractograms for Sb, showing that Sb binds to colloids of a specific size in pore water of contaminated soils.

These Sb-bearing colloids changed with time after flooding by becoming larger and more diverse. This transformation is most probably linked to changes in the redox regime of the system. Sb coeluted with organic acid and Iron (Fe), indicating an affinity for both, organic and inorganic colloids. In absolute values, colloidal Sb made up only a minor amount of the total Sb concentrations, putting the role of colloid-facilitated transport in Sb mobility into perspective. Nevertheless, our results are the first that describe and quantify colloidal Sb in soil pore water and therefore help to further understand the complex chemistry of Sb in the soil-water interface.

## 4.9

# Effects of dissolved organic compounds on phosphate uptake of Fe(III)-precipitates formed by Fe(II) oxidation.

Ville Nenonen<sup>1,2</sup>, Ralf Kaegi<sup>1</sup>, Stephan J. Hug<sup>1</sup>, Stefan Mangold<sup>3</sup>, Jörg Göttlicher<sup>3</sup>, Lenny H.E. Winkel<sup>1,2</sup> & Andreas Voegelin<sup>1</sup>

<sup>1</sup> Eawag, Swiss Federal Institute of Aquatic Science and Technology, Ueberlandstrasse 133, CH-8600 Duebendorf, Switzerland ([ville.nenonen@eawag.ch](mailto:ville.nenonen@eawag.ch))

<sup>2</sup> Department of Environmental Sciences, Institute of Biogeochemistry and Pollutant Dynamics, ETH, Swiss Federal Institute of Technology, Zurich, Switzerland.

<sup>3</sup> Karlsruhe Institute of Technology, Institute of Synchrotron Radiation, Hermann-von-Helmholtz Platz 1, D-76344 Eggenstein-Leopoldshafen, Germany

Phosphorus as phosphate ( $\text{PO}_4$ ) is an essential and often growth-limiting nutrient, but excessive inputs of  $\text{PO}_4$  into surface waters can lead to eutrophication. The fate of  $\text{PO}_4$  in the environment is coupled to the redox-cycling of iron (Fe). The oxidation of Fe(II) in natural waters leads to the precipitation of amorphous to poorly crystalline Fe(III)-solids that can bind  $\text{PO}_4$  (Senn et al. 2015). Dissolved organic matter (DOM) may affect the structure, colloidal mobility, and  $\text{PO}_4$  uptake of Fe(III)-precipitates (Vindedahl et al. 2016). To date, mechanistic insights on the effect of DOM on the formation, properties, and  $\text{PO}_4$  uptake of Fe(III)-precipitates formed by Fe(II) oxidation in the presence of DOM and other interfering solutes (Ca,  $\text{PO}_4$ ) in natural waters are still scarce.

The aim of this work was to study the effects of model organic ligands (citrate, 2,4-dihydroxybenzoate, galacturonate, humate) on the structure, colloidal stability, and  $\text{PO}_4$  uptake of Fe(III)-precipitates. Laboratory experiments were performed in bicarbonate-buffered (pH 7.0) aqueous solutions, with Na or Ca as electrolyte cation,  $\text{PO}_4$  (molar P/Fe ratios of 0.25 or 0.05), and organic ligands (molar C/Fe ratios of 0.1 to 9.6). Precipitate formation was initiated by spiking 0.5 mM Fe(II) to the aerated solutions; followed by a 18-h reaction time. Solutions were analyzed for Fe, P, Ca and organic C. Suspended solids were analyzed for their particle sizes and zeta potentials by dynamic and electrophoretic light scattering. The local coordination of Fe in the dried solids was characterized by extended X-ray absorption fine structure spectroscopy, molecular bonding of Fe,  $\text{PO}_4$ , and OM by Fourier-transform infrared spectroscopy, and particle morphology and composition distribution by transmission electron microscopy coupled to energy dispersive X-ray detection.

Fe(III)-precipitates formed without DOM were mixtures of amorphous Fe(III)-phosphate and poorly-crystalline lepidocrocite (Senn et al. 2015). Increasing levels of the organic ligands lead to increasing formation of ferrihydrite instead of lepidocrocite and to decreasing lepidocrocite crystallinity, resulting in more effective  $\text{PO}_4$  binding. On the other hand, higher C/Fe ratios resulted in lower aggregate sizes and more negative zeta potentials, i.e., higher colloidal stability. These effects decreased in the order citrate > galacturonate > humate  $\geq$  2,4-dihydroxybenzoate. At C/Fe  $>$  0.6, citrate inhibited precipitate formation. In conclusion, this study shows that organic ligands can enhance the  $\text{PO}_4$  binding and colloidal stability of Fe(III)-precipitates to variable degree and thereby impact Fe-related  $\text{PO}_4$  cycling in environmental systems.

## REFERENCES

- Senn, A.-C.; Kaegi, R.; Hug, S. J.; Hering, J. G.; Mangold, S.; Voegelin, A., *Composition and structure of Fe(III)-precipitates formed by Fe(II) oxidation in near-neutral water: Interdependent effects of phosphate, silicate and Ca*. Geochim. Cosmochim. Acta 2015, 162, 220–246.
- Vindedahl, A. M., Strehlau, J. H., Arnold, W. A., Penn, R. L. *Organic matter and iron oxide nanoparticles: aggregation, interactions, and reactivity*. Environmental Science: Nano 2016, 3, 494–505.

## 4.10

### Retention of Tc on Fe-bearing Clay Minerals

Yanting Qian<sup>1,2</sup>, Andreas C. Scheinost<sup>3a,b</sup>, Sylvain Grangeon<sup>4</sup>, Alwina Hoving<sup>5</sup>, Jean-marc Greneche<sup>6</sup>, Maria Marques Fernandes<sup>1</sup>, Sergey V. Churakov<sup>1,2</sup>

<sup>1</sup> Laboratory for Waste Management, Paul Scherrer Institut, CH-5232 Villigen PSI

(yanting.qian@psi.ch) (maria.marques@psi.ch) (sergey.churakov@psi.ch)

<sup>2</sup> Institute for Geological Sciences, University of Bern, CH-3012 Bern

<sup>3a</sup> The Rossendorf Beamline at the European Synchrotron Radiation Facility (ESRF), Avenue des Martyrs 71, 38043, Grenoble (scheinost@esrf.fr)

<sup>3b</sup> Helmholtz Zentrum Dresden Rossendorf, Institute of Resource Ecology, Bautzner Landstrasse 400, 01328, Dresden

<sup>4</sup> BRGM – French Geological Survey, 45060 Orléans (S.Graneon@brgm.fr)

<sup>5</sup> TNO Geological Survey of the Netherlands, PO Box 80015, 3508 TA Utrecht (alwina.hoving@tno.nl)

<sup>6</sup> Institut des Molécules et Matériaux du Mans IMMM UMR CNRS 6283, Le Mans Université, 72085, Le Mans Cedex 9 (jean-marc.greneche@univ-lemans.fr)

<sup>99</sup>Tc is one of the redox-sensitive fission products with a long half-life ( $2.1 \times 10^5$  years) and high toxicity. Tc in its most oxidized heptavalent anionic form ( $\text{TcO}_4^-$ ) is highly mobile, whereas under reducing conditions the mobility of Tc is greatly decreased as it is reduced to insoluble  $\text{TCO}_2 \cdot n\text{H}_2\text{O}$ -like species. The migration of <sup>99</sup>Tc contaminants in the deep geological repository is essentially controlled by geochemical factors such as mineralogical and chemical composition of the environment, pH, redox potential (Eh), solubility, biological (microbial) interactions, and (redox) reaction kinetics. Clay minerals, as the main components of the engineered barrier in several deep geological repository concepts, play a key role in retarding the migration of <sup>99</sup>Tc to the biosphere. Especially iron-containing clay minerals, depending on the amount and location of redox-active Fe, might cover a large range of reducing potentials (Gorski et al. 2013), and thus potentially affect the mobility and (bio)availability of <sup>99</sup>Tc by changing its oxidation state.

Here, we will systematically address the retention of  $\text{Tc}^{VII}$  by  $\text{Fe}^{II}/\text{Fe}^{III}$  containing clay minerals. We perform Tc sorption experiments on native and reduced smectite clay samples with different  $\text{Fe}^{II}/\text{Fe}^{III}$  ratios. The  $\text{Fe}^{II}/\text{Fe}^{III}$  ratio and its local coordination in the clay mineral structure are determined by both Mössbauer and Fe K-edge XAFS spectroscopy. The reduced species after sorption experiments are identified by Tc K-edge XANES and EXAFS. Reduction of  $\text{Tc}^{VII}$  to  $\text{Tc}^{IV}$  by Fe-bearing minerals has been observed, mainly forming  $\text{TCO}_2 \cdot n\text{H}_2\text{O}$  surface precipitates (Jaisi et al. 2009; Peretyazhko et al. 2008). Most of these studies, however, were carried out at rather high Tc loadings. The focus of our study is on low Tc loadings, which are more environmentally relevant. By identifying the reduced surface products at low loading, we expect to have a better understanding of the geochemical redox reaction between Fe and Tc, and thus contribute to a more reliable prediction of Tc retention in radioactive waste repositories.

#### REFERENCES

- Gorski, C.A., et al. 2013: Redox properties of structural Fe in clay minerals: 3. Relationships between smectite redox and structural properties. Environ Sci Technol., 47(23): p. 13477-85.
- Jaisi, D.P., et al. 2009: Reduction and long-term immobilization of technetium by Fe(II) associated with clay mineral nontronite. Chemical Geology, 264(1): p. 127-138.
- Peretyazhko, T., et al. 2008: Heterogeneous reduction of Tc(VII) by Fe(II) at the solid–water interface. Geochimica et Cosmochimica Acta., 72(6): p. 1521-1539

## 4.11

# Assessing trace element concentrations in surface soils across Switzerland

Jolanda E. Reusser<sup>1,2</sup>, Maja B. Siegenthaler<sup>1,3</sup>, Lenny H.E. Winkel<sup>2,3</sup>, Ruben Kretzschmar<sup>2</sup>, Daniel Wächter<sup>1</sup>, Reto G. Meuli<sup>1</sup>

<sup>1</sup> Swiss Soil Monitoring Network NABO, Agroscope, CH-8046 Zurich ([jolanda.reusser@agroscope.admin.ch](mailto:jolanda.reusser@agroscope.admin.ch))

<sup>2</sup> Institute of Biogeochemistry and Pollutant Dynamics, ETH Zurich, CH-8092 Zurich

<sup>3</sup> Department Water Resources and Drinking Water, Swiss Federal Institute of Aquatic Science and Technology, Eawag, CH-8600 Dübendorf

Trace elements such as Se, Cu and Zn are essential for humans, plants, and other organisms. However, depending on the concentration range, trace elements can pose a potential threat to plant and/or human health. Knowledge of the concentrations and spatial distributions of trace elements in soils is a prerequisite for defining regions with potentially deficient or contaminated soils.

For this purpose, we are creating a soil geochemical atlas presenting the spatial distribution of 22 elements in Swiss surface soils.

The atlas is based on 1'082 sampling sites distributed on a regular 6 by 4 km grid across Switzerland. Samples of the topsoils (0-20 cm) have been collected between 2011 and 2015 within the framework of the Swiss Biodiversity Monitoring (BDM) program (Meuli et al., 2017). Element concentrations including As, B, Ca, Cd, Co, Cr, Cu, Fe, Hg, Mg, Mn, Mo, Na, Ni, Pb, S, Sb, Se, Ti, U, V, and Zn were measured in aqua regia digests of dried and sieved (<2 mm) soil samples using ICP-MS. In addition, parameters describing chemical and physical soil properties such as pH,  $\text{CaCO}_3$  content, total C and N, the content of clay, silt and sand, organic C, etc. have been measured. The dataset was completed by auxiliary data from various sources (precipitation, lithology, elevation, atmospheric deposition, etc.).

Based on these data, we carried out multivariate statistics using different machine learning techniques (random forest, gradient boosting) in combination with expert knowledge in order to evaluate factors influencing the distribution of trace elements across Swiss surface soils. First results indicate that the proportion of overall variance explainable by these factors depends on the element and on the chosen method. For example, less than 30 % of the overall variance can be explained for Sb, but more than 90 % for Ca. Furthermore, main predictors vary markedly between elements, e.g. the importance of pH, the importance of variables representing the soil organic matter, or the importance of the soil mineralogy is different for each element.

Here we will present the current state of the geochemical soil atlas as well as the results of multivariate analyses.

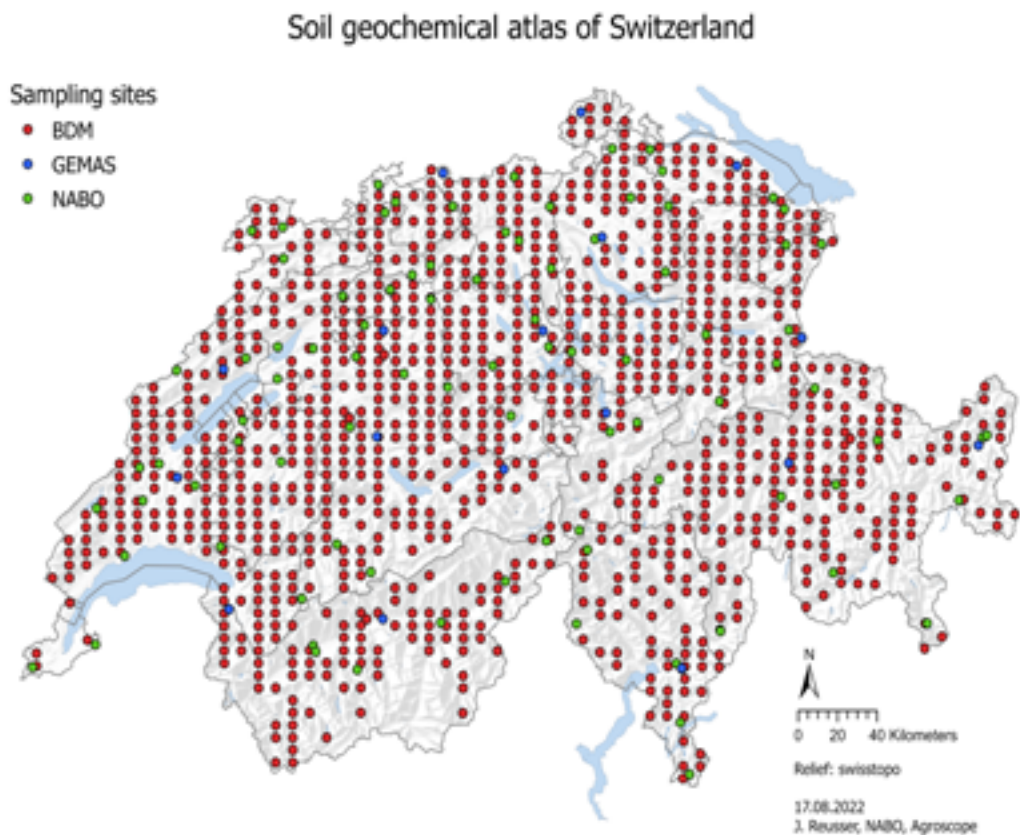


Figure 1. Sampling sites of the soil geochemical atlas. BDM: Swiss Biodiversity Monitoring program, up to 4 samples per site; GEMAS: sampling sites of the “Geochemical Mapping of Agricultural and Grazing Land Soil in Europe” (Reimann et al., 2014); NABO: sampling sites of the Swiss Soil Monitoring Network.

## REFERENCES

- Meuli, R.G., Wächter, D., Schwab, P., Kohli, L., Zimmermann, R., 2017. Connecting Biodiversity Monitoring with Soil Inventory Data – A Swiss Case Study. *Bulletin BGS* 38, 65–69.
- Reimann, C., Birke, M., Demetriades, A., Filzmoser, P., O'Connor, P., Akinfiev, G., Albanese, S., Amashukeli, Y., Andersson, M., Arnoldussen, A., Artamonov, Y., Audion, A., Baritz, R., Barker, K., Batista, M., Bellan, A., Belougovschev, V., Bitz, I., Branellec, M., Zomeni, Z., 2014. Chemistry of Europe's agricultural soils - Part A: Methodology and interpretation of the GEMAS data set.

## 4.12

# Estuarine biogeochemical processes influencing the potentially bioavailable fraction of a range of trace metals

Mary-Lou Tercier-Waeber<sup>1</sup>, Melina Abdou<sup>1,2</sup>, Abra Penezic<sup>1</sup>, Fabio Confalonieri<sup>3</sup>, Alexandra Coynel, Jörg Schäfer<sup>2</sup>

<sup>1</sup> University of Geneva, Sciences II, 30 Quai E.-Ansermet, 1221 Geneva 4, Switzerland ([marie-louise.tercier@unige.ch](mailto:marie-louise.tercier@unige.ch))

<sup>2</sup> University of Bordeaux, UMR CNRS 5805 EPOC, 3315 Pessac, France

<sup>3</sup> Idronaut Srl, Via Monte Amiata 10, 20047 Brugherio (MB), Italy

Trace metals play critical role in aquatic ecosystems. Understanding their impact is however challenging. Trace metals are distributed in a variety of redox states and chemical species that may vary continuously in space and time [1,2]. Only some trace metal species are bioavailable. The development of robust and adaptive submersible sensitive trace metal bioavailability-assessment tools is therefore required to support the establishment of guidelines based on realistic risk assessment to protect aquatic life and biodiversity, and ultimately human health.

Toward this aim, we developed a unique submersible compact integrated multichannel trace metal sensing probe (TracMetal) [2]. Innovative antifouling gel-integrated microelectrode arrays (GIMEs) are incorporated in the TracMetal. These sensors enable *in situ* autonomous and simultaneous measurements of the dynamic (potentially bioavailable) fraction of a range of EU and US-EPA (priority) hazardous metals: Hg(II), As(III), As(V), Cd(II), Pb(II), Cu(II), Zn(II) with sensitivity at sub-nanomolar to low picomolar levels.

We report here the application of the TracMetal in coastal aquatic systems characterized by contrasting conditions (salinity gradient, high turbidity) and hosting major coastal protected areas and economic activities. In parallel, master variables were monitored in situ, and water samples were collected for complementary analyses of total dissolved metal concentrations in the operationally defined dissolved <0.2 µm and <0.02 µm fractions; water composition and proxies for primary production. The combination of all data provided the first assessment of the spatial concentrations of the potentially available fractions of the targeted metals in estuarine complex systems and enabled to identify abiotic and biotic processes that control metal fate and potential impact [3].

## REFERENCES

- [1] Tercier-Waeber, M.-L., Stoll, S., Slaveykova, V.I. 2012: Trace metal behavior in surface waters: emphasis on dynamic speciation, sorption processes and bioavailability (Review), *Archive of Sciences*, 65, 119-142.
- [2] Tercier-Waeber, M.-L., Confalonieri, F., Abdou, M., Dutruch, L., Bossy, C., Fighera, M., Bakker, E., Schäfer, J., 2021: Advanced multichannel submersible probe for autonomous high-resolution *in situ* monitoring of the cycling of the potentially bioavailable fraction of a range of trace metals, *Chemosphere* 282, <https://doi.org/10.1016/j.chemosphere.2021.131014>.
- [3] Abdou M., Tercier-Waeber, M.-L., Dutruch, L., Bossy, C., Coynel, A., Bakker, E. Blanc, G., Schäfer, J., 2022: Estuarine dissolved speciation and partitioning of trace metals: a novel approach to study biogeochemical processes. *Environ. Res.*, 208, 112596,, <https://doi.org/10.1016/j.envres.2021.112596>

## 4.13

### Spatially and temporally resolved mineral phase evolution and arsenic retention in microfluidic models of zerovalent iron-based water treatment

Jonas Wielinski<sup>1</sup>, Joaquin Jimenez-Martinez<sup>1,2</sup>, Jörg Göttlicher<sup>3</sup>, Ralph Steininger<sup>3</sup>, Stefan Mangold<sup>3</sup>, Stephan J. Hug<sup>1</sup>, Michael Berg<sup>1</sup>, and Andreas Voegelin<sup>1</sup>

<sup>1</sup> Eawag, Swiss Federal Institute of Aquatic Science and Technology, Ueberlandstrasse 133, CH-8600 Dübendorf, Switzerland.

<sup>2</sup> ETH Zurich, Department of Civil, Environmental and Geomatic Engineering, CH-8092 Zürich, Switzerland.

<sup>3</sup> Karlsruhe Institute of Technology, Institute of Synchrotron Radiation, Hermann-von-Helmholtz Platz 1, D-76344 Eggenstein-Leopoldshafen, Germany

Arsenic (As) is a toxic element, and elevated levels of geogenic As in drinking water pose a threat to the health of several hundred million people worldwide. In this study, we used microfluidics in combination with optical microscopy and X-ray spectroscopy to investigate zerovalent iron (ZVI) corrosion, secondary iron (Fe) phase formation, and As retention processes at the pore scale in ZVI-based water treatment filters.

Two 250 µm thick microchannels filled with single ZVI and quartz grain layers were operated intermittently (12 h flow/12 h no-flow) with synthetic groundwater (pH 7.5; 570 µg/L As(III)) over 13 and 49 days. During operation, the corrosion of ZVI and the formation and transformation of Fe mineral phases was followed with spatiotemporal resolution using optical microscopy. After operation, the microchannel was resin-embedded for analysis by synchrotron-based micro-focused X-ray fluorescence spectrometry ( $\mu$ -XRF) and X-ray absorption spectroscopy ( $\mu$ -XAS), chemical imaging and fullfield XAS to gain insights into the spatial distribution of Fe, As and other elements, the distribution of Fe mineral phases, and the redox speciation of As.

At the start of filter operation, lepidocrocite (Lp) and carbonate green rust (GRC) were the dominant secondary Fe-phases. They underwent cyclic transformation over intermittent periods of water flow and stagnation. During no-flow, lepidocrocite partially transformed into GRC and into small fractions of magnetite, kinetically limited by Fe(II) diffusion or by decreasing corrosion rates. When water flow was resumed, GRC rapidly and nearly completely transformed back into lepidocrocite. Longer filter operation combined with a prolonged no-flow period accelerated magnetite formation. Phosphate adsorption onto Fe-phases allowed for spatially separated downstream precipitation of calcium carbonate and, consequently, accelerated anoxic ZVI corrosion. Arsenic was retained on Fe-coated quartz grains and in zones of cyclic Lp-GRC transformation, as both As(V) and As(III). Our results suggest that intermittent filter operation and the resulting redox cycles promote the formation of denser secondary Fe-solids and thereby ensure prolonged filter performance.

Methodologically, this work highlights the potential of spatially and temporally resolved studies on micromodels to offer new insights into geochemical processes at the pore scale under conditions of kinetic and transport limitations.

#### REFERENCE

Wielinski, J., Jimenez-Martinez, J., Göttlicher, J., Steininger, R., Mangold, S., Hug, S. J., Berg, M., Voegelin, A., *Spatiotemporal mineral phase evolution and arsenic retention in microfluidic models of zerovalent iron-based water treatment*. Environ. Sci. Technol. 2022, DOI: 10.1021/acs.est.2c02189.

## P 4.1

# Multidisciplinary Perspectives on Early Triassic Pyrogenic Carbon Cycling

Franziska R. Blattmann\*, Charline Ragon\*\*, Torsten Vennemann\*, Christian Vérard\*\*\*, Jérôme Kasparian\*\*, Maura Brunetti\*\*, Thierry Adatte\*\*\*\*, Hugo Bucher\*\*\*\*\* & Clayton R. Magill\*\*\*\*\*

\* Institute of Earth Surface Dynamics, University of Lausanne, Quartier UNIL-Mouline, 1015 Lausanne, Switzerland (Franziska.Blaettmann@unil.ch)

\*\* Group of Applied Physics and Institute for Environmental Sciences, Bd Carl-Vogt 66, 1205 Geneva, University of Geneva, Switzerland

\*\*\* Section of Earth and Environmental Sciences, University of Geneva, Rue des Maraîchers 13, CH-1205 Geneva, Switzerland

\*\*\*\* Institute of Earth Sciences, University of Lausanne, Quartier UNIL-Mouline, CH-1015 Lausanne, Switzerland

\*\*\*\*\* Paläontologisches Institut und Museum, Universität Zürich, Karl-Schmid-Strasse 4, 8006 Zürich, Switzerland

\*\*\*\*\* The Lyell Center, Heriot-Watt University, Research Avenue South, Edinburgh EH14 4AP, Scotland

Pyrogenic carbon (PyC) is produced by the incomplete combustion of organic matter. It is a poorly understood and potentially slow-cycling component of the organic carbon cycle (Bird et al. 2015). Across geological time, little is known about how PyC cycling has evolved and modulated the organic carbon cycle. In this study, the PyC cycle is examined for the Early Triassic (Smithian, Spathian), a time interval characterized by global carbon cycle perturbations and biological radiation and extinction pulses. Polycyclic aromatic hydrocarbon (PAH) biomarkers, which can differentiate sources of PyC, were analyzed and then compared with evaporation, precipitation, wind, biomes and temperature maps simulated through the MIT general circulation and Biome 4 models. Initial biomarker results from Spitzbergen show an increase in the PAH concentrations across the Smithian-Spathian boundary (SSB), in particular phenanthrene (Ph), chrysene (Chr), benz[a]anthracene (BaA), fluoranthene (FLA) and pyrene (PYR). Calculated ratios FLA/(FLA+PYR) and BaA/(Chr+BaA) indicate that fresh biomass and not coal combustion was the dominant PAH source; the latter is frequently considered to be the main source as a consequence of Siberian Traps volcanism (Payne & Clapham 2012). As temperature declined during the latest Smithian (Goudemand et al. 2019), our data and climate simulation output suggest that a cooler climate is associated to a weaker hydrological cycle with less precipitation, which in turn would have an impact on wildfire activity, particularly in high latitude regions. These findings contradict previous model-based studies, which have argued that wildfire activity was particularly low during the Early and Middle Triassic (Belcher et al. 2010).

## REFERENCES

- Belcher, C. M., Yearsley, J. M., Hadden, R. M., McElwain, J. C., & Rein, G. (2010). Baseline intrinsic flammability of Earth's ecosystems estimated from paleoatmospheric oxygen over the past 350 million years. *Proceedings of the National Academy of Sciences*, 107(52), 22448-22453.
- Bird, M. I., Wynn, J. G., Saiz, G., Wurster, C. M., & McBeath, A. (2015). The pyrogenic carbon cycle. *Annual Review of Earth and Planetary Sciences*, 43, 273-298.
- Goudemand, N., Romano, C., Leu, M., Bucher, H., Trotter, J., and Williams, I. (2019). Dynamic interplay between climate and marine biodiversity upheavals during the Early Triassic Smithian-Spathian biotic crisis. *Earth Sci. Rev.* 195, 169–178.
- Payne, J. L., & Clapham, M. E. (2012). End-Permian mass extinction in the oceans: an ancient analog for the twenty-first century? *Annual Review of Earth and Planetary Sciences*, 40, 89-111.

## P 4.2

### Microbial-Mineral Chips: a closer look at Fe reduction

Alice Bosco-Santos<sup>1</sup>, Giulia Ceriotti<sup>1</sup>, Jasmine Berg<sup>1</sup>

<sup>1</sup> Institute of Earth Surface Dynamics, University of Lausanne, Batiment Geopolis, Unil-Mouline, CH-1015 (alice.boscosantos@unil.ch, Giulia.Ceriotti@unil.ch)

Microbial iron (Fe) oxide reduction is a critical process regulating nutrient and contaminant cycling in subsurface environments. Batch cultures have traditionally been used to study microbial Fe reduction, but they fail to replicate the physical and geochemical micro-scale heterogeneity of natural sediment and soil environments. Here we argue that neglecting this microscale heterogeneity can be an obstacle to explaining the previously observed biomass of dissimilatory Fe reducers bacteria in marine and freshwater sediments decoupled from geochemical gradients (Otte et al., 2018). We have developed two experimental setups relying on microfluidic devices to directly visualize and monitor the evolving spatial organization of Fe reducers in response to O<sub>2</sub> gradients, mineral distribution, and porous architecture. In a stagnant straight channel, initially anoxic and allowing O<sub>2</sub> diffusion along the longitudinal direction, we tracked the spatial distribution evolution of a facultative Fe reducer bacteria (*Shewanella oneidensis* MR1) and, simultaneously, O<sub>2</sub> concentrations (Ceriotti et al., 2022). We observed that the initial tendency for sessile-clustering behavior of the cells around the Fe-oxides progressively shifts towards a planktonic-like spatial distribution over a few hours. We mimicked anoxic porewater flow in natural-like sediment structures using a microfluidics device etched with a heterogeneous porous structure. In addition to the Fe-oxides localization, we observed that filtration affects bacteria spatiality when a porous matrix is present, resulting in cell clusters trapped between no-reactive grains. Our preliminary microfluidic experiments indicate that O<sub>2</sub> concentration (<0.1 mg/L) in anoxic conditions (<0.5 mg/L, Burton et al., 2013) can potentially impact microbial-minerals aggregation; and that bacteria biomass is not a direct proxy for Fe reduction. As the organization of bacteria impacts function, we expect the use of microfluidic devices to continue enlightening aspects of microbial-mineral interactions blinded on batch experiments, that ultimately can impact strategies of bioremediation.

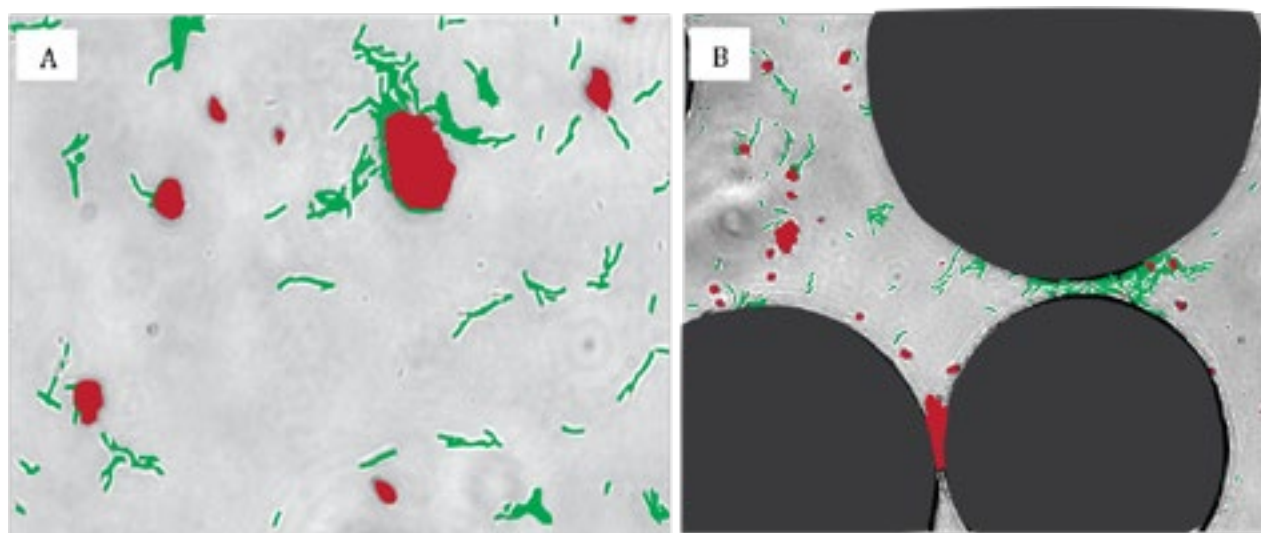


Figure 1. Bacteria (green) and Fe-oxides (red) in a microfluidic device. A. In a flowing system without a porous matrix, bacteria gather and grow prevalently around Fe-oxides with patterns similar to those observed in stagnant systems. B. In a porous matrix is present, the colonization of the Fe-oxide surfaces co-occurs with filtration.

#### REFERENCES

- Otte, J.m., Harter, J., Laufer, K., Blackwell, N., Straub, D., Kappler, A. And Kleindienst, S. 2018: The Distribution Of Active Iron-Cycling Bacteria In Marine And Freshwater Sediments Is Decoupled From Geochemical Gradients, Environ Microbiol, 20, 2483-2493.
- Ceriotti, G., Borisov, S.m., Berg, J.s., De Anna, P. 2022: Morphology And Size Of Bacteria Colonies Control Anoxic Microenvironment Formation In Porous Media, Arxiviv: 2208.05733v1
- Burton, C.a., Land, M., And Belitz, K. 2013: Status And Understanding Of Groundwater Quality In The South Coast Range-Coastal Study Unit, 2008: California Gama Priority Basin Project (No. 2013-5053). Us Geological Survey

## P 4.3

### On the behaviour of W and Re in pore fluids and sediments from a continental margin

Sylvie Bruggmann<sup>1,2</sup>, James McManus<sup>3</sup>, Silke Severmann<sup>2</sup>

<sup>1</sup> Institute of Earth Sciences, University of Lausanne, Géopolis, Quartier UNIL – Mouline, CH-1015 Lausanne  
(sylvie.bruggmann@unil.ch)

<sup>2</sup> Department of Marine and Coastal Sciences, Rutgers University, 71 Dudley Road, USA-08901 New Brunswick, New Jersey

<sup>3</sup> Bigelow Laboratory for Ocean Sciences, 60 Bigelow Drive, USA-04544 East Boothbay, Maine

The trace metals tungsten (W) and rhenium (Re) are promising tools to track redox changes in past environments. Interpretations of W and Re concentrations in sediments and sedimentary rocks rely on our understanding of the processes driving the cycling of these metals from water column to pore fluids, and eventually to the sediment. While recent studies are focusing on deciphering the behaviour of W and Re in modern oceans and sediments, information on their behaviour in pore fluids is scarce. We contribute new W and Re concentration data from pore fluids and sediments from six sites on the California and Mexico continental margin. These sites span a range of geochemical conditions, including organic-rich anoxic sites as well as Mn-rich oxic sites.

Our results show that W closely follows the distribution of Mn, showing positive correlations of W and Mn in both solid and dissolved phases at the Mn-rich oxic sites. Dissolved Re concentrations decrease with depth at stations with oxygenated surface sediments, indicating that Re is removed from the pore fluids to the sediment under reducing conditions. At organic-poor sites, Re follows a similar pattern as U.

This study provides new insights into the cycling of W and Re under a range of geochemical conditions, helping to improve interpretations of W and Re variations in the geological record.

## P 4.4

# Isotope Fingerprints for Deciphering the Role of Chelating Thiols to Separate Zinc from Cadmium in Plants (IsoThiolPrint)

Fernando Antônio Gomes Brito<sup>1</sup>, Matthias Wiggenhauser<sup>1</sup>

<sup>1</sup> Group of Plant Nutrition, ETH Zürich, Eschikon 33, CH-8315 Lindau (fgomes@ethz.ch)

Cadmium (Cd) and zinc (Zn) occur naturally in soils and through anthropogenic activities. Even though Cd plays no role in plant metabolism, it is easily absorbed by plants because it is chemically similar to Zn. In the plant, Cd accumulates in the edible parts and eventually enters the food chain posing a serious risk to human health in the long run. Zinc is essential for plants and humans but is toxic in high concentrations. To cope with these metals, plants have tools such as thiols (R-SH). These organic molecules bind and/or chelate metals (i.e. detoxify) and thereby immobilize and/or transport them. Thiols can further separate these metals by sequestering them into the vacuole of different organs such as roots and leaves. As a result, not all metals that are taken up by the plant end up in edible parts. To further investigate the uptake and separation mechanisms of Cadmium and Zinc, natural stable isotope variations of these metals could be used. This isotope fractionation is caused by biological and physico-chemical processes within the plant. Thiols typically bind light Cd and Zn isotopes, so processes involving thiols may lead to a unique isotope fingerprint. We expect that linking the isotope fingerprint of thiols with isotope ratios in different plant organs can advance the understanding of the different functions of metal chelating thiols. The goal of this Ph.D. project is to investigate the role of chelating thiols, for the separation of Cd and Zn in plants.

To achieve this goal, we will step-by-step study the Cd and Zn isotope ratio in different systems, starting at a molecular level and ending at a whole plant level. **We will use cutting-edge analytical techniques to determine isotope ratios** (MC-ICPMS) and speciation techniques (SEC-ICP-MS, XANES). This set of methods will be originally combined to determine, in extracted and solid samples, the Cd and Zn natural stable isotope variations as well as the speciation of these metals. The objective of the first work package (WP) is to investigate if the binding of Cd and Zn to thiols controls the overall isotope fingerprint on a cellular level. To achieve this, we will express plant metallothionein (MT), a sulfur-rich protein, in a modified *E.coli* strain to determine precise isotope fractionation factors for thiols and compare it with its wild type. The objective of WP2 is to identify species-specific isotope fingerprints of MT and phytochelatin (PC) in plant organs. Plants will be grown hydroponically in different concentrations of Cd and Zn. We will develop a method to measure species-specific isotope ratios in plants by combining size exclusion chromatography (SEC) and isotope mass spectroscopy. We expect the fingerprints in the leaves to correspond to the isotope fractionation in WP1. The objective of WP3 is to bring all knowledge and developed techniques from the previous WPs together, linking Cd and Zn binding to MT and PC to the distribution of Cd and Zn isotopes on a whole plant. We will harvest plants at two different stages, full maturity and flowering, and collect different organs. With these experiments, we seek to advance the understanding of the functions of chelating thiols in separating Cd and Zn in the plant. Thereby, we hope to contribute knowledge that highly nutritious crops can be produced by enriching them in Zn and minimizing their Cd content.

## P 4.5

### “Enzyme or Manganese latch”: Fungal-mediated litter-C turnover coupled to Manganese biogeochemistry

Chunlan Ni<sup>1,2</sup>, Jingtao Hou<sup>1</sup>, Wenfeng Tan<sup>1</sup>, Marco Keiluweit<sup>2</sup>

<sup>1</sup> State Environmental Protection Key Laboratory of Soil Health and Green Remediation, College of Resources and Environment, Huazhong Agricultural University, Wuhan, 430070, China (Ncl@webmail.hzau.edu.cn)

<sup>2</sup> Faculty of Geosciences and Environment, University of Lausanne, Unicentre, CH-1015 Lausanne (Marco.keiluweit@unil.ch)

Decomposition of plant litter is a key biogeochemical process regulating the element cycles in forest ecosystem. The pool size of soil organic matter (SOM) largely depends on the partial decay and transformation of plant input. Litter decomposition rates are influenced by initial litter chemistry and climate factors. Among all other parameters adopted for decomposition models (water soluble C, lignin, N, P, K, Ca, and Mg contents), Mn content of litter best predicts late-stage litter mass loss. The degradation of lignin and lignified tissue, dominating in the late stage, requires a new set of enzymes and redox mediators. However, the functional roles of biotic enzyme and abiotic Mn redox intermediates on lignin decomposition remains highly unclear. Herein, the coupled process of oxidases and reactive Mn species was experimentally examined using a coniferous and a deciduous forest site. The response of manganese peroxidase (MnP) and functional taxa for Mn fertilization stimulation was captured by 6 months incubation in lab. A significant positive correlation between Mn availability and lignin-decay enzyme activities was built. Mn limitation was considered to be a regulator of plant-derived C turnover, playing the role of a co-factor of “Enzyme latch”.

#### REFERENCES

- Berg, B., Steffen, K., McClaugherty, C., 2007: Litter decomposition rates as dependent on litter Mn concentration. *Biogeochemistry*, 85, 29–39.
- Berg, B., 2014: Decomposition patterns for foliar litter- A theory for influencing factors. *Soil Biol. Biochem.*, 78, 222–232.
- Keiluweit, M., Nico, P., Harmon, M. E., Mao, J., Pett-Ridge, J., Kleber, M., 2015: Long-term litter decomposition controlled by manganese redox cycling. *Proc. Natl. Acad. Sci. U. S. A.*, 112(38), E5253-E5260.
- Sinsabaugh, R. L., 2010: Phenol Oxidase, Peroxidase and Organic Matter Dynamics of Soil. *Soil Biol. Biochem.*, 42 (3), 391–404.
- Sun, T., Cui, Y., Berg, B., 2017: A test of manganese effects on decomposition in forest and cropland sites. *Soil Biol. Biochem.*, 129, 178–183.

## P 4.6

# The green microalga *Tetraselmis chui*, a potential $^{90}\text{Sr}$ bioremediation agent

Inés Segovia-Campos<sup>1</sup>, Anastasios Kanellakopoulos<sup>2</sup>, Ivan Barrozo<sup>2</sup>, Edouard Fock-Chin-Ming<sup>2</sup>, Axel Baxarias Fontaine<sup>2</sup>, Stavroula Pallada<sup>2</sup>, Gilles Triscone<sup>2</sup>, Karl Perron<sup>3</sup>, Montserrat Filella<sup>4</sup>, Daniel Ariztegui<sup>1</sup>.

<sup>1</sup> Department of Earth Sciences, University of Geneva, 1205 Geneva, Switzerland (ines.segoviacampos@unige.ch)

<sup>2</sup> HEPIA/HES-SO, University of Applied Sciences of Western Switzerland, 1202 Geneva, Switzerland

<sup>3</sup> Microbiology Unit, University of Geneva, 1205 Geneva, Switzerland

<sup>4</sup> Department F.-A. Forel, University of Geneva, 1205 Geneva, Switzerland

Many species of green microalgae within the class Chlorodendrophyceae form intracellular mineral inclusions of amorphous calcium carbonate (ACC) that can be highly enriched in strontium (Sr) (Martignier *et al.*, 2018; Segovia-Campos *et al.*, 2021). This suggests that these species may have evolved cellular mechanisms to specifically absorb Sr from their living medium. Stable Sr is naturally present in the environment and shows low toxicity. However, radioactive  $^{90}\text{Sr}$  is an artificial unstable isotope ( $t_{1/2} = 28.8$  years) produced by nuclear fission that can be released into the environment in the event of a nuclear accident and that poses a major health risk.

In this study, we investigated the capacity of the species *Tetraselmis chui* (within the class Chlorodendrophyceae) to sequester radioactive  $^{90}\text{Sr}$  in view of its application in the development of new bioremediation techniques targeting this contaminant.

Experiments were performed with laboratory cultures of *T. chui* containing a range of  $^{90}\text{Sr}$  concentrations. The assessment of the  $^{90}\text{Sr}$  uptake capacity of *T. chui* cells was performed by following the variation over time of the radioactivity of the culture media using liquid scintillation spectrometry.

The results obtained show the ability of *T. chui* to effectively sequester  $^{90}\text{Sr}$ , proving its potential as a bioremediation agent to treat  $^{90}\text{Sr}$  contamination.

## REFERENCES

- Martignier, A., et al. (2018). «Marine and freshwater micropearls: Biomimicry producing strontium-rich amorphous calcium carbonate inclusions is widespread in the genus *Tetraselmis* (Chlorophyta).» *Biogeosciences Discuss.* 2018: 1-22.  
Segovia-Campos, I., et al. (2022). «Micropearls and other intracellular inclusions of amorphous calcium carbonate: an unsuspected biomimicry capacity shared by diverse microorganisms.» *Environmental Microbiology* 24.2: 537-550.

## P 4.7

### Localized heavy arsenic enrichment in Dead Sea microbial mats

Camille Thomas<sup>1</sup>, Montserrat Filella<sup>2</sup>, Danny Ionescu<sup>3</sup>, Stéphanie Sorieul<sup>4</sup>, Amanda Oehlert<sup>5</sup>, Petra Zahajská<sup>6</sup>, Dario Ferreira Sanchez<sup>7</sup>, Nuphar Gedulter<sup>8</sup>, Amotz Agnon<sup>8</sup>, Daniel Ariztegui<sup>1</sup>

<sup>1</sup> Department of Earth Sciences, University of Geneva, Geneva, Switzerland ([camille.thomas@unige.ch](mailto:camille.thomas@unige.ch))

<sup>2</sup> Department F.-A. Forel, University of Geneva, Geneva, Switzerland

<sup>3</sup> Leibniz Institute for Freshwater Ecology and Inland Fisheries, Stechlin, Germany

<sup>4</sup> University of Bordeaux, CNRS, IN2P3, CENBG, Gradignan, France

<sup>5</sup> Rosenstiel School of Marine and Atmospheric Science, University of Miami, Miami, USA

<sup>6</sup> Institute of Geography & Oeschger Centre for Climate Change Research, University of Bern, Bern, Switzerland

<sup>7</sup> Paul Scherrer Institut – PSI, Forschungsstrasse 111, 5232 Villigen, Switzerland

<sup>8</sup> Hebrew University of Jerusalem, Institute of Earth Sciences, Jerusalem, Israel

A microbial mat was collected from the sinkhole systems of the western shores of the Dead Sea to better understand how microbial communities cycle trace elements and immobilize some of them into biofilms and microbialites used for the reconstruction of early life and associated environments. Heavy arsenic enrichment (up to 10000 times compared to water chemistry) was measured in one specific layer of this microbial mat. Arsenic was almost uniquely found under the form of organo-arsenic (As(V)) co-occurring with manganese, as shown by XANES spectra and high resolution elemental mapping. In the whole mat, arsenic cycling genes are associated to arsenic detoxification almost exclusively, supporting an overall active arsenic enrichment in the layer by detoxification process transforming As(V) in organo-arsenic compounds. Organisms responsible for this detoxification process have not yet been identified but may encompass photoautotrophic and heterotrophic communities. The reason for a localized enrichment can tentatively be attributed to a temporal increase in arsenic V concentrations in the subsurface circulating water of the Dead Sea shore.

Our dataset supports the possibility for very intense and localized arsenic enrichment within microbial mats, without showing evidence of the use of arsenic for energy-gaining metabolic activity. In this context, the Dead Sea system example calls for caution when interpreting metal(lloid) enrichment (including arsenic) from microbialites-stromatolite or organic matter-rich layers of Precambrian origins. Metallic enrichments may be recorded even in very localized facies due to temporal fluctuations of environmental chemistry. With this respect, metallic signatures in Precambrian organic matter and carbonate rocks may host biosignatures (EPS production and As- binding and detoxification process) without supporting arsenotrophy. They however provide clues to better assess paleoenvironmental conditions at the time of microbial mat formation and sedimentation.

**P 4.8****Mobilisation and chemical speciation of antimony upon flooding of shooting range soil**

Karen Viacava<sup>1\*</sup>, Ursina Morgenthaler<sup>1</sup>, Dominik Dubach<sup>1</sup>, Adrien Mestrot<sup>1</sup>

<sup>1</sup>Institute of Geography, University of Bern, 3012, Bern, Switzerland (\*correspondence: karen.viacava@giub.unibe.ch)

In Switzerland, approximately 4000 shooting ranges are currently registered as polluted sites (Kettler & Schenk, 2020). Besides being the greatest contribution of lead to the environment, shooting also results in the propagation of antimony (Sb), a carcinogenic element classified as a priority pollutant (European Communities, 1998 & USEPA, 1980). Upon soil flooding, Sb rapidly remobilises into the soil solution. Thus, in Sb-polluted sites prone to waterlogging, Sb can enter the groundwater and nearby surface waters spreading the pollution. Sb remobilisation into the soil solution has been divided in three phases: a steep immediate Sb release followed by a rapid decrease and a final more gradual release (Caplette et al., 2022). The dissolution of iron and manganese oxy-hydroxides has been pointed as the cause of the final Sb release. However, to date there is few information about the dynamics of the decrease which may be used as a stabilisation strategy. We hypothesize that Sb sorbs to organic matter macromolecules or to iron aggregates causing the decrease in concentration.

Using soil from a shooting range prone to waterlogging, we performed a three-month mesocosm experiment under flooded conditions. The Sb concentration in the soil solution was analysed in three different size fractions ( $<0.02\mu\text{m}$ ,  $<0.45\mu\text{m}$  and  $<10\mu\text{m}$ ) using ICP-MS. In addition, the medium fraction was analysed by size exclusion chromatography (SEC) coupled to ICP-MS and the smallest fraction for Sb species by HPLC-ICP-MS (antimonate (Sb(V)), antimonite (Sb(III)) and trimethylated antimony (TMSb)). Eventually, a 7-steps sequential extraction procedure (SEP) was done to study the dynamics behind the immediate Sb release.

During the three-month experiment, the analysed metals and metalloids ubiquitously present in the soil (arsenic, cobalt, uranium and nickel) were progressively re-mobilised together with iron and manganese into solution ( $<0.02\mu\text{m}$ ). Sb concentration peaked after two days of flooding, first phase of release, decreasing to its minimum after seven days. During the first release phase, Sb was present as soluble ( $<0.02\mu\text{m}$ ) Sb(V). During the final release and with the development of anaerobic conditions (redox potential  $<0$ ), up to 15% and 5% of Sb(III) and TMSb, respectively, were detected in the soil solution. This most probably occurred as a result of microbial activity which was evidenced by the consumption of electron acceptors (nitrate and sulfate), the production of ammonia and the increment in dissolved organic carbon. An increase of Sb bound to macromolecules was evidenced with SEC. However this was not enough to explain the observed decrease of the Sb concentration in the soil solution. Finally, the SEP showed the greatest Sb fraction in the soil is indeed bound to low-crystallinity oxy-hydroxides, one of the most reactive fractions. These results show the mobilisation and microbial transformation of Sb under iron-reducing conditions. Thus, Sb-polluted soils prone to waterlogging are particularly at risk of Sb migration into the environment.

**REFERENCES**

- Kettler & Schenk, 2020: Indemnisations en vertu de l'OTAS pour les installations de tir. Communication de l'OFEV en tant qu'autorité d'exécution. 4e édition actualisée 2020 ; 1re édition 2006. Office fédéral de l'environnement. L'environnement pratique no 0634: 36 p.
- European Communities, 1998: Richtlinie 98/83/EG des Rates vom 3. November 1998 Über die Qualität von Wasser für den Menschlichen Gebrauch.
- USEPA, 1980: Ambient Water Quality Criteria Document for Antimony. Prepared by the Office of Health and Environmental Assessment, Environmental Criteria and Assessment Office Cincinnati, OH for the Office of Air Quality Planning and Standards; EPA 440/5-80-020. Washington, DC, USA.
- Caplette et al., 2022: Antimony release and volatilization from rice paddy soils: Field and microcosm study. Sci. Total Environ. 842, 156631.

## P 4.9

### Geochemical imprints of volcanic ash leaching in coral skeletons

James Vincent<sup>1</sup>, Elias Samankassou<sup>1</sup>, Tom Sheldrake<sup>1</sup>

<sup>1</sup> Department of Earth Sciences, University of Geneva, Rue des Maraîchers, 1205 Geneva (james.vincent@unige.ch)

Explosive volcanic eruptions are capable of depositing large quantities of nutrient-rich ash over sizable areas of the ocean. Ash particles are known to rapidly leach high concentrations of major, minor and trace elements in water, although the influence of this process on corals is poorly studied. Chemical proxies in the skeletons of tropical reef-building corals have been widely used to reconstruct oceanic parameters, such as sea surface temperature, salinity, light intensity, pH, sedimentation and seawater composition. Seeing as though many of these parameters are affected by ash deposition, we hypothesise that the effects of volcanic ash leaching can leave a geochemical imprint on the chemical composition of the coral skeleton.

To test this hypothesis, we measured LA-ICP-MS profiles on coral core samples taken from the northwest fringing reefs of Barbados, Lesser Antilles. Massive colonies of *Diploria strigosa* and *Siderastrea siderea* were cored 15 months following the April 2021 eruption of La Soufrière, St. Vincent (192 km east of Barbados), which deposited volcanic ash on Barbados. Each core sample is approximately 6cm in depth, and thus represents skeleton precipitated before, during and after the eruption. Four different locations were chosen to compare skeletal geochemistry between each colony, focusing on contrasting energy regimes and coastal currents. In addition, colony morphology were considered for ash sedimentation effects. Our results may provide crucial information regarding distinguishing volcanic eruptions in coral archives.

## P 4.10

### Transformation of plant-derived carbon by Manganese oxides

Isabella O. Zelano<sup>1</sup>, Debra Hausalden<sup>2</sup>, Jasquelin Pena<sup>3</sup>

<sup>1</sup> Université de Lausanne, CH-1015 Lausanne, Switzerland ([isabella.zelano@unil.ch](mailto:isabella.zelano@unil.ch))

<sup>2</sup> Université de Sherbrooke, Sherbrooke (Québec) J1K 2R1, 819 8218000

<sup>3</sup> University of California, Davis, One Shields Avenue, Davis, CA 95616

The interaction of organic carbon (C) substrates with microorganisms and mineral phases is a key factor regulating the fate of organic matter in soils. While carbon substrates can be transformed into biomass or mineralized to CO<sub>2</sub> by microbial metabolism, mineral phases can stabilize organic compounds through sorption processes or promote their oxidation through redox reactions (Kleber et al.). Manganese oxides, in particular, are among the strongest natural oxidants in soils, able to drive the oxidation of a broad range of organic molecules, changing the speciation of bioavailable organic C. However, depending on the aliphatic or aromatic nature of the organic molecules, Mn oxides can also support C stabilization through adsorption or polymerization processes. At present, the mechanisms through which Mn oxides affect the pool of bioavailable C in soils are not fully understood.

In this study, we investigate the extent and mechanisms of the reactions between a layer-type Mn oxides ( $\delta\text{-MnO}_2$ ) and four organic substrates as model components of plant litter. We select cellobiose and arabinose as aliphatic molecules, constitutive of cellulose and hemicellulose, respectively, and two substrates containing aromatic rings as coumaric acid and lignin. The selected organic substrates are added to continuously-stirred batch reactors containing  $\delta\text{-MnO}_2$  in three different Mn : C molar ratios, ranging from excess electron donating capacity (EDC) to excess electron accepting capacity (EAC), with an initial pH value adjusted to 7. The reaction products derived from the oxidation/transformation of the studied organic molecules are tracked over four days through liquid chromatography-mass spectrometry (LC-MS) and ion chromatography (IC). Eventual sorption or mineralization of C are estimated by measuring the concentration of dissolved organic carbon (DOC) and of CO<sub>2</sub> evolved from parallel experiments performed in closed conditions. To monitor the concomitant reduction of  $\delta\text{-MnO}_2$  and the electron flux occurring during the reaction, solid-phase Mn(III) generation is quantified over time through a pyrophosphate extraction, and the average Mn oxidation number (AMON) is measured by a three step potentiometric titration. The soluble Mn(II) concentration is measured in solution after filtration at 0.2  $\mu\text{m}$ .

Preliminary results show that the reaction between  $\delta\text{-MnO}_2$  and aliphatic substrates produces formic acid as main oxidation product. No loss of carbon is observed, indicating incomplete mineralization. While solid-phase Mn(III) is generated within all treatments, the increasing concentration of Mn(II) in the aqueous phase is not a good predictor of the overall Mn reduction and is only observed when EDC exceeds EAC. Further research is on-going to assess the extent to which redox-sensitive minerals as Mn oxides can modulate the bioavailability of carbon substrates with aromatic structures.

#### REFERENCES

- Kleber, et al. 2021: Dynamic Interactions at the Mineral–Organic Matter Interface, *Nature Reviews Earth & Environment*, 2, 402–21.



## 5 Palaeontology

Allison Daley, Harriet Drage, Christian Klug, Torsten Scheyer

*Schweizerische Paläontologische Gesellschaft,  
Kommission des Swiss Journal of Palaeontology (KSJP)*

TALKS:

- 5.1 Baumgartner P.O., Baumgartner-Mora C., Epard J-L., Ferràndez-Cañadell C., Derron M-H., Andjic G.: Pycnodonte gigantica oyster banks in a short-lived Priabonian Palaeogeography of the Helvetic Nappes (W-Switzerland and Haute Savoie)
- 5.2 Daley A.C., Bath Enright B., Gueriau P., Laibl L., Lutri L., Pérez-Peris F., Potin G., Saleh F.: Arthropod Evolution During the Palaeozoic : Insights from the Fezouata Biota
- 5.3 Drage H.B., Pates S.: Cephalic shape has little association with trilobite moulting behaviour
- 5.4 Etter, W.: Eozoon and the strange case of Otto Hahn
- 5.5 Evers S.W., Hermanson G.: Phylogenetic comparative analysis of histological long bone complexity in turtles
- 5.6 Gardiner A., Kocáková K., Cooper R., Silvestro D., Pimiento C.: Neoselachian Diversity through Deep Time
- 5.7 Girard L., De sousa oliveira S., Raselli I., Martin J-E., Anquetin J.: A new specimen of Metriorhynchidae (Crocodylomorpha, Thalattosuchia) from the Kimmeridgian of Switzerland: Description, phylogenetic relationships and evolution.
- 5.8 Hautmann M., Ferrari M.: Mollusc extinction during the end-Triassic crisis
- 5.9 Hermanson G., Dziomber L., Joyce W.G., Foth C., Evers S.W.: Evaluating turtle shell ecomorphology patterns using phylogenetic comparative analyses
- 5.10 Kocakova K., Gardiner A., Silvestro D., Pimiento C.: FINS database and the diversification dynamics of sharks, rays, and skates
- 5.11 Kocsis L., Briguglio A., Roslim A., Goeting S.: Palaeontological discoveries from North Borneo
- 5.12 Le Verger K., Sánchez-Villagra M.R.: Xenarthrans of the Santiago Roth collection from the Pampean region of Argentina (Pleistocene), in Zurich, Switzerland
- 5.13 Lynch S., Drage H.B., Daley A.C., Źylińska A.: Enrolment and flexures in the trilobite Strenuella polonica Czarnocki, 1926 from the Cambrian of Poland
- 5.14 Plateau O., Green T., Gignac P., Foth C.: Comparative digital reconstruction of ontogenetic skull variation in altricial (*Pica pica*) and precocial birds (*Struthio camelus*)
- 5.15 Pohle A., Stevens K., Klug C.: Fossil cephalopod phylogenetics: recent advances, remaining challenges and future perspectives
- 5.16 Potin G.J.-M., Claisse P., Gueriau P., Pates S., Daley A.C.: Frontal appendages from the Fezouata Shale (Early Ordovician, Morocco) reveal high diversity and ecological adaptations in radiodonts after the Cambrian.

- 5.17 Raselli I., Foth C., Anquetin J.: From the past to the future: Unraveling the complexity of the crocodylian skull morphology
- 5.18 Rollot Y., Evers S.W., Pierce S.E., Joyce W.G.: Cranial osteology of the Early Cretaceous baenid turtle *Trinitichelys* hiatti and new insights into the evolution of the basicranium of turtles
- 5.19 Saleh F.: New fossil assemblages from the Early Ordovician Fezouata Biota
- 5.20 Santodomingo N., Waheed Z., Syed Hussein M.A., Rosedy A., Johnson K.: Resilience of platy corals (Scleractinia, Agariciidae) over the past 30 million years in the Coral Triangle
- 5.21 Schneebeli-Hermann E., Leu M., Hansen B.B., Hammer Ø., Lindemann F.-J., Bucher H.: Early Triassic conodonts and palyonomorphs from Stensiöfjellet, Svalbard
- 5.22 Torchet A., Shaw J., Stockar R., Scheyer T.: Trophic network reconstruction and analysis of the different fossiliferous layers of the Middle Triassic Monte San Giorgio world heritage (Switzerland/ Italy)

## 5.1

# ***Pycnodonte gigantica* oyster banks in a short-lived Priabonian Palaeogeography of the Helvetic Nappes (W-Switzerland and Haute Savoie)**

Peter O. Baumgartner<sup>1</sup>, Claudia Baumgartner-Mora<sup>1</sup>, Jean-Luc Epard<sup>1</sup>, Carles Ferràndez-Cañadell<sup>2</sup>, Marc-Henri Derron<sup>1</sup>, Goran Andjic<sup>1</sup>.

<sup>1</sup> Institut des Sciences de la Terre, Géopolis, CH-1015 Lausanne (Switzerland)  
 (peter.baumgartner@unil.ch)

<sup>2</sup> Departament Dinàmica de la Terra i de l'Oceà, Facultat de Ciències de la Terra, Universitat de Barcelona,  
 Martí Franquès s/n, 08028 Barcelona (Spain)

Upper Eocene paralic and marine sediments exposed in the Helvetic nappes comprise quartz-rich siliciclastic and shallow carbonate rocks that accumulated in a foreland basin located on the European margin in front of the early Paleogene Alpine orogen. Banks of *Pycnodonte gigantica* (Solander in Brander 1766) occur in the Priabonian Sanetsch Formation, in an overall transgressive succession, resting with a regional, erosive unconformity on a Cretaceous substrate. Facies range from lacustrine-paralic (Diablerets Member) to neritic alternations of quartzose sandstones and sandy calcarenites (Tsanfleuron Member), followed by shallow water carbonates made of coralline algae, abundant larger benthic foraminifera (LBF) and upwards decreasing amounts of detrital quartz (Pierredar Limestone Member).

We found *P. gigantica* banks in two different stratigraphic positions:

**1. Top of Tsanfleuron Member.** The sofar largest and best preserved *P. gigantica* bank is located in the Sex Rouge section on the Lapis de Genève (VS, Fig. 1), in the Mont Gond Nappe (Wildhorn Nappe Complex). The bank extends over 1 km on a ledge that forms the top of the Tsanfleuron Member, recently assigned by us to the Early Priabonian Shallow Benthic Zone 19 (Ferràndez et al. accepted). It was deposited in a high energy environment between seastacks of Cretaceous Schrattenkalk. The oyster bank of 10-100 cm thickness shows wavy planar bedding with a grainsone to packstone matrix of coralline algae, orthophragmines, nummulites, and a minor ditrial content. The surface of the bank, polished by the Tsanfleuron glacier in postglacial times, only presents cuts. Most oyster shells measure 13-20 cm, are oriented parallel to bedding and are separated by areas of matrix, except in zones where densely packed, broken shells grade into a breccia. Sagittal cuts occur in vertical sections along open fractures (Fig. 1c). About 20% of shells are articulated, as seen in vertical sections and tilted specimens on the surface. Ligamental areas are rarely observable, while the scar of the adductor muscle apperas frequently as sediment-filled round spot.

In the Grand Platé area (Flaine, Haute Savoie) in an anticline of the Morcles Nappe, we found scattered shells also at the top of the Tsanfleuron Member.

**2. Near top of the Pierredar Limestone.** A similar bank occurs in the Grand Platé area on the "Cisral" ski track in an area of 20x30 m, as well as scattered shells in outcrops of the same level, about 2 m below the top of the limestone. The matrix is again a LBF-coralline packstone with some detrital component. This bank must be of latest Priabonian age. Even small fragments can be recognized by the particular shell architecture (Fig1, b, d, e) composed of thin (50-200 µm) foliate (fl) layers and thick (400-1600 µm) vesicular layers (vl) built of a framework on thin slats that enclose up to 60% of originally water-filled porosity of the shell. In our fossil specimens this pore space is filled with sparitic cement with a cement stratigraphy, characte-ristic of the bank, seen under cathodoluminescence (Fig.1 e).

*P. gigantica* is secondary soft-bottom dweller according to Seialcher (1984, p. 215), who wrote that "a very dense shell structure contributes to the stabilizing weight of the oysters". He probably was not aware of the fact that in Modern *Neopycnodonte* shells the vesicular structure is water-filled (Wissak et al. 2008). Our preliminary calculation indicates that the immersed bulk density of a live *P. gigantica* shell is close to that of a carbonate sand. We speculate that the shells could stay afloat in non-cohesive, moving sediment during storms.



Figure 1. a., c. Outcrop of oyster bed, vertical cut (c), Lapis de Genève (VS). b., d., e. Thin section of shell in normal (b) and cross-polarized light(d), and cathodoluminescence (e). Vesicular layer (vl), foliated layer (fl).

#### REFERENCES

- Ferràndez-Cañadell, C., Baumgartner-Mora, C., Baumgartner, P. O., Epard J-L. accepted: Priabonian (upper Eocene) larger foraminifera from the Helvetic Nappes of the Alps (Western Switzerland): New markers for Shallow Benthic zones 19–20. *Micropaleontology* 2023.
- Seilacher A. 1993: Constructional morphology of bivalves: Evolutionary pathways in primary versus secondary soft-bottom dwellers. *Palaeontology*, Vol. 27/2, 207-237.
- Wissak, M., Lopez Correa, M., Gofas, S., Salas, C., Taviani, M., Jakobsen, J., Freiwald, A. 2008: Shell architecture, *Neopycnodonte zibrowii* sp. n. from the NE Atlantic. *Deep Sea Research*, 1, 56, 374–407.

Funded by: Swiss National Science Foundation, No. 200021-185067.

## 5.2

### Diversity and Evolution of Radiodonta during the Early Paleozoic

Allison C. Daley \*

\* Institute of Earth Sciences, University of Lausanne, Geopolis, CH-1-15 Lausanne, Switzerland (allison.daley@unil.ch)

Radiodonta is an early Paleozoic group of stem lineage arthropods that includes *Anomalocaris* and over 25 other taxa. These animals are reknown amongst Cambrian Explosion taxa owing to their large body size, inferred predatory lifestyle, and complicated history of description. Radiodonts have been described from every major Cambrian and Ordovician Burgess Shale-type (BST) lagerstätten, showing that they were globally distributed and relatively abundant. They most commonly preserve as isolated cuticularised frontal appendages, oral cones, and cephalic carapaces of the head region, but rare complete specimens show the body trunk was segmented and consisted of swim flaps associated with setal blades. Study of these morphological features in radiodonts has helped clarify the evolutionary pathway of key anatomical structures in Arthropoda, for example the biramous limbs, compound eyes, and cephalic structures (Daley et al. 2009; 2018; Van Roy et al. 2015).

As the name suggests, Radiodonta was originally described as a clade uniting taxa with a radially-arranged oral structure of 32 plates with a central opening, which was thought to be a highly conserved element of radiodont anatomy (Collins 1996). More recent work has shown that the oral structures are more diverse, with some taxa possessing a variable number of radially-arranged plates (Daley & Bergstrom 2012), and others showing a series of gnathobase-like plates that do not form a solid oral cone (Cong et al. 2017). Likewise, the frontal appendages show a great diversity of feeding ecologies, including adaptations for active predation, sediment-sifting, and even suspension feeding (Van Roy et al. 2015). Cephalic carapaces range from small dorsal carapaces to elaborate carapace complexes that make up nearly half the total body length (Daley et al. 2009; Van Roy et al. 2015). We can trace the evolution of these structures and use their functional morphology to make inferences about how ecological function changed in response to evolutionary pressures.

Here I review the recent work revealing the diversity of radiodont taxa in major fossil lagerstätten. Four major families of Radiodonta have been established, with the relationships between them coming into focus and revealing the evolutionary history of the major anatomical features, specifically the frontal appendages and oral structures (Pates et al. 2019; Pates & Daley 2019). During the early stage of their evolution, radiodont diversity was dominated by members of the Anomalocarididae and Amplectobeluidae, all of whom were active predators. Later stages of radiodont evolution were dominated by Huriidae, most of which are interpreted as generalised predators and sediment-sifters. Suspension feeding evolved multiple times during their evolution, presumably in response to increasing levels of competition in the ecosystem. This work highlights that radiodonts were important components of early animal ecosystems.

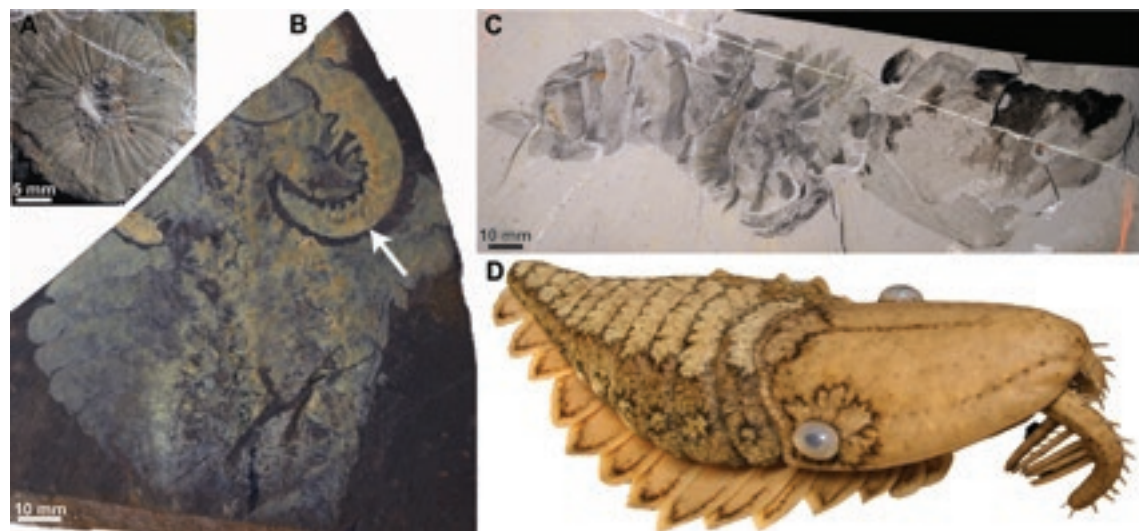


Figure 1. Cambrian radiodonts from the Burgess Shale, Canada. A: Oral cone showing 32-plate morphology of *Peytoia nathorsti*. B: Whole body specimen of *Anomalocaris canadensis*, with a raptorial frontal appendage indicated with white arrow. C: Whole body specimen of *Hurdia victoria*, showing large frontal carapace. D: Model of *Peytoia nathorsti* by E. Horn. Modified from Daley (2013).

## REFERENCES

- Collins, D. 1996: The “evolution” of Anomalocaris and its classification in the arthropod Class Dinocarida (nov.) and order Radiodonta (nov.). *J. Paleontol.* 70, 280–293.
- Cong, P., Daley, A. C., Edgecombe, G. D. & Hou, X. 2017: The functional head of the Cambrian radiodontan (stem-group Euarthropoda) *Amplectobelua symbiocrinata*. *BMC Evolutionary Biology* 17, 208.
- Daley, A. C. 2013: Anomalocaridids. *Curr. Biol.* 23, R860–1.
- Daley, A. C. & Bergström, J. 2012: The oral cone of Anomalocaris is not a classic ‘Peytoia’. *Naturwissenschaften* 99, 501–504.
- Daley, A. C., Budd, G. E., Caron, J.-B., Edgecombe, G. D. & Collins, D. 2009: The Burgess Shale anomalocaridid *Hurdia* and its significance for early euarthropod evolution. *Science* 323, 1597–1600.
- Daley, A. C., Antcliffe, J. B., Drage, H. B. & Pates, S. 2018: Early fossil record of Euarthropoda and the Cambrian Explosion. *Proc. Nat. Acad. Sci.* 115, 5323–5331.
- Pates, S., Daley, A. C. & Butterfield, N. J. 2019: First report of paired ventral endites in a hurdiid radiodont. *Zoological Letters* 5, 18.
- Van Roy, P., Daley, A. C. & Briggs, D. E. 2015: Anomalocaridid trunk limb homology revealed by a giant filter-feeder with paired flaps. *Nature* 522, 77–80.

## 5.3

### Cephalic shape has little association with trilobite moulting behaviour

Harriet B. Drage<sup>1</sup>, Stephen Pates<sup>2</sup>

<sup>1</sup> Institute of Earth Sciences, University of Lausanne, Switzerland ([harriet.drage@unil.ch](mailto:harriet.drage@unil.ch))

<sup>2</sup> Department of Zoology, University of Cambridge, UK

Trilobites had strongly biomineralised exoskeletons with a diversity of morphological adaptations to different ecological niches across the Palaeozoic. Like all euarthropods, trilobites moulted their exoskeletons repeatedly throughout their lives to grow and develop. Exoskeleton moulting behaviour in trilobites appears to have been uniquely variable compared to modern arthropod groups, partly because of their cephalon morphological diversity. Previous work has suggested that trilobites were both highly inter- and intraspecifically variable in moulting behaviour, producing a variety of moult configurations preserved in the fossil record (Drage et al. 2018a). For some species this was related to cephalic morphology at ontogenetic stage (Drage et al. 2018b). Variation in moulting during adulthood might be expected to be related to morphometry; the shape and proportions of exoskeleton sclerites. However, proportions at least appear largely unrelated to moulting behaviour interspecifically, and intraspecifically in at least one species (Drage et al. submitted).

We tested for an association between cephalic shape and moulting behaviour to confirm whether broad-scale trilobite moulting variability was indeed unrelated to morphometry. Cephalic shape has been shown to relate to variation in other trilobite behaviours, such as enrolment (Suárez & Esteve 2021). We used a dataset of cephalon outline semi-landmarks of ~200 trilobite species with moulting behaviour information to test this potential association.

Elliptical Fourier Analysis suggests cephalon shape has little impact on moulting behaviour, with different behavioural groups almost entirely nested in morphospace. Species showing the Sutural Gape mode of moulting, using only the facial and/or rostral sutures, may occupy a slightly greater amount of morphospace, though this is unsurprising given the facial sutures were likely adaptive for moulting and are found throughout the trilobite orders. There is otherwise little difference in the area or location of cephalic outline morphospace occupied by different moulting behaviour groups. Perhaps trilobites indeed demonstrated high phenotypic plasticity in moulting across the group that cannot be explained by individual variables or evolutionary drivers such as morphometry or ontogeny.

#### REFERENCES

- Drage, H. B., Holmes, J. D., García-Bellido, D. C. & Daley, A. C. 2018a: An exceptional record of Cambrian trilobite moulting behaviour preserved in the Emu Bay Shale, South Australia. *Lethaia* 51, 473–492.
- Drage, H. B., Laibl, L. & Budil, P. 2018b: Postembryonic development of *Dalmanitina*, and the evolution of facial suture fusion in Phacopina. *Paleobiology* 44, 638–659.
- Drage, H. B., Holmes, J. D., García-Bellido, D. C. & Paterson, J. R. Submitted: Associations between trilobite intraspecific moulting variability and body proportions: *Estaiungia bilobata* from the Cambrian Emu Bay Shale, Australia.
- Suárez, M. G. & Esteve, J. 2021: Morphological diversity and disparity in trilobite cephalon and the evolution of trilobite enrolment throughout the Palaeozoic. *Lethaia* 54, 752–761.

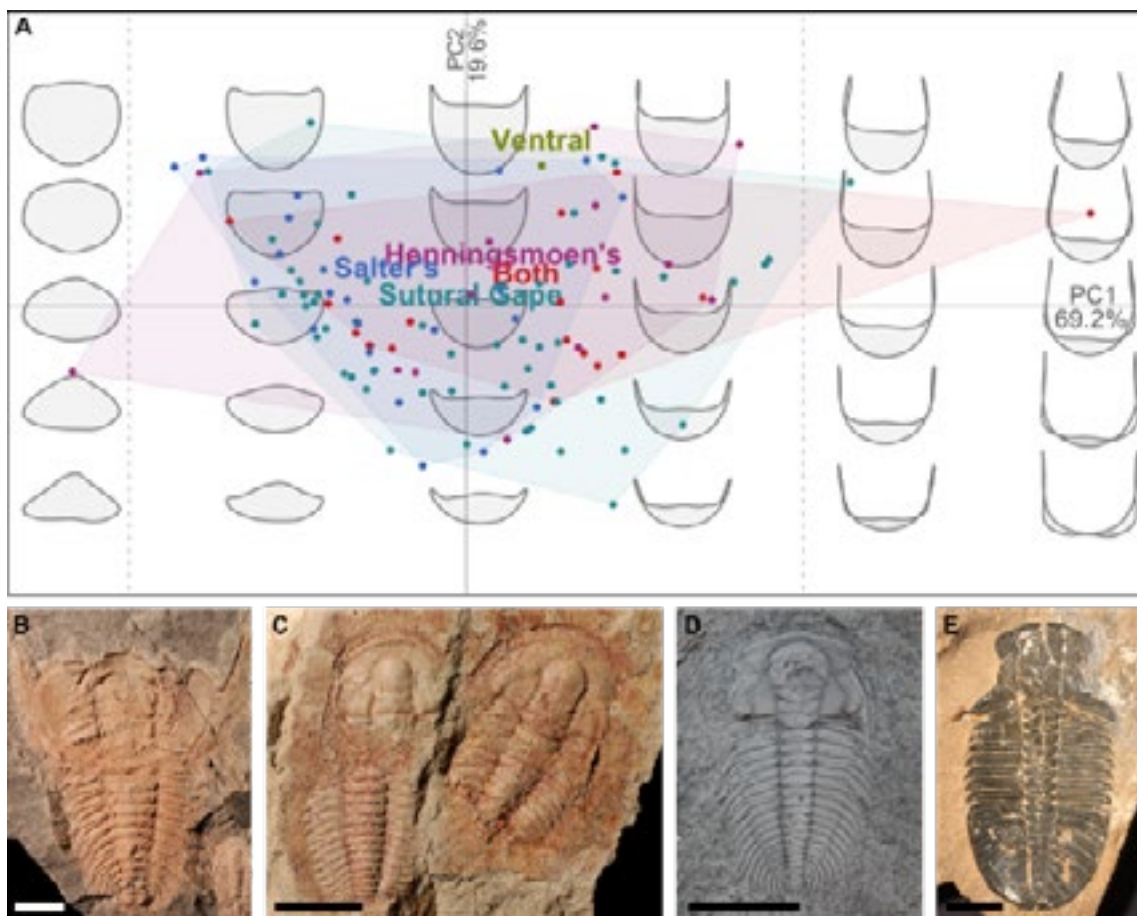


Figure 1. Preliminary morphospace of trilobite cephalic outlines (A), exploring a potential association between morphospace occupation and exoskeleton moulting behaviour. Coloured polygons correspond to the different generalised moult configurations analysed. B–E show example trilobite moults. A, *Redlichia takooensis*, SAM-P 43593; B, *Estaingia bilobata*, SAM-P 45697; C, *Paradoxides* sp., UUM 25711-37; D, *Ogygopsis klotzi*, OUMNH AT205. A, D scales 10 mm; B, C scales 5 mm.

## 5.4

### **Eozoon and the strange case Otto Hahn**

Walter Etter<sup>1</sup>

<sup>1</sup> Naturhistorisches Museum Basel, CH-4001 Basel (walter.etter@bs.ch)

It was in 1864 that at the Meeting of the British Association for the Advancement of Science in Bath a sensation was presented: the presumably oldest fossils of the world, from Precambrian Strata in Eastern Canada. First finds were made already in 1858 but generally not accepted as organic remains. This had now changed, and scientists as prominent as John William Dawson, Charles Lyell, William B. Carpenter and even Charles Darwin were in support of the organic nature of these structures.

These were formally described as *Eozoon* (originally *Eozoön*) *canadense* and assigned as Rhizopoda, more precisely as giant Foraminifera. The then world leading expert on Foraminifera was William B. Carpenter and he supported this interpretation from the beginning. *Eozoon canadense* consisted of banded, concentric structures of coarse-grained calcite, alternating with serpentine or pyroxene. In thin sections small canals and cavities were visible, again interpreted as typical of foraminifers. The finds were hailed as “the most important discovery in geology for at least half a century” and “the brightest gem in the crown of the geological survey of Canada”.

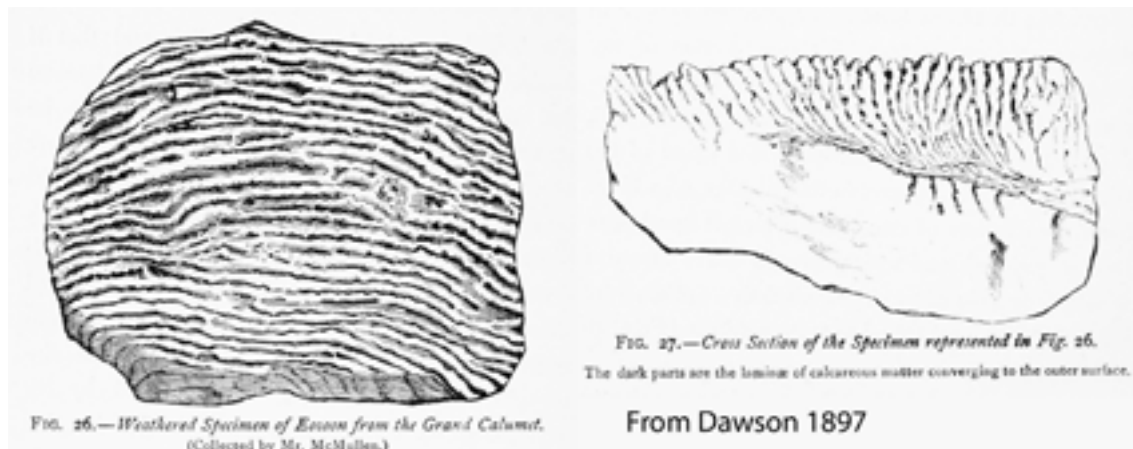


Figure 1. Macroscopic appearance of *Eozoon canadense*.

It was not for long, though, that doubts about the organic nature of *Eozoon* were expressed, not the least because it occurred in metamorphic rocks. Apart from 1870, the debates became more and more heated. At first, those convinced of an inorganic nature were vastly outnumbered by those seeing *Eozoon* as giant foraminifer, but as time went by, the tide turned. After the death of Carpenter in 1885, Dawson remained the only proponent of the organic nature of *Eozoon* until his death in 1899.

Perhaps the most interesting figure in this debate was Otto Hahn (has nothing to do with the radiochemist and discoverer of Uranium fission with the same name). He at first was a decided opponent of the organic theory. But just a few years later he made a complete turnaround. He interpreted the structures not as foraminifers but mostly as algae. Then he somehow lost the ordinary judgement. He started to see *Eozoon*-like structures everywhere, also in magmatic and metamorphic rocks, and later even in meteorites. He published two books on the subject, both richly illustrated with photographs and drawings, and described countless new species and named them e.g., after Reich Chancellor Otto Bismarck, after Darwin, and even after the German Emperor Wilhelm. His theories had, not surprisingly, very few support, and then he somehow lost interest in the subject and emigrated to Canada.

The story could end here, but there is an epilogue. Randolph Kirkpatrick was a palaeontologist working at the British Natural History Museum from 1886 until 1927. He collected and described new sponges while working in the Azores, Madeira and Canaries, and these studies are considered nowadays excellent. These were the first descriptions of so-called sclerosponges. Yet he also undertook extensive hikes and ascended to the mountaintops on these islands. And here he started to see, in the rocks of these volcanic islands, everywhere foraminifers of the genus *Nummulites*. His further studies showed, in his eyes, that almost the whole lithosphere was composed of *Nummulites* shells. He published his views in the books “The Nummulosphere”, the first volume appearing in 1913. Because, little surprising, support for his theory was weak, he had to pay the printing costs himself. By the end of his life, he had almost no savings.



Figure 2. Title page of Kirkpatrick's first volume of "The Nummulosphere".

## 5.5

# Phylogenetic comparative analysis of histological long bone complexity in turtles

Serjoscha W. Evers<sup>1</sup>, Guilherme Hermanson<sup>1</sup>

<sup>1</sup> Department of Geosciences, University of Fribourg, Chemin du Musée 4, 1700 Fribourg, Switzerland (serjoscha.evers@googlemail.com)

Bone compactness has been used to infer aquaticness in tetrapods, and to discriminate between aquatic and terrestrial lifestyles. The relationships between bone compactness and aquaticness have not been tested with phylogenetic comparative methods for turtles, and turtles have been omitted from studies that compare compactness across otherwise broad comparisons of secondarily aquatic tetrapods.

We use the Nakajima et al. (2014) dataset, which is a compilation of bone compactness for 51 extant turtle species, to explore the relationships of ecological variables and body size (i.e., allometry) with bone compactness in multiple phylogenetic regression models. Using bone compactness as the response variable, we built phylogenetic generalized least squares (pgls) regression models. The statistical associations of allometry and ecological variables with bone compactness were modelled in bivariate and multiple regression models.

Model comparison of phylogenetic generalized least squares (pgls) regressions using Akaike's Information Criterion for small sample sizes (AICc) indicate independent effects of body size (i.e., allometry) and highly aquatic ecology on bone compactness. The AICc-best model takes the form "bone compactness ~ humerus size + aquatic". The model indicates strong negative evolutionary allometry (slope = -0.18; p < 0.01), meaning that bone compactness decreases with body size in turtles. This effect is independent of further bone compactness reduction in highly aquatic turtles (slope = -0.11; p < 0.01). This best model explains 23.6% of the bone compactness variation observed in the data, whereby 14.0% can be attributed to the allometric effect as indicated by a bivariate allometric regression. Thus, 9.6% of the bone compactness variation can be explained by the effect of being highly aquatic. The residual variation in bone compactness is negatively phylogenetically correlated in all non-negligible AICc models that include ecological effects as covariates, so that closely related species have less similar bone compactness than distantly related ones. The effect of aquatic foraging (i.e., combining semiaquatic+aquatic explanatory variables) and terrestriality are non-significant and not among non-negligible AICc models.

Although highly aquatic turtles can potentially be identified based on long bone complexity, our results indicate that bone compactness is not useful for distinguishing terrestrial and semiaquatic turtles. Thus, the usefulness of this tool is limited for habitat interpretations of fossil turtles. Interestingly, turtles break the tetrapod-wide trend of increasing bone compactness with increased aquaticness. This can potentially be explained by the presence of a bony shell in turtles, which may partially fulfil a buoyancy control function that is otherwise attributed to compact bones in aquatic elements that lack a shell.

## REFERENCES

- Nakajima, Y., Hirayama, R., & Endo, H. 2014: Turtle humeral microanatomy and its relationships to lifestyle, *Biological Journal of the Linnean Society*, 112(4), 719-734.

## 5.6

### Neoselachian Diversity through Deep Time

Amanda Gardiner<sup>1</sup>, Kristína Kocáková<sup>1</sup>, Rebecca Cooper<sup>3</sup>, Daniele Silvestro<sup>3</sup>, Catalina Pimiento<sup>1,2,4</sup>

<sup>1</sup> Paleontological Institute and Museum, University of Zurich, Rämistrasse 71, CH-8006 Zürich  
(amandamichaela.gardiner@uzh.ch)

<sup>2</sup> Department of Biosciences, Swansea University, Singleton Park, Sketty, Swansea SA2 8PP, United Kingdom

<sup>3</sup> Department of Biology, Université de Fribourg, Av. de l'Europe 20, CH-1700 Fribourg <sup>4</sup> Smithsonian Tropical Research Institution, Balboa, Panama

Neoselachians are a cosmopolitan clade of Chondrichthyes that contain all sharks, skates, and rays together with their closely related extinct ancestors. After arising in the Lower Triassic (251Ma), they survived the Triassic-Jurassic and Cretaceous-Paleogene mass extinctions before reaching their current diversity, with 1,147 recognized species and more being identified each year. Numerous species throughout the past and into the present have essential roles in ecosystems as apex- and meso-predators, with the loss of some extant neoselachians leading to trophic cascades. Despite their extensive fossil history and ecological importance, it has only been in the last several decades that we have begun to fathom their past diversity and how it has changed through time. Initial works relied upon first and last appearance datum, which are biased as a result of the Signor-Lipps effect. More recent research utilized ghost ranges in time-calibrated phylogenies, which can account for this bias but fail to address sampling and spatiotemporal preservation biases. Accordingly, despite the advances made in recent years, our current understanding of neoselachian diversity may still be biased, with some patterns remaining illusive.

Here we utilize DeepDive, a novel deep learning neural network, to estimate neoselachian diversity over time while accounting for multiple biases in the fossil record. To do so, we built the most comprehensive neoselachian database to date, which spans from the Cretaceous to the Holocene and contains over 5,800 collections and 29,000 occurrences, 53% of which are new with the remaining downloaded from the Paleobiology Database. DeepDive can account for the Signor-Lipps effect in addition to spatiotemporal and sampling biases due to the neural network being trained with simulated ‘perfect’ data sets, which are impossible to achieve in the fossil record. The neural network training consists of introducing gaps to the simulated data, thereby replicating known biases, and allowing us to compare the obtained results with the initial perfect diversity to correct them. The results of this research are expected to refine and correct previous diversity estimates along with revealing new patterns previously unknown. This knowledge will be used to test hypotheses on the relationships between neoselachian diversity and past climatic and biotic events, thereby improving our understanding of how sharks and rays respond to various environmental stressors and contributing to a better understanding of the paleobiology of this charismatic clade.

## 5.7

# A new specimen of Metriorhynchidae (Crocodylomorpha, Thalattosuchia) from the Kimmeridgian of Switzerland: Description, phylogenetic relationships and evolution.

Léa Girard<sup>1,2</sup> Sophie De sousa oliveira<sup>2</sup>, Irena Raselli<sup>3,1</sup>, Jeremy E. Martin<sup>4</sup>, Jérémie Anquetin<sup>3,1</sup>

<sup>1</sup> Department of Geosciences, University of Fribourg, Chemin du Musée 6, CH-1700 Fribourg ([lea.girard@unifr.ch](mailto:lea.girard@unifr.ch))

<sup>2</sup> Université de Rennes 1, Rennes 35000, France

<sup>3</sup> JURASSICA Museum, 2900 Porrentruy, Switzerland

<sup>4</sup> Laboratoire de géologie de Lyon, terre, planète, environnement, UMR CNRS 5276 (CNRS, ENS, Université Lyon 1), École normale supérieure de Lyon, 69364 Lyon cedex 07, France

The paleontological excavations conducted during the building of the A16 Highway in the Swiss canton of Jura uncovered many fossils of Jurassic marine reptiles in a proximal environment. Among these finds were the rare remains of strictly pelagic crocodylomorphs belonging to the Metriorhynchidae family. Metriorhynchids are found all across Jurassic deposits of Europe, Central and South America, mostly as isolated and fragmentary remains, yet their fossil record is relatively poor in Switzerland compared to England or Germany. The group have been subject to an intensive revision over the past fifteen years but the phylogenetic relationships within Metriorhynchidae are still under debate.

We describe a new specimen of Metriorhynchidae from the Kimmeridgian of the region of Porrentruy, Switzerland. The material consists of a subcomplete, disarticulated skeleton preserving most pieces of the cranium, mandibles, and many remains of the axial and appendicular skeleton (Fig.1). This new specimen is referred to large-bodied macrophagous tribe Geosaurini and to the poorly represented genus *Torvoneustes*, and replaced in the phylogenetic context of the group.

The study of this disarticulated specimen was particularly improved by a process of 3D surface rendering and modeling of the cranial bones that allowed us to reconstruct the skull itself. This approach gave us a better understanding of the cranial anatomy of the specimen without risking damaging its fragile pieces by intensive manipulation. The study of this specimen allows us to take a critical look at the currently proposed evolutionary trends within the genus *Torvoneustes* in addition to providing new informations on the variations and evolution of this poorly known taxon.

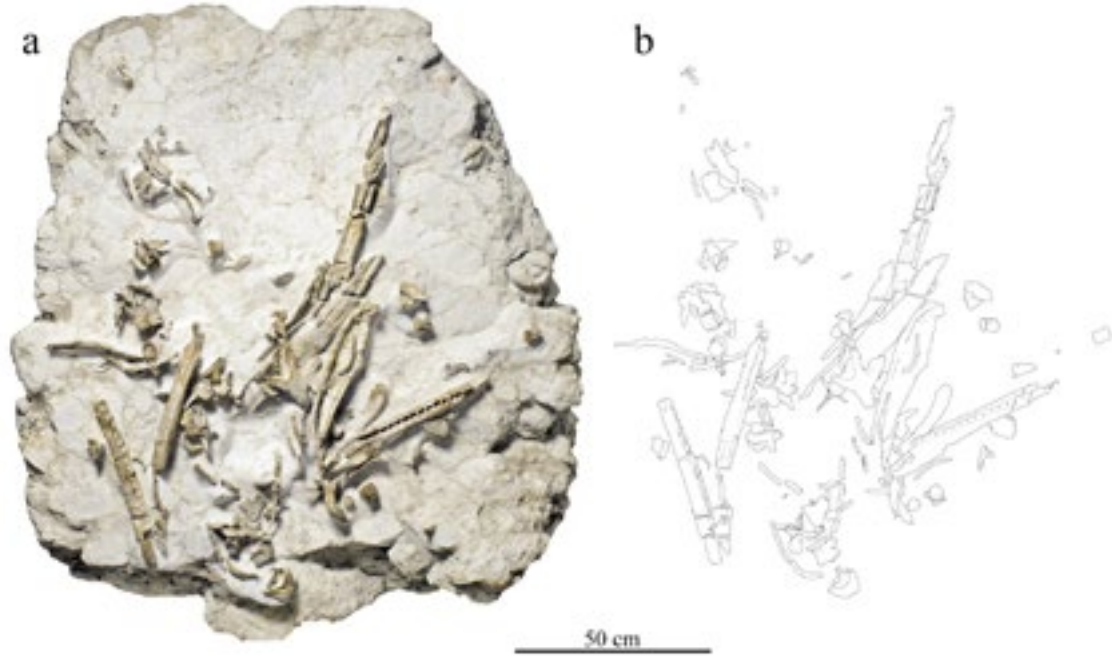


Figure 1. Taphonomical disposition of the metriorhynchid skeleton MJSN BSY008-465. (a) photograph of the skeleton still embedded in the limestone block; (b) drawing of the bones in their taphonomical position.

## 5.8

### Mollusc extinction during the end-Triassic crisis

Michael Hautmann<sup>1</sup>, Mariel Ferrari<sup>2</sup>

<sup>1</sup> Paläontologisches Institut und Museum, University of Zurich, Karl-Schmid-Strasse 4, CH-8006 Zürich  
(michael.hautmann@pim.uzh.ch)

<sup>2</sup> Instituto Patagónico de Geología y Paleontología, IPGP (CCT CONICET-CENPAT), Boulevard Alte. Brown 2915, (9120) Puerto Madryn, Provincia de Chubut, Argentina

The end-Triassic mass extinction is commonly ranked among the “big five” extinction events of the Phanerozoic and has attracted considerable scientific attention, but surprisingly, there is still a lack of comprehensive studies on the taxonomic turnover of many major taxa (Hautmann 2021). This presentation provides the first in-depth analysis of diversity changes of gastropods during the Triassic–Jurassic transition and a comparison with the diversity trajectories of other molluscs. Gastropods suffered a loss of 56.8 % of genera and subgenera during the crisis, which was higher than the average of marine life (46.8 %). The most strongly affected subclass was the Neritimorpha, which lost 72.7 % of their Rhaetian genera; on the other extreme, the Heterobranchia remained nearly unaffected (11 % loss). We analysed this extinction pattern with respect to larval development, palaeobiogeography, shell size, and anatomy and found that putative feeding of the pelagic larval stage, adaptation to tropical-temperate water temperatures, and flexibility of the mantle attachment were among the factors that might explain extinction resilience of heterobranchs during the end-Triassic crisis. Among molluscs, gastropods were more strongly affected than bivalves (43.4 % extinction) but less than ammonoids, which were nearly annihilated. These differences in extinction magnitude roughly correlates with locomotion activity and thus metabolic rates. We suggest three potential kill mechanisms that could account for the observed extinction patterns: global warming, ocean acidification, and extinction of marine plankton. The end-Triassic extinction of gastropods fits to proposed extinction scenarios for this event, which invoke the magmatic activity of the Central Atlantic Magmatic Province as the ultimate cause of death.

#### REFERENCES

- Hautmann, M. 2021: Extinction: End-Triassic Mass Extinction, eLS, Vol 2: 1–15, 2021. DOI: 10.1002/9780470015902. a0029378

## 5.9

# Evaluating turtle shell ecomorphology patterns using phylogenetic comparative analyses

Guilherme Hermanson<sup>1</sup>, Laura Dziomber<sup>2</sup>, Walter G. Joyce<sup>1</sup>, Christian Foth<sup>1</sup>, Serjoscha W. Evers<sup>1</sup>

<sup>1</sup> Department of Geosciences, University of Fribourg, Chemin du Musée 6, CH 1700 Fribourg

(guilhermehermanson@gmail.com)

<sup>2</sup> Institute of Plant Sciences & Oeschger Centre for Climate Change Research, University of Bern,

Hochschulstrasse 4, CH 3012 Bern

The shell is the most striking evolutionary novelty of turtles, likely placing different constraints on other parts of their skeleton, such as the limbs and neck. Extant turtles exhibit notable variation in shell shapes, ranging from highly domed carapaces of terrestrial species to flattened and broad instances as in most aquatic taxa. Hypotheses around the evolution of this variation have been mainly concentrated on ecological (e.g. habitat differences; Claude et al. 2003; Benson et al. 2011; Dziomber et al. 2020) and functional explanations (e.g. hydrodynamicity; Rivera et al. 2006; Butterfield et al. 2021). Explicit tests of other potential influences have, however, remained overlooked, such as the enlargement of the shell accommodating larger guts in herbivorous species (Bjorndal 1997) or the effect of the size of the anterior shell space as to their capacity of neck retraction, given it is within the shell where the neck is withdrawn. Past investigations of turtle shell ecomorphology also aimed to characterize extant turtle shell shape variation in contrast to their habitats as a means to infer the ecological preferences of extinct taxa (e.g. Benson et al. 2011; Dziomber et al. 2020). This is central to understanding the ecological transitions in the group, since the ecology of the earliest stem-turtles is disputed (Joyce & Gauthier 2004; Scheyer & Sander 2007; Benson et al. 2011; Dziomber et al. 2020). However, most of these studies neglected or did not properly account for species interrelationships in their analyses, which is crucial when dealing with species-trait data (Felsenstein 1985).

In this study, we re-analyze a previously collected 3D shape dataset of turtle shells and make explicit use of phylogenetic statistical tools to test hypotheses of turtle shell ecomorphology. We assess the effects of evolutionary allometry, general and specific habitat ecologies, dietary specializations to herbivory as well as neck retraction capacity on extant turtle shell shape variation. Different from previous surveys, we take the uncertainty in branch length variation of time-calibrated trees into account when predicting the ecology of turtles based on shell shape. For three extinct taxa, the stem-turtles *Proganochelys quenstedtii* and *Proterochersis robusta*, and the thalassocchelydian *Plesiochelys bigleri*, previous paleoecology hypotheses are re-evaluated. Additionally, we inspected rates of shell shape evolution to verify whether these are different between specific clades or ecological groups.

We show that allometry has a strong effect on turtle shell shape variation, with large-bodied species exhibiting a more embayed anterior shell region that likely provides more space to bigger heads. On the other hand, none of our other explanatory variables (habitat, diet, function) was retrieved as having significant effects on shell shape variation. Phylogenetic signal of shell shape and of ecology-specific shapes is moderate but significant across turtles, indicating that besides closely related species being more similar, they also often show similar ecologies. This is further corroborated by our analysis of shell shape rate evolution, with which we detect rate heterogeneity between clades. Furthermore, as ecology and shape evolve on the same tree, our iterative phylogenetic discriminant analysis had high success rates of predicting ecology, despite the clear absence of a form-function signal. Our iterative predictions are consistent with an independent origin of a flippered, highly-aquatic mode in thalassocchelydians and an intermediate, semiaquatic habitat for the Triassic stem-turtle *Proterochersis robusta*. For *Proganochelys quenstedtii*, our analyses detect ambiguity for habitat predictions, as its shell shape can either support terrestrial or semiaquatic ecologies.

## REFERENCES

- Benson, R.B.J., Domokos, G., Várkonyi, P.L., & Reisz, R.R. 2011. Shell geometry and habitat determination in extinct and extant turtles (Reptilia: Testudinata), *Paleobiology*, 37(4), 547-562.
- Bjorndal, K.A. 1997. Fermentation in reptiles and amphibians. In: *Gastrointestinal Microbiology. Volume 1: Gastrointestinal Ecosystems and Fermentations* (Eds. Mackie, R.I. & White, B.A.), Chapman & Hall, New York, 199-230.
- Butterfield, T.G., Herrel, A., Olson, M.E., Contreras-Garduño, J., & Macip-Rios, R. 2021. Morphology of the limb, shell and head explain the variation in performance and ecology across 14 turtle taxa (12 species), *Biological Journal of the Linnean Society*, 134(4), 879-891.
- Claude, J., Paradis, Tong, H., & Auffray, J.C. 2003. A geometric morphometric assessment of the effects of environment and cladogenesis on the evolution of the turtle shell, *Biological Journal of the Linnean Society*, 79(3), 485-501.
- Dziomber, L., Joyce, W.G., & Foth, C. 2020. The ecomorphology of the shell of extant turtles and its applications for fossil turtles, *PeerJ*, 8, e10490.

- Felsenstein, J. 1985. Phylogenies and the comparative method, *The American Naturalist*, 125(1), 1-15.
- Joyce, W.G., & Gauthier, J.A. 2004. Palaeoecology of Triassic stem turtles sheds new light on turtle origins, *Proceedings of the Royal Society of London. Series B: Biological Sciences*, 271(1534), 1-5.
- Rivera, G., Rivera, A.R., Dougherty, E.E., & Blob, R.W. 2006. Aquatic turning performance of painted turtles (*Chrysemys picta*) and functional consequences of a rigid body design, *Journal of Experimental Biology*, 209(21), 4203-4213.
- Scheyer, T.M., & Sander, P.M. 2007. Shell bone histology indicates terrestrial palaeoecology of basal turtles, *Proceedings of the Royal Society B: Biological Sciences*, 274(1620), 1885-1893.

## 5.10

# FINS database and the diversification dynamics of modern sharks, rays and skates

Kristína Kocáková<sup>1</sup>, Amanda Gardiner<sup>1</sup>, Daniele Silvestro<sup>2</sup>, Catalina Pimienta<sup>1,3,4</sup>

<sup>1</sup> Palaeontology Institute and Museum, University of Zurich, Zurich, Karl-Schmid-Strasse 4, 8006, Switzerland

<sup>2</sup> Department of Biology, University of Fribourg, Fribourg, Ch. du Musée 10 1700, Switzerland

<sup>3</sup> Department of Biosciences, Swansea University, Swansea SA2 8PP, UK

<sup>4</sup> Smithsonian Tropical Research Institute, Balboa, Republic of Panama

Neoselachians are a monophyletic group encompassing all extant sharks, rays, skates, and many of their extinct relatives. Originating in the Triassic (251 Ma), this group persevered throughout two mass extinction events, the Triassic-Jurassic and the Cretaceous-Paleogene mass extinctions. In the present, this group represents a specious cosmopolitan lineage, members of which play essential roles in modern marine ecosystems, many having high or even apex trophic positions. They are also one of the marine groups most severely impacted by human pressures with at least one third of species currently threatened with extinction. Understanding of the underlying factors which affect extinction susceptibility, and insight into the past responses to extinction events could provide important pointers for current conservation efforts, by identifying the most at-risk species, based on factors other than the ones traditionally used in conservation. The neoselachian fossil record has the potential to be a significant resource in obtaining such understanding, as it is exceptionally rich. Neoselachians are one of the most prominent vertebrate groups in the marine fossil record as the result of their teeth, which have high fossilization potential due to their composition, and are continuously produced and shed throughout their lifetimes. The abundance and ubiquity of the neoselachian fossil record is underlined by the number of descriptions of neoselachian remains present in literature, with the first records dating to as early as the 1800's. Despite this, there has not been an attempt to compile the available knowledge into a comprehensive database to this day. Consequently, research on neoselachian evolution available today provides only an incomplete picture of the history of this clade, usually only focusing on a specific time period, geographical area, or taxon (e.g. Kriwet & Benton, 2004, Condamine et al., 2019). Global studies covering an entire era or longer time frames are lacking, thus a more holistic and complete understanding of the history of the group is yet to be achieved.

Here we present the *Fossil Neoselachian* (FINS) database which compiles all available data of the neoselachian fossil record from the last 145 Myr. This database was compiled extracting data from an extensive literature research using SharkReferences (Pollerspöck & Straube, 2022) as a foundational source, spanning all published material from the 1970's to the present, including research articles, theses, and conference abstracts in a variety of languages. This data was then complemented with information downloaded from the PaleoBiology Database (PBDB). The final database contains more than a double the number of data obtained from PBDB alone. The primary types of data collected were the information on localities where neoselachian fossils were found (collections) and the taxa identified from these localities (occurrences). The FINS database currently contains 5,895 collections and 29,853 occurrences. We identified 2,239 unique taxa, out of which 1,598 are species, 520 are genera, 93 are families, and 28 are orders, with 71% of the occurrences being identified to the species level and 96% to the genus level. Occurrences were found globally, with particular abundance in North America and Europe.

We are capitalizing on this unprecedented database by examining the diversification dynamics of neoselachians. For the first time, we aim to quantify their speciation and extinction rates over the past 145 million years to illustrate the patterns of their macroevolution on a global scale. To achieve this, a Bayesian approach which accounts for preservation and sampling biases and age uncertainties will be used (Silvestro et al. 2019). Results of these analyses are presented here, alongside with plans for the future application of this dataset. These analyses will focus on modelling the relationship between taxon duration and likelihood of extinction, adding information on the intrinsic characteristics of individual taxa, to model the relationship between traits and extinction probability, and incorporation of these models of past extinction mechanism with paleoclimate data, to produce a holistic model of the neoselachian mechanisms of extinction throughout the Cretaceous and the Cenozoic. These models will have the potential to provide valuable insights for the conservation efforts as implied above, by using the knowledge about the factors contributing to the extinction probability in the past, resulting in an improvement in the ability to identify the species which require the most urgent conservation attention in the present.

## REFERENCES

- Kriwet, J., Benton, M., J. (2004) Neoselachian (Chondrichthyes, Elasmobranchii) diversity across the Cretaceous-Tertiary boundary. *Palaeogeography, Palaeoclimatology, Palaeoecology*. 214(3), 181-194.

- Condamine, F., L., Romieu, J., Guinot, G. (2019) Climate cooling and clade competition likely drove the decline of lamniform sharks. PNAS. 116(41). 20584-20590
- Pollerspöck, J., Straube, N. (2022) [www.shark-references.com](http://www.shark-references.com). World Wide Web electronic publication. Version 2021.
- Silvestro, D., Schnitzler, J., Liow, L.H., Antonelli, A. & Salamin, N. (2014) Bayesian Estimation of Speciation and Extinction from Incomplete Fossil Occurrence Data. Systematic Biology, 63, 349–367.

## 5.11

### Palaeontological discoveries from North Borneo

László Kocsis<sup>1</sup>, Antonino Briguglio<sup>2</sup>, Amajida Roslim<sup>3</sup>, Sulia Goeting<sup>3</sup>

<sup>1</sup> Institute of Earth Surface Dynamics, University of Lausanne, Rue de la Mouline, 1015 Lausanne, Switzerland  
(laszlo.kocsis@unil.ch)

<sup>2</sup> DI.S.T.A.V. Dipartimento di Scienze della Terra, dell'Ambiente e della Vita Università degli Studi di Genova, Corso Europa, 26, I – 16132 Genova, Italy (

<sup>3</sup> Geology Group, Faculty of Science, Universiti Brunei Darussalam, Jalan Tungku Link, Gadong BE1410, Brunei Darussalam

Borneo is the world's third largest island, situated in Southeast Asia in the centre of the Coral Triangle, which region displays the highest biodiversity today. Via investigating the fossil record in the area, new data can be added about how this rich diversity developed and evolved in the past. Palaeontology focused researches in Borneo are rare, and most of the knowledge comes from samples collected during geological mappings in 1960ies.

Since 2014, we are investigating Neogene shallow marine sediments and their fossil contents in Northern Borneo, especially in Brunei Darussalam. Our field surveys yielded many exceptional fossils and here the most remarkable discoveries are shown to give a taste of ancient biodiversity of the region. Some of the results are already published by our wider group with the involvement of experts, but preliminary new finds will also be briefly presented. Among the vertebrates, fish fossils such as teeth, bones, and otoliths can occur frequently, and until now the most diverse Southeast Asian chondrichthyan fossil record comes from Brunei with many sealchian and batoid taxa including the famed *Otodus (Megaselachus) megalodon* (Kocsis et al. 2019). The over 1200 teleost otoliths are currently under investigation, but the picture of a diverse coastal fish fauna can be drawn that was dominated by family Sciaenidae and Ariidae with many taxa new to science. Turtle bones, and rarely crocodile teeth and scutes were also found in the rocks, but they are more often found reworked along the coastlines. Certain outcrops can be very rich in invertebrates. Molluscs are the most widespread, among which gastropods were studied in detail with 23 new species described so far (Harzhauser et al. 2018). Other taxa such as bivalves, crustaceans, and corals can be also very common, and their descriptions are in progress. Microfossils such as pollen and foraminifera have been also studied and described from both fossil and modern settings (Goeting et al. 2021; Roslim et al. 2021). Many sedimentary successions in the region yield macroplant remains as well, and dipterocarp fossil-leaf floras and dipterocarp originated fossil tree resins (amber) were recently reported (Kocsis et al. 2020, Wilf et al. 2022). Amber can be abundant in certain layers, and they come with different size and colour. They often show the sign of bioerosion, while some contain trapped insects that wait for further studies.

#### REFERENCES

- Harzhauser, M., Raven, H., Landau, B., Kocsis, L., Adnan, A., Zuschin, M., Mandic, O., Briguglio, A. 2018: Late Miocene gastropods from northern Borneo (Brunei Darussalam, Seria Formation). *Palaeontographica, abt. A: Palaeozoology-Stratigraphy*, 313, 1-79.
- Kocsis, L., Razak, H., Briguglio, A., Szabó, M., 2019: First report on a diverse Neogene fossil cartilaginous fish fauna from Borneo (Ambig Hill, Brunei Darussalam). *Journal of Systematic Palaeontology*, 17(10), 791-819.
- Kocsis, L., Usman, A., Jourdan, A.-L., Haji Hassan, S., Jumat, N., Daud, D., Briguglio, A., Slik, F., Rinyu, L., Futó, I. 2020: The Bruneian record of "Borneo Amber": a regional review of fossil tree resins in the Indo-Australian Archipelago. *Earth-Science Review*, 201 - 103005
- Roslim, A., Briguglio, A., Kocsis, L., Goeting, S., Hofmann, Ch.-Ch. 2021. Palynology of Miocene sediments in Brunei Darussalam: first SEM investigations of pollen and spores, and their taxonomy and palaeoenvironmental interpretation. *Palaeontographica Abteilung B Palaeobotany–Palaeophytology*. 301, 77-139.
- Wilf, P., Zou, X., Donovan, M.P., Kocsis, L., Briguglio, A., Shaw, D., Slik, J.W.F., Lambiase, J.J. 2022: First fossil-leaf floras from Brunei Darussalam show dipterocarp dominance in Borneo by the Pliocene. *PeerJ* – 12949.

## 5.12

# Xenarthrans of The Santiago Roth Collection From The Pampean Region of Argentina (Pleistocene), in Zurich, Switzerland.

Kévin LE VERGER<sup>1</sup>; Marcelo R. SÁNCHEZ-VILLAGRA<sup>1</sup>.

<sup>1</sup> Palaeontological Institute and Museum, University of Zurich, Karl-Schmid-Strasse 4, 8006 Zurich, Switzerland  
(kevin.leverger@pim.uzh.ch).

Santiago Roth was an illustrious Swiss paleontologist who prospected and collected an extensive amount of fossil mammals belonging mainly to the Pleistocene South American Megafauna of the Pampean Region of Argentina. In Switzerland, the material is housed in several institutions across the country, the largest parts being stored at the Museum of Natural History of Geneva and the Paleontological Institute and Museum of the University of Zurich (= PIMUZ).

The present work is a revision of the xenarthrans from the Santiago Roth Collection and focuses on material housed at PIMUZ (Roth, 1889). Among the specimens present, xenarthrans are the main representatives with a total of 150 specimens out of 284. Since the work of Schulthess (1920), this material has not been revised and practically not studied. From the isolated tooth fragment to the complete skeleton, we have carried out in the present study a complete taxonomic revision of these specimens (= 110 taxonomic reassessments) with a mention of their exceptional completeness and of the scientific interests they could bring for the study of this clade. We were thus able to confirm the presence of 27 species with disparate distributions in the three temporal subdivisions of the Pleistocene Pampean Region of Argentina (Figure 1). As an ecotone marked by the transition between the subtropical forest of Brazil and the arid steppes of Patagonia, the Pampean Region was drastically impacted by Quaternary climate fluctuations (Prado et al., 2021). Consequently, this review has allowed us to highlight the exceptional diversity of xenarthrans present in the PIMUZ Santiago Roth Collection and to relate this high diversity to the different abiotic events impacting the paleoenvironment of the Pampean Region during the Pleistocene. With the present study, our objective is threefold: i) to shed new light on the material available for the study of xenarthrans; ii) to propose a basis for the revision of specimens from the Santiago Roth Collection housed in other institutions, iii) and to encourage the work of expertise in mammal collections for the paleontological community.

## REFERENCES

- Pascual, R., Ortiz Jaureguizar, E., and Prado, J.L. 1996. Land mammals: Paradigm for Cenozoic South American Geobiotic evolution. Münchener Geowissenschaftliche Abhandlungen (A), 30, 265–320.
- Prado, J.L., Alberdi, M.T., and Bellinzoni, J. 2021. Pleistocene mammals from Pampean region (Argentina). Biostratigraphic, biogeographic, and environmental implications. Quaternary, 4(2), 16.
- Roth, S. 1889. Fossiles de La Pampa, Amérique du Sud, collectionnés par Santiago Roth. Ed. Jean Meyer, Zürich, 5, 16
- Schulthess, B. 1920. Beiträge zur Kenntnis der Xenarthra auf Grund der Santiago Roth'schen Sammlung des Zoologischen Museums der Universität Zürich. Ed. Albert Kundig, Zürich, 44, 119.
- Soibelzon, E. 2019. Using paleoclimate and the fossil record to explain past and present distributions of armadillos (Xenarthra, Dasypodidae). Journal of Mammalian Evolution, 26(1), 61–70.

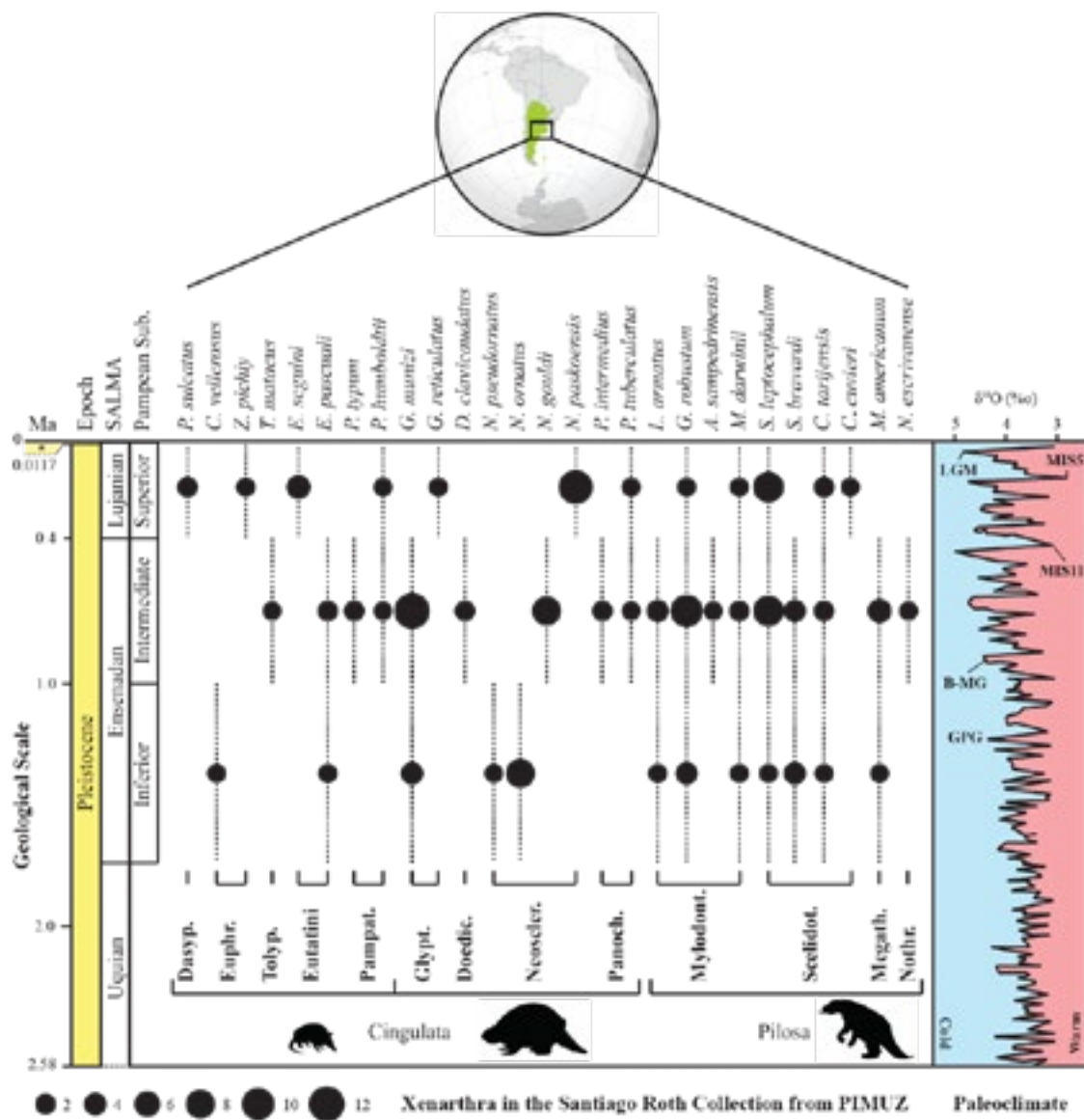


Figure 1. Location of the Pampean Region and list of the 27 species of Xenarthra identified in the collection of Santiago Roth hosted at PIMUZ associated with their belonging to the Pampean subdivisions, the geological scale sensu SALMA (Pascual et al., 1996), and the paleoclimatic curve of Soibelzon (2019). Abbreviations: B-MG, Matuyama/Brunhes Glaciation; GPG, Great Patagonian Glaciation; LGM, Last Glacial Maximum; MIS, Marine Isotopic Stage.

## 5.13

# Enrolment and flexures in the trilobite *Strenuella polonica* Czarnocki, 1926 from the Cambrian of Poland

Sinéad Lynch<sup>1</sup>, Harriet B. Drage<sup>1</sup>, Allison C. Daley<sup>1</sup>, Anna Źylińska<sup>2</sup>

<sup>1</sup>Institute of Earth Sciences, University of Lausanne, Géopolis, CH-1015, Lausanne (sinead.lynch@unil.ch)

<sup>2</sup>Faculty of Geology, University of Warsaw, Żwirki i Wigury 93, 02-089 Warszawa

Enrolment in trilobites has been hypothesised to be a protective response against predation, or extreme environmental conditions (Babcock and Speyer, 1987). Other postures, such as dorsal flexures, may assist with the moulting process by facilitating the breakage of sutures that allowed the trilobite to exit from its old exoskeleton (McNamara and Rudkin, 1984). In some cases, these positions could also have positioned pleural spines to strengthen anchorage during the moulting process (Drage et al., 2018).

This study is a continuation of the project presented by Źylińska and Daley (2019). Here, we investigate if moults of the ellipsocephalic trilobite *Strenuella polonica* Czarnocki, 1926 are more often found in postures theorized to help with moulting, and correspondingly if carcasses are more often found in postures associated with protection. Our sample comprises 85 specimens of *S. polonica* from the Cambrian Series 2 of the Holy Cross Mountains in Poland (Źylińska, 2013). Each specimen in this study was categorized into one, or a combination of the following posture categories: fully enrolled, outstretched, cranidium flexed, and pygidium flexed. We also identified each of these specimens either as a moult or a carcass.

The moults of *S. polonica* were mainly recognizable by their detached librigenae because this species predominantly moulted through a cephalic opening. We also describe some parts of the morphology of *S. polonica*, such as the axial spines and the hypostome. The preliminary results indicate an association between the different postures and their proportions in moults and carcasses. We found more carcasses in postures with the thorax enrolled, and more exuviae in the outstretched and flexed postures. This suggests a possible evolutionary link between enrolment and moulting.

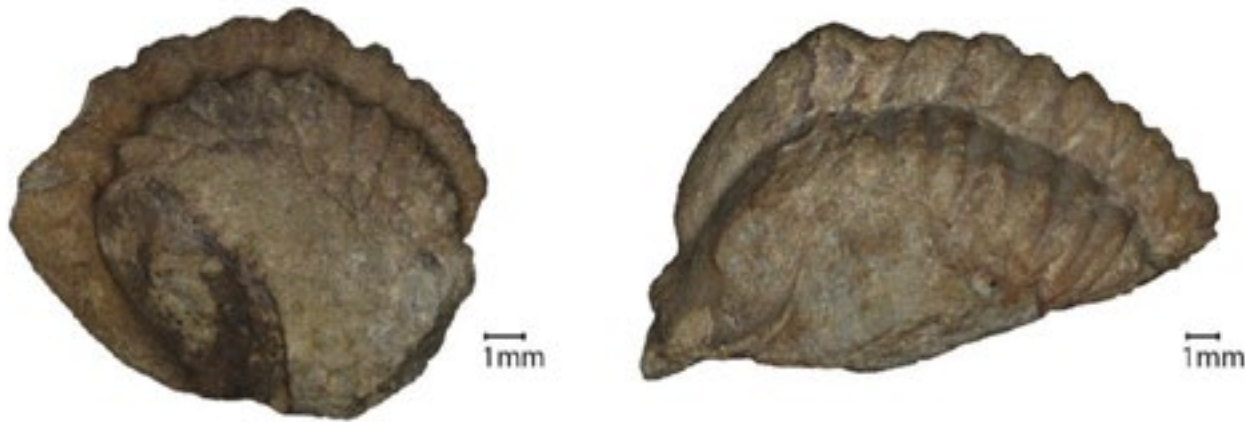


Figure 1. Two of the postures observed in *Strenuella polonica*. Left: Fully enrolled specimen with flexed cranidium (MWG ZI/42/073, Probable carcass). Right: Fully enrolled specimen with slightly flexed cranidium (MWG ZI/107/50, Probable moult).

## REFERENCES

- Babcock, L. E., & Speyer, S. E. 1987: Enrolled trilobites from the Alder Pyrite Bed, Ledyard Shale (Middle Devonian) of western New York. *Journal of Paleontology*, 61(3), 539-548.
- Drage, H. B., Holmes, J. D., García-Bellido, D. C., & Daley, A. C. 2018: An exceptional record of Cambrian trilobite moulting behaviour preserved in the Emu Bay Shale, South Australia. *Lethaia*, 51(4), 473-492.
- McNamara, K. J. & Rudkin, D. M. 1984: Techniques of trilobite exuviation. *Lethaia*, 17(2), 153-173.
- Źylińska, A. 2013: The oldest Cambrian trilobites from the Holy Cross Mountains, Poland: taxonomic, stratigraphic and biogeographic reappraisal. *Acta Geologica Polonica*, 63(1), 57-87.
- Źylińska, A., & Daley, A. C. 2019: Moulting or protection-enrolment strategies in *Strenuella polonica* Czarnocki, 1926 (Ellipsocephalida, Trilobita) from Cambrian Series 2 of the Holy Cross Mountains, Poland. 17th Swiss Geoscience Meeting, Fribourg 2019.

## 5.14

### Comparative digital reconstruction of ontogenetic skull variation in altricial (*Pica pica*) and precocial birds (*Struthio camelus*)

Olivia Plateau<sup>1</sup>, Todd Green<sup>2</sup>, Paul Gignac<sup>3</sup>, Christian Foth<sup>1</sup>

<sup>1</sup> Department of Geosciences, University of Fribourg, Chemin du Musée 6, CH-1700 Fribourg (olivia.plateau@gmail.com)

<sup>2</sup> Department of Anatomy, New York Institute of Technology College of Osteopathic Medicine, Box 8000, Old Westbury, NY

<sup>3</sup> Department of Cellular & Molecular Medicine, University of Arizona College of Medicine, Box 245044, Tucson, Arizona

The ontogeny of birds has been studied since the 19th century but focused primarily on embryonic development. Until to date, only a few case studies describe post-hatching ontogenetic variation of single species (Mayr, 2020; Mayr & Manegold, 2021 Sosa & Hospitaleche, 2018; Piro & Hospitaleche, 2019). The application of CT based 3D digital reconstructions allows to highlight the internal morphology of an object, but also the documentation of delicate structures in a non-invasive manner (Lautenschlager *et al.*, 2014; Beyrand *et al.*, 2019), making this method useful for studying ontogenetic variation. Here, we investigated the ontogenetic skull variation of two bird species with very different ecologies, *Pica pica* and *Struthio camelus*, using µCT based 3D reconstructions. For each specimen, we performed bone-by-bone segmentation in order to visualize and describe the ontogenetic shape variation, calculated the average sutural closure based on the degree of bone fusion, and estimated overall skull volume.

Based on subsequent comparisons, bone fusion of *Pica pica* occurs more rapidly than that of *Struthio camelus*, but both species follow a similar order of skull fusion events. The general shape of the skull roof is more rounded in juvenile stages and becomes more dorsally flattened and posteriorly elongated in adult stages. Some bones, such as the lacrimals and quadrates, show great shape variation, which are related to the formation of different bony processes during ontogeny. Although skull growth lasts longer in *Struthio camelus* than in *Pica pica*, the skull of the most mature *Struthio camelus* is still less fused than that of *Pica pica*. Growth and fusion patterns indicate that the interspecific variation in ontogeny could be related to heterochrony, i.e., a shift in rates or timing of developmental. Nevertheless, this hypothesis needs to be tested in a broader phylogenetic framework in order to detect the evolutionary direction of the potential heterochronic transformation.

Due to the ontogenetic process of bone fusion (see Plateau & Foth, 2021), the skull morphology of adult crown birds is somehow improper to understand details of skull evolution between stem and crown, as major morphological differences are simply a result of bone fusion. In contrast, using juvenile crown birds allows for a broader comparison with the skull bone morphology of stem birds, generating more detailed insights into this evolutionary process.

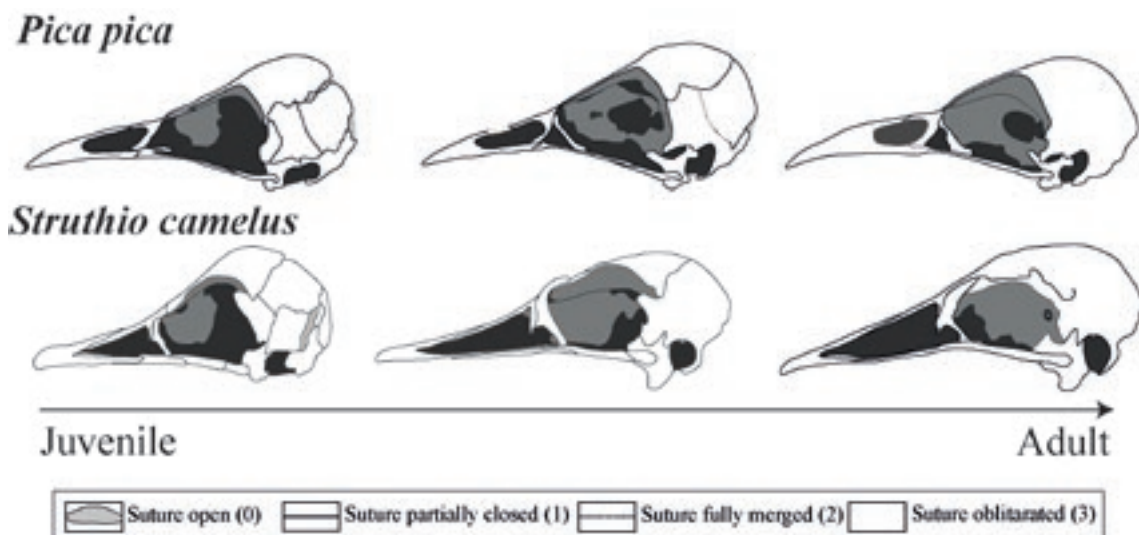


Figure 1. Overview of the ontogenetic variation of the cranium of *Pica pica* and *Struthio camelus* in lateral view.

## REFERENCES

- Beyrand, V., Voeten, D. F., Bureš, S., Fernandez, V., Janáček, J., Jirák, D., Rauhut, O., and Tafforeau, P. 2019: Multiphase progenetic development shaped the brain of flying archosaurs. *Scientific Reports*, 9, 1-15.
- Lautenschlager, S., Bright, J. A., and Rayfield, E. J. 2014: Digital dissection—using contrastenhanced computed tomography scanning to elucidate hard-and soft-tissue anatomy in the Common Buzzard *Buteo buteo*. *Journal of Anatomy*, 224, 412-431.
- Mayr, G. 2020: Comparative morphology of the avian maxillary bone (os maxillare) based on an examination of macerated juvenile skeletons. *Acta Zoologica*, 101, 24-38.
- Mayr, G., & Manegold, A. 2021: On the comparative morphology of the juvenile avian skull: An assessment of squamosal shape across avian higher-level taxa. *Anatomical Record*, 304, 845-859.
- Piro, A., & Acosta Hospitaleche, C. 2019: Skull morphology and ontogenetic variation of the Southern Giant Petrel *Macronectes giganteus* (Aves: Procellariiformes). *Polar Biology*, 42, 27-45.
- Plateau, O., & Foth, C. 2021: Common patterns of skull bone fusion and their potential to discriminate differentontogenetic stages in extant birds. *Frontiers in ecology and evolution*, 9, 1-15.
- Sosa, M. A., & Acosta Hospitaleche, C. 2018: Ontogenetic variations of the head of *Aptenodytes forsteri* (Aves, Sphenisciformes): muscular and skull morphology. *Polar Biology*, 41, 225-235.

## 5.15

# Fossil cephalopod phylogenetics: recent advances, remaining challenges and future perspectives

Alexander Pohle<sup>1</sup>, Kevin Stevens<sup>2</sup>, Christian Klug<sup>1</sup>

<sup>1</sup> Paläontologisches Institut und Museum, Universität Zürich, Karl-Schmid-Strasse 4, CH-8006 Zürich

(alexander.pohle@pim.uzh.ch)

<sup>2</sup> Institut für Geologie, Mineralogie und Geophysik, Ruhr-Universität Bochum, Universitätsstraße 150, DE-44801 Bochum

Fossil cephalopods represent one of the most important classical topics in palaeontology and are part of almost any undergraduate geoscience programme. However, despite their great abundance in the fossil record and their biostratigraphical importance, phylogenetic methods have historically only reluctantly been applied to cephalopods when compared to most other groups of fossil organisms (Neige et al. 2007). Here, we present some of the recent advances that have been made in this regard, exemplified by phylogenetic studies on early Palaeozoic cephalopods (Pohle et al. 2022) and belemnites (Stevens et al. 2022). These studies allow for modernised systematic classifications that more accurately reflect phylogenetic relationships and open the door for further macroevolutionary studies. We identify gaps in our current understanding of fossil cephalopod phylogeny, e.g., the origin of the Nautilida or the phylogenetic relationships between “belemnoid” coleoids (Figure 1). We use these examples to call for a wider application of modern Bayesian phylogenetic tools in other groups of fossil cephalopods, in particular through the use of the fossilized birth-death process (Stadler 2010; Heath et al. 2014), which is one of the few available phylogenetic tools that explicitly take into account stratigraphic data a priori, besides offering several other advantages. The outstanding fossil record in combination with numerous cases of homoplasies including cases of parallelism have often been used as a justification why the application of phylogenetic methods were considered inappropriate for cephalopods, leading to the widespread use of a “stratophenetic” approach. However, this approach ultimately relies on subjective opinions, which characters are deemed to be of importance for evolutionary relationships. In contrast, quantitative methods allow for rigorous hypothesis testing and are now able to explicitly account for these perceived problems, i.e., stratigraphic ages and variable rates of evolution. Thus, cephalopods are ideally suited to exploit these methods to reconstruct evolutionary time trees, but also to test macroevolutionary hypotheses more generally. At the same time, core taxonomic work and expertise is more important than ever for constructing the large morphological character matrices that are necessary for these phylogenetic studies.

## REFERENCES

- Heath, T.A., Huelsenbeck, J.P. & Stadler, T. 2014: The fossilized birth-death process for coherent calibration of divergence-time estimates, *Proceedings of the National Academy of Sciences*, 111, E2957-2966.
- Neige, P., Rouget, I., & Moyne, S. 2007: Phylogenetic practices among scholars of fossil cephalopods, with special reference to cladistics. In: *Cephalopods Present and Past: New Insights and Fresh Perspectives* (Ed. by Landman, N.H., Davis, R.A. & Mapes, R.H.). Springer, Dordrecht, 3-14.
- Pohle, A., Kröger, B., Warnock, R.C.M., King, A.H., Evans, D.H., Aubrechtová, M., Cichowski, M., Fang, X., & Klug, C. 2022: Early cephalopod evolution clarified through Bayesian phylogenetic inference, *BMC Biology*, 20, 88.
- Stadler, T. 2010: Sampling-through-time in birth-death trees, *Journal of Theoretical Biology*, 267, 396-404.
- Stevens, K., Pohle, A., Hoffmann, R. & Immenhauser, A. 2022: Bayesian inference reveals a complex evolutionary history of belemnites, *bioRxiv*, doi: 10.1101/2022.08.22.504746.

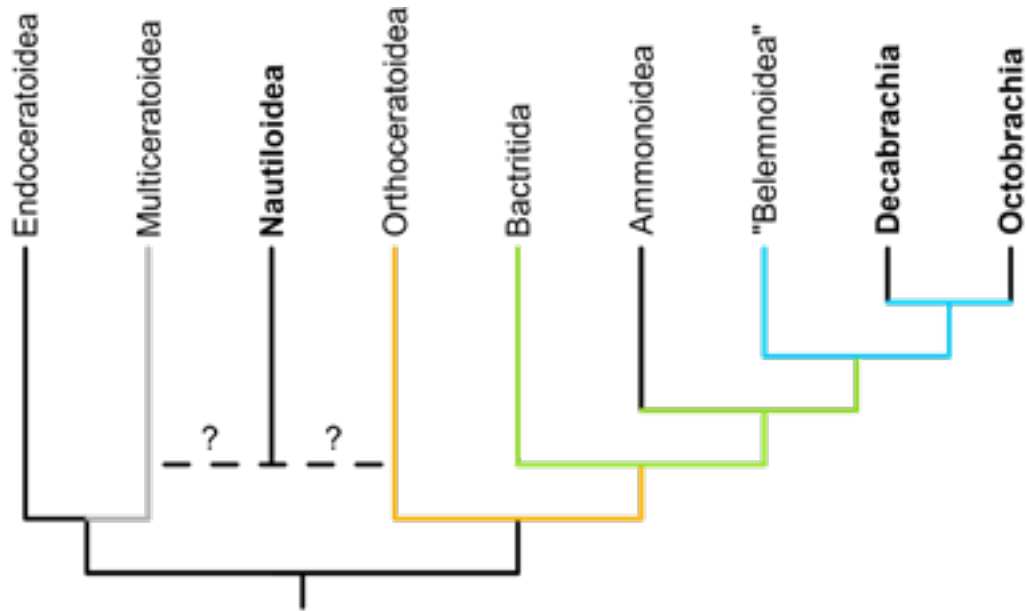


Figure 1. Phylogenetic relationships between major groups of cephalopods. Groups with living members are shown in bold text. The Orthoceratoidea, Bactritida and Belemnoidea are paraphyletic with respect to their descendants, as shown by coloured branches. The Multiceratoidea (grey) are potentially paraphyletic, because they may include the ancestors of the living Nautiloidea.

## 5.16

# Frontal appendages from the Fezouata Shale (Early Ordovician, Morocco) reveal high diversity and ecological adaptations in radiodonts after the Cambrian.

Gaëtan J.-M. Potin<sup>1</sup>, Pénélope Claisse<sup>1,2</sup>, Pierre Gueriau<sup>3</sup>, Stephen Pates<sup>4</sup>, Allison C. Daley<sup>1</sup>

<sup>1</sup> Institute of Earth Sciences, University of Lausanne, Géopolis, CH-1015 Lausanne, Switzerland (gaetan.potin@unil.ch)

<sup>2</sup> Université de Lille, CNRS, UMR 8198 – Evo-Eco-Paleo, F-59000 Lille, France

<sup>3</sup> Université Paris-Saclay, CNRS, ministère de la Culture, UVSQ, MNHN, Institut photonique d'analyse non-destructive européen des matériaux anciens, 91192, Saint-Aubin, France

<sup>4</sup> Department of Zoology, University of Cambridge, Downing Street, Cambridge CB2 3EJ, United Kingdom

The Fezouata Biota (Early Ordovician, Tremadocian) of Morocco highlights the transition between the Cambrian Explosion and the Great Ordovician Biodiversification Event (GOBE) because it yields exceptionally preserved remains of marine organisms (Saleh et al. 2020). This *Lagerstätte* is rich in arthropod remains, especially radiodonts (informally known as anomalocaridids) (Van Roy et al. 2015a). Radiodonta is a clade of stem-lineage arthropods characterised by a segmented body with wide swimming flaps, and a head bearing a pair of appendages, a pair of eyes on stalks, and a mouth surrounded by spiny plates. Their frontal appendages are sclerotized and have a high preservation potential, meaning they are often found in isolation, providing both taxonomic identification and palaeoecological information on feeding behaviour (Daley & Budd 2010), even in the absence of complete bodies. We examined 105 radiodont frontal appendages specimens in the collections of the Musée Cantonal de Géologie de Lausanne and the Yale Peabody Museum, allowing us to revise *Aegirocassis*, (Van Roy et al. 2015b), the first and only named radiodont yet described from the Fezouata Shale, and to identify several new taxa, most belonging to Hurdidae. The enigmatic fossil *Pseudoangustidontus* (Van Roy & Tetlie 2006), previously described as a single spinose fragment of an unknown raptorial appendage, is also identified as a hurdiid radiodont. Using computer tomography (CT-scanning), we were able to reconstruct a specimen showing several *Pseudoangustidontus* spinose fragments articulated together as endites attached to podomeres of an appendage with an arrangement typical for hurdiids. Radiodonts in the Fezouata Shale were highly diverse and employed a variety of different feeding strategies. Suspension feeding is interpreted as the feeding strategy for 96 specimens, whereas there are only 9 sediment sifters. This abundance in suspension feeding may be linked to the “Ordovician Plankton Revolution”, which saw a huge radiation in plankton diversity during the GOBE (Perrier et al. 2015). The study also points the decline of active raptorial predation in radiodonts, as suggested by their absence, so far, in the Fezouata Shale Formation.

## REFERENCES

- Daley, A.C., Budd, G. 2010. Morphology and systematics of the anomalocaridid arthropod *Hurdia* from the Middle Cambrian of British Columbia and Utah. *Journal of Systematic Palaeontology*, 11, 7, 743-787.
- Perrier, V., Williams, M., & Siveter, D.J. 2015: The fossil record and palaeoenvironmental significance of marine arthropod zooplankton, *Earth-Science Reviews*, 146, 146-162.
- Saleh, F., Antcliffe, J.B., Lefebvre, B., Pittet, B., Laibl, L., Perez-Peris, F., Lustri, L., Gueriau, P., & Daley, A.C. 2020: Taphonomic bias in exceptionally preserved biotas, *Earth and Planetary Science Letters*, 529, 1-6.
- Van Roy, P., Briggs, D.E.G., & Gaines, R.R. 2015a: The Fezouata fossils of Morocco; an extraordinary record of marine life in the Early Ordovician, *Journal of the Geological Society*, 172, 541-549.
- Van Roy, P., Daley, A.C., & Briggs, D.E.G. 2015b: Anomalocaridid trunk limb homology revealed by a giant filter-feeder with paired flaps, *Nature*, 522, 77-80.
- Van Roy, P., & Tetlie, O.E. 2006. A spinose appendage fragment of a problematic arthropod from the Early Ordovician of Morocco. *Acta Palaeontologica Polonica* 51 (2): 239–246.

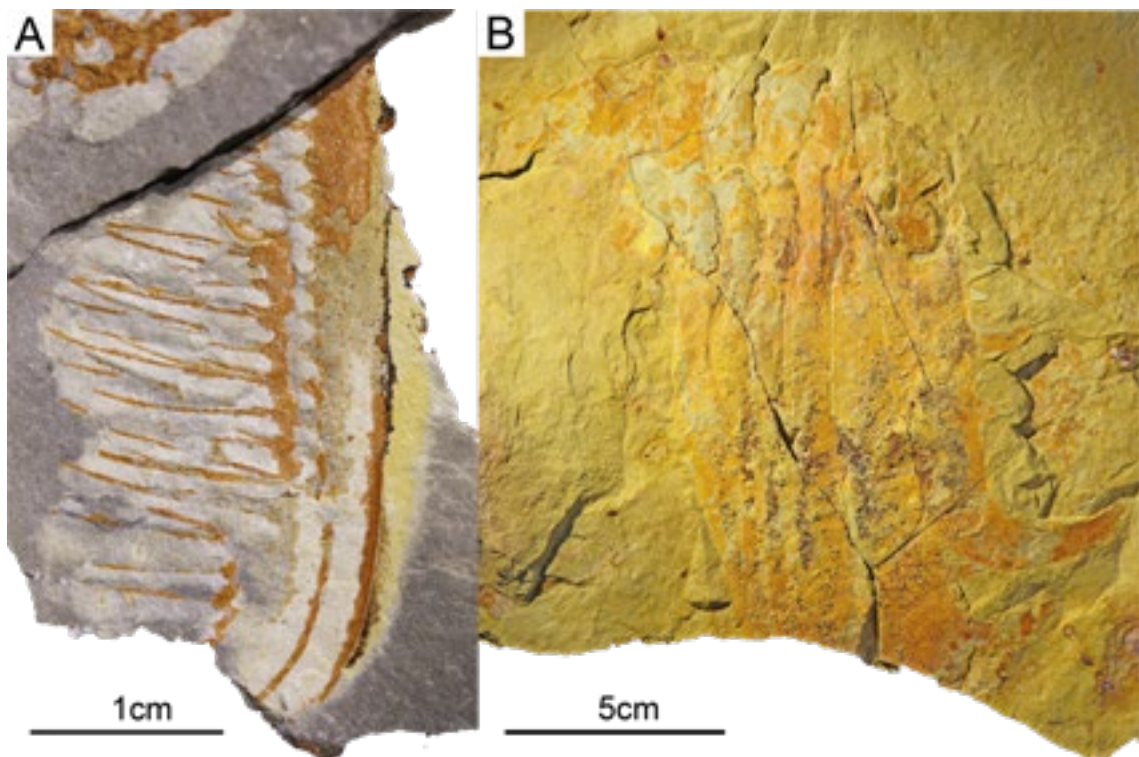


Figure 1. New hurdiid frontal appendages (Radiodonta) from the Fezouata Biota (Early Ordovician, Morocco). A – *Pseudoangustidontus* sp. nov., suspension feeder. B – Gen. nov. sp. nov., sediment sifter.

## 5.17

# From the past to the future: Unraveling the complexity of the crocodylian skull morphology

Irena Raselli<sup>1,2</sup>, Christian Foth<sup>2</sup>, Jérémie Anquetin<sup>1,2</sup>

<sup>1</sup> Jurassica Museum, Route de Fontenais 21, 2900 Porrentruy, Switzerland

(irena.raselli@hotmail.com)

<sup>2</sup> Department of Geosciences, University of Fribourg, Chemin du Musée 6, 1700 Fribourg, Switzerland

Evolvability, as the ability of organisms to produce selectively advantageous variation in order to adapt to new environments (Wagner et al. 2007; Pigliucci 2008), is progressively taking center stage in biological studies addressing the challenges of the modern environmental crisis (e.g. Campbell et al. 2021). To date, over 8'000 life forms are critically endangered (IUCN 2022) and although the fast environmental changes are not the only threat, a better understanding of a species' capability to adapt is crucial to support and improve conservation work. A way of gaining insights into the evolvability of a group of organisms is to examine the modularity and integration of their phenotypic traits. Modularity is a key driver of evolvability (Clune et al. 2013) and it is understood as the organization of an organism into nearly independent subunits (e.g. Wagner 1996). A strong integration between subunits can lead to an organism that is functionally better coordinated, however would simultaneously constrain its evolvability (Kirschner and Gerhart 1998). In contrast, an organism which is rather modular in organization remains more flexible and adaptable when environmental changes occur.

To date 27 living species of Crocodylia are recognized and for over a third of them, their existence in the wild is threatened (32% critically endangered, 14% vulnerable; IUCN 2022). The clade comprises three monophyletic families (Alligatoridae, Crocodylidae and Gavialidae) and originates in the Upper Cretaceous. The time to the most recent common ancestor of Alligatoridae dates back to approximately 53 Mya and that of Crocodylidae and Gavialidae around 50 Mya (Pan et al. 2021) predatory and semi-aquatic reptiles. Crocodylia, the closest living relatives of birds, first appeared in the Late Cretaceous period. In the present study, the complete mitochondrial (mt. Even though extant Crocodylia only represent a fraction of the Crocodylomorpha's rich taxonomic diversity and morphological disparity (Godoy 2020), they are still being wrongly labelled as 'living fossils' (Langston 1973). Their seemingly primeval morphology appears to vary in exclusively one aspect, namely the proportions of the rostrum. However, in order to gain a better understanding of the morphological evolution of the crocodylian skull, it is necessary to put behind simplistic perceptions and embrace its complexity instead.

In this study, we capture a comprehensive part of the clade's morphological disparity and taxonomic diversity based on over 170 three-dimensional, high-quality surface scans of skulls and mandibles from 26 extant crocodylian species. With the tools of Geometric Morphometrics and multivariate statistics we dissect the aspects of modularity and integration, morphological disparity, evolutionary allometry, phylogenetic inertia and the influence of functionality and abiotic factors, in order to understand the driving forces in the morphological evolution of the crocodylian skull. Our results show amongst other that the crocodylian mandible consists of two modules, while the morphologically more complex cranium is a constellation of three general morphological units which split into a total of five sub-modules. These sub-modules form family-specific clusters. The combined cranial and mandibular modularity pattern of each family reflects a different ratio of phylogenetic constraint and ecological factor. With these and other new insights into the driving forces and constraints of the morphological evolution of Crocodylia, we discuss the evolutionary conditioning and long-term survival chances of extant crocodylian species in the light of the increasingly rapid environmental changes. Furthermore our study provides a breadth of new aspects of the crocodylian skull morphology, which will serve as a solid base for future studies elucidating the fossil record of Crocodylia.

## REFERENCES

- Campbell, C. S., Adams, C.E., Bean, C.W., Pilakouta, N. & Parsons, K. J. 2021. "Evolvability under Climate Change: Bone Development and Shape Plasticity Are Heritable and Correspond with Performance in Arctic Charr (*Salvelinus Alpinus*)."  
*Evolution & Development* 23 (4): 333–50. <https://doi.org/10.1111/ede.12379>.
- Clune, J., Mouret, J.-B. & Lipson, H. 2013. "The Evolutionary Origins of Modularity." *Proceedings of the Royal Society B: Biological Sciences* 280 (1755): 20122863. <https://doi.org/10.1098/rspb.2012.2863>.
- Godoy, P. L. 2020. "Crocodylomorph Cranial Shape Evolution and Its Relationship with Body Size and Ecology." *Journal of Evolutionary Biology* 33 (1): 4–21. <https://doi.org/10.1111/jeb.13540>.
- IUCN. 2022. The IUCN Red List of Threatened Species. Version 2022-1. <https://www.iucnredlist.org>. Accessed on 30.08.2022
- Kirschner, M., & Gerhart, J. 1998. "Evolvability." *Proceedings of the National Academy of Sciences* 95 (15): 8420–27. <https://doi.org/10.1073/pnas.95.15.8420>.
- Langston, W. 1973. "The Crocodilian Skull in Historical Perspective." In *Biology of the Reptilia* (Ed. Gans C), 263–284. New York: Academic Press. [https://scholar.google.com/scholar\\_lookup?hl=en&publication\\_year=1973&pages=263-284&author=W+Langston&title=Biology+of+the+reptilia](https://scholar.google.com/scholar_lookup?hl=en&publication_year=1973&pages=263-284&author=W+Langston&title=Biology+of+the+reptilia).

- Pan, T., Miao, J.-S., Zhang, H.-B., Yan, P., Lee, P.-S., Jiang, X.-Y., Ouyang, J.-H., Deng, J.-P., Zhang, B.-W. & Wu, X.-B. 2021. "Near-Complete Phylogeny of Extant Crocodylia (Reptilia) Using Mitogenome-Based Data." *Zoological Journal of the Linnean Society* 191 (4): 1075–89. <https://doi.org/10.1093/zoolinnean/zlaa074>.
- Pigliucci, M. 2008. "Is Evolvability Evolvable?" *Nature Reviews Genetics* 9 (1): 75–82. <https://doi.org/10.1038/nrg2278>.
- Wagner, G. P. 1996. "Homologues, Natural Kinds and the Evolution of Modularity1." *American Zoologist* 36 (1): 36–43. <https://doi.org/10.1093/icb/36.1.36>.
- Wagner, G. P., Pavlicev, M. & Cheverud, J. M. 2007. "The Road to Modularity." *Nature Reviews Genetics* 8 (12): 921–31. <https://doi.org/10.1038/nrg2267>.

## 5.18

# Cranial osteology of the Early Cretaceous baenid turtle *Trinitichelys hiatti* and new insights into the evolution of the basicranium of turtles

Yann Rollot<sup>1</sup>, Serjoscha W. Evers<sup>1</sup>, Stephanie E. Pierce<sup>2</sup>, Walter G. Joyce<sup>1</sup>

<sup>1</sup> Department of Geosciences, University of Fribourg, Chemin du Musée 6, CH-1700 Fribourg (yann.rollot@gmail.com)

<sup>2</sup> Museum of Comparative Zoology and Department of Organismic and Evolutionary Biology, Harvard University, 26 Oxford Street, MA 02138, USA

Paracryptodira is a clade of freshwater turtles that lived from the Late Jurassic to the Eocene in North America and Europe. Three clades of paracryptodiran turtles are commonly identified. The Compsemydidae were recently recognized as the most basal branching clade of paracryptodires, whereas the Pleurosternidae and Baenidae are grouped into the Baenoidea. Baenidae are particularly diverse from the Late Cretaceous to the Eocene in North America but, despite plenty of material has been described over the last 20 years, little is known from its early branching representatives in the Early Cretaceous. The Early Cretaceous fossil record of Baenidae consists of four valid taxa: *Arundelemys dardeni* from the Aptian-Albian of Maryland, *Lakotemys australodakotensis* from the Berriasian-Valanginian of South Dakota, *Protobaena wyomingensis* from the Albian of Wyoming, and *Trinitichelys hiatti* from the Aptian-Albian of Texas. While the former two taxa have recently benefited from new insights, the anatomy of *Protobaena wyomingensis* and *Trinitichelys hiatti* still remains poorly known to date.

As a better understanding of the cranial anatomy of the early representatives of Baenidae is critical for more confidently assessing the evolution of paracryptodires but also turtles in general, we described the skull of the holotype of *Trinitichelys hiatti* using micro-computed tomography. The segmentation of the skull reveals a different arrangement of cranial bones from the original illustrations provided half a century ago for that same specimen (see Gaffney, 1972). We document that the basicranium of *Trinitichelys hiatti* represents an intermediate ossification stage of that area between that of Pleurosternidae and more advanced baenids, also providing evidence for a new way of enclosing the internal carotid artery in bone. The circulatory system of turtles was progressively enclosed by bone during the evolutionary history of the group, notably with the closure of the intrapterygoid vacuity and increasing ossification of the basicranium. The encapsulation of the internal carotid artery in bone was shown to have occurred from the most posterior aspect of the basicranium in several turtle clades, but the basicranial area of *Trinitichelys hiatti* suggests that a different mechanism occurred within paracryptodires, in which the enclosing of the circulatory system occurred from anterior instead.

## REFERENCES

- Gaffney, E.S. 1972: The systematics of the North American family Baenidae (Reptilia, Cryptodira), Bulletin of the American Museum of Natural History, 147, 241-320.

## 5.19

### New fossil assemblages from the Early Ordovician Fezouata Biota

Farid Saleh<sup>1,2,3</sup>, Romain Vaucher<sup>3</sup>, Muriel Vidal<sup>4</sup>, Khadija El Hariri<sup>5</sup>, Lukáš Laibl<sup>6</sup>, Allison C. Daley<sup>3</sup>, Juan Carlos Gutiérrez-Marco<sup>7</sup>, Yves Candela<sup>8</sup>, David A.T. Harper<sup>9</sup>, Javier Ortega-Hernández<sup>10</sup>, Xiaoya Ma<sup>1,2,11</sup>, Ariba Rida<sup>12</sup>, Daniel Vizcaíno<sup>13</sup> and Bertrand Lefebvre<sup>14</sup>

<sup>1</sup> *Yunnan Key Laboratory for Palaeobiology, Institute of Palaeontology, Yunnan University, Kunming, China*

<sup>2</sup> *MEC International Joint Laboratory for Palaeobiology and Palaeoenvironment, Institute of Palaeontology, Yunnan University, Kunming, China*

<sup>3</sup> *Institute of Earth Sciences (ISTE), University of Lausanne, Geopolis, CH-1015 Lausanne, Switzerland*

<sup>4</sup> *University of Brest, CNRS, IUEM Institut Universitaire Européen de la Mer, UMR 6538 Laboratoire Géosciences Océan, Place Nicolas Copernic, 29280 Plouzané, France*

<sup>5</sup> *Laboratoire de Géoressources, Géoenvironnement et Génie Civil 'L3G', Faculté des Sciences et Techniques, Université Cadi-Ayyad, BP 549, 40000 Marrakesh, Morocco*

<sup>6</sup> *Czech Academy of Sciences, Institute of Geology, Rozvojová 269, 165 00 Prague 6, Czech Republic*

<sup>7</sup> *Instituto de Geociencias (CSIC, UCM) and Departamento GEODESPAL, Facultad de Ciencias Geológicas, José Antonio Novais 12, 28040 Madrid, Spain*

<sup>8</sup> *Department of Natural Sciences, National Museums Scotland, Edinburgh EH1 1JF, UK*

<sup>9</sup> *Palaeoecosystems Group, Department of Earth Sciences, Durham University, Durham DH1 3LE, UK*

<sup>10</sup> *Museum of Comparative Zoology and Department of Organismic and Evolutionary Biology, Harvard University, Cambridge, MA 02138, USA*

<sup>11</sup> *Centre for Ecology and Conservation, University of Exeter, Penryn, UK*

<sup>12</sup> *Université Cadi Ayyad, École Normale Supérieure, Marrakech, Morocco*

<sup>13</sup> *Independent – 7 rue Chardin, Maquens, F-11090 Carcassonne, France*

<sup>14</sup> *Université de Lyon, Université Claude Bernard Lyon 1, École Normale Supérieure de Lyon, CNRS, UMR5276, LGL-TPE, Villeurbanne, France*

The Fezouata Biota (Morocco) is a unique Early Ordovician fossil assemblage. The discovery of this biota revolutionized our understanding of Earth's early animal diversifications – the Cambrian Explosion and the Ordovician Radiation – by suggesting an evolutionary continuum between both events. Herein, we describe Taichoute, a new fossil locality from the Fezouata Shale. This locality extends the temporal distribution of fossil preservation from this formation into the upper Floian, while also expanding the range of depositional environments to more distal parts of the shelf. In Taichoute, most animals were transported by density flows, unlike the *in-situ* preservation of animals recovered in previously investigated Fezouata sites. Taichoute is dominated by three-dimensionally preserved, and heavily sclerotized fragments of large euarthropods – possibly representing nektobenthic/nektic bivalved taxa and/or radiodonts. Resolving whether this dominance reflects a legitimate aspect of the original ecosystem or a preservational bias requires an in-depth assessment of the environmental conditions at this site. Nevertheless, Taichoute provides novel preservational and palaeontological insights during a key evolutionary transition in the history of life on Earth.

## 5.20

# Resilience of platy corals (Scleractinia, Agariciidae) over the past 30 million years in the Coral Triangle

Nadia Santodomingo<sup>1,2</sup>, Zarinah Waheed<sup>3</sup>, M. Ali Syed Hussein<sup>3</sup>, Allia Rosedy<sup>3</sup>, Kenneth Johnson<sup>1</sup>

<sup>1</sup> Natural History Museum, Cromwell Road, SW7 5BD, London, UK

(n.santodomingo@nhm.ac.uk; nsantodomingo@gmail.com)

<sup>2</sup> Institute of Earth Sciences (ISTE), Quartier UNIL-Mouline, Bâtiment Géopolis CH-1015 Lausanne, Switzerland

<sup>3</sup> Endangered Marine Species Research Unit, Borneo Marine Research Institute, Universiti Malaysia Sabah, Kota Kinabalu, Malaysia

The origins of the Coral Triangle region date from 30 million years ago, from which the oldest coral assemblages are from northeast Borneo. These ancient reefs were low-relief patch reefs that developed under low light and high sediment input, i.e. turbid conditions (Santodomingo et al. 2016). Paleontological studies have revealed that platy corals of the family Agariciidae are among the most common corals on these ancient Oligocene and Miocene turbid habitats (McMonagle et al. 2011, Santodomingo et al. 2016). Today, agariciids are known to flourish at low light and deep mesophotic environments, but most species distribute over a wide bathymetric range (Waheed et al. 2013). We assessed modern turbid reefs, analogous to their ancient counterparts, in order to better understand the diversity and dominance of agariciids in these marginal environments through time. Surveys on mosaic of turbid reefs in Darvel Bay (Sabah, NE Borneo) were done up to 30 m depth between January 2019 to October 2021. Fossil specimens were examined from the collections of the Natural History Museum (NHM, London, UK) and Naturalis Biodiversity Centre (Leiden, The Netherlands). Our findings show a high coral diversity in turbid environments (27 species), with foliose and platy forms of *Leptoseris* dominant in the most turbid localities. Our revision of the fossil record in the Coral Triangle region includes six species dated from the late Oligocene, 32 species along the Miocene, from which most them are still living today in this region (18 spp.). These outcomes show that agariciids that were common during the Oligo-Miocene remain dominant in modern turbid reefs, highlighting the role of these marginal habitats as refugia by hosting high species richness over the past 30 million years. Ongoing research on the genetic diversity of agariciids and time-calibrated phylogenies will allow to further explore the lability of species to shift from turbid to clear-waters through time.

## REFERENCES

- McMonagle, L. B., Lunt, P., Wilson, M. E. J., Johnson, K. G., Manning, C., & Young, J. 2011: A re-assessment of age dating of fossiliferous limestones in eastern Sabah, Borneo: Implications for understanding the origins of the Indo-Pacific marine biodiversity hotspot. *Palaeogeography, Palaeoclimatology, Palaeoecology*, 305(1–4), 28–42.
- Santodomingo, N., Renema, W., & Johnson, K.G. 2016: Understanding the murky history of the Coral Triangle: Miocene corals and reef habitats in East Kalimantan (Indonesia). *Coral Reefs*, 35, 765–781
- Waheed, Z., & Hoeksema, B. W. 2013: A tale of two winds: species richness patterns of reef corals around the Semporna peninsula, Malaysia. *Marine Biodiversity*, 43, 37–51.

## 5.21

# Early Triassic conodonts and palynomorphs from Stensiöfjellet, Svalbard

Elke Schneebeli-Hermann<sup>1</sup>, Marc Leu<sup>1</sup>, Bitten Bolvig Hansen<sup>2</sup>, Øyvind Hammer<sup>3</sup>, Franz-Josef Lindemann<sup>3</sup>, Hugo Bucher<sup>1</sup>

<sup>1</sup> Paläontologisches Institut und Museum, Universität Zürich, Karl Schmid-Strasse 4, CH-8006 Zürich  
(elke.schneebeli@pim.uzh.ch)

<sup>2</sup> Kobberbæksvej 80, 5700 Svendborg, Denmark

<sup>3</sup> Natural History Museum, University of Oslo, Pb. 1172 Blindern, 0318 Oslo, Norway

The Smithian–Spathian transition (~249.2 Ma Widmann et al., 2020) is marked by profound environmental changes, carbon cycle perturbations, and the stepwise loss of nektonic biodiversity (ammonoids and conodonts) during the ~600 Ky long late Smithian (Widmann et al., 2020). From the subtropics, climatic conditions have been described as being highly unstable. The warm conditions during the middle Smithian and early late Smithian were followed by a cooling episode starting during the late late Smithian and extended into the earliest Spathian (Goudemand et al., 2019). Moreover, a global unconformity at the Smithian–Spathian boundary can only be explained by a regression of glacio-eustatic origin (Widmann et al., 2020). How these climatic conditions influenced boreal biota is poorly known.

Here we present conodont and palynomorph data from the Lower Triassic Vikinghøgda Formation from the Stensiöfjellet section, Svalbard.

In the studied succession, palynomorphs are poorly preserved but allow the description of three distinct assemblages. The first assemblage in the upper part of the Lusitaniadalen Member is spore-dominated. Co-occurring ammonoids indicate a middle Smithian age (mainly *Arctoceras blomstrandii*). In the Vendomdalen Member two assemblages are described, both being dominated by bisaccate pollen grains. The second assemblage is found ca. 5m above the earliest Spathian ammonoid *Bajarunia* sp. However, the consistent occurrence of gymnosperm pollen below this assemblage indicates that the base of second assemblages is located right above the *Wasatchites tardus* Zone. For the third assemblage from the upper part of the Vendomdalen Member, the ammonoids *Keyserlingites subrobustus* and *Svalbardiceras spitzbergensis* indicate a late Spathian age. The three assemblages correspond well with previously established palynomorph biozones for the boreal realm. They indicate a distinct change from a lycophyte-dominated vegetation to a gymnosperm-dominated vegetation just above the *Wasachites tardus* Zone, in concomitance with the onset of the late Smithian cooling.

Conodonts survived the Permian–Triassic mass extinction almost unscathed but underwent a major turnover around the Smithian–Spathian boundary (Orchard 2007). Conodont samples from the studied succession yielded relatively few specimens. Most conodont samples of the Lusitaniadalen Member are typically dominated by middle to late Smithian segminiplanate forms, such as *Scythogondolella* spp. (e.g. see Nakrem et al. 2008). Due to low abundance and low diversity, the latest Smithian extinction event is hardly discernible. An exceptionally abundant and diverse horizon occurs in the basal Vendomdalen Member in association with the cosmopolitan ammonoid *Bajarunia* of earliest Spathian age. This sample associates segminiplanate forms with numerous segminate forms. The latter are usually regarded as warm water dwellers (Leu et al., 2019 and references therein). The unusual high abundance and taxonomic diversity of this single sample strongly suggests condensation. Moreover, the presence of segminate forms in the Boreal during the Early Triassic suggests that temperature is not an important parameter regulating their distributions, as opposed to segminiplanate forms which were apparently restricted to cold waters. Size variation of P1 elements of segminate forms was also documented to be unrelated to temperature (Leu et al 2019).

Thus, the swap in the ecological dominance of land plants correlates well with the transition from warmer to cooler climate during the late Smithian and segminate condonts cannot univocally be interpreted as indicators of warm waters.

## REFERENCES

- Goudemand, N., Romano, C., Leu, M., Bucher, H., Trotter, J. A., & Williams, I. S. 2019. Dynamic interplay between climate and marine biodiversity upheavals during the early Triassic Smithian -Spathian biotic crisis. *Earth-Science Reviews*, 195, 169–178. <https://doi.org/10.1016/j.earscirev.2019.01.013>
- Leu, M., Bucher, H., & Goudemand, N. 2019. Clade-dependent size response of conodonts to environmental changes during the late Smithian extinction. *Earth-Science Reviews*, 195, 52-67. <https://doi.org/10.1016/j.earscirev.2018.11.003>
- Nakrem, H. A., Orchard, M. J., Weitschat, W., Hounslow, M. W., Beatty, T. W., & Mørk, A. (2008). Triassic conodonts from Svalbard and their Boreal correlations. *Polar Research*, 27(3), 523-539.
- Orchard, M. J. (2007). Conodont diversity and evolution through the latest Permian and Early Triassic upheavals. *Palaeogeography, Palaeoclimatology, Palaeoecology*, 252(1-2), 93-117. <https://doi.org/10.1016/j.palaeo.2006.11.037>
- Widmann, P., Bucher, H., Leu, M., Vennemann, T., Bagherpour, B., Schneebeli-He, Ermann, E., Goudemand, N., Clare, M. A., & Burgess, S. 2020. Dynamics of the Largest Carbon Isotope Excursion During the Early Triassic Biotic Recovery. *Frontiers in Earth Sciences* 8, 1–16. <https://doi.org/10.3389/feart.2020.00196>

## 5.22

# Trophic Network Reconstruction And Analysis Of The Different Fossiliferous Layers Of The Middle Triassic Monte San Giorgio World Heritage (Switzerland/Italy)

A. Torchet<sup>1</sup>, J. Shaw<sup>2</sup>, R. Stockar<sup>4</sup>, T. Scheyer<sup>1</sup>

<sup>1</sup> Institut und Museum, Universität Zürich, 8006 Zürich, Switzerland

<sup>2</sup> Department of Geology and Geophysics, Yale University, CT 06520 New Haven, United States of America

<sup>3</sup> Museo Cantonale di Storia Naturale, Viale Cattaneo 4, 6900 Lugano, Switzerland

Alexandre Torchet, alexandre.torchet@uzh.ch

**Keywords:** trophic networks, ecological interactions, Middle Triassic, marine fauna.

Since its discovery, the Middle Triassic Monte San Giorgio (MSG) lagerstätte near Meride (Canton Ticino, Switzerland) has revealed an enormous quantity of exceptionally preserved fossils. Distinct changes in faunal composition have been identified in the MSG lagerstätte, illustrating significant ecological changes of this extinct ecosystem over a time-lapse of 3 Ma. However, there has never been a detailed study on the network of trophic interactions among the organisms of the MSG Faunas. Here we present the most complete database on MSG fossils with specimens from museums in Zurich and Lugano in Switzerland and Milano in Italy. These initial results will be expanded to reconstruct a succession of 8 trophic networks for 8 distinct fossil layers of the MSG lagerstätte. We are using well-documented feeding behaviours and interactions of several hundreds of different taxa collected and a new Rstudio package called PFIM (Paleo Food Web Inference Model). The aim of this project is twofold. Firstly, our study will shed a new light on the ecological changes of a Middle Triassic marine fauna set between two of the deadliest mass extinction events in Earth history. Secondly, we will add a new element to the growing list of fossil faunas studied for trophic network reconstruction. This will open new research opportunities for the understanding of extinct ecosystem complexities and organizations and how these evolve through deep time.



# 6 Stratigraphy and Sedimentology: processes and deposits through time

Alain Morard, Sébastien Castelltort, Ursula Menkveld-Gfeller, Reto Burkhalter, Oliver Kempf

*Swiss Committee for Stratigraphy (SKS/CSS)  
 Swiss Palaeontological Society (SPG/SPS)  
 Swiss Geological Survey – swisstopo*

## TALKS:

- 6.1 Baud A.: Paleoecology and timing of the middle Triassic microbial mats to sponge-microbial buildups, and bio-events in the Briançonnais epeiric sea, links to the Permian–Triassic crisis aftermath.
- 6.2 Carraro D., Gaynor S., Ventra D., Moscariello A.: Testing the fidelity of zircon as a provenance indicator: an example from the Paleogene Wasatch/Colton alluvial system (central Utah, USA).
- 6.3 Fantasia A., Adatte T., Spangenberg J.E., Mattioli E., Millot R., Melleton J., Salazar C., Rogov M., Zverkov N., Lutikov O., Ippolitov A., Bodin S., Letulle T., Suan G.: Understanding Earth system recovery after the early Toarcian hyperthermal event.
- 6.4 Karabeyoglu U., Spangenberg J., Adatte T.: At the dawn of a big mass extinction: Multi-proxy studies across the Cretaceous-Paleogene (K/Pg) boundary in Central Anatolia, Turkey.
- 6.5 Krizova B., Consorti L., Tunis G., Bonini L., Franceschi M., Cardelli S., Schmitt K., Brombin V., Frija G.: High-resolution Stratigraphy and Paleoenvironmental Reconstructions of Cenomanian-Coniacian (Upper Cretaceous) Interval of the Adriatic Carbonate Platform (Friuli; NE Italy).
- 6.6 Lazarev S., Stoica M., Koiava K., Mandic, O., Vasilyan D.: Timing and faunal responses to extreme water-level changes of the Eastern Paratethys in the Caspian Basin during the Sarmatian Stage (late Serravalian-Tortonian).
- 6.7 Nuriel P., Weinberger R., Calvo R., Kylander-Clark A.R.C.: Invited talk: Dating terrestrial sediments by in situ U-Pb dating of carbonates.
- 6.8 Pietsch J., Wetzel A., Deplazes G., Filippioni M.: Lithofacies and depositional history of Middle Muschelkalk evaporites (Zeglingen Formation) in a regional stratigraphic context.
- 6.9 Ruchat A., Lathuilière B., Wohlwend S., Deplazes G., Madritsch H., Eberli G., Feist-Burkhardt S., Samankassou E.: A global coral reef event in the Bajocian: Evidence from a new coral reef in Northern Switzerland.
- 6.10 van de Schootbrugge B., Bos R.: Guest speaker: Reworking of organic matter associated with the end-Triassic mass-extinction and implications for other paleo-proxy records.
- 6.11 Vaucher R., Chiarella D., Marchegiano M., Poyatos-Moré M., Privat A., Spyrala Y., Thomas C., Zuchuat V.: Sedimentologika: a new community-driven DOA journal.
- 6.12 Wohlwend S., Feist-Burkhardt S., Hostettler B., Menkveld-Gfeller U., Bläsi H., Bernasconi S., Deplazes G.: Combined Middle Jurassic C-isotope chemo- and biostratigraphic correlation from Northern Switzerland through the new Nagra drill cores.
- 6.13 Zeyen N., Benzerara K., Beyssac O., Daval D., Muller E., Thomazo C., Tavera R., López-García P., Moreira D., Duprat E.: Invited talk: Integrative analysis of the mineralogical and chemical composition of modern microbialites from ten Mexican lakes: what do we learn about their formation?

## POSTERS:

- P 6.1 Baumgartner P.O., Epard J-L., Andjic G., Schmalholz S-M.: Paleogene Paleoenvironments of the Doldenhorn Nappe: from short-lived carbonate shoals to hemipelagic slope (Lämmerenalp, VS).
- P 6.2 Bomou B., Adatte T., Spangenberg J.E.: Expression of the Coniacian-Santonian oceanic anoxic event 3 in the Gabal Ekma section, Egypt.
- P 6.3 Jaimes-Gutierrez R., Adatte T., Puceat E., Vennemann T., Castelltort S.: Responding to change: Chemical weathering in the aftermath of the PETM, a case study in the Spanish Pyrenees.
- P 6.4 Jamart V., Pas D., Adatte T., Spangenberg J.E., Daley A.C.: Carbon geochemical insight at the Lower-Middle Cambrian (LMC) boundary in Southern Montagne Noire, SW France.
- P 6.5 Saintilan N.J., McLoughlin N., Beukes N.J., Spangenberg J.E., Banks D.A., Selby D.: Oxidation of organic matter in Neoarchean microbialite coincident with the Great Oxidation Event: Evidence from Re-Os geochronology and elemental proxies.
- P 6.6 Sharma N., Spangenberg J., Vérité J., Adatte T., Castelltort S.: Climatic imprint of the Middle Eocene Climatic Optimum (MECO) in the Escanilla formation, Spain.
- P 6.7 Vaucher R., Musajo C., Spangenberg J.E., Poyatos-Moré M., Puigdefàbregas C., Castelltort S., Adatte T.: Sedimentary record of hyperthermal events during the Early Eocene Climatic Optimum in the South Pyrenean Foreland Basin.
- P 6.8 Weidlich R., Bialik O.M., Pettke T., Rüggeberg A., Grobety B., Vennemann T., Makovsky Y., Foubert A.: Understanding seepage activity and formation of cold-seep carbonates in the south-eastern Mediterranean Sea.
- P 6.9 Zimmerli G., Lauper B., Deplazes G., Jaeggi D., Wohlwend S., Foubert A.: Lateral facies correlation of Opalinus Clay in central northern Switzerland using geochemical core logging data.
- P 6.10 Bomolomo M., Bessong M., Adatte T., Ossa Ossa F.-G.: Chrono-chemo-lithostratigraphic reconstruction and organic geochemistry of a carbonate reservoir in the Mintom “Neoproterozoic ?” Formation, South-East Cameroon.

## 6.1

# Paleoecology and timing of the middle Triassic microbial mats to sponge-microbial buildups, and bio- events in the Briançonnais epeiric sea, links to the Permian–Triassic crisis aftermath

Aymon Baud

*Institut des sciences de la Terre, Université de Lausanne, Geopolis, CH-1015 Lausanne (aymon.baud@unil.ch)*

Recent works on classic stromatolite (Lee & Riding, 2020), on sponge take over following the end-Permian mass extinction (Baud et al., 2021) and the possible extension of the sponge-microbial buildups in the Germanic basin Triassic carbonate (Pei & Reitner, 2022), led us to question and actualize the so called “algal mats, crypto-sponge and mudmound” of our published work on the middle Triassic carbonate of the neighboring Briançonnais epeiric sea (Baud, 1987; Baud et al., 2016). In this adjacent sea, recorded from central Switzerland to Franco-Italian maritime Alps, a first marine transgression occurred during the Lower-Middle Triassic transition about 247 My ago, characterized by a very large scale, dolomitic microbial mat deposition (a, fig. 1) a first similarity with the post extinction basal Triassic stromatolites of the Tethys. But the presence of nonspicular demosponges in the Briançonnais stromatolites with a mutualistic relationship is here to be resolved.

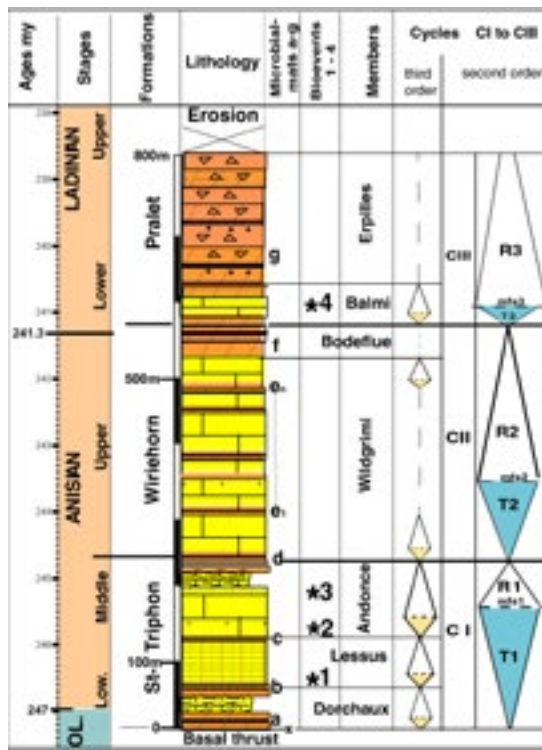


Figure 1: Stratigraphical sketch of the Middle Triassic succession of the Briançonnais domain in Western Switzerland with microbial mats levels and bioevents. Captions: limestone in yellow and dolomite in brown. T=transgressive system-track; R=regressive s-t; mfs=main flooding surface; Absolute ages in millions of years (My) according to recent chronostratigraphic charts.

During the Lower Anisian time (247-246 My), a new, large scale dolomitic microbial mat, caps (b, fig. 1) the open shallow marine deposition of the 20m thick vermicular limestone of the Dorchaux Member. The next third order transgressive cycle (Lessus Member) is showing a first bio-event (\*1, fig. 1) with the lower Anisian sudden recovery of abundant calcareous algae, which disappeared during the end-Permian great extinction and were absent during Early Triassic time. At the top this Lessus Member (middle Anisian about 246 My ago), a local dolomitic microbial mat was well recorded (c, fig. 1). The new transgressive system track of the Andonce Member brought two bio-events (\*2 and \*3, fig. 1): the first concerns the resurgence and abundance of siliceous sponges, bio-event at the origin of the first chert bands in the limestones. Due to an Ammonoid finding, the second bio-event is well dated of the middle Anisian *B. cadoricus* zone and consists of the recovery of a corals type *Thamnastrea*, and of calcareous and non-calcareous spicular sponges' growth. Also, unique and close in time, a level of a thrombolitic buildup up to 4 m thick were found in the Rothorn section, all described in Baud, 1987, “mudmound” showing similarity to the post extinction basal Triassic sponge microbial buildups (Baud et al., 2021).

At the middle-upper Anisian transition between 245 and 244 My ago, the regressive top of the Saint-Triphon Formation is characterized by a very large scale, dolomitic microbial mats deposition (d, fig. 1) recorded within the whole Briançonnais domain. The overlying Wildgrimmi Member of the Wiriehorn Formation consists of a 220 to 340 m succession of peritidal carbonate deposits with a shift to decametric scale shallowing-upward cycles, each topped by a dolomite bed possibly of microbial origin (e<sub>1</sub> to e<sub>n</sub>, fig. 1), like to same age South Alpine lagoonal Latemar shorter cycles. The upper regressive part of the Wiriehorn Formation is characterized by dolomitic beds partly built by stromatolites (f, fig. 1). In the following transgressive part of the Pralet Formation, the recorded conodont *trumptyi* allowed us to date the upper bio-event (\*4 fig. 1) of the basal Lower Ladinien, about 241 My ago. It consists of a short living rich assemblage of crinoids, gastropods, brachiopods, bivalves, and siliceous sponges. Then due to aridity and higher salinity, the carbonate factory moves to dolomitic production with increase in microbial activities (g, fig. 1) and loss of skeletal material in the upper Pralet Formation still Ladinien in age (240-238 My).

## REFERENCES

- Baud, A. (1987). Stratigraphie et sédimentologie des calcaires de Saint-Triphon (Trias, Préalpes, Suisse et France). Mémoires de Géologie, Lausanne, 1, 1-322.
- Baud, A., Plasencia, P., Hirsch, F., & Richoz, S. (2016). Revised middle Triassic stratigraphy of the Swiss Prealps based on conodonts and correlation to the Briançonnais (Western Alps). Swiss Journal of Geosciences, 109, 365-377.
- Baud, A., Richoz, S., Brandner, R., Krystyn, L., Heindel, K., Mohtat, T., Mohtat-Aghai, P., and Horacek, M., 2021. Sponge takeover from End-Permian mass extinction to early Induan time: Records in Central Iran microbial buildups, *Front. Earth Sci.*, 9, 1-23.
- Lee, J. H., & Riding, R. (2021). The 'classic stromatolite' *Cryptozoön* is a keratose sponge-microbial consortium. *Geobiology*, 19(2), 189-198.
- Pei, Y., Hagdorn, H., Voigt, T., Duda, J. P., & Reitner, J. (2022). Palaeoecological Implications of Lower-Middle Triassic Stromatolites and Microbe-Metazoan Build-Ups in the Germanic Basin: Insights into the Aftermath of the Permian–Triassic Crisis. *Geosciences*, 12(3), 1-19.

## 6.2

### Testing the fidelity of zircon as a provenance indicator: an example from the Paleogene Wasatch/Colton alluvial system (central Utah, U.S.A.)

Davide Carraro<sup>1</sup>, Sean Gaynor<sup>1,2</sup>, Dario Ventra<sup>1</sup>, Andrea Moscariello<sup>1</sup>

<sup>1</sup> *Département des sciences de la Terre, University of Geneva, 13 Rue des Maraîchers, CH-1205 Geneva (davide.carraro@unige.ch)*

<sup>2</sup> *Department of Geosciences, Princeton University, Princeton, New Jersey 08544, U.S.A.*

Understanding how depositional systems redistribute and store sediments is critical for interpreting basin-scale trends in provenance. Detrital zircon analyses are a classical approach to derive detailed records of basin paleogeographic and paleotectonic evolution by revealing temporal and spatial variability of detrital zircon ages within clastic successions. However, classic source-to-sink sedimentary models mainly focus on broad changes in zircon population through the entire stratigraphy of a basin, and do not typically consider how spatial variations in sediment transport processes across a sedimentary environment might affect provenance signatures. We present the result of U-Pb geochronology for zircon from 7 sandstone samples collected from the proximal and medial-to-distal sectors of the Paleocene-Eocene Wasatch/Colton paleodrainage system in the Uinta Basin (central Utah, USA). We used a systematic sampling strategy to examine the spatial and temporal variability of detrital zircon geochronology across the system's regional extent. These data can be used to interpret clastic provenance throughout fan development. Furthermore, we can also assess if potential shifts in zircon age spectra are associated with a change in provenance or by autogenic factors during the accumulation of this dominantly fluvial succession.

Our data from the Wasatch/Colton system provide a provenance reconstruction for the early clastic infill along the south-central margin of the Uinta Basin. These data also show that the modal abundances of detrital age populations present minor variations throughout the stratigraphy. In contrast, across-strike trends are more challenging to interpret, and we propose that system-scale compensational stacking that controlled aggradational of the alluvial wedge might be responsible for the lateral scattering of the observed data. This suggests that detrital zircon geochronology might have limited application in addressing detailed questions regarding the evolution of depositional systems at intra-basinal scale.

## 6.3

# Understanding Earth system recovery after the early Toarcian hyperthermal event

Alicia Fantasia<sup>1</sup>, Thierry Adatte<sup>2</sup>, Jorge E. Spangenberg<sup>3</sup>, Emanuela Mattioli<sup>1</sup>, Romain Millot<sup>4</sup>, Jérémie Melletton<sup>4</sup>, Christian Salazar<sup>5</sup>, Mikhail Rogov<sup>6</sup>, Nikolay Zverkov<sup>6</sup>, Oleg Lutikov<sup>6</sup>, Alexei Ippolitov<sup>6</sup>, Stéphane Bodin<sup>7</sup>, Thomas Letulle<sup>1</sup>, Guillaume Suan<sup>1</sup>

<sup>1</sup> Univ Lyon, UCBL, ENSL, CNRS, LGL-TPE, F-69622, Villeurbanne, France, (alicia.fantasia@univ-lyon1.fr)

<sup>2</sup> Institute of Earth Sciences, University of Lausanne, 1015 Lausanne, Switzerland

<sup>3</sup> Institute of Earth Surface Dynamics, University of Lausanne, 1015 Lausanne, Switzerland

<sup>4</sup> Bureau de Recherches Géologiques et Minières, F-45060 Orléans, France

<sup>5</sup> Facultad de Ciencias, Ingeniería y Tecnología, Universidad Mayor, Santiago, Chile

<sup>6</sup> Geological Institute of Russian Academy of Sciences, Moscow, Russia

<sup>7</sup> Department of Geoscience, Aarhus University, Høegh-Guldbergs Gade 2, 8000 Aarhus C, Denmark

Extreme climatic and environmental perturbations have punctuated Earth history. Given the pressing challenges associated with current climate change, most studies are generally focused on understanding the causes and consequences of these past global warming events. On the other hand, how the Earth system can recover and what is its self-regeneration capacity after these past extreme events is still understudied. The Toarcian in the Early Jurassic is an ideal time interval to understand the recovery phase after an extreme crisis. Indeed, it was marked by one of the most extreme hyperthermal events of the Phanerozoic accompanied by major environmental changes and the Toarcian Oceanic Anoxic Event (T-OAE, ca. 183 Ma). The onset of the Toarcian hyperthermal is relatively well understood, whereas the recovery phase, the mechanisms associated with this recovery, their efficiency, and the timing are still poorly constrained. Global warming is thought to have increased chemical weathering and favored organic carbon burial, leading to Earth climate recovery through atmospheric CO<sub>2</sub> drawdown. However, to date, there is a lack of empirical data to quantify the efficiency of both processes. The goal of this multi-proxy study is to combine sedimentological observations, mineralogical (whole-rock and clays) and geochemical analyses (inorganic and organic carbon isotopes, total organic carbon content, total phosphorus content, lithium isotopes) to reconstruct the long-term palaeoenvironmental evolution through the Toarcian and to constrain the efficiency of the mechanisms leading to the recovery of Earth system. Four worldwide distributed sites have been selected for this study: Fontaineilles in France (Grand Causses Basin), Vilyui in Siberia (Siberian Basin), Agua de la Falda in Chile (Andean Basin), and Ait Athmane in Morocco (High Atlas Basin). Our unprecedented high-resolution carbon isotope records allow us to correlate the studied sites to trace the global carbon cycle dynamics in the aftermath of the Toarcian event. Lithium isotope ratios are used to trace global weathering rates and to understand processes that control the long-term carbon cycle. Our results indicate that higher silicate weathering rates during the Toarcian hyperthermal likely helped the climate system recover and return to cooler climatic conditions.

## 6.4

# At the dawn of a big mass extinction: Multi-proxy studies across the Cretaceous-Paleogene (K/Pg) boundary in Central Anatolia, Turkey

Uygar Karabeyoglu<sup>1</sup>, Jorge Spangenberg<sup>2</sup>, Thierry Adatte<sup>1</sup>

<sup>1</sup> ISTE, Institute of Earth Sciences, University of Lausanne, Lausanne, Switzerland ([aliuygar.karabeyoglu@unil.ch](mailto:aliuygar.karabeyoglu@unil.ch))

<sup>2</sup> IDYST, Institute of Surface Dynamics, University of Lausanne, Lausanne, Switzerland Institut, University of Vienna, Innrain 52, A-6020 Innsbruck

The causation between continental flood basalt volcanisms and major mass extinctions has been known for long (e.g., Courtillot and Renne, 2003). The popularity of the K/Pg boundary (KPB) mass extinction stems from having two cataclysmic events in a very short time (i.e., the Deccan volcanism and the Chicxulub impact). In this aspect, Deccan-volcanism-related ecosystem changes need to be scrutinized in order to comprehend the interplay between volcanic eruptions and associated environmental stress. Therefore, here we document this relationship in terms of high-resolution quantitative species analysis coupled with geochemical and isotopic data on two complete sections in the Mudurnu-Göynük and the Haymana basins of central Anatolia (Turkey).

Throughout the late Maastrichtian, our  $\delta^{13}\text{C}$  measurements in the Haymana Basin show cyclical patterns highlighting the effects of precession cycles on the  $\delta^{13}\text{C}$  record. Remarkably, each cycle terminates by a less stratified ocean (i.e., similar benthic and planktonic  $\delta^{13}\text{C}$  values), and with a cooling spike (i.e., a positive shift in  $\delta^{18}\text{O}$  values).

On the other hand, it has been shown that the Deccan eruptions accelerates before the KPB (Schoene et al., 2019). In the Haymana basin we detected this acceleration-related environmental perturbation in terms of rapid drop in the planktonic foraminifera species diversity (Karabeyoglu et al. 2019). In fact, our magnetic susceptibility data from two different localities of Göynük and Okçular sections strongly testify this phenomenon. Such that, the ongoing late Maastrichtian reduction in the magnetic susceptibility suddenly accelerates right before the KPB corresponding exactly the same level of the species diversity loss.

Apart from these findings, the KPB itself is characterized by a 2-3 mm-thick reddish oxidized layer. It demonstrates a series of events, such as, sudden annihilation of large, ornamented ecological specialists (e.g. globotruncanids, racemiguembelinids, planoglobulinids), a Hg anomaly, and enrichments in Ir, Te, Ba, Ni, Cr and Co. Among these, Hg/Te shows a good correlation implying that Te may be used as another proxy for volcanic activity.

Overall, our detailed paleontological, isotopic, and geochemical records show that the deteriorating effects of Deccan volcanism had already started before the Chicxulub impact which predisposed faunas to eventual extinction at the KPB.

## REFERENCES

- Courtillot, V.E., Renne, P.R. 2003: On the ages of flood basalt events. *Comptes Rendus Geoscience*, 335, 113–140.  
 Schoene, B., Eddy, M.P., Samperton, K.M., Keller, C.B., Keller, G., Adatte, T., Khadri, S.F.R. 2019: U-Pb constraints on pulsed eruption of the Deccan Traps across the end-Cretaceous mass extinction, *Science*, 363, 862-866.  
 Karabeyoglu, A.U., Özkan-Altiner, S., Altiner, D. 2019: Quantitative analysis of planktonic foraminifera across the Cretaceous-Paleogene transition and observations on the extinction horizon, Haymana Basin, Turkey, *Cretaceous Research*, 104, 104169.

## 6.5

# High-resolution Stratigraphy and Paleoenvironmental Reconstructions of Cenomanian-Coniacian (Upper Cretaceous) Interval of the Adriatic Carbonate Platform (Friuli; NE Italy)

Barbora Krizova<sup>1</sup>, Lorenzo Consorti<sup>2</sup>, Giorgio Tunis<sup>3</sup>, Lorenzo Bonini<sup>4</sup>, Marco Franceschi<sup>4</sup>, Sahara Cardelli<sup>1</sup>, Katharina Schmitt<sup>5</sup>, Valentina Brombin<sup>1</sup> and Gianluca Frijia<sup>1</sup>

<sup>1</sup> Department of Physics and Earth Sciences, University of Ferrara, Via Saragat 1, 44122 Ferrara  
(barbora.krizova@unife.it)

<sup>2</sup> Italian National Research Council (ISMAR-CNR), Viale Romolo Gessi 2, 34123 Trieste

<sup>3</sup> Via Margotti 19, 34170 Gorizia

<sup>4</sup> Department of Mathematics and Geosciences, University of Trieste, Via Valerio 12/1, 34127 Trieste

<sup>5</sup> Institute of Geosciences, University of Mainz, Johann-Joachim-Becher-Weg 21, 55128 Mainz

Evidence based on climate modeling and temperature reconstructions derived by several proxies ( $\text{TEX}_{86}$ ,  $\delta^{18}\text{O}$ ) suggest that Late Cretaceous was one of the warmest periods in Earth history. The early Turonian experienced a temperature maximum with the highest ocean temperatures of the entire Cretaceous, as well as the highest sea level of the whole Phanerozoic (Jarvis et al. 2015 and references therein). This interval was followed by a general cooling trend, punctuated by short-term hot-snaps and relative lowering of sea level (Wiese and Voigt 2002). Paleotemperature and paleoenvironmental changes are well documented from deep-water carbonate deposits. They are reflected by variations in geochemical proxies and distribution patterns of macro- and microfauna. However, such climatic and environmental fluctuations must have had severe impacts on carbonate platforms, sedimentary environments that are particularly sensitive to external perturbations. Indeed, paleontological data show major changes within group of the main carbonate platform producers during early Late Cretaceous. Rudist bivalves experienced collapse in diversity during the early Turonian, that was followed by a further re-radiation in the late Turonian, continuing into the Coniacian (Skelton 2003). In the present study, we integrated geochemical, sedimentological, and paleontological data from several outcrops in the Adriatic Carbonate Platform (Friuli; north-east Italy), where continuous Upper Cretaceous shallow-water carbonate successions are exposed. Foraminifera biostratigraphy, along with isotope stratigraphy ( $\delta^{13}\text{C}$  and  $^{87}\text{Sr}/^{86}\text{Sr}$ ) was used to precisely constrain the stratigraphy; whereas  $\delta^{18}\text{O}$  analyses on both well-preserved rudist shells and bulk rock samples allowed us to build high-resolution paleotemperature curves. The resulting paleotemperature trends are comparable with those from the deep-water record and allow to investigate the relationship between paleoclimate/paleoenvironmental changes and the distribution patterns of the main carbonate platform producers.

## REFERENCES

- Jarvis, I., Trabucho-Alexandre, J., Gröcke, D.R., Uličný, D. & Laurin, J. 2015: Intercontinental correlation of organic carbon and carbonate stable-isotope records: evidence of climate and sea-level change during the Turonian (Cretaceous). *The Depositional Record*, 1 (2), 53–90.
- Skelton, P.W. 2003: Rudist evolution and extinction — a North African perspective. In: Gili, E., El Hédi Negra, M. and Skelton, P.W. (eds). North African Cretaceous carbonate platform systems. NATO Science Series, 28, 215–227. Springer, Dordrecht.
- Wiese, F. & Voigt, S. 2002: Late Turonian (Cretaceous) climate cooling in Europe: faunal response and possible causes. *Geobios*, 35, 65–77.

## 6.6

# Timing and faunal responses to extreme water-level changes of the Eastern Paratethys in the Caspian Basin during the Sarmatian Stage (late Serravalian-Tortonian).

Sergei Lazarev<sup>1,2</sup>, Marius Stoica<sup>3</sup>, Kakhaber Koiava<sup>4</sup>, Oleg Mandic<sup>5</sup>, Davit Vasilyan<sup>2,1</sup>

<sup>1</sup> Department of Geosciences, University of Fribourg, Chemin du Musée 6, 1700 Fribourg, Switzerland

<sup>2</sup> JURASSICA Museum, Route de Fontenais, 21, 2900 Porrentruy, Switzerland

<sup>3</sup> Faculty of Geology and Geophysics, University of Bucharest, Balcescu Bd. 1, 010041 Bucharest, Romania

<sup>4</sup> Ivane Javakhishvili Tbilisi State University, Alexandre Janelidze Institute of Geology, A. Politkovskaia str. 31, 0186 Tbilisi, Georgia

<sup>5</sup> Geological-Paleontological Department, Natural History Museum Vienna, Burgring 7, 1010, Vienna, Austria

The Eastern Paratethys is a former epicontinental Sea that during the Cenozoic occupied large territories of West Eurasia – from the Carpathian foreland on the west to the Central Asia on the east. Comprising three major subbasins - The Dacian (Carpathian foreland), the Euxinian (Black Sea) and the Caspian basins, the Eastern Paratethys played a crucial role in Eurasian climate, paleobiogeography and ecosystem sustainability.

During the so-called Sarmatian s.l. Stage (12.6–7.65 Ma), the Eastern Paratethys underwent a series of paleohydrological changes that gradually transformed this sea into the largest megalake.

During the early Sarmatian (Volhyanian), the Eastern Paratethys was hydrologically connected with the Central Paratethys and global ocean, while during the middle Sarmatian (Bessarabian), tectonic closure of the major Carpathian gateways made the Eastern Paratethys hydrologically isolated. The simultaneous warming and drying of the global climate together with hydrological isolation disrupted the hydrological water budget of the Eastern Paratethys resulting in several extreme water-level fluctuations. Accompanying changes in water chemistry led to a high-level of aquatic ecosystem endemism and later to their extinction.

These basic paleoenvironmental changes have been observed in the Dacian and Euxinian basins, leaving the Sarmatian s.l. paleoenvironmental, paleobiogeographic and geochronological constraints in the Caspian Basin unknown.

Here, we present our new magneto- and biostratigraphic data from the Sarmatian s.l. deposits of two outcrops – Nadarbazevi (Georgia) and Karagiya (Kazakhstan). The Sarmatian s.l. in Nadarbazevi begins around 12.6 Ma (correlated to the middle of C5Ar.1r), while in Karagiya the base is rather incomplete. The Middle Sarmatian s.l. (Bessarabian) in both sections is marked by a wide transgression around 11.6 – 11.8 Ma (around C5r.2n). The upper Sarmatian s.l. (Khersonian) in Karagiya is marked by a small-scale transgression at ~9.6 Ma (correlated to the middle of C4Ar.2r), while in Nadarbazevi, the post-Bessarabian record becomes continental.

Our ongoing study for the first time provides well-dated mollusc and microfauna zonations of the Sarmatian s.l. substages in the Caspian Basin. The new age constraints may also help to understand the drivers of paleohydrological and biotic changes during the Sarmatian s.l. Stage.

## 6.7

### Dating terrestrial sediments by in situ U-Pb dating of carbonates

Perach Nuriel<sup>1</sup>, Ram Weinberger<sup>2</sup>, Rani Calvo<sup>2</sup>, Andrew R.C. Kylander-Clark<sup>3</sup>

<sup>1</sup> Department of Earth Sciences, University of Geneva, Rue des Maraîchers 13, CH-1205 Genève, Switzerland  
(perach.nuriel@unige.ch)

<sup>2</sup> Geological Survey of Israel, 32 Yeshayahu Leibowitz St., 9692100 Jerusalem, Israel

<sup>3</sup> Department of Earth Science, University of California Santa Barbara, Santa Barbara, CA 93106, USA.

Carbonate precipitation occurs in various geological environments including marine, lacustrine, terrestrial, and hydrothermal systems. Their precipitation as vein filling, breccia cement and fault coating also accompanied tectonic processes. Traditional U-Pb bulk analyses are challenging, because such samples are often texturally complex at the sub-millimeter scale, with either slow continues or multi-phase growth. The in-situ approach allows accurate analyses while avoiding possible mixing or averaging ages of different phases.

New results of in-situ U Pb dating of carbonate precipitates within terrestrial sediments such as cements, stromatolites, dolomites, and lake sediments demonstrate the applicability of this method to various types of carbonate samples. Absolute ages of these carbonates constrain the timing and rate of >2000 m thick sediments deposition to the Early and Middle Miocene, and open new frontiers in dating terrestrial sediments.



Figure 1. Carbonate deposit within terestrial sediments that can be dated by *in-situ* U-Pb geochronology; (a) shells; (b) stromatolite; (c) Oncoids; (d) Calcite cement; and (e) lake sediments.

#### REFERENCES

Nuriel, P., Weinberger, R., Kylander-Clark, A.R.C., Hacker, B.R., & Craddock, J.P.;2017: The onset of the Dead Sea transform based on calcite age-strain analyses. *Geology*, 45 (7): 587–590. doi: <https://doi.org/10.1130/G38903.1>

## 6.8

# Lithofacies and depositional history of Middle Muschelkalk evaporites (Zeglingen Formation) in a regional stratigraphic context

Johannes Pietsch<sup>1,2</sup>, Andreas Wetzel<sup>1</sup>, Gaudenz Deplazes<sup>3</sup>, Marco Filippioni<sup>3</sup>

<sup>1</sup> University of Basel, Department of Environmental Sciences, Bernoullistrasse 32, CH-4056 Basel, Switzerland

(johannes.pietsch@unibas.ch)

<sup>2</sup> Schweizer Salinen AG, Rheinstrasse 52, CH-4133 Pratteln, Switzerland

<sup>3</sup> Nagra, Hardstrasse 73, CH-5430 Wettingen, Switzerland

The Middle Muschelkalk Zeglingen Formation in northern Switzerland consists of evaporites that formed during times of enhanced subsidence and halite beds up to more than 100 m thick accumulated. These deposits have been mined for about 180 years in northern Switzerland and provided nearly the entire salt supply for Switzerland. Since these sediments are of economic as well as academic interest, many investigations dealt with the Middle Muschelkalk evaporites and, especially, the halite deposits in northern Switzerland and Germany. These studies resulted in a model of a highly dynamic depositional environment. In Germany, they provided, furthermore, detailed concepts about evaporite formation and a sequence-stratigraphic subdivision for interior parts of the Central European Basin. However, the last studies on Middle Muschelkalk evaporites in northern Switzerland, representing a rather peripheral position with respect to the Central European Basin, date back about 30 years. Due to the new, extensive deep drilling campaign by Nagra («National Cooperative for the Disposal of Radioactive Waste») in northern Switzerland and recent findings in the interior part of the basin, a re-evaluation of the peripheral facies towards the basin margin is necessary.

For this purpose, 640 m of newly drilled and already available cores of the Middle Muschelkalk Zeglingen Formation from 10 deep boreholes were sedimentologically logged. This analysis resulted in a more detailed understanding of the Middle Triassic Muschelkalk formations in NW Switzerland.

Based on the detailed logging, 22 lithofacies and 10 lithofacies associations of Middle Muschelkalk evaporites were defined. High-resolution regional correlations of gamma-ray logs from the different boreholes as well as sequence stratigraphic considerations provide a detailed stratigraphic framework of the Middle Muschelkalk sediments in the study area and form the base to correlate and to compare them with equivalents in more interior parts of the basin and to analyse apparent variations in sediment thickness in detail.

Lithofacies and isopach patterns point towards a tectonically active depositional setting during the Middle Triassic. Nevertheless, short-term changes in subaqueous topography were rapidly compensated for by high rates of sedimentation. Most lithofacies encountered appear to have nearly flat bounding surfaces. Marine transgressions, thus, flooded wide areas in rather short time, nearly simultaneously. Thus, the corresponding deposits can be considered isochronous over wide parts of the basin and serve as reference levels to integrate the peripheral facies into the supraregional context.

## 6.9

# A global coral reef event in the Bajocian: Evidence from a new coral reef in Northern Switzerland.

Arnaud Ruchat<sup>1</sup>, Bernard Lathuilière<sup>2</sup>, Stephan Wohlwend<sup>3</sup>, Gaudenz Deplazes<sup>4</sup>, Herfried Madritsch<sup>4</sup>, Gregor P. Eberli<sup>5</sup>, Susanne Feist-Burkhardt<sup>1</sup>, Elias Samankassou<sup>1</sup>

<sup>1</sup> Department of Earth Sciences, University of Geneva, Rue des Maraîchers 13, 1205 Geneva, Switzerland

<sup>2</sup> Université de Lorraine, CNRS, Lab. GeoRessources, UMR 7359, BP 70239, 54506 Vandoeuvre-lès-Nancy Cedex, France

<sup>3</sup> Geological Institute, ETH Zürich, Sonneggstrasse 5, 8092 Zürich, Switzerland

<sup>4</sup> National Cooperative for the Disposal of Radioactive Waste (Nagra), Hardstrasse 73, 5430 Wettingen, Switzerland

<sup>5</sup> Department of Marine Geosciences, Rosenstiel School of Marine and Atmospheric Science, University of Miami, FL 33149, USA

On a global scale, the Middle Jurassic (Bajocian, Bathonian, Callovian) is currently not considered favourable for coral reef growth. At this time, most reef constructors and corals in particular are still recovering from the devastating climate-induced crisis of the Early Jurassic (Pliensbachian-Toarcian events) (Krencker et al., 2020). Climate warming, a global perturbation of the carbon cycle and increased continental weathering produced one of the most intense extinction events for corals (Vasseur et al., 2021). Therefore, the Middle Jurassic was not yet an opportune time for coral reef development, perhaps due to environmental factors slowing the recovery of reef-constructing organisms. In updating the previous bibliographic syntheses (Beauvais, 1976; Leinfelder, 2002), it is possible to show a substantial number of Bajocian locations that have been mapped. Most of these Bajocian localities are distributed along a hypothetical paleo-geographical belt on the northern margin of the Tethys. The number of reefs and their presence in a pattern could be indicative of a global coral reef event during the early Bajocian, substantially greater growth of reef builders (Leinfelder et al., 2002) and a quicker than expected recovery of those organisms in the Tethyan realm and across the globe.

Here we present a recently discovered Bajocian reef in the so-called «Herrenwis Unit». It was identified in the northern part of Switzerland as part of the exploration program of Nagra, which is currently investigating three siting regions in northern Switzerland as potential repositories for radioactive waste. In the Nördlich Lägern siting region, the boreholes Bülach-1 and Stadel-3 show well-preserved corals.

In central Europe Bajocian coral reefs are mainly known from the western and central part of the Burgundy Platform, a large platform covering most of eastern France and Luxembourg (Gonzalez & Wetzel, 1996). Bajocian reefs are however uncommonly found on the eastern margin of the Burgundy Platform (Switzerland e.g., in Jura Mountains at Gisliflue, Wullschleger, 1966). Furthermore, little is known about the eastern part closer to the Tethys in deeper environments, corresponding today to Switzerland, where outcrops are rare or absent (Gonzalez & Wetzel, 1996). Because of this scarcity, the «Herrenwis Unit» offers a rare point of comparison for coral reef growth outside the large carbonate platforms during the Bajocian. The establishment of an accurate biostratigraphy with robust dating is necessary to assess the possibility of a global reef event during the Bajocian. This new reef was studied from two cores drilled in a paleo-relief feature revealed by seismic exploration. Core description, with particular attention to the well-preserved corals was performed, along with lithostratigraphic description and additional data on microfacies and biostratigraphy. The use of well calibrated palynological assemblages allowed precise dating of the reef using the intervals established by Feist-Burkhardt & Wille, (1992), which were also cross referenced with the standard scales established by Cariou & Hantzpergue (1997).

## REFERENCES:

- Beauvais, L. (1976). Paléobiogéographie des Madréporaires du Dogger. *Réunion Annuelle Des Science de La Terre, Paris*, 4, 40.
- Cariou, E., & Hantzpergue, P. (1997). Biostratigraphie du Jurassique ouest-européen et méditerranéen: Zonations parallèles et distribution des invertébrés et microfossiles. Elf Aquitaine.
- Feist-Burkhardt, S., & Wille, W. (1992). Jurassic palynology in southwest Germany—State of the art. *Cahiers de Micropaléontologie*, 7(1/2), 141–164.
- Gonzalez, R., & Wetzel, A. (1996). Stratigraphy and paleogeography of the Hauptrogenstein and Klingnau Formations (middle Bajocian to late Bathonian), northern Switzerland. *Eclogae Geologicae Helvetiae : Recueil Périodique de La Société Géologique Suisse*, vol. 89(no. 1), p. 695-720. <https://doi.org/10.5169/SEALS-167921>
- Krencker, F.-N., Fantasia, A., Danisch, J., Martindale, R., Kabiri, L., El Ouali, M., & Bodin, S. (2020). Two-phased collapse of the shallow-water carbonate factory during the late Pliensbachian–Toarcian driven by changing climate and enhanced continental weathering in the Northwestern Gondwana Margin. *Earth-Science Reviews*, 208, 103254. <https://doi.org/10.1016/j.earscirev.2020.103254>

- Leinfelder, R. R., Schmid, D. U., Nose, M., & Werner, W. (2002). Jurassic reef patterns—The expression of a changing globe. Society for Sedimentary Geology.
- Vasseur, R., Lathuilière, B., Lazăr, I., Martindale, R. C., Bodin, S., & Durlet, C. (2021). Major coral extinctions during the early Toarcian global warming event. *Global and Planetary Change*, 207, 103647. <https://doi.org/10.1016/j.gloplacha.2021.103647>
- Wullschleger, E. (1966). Bermerkungen zum fossilen Korallenriff Gisliflue-Homberg. Aargauische Naturforschende Gesellschaft, Mitteilungen v. 27, 101–152.

## 6.10

### Reworking of organic matter associated with the end-Triassic mass-extinction and implications for other paleo-proxy records

Bas van de Schootbrugge<sup>1</sup>, Remco Bos<sup>1</sup>

<sup>1</sup> Department of Earth Sciences, Utrecht University, Princetonlaan 8A, 3584CS Utrecht, The Netherlands  
([b.vanderschootbrugge@uu.nl](mailto:b.vanderschootbrugge@uu.nl))

The end-Triassic mass-extinction (ETME; 201.6 Ma) led to widespread collapse of tree-forming vegetation across continental landmasses in northwest Europe resulting from large scale volcanic activity in the Central Atlantic Magmatic Province (CAMP). In palynological records obtained from numerous drill cores and outcrops, declines in Rhaetian tree pollen are accompanied by a marked increase in reworked organic matter, including Permian and Carboniferous pollen and spores, and Devonian, Silurian, Ordovician and Cambrian acritarchs (van de Schootbrugge et al., 2020). Intense reworking occurs in sediments that also preserve a record of widespread seismic activity that is likely linked to CAMP activity. A scenario is thus envisioned in which tectonic activity, vegetation dieback, and increases in pCO<sub>2</sub> drove enhanced weathering and erosion on the continents. Even though the biggest pulse in weathering occurred in direct connection to the ETME, further episodes of enhanced weathering are noted during the Hettangian that appear to be modulated by orbital forcing. The reworking signal is lost at the start of the Sinemurian as tree-forming vegetation recovered. Here, we will also discuss the implications of the strong reworking of Paleozoic material for the interpretation of commonly used paleo-proxy records, such as organic C-isotope records and elemental records, including Hg.

## REFERENCES

- B van de Schootbrugge, CMH Van Der Weijst, TP Hollaar, M Vecoli, PK Strother, N Kuhlmann, J Thein, H Visscher, H Van Konijnenburg-van Cittert, MAN Schobben, A Sluijs, S Lindström 2020: Catastrophic soil loss associated with end-Triassic deforestation, *Earth-Science Reviews*, 210, 103332.

## 6.11

# Sedimentologika: a new community-driven DOA journal

Romain Vaucher<sup>1</sup>, Domenico Chiarella<sup>2</sup>, Marta Marchegiano<sup>3</sup>, Miquel Poyatos-Moré<sup>4</sup>, Aurélia Privat<sup>5</sup>, Yvonne Spychala<sup>6</sup>, Camille Thomas<sup>7</sup>, Valentin Zuchuat<sup>8</sup>

<sup>1</sup> Institute of Earth Sciences (ISTE), University of Lausanne, Geopolis, Lausanne, Switzerland ([romain.vaucher@unil.ch](mailto:romain.vaucher@unil.ch))

<sup>2</sup> Clastic Sedimentology Investigation (CSI), Department of Earth Sciences, Royal Holloway, University of London, Egham, UK

<sup>3</sup> Analytical, Environmental and GeoChemistry, Vrije Universiteit Brussel, Brussel, Belgium

<sup>4</sup> Departament de Geologia, Universitat Autònoma de Barcelona, Barcelona, Spain

<sup>5</sup> University of Aberdeen, Department of Geosciences, Meston Building Kings College, Aberdeen, UK

<sup>6</sup> Institute of Geology, Leibniz University Hannover, Hannover, Germany

<sup>7</sup> Department of Earth Sciences, University of Geneva, Geneva, Switzerland

<sup>8</sup> Geological Institute, RWTH Aachen University, Aachen, Germany

*Sedimentologika* is a community-driven Diamond Open Access (DOA) scientific journal about sedimentology. The journal aims to create a place where people can publish their research and access scientific studies on all types of sedimentary processes, methods, deposits, and environments, across all spatial and temporal scales, on Earth or any other planetary body, for free. The published material will be free to share (i.e., no embargo period) since the authors retain the copyright. *Sedimentologika* is driven by the community for the community and is part of a broader DOA movement in geosciences. *Sedimentologika* aspires to emancipate from private publishing houses to provide free, ethical, and equal access to science to all citizens, scientists, and institutions all over the globe. This journal is hosted at the University of Geneva Library and will be defined by Open Science principles to promote ethical dissemination of science and knowledge, following high equality, diversity, and inclusion standards (EDI). Each step of the review and publication process will be visible and easy to follow for authors, reviewers, and the community. *Sedimentologika* will be launched by late 2022, and it is always looking for motivated people keen on integrating and supporting its development to make it a viable and recognized peer-reviewed scientific journal. Interested in this initiative? Come discuss with us!

## 6.12

# Combined Middle Jurassic C-isotope chemo- and biostratigraphic correlation from Northern Switzerland through the new Nagra drill cores

Stephan Wohlwend<sup>1</sup>, Susanne Feist-Burkhardt<sup>2</sup>, Bernhard Hostettler<sup>3</sup>, Ursula Menkveld-Gfeller<sup>3</sup>, Hansruedi Bläsi<sup>4</sup>, Stefano M. Bernasconi<sup>1</sup>, Gaudenz Deplazes<sup>5</sup>

<sup>1</sup> Geological Institute, ETH Zurich, Sonneggstrasse 5, CH-8092 Zürich ([stephan.wohlwend@erdw.ethz.ch](mailto:stephan.wohlwend@erdw.ethz.ch))

<sup>2</sup> SFB Geological Consulting & Services, Odenwaldstrasse 18, D-64372 Ober-Ramstadt

<sup>3</sup> Natural History Museum Bern, Bernastrasse 15, CH-3005 Bern

<sup>4</sup> Geo-Consulting, Steinackerstrasse 2, CH-3184 Wünnewil

<sup>5</sup> Nagra, Hardstrasse 73, CH-5430 Wettingen

The Opalinus Clay, an argillaceous to silty claystone formation deposited mainly during the latest Toarcian to Early Aalenian, is the selected host rock for disposal of radioactive waste in Switzerland. With the aim of finding the best suited site for a deep geological repository, in recent years Nagra (National Cooperative for the Disposal of Radioactive Waste) has drilled nine deep boreholes in northern Switzerland.

To establish a chronology in the Opalinus Clay and the overlying more variable succession of Middle to earliest Late Jurassic period, we used carbon-isotope chemostratigraphy in combination with ammonite and palynomorph biostratigraphy. The metre-resolution of the sampling for isotope geochemical investigations allows a very detailed correlation and thus complements the biostratigraphic findings in intervals with increased sedimentation rates, such as in the Opalinus Clay. In this study we took advantage of the fact that nine new deep boreholes were drilled over a distance of around 50 km, which could be compared with four existing drill cores (Riniken, Weiach, Benken to Schlattingen-1). The dense underground recovery allows a detailed and unique investigation. The newly established C-isotope chemostratigraphy measured on carbonates and organic matter provides sufficient variability to establish a very high-resolution correlation for the Toarcian to the Middle Oxfordian which can be followed throughout the drill cores. The major perturbations in the C-isotopes, such as the Toarcian Oceanic Anoxic Event (T OAE), the positive shift during the Early Bajocian (Laeviuscula to Humphriesianum ammonite zones), as well as the Middle Oxfordian positive excursion are nicely documented and therefore allow a detailed correlation and interpretation of environmental change in the Middle Jurassic.

## 6.13

# Integrative analysis of the mineralogical and chemical composition of modern microbialites from ten Mexican lakes: what do we learn about their formation?

Nina Zeyen<sup>1,2</sup>, Karim Benzerara<sup>2</sup>, Olivier Beyssac<sup>2</sup>, Damien Daval<sup>3</sup>, Elodie Muller<sup>2</sup>, Christophe Thomazo<sup>4,5</sup>, Rosaluz Tavera<sup>6</sup>, Purificación López-García<sup>7</sup>, David Moreira<sup>7</sup> and Elodie Duprat<sup>2</sup>

<sup>1</sup> Department of Earth Sciences, University of Geneva, Rue des Maraîchers 13, 1205 Geneva, Switzerland  
*(Nina.Zeyen@unige.ch)*

<sup>2</sup> Sorbonne Université, Muséum National d'Histoire Naturelle, UMR CNRS 7590. Institut de Minéralogie, de Physique des Matériaux et de Cosmochimie (IMPMC), 4 Place Jussieu, 75005 Paris, France

<sup>3</sup> Laboratoire d'Hydrologie et de Géochimie de Strasbourg, EOST-ENGEES, Univ Strasbourg, EOST CNRS UMR 7517, 67084 Strasbourg, France

<sup>4</sup> UMR CNRS/uB6282 Biogéosciences, Université de Bourgogne Franche-Comté, 6 Bd Gabriel, 21000, Dijon, France

<sup>5</sup> Institut Universitaire de France

<sup>6</sup> Departamento de Ecología y Recursos Naturales, Universidad Nacional Autónoma de México, DF México, México

<sup>7</sup> Ecologie, Systématique et Evolution, CNRS, Université Paris-Saclay, AgroParisTech, Orsay, France

Interpreting the environmental conditions under which ancient microbialites formed relies upon comparisons with modern analogues. This is why we need a detailed reference framework relating the chemical and mineralogical compositions of modern microbialites to the physical and chemical parameters prevailing in the environments where they form. Here, we measured the chemical, including major and trace elements, and mineralogical composition of microbialites from ten Mexican lakes as well as the chemical composition of the surrounding waters. Saturation states of lakes with different mineral phases were systematically determined and correlations between solution and solid chemical analyses were assessed using multivariate analyses. I will show that a large diversity of microbialites was observed in terms of mineralogical composition, with occurrence of diverse carbonate phases such as (Mg-)calcite, monohydrocalcite, aragonite, hydromagnesite, and dolomite as well as authigenic poorly crystalline Mg-silicate phases (kerolite and/or stevensite). Interestingly, all lakes harboring microbialites were saturated or supersaturated with monohydrocalcite, suggesting that such a saturation state might be required for the onset of microbialite formation and that precursor soluble phases such as amorphous calcium carbonate and monohydrocalcite play a pivotal role in these lakes. Subsequently, monohydrocalcite transforms partly or completely to aragonite or Mg-calcite, depending on the lake (Mg/Ca)aq. Moreover, lakes harboring hydromagnesite-containing microbialites were saturated with an amorphous magnesium carbonate phase, supporting again the involvement of precursor carbonate phases. Authigenic Mg-silicates formed by homogenous or heterogenous nucleation in lakes saturated or supersaturated with a phase reported in the literature as "amorphous sepiolite" and with a H<sub>4</sub>SiO<sub>4</sub> concentration superior to 0.2 mM. A strong correlation between the alkalinity and the salinity of all the lakes was observed. The observed large variations of alkalinity between the lakes relate to varying concentration stages of an initial alkaline dilute water, due to a varying hydrochemical functioning. In all cases, the size of microbialites in the lakes correlated positively with salinity, (Mg/Ca)aq and alkalinity (Figure 1). Last, some microbialites poorly affected by detrital contamination showed (REE+Y) patterns with features commonly reported for marine microbialites, questioning the possibility to infer the marine versus lacustrine origin of a microbialite only based on (REE+Y). Overall, while microorganisms can impact nucleation processes and textural arrangements in microbialites, we observed that the hydrogeochemical evolution of lakes exerts a primary control over the onset of microbialite formation and the evolution of their chemical and mineralogical composition.

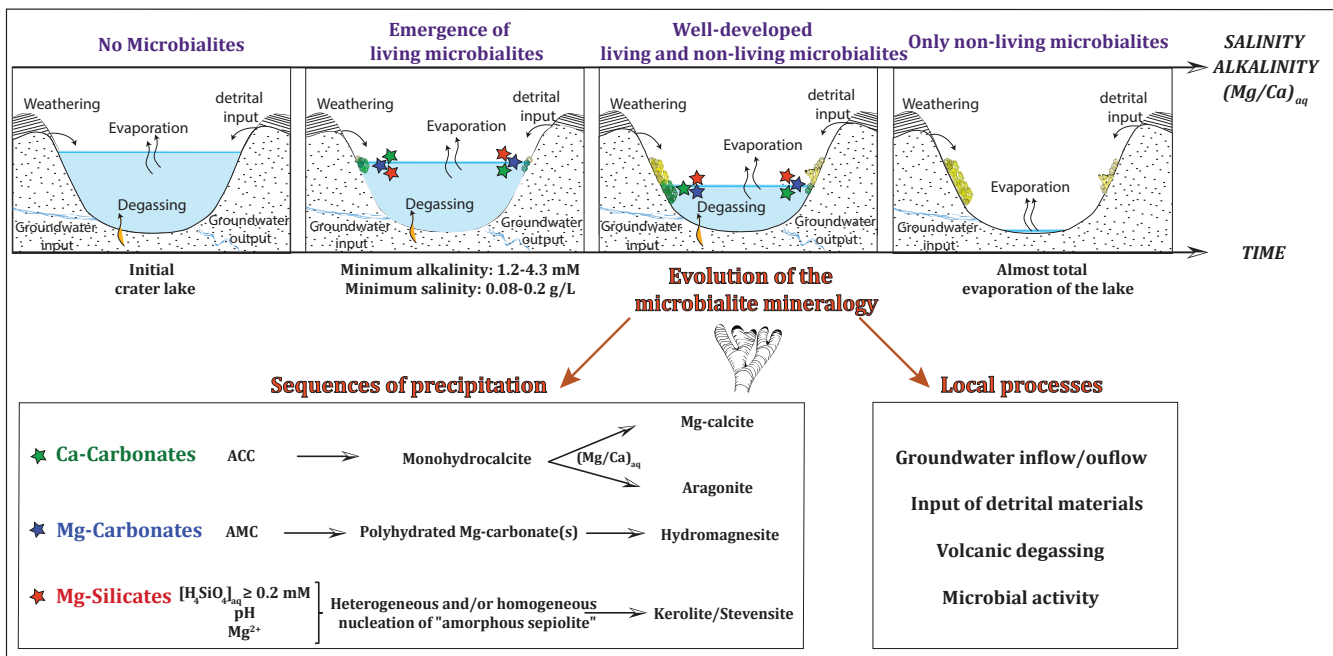


Figure 1. Model of lake evolution over time. Microbialites start emerging at a certain stage of evaporation and/or weathering of the lake (when  $[Na^+]_{aq}$  and alkalinity become higher than certain threshold values). Then microbialite mineralogy changes according to key parameters such as the aqueous ( $Mg/Ca$ ), which controls carbonate mineralogy, and aqueous  $[H_4SiO_4]$  controlling the precipitation of authigenic Mg-silicate.

## P 6.1

# Paleogene Paleoenvironments of the Doldenhorn Nappe: from short-lived carbonate shoals to hemipelagic slope (Lämmernenalp, VS)

Claudia Baumgartner-Mora, Peter O. Baumgartner, Jean-Luc Epard, Goran Andjic, Stefan M. Schmalholz

*Institut des Sciences de la Terre, Université de Lausanne, Géopolis, CH-1015 Lausanne (Claudia.baumgartner@unil.ch)*

The Paleogene of the Doldenhorn Nappe in the Gemmi-Lämmernenalp area has not been assigned to lithostratigraphic formations and lacks precise biochronology and paleoenvironmental interpretation. Furrer (1962) briefly described the Eocene formations of the area and mentioned *Nummulites incrassatus* De La Harpe, typical of the Late Eocene, among other fossils from the NW-slopes of the Doldenhorn. Herb in Masson et al. (1980) gave an excellent description of the Jurassic to Eocene section of the Doldenhorn nappe in the area. Gansner (2000) described the Eocene sections of the Lämmernenalp. Here, we assign the Paleogene sediments in stratigraphic order to: the Siderolithic, the Santesch and the Stad Formations.

The **Siderolithic** Formation is characterized by terrestrial Fe-hydroxide crusts and red shales with pisolites, occurring in paleo-karst pockets in the underlying Lower Cretaceous formations (Schrattenkalk and Thierwis), which are often pervasively invested by *Microcodium*.

The Priabonian **Sanetsch** Formation (Menkveld-Gfeller, 1994) onlaps unconformably on a paleorelief with several facies: The lowest (and in places oldest) facies consist of dark grey shaly limestones rich in fossils, including solitary and hermatypic corals, oysters and other bivalves, sponges, and in some places *Cerithium* sp. This facies ("Cerithium beds") can be assigned to the **Diablerets Member** of the Sanetsch Formation. It represents a paralic to brackish paleo-environment containing terrestrial and coastal organic matter. This facies occurs with up to 10 m thickness at Rote Chumme (Herb in Masson et al. 1980) and interfingers with lithothamnid limestones S of the Lämmernensee. At Lämmernplatten normal marine facies assignable to the **Tsanfleuron Member** of the Sanetsch Formation onlap on the Lower Cretaceous substrate with marine conglomerates containing bored limestone clasts in a sandy matrix, and coral colonies in former karst depressions. Well washed, carbonate poor, parallel and cross-bedded quartz sandstone sheets alternate with massive, sometimes sandy limestones composed of both geniculate and melobesian red algae, corals, bivalves and echinids (*Clypeaster* sp). Rare, small nummulites such as *Nummulites retiatus* Roveda (Fig. 1a) indicate a Priabonian age, already mentioned by Herb (1988) in the Priabonian of the Doldenhorn nappe of the Kiental. Some levels may correspond to algal boundstones, others represent micrite-rich packstones with miliolids, representing lagoonal facies. Sharp bases of the sandstone sheets suggest sudden demise of the short-lived carbonate shoals and onset of quartz sand-dominated sealevel lowstand sedimentation. The topmost, massive, 6-8 m thick limestone bed is richer in *Nummulites* spp. and contains less quartz sand. Well preserved colonies of the coral *Cladocora* sp. (Fig. 1b) attest for a blue water shallow carbonate environment, assignable to the **Pierredar Limestone Member** of the Sanetsch Formation.

To the NE of the Lämmernensee, along a vertical cliff (Fig. 1c), the topmost Pierredar Limestone bed folds into a narrow, overturned limb and is stratigraphically overlain by a light yellowish-grey shaly hemipelagic limestone with globigerinids, assignable to the **Stad Formation**. The sharp change from shallow carbonate to pelagic facies is interpreted as tectonic drowning in front of the Alpine orogen, close to the Eocene/Oligocene boundary.

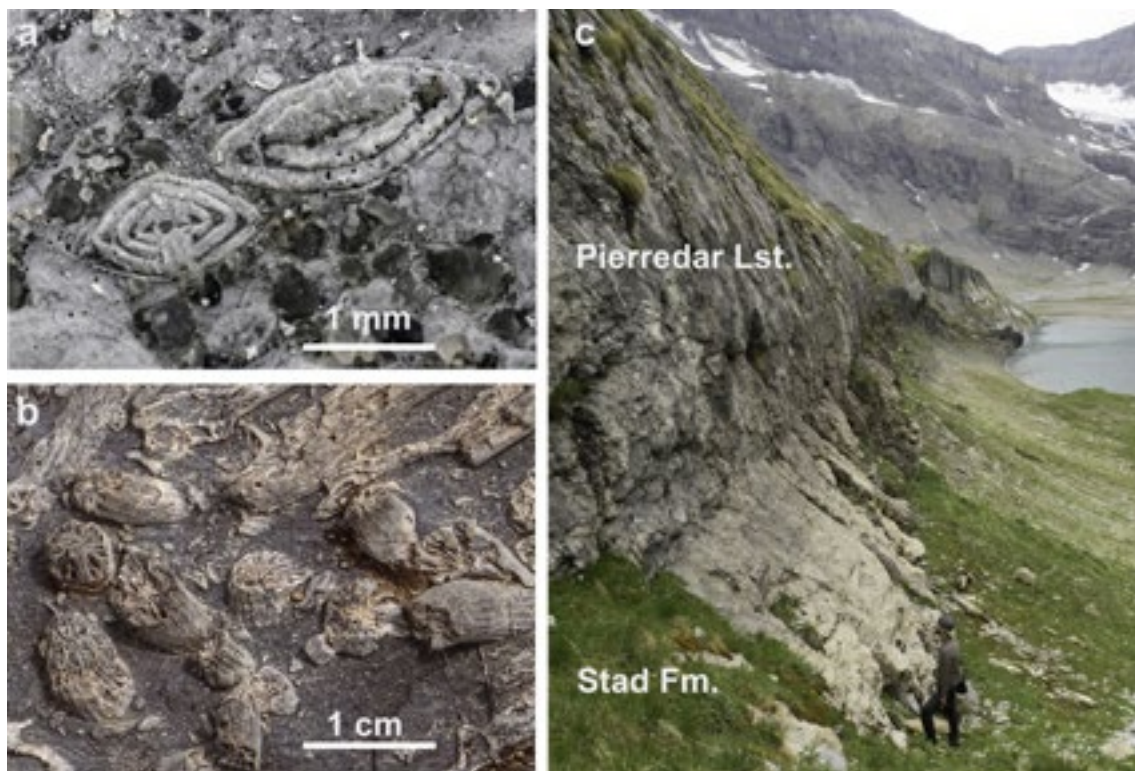


Figure 1. a.- b Outcrop images of the Pierredar Limestone fossils, Lämmerenalp (VS). a. *Nummulites retiatus* axial sections in quartzose (dark grey) limestone. b. *Cladocora* sp. shallow water coral colony, topmost Pierredar Limestone. c. Top of Pierredar Lst. and overturned stratigraphic contact with hemipelagic Stad Formation, NE of Lämmerensee (middle right).

## REFERENCES

- Furrer, H. 1962: Erläuterungen zum geologischen Atlas der Schweiz, Blatt: Gemmi, 1 :25'000. - Schweizerische geologische Kommission.
- Gansner, C. 2000: Geologische Untersuchungen im Gebiet Gemmipass-Lömmerenboden-Lämmerenalp-Kummen, Leukerbad Kanton Wallis. Diploarbeit, Geologisches Institut ETH.
- Menkveld-Gfeller, U. 1994: Die Wildstrubel-, die Hohgant- und die Sanetsch-Formation: Drei neue lithostratigraphische Einheiten des Eocaens der helvetischen Decken. *Eclogae Geologicae Helvetiae*, 87: 789–809.
- Herb, R. 1988: Eozäne Paläogeographie und Paläotektonik des Helvetikums. *Eclogae geol. Helv.* 81/3, 611-657.
- Masson, H., Herb, R., Steck, A. 1980: Helvetic Alps of Western Switzerland. In: (Ed) Trümpy, R. *Geology of Switzerland*. part B. Basel. Wepf & Co. 109-135.

Funded by: Swiss National Science Foundation, No. 200021-185067, and UNIL

## P 6.2

### Expression of the Coniacian-Santonian oceanic anoxic event 3 in the Gabal Ekma section, Egypt.

Brahimsamba Bomou<sup>1</sup>, Thierry Adatte<sup>1</sup> and Jorge E. Spangenberg<sup>2</sup>

<sup>1</sup> Institute of Earth Sciences (ISTE), University of Lausanne, Geopolis, CH-1015 Lausanne, Switzerland

(brahimsamba.bomou@unil.ch)

<sup>2</sup> Institute of Earth Surface Dynamics (IDYST), University of Lausanne, Geopolis, CH-1015 Lausanne, Switzerland

The Gabal Ekma section, located in the Sinai desert (Egypt), is characterised by shallow marine deposits of mixed siliciclastic/carbonate sediments of the Matulla Formation which includes the Coniacian and Santonian stages (El-Azabi and El-Araby, 2007). The section exhibits significant accumulation of organic-rich intervals and phosphatic layers associated with fossiliferous vertebrate remains. The Coniacian-Santonian (CS) carbon isotopic patterns appear to be recognised in the Egyptian section and is used to characterise the interval of the CS oceanic anoxic event (OAE 3). However, this latest Cretaceous OAE appears not to be truly important on a global scale but was more dependent on local or regional conditions (Wagreich, 2012). These are mainly limited to shallow-water environments and epicontinental seas of the equatorial and South Atlantic basins and the Western Interior Seaway. Based on a weathering index and mineralogy, climate gradually evolved from warm and seasonal climate to arid conditions during the late Coniacian up to the base of the Santonian (Michel Dean Event). Then a significant change to more humid and tropical conditions is observed above the Michel Dean Event (early Santonian), which persisted up to the Buckle Event (base on the late Santonian), coinciding with the organic-rich shales deposits in deeper environments. Fluctuations in total phosphorus (Total-P) contents are clearly independent from detrital input but seem to be controlled by regional anoxia and phosphogenesis. Total-P contents is indeed depleted in the organic-rich interval, suggesting intense P regeneration due to anoxic conditions. This type of P regeneration may explain the formation of the bone-bed located at the C-S boundary characterised by very well-preserved shark teeth and vertebra, associated with phosphatised nodules in a sandy phosphatic matrix.

## REFERENCES

- El-Azabi, M.H., El-Araby, A. 2007: Depositional framework and sequence stratigraphic aspects of the Coniacian-Santonian mixed siliciclastic/carbonate Matulla sediments in Nezzazat and Ekma blocks, Gulf of Suez, Egypt. Journal of African Earth Sciences, 47, 179–202.
- Wagreich, M. 2012: “OAE 3” – regional Atlantic organic carbon burial during the Coniacian-Santonian. Clim. Past, 8, 1447–1455.

## P 6.3

### Seismic evaluation of an existing pile group on liquefiable soil

Konstantinos Kassas<sup>1</sup>, Lampros Sakelariadis<sup>1</sup>, Alexandru Marin<sup>1</sup>, Ioannis Anastopoulos<sup>1</sup>

<sup>1</sup> Institute of Geotechnical Engineering, ETH Zürich, Stefano-Francini-Platz 5, CH-8093 Zürich (kkassas@ethz.ch)

This study outlines the seismic evaluation of an existing pile group supporting a motorway bridge. The critical aspects are related to the strength and stiffness parameters of the local soil, which appear to be decreasing significantly with depth. Moreover, some of the soil layers at the location of the pile group may be susceptible to pore pressure build-up or soil liquefaction during seismic shaking. Based on the available geotechnical data (borehole logs, classification tests, and Standard Penetration Test) the soil profile is described and the required soil parameters for the subsequent analyses are determined. Two scenarios are considered; (a) non-liquefied layers; and (b) presence of liquefied layers.

The seismic bearing capacity, the stiffness of the pile group and its performance is assessed. The vertical and moment capacity of the pile group are compared to the provided design loads. The assessment is performed through thoroughly validated 3D nonlinear finite element (FE) analyses. To this end, the reinforced concrete piles are modelled with the Concrete Damaged Plasticity (CDP) model (Abaqus, 2014). The FE analysis results for each structural member are verified against RC section analysis. Nonlinear soil behaviour is modelled with nonlinear constitutive models, appropriately selected for the soil materials encountered in the local stratigraphy (Fig. 1). Appropriate interface elements are used, capable of modelling the geometric nonlinearities due to sliding and detachment at the soil-pile, and soil-pile cap interface.

The liquefaction susceptibility assessment is conducted using different approaches of increasing level of complexity. Initially, the liquefaction susceptibility is investigated through hand calculations (Idriss & Boulanger, 2008). Subsequently, detailed effective stress 1D site response analysis is conducted. It is concluded that the liquefaction risk is limited, but cannot be fully excluded in view of the uncertainties related to insufficient soil investigation. Based on the worst case scenario investigated, the settlements solely due to partial soil liquefaction may reach 10 cm. The structural verification of the bridge superstructure should be conducted for this level of deformation.

Although the risk of liquefaction is limited, the seismic performance of the foundation is further assessed, conservatively assuming full liquefaction of the critical layer and a residual undrained shear strength (Stark & Mesri 1992). The performance of the pile group foundation under these conditions is evaluated for vertical (static) and horizontal (seismic) loading in both directions (longitudinal and transverse). It is shown that even under such conservative assumptions, retrofit measures are not justified since the critical compliance factor  $> 0.75$ .

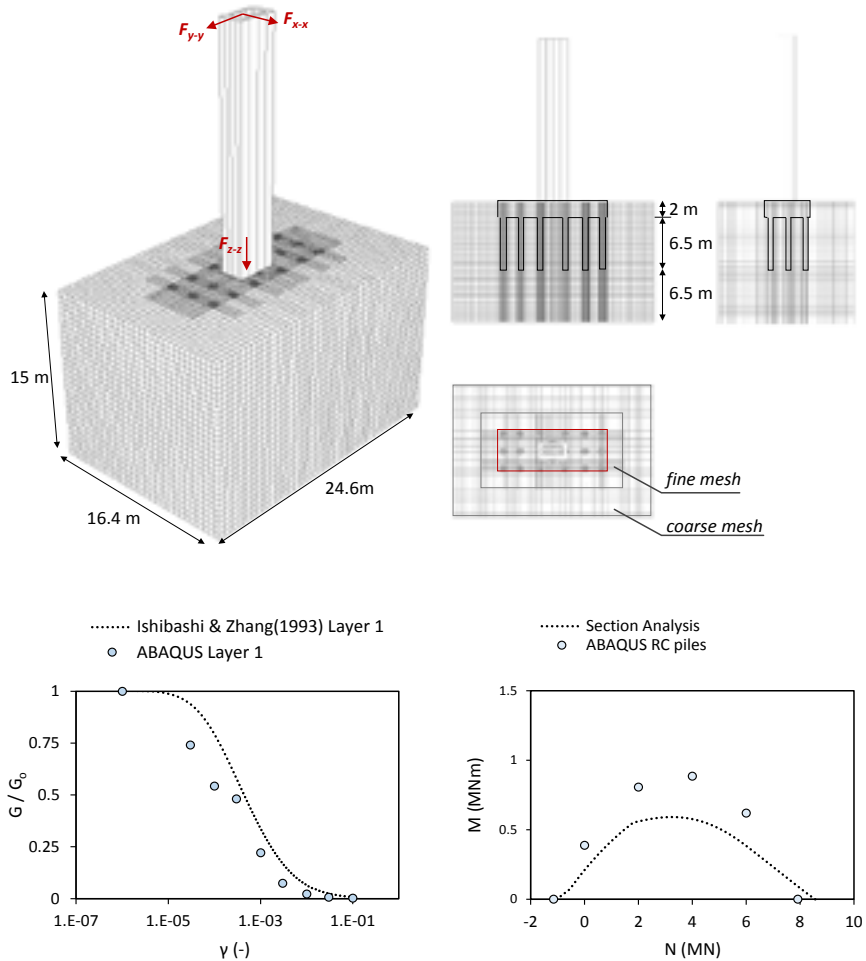


Figure 1: Overview, calibration and validation results of the Finite Element model in ABAQUS.

## REFERENCES

- ABAQUS 6.11. (2014). Standard user's manual. Dassault Systèmes Simulia Corp., Providence, RI, USA.
- Idriss, I. M. & Boulanger, R. W. (2008). Soil liquefaction during earthquakes. Monograph MNO-12, Earthquake Engineering Research Institute, Oakland, CA.
- Stark, T.D. & Mesri, G. (1992). Undrained shear strength of liquefied sand for stability analysis. Journal of Geotechnical Engineering 118(11): 1727-1747
- Martin G. R., Lam I.P. (2000). Earthquake resistant design of foundations: retrofit of existing foundations. In: ISRM International Symposium, OnePetro, Melbourne, Australia.

**P 6.4****Carbon geochemical insight at the Lower-Middle Cambrian (LMC) boundary in Southern Montagne Noire, SW France.**

Valentin Jamart<sup>1</sup>, Damien Pas<sup>1</sup>, Thierry Adatte<sup>1</sup>, Jorge E. Spangenberg<sup>2</sup>, Allison C. Daley<sup>1</sup>

<sup>1</sup> Institute of Earth Sciences (ISTE), University of Lausanne, CH-1015 Lausanne, Switzerland (Valentin.Jamart@unil.ch)

<sup>2</sup> Institute of Earth surface Dynamics (IDYST), University of Lausanne, CH-1015 Lausanne, Switzerland.

Identifying and refining stage boundaries within the Cambrian Period is fundamental for global stratigraphic correlations and for increasing knowledge on the major biodiversity and geochemical changes recorded during this critical time interval. These changes are either multimillion year-long such as the so-called “Cambrian Explosion” (Briggs, 2015; Peng *et al.*, 2020) or the “Cambrian Substrate Revolution” (Mángano & Buatois, 2017; Peng *et al.*, 2020) or as short as an anoxic event or a carbon isotope excursion. As a result of the severe lack of biostratigraphically-correlatable fossils (endemism was the rule during the Cambrian) and very rare high-precision radioisotope dates, the Cambrian time scale remains among the least precise in all the Phanerozoic Eon with a minimum uncertainty of ±2 million years at stage boundaries. These two obstacles make global correlations extremely difficult. Nevertheless, the Cambrian interval records major carbon isotope excursions that can be traced on a global scale, making  $\delta^{13}\text{C}$  a tremendously valuable tool for developing a correlation framework. To resolve the identification of the Lower Middle Cambrian boundary, we focused on a 78.5 m-thick well-known section located in southern France (Ferrals-les-Montagnes, Montagne Noire). This section shows a deepening sequence starting with pure limestone, then passing to an alternation of limestone nodules and purple shales (“grotte” like facies) and ending with green shales. A total of eighty-three samples for TOC and  $\delta^{13}\text{C}$  were collected. The TOC values range from 0.01 to 0.21 wt %, with most values  $\leq 0.1$  wt %. The very low content of TOC would suggest low primary productivity and poor preservation probably due to diagenetic and low-grade metamorphisms processes. The very low content of organic matter in most of the samples made the analysis of organic carbon isotopes ( $\delta^{13}\text{C}_{\text{org}}$ ) difficult. The carbonate content values range from 0.1 to 100 wt % with the lowest values in the upper part of the section (i.e., green shales). The carbonate carbon isotope composition ( $\delta^{13}\text{C}_{\text{carb}}$ ) of the samples in the lower part of the section (i.e., the first forty-two meters) show a negative  $\delta^{13}\text{C}_{\text{carb}}$  spike of -1.66‰. This excursion allowed the identification of the Redlichia-Olenellid Extinction Carbon isotope Excursion (ROECE), characterized by a strong negative carbon isotope excursion at the Lower Middle Cambrian boundary (Zhu *et al.*, 2006). Recognition of this C isotope excursion allows to place the section within the global Cambrian chemostratigraphic framework of Cramer & Jarvis (2020). The Middle Cambrian Drumlun Carbon isotope Excursion (DICE) could not be identified due to the very low carbonate content of the analyzed samples.

**REFERENCES**

- Briggs, D. E. G. (2015). The Cambrian explosion. *Current Biology*, 25(19), R864-R868. <https://doi.org/10.1016/j.cub.2015.04.047>
- Cramer, B. D., & Jarvis, I. (2020). Carbon Isotope Stratigraphy. In F. M. Gradstein, J. G. Ogg, M. D. Schmitz, & G. M. Ogg (Eds.), *Geological Time Scale 2020* (Vol. 2, pp. 309-343). Elsevier. <https://doi.org/https://doi.org/10.1016/B978-0-12-824360-2.00011-5>
- Mángano, M. G., & Buatois, L. A. (2017). The Cambrian revolutions: Trace-fossil record, timing, links and geobiological impact. *Earth-Science Reviews*, 173, 96-108. <https://doi.org/10.1016/j.earscirev.2017.08.009>
- Peng, S.-C., Babcock, L. E., & Ahlberg, P. (2020). The Cambrian Period. In F. M. Gradstein, J. G. Ogg, M. D. Schmitz, & G. M. Ogg (Eds.), *Geological Time Scale 2020* (Vol. 2, pp. 565-629). Elsevier. <https://doi.org/10.1016/B978-0-12-824360-2.00019-X>
- Zhu, M.-Y., Babcock, L. E., & Peng, S.-C. (2006). Advances in Cambrian stratigraphy and paleontology: Integrating correlation techniques, paleobiology, taphonomy and paleoenvironmental reconstruction. *Palaeoworld*, 15(3-4), 217-222. <https://doi.org/10.1016/j.palwor.2006.10.016>

## P 6.5

# Oxidation of organic matter in Neoarchean microbialite coincident with the Great Oxidation Event: Evidence from Re-Os geochronology and elemental proxies.

Nicolas J. Saintilan<sup>1</sup>, Nicola McLoughlin<sup>2,3</sup>, Nicolas J. Beukes<sup>3</sup>, Jorge E. Spangenberg<sup>4</sup>, David A. Banks<sup>5,6</sup>, David Selby<sup>7</sup>

<sup>1</sup> Institute of Geochemistry and Petrology, Department of Earth Sciences, ETH Zürich, Clausiusstrasse 25, 8092, Zürich, Switzerland

<sup>2</sup> Geology Department, Rhodes University, Makhanda/Grahamstown, Artillery Road, 6140 South Africa

<sup>3</sup> DSi-NRF CIMERA, Department of Geology, APK Campus, University of Johannesburg, 2006 Auckland Park, South Africa

<sup>4</sup> Institute of Earth Surface Dynamics, University of Lausanne, Building Geopolis, 1015 Lausanne, Switzerland

<sup>5</sup> School of Earth and Environment, University of Leeds, Leeds LS2 9JT, UK

<sup>6</sup> Department of Geological Engineering, Pamukkale University, TR-20020 Denizli, Turkiye

<sup>7</sup> Department of Earth Sciences, University of Durham, Durham DH1 3LE, UK

The Earth is an active, dynamic, open system in which the geosphere, atmosphere, hydrosphere and biosphere interact to shape the state of the planet. Understanding long-term and rapid environmental changes in Earth's history helps to elucidate Earth system dynamics and the complex nature of the evolution of life on Earth. Improved constraints on the ages and rates of geological processes are therefore paramount to address and quantify the role of biogeochemical cycles through time in rock and mineral formation and weathering, and carbon cycling. Here we combine petrographical observations, rhenium-osmium (Re-Os) radiogenic isotope geochemistry and elemental proxies ( $d^{13}C_{carb}$ ,  $d^{18}O_{carb}$ , total organic carbon content – TOC, and  $d^{13}C_{TOC}$ ) of microbialites from drillcore AHL-4 across the Gamohaan Formation of the Campbellrand Subgroup, Transvaal Supergroup, South Africa. Carbonaceous carbonates including microbialites accumulated on the slope of shallow-shelf platform carbonates [Beukes and Gutzmer, 2008]. Our samples come from 37 to 41 m below a ca. 2521 Ma (multi-grain zircon uranium-lead geochronology; Sumner and Bowring, 1996) volcanic tuff horizon. Another volcanic tuff horizon at the base of the Nauga Formation, which represents deeper water to lower slope iron-rich limestones and shales [Beukes, 1987; Beukes and Gutzmer, 2008], could indicate a maximum depositional age of ca. 2588 Ma [Martin et al., 1998] for the cuspatate microbialites of the Gamohaan Formation [Beukes and Gutzmer, 2008].

Carbonates in the microbialites have  $d^{13}C$  and  $d^{18}O$  values ( $+0.02 \pm 0.07\text{‰}$  and  $-8.55 \pm 0.15\text{‰}$  VPDB, respectively, average  $\pm 1$  SD,  $n = 32$ ) that are typical for marine carbonates. The  $d^{13}C_{TOC}$  values ( $-38.8$  to  $-36.3\text{‰}$ ;  $-37.5 \pm 0.7\text{‰}$ ; TOC = 0.43 to 1.02 wt.% C) are typical of  $C_3$  photosynthetic bacterial origin [Spangenberg and Frimmel, 2001]. The first Re-Os results demonstrate that the sample set ( $n = 16$ ) taken from a 0.73 m interval of core possess between 0.6 and 9.5 ng g<sup>-1</sup> Re and 14.5 and 503.0 pg g<sup>-1</sup> total Os. Although the  $^{187}\text{Re}/^{188}\text{Os}$  and  $^{187}\text{Os}/^{188}\text{Os}$  broadly correlate positively, linear regression analysis using IsoplotR [Vermeesch, 2018] shows that the Re-Os isotopic data scatter about a 2.2 Ga errorchron. Thus, collectively the Re-Os systematics do not record the timing of deposition and suggest post deposition disturbance. Finite mixture model analysis [Davies et al., 2018] of the Re-Os data set defines six samples that represent a linear regression with an intercept and slope (i.e., age). The Re-Os data of these six samples yield a statistically meaningful date of 2.42 Ga, with a moderately radiogenic initial  $^{187}\text{Os}/^{188}\text{Os}$  ( $\text{Os}_i$ ) of 0.6. Interestingly, the 2.42 Ga Re-Os date overlaps with the age of the Ongeluk Large Igneous Province (OLIP,  $2426 \pm 3$  Ma) from the Kaapvaal Craton of southern Africa, which is taken to bracket the onset of the Great Oxidation Event between 2460 and 2426 Ma [Gumsley et al., 2017]. The disturbance and reset of the redox-sensitive Re-Os systematics of >2.52 Ga microbialites in the Gamohaan Formation could thus relate to the onset of the GOE at the time of significant ( $>10^{-5}$  PAL) atmospheric oxygenation.

## REFERENCES

- Beukes, N.J., 1987: Facies relations, depositional environments and diagenesis in a major early Proterozoic stromatolitic carbonate platform to basinal sequence, Campbellrand Subgroup, Transvaal Supergroup, Southern Africa, *Sedimentary Geology*, 54, 1-46.
- Beukes, N.J., and Gutzmer, J., 2008: Origin and paleoenvironmental significance of major iron formations at the Archean-Paleoproterozoic boundary, *Economic Geology Reviews*, 15, 5-47.
- Davies, J. H. F. L., Sheldrake, T. E., Reimink, J. R., Wotzlaw, J.-F., Moeck, C., & Finlay, A., 2018: Investigating complex isochron data using mixture models, *Geochemistry, Geophysics, Geosystems*, 19, 4035–4047.
- Gumsley, A., Chamberlain, K.R., Bleeker, W., Söderlund, U., de Kock, M., Larsson, E., Bekker, A., 2017: Timing and tempo of the Great Oxidation Event, *Proceedings of the National Academy of Science*, 114, 1811-1816.
- Martin, D.M., Clendenin, C.W., Krapez, B., Mcnaughton, N.J., 1998: Tectonic and geochronological constraints on late Archaean and Palaeoproterozoic stratigraphic correlation within and between the Kaapvaal and Pilbara Cratons, *Journal of the Geological Society of Australia*, 155, 311–322.

- Spangenberg, J.E., & Frimmel, H.E., 2001: Basin-internal derivation of hydrocarbons in the Witwatersrand Basin, South Africa: evidence from bulk and molecular  $\delta^{13}\text{C}$  data, *Chemical Geology*, 173, 339-355.
- Sumner, D.Y., & Bowring, S.A., 1996: U-Pb geochronologic constraints on deposition of the Campbellrand Subgroup, Transvaal Supergroup, South Africa, *Precambrian Research*, 79, 25-35.
- Vermeesch, P., 2018: IsoplotR: a free and open toolbox for geochronology. *Geoscience Frontiers* 9, 1479-1493.

## P 6.6

# Climatic imprint of the Middle Eocene Climatic Optimum (MECO) in the Escanilla formation, Spain

Nikhil Sharma<sup>1</sup>, Jorge Spangenberg<sup>2</sup>, Jean Vérité<sup>3</sup>, Thierry Adatte<sup>4</sup>, Sébastien Castelltort<sup>1</sup>

<sup>1</sup> University of Geneva, Department of Earth Sciences, Rue des Maraîchers 13, 1205 Geneva, Switzerland  
(nikhil.sharma@unige.ch)

<sup>2</sup> Institute of Earth Surface Dynamics (IDYST), University of Lausanne, Quartier UNIL-Mouline, Bâtiment Géopolis, 1015 Lausanne, Switzerland

<sup>3</sup> LPG – Le Mans, UFR Sciences et Techniques, Université du Maine, 72089 Le Mans cedex 9, France

<sup>4</sup> Institute of Earth Sciences (ISTE), University of Lausanne, Quartier UNIL-Mouline, Bâtiment Géopolis, 1015 Lausanne, Switzerland

The Middle Eocene Climatic Optimum (MECO) was a global warming event mainly described in the marine domain but significantly lacks records from terrestrial sections. Here we present a new comprehensive record of MECO based on a suite of middle Eocene paleosols sampled from the fluvial Escanilla formation in the south Pyrenean foreland basin, Spain. Our framework of geochemical analyses focuses on reconstructing weathering indices, mean annual precipitation and temperature, and stable isotope analyses on paleosol carbonates and preserved organic matter. The middle Eocene interval in northern Spain was characterized by temperate, arid (semi-arid) climatic conditions where peak precipitation and temperature occur during the peak warming event at ~40.0 Ma. Importantly, stable isotope excursions indicate the regional preservation of the MECO and highlights fluvial sedimentary successions as key archives to past global warming events.

## P 6.7

# Sedimentary record of hyperthermal events during the Early Eocene Climatic Optimum in the South Pyrenean Foreland Basin

Romain Vaucher<sup>1</sup>, Claire Musajo<sup>1</sup>, Jorge E. Spangenberg<sup>2</sup>, Miquel Poyatos-Moré<sup>3</sup>, Cai Puigdefàbregas<sup>4</sup>, Sébastien Castelltort<sup>5</sup>, Thierry Adatte<sup>1</sup>

<sup>1</sup> Institute of Earth Sciences (ISTE), University of Lausanne, Geopolis, 1015 Lausanne, Switzerland ([romain.vaucher@unil.ch](mailto:romain.vaucher@unil.ch))

<sup>2</sup> Institute of Earth Surface Dynamics (IDYST), Géopolis, University of Lausanne, 1015 Lausanne, Switzerland

<sup>3</sup> Departament de Geologia, Universitat Autònoma de Barcelona, Barcelona, Spain

<sup>4</sup> Department of Earth and Ocean Dynamics, University of Barcelona, C/ Martí i Franquès, s/n, 08028 Barcelona, Spain

<sup>5</sup> Department of Earth Sciences, University of Geneva, Rue des Marîchers 13, 1205 Geneva, Switzerland

The Early Eocene Climate Optimum (EECO; ~ 54-49 Ma ago) is a time interval defined by high CO<sub>2</sub> concentration in the atmosphere and high global temperature. The EECO is also associated with multiple hyperthermal events, which are abrupt and massive releases of isotopically-depleted carbon in the atmosphere, leading to rapid temperature and precipitation increases, thereby enhancing erosion and chemical weathering on land. Here, we analyse the sedimentological and stratigraphic record of the Castigaleu Sequence (Early Eocene; Ypresian; 52-50.2 Ma) cropping out in the South Pyrenean Foreland Basin (SPFB) near the location of Navarri (Aragon, Spain). The stratigraphic interval was chosen because i) its deposition took place during the EECO, and ii) accommodation creation and sediment delivery into the basin were both high, promoting the completeness of the stratigraphy and, therefore, the record and preservation of a high-resolution climate signal. A 643.5 m-thick mixed siliciclastic-carbonate section was logged and sampled (n = 301). The sedimentary facies analysis was complemented with mineralogical (XRD of whole rock and clay minerals) and geochemical (organic carbon stable isotopes, d<sup>13</sup>C<sub>org</sub>, and organic matter characterization by Rock-Eval pyrolysis) analysis. The first results suggest that deposition started in a mid-ramp bioclastic-rich environment and vertically evolved into a siliciclastic-prone fluvial-dominated deltaic system with a subordinate influence of waves. The onset and progradation of this deltaic system coincide with the first negative carbon isotope excursion recorded in the stratigraphic section. In turn, it suggests that the clastic input into the basin may represent the direct environmental response of the SPFB sedimentary routing systems to hyperthermal events in the EECO.

## P 6.8

# Understanding seepage activity and formation of cold-seep carbonates in the south-eastern Mediterranean Sea

Reinhard Weidlich<sup>1</sup>, Or M. Bialik<sup>2,3</sup>, Thomas Pettke<sup>4</sup>, Andres Rüggeberg<sup>1</sup>, Bernard Grobety<sup>1</sup>, Torsten Vennemann<sup>5</sup>, Yizhaq Makovsky<sup>3,6</sup>, Anneleen Fouber<sup>1</sup>

<sup>1</sup> University of Fribourg, Department of Geosciences, Chemin du Musée 6, CH-1700 Fribourg ([reinhard.weidlich@unifr.ch](mailto:reinhard.weidlich@unifr.ch))

<sup>2</sup> Marine Geology & Seafloor Surveying, Department of Geosciences, University of Malta, Msida, MSD, 2080 Malta

<sup>3</sup> The Dr. Moses Strauss Department of Marine Geosciences, Leon H. Charney School of Marine Sciences, University of Haifa, ISR-3498838 Haifa

<sup>4</sup> University of Bern, Department of Earth Sciences, Baltzerstrasse 1+3, CH-3012 Bern

<sup>5</sup> University of Lausanne, Institut des dynamiques de la surface terrestre, Bâtiment Géopolis, CH-1015 Lausanne

<sup>6</sup> The Hatter Department of Marine Technologies, Leon H. Charney School of Marine Sciences, University of Haifa, ISR-3498838 Haifa

Authigenic seep carbonates are unique archives to characterise the paleo-seepage activity of hydrocarbon-enriched fluids through the subsurface towards the seafloor. This study aims to identify past seepage activity in the south-eastern Mediterranean Sea and the formation conditions of authigenic seep carbonates sampled during the 2016 EUROTLETS 2 SEMSEEP expedition aboard the RV AEGEO and the 2011 Nautilus expedition. Seep carbonates with three different morphologies (chimneys, crusts, and, pavements), are studied using sediment petrography, X-ray diffraction, LA-ICP-MS, Raman spectroscopy, and stable isotope geochemistry. Recurrent cement and replacement phases contain aragonite, low-magnesium calcite (LMC), high-magnesium calcite (HMC) and dolomite. Chimneys consist of micrite ( $\delta^{13}\text{C}_{\text{VPDB}}$  of -10 to +5 ‰), fan-shaped aragonite ( $\delta^{13}\text{C}_{\text{VPDB}}$  of -52 to -30 ‰), botryoidal LMC cements and blocky HMC replacements. Crusts consist mainly of micrite, LMC breccias, HMC nodules ( $\delta^{13}\text{C}_{\text{VPDB}}$  of -35 to -20 ‰) and HMC cements, and several stages of fan-shaped aragonite cement. Pavements consist of micritic dolomite and clotted HMC as well as LMC microsparite and locally fan-shaped aragonite. Fe-oxy-hydroxides are coating the low- and high-Mg calcite and dolomite. Raman spectroscopic analysis indicate the presence of aliphatic, methyl and aromatic organic compounds associated with aragonite and dolomite. LA-ICP-MS analyses give distinct REY patterns for each phase.

Combined sediment petrography, XRD, and stable isotope analysis support several pulses of methane seepage through time. Distinct mineralogies (dolomite vs aragonite) within the seep carbonate morphologies result from different formation mechanisms. LA-ICP-MS analysis, combined with Raman spectroscopy suggests that distinct carbonate mineralogies formed from different fluids under variable redox conditions and in the presence of specific organic compounds.

**P 6.9****Lateral facies correlation of Opalinus Clay in central northern Switzerland using geochemical core logging data**

Géraldine Zimmerli<sup>1</sup>, Bruno Lauper<sup>1</sup>, Gaudenz Deplazes<sup>2</sup>, David Jaeggi<sup>3</sup>, Stephan Wohlwend<sup>4</sup>, Anneleen Foubert<sup>1</sup>

<sup>1</sup> Department of Geosciences, University of Fribourg, 1700 Fribourg, Switzerland ([geraldine.zimmerli@unifr.ch](mailto:geraldine.zimmerli@unifr.ch))

<sup>2</sup> Nagra, 5430 Wettingen, Switzerland

<sup>3</sup> Federal Office of Topography swisstopo, 3084 Wabern, Switzerland

<sup>4</sup> Geological Institute, ETH Zurich, 8092 Zürich, Switzerland

The Opalinus Clay, an argillaceous to silty claystone formation, is known in Switzerland as being the selected host rock for deep geological disposal of high-, intermediate- and low-level radioactive waste. Since the 1990's, various geotechnical, mineralogical and sedimentological properties of the Opalinus Clay have been studied within the framework of the Nagra (National Cooperative for the Disposal of Radioactive Waste) deep drilling campaigns and the Mont Terri Project (international research program dedicated to the investigation of claystone). The Opalinus Clay succession was deposited during the Late Toarcian to Early Aalenian in an epicontinental sea covering central Europe.

The Opalinus Clay is relatively homogeneous at formation-scale compared to other Mesozoic formations in northern Switzerland. At higher spatial resolution however, sedimentological facies variations do occur. Besides m-scale lithofacies variations, high, intra-facies lithological variability occur at dm- to cm-scale. The facies diversity is primarily attributed to regional differences in depositional, environmental and diagenetic conditions. In order to harmonize petrographic descriptions in an objective and quantitative way within all fields of research related to the Opalinus Clay, a subfacies classification scheme has been developed (Lauper et al. 2018; 2021). Five subfacies are distinguished by texture (grain size, bedding, fabric and colour) and composition (nature and mineralogy of components). Accurate petrographic descriptions are an important prerequisite to many geotechnical studies and the predictive modelling of petrophysical properties.

The aim of the present study is to compare geochemical core logging data (x-ray fluorescence) to petrographic descriptions and the defined subfacies for nine newly acquired Nagra drillings using multivariate statistics and end-member modelling. Results evidence that XRF core logging data can be used to quantify the lithological variability of Opalinus Clay. Small-scaled vertical variations and marker horizons are identified which can be correlated at regional scale. The new descriptions, combined with geochemical core logging, will form the base for the revision of depositional models for the Opalinus Clay at basin-scale.

**REFERENCES**

- Lauper, B., Jaeggi, D., Deplazes, G., & Foubert, A. (2018). Multi-proxy facies analysis of the Opalinus Clay and depositional implications (Mont Terri rock laboratory, Switzerland). Swiss Journal of Geosciences, 111, 383-398. <https://doi.org/10.1007/s00015-018-0303-x>.
- Lauper, B., Zimmerli, G.N., Jaeggi, D., Deplazes, G., Wohlwend, S., Rempfer, J., & Foubert, A. (2021). Quantification of lithological heterogeneity within Opalinus Clay: toward a uniform subfacies classification scheme using a novel automated core image recognition tool. Frontiers in Earth Science, 9, 645596. <https://doi.org/10.3389/feart.2021.645596>.

**P 6.10**

# **Chrono-chemo-lithostratigraphic reconstruction and organic geochemistry of a carbonate reservoir in the Mintom “Neoproterozoic ?” Formation, South-East Cameroon**

Bomolomo Michèle Vanessa<sup>1,2</sup>, Bessong Moïse<sup>2</sup>, Adatte Thierry<sup>3</sup>, Ossa Ossa Frantz-Gerard<sup>4</sup>

<sup>1</sup> Department of Earth Sciences, University of Yaoundé 1, P.O. Box 812 Yaounde (*michelebomolomo@yahoo.fr*)

<sup>2</sup> Institute of Geological and Mining Research, P.O. Box 4110 Nlongkak Yaounde

<sup>3</sup> Institute of Earth Sciences, Lausanne University, CH 1015 Lausanne

<sup>4</sup> Cardiff University, School of Earth and Environmental Sciences

The Neoproterozoic was one of the most significant geological periods in Earth history. It was marked by many important tectonic, climatic and biological changes such as Great Oxygenation Event, the formation and destruction of the supercontinents Nuña and Rodinia, appearance of the first metazoans, and glaciations. The Sturtian and Marinoan were Neoproterozoic Snowball glaciations and the Gaskiers, a less extensive event. Glacial deposits have been sufficiently documented in the western and southwestern parts of Africa (e.g., Taoudenni basin in Mauritania, Otavie sequence in Namibia, ...), unlike the central part where very few data exist. The Mintom, study area, is a Central African basin located at the boundary between the North-Equatorial Pan-African Belt and the Congo craton, in southeast Cameroon. Several petrographic types, grouped into three major groups, are recognized in this area. They include: a granite-gneiss complex; a metasedimentary ensemble comprising limestone and dolostone; and a sedimentary ensemble represented by conglomerate, quartzite sandstone, and red pelite that is overlain by a thick layer of locally brecciated laterite. The Mintom Formation is subdivided into four lithological units (Kol, Metou, Momibolé and Atog-Adjap) and consists of diamictite, dolostone, pelite, and limestone from bottom to top. The position of this formation in relation to neighboring formations remains very problematic. It is represented on geological maps as either resting unconformably on the Yaounde Group and thrust onto the Congo Craton, or as unconformably overlying both these major tectonic units. According to Caron et al. (2010, 2011), the Mintom Formation would be Neoproterozoic, would have been affected by one or two glaciations (Hirnantian and/or Gaskiers), and would be composed of cap carbonate. Presently, these are only preliminary hypotheses which we examine in this study using a first borehole of about 100.30m depth that was drilled in East of the Mintom sedimentary basin. The total core recovered is 101 m thick, with about 1 m of culminating core loss. Soil and recent alluvium are approximately 5.70 m and lie directly above the limestone. Lithostratigraphic studies and Rock-Eval pyrolysis were previously conducted on the first 100 m drilled.  $\delta^{13}\text{C}$  and  $\delta^{18}\text{O}$  isotope analyses are underway, as well as geochemical and Uranium analyses. Based on lithostratigraphic studies and field data, the first 100 meters are generally light to dark grey, finely stratified limestone that alternate with thin and dark claystone. Above 70 m, there are pyrite-rich levels, which become more and more common and abundant with depth. The first pyrolysis results reveal that the first drilled meters of the Mintom Formation contain low amounts of organic matter and the maximum pyrolysis temperatures (Tmax) are ~309 to 520°C. According to their TOC, they cannot generate petroleum. Moreover, the presence of pyrite suggest that the environment would have been reductive and anoxic during the deposition.

**REFERENCES**

- Caron, V., Ekomane, E., Mahieux, G., Moussango, P. & Ndjeng, E. 2010: The Mintom Formation (new): sedimentology and geochemistry of a Neoproterozoic, Paralic succession in south-east Cameroon. Journal of African Earth Sciences 57, 367-385.
- Caron, V., Mahieux, G., Ekomane, E., Moussango, P. & Babinski, M. 2011: One, two or no record of late neoproterozoic glaciation in South-East Cameroon? Journal of African Earth Sciences 59, 111-124.



# 7 Seismic Hazard and Risk in Switzerland: From Science to Mitigation

Donat Fäh, Blaise Duvernay, Savvas Saloustros

## TALKS:

- 7.1 Arslantürkoglu S., Stojadinovic B.: Praktische Ermittlung des Todesfallrisikos bezüglich Erdbeben für bestehende Bauten in der Schweiz
- 7.2 Bellwald B., Nigg V., Fabbri S.C., Becker L.W.M., Gilli A., Anselmetti F.S.: Holocene seismic activity in southeastern Switzerland: Evidence from the sedimentary record of Lake Silvaplana
- 7.3 Bergamo P., Panzera F., Cauzzi C., Glüer F., Perron V., Fäh D.: A ground-motion amplification model for Switzerland based on site condition indicators and measured local response
- 7.4 Hallo M., Koroni M., Imtiaz A., Fäh D.: Prediction of broadband waveforms at depth from earthquake recordings on the surface in Switzerland
- 7.5 Imtiaz A., Panzera F., Fäh D.: Assessing site amplification from canonical correlation for Basel, Switzerland
- 7.6 Janusz P., Bonilla L.F., Perron V., Bergamo P., Panzera F., Fäh D.: Preliminary results of estimating the non-linear site response in the Lucerne area
- 7.7 Kassas K., Sakelariadis L., Marin A., Anastopoulos I.: Seismic evaluation of an existing pile group on liquefiable soil
- 7.8 Khodaverdian A., Lestuzzi P.: Sa-based Fragility Model for Swiss Buildings
- 7.9 Koroni M., Hallo M., Imtiaz A., Fäh D.: Broadband waveform simulations of earthquake scenarios in the Swiss Molasse basin
- 7.10 Panzera F., Bergamo P., Danciu L., Fäh D.: On the selection of design-compatible waveforms for microzonation purpose in Switzerland
- 7.11 Saloustros S., Beyer K.: Experimental testing of rubble stone masonry walls of varying size under in-plane quasi static loading
- 7.12 Shynkarenko A., Cauzzi C., Kremer K., Bergamo P., Lontsi A.M., Janusz P., Fäh D.: Seismic response of subaqueous slopes in Lake Lucerne
- 7.13 Sieber M., Anastopoulos I.: On the development of a simplified analysis method for piled foundations subjected to seismic excitation

## POSTERS:

- P 7.1 Hetényi G., Sauron A., Böse M., Roduit R., Subedi S., Dallo I.: Seismology-at-School across Switzerland: project nucleation and growth
- P 7.2 Mesimeri M., Diehl T., Clinton J., Herwegh M., Wiemer S.: Moment Tensors for small to moderate magnitude earthquakes in Switzerland

## 7.1

# Praktische Ermittlung des Todesfallrisikos bezüglich Erdbeben für bestehende Bauten in der Schweiz

Safak Arslantürkoglu<sup>1</sup>, Bozidar Stojadinovic<sup>1</sup>

<sup>1</sup> Departement Bau, Umwelt und Geomatik, ETH Zurich, Stefano-Francini-Platz 5, CH-8093 Zurich (safak@ibk.baug.ethz.ch)

Unter den Naturgefahren haben Erdbeben das grösste Katastrophenpotenzial in der Schweiz. Für den Umgang mit dieser Gefahr und zur Minderung der damit gebundenen Risiken regelt die SIA 269/8 die Überprüfung bestehender Bauten bezüglich Erdbeben. Der im Schwerpunkt liegende Erfüllungsfaktor gibt an, inwiefern das untersuchte Gebäude die Anforderungen der aktuellen SIA Normen erfüllt. Rechnerisch gesehen, entspricht dieser Faktor dem Verhältnis zwischen der seismischen Kapazität eines Gebäudes und der Anforderung der zum Zeitpunkt der Überprüfung gültigen SIA Normen. Mittels einer Risikokurve wird jedem Erfüllungsfaktor ein Personenrisikofaktor zugewiesen, welcher das jährliche Todesfallrisiko eines Individuums bezüglich Erdbeben darstellt. Durch den Personenrisikofaktor wird entschieden, ob und in welchem Umfang Massnahmen zur Erdbebenertüchtigung fällig sind. Dank der direkten Beziehung zwischen dem Erfüllungsfaktor und dem Personenrisikofaktor ist die Risikokurve zwar nützlich für Ingenieure in der Praxis, es lässt sich jedoch nicht herleiten, wie die einzelnen Risikocomponenten auf das totale Risiko wirken. Zudem beruht die Form der Risikokurve auf der statistischen Auswertung von Risikoanalysen für eine begrenzte Anzahl an Fallbeispielen, weswegen Fragen bezüglich ihrer Gültigkeit für weitere Gebäudetypen auftauchen.

Eine robuste Methode für die risikobasierte Ermittlung bezüglich Erdbeben ist die leistungsorientierte Methodik (PBEE) vom Pacific Earthquake Engineering Research Center (PEER). Die Überschreitungsrate einer Entscheidungsvariable ) wird mit folgendem Dreifachintegral berechnet, indem die probabilistische Natur des seismischen Gefährdungs-, Anforderungs-, Schadens- sowie des Verlustmodells mit dem Satz der totalen Wahrscheinlichkeit kombiniert werden (Moehle & Deierlein 2004; Mackie & Stojadinovic 2006).

$$v_{DV} = \int_{dm} \int_{edp} \int_{im} G_{DV|DM}(DV|DM) |dG_{DM|EDP}(DM|EDP)| |dG_{EDP|IM}(EDP|IM)| |dv(IM)|$$

Die komplementäre kumulative Dichtefunktion (CCDF) und die Wahrscheinlichkeitsdichtefunktion (PDF) von der Variable unter der Bedingung der Variable , wird mit respektive bezeichnet. Die entkoppelte Natur des PEER PBEE Dreifachintegrals lässt die Risikoverteilung zwar in kleinere Bereiche aufteilen, seine numerische Lösung ist jedoch nicht geradlinig, weshalb seine Anwendung vorwiegend auf die Forschung beschränkt ist.

Als Alternative zur SIA 269/8 und numerischen Lösung des PEER PBEE Integrals, präsentiert diese Arbeit eine praxisorientierte Methode für die Ermittlung des Todesfallrisikos infolge Erdbeben, welche auf der geschlossenen Lösung des PEER PBEE Integrals und der grafischen Veranschaulichung der probabilistischen Modelle beruhen (Figure 1). Die Vorteile liegen in der benutzerfreundlichen Anwendung sowie der Rückverfolgbarkeit der Risikocomponenten, wodurch die Identifizierung jeder einzelnen Komponente hinsichtlich ihres Beitrags zu dem totalen Risiko möglich wird. Kombiniert mit dem seismischen Gefährdungsmodell SULhaz2015 (Wiemer et al. 2015), kann die jährliche Überschreitungsrate der Todesopfer in einer Verlustkurve zusammengefasst werden, um risikobasierte Entscheidungen bezüglich der Erdbebenertüchtigung zu treffen.

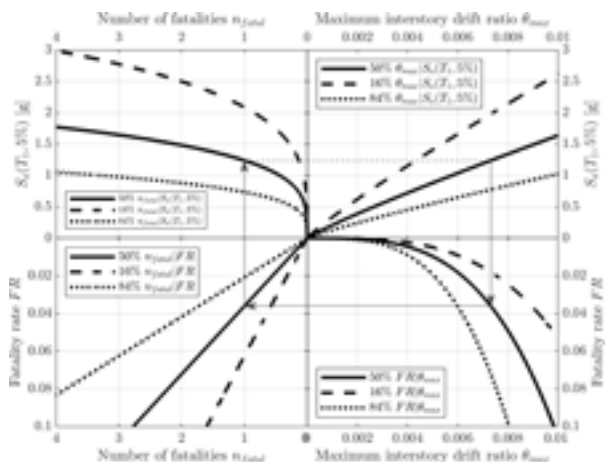


Figure 1. Grafische Darstellung der Methode für die Ermittlung des Todesfallrisikos bezüglich Erdbeben (Arslantürkoglu & Stojadinovic 2022)

Zur Demonstration der Methode wird ein Fallbeispiel eines unbewehrten Mauerwerksgebäudes unter Verwendung diverser Kombinationen bezüglich den Überprüfungsmethoden (statisch nichtlinear gegen dynamisch nichtlinear), der Behandlung der Unsicherheiten (Zufälligkeit der Bodenbewegung mit oder ohne Baustoffparameter-Unsicherheiten) sowie die Lösungsstrategien des PEER PBEE Integrals (numerisch gegen geschlossen) mit dem Ziel einen praktischen Kompromiss zwischen der Ergebnisgenauigkeit und dem Rechenaufwand zu finden. Die Verlustkurve aus der dynamisch nichlinearen Analyse und der numerischen Lösung des PEER PBEE Integrals wurde als Benchmark verwendet, um die Zuverlässigkeit der Ergebnisse auszuwerten.

Die vorliegende grafische Methode hat sich als eine praktische und eine transparente Alternative zur SIA 269/8 erwiesen. Um genau zu sein hat der Erfüllungsfaktor das Todesfallrisiko mindestens um den Faktor 6 unterschätzt, während es durch die präsentierte Methode nur geringfügig überschätzt wurde.

## REFERENZEN

- Arslantürkoglu S. & Stojadinovic B. 2022: Seismic Fatality Risk Evaluation Framework for Existing Buildings in Switzerland  
(Zur Veröffentlichung eingereicht)
- Mackie K. R. & Stojadinovic B. 2006: Fourway: Graphical Tool for PBEE
- Moehle J. P. & Deierlein G. 2004: A framework methodology for Performance-Based Earthquake Engineering, 13<sup>th</sup> World Conf Earthq Eng
- Wiemer S., Danciu L., Edwards B., et al. 2015: Seismic Hazard Model 2015 for Switzerland (SUIhaz2015), Swiss Seismological Service (SED)

## 7.2

# Holocene seismic activity in southeastern Switzerland: Evidence from the sedimentary record of Lake Silvaplana

Benjamin Bellwald<sup>1,2</sup>, Valentin Nigg<sup>3</sup>, Stefano C. Fabbri<sup>3</sup>, Lukas W.M. Becker<sup>4</sup>, Adrian Gilli<sup>2</sup>, Flavio S. Anselmetti<sup>3</sup>

<sup>1</sup> Department of Geosciences, University of Oslo, Sem Sælands vei 1, NO-0371 Oslo ([benjamin.bellwald@gmail.com](mailto:benjamin.bellwald@gmail.com))

<sup>2</sup> Geological Institute, ETH Zurich, Sonneggstrasse 5, CH-8092 Zurich

<sup>3</sup> Institute of Geological Sciences and Oeschger Centre for Climate Change Research, University of Bern, Baltzerstrasse 1+3, CH-3012 Bern

<sup>4</sup> Rambøll Norway, Folke Bernadottes vei 50, Fyllingsdalen, NO-5845 Bergen

High-alpine regions are prone to a large variety of geohazards, among which earthquakes have the strongest impact on landscape and local population. Historic records indicate a moderate to high seismic activity in the northern, southwestern and central parts of Switzerland. In contrast, southeastern Switzerland has less historic earthquake chronicles due to the low population density, resulting in a poorly constrained seismic event catalogue. The aim of this study is to evaluate the paleoseismic activity for southeastern Switzerland by using the sedimentary record of Lake Silvaplana in the Engadine Valley. We use a dense grid of high-resolution 2D seismic profiles, high-resolution bathymetry, and a 10 m long sediment core from the deepest basin to investigate the lake stratigraphy. The bathymetry reveals a flat basin, flanked by steep slopes to the northwest and southeast. The acoustic basement consists of four ridges, and gently-dipping fans to the southwest and northeast. Expressions of slope failure can be identified in all domains of the lake floor and the subsurface data. Multiple coevally-triggered chaotic mass-flow deposits, overlain by megaturbidites with a coarse-sand base, have been detected along ten horizons in the seismic data. We interpret these ten event layers to be triggered by paleo-earthquakes in eastern Switzerland or northern Italy. The four most recent of these deposits are cored and radiocarbon dated to ~230, 310, 960, and 1330 cal yr BP, indicating four overregional seismic events that triggered large slope failures in Lake Silvaplana in the last 1400 years. Correlation with sedimentary deposits of Lake Sils, Lake Como and Lake Ledro within radiocarbon uncertainties indicate a large earthquake around 1330 cal yr BP. Within their age ranges, the postulated earthquake at 310 cal yr BP (1640 CE) further correlates with a moment magnitude Mw ~5.4 event in Ftan in 1622 CE, and the 960 cal yr BP (990 CE) with a Mw ~5.2 earthquake in Brescia in 1065 CE. Six mass-movement deposits that were not reached by the sediment core have a suggested age between 7800 and 11300 cal yr BP, and are also suggested to be caused by earthquakes. Thus, Lake Silvaplana sediments provide the first reliable record of seismic activity for the mid- and Late Holocene in this region. Basement ridges following the Engadine Line, a major fault zone running along the main valley, further indicate the potential that the Engadine Line is a neotectonically active structure.

## REFERENCES

- Bellwald, B., Nigg, V., Fabbri, S.C., Becker, L.M.W., Gilli, A., & Anselmetti, F.S. in review: Holocene seismic and flood activity in southeastern Switzerland: Evidence from the sedimentary record of Lake Silvaplana, *Sedimentology*.
- Blass, A., Anselmetti, F.S., Grosjean, M., & Sturm, M. 2005: The last 1300 years of environmental history recorded in the sediments of Lake Sils (Engadine, Switzerland), *Eclogae Geologicae Helvetiae*, 98(3), 319-332.
- Fanetti, D., Anselmetti, F.S., Chapron, E., Sturm, M., & Vezzoli, L. 2008: Megaturbidite deposits in the Holocene basin fill of Lake Como (southern Alps, Italy), *Palaeogeography, Palaeoclimatology, Palaeoecology*, 259(2-3), 323-340.
- Gobet, E., Tinner, W., Hochuli, P.A., Van Leeuwen, J.F.N., & Ammann, B. 2003: Middle to Late Holocene vegetation history of the Upper Engadine (Swiss Alps): the role of man and fire, *Vegetation History and Archaeobotany*, 12(3), 143-163.
- Kremer, K., Wirth, S.B., Reusch, A., Fäh, D., Bellwald, B., Anselmetti, F.S., ... & Strasser, M. 2017: Lake-sediment based paleoseismology: Limitations and perspectives from the Swiss Alps, *Quaternary Science Reviews*, 168, 1-18.
- Lauterbach, S., Chapron, E., Brauer, A., Hüls, M., Gilli, A., Arnaud, F., ... & Participants, D. 2012: A sedimentary record of Holocene surface runoff events and earthquake activity from Lake Iseo (Southern Alps, Italy), *The Holocene*, 22(7), 749-760.
- Leemann, A., & Niessen, F. 1994: Holocene glacial activity and climatic variations in the Swiss Alps: reconstructing a continuous record from proglacial lake sediments. *The Holocene*, 4(3), 259-268.
- Nigg, V., Wohlwend, S., Hilbe, M., Bellwald, B., Fabbri, S.C., de Souza, G.F., ... & Anselmetti, F.S. 2021: A tsunamigenic delta collapse and its associated tsunami deposits in and around Lake Sils, Switzerland, *Natural Hazards*, 107(2), 1069-1103.
- Rapuc, W., Arnaud, F., Sabatier, P., Anselmetti, F., Piccin, A., Peruzza, L., ... & Straub, K. 2022: Instant sedimentation in a deep Alpine lake (Iseo, Italy) controlled by climate, human and geodynamic forcing, *Sedimentology*, 12972.
- Schlüchter, C., Bonani, G., Donau, F., Grischott, R., Nicolussi, K., Pfenninger, A., Schlüchter, B., Seifert, M., Vattioni, S., & Hajdas, I. 2018: Rätselhafte Unterwasserbäume in den Oberengadiner Seen, *Jahresbericht der Naturforschenden Gesellschaft Graubünden* 120, 41-49.

## 7.3

# A ground-motion amplification model for Switzerland based on site condition indicators and measured local response

Paolo Bergamo<sup>1</sup>, Francesco Panzera<sup>1</sup>, Carlo Cauzzi<sup>1</sup>, Franziska Glüer<sup>1</sup>, Vincent Perron<sup>1,2</sup>, Donat Fäh<sup>1</sup>

<sup>1</sup> Swiss Seismological Service (SED) at ETH Zurich, Sonneggstrasse 5, CH-8092 Zürich ([paolo.bergamo@sed.ethz.ch](mailto:paolo.bergamo@sed.ethz.ch))

<sup>2</sup> presently at French Alternative Energies and Atomic Energy Commission (CEA), FR-13108, Saint-Paul-les-Durance, France.

Mapping the local seismic response is one of the key elements for seismic risk estimation studies. In the framework of the “Earthquake Risk Model Switzerland” project (ERM-CH, <http://www.seismo.ethz.ch/en/knowledge/seismic-risk-switzerland/>), presently in its final stage, we developed a new ground-motion soil amplification model covering homogeneously the entire Switzerland.

The model is based on two datasets:

- Site amplification functions measured at Swiss seismic stations estimated processing earthquake records (years 2000 – 2021) by means of the empirical spectral modeling technique (ESM, Edwards et al. 2013). Among the permanent and temporary seismic networks of Switzerland, we selected ~260 (urban) free-field installations with sufficient events’ coverage (at least 5 recorded earthquakes with S/N ratio > 3 in the frequency band 0.5 – 10 Hz).
- Several layers of site condition indicators, of proven correlation with local seismic response (Bergamo et al., 2022): i) a lithological classification of Switzerland derived from the Swiss National Geological map, ii) multi-scale topographic slope and iii) the depth-to-bedrock as estimated by the national bedrock elevation model of Swisstopo (2019).

The two datasets were cross-referenced to extrapolate the local measures of soil response at seismic stations over the entire Switzerland, applying the regression-kriging algorithm (RK, Hengl et al. 2007). The obtained amplification model consists of four soil response maps, for PGV, PSA(1.0s), PSA(0.6s) and PSA(0.3s), respectively (e.g. Fig. 1a). These maps are accompanied by an estimate of the corresponding uncertainty terms (Edwards & Fäh, 2013): the “site-to-site variability” ( $\phi_{S2S}$ ) and the “single-site, within-event variability” ( $\phi_{SS}$ ; Fig. 1b-c). The complete modeling of the soil response with uncertainties allows their coherent integration in the ERM-CH architecture, avoiding double-counting of uncertainties. The amplification maps are currently being validated through the comparison with macroseismic intensity observations from historical earthquakes (Fäh et al., 2011), with local amplification models covering specific urban areas (e.g. Panzera et al. 2022, Janusz et al., 2022, Perron et al., 2022), and finally with site response measurements from stations not included in the calibration dataset.

## REFERENCES

- Bergamo P. et al. 2022: Correspondence between Site Amplification and Topographical, Geological Parameters: Collation of Data from Swiss and Japanese Stations, and Neural Networks-Based Prediction of Local Response, BSSA, 112(2), 1008 – 1030.
- Edwards B. and Fäh D. 2013: A stochastic ground-motion model for Switzerland, BSSA, 103 (1), 78–98
- Edwards B. et al. 2013: Determination of Site Amplification from Regional Seismicity: Application to the Swiss National Seismic Networks, SRL, 84(4), 611-621.
- Fäh D et al. 2011: ECOS-09 earthquake catalogue of Switzerland release 2011. Report and database. Sed/Ecos/R/001/20110417.
- Panzera F. et al. 2022: Reconstructing a 3D model from geophysical data for local amplification modelling: The study case of the upper Rhone Valley, Switzerland. SDEE, 155, 107163.
- Perron V. et al. 2022: Site Amplification at High Spatial Resolution from Combined Ambient Noise and Earthquake Recordings in Sion, Switzerland. SRL, <https://doi.org/10.1785/0220210289>
- Janusz, P., et al. 2022: Combining Earthquake Ground Motion and Ambient Vibration Recordings to Evaluate a Local High-Resolution Amplification Model—Insight From the Lucerne Area, Switzerland. Front. Earth Sci., <https://doi.org/10.3389/feart.2022.885724>
- Swisstopo, Swiss Federal Office of Topography 2019. Bedrock elevation model.

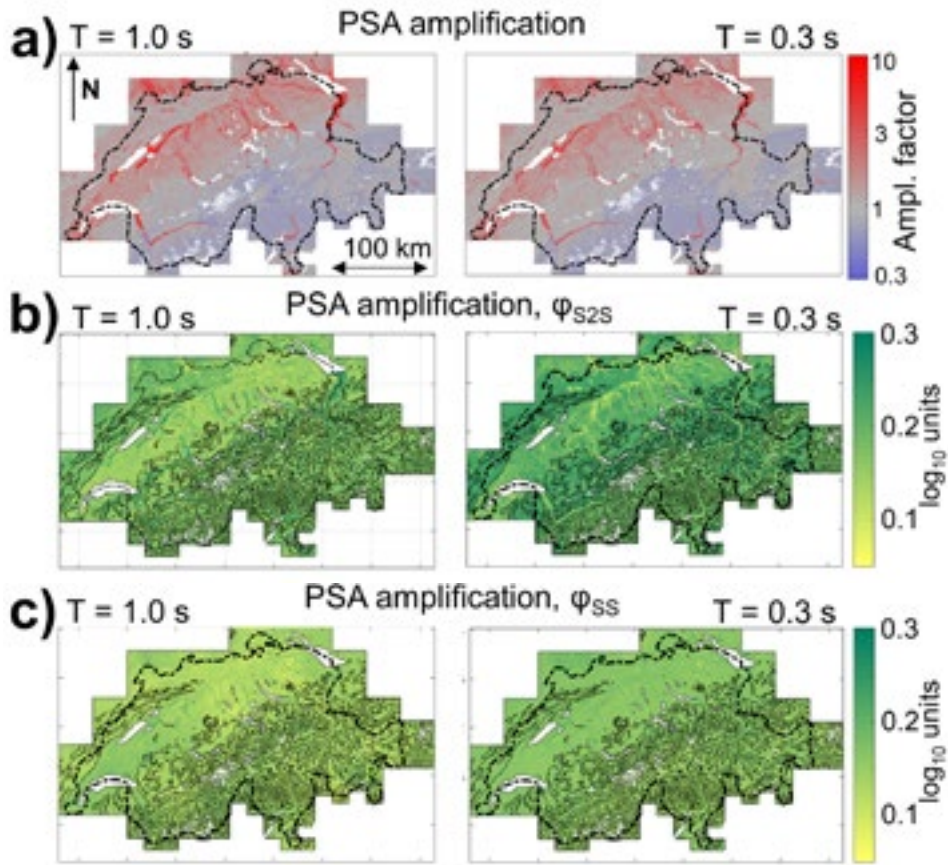


Figure 1. a) Obtained amplification maps for PSA(1.0s), left, and PSA(0.3s), right. b) Corresponding  $\varphi_{S2S}$  (site-to-site variability) maps. c) Corresponding  $\varphi_{SS}$  (single-site, within event variability) maps.

## 7.4

# Prediction of broadband waveforms at depth from earthquake recordings on the surface in Switzerland

Miroslav Hallo<sup>1</sup>, Maria Koroni<sup>1</sup>, Afifa Imtiaz<sup>1</sup>, Donat Fäh<sup>1</sup>

<sup>1</sup> Swiss Seismological Service (SED), ETH Zürich, Sonneggstrasse 5, CH-8092 Zürich ([miroslav.hallo@sed.ethz.ch](mailto:miroslav.hallo@sed.ethz.ch))

In order to minimize the damage and fatalities caused by future earthquakes, many countries imposed seismic design in their building codes (CEN 2004, SIA 2020). In Europe, there are several classes of buildings with different earthquake resistance requirements (agricultural, ordinary, institutional, and buildings of special importance). In the case of structures of special importance, the seismic hazard is evaluated for long return periods and should take into account the conditions of the rock and soil at the foundation of the construction. Next, the earthquake shaking observed on the ground surface differs from the shaking at a depth beneath. This applies to observed temporal waveforms as well as intensity measure types such as peak ground acceleration (PGA), peak ground velocity (PGV), and cumulative absolute velocity (CAV). Such phenomenon originates from the near-surface soft rock and soil layers that cause amplification and attenuation of seismic waves. The prediction of a possible ground motion at depth is important for earthquake resistance design of deep geological disposals (i.e., nuclear waste repositories), buildings with deep foundations, or for studies of soil-structure interaction.

Recently, Hallo et al. (2022) proposed a new method to characterize high-frequency (>1 Hz) ground motion at a depth that is also suitable for broadband waveform predictions. The method makes use of a new stochastic model (SM) that relates the ground motion at depth and on the surface in the Fourier domain (Borcherdt 1970). The surface-borehole SM is based on a response of a layered 1D medium to incident body waves, it resembles an empirical surface-borehole response, and it can be used for the full-waveform prediction of ground motion at depth from waveforms observed on the surface. This method was successfully applied to borehole installations of the KiK-net network in Japan already.

In this contribution, we demonstrate this recently developed method in the Swiss molasse basin. In particular, we apply the method to predict borehole waveforms from surface recordings of the 2017 Urnerboden  $M_w 4.1$  earthquake in Switzerland (Diehl et al. 2021). Full-waveform predictions are performed at BOBI and HAMIK sites equipped with surface and bore sensors, which allow direct comparison with empirical data (see an example in Fig.1). A comparison of predicted and observed acceleration waveforms shows a high level of similarity in the broadband frequency range and well-predicted values of PGA and PGV at depth. The latter demonstrates the capability of the method to predict broadband waveforms that can be used for the earthquake-resistant design of deep geological disposals in Switzerland.

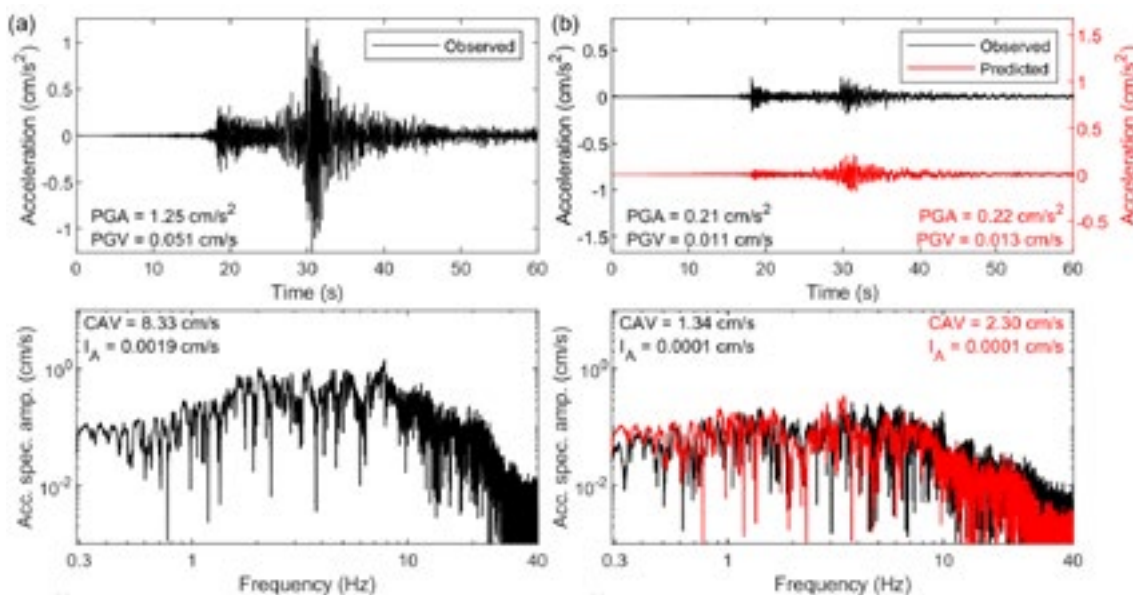


Figure 1. The 2017 Urnerboden  $M_w 4.1$  earthquake: Prediction of the ground motion at depth at the BOBI site in Switzerland. (a) Transverse component of the horizontal ground motion observed on the surface. (b) Observed (black) and predicted (red) horizontal ground motion in the borehole at 153 m depth.

## REFERENCES

- Borcherdt, R.D. 1970: Effects of local geology on ground motion near San Francisco Bay, Bull. Seismol. Soc. Am., 60, 29-61.
- CEN 2004: Eurocode 8: Design of structures for earthquake resistance – Part 1: General rules, seismic actions and rules for buildings, European Committee for Standardization, EN 1998-1 edition, Brussels, Belgium.
- Diehl, T., Clinton, J., Cauzzi, C., Kraft, T., Kästli, P., Deichmann, N., Massin, F., Grigoli, F., Molinari, I., Böse, M., Hobiger, M., Haslinger, F., Fäh, D., & Wiemer, S. 2021: Earthquakes in Switzerland and surrounding regions during 2017 and 2018, Swiss J. Geosci., 114, 4, doi: 10.1186/s00015-020-00382-2.
- Hallo, M., Bergamo, P., & Fäh, D. 2022: Stochastic model to characterize high-frequency ground motion at depth validated by KiK-net vertical array data, Bull. Seismol. Soc. Am., 112, 1997-2017.
- SIA 2020: SIA 261 Einwirkungen auf Tragwerke. Société Suisse des ingénieurs et des architectes, Zurich, Switzerland.

## 7.5

# Assessing site amplification from canonical correlation for Basel, Switzerland

Afifa Imtiaz<sup>1</sup>, Francesco Panzera<sup>1</sup>, Donat Fäh<sup>1</sup>

<sup>1</sup> Swiss Seismological Service (SED), ETHZ, Switzerland ([afifa.imtiaz@sed.ethz.ch](mailto:afifa.imtiaz@sed.ethz.ch))

An a priori estimation of the effects of shallow geology on the earthquake ground motion, termed as site-amplification, is essential in seismic risk studies. Generally, it is estimated by using techniques such as Standard Spectral Ratio (SSR), Empirical Spectral Modelling (ESM) or Horizontal-to-Vertical Spectral Ratio (HVSR), based on the analysis of earthquake recordings. However, it is not always feasible to apply them in areas where sufficient earthquake recordings are not available due to a lack of seismic stations or seismicity or where ground motion needs to be estimated with high spatial resolution. As ambient noise measurements at single stations can be obtained relatively easily, many recent studies (e.g., Cultrera et al.; 2014, Panzera et al., 2021) have investigated a statistical association between Horizontal-to-Vertical Noise Ratios (HVNRs) and empirical amplification functions (EAFs). This is performed over the frequency band of engineering interest (0.5-10 Hz) and for locations of a site where both single-station noise measurements and earthquake recordings and amplification functions are available. Then they predicted amplification functions (PAFs) at locations where only ambient noise measurements are available. Their results highlighted the improvement in resolution achieved in the assessment of site-amplification through the application of such an approach.

This study presents an ongoing work on developing a high-resolution site-amplification model at an urban scale for the canton of Basel-City in Switzerland. Michel et al. (2017) estimated amplification functions for Basel by using a hybrid ESM method. Even though it overcomes limitations of using only SSRs, it falls short of providing the necessary resolution to capture the effects of complex shallow geology of Basel. Taking advantage of EAFs estimated from stations of the national seismic networks of Switzerland along with their shear-wave velocity (Vs) profiles, and HVNRs available from numerous single stations (Figure 1, top), we apply a multivariate statistical approach, proposed by Panzera et al. (2021), based on the canonical correlation. We use the training dataset of about 200 seismic station from all over Switzerland, applied by Panzera et al. (2021), to obtain the statistical correlation between EAFs and HVNRs. The authors also considered adjustment factors in the form of geological and geophysical predictor proxies, such as, the last glacial maximum thickness (LGM) and the average Vs down to 30 m depth ( $Vs_{30}$ ), in order to improve their predictions. At first, we evaluate PAFs at the locations of seismic stations in Basel. Once the accuracy of the prediction is verified (Figure 1, bottom), we estimate PAFs at the scale of the city where we have a rich database of ambient noise recordings. Vs profiles for these target locations are obtained from the three-dimensional geological-geophysical model for Basel (Imtiaz et al., 2021). Results of the validation phase indicate that the canonical correlation method can be promising in predicting amplification. The generated amplification map, at any period of interest for earthquake engineering, seems to efficiently capture the spatial variability of the surface geology and the consequent site-amplification.

## REFERENCES

- Cultrera, G. V., De Rubeis, V., Theodoulidis, N., Cadet, H., and Bard, P.-Y. 2014: Statistical correlation of earthquake and ambient noise spectral ratios, *Bull. Earthq. Eng.* 12, 1493–1514.
- Imtiaz, A., Panzera, F., Hallo, M., Dresmann, H., Steiner, B., Fäh, D. 2021: An integrated 3D geological-seismological model at urban scale in Basel, Switzerland. *Proceedings of the 6th IASPEI / IAEE International Symposium: Effects of Surface Geology on Seismic Motion*, online, 30 August – 1 September 2021.
- Michel, C., Fäh, D., Edwards, B., Cauzzi, C. 2017: Site amplification at the city scale in Basel (Switzerland) from geophysical site characterization and spectral modelling of recorded earthquakes. *Phys Chem Earth, Parts A/B/C*, 98, 27–40, doi: 10.1016/j.pce.2016.07.005.
- Panzera, F., Bergamo, P., Fäh, D. 2021: Canonical Correlation Analysis Based on Site-Response Proxies to Predict Site-Specific Amplification Functions in Switzerland. *Bull. Seismol. Soc. Am.* 111(4): 1905–1920, doi: <https://doi.org/10.1785/0120200326>

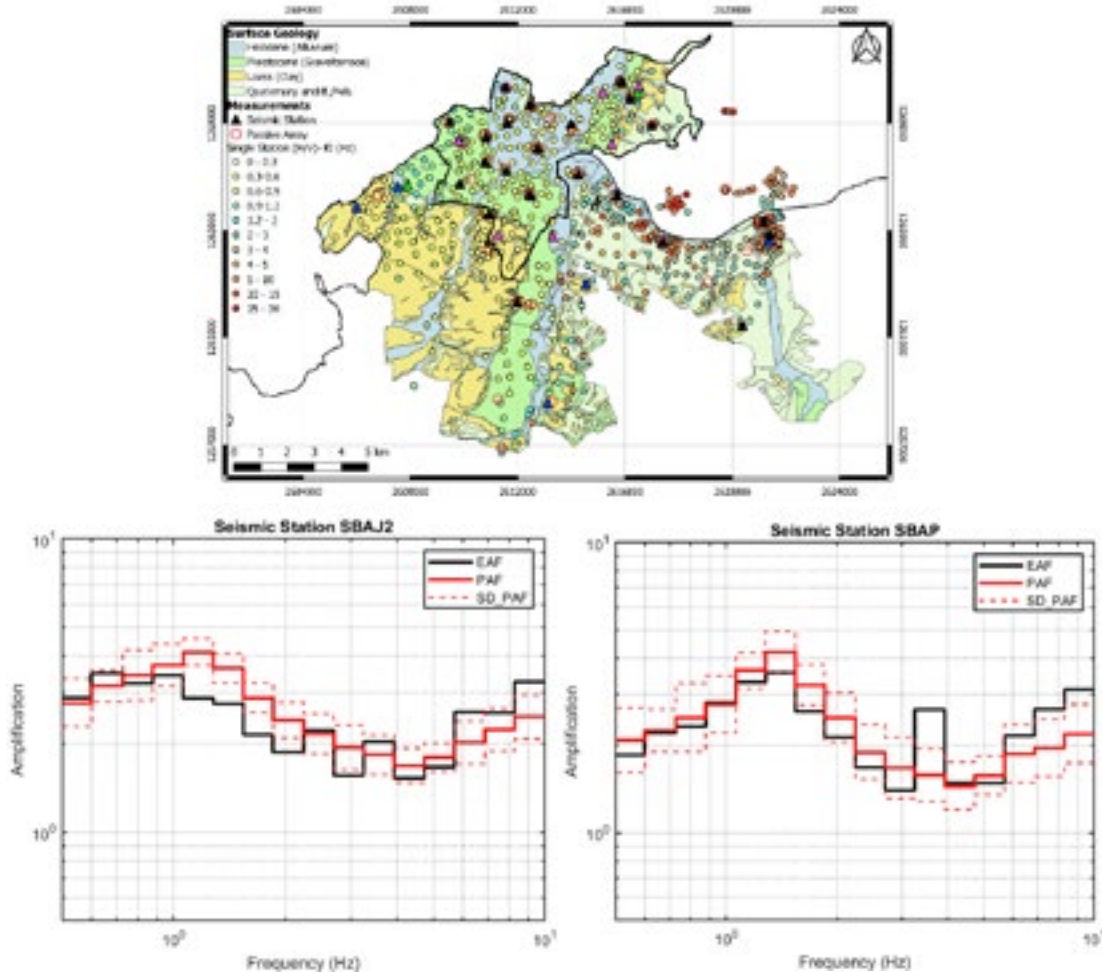


Figure 1. Surface geology of Basel along with locations of seismic stations, and ambient vibration array and single station measurements (top). Comparison between the EAF and the PAF at two different station locations from the validation dataset (bottom).

## 7.6

# Preliminary results of estimating the non-linear site response in the Lucerne area

Paulina Janusz<sup>1</sup>, Luis Fabian Bonilla<sup>2</sup>, Vincent Perron<sup>3</sup>, Paolo Bergamo<sup>1</sup>, Francesco Panzera<sup>1</sup>, Donat Fäh<sup>1</sup>

<sup>1</sup> Swiss Seismological Service, ETH Zürich, Sonneggstrasse 5, 8092 Zürich, Switzerland ([paulina.janusz@sed.ethz.ch](mailto:paulina.janusz@sed.ethz.ch))

<sup>2</sup> Université Gustave Eiffel, 14-20 Boulevard Newton, Cité Descartes, 77447 Marne-la-Vallée Cedex 2, France

<sup>3</sup> Atomic Energy and Alternative Energies Commission (CEA), centre d'étude de Cadarache, 13108 St Paul lez Durance Cedex, France

The importance of non-linear site effects is often debated, especially in a low-to-moderate seismicity area like central Switzerland. The city of Lucerne is located on very soft, unconsolidated water-saturated deposits that are prone to strong amplification (Janusz et al., 2022) especially in low-seismicity urban areas, recording a statistically representative number of high-quality signals may take years. Hence, the attempts to use ambient vibration instead have progressed. This includes the development of the hybrid site-to-reference spectral ratio (SSRh, enhancing the possibility of non-linear soil behaviour and liquefaction during strong earthquakes.

We perform fully non-linear wave propagation modelling which requires complex soil models and calibration of many geophysical and geotechnical parameters, including soil dilatancy parameters (Iai et al., 1990) if pore pressure development and cyclic loading of the sands are to be considered. In this study, we use mainly CPT (Cone Penetration Test) data to define the geotechnical parameters of the soil columns by employing different empirical relations (e.g. Robertson, 2009), and combining them with shear-wave velocity measurements. While dilatancy parameters are typically estimated using triaxial experiments and a trial-and-error method, we use the inversion procedure introduced by Roten (2014) that uses the Neighbourhood algorithm (Sambridge, 1999) to retrieve them directly from CPT. We extensively tested the procedure and conclude that a realistic set of dilatancy parameters can be found in most cases if reasonable model space search ranges are defined. However, the inversion is sometimes highly non-linear and non-unique. Hence, it is important to calibrate the inversion algorithm to be explorative to find several local minima and test their influence.

For modelling the wave propagation in complex media, we use a fully-nonlinear finite-difference code NOAH (Bonilla et al., 2005) and apply input ground motions from 11 scaled waveforms. The waveforms are compatible with the elastic response spectrum for a return period of 975 years and a class "A" soil, as defined in the Swiss building code SIA261 (2020). We observe large variability of the results depending on the input ground motion. The preliminary results show some impact of non-linearity at low frequency compared to the linear response. In addition, for some fully-saturated sandy layers, we observe the onset of liquefaction (Figure 1). Because of the lack of strong motion observation in the area, the results cannot be verified against real data. To assess the impact of dilatancy parameters, we tested the 30 best sets obtained from the inversion. Mainly because of the thinness of the layers for which we consider the pore pressure effects, the influence is negligible. Nevertheless, the effect cannot be ignored for all sites and the experiments with randomized sets of dilatancy parameters show a much greater influence of the choice of dilatancy parameters.

## REFERENCES

- Bonilla, L. F., Archuleta, R., & Lavallée, D. 2005: Hysteretic and dilatant behavior of cohesionless soils and their effects on nonlinear site response: Field data observations and modeling. *Bulletin of the Seismological Society of America*, 95, 2373–2395.
- Iai, S., Matsunaga, Y., & Kameoka, T. 1990: Parameter Identification for a Cyclic Mobility Model (Report of the Port and Harbour Research Institute Vol. 29, No. 4, pp. 57–83).
- Janusz, P., Perron, V., Knellwolf, C., & Fäh, D. 2022: Combining Earthquake Ground Motion and Ambient Vibration Recordings to Evaluate a Local High-Resolution Amplification Model—Insight From the Lucerne Area, Switzerland. *Frontiers in Earth Science*, 10. <https://doi.org/10.3389/feart.2022.885724>
- Robertson, P. 2009: Interpretation of cone penetration tests—A unified approach. *Canadian Geotechnical Journal*, 46, 1337–1355. <https://doi.org/10.1139/T09-065>
- Roten, D. 2014: Documentation of tools for analysis of nonlinear soil behavior.
- Sambridge, M. 1999: Geophysical inversion with a neighbourhood algorithm—I. Searching a parameter space. *Geophysical Journal International*, 138(2), 479–494. <https://doi.org/10.1046/j.1365-246X.1999.00876.x>
- SIA261. 2020: Actions on Structures, SIA 261. Swiss Standards, Swiss Society of Engineers and Architects.

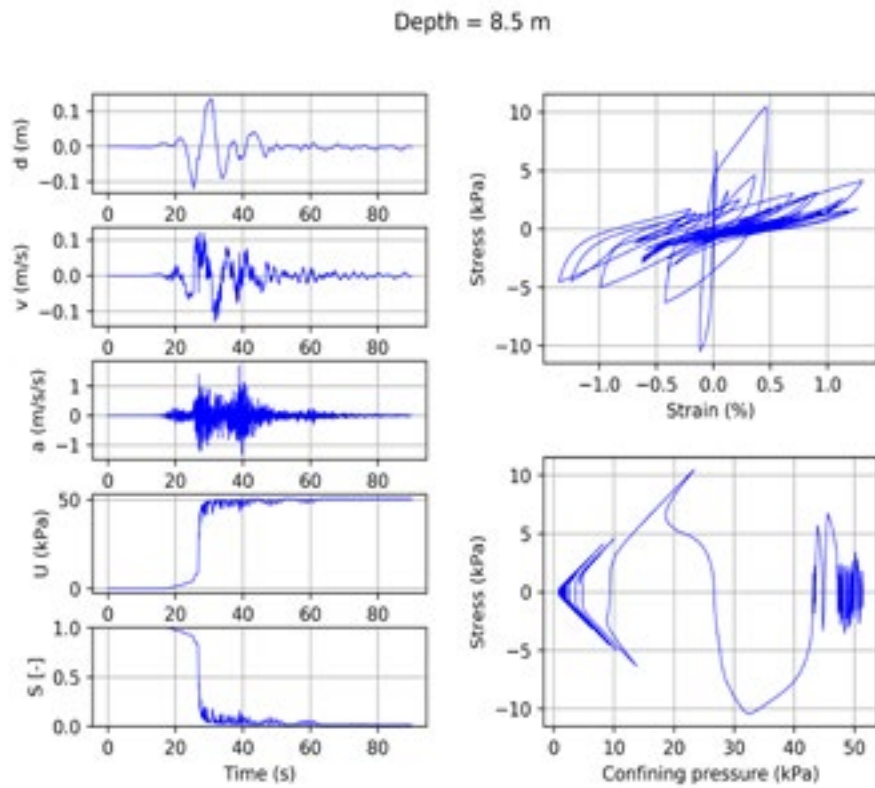


Figure 1. An example of 1D non-linear wave propagation simulation for a fully-saturated sandy layer at depth of 8.5 m. Left panel from the top: displacement, velocity, acceleration, pore pressure, and dimensionless dilatancy parameter  $S$  ( $S=0$  when pore pressure exceeds confining pressure and liquefaction starts). Right panel from the top: stress-strain relation and stress-confining pressure relation.

## 7.7

# Seismic evaluation of an existing pile group on liquefiable soil

Konstantinos Kassas<sup>1</sup>, Lampros Sakelariadis<sup>1</sup>, Alexandru Marin<sup>1</sup>, Ioannis Anastopoulos<sup>1</sup>

<sup>1</sup> Institute of Geotechnical Engineering, ETH Zürich, Stefano-Francini-Platz 5, CH-8093 Zürich (kkassas@ethz.ch)

This study outlines the seismic evaluation of an existing pile group supporting a motorway bridge. The critical aspects are related to the strength and stiffness parameters of the local soil, which appear to be decreasing significantly with depth. Moreover, some of the soil layers at the location of the pile group may be susceptible to pore pressure build-up or soil liquefaction during seismic shaking. Based on the available geotechnical data (borehole logs, classification tests, and Standard Penetration Test) the soil profile is described and the required soil parameters for the subsequent analyses are determined. Two scenarios are considered; (a) non-liquefied layers; and (b) presence of liquefied layers.

The seismic bearing capacity, the stiffness of the pile group and its performance is assessed. The vertical and moment capacity of the pile group are compared to the provided design loads. The assessment is performed through thoroughly validated 3D nonlinear finite element (FE) analyses. To this end, the reinforced concrete piles are modelled with the Concrete Damaged Plasticity (CDP) model (Abaqus, 2014). The FE analysis results for each structural member are verified against RC section analysis. Nonlinear soil behaviour is modelled with nonlinear constitutive models, appropriately selected for the soil materials encountered in the local stratigraphy (Fig. 1). Appropriate interface elements are used, capable of modelling the geometric nonlinearities due to sliding and detachment at the soil-pile, and soil-pile cap interface.

The liquefaction susceptibility assessment is conducted using different approaches of increasing level of complexity. Initially, the liquefaction susceptibility is investigated through hand calculations (Idriss & Boulanger, 2008). Subsequently, detailed effective stress 1D site response analysis is conducted. It is concluded that the liquefaction risk is limited, but cannot be fully excluded in view of the uncertainties related to insufficient soil investigation. Based on the worst case scenario investigated, the settlements solely due to partial soil liquefaction may reach 10 cm. The structural verification of the bridge superstructure should be conducted for this level of deformation.

Although the risk of liquefaction is limited, the seismic performance of the foundation is further assessed, conservatively assuming full liquefaction of the critical layer and a residual undrained shear strength (Stark & Mesri 1992). The performance of the pile group foundation under these conditions is evaluated for vertical (static) and horizontal (seismic) loading in both directions (longitudinal and transverse). It is shown that even under such conservative assumptions, retrofit measures are not justified since the critical compliance factor  $> 0.75$ .

## REFERENCES

- ABAQUS 6.11. (2014). Standard user's manual. Dassault Systèmes Simulia Corp., Providence, RI, USA.
- Idriss, I. M. & Boulanger, R. W. (2008). Soil liquefaction during earthquakes. Monograph MNO-12, Earthquake Engineering Research Institute, Oakland, CA.
- Stark, T.D. & Mesri, G. (1992). Undrained shear strength of liquefied sand for stability analysis. Journal of Geotechnical Engineering 118(11): 1727-1747
- Martin G. R., Lam I.P. (2000). Earthquake resistant design of foundations: retrofit of existing foundations. In: ISRM International Symposium, OnePetro, Melbourne, Australia.

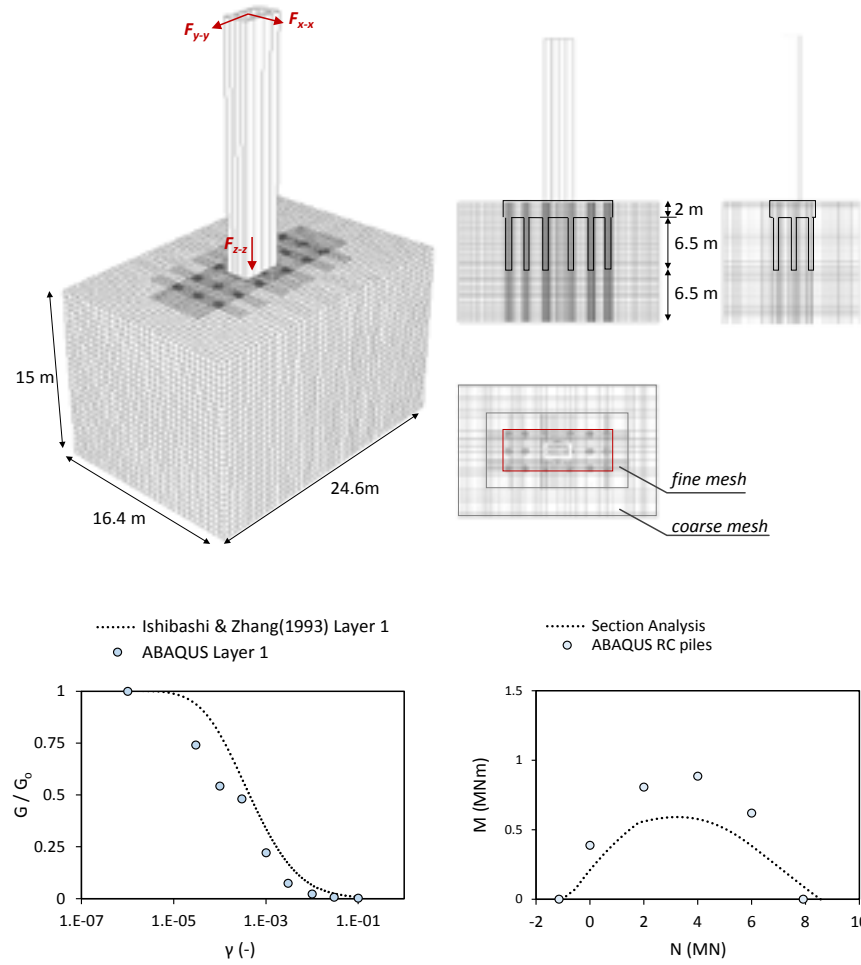


Figure 1: Overview, calibration and validation results of the Finite Element model in ABAQUS.

## 7.8

### Sa-based Fragility Model for Swiss Buildings

Alireza Khodaverdian<sup>1,2</sup>, Pierino Lestuzzi<sup>1</sup>

<sup>1</sup> EESD, Ecole Polytechnique Fédérale Lausanne (EPFL), Station 18, CH-1015 Lausanne, Switzerland.  
(alireza.khodaverdian@epfl.ch)

Earthquake is one of the most devastating natural disasters, which may cause adverse economic repercussions because of considerable damage to vulnerable structures. Although Switzerland is categorized as a low-to-moderate seismic zone in Europe, historical records show occurrence of large-magnitude earthquakes in Switzerland is probable and Swiss buildings are vulnerable to such events. Seismic risk assessment at the urban scale is of great importance as it paves the path for disaster preparedness measures, including pre-earthquake retrofitting and setting up insurance policies. Fragility model for existing buildings is one of the essential elements of risk assessment and plays a major role in a proper estimate of damages. In the framework of Earthquake Risk Model for Switzerland (ERM-CH), we considered different classes of Swiss buildings and their seismic performance is investigated by having several 3D numerical models with different numbers of stories. Sets of capacity curves are generated and then used for deriving fragility curves based on the methodology, with which different types of uncertainties in hazard and capacity of structures are captured. The fragility model, covering almost the whole portfolio of Swiss buildings, links the different damage grades to a measure of the ground motion intensity (i.e., spectral acceleration). The presented fragility curves have been also compared with those from independent studies as well as with I-based fragility curves, and well consistency has been observed, which indicates the robustness of the presented fragility model.

## 7.9

# Broadband waveform simulations of earthquake scenarios in the Swiss Molasse basin

Maria Koroni<sup>1</sup>, Miroslav Hallo<sup>1</sup>, Afifa Imtiaz<sup>1</sup>, Donat Fäh<sup>1</sup>

<sup>1</sup> Schweizerischer Erdbebendienst, Sonneggstrasse 5, CH-8092 Zürich ([maria.koroni@sed.ethz.ch](mailto:maria.koroni@sed.ethz.ch))

Numerical modelling of strong ground motion is an essential part of understanding earthquake recordings and explaining processes that affect seismic wave propagation. Moreover, the prediction and modelling of strong ground motions is an important input for seismic hazard assessment in particular when considering long return periods as required for buildings of special importance like hospitals, dams, power plants, or nuclear facilities. Switzerland is a country characterized by moderate seismic hazard, although the risk can be significant due to potential damage and financial losses. As we are missing strong motion recordings in Switzerland, numerical modelling is necessary to characterize future potentially damaging earthquakes. In this preliminary study, we first aim at modelling broadband waveforms originating from regional, small-to-moderate (roughly  $4 \leq Mw < 5.5$ ) earthquakes recorded in the Swiss Molasse basin. To achieve this, a numerical tool for simulating broadband waveforms is needed. We, therefore, use the SCEC hybrid broadband tool, which synthesizes low and high frequency waveforms and then combines them to obtain broadband waveforms. The goal of our study is twofold: i) to validate the method and models based on existing recorded events and ii) to simulate scenario earthquakes for frequencies up to 40 Hz, if possible. Firstly, we perform broadband waveform modelling for validation purpose by using the Mw 4.1 Urnerboden earthquake that occurred in central Switzerland on 6th of March 2017. The modelling is done for specific seismic stations with their shear-wave velocity models inferred from site characterization measurements. The simulations will allow us to properly apply the tool by comparing the synthetics to the recorded waveforms in both temporal and spectral domains and assess their level of similarity in order to proceed to the second goal of our research. We intend to use the broadband tool to simulate scenario earthquakes (i.e. Mw=5.5-6.5) which could occur in the future. Such events are of particular interest for assessing the seismic hazard of locations where geological disposal facilities will potentially be constructed.

## 7.10

# On the selection of design-compatible waveforms for microzonation purpose in Switzerland

Francesco Panzera<sup>1</sup>, Paolo Bergamo<sup>1</sup>, Laurentiu Danciu<sup>1</sup>, Donat Fäh<sup>1</sup>

<sup>1</sup> Swiss Seismological Service (SED) at ETH Zurich, Sonneggstrasse 5, CH-8092 Zürich ([francesco.panzera@sed.ethz.ch](mailto:francesco.panzera@sed.ethz.ch))

Ground motion selection is a key step of many applications in engineering seismology, such as seismic microzonation, which aims at identifying and characterizing the expected ground-motion level within risk-relevant areas.

In this contribution, we first determine the earthquake scenarios (i.e. magnitude-distance) relevant for the five seismic zones (Z1a, Z1b, Z2 Z3a and Z3b) defined in the Swiss seismic design code (SIA-261 2020); Such magnitude distance scenarios were obtained by disaggregating the ground shaking hazard of SUIhaz2015 (Wiemer et al 2016) for a return period of 475 years. These scenarios were reported at 774 geographical locations defined over a regular spatial grid (hereinafter referred to as “nodes”), later grouped by seismic zone.

Second, we examine the waveforms and associated metadata of globally accessible strong-motion databases to define standards associated with the quality of three-component (3C) waveforms (compatibility to GMPE, adequate frequency content, absence of non-physical drift in velocity and displacement) and quality of metadata (reliability of magnitude, distance, site condition information, housing type, etc.).

The purpose of the analysis is to assess which site metadata are provided, to compare them across different databases, and to assess the feasibility of a sub-selection of stations which meet the pre-defined criteria (i.e. free-field stations with a reliable soil classification). Finally, in accordance with a common assumption in Europe (Eurocode8) we choose waveforms for soil class A.

In the next step, we define a strategy for the selection of ground motions for each seismic zone. Among the existing algorithms used to select waveforms, the most adaptable is the one proposed by Baker and Lee (2018). The key steps of the algorithm include the screening of the ground motion database for suitable motions, the simulation of response spectra from a target, the identification of ground motions whose spectra match each statistically simulated response spectrum, and the optimization to further improve their consistency with the target distribution (more details in Baker and Lee, 2018).

The Eurocode8 criteria are also used in this procedure to choose response spectra that are compatible with the seismic design recommendations. Since our selection is made for the purpose of microzonation, we fitted the target response spectrum i.e. the elastic response spectrum within the period range 0.02-2.0 s. The selection is made allowing linear scaling of the amplitudes. The maximum scaling factor is 2, the minimum is 0.5.

For each zone we selected all the possible combinations of 11 scaled waveforms. For instance, 53 compatible sets were found for Z1a with RMSE in the range 0.097 to 0.154 (e.g. left panel in Fig. 1).

Among these we select the dataset with the lowest RMSE if the majority waveforms fall within or nearby the disaggregation borders; otherwise we search for another dataset (e.g. right panel in Fig. 1).

## ACKNOWLEDGEMENTS

This work is made in the frame of the project Database for design-compatible waveforms financed by Federal Office for the Environment (FOEN).

## REFERENCES

- Baker J. and C. Lee, 2018. An improved algorithm for selecting ground motions to match a conditional spectrum. *Journal of Earthquake Engineering*, 22(4), 708-723.
- Eurocode 8, 2004, Design of structures for earthquake resistance, General rules, seismic actions and rules for buildings, European Standard, European Committee for Standardization.
- SIA261 (Società svizzera degli ingegneri e degli architetti), 2020. Azioni sulle strutture portanti. Società svizzera degli ingegneri e degli architetti, Zurigo, 2020.
- Wiemer S., Danciu L., Edwards B., Marti M., Fäh D., Hiemer S., Wössner J., Cauzzi C., Kästli P., Kremer K., 2016. Seismic Hazard Model 2015 for Switzerland (SUIhaz2015). Swiss Seismological Service (SED) at ETH Zurich, DOI: 10.12686/a2

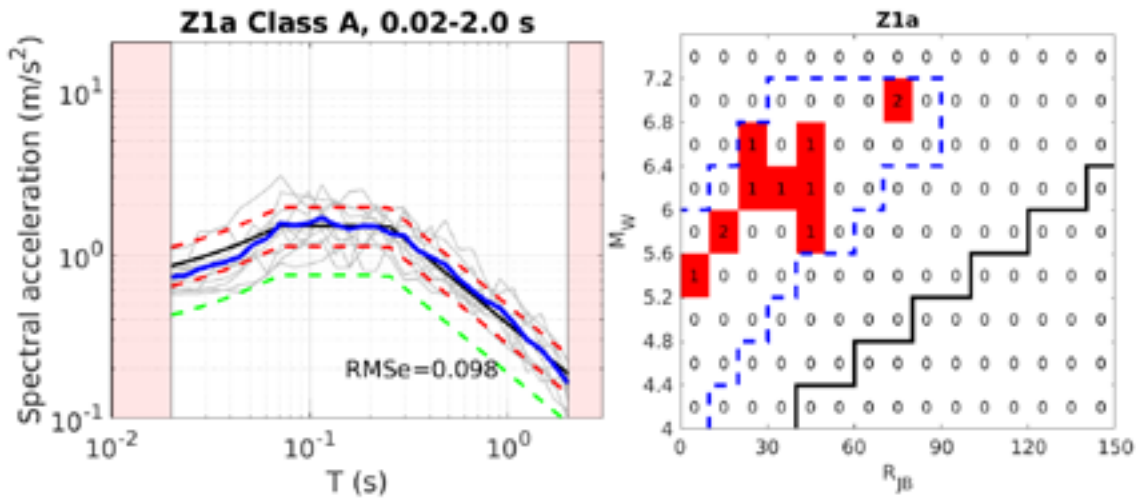


Figure 1. Left panel extracted sets of  $n=11$  response spectra from scaled waveforms (gray lines) using as target the SIA261 elastic response spectrum for the seismic zone Z1a (black line). Red dashed lines indicate the 1.3 and 0.75 ratio threshold for the average (blue line); the green dashed line indicates the 0.5 ratio threshold. Right panel selected number of recordings by bin of Joyner-Boore distances (10 km width) and M<sub>w</sub> (0.4 unit) for the selected set of waveforms for zone Z1a. The dashed blue line defines the range of scenarios from the disaggregation.

## 7.11

# Experimental testing of rubble stone masonry walls of varying size under in-plane quasi static loading

Savvas Saloustros<sup>1</sup>, Katrin Beyer<sup>1</sup>

<sup>1</sup>Laboratory of Earthquake Engineering and Structural Dynamics (EESD), School of Architecture, Civil and Environmental Engineering (ENAC), École Polytechnique Fédérale de Lausanne (EPFL), 1015 Lausanne, Switzerland  
 (savvas.saloustros@epfl.ch, katrin.beyer@epfl.ch)

Rubble stone masonry is a common construction typology of historical city centres and vernacular architecture. While past earthquakes have shown that it is one of the most vulnerable masonry typologies, there are few experimental campaigns giving quantitative information on the strength and displacement capacity, as well as on the damage pattern under in-plane horizontal loading (Rezaie et al., 2020; Vanin et al., 2017) existing criteria for estimating lateral strength and stiffness of stone masonry walls are reviewed and improvements proposed. The drift capacity of stone masonry walls is evaluated at six different limit states that characterise the response from the onset of cracking to the collapse of the wall. To provide input data for probabilistic assessments of stone masonry buildings, not only median values but also the corresponding coefficients of variation are determined. In addition, analytical expressions that estimate the ultimate drift capacity either as a function of masonry typology and failure mode or as a function of masonry typology, shear span and axial load ratio are proposed. The paper provides also estimates of the uncertainty related to the natural variability of stone masonry by analysing repeated tests and investigates the effect of mortar injections and the effect of the loading history (monotonic vs cyclic). Additionally, there is a lack of experimental studies looking into the role of the size of the structural element on the structural response of rubble stone masonry walls.

Here we present the results of an experimental campaign carried out at École Polytechnique Fédérale de Lausanne (EPFL) for the investigation of the in-plane seismic response of rubble stone masonry walls. Nine rectangular walls of three different sizes were constructed by experienced masons using irregular limestone units and lime mortar. The variation of the size aimed at investigating the potential size effect on the pre- and post-peak response of rubble stone masonry. The mechanical properties on the unit and wall level were obtained through mechanical characterization tests on mortar samples and wallets. The walls were tested at the Structural Engineering laboratory of EPFL under quasi-static loading using the same load and boundary conditions. All walls were tested up to axial load failure (i.e. up to the point where the walls cannot bear any vertical load), providing information on the drift levels at collapse of the wall. Digital image correlation measurements were used to obtain displacement fields and extract crack patterns during the load history. The results of this experimental campaign offer a first insight on the size effect on the in-plane response of rubble stone masonry walls. The experimental dataset, as well as the geometrical digital twinning of five of the nine tested walls, are valuable for the calibration of numerical models for rubble stone masonry.

## REFERENCES

- Rezaie, A., Godio, M., & Beyer, K. (2020). Experimental investigation of strength, stiffness and drift capacity of rubble stone masonry walls. *Construction and Building Materials*, 251, 118972. <https://doi.org/10.1016/j.conbuildmat.2020.118972>
- Vanin, F., Zaganelli, D., Penna, A., & Beyer, K. (2017). Estimates for the stiffness, strength and drift capacity of stone masonry walls based on 123 quasi-static cyclic tests reported in the literature. *Bulletin of Earthquake Engineering*, 15(12), 5435–5479. <https://doi.org/10.1007/s10518-017-0188-5>

## 7.12

### Seismic response of subaqueous slopes in Lake Lucerne

Anastasiia Shynkarenko<sup>1</sup>, Carlo Cauzzi<sup>1</sup>, Katrina Kremer<sup>1,2</sup>, Paolo Bergamo<sup>1</sup>, Agostiny Marrios Lontsi<sup>1</sup>, Paulina Janusz<sup>1</sup>, Donat Fäh<sup>1</sup>

<sup>1</sup> Swiss Seismological Service, ETH Zurich, Sonneggstrasse 5, CH-8092, Zurich ([a.shynkarenko@sed.ethz.ch](mailto:a.shynkarenko@sed.ethz.ch))

<sup>2</sup> Institute of Geological Sciences and Oeschger Centre for Climate Change Research, Baltzerstrasse 1+3, CH-3012, Bern, Switzerland

Subaqueous lake slopes can experience seismically- and aseismically-triggered failures with potential for tsunami generation. Worldwide, most of historically- and sedimentologically-documented lake slope failures and tsunamis are associated with seismic activity (e.g., Kremer et al. 2021). In Switzerland, the occurrence of such events during the past 20'000 years was confirmed for several lakes, e.g., for Lake Geneva in 1584 and for Lake Lucerne in 1601 (e.g., Hilbe and Anselmetti 2014; Schwarz-Zanetti et al. 2018). Nowadays, lake shores are highly vulnerable to such events due to their dense population and developed infrastructure. Thus, the investigation of seismic response of subaqueous lake slopes plays a key role in the evaluation of their failure potential and tsunami hazard assessment for the lake shores.

During 2018-2022, we performed more than 160 single-station measurements in Lake Lucerne (Fig. 1) with Ocean Bottom Seismometers (OBS). During these measurements, both ambient vibrations and earthquake signals were recorded. The main goals of these measurements were to assess the subsurface structure and shear-wave velocity profiles at selected lake slopes (Shynkarenko et al. 2021) and to evaluate their seismic response (Shynkarenko et al. 2022).

Primary descriptors of the seismic response measured at investigated locations are the fundamental frequency of resonance (from the H/V ratio) and the frequency-dependent amplification function (at locations with enough earthquake records; Fig. 1). Overall, we observe spatially variable site response even on a local scale. Resonance frequencies are within the range of 0.5–4 Hz. Estimated amplification factors are very high and often exceed the value of 50–100 in the frequency range of 1–10 Hz. These results are supplementary to previously retrieved shear-wave velocity profiles which resolve the subsurface structure and lithological composition at six sites down to the depths of 60–150 m.

Next, we performed a back-analysis of past seismically-triggered slope failures and lake tsunamis in Switzerland. We estimated the return period for such events to be in the range of 36–224 years. Also, we evaluated the lake slope failure-triggering threshold in terms of moment magnitude and epicentral distance; macroseismic intensity; and earthquake ground motion intensity measures at reference rock conditions ( $v_{s30} = 1105 \text{ m/s}$ ). More specifically, the most probable minimum critical values of PGA and PGV at the rock reference are  $0.176 \text{ m/s}^2$  and  $0.013 \text{ m/s}$ , respectively. Corresponding macroseismic intensities in the EMS scale are in the range of IV 9/10 – V 2/5 at the rock reference or V 2/5 – V 4/5 at a soil reference with  $v_{s30} = 600 \text{ m/s}$ .

To summarize, obtained results provide a qualitative and quantitative description of the seismic response of subaqueous lake slopes which is crucial for the future 2D or 3D numerical modeling of site behavior under seismic impact.

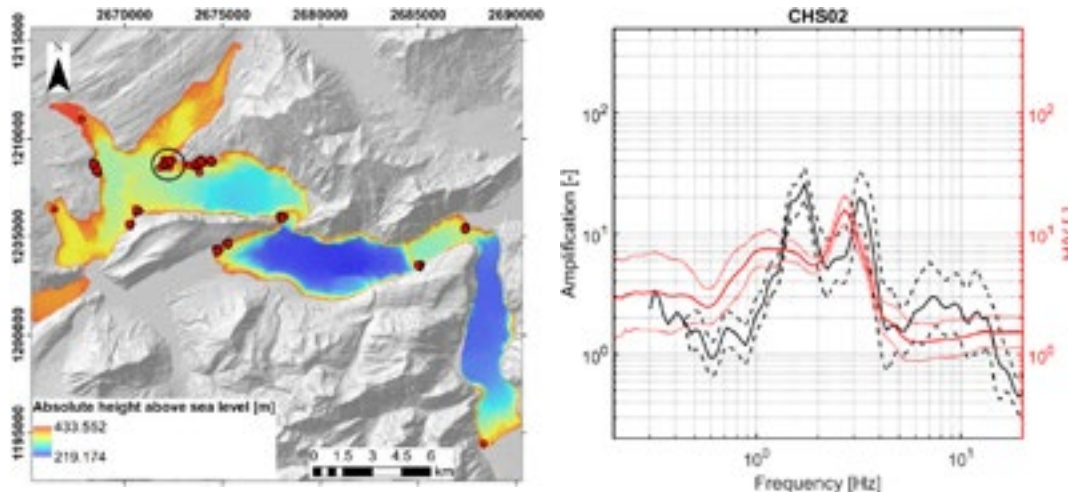


Figure 1. Left – a map with the locations of OBS measurements (red circles) in Lake Lucerne; right – amplification function and H/V ratio at site CHS02 located inside the black circle on the left figure.

## REFERENCES

- Hilbe, M. & Anselmetti, F.S. (2014). Signatures of slope failures and river-delta collapses in a perialpine lake (Lake Lucerne, Switzerland), *Sedimentology*, 61(7), 1883–1907, doi: 10.1111/sed.12120.
- Schwarz-Zanetti, G., Fäh, D., Gache, S., Kästli, P., Loizeau, J., Masciadri, V., & Zenhäusern, G. (2018). Two large earthquakes in western Switzerland in the sixteenth century: 1524 in Ardon (VS) and 1584 in Aigle (VD). *Journal of Seismology*, 22, 439–454, doi:10.1007/s10950-017-9715-8.
- Kremer, K., Anselmetti, F.S., Evers, F.M., Goff, J., & Nigg, V. (2021). Freshwater (paleo)tsunamis – a review, *Earth-Science Reviews*, 212, 103447, doi: 10.1016/j.earscirev.2020.103447.
- Shynkarenko, A., Lontsi, A.M., Kremer, K., Bergamo, P., Hobiger, M., Hallo, M., & Fäh, D. (2021). Investigating the subsurface in a shallow water environment using array and single-station ambient vibration techniques, *Geophysical Journal International*, 227(3), 1857–1878, doi:10.1093/gji/ggab314.
- Shynkarenko, A., Cauzzi, C., Kremer, K., Bergamo, P., Lontsi, A.M., Janusz, P., & Fäh, D. On the seismic response and earthquake-triggered failures of subaqueous slopes in Swiss lakes, subm. to *Geophysical Journal International*.

## 7.13

# On the development of a simplified analysis method for piled foundations subjected to seismic excitation

Max Sieber<sup>1</sup>, Ioannis Anastasopoulos<sup>1</sup>

<sup>1</sup> Institute of Geotechnical Engineering, ETH Zürich, Stefano-Francini-Platz 5, CH-8093 Zürich  
 (max.sieber@igt.baug.ethz.ch)

Relatively recent research on the response of surface foundations to seismic shaking indicates that full mobilisation of bearing capacity or sliding at the soil-foundation interface may have a beneficial effect on structural integrity – especially in the case of seismic motions that exceed the design limits (Martin & Lam, 2000; Pecker, 2003; Gajan et al., 2005; Anastasopoulos et al., 2010; Sakellariadis et al., 2020). Similar observations have been made for piled foundations that are allowed to fully mobilise their moment capacity (Sakellariadis et al., 2019). Unlike the conventional seismic design (Fig. 1, on the left), where failure is guided to the superstructure by “overdesigning” the foundation, allowing full mobilisation of the foundation moment capacity guides failure to the soil and the soil-pile interface (Fig. 1, on the right). Such a mechanism acts as a safety valve protecting the superstructure, as it limits the inertia loading, which can be transmitted to the superstructure. This is of particular interest for the retrofit of existing structures, which were typically designed and constructed long before the adoption of modern seismic design provisions. Due to the historical development in central Europe (for example), this includes a large share of existing bridges. In this context, full mobilisation of foundation moment capacity may prevent foundation strengthening, leading to significant savings in the construction effort.

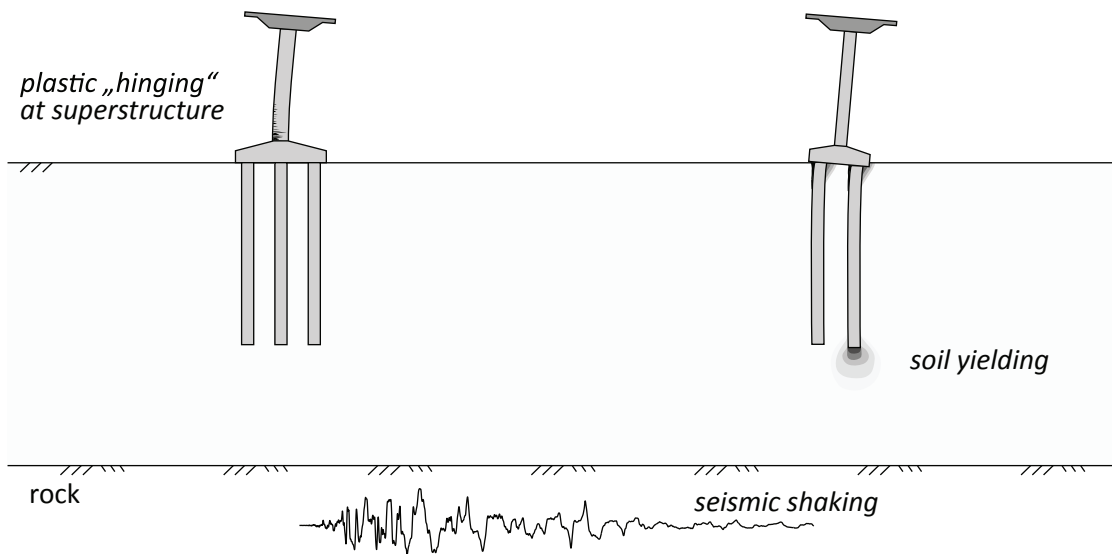


Figure 1: Schematic illustration of the: conventional seismic design (left); and allowing full mobilisation of the foundation moment capacity (right).

However, to allow full mobilisation of foundation moment capacity, dynamic time history analysis is necessary to ensure that permanent foundation rotation and settlement are within serviceability limits. This calls for nonlinear 3D finite element (FE) analysis of the entire soil-foundation-structure system. Especially in the case of pile groups, such 3D FE models are computationally intensive, as there is a need for mesh refinement in the vicinity of the pile tip. As a result, the required computational effort is excessive, even for pile groups containing a small number of piles.

Furthermore, developing such rigorous 3D FE models is a complex task requiring expert knowledge. This study makes a first step towards developing a simplified analysis method, where the entire soil-pile-foundation system is replaced with an assembly of hysteretic elements. Comparison with a benchmark 3D FE analysis reveals the key limitations and the potential of such an approach.

## REFERENCES

- Anastasopoulos I., Gazetas G., Loli M., Apostolou M., Gerolymos N. (2010). Soil failure can be used for seismic protection of structures. *Bulletin of Earthquake Engineering*, 8, 309-326.
- Gajan S., Kutter B. L., Phalen J. D., Hutchinson T. C., Martin G. R. (2005). Centrifuge modeling of load-deformation behavior of rocking shallow foundations. *Soil Dynamics and Earthquake Engineering*, 25(7-10), 773-783.
- Martin G. R., Lam I.P. (2000). Earthquake resistant design of foundations: retrofit of existing foundations. In: ISRM International Symposium, OnePetro, Melbourne, Australia.
- Pecker A. (2003). Aseismic foundation design process, lessons learned from two major projects: the Vasco de Gama and the Rion Antirion bridges. In: ACI international conference on seismic bridge design and retrofit, University of California at San Diego, La Jolla, USA.
- Sakellariadis L., Marin A., Anastasopoulos I. (2019). Widening of existing motorway bridges: pile group retrofit versus nonlinear pile soil response. *Journal of Geotechnical and Geoenvironmental Engineering*, 145(12), 04019107
- Sakellariadis L., Anastasopoulos I., Gazetas G. (2020). Fukae bridge collapse (Kobe 1995) revisited: New insights. *Soils and Foundations*, 60(6), 1450-1467

## P 7.1

# Seismology-at-School across Switzerland: project nucleation and growth

György Hetényi<sup>1,2</sup>, Anne Sauron<sup>3</sup>, Maren Böse<sup>4</sup>, Romain Roduit<sup>3,5</sup>, Shiba Subedi<sup>1,6</sup>, Irina Dallo<sup>4</sup>, and the already involved teachers of Swiss schools

<sup>1</sup> Institute of Earth Sciences, University of Lausanne, CH-1015 Lausanne ([gyorgy.hetenyi@unil.ch](mailto:gyorgy.hetenyi@unil.ch))

<sup>2</sup> Centre Interdisciplinaire de Recherche sur la Montagne (CIRM), University of Lausanne, CH-1967 Bramois/Sion

<sup>3</sup> HES-SO Valais-Wallis, CH-1950 Sion

<sup>4</sup> Swiss Seismological Service, ETH Zürich, CH-8092 Zürich

<sup>5</sup> Espace des Inventions, CH-1007 Lausanne

<sup>6</sup> Seismology-at-School in Nepal, NP-33700 Pokhara, Nepal

One of the most direct and also longest lasting impact of research on society is providing correct education material to schools. This requires not only the selection of content and tailoring the format to the level of the respective classes, but also training the teachers and supporting them in the implementation of teaching tasks.

Teaching seismology in the classroom carries a lot of potential, not only in countries with a high level of seismic activity. Beyond the discussion of what earthquakes are, why and how they happen, and how to behave before, during and after an earthquake, a variety of other topics can be presented in the classroom. What is a probability? What is the difference between hazard and risk? What kind of tools exist to detect and locate earthquakes? What is the IT background to run an observation and alerting network? What are the societal impacts of seismicity and how to communicate around earthquakes?

For these reasons, based on our own experiences and a few international examples, we have (re)launched the seismology-at-school program throughout Switzerland. The program is strongly rooted in the activities and history of the Centre Pédagogique Prévention Séisme (Sion) since 2014 ([www.cpps-vs.ch](http://www.cpps-vs.ch)) and the Seismology-at-School in Nepal program (Subedi et al. 2020) co-run by the University of Lausanne, and also benefits from the recent exhibit “Tic-Tac-Tectonique” at the “Espace des Inventions” in Lausanne.

The program stands on two main pillars. First, we install low-cost seismic sensors at schools which serve both educational and observational purposes. In quiet conditions these sensors can detect waves from a magnitude 1 earthquake at 50 km distance. Second, we prepare educational material and activities for teachers to teach seismology in the classroom, including demonstrations and hands-on work for students with the seismometers. Following an initial training session for interested teachers, our team continues to support them for both technical and scientific matters.

In practice, a first RaspberryShake seismometer was installed in the Valais for testing purposes in March 2019, and its operation has convinced us that this type of sensor is best suited for our program: it is easy to install, provides good quality data right out of the box, and is affordable (500 USD for a 1-component sensor). In the nucleation phase of the project, an invitation was sent to 9th grade teachers in the cantons of Valais and Vaud to participate in the program. Over 30 teachers from 22 schools responded, and by Spring 2022 seismometers in 21 schools have been installed. First feedback from the teachers is positive, and a joint discussion on the educational part is planned in November 2022. Further growth is planned by involving German speaking schools, an effort led by the Swiss Seismological Service at ETH Zurich. The low-cost seismic network also grows thanks to interested institutions and geoscience researchers, and currently counts 26 operational stations. All RaspberryShake seismometers are visible at [stationview.raspberryshake.org](http://stationview.raspberryshake.org) or in the ShakeNet app, and all data is freely and openly available.

Challenges for further growth exist, and include coordination between French and German speaking parts. Further challenges arise from the diversity of cantonal educational programs (i.e. content and timing of teaching curricula), which will require adaptations and flexibility of our program. Technical improvements to find lower noise-level spots within the respective school domains, as well as direct data transfer to the Swiss Seismological Service are also on our agenda.

Participation of further schools is warmly welcome, and we invite any interested teacher or school director to contact us.

## REFERENCES

- Subedi, S., Hetényi, G., Denton, P., & Sauron, A. 2020: Seismology at School in Nepal: a program for educational and citizen seismology through a low-cost seismic network, *Front Earth Sci*, 8, 73. doi:10.3389/feart.2020.00073

## P 7.2

# Moment Tensors for small to moderate magnitude earthquakes in Switzerland

Maria Mesimeri<sup>1</sup>, Tobias Diehl<sup>1</sup>, John Clinton<sup>1</sup>, Marco Herwegh<sup>2</sup>, and Stefan Wiemer<sup>1</sup>

<sup>1</sup> Swiss Seismological Service, ETH Zurich, Zurich, Switzerland

(maria.mesimeri@sed.ethz.ch, tobias.diehl@sed.ethz.ch, john.clinton@sed.ethz.ch, Stefan.wiemer@sed.ethz.ch)

<sup>2</sup> Institute of Geological Sciences, University of Bern, Bern, Switzerland (marco.herwegh@geo.unibe.ch)

Computing moment tensors (MT) after a big earthquake is crucial for identifying the faulting mechanism and to determine the moment magnitude (Mw), especially when other magnitude scales saturate. For small to moderate magnitude earthquakes (usually M<3.5) it is challenging to derive MTs from full waveform inversion and known methods are hampered by insufficient crustal models lacking the necessary resolution. However, it is equally important for the seismic hazard assessment to be able to compute MTs and especially Mw for small earthquakes, e.g. to derive improved scaling relationships between Mw and ML (local magnitude). To overcome problems associated with waveform modelling, we explored a method to compute MTs based only on amplitudes and first-motion P-wave polarities, which is implemented in the HybridMT algorithm (Kwiatek *et al.* 2016). Overall, we compile a database with more than a hundred stable and manually reviewed hybrid MTs spanning the last decade (2012–2021). The high-quality, dense seismic network in Switzerland maintained by the Swiss Seismological Service (SED) allowed us to successfully compute hybrid MTs for earthquakes with magnitude as low as M1.9. We compare the results of the hybridMT method with traditional waveform inversion techniques in terms of CLVD component, which describes the non double-couple part of the MT solution, and Mw. To check whether such CLVD component is real and not an artifact caused, for instance, by unmodeled heterogeneities or insufficient data, we compare the CLVD percentage from hybridMT solutions to the ones derived from waveform inversion methods that used multiple 1D velocity models. For the Mw, we compare the results from hybridMT to other inversion methods, as well as to Mw that is calculated routinely at the SED using a spectral method. In addition, we compare the MT solutions (fault planes) to existing high-quality focal mechanisms computed using first motion polarities and to high-precision double difference locations. Uncertainties of hybrid MT solutions are estimated using both jackknife and resampling methods. This work was carried out in the framework of the SeismoTeCH project funded by the Swiss Geophysical Commission (SGPK) and contributes towards an enriched high-quality focal mechanisms database for Switzerland. This catalogue could be used to revisit the regional to local stress field at unprecedented resolution and provides new insights into the complexities of active fault systems in the Central Alps region.

## REFERENCES

- Kwiatek, G., Martínez-Garzón, P. & Bohnhoff, M. (2016) HybridMT: A MATLAB/Shell Environment Package for Seismic Moment Tensor Inversion and Refinement. *Seismol. Res. Lett.*, 87, 964–976. doi:10.1785/0220150251



# 8 Deep geothermal energy, CO<sub>2</sub>-storage and energy-related exploration of the subsurface

Christophe Nussbaum, Marie Violay, Daniela van den Heuvel, Benoît Valley

TALKS:

- 8.1 Carbajal-Martínez D., Wanner C., Diamond L.W.: Fault-hosted non-magmatic coastal geothermal systems, insights from La Jolla Beach, Baja California, Mexico
- 8.2 Crinière A., Eruteya O.E., Moscariello A.: Characterization of the seismic morphology and sedimentary infill of karsts occurring at the Cretaceous Cenozoic Transition sequence boundary in the Geneva Basin and neighbouring France – Implication for Geo-energy prospectivity
- 8.3 Decker K., Levi N., Oppenauer L., Weissl M.: Active faults and the hazard of triggered seismicity in the exploration and production of deep geothermal reservoirs: the Vienna case study
- 8.4 Ermert L., Lanza F., Shi P., Tuinstra K., Wiemer S.: Modeling induced micro-earthquakes for an experimental enhanced geothermal system site
- 8.5 Guglielmetti L., Danillidis A., Valley B., Moscariello A.: Application of spatial multi-criteria play-based analysis to high-temperature aquifer thermal energy storage. The Swiss Molasse Basin case study
- 8.6 Heuberger S., Morgenthaler J. & Galfetti T.: Lithium extraction from geothermal brines in Switzerland?
- 8.7 Jiménez J., Blasco M., Auqué L.F., Gimeno M.J.: Geothermometrical modelling applied to the CO<sub>2</sub>-rich thermal waters of the Caldas de Malavella hydrothermal system in Gerona (Spain) and lessons learnt for the geological storage of CO<sub>2</sub> in granitic rocks.
- 8.8 Kong X.-Z., Wang X., Lima M.G., Kuhn K., Mangold D., Ma J., Saar M.O.: Core-scale chemical and hydraulic stimulations on fractured rocks
- 8.9 Makhlofi Y., Guglielmetti L., Mondino F.: Multi-criteria play based analysis for geothermal energy potential evaluation in sedimentary basins: an example from North-Eastern Switzerland.
- 8.10 Mondino F., Giroud N., Marchant R.: Analysis of the regional structural elements of the Lausanne region (VD) in support of geothermal exploration
- 8.11 Moscariello A., Haas M., Meftah E., Le Cotonnec A., Makhlofi Y.: 3D geological modelling in support of CERN's Future Circular Collider ~100-km long tunnel infrastructure (Geneva Basin, Switzerland-France): synergies or conflicts with geo-energy resources?
- 8.12 Munoz-Burbano F., Calo M., Reyes-Orozco V., Lupi M.: Monitoring geothermal operations with noise interferometry at the Domo de San Pedro, Nayarit – Mexico
- 8.13 Schwendener D., Naets I., Kong X.-Z.: Velocity Quantification (PIV) in Two-Phase Drainage and Imbibition Processes in Rough Wall Fractures.
- 8.14 Spillmann T., Hoelker A., Madritsch H., Merz K., Hertrich M., Birkhäuser Ph.: 3D-seismic exploration for radioactive waste repository siting in Switzerland: acquisition and processing strategy
- 8.15 Stavropoulou E., Moscariello A., Zappone A., De Haller A., Eruteya O.E., Madonna C., Guglielmetti L., Laloui L., Mazzotti M., Wiemer S.: DemoUpStorage: Storing Swiss CO<sub>2</sub> in Basalts
- 8.16 van den Heuvel D.B., Wanner C., Guglielmetti L., Martin F., Meyer M., Lutz S., Benning L.G., Diamond L.D.: Corrosion and scaling inside a low-enthalpy geothermal well during shut-in

- 8.17 Vietor T., Schnellmann M., Giger S., Landgraf A., Traber D., Madritsch H., Braun M.: Keynote presentation: Geological Reasoning for the Site of the Swiss Nuclear Waste Repository
- 8.18 Yapparova A., Lamy-Chappuis B., Driesner T.: Numerical simulations of supercritical geothermal resource utilization
- 8.19 Zabihian F., Sohrabi R., Alcolea A., Meier P., Valley B.: Deriving full stress tensor profile from borehole failure observations

**POSTERS:**

- P 8.1 Fakhretdinova R., Sáez A., Lecampion B.: Semi-analytical solution for the asymmetrical propagation of fluid-induced frictional shear rupture due to an in-situ linear stress gradient.
- P 8.2 Gallyamov E., Lecampion B., Molinari J-F.: Numerical Scheme for the Large-scale Geomechanical Simulations of CO<sub>2</sub>-storage
- P 8.3 Liardon T., Kolinski J., Lecampion B.: Influence of roughness on the stress dependent permeability of a fracture: Experimental evidences
- P 8.4 Pezzulli E., Matthai S.K., Driesner T.: Fracture aperture distributions of geomechanically-stressed fractured reservoirs
- P 8.5 Savard G., Planès T., Lupi M. and the Crustal Deformation and Fluid Flow Group: Imaging deep shear-wave velocity structures for geothermal exploration with Ambient Noise Tomography and dense geophone arrays: a tale of two case studies at Aargau and Riehen, Switzerland
- P 8.6 Scheidler S., Dreßmann H., Epting J.: Regional-Scale Thermal Hydraulic Modeling for Preliminary Geothermal Potential Assessment – A Theoretical Approach using the example of Riehen
- P 8.7 Toussaint G., Sohrabi R., Duhamel R., Perez R., Jolivet M., Valley B.: Induced seismicity in Enhanced Geothermal System (EGS): Insights from the Vendenheim project, France

## 8.1

# Fault-hosted non-magmatic coastal geothermal systems, insights from La Jolla Beach, Baja California, Mexico

Daniel Carbajal<sup>1</sup>, Christoph Wanner<sup>1</sup>, Larryn W. Diamond<sup>1</sup>

<sup>1</sup> Institut für Geologie, Universität Bern, Baltzerstrasse 1+3, CH-3012 Bern (daniel.carbajal@geo.unibe.ch)

Non-magmatic coastal geothermal systems are linked to orogenic belts and permeable fault zones that allow the infiltration of meteoric water and the diffuse discharge of Na-Cl hot water visible at low tide in the intertidal zone. In order to assess their potential for geothermal power production or seawater desalination, more fundamental insights are needed to understand how these systems work and why they are located in the coastal zone. This study focuses on the non-magmatic geothermal system of La Jolla beach hosted by the dextral Agua Blanca Fault (ABF) in Baja California, Mexico. Thermal-InfraRed drone surveys and thermocouple measurements record temperatures up to 94 °C at 20 cm below La Jolla beach (Carbajal-Martínez et al., 2020). This represents one of the hottest observed for non-magmatic systems worldwide. Here, we present 3D coupled thermal-hydraulic simulations carried out with the software Toughreact. Our numerical model covers a large 3D domain of 34×12×11.5 km (x, y, z) (i) to assess the role of surface topography and nearshore seafloor bathymetry in controlling regional water circulation in the ABF and (ii) to obtain a fundamental understanding of the processes that cause the strong thermal anomaly at La Jolla beach. Modeling results indicate that the hydrostatic pressure from the mountains and the Pacific Ocean and the high permeability of the ABF (e.g., fault width 45 m and  $k = 4 \times 10^{-14} \text{ m}^2$ ) lead to hot water upflow beneath La Jolla Beach (<100 °C), which occurs independently of the fault width and permeability. However, the permeability of the ABF along the Pacific Ocean must be lower than inland (e.g., fault width 45 m and  $k = 4 \times 10^{-15} \text{ m}^2$ ). In conclusion, the topography induces strong hydraulic head gradients, driving the infiltration of meteoric water deep into the crystalline basement. The extended hydraulic connectivity along the permeable ABF plane then facilitates the collection and circulation of meteoric water at greater depths. Finally, the hydrostatic pressure of the Pacific Ocean acts as a barrier that prevents the circulation of meteoric water beyond the coastline. For that reason, the highest hydraulic head gradient along the entire ABF is in the coastal zone, which, combined with the high permeability of the ABF, generates an upflow zone of hot water beneath La Jolla beach.

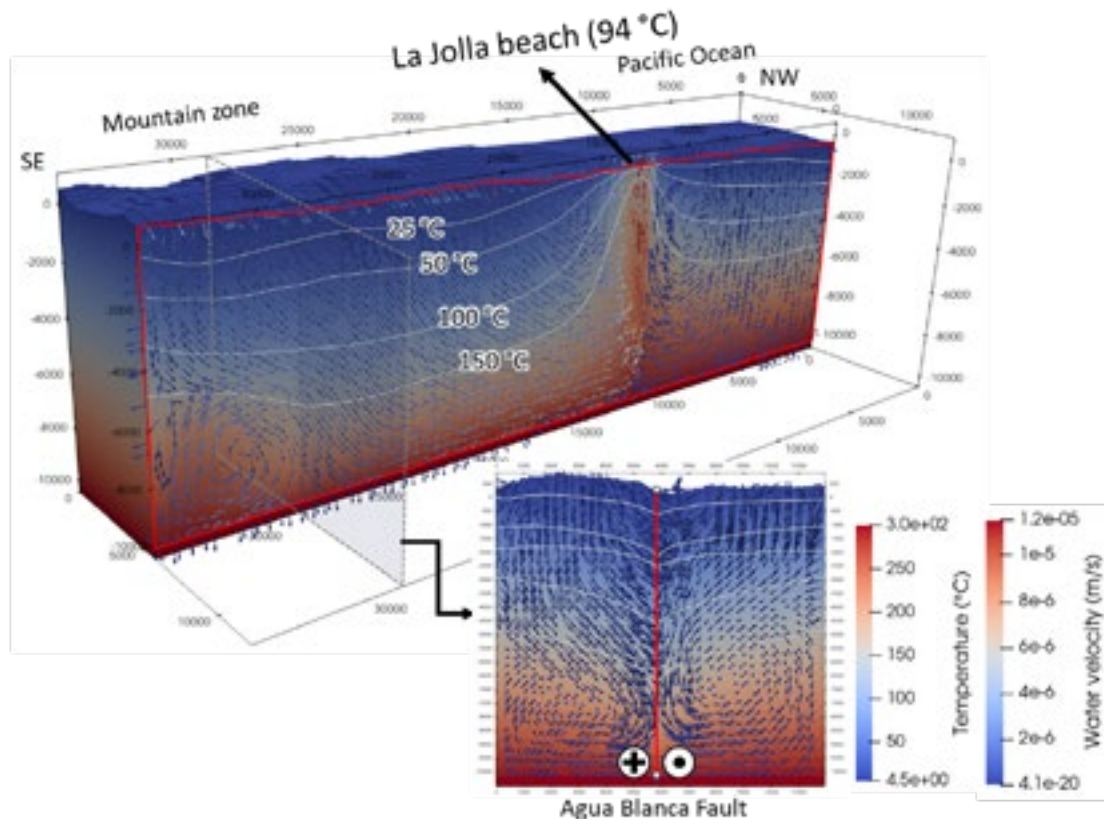


Figure 1. 3D thermal and hydraulic simulation of La Jolla beach, Baja California, Mexico.

## REFERENCES

- Carbajal-Martínez, D., Peiffer, L., Hinojosa-Corona, A., Trasviña-Castro, A., Arregui-Ojeda, S.M., Carranza-Chávez, F.J., Flores-Luna, C., Méndez-Alonso, R., Inguaggiato, C., Casallas-Moreno, K.L., 2020. UAV-based thermal imaging and heat output estimation of a coastal geothermal resource: La Jolla beach, Baja California, Mexico. *Renewable Energy*, 168, 1364-1376.

## 8.2

# Characterization of the seismic morphology and sedimentary infill of karsts occurring at the Cretaceous Cenozoic Transition sequence boundary in the Geneva Basin and neighbouring France – Implication for Geo-energy prospectivity

Aurélia Crinière<sup>1</sup>, Ovie Emmanuel Eruteya<sup>1</sup>, Andrea Moscariello<sup>1</sup>

<sup>1</sup> GE-RGBA Group, Department of Earth Sciences, University of Geneva, Rue des Maraîchers 13, CH-1205 Geneva, Switzerland (ovie.eruteya@unige.ch; aurelia.criniere@unige.ch; andrea.moscariello@unige.ch )

Since 2014, the Geneva Basin has become a region where intense geothermal exploration activities have been carried out to achieve the energy-transition goals towards an ultimate net-zero future by 2050. One of the challenges in identifying economically viable drilling locations is to understand and predict the subsurface heterogeneities. This has been well demonstrated by the result of the newly drilled GGeo-02 borehole which encountered a surprising c. 150 m thick Siderolithic sediments, presumably of Eocene age, known to likely infill karst structures developed in the Molasse Basin at the Cretaceous Cenozoic Transition (CCT). Here, we investigate the seismic characteristics of karst features and their infill by adopting a workflow integrating outcrop analogues, e-logs and cuttings's petrographical and geochemical composition from the GGeo-02 well, seismic interpretation, and seismic attribute analysis using a 2D seismic reflection dataset.

In the study area, karsts developed over the CCT sequence boundary are characterized by different-end member seismic morphologies ranging from dissolution-based collapse features to large scale collapse structure and fault-bounded depressions. The karst infill encountered in the GGeo-02 well and interpreted as Siderolithic deposits, have distinct seismic facies characterized by both higher and lower seismic/RMS amplitude compared to the host Lower Cretaceous carbonates unit. This arises from the discrepancies in the acoustic properties of the infill and the surrounding cretaceous sediments material and possible fluid content.

Karstification along the CCT is modulated by the structural re-organization of the Molasse foreland during the early phase of the Alpine orogeny resulting in the subaerial exposure of the Cretaceous carbonate substratum, change in base-level and the development of dissolution processes by meteoritic water which generated both epigeus and ipogeus karst features. Understanding their distribution, vertical and lateral extension and the nature of their infill is critical to assess correctly the role they can play in assessing the overall opportunities and risks of geothermal prospectivity of the study area. As an example, the results from the GGeo-02 borehole reveal that the Siderolithic karst-infill can consist of remarkable thickness of highly porous sandstone which would therefore form an excellent reservoir. On the other hand karsts may also represent geohazards during drilling operations because possible high fluid pressure or the presence of empty cavities where drilling tools can be damaged or lost with negative impact on the overall exploration campaign.

## 8.3

# Active faults and the hazard of triggered seismicity in the exploration and production of deep geothermal reservoirs: the Vienna case study

Kurt Decker<sup>1</sup>, Nicola Levi<sup>1</sup>, Lisa Oppenauer<sup>1</sup>, Michael Weiss<sup>1</sup>

<sup>1</sup> Department of Geology, University of Vienna, Josef Holaubek-Platz 2, A-1090 Vienna ([kurt.decker@univie.ac.at](mailto:kurt.decker@univie.ac.at))

In the last decades, the increasing need for renewable energies led to an exponential growth of enhanced geothermal projects in many parts of the World, including continental Europe. This led to several episodes of unpredicted seismicity, which in some instances brought to the temporary interruption of the geothermal activities or even to the complete cancelation of projects. The presumably most important mechanism causing unwanted seismicity is the injection of fluids into the subsurface, resulting in pore pressure build-up associated with the decrease of the effective normal stress acting on faults. The effect can lead to unpredicted fault slip and triggered seismicity, in which human intervention causes the initiation of the seismic rupture process while the subsequent rupture propagation is controlled by natural stress. In combination, both have the potential to trigger strong earthquakes with magnitudes that are only limited by the size of the triggered fault. Triggered seismicity is therefore an important issue for developing deep geothermal resources in tectonically active regions and in urban areas where both, the acceptance level and risk tolerance for unwanted seismic events is very low.

Exploration for deep geothermal resources in the city of Vienna therefore accounted for the hazard of triggered seismicity from an early stage of the project on. The aim was to exclude re-injection sites in the vicinity of active faults which must be assumed to be close to critical stress. The workflow included assessments of the recent geodynamic setting, the identification and mapping of active faults from a combination of 3D seismic data, high-resolution near-surface geophysics and paleoseismological techniques. In addition, a 1D-stress model was developed using data from an existing exploration well in the area. The results highlight a system of "conjugated" normal faults. Both of the "conjugated" fault sets contain active faults. Fault activity is proved by offset Quaternary sediments, geomorphological fault expressions and paleoseismological trenching that revealed evidence of repeated strong paleoearthquakes causing surface rupture. Image log data from the existing well proved a change of the SHmax orientation at a fault which parallels one of the active faults. The 1D-stress model from the same well indicates that this fault is close to critical stress.

The identified faults require to develop geothermal heat production with caution, to select a layout of production-reinjection wells that prevents injection in the intimate vicinity of critically stressed faults, and to reduce the pore pressure buildup at the injection sites to a minimum. Finally, we conclude that due to the high vulnerability of the urban environment where heat production should be established, a safety case has to be made prior to a geothermal use of deep reservoirs to exclude fault triggering.

## 8.4

# Modeling induced micro-earthquakes for an experimental enhanced geothermal system site

Laura Erment<sup>1</sup>, Federica Lanza<sup>1</sup>, Peidong Shi<sup>1</sup>, Katinka Tuinstra<sup>1</sup>, Stefan Wiemer<sup>1</sup>

<sup>1</sup> Schweizerischer Erdbebendienst, Sonneggstr. 5, 8092 Zürich

Induced seismicity is one of the great challenges on the way to creating enhanced geothermal systems (EGS). Past induced events have caused building damage, injuries, and concern among the general population (Zang et al., 2014; Grigoli et al., 2018). Two Swiss EGS projects had to be abandoned after induced earthquakes. Nevertheless, Switzerland is hoping to cover more than 4 TWh of its electricity demand through EGS by the year 2050 (Ejderyan et al., 2019). The DEEP project run by the Swiss Seismological Service (SED) in collaboration with several international institutes aims to de-risk hydraulic fracturing through real-time monitoring (<http://deepgeothermal.org/home/>).

One crucial step towards successful de-risking is to gain an understanding of seismic wave propagation effects in EGS settings. These determine ground motion and associated hazard, as well as dynamic stress changes. Moreover, an accurate understanding of wave propagation will improve our capabilities to monitor induced seismicity in real time, which is one of the central goals of DEEP. For example, numerical wave propagation modeling can be used to generate synthetic ground-truth testing and training data for microseismic event detection, phase picking, and relocation. This is useful because manually labeled data are much scarcer for induced microseismicity than for local and teleseismic earthquakes.

The DEEP project focuses among others on the Utah FORGE site, where several hydraulic stimulations have been performed in a heavily instrumented granitoid volume overlain by volcanic and alluvial sediment. The FORGE site is thus our first target for creating an EGS site seismic wave propagation model. We will generate a large set of numerically simulated micro-earthquakes with known origin times, locations and moment tensors recorded by different types of receivers (borehole, surface; geophone, distributed acoustic sensing). These can then for example be used to train machine learning algorithms. The wave propagation setup will furthermore become part of an integrated modeling workflow for EGS sites that includes various other models e.g. of stress change and seismicity.

To numerically model wave propagation, we harness existing geologic and geophysical knowledge of the FORGE site: Our representations of the subsurface structure are based on a pseudo-3D shear wave velocity model obtained from ambient seismic noise analysis (Zhang et al., 2019), characterization of faults and the sediment-bedrock interface from vertical seismic profiling in addition to high-resolution site topography and stochastic small-scale variations of subsurface elastic properties, which result in wave scattering (see Fig. 1). In this way, we create multiple “digital siblings”, which allows us to include (a) uncertainty and plausible ranges for parameters that are currently poorly constrained at the FORGE site (e.g. anelastic attenuation), (b) multiple realizations of the stochastic medium and (c) realistic, varying ambient noise extracted from recordings at the site.

Wave propagation is modeled using numerical solutions of the (visco-) elastic wave equation through explicit time stepping and spectral element discretization with Salvus (Afanasiev et al., 2019). A challenge in this context is to match the high frequency content of microseismic events, which requires substantial computational resources. Three-dimensional simulations are conducted at the Swiss National Supercomputing Centre.

We will showcase different modeled microseismic events and discuss how we intend to simulate the continuous full seismic wavefield containing catalogued events and ambient noise, and how the output can be used for testing monitoring algorithms at FORGE and other sites.

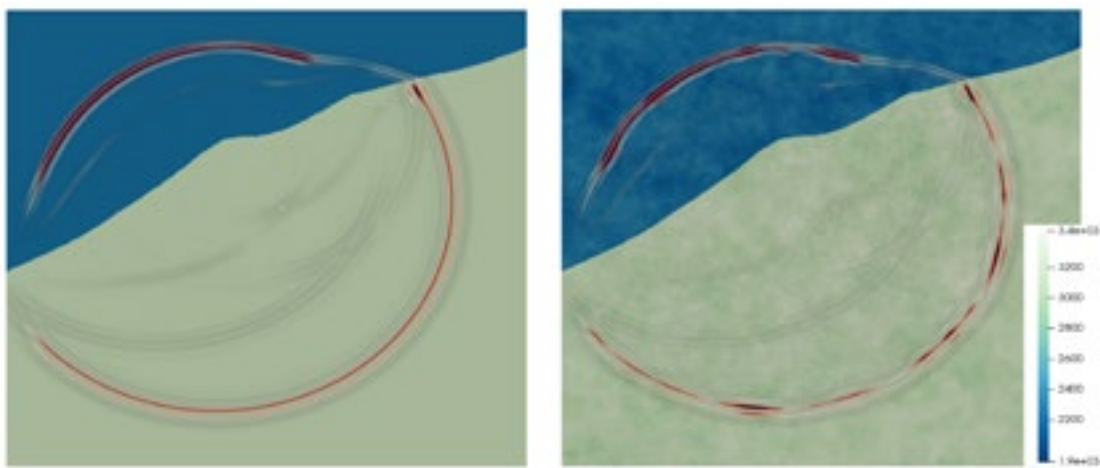


Figure 1. Illustration of vertical cuts through the velocity structure and wavefield. *Left panel:* In the sediment above and the bedrock below the interface, the respective shear wave velocity  $v_s$  is constant. *Right panel:* Shear wave velocity  $v_s$  of the sediment and bedrock is perturbed by random heterogeneities, which introduce small-scale scattering.

## REFERENCES

- Zang, A., Oye, V., Jousset, P., Deichmann, N., Gritto, R., McGarr, A., ... & Bruhn, D. 2014: Analysis of induced seismicity in geothermal reservoirs—An overview. *Geothermics*, 52, 6-21.
- Grigoli, F., Cesca, S., Rinaldi, A. P., Manconi, A., Lopez-Comino, J. A., Clinton, J. F., ... & Wiemer, S. 2018: The November 2017 M w 5.5 Pohang earthquake: A possible case of induced seismicity in South Korea. *Science*, 360(6392), 1003-1006.
- Ejderyan, O., Ruef, F., & Stauffacher, M. 2019: Geothermal energy in Switzerland: highlighting the role of context. In *Geothermal Energy and Society* (pp. 239-257). Springer, Cham.
- Zhang, H., Pankow, K., & Stephenson, W. 2019: A Bayesian Monte Carlo inversion of spatial auto-correlation (SPAC) for near-surface Vs structure applied to both broad-band and geophone data. *Geophysical Journal International*, 217(3), 2056-2070.
- Afanasiev, M., Boehm, C., van Driel, M., Krischer, L., Rietmann, M., May, D. A., ... & Fichtner, A. 2019: Modular and flexible spectral-element waveform modelling in two and three dimensions. *Geophysical Journal International*, 216(3), 1675-1692.

## 8.5

# Application of spatial multi-criteria play-based analysis to high-temperature aquifer thermal energy storage. The Swiss Molasse Basin case study

Luca Guglielmetti<sup>1</sup>, Alexandros Danillidis<sup>2</sup>, Benoît Valley<sup>3</sup>, Andrea Moscariello<sup>1</sup>

<sup>1</sup> Department of Earth Sciences, University of Geneva, Rue des Maraîchers 13, CH-1205 Geneva  
(luca.guglielmetti@unige.ch)

<sup>2</sup> Department of Civil Engineering and Geosciences (GSE), Technical University of Delft, Building 23, Stevinweg 1 / PO-box 5048, Delft (The Netherlands)

<sup>3</sup> Center for hydrogeology and geothermics CHYN, University of Neuchâtel, Rue Emile Argand 11, 2000 Neuchâtel

The work carried out in this study comprises of screening the potential for high temperature aquifer thermal energy storage (HT-ATES) across the Swiss Molasse Basin (SMB).

HT-ATES systems can provide a solution to contribute reaching the Swiss 2050 energy strategy, however in Switzerland, despite having one of largest market for ground-source heat pumps, only few examples of HT-ATES have been tested or implemented in the past (Guglielmetti et al., 2021; Kallesøe et al., 2019). Additionally, a screening of the potential has never been carried out since now. In the framework of the European GEOTHERMICA project HEATSTORE, the Swiss potential of HT-ATES is evaluated according to the publicly available data, by combining subsurface data (e.g. depth of the targets, thickness of the targets, petrophysical parameters, temperature distribution at different depth) and energy data (e.g. heat demand and excess heat configurations and distributions, thermal network distribution) in order to identify the most promising areas for HT-ATES potential. At this stage economical, regulatory and socio-environmental constraints were not taken into account, but the presented framework can be easily expanded to include such criteria in order to perform a more comprehensive analysis based on sustainability performance evaluation.

The choice of focussing on the SMB was driven by the availability of subsurface data as the 3D geologic model available from Swisstopo (Allenbach et al., 2017; Geowatt AG, 2015; Sommaruga et al., 2012) only covers this region.

Two main reservoirs have been identified in the Cenozoic Molasse and the Upper Mesozoic carbonates. Additionally, a minimal underground temperature threshold is set to 25°C which is the temperature commonly considered as separating low temperature ATES from HT-ATES systems (Fleuchaus et al., 2020; SIA 384/7, 2015). These two units show different lithological, petrophysical, geomechanical and hydraulic conditions, locally enhanced by lithological heterogeneities in the Cenozoic Molasse and by enhanced fracture conditions thanks to the presence of fault corridors in the Mesozoic. A maximal depth of 2000m was set as boundary as it was considered as a reasonable depth for favourable implementation of HT-ATES systems in terms of the techno-economic performance. We also considered a temperature threshold of 70°C which gives a reasonable temperature difference between aquifer ambient temperature and excess heat temperature injected into the aquifer (90°C), to allow effective thermal storage.

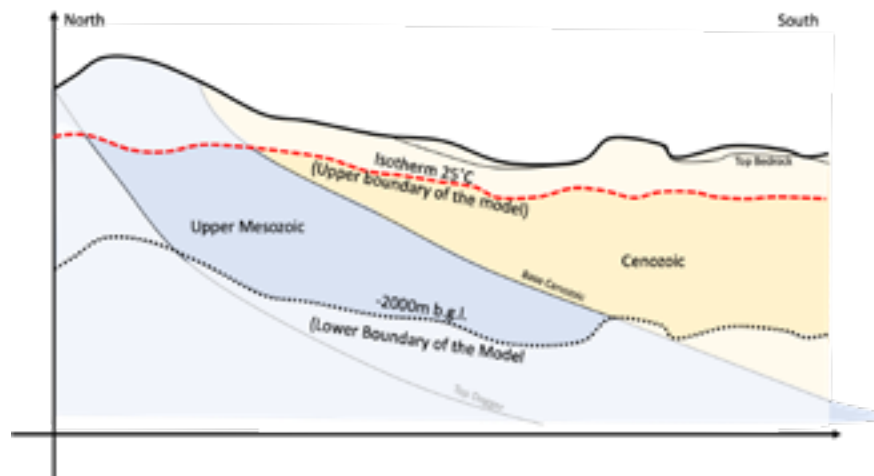


Figure 1. Sketch of the subsurface of interest along a hypothetical N-S oriented cross-section across the SMP

The results of the study show how the Cenozoic has some theoretical potential storage in the southern part the study area, where also some major cities are located (Zurich, Bern, Lausanne). Regarding the faulted Mesozoic, fault structures can be suitable as targets in Aarau, Biel and Geneva. However, as demonstrated by the GGeo-01 well in Geneva, high permeabilities

characterizing fault corridors and important elevation differences between the recharge and reservoir area lead to high wellhead pressure and important natural artesian flow. Such conditions are therefore a limiting factor for storage, due to flow management and injection pressure limitations. On the contrary, the same targets in the Mesozoic carbonates can be unsuitable for HT-ATES, as shown by the poor hydraulic performances of the GGeo-02 well, which however, can be suitable for borehole thermal energy storage.

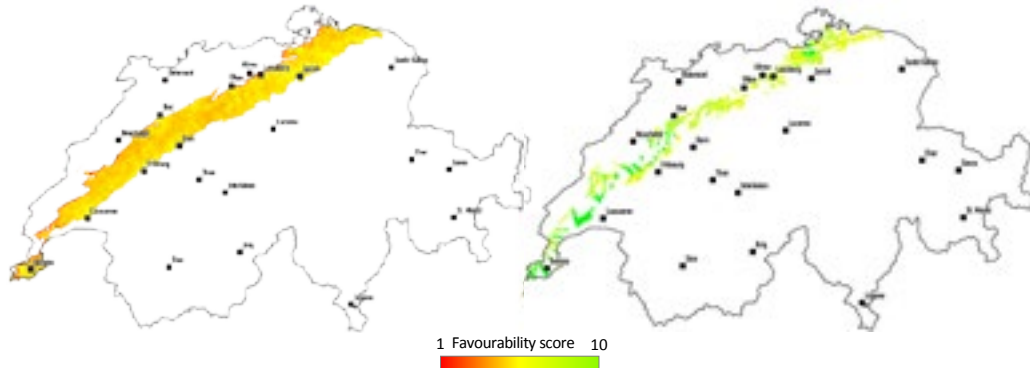


Figure 2 – Favourability assessment for the Cenozoic and fault

## REFERENCES

- Allenbach, R., Baumberger, R., Kurman, E., Michale, C. S., & Reynolds, L. (2017). GeoMol: Geologisches 3D-Modell des Schweizer Molassebeckens : Schlussbericht. *Berichte Der Landesgeologie*, 10, 128.
- Fleuchaus, P., Schüppler, S., Bloemendaal, M., Guglielmetti, L., Opel, O., & Blum, P. (2020). Risk analysis of High-Temperature Aquifer Thermal Energy Storage (HT-ATES). *Renewable and Sustainable Energy Reviews*, 133. <https://doi.org/10.1016/j.rser.2020.110153>
- Geowatt AG. (2015). *Temperaturmodell des Schweizerischen Molassebeckens*.
- Guglielmetti, L., Daniilidis, A., Valley, B., Maragna, C., Maurel, C., Dinkelman, D., Koornneef, J., Oerlemans, P., Drijver, B., Kallesøe, A. J., Mortensen, M. H., Ditlefsen, C., & Vangkilde-Pedersen, T. (2021). *Screening for national potential for UTES*. 87. [https://www.heatstore.eu/documents/HEATSTORE\\_WP1\\_D1.3\\_Final\\_2021.10.28.pdf](https://www.heatstore.eu/documents/HEATSTORE_WP1_D1.3_Final_2021.10.28.pdf)
- Kallesøe, A. J., Vangkilde-Pedersen, T., Nielsen, J. E., Sørensen, P. A., Bakema, G., Drijver, B., Pittens, B., Buik, N., Egermann, P., Rey, C., Maragna, C., Hamm, V., Guglielmetti, L., Hahn, F., Nardini, I., Koornneef, J., & Dideriksen, K. (2019). Underground Thermal Energy Storage (UTES) - state-of-the-art, example cases and lessons learned. In *Deliverable 1.1 - HEATSTORE Project: Vol. D1.1*. [https://www.heatstore.eu/documents/HEATSTOREUTES State of the Art\\_WP1\\_D1.1\\_Final\\_2019.04.26.pdf](https://www.heatstore.eu/documents/HEATSTOREUTES State of the Art_WP1_D1.1_Final_2019.04.26.pdf)
- SIA 384/7. (2015). *Grundwasserwärmennutzung* (p. 84).
- Sommaruga, A., Eichenberger, U., & Marillier, F. (2012). Seismic Atlas of the Swiss Molasse Basin. *Matériaux Pour La Géologie de La Suisse - Géophysique*, 44. Bibliotheque%5CnUrs

## 8.6

### Lithium extraction from geothermal brines in Switzerland?

Stefan Heuberger<sup>1</sup>, Joël Morgenthaler<sup>1</sup>, Thomas Galfetti<sup>2</sup>

<sup>1</sup> Georesources Switzerland Group, Department of Earth Sciences, ETH Zurich, Sonneggstrasse 5, 8092 Zürich, Switzerland  
(stefan.heuberger@erdw.ethz.ch)

<sup>2</sup> Swiss Geological Survey, Swiss Federal Office of Topography swisstopo, Seftigenstrasse 264, 3084 Wabern Switzerland.

Deep geothermal aquifers are known to occasionally contain significant concentrations of lithium and other critical metals (e.g. in the Upper Rhine Graben, Sanjuan et al. 2016, 2022). In collaboration with the Swiss Geological Survey and the Swiss Federal Office of Energy, we are evaluating the occurrence and distribution of these metals based on deep well records in Switzerland with a focus on lithium. To this end, we review and update the existing hydrogeochemical database by Sonney & Vuataz (2008) with new hydrochemistry well data from geothermal exploration projects and from Nagra (Waber et al. 2014).

Here we present the preliminary results from our analysis of this new well database. The lithium concentration was measured in 64 of the available 100 (deep) wells. Na-Cl brines from Keuper-, Muschelkalk and Permian aquifers in northern Switzerland have slightly elevated lithium concentrations (5-30 mg/l) with 2 wells having lithium concentrations of 80-145 mg/l in the Muschelkalk aquifer (Biehler et al. 1993). Compared to the concentrations in the Upper Rhine Graben, reaching up to 150-210 mg/l (Sanjuan et al. 2022), the lithium concentrations in the currently available Swiss wells are clearly lower.

The production of geothermal energy, coupled with the extraction of lithium, or other critical metals from deep aquifers (drilled in future geothermal projects) could provide, if successful, an important economic incentive to scale up geothermal exploration and production in Switzerland. However, to better characterise and understand the deeper Swiss underground and its geothermal and hydrochemical properties, significantly more deep and spatially distributed wells are needed.

#### REFERENCES

- Biehler, D., Schmassmann, H., Schneeman, K. & Sillanpää, J. (1993). Hydrochemische Synthese Nordschweiz: Dogger-, Lias-, Keuper und Muschelkalk-Aquifere. Nagra Technischer Bericht, NTB 92-08.
- Sanjuan, B., Millot, R., Innocent, C., Dezayes, C., Scheiber, J. & Brach, M. (2016). Major geochemical characteristics of geothermal brines from the Upper Rhine Graben granitic basement with constraints on temperature and circulation. *Chemical Geology* 428, 27-47.
- Sanjuan, B., Gourcerol, B., Millot, R., Rettenmaier, D., Jeandel, E. and Rombaut, A. (2022). Lithium-rich geothermal brines in Europe: An up-date about geochemical characteristics and implications for potential Li resources. *Geothermics* 101, 102385.
- Sonney, R. & Vuataz, F.-D. (2008). Properties of geothermal fluids in Switzerland: A new interactive database. *Geothermics* 37, 496-509.
- Waber, H. N., Heidinger, M., Lorenz, G. & Traber, D. (2014). Hydrochemie und Isotopenhydrogeologie von Tiefengrundwässern in der Nordschweiz und im angrenzenden Süddeutschland. Nagra Arbeitsbericht, NAB 13-63.

## 8.7

# Geothermometrical modelling applied to the CO<sub>2</sub>-rich thermal waters of the Caldas de Malavella hydrothermal system in Gerona (Spain) and lessons learnt for the geological storage of CO<sub>2</sub> in granitic rocks.

Jon Jiménez<sup>1</sup>, Mónica Blasco<sup>1</sup>, Luis F. Auqué<sup>1</sup>, María J. Gimeno<sup>1</sup>

<sup>1</sup> University of Zaragoza, Earth Sciences Department, C/Pedro Cerbuna, 50009, Zaragoza, Spain. (jimenezbjon@unizar.es)

The interest in CO<sub>2</sub>-rich hydrothermal systems has raised significantly in the last decades due to their potential as natural analogues of the expected geochemical processes during the geological storage of CO<sub>2</sub>. The Malavella hydrothermal system, characterized by its CO<sub>2</sub>-rich thermal waters, is one of these systems and the characterization of the temperature and mineral equilibrium conditions in the deep reservoir is presented in this work. The system is located in Caldas de Malavella (Gerona), along the southern margin of La Selva Graben (Figure 1). The CO<sub>2</sub> dissolved in these groundwaters at depth is mostly endogenous, and the water reservoir is hosted in a basement of late Hercynian granodiorites and leucogranites that intrude the metasedimentary Paleozoic rocks (Navarro et al., 2011).

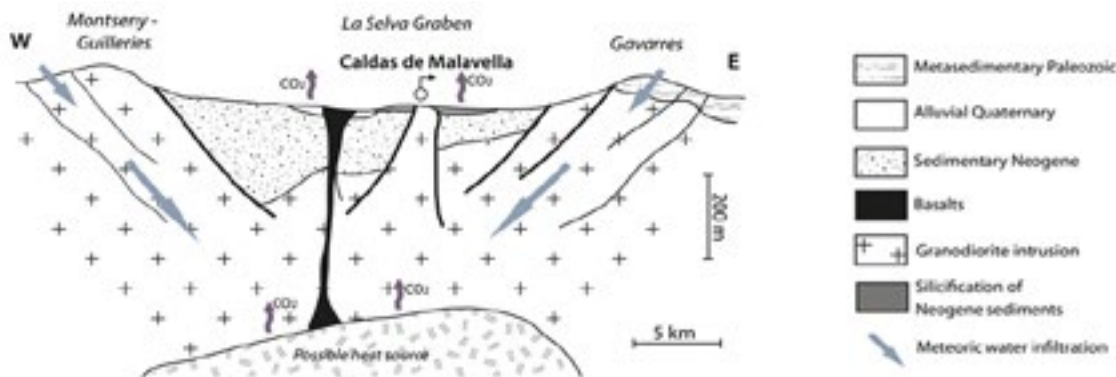


Figure 1. Simplified geological model of the Malavella geothermal system (modified from Navarro et al., 2011).

Analytical data of two water samples taken in Caldas de Malavella from the thermal springs Font de la Mina (GE-1: sampled in 2021) and Vichy Spa (M1: sampled in 2009), have been used. Temperature, pH and conductivity were measured in situ. Total alkalinity was determined by titration. Cl<sup>-</sup> and F<sup>-</sup> were analysed by the electrodes of chloride ORION 94-17B and fluoride ORION 94-09, respectively. SO<sub>4</sub><sup>2-</sup> has been determined by turbidimetry. Ca, Mg, Na, K, Si, Ba, Sr and Li were analysed by ICP-OES. The geothermometrical modelling consists of evaluating the evolution of selected saturation indices (SI) as the temperature increases, until they reach the equilibrium at the water temperature of the deep reservoir. This modelling has been performed with PHREEQC (Parkhurst and Appelo, 2013) and the LLNL thermodynamic database. Several simulation conditions have been tested for both samples: 1) Closed system: no mass transfer considered; 2) Open system: re-equilibriums with certain mineral phases, as well as CO<sub>2</sub> input to restore the outgassing effect, are imposed. Only the results of those simulation conditions that better restore the SI evolution are shown in this abstract in Figure 2.

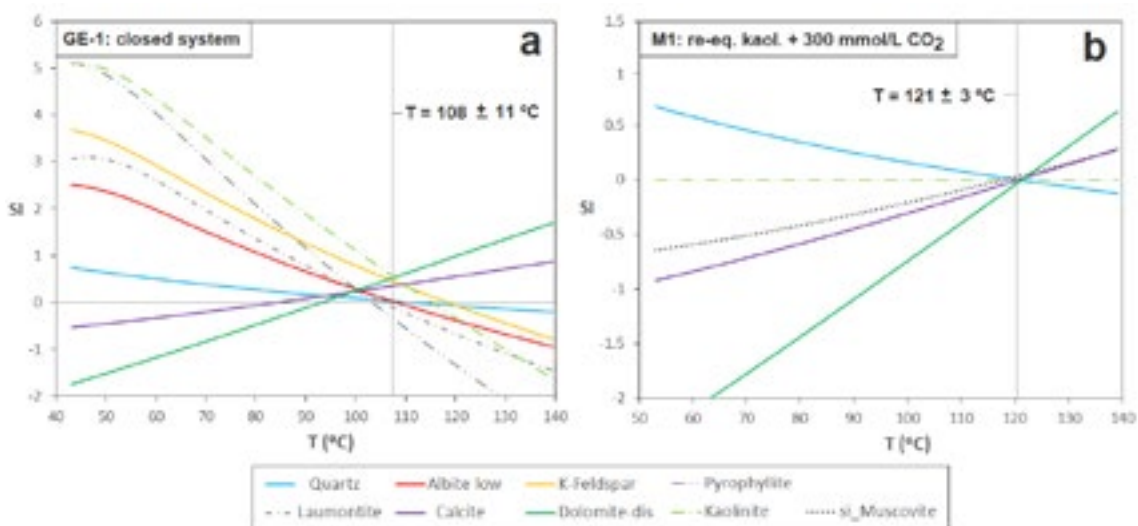


Figure 2. Geothermometrical simulation results obtained for samples GE-1 in closed system conditions (Figure 2a) and M1 imposing a re-equilibrium with kaolinite and a CO<sub>2</sub> input of 300 mmol/L (Figure 2b). The mean equilibrium temperature is provided together with the standard deviation.

The results obtained for sample GE-1 in closed system conditions show a convergence at a temperature of  $108 \pm 11^\circ\text{C}$ , with an equilibrium assemblage constituted by quartz, albite, K-feldspar, calcite, dolomite and the auxiliary phases pyrophyllite and laumontite. The results are almost identical considering a re-equilibrium with calcite. In the case of sample M1, the convergence is only obtained under open system conditions, assuming a re-equilibrium with kaolinite (previously observed in other granitic systems) and compensating the CO<sub>2</sub> outgassing by an input of 300 mmol/L of CO<sub>2</sub>. In this sample, the equilibrium assemblage is represented by quartz, calcite, dolomite and muscovite, and it is obtained at  $121 \pm 3^\circ\text{C}$ . This suggests that the reservoir of the water M1 could be different from the one of GE-1, explaining different mineral equilibrium conditions reached. Furthermore, an important common outcome of the deduced equilibrium assemblages is that, despite calcite is not present in the granitic hosting rocks, it takes part in the equilibrium assemblage of both groundwaters. This indicates that calcite is precipitating at depth as a secondary phase, which entails that this precipitation could be feasible as a CO<sub>2</sub> mineral trapping process in a deep geological storage of CO<sub>2</sub> in similar granitic rocks.

## REFERENCES

- Navarro, A., Font, X., & Viladevall, M. (2011). Geochemistry and groundwater contamination in the La Selva geothermal system (Girona, Northeast Spain). *Geothermics*, 40(4), 275-285.  
 Parkhurst, D. L., & Appelo, C. A. J. (2013). Description of input and examples for PHREEQC version 3—a computer program for speciation, batch-reaction, one-dimensional transport, and inverse geochemical calculations. US geological survey techniques and methods, 6(A43), 497.

## 8.8

### What can pore-scale optical measurements do?

Xiang-Zhao Kong<sup>1,+</sup>, Isamu Naets<sup>1</sup>, Mehrdad Ahkami<sup>1,2</sup>, Pierre Leard<sup>1</sup>, Dario Schwendener<sup>1</sup>, Martin O. Saar<sup>1,3</sup>

<sup>1</sup> Geothermal Energy and Geofluids (GEG) Group, Department of Earth Sciences, ETH Zurich, Sonneggstrasse 5, CH-8092 Zurich, Switzerland (+xkong@ethz.ch)

<sup>2</sup> Department of Engineering Geology and Hydrogeology, RWTH Aachen University, 52056, Aachen, Germany

<sup>3</sup> Department of Earth and Environmental Sciences, University of Minnesota, Minneapolis, USA

Despite progress in recent years, it is still a challenging task to understand the fundamental behaviour of fluid flow and transport at the pore scale, because pore-scale processes are often difficult to capture due to the opacity of porous media. In this presentation, we show our recent pore-scale optical measurements on fluid flow and solute/heat transport.

In a 3D-printed fractured porous medium, we measure pore-scale fluid velocities using both Magnetic Resonance Imaging (MRI) and Particle Image Velocimetry (PIV) techniques and analyse the stress jump and velocity slip coefficients at fracture-matrix interfaces. In addition to fluid flow quantifications, we use laser-induced fluorescence (LIF) techniques to quantify a pulse-like injection of fluorescent dye into the same fractured porous medium and to understand the role of permeability heterogeneity on solute transport. We also capture the development of the thermal plume and the corresponding fluid velocities using combined PIV and two-colour LIF methods when a heat flux is introduced into porous media.

We also use PIV-measured fluid velocities to characterize the evolution of fluid flow paths in a single, self-affine fracture with rough walls, as the fracture undergoes shear displacement. Moreover, we capture both drainage and imbibition processes when immiscible dual-phase flows are injected into the same fracture, which experienced shear displacements. These experiments enable us to delineate the effect of fracture aperture heterogeneity on fracture fluid flow, induced by shear displacement. We extend our measurements on fluid flow and solute transport to a bifurcating fracture to quantify the distribution of fluid and solute mass at fracture intersections.

#### REFERENCES

- Ahkami, M., Roesgen, T., Saar, M. O., Kong, X.-Z. 2019: High-Resolution Temporo-Ensemble PIV to Resolve Pore-Scale Flow in 3D-Printed Fractured Porous Media. *Transp. Porous Media*.
- Naets, I., Ahkami, M., Huang, P.-W., Saar, M. O., Kong, X.-Z. 2022: Shear induced fluid flow path evolution in rough-wall fractures: A particle image velocimetry examination. *Journal of Hydrology*.
- Kong, X.-Z., Ahkami, M., Naets, I., Saar, M. O., 2022: The role of high-permeability inclusion on solute transport in a 3D-printed fractured porous medium: An LIF-PIV integrated study. *Transp. Porous Media*.
- Schwendener, D. 2022: Velocity quantification of two-phase drainage and imbibition processes in rough wall fractures. MSc thesis.
- Ahkami, M. 2020: Experimental and numerical study of fluid flow, solute transport, and mineral precipitation in fractured porous media. PhD thesis.
- Naets, I. 2022: Fluid flow heterogeneity and solute transport in rough-walled fractures. PhD thesis.

## 8.9

# Multi-criteria play based analysis for geothermal energy potential evaluation in sedimentary basins: an example from North-Eastern Switzerland.

Yasin Makhloufi<sup>1,2</sup>, Luca Guglielmetti<sup>2</sup>, Fiammetta Mondino<sup>1</sup>

<sup>1</sup> Geneva Earth Resources SA, Rue Jean Jaquet 10, 1201 Geneva ([yasin.makhloufi@geneva-er.com](mailto:yasin.makhloufi@geneva-er.com))

<sup>2</sup> Geo-Energy Reservoir Geology and Sedimentary Basin Analysis, Université de Genève, Rue des Maraîchers 13, 1205, Geneva, Switzerland

In a context of growing demand for diversification in energy sources, Switzerland has seen in the last decade the development of several projects for exploration and production of geothermal resources in the Molasse Basin. Geothermal energy is characterized by a variety of form and usage and large versatility where: low temperatures at shallow depths that can provide unlimited usage for domestic heating; direct use of heat from medium depth with higher temperature distributed to households' districts, industry and agricultural installations and high-temperature production (>100 °C) that can lead to electricity production. However, a common pre-requisite for geothermal energy production is the preliminary evaluation of geothermal potential.

A spatial multi-criteria play based analysis was used to evaluate the geothermal potential of a large area in NE Switzerland. This is a "source to sink" methodology where the evaluation of the subsurface geothermal potential (source), integrated analysis and modelling of geophysical, geological and fluid-flow data, is carried out in parallel to the energy demand (sink) characterization. This methodology also imply the understanding of the energy demand portfolio and consumption distribution over time such as: current vs future customers, seasonal variations, business demands. This method imply the collection of all available surface and subsurface data relevant to the project i.e.: household and industrial energy demands, district heating networks loads in space and time, geological maps, seismic, borehole data, water chemistry, scientific reports, etc... In order to identify the most favourable sites with a geothermal potential, a GIS-based geo-processing technique was developed. This technique consists of compiling several GIS layers of spatial repartition of elements in favour of the presence of a geothermal system. Results are synthesized as *Favourability Maps* summarizing a large critical number of aspects including both the subsurface and surface.

Based on the limited data set analysed in this project, the favourability maps indicated the possibility, in the studied area, for the application of closed systems such as Deep Borehole Heat Exchangers (DBHE) as the most suitable solution to extract heat from the Cainozoic sediments with temperature up to ca. 80°C. Moreover, two main reservoirs have been identified in the Mesozoic carbonates: the Upper Jurassic Malm and the Triassic Muschelkalk, presenting fracture-controlled hydraulic conductivities as well as temperatures up to 100°C. In addition, the top of the crystalline basement exhibits potential for direct use of hydrothermal resources, favourable for co-generation of heat and power.

In this project, the spatial multi-criteria play based analysis proved to be a cost-effective and time efficient method. The favourability maps are a key product for stakeholders during the decision making phase, helping in new data acquisition planning; exploration site selection and risk vs opportunity assessment.

## 8.10

# Analysis of the regional structural elements of the Lausanne region (VD) in support of geothermal exploration

Fiammetta Mondino<sup>1</sup>, Niels Giroud<sup>2</sup>, Robin Marchant<sup>3</sup>

<sup>1</sup> Geneva Earth Resources SA, Rue Jean Jaquet 10, 1201 Geneva

<sup>2</sup> GEOOL (Géothermie de l'Ouest Lausannois), Place Chauderon 27, 1003 Lausanne

<sup>3</sup> Musée Cantonal de Géologie, Batiment Anthropole, Université de Lausanne, CH1015 Lausanne

Major structural elements such as faults or fracture corridors are known to have a significant role in the circulation of fluids, as they can act as conduits or barriers to fluid flow. In carbonate rocks they represent a major uncertainty in geo-energy exploration and production as fluid flow properties result from the combination of mechanical and diagenetic processes controlled by the brittle and reactive characteristics of carbonate rocks.

The public utility of Lausanne (Services industriels de Lausanne - SIL), Romande Energie Holding SA, and SIE SA – Service intercommunal de l'énergie decided to combine forces to develop medium-depth geothermal energy in the western part of the Lausanne area. The objective of the newly founded company, GEOOL SA, is to explore at least three sites and develop one to two doublets. The heat will feed into the existing district heating networks and support their shift towards carbon neutrality. In support of the geothermal exploration carried out by GEOOL, a regional analysis of major structural elements has been performed in the Lausanne-Echallens-Cossonay-Morges areas (Canton of Vaud).

For this study 2D seismic surveys acquired for hydrocarbon exploration during the 1970s and 80s, and more recent lines acquired later by the SIL (2016) and the University of Lausanne (2014) were made available. The structural interpretation of the study area was based on the stratigraphic interpretation established for the GeoMol project (Marchant, 2017). Similarly the major structural lineaments, such as the "La Sarraz Fault" and the "Decrochement Pontarlier-Aubonne", already described by previous studies (see Gruber, 2017 and references therein) were taken as reference elements for the area.

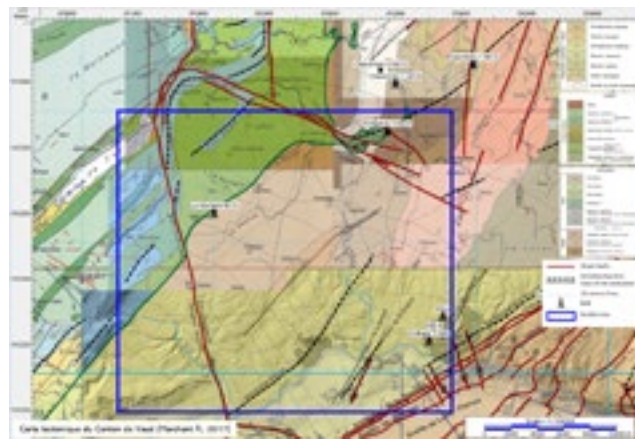


Fig. 1. Detail of the studied area (after Marchant R., 2017)

In this study particular attention was given to areas where no lineaments were previously investigated (Fig.1) resulting in the identification of a complex network of discontinuities organised in structural compartments (Fig.2). Within the latter, lineaments have similar seismic expression and they are organised in Riedel shears (synthetic and antithetic). Important implications for deep water circulation can be linked with the presence of these newly interpreted lineaments and help developing a predictive model to assist future exploration in this area for geothermal resources.

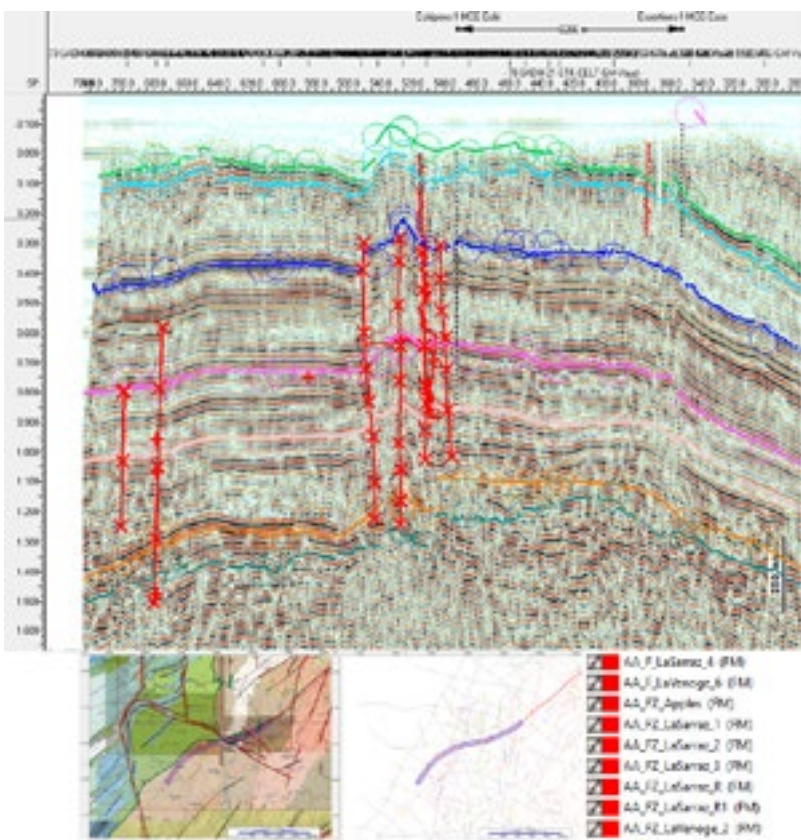


Fig. 2. Example of the seismic interpretation of the "La Sarraz" Fault Zone

## REFERENCES

- Marchant, R. 2017: Interprétation de la campagne sismique 2016 pour la géothermie de moyenne profondeur à Lausanne, Musee Cantonal de Geologie (VD).
- Gruber, M. 2017: Structural Investigations of the Western Swiss Molasse Basin, From 2D Seismic Interpretation to a 3D Geological Model, Thesis presented to the Faculty of Science of the University of Fribourg (Switzerland).

## 8.11

# 3D geological modelling in support of CERN's Future Circular Collider ~100-km long tunnel infrastructure (Geneva Basin, Switzerland-France): synergies or conflicts with geo-energy resources?

Andrea Moscariello<sup>1</sup>, Max Haas<sup>2</sup>, Emna Meftah<sup>1</sup>, Aymeric Le Cottenc<sup>1</sup>, Yasin Makhlofi<sup>1</sup>

<sup>1</sup> Geo-Energy Reservoir Geology and Sedimentary Basin Analysis, Université de Genève, Rue des Maraîchers 13, 1205, Geneva, Switzerland

<sup>2</sup> European Organization for Nuclear Research (CERN), Espl. Des Particules 1, 1211 Geneva, Switzerland

The European Organization for Nuclear Research (CERN) is currently undertaking a feasibility study to build the next-generation particle accelerator, named the Future Circular Collider (FCC), hosted in a 90–100 km subsurface infrastructure in the Geneva Basin, extending across western Switzerland and adjacent France.

For the design of FCC trajectory, a full understanding of the subsurface geology that will be crossed by both the tunnel and the access shafts is required. For this purpose a detailed knowledge of the regional distribution of rock mass composition and structural elements as well as the hydrogeological characteristics of the area should be achieved and summarised in a full-scale 3D geological model. In order to accomplish this task, a research project is being carried out by UNIGE with two goals: I) establish a Geographic Information System (GIS)-based subsurface data set and data base architecture in support of the feasibility and execution of the FCC tunnelling work by defining a standard data set framework for new data and II) establish a consistent high-resolution 3D geological model, supported by quantitative geological analytical investigations along the FCC trace aimed at predicting geological features and possible.

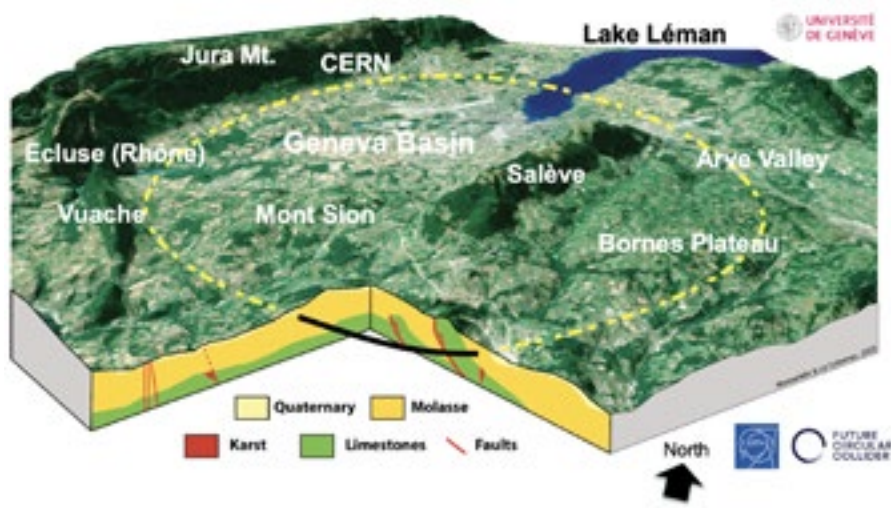


Figure 1: schematic block diagram showing the planned trace of the Future Circular Collider ~ 100-km long tunnel.

The 3D geological model to date provides a solid knowledge framework based on all available data known to date, highlighting the different lithological and structural heterogeneities crossed by the planned trace of the FCC tunnel. Specifically, the model allows the visualisation of the subsurface conditions known to date in the high-risk areas identified enabling to take informed decisions during the forthcoming geotechnical and seismic investigation campaign which will take place across the French and Swiss border. Following this investigation campaign the geological 3D model will be updated with the new acquired data and will therefore provide more accurate view of the subsurface.

This tool will be also used to map distribution of underground geo-resources and help the decision makers to identify possible opportunities and/or conflicts with exploration and exploitation of geothermal energy (heat pumps, heat storage) and/or underground water. The model will also be used to predict possible risks of high-pressure water flows (i.e. karst, fault and fracture network) and venues of hydrocarbons which might represent a geo-hazard during tunnel excavation.

This 3D model represents therefore a practical and 'live' working tool which will support the FCC project throughout the different phases of tunnelling design, planning and execution.

## REFERENCES

- Haas, M., Carraro, D., Ventra, D., Plötze, M., De Haller A., Moscariello A. et al. Integrated stratigraphic, sedimentological and petrographical evaluation for CERN's Future Circular Collider subsurface infrastructure (Geneva Basin, Switzerland-France). *Swiss J Geosci* 115, 16 (2022). <https://doi.org/10.1186/s00015-022-00407-y>

## 8.12

# Monitoring geothermal operations with noise interferometry at the Domo de San Pedro, Nayarit – Mexico

Francisco Muñoz-Burbano<sup>1</sup>, Marco Calò<sup>2</sup>, Violeta Reyes-Orozco<sup>3</sup>, Matteo Lupi<sup>1</sup>

<sup>1</sup> Université de Genève UNIGE, 13 Rue des Maraîchers, 1205, Genève, Suisse

(francisco.munozburbano@unige.ch, matteo.lupi@unige.ch)

<sup>2</sup> Universidad Nacional Autónoma de México UNAM, Ciudad Universitaria, 04510, Ciudad de México, México

(calo@igeofisica.unam.mx)

<sup>3</sup> Grupo Dragón, Km 12 Carr. Chapalilla-Compostela. San Pedro Lagunillas, Nayarit. México (vreyeso@gdragon.com.mx)

The Domo de San Pedro (DSP) is part of a silicic volcanic complex located at the westernmost part of the trans-Mexican volcanic belt. The DSP dates between  $27 \pm 7$  and  $55 \pm 8$  Ka with an estimated sub-aerial volume of  $4.5 \text{ km}^3$  emplaced over an extensional basin dominated by sodic-alkaline and calc-alkaline volcanism since the Late Miocene. The geothermal potential of the DSP has been investigated since 1980 and exploited since 2015 and now produces 35 MW. Multidisciplinary studies suggest the presence of a high enthalpy hydrothermal system where circulation of meteoric and deep fluids is fuelled by a plutonic source at depth. Fluid flow is suggested to be controlled by a regional fault system known as Compostela-Pedernales oriented NW-SE and local fault systems trending N-S and NE-SW.

In 2021 a joint effort between the University of Geneva, The Universidad Nacional Autónoma de México, the company Grupo Dragón, and the Swiss platform REPIC\* allowed deploying a temporary broadband seismic network composed of 20 stations in the surroundings of the DSP. The goal of the project is to monitor the seismic activity of the region and to study possible seismic responses to the geothermal operations.

We compiled a seismic catalog of the events that occurred at the DSP from March 2021 to January 2022. We also analyze the temporal changes in the seismic velocity using passive seismic methods. In particular, we implemented seismic ambient noise interferometry from cross-correlating station pair signals to retrieve the Green Function and analyze the coda velocity changes. These velocity changes are often associated with changes in the effective stress beneath the volcanic system. In particular, we identify velocity changes prior and during the occurrence of three groups of seismic events. The velocity changes vary up to 0.1 % from the mean velocities recorded for the station pairs. Additional velocity changes were observed for station pairs inside the geothermal field and might suggest a causal relation with re-injection of fluids into the geothermal system.

\* <https://www.replic.ch/en/domo-san-pedro-dos-pegas/>

## 8.13

# Velocity Quantification (PIV) in Two-Phase Drainage and Imbibition Processes in Rough Wall Fractures.

Dario Schwendener<sup>1,\*</sup>, Isamu Naets<sup>1</sup>, Xiang-Zhao Kong<sup>1,\*</sup>

<sup>1</sup> Geothermal Energy and Geofluids (GEG) Group, Department of Earth Sciences, ETH Zurich, Sonneggstrasse 5, CH-8092 Zurich, Switzerland  
 (+dariosc@ethz.ch and \*xkong@ethz.ch)

The research of two-phase fluid flow through rough-walled fractures is of importance to understand the (multiphase) fluid flow and solute/thermal transport along the predominant pathways in the subsurface. Applications are of academic and technological interest, such as the phase exsolution above magmatic intrusions, oil and gas production in fractured reservoirs, and carbon capture utilisation and storage (CCS/CCUS).

The main objective of this study is using particle image velocimetry (PIV) to measure the fluid velocity fields of high resolution during the drainage and imbibition processes, the two major processes during multiphase flow. During the experiments, both the defending and invading fluids are refractive index matched fluids, and they migrate within a transparent, 3D-printed, shearable fracture model. By seeding fluorescent additives (dye and particles) under laser illumination, the motion of fluorescent particles is tracked with a high-resolution camera. Fluid velocities are then extracted from the incremental particle displacement using the PIV algorithm *sliding sum-of-correlation*.

The detailed dynamics during both drainage and imbibition processes are evaluated to elucidate viscous fingering and stable displacement. In addition, the influence of aperture field on the drainage and imbibition processes is examined by shearing the fracture model at three different positions. By mapping the fluid velocity vectors on top of the fracture aperture fields, the influence of local aperture on invasion pattern and flow dynamics can be directly illustrated. The integration of fracture aperture allows us to classify flow regimes on the basis of their dynamics in addition to their invasion pattern fractality. Our measurements and analyses should further provide the quantitative measure to estimate interface instability and competition between viscous and capillary forces for different flow regimes and fractures types. The use of 3D-printing techniques allows to extend this work across a wide set of natural geometries. The characteristic dimensionless quantities, such as capillary number and viscosity ratio, enable comparisons of our experimental results to numerical simulation. We also discuss the full potential of the applied approach and its limitations in this presentation.

## REFERENCES

- Bob Harrison and Gioia Falcone. Carbon capture and sequestration versus carbon capture utilisation and storage for enhanced oil recovery. *Acta Geotechnica*, 9(1):29–38, 2014.
- AA Alturki, BB Maini, and ID Gates. The effect of wall roughness on two-phase flow in a rough-walled hele-shaw cell. *Journal of Petroleum Exploration and Production Technology*, 4(4):397–426, 2014.
- Yi-Feng Chen, Shu Fang, Dong-Sheng Wu, and Ran Hu. Visualizing and quantifying the crossover from capillary fingering to viscous fingering in a rough fracture. *Water Resources Research*, 53(9):7756–7772, 2017
- Ran Hu, Chen-Xing Zhou, Dong-Sheng Wu, Zhibing Yang, and Yi-Feng Chen. Roughness control on multiphase flow in rock fractures. *Geophysical Research Letters*, 46(21):12002–12011, 2019.
- Isamu Naets, Mehrdad Ahkami, Po-Wei Huang, Martin O Saar, and Xiang-Zhao Kong. Shear induced fluid flow path evolution in rough-wall fractures: A particle image velocimetry examination. *Journal of Hydrology*, 610:127793, 2022.

## 8.14

# 3D-seismic exploration for radioactive waste repository siting in Switzerland: acquisition and processing strategy

Thomas Spillmann<sup>1</sup>, Andreas Hoelker<sup>2</sup>, Herfried Madritsch<sup>1</sup>, Kaspar Merz<sup>1</sup>, Marian Hertrich<sup>3</sup>, Philip Birkhäuser<sup>1</sup>

<sup>1</sup> Nagra, Hardstrasse 73, CH-5630 Wettingen ([thomas.spillmann@nagra.ch](mailto:thomas.spillmann@nagra.ch))

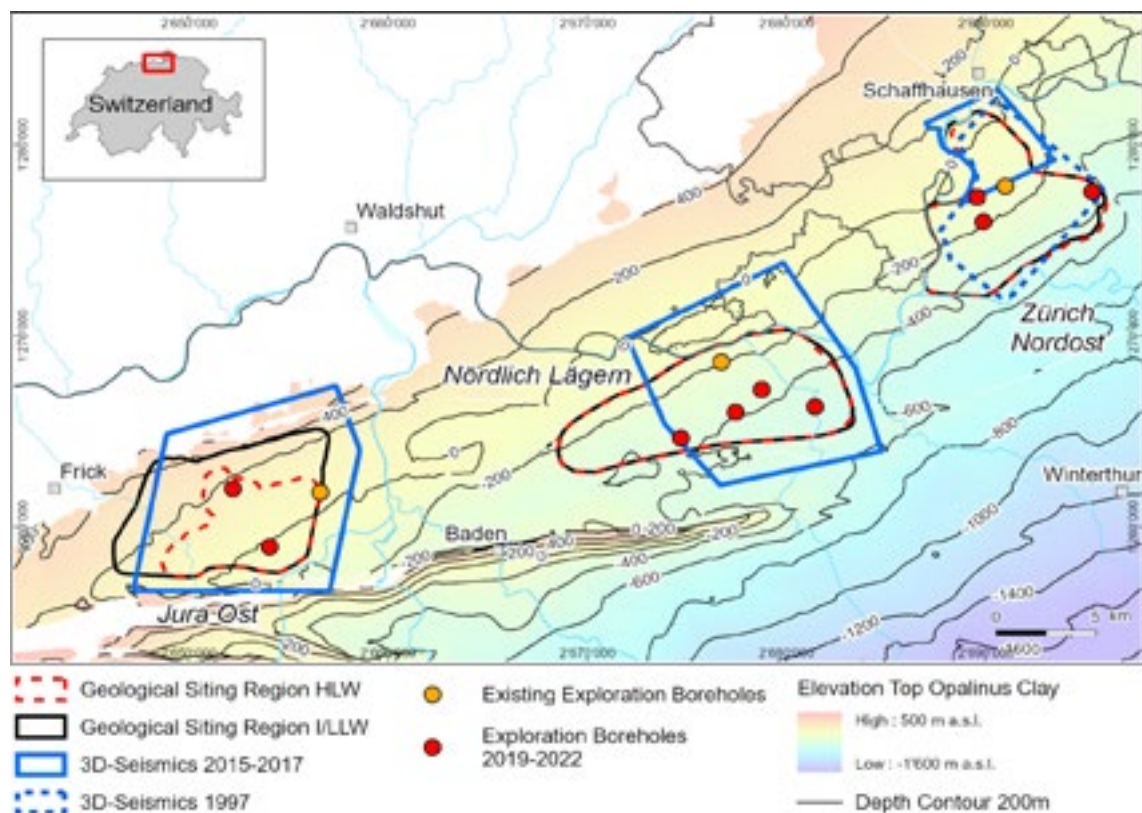
<sup>3</sup> ETH Zürich, Sonneggstrasse 5, CH-8092 Zürich

The area of northern Switzerland has been regarded as potential target zone for a radioactive waste repository since the early 1980s. In 2008, the so-called Sectoral Plan Deep Geological Repository (SGT) was launched aiming to systematically define, characterize and finally select the most suitable site to construct such a repository (BFE, 2011). Being in charge for the technical project management, the Swiss National Cooperative for the Disposal of radioactive waste (Nagra) developed and led the exploration activities. Recent 3D-seismic surveys played a significant role in the final stage 3 of the selection process. This contribution summarizes acquisition and processing.

As a result of stages 1 and 2, the Opalinus Clay was selected as target formation to host repositories for high-level (HLW) and low-/intermediate level waste(L/ILW). From 2D-seismic data and sparse borehole information lateral variations of Opalinus Clay depth were identified, as well as the stratigraphic sequence down to basement. This information played a crucial role in the development of appropriate layouts and specifications for new exploration surveys as part of the SGT. Figure 1 illustrates the location of the survey boundaries. While a conventional cross-spread layout was applied in the first ZNO survey (1997), the three recent surveys, named JO-2015, ZNO-2016 and NO-2016 (Hölker & Birkhäuser, 2018), employed quasi straight receiver lines parallel to the geological dip direction. The source points pragmatically followed accessible roads and paths with explosive infills when required. The pragmatic source point layout allowed an efficient operation of seismic vibrator sources. The resulting semi-irregular geometry yields further advantages like more homogeneous azimuth and coverage distribution, and disadvantages (lapse of cross-spread domain processing modules).

The sumptuous acquisition of the 3D-seismic across densely populated areas was just one of several acquisition challenges. Cross-frontier acquisition, pronounced topography, river crossings and airplane noise are mentioned here as examples of untypical challenges to be mastered by the acquisition crew. It is noteworthy that seismic acquisition was met with great acceptance, which resulted in nearly complete realisation of the planned surveys. The confidence gained in the field is considered very valuable for successful communication in later SGT stages.

Geological challenges were posed by the rather shallow target formation (Opalinus Clay depth is ~200-1000 m within the seismic surveys, and by the heterogeneous and heavily varying near surface layer (Quaternary). Strong attenuation in consolidated gravel (Deckenschotter) and the complicated geometry of backfilled overdeepend glacial channels negatively affected the S/N and focusing in the prestack data processing. Sophisticated 3D travelttime inversions were performed to accurately model the near surface geology before 3D-seismic depth processing was endeavored. Benefiting from these analyses, highly accurate determination of static solutions proved to be key in obtaining detailed seismic images in both time and depth domain. The resulting stratigraphic and structural images, in combination with the underlying 3D velocity models, provided the input for the comparison of site-specific geological models, which lead to the selection of the most suitable site for a future repository.



APRX: T1\_alle\Projekte\_Personenbezogen\Spfh\20220829\_TBO\_OPA\3D-Seismik\_TBO\_TOPA\_20220829.aprx

Figure 1. Map showing top Opalinus Clay elevation, sectoral plan siting regions, 3D-seismic boundaries and location of exploration boreholes

## REFERENCES

- BFE 2011: Sachplan geologische Tiefenlager: Konzeptteil. Bundesamt für Energie BFE, Bern, Schweiz.  
 Höcker, A. & Birkhäuser, Ph. 2018: 3D-Seismik Datenbearbeitung 2016-2017: Jura Ost, JO-15, Nördlich Lägern, NL-16, Zürich Nordost, ZNO-97/16. Nagra Working Report NAB 17-36. Wettingen, Switzerland.

## 8.15

### DemoUpStorage: Storing Swiss CO<sub>2</sub> in Basalts

Eleni Stavropoulou<sup>1</sup>, Andrea Moscariello<sup>2</sup>, Alba Zappone<sup>3,4</sup>, Antoine De Haller<sup>2</sup>, Ovie Emmanuel Erutuya<sup>2</sup>, Claudio Madonna<sup>3,4</sup>, Luca Guglielmetti<sup>2</sup>, Lyesse Laloui<sup>1</sup>, Marco Mazzotti<sup>4</sup>, Stefan Wiemer<sup>3</sup>

<sup>1</sup> Ecole Polytechnique Fédérale de Lausanne (EPFL), Laboratory for Soil Mechanics (LMS), EPFL-ENAC-LMS, Station 18, CH-1015 Lausanne, Switzerland (eleni.stavropoulou@epfl.ch)

<sup>2</sup> Geo-Energy Reservoir Geology and Sedimentary Basin Analysis, Université de Genève, Rue des Maraîchers 13, 1205, Geneva, Switzerland

<sup>3</sup> Swiss Seismological Service, ETHZ, Zurich, 8092, Switzerland

<sup>4</sup> Department of Mechanical and Process Engineering, ETHZ, Zurich, 8092, Switzerland

To achieve climate goals of net-zero emissions by 2050, Switzerland will soon need to capture from non-avoidable sources and sequester geologically several millions of tons of CO<sub>2</sub> every year. The DemoUpStorage project, partner project with DemoUpCarma (Demonstration and Upscaling of CARbon dioxide Management solutions for a net-zero Switzerland), aims at: i. Demonstrating the safe, permanent as well as ecologically and economically viable storage of 1 kt of biogenic CO<sub>2</sub> captured in Switzerland, and ii. Advancing the Swiss Roadmap for geological CO<sub>2</sub> storage through knowledge transfer, capacity building and acceptance research. The Swiss CO<sub>2</sub> will be injected and stored permanently in a Basalt reservoir in Iceland, using a novel injection strategy accompanied by dense geophysical and geochemical monitoring.

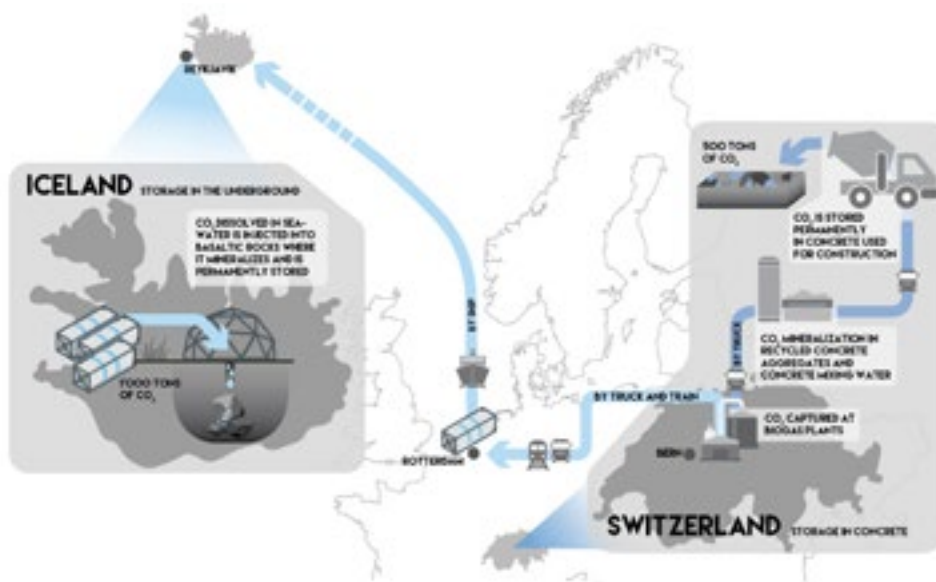


**Figure 1.** Overview of the DemoUpCarma and DemoUpStorage projects for Capture, Utilisation, Transport and Storage of Swiss CO<sub>2</sub> (<http://www.demouparma.ethz.ch/en/home/>)

Storage in basalts may represent an important and cost-effective CO<sub>2</sub> storage technology using suitable formations (off-shore or on-shore) located over the entire globe (Snæbjörnsdóttir et al., 2020; Goldberg et al., 2010). This technology, where CO<sub>2</sub> is permanently stored through mineralisation, has been explored by Carbfix during the last few years by injecting dissolved CO<sub>2</sub> in water in a Basalt reservoir. In DemoUpStorage, CO<sub>2</sub> is dissolved for the first time in seawater and it is then injected in low over-pressure at a few hundred meters overburden. Carbon trapping through mineralisation has the great advantage of occurring very rapidly (1-2 years as per Matter et al., 2016; Clark et al., 2019) when compared to standard CCTS solutions in sedimentary basins, i.e. thousands of years (see Figure 2).

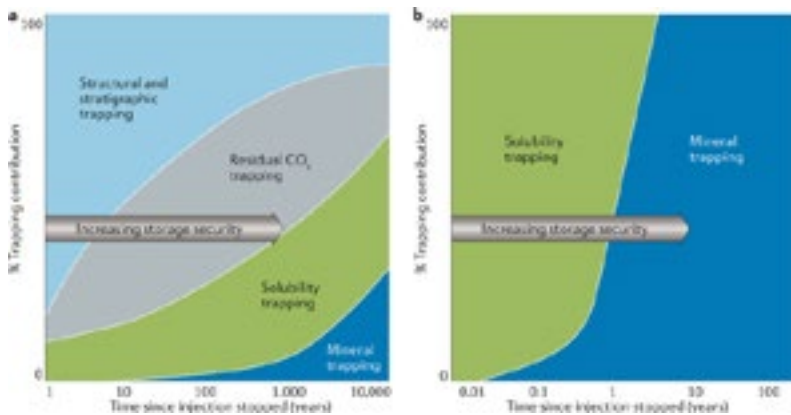


Figure 2. Change in the relative contribution of the carbon-trapping mechanism of CO<sub>2</sub> storage over time when injecting supercritical CO<sub>2</sub> into sedimentary basins (left), and when injecting water-dissolved CO<sub>2</sub> for mineralisation (right), based on data from field experiments (Matter et al., 2016). From Snæbjörnsdóttir et al. (2020).

To achieve the targets of DemoUpStorage, a set of advanced geophysical and geochemical measurements prior, during and after CO<sub>2</sub> injection will be conducted in Iceland. These real-scale field observations and data will be accompanied and supported by ongoing laboratory work carried out by EPFL, ETHZ and UNIGE where high-resolution geomechanical, geochemical and petrophysical analysis will be integrated in a seamless workflow with 3D computational modelling and advanced image analysis for enhancing process understanding, risk and environmental impact assessment, and validation to enable flow model upscaling. The encouraging preliminary results are presented and discussed, the challenges at the various scales of observations are evaluated and the next steps are highlighted.

## REFERENCES

- Clark, D. E., Galeczka, I. M., Dideriksen, K., Voigt, M. J., Wolff-Boenisch, D., & Gislason, S. R. (2019). Experimental observations of CO<sub>2</sub>-water-basaltic glass interaction in a large column reactor experiment at 50 C. *International Journal of Greenhouse Gas Control*, 89, 9-19.
- Matter, J. M., Stute, M., Snæbjörnsdóttir, S. Ó., Oelkers, E. H., Gislason, S. R., Aradottir, E. S., et al. (2016). Rapid carbon mineralization for permanent disposal of anthropogenic carbon dioxide emissions. *Science*, 352(6291), 1312-1314.
- Snæbjörnsdóttir, S. Ó., Sigfusson, B., Marieni, C., Goldberg, D., Gislason, S. R., & Oelkers, E. H. (2020). Carbon dioxide storage through mineral carbonation. *Nature Reviews Earth & Environment*, 1(2), 90-102.

## 8.16

# Corrosion and scaling inside a low-enthalpy geothermal well during shut-in

Daniela B. van den Heuvel<sup>1</sup>, Christoph Wanner<sup>1</sup>, Luca Guglielmetti<sup>2</sup>, François Martin<sup>3</sup>, Michel Meyer<sup>3</sup>, Stefanie Lutz<sup>4</sup>, Liane G. Benning<sup>4</sup>, Larryn W. Diamond<sup>1</sup>

<sup>1</sup> Institute of Geological Sciences, University of Bern, Baltzerstrasse 3, CH-3012 Bern (daniela.vandenheuvel@geo.unibe.ch)

<sup>2</sup> Section des sciences de la Terre et de l'environnement, Université de Genève, Rue des Maraîchers 13, CH-Geneva

<sup>3</sup> Services Industriels de Genève, Chemin du Château-Bloch 2, CH-1219 Vernier

<sup>4</sup> Deutsches GeoForschungsZentrum GFZ, Telegrafenberg, D-14473 Potsdam

In 2018, the 750 m deep GEo-01 well was drilled into Lower Cretaceous lime-stones in the Geneva Basin as part of the "Géothermies 2020" exploration program. The well produces currently 55 L/s of 35 °C water under artesian flow. As of now, the water remains unused and the well is often closed over periods of weeks to months. Upon re-opening the well after such a shut-in period, black suspended particles identified as pyrite were observed in the produced water. In order to assess the source of the pyrite and the processes controlling its formation, water samples were collected at various time intervals (2 min to 2 h) while producing at 35 L/s. The samples were analysed for their solute composition, amount and type of suspended solids and microbial diversity.

The concentrations of major ions (Na, K, Mg, Cl) remained constant and identical to groundwater samples obtained during previous hydrotests at GEo-01. However, the sulphur system proved to be highly reactive during the shut-in period. The reservoir water originally contained around 3-4 mg/L of both oxidised and reduced sulphur species. During shut-in, these concentrations essentially dropped to zero as sulphur was consumed by the corrosion of the steel casing and by the formation of pyrite. In the top of the well, pH and Eh shifts led to transformation of pyrite into nano-crystalline Fe-oxyhydroxides and elemental sulphur. All of these solids were produced with the water upon re-opening of the well. After 15 min of production (equivalent to two well volumes), the amount of suspended solids decreased drastically, suggesting that the corrosion products were detached rapidly from the well casing. This was later confirmed by visual inspection of the casing using a downhole televiwer, which showed no macroscopic signs of corrosion.

All of the observed chemical processes were presumably affected by microbes, as oxidisers and reducers iron and sulphur have been identified in the samples and their abundance correlates with the amount of suspended solids produced. In addition to pyrite formation, the water chemistry suggests that calcite precipitated in the upper section of the well during the shut-in period, removing Ca and HCO<sub>3</sub> from solution. Further dissolved CO<sub>2</sub>, together with H<sub>2</sub> produced as a by-product of corrosion, was likely converted to CH<sub>4</sub> by methanogenic microbes.

Our results suggest that corrosion of the casing, mediated by microbes, and precipitation of precipitation are taking place during shut-ins in low-enthalpy geothermal wells. Similar conditions are expected in wells drilled for seasonal heat storage where shut-in periods of several months are normal. Corrosion and, to a lesser degree, scaling could therefore have a significant impact on the operation of heat storage sites.

## 8.17

# Geological Reasoning for the Site of the Swiss Nuclear Waste Repository

Tim Vietor<sup>1</sup>, Michael Schnellmann<sup>1</sup>, Silvio Giger<sup>1</sup>, Angela Landgraf<sup>1</sup>, Daniel Traber<sup>1</sup>, Herfried Madritsch<sup>1</sup>, Matthias Braun<sup>1</sup> & Nagra's site selection team

<sup>1</sup> Nagra, Hardstrasse 73, 5430 Wettingen

The site selection process for the deep geological repository for radioactive waste of Switzerland is in its final phase. All three remaining sites fulfill the requirements of the repositories for low level waste as well as for high level waste and spent fuel. Using surface-based exploration methods, including 3D-seismics and deep boreholes, Nagra has recently collected the necessary data to select and announce the most suitable site.

The sites are compared based on technical criteria already used in the two previous phases of the selection process. The criteria comprise safety-related aspects including the barrier properties and their long-term stability, as well as the construction suitability of the repository and its access facilities.

All three sites feature a roughly 200 m thick sequence of claystones and marls. The host rock at the centre of the sequence, the Opalinus Clay, is a homogenous claystone around 100 m thick. It has been deposited under shallow marine conditions with little lateral changes. Overlying and underlying units are less homogenous and lateral facies changes between marls, claystones and limestones are common. Hence the thickness and quality of the geological barrier can be different at the three sites. 3D-seismic surveys in the three siting regions acquired between 2015 and 2017 already revealed differences in the depth of the host rock layer, the structural setting and the lithofacies of the rocks surrounding the Opalinus Clay.

From 2019 to spring 2022 Nagra has followed-up on the 3D-seismic surveys with 9 deep boreholes. The boreholes had been positioned around the most promising zones to assess the barrier properties of the clay-mineral rich rock sequence including the bounding aquifers. Some boreholes also reached the underlying Pre-Mesozoic basement. Depending on the local situation and the exploration aims the boreholes were drilled to depths between 650 and 1350 m.

Using mostly continuous wireline coring, the rock sequence at each drillsite was characterized with respect to lithology and barrier relevant parameters such as clay mineral content, porosity, and fault density. Hydraulic properties and stress conditions were determined by in situ tests. Laboratory investigations included rock microfacies, macro- and micropaleontology, mineralogy, strength, ground water and pore water composition, fission track and isotope dating and many more.

In our contribution we present an overview of key results and data sets from the seismic surveying and the boreholes in the three siting regions. The data confirm the high quality of the barrier rocks and the low vertical and lateral variability of the host rock.

To address the long-term stability of the barrier, the Quaternary erosion history was investigated with 11 cored boreholes into overdeepened valleys.

Based on these investigations we present and discuss the geological differences between the regions that have led to the proposed site. As the selected site offers optimal conditions for both HLW and LLW and the space requirements can be met at that site, a co-disposal facility is proposed. This facility will comprise separate emplacement areas with specific safety concepts for the two waste categories.

## 8.18

# Numerical simulations of supercritical geothermal resource utilization

Alina Yapparova<sup>1</sup>, Benoit Lamy-Chappuis<sup>1</sup>, Thomas Driesner<sup>1</sup>

<sup>1</sup> Institute of Geochemistry and Petrology, ETH Zurich, Clausiusstrasse 25, CH-8092 Zurich (alina.yapparova@erdw.ethz.ch)

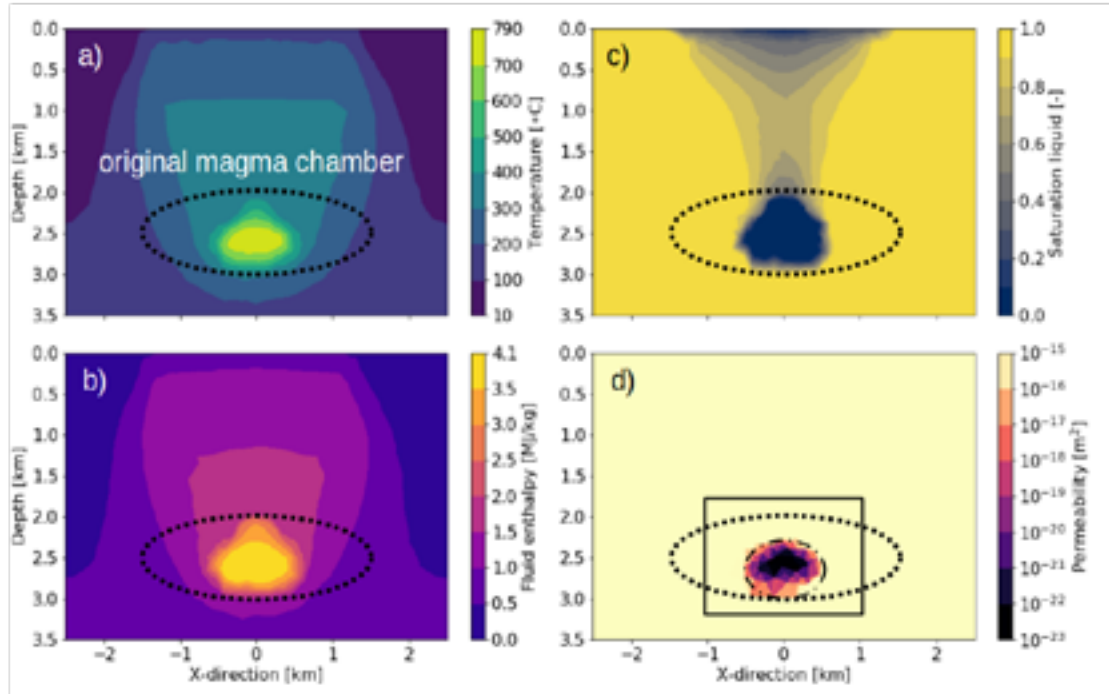
High enthalpy geothermal systems have been harnessed for electrical power generation for over 100 years. An average geothermal well in Iceland, drilled to 1.5-2 km depth, would produce up to 5 Mwe from a two-phase boiling reservoir. A deeper well producing single-phase supercritical water ( $T > 374^\circ\text{C}$ ) could have an order of magnitude higher power output. However, direct production of supercritical fluid can be challenging to the well equipment, and cold water injection into the deep well in order to recharge the conventional resource from below might be a better utilization strategy.

In this work we present numerical simulations of transient geothermal system evolution from the time of magma emplacement through a subsequent formation of a potential supercritical geothermal resource (Fig. 1). The modelling is performed using the 3D Control Volume Finite Element Method (CVFEM; Weis et al., 2014). The numerical scheme is locally mass-conservative and is able to capture strong gradients in fluid properties arising at the contact between a magmatic intrusion and the host rock. The magmatic heat source is explicitly represented as a region of an unstructured mesh and its permeability varies with temperature mimicking the brittle-ductile transition of a basaltic rock.

Direct fluid production from and cold water injection into a supercritical resource is simulated using a newly implemented a well model for the 3D CVFEM (Yapparova et al., 2022; Lamy-Chappuis et al., 2022). Our reconnaissance simulations provide the first glimpse into the response of a supercritical resource to operation with wells.

## REFERENCES

- Lamy-Chappuis, B. et al. 2022: Advanced well model for superhot and saline geothermal reservoirs, *Geothermics*, 105, 102529.
- Weis, P. et al. 2014: Hydrothermal, multiphase convection of H<sub>2</sub>O-NaCl fluids from ambient to magmatic temperatures: A new numerical scheme and benchmarks for code comparison, *Geofluids*, 14, 347–371.
- Yapparova, A. et al. 2022: A Peaceman-type well model for the 3D Control Volume Finite Element Method and numerical simulations of supercritical geothermal resource utilization, *Geothermics*, 105, 102516.



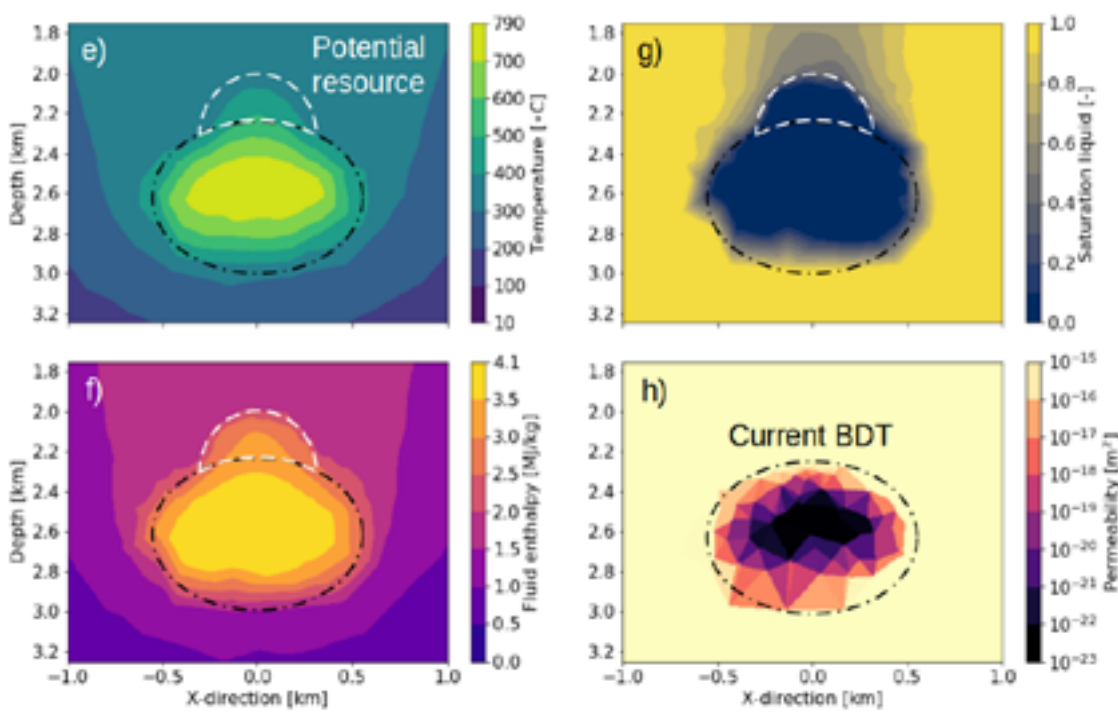


Figure 1. Geothermal system 2.7 ka after magma emplacement, a vertical slice through a 3D model showing temperature (a, e), fluid enthalpy (b, f), liquid saturation (c, g) and rock permeability (d, h). Subfigures e, f, g and h present the area inside a black rectangle on d. From Yapparova et al., (2022).

## 8.19

### Deriving full stress tensor profile from borehole failure observations

Farid Zabihian<sup>1</sup>, Reza Sohrabi<sup>1</sup>, Andrés Alcolea<sup>2</sup>, Peter Meier<sup>2</sup>, Benoît Valley<sup>1</sup>

<sup>1</sup> Centre for Hydrogeology and Geothermics (CHYN), University of Neuchâtel, Neuchâtel, Switzerland  
 (farid.zabihian@unine.ch)

<sup>2</sup> Geo-Energie Suisse AG, Zürich, Switzerland

The potential for harnessing electricity from Enhanced Geothermal Systems (EGS) has long been recognised. However, the technical challenges, risks and associated costs of drilling the boreholes of an EGS rise steeply with increasing depth and must be reduced towards a broad deployment of deep geothermal energy. Characterising the in-situ stresses and assessing wellbore failure is critical for de-risking deep drilling, which comes along with borehole breakouts and drilling induced tensile fractures (Figure 1) that affect borehole integrity, thus increasing risk of failure.

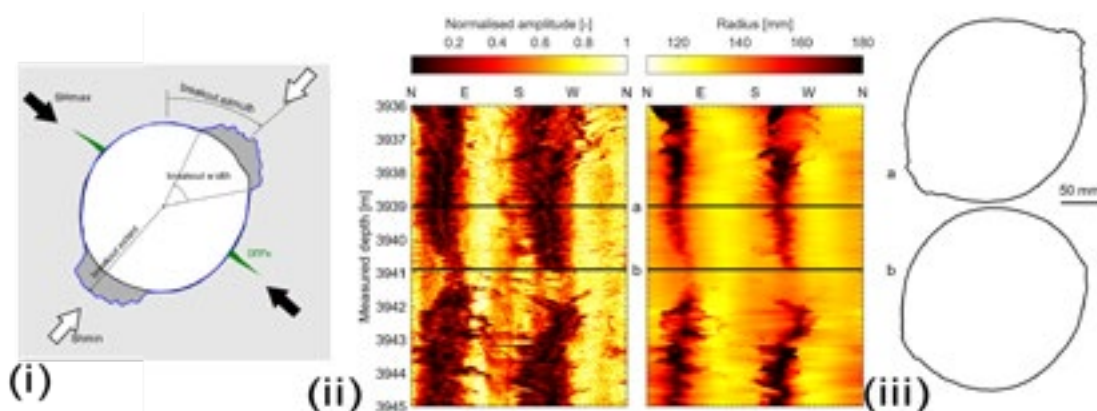


Figure 1. (i) Geometry of typical borehole breakouts and drilling induced tensile fractures, (ii) image-logs of an interval along borehole BS-1 in Basel (Switzerland); (iii) interpreted cross-sections of the borehole, showing the small scale heterogeneity of breakout geometry over short distances.

Borehole instability leads not only to increase drilling costs and risks. Breakouts and tensile fractures may make difficult, or even preclude, borehole completion, e.g., casing or logging, and EGS completion, e.g., the installation of packers for zonal isolation. On the other hand, breakouts or tensile fractures -limited to a certain extent- provide crucial information on rock strength, state of stress and their interactions around the borehole. Contrary to most stress measurement techniques that are essentially point measurements, e.g., mini-fracture tests, interpretation of borehole failure allows to characterise both stress and strength along continuous 1D profiles.

We enhanced the workflow developed by Dahrabou et al. (2022) for interpreting borehole failure information. The main outcomes of the workflow are the heterogeneous distributions of (1) the values and directions of the principal components of the stress tensor and, (2) the rock strength properties (e.g., cohesion and friction). Measurements obtained during or shortly after drilling (i.e., breakout width, breakout extent/depth of penetration, breakout orientation and presence or absence of drilling induced tensile fractures) are used to calibrate the aforementioned model parameters. The use of a computationally efficient semi-analytical solution for evaluating wellbore failure, based on Kirsch analytical solution, allows us to perform a systematic parameter estimation and also to go beyond analyses based on a limited number of scenarios that are typically proposed in borehole failure analyses.

Parameter estimation is carried out using the Regularized Pilot Points Method (Alcolea et al., 2006), as implemented in the software package PEST in two main steps. Firstly, we evaluate coherent depth trends of parameters. Secondly, we evaluate deviations from the trend (i.e., heterogeneity). This approach allows to ultimately propose stress and strength profiles along the borehole including an estimation of the spatial variability. Notably, direct measurements of parameters (e.g., out of laboratory tests or field tests like mini-fracture tests) can be easily accommodated in the workflow to better constrain model outcomes. The estimated profiles open new perspectives for a better understanding of the sources of, e.g., stress or strength variability and their interplays in the upper crust.

## REFERENCES

- Alcolea A., Carrera J., Medina A. 2006: Pilot points method incorporating prior information for solving the groundwater flow inverse problem, *Advances in Water Resources*, 29, 1678–1689.
- Dahrabou A., Valley B., Meier P., Brunner Ph., Alcolea A. 2022: A systematic methodology to calibrate wellbore failure models, estimate the in-situ stress tensor and evaluate wellbore cross-sectional geometry, *International Journal of Rock Mechanics & Mining Sciences*, 149, <https://doi.org/10.1016/j.ijrmms.2021.104935>.

## P 8.1

# Semi-analytical solution for the asymmetrical propagation of fluid-induced frictional shear rupture due to an in-situ linear stress gradient

Regina Fakhretdinova<sup>1</sup>, Alexis Sáez<sup>1</sup>, Brice Lecampion<sup>1</sup>

<sup>1</sup> Geo-Energy Lab – Gaznat Chair, EPFL ([regina.fakhretdinova@epfl.ch](mailto:regina.fakhretdinova@epfl.ch), [alexis.saez@epfl.ch](mailto:alexis.saez@epfl.ch), [brice.lecampion@epfl.ch](mailto:brice.lecampion@epfl.ch))

Many industrial applications like deep heat mining require activation of slip on pre-existing geological discontinuities and creation of hydraulically conductive fracture networks. The fracturing process depends strongly on the initial stress conditions. It is known that the in-situ principal stresses increase linearly with depth [1]. Tensions acting on pre-existing discontinuities depend on depth and orientation of the rupture planes. Fluid injection or diffusion of ground waters can rise the fluid pressure near pre-existing fractures and faults, which may induce frictional slip. In the work [2], it was shown that for a planar rupture when the initial state of stress is uniform and the fluid is pumped under a constant overpressure, a symmetrical frictional shear rupture propagates in a self-similar way. Moreover, there exists a sole dimensionless parameter  $T_o$  that governs the problem.

In this work, we investigate the influence of a linear stress gradient acting initially on the fault, and how this breaks the symmetry of the growing frictional rupture. The problem couples quasi-static elastic equilibrium and fluid flow on the fault plane via a Coulomb shear failure criterion. From a scaling analysis, it is shown that the problem is governed by two dimensionless parameters one of which is the same as in [2]. Initially, when the term associated with the linear gradient of stress is small compared to the rupture length, the solution is similar to the homogeneous stress case ([2] or [3] depending on the injection type). As the time/rupture length increases, the non-uniform stress distribution will start to have an effect and renders the crack growth become asymmetrical as soon as the crack reaches a transition lengthscale. We investigate the crack transition scenarios and provide a benchmark solution for numerical solvers like the one discussed in [3].

## REFERENCES

- [1] Jaeger, J., Cook, N., Zimmerman, R., 2007 Fundamentals of Rock Mechanics, 4th edn. Blackwell Publishing.
- [2] Viesca, R., 2021 Self-similar fault slip in response to fluid injection, *Journal of Fluid Mechanics*, vol. 928
- [3] Sáez, A., Lecampion, B., Bhattacharya, P., Viesca, R., 2022 Three-dimensional fluid-driven stable frictional ruptures, *Journal of the Mechanics and Physics of Solids*, vol. 160

## P 8.2

# Numerical Scheme for the Large-scale Geomechanical Simulations of CO<sub>2</sub>-storage

Emil Gallyamov<sup>1,2,\*</sup>, Brice Lecampion<sup>1</sup>, Jean-François Molinari<sup>2</sup>

<sup>1</sup> Geo-Energy Laboratory, EPFL, Rte Cantonale, 1015 Lausanne

<sup>2</sup> Computational Solid Mechanics Laboratory Institut, EPFL, Rte Cantonale, 1015 Lausanne

\* Corresponding author, e-mail: emil.gallyamov@epfl.ch

CO<sub>2</sub> geological storage is currently the only available Negative Emission Technology with sufficient proven capabilities to significantly contribute to the removal of carbon dioxide from the atmosphere. The design and operations of a storage site are based on the combination of measurements (intrinsically limited to the surface and few wells) and the use of physics-based computational models. A digital twin of the subsurface is indeed the corner stone of all performance and risks assessments. This study aims at addressing a critical gap in the currently available solutions for CO<sub>2</sub> injection modelling.

In this work we develop a fully-coupled hydro-mechanical simulator, which accounts both for the fluid flow and the induced rock deformation. As the high computational efficiency is crucial, we implement and compare several solution schemes such as monolithic scheme, block conjugate gradient<sup>1</sup> and fixed-stress split<sup>2</sup>. The efficiency of each scheme is evaluated on its convergence rate and the code architecture flexibility.

After choosing the most efficient solution scheme, we implement the poroelastic model as an extension of the open-source finite element library Akantu<sup>3</sup> to simulate the time-dependent hydro-mechanical changes associated with CO<sub>2</sub> injection. An implicit time-integration scheme is employed with adaptive time-stepping. In such schemes a large linear system (for displacement and pressure increments) needs to be solved at each time-step. We use well-known pre-conditioners for the solution of mechanical and flow problems by iterative methods.

The hydro-mechanical behaviour of fracture is highly non-linear as fracture permeability strongly depends on its aperture. We work on development of a pore-pressure cohesive element with interface flow following previous work<sup>4,5</sup>. Such a hydro-mechanical cohesive element follows the same principles as the matrix poroelastic solver, resulting in a consistent and robust hydro-mechanical solver. Note that the non-linearity brought by the constitutive behaviour of rock fracture is solved using classical Newton-Raphson algorithm.

A suite of verification problems is implemented to test and validate the numerical developments. For matrix poroelasticity, several analytical solutions in planar and spherical geometries are used<sup>6</sup>. For hydro-mechanical problems, a solution for an open fracture<sup>7</sup> is employed. These different test problems provide a very thorough and robust suite of verification and example problems that are crucial, yet often lacking for highly non-linear multi-physics solvers.

## REFERENCES

1. Prevost, J. H., 1997: Partitioned solution procedure for simultaneous integration of coupled-field problems, Communications in Numerical Methods in Engineering, 13(4), 239-247.
2. Kim, J., Tchelepi, H. A. 2009: Stability, Accuracy and Efficiency of Sequential Methods for Coupled Flow and Geomechanics, SPE 119084.
3. Richart, N., & Molinari, J.-F. 2015: Implementation of a parallel finite-element library: Test case on a non-local continuum damage model, Finite Elements in Analysis and Design, 100, 41-46.
4. Segura, J. M., Carol, I. 2008: Coupled HM analysis using zero-thickness interface elements with double nodes. Part I: Theoretical model. International journal for numerical and analytical methods in geomechanics, 32(18), 2083–2101.
5. Nguyen, T., Selvadurai, A. 1998: A model for coupled mechanical and hydraulic behaviour of a rock joint, International Journal for Numerical and Analytical Methods in Geomechanics, 22(1), 29–48.
6. Cheng, A. H.-D. 2016: Poroelasticity, Springer, 27.
7. Detournay, E. 2016: Mechanics of hydraulic fractures, Annual Review of Fluid Mechanics, 48, 311–339.

**P 8.3****Influence of roughness on the stress dependent permeability of a fracture: Experimental evidences**

Tristan Liardon<sup>1</sup>, John Kolinski<sup>2</sup>, Brice Lecampion<sup>1</sup>

<sup>1</sup> Geo-Energy Lab - Gaznat Chair on GeoEnergy, École Polytechnique Fédérale de Lausanne, CH-1015 Lausanne  
(tristan.liardon@epfl.ch)

<sup>2</sup> Engineering Mechanics of Soft Interfaces, École Polytechnique Fédérale de Lausanne, CH-1015 Lausanne

The hydraulic properties of fractures/joints at depth are known to be highly non-linear with effective stress [Rutqvist and Stephansson 2003]. In order to have a complete description of fluid flow in fracture under compressive stress, the relationship between pressure and permeability must be quantified through the contact mechanics of the interface.

Experimental evidences indicate that the cubic law, that relates the permeability to the cube of the interface aperture, is valid with rock joints with areas in contact [Witherspoon et al 1980]. A number of relationships between normal loading, contact area and aperture distribution have been obtained from both experimental or theoretical investigations [Greenwood et al. 1966, Barton et al. 1985, Persson 2001, Persson 2007].

It is however unclear how these results translate across scales and their domain of validity. For that purpose, experiments at the laboratory scale allow to control closely the relevant properties of the material, interface and fluid.

We investigate the impact of roughness on the permeability of an interface between a layer of Polydimethylsiloxane (PDMS) and glass. The PDMS layers are casted with pre-determined roughness (amplitude of the height and spatial distribution). By injecting fluid from a central point in the interface, and performing pulse tests at different rates, measuring the pressure at the well and elsewhere in the interface, we assess the relation between permeability, surface roughness and the effective stress acting on the interface.

**REFERENCES**

- Barton, N., Bandis, S., Bakhtar,K. 1985: Strength, Deformation and Conductivity Coupling of Rock Joints, International Journal of Rock Mechanics and Mining Sciences & Geomechanics Abstracts, Vol. 20, Num. 6, pp 249-268.
- Greenwood, J. A., Williamson, J. P. B., Bowden, F. P., 1966, Contact of nominally flat surfaces, Proceedings of the Royal Society of London. Series A. Mathematical and Physical Sciences, Vol. 95, Num. 1442, pp 300-319.
- Persson, B. N. J. 2001: Elastoplastic Contact between Randomly Rough Surfaces, Physical Review Letters, Vol. 87, Num. 11.
- Persson, B. N. J. 2007: Relation between Interfacial Separation and Load: A General Theory of Contact Mechanics, Physical Review Letters, Vol. 99, Num. 12.
- Rutqvist, J. & Stephansson, O. 2003: The role of hydromechanical coupling in fractured rock engineering, Hydrogeology Journal, Vol. 11, Num. 11, pp 7-40.
- Witherspoon, P. A., Wang, J. S. Y., Iwai, K., Gale, J.-E. 1980, Validity of Cubic Law for fluid flow in a deformable rock fracture, International Journal of Rock Mechanics and Mining Sciences & Geomechanics Abstracts, Vol. 18, Num. 1, pp 1-21.

## P 8.4

# Fracture aperture distributions of geomechanically-stressed fractured reservoirs

Edoardo Pezzulli<sup>1</sup>, Stephan Matthai<sup>2</sup>, Thomas Driesner<sup>1</sup>

<sup>1</sup> Department of Earth Sciences, ETH Zurich, Clausiusstrasse 25 CH-8092, Zurich (edoardo.pezzulli@erdw.ethz.ch)

<sup>2</sup> Department of Infrastructure Engineering, University of Melbourne, Victoria, Australia

The hydraulic conductivity of a fractured reservoir determines the reservoirs suitability for extracting geothermal energy or sequestering carbon dioxide. Deep geothermal reservoirs require conductive fracture networks to act as efficient heat exchangers for fluids, while conductive fracture networks can negatively affect the sweep characteristics of CO<sub>2</sub> plumes and the resultant CO<sub>2</sub> volume stored. Consequently, the hydraulic conductivity of fractured rock masses significantly affects the success of such engineering projects. The opening and dilatancy of individual fractures strongly affects the fracture's hydraulic conductivity, and provides a fundamental prerequisite for understanding the hydraulic conductivity of the combined fracture network (Lei et al., 2017; Jing et al., 2013; Tsang et al., 2007). In this work, we investigate the role the geomechanical setting plays in opening and dilating fractures within a fracture network. Mechanical simulations are conducted with multiple intersecting and mechanically interacting fracture sets using the numerical multi-physics solver, Open-CSMP++. Each fracture is explicitly captured by a discontinuous finite element mesh which conforms with the fracture geometry. Consequently, the opening and dilatancy of each fracture is a natural mechanical consequence of the discontinuous displacement that develops across the fracture. To inhibit the fictitious interpenetration of fracture surfaces, a penalty-based contact algorithm is used. For a given tectonic setting, the cumulative opening volume is estimated, along with its spatial distribution within the fracture network. Finally, the role of the differential tectonic stress is investigated, along with the orientation of the principle tectonic stresses relative to the orientation of the fracture sets.

## REFERENCES

- L. Jing, K.-B. Min, A. Baghbanan, and Z. Zhao. Understanding coupled stress, flow and transport processes in fractured rocks. *Geosystem Engineering*, 16 (1):2–25, Mar. 2013.
- Q. Lei, J.-P. Latham, and C.-F. Tsang. The use of discrete fracture networks for modelling coupled geomechanical and hydrological behaviour of fractured rocks. *Computers and Geotechnics*, 85:151–176, May 2017.
- C.-F. Tsang, J. Rutqvist, and K.-B. Min. Fractured rock hydromechanics: from borehole testing to solute transport and CO<sub>2</sub> storage. *Geological Society, London, Special Publications*, 284(1):15–34, Jan. 2007.

## P 8.5

# Imaging deep shear-wave velocity structures for geothermal exploration with Ambient Noise Tomography and dense geophone arrays: a tale of two case studies at Aargau and Riehen, Switzerland

Genevieve Savard<sup>1</sup>, Thomas Planes<sup>2</sup>, Matteo Lupi<sup>1</sup> and the Crustal Deformation and Fluid Flow Group<sup>1</sup>

<sup>1</sup> Department of Earth Sciences, University of Geneva, Des Marais 13, CH-1213 Geneva ([genevieve.savard@unige.ch](mailto:genevieve.savard@unige.ch))

<sup>2</sup> Formerly at Department of Earth Sciences, University of Geneva, Des Marais 13, CH-1213 Geneva

Ambient Noise Tomography (ANT) shows great promise as a geothermal exploration method because of its ability to image deeper earth structure including the crystalline basement that is the target of deep geothermal projects for electricity. A shear-wave velocity (Vs) structure is constructed from surface wave dispersion measurements extracted from ambient noise cross-correlations, with the degree of horizontal resolution dictated by the density of the network and inter-station spacing. We have been developing and assessing the performance of ANT with two dense nodal networks of 200 3-C geophones deployed in the canton of Aargau in December 2019 and more recently in Riehen (Basel-Stadt) in September 2022. The two different surveys cover a circular area of approximately 25 and 18 km in diameter respectively, and encompass different environments, with the former including mostly farmland and the latter a mostly urban environment.

In this presentation, we will compare data from these two experiments and discuss how these different environments affect the retrieval of different surface wave and body wave measurements. Results of the Aargau experiment shows ANT can successfully retrieve deep Vs structures consistent with known deep Permo-Carboniferous throughs. For the Riehen experiment, a primary motivation is to compare the wealth of existing geophysical studies in this area with our ANT results. We will show preliminary results of this study and discuss how a high-noise urban environment affects the retrieval of coherent waves from ambient noise. These two experiments are an important step forward to evaluate the reliability and performance of ANT as a valuable early (geothermal) exploration tool.

## P 8.6

# Regional-Scale Thermal Hydraulic Modeling for Preliminary Geothermal Potential Assessment – A

## Theoretical Approach using the example of Riehen

Stefan Scheidler<sup>1</sup>, Horst Dresmann<sup>1</sup>, Jannis Epting<sup>1</sup>

<sup>1</sup> Applied and Environmental Geology, Hydrogeology Research Group, Department of Environmental Sciences, University of Basel, Bernoullistrasse 32, CH-4056 Basel (stefan.scheidler@unibas.ch)

Based on the approach of Tóth et al. (2020), we demonstrate how conceptual, generalized, and simplified Thermal Hydraulic Models (THM) can be used to simulate groundwater flow and heat transport and to support the identification of potential areas for the planned new medium-depth geothermal wells in the municipality of Riehen, Northwestern Switzerland. Regional-scale 2D THM were developed using COMSOL® based on geological section interpretations followed by an assessment of the influence of geological structures as well as the sensitivity of hydraulic and thermal parameters and boundary conditions. Preliminary modeling results show that the thermal regime can be modelled relatively accurately and reproduces measured temperature data (Figure). Furthermore, the most sensitive geologic units and parameters could be identified, which are faults (k-value and aperture) and aquitard (k-value, thermal conductivity) whereas the hydraulic parameters of aquifers have been recognized as not very sensitive.

The next step would be to use the gained experience and to update our existing high-resolution regional 3D geologic model, augment it with the recorded 3D seismic data, and develop a 3D THM. Information on 3D geothermal potential and groundwater flow regime would allow optimization of the location of production and injection wells for an efficient long-term use and to address groundwater protection issues already in the exploratory phase.

## REFERENCES

- Tóth, A., Gallo, A., Mádl-Szönyi, J. (2020) "Significance of basin asymmetry and regional groundwater flow conditions in preliminary geothermal potential assessment – Implications on extensional geothermal plays", Global and Planetary Change 195. DOI: doi.org/10.1016/j.gloplacha.2020.103344

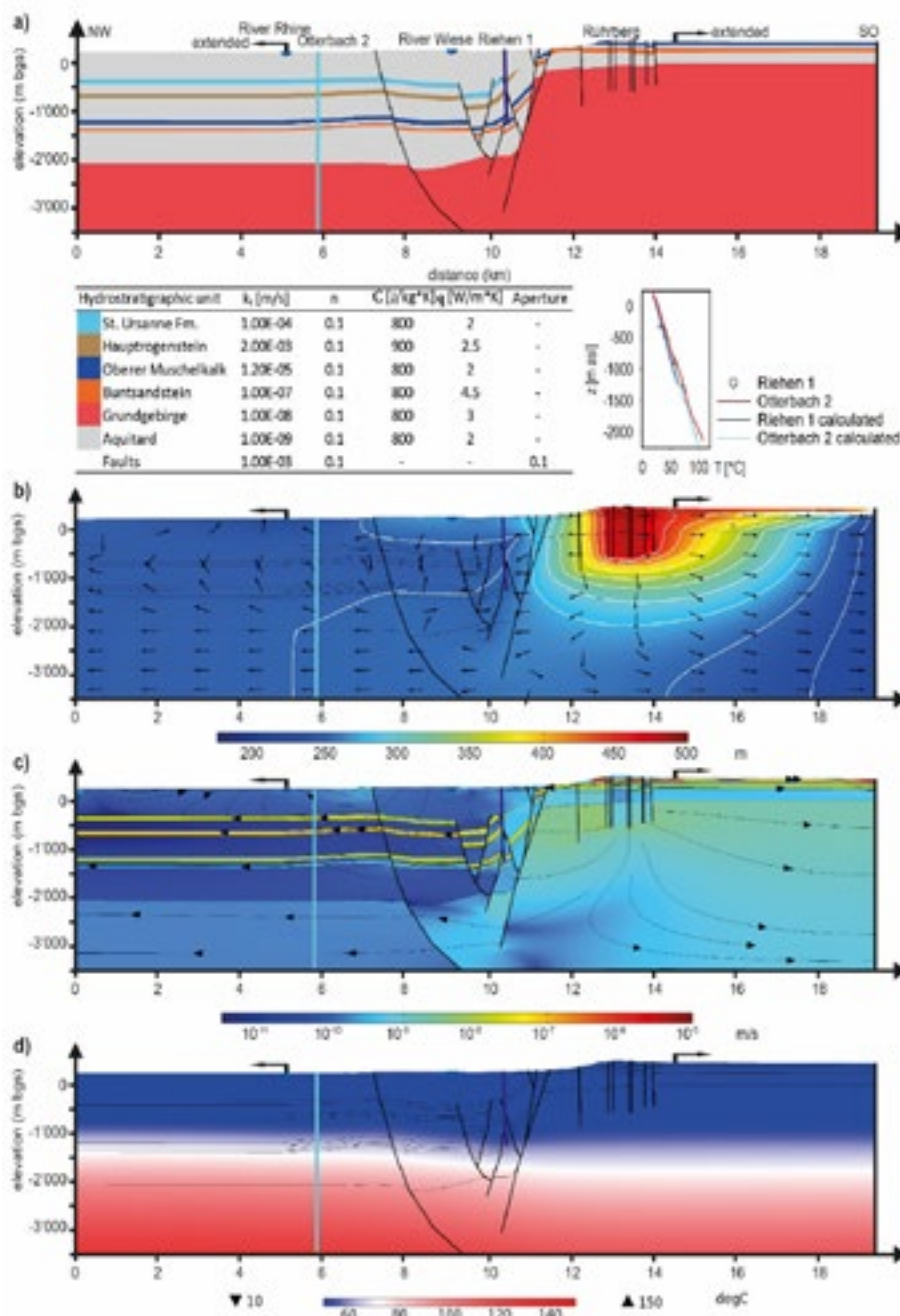


Figure: Regional-scale 2D THM: a) geologic profile extended on both sides to avoid boundary effects; b) simulated groundwater flow and thermal regime showing the hydraulic head and uniform Darcy velocity vector field; c) Darcy velocity magnitude with characteristic streamlines; d) simulated temperature field. The graph shows the measured and calculated vertical temperature profiles from the deep borehole Otterbach 2 in Basel and the existing geothermal well Riehen 1.

## P 8.7

# Induced seismicity in Enhanced Geothermal System (EGS): Insights from the Vendenheim project, France

Gaëlle Toussaint<sup>1</sup>, Reza Sohrabi<sup>1</sup>, Romain Duhamel<sup>2</sup>, Ricardo Perez<sup>2</sup>, Marine Jolivet<sup>2</sup>, Benoît Valley<sup>1</sup>

<sup>1</sup> Centre for Hydrogeology and Geothermics (CHYN), University of Neuchâtel, Neuchâtel, Switzerland

(gaelle.toussaint@unine.ch)

<sup>2</sup> Georhin, zac des Champs de Lescaze, 47310 Roquefort, France

The main challenge of Enhanced Geothermal system (EGS) is to find the most adequate means to develop a network of sufficient permeability to allow circulation and extraction of fluids and heat at economically exploitable rates. Massive fluids injections, usually accomplished to improve the natural permeability of the rock mass, induce seismicity that can sometimes reach magnitude levels felt at the surface. This was the case of the EGS project of Vendenheim, France where seismic events with magnitude up to 3.7 were induced, leading to the project stand by. To allow a future for this technology, it is therefore essential to better understand the development of seismicity induced by EGS as well as the factors that influence its triggering.

Seismicity is generated by shear failure and result of the interlink between in-situ stress state and hydrodynamic conditions in the reservoir. In this work, we determined two possible in situ stress state scenarios based on borehole failure observation and hydraulic data. We characterized the initial hydraulic state of the reservoir and its evolution following the stimulation operations by determining the evolution of the injectivity indices. We also analyzed hydraulic tests to estimate the hydraulic conductivity of the reservoir. These analyses reveal quite good hydraulic conductivities and intermediate injectivity indices compared to other EGS project of the region but it also highlighted a different behaviour of the reservoir around each of the two wells. This different behaviour was also confirmed by spatio-temporal analysis of the induced seismic events. Injection parameters such as cumulative injection volume or pressure were also compared to induced seismicity and interpreted using fracture mechanics-based relations, indicating that larger magnitude seismic events are rather controlled by rupture on unstable fault patches and not by pore pressure diffusion.

All these observations were combined with slip tendency and dilation tendency analyses to refine the conceptual model of the reservoir and to better understand the impact of stimulation operations. This new conceptual model showed that the development of the reservoir, and therefore the viability of the project is strongly influenced by the kinematic structure of the targeted fault zone, i.e. a compressional step-over in a regional strike-slip fault. The relay faults likely act as an hydraulic barrier between the injection and production well while unstable conjugated structures are responsible for the higher magnitude seismic events.



# 9 Scientific Drilling Through Time and Space: On Land and Under the Sea

Miriam Andres, Judith McKenzie, Camille Thomas, Helmut Weissert

## TALKS:

- 9.1 Ariztegui D.: Keynote presentation: Scientific drilling in lacustrine basins: Uncovering while innovating
- 9.2 Baumgartner P.O., Li X., Matsuoka A., Vérard C.: Keynote presentation: Leg 123, Site 765, Argo Abyssal Plain revisited: Austral and subtropical gyre Radiolaria – Late Jurassic/Early Cretaceous southern hemisphere paleobiogeography and global climate change
- 9.3 Früh-Green G.L., Orcutt B.N., Ternietan L., Bernasconi S.M., Lilley, M.D., IODP Exp. 357 Science Party: Keynote presentation: Magmatism, hydrothermal alteration and life at slow-spreading ridges: Insights from Lost City and drilling the Atlantis Massif
- 9.4 Hernández-Almeida I., Gutián J., Tanner T., Zhang H., Stoll H.M.: Hydrographic control of carbon isotope fractionation in coccolithophores in the North Atlantic during the Mid-Pleistocene
- 9.5 Pasquier V., Fike D., Halevy I.: A global reassessment of the controls on iron speciation in modern sediment sand sedimentary rocks: A dominant role for diagenesis

## POSTERS:

- P 9.1 Gerotto A., Zhang H., Stoll H.M., Lopes Figueira R.C., Liu C., Nagai R.H., Hernández-Almeida I.: Calibration of coccoliths morphological attributes as past ocean carbonate chemistry proxies and its application in the South China Sea (ODP Site 1146)

## 9.1

# Scientific drilling in lacustrine basins: Uncovering while innovating

Daniel Ariztegui<sup>1</sup>

<sup>1</sup> Department of Earth sciences, University of Geneva, rue des Maraîchers 13, 1205 Geneva (daniel.ariztegui@unige.ch)

An appreciation of lakes as small oceans in landlocked Switzerland began very early. In 1705, the Italian scholar and eminent natural scientist Count Luigi Ferdinando Marsili, while visiting the region around Lake Urner, referred to it as "piccolo mare" or a "small brother" of the Mediterranean Sea. Almost two centuries later, by the end of the 19<sup>th</sup> century, François-Alphonse Forel initiated the study of many processes in modern Lake Geneva with a pioneering approach that amalgamated physical, biological and chemical aspects of lakes.

However, it was during the 20<sup>th</sup> century that lakes began to be considered as both natural laboratories and archives of climate initiating a bloom of lake studies in several Swiss institutions. Many methods and approaches were borrowed from paleoceanography, including "deep" drilling that was first applied to Lake Zürich (Zübo project) by ETH Professor of Experimental Geology Kenneth J. Hsü. The idea of a drilling rig especially tailored to retrieve long cores from lacustrine settings worldwide started to mature under the leadership of Kerry Kelts, who moved from Switzerland to the US in the early 90's. The Global Lake Drilling (GLAD) project was finally born and tested in the Great Salt Lake, Utah, and a decade later became a major part of the International Continental Drilling Program (ICDP). Relatively long lake coring was already a reality in Swiss institutions and several projects were developed in Asia, Africa, Europe and South America. It was precisely after a very successful project in Lago Cardiel, Argentinean Patagonia, that a Swiss team was invited to participate in the first ICDP project in Guatemala. In 2008, after the successful coring of Lake Petén-Itza, Swiss scientists participated in the Potrok Aike Drilling Project (PASADO) in southernmost Patagonia. This project was very important because it marks the beginning of continuous Swiss membership in ICDP, as well as the beginning of subsurface biosphere studies in deep lacustrine sediments.

Swiss scientists developed a tailor-made methodology for sampling living microbes during lake drilling, which provided the possibility to unveil hidden aspects of microbe-sediment interactions and their potential relationship with climate. ICDP established this new sampling approach as a standard methodology for subsequent lacustrine drilling. Researchers based in Swiss institutions participated and were often leaders of successful lake drilling projects from Patagonia to Indonesia, such as in Lake Ohrid, Lake Van, Lake Towuti and the Dead Sea among other. These drilling expeditions resulted in not only the reconstruction of diverse aspects of past climates but also in the development and application of new approaches and techniques. Many pending lake projects involving researchers based in Swiss institutions are in the pipeline and will possibly be drilled in the near future.

In the same fashion as their bigger brothers, that is, scientific drilling expeditions in the oceans, lake drilling projects have continued to surprise us. Unveiling new aspects of past environments while generating innovative approaches, two critical ingredients for the development of science, scientific drilling in lakes has furthered much of our understanding of the different processes shaping major global events over time. Undoubtedly, a lot more exciting results will come with future lake drilling projects!

## 9.2

# Leg 123, Site 765, Argo Abyssal Plain revisited: Austral and subtropical gyre Radiolaria - Late Jurassic/Early Cretaceous southern hemisphere paleo-biogeography and global climate change

Peter O. Baumgartner<sup>1</sup>, Xin Li<sup>2</sup>, Atsushi Matsuoka<sup>3</sup> and Christian Vérard<sup>4</sup>

<sup>1</sup>Institut des Sciences de la Terre, Université de Lausanne, Géopolis, CH 1015 Lausanne (peter.baumgartner@unil.ch)

<sup>2</sup>Nanjing Institute of Geology and Palaeontology, 39 East Beijing Road, Nanjing 210008, China.

<sup>3</sup>Department of Geology, Niigata University, Niigata 950-2181, Japan. e-mail

<sup>4</sup>Department of Earth Sciences, University of Geneva, Rue des Maraîchers, 13, CH -1205 Genève

The Jurassic/Cretaceous (J/K) boundary, unlike other system boundaries, cannot be linked to a catastrophic paleoenvironmental crisis, but to a gradual palaeoceanographic change recorded in the Western Tethyan intra-Pangean basins by a shift from bio-siliceous (radiolarian) to calcareous (nannoplankton) pelagic sedimentation.

The Tithonian to Aptian/early Albian radiolarian record recovered from Hole 765C-Cores 62R-36R in the Argo Abyssal Plain off the North-western Australian margin is unique by its density of well-preserved radiolarian assemblages and by its faunal contents (Baumgartner, 1992, Baumgartner et al. 2022). The integration with published records of southern hemisphere “non-Tethyan” radiolarian assemblages from Timor/Indonesia, Southern Tibet, Antarctica, Patagonia, New Zealand and the West Pacific allows to define radiolarian paleobiogeography of the southern hemisphere and its implications for the early opening of oceanic gateways within Pangea and global climate change during the J/K- transition.

Radiolaria recovered from claystone yielded the low diversity, “Crypto-Archaeo” Assemblage (chiefly cryptocephalic/cryptothoracic nassellarians and *Archeodictyomitra* spp.) interpreted as tolerant to oligotrophy, originated in the Subtropical Gyre (STG). In contrast, assemblages extracted from radiolarite layers, interpreted as pelagic turbidites/contourites derived from the deeper W-Australian margin, are dominated by Austral taxa, related to an influx of S-polar cold water into the early Argo Basin since the earliest Cretaceous (Fig. 1). Neotethyan taxa are very rare to absent before the late Hauterivian/Barremian, when they gradually gain in diversity and abundance.

Radiolarian biogeography and plate tectonic models support a scenario of palaeoceanographic and global climatic change during the Jurassic-Cretaceous transition related to progressive Pangea break-up: Oceanization between Africa and Madagascar-India-E-Antarctica and the connection of the Proto-Caribbean with S-high latitudes via the S-American Quebrada Grande and Rocas Verdes back-arc basins resulted in: 1. An increased heat transfer to the Southern hemisphere which caused cooling and less nutrient flux in Neotethyan regions during the Late Tithonian dry event. 2. A northward shift of the northern winter Intertropical Convergence Zone reduced the Neotethyan mega-monsoon area and allowed the establishment of a southern Neotethyan subtropical gyre, documented by the “Crypto-Archaeo” Assemblage. 3. The south-polar West Wind Drift may have forced a circum-S-polar cold current through the epicontinental rift between India and Antarctica-Australia, since the Berriasian (140 my) transporting Austral radiolaria into the Argo Abyssal Plain, where they accumulated in radiolarite layers.

## REFERENCES

- Baumgartner P. O. 1992. Lower Cretaceous Radiolarian biostratigraphy and biogeography off northwestern Australian (ODP sites 765 and 766 and DSDP site 261), Argo abyssal plain and lower Exmouth plateau. *Proceedings of the Ocean Drilling Program, Scientific Results*, 123: 299–342.
- Baumgartner P. O., Xin Li, Matsuoka A., Vérard C. 2022: submitted. Austral and Subtropical Gyre Radiolaria - latest Jurassic-Early Cretaceous Leg 123, Site 765, Argo Abyssal Plain revisited– Southern hemisphere paleobiogeography and global climate change. *Micropaleontology*.

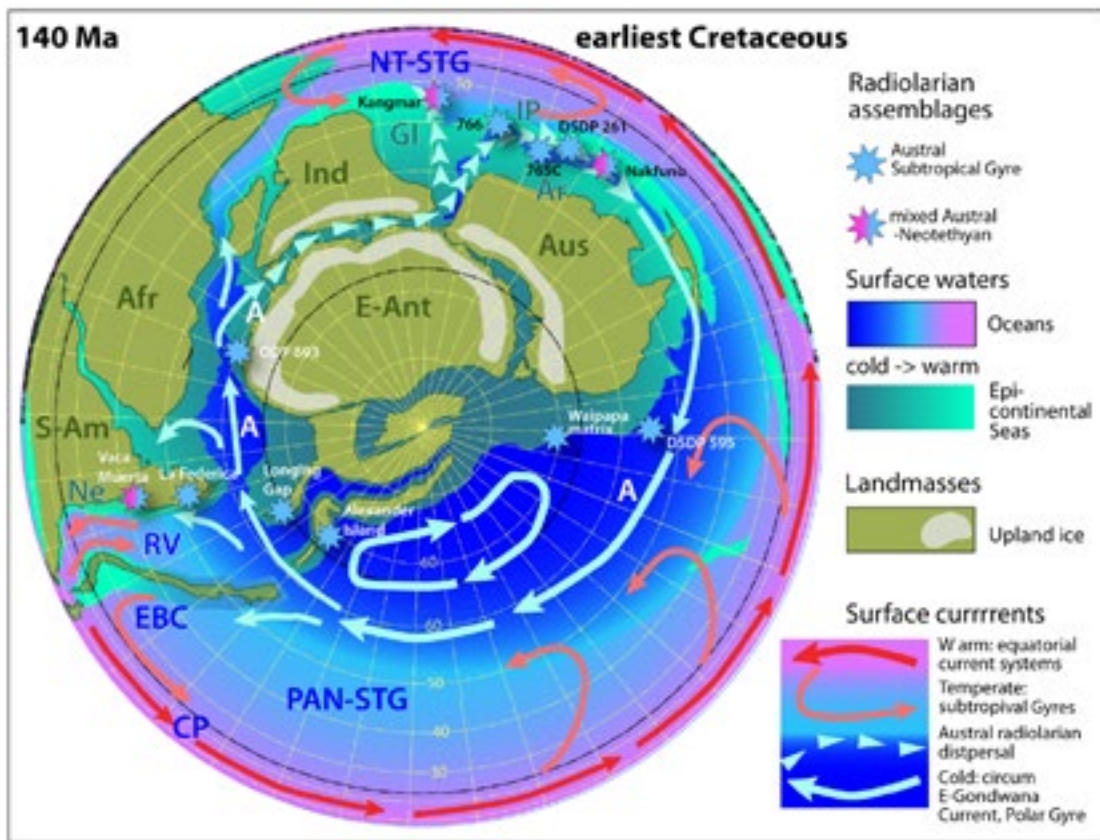


**Figure 1.** 140 Ma (earliest Cretaceous) Paleogeography of S-Gondwana centred on the South Pole, after Baumgartner et al. (2022), with indications of ocean surface currents, latest Jurassic-Early Cretaceous Austral radiolarian dispersal routes and known localities yielding “non-Tethyan”, Austral radiolarian taxa. **Ar:** Argo Abyssal Plan, **GI:** Greater India, **IP:** Indian Promontory, **Ne:** Neuquen Basin, **RV:** Rocas Verdes Ocean (Vérard et al. 2012). Circum- East Gondwanian surface ocean current system inspired by Gordon (1972). Dispersal routes of Austral radiolarian adapted from Baumgartner (1992). **A:** Austral, Circum-S.-polar current system. **EBC:** Eastern Boundary Current. **CP:** Central Panthalassan Current. **NT-STG:** Neotethyan Subtropical Gyre. **PAN-STG:** Panthalassan Subtropical Gyre. **RV:** Rocas Verdes monsoonal circulation.

### 9.3

## Magmatism, hydrothermal alteration and life at slow-spreading ridges: Insights from Lost City and drilling the Atlantis Massif

Gretchen L. Früh-Green<sup>1</sup>, Beth N. Orcutt<sup>2</sup>, Lotta Ternieten<sup>1</sup>, Stefano M. Bernasconi<sup>1</sup>, Marvin D. Lilley<sup>3</sup>, IODP Expedition 357 Science Party

<sup>1</sup> Department of Earth Sciences, ETH Zurich, Sonneggstrasse 5, CH-8092 Zurich ([frueh-green@erdw.ethz.ch](mailto:frueh-green@erdw.ethz.ch))

<sup>2</sup> Bigelow Laboratory for Ocean Sciences, East Boothbay, Maine, 04544, USA

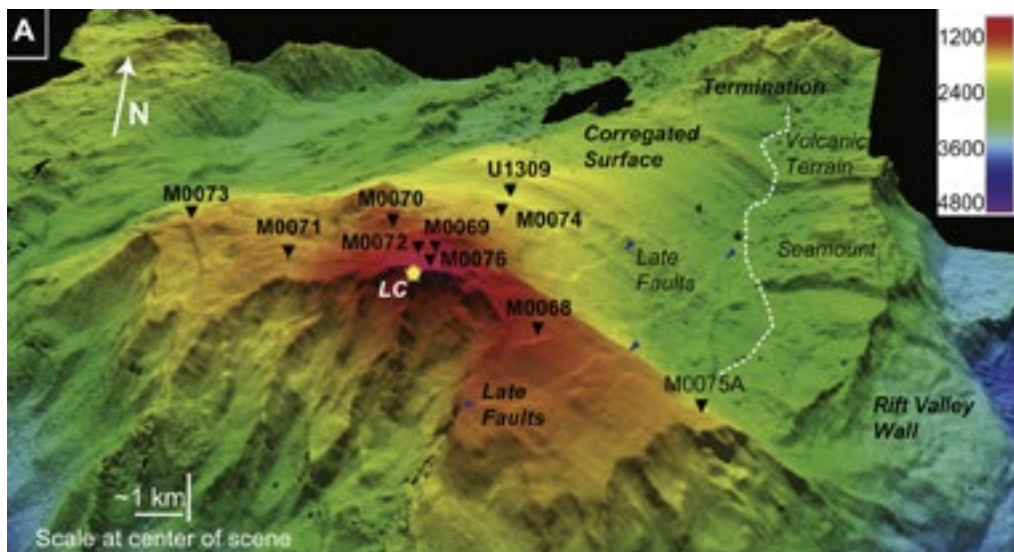
<sup>3</sup> School of Oceanography, Univ. of Washington, Seattle, Washington, 98105, USA

Ultramafic and lower crustal rocks are exposed on the seafloor in different tectonic settings and have been the target of a number of expeditions throughout the history of ocean drilling. Progressive interaction of seawater with mantle-dominated lithosphere during serpentinization is a fundamental process that controls rheology and geophysical properties of the oceanic lithosphere and has major consequences for heat flux, geochemical cycles and microbial activity. At slow spreading ridge environments, serpentinization occurs along detachment faults (major, large-scale offset normal faults), as mantle rocks are uplifted to the seafloor and are incorporated in dome-shaped massifs known as oceanic core complexes. The processes controlling hydrothermal activity and a deep biosphere are intimately linked, however, the spatial scale of lithological variability, the implications for geochemical cycles and the consequences for subsurface ecosystems supported by these systems remain poorly constrained. This presentation provides an overview of magmatic and alteration processes at the Atlantis Massif (Mid-Atlantic Ridge, 30°N, Fig. 1A) and highlights the importance of the discovery of the spectacular Lost City hydrothermal field and recent results of drilling during IODP Expedition 357.

The Atlantis Massif is one of the best-studied oceanic core complexes and hosts the low-temperature Lost City hydrothermal field on its southern wall (Fig.1). Serpentinization reactions in the underlying mantle rocks produce high pH fluids that form intricate carbonate-brucite structures upon venting on the seafloor. The fluids have high concentrations of hydrogen, methane and formate that support novel microbial communities dominated by methane-cycling archaea in the hydrothermal carbonate deposits (Kelley et al., 2005). Understanding the links between serpentinization processes and microbial activity in the shallow subsurface of the Atlantis Massif was one focus of IODP Expedition 357, which used seabed rock drilling technology for the first time in the history of ocean drilling to recover ultramafic and mafic rock sequences and fluids along a detachment fault zone (Früh-Green et al., 2018). The cores show highly heterogeneous rock type, bulk rock chemistry and alteration that reflect multiple phases of magmatism and fluid-rock interaction within the detachment fault zone. The expedition also successfully applied new technologies that provide insights into active serpentinizing systems at slow-spreading ridges. An *in-situ* sensor package and water sampling system recorded real-time variations in dissolved methane and hydrogen, oxygen, pH, oxidation reduction potential, temperature and conductivity during drilling and sampled bottom water after drilling. Systematic excursions in these parameters together with elevated hydrogen and methane concentrations in post-drilling fluids provide evidence for active serpentinization at all sites (Früh-Green et al., 2018). A major achievement was to obtain microbiological samples along a west–east profile to better understand how microbial communities are sustained as ultramafic rocks are altered and emplaced on the seafloor. The presence of a limited biosphere in this subseafloor environment is confirmed by cell counts, which revealed cell densities on the order of  $10\text{--}10^4$  cells per cubic centimetre of rock.

### REFERENCES

- Früh-Green, G.L., et al. 2018: Magmatism, serpentinization and life: Insights through drilling the Atlantis Massif (IODP Exp. 357): *Lithos*, 323, 137–155.  
 Kelley, D.S., et al., 2005, A serpentinite-hosted ecosystem: The Lost City Hydrothermal Field: *Science*, 307, 1428–1434.



B.



Figure 1. (A): 3-D bathymetric model of the Atlantis Massif with a northward view of the detachment fault surface showing striations associated with detachment faulting and locations of IODP Expedition 357 drill sites, the Lost City hydrothermal field (LC: yellow star) and IODP Site U1309. (B): Carbonate-brucite minerals are deposited from high pH fluids at temperatures of 40–95°C, forming elaborate towers and structures of the Lost City hydrothermal field.

## 9.4

# Hydrographic control of carbon isotope fractionation in coccolithophores in the North Atlantic during the Mid-Pleistocene

I. Hernández-Almeida<sup>1</sup>, J. Gutián<sup>1</sup>, T. Tanner<sup>1</sup>, H. Zhang<sup>1, 2</sup>, H. Stoll<sup>1</sup>

<sup>1</sup> Department of Earth Sciences, ETH Zurich ([ivan.hernandez@erdw.ethz.ch](mailto:ivan.hernandez@erdw.ethz.ch)).

<sup>2</sup> State Key Laboratory of Marine Geology, Tongji University

The carbon isotopic fractionation during photosynthesis ( $\varepsilon_p$ ) from sedimentary alkenone biomarkers produced by coccolithophores are a widely used proxy for concentrations of past dissolved CO<sub>2</sub> in seawater (CO<sub>2[aq]</sub>). Currently,  $\varepsilon_p$  records covering the last 1 Myr exist only for oligotrophic locations at low-latitudes regions. Higher latitudes are affected by more variable hydrographic conditions which are expected to produce larger changes in factors which are important for  $\varepsilon_p$ , such as light, temperature, CO<sub>2</sub> and growth rate. Understanding these processes at high latitudes is important in order to derive correct estimates of past CO<sub>2</sub> concentrations. Here we present a new  $\varepsilon_p$  records, alkenone-based temperature reconstructions and review previously published micropaleontological and geochemical records sensitive to hydrographic circulation changes, from sites across a latitudinal transect in the eastern North Atlantic (66°-37°N) for the 800-400 ka time interval. During this period, the subpolar hydrographic fronts shifted latitudinally at orbital and sub-orbital time-scales, leading to large zonal and meridional environmental gradients in the North Atlantic. We observe that  $\varepsilon_p$  and climate-state relationships (depicted by δ<sup>18</sup>O<sub>b</sub>) are similar across different regions.  $\varepsilon_p$  are lower at mid-latitude regions (sites U1385 and U1313), due a higher growth rate during colder intervals. In the high-latitude sites, a longitudinal gradient is observed, with higher  $\varepsilon_p$  during glacial intervals eastward (Site 982) compared to interglacials, as opposite to sites located westward (sites U1314 and 984). We suggest that this is the result of the uninterrupted northward flow of warm atlantic waters through towards the east, which sustained high coccolithophore productivity and growth rate, depressing  $\varepsilon_p$  values at Site 982 during interglacial intervals. Combining high-latitude planktonic foraminifera species and calcium carbonate records, we reconstruct the effect of non-CO<sub>2</sub> factors on  $\varepsilon_p$ .

## 9.5

# A global reassessment of the controls on iron speciation in modern sediments and sedimentary rocks: A dominant role for diagenesis

Virgil Pasquier<sup>1</sup>, David Fike<sup>2</sup>, Itay Halevy<sup>3</sup>

<sup>1</sup> Institute of Earth Sciences, Université de Lausanne, Geopolis, Mouline 1015 Lausanne, Switzerland

(virgil.pasquier@unil.ch)

<sup>2</sup> Earth and Planetary Sciences, Washington University in St. Louis, St. Louis, MO, USA

<sup>3</sup> Earth and Planetary Sciences, Weizmann Institute of Science, Rehovot, Israel

The speciation of iron in sediments and sedimentary rocks is a widely used proxy for the chemistry and oxidation state of ancient water bodies. Specifically, the fraction of reactive iron out of the total iron ( $\text{Fe}_{\text{HR}}/\text{Fe}_{\text{T}}$ ) and the fraction of pyrite iron out of the reactive iron pool ( $\text{Fe}_{\text{PYR}}/\text{Fe}_{\text{HR}}$ ) are thought to constrain the oxidation state and the presence of sulfide in the water column, respectively. This approach was developed and tested against modern core-top sediments, but application to sedimentary rocks requires consideration of the effects of diagenesis and lithification on iron speciation. Furthermore, the effects of deep burial, metamorphism, and late-stage alteration during exhumation or sampling (e.g., oxidative weathering) have not been systematically explored. To bridge this gap, we combined new data from four sediment cores ( $n=54$ ) with an extensive literature compilation of modern sediments (2936 measurements from 316 cores) and ancient sedimentary rocks (12173 measurements spanning the Neoarchean to Quaternary). The modern data include both surface and buried sediments, allowing an investigation of the effects of diagenesis on iron speciation. Depending on the thresholds used to distinguish oxic from anoxic environments and ferruginous from euxinic environments, interpretation of the modern sedimentary iron speciation data within the existing framework yields incorrect environmental classifications up to  $\approx 70\%$  of the time. In modern sediments, diagenesis is the main reason that iron speciation does not represent the chemistry and oxidation state of the water column. We find that iron speciation correlates with porewater chemistry and that it changes with progressive burial along three distinctive  $\text{Fe}_{\text{HR}}/\text{Fe}_{\text{T}}$ – $\text{Fe}_{\text{PYR}}/\text{Fe}_{\text{HR}}$  arrays, each of which represents a different set of diagenetic processes. We suggest that similarly to modern sediments, stratigraphic variation in iron speciation in sedimentary rocks primarily reflects progressive burial diagenesis or variation in depositional conditions rather than temporal variation in water-column chemistry and oxidation state. Indeed, analysis of the geologic iron speciation data reveals no statistically significant trends in either  $\text{Fe}_{\text{HR}}/\text{Fe}_{\text{T}}$  or  $\text{Fe}_{\text{PYR}}/\text{Fe}_{\text{HR}}$  from the Archean to the present day. The diagenetic  $\text{Fe}_{\text{HR}}/\text{Fe}_{\text{T}}$ – $\text{Fe}_{\text{PYR}}/\text{Fe}_{\text{HR}}$  arrays that we identified in modern marine sediments suggest that under certain conditions, iron speciation analyses may be used to constrain  $\text{Fe}_{\text{HR}}/\text{Fe}_{\text{T}}$  in the local sediment source(s). Hence, we suggest that iron speciation data, together with complementary petrographic, mineralogical and geochemical constraints, may be used to constrain the local iron source(s) and early and late diagenetic processes, but rarely the chemistry or oxidation state of ancient water columns.

## P 9.1

# Calibration of coccoliths morphological attributes as past ocean carbonate chemistry proxies and its application in the South China Sea (ODP Site 1146)

Amanda Gerotto<sup>1</sup>, Hongrui Zhang<sup>2,3</sup>, Heather Stoll<sup>2</sup>, Rubens César Lopes Figueira<sup>1</sup>, Chuanlian Liu<sup>3</sup>, Renata Hanae Nagai<sup>4</sup>, Iván Hernandez-Almeida<sup>2</sup>

<sup>1</sup> Oceanographic Institute, University of São Paulo, Praça do Oceanográfico, 191, São Paulo, SP, Brazil

<sup>2</sup> Department of Earth Sciences, ETH Zurich ([ivan.hernandez@erdw.ethz.ch](mailto:ivan.hernandez@erdw.ethz.ch)).

<sup>3</sup> State Key Laboratory of Marine Geology, Tongji University

<sup>4</sup> Center for Marine Studies, Federal University of Paraná, Av. Beira Mar, s/n, Pontal do Paraná, PR, Brazil

Understanding the variations in past ocean carbonate chemistry is critical in elucidating the role of the oceans in balancing the global carbon cycle. Marine calcifiers tests are widely used as past ocean carbonate chemistry proxies, however, the complexity of the carbonate system and ecological aspects limit the interpretation of these proxies. Therefore, there is a need to calibrate existing or develop new proxies to improve our past ocean chemistry changes reconstruction capacity. Here we present a new dissolution proxy based on the morphological attributes of fossil coccolithophores from surface sediments of the South China Sea (SCS). We applied morphological attributes (length, volume, thickness, and shape factor "ks") from the Noelaerhabdaceae group (*Emiliana huxleyi* and *Gephyrocapsa* spp.) to evaluate coccolithophore calcification and preservation aspects. Surface sediments samples were retrieved along a depth gradient (629 – 3809 m) in the SCS. The morphological attributes and environmental data, including mean annual seawater temperature, salinity, nutrients, total alkalinity and CO<sub>2</sub>, pH, and CO<sub>3</sub><sup>-</sup> at 50 m depth, and calcium carbonate saturation ( $\Omega$ Ca) at bottom depth from surface samples site locations, were normalized using a box-cox transformation and combined in a redundancy analysis (RDA) to assess potential relationships. The RDA results presented samples mainly distributed along the first axis (RDA1) which explained 54.6% of the total variation in the morphological data. The RDA1 was highly correlated with the  $\Omega$ Ca at bottom depth ( $R=0.62$ ). The variance of the morphological data was primarily explained by the Wca saturation at depth. The mean  $\Omega$ Ca was the environmental variable that explained the highest amount of variance on the ks shape factor ( $R^2=0.47$ ). Our results show that the mean ks in fossil coccolithophores have the potential to be used as quantitative indicators of past carbonate dissolution changes. We applied this approach to fossil coccolithophores assemblages from ODP Site 184-1146 (1451 m depth) samples, to reconstruct  $\Omega$ Ca changes in the northern SCS since MIS 6.



# 10 Quaternary environments: landscapes, climate, ecosystems and human activity during the past 2.6 million years

Catharina Dieleman, Loren Eggenschwiler, Bigna Steiner, Marius Buechi, René Löpfe, Marc Luetscher, Stefanie Wirth

*Swiss Society for Quaternary Research (CH-QUAT)*

## TALKS:

- 10.1 Czerski D., Giacomazzi D., Scapozza C.: Evolution of fluvial environments and history of human settlements on the Ticino river alluvial plain (Southern Switzerland)
- 10.2 Dieleman C., Christl M., Vockenhuber C., Gautschi P., Akçar N.: Complex Deckenschotter architecture at Irchel – An endeavor to reconstruct detailed chronology and stratigraphy
- 10.3 Jouvet G., Cohen D., Russo E., Buzan F., Raible C.C., Fischer U.H., Haeberli W., Imhof M., Becker J.K., Landgraf A.: Coupled climate-glacier modelling of the last glaciation in the Alps
- 10.4 Mey J., Schwanghart W., Landgraf A., Davy P.: Fluvial response to glacial-interglacial cycles – modelling the evolution of the Hochrhein using EROS
- 10.5 Musso Piantelli F., Truttmann S., Herwegh M.: Structural-controlled valley erosion in high erosion-resistance crystalline bedrock
- 10.6 Schaeppman-Strub G., Kassens H., Jaccard S.L., Makhotin M., Arctic Century science team: Arctic Century – an interdisciplinary expedition to the Kara and Laptev Sea to study ocean, atmosphere and land processes in the changing Arctic
- 10.7 Vendettioli D., Strupler M., Anselmetti F.S., Fabbri S.C., Shynkarenko A., Kremer K.: Understanding tsunamigenic delta collapses in the perialpine lakes of Switzerland

## POSTERS:

- P 10.1 Dieleman C., Eggenschwiler L., Steiner B., Buechi M., Löpfe R., Luetscher M., Wirth S., Haas J.N.: Swiss Society for Quaternary Research (CH-QUAT)
- P 10.2 Kamleitner S., Ivy-Ochs S., Manatschal L., Akçar N., Christl M., Vockenhuber C., Hajdas I., Synal H.-A.: Last Glacial Maximum glacier fluctuations of the Rhine and Reuss glacier systems
- P 10.3 Kober F., Pollhammer T., Salcher B., Deplazes G.: Glaciofluvial terrace hypsometry in the Swiss Alpine Foreland compared with stratigraphic, glacio- and geodynamic and absolute dating information
- P 10.4 Maier F., Haeberli W., Fischer U.H., Landgraf A.: Deep erosion by glaciers – Analysing morphological characteristics of global glacier-bed overdeepenings
- P 10.5 Kremer K., Fabbri S.C., Vendetuolli D., Affentranger C., Anselmetti F.S.: What controls delta failures?
- P 10.6 Millet J.F.L., Rydberg J., Bigler C., Dubois N., Lehmann M.F., Studer A.S.: Diatom-bound nitrogen isotopes as a paleo-proxy in lacustrine environments: a preliminary report
- P 10.7 Blattmann T.: Enhanced petrogenic organic carbon oxidation at glacial terminations?
- P 10.8 Thomas C.L., Galka M., Czerwiński S., Knorr K.-H., Jansen B., Wiesenberg G.L.B.: Insights into Central European environmental changes during the last 2500 years by multi-proxy analysis of the undisturbed Beerberg peatland, Thuringia, Germany
- P 10.9 Broś E., Ivy-Ochs S., Grischott R., Kober F., Vockenhuber C., Christl M., Gautschi P., Maden C., Ylä-Mella L., Jansen J.D., Knudsen M.F., Synal H.A.: Age of the oldest sediments in the northern Swiss Alpine Foreland
- P 10.10 Ott R., Ivy-Ochs S., Kober F., Christl M., Vockenhuber C.: Paired cosmogenic-nuclide measurements improve denudation rate estimates of northern Switzerland
- P 10.11 Schmidt C., Halter T., King G., Hanson P., Kreutzer S.: Zircon luminescence as a geochronological tool for (sub-) recent sediments – First results
- P 10.12 Morgan A., Fleitmann D., Cheng H., Edwards L.R., Matter A., Hofmeister E., Tuysuz O., Altaweel M.: Late Holocene speleothem reconstructions from SW Asia
- P 10.13 Rowan S., Luetscher M., Szidat S., Laemmeli T., Kost O., Lechleitner F.: Constraining the sources of cave CO<sub>2</sub> through multipool <sup>14</sup>C and δ<sup>13</sup>C analysis at Milandre cave, Switzerland.
- P 10.14 Held F., Cheng H., Edwards R.L., Tüysüz O., Fleitmann D.: Holocene to Late-Pleistocene climate variability in Turkey and the Eastern Mediterranean recorded in speleothems10.

## 10.1

# Evolution of fluvial environments and history of human settlements on the Ticino river alluvial plain (Southern Switzerland)

Dorota Czerski<sup>1</sup>, Daphné Giacomazzi<sup>1</sup>, and Cristian Scapozza<sup>1</sup>

<sup>1</sup> Institute of Earth Sciences, University of Applied Sciences and Arts of Southern Switzerland (SUPSI), Campus Mendrisio, Via Flora Ruchat-Roncati 15, CH-6850 Mendrisio

In recent times many studies were carried out to determine the evolution of the hydro-sedimentary dynamics of Alpine rivers in the past, in order to understand the river dynamics, their relationship with the climate oscillations, and their impact on humans as a resource and/or natural risk.

The present contribution is the object of a recent publication (Czerski et al. 2022, Geogr. Helv. 77) on the evolution of the fluvial environments of the Ticino river alluvial plain (Southern Switzerland). The research is based on historical sources, previous investigations on three sites based in the Ticino river floodplain, and data collected on six archaeological sites located on four alluvial fans. The results revealed a complex interaction of the Ticino river and its lateral tributaries with the human communities since the Neolithic (5400–2200 BCE). Lithostratigraphic sequences and archaeological evidence described in the field were constrained by radiocarbon dating, providing the interpretation of the depositional context in relationship with the geological epochs and the cultural periods defined for the Southern Swiss Alps. The combined approach allowed for the definition of 13 phases of enhanced hydro-sedimentary activity covering a period between the Neolithic and the contemporary period. The palaeoenvironmental and palaeoclimatic causes of these phases and their impacts on human settlements are evaluated.

Most of the enhanced hydro-sedimentary phases are linked to the regional or continental palaeoenvironmental and palaeoclimatic context, recorded in correspondence with periods of climate degradation with the establishment of cold and humid conditions, evidence of glacier advances in the Swiss Alps, and/or by an increase in the flood activity on the southern side of the Alps. The more recent phases, in particular, are attributed to the coldest and moistest phases of the Little Ice Age (LIA) climate oscillation. The collected data allowed us also to assess the impacts of these enhanced alluvial phases on the human communities and to explain many of the sedimentological and archaeological observations in the field, e.g. the torrential events attributed to the LIA had a strong impact on the construction and destruction phases observed for the archaeological site of Giubiasco Palasio.

The study is still ongoing; the summary of the evolution of the hydro-sedimentary dynamics of the Ticino river and its tributaries presented herein will be continuously refined and updated with further sedimentological and archaeological observations.

## 10.2

# Complex Deckenschotter architecture at Irchel – An endeavor to reconstruct detailed chronology and stratigraphy

Catharina Dieleman<sup>1</sup>, Marcus Christl<sup>2</sup>, Christof Vockenhuber<sup>2</sup>, Philip Gautschi<sup>2</sup>, Naki Akçar<sup>1</sup>

<sup>1</sup> Institut für Geologie, University of Bern, Baltzerstrasse 1+3, CH-3012 Bern (catharina.dieleman@geo.unibe.ch)

<sup>2</sup> Labor für Ionenstrahlphysik, ETH Zürich, Otto-Stern-Weg 5, CH-8093 Zürich

The Lower Pleistocene of the northern Swiss Alpine Foreland is characterized by a succession of glaciofluvial sediments intercalated with glacial and/or overbank deposits (*Deckenschotter* in German), which are accumulated in three phases between ca. 2.5 and ca. 1 Ma (Graf 1993; Akçar et al. 2014, 2017; Claude et al. 2017; 2019; Knudsen et al., 2020; Dieleman et al. 2022). The topographically highest Deckenschotter site is located at Irchel in the Canton of Zurich, where the recently established chronostratigraphy indicates a cut-and-fill system that prevailed during the Early Pleistocene and disagrees with the existing morphostratigraphy (Claude et al. 2019; Dieleman et al. 2022). Mammal fossils discovered in the Hasli Formation in the early 90's were ascribed to the Mammal Neogene Zone 17 (2.5 – 1.8 Ma; Bolliger et al., 1996) and the Hasli Formation overlies the ca. 1 Ma old gravels at the spot of discovery. In brief, the lines of evidence show that the Deckenschotter at Irchel have a more complex architecture than assumed so far.

This study aims at getting a better understanding of the environment responsible for this complex architecture and at reconciling the lithostratigraphy, chronology, and biostratigraphy. To achieve these goals, a set of methods is applied. Outcrops are mapped and their sedimentology analyzed to reconstruct the origin, transport mechanism, and depositional environment as well as to improve the lithostratigraphical framework. To validate the existing chronology, at least six outcrops above and below the Hasli Formation are sampled along a stratigraphic profile for isochron-burial dating with cosmogenic <sup>10</sup>Be and <sup>26</sup>Al. In addition, three boreholes and shallow trenches will provide further insights into the complex architecture. Besides, the Hasli Formation, if encountered, and gravels under and above will be sampled for isochron-burial and burial dating. In the boreholes and surroundings, geophysical measurements will be performed to complement our comprehension of the internal structure of the Deckenschotter at Irchel. First results will be presented.

## REFERENCES

- Akçar, N., Ivy-Ochs, S., Alfimov, V., Claude, A., Graf, H.R., Dehnert, A., Kubik, P.W., Rahn, M., Kuhlemann, J., and Schlüchter, C. 2014: The first major incision of the Swiss Deckenschotter landscape: Swiss Journal of Geosciences, v. 107, p. 337–347, doi: 10.1007/s00015-014-0176-6.
- Akçar, N., Ivy-Ochs, S., Alfimov, V., Schlunegger, F., Claude, A., Reber, R., Christl, M., Vockenhuber, C., Dehnert, A., Rahn, M., and Schlüchter, C. 2017: Isochron-burial dating of glaciofluvial deposits: First results from the Swiss Alps: Earth Surface Processes and Landforms, v. 42, p. 2414–2425, doi: 10.1002/esp.4201.
- Claude, A., Akçar, N., Ivy-Ochs, S.D., Schlunegger, F., Kubik, P.W., Dehnert, A., Kuhlemann, J., Rahn, M., and Schlüchter, C. 2017: Timing of early Quaternary gravel accumulation in the Swiss Alpine Foreland: Geomorphology, v. 276, p. 71–85, doi: 10.1016/j.geomorph.2016.10.016.
- Dieleman, C., Christl, M., Vockenhuber, C., Gautschi, P. and Akçar, N. 2022: Early Pleistocene complex cut-and-fill sequences in the Alps, Swiss Journal of Geosciences, 115, 11.
- Graf, H.R. 1993: Die Deckenschotter der zentralen Nordschweiz: ETH Zurich, 187 p.
- Knudsen, M. F., Nørgaard, J., Grischott, R., Kober, F., Egholm, D. L., Hansen, T. M. and Jansen, J. D. 2020: New cosmogenic nuclide burial-dating model indicates onset of major glaciations in the Alps during Middle Pleistocene Transition, Earth and Planetary Science Letters, 549, 11649.
- Schlüchter, C. 2004: The Swiss glacial record – a schematic summary, in Ehlers, J. & Gibbard, P. eds., Quaternary Glaciations - Extent and Chronology, Amsterdam: Elsevier, p. 431-418.

## 10.3

### Coupled climate-glacier modelling of the last glaciation in the Alps

Guillaume Jouvet<sup>1,2</sup>, Denis Cohen<sup>3,4</sup>, Emmanuele Russo<sup>5,6,7</sup>, Jonathan Buzan<sup>5,6</sup>, Christoph C. Raible<sup>5,6</sup>, Urs H. Fischer<sup>8</sup>, Wilfried Haeberli<sup>2</sup>, Michael Imhof, Jens K. Becker<sup>8</sup>, Angela Landgraf<sup>8</sup>

<sup>1</sup> Institute of Earth Surface Dynamics, University of Lausanne, Lausanne, Switzerland

<sup>2</sup> Department of Geography, University of Zurich, Zurich, Switzerland

<sup>3</sup> Department of Earth and Environmental Science, New Mexico Tech, Socorro, NM, USA

<sup>4</sup> CoSci LLC, Placitas, NM, USA

<sup>5</sup> Climate and Environmental Physics, University of Bern, Sidlerstrasse 5, 3012, Bern, Switzerland

<sup>6</sup> Oeschger Centre for Climate Change Research, University of Bern, Hochschulstrasse 4, 3012, Bern, Switzerland

<sup>7</sup> now at Institute for Atmospheric and Climate Science (IAC), ETH Zurich, Universitätstrasse 16, 8092 Zürich, Switzerland.

<sup>8</sup> Nagra, Wettingen, Switzerland

Our limited knowledge of the climate prevailing over Europe during former glaciations is the main obstacle to reconstruct the past evolution of the ice coverage over the Alps by numerical modelling. To address this challenge, we perform a two-step modelling approach: First, a regional climate model is used to downscale the time slice simulations of a global earth system model in high-resolution leading to climate snapshots during the Last Glacial Maximum (LGM) and the Marine Isotope Stage 4 (MIS4). Second, we combine these snapshots and a climate signal proxy to build a transient climate over the last glacial period and force the Parallel Ice Sheet Model to simulate the dynamical evolution of glaciers in the Alps. The results show that the extent of modelled glaciers during the LGM agrees quite well with several independent key geological imprints including moraine-based and trimline-based maximal reconstructed glacial extents, known ice transfluences, and trajectories of erratic boulders of known origin and deposition. Our results show the significant added-value of multiphysical coupled climate and glacier transient modelling over simpler approaches to help with reconstructing paleo-glacier fluctuations in agreement with the traces they have left on the landscape.

## 10.4

# Fluvial response to glacial-interglacial cycles - modelling the evolution of the Hochrhein using EROS

Jürgen Mey<sup>1</sup>, Wolfgang Schwanghart<sup>1</sup>, Angela Landgraf<sup>2</sup>, Philippe Davy<sup>3</sup>

<sup>1</sup> Institute of Environmental Science and Geography, University of Potsdam, Karl-Liebknecht-Str. 24-25, 14476 Potsdam, Germany (juemey@uni-potsdam.de)

<sup>2</sup> Nationale Genossenschaft für die Lagerung radioaktiver Abfälle (Nagra), Hardstrasse 73, Postfach, 5430 Wettingen/Schweiz

<sup>3</sup> Géosciences Rennes, Université de Rennes 1, Rennes 35042, France

Repeated alpine glaciations during the Quaternary partly reached far into the foreland and caused profound landscape changes beyond glacial margins in northern Switzerland. Climate-driven glacier growth and decay and commensurate variations in water and sediment delivery caused river systems to aggrade and to incise, leading to the widespread occurrence of glacio-fluvial deposits (Deckenschotter) and associated terraces. Mapping and numerical dating of these depositional complexes increasingly offer insights into the spatial patterns and timing of Quaternary glaciations, and associated changes in (glacio-)fluvial dynamics. An improved understanding of how fluvial systems respond to glacial-interglacial cycles will help to assess the erosion potential around repository sites of nuclear waste over the next one million years. In this study, we contribute to close this research gap using numerical landscape evolution modelling (LEM).

We use EROS, a numerical landscape evolution model, which implements a particle-based approach to simulate water and sediment fluxes that interact with topography through erosive and depositional actions. Unlike LEMs based on the stream-power incision law, the method solves the 2D shallow water equations with both basal and lateral erosion and deposition, which allows for variations in width and lateral mobility of rivers; these variations induce changes in the transport capacity of the sediments that cause specific patterns of deposition and erosion to emerge. We adjusted the model so that it is capable to run over 1 Myrs, and imposed boundary conditions that – informed by estimates on long-term erosion rates – reflect rock uplift and plausible variations in water and sediment fluxes following a 100-kyrs glacial cycle. Our model relies on digital elevation models and sediment thickness data with 60 m spatial resolution and is applied to the Hochrhein river between Stein am Rhein and Basel and the Aare river downstream of the area, where Limmat and Reuss enter.

Our simulations show that the model reproduces widespread aggradation of up to several tens of meters along the entire Hochrhein and Aare during the onset of glaciations when increased sediment availability combines with reduced runoff due to decreasing precipitation and water-storage in growing ice-masses. During the main glacial phase, the model predicts large reworking of the sediments by highly laterally mobile, braided river systems. An additional aggradational phase is caused during glacial readvance. During deglaciation and the interglacial, increased runoff and low sediment availability due to trapping in perialpine lakes cause rivers to incise into their deposits.

Our model setup and parametrization features several uncertainties. For example, the capacity of rivers to laterally erode strongly determines the thickness and extent of depositional complexes lining the Hochrhein and Aare system. Also, our model is sensitive to temporally varying boundary conditions of water and sediment input about which precise estimates are lacking. Regardless, the more detailed and realistic representation of hydraulic and sediment transport processes by EROS compared to conventionally used landscape evolution models at this spatial and temporal scale provide the opportunity to test different hypotheses using numerical experiments and link the results to field evidence. Further sensitivity analyses and uncertainty quantification will enable us to use our model as simulation tool to hindcast and investigate the behaviour of fluvial system in response to different tectonic and climatic scenarios, thus helping to better understand potential spatial patterns of and sediment assemblages within widespread glacio-fluvial deposits.

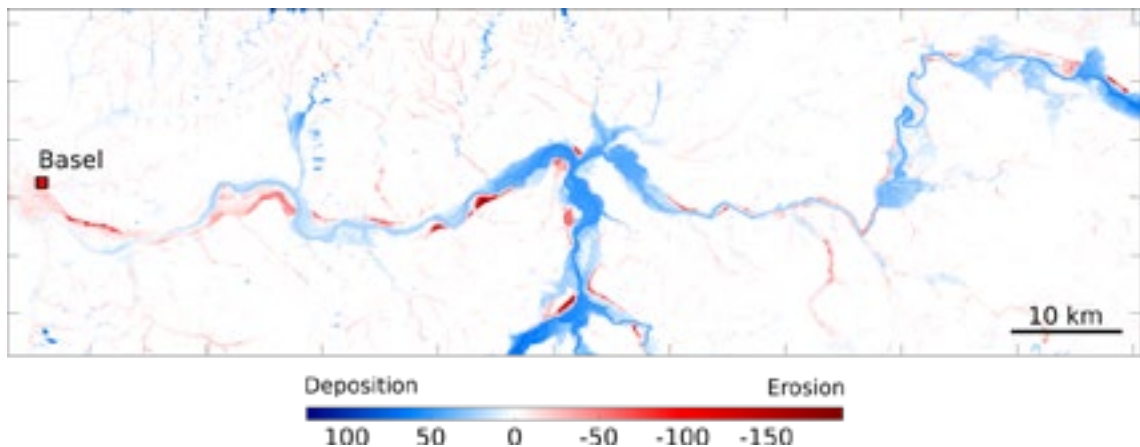


Figure 1. Erosion/deposition pattern (in m) after 1 Myrs into the future. Background rock uplift and subsidence have been subtracted from the grid for clarity.

## 10.5

# Structural-controlled valley erosion in high erosion-resistance crystalline bedrock

Ferdinando Musso Piantelli<sup>1</sup>, Sandro Truttmann<sup>1</sup>, and Marco Herwegen<sup>1</sup>

<sup>1</sup> Institute of Geological Sciences University of Bern, Switzerland

The susceptibility of catchment rocks to glacial erosion may control the evolution of valley morphology in high-relief mountain ranges such as the Alps. Non-uniform proneness to bedrock erosion may indeed localize abrupt changes in the glacier flow direction and overdeepenings characteristic of glacial valleys. Yet, little is known about the explicit influence of bedrock properties (i.e., lithology, hardness, and geological structures) on glacial erosion processes. In this study, we select the Great Aletsch Glacier (Swiss Alps) as a natural laboratory to document and investigate the relationship between bedrock properties and subglacial erosion mechanisms. The Great Aletsch Glacier with a length of more than 20km and an ice thickness of up to 800m is the largest glacier in Central Europe. The underlying bedrock consists of the crystalline basement units of the Aar massif (gneiss, granite, and granodiorite) and is dissected by a large number of steep faults and former ductile shear zones. Geological and remote sensing lineament mapping combined with 3D geological modelling allowed us to make a large-scale characterization of the lithologies and structures' spatial frequency over the entire length of the glacier. Additionally, we performed field structural mapping and field-based rock hardness analyses (Schmidt hammer) along the glacier's bedrocks (intact rock and faulted/sheared domains) to testify for structure-controlled erosion behaviour. Obtained results demonstrate that: (i) the typology and distribution of faults and shear zones are not uniform over the entire length of the glacier; (ii) high-frequency structure domains correlate with overdeepenings and/or abrupt glacier flow deflection in the direction of the strike of the structures; (iii) low-frequency structure domains correlate to the absence of overdeepenings and a straight glacier trajectory. In terms of erosive resistance domains of intact rock masses show high hardness values for each of the investigated lithologies without substantial variability between the different basement rocks. On the contrary, faulted or sheared domains show a significant drop in hardness value. Based on these results we propose that differences in the mapped crystalline basement lithologies do not exert an important role in glacial erosion. We postulate instead that the non-uniform spatial distribution of geological structures imposes a major control on the development of the glacial valley. The substantially reduced bulk hardness within high-frequency structure domains renders indeed the bedrock to be more prone to efficient glacial erosion process at these sites (i.e., glacial quarrying) and therefore to the development of large-scale overdeepenings, local scouring, or changes in the glacier flow direction. By contrast, the more massive undeformed and therefore less erosive low-frequency structure domains coincide with sections with no knickpoints or overdeepenings.

*Keywords:* glacial erosion; crystalline bedrock; structural preconditioning

## 10.6

# Arctic Century – an interdisciplinary expedition to the Kara and Laptev Sea to study ocean, atmosphere and land processes in the changing Arctic

Gabriela Schaeppman-Strub<sup>1,2</sup>, Heidemarie Kassens<sup>3</sup>, Samuel L. Jaccard<sup>4</sup>, Mikhail Makhotin<sup>5</sup>, Arctic Century science team

<sup>1</sup> Department of Evolutionary Biology and Environmental Studies, University of Zurich, Winterthurerstr. 190, CH-8057 Zurich ([gabriela.schaeppman@ieu.uzh.ch](mailto:gabriela.schaeppman@ieu.uzh.ch))

<sup>2</sup> Swiss Polar Institute, Rue de l'Industrie 17, CH-1950 Sion

<sup>3</sup> Research Center for Marine Geosciences, GEOMAR, D-Kiel

<sup>4</sup> Institute of Earth Sciences, University of Lausanne, CH-1015 Lausanne

<sup>5</sup> Arctic and Antarctic Research Institute, RU-St. Petersburg

The region of the Kara and Laptev Sea in the Russian Arctic experienced one of the highest warming rates globally during past decades. From 5 August – 6 September 2021, the Arctic Century science team gathered unique data during a ship expedition, along marine transects and on seven high Arctic islands that are very rarely accessible. The aim of the expedition is to contribute to the understanding of the dynamics and interactions between the sea, land and the atmosphere under global change. Here we provide an overview of the main research topics and measurements performed: 1. physical dynamics of Atlantic water masses and their mixing with Arctic waters, 2. biodiversity and ecosystem productivity in the sea and on high Arctic islands, at the margin of life, 3. dynamics of the atmosphere and interactions with the sea and land, 4. climate change and sea level change through coring ice, coastal and sea sediments, and 5. amount and flow of macro- and microplastic in the sea and at shore. First sample and data analyses are currently being performed by the expedition consortium. After an initial moratorium, the data will be made openly accessible to the wider science community.

## 10.7

# Understanding tsunamigenic delta collapses in the perialpine lakes of Switzerland

Daniela Vendettuoli<sup>1</sup>, Michael Strupler<sup>2</sup>, Flavio S. Anselmetti<sup>1</sup>, Stefano C. Fabbri<sup>1</sup>, Anastasiia Shynkarenko<sup>2</sup>, Katrina Kremer<sup>1</sup>

<sup>1</sup> Institute of Geological Sciences and Oeschger Centre for Climate Change Research, Baltzerstrasse 1+3, 3012 Bern (katrina.kremer@geo.unibe.ch)

<sup>2</sup> Swiss Seismological Service, ETH Zurich, Sonneggstrasse 5, 8092 Zurich

Large lacustrine mass movements and delta collapses are increasingly being considered as potential tsunamigenic sources. They are therefore hazardous for the population and infrastructure along lakeshores (Nigg et al., 2021 and reference therein). In most studies of slope stability and triggered tsunamis, however, subaqueous deltas have largely been excluded because of lacking information on their morphodynamic evolution. Thus, a holistic assessment of tsunami hazard in lacustrine environment is required leading to an understanding on the how lake deltas evolve through time and space.

Within a study funded by the Federal Office of the Environment, we aim to understand what type of deltas are susceptible to slope failure within the Swiss landscape. To achieve our goal, we will primarily focus on those deltas that present an increased potential for subaqueous erosion. For this purpose, we will analyse their morphological, morphometric and sedimentological characteristics taking advantage of the existing and publically available datasets (high-resolution bathymetry, hydrological data and historical and sedimentological records).

In this contribution, we will present the designed approach and preliminary results, using Lake Lucerne as case study. This approach will then be applied to all lakes with a surface > 1km<sup>2</sup>, for which high-resolution bathymetric data is available. The final product and results of this analysis will be summarized in a geodatabase of the different delta-types of the Swiss lakes representing an important milestone for the assessment of tsunami hazard in the peri-alpine lakes of Switzerland.

## REFERENCES

- Nigg, V., Wohlwend, S., Hilbe, M., Bellwald, B., Fabbri, S., Strasser, M., de Souza, G.F., Anselmetti F. S. 2021: A tsunamigenic delta collapse and its associated tsunami deposits in and around Lake Sils, Switzerland. Natural Hazards (2021) 107:1069–1103 <https://doi.org/10.1007/s11069-021-04533-y>

**P 10.1****Complex Deckenschotter architecture at Irchel – An endeavor to reconstruct detailed chronology and stratigraphy**

Catharina Dieleman<sup>1</sup>, Marcus Christl<sup>2</sup>, Christof Vockenhuber<sup>2</sup>, Philip Gautschi<sup>2</sup>, Naki Akçar<sup>1</sup>

<sup>1</sup> Institut für Geologie, University of Bern, Baltzerstrasse 1+3, CH-3012 Bern (catharina.dieleman@geo.unibe.ch)

<sup>2</sup> Labor für Ionenstrahlphysik, ETH Zürich, Otto-Stern-Weg 5, CH-8093 Zürich

The Lower Pleistocene of the northern Swiss Alpine Foreland is characterized by a succession of glaciofluvial sediments intercalated with glacial and/or overbank deposits (*Deckenschotter* in German), which are accumulated in three phases between ca. 2.5 and ca. 1 Ma (Graf 1993; Akçar et al. 2014, 2017; Claude et al. 2017; Knudsen et al., 2020; Dieleman et al. 2022). The topographically highest Deckenschotter site is located at Irchel in the Canton of Zurich, where the recently established chronostratigraphy indicates a cut-and-fill system that prevailed during the Early Pleistocene and disagrees with the existing morphostratigraphy (Claude et al. 2019; Dieleman et al. 2022). Mammal fossils discovered in the Hasli Formation in the early 90's were ascribed to the Mammal Neogene Zone 17 (2.5 – 1.8 Ma; Bolliger et al., 1996) and the Hasli Formation overlies the ca. 1 Ma old gravels at the spot of discovery. In brief, the lines of evidence show that the Deckenschotter at Irchel have a more complex architecture than assumed so far.

This study aims at getting a better understanding of the environment responsible for this complex architecture and at reconciling the lithostratigraphy, chronology, and biostratigraphy. To achieve these goals, a set of methods is applied. Outcrops are mapped and their sedimentology analyzed to reconstruct the origin, transport mechanism, and depositional environment as well as to improve the lithostratigraphical framework. To validate the existing chronology, at least six outcrops above and below the Hasli Formation are sampled along a stratigraphic profile for isochron-burial dating with cosmogenic <sup>10</sup>Be and <sup>26</sup>Al. In addition, three boreholes and shallow trenches will provide further insights into the complex architecture. Besides, the Hasli Formation, if encountered, and gravels under and above will be sampled for isochron-burial and burial dating. In the boreholes and surroundings, geophysical measurements will be performed to complement our comprehension of the internal structure of the Deckenschotter at Irchel. First results will be presented.

**REFERENCES**

- Akçar, N., Ivy-Ochs, S., Alfimov, V., Claude, A., Graf, H.R., Dehnert, A., Kubik, P.W., Rahn, M., Kuhlemann, J., and Schlüchter, C. 2014: The first major incision of the Swiss Deckenschotter landscape: Swiss Journal of Geosciences, v. 107, p. 337–347, doi: 10.1007/s00015-014-0176-6.
- Akçar, N., Ivy-Ochs, S., Alfimov, V., Schlunegger, F., Claude, A., Reber, R., Christl, M., Vockenhuber, C., Dehnert, A., Rahn, M., and Schlüchter, C. 2017: Isochron-burial dating of glaciofluvial deposits: First results from the Swiss Alps: Earth Surface Processes and Landforms, v. 42, p. 2414–2425, doi: 10.1002/esp.4201.
- Claude, A., Akçar, N., Ivy-Ochs, S.D., Schlunegger, F., Kubik, P.W., Dehnert, A., Kuhlemann, J., Rahn, M., and Schlüchter, C. 2017: Timing of early Quaternary gravel accumulation in the Swiss Alpine Foreland: Geomorphology, v. 276, p. 71–85, doi: 10.1016/j.geomorph.2016.10.016.
- Dieleman, C., Christl, M., Vockenhuber, C., Gautschi, P. and Akçar, N. 2022: Early Pleistocene complex cut-and-fill sequences in the Alps, Swiss Journal of Geosciences, 115, 11.
- Graf, H.R. 1993: Die Deckenschotter der zentralen Nordschweiz: ETH Zurich, 187 p.
- Knudsen, M. F., Nørgaard, J., Grischott, R., Kober, F., Egholm, D. L., Hansen, T. M. and Jansen, J. D. 2020: New cosmogenic nuclide burial-dating model indicates onset of major glaciations in the Alps during Middle Pleistocene Transition, Earth and Planetary Science Letters, 549, 11649.
- Schlüchter, C. 2004: The Swiss glacial record – a schematic summary, in Ehlers, J. & Gibbard, P. eds., Quaternary Glaciations - Extent and Chronology, Amsterdam: Elsevier, p. 431-418.

## P 10.2

# Last Glacial Maximum glacier fluctuations of the Rhine and Reuss glacier systems

Sarah Kamleitner<sup>1</sup>, Susan Ivy-Ochs<sup>1</sup>, Lucia Manatschal<sup>2</sup>, Naki Akçar<sup>3</sup>, Marcus Christl<sup>1</sup>, Christof Vockenhuber<sup>1</sup>, Irka Hajdas<sup>1</sup>, Hans-Arno Synal<sup>1</sup>

<sup>1</sup> Laboratory of Ion Beam Physics, ETH Zurich, Otto-Stern-Weg 5, CH-8093 Zürich ([kamsarah@phys.ethz.ch](mailto:kamsarah@phys.ethz.ch))

<sup>2</sup> Department of Earth Sciences, ETH Zurich, Sonneggstrasse 5, CH-8092 Zürich

<sup>3</sup> Institute of Geological Sciences, University of Bern, Baltzerstrasse 1+3, CH-3012 Bern

Glacial landforms are pervasive geomorphic features of Swiss landscapes. On the northern Alpine foreland, fresh ice marginal landforms are associated with the latest episode of Pleistocene glaciation and yield key information on the succession and termination of Last Glacial Maximum (LGM) glaciers. Our new, high resolution geomorphological mappings from NE Switzerland and SW Germany provide an excellent base to reconstruct LGM glacier evolution of the area in profound detail and over large scales. This study focusses on the deposits of the broad, more than 100 km wide, LGM Rhine glacier piedmont lobe and the comparably narrow eastern lobes of the LGM Reuss glacier system. The formation of distinguished ice margins is chronologically tied to new  $^{10}\text{Be}$  and  $^{36}\text{Cl}$  surface exposure as well as new radiocarbon dates (Kamleitner et al., in revision). The latter include redated mammoth specimens of the existing LGM Rhine glacier chronology firstly determined in the 1980s. By combining our new results with recent dates from published exposure- and luminescence dating studies we were able to build a robust chronological framework for the advance and decay of the LGM Rhine and Reuss glaciers that show remarkable similarities. Chronological evidence suggests that the Rhine glacier advanced to and reached its LGM maximum position between 26-22 ka. A time period during which the prominent and largely continuous frontal moraines of the outer Schaffhausen stadial were built up. To the west, the Reuss lobe likely advanced to its LGM maximum by  $25/24 \pm 2$ . The corresponding Untertannwald ice margin and the more prominent but slightly internal ridges of the Mellingen stadial stabilized no later than ca. 22 ka and ca. 21 ka, respectively. After the retreat from the maximum positions, oscillations of the glacier fronts are observed in both Rhine and Reuss glacier systems, although preservation of intermediate ice positions is better in the Reuss area (Stetten stadial). Largely continuous internal ice margins are the results of late LGM readvances of Rhine (Stein am Rhein stadial) and Reuss (Bremgarten stadial) glaciers after ca. 21 ka. Missing geomorphic evidence upstream suggests that both foreland glaciers decayed rapidly and without marked stabilization thereafter.

## REFERENCES

- Kamleitner, S., Ivy-Ochs, S., Manatschal, L., Akçar, N., Christl, M., Vockenhuber, C., Hajdas, I., Synal, H.-A. in revision: Last Glacial Maximum glacier fluctuations on the northern Alpine foreland: geomorphological and chronological reconstructions from the Rhine and Reuss glacier systems, submitted to Geomorphology.

## P 10.3

# Glaciofluvial terrace hypsometry in the Swiss Alpine Foreland compared with stratigraphic, glacio- and geodynamic and absolute dating information

Florian Kober<sup>1</sup>, Thomas Pollhammer<sup>2</sup>, Bernhard Salcher<sup>2</sup>, Gaudenz Deplazes<sup>1</sup>

<sup>1</sup> NAGRA Switzerland, Hardstrasse 73, 5430 Wettingen, Switzerland ([florian.kober@nagra.ch](mailto:florian.kober@nagra.ch))

<sup>2</sup> University of Salzburg, Dept. of Environment and Biodiversity, Salzburg, Austria

Glaciofluvial terraces of the North Alpine Swiss Foreland have been subjected to Quaternary research for numerous decades but have just recently gained interest for various absolute dating attempts and updated landscape evolution scenario interpretations (e.g., Claude et al. 2019, Dieleman et al. 2022, Knudsen et al. 2020). Conflicts in absolute age constraints pose further difficulties in deriving incision histories and their potential corresponding drivers (i.e. tectonic, climate, intrinsic river dynamics, glacial dynamics). Specific focus has been given to the Deckenschotter deposits. Their fragmentary to isolated preservation and often unclear paleo-flow paths due to the lack of bounding topography pose a particular challenge for morphostratigraphic correlations.

Based on a GIS compilation of existing data (digital elevation models, geologic maps, sedimentologic data), we used a novel self-developed morphostratigraphic method, within the software R, to create 2D paleo-river-long-profiles to i) test the existing terrace stratigraphy, ii) test possible terrace parallelizations across the major catchments of Rhine and Danube, and iii) with the help of existing relative and absolute age constraints, collect evidence based data on Quaternary uplift rates across the foreland.

By generating supra-regional profiles along possible paleo-flow courses of the Deckenschotter, possible relationships and correlations of terraces could be traced and verified, and deviations to existing models can be discussed. A comprehensive compiled data set (profiles) will be presented providing a valuable tool for further and complementary analysis and shedding light on potential areas to investigate and date in further detail.

## REFERENCES

- Claude, A., Akçar, N., Ivy-Ochs, S., Schlunegger, F., Kubik, P. W., Christl, M., Vockenhuber, C., Kuhlemann, J., Rahn, M., Schlüchter, C. 2019: Changes in landscape evolution patterns in the northern Swiss Alpine Foreland during the mid-Pleistocene revolution. *GSA Bulletin*, Geological Society of America, <https://doi.org/10.1130/B31880.1>
- Dieleman, C., Christl, M., Vockenhuber, C., Gautschi, P., Akçar, N. 2022: Early Pleistocene complex cut-and-fill sequences in the Alps. *Swiss Journal of Geosciences* 115, <https://doi.org/10.1186/s00015-022-00411-2>
- Knudsen, M.F., Nørgaard, J., Grischott, R., Kober, F., Egholm, D.L., Hansen, T.M., Jansen, J.D. 2020: New cosmogenic nuclide burial-dating model indicates onset of major glaciations in the Alps during Middle Pleistocene Transition. *Earth and Planetary Science Letters* 549, <https://doi.org/10.1016/j.epsl.2020.116491>

## P 10.4

# Deep erosion by glaciers – Analysing morphological characteristics of global glacier-bed overdeepenings

Fabian Maier<sup>1</sup>, Wilfried Haeberli<sup>2</sup>, Urs H. Fischer<sup>1</sup>, Angela Landgraf<sup>1</sup>

<sup>1</sup> National Cooperative for the Disposal of Radioactive Waste (Nagra), Hardstrasse 73, CH-5430 Wettingen, Switzerland  
(fabian.maier@nagra.ch)

<sup>2</sup> Department of Geography, University of Zurich, Winterthurerstrasse 190, CH-8057 Zurich, Switzerland  
(wilfried.haeberli@geo.uzh.ch)

Glacial overdeepening is a worldwide phenomenon, yet their relation to specific erosion processes, driving mechanisms, or comparability is poorly understood. Scientific challenges include, for instance, the limited availability of quantitative information about subsurface bedrock topography and erodibility, or the lack of absolute age dating of the infill of such troughs. This in turn hampers the estimation of erosion rates, their variation through time, or the assignment of an associated glaciation.

To approach some of these questions, a GIS-based methodology was used to assess the variability of such analogue landforms from selected global locations. The analysis includes morphometric characterisations like elongation ratios, mean or maxima of geometric dimensions, and form indices. In addition, boundary conditions, such as tectonic, lithologic, topographic, climatic, and paleo-glaciological settings were compared amongst the different locations and put into relation with the morphometry of the overdeepenings.

Comparing planimetric characteristics of worldwide features documents extraordinary lengths/elongations for piedmont overdeepenings and overdeepenings in inneralpine valleys (e.g., Swiss Piedmont, Patagonia, New Zealand) with larger maximum depths for the latter (median: ~90 vs. 170 m, respectively), presumably due to topographic steering. In contrast, overdeepenings in high mountain areas (e.g., Swiss Alps, Cordillera Blanca) exhibit rather shallow and more rotund shapes. Results of longitudinal and cross-sectional analyses indicate rather V-shaped cross sections in piedmont conditions, pointing to predominant pro-, sub-, and interglacial fluvial components of the overall erosive processes. Moreover, the observed relation between more V-shaped, strongly elongated features under foreland conditions and more U-shaped, less elongated alpine features seems to agree with modelled spatial patterns of sliding distance as an indication of time-integrated ice occupancy and related abrasion/plucking effects.

The study allows an improved comparability of glacial overdeepenings, but deriving quantitative information remains challenging due to the worldwide unequal data availability. Erodibility seems to exert a key influence and thus is expected to support re-excavation during subsequent ice ages. In comparison with this, it appears reasonable to attribute a protective function to less erodible rocks.

## P 10.5

### What controls delta failures?

Katrina Kremer<sup>1,2</sup>, Stefano C. Fabbri<sup>1,3</sup>, Daniela Vendituoli<sup>1</sup>, Carlo Affentranger<sup>1</sup>, Flavio S. Anselmetti<sup>1</sup>

<sup>1</sup> Institute of Geological Sciences and Oeschger Centre for Climate Change Research, Baltzerstrasse 1+3, 3012 Bern (katrina.kremer@geo.unibe.ch)

<sup>2</sup> Swiss Seismological Service, ETH Zurich, Sonneggstrasse 5, 8092 Zurich

<sup>3</sup> Université Savoie Mont Blanc, Laboratoire EDYTEM, 5 bd de la Mer Caspienne, Le Bourget du Lac, France

Deltas represent transfer zones where sediment is moved from terrestrial to the subaqueous domains. They represent a depositional area as well as a source for sediments. One of the aspects in this highly dynamic environment that has experienced so far little attention are slope failures in deltas. Such failures are, however, mentioned as potential cause for large (up to m-scale deposits), graded deposits, in the sedimentary record often termed as megaturbidites or homogenites. In some cases, they may have generated tsunamis in the near-shore area. These delta failures can be triggered, amongst other causes, by spontaneous slope collapses (e.g. Muota delta 1687 in Lake Lucerne; Hilbe et al., 2014). To better understand the controlling factors of slope stability in deltas, we need to understand interplay between deltaic deposition and erosion through time and monitor their evolution.

Repeated bathymetric mapping has been used as powerful tool to better understand the short-term processes occurring in deltas as shown at the Squamish delta, Canada (Hughes-Clarke et al., 2014), for example. In this contribution, repeated bathymetric mapping is used to better understand, which short-term processes may shape subaqueous delta fronts. Using the dataset acquired in recent years in Swiss lakes, we seek to answer (1) what processes can be visualized based on repeated bathymetric mapping?; (2) which areas are prone to depositional/erosion processes?; and (3) what type of delta is more prone to slope failures? We present the first datasets of differential maps from four deltas in Switzerland that show different processes of erosion and deposition on short and long time scales.

### REFERENCES

- Clarke, J. E. H., Marques, C. R. V., & Pratomo, D. 2014 : Imaging active mass-wasting and sediment flows on a fjord delta, Squamish, British Columbia. In Submarine mass movements and their consequences (pp. 249-260), Springer, Cham.  
Hilbe, M., & Anselmetti, F. S. 2014: Signatures of slope failures and river-delta collapses in a perialpine lake (Lake Lucerne, Switzerland), *Sedimentology*, 61(7), 1883-1907.

## P 10.6

# Diatom-bound nitrogen isotopes as a paleo-proxy in lacustrine environments: a preliminary report

Jules F.L. Millet<sup>1\*</sup>, Johan Rydberg<sup>2</sup>, Christian Bigler<sup>2</sup>, Nathalie Dubois<sup>3</sup>, Moritz F. Lehmann<sup>1</sup>, Anja S. Studer<sup>1</sup>

<sup>1</sup> Department of Environmental Sciences, University of Basel, Bernoullistrasse 30, 4056 Basel, Switzerland,

\*jules.millet@unibas.ch

<sup>2</sup> Department of Ecology and Environmental Science, Umeå University, Linneus väg 6, 901 87 Umeå, Sweden

<sup>3</sup> Swiss Federal Institute of Aquatic Science and Technology (Eawag), CH-8600 Dübendorf, Switzerland

Diatom frustules are well preserved in marine and lacustrine sediments over hundreds or even thousands of years. They contain minute amounts of intra-crystalline organic matter that is thought to be protected by the silica against diagenetic alteration. Previous applications of the diatom-bound nitrogen isotope paleo-proxy in palaeoceanographic studies have shown that the  $^{15}\text{N}/^{14}\text{N}$  ratio of the nitrogen contained in these frustules (the diatom-bound  $\delta^{15}\text{N}$ , or  $\delta^{15}\text{N}_{\text{DB}}$ ) can be used as a proxy for nutrient cycling in the polar oceans, and that it is unbiased by the diagenetic effects. However, the applicability of this paleo-proxy to lacustrine sediments has never been tested.

One goal of this study is to validate whether the organic nitrogen contained in diatom frustules is indeed protected against diagenetic alteration. For this purpose, we will analyse and compare the  $\delta^{15}\text{N}_{\text{DB}}$  and  $\text{N}_{\text{DB}}$  content of sediment trap, surface sediment and downcore sediment material from a time-series study of varved sediment cores from the lake Nylandssjön (Sweden). We will also measure the  $\delta^{15}\text{N}_{\text{DB}}$  and  $\text{N}_{\text{DB}}$  content from degradation experiments of diatom cultures.

Another goal of this study is to explore the use of  $\delta^{15}\text{N}_{\text{DB}}$  to reconstruct the history of nitrogen dynamics in Swiss lakes in the past. Provided that the  $\delta^{15}\text{N}_{\text{DB}}$  record is unaffected by diagenesis, it should record past changes in the N input/output processes and/or internal N cycling processes within a given lake. We chose to investigate the sedimentary record of the well-studied Lake Baldegg in Switzerland, which underwent severe eutrophication in the middle of the 20th century, and which is being artificially ventilated since 1982. We will measure the  $\delta^{15}\text{N}_{\text{DB}}$  in Lake Baldegg sediments, and will compare the  $\delta^{15}\text{N}_{\text{DB}}$  down-core record to other sedimentary proxies (e.g., bulk isotopic composition, elemental composition and chlorophyll a), as well as hydrochemical datasets from the lakes' monitoring program (e.g., nutrient concentrations), allowing us to constrain the environmental context of sedimentation, and to disentangle the multiple controls that led to expected fluctuations in  $\delta^{15}\text{N}_{\text{DB}}$  in Lake Baldegg in the recent past.

**P 10.7****Enhanced petrogenic organic carbon oxidation at glacial terminations?**

Thomas M. Blattmann<sup>1,2</sup>

<sup>1</sup> Geological Institute, ETH Zurich, Sonneggstrasse 5, CH-8092 Zurich ([thomas.blattmann@erdw.ethz.ch](mailto:thomas.blattmann@erdw.ethz.ch))

<sup>2</sup> Biogeochemistry Research Center, Japan Agency for Marine-Earth Science and Technology, 2-15 Natsushima-cho, JP-237-0061 Yokosuka

Petrogenic organic carbon comprises the largest body of reduced carbon on Earth. Geochemical, organic petrological, and palynological studies indicate that the efficiency of petrogenic organic carbon reburial varied through geologic time with greater quantities of kerogen reburied during glacial interludes in Earth history. Blattmann (2022) hypothesized that petrogenic organic carbon exposed upon deglaciation oxidizes rapidly, thereby contributing to rapid atmospheric carbon dioxide increase at glacial-interglacial transitions. Disentangling this potential source of carbon dioxide to the atmosphere from the established major pathway of degassing from the oceans will require quantitative constraints on petrogenic organic carbon oxidation, the study of which is in its infancy. However, retreat of the Laurentide Ice Sheet across North America shows spatiotemporal synchronization between carbon dioxide increase, also consistent with carbon isotope patterns of atmospheric carbon dioxide for both stable ( $^{13}\text{C}$ ) and radiocarbon ( $^{14}\text{C}$ ), and exposure of the petrogenic organic carbon-rich Western Canadian Sedimentary Basin, suggesting a connection. To evaluate the hypothesized role of petrogenic organic cycling over glacial-interglacial cycles, systematic chronosequence studies in the forefields of glaciers are needed to constrain oxidation rates of petrogenic organic carbon.

**REFERENCES**

- Blattmann, T.M. 2022: Ideas and perspectives: Emerging contours of a dynamic exogenous kerogen cycle, *Biogeosciences*, 19, 359-373.

## P 10.8

# Insights into Central European environmental changes during the last 2500 years by multi-proxy analysis of the undisturbed Beerberg peatland, Thuringia, Germany

Carrie L. Thomas<sup>1,2</sup>, Mariusz Galka<sup>3</sup>, Sambor Czerwiński<sup>4</sup>, Klaus-Holger Knorr<sup>5</sup>, Boris Jansen<sup>2</sup>, and Guido L. B. Wiesenberg<sup>1</sup>

<sup>1</sup> University of Zurich, Winterthurerstrasse 190, CH-8057 Zurich (carrie.thomas@geo.uzh.ch)

<sup>2</sup> University of Amsterdam, Netherlands

<sup>3</sup> University of Lodz, Poland

<sup>4</sup> Adam Mickiewicz University, Poland

<sup>5</sup> University of Muenster, Germany

Peatlands are an important ecosystem for many reasons, including their function as carbon sinks essential for mitigating climate change. Additionally, due to the anaerobic conditions in which peatlands form, decomposition of their constituent plant material is inhibited, making peatlands valuable archives for paleoenvironmental reconstructions. In this study, we examined a new 3.4 m core from the ombrotrophic Beerberg peatland located in the Vessertal-Thuringian Forest Biosphere Reserve in Germany. While paleo-archives at this peatland have been studied in the past (e.g., Jahn, 1930; Lange, 1967), we aim to apply newer techniques at a higher resolution to obtain more detailed results. Radiocarbon dating indicates that the core spans approximately the last 2500 years. Samples from the core were analyzed for pollen, macrofossils, and biomarkers, in particular, free extractable lipids including *n*-alkanes, *n*-alcohols, and *n*-fatty acids. These proxy data were used both to perform a vegetation reconstruction as well as to compare the results of the different proxies to each other to determine accuracy as well as create a more complete picture of the environment over time at the Beerberg peatland. The current dominant vegetation at the moor are *Sphagnum* mosses as well as *Calluna vulgaris*. Additionally, *Eriophorum vaginatum*, *Empetrum nigrum*, *Oxycoccus palustris*, and various *Vaccinium* species were abundant. Preliminary results from the macrofossil and pollen analyses indicate that through time, the peatland has been primarily dominated by *Sphagnum* mosses, particularly *Sphagnum fuscum*. However, there are also conflicting results of when transitions to other dominant vegetation, such as *Eriophorum vaginatum*, occurred, as well as the contributions of species, such as *Calluna vulgaris*, over time. We aim to clarify these results through the addition of the biomarker analysis to develop a robust picture of evolution of vegetation during the Holocene at Beerberg peatland. Data from this study will also be used to improve a future iteration of the VERHIB (VEgetation Reconstruction with the Help of Inverse modeling and Biomarkers) model (Jansen et al., 2010).

## REFERENCES

- Jahn, R. (1930). Pollenanalytische Untersuchungen an Hochmooren des Thüringer Waldes. Forstwissenschaftliches Centralblatt, 52, 761-774.
- Jansen, B., van Loon, E. E., Hooghiemstra, H., & Verstraten, J. M. (2010). Improved reconstruction of palaeo-environments through unravelling of preserved vegetation biomarker patterns. Palaeogeography, Palaeoclimatology, Palaeoecology, 285(1-2), 119-130.
- Lange, E. (1967). Zur Vegetationsgeschichte des Beerberggebietes im Thüringer Wald. Feddes Repertorium, 76(3), 205-219.

**P 10.9****Age of the oldest sediments in the northern Swiss Alpine Foreland**

Ewelina Broś<sup>1</sup>, Susan Ivy-Ochs<sup>1</sup>, Reto Grischott<sup>2</sup>, Florian Kober<sup>3</sup>, Christof Vockenhuber<sup>1</sup>, Marcus Christl<sup>1</sup>, Philip Gauthsch<sup>1</sup>, Colin Maden<sup>4</sup>, Lotta Ylä-Mella<sup>5</sup>, John D. Jansen<sup>5</sup>, Mads F. Knudsen<sup>6</sup>, Hans-Arno Synal<sup>1</sup>

<sup>1</sup> Laboratory of Ion Beam Physics, ETH Zurich, Otto-Stern-Weg 5, CH-8093 Zurich (ewelinao@ethz.ch)

<sup>2</sup> BTG Büro für Technische Geologie AG, Grossfeldstrasse 74, CH-7320 Sargans

<sup>3</sup> NAGRA Nationale Genossenschaft für die Lagerung radioaktiver Abfälle, Hardstrasse 73, CH-5430 Wettingen

<sup>4</sup> Geochemistry and Petrology, ETH Zurich, Clausiusstrasse 25, CH-8092 Zurich

<sup>5</sup> Institute of Geophysics, Czech Academy of Science, Boční II/1401, CZ-14131 Prague

<sup>6</sup> Department of Geoscience, Aarhus University, Høegh-Guldbergs Gade 2, DK-8000 Aarhus

In the Middle and Early Pleistocene, the northern Alpine Foreland witnessed several phases of alternating deposition and incision, shaping the present-day landscape. High elevated plateaus separated by deeply incised overdeepened valleys, create a topography with relief of several hundred meters. On top of these plateaus can be found the oldest glaciofluvial sediments in Switzerland, the Deckenschotter (DS). These Deckenschotter deposits consist mainly of glaciofluvial sediments intercalated with glacial sediments. The DS have traditionally been divided into two morphostratigraphic units, the Higher (older; HDS) and the Lower (younger; TDS) Deckenschotter. Both units form gravel plateaus or terraces located up to about 250 m above the modern valley bottom. A significant altitude difference of approximately 100-150 m separates the HDS from the TDS deposits. Their exact time of deposition is important for understanding long-term landscape evolution scenarios of the northern Foreland during the Middle and Early Pleistocene and was addressed in a number of recent studies (Akçar et al. 2017, Claude et al. 2019, Grischott et al. 2020, Knudsen et al. 2020, Dieleman et al. 2022).

In this study we implement the isochron-burial dating technique with the pair of cosmogenic nuclides, <sup>26</sup>Al and <sup>10</sup>Be, to date the Deckenschotter sediments. Furthermore, we utilize a new burial-dating model proposed by Knudsen et al. (2020) implementing the source-to-sink approach to further examine and refine the question of the age of the Deckenschotter. We aim to reconstruct the chronology of the alternating phases of deposition and incision of the gravel units. Our focus is placed on similar and complementary Deckenschotter deposits outcropping in several sites across the Northern Alpine Foreland. The first preliminary age estimates point to deposition in the latter part of the Early Pleistocene. With the objective to determine the age of these oldest glaciofluvial sediments, our results will also complement the knowledge about their sedimentology, as well as inform our understanding of landscape change during and after Deckenschotter times.

**REFERENCES**

- Akçar N., Ivy-Ochs S., Alfimov V., Schlunegger F., Claude A., Reber R., Christl M., Vockenhuber C., Dehnert A., Rahn M. & Schlüchter C. 2017: Isochron-burial dating of glaciofluvial deposits: First results from the Swiss Alps, Earth Surface Processes and Landforms, 42 (14), pp. 2414-2425.
- Claude A., Akçar N., Ivy-Ochs S., Schlunegger F., Kubik P.W., Christl M., Vockenhuber C., Kuhlemann J., Rahn M. & Schlüchter C. 2019: Changes in landscape evolution patterns in the northern Swiss Alpine Foreland during the mid-Pleistocene revolution, GSA Bulletin, 131 (11-12), pp. 2056–2078.
- Dieleman C., Christl M., Vockenhuber C., Gauthsch P. & Akçar N. 2022: Early Pleistocene complex cut-and-fill sequences in the Alps, Swiss Journal of Geosciences, 115 (1), pp. 1-25.
- Grischott R., Kober F., Ivy-Ochs S., Hippe K., Lupker M., Broś E., Maden C., Christl M. & Vockenhuber C. 2020: Dating Quaternary Terraces in Northern Switzerland with Cosmogenic Nuclides, Nagra Arbeitsbericht NAB 19-025.
- Knudsen M.F., Nørgaard J., Grischott R., Kober F., Egholm D.L., Hansen T.M. & Jansen J.D. 2020: New cosmogenic nuclide burial-dating model indicates onset of major glaciations in the Alps during Middle Pleistocene Transition, Earth and Planetary Science Letters, 549: 116491.

## P 10.10

# Paired cosmogenic-nuclide measurements improve denudation rate estimates of northern Switzerland

Richard F. Ott<sup>1</sup>, Susan Ivy-Ochs<sup>2</sup>, Florian Kober<sup>3</sup>, Marcus Christl<sup>2</sup>, Christof Vockenhuber<sup>2</sup>

<sup>1</sup> Earth Surface Geochemistry, GFZ German Research Centre for Geosciences, Telegrafenberg, D-14473 Potsdam ([richard.ott@gfz-potsdam.de](mailto:richard.ott@gfz-potsdam.de))

<sup>2</sup> Laboratory of Ion Beam Physics, ETH Zürich, Otto-Stern-Weg 5, CH-8093 Zürich

<sup>3</sup> Nationale Genossenschaft für die Lagerung Radioaktiver Abfälle (Nagra), Hardstrasse 73, CH-5430 Wettingen

Denudation is the main process sculpting landscapes and generating sediment. Millennial time-scale denudation rates are most commonly derived from cosmogenic nuclide concentrations, especially from <sup>10</sup>Be measurements. However, most sediments in northern Switzerland and southwestern Germany are calcareous and Ott et al. (2022a) showed that cosmogenic <sup>10</sup>Be concentrations can be strongly biased if weathering is non-negligible. To produce more reliable estimates of long-term denudation, we conducted paired <sup>10</sup>Be and <sup>36</sup>Cl cosmogenic nuclide measurements on alluvial sediment samples, complemented with amalgamated samples of hillslope colluvium. Sampling sites include the Bözberg plateau, Randen, and the Wutach region. We use the WeCode software (Ott et al., 2022b) to predict long-term denudation and weathering rates from paired nuclide concentrations. Furthermore, weathering rates were calculated from stream water chemistry data for the three study regions to independently verify weathering estimates from the cosmogenic nuclides. Preliminary results from Wutach, Bözberg, and Randen catchments show the highest denudation rates in the Wutach region. Weathering rates predicted from cosmogenic nuclides for all catchments agree within uncertainty with weathering rates from stream water chemistry. Conventional <sup>10</sup>Be denudation rates would have underestimated denudation by a factor of 2.2, 2.3, and 2.6 for the Randen, Wutach and Bözberg sample, respectively. These preliminary results indicate that accounting for weathering biases is very important when quantifying denudation, and highlight the promise of paired nuclide measurements in doing so.

## REFERENCES

- Ott, R. F., Gallen, S. F., & Granger, D. E. 2022a: Cosmogenic nuclide weathering biases: corrections and potential for denudation and weathering rate measurements. *Geochronology*, 4(2), 455-470, <https://doi.org/10.5194/gchron-4-455-2022>
- Ott, R. F. 2022b: WeCode – Weathering Corrections for denudation rates V. 1.0, GFZ Data Serv. [code], <https://doi.org/10.5880/GFZ.4.6.2022.001>, 2022

## P 10.11

### Zircon luminescence as a geochronological tool for (sub-) recent sediments – First results

Christoph Schmidt<sup>1</sup>, Théo Halter<sup>1</sup>, Georgina King<sup>1</sup>, Paul Hanson<sup>2</sup>, Sebastian Kreutzer<sup>3,4</sup>

<sup>1</sup> Institute of Earth Surface Dynamics, University of Lausanne, Quartier UNIL-Mouline, Géopolis, CH-1015 Lausanne ([christoph.schmidt@unil.ch](mailto:christoph.schmidt@unil.ch))

<sup>2</sup> School of Natural Resources, University of Nebraska-Lincoln, Lincoln, US-NE 68583-0996

<sup>3</sup> Institute of Geography, Ruprecht-Karls Universität Heidelberg, Im Neuenheimer Feld 348, DE-69120 Heidelberg

<sup>4</sup> Archéosciences Bordeaux, UMR 6034, CNRS-Université Bordeaux Montaigne, Esplanade des Antilles, FR-33607 Pessac

Constraining the timing of sediment re-deposition in geomorphological and (geo-)archaeological studies over the past 1,000–2,000 years remains challenging, particularly in arid environments and in the absence of organic material for radiocarbon dating and dendrochronology. Detrital zircons occur commonly in sediments (albeit at low concentration). Their time-dependent luminescence signal accumulation offers a new opportunity to develop a geochronometer at recent to sub-recent timescales. The dated event is the last light exposure of zircon grains, corresponding to the burial time following (re-)mobilisation. Unlike quartz and feldspar, zircon minerals contain high concentrations of U and Th, exceeding by far the radionuclide concentrations from the surrounding sediment matrix. This intense ‘self-irradiation’ facilitates the ‘auto-regeneration’ technique, in which the zircon grains, after readout of the natural signal, are stored in the dark for several months, followed by measuring their auto-regenerated signal. The age is then obtained by dividing the natural signal by the auto-regenerated signal multiplied by the storage time (Templer 1985; Smith 1988). With this methodology, a dating precision on the order of a few years appears possible.

Our contribution presents the first results from a new project on reconstructing droughts in the Great Plains (USA) within the past 1,500 years using the zircon luminescence chronometer. We share our experiences in extracting zircons from sediments using a range of methodologies. Laboratory experiments using green laser stimulation and detection of the UV signal of zircons indicate signal resetting rates under sunlight exposure almost as high as those of quartz. This characteristic facilitates accurate dating, even of events associated with short sunlight exposure. Measured rates of athermal signal loss are high but irrelevant for the auto-regeneration technique. Finally, we present preliminary results from a storage experiment to assess the minimum storage time required to induce a detectable auto-regenerated signal.

## REFERENCES

- Smith, B. 1988: Zircon from sediments: a combined OSL and TL auto-regenerative dating technique. *Quaternary Science Reviews* 7, 401-406.  
Templer, R. 1985: The dating of zircons by auto-regenerated TL at low temperatures. *Nuclear Tracks and Radiation Measurements* 10, 789-798.

**P 10.12****Late Holocene speleothem-reconstructions from SW Asia**

Alistair Morgan<sup>1</sup>, Dominik Fleitmann<sup>1</sup>, Hai Cheng<sup>2</sup>, Lawrence R. Edwards<sup>3</sup>, Albert Matter<sup>4</sup>, Elisa Hofmeister<sup>1</sup>, Okan Tuysuz<sup>5</sup>, Mark Altaweel<sup>6</sup>

<sup>1</sup> Department of Quaternary Geology, University of Basel, Bernoullistrasse 32, CH-4056 Basel, Switzerland

(alistair.morgan@unibas.ch, dominik.fleitmann@unibas.ch, elisa.hofmeister@unibas.ch)

<sup>2</sup> Institute of Glocal Environmental Change, Xi'an Jiaotong University, 710049 Xi'an, China (m.altaweel@ucl.ac.uk).

<sup>3</sup> Earth & Environmental Sciences, University of Minnesota, MN 55455 Minneapolis, USA (m.altaweel@ucl.ac.uk).

<sup>4</sup> Institute of Geological Sciences, University of Bern, CH-3012 Bern, Switzerland (m.altaweel@ucl.ac.uk).

<sup>5</sup> Eurasia Institute of Earth Sciences and the Department of Geological Engineering, Istanbul Technical University, 34467 Istanbul, Turkey (m.altaweel@ucl.ac.uk).

<sup>6</sup> Institute of Archeology, UCL, WC1H 0PY London, UK (m.altaweel@ucl.ac.uk).

East Thrace and Northern Mesopotamia are significant regions to study palaeoclimatology considering their geographical and historical significance over the last 3,000 years as a place of societal change and conquest; including the collapse of the Neo-Assyrian Empire, Thracian tribal tensions and the rise of the Persian Empire, Ancient Greek colonisation, the rise and fall of the Roman Byzantine Empire, and rise of Islam.

The region is also in a unique position between the major climatic systems of the Black Sea, North Atlantic, Mediterranean and Eurasia. Changes in these climate systems have driven several 'rapid climate change' episodes through the Late Holocene (Weninger et. al., 2009) that are believed to have directly influenced major historical transitions including the 3.1 to 2.9 ka 'Bronze Age Collapse' and 0.75 to 0.1 ka 'Little Ice Age'. With major populated areas such as Istanbul at risk from future extreme weather events (Aygün & Baycan, 2020), and the greater Eastern Mediterranean at risk from agricultural drought (Dabanlı et. al., 2017), which has proven to cause significant societal impacts through history (Jones et. al., 2019), this region warrants the study of potential climatically driven cultural and societal changes through time.

Given the lack of meteorological data past 100-years, and heterogeneity of Eastern Mediterranean climate in general (Jacobson et. al., 2021), this is best accomplished through high-resolution and well-resolved records, to better understand spatio-temporal climate change. Uzuntarla cave (Thracian region of NW Turkey) and Shallai Cave (Iraqi Kurdistan) are in unique positions with few annual to sub-annual palaeoclimate records locally, that could potentially fill in these regional gaps. Presented is preliminary data of new U/Th and <sup>14</sup>C chronologies against stable isotope ( $\delta^{13}\text{C}$ ,  $\delta^{18}\text{O}$ ), and trace element, records that was first calibrated against contemporary meteorological data for the region. This was then compared against regional and global palaeoclimate data through time, linked with key historical events.

**REFERENCES**

- Aygün, A. and Baycan, T., 2020: Risk assessment of urban sectors to climate change in Istanbul. *Ekonomicheskie i Sotsialnye Peremeny*, 13(3), pp.211-227.
- Dabanlı, İ., Mishra, A.K. and Şen, Z., 2017: Long-term spatio-temporal drought variability in Turkey. *Journal of Hydrology*, 552, pp.779-792.
- Jacobson MJ, Pickett J, Gascoigne AL, Fleitmann D, Elton H., 2022: Settlement, environment, and climate change in SW Anatolia: Dynamics of regional variation and the end of Antiquity. *PLoS ONE* 17(6): e0270295.
- Jones, M.D., Roberts, C.N., Leng, M.J., Turkes, M., 2006: A high-resolution late Holocene lake isotope record from Turkey and links to North Atlantic and monsoon climate. *Geology* 34, 361-364.

**P 10.13****Constraining the sources of cave CO<sub>2</sub> through multipool <sup>14</sup>C and δ<sup>13</sup>C analysis at Milandre cave, Switzerland.**

Sarah Rowan<sup>1</sup>, Marc Luetscher<sup>2</sup>, Sönke Szwedat<sup>1</sup>, Thomas Laemmel<sup>1</sup>, Oliver Kost<sup>3</sup>, Franziska A. Lechleitner<sup>1</sup>.

<sup>1</sup> Department of Chemistry, Biochemistry and Pharmaceutical Sciences & Oeschger Centre for Climate Change Research, University of Bern, Freiestrasse 3, 3012 Bern, Switzerland (sarah.rowan@unibe.ch).

<sup>2</sup> Swiss Institute for Speleology and Karst Studies. Rue de la Serre 68, 2300 La Chaux-de-Fonds, Switzerland.

<sup>3</sup> Department of Earth Sciences, ETH Zurich, Sonneggstrasse 5, 8092 Zurich, Switzerland.

Karst landscapes make up 15% of the terrestrial geological coverage (Goldscheider et al., 2020). An accurate understanding of how carbon is cycled in these environments is therefore essential to our understanding of global carbon fluxes. However, the contributing sources and mechanisms of delivery of subsurface CO<sub>2</sub> in karst systems are not well understood. The traditional cave carbon cycle model proposes that the dominant source of vadose CO<sub>2</sub> originates from the respiration of catchment soils (Hendy, 1971). In contrast, a growing body of recent studies have suggested the presence of additional, comparatively older and deeper sources of cave CO<sub>2</sub> (Bergel et al., 2017, Tune et al., 2020).

We evaluated the <sup>14</sup>CO<sub>2</sub> and δ<sup>13</sup>CO<sub>2</sub> composition of the atmosphere in the overlying cave catchment, catchment soil gas, well gas, and cave air of Milandre cave in Switzerland as part of an ongoing two year monitoring campaign. The <sup>14</sup>C signature in cave gas samples is more depleted compared to soil and well gas. However, the δ<sup>13</sup>C of cave and soil/well gas samples show similarly depleted signatures, indicating a dominant contribution from biological respiration. This discrepancy could hint towards an aged deep reservoir of CO<sub>2</sub> contributing to the cave gas, or significant input from degassing of <sup>14</sup>C fossil carbonate CO<sub>2</sub> from drip water. Dissolved inorganic carbon δ<sup>13</sup>C from drip waters is depleted implying that the cave is an open system with a considerable contribution of biologically respiration CO<sub>2</sub> feeding speleothem growth. These results have implications for the understanding of the subterranean carbon cycle and the interpretation of speleothem carbon isotope records for paleoclimate studies.

**REFERENCES**

- Bergel, S., Carlson, P., Larson, T., Wood, C., Johnson, K., Banner, J. and Breecker, D., 2017. Constraining the subsoil carbon source to cave-air CO<sub>2</sub> and speleothem calcite in central Texas. *Geochimica et Cosmochimica Acta*, 217, pp.112-127.
- Goldscheider, N., Chen, Z., Auler, A., Bakalowicz, M., Broda, S., Drew, D., Hartmann, J., Jiang, G., Moosdorf, N., Stevanovic, Z. and Veni, G., 2020. Global distribution of carbonate rocks and karst water resources. *Hydrogeology Journal*, 28(5), pp.1661-1677.
- Hendy, C., 1971. The isotopic geochemistry of speleothems—I. The calculation of the effects of different modes of formation on the isotopic composition of speleothems and their applicability as palaeoclimatic indicators. *Geochimica et Cosmochimica Acta*, 35(8), pp.801-824.
- Tune, A., Druhan, J., Wang, J., Bennett, P. and Rempe, D., 2020. Carbon Dioxide Production in Bedrock Beneath Soils Substantially Contributes to Forest Carbon Cycling. *Journal of Geophysical Research: Biogeosciences*, 125(12).

**P 10.14****Holocene to Late-Pleistocene climate variability in Turkey and the Eastern Mediterranean recorded in speleothems**

Frederick Held<sup>1</sup>, Hai Cheng<sup>2</sup>, R. Lawrence Edwards<sup>3</sup>, Okan Tüysüz<sup>4</sup>, Dominik Fleitmann<sup>1</sup>

<sup>1</sup> Department Environmental Sciences, University of Basel, Bernoullistrasse 32, CH-4056 Basel  
(frederick.held@unibas.ch, dominik.fleitmann@unibas.ch)

<sup>2</sup> Institute of Global Environmental Change, Xi'an Jiaotong University, 710049 Xi'an, Shaanxi, China (xjtu.edu.cn)

<sup>3</sup> Department of Geology and Geophysics, University of Minnesota, 310 Pillsbury Drive SE, Minneapolis, Minnesota 55455-0231, USA (edwar001@umn.edu)

<sup>4</sup> Eurasia Institute of Earth Sciences, Istanbul Technical University, Maslak 34469 Istanbul, Turkey (tuysuz@itu.edu.tr)

Climatically, the eastern Mediterranean region, including Turkey, is a transition zone for different climatic systems, influenced by the North Atlantic/Siberian High Pressure System in winter and by the Asian monsoon in summer. Detailed paleoclimate archives recording the interaction of those systems during the Holocene and Pleistocene are pivotal for resolving the driving mechanisms of climate change on regional and global scales. Precisely dated and highly resolved multi-proxy speleothem records from Sofular cave in northeastern Turkey provide information on fluctuations in precipitation, temperature and ecosystem in unprecedented detail. To date, more than 60 stalagmites have been collected and partly investigated in close detail. Based on numerous 230Th-dates, collected stalagmites cover much of the last 700,000 years, allowing us to close many temporal gaps in the previously published records from Sofular Cave (Fleitmann et al., 2009; Badertscher et al., 2011). A key research interest focuses on climate variability during the last, penultimate and older glacial cycles. Sofular speleothem stable isotope profiles reveal climate variability on millennial and centennial time scales in response to global climate impacts, such as Dansgaard-Oeschger events or Heinrich events. The very precise chronology of D-O events enhances our ability to add information on the physical mechanisms of climate change. The isotopic signature of Black Sea surface water, the dominant moisture source for Sofular Cave, is recorded in speleothem  $\delta^{18}\text{O}$ . Changes in the  $\delta^{18}\text{O}$  of Black Sea water is caused by changes in riverine discharge and exchange with the Caspian or Mediterranean Seas are closely recorded in Sofular Cave speleothems, contributing to the reconstruction of the hydrological history of the Black Sea during the Holocene and Pleistocene (Badertscher et al., 2011). In addition, isotope measurements on speleothem fluid inclusions enables us to reconstruct temperature changes across glacial and interglacial cycles.

**REFERENCES**

- Badertscher, S., Fleitmann, D., Cheng, H., Edwards, R.L., Göktürk, O.M., Zumbühl, A., Leuenberger, M., Tüysüz, O. 2011: Pleistocene water intrusions from the mediterranean and caspian seas into the Black Sea, *Nature Geoscience*, 4 (4), 236–239.
- Fleitmann, D., Cheng, H., Badertscher, S., Edwards, R.L., Mudelsee, M., Göktürk, O.M., Fankhauser, A., Pickering, R., Raible, C.C., Matter, A., Kramers, J., Tüysüz, O. 2009: Timing and climatic impact of Greenland interstadials recorded in stalagmites from northern Turkey, *Geophysical Research Letters*, 36 (19), L19707.

# 11 Geomorphology

Caroline Bolliger, Jonathan Bussard, Dorota Czerski, Reynald Delaloye, Isabelle Gärtner-Roer, Christoph Graf, Nikolaus Kuhn, Isabelle Kull, Christophe Lambiel, Géraldine Regolini, Cristian Scapozza, Julie Wee, Andreas Zischg

*Swiss Geomorphological Society (SGmS)*

## TALKS:

- 11.1 Bandou D., Kissling E., Schlunegger F., Marti U., Schwenk M., Schläfli P., Douillet G.A., Mair D.: Evidence for water erosion forming overdeepenings
- 11.2 Bonetti S., Anand S.K., Camporeale C., Porporato A.: Formation of ridge and valley patterns in fluvial landscapes
- 11.3 Cache T., Ramirez J.A., Molnar P., Ruiz-Villanueva V., Peleg N.: The hydromorphological response of a pre-Alpine catchment to climate change
- 11.4 Del Siro C., Scapozza C., Perga M.E., Lambiel C.: Water origin and quality of rock glacier springs. Case studies in the Swiss Alps.
- 11.5 Delaney I. , Felix D., Werder M.A., Boes R., Albayrak I., Farinotti ..: Sediment transport processes during glacier retreat-insights from a decadal record of sediment discharge
- 11.6 Nyathi N.A., Kuhn N.J., Delzeit R..: Potential for Earth Observation to map and model Soil Erosion
- 11.7 Spielmann R., Aaron J., Graf Ch., Mc Ardell B.W.: Inferring hazard-related parameters of a natural debris flow based on high-frequency 3D LiDAR point clouds; Illgraben, Switzerland
- 11.8 Wee J., Hauck C., Lambiel C.: Assessing the properties of ground ice and its influence on surface dynamics at Gruben, Swiss Alps

## POSTERS:

- P 11.1 Aksay S., Schoorl J.M., Veldkamp A., Versendaal A., Wallinga J., Demir T., Aytaç A.S., Maddy M.: Geomorphological development of a Mediterranean badland landscape, western Turkey
- P 11.2 Bobillier G., Ciciora A., Epard J.-L., Kenner R., Lambiel C., Gaume J.: Investigation of permafrost instability based on a thermo-mechanical numerical model
- P 11.3 Chairi R.: Granulometric distribution and sedimentary dynamics in the Rejel Chiba wadi. Sahel region of Tunisia
- P 11.4 De Pedrini A., Del Siro C., Giacomazzi D., Scapozza C.: Schmidt hammer exposure-age dating of large rock slope failure deposits in the Southern Swiss Alps
- P 11.5 Graf E., Mudd S., Ludwig A., Landgraf A.: To what extent does 3D lithological structure drive divide migration?
- P 11.6 Mawet S., Mair D., Strupler M., Kremer K.: Assessment of the use of Unmanned Aerial Vehicle (UAV) for the analysis of lake bottom sediment features
- P 11.7 Turowski J.M., Prüß G., Voigtländer A., Ludwig A., Landgraf A., Kober F., Bonnelye A.: Geotechnical controls on erodibility in fluvial impact erosion
- P 11.8 Vivero S., Pellet C., Echelard T., Barboux C., Delaloye R.: The Rock Glacier Inventories and Kinematics (RGIK) Action Group: Recent Progress and Overview

## 11.1

### Evidence for water erosion forming overdeepenings

D. Bandou<sup>1</sup>, E. Kissling<sup>2</sup>, F. Schlunegger<sup>1</sup>, U. Marti<sup>3</sup>, M. Schwenk<sup>1</sup>, P. Schläfli<sup>1,4</sup>, G. A. Douillet<sup>1</sup>, D. Mair<sup>1</sup>

<sup>1</sup> Institute of Geological Sciences, University of Bern

<sup>2</sup> Department of Earth Sciences, ETH Zürich

<sup>3</sup> Landesgeologie Swisstopo, Bern

<sup>4</sup> Institute of Plant Sciences, University of Bern

We investigated the formation mechanism of tunnel valleys, by producing 3D models of bedrock topography using gravimetry. We obtained the cross-sectional geometry of tunnel valleys in the Swiss foreland, near Bern. The combination of information about the densities of the sedimentary fill and of the bedrock, together with borehole data and gravity surveys, along profiles across the valleys, served as input for our 3D gravity modelling software, Prisma. This finally allowed us to model the gravity effect of the Quaternary fill of the overdeepenings and to produce cross-sectional geometries of the overdeepenings.

The results show that upstream of the city of Bern, the overdeepenings are characterised by a U-shaped cross-sectional geometry, with steep to over-steepened lateral flanks and a wide flat base. Along this portion, the maximum residual anomaly ranges between -3 to -4 mGal for the Aare valley which is the main overdeepening of the region. Modelling shows that this corresponds to a depth of c. 200m to 250m. Farther downstream, approaching Bern, the erosional trough narrows by c. 1km and flattens by c. 100m as revealed by drillings. This is supported by the results of our gravity surveys, which disclose a maximum gravity effect of c. -1.0 to -1.7 mGal. Interestingly, this area with shallower troughs shows evidence for the presence of one or multiple inner gorges, which are at least 100m deep and a few tens of meters wide. At the downstream end of the Bern area, we observe that the trough widens from 4km North of Bern to c. 7 km approximately 2km farther downstream. Our gravity survey implies that this change is associated with an increase in the maximum residual anomaly, reaching values of -2.5 mGal. Modelling has not been accomplished yet but based on the results of a scientific drilling nearby, the depth is deeper than 210 m (Schwenk et al., 2021).

Interestingly, the overdeepening cross-sectional geometry in this area is V-shaped at its base. We attribute this to erosion by water, forming a gorge. This narrow bedrock depression was subsequently widened by glacial carving. In this context, strong glacial erosion upstream of the Bern area appears to have overprinted these traces. In contrast, beneath the city of Bern and farther downstream these V-shaped features have been preserved. We thus consider the Bern area as a paleo-equivalent of the modern Aare gorge near Meiringen, where the Aare River cuts through a bedrock ridge thereby forming a narrow gorge, linking two U-shaped valleys.

### REFERENCES

- Schwenk, M. A., Schläfli, P., Bandou, D., Gribenski, N., Douillet, G. A., and Schlunegger, F.: From glacial erosion to basin overfill: a 240 m-thick overdeepening–fill sequence in Bern, Switzerland, Sci. Dril., 30, 17–42, <https://doi.org/10.5194/sd-30-17-2022>, 2022.

## 11.2

### Formation of ridge and valley patterns in fluvial landscapes

Sara Bonetti<sup>1</sup>, Shashank Kumar Anand<sup>2</sup>, Carlo Camporeale<sup>3</sup>, Amilcare Porporato<sup>2,4</sup>

<sup>1</sup> School of Architecture, Civil and Environmental Engineering, École Polytechnique Fédérale de Lausanne, Lausanne, Switzerland (sara.bonetti@epfl.ch)

<sup>2</sup> Department of Civil and Environmental Engineering, Princeton University, Princeton, USA

<sup>3</sup> Department of Environment, Land and Infrastructure Engineering, Politecnico di Torino, Italy

<sup>4</sup> High Meadows Environmental Institute, Princeton University, Princeton, USA

The morphology and space-time evolution of drainage basins are key features of the Earth's surface, regulating ecosystem functions and services and creating visually striking patterns across various scales. However, a comprehensive understanding of the physical processes leading to the formation of such ridge and valley patterns and a rigorous theoretical examination of the underlying governing equations are still elusive. Here we start from the derivation of a differential equation for the definition of the specific drainage area, a key non-local property of catchments, controlling surface and subsurface hydrological fluxes. Such a drainage area equation, when coupled to landscape evolution dynamics, is shown to produce a branching cascade which exhibits remarkable similarities with other complex systems found in Nature. By means of a linear stability analysis we identify the critical conditions triggering channel formation and the emergence of a characteristic valley spacing. The spatial organization of the resulting ridge and valley patterns is shown to be in good agreement with both numerical simulations and topographic data from natural landscapes, and to be strongly dependent on the boundary conditions and runoff-erosion laws assumed.

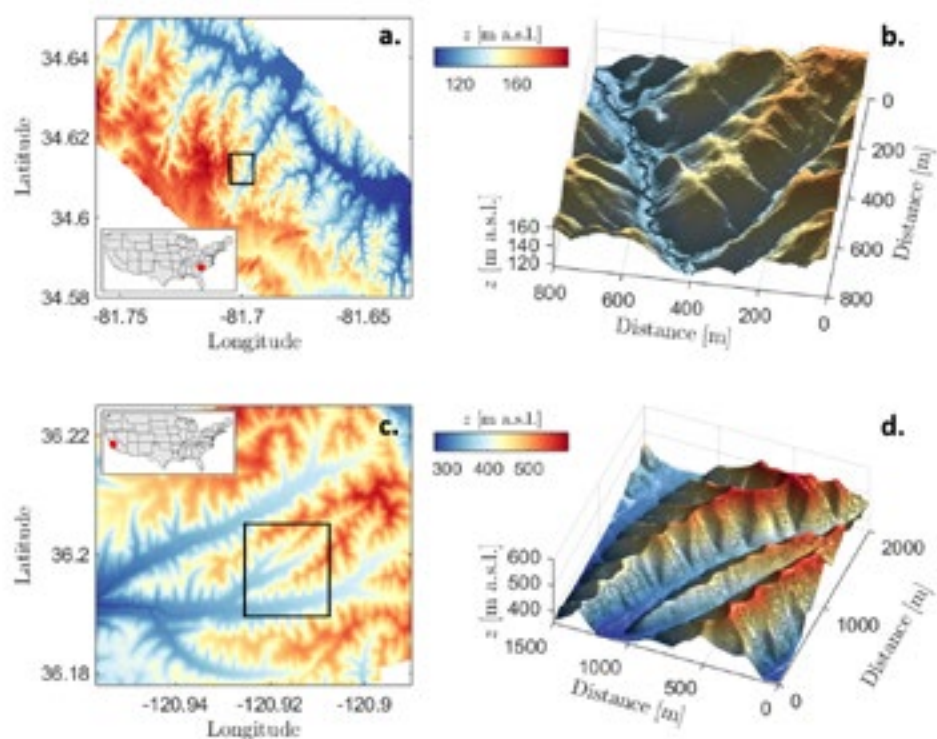


Figure 1. Ridge and valley patterns in natural landscapes (modified from Bonetti et al. 2020). One-meter resolution LiDAR topographies of (a) the Calhoun Critical Zone landscape in South Carolina and (c) Gabilan Mesa in California. Panels b and d show 3D surfaces for 2 subsets (black rectangles in panels a and c) where regular evenly spaced valleys are visible.

#### REFERENCES

- Bonetti, S., Hooshyar M., Camporeale C. & Porporato A. 2020: Channelization cascade in landscape evolution, Proceedings of the National Academy of Sciences, 117, 1375-1382.

## 11.3

### The hydromorphological response of a pre-Alpine catchment to climate change

Tabea Cache<sup>1</sup>, Jorge A. Ramirez<sup>2</sup>, Peter Molnar<sup>3</sup>, Virginia Ruiz-Villanueva<sup>1</sup>, Nadav Peleg<sup>1</sup>

<sup>1</sup> Institute of Earth Surface Dynamics, University of Lausanne, 1015 Lausanne, Switzerland ([tabea.cache@unil.ch](mailto:tabea.cache@unil.ch))

<sup>2</sup> Department of Geography, University of Exeter, Exeter, UK

<sup>3</sup> ETH Zurich, Institute of Environmental Engineering, Hydrology and Water Resources Management, Zurich, Switzerland

Geomorphological changes can threaten infrastructure, increase flood impact, or affect water quality. Climate change is expected to alter precipitation intensities and frequencies and increase temperature, which will have a direct impact on streamflow and sediment transport. The impact of climate change is particularly relevant in mountainous environments that play a crucial role in water resources and sediment supply for downstream reaches and are vulnerable to warming temperatures. The main objectives of this study were to understand how changes to rainfall and snow accumulation affect sediment erosion, transport, and deposition in a pre-Alpine catchment by exploring (a) how elevation-dependent precipitations impact the hydromorphological response, and (b) how a warming climate impacts rainfall extremes that play a crucial role in sediment transport.

We explored the hydromorphological response of the upper Emme River, a small pre-Alpine catchment (127 km<sup>2</sup>) located in the Swiss cantons of Bern and Lucerne, to different climate scenarios. The landscape evolution model CAESAR-Lisflood was used to simulate the hydromorphological response for the present (1981-2010) and future (2071-2100) climates at relatively high spatial (50 m) and temporal (hourly) resolutions. Future climate data were simulated by modifying the present climate data for three possible emission scenarios: RCP2.6, RCP4.5, and RCP8.5. Mean seasonal changes in temperature and precipitation were based on information from the official Swiss climate change scenarios (CH2018). In addition, we explicitly modeled the expected intensification of short-duration rainfall extremes in the catchment, which is not commonly added in geomorphological impact studies. Precipitation was pre-processed to distinguish between 'net precipitation' (rainfall and snowmelt) and snow accumulation.

The results reveal different hydromorphological responses between climate scenarios and between seasons. For example, the almost 4°C increase in winter and spring temperatures projected for RCP8.5 at the end of the century leads to a decrease in snow accumulation, as expected. This, along with a 7% increase in winter precipitations, resulted in streamflow and sediment yield increasing respectively by 161% and 312% in winter and reducing by 20% and 10% in spring. The results also highlight the importance of the magnitude of the rainfall events, and their future changes, to transport sediments at the outlet as most of the sediments are flushed out of the catchment during high flows. In RCP4.5 for example, despite a 4% reduction in summer precipitation at the end of the century, the sediment yield increases by 13% due to the intensification of short-duration rainfall events.

## 11.4

### Water origin and quality of rock glacier springs. Case studies in the Swiss Alps.

Chantal Del Siro<sup>1</sup>, Cristian Scapozza<sup>1</sup>, Marie-Elodie Perga<sup>2</sup>, Christophe Lambiel<sup>2</sup>

<sup>1</sup> Institute of Earth Sciences, University of Applied Sciences and Arts of Southern Switzerland (SUPSI), Campus Mendrisio, Via Flora Ruchat-Roncati 15, CH-6850 Mendrisio (chantal.delsiro@supsi.ch)

<sup>2</sup> Institute of Earth Surface Dynamics, University of Lausanne, UNIL Mouline, CH-1015 Lausanne

In the current context of climate warming, rock glaciers represent potentially important water resources due to the melting of ice they contain and/or their role as high mountain aquifers. However, little is still known about the hydrological role of rock glaciers in periglacial watersheds. For this reason, this study aimed at improving knowledge about the origin and quality of rock glacier springs in order to evaluate their contribution and impact on aquatic systems. A conceptual model was developed to explain the hydro-chemical processes taking place in active rock glaciers in the current context of air, ground and permafrost temperature warming. This conceptual model is based on physico-chemical and isotopic analyses performed on water emerging from six rock glacier (of different degree of activity) in the Swiss Alps during the warm season. Similar chemical and isotopic analyses were also performed in springs located in the same catchments but fed by other water supplies. The ion content ( $\text{SO}_4^{2-}$ ,  $\text{Ca}^{2+}$ ,  $\text{Mg}^{2+}$  and  $\text{NO}_3^-$ ) of the water emerging from rock glaciers was significantly higher than that of sources not fed by rock glaciers. Besides, ion ( $\text{SO}_4^{2-}$ ,  $\text{Ca}^{2+}$  and  $\text{Mg}^{2+}$ ) and isotopic ( $\delta^{18}\text{O}$ ) values of rock glacier springs increased significantly during the warm season. Inter-site comparison showed that these differences were more pronounced in the water emerging from active rock glaciers. In addition, a seasonal increase in electrical conductivity was also observed in these springs. We assume that the seasonal rise in physico-chemical parameters (especially electrical conductivity,  $\text{SO}_4^{2-}$ ,  $\text{Ca}^{2+}$  and  $\text{Mg}^{2+}$ ) could trace the increase of ground ice melting in active rock glacier outflows from the summer to the autumn. We suggest that the cryosphere stocked chemical compounds arising from atmospheric fallout during a colder period in the recent past (1960s-1980s) and that the current ground ice melting partially releases these compounds in the Alpine water systems.

## 11.5

# Sediment transport processes during glacier retreat-insights from a decadal record of sediment discharge

Ian Delaney<sup>1</sup>, David Felix<sup>2,\*</sup> Mauro A. Werder<sup>3,4</sup>, Robert Boes<sup>3</sup>, Ismail Albayrak<sup>3</sup>, Daniel Farinotti<sup>3,4</sup>

<sup>1</sup> Institut des dynamiques de la surface terrestre, Université de Lausanne, Bâtiment Géopolis, CH-1015 Lausanne (ianarburua.delaney@unil.ch)

<sup>2</sup>Aquased.ch, 8408 Winterthur. Formerly at Laboratory of Hydraulics, Hydrology and Glaciology (VAW), ETH Zürich.

<sup>3</sup>Laboratory of Hydraulics, Hydrology and Glaciology (VAW), ETH Zürich, Hönggerbergring 26, CH-8093 Zürich

<sup>4</sup>Eidg. Forschungsanstalt WSL, Zürcherstrasse 11, CH-8903 Brümsdorf

Glacierized catchments are well known to expel massive quantities of sediment. Since glaciers form the head of catchments, changes to the amount of sediment mobilized below and around glaciers following glacier retreat will impact the downstream ecosystems, hydropower operations, and river dynamics below (Lane et al., 2019). Yet evaluating the role of different erosional processes remains difficult. Over long timescales, or on glaciers with minimal sediment stored beneath them, sediment discharge may come from glacier sliding that erodes bedrock and produce sediment. On shorter timescales, fluvial sediment transport controls sediment discharge, and discharge is impacted by hydrology and sediment distribution (Delaney et al., 2019). Furthermore, as glaciers retreat the relative role of these processes evolve, sediment discharge is impacted by changes in the catchment's sediment storage along with the exposure of proglacial areas.

In an attempt to disentangle these processes, we make use of a decade long timeseries of suspended sediment discharge (Felix, 2017; Abgottspoon et al., 2022). This timeseries has been collected from Fieschergletscher in Canton Valais. As the glacier retreated and its melt increased, glacier dynamics changed and a proglacial area grew. First, we use the data to evaluate changes to sediment transport from the catchment as climate has warmed. We then apply a model of subglacial erosion, sediment transport and proglacial processes to the data. The model only contains two elements for subglacial and proglacial processes. Its simplicity means that it can be run iteratively over the model's parameters space, allowing outputs to be compared to the sediment discharge data. By examining favorable model parameters and their resultant model outputs, we evaluate the key processes that impact the sediment discharge from Fieschergletscher's catchment. We then discuss both the limitations of this technique and the implications of these evolving processes for sediment discharge as glaciers retreat and climate warms.

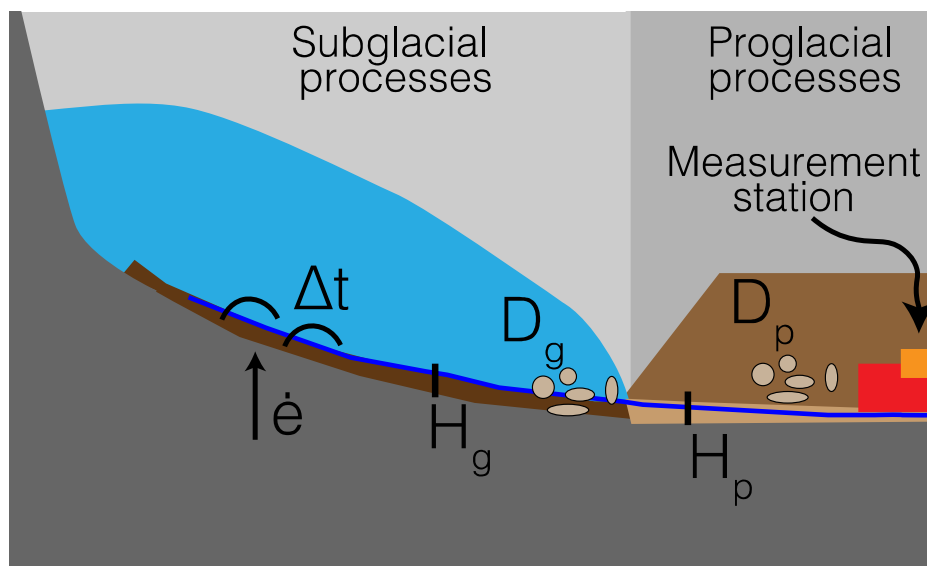


Figure 1. Cartoon representation of Fieschergletscher catchment and model design. The model represents subglacial and proglacial sediment transport processes, depending on erosion rate ( $e$ ), time scale of change to the subglacial conduit ( $\Delta t$ ), initial till height in the subglacial and proglacial areas ( $H_g$ ,  $H_p$ ), and grain size in the subglacial and proglacial areas ( $D_g$ ,  $D_p$ ). Model outputs with these parameters are tested against sediment discharge data collected at the end of the proglacial area.

## REFERENCES

- Abgottsporn, A., Felix, D., Staubli, T., Boes, R. (2022). Betriebs- und Unterhaltsoptimierung von beschichteten Pelonturbinen mit hydro-abrasivem Verschleiss - Erkenntnisse aus einem Forschungsprojekt am KW Fieschertal. *Wasser, Energie, Luft* 114(2): 105-117 (in German).
- Delaney, I., Werder, M.A., Farinotti, D. 2019: A numerical model for fluvial transport of subglacial sediment, *Journal of Geophysical Research: Earth Surface*, 124 (8), 2197-2223.
- Felix, D. (2017). Experimental investigation on suspended sediment, hydro-abrasive erosion and efficiency reductions of coated Pelton turbines. *VAW-Mitteilung 238* (R. Boes, ed.), Laboratory of Hydraulics and Glaciology, ETH Zurich.
- Lane, S. N., Bakker, M., Costa, A. et al. 2019: Making stratigraphy in the Anthropocene: climate change impacts and economic conditions controlling the supply of sediment to Lake Geneva, *Scientific Reports*, 9,8904.

## 11.6

### Potential for Earth Observation to map and model Soil Erosion

Nesisa Analisa Nyathi<sup>1</sup>, Nikolaus J. Kuhn<sup>1</sup>, Ruth Delzeit<sup>2</sup>

<sup>1</sup> Physical Geography and Environmental Change Research Group, Department of Geography and Physical Sciences, Faculty of Philosophy and Natural Sciences, University of Basel, Basel, 4056 (nesisa.nyathi@unibas.ch)

<sup>1</sup> Physical Geography and Environmental Change Research Group, Department of Geography and Physical Sciences, Faculty of Philosophy and Natural Sciences, University of Basel, Basel, 4056 (Nikolaus.kuhn@unibas.ch)

<sup>2</sup> Land Use Change Research Group, Department Umweltwissenschaften, Faculty of Philosophy and Natural Sciences, University of Basel, Basel, 4056 (ruth.delzeit@unibas.ch)

Globally, there is an increasing interest in modelling Ecosystem Services (ESS), the benefits that nature provides to people. Sediment retention is one such service that is affected by soil erosion due to land use land cover dynamics, landscape management and climate change. Such scenarios contribute to hydrological responses of river and sediment outputs thus, necessitates the need for greater attention to the fact that the rate of soil loss outweighs the soil formation rate. This problem triggered the objective of the study, to assess the potential of earth observation to map soil erosion within the Greater Limpopo Transfrontier Park catchment area. This study assesses sensitive parameters of simulated data such as discharge and sediment load which will be calibrated and validated using the modified version of Soil and Water Assessment Tool (SWAT). The envisaged results derived from the study will show that the prediction of sediment yield is sensitive to varied sizes of sub-basins which will also be associated with the sensitivity of topographic factors used in the model. Furthermore, results will indicate that the model can identify critical soil erosion susceptible areas within the catchment area on sub-watershed scales thus enabling the introduction of effective management practices at the lowest cost. Finally, it is predicted that a considerable area of the catchment can be categorized as above increased soil erosion zones with the combination of coarse loamy type of soil and agricultural type of land use and land cover condition within the study area.

## 11.7

# Inferring hazard-related parameters of a natural debris flow based on high-frequency 3D LiDAR point clouds; Illgraben, Switzerland

Raffaele Spielmann<sup>1,2</sup>, Jordan Aaron<sup>2</sup>, Christoph Graf<sup>2</sup>, Brian W. Mcardell<sup>2</sup>

<sup>1</sup> Engineering Geology Group, Geological Institute, Department of Earth Sciences, ETH Zürich, Sonneggstrasse 5, CH-8092 Zürich (raffaele.spielmann@alumni.ethz.ch)

<sup>2</sup> Swiss Federal Institute for Forest, Snow and Landscape Research WSL, Zürcherstrasse 111, CH-8903 Birmensdorf

Debris flows are extremely rapid, flow-like landslides with large impact forces and long runout distances (Hungr et al., 2014), and they are one of the most dangerous types of mass movements in mountainous regions. More detailed field-scale measurements of natural debris flows are required to better understand the fundamental mechanisms governing their motion and, ultimately, reduce the associated risks.

In this work, we analyzed a debris-flow event using timelapse point clouds from a high-resolution, high-frequency 3D LiDAR sensor (*Ouster OS1-64 Gen. 1*), which we installed at the WSL debris-flow monitoring station in the Illgraben catchment, Valais, Switzerland (Fig. 1). We developed and applied both manual and automated algorithms to derive critical hazard-related parameters, including front and surface velocities, cross-sectional area, discharge and event volume.

We observed that surface velocities measured directly behind the front exceeded the front velocity, which likely led to the formation of the bouldery front present in this event. We further found that different objects (including large boulders and woody debris) traveled at systematically different velocities, which provided quantitative information about the vertical velocity profile of the debris flow. Finally, we estimated the discharge at three different channel sections upstream of a check dam (Fig. 1) based on surface velocity and cross-sectional area measurements. We quantified systematic differences in these discharge estimates for the three sections. This “discharge paradox” could be explained by spatial and temporal variations in the velocity profile and in the channel bed geometry.

The LiDAR data analyzed in this project is unique because it allows for a truly 3D, high-resolution investigation of moving debris flows at sub-second intervals. The developed methods will be applied to LiDAR data from additional monitoring stations and events at the Illgraben, which should allow for further inference into the internal dynamics of debris flows. Eventually, this might enhance our understanding of the fundamental debris-flow mechanisms, help to optimize numerical as well as empirical modeling approaches, improve hazard mitigation in general and reduce the risk posed by flow-like landslides in the future.

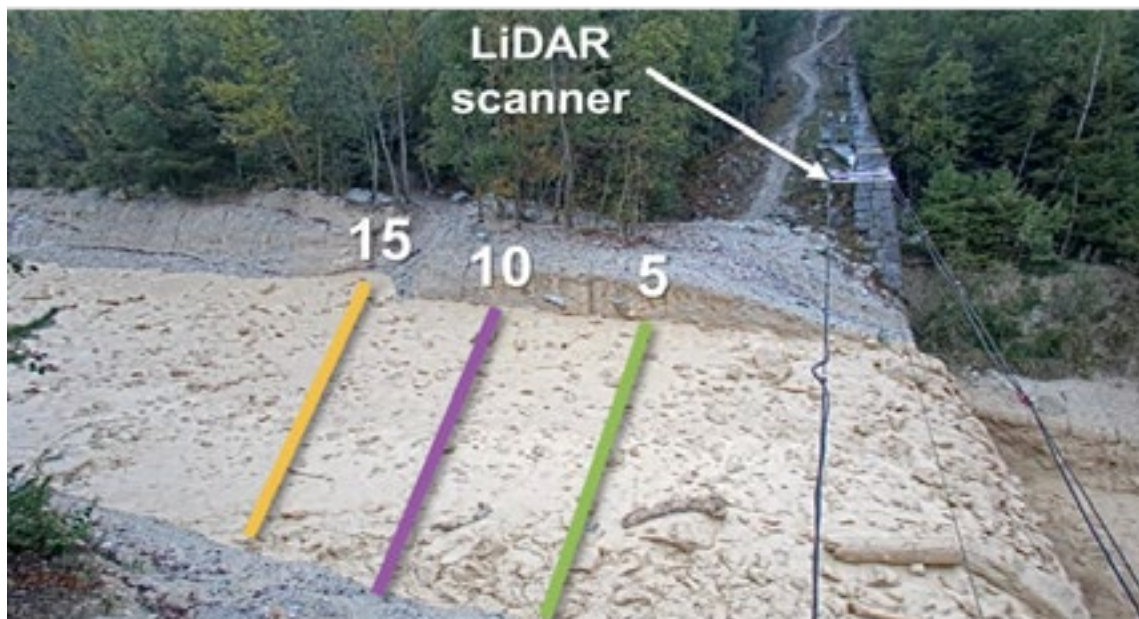


Figure 1. LiDAR scanner suspended above a check dam at the WSL debris-flow monitoring station in the Illgraben during the analyzed debris-flow event. We quantified various hazard-related debris-flow parameters within this channel segment based on high-frequency, 3D LiDAR point clouds. In particular, the discharge was estimated over the event for the three indicated channel sections (upstream of the sensor distance in meters).

**REFERENCES**

- Hungr, O., Leroueil S., & Picarelli L. 2014: The Varnes classification of landslide types, an update. *Landslides* 11(2), 167–94.  
<https://doi.org/10.1007/s10346-013-0436-y>

## 11.8

### Assessing the properties of ground ice and its influence on surface dynamics at Gruben, Swiss Alps

Julie Wee\*, Christian Hauck\*, Christophe Lambiel\*\*

\* Department of Geosciences, University of Fribourg, Ch. du Musée 4, CH-1700 Fribourg (julie.wee@unifr.ch)

\*\* Institute of Earth Surface Dynamics (IDYST), University of Lausanne, Bâtiment Géopolis UNIL Mouline, CH-1015 Lausanne

High alpine environments are characterized by glacial and periglacial landforms that are currently undergoing transformations that illustrate a degrading cryosphere. While glacier shrinkage stands among the most evident signs of a transitioning alpine landscape, visible changes in the periglacial belt such as the degradation of permafrost or the melt of ground ice are more subtle, especially in environments where both glacial and periglacial processes have occurred or still occur simultaneously. From a geomorphological perspective, they constitute complex environments sitting astride the glacial and periglacial domains, whose consecutive response to atmospheric forcing is little known and deserve in-depth investigation.

This contribution aims at understanding the extent to which ground ice properties influence the surface dynamics of a) a rock glacier disturbed by the advance of a glacier during the Little Ice Age and b) a nearby debris-covered glacier at Gruben (VS), on the basis of long-term time series of ground surface temperature, together with in-situ geodetic and geophysical measurements.

In the glacier-affected upper part of the rock glacier, where surface elevation changes are the highest (from 0.2 m/y up to more than 0.5 m/y), preliminary results reveal the presence of ground ice with high electrical resistivities close to the subsurface. On the other hand, in the undisturbed lower part of the rock glacier the uppermost boundary of the permafrost body can be observed at a depth of approximately 5-7 meters. In contrast to the upper zone, this area expresses surface elevation changes solely due to downslope movement along the topographical slope, enhanced by an extensive flow pattern. The debris-covered zone of the Gruben glacier expresses a non-uniform kinematic behaviour: the upper zone shows important surface displacement velocities, while in the lower zone, close to the margins, velocities tend to strongly decrease (Gärtner-Roer et al., 2022).

These observations confirm the heterogeneous distribution of the ground ice content throughout the investigated rock glacier as well as the non-uniform geometrical behaviour of the landform. The undisturbed zone of the rock glacier expresses a constant behaviour of downslope creep movement, while the glacier-affected zone of the rock glacier suffers a melt-induced subsidence, not only indicating the presence of buried glacier ice in this zone, but also the insufficiency of the debris-cover thickness to ensure a long-term preservation of the ice under the current climate conditions. The debris-covered part of the Gruben glacier shows strong signs of downwasting, particularly in its margins inferring the absence of ice.

#### REFERENCES

- Gärtner-Roer, I., Brunner, N., Delaloye, R., Haeberli, W., Kääb, A. and Thee, P. (2022). Glacier-permafrost relations in a high-mountain environment: 5 decades of kinematic monitoring at the Gruben site, Swiss Alps. *The Cryosphere*, 16, 2083–2101.

**P 11.1****Geomorphological development of a Mediterranean badland landscape, western Turkey**

Selçuk Aksay<sup>1</sup>, Jeroen M. Schoorl<sup>1</sup>, Antonie Veldkamp<sup>2</sup>, Alice Versendaal<sup>1,3</sup>, Jakob Wallinga<sup>1,3</sup>, Tuncer Demir<sup>4</sup>, Serdar Aytaç<sup>5</sup>, Darrel Maddy<sup>6</sup>

<sup>1</sup> SGL, Wageningen University, NL-6700 AA Wageningen ([selcuk.aksay@wur.nl](mailto:selcuk.aksay@wur.nl))

<sup>2</sup> ITC, Twente University, NL-7514 AE Enschede

<sup>3</sup> NCL, Wageningen University, NL-6708 PB Wageningen

<sup>4</sup> Geography Department, Akdeniz University, TR-07058 Antalya

<sup>5</sup> Department of Geography, Harran University, TR-63300 Şanlıurfa

<sup>6</sup> School of Geography, Newcastle University, UK-NE1 7RU Newcastle upon Tyne

Badlands are extensively eroded landscapes, typically recognised with surface features such as deeply incising gullies, steep slopes, cracks and piping structures affecting weakly consolidated deposits. The origin of semi-arid Mediterranean badlands is associated with a range of forming processes and controlling factors that are not always well-understood. These controlling factors vary and are often categorised within short-term effects such as land-use and high population densities, and long-term natural causes such as tectonic activity and climate conditions (Mather et al., 2002). Due to the existence of fine grain sediments and poor preservation of material in rapidly incising gullies in short travelling distances, assessing badland landscapes is a challenge (van Gorp et al., 2013). To address the short-term and long-term effects and natural causes, and understand spatio-temporal landscape evolution, a systematic assessment of badlands with geological mapping, morphometric analysis, age control and dynamic landscape evolution modelling is essential.

This study focuses on understanding the development of Kula badlands (Manisa, Turkey), recognised with eroded surface features and deepened gullies incising into Miocene and Quaternary sand-clay sediments within the extensional tectonic regime of western Turkey. Our multidisciplinary approach involves geomorphological assessment of the badland topography by combining geological and structural mapping with morphometric analysis using *SLk* indexes. Furthermore, age control of the Quaternary badland gully erosion, and consequent gully sedimentation will be provided using primarily pIRIR feldspar, OSL quartz and <sup>14</sup>C dating methods, particularly within the context of establishing a framework with short- and long-term (natural) causes as climate or tectonics. Dynamic numerical modelling will be performed within given time scales with supporting geological evidence to understand net erosion-deposition, incision rates and landscape evolution of this badland topography.

**REFERENCES**

- Mather, A.E., Stokes, M., Griffiths, J.S. 2002: Quaternary landscape evolution: A framework for understanding contemporary erosion, southeast Spain. Land degradation and development 13(2), pp. 89-109.  
 van Gorp, W., Veldkamp, A., Temme, A.J.A.M., Maddy, D., Demir, T., van der Schriek, T., Reimann, T., Wallinga, J., Wijbrans, J., Schoorl, J.M. 2013: Fluvial response to Holocene volcanic damming and breaching in the Gediz and Geren rivers, western Turkey. *Geomorphology*, 201, 430–448.

## P 11.2

# Investigation of permafrost instability based on a thermo-mechanical numerical model

Grégoire Bobillier<sup>1, 2\*</sup>, Alessandro Ciciora<sup>3</sup>, Jean-Luc Epard<sup>4</sup>, Robert Kenner<sup>1</sup>, Christophe Lambiel<sup>5</sup>, Johan Gaume<sup>1, 2</sup>

<sup>1</sup> WSL Institute for Snow and Avalanche Research SLF, Davos, Switzerland

<sup>2</sup> Swiss Federal Institute of Technology EPFL, Lausanne, Switzerland

<sup>3</sup> Department of Geography, University of Zurich, Zurich, Switzerland

<sup>4</sup> Institute of Earth Sciences, University of Lausanne, Lausanne, Switzerland

<sup>5</sup> Institute of Earth Surface Dynamics, University of Lausanne, Lausanne, Switzerland

\*Correspondence: Grégoire Bobillier ([gregoire.bobillier@slf.ch](mailto:gregoire.bobillier@slf.ch))

The rise in global mean temperatures induced by climate change causes accelerated permafrost degradation. In high mountain rock slopes, rock falls in permafrost areas are triggered by decreasing restraining forces such as friction loss in joints or fatigue of rock bridges, as well as increasing destabilizing forces such as hydrostatic or cryostatic pressure. Although our knowledge of the thermal influence on permafrost degradation has improved over the last decades, its mechanical effect on rock slope destabilization remains rather poorly understood.

In this work, we modeled the Mont fort geological structure (Verbier, CH) using the 3D Distinct Elements Numerical Method (3DEC software) to simulate and analyze rock failure processes. A simplified rock joint network is defined based on field observations by modeling different rock joint types (water-filled-, ice-filled-rock joints, and rock joints with a high cohesion representing rock bridges). Our developed thermo-mechanical joint model simulates the main permafrost rock destabilization processes, i.e. joint strength temperature dependency, hydrostatic and cryostatic pressures. The process-based numerical failure analysis emphasizes the contribution of each destabilization process to the fracture depth. The results show that temperature changes affect the rock stability deeper than the active layer. In addition, our results shed light on the three-dimensional influence of the water/ice-filled-joint network configuration on permafrost rock slope stability.

Overall, our results highlight the effect of the geometrical joint network configuration and the temperature influence on rock joint failure propagation. Our study advances our understanding of thermo-mechanical failure processes in permafrost rock slopes, with several potential applications in structural engineering and natural hazards.

## P 11.3

# Granulometric distribution and sedimentary dynamics in the Rejel Chiba wadi. Sahel region of Tunisia

Raja Chairi<sup>1</sup>

<sup>1</sup>Georeaserch Laboratory, Center of Research and Technologies of water. University Carthage.

Smartek Borj Cedria BP 273, 8020 Soliman, Tunisia (raja.chairi6468@gmail.com)

Located in the region of Moknine, wadi Rejel Chiba is a watercourse that has a non-permanent flow. Moknine, Gotatai, and Eliane sebkhas are connected by this wadi (Figure 1). A watershed of this wadi is about 100km and includes the tributaries Echrahil, Bennour, Chiba, and Garraf (Chairi, 2005, Chairi & Abdeljaoued, 2019).

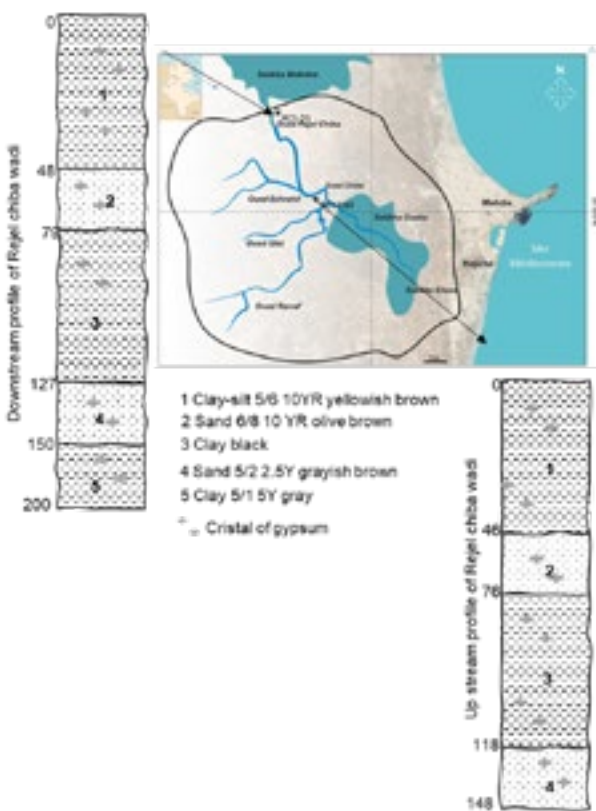


Figure 1: Sedimentary profiles of wadi Rejel Chiba and its geographical location.

A similar distribution is observed in the core profile take in downstream of the wadi (ORcAv) to that seen in the Moknine sebkha and the Eliane sebkha middle zones. The ORcAm core located at the upstream end of the wadi is comparable to the periphery of the Gotaia sebkha. An alternating sequence of clayey silt and sandy deposits forms both profiles. In terms of sedimentation, the silty-clay phase is more important than the sandy layers downstream of the wadi. The fine fraction of a sedimentation phase is about 3/4, and the coarse fraction about 1/4 (Figure 1). The mineral assemblage in the Rejel Chiba wadi consists of quartz, calcite, gypsum, and halite. Halite is less abundant at the upstream, feldspars are recognized at the downstream of the wadi in very low percentage. The clay deposits are made of smectite, illite and kaolinite. Thus, smectite is the most abundant mineral downstream, representing 42% of the total. Kaolinite, less abundant, represents 25% and illite, 33%. In the upstream wadi, kaolinite dominates (60%) while illite and smectite are comparable. In the upstream ORch area, the coarse fraction ( $FG > 63 \text{ m}$ ) is abundant at the base (100%). The facies is noted as very fine, medium-grained sands ( $\sigma = 0.89 \phi$ ). Based on the 50% average, the fine fraction becomes richer at the surface and the facies is clayey-silty. The logarithmic curves indicate that the currents transport the particles and the excess charge deposits them as the velocity of these currents decreases (Figure2).

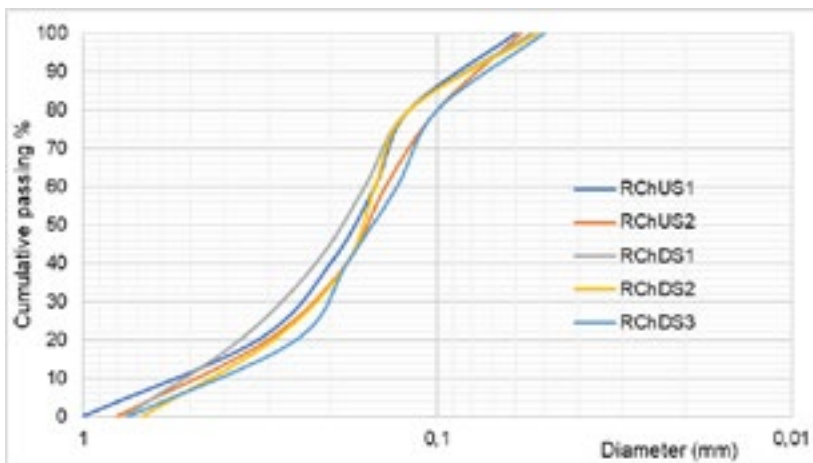


Figure 2: the granulometric curves of sandy sediments deposited in the wadi Rejel Chiba

In the downstream region of wadi Rejel Chiba, the sands appear quite fine, moderately graded ( $\sigma = 0.23 \text{--} 0.52$ ) and almost symmetrical (SKI: 0.58 1.2). The uniformity of the sands was proved by the U coefficient <2. The sands in this area are very fine, as indicated by the average Mz of 2.38 to 3.1. The mouth of the wadi is a low-energy environment (Md 110 180m). A sandy facies is characterized by sub-logarithmic cumulative curves found in protected areas, mouths, lagoons and sites with lagoons (Rivière, 1977). The same facies characterizes the sands deposited in the Eliane sebkha (Figure 2).

## REFERENCES

- Chairi, R. 2005: Sedimentological study of sediment from an hypersaline system of oriental Tunisia in recent Quaternary: Moknine Sebkha. *Quaternaire*, 16 (2), 107117. DOI : 10.4000/quaternaire.328
- Chairi, R. & Abdeljaoued S. 2019 : Environmental and geomorphological study of the Gotaia and Eliane Sebkhas in relation to the evolution of the Moknine Sebkha (Eastern Tunisia). <https://doi.org/10.4000/geomorphologie.13086>
- Rivière, A. 1977 :Méthodes granulométriques techniques et interprétation. Ed. Masson, Paris, 167 p.

## P 11.4

# Schmidt hammer exposure-age dating of large rock slope failure deposits in the Southern Swiss Alps

Alessandro De Pedrini<sup>1,2</sup>, Chantal Del Siro<sup>1</sup>, Daphné Giacomazzi<sup>1</sup>, Cristian Scapozza<sup>1</sup>

<sup>1</sup> Institute of Earth Sciences, University of Applied Sciences and Arts of Southern Switzerland, Via Flora Ruchat-Roncati 15, CH-6850 Mendrisio ([alessandro.depedrini@supsi.ch](mailto:alessandro.depedrini@supsi.ch))

<sup>2</sup> Department of Earth Sciences, Swiss Federal Institute of Technology, Sonneggstrasse 5, CH-8092 Zürich

In an Alpine environment, the occurrence of large rock slope failures is largely conditioned by glacial and paraglacial processes, which role on the timing of slope collapse has not been fully understood yet. To comprehend the strong relationship between the deglaciation and the large rock slope failures following it, a detailed geochronological assessment of both processes is essential. In the Southern Swiss Alps, between the five valleys north of Bellinzona (Riviera, Valle Leventina and Valle di Blenio in Canton of Ticino, Val Calanca and Valle Mesolcina in Canton of Graubünden), several debris accumulations of large rock slope failures can be observed. The objective of this research is to define the age of failure of four rockslide/rock avalanche deposits located close to the villages of Ludiano (Valle di Blenio), Bodio-Cauco (Val Calanca), Norantola and Centena (Valle Mesolcina) through Schmidt hammer exposure-age dating (SHD).

The Schmidt hammer, also called concrete sclerometer, measures a rebound value (R-value) which is proportional to the compressive strength of the rock surface. For a given lithology subject to similar climate conditions, the R-value can be considered as proportional to the weathering degree of the rock surface. As a consequence, R-values allow to determine a relative exposure-age of the rock surface, with high values indicating young ages, and vice versa. In case of R-values determined on two or more rock surfaces of known age, an age-calibration can be performed by regression analysis. In this study, we performed a calibration curve thanks to cosmogenic nuclide dating of the surfaces of 4 erratic boulders deposited by the Ticino glacier in Riviera valley (Scapozza et al. 2022) and 13 boulders of the prehistoric rock avalanche of Chironico (Claude et al. 2014).

By linear regression, we calculated the following SHD of the investigated rock slope deposits: 17.90–15.86 ka for the Centena rockslide, 17.14–15.17 ka for the Ludiano rock avalanche; 17.00–14.93 ka for the Norantola rock avalanche, 15.24–12.72 ka for the Bodio-Cauco rockslide, 13.86–12.25 for the Chironico rock avalanche (Fig. 1).

Considering that the Last deglaciations of the Ticino and Moesa valleys started between 16.94 and 16.39 ka b2k and ended between 15.96 and 14.87 ka b2k, it is possible to observe two clusters of rock slope deformations: Centena, Ludiano and Norantola took place immediately during the deglaciation (delay of 0 to 2.03 ka according to the dating uncertainties) and represent an “early paraglacial” response (Cat. A in Fig. 1) occurred during the Greenland Stadial GS-2.1a of the INTIMATE event stratigraphy, dated between 17.48 and 14.69 ka b2k (Rasmussen et al. 2014). Bodio-Cauco and Chironico occurred 1.03 to 4.16 ka after the deglaciation, and represent a few millennia “delayed response” to the deglaciation (Cat. B in Fig. 1). Indeed, these two rockslides fell during the Greenland Interstadial GI-1 (14.69–12.90 ka b2k), which was characterized by the first significant temperature increase after the Last Glacial Maximum. If we consider also four rock slope deformations fell in historical times (Monte Crenone, Sasso Rosso, Valegión) or not yet collapsed (Simano), it is possible to observe a third cluster (Cat. C in Fig. 1), with a very long delay (more than 14 millennia) after the deglaciation.

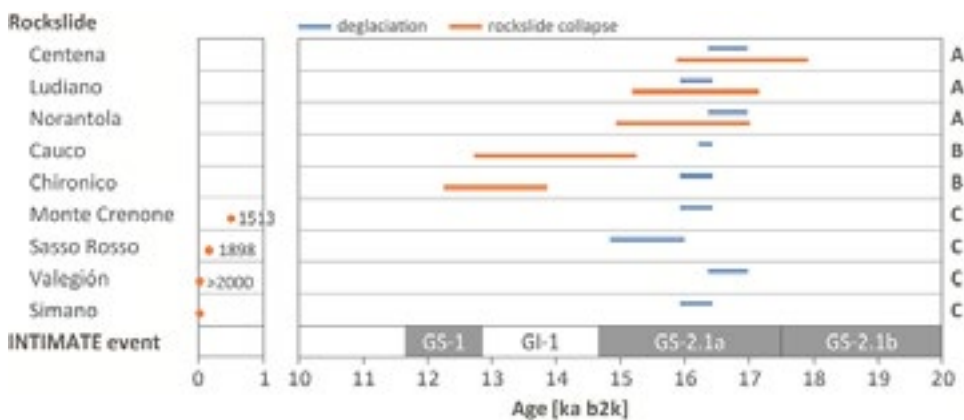


Figure 1. Comparison between the ages of rockslide collapses for 9 sites of the Lepontine Alps and the age of deglaciation of the valley slope that generated the instability. INTIMATE events from Rasmussen et al. (2014).

## REFERENCES

- Claude, A., Ivy-Ochs, S., Kober, F., Antognini, M., Salcher, B., & Kubik, P.W. 2014: The Chironico landslide (Valle Leventina, southern Swiss Alps): age and evolution, *Swiss Journal of Geosciences*, 107, 273–291. <https://doi.org/10.1007/s00015-014-0170-z>
- Rasmussen, S.O., Bigler, M., Blockley, S.P., Blunier, T., Buchard, S., Clausen, H.B., ... & Winstrup, M. 2014. A stratigraphic framework for abrupt climatic changes during the Last Glacial period based on three synchronized Greenland ice-core records: refining and extending the INTIMATE event stratigraphy, *Quaternary Science Reviews*, 106, 14–28. <https://doi.org/10.1016/j.quascirev.2014.09.007>
- Scapozza, C., Giacomazzi, D., Czerski, D., Kamleitner, S., Ivy-Ochs, S., Mazzaglia, D., Patocchi, N., & Antognini, M. 2022: Timing of deglaciation and Late Glacial and Holocene infilling of the Ticino valley between Biasca and Lago Maggiore (Southern Switzerland), ICG2022-118. <https://doi.org/10.5194/icg2022-118>

## P 11.5

### To what extent does 3D lithological structure drive divide migration?

Emma Graf<sup>1</sup>, Simon Mudd<sup>1</sup>, Andreas Ludwig<sup>2</sup>, Angela Landgraf<sup>2</sup>

<sup>1</sup> School of Geosciences, University of Edinburgh, Drummond Street, EH8 9XP Edinburgh, UK ([Emma.Graf@ed.ac.uk](mailto:Emma.Graf@ed.ac.uk))

<sup>2</sup> Nationale Genossenschaft für die Lagerung radioaktiver Abfälle (Nagra), Hardstrasse 73, CH-5430 Wettingen

Estimating future relief is a longstanding challenge in the field of geomorphology. Past denudation and incision rates can be reconstructed and modelled from field data such as thermochronometers, cosmogenic nuclides or optically stimulated luminescence, whereas future rates are then, by definition, fully unknown. Modelling future landscape evolution is further complicated by the dynamic nature of drainage networks, as well as the necessity of constraining properties such as erodibility in order to make sensible estimates. One of the few constraints available for future landscape properties is the underground stratigraphy imaged by wells or geophysical methods. The 3D rock structure will eventually be exhumed and can be utilised to constrain the future states of model simulations.

In this contribution, we present a landscape evolution model capable of ingesting 3D lithologic information and adapting to alternative channel networks, and demonstrate it using a study area in the Swiss Jura Mountains. The model calculates local relief using steady state solutions of the stream power incision model, and also quantifies hillslope relief using a very simple critical slope gradient where hillslope angles are set to a critical value on pixels that have a small drainage area. Further, drainage divides are allowed to migrate to minimize sharp breaks in relief across drainage divides.

We calibrate the values of the erodibility coefficient,  $K$ , for each lithological unit by extracting ranges of apparent  $K$  values from the present-day landscape based on drainage area and gradient along the drainage network. This is then further refined by i) using a Monte Carlo approach to create combinations of  $K$  based on these ranges, and ii) comparing the real and model landscape for each combination with the aim to minimise the difference between the two. We then test the best fit  $K$  combinations by running selected model simulations of future base level fall and potential drainage reorganisation events, highlighting the effects of i.) spatially variable erodibility and ii.) lateral changes of the main channel axis on divide migration.

## P 11.6

# Assessment of the use of Unmanned Aerial Vehicle (UAV) for the analysis of lake bottom sediment features

Sabine Mawet<sup>1</sup>, David Mair<sup>2</sup>, Michael Strupler<sup>3</sup>, Katrina Kremer<sup>2,3</sup>

<sup>1</sup> Department of Geology, Ghent University, Krijgslaan 28, B-9000 Gent ([sabine.mawet@ugent.be](mailto:sabine.mawet@ugent.be))

<sup>2</sup> Institute of Geological Sciences and Oeschger Centre for Climate Change Research, Baltzerstrasse 1+3, 3012 Bern

<sup>3</sup> Swiss Seismological Service (SED), ETH Zurich, Sonneggstrasse 5, CH-8092 Zurich

High-resolution bathymetric mapping allows imaging features that are located underwater. Imaging and characterisation of these features is crucial for process understanding and in some cases allows to better constrain natural hazards in the studied region (e.g. by visualizing underwater mass movements). However, due to often big time and cost-efforts, in some lakes high-resolution bathymetric are (still) not available.

Here, we use an unmanned aerial vehicle (UAV) to obtain orthophotos of the drained lake Kloental (Switzerland) and conduct a detailed geomorphological analysis. We investigate the lake bottom features, both sedimentologically and morphologically and later compare them to existing digital data.

Application of this method revealed relicts of houses, roads and cut forests, which show a clear imprint of human activities on the environment. The more naturally influenced parts of the lake are located in lacustrine or riverine settings or along slopes influenced by rockfalls. A small hill in a region influenced by all three settings will need some further investigation to unravel its actual origin. We found that the method of using drones is useful for rapidly acquiring, mapping, and interpreting the bottom features of emptied lakes. However, minor challenges occurred during the calibration of the colours, which differ from one image to another. The colour of the image can depend on the drone, its camera, the lighting conditions, and the meteorological conditions prevailing at that time.

For the comparison of two images, it is recommended to use the same drone, to calibrate the colours and to make sure that similar weather conditions prevail that day, and the days before the images are taken.

In this contribution, we present (1) the approach used, (2) the main observed features of lake Klöntal, their dimensions and their interpretation, (3) the challenges and the limitations encountered.

## P 11.7

### Geotechnical controls on erodibility in fluvial impact erosion

Jens M. Turowski<sup>1</sup>, Gunnar Prüß<sup>1</sup>, Anne Voigtländer<sup>1</sup>, Andreas Ludwig<sup>2</sup>, Angela Landgraf<sup>2</sup>, Florian Kober<sup>2</sup>, Audrey Bonnelye<sup>1</sup>

<sup>1</sup> Helmholtzzentrum Potsdam, GFZ German Research Centre for Geosciences, Telegrafenberg, 14473 Potsdam, Germany  
(jens.turowski@gfz-potsdam.de)

<sup>2</sup> Nationale Genossenschaft für die Lagerung Radioaktiver Abfälle (NAGRA), 5430 Wettingen, Switzerland

Bedrock incision by rivers is commonly driven by the impacts of moving bedload particles. The speed of incision is modulated by rock properties, which is quantified within a parameter known as erodibility that scales the erosion rate to the erosive action of the flow. Although basic models for the geotechnical controls on rock erodibility have been suggested, large scatter and trends in the remaining relationships indicate that they are incompletely understood. Here, we conducted dedicated laboratory experiments to investigate these controls using erosion mills. In parallel, we measured compressive strength, tensile strength, Young's modulus, bulk density and the Poisson ratio for the tested lithologies. We find that under the same flow conditions, erosion rates of samples from the same lithology can vary by a factor of up to sixty. This indicates that rock properties that can vary over short distances within the same rock can exert a strong control on its erosional properties. The geotechnical properties of the tested lithologies are strongly cross-correlated, preventing a purely empirical determination of their controls on erodibility. The currently prevailing model predicts that erosion rates should scale linearly with Young's modulus and inversely with the square of the tensile strength. We extend this model using first-principle physical arguments, taking into account the geotechnical properties of the impactor. The extended model provides a better description of the data than the existing model, yet, the fit is far from satisfactory. We will also demonstrate that the ratio of mineral grain size to the impactor diameter present a strong control on erodibility that has not been quantified so far. Finally, we also discuss how our laboratory results upscale to real landscapes and long timescales.

## P 11.8

# The Rock Glacier Inventories and Kinematics (RGIK) Action Group: Recent Progress and Overview

Sebastián Vivero<sup>1</sup>, Cécile Pellet<sup>1</sup>, Thomas Echelard<sup>1</sup>, Chloé Barboux<sup>1</sup>, Reynald Delaloye<sup>1</sup>

<sup>1</sup> Department of Geosciences, University of Fribourg, CH-1700 Fribourg ([sebastian.viveroandrade@unifr.ch](mailto:sebastian.viveroandrade@unifr.ch))

Rock glaciers are widespread landforms associated with periglacial environments and derived from the past or present creep of mountain permafrost. Considerable volumes of fine- and coarse-grained debris are involved in building rock glaciers as typical morphological features of the mountain periglacial zone. Since the late 1990s, there has been an increasing interest in their dynamics in the face of climate change, highlighting a general acceleration and growing occurrences of rock glacier destabilisation. Changes in the creep rate at short-term, seasonal and multiyear scales can affect: sediment transfer rates along mountain slopes, landscape evolution, localised hazard situations and hydrologic regime.

Numerous rock glacier inventories have been executed over several mountain regions for decades but without meaningful coordination. Whereas rock glaciers have to be primarily identified as geomorphological items of the mountain landscape, the general progress in remote sensing technologies and the ever-increasing availability of appropriate optical and radar satellite images permit the incorporation of kinematic information within rock glacier inventories. New and sometimes overlapping initiatives for inventorying and monitoring rock glaciers are expanding in many regions with various methodologies. Similarly, there is a growing number of studies focusing on the computation of rock glacier velocity using diverse methods ranging from in-situ geodetic measurements to space-borne radar and optical imagery at different time scales (i.e. seasonal to centennial-scale).

In this context, there is an obvious need for coordination and, as far as possible, the application standardisation procedures. In these circumstances, the Rock Glacier Inventories and Kinematics (RGIK) Action Group (2018-2023) aims to (1) coordinate the definition of standard guidelines for global inventorying and mapping rock glaciers (RoGI), including information on their activity rate, and (2) promote rock glacier velocities (RGV) as a new associated product to the Essential Climate Variable (ECV) permafrost in the frame of the Global Climate Observation System (GCOS). Here, we give an overview of the RGIK Action Group and an insight into the current developments and foreseen activities. This presentation is a community effort of the RGIK Action Group. For more information about the Action Group, please visit [www.rgik.org](http://www.rgik.org).

# 12 Soil: Formation, Processes and Conservation

Tobias Sprafke, Ophélie Sauzet, Klaus Jarosch, Stéphanie Grand, Tatenda Lemann, Madlene Nussbaum

*Bodenkundliche Gesellschaft der Schweiz (Swiss Soil Science Society)*

## TALKS:

- 12.1 Ceriotti G., Borisov S.M., Berg J., de Anna P.: Soil on a Chip: Visualizing microscale O<sub>2</sub> and Biomass Heterogeneity to explain anoxic Microsite Formation
- 12.2 Dupla X., Möller B., Baveye P., Grand S.: Will enhanced rock weathering practices lead to soil pollution?
- 12.3 Keiluweit M., Anderson G.G.: Hydrological extremes shift controls and pathways of carbon loss from floodplain soils
- 12.4 Lin Lin Yemeli P., Lonla Vijayakumar J., Cornelis W.: Effect of soil sealing on soil properties under simulated rainfall experiments
- 12.5 Lu Li Krenz J., Kuhn N.J.: The potential to reconstruct 20th century soil carbon erosion in rangelands from small reservoir sediments
- 12.6 Metzger K., Liebisch F., Herrera JM., Walder F., Bragazza L.: Field-based application of visible and near-infrared (vis-NIR) spectroscopy for soil chemical and physical characterization
- 12.7 Minich L.I., Meusburger Di Bella K., Haghipour N., Moreno Duborgel M., Eglinton T., Hagedorn F.: A radiocarbon-based approach to explore dissolved organic carbon cycling in Swiss forest soils
- 12.8 Oberholzer S., Steffens M., Jarosch K.A., Harder N., Ifejika Speranza C.: Maximizing biomass input or soil cover? Immediate effects of different cover cropping strategies on soil carbon and nitrogen fractions in organic reduced tillage systems in Switzerland
- 12.9 Semeraro S., Rasmann S., Le Bayon C.: The use of physical soil profile collections to measure the impact of climate change on soil properties
- 12.10 Siegenthaler M.B., McLaren T.I., Frossard E., Tamburini F.: Microbial synthesis of organic phosphorus induced by inorganic phosphorus addition in organic soil horizons of beech forests
- 12.11 Van Thuyne J., Verrecchia E.P.: Are termite mounds the calcium reactor of silica-rich landscapes? A research perspective.

**POSTERS:**

- P 12.1 Jarosch K., EJP SOIL team: EJP SOIL: Towards Climate Smart Agricultural Soils
- P 12.2 Hildbrand C., Sprafke T.: Soilscape information and sustainable land use – a case study in the canton of Bern, Switzerland
- P 12.3 Musso A., Tikhomirov D., Plötze M., Greinwald K., Hartmann A., Geitner C., Maier F., Petibon F., Egli M.: Siliceous and calcareous soil development in the Swiss Alps: weathering, erosion, and mineralogical data from two Holocene chronosequences
- P 12.4 Charles C., Khelidj N., Grand S., Losapio G.: Impact of glacier retreat on plant diversity and soil functioning
- P 12.5 Wasner D., Abramoff R., Griepentrog M., Zagal Venegas E., Boeckx P., Doetterl S.: The changing importance of controls on soil carbon stabilization across soil types
- P 12.6 Siegfried L., Vittoz P., Verrecchia E.: From vegetation to soil: Organic matter dynamics in riparian forests in the Grand Cariçaie (Switzerland)
- P 12.7 Bonvin E., Claustre R., Dupla X., Grand S.: Soil and rock mineralogical transformations resulting from enhanced rock weathering under temperate climate
- P 12.8 Claustre R., Bonvin E., Dupla X., Grand S.: Making sure climate mitigation promises are safe: Impact of enhanced rock weathering on soil organisms and edaphic factors
- P 12.9 Deluz A., Hartmann M., Boivin P., Fliessbach A., Six J.: Microbial communities in Swiss croplands
- P 12.10 Grunder A., Bigalke M., Beriot N.: Soil Micro Plastic: A standardized extraction & analysis protocol for MINAGRIS

## 12.1

# Soil on a Chip: Visualizing microscale O<sub>2</sub> and Biomass Heterogeneity to explain anoxic Microsite Formation

Giulia Ceriotti<sup>1</sup>, Sergey M. Borisov<sup>2</sup>, Jasmine Berg<sup>1</sup>, Pietro de Anna<sup>3</sup>

<sup>1</sup>Institute of Earth Surface Dynamics, University of Lausanne, Batiment Geopolis, UNIL-Mouline, CH-1015 Lausanne  
(giulia.ceriotti@unil.ch)

<sup>2</sup>Institute of Analytical Chemistry and Food Chemistry, Graz University of Technology, Rechbauerstrasse 12, 8010 Graz, Austria

<sup>3</sup>Institute of Earth Sciences, University of Lausanne, Batiment Geopolis, UNIL-Mouline, CH-1015 Lausanne

The cycling of nutrients and other elements and the natural attenuation of contaminants in soils and aquifers are often mediated by anaerobic microbial processes under anoxic conditions. Surprisingly, recent studies have provided evidence that facultative and obligately anaerobic bacteria also proliferate in oxic subsurface systems (such as well-drained soils and shallow groundwater), and they largely contribute to methane (Keiluweit et al. 2017) and NO<sub>x</sub> emissions (Kravchenko et al. 2017), Mn and Fe reduction, and reductive dehalogenation (Herrero et al. 2022). This paradox can be explained by the formation of anoxic microsites due to heterogeneous pore water flow and matrix tortuosity limiting O<sub>2</sub> diffusion rates coupled with bacterial aerobic respiration (Kuzyakov & Blagodatskaya 2015; Baveye et al. 2018). Thus, understanding microscale O<sub>2</sub> heterogeneity is crucial to improving the predictability of anaerobic processes and the associated element cycling and contaminant attenuation.

This work presents a novel experimental setup combining microfluidic devices mimicking a sandy structure and transparent O<sub>2</sub> planar sensors to explore and directly visualize anoxic microsite formation. An automated microscope allows us to simultaneously monitor biomass distribution and O<sub>2</sub> concentration over the entire chosen porous landscape with a microscale resolution over time (see Figure 1).

Our results reveal the relevance of bacterial colony morphology and growth regime in controlling anoxic microsite formation. Based on our quantitative assessment of O<sub>2</sub> fluxed within each bacterial colony, we demonstrate that a change in colony morphology is sufficient to tip the balance between O<sub>2</sub> diffusion and bacterial uptake and thus trigger the formation of an anoxic microsite in well-oxygenated soils and aquifers.

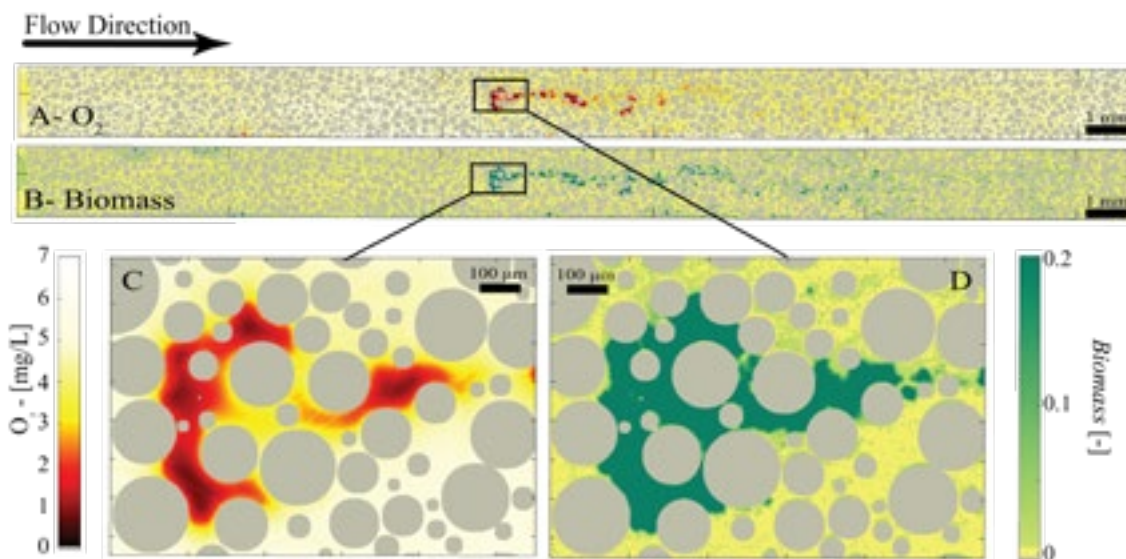


Figure 1. O<sub>2</sub> concentrations (A) and biomass distribution (B) and over the entire porous landscape after 26 hours. (C) and (D) Zoom in on an anoxic microsite and the corresponding biomass map.

## REFERENCES

- Keiluweit, M.; Wanzek, T.; Kleber, M.; Nico, P.; Fendorf, S. Anaerobic microsites have an unaccounted role in soil carbon stabilization. *Nature communications* 2017, 8, 1–10.
- Kravchenko, A.; Toosi, E.; Guber, A.; Ostrom, N.; Yu, J.; Azeem, K.; Rivers, M., Robertson, G. Hotspots of soil N<sub>2</sub>O emission enhanced through water absorption by plant residue. *Nature Geoscience* 2017, 10, 496–500.
- Herrero, J.; Puigserver, D.; Nijenhuis, I.; Kuntze, K.; Carmona, J. M. Key factors controlling microbial distribution on a DNAPL source area. *Environmental Science and Pollution Research* 2022, 29, 1508–1520.
- Kuzyakov, Y.; Blagodatskaya, E. Microbial hotspots and hot moments in soil: concept & review. *Soil Biology and Biochemistry* 2015, 83, 184–199.
- Baveye, P. C.; Otten, W.; Kravchenko, A.; Balseiro-Romero, M.; Beckers, 'E.; Chalhoub, M.; Darnault, C.; Eickhorst, T.; Garnier, P.; Hapca, S., et al. Emergent properties of microbial activity in heterogeneous soil microenvironments: different research approaches are slowly converging, yet major challenges remain. *Frontiers in Microbiology* 2018, 9, 1929.

## 12.2

### Will enhanced rock weathering practices lead to soil pollution?

Xavier Dupla<sup>1</sup>, Benjamin Möller<sup>2</sup>, Philippe C. Baveye<sup>3</sup> and Stéphanie Grand<sup>1</sup>

<sup>1</sup> University of Lausanne, Institute of Earth Surface Dynamics, CH-1015 Lausanne, Switzerland ([xavier.dupla@unil.ch](mailto:xavier.dupla@unil.ch))

<sup>2</sup> University of Bayreuth, Universitätsstraße 30, 95447 Bayreuth, Germany

<sup>3</sup> Saint Loup Research Institute, 79600 Saint Loup Lamairé, France

Terrestrial enhanced rock weathering (ERW) is a carbon dioxide removal technology that aims at accelerating one of the most powerful negative feedbacks on Earth's climate, the chemical weathering of silicates. To achieve this, ERW proposes to spread ground rock on agricultural soils. According to many models, global applications rates of 40 tons of ground basaltic rock per hectare and per year would be necessary to reach a sequestration of 0.2 to 4.0 gigaton of CO<sub>2</sub>-equivalent per year. When assessing the viability of ERW as a global geo-engineering strategy, a pivotal question to address is whether ERW may lead to toxic trace element accumulation in soils at potentially harmful levels.

This study evaluates the legal sustainability of ERW with regard to trace element contents in soils. We compare different trace element accumulation scenarios considering a range of rock sources, application rates and national regulatory limits. The results indicate that suggested application rates will likely lead to the overrun of existing regulatory limits for copper and nickel in less than 20 years and could, in unfavorable contexts, prevent ERW from being implemented altogether. This study argues in favor of a close tailoring of ERW deployment to local conditions in order to tap into its climate mitigation potential while preserving long-term sustainable soil uses.

## 12.3

### Hydrological extremes shift controls and pathways of carbon loss from floodplain soils

Marco Keiluweit<sup>1</sup> and Cam G. Anderson<sup>2</sup>

<sup>1</sup> Institute of Earth Surface Dynamics, University of Lausanne, Lausanne ([marco.keiluweit@unil.ch](mailto:marco.keiluweit@unil.ch))

<sup>2</sup> School of Earth and Sustainability, University of Massachusetts, Amherst

Floodplains within mountainous watersheds are dynamic reservoirs of carbon that experience seasonal flooding due to snowmelt and drainage. Climate change dramatically alters snowpack levels across alpine ecosystems within the Western US, which results in more extreme flood and drought years. The variable hydrology drives spatial and temporal redox gradients within floodplain soils, with unknown consequences for carbon storage and export. In this presentation, I will show how extreme flooding and drought events alter controls and pathways of soil carbon loss within a mountainous floodplain system. Specifically, we aimed to resolve the balance between mineral and metabolic constraints on floodplain carbon loss. I will report on an extensive monitoring campaign and associated biogeochemical measurements across extremely low and high river discharge years, which foreshadow climate change predictions across mountainous ecosystems in the Western US. Combining in-field geochemical measurements and DOC and CO<sub>2</sub> flux measurements, we showed that reducing conditions during extreme flooding decrease the stability of mineral-organic associations, causing concomitant mobilization of metals and DOC. However, extensive metabolomic and metagenomic analysis showed that newly liberated reduced DOC compounds were subject to metabolic constraints, decreasing CO<sub>2</sub> fluxes. Conversely, during the extreme drought year, the stability of mineral-organic associations was increased due to sediment oxygenation, diminishing DOC export. Our results suggest that hydrological extremes alter the magnitude and pathways of CO<sub>2</sub> and DOC export in mountainous watersheds. Implications for carbon storage potential of floodplain soils will be discussed.

## 12.4

### Effect of soil sealing on soil properties under simulated rainfall experiments

Lin Lin<sup>1</sup>, Patric Yemeli Lonla<sup>1</sup>, Jaianth Vijayakumar<sup>2</sup>, Wim Cornelis<sup>1</sup>

<sup>1</sup> Department of Environment - Soil Physics Unit, Ghent University, Gent, Belgium. ([Lin.Lin@UGent.be](mailto:Lin.Lin@UGent.be))

<sup>2</sup> Centre of X-ray Tomography UGCT, Ghent University, Gent, Belgium.

Soil surface crusting is a common phenomenon on agricultural soils susceptible to raindrop impact. Crusts affect soil hydrological properties, erosion, crop quality and yield, which implicates both agriculture and the environment. Whereas methods for determining hydraulic or basic properties of soil layers (thicker than 2 cm) are well established, measuring the soil characteristics of a thin crust (< 5 mm) remains a challenge. Therefore, in this study, we combine traditional lab methods and advanced techniques to test the variation in soil properties during the crust forming process. The overall purpose of this study was to reveal temporal variations of seal micro-morphology and their effect on soil properties with increasing rainfall amount. Composite samples from two soil textures were collected, dry-sieved at 8 mm, packed in soil pans and exposed to a range of rainfall amounts and two rainfall intensities, using a laboratory nozzle-type rainulator. Intact soil ring samples were collected after each rainfall even. They were scanned using X-ray Computed Tomography (CT) to determine the evolution of soil porosity, bulk density and crust thickness during the crust formation process. In addition, the water retention, permeability and infiltration dynamics of the developing seals were investigated with a minidisk infiltrometer placed on the crusts developed in the pans and with a falling head permeameter (KSAT®), and the evaporation method (HYPROP®) on soil cores taken. Shear strength was evaluated by a hand vane. Disturbed soil was collected to explore variation in organic matter content and texture with rainfall. During the simulated rain events, soil loss, splash and runoff were recorded as well. We found that runoff volume and sediment mass increased, while splash and infiltration volume decreased with increasing rainfall amount. Shear strength increased until 200 mm of rainfall. Additionally, rainfall that resulted in crust formation had a rapid and strong effect on the hydraulic properties, with the unsaturated hydraulic conductivity being reduced as rainfall duration increased. The relatively high rainfall intensity was shown to have a greater impact than the relatively low intensity. These results were associated with rainfall-induced aggregate breakdown processes, which was confirmed by CT images. CT images showed that the porosity reached a minimum value after 50 mm rainfall, while bulk density reached a maximum value. The dense crust was then relieved/dissolved by further rainfall events. Crust thicknesses were about 3.19 and 4.85 mm, and the mean porosity of the crust layers was about 76% and 73% of the underlying layer, at relatively high and low rainfall intensity, respectively. In summary, it was possible to illustrate the structural seal formation process, and the temporal interrelated dominance and significance of the associated sub-processes which contribute to overcoming the challenge of testing the thin crust (< 5 mm).

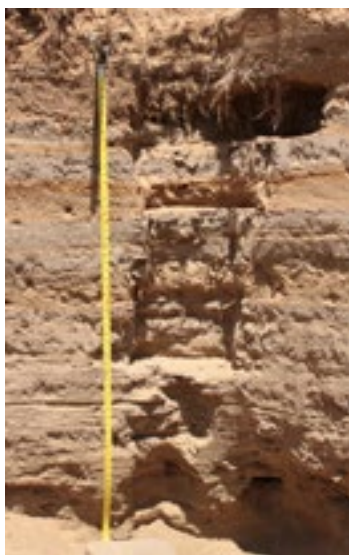
## 12.5

### The potential to reconstruct 20<sup>th</sup> century soil carbon erosion in rangelands from small reservoir sediments

Lu Li<sup>1</sup>, Juliane Krenz<sup>1</sup>, Nikolaus J. Kuhn<sup>1</sup>

<sup>1</sup> University of Basel, Physical Geography and Environmental Change, Klingelbergstrasse 27, 4056, Basel, Switzerland

Land degradation affects the productivity of the land, but is also associated with a flux of greenhouse gases (GHGs) from soil and vegetation into the atmosphere. This flux is fairly well-studied for cropland, but large spatial and temporal gaps exist for soil organic matter loss of rangelands. The large area of rangelands (35 million km<sup>2</sup>, cover about 40% of earth's surface) can contribute significantly to changes of atmospheric CO<sub>2</sub> concentrations following even a minor alteration of the rangeland soil C pool (Wang et al. 2002). Therefore, studying the rangeland soil C cycle in the past is highly relevant to understand the development of atmospheric CO<sub>2</sub>, in particular as a consequence of the intense livestock production during the 20<sup>th</sup> century (Jones and Donnelly 2004). Degradation of South African rangelands has been a concern for more than 100 years (Rowntree, 2013). The Karoo drylands, covering 30% of the land surface of South Africa, have experienced particular intense soil erosion and thus loss of topsoil C. To sustain the large number of animals, many small farm dams have been constructed mainly in the first half of the twentieth century. As a consequence of the soil erosion, they are now often silted-up and have breached (Boardman, 2014). The sediment deposited behind such small dams offers the possibility to reconstruct the loss soil C for the time period between construction and breaching of dams. Five dams were chosen to explore the possibility to use their sediment as an environmental archive for 20<sup>th</sup> century rangeland soil Carbon loss. The specific aims of our study are to 1) find out whether distinct C profiles can be discerned in dam sediments; 2) identify whether these changes potentially reflect erosion and soil C loss in the dam catchments; and 3) to discuss whether the dam sediments can serve as an environmental archive to reconstruct soil-atmosphere interaction during recent decades. The initial survey of the dams involved the sampling of individual sediment strata and the analysis of their organic and nitrogen content, as well as the Caesium 137 activity of selected samples to gain an insight into the time of deposition. Two dams showed a profile that indicates a loss of soil C during the first decreased after their construction, while the other dams showed no clear signal or even an increase of sediment C in the younger sediment. One dam showed no Caesium 137 activity, indicating that it was filled with sediment very quickly after construction. These results illustrate that soil degradation and associated loss of soil C stocks can potentially be reconstructed based on the small dam sediments. However, the source of the sediment C has to be tested, as well as the individual land use and erosion history of each dam catchment.



The Dam profile



**REFERENCE:**

- Wang G, Qian J, Cheng G, Lai Y (2002) Soil organic carbon pool of grassland soils on the Qinghai-Tibetan Plateau and its global implication. *Sci Total Environ* 291:207–217.
- Jones M, Donnelly A (2004) Carbon sequestration in temperate grassland ecosystems and the influence of management, climate and elevated CO<sub>2</sub>. *New Phytol* 164:423–439.
- Rowntree KM. 2013. The evil of 'sluits'. *Journal of Environmental Management* 130: 98-105.
- Boardman, J. 2014. How old are the gullies (dongas) of the Sneeuberg uplands, eastern Karoo, South Africa? *Catena* 113: 79-85.
- Boardman, J. 2014. How old are the gullies (dongas) of the Sneeuberg uplands, eastern Karoo, South Africa? *Catena* 113: 79-85.

## 12.6

# Field-based application of visible and near-infrared (vis-NIR) spectroscopy for soil chemical and physical characterization

Konrad Metzger<sup>1</sup>, Frank Liebisch<sup>2</sup>, Juan Manuel Herrera<sup>3</sup>, Florian Walder<sup>4</sup>, Luca Bragazza<sup>1</sup>

<sup>1</sup>Agroscope, Field-Crop Systems and Plant Nutrition, Nyon, Switzerland ([Konrad.metzger@agroscope.admin.ch](mailto:Konrad.metzger@agroscope.admin.ch))

<sup>2</sup>Agroscope, Water Protection and Substance Flows, Zurich, Switzerland

<sup>3</sup>Agroscope, Cultivation Techniques and Varieties in Arable Farming, Nyon, Switzerland

<sup>4</sup>Agroscope, Soil Quality and Soil Use, Zurich, Switzerland

In the last decades, the use of visible and near-infrared (350 – 2500 nm) spectroscopy (vis-NIR) to characterise agricultural soils has gained increased interest. The absorption of light in this range by several soil components, such as organic matter, clay minerals, and iron oxides, makes vis-NIR a potential alternative to tedious and expensive laboratory analyses, especially having in mind the future challenges of having high-resolution soil data for precision agriculture and sustainable soil use.

Recently, portable and handheld devices have been developed to obtain vis-NIR soil spectra directly in-situ. However, operational questions are still open, in particular concerning the reliability of different portable instruments and the best practice to collect soil spectra in the field. Accordingly, the main goal of this study is to propose a best practice for soil spectra acquisition in the field by comparing two different portable instruments. More precisely, we used a miniature spectrometer (NeoSpectra-Scanner, Si-Ware Systems, Egypt) with a range of 1350 – 2500 nm and a research grade portable spectroradiometer (PSR+ 3500, Spectral Evolution, Lawrence, USA) with a range of 350 – 2500 nm. Soil samples were scanned according to the following procedures in five replicate scans: on both sides of a 20 cm helical corer (side\_a and side\_b); on the undisturbed soil surface around the corer hole, avoiding stones, roots and cracks where possible (surface\_raw) and on the smooth soil surface by compacting and smoothing the soil (surface\_smooth).

In total, 134 sampling points in 9 experimental agricultural fields in Switzerland were scanned, and soil samples were analysed for texture (sand, silt, clay), C content (organic C (OC), carbonates), N content (N\_total, C/N ratio), pH, cation exchange capacity (CEC) and total and exchangeable nutrients (P, K, Mg, Ca).

Spectral outliers were removed and several pre-processing methods were applied, namely standard normal variate (SNV), multiplicative scatter correction (MSC) and Savitzky-Golay smoothing without, only with the first and only with the second derivative. With the raw and the pre-processed spectra, a partial least squares regression (PLSR) model was built for each of the scan procedures (side\_a, side\_b, surface\_raw, surface\_smooth) for clay, sand, OC, Ntot, C/N ratio, pH and CEC. For each model, the dataset was split into a calibration and validation set by using the data from one field to test the calibration built with the data from the remaining fields. This was repeated nine times and the resulting model parameters (R2, RMSECV, RMSEP, latent variables) were averaged. The selection of the ideal amount of latent variables was facilitated in the pls package based on the one-sigma heuristic and with 8-fold stratified internal cross validation.

Preliminary results showed that the PSR+ spectrometer provided the best results for clay content (R2 0.95, RMSEP 3%) and OC (R2 0.81, RMSEP 0.33 %), with the scan procedure along the core (a and b) leading to the best models. Conversely, for the NeoSpectra Scanner, the best results were obtained on the scans at the soil surface (clay: R2 0.79, RMSEP 6.7%, surface\_raw, OC: R2 0.62, RMSEP 0.45%, surface\_smooth). To simplify the spectral acquisition method, the possibility of using more spectral replicates to obtain more stable spectra with the NeoSpectra Scanner was tested by averaging the scans from both sides of the corer (side\_a, side\_b, n=10, side\_mean). This improved the prediction and brought the performance indicators (RPIQ, R<sup>2</sup>, RMSEP) close to the results from other scanning positions. Based on these results and the fact that the core covers the upper 20 cm of the soil, i.e. the area most important for crops, scanning the sides of a 20 cm corer was determined as best practice for soil spectra acquisition. Overall, the PSR+ performed better than the NeoSpectra, even though the latter showed potential as a low-cost alternative for selected parameters (clay, OC).

## 12.7

# A radiocarbon-based approach to explore dissolved organic carbon cycling in Swiss forest soils

Luisa I. Minich<sup>1,2</sup>, Katrin Meusburger Di Bella<sup>1</sup>, Negar Haghipour<sup>2,3</sup>, Margaux Moreno Duborgel<sup>1,2</sup>, Timothy I. Eglinton<sup>2</sup>, Frank Hagedorn<sup>1</sup>

<sup>1</sup> Swiss Federal Institute for Forest, Snow and Landscape Research (WSL), Switzerland

<sup>2</sup> Biogeoscience, Department of Earth Sciences, ETH Zurich, Switzerland

<sup>3</sup> Laboratory for Ion Beam Physics, Department of Physics, ETH Zurich, Switzerland

Fluxes of dissolved organic carbon (DOC) transfer carbon (C) from topsoils into subsoils. The downward transport of DOC and subsequent sorption to soil minerals is assumed to be one of the key processes for long-term C stabilization in soils. Furthermore, DOC fluxes are one transport vector for the export of carbon from terrestrial to aquatic systems. However, the pathways and magnitude of these fluxes are still uncertain. Our objectives are to better understand the importance of DOC fluxes for the linkage between terrestrial and aquatic carbon pools by (i) quantifying DOC fluxes in Swiss forest soils, (ii) by elucidating the spatial variation of DOC sources and turnover times in soils and its drivers, and by (iii) estimating the role of DOC for soil carbon stabilization and carbon export to aquatic ecosystems.

Here, we quantify DOC fluxes at five sites of the Long-term Forest Monitoring (LWF) program of WSL where soil solution is continuously sampled at four depths using tension-lysimeters. Samples are collected on a biweekly basis and analysed for pH, DOC concentration, and other element concentrations. For two time periods (archived samples: spring 2007; contemporary samples: spring 2022), we further measure radiocarbon (<sup>14</sup>C) in DOC which inform about the carbon age and turnover times of DOC. We further conduct optical measurements (UV-Vis spectroscopy, Fluorescence spectroscopy) which inform about the DOC composition. We combine the <sup>14</sup>C signatures of DOC with long-term records of DOC concentration and DOC flux rates that are modeled with the Brook90 R Package.

Our preliminary data showed an up to 27-times decrease in DOC concentrations and fluxes from the forest floor to the subsoils, signifying a net retention of DOC in mineral soils. Also, the <sup>14</sup>C contents strongly decreased with increasing soil depth, reaching radiocarbon ages up to several thousand years at 80 cm soil depth. The depth pattern of DOC concentrations and DO<sup>14</sup>C values support the concept of DOC cycling downwards (Kaiser & Kalbitz 2012). Leached, “young” DOC is likely to be sorbed to soil minerals. During microbial processing, previously sorbed DOC is remobilized and contributing to an “older” DOC source, which is then transported to greater depth. Site comparison data further suggest that the spatial variation of DO<sup>14</sup>C may rather be driven by physico-chemical differences in soils (i.e. Fe-, Al-, clay content, loess) than by climatic differences among sites. DOC losses from forest soils, here estimated by the leaching beyond 80 cm depth, are small (< 2 g C m<sup>-2</sup> y<sup>-1</sup>) as compared to other C fluxes such as soil respiration (500 – 1000 g C m<sup>-2</sup> y<sup>-1</sup>) and litterfall (200 – 500 g C m<sup>-2</sup> y<sup>-1</sup>). Although the net retention of DOC is also smaller than these fluxes, it might contribute to the C stabilization and accumulation of soil organic carbon on the centennial and millennial time scales.

This study demonstrates that physico-chemical soil properties are important drivers of DOC dynamics and age distribution across soil profiles.

## REFERENCES:

- Kaiser, K., & Kalbitz , K. (2012). Cycling downwards dissolved organic matter in soils. *Soil Biology & Biochemistry*, 52, 29–32.  
doi:10.1016/j.soilbio.2012.04.002

## 12.8

# Maximizing biomass input or soil cover? Immediate effects of different cover cropping strategies on soil carbon and nitrogen fractions in organic reduced tillage systems in Switzerland

Simon Oberholzer<sup>1</sup>, Markus Steffens<sup>1,2</sup>, Klaus A. Jarosch<sup>1,3</sup>, Nadine Harder<sup>1</sup>, Chinwe Ifejika Speranza<sup>1</sup>

<sup>1</sup> University of Bern, Institute of Geography, Hallerstrasse 12, CH-3012 Switzerland

<sup>2</sup> Research Institute of Organic Agriculture, Department of Soil Sciences, Ackerstrasse 113, CH-5070 Frick, Switzerland

<sup>3</sup> Agroecology and Environment, Agroscope, Reckenholzstrasse 191, CH-8046, Switzerland

Cover crops are grown to reduce periods of bare fallow for avoiding soil erosion and maximizing organic matter input into the soil. In reduced tillage systems under organic farming conditions, cover cropping is gaining increasing attention because of its alleged positive effects on soil organic matter formation and nutrient cycling. Yet different strategies of cover cropping are currently implemented, where detailed knowledge on their individual effects on soil properties are lacking.

Therefore, two different cover cropping approaches were compared to determine the immediate effects on different soil fertility parameters. The trial was conducted on six fields in Eastern Switzerland in the long period between harvest of winter wheat and sowing of spring crops, in which bare soil fallows are legally prohibited. Tested treatments were a) double cover cropping (DCC) where two cover crops are grown subsequently and shallowly (3 cm) incorporated into the soil or b) permanent soil cover (PSC) with one cover crop, which was harvested and thus not incorporated into the soil.

Samples were taken in high spatial and temporal resolution and a combination of near infrared spectroscopy and conventional lab methods was applied to determine different soil carbon (C) and nitrogen (N) fractions. Irrespective of the treatment, stocks of soil organic C (SOC) increased up to 8.5 %, total N up to 7.6 % and permanganate oxidizable C (POXC) up to 10.5 % over the investigated period of nine months. In 5-10 cm soil depth, the PSC treatment showed a higher increase in SOC stocks than the DCC treatment but in both treatments the increases in SOC and POXC stocks were higher in 5-10 than 0-5 cm soil depth. The DCC treatment generally showed significantly higher changes in microbial C, microbial N, and mineral N than the PSC treatment. However, the results differed largely between the fields and only in the case of microbial C and microbial N there was a correlation with cover crop aboveground biomass input. We conclude that maximizing soil cover such as in the PSC approach is a better choice when aiming for immediate SOC accumulation. Nevertheless, the aboveground plant biomass in the DCC approach increased soil microbial biomass that might have beneficial effects on soil health and long-term soil organic matter formation. Considering the higher labor and capital input in the DCC approach we would rather recommend the PSC approach for practice if the undersown cover crop in the cereal stand shows a good development.

## 12.9

### The use of physical soil profile collections to measure the impact of climate change on soil properties

Sarah Semeraro<sup>1</sup>, Sergio Rasmani<sup>2</sup>, Claire Le Bayon<sup>3</sup>

<sup>1</sup> Institute of biology, Functional Ecology Laboratory, University of Neuchâtel, Emile-Argand 11, CH-2000 Neuchâtel  
(sarah.semeraro@unine.ch)

<sup>2</sup> Institute of biology, Functional Ecology Laboratory, University of Neuchâtel, Emile-Argand 11, CH-2000 Neuchâtel  
(sergio.rasmani@unine.ch)

<sup>3</sup> Institute of biology, Functional Ecology Laboratory, University of Neuchâtel, Emile-Argand 11, CH-2000 Neuchâtel  
(claire.lebayon@unine.ch)

Along with the current climatic crisis, terrestrial ecosystems are undergoing significant modifications, both above and belowground. However, such modification might be ecosystem-dependent, likely vary depending on the local biotic and abiotic factors. Thus, climate change might disrupt the role of mountain soils acting as carbon sinks. To address whether recent climate change affected soil qualities differently across habitats, we took advantage of a physical soil profile collection currently existing at the University of Neuchâtel. We were able to re-sample 28 soil profiles that were sampled > 20 years ago, and across a wide range of habitats. We found that in average, across all soils, the carbon-to-nitrogen ration increased over this time period. Together, the results of this research address how climatic gradients, spanning collinear to alpine elevations, might affect the evolution of soils, and it will allow deciphering the ecosystem components that will majorly drive these changes.

## 12.10

# Microbial synthesis of organic phosphorus induced by inorganic phosphorus addition in organic soil horizons of beech forests

Maja B. Siegenthaler<sup>1,2</sup>, Timothy I. McLaren<sup>2,3</sup>, Emmanuel Frossard<sup>2</sup>, Federica Tamburini<sup>2</sup>

<sup>1</sup> Swiss Soil Monitoring Network NABO, Agroscope, CH-8046 Zurich ([maja.siegenthaler@agroscope.admin.ch](mailto:maja.siegenthaler@agroscope.admin.ch))

<sup>2</sup> Institute of Agricultural Sciences, ETH Zurich, CH-8215 Lindau

<sup>3</sup> School of Agriculture and Food Sciences, The University of Queensland, AU-QLD-4072 St Lucia

In European forests, which are experiencing increased phosphorus (P) limitation (Jonard et al. 2015, Talkner et al. 2015), trees and microorganisms take up phosphate from the soil solution. The soil solution represents a small proportion of total P in soil and must be replenished with P from less labile soil P pools to meet P demands. One process that replenishes the soil solution with P is the mineralization of organic P. Microorganisms stimulate organic P mineralization through the release of enzymes like phosphatases. Besides, microorganisms synthesize organic P species, which, upon microbial cell death, can return to the soil. However, there is limited knowledge on microbial synthesis of organic P in organic soil horizons.

Our study was part of the German priority program "SPP 1685 - Ecosystem Nutrition" (Lang et al., 2017). In this framework, we investigated if inorganic P addition could induce the synthesis of soil organic P. The organic soil horizons of two beech (*Fagus sylvatica* L.) forest sites in Germany with contrasting P stocks (low-P site Lüss and high-P site Vessertal) were subjected to four nutrient addition treatments (control, P addition, combined carbon (C) and nitrogen (N) addition, combined CNP addition) and incubated for 103 days. Phosphorus pools in soil were quantified by well-established chemical extractions. Phosphorus fluxes into these sequentially extracted soil P pools were traced by labelling the added water-soluble P with <sup>33</sup>P. Furthermore, the chemical nature of P in NaOH/EDTA extracts was studied with solution <sup>31</sup>P nuclear magnetic resonance (NMR) spectroscopy.

In the Lüss O horizon, half of the added P was recovered in the microbial and soil organic P pools, while increases in the P classes polyphosphates, phosphonates, and phosphodiesters upon inorganic P addition were revealed by <sup>31</sup>P NMR. In contrast, in the Vessertal O horizon, added P recovery in the soil organic P pool was minor. Thus, inorganic P addition has the potential to stimulate microbial P uptake, microbial synthesis of organic P species and polyphosphates, and P transfer into the soil organic P pool under low-P conditions.

## REFERENCES

- Jonard, M., Furst, A., Verstraeten, A., Thimonier, A., Timmermann, V., Potocic, N., Waldner, P., Benham, S., Hansen, K., Merila, P., Ponette, Q., De La Cruz, A.C., Roskams, P., Nicolas, M., Croise, L., Ingerslev, M., Matteucci, G., Decinti, B., Bascietto, M. & Rautio, P. 2015: Tree mineral nutrition is deteriorating in Europe, *Global Change Biology*, 21, 418-430.
- Lang, F., Kruger, J., Amelung, W., Willbold, S., Frossard, E., Büinemann, E.K., Bauhus, J., Nitschke, R., Kandeler, E., Marhan, S., Schulz, S., Bergkemper, F., Schloter, M., Luster, J., Guggisberg, F., Kaiser, K., Mikutta, R., Guggenberger, G., Polle, A., Pena, R., Prietzel, J., Rodionov, A., Talkner, U., Meesenburg, H., von Wilpert, K., Holscher, A., Dietrich, H.P. & Chmara, I. 2017: Soil phosphorus supply controls P nutrition strategies of beech forest ecosystems in Central Europe. *Biogeochemistry*, 136, 5-29.
- Talkner, U., Meiwas, K.J., Potocic, N., Seletkovic, I., Cools, N., De Vos, B. & Rautio, P. 2015: Phosphorus nutrition of beech (*Fagus sylvatica* L.) is decreasing in Europe, *Annals of Forest Science*, 72, 919-928.

## 12.11

### « Are termite mounds the calcium reactor of silica-rich landscapes? A research perspective».

John Van Thuyne<sup>1,2</sup>, Eric P. Verrecchia<sup>1,2</sup>

<sup>1</sup> Institute of Earth Surface Dynamics, Faculty of Geosciences and the Environment, University of Lausanne, Geopolis, 1015 Lausanne, Switzerland. (john.vanthuyne@unil.ch)

<sup>2</sup> Van Thuyne Ridge Research Center, PO box 301, Kasane, Botswana.

Termite mounds are well-recognized features of subtropical regions for their capacity to concentrate nutrients, store water, increase the proportion of silt and clay, modify the soil structure, and enhance the soil pH. They serve as fire buffers, plant hotspots, seedling rebound after droughts and can be used by local as soil amendment for agriculture and for traditional medicine. It is worth mentioning that the recent literature related to fungus-growing termites and their mounds does not specifically tackle the subject of the calcium element at the exception of (Mujinya et al., 2011) who discuss the origins of carbonates in termite mounds. Consequently, this study intends to fill a critical gap, and proposes to consider termite mounds as calcium reactors in silica-rich landscapes. Calcium is supposed to be a trace and rare element in the study area (Northern Botswana) as a thick arenic layer, sometimes a few hundred of meters deep, cover most of the territory. There are no proximate geological calcium-rich outcrops closer than a hundred of kilometers, i.e. in the Karroo Bedrock. Calcium is a fundamental element for plant growth, for soil organic matter (SOM) stabilization and for organic matter preservation (Rowley et al., 2018). It influences directly the pH of the soil and the cation exchange capacity (CEC), as well as the total organic carbon (TOC) content, which both have positive known effects on the soil fertility for all types of plants in savanna landscapes. As the widespread regional arenic soils are deprived of many nutrients, the unexpected concentration of calcium could foster new type of soil development, i.e. Kastanozem and Phaeozem (Romanens et al., 2019). Therefore, the aim of this study is to evaluate the role of fungus-growing termite (FGT) mounds in silica-rich landscapes regarding the elemental calcium distribution, from its capture and accumulation to its redistribution in adjacent sandy sediments. First, the various sources of calcium in the studied semiarid environment are assessed: three main sources are proposed (i) airborne dust, (ii) groundwater, and (iii) plants. In the Chobe Enclave, quartz (Kalahari sands) and diatomites form the geological surficial material, the landscape being almost exclusively a silica-rich environment of fluvial and eolian sands. In addition, carbonate paleo-islands, randomly outcropping in the region (Diaz et al., 2019), constitute a potential fourth source of calcium. Although their origin is still unclear, they remain in a limited extent in the study area but their role as a calcium contributor cannot be totally discarded. Consequently, four sources of calcium are identified, but only three of them are considered to be directly associated to termite mounds. Indeed, the termites of the Chobe Enclave cannot reach the distant carbonate paleo-islands, although the latter can contribute to calcium included in airborne dust or groundwater. In order to conduct this research, an FGT mound is selected in an open ground, previously identified as an Arenosol area (Romanens et al., 2019), away from carbonate paleo-islands in order to avoid any contamination. The second step consists into the description of the main physicochemical properties observed inside the mound, which are fostering the association of calcium to other phases and properties, such as cation saturation, cation exchange capacity or alkalinity. This step includes the identification of the various biogeochemical reactions involved in the formation of carbonate and bicarbonate ions, as well as carbonate phases. The third step involves the mechanistic approach of the biogeochemical processes acting in the interior of the mound and triggering the accumulation of calcium in the mound, such as differential leaching, calcite precipitation, as well as the oxalate-carbonate pathway (Mujinya et al., 2011). The last step of this study evaluates the environmental consequences of the redistribution of this calcium-enriched material in semiarid subtropical savannas. This material could have implications into plant expansion and soil forming processes. As a result, this research proposes to answer four main questions: (i) where are the main calcium sources in the fungus-growing-termite environment? (ii) What are the conditions in a fungus-growing-termite mound permitting calcium to associate with various other chemical species (such as carbonate and bicarbonate ions)? (iii) what are the chemical processes taking place in a fungus-growing-termite mound allowing calcium to accumulate? (iv) Finally, what are the effects of the calcium ions on the surrounding environment after the termitaria is abandoned and eroded?

#### REFERENCES

- Diaz, N., Armitage, S. J., Verrecchia, E.P., Herman, F., 2019: OSL dating of a carbonate island in the Chobe Enclave, NW Botswana. Quaternary Geochronology 49 172–176.
- Mujinya, B.B., Mees, F., Boeckx, P., Bodé, S., Baert, G., Erens, H., Delefortrie, S., Verdoodt, A., Ngongo, M., Van Ranst, E., 2011: The origin of carbonates in termite mounds of the Lubumbashi area, D.R. Congo. Geoderma 165, 95-105.
- Romanens, R., Pellacani, F., Mainga, A., Fynn, R., Vittoz, P., Verrecchia, E.P., 2019 : Soil diversity and major soil processes in the Kalahari basin, Botswana. Geoderma Regional 19, e00236.
- Rowley, M., Grand, S., Verrecchia, E.P., 2018: Calcium-mediated stabilization of soil organic carbon. Biogeochemistry 137, 27–49.

## P 12.1

### EJP SOIL: Towards Climate Smart Agricultural Soils

Klaus A. Jarosch<sup>1</sup>, Thomas Bucheli<sup>1</sup>, Nompumelelo Dammie<sup>1</sup>, Gina Garland<sup>1</sup>, Miriam Gross-Schmölders<sup>1</sup>, Nikolas Hagemann<sup>1</sup>, Marcel van der Heijden<sup>1</sup>, Olivier Heller<sup>1</sup>, Juliane Hirte<sup>1</sup>, Sonja Kay<sup>1</sup>, Sonja G. Keelv, Thomas Keller<sup>1</sup>, Kristy Klein<sup>1</sup>, John Koestel<sup>1</sup>, Jens Leifeld<sup>1</sup>, Frank Liebisch<sup>1</sup>, Jochen Mayer<sup>1</sup>, Reto Meuli<sup>1</sup>, Noemi Peter<sup>1</sup>, Kirsten Rehbein<sup>1</sup>, Leonor Rodrigues<sup>1</sup>, Ferran Romero<sup>1</sup>, Michael Simmler<sup>1</sup>, Florian Walder<sup>1</sup>, Shengchang Zhang<sup>1</sup>, Lutz Merbold<sup>1</sup>

<sup>1</sup> Agroecology and Environment, Agroscope, Reckenholzstrasse 191, 8045-Zurich, Switzerland,  
(klaus.jarosch@agroscope.admin.ch).

Agricultural soils are the basis for a variety of ecosystem services and store considerable amounts of carbon in the soil organic matter. At the same time, many agricultural practices contribute to the emission of climate-relevant greenhouse gases. The European Joint Programme SOIL (EJP Soil) aims, to improve the understanding of agricultural soils in relation to climate change. A total of 24 European countries are involved in this co-fund project. Through individual projects within EJP Soil, researchers are networked with each other internationally, and through the “National Hub” are brought into dialogue with national stakeholders such as cantonal and federal authorities, in order to contribute effectively to the sustainable use of soil as a resource.

The projects carried out within the framework of the EYP Soil with Swiss participation include the following areas:

- a) Inventories of national soil information systems, long-term field trials and practised land use methods, used recommendation and enforcement instruments
- b) Field studies on methods and quantification of carbon fixation in peatland soils and on the importance of root systems for carbon inputs into soils and adaptation to drought stress
- c) Further development of remote sensing methods for the determination of soil parameters and their use in the agricultural context as well as further development of soil carbon modelling.

The selection and implementation of the research projects is carried out in continuous consultation with colleagues from different interest groups (public administration, research institutions, etc.) in order to achieve the fastest possible application of the research results obtained.

The aim of this poster contribution is to give an overview of the different research projects within EJP Soil and to identify possible synergies with other projects.

## P 12.2

# Soilscape information and sustainable land use – a case study in the canton of Bern, Switzerland

Céline Hildbrand<sup>1</sup>, Tobias Sprafke<sup>1,2</sup>

<sup>1</sup> Institute of Geography, University of Bern, Hallerstrasse 12, CH-3012 Bern (celine.hildbrand@students.unibe.ch)

<sup>2</sup> Center of Competence for Soils (KOBO), BFH-HAFL, Länggasse 85, CH-3052 Zollikofen (tobias.sprafke@bfh.ch)

Soil provides the basis for life on land and fulfills indispensable economic and ecological functions. Soils vary in landscape as result of spatially varying soil-forming factors, which may change through its evolution. Soil information is the indispensable basis for sustainable land use, therefore stakeholders and politics are interested in spatially distinct soil data (i.e. soil maps). Information about soil properties is of central importance for taking measures to protect or restore site-typical and functional soils. Currently, there are gaps in knowledge about the type, extent and quality of soils in many Swiss cantons. The aim of the present work is to find out whether and how soil information can help to create a better basis for the sustainable use of soil as a resource. To answer the research question, soil information was collected in two landscape transects in the Bernese part of the Swiss Plateau using hand augers and the Swiss soil mapping instructions and classification. Based on interviews with experts who are directly involved with soils, the collected soil properties were discussed and the needs and requirements for soil information of different user groups were addressed. The fieldwork has shown that despite rather similar topsoils, subsoils vary considerably and so do the potentials for certain types of land use. In ongoing interviews, we evaluate varying perspectives on how different aspects of soil information guide planning and decision-making. On this poster we will present the final results of this work in progress.

## P 12.3

# Siliceous and calcareous soil development in the Swiss Alps: weathering, erosion, and mineralogical data from two Holocene chronosequences

Alessandra Musso<sup>1,2</sup>, Dmitry Tikhomirov<sup>1</sup>, Michael L. Plötze<sup>3</sup>, Konrad Greinwald<sup>4</sup>, Anne Hartmann<sup>5</sup>, Clemens Geitner<sup>6</sup>, Fabian Maier<sup>1</sup>, Fanny Petibon<sup>1</sup>, Markus Egli<sup>1</sup>

<sup>1</sup> Department of Geography, University of Zurich, Winterthurerstrasse 190, 8057 Zurich, Switzerland

<sup>2</sup> Eidgenössische Forschungsanstalt für Wald, Schnee, und Landschaft, Zürcherstrasse 111, 8903 Birmensdorf ZH, Switzerland (alessandra.musso@wsl.ch)

<sup>3</sup> Department of Civil, Environmental and Geomatic Engineering, ETH Zurich, Stefano-Francini-Platz 3, 8093 Zurich, Switzerland

<sup>4</sup> Institute of Hydrology, Albert-Ludwig University Freiburg, Friedrichstraße 39, 79104 Freiburg, Germany

<sup>5</sup> Section Hydrology, GFZ German Research Centre for Geosciences, Telegrafenberg, 14473 Potsdam, Germany

<sup>6</sup> Institute of Geography, University of Innsbruck, Innrain 52, 6020 Innsbruck, Austria

The evolution of mountain landscapes is strongly influenced by the balance between soil production and erosion. The abundance of fresh glacial sediments in combination with an oftentimes sparse vegetation cover enable high erosion and sedimentation rates. The physical and chemical alteration of this material, i.e., soil formation, is also especially rapid in such young and dynamic landscapes.

Soil formation on parent materials of different mineralogical compositons can be expected to run at different rates and to take different pathways. While siliceous soil formation has been widely studies in the Alps, there is a need for more studies about calcareous soil formation, as only very few exist to date. To address this resarch gap, we studied and compared two moraine chronosequences that cover the entire Holocene.

We determined weathering rates, short- and long-term erosion rates and also studied the bulk mineralogy of the soils. Both chronosequences exhibited very high erosion rates in the first century of soil formation, which then decreased rapidly after 3–5 kyr. The chemical weathering rates followed a similar pattern, especially in the calcareous chronosequence, which chronicled high losses in calcite. The calculated soil production rates, while also decreasing with higher soil age, almost always outpaced the denudation, indicating that the soil formation was prograde throughout most of the Holocene.

In conclusion: it took up to 10 kyr to reach soil stability, depending on the topography and the development of the vegetation. We could see that in the early stages of soil formation (i.e., decades, centuries), the parent material was the dominating factor. In the later stages, however, the influence of the vegetation dominated as it influenced many soil properties: increased surface stability, complex hydrological pathways and increased chemical weathering.

## P 12.4

### Impact of glacier retreat on plant diversity and soil functioning

Cécile Charles<sup>1</sup>, Nora Khelidj<sup>1</sup>, Stéphanie Grand<sup>1</sup>, Gianalberto Losapio<sup>1</sup>

<sup>1</sup> Institut des dynamiques de la surface terrestre (IDYST), University of Lausanne, Bâtiment Géopolis, CH-1015 Lausanne (cecile.charles@unil.ch)

An emblematic sign of climate change in Switzerland is the retreat and extinction of glaciers. As glaciers retreat, new terrain is exposed to colonization by a variety of organisms, leading to changes in ecological communities and soil properties. Indeed, glacier retreats involve three major ecological changes at the local scale: a loss of glacial habitat, a gain of soil habitat, and a decrease in the influence of glacier microclimate on surrounding habitats. However, little is known about the development of soils, their physico-chemical changes and their influence on plant diversity after glacier retreat. This undermines our ability to mitigate the dual impact of glacier retreat on plant communities and soil functioning. Here, we aim to understand and predict the development of plant diversity and soil functioning after glacier retreat in the Mont Miné and Ferrière glaciers (Valais Alps, Switzerland). We examined species composition and species abundance of plant communities across four glacier retreat stages. Then, we analyzed soil CO<sub>2</sub> respiration, soil texture and soil physico-chemical properties. Our expectation is that the increase in plant diversity is associated to soil development. In turn, the increase in plant diversity will lead to an increase in soil organic matter and CO<sub>2</sub> respiration, which will further promote plant colonization and diversity. Yet, we also expect that the dominance of few plant species will stabilize soil development but decrease plant diversity. The outcome of this project intends to contribute to our understanding of the consequences of global warming on mountain ecosystems, and ways to anticipate its impact.

## P 12.5

# The changing importance of controls on soil carbon stabilization across soil types

Daniel Wasner<sup>1</sup>, Rose Abramoff<sup>2</sup>, Marco Griepentrog<sup>1</sup>, Erick Zagal Venegas<sup>3</sup>, Pascal Boeckx<sup>4</sup>, Sebastian Doetterl<sup>1</sup>

<sup>1</sup> Soil Resources, Department of Environmental Systems Science, ETH Zurich, Switzerland

<sup>2</sup> Environmental Sciences Division & Climate Change Science Institute, Oak Ridge National Laboratory, Oak Ridge, Tennessee, USA

<sup>3</sup> Department of Soil and Natural Resources, Faculty of Agronomy, University of Concepción, Concepción, Chile

<sup>4</sup> Department of Green Chemistry and Technology, Faculty of Bioscience Engineering, Ghent University, Coupure Links 653, 9000 Gent, Belgium

The concept of distinct soil organic matter (SOM) fractions – with differing formation pathways, stabilization mechanisms and responses to change – is promising to improve our understanding of soil carbon (C) dynamics. While there is widespread consensus on the general usefulness of conceptual fractions with specific functional implications, there is still a lack of information on the patterns with which they contribute to bulk soil organic carbon (SOC) at larger scales and across climatic and soil physicochemical gradients. In this study, we aimed to assess first the quantitative importance of three key SOM fractions across a diverse range of 11 soil groups with global significance. Secondly, we wanted to gain insights on the environmental controls that shape the contribution of these fractions to total SOC amounts.

Here we sampled a set of 35 grassland topsoils (0 – 10 cm) along a 2300 km north-south transect in Chile ranging from tundra to arid steppe climate, and covering 11 WRB major soil groups. Following a modified version of the protocol in Zimmermann et. al (2007), we partitioned the soils into three functional SOM fractions defined by particle size and density (free silt and clay, free particulate organic matter, stable microaggregates), enabling us to quantify fraction-specific total SOC amounts and their relative contribution to bulk SOC. In order to identify links between fractions and potential drivers of C stabilization, we further characterized extensively relevant physico-chemical properties of the soils, compiled climatic data of the sites and characterized OM maturity (DRIFT spectroscopy and Rock-Eval pyrolysis) as well as pedogenic, secondary Fe-, Al- and Mn-oxide concentrations through sequential extraction.

We found that the contributions of mineral-associated SOM fractions to bulk SOC varied strongly across the soil gradient, while the contribution of free particulate organic matter was comparatively stable and low. SOM associated with free silt and clay sized particles are the most important C reservoir in soils with less than 4 % SOC, whereas in soils with higher SOC content, the majority of the SOC is contained in stable microaggregates. The amount of SOC in various fractions was sensitive to changes in temperature, pedogenic oxides, and OM input vs. decomposition. Comparison of OM maturity showed that free particulate OM and free silt and clay associated OM can be clearly distinguished, while OM in microaggregates is likely a mixture of both.

This study demonstrates that in SOC-rich soils, microaggregates represent a major fraction of bulk SOC, and that SOC in key SOM fractions can be linked to distinct climatic and soil physicochemical factors.

## REFERENCES:

- Zimmermann, M., Leifeld, J., Schmidt, M. W. I., Smith, P. & Fuhrer, J. Measured soil organic matter fractions can be related to pools in the RothC model. Eur. J. Soil Sci. 58, 658–667 (2007).

## P 12.6

# From vegetation to soil: Organic matter dynamics in riparian forests in the Grand Cariçaie (Switzerland)

Lila Siegfried<sup>1</sup>, Pascal Vittoz<sup>1</sup>, Eric Verrecchia<sup>1</sup>

<sup>1</sup> Institute of Earth Surface Dynamics, Faculty of Geosciences and Environment, University of Lausanne, Géopolis, CH-1015 Lausanne ([lila.siegfried@unil.ch](mailto:lila.siegfried@unil.ch))

The wetland forests in the Grande Cariçaie have an unique origin. Their substrate emerged at the southern shores of Lake Neuchâtel up to the 3-m lowering of the lake level (1868-1891)(Vischer, 2003). Afterwards, different types of forests colonized the newly available area, and soils developed, according to their relative position to the lake and rivers. A large proportion of these forests have never been exploited and can be considered as riparian forests in a post-pioneer stage or transition to a still poorly known climax. Some of these forests are rare in Europe, such as black alder forests.

This project aims at better understanding the dynamics of vegetation and soils in wetland forests in the context of climate change and biodiversity loss. Part of this project focuses on carbon cycle. Indeed wetlands are known to be carbon sinks, but what about the riparian forests of the Grande Cariçaie? To answer this question, we are studying the pathway of organic matter in four different forestry alliances: *Alnion glutinosae*, *Alnion incanae*, *Fraxinion* and *Molinion-Pinion*. Measurements include vegetation surveys, water table fluctuations, soil litter inputs, organic matter decomposition rates, soil respiration, and soil organic matter analysis. The preliminary results show a difference in the organic matter pathways between the four habitats and will contribute to improve the management practices and conservation of these threatened ecosystems.

## REFERENCES

- Vischer, D. 2003: Histoire de la protection contre les crues en Suisse, Rapports de l'OFEG, Série Eaux. Office fédéral des eaux et de la géologie, OFEG. Bienne. 208 p.

## P 12.7

# Soil and rock mineralogical transformations resulting from enhanced rock weathering under temperate climate

Emma Bonvin<sup>1</sup>, Romane Claustre<sup>1</sup>, Xavier Dupla<sup>1</sup>, Stéphanie Grand<sup>1</sup>

<sup>1</sup> IDYST, University of Lausanne, CH-1015 Lausanne ([emma.bonvin@unil.ch](mailto:emma.bonvin@unil.ch))

Soils are the largest terrestrial reservoir of carbon and store three times more carbon than the atmosphere or biomass. In the current context of global warming and increasing atmospheric CO<sub>2</sub> levels, the idea of using the capacity of soils to store carbon and even amplifying it has emerged in the thinking surrounding the development of policies against global warming. In addition to better management of soils and agricultural practices, the IPCC (Intergovernmental Panel on Climate Change) has identified the need to develop technologies to remove CO<sub>2</sub> from the atmosphere (Negative Emission Technologies or NETs). One of these technologies, Enhanced Weathering (EW), is based on the ability of soils to sequester carbon through the chemical weathering of silicate minerals. More specifically, this technology aims to accelerate the natural activity of the silicate-carbonate pump, which regulates, on a geological scale, the carbon rate in the atmosphere.

While one part of the published literature considers enhanced weathering as a promising technology, stating that up to 5 to 30% of the current annual CO<sub>2</sub> rise could be negated, the other refutes these claims by arguing that silicate dissolution is limited by mineral saturation and the formation of a leached layer on the minerals surfaces and thus should be reconsidered as a strategy for mitigating global warming. To verify the effectiveness of the latter, we conducted a field trial in two Swiss vineyards that received 20 tons of basalt per hectare in 2021. We combined scanning electron microscopy observations with the electron microprobe to characterize the extent of mineral weathering and potential coatings. The formation of secondary phases and minerals was evaluated via infrared spectroscopy, ammonium oxalate extractions and X-ray diffraction analysis. This study allowed us to identify the dissolution and reprecipitation extent of mineralogical phases. These observations enabled the monitoring of the alteration processes of basalt at the micro- and even nanometer scale leading to a better understanding of the interactions at the interface between the mineral and the soil solution.

## P 12.8

### Making sure climate mitigation promises are safe: Impact of enhanced rock weathering on soil organisms and edaphic factors

Romane Claustre<sup>1</sup>, Emma Bonvin<sup>1</sup>, Xavier Dupla<sup>1</sup>, Stéphanie Grand<sup>1</sup>

<sup>1</sup> IDYST, University of Lausanne, CH-1015 Lausanne ([romane.claustre@unil.ch](mailto:romane.claustre@unil.ch))

In order to reduce the CO<sub>2</sub> concentrations in the atmosphere, technologies which enable CO<sub>2</sub> capture are in active development. One of them, called enhanced rock weathering (ERW), works as a fast-track silicate-carbonate cycle. Silicate mineral powder is spread on agricultural land and the reaction with the organic and carbonic acids within the soil's solution leads to chemical weathering and acts therefore as a potential significant carbon sink.

This technology has been highlighted as very promising by the scientific community, with a focus put on the effectiveness of the method in terms of CO<sub>2</sub> storage (up to 10% of annual CO<sub>2</sub> emissions stored). But the potential impact of the ERW application on the soil's ecosystem, in particular when knowing the intakes of heavy metals like nickel, copper and chromium, is largely unexplored.

To measure this impact, we conducted a field trial in two Swiss vineyards that received 20 tons of basalt per hectare in 2021. Changes in composition of microbial, arthropods and earthworm communities were evaluated by field extraction and species identification. The impact of ERW on three key soil functions (carbon transformation, nutrient cycling and structure maintenance) were assessed via the Biofunctool® methodology. Our study allowed us to obtain a first assessment of the impact of ERW on soil biological processes and organisms and highlights the importance of broadscale evaluations of climate mitigation strategies.

**P 12.9****Microbial communities in Swiss croplands**

Alyssa Deluz<sup>1,2</sup>, Martin Hartmann<sup>2</sup>, Pascal Boivin<sup>1</sup>, Andreas Fliessbach<sup>3</sup>, Johan Six<sup>2</sup>

<sup>1</sup> HEPIA Soils and Substrates, University of Applied Sciences and Arts Western Switzerland, Geneva (alyssa.deluz@hesge.ch)

<sup>2</sup> Sustainable Agroecosystems, ETH Zurich

<sup>3</sup> Research Institute of Organic Agriculture, Frick, Switzerland

Soil microbial communities contribute to agricultural production by performing key functions for the soil-plant system such as nutrient cycling, soil structure formation, and pest and disease regulation. Agricultural practices influence soil microbial communities by shaping their physical and chemical habitat. Intensive farming can degrade soil structure and lead to soil organic matter loss, directly affecting the water-air equilibrium in soil pores and the energy available for soil microbes. Previous studies have identified a preferential colonization of soil microstructures with enhanced microbial activity in the 30–90µm structural pore size range (Kravchenko & Guber, 2017). This mesopore size range is highly correlated to soil organic carbon content. Furthermore, thresholds of clay saturation by soil organic carbon have been defined to assess soil structure vulnerability (Johannes et al., 2017). This work will evaluate the relevance of these thresholds for predicting alterations in soil microbial communities. We hypothesized that a higher proportion of fine structural pores and higher soil organic carbon saturation translate into changes in microbial community composition.

To discuss the relationships between bio-physical properties, soil organic carbon and cropping practices, we assessed soil microbial communities (activity, abundance and diversity), soil structure and soil organic matter in farm fields across 60 cropland sites in the Swiss Plateau. Microbial activity and abundance were assessed measuring respectively soil basal respiration and microbial carbon from chloroform fumigation. Soil bacterial and fungal diversity were assessed by metabarcoding of 16S rRNA genes and ITS rrn regions. Soil structure was studied at core scale (100 cm<sup>3</sup>) using shrinkage curve modeling to quantify the structural porosity and the hydro-structural properties of the soils. Soil organic carbon content and forms were assessed measuring thermal properties. This project aims to investigate the relevance of soil quality standards used in agriculture for soil microbial communities.

**REFERENCES**

- Johannes, A., Matter, A., Schulin, R., Weisskopf, P., Baveye, P., & Boivin, P. 2017: Optimal organic carbon values for soil structure quality of arable soils. Does clay content matter? Geoderma, 302, 14–21  
 Kravchenko, A. & Guber, A. 2017: Soil pores and their contributions to soil carbon processes, Geoderma, 287, 31–39.

## P 12.10

# Soil Micro Plastic: A standardized extraction & analysis protocol for MINAGRIS

Adrian Grunder<sup>1</sup>, Moritz Bigalke<sup>1,2</sup>, Nicolas Beriot<sup>3</sup>

<sup>1</sup> Geographisches Institut Universität Bern, Universität Bern, Hallerstrasse 12, CH-3012 Bern (adrian.grunderiub.unibe.ch)

<sup>2</sup> Institut für Angewandte Geowissenschaften, Technische Universität Darmstadt, Schnittspahnstrasse 9, DE-64287 Darmstadt

<sup>3</sup> Department of Environmental Sciences, Wageningen University & Research, Droevedaalsesteeg 4, NL-6708 PB Wageningen

World plastic production is steadily increasing with most of the plastic waste being mismanaged. When in the environment, plastic degrades and can be fragmented in smaller pieces. Micro plastic (MPs, < 5mm diameter) concentrations and fates in aqueous systems have been getting significant attention, while terrestrial systems are being neglected. The various polymers are ubiquitous and pose serious threats to environmental systems worldwide. Soils as a pollutant sink and a site of accumulation will be affected – especially given the non-degradability of most plastics. In order to assess how contaminated the pedosphere really is, comparability in results is needed. To ensure this, the development of a standardized method for plastic extraction from different soils and its quantification is necessary. The present work aims at addressing this as part of the MINAGRIS project by unifying previous research and developing one harmonized protocol based on earlier studies (Scheurer & Bigalke, 2018, Olson et al. 2020). The developed method consists of a sequence of density separations and filtrations including an OM oxidation step resulting in the deposition of the particles on an aluminum oxide filter. NaBr 48% ( $\rho = 1.5\text{g/cm}^3$ ) was chosen as the density separation solution allowing for an extraction of most common polymers. To avoid an interference of  $\text{CaCO}_3$  during the OM oxidation, small quantities of HCl 1% were added for a short time. A NaUT (Natriumhydroxide, Urea, Theourea) treatment coupled with an OM oxidation was implemented, substantially reducing OM content and thus greatly reducing background noise. In order to counter-balance an iron oxide triggered coloration of the sample,  $\text{H}_2\text{SO}_4$  (2M) was applied on the filter removing residual iron oxides. This is followed by an FTIR/LDIR analysis of the samples and a further improved automatized identification of the retrieved spectra (Löder et al. 2015, Bigalke et al. 2022). Using this extraction and analysis protocol no significant alteration of the MPs was observed and a recovery rate of >85% determined. Until the end of this year and as part of MINAGRIS, 220 agricultural soils across 11 European countries will be analyzed using this protocol. This will allow a big scale soil MP comparison across cropping systems and cultures in Europe.

## REFERENCES

- Bigalke et al., 2022: Microplastics in agricultural drainage water: A link between terrestrial and aquatic microplastic pollution, *Science of the Total Environment*, 806.
- Löder et al., 2015: Focal plane array detector-based micro-Fouriertransform infrared imaging for the analysis of microplastics in environmental samples. *Environ. Chem.*, 12, 563–581.
- Olson et al. 2020; Facilitating microplastic quantification through the introduction of a cellulose dissolution step prior to oxidation: Proof-of-concept and demonstration using diverse samples from the Inner Oslofjord, Norway, *Marine Environment Research*, 161.
- Scheurer, M. & Bigalke, M. 2018: Microplastics in Swiss Floodplain Soils, *Environmental Science & Technology*, 52, 3591–3598.



# 13 Hydrology and Hydrogeology

Sandra Pool, Peter Molnar, Daniel Hunkeler, Christophe Lienert, Nadav Peleg, Michael Sinreich, Massimiliano Zappa, Sanja Hosi

*Swiss Hydrological Commission CHy,  
Swiss Society for Hydrology and Limnology SGHL,  
Swiss Hydrogeological Society SGH*

## TALKS:

- 13.1 Arnoux M., Sonney R., Gillioz A.: Mountain springs and climate change
- 13.2 Blanc T., Peel M., Brennwald M., Kipfer R., Brunner P.: Novel approach for efficient injection of tracer gases into a flowing river
- 13.3 Brunner M. I., Voan Loon A. J., Stahl K.: Extreme and moderate streamflow droughts are governed by different hydro-meteorological processes
- 13.4 Epting J., Råman Vinnå L., Affolter A., Scheidler S.: Impacts of Climate Change on Swiss Alluvial Aquifers – Adaptation and Mitigation Measures using MAR and MSWR
- 13.5 Guglielmetti L., Moscariello A.: Hydrochemical evolution of geothermal waters in the Geneva Basin
- 13.6 Halloran L., Millwater J., Arnoux M., Hunkeler D.: Understanding the present and future state of groundwater in alpine headwater catchments using hydrogeophysics
- 13.7 Pastore C., Luetscher M., Doumenc F., Sedaghaktish A., Weber E., Jeannin P.-Y.: Consequences of intermittent ventilation on the energy balance of a karst system
- 13.8 Roques C., Rupp D.E.; de Dreuzy J.-R., Abhervé R., Leith K., Leray S., Longuevergne L., Thornton J., Brunner P., Grant G., Selker J.S.: Predicting streamflow recession in alpine catchments: how does bedrock morphology control the dynamics?
- 13.9 Schilling O.S., Partington D.J., Doherty J., Kipfer R., Hunkeler D., Brunner P.: Buried paleo-channel detection with a groundwater model, tracer-based observations, and spatially varying, preferred anisotropy pilot point calibration
- 13.10 Schirmer M., Magnusson J., Jonas T.: GCOS project: Enhance snowfall estimates in existing Swiss precipitation products
- 13.11 Torelló H., Marra F., Peleg N.: Changing patterns of heavy rainfall events across an urban area (Milan, Italy)
- 13.12 Wakjira T. M., Peleg N., Molnar P.: Changes in rainwater productivity across the rainfed agricultural areas in Ethiopia
- 13.13 Wiersma P., Aerts J., Zekollari H., Hrachowitz M., Drost N., Huss M., Sutanudjaja E., Hut R.: Coupling a global glacier model to a global hydrological model prevents underestimation of glacier runoff

## POSTERS:

- P 13.1 Binder M., Engelmann C., Epting J.: Implementation of Sewer Network Structures into Numerical Heat Transport Models via an Adaptive Surrogate Approach
- P 13.2 Chang A.Y.-Y., Bogner K., Domeisen D.I.V., Zappa M.: Hybrid Forecasting of Sub-seasonal Streamflow and Lake Level in Switzerland
- P 13.3 Collenteur R.A., Moeck C., Birk S., Schirmer M.: Analysis of the Swiss groundwater monitoring network using Pastas models and groundwater signatures
- P 13.4 Roth E., Dresmann H., Ebert A., Scheidler S., Epting J.: Geothermal Modeling – Interrelated Evaluation of Measured Temperature Data from Borehole Heat Exchangers and Heat Transport in the Geological Subsurface
- P 13.5 Götte J., Brunner M.: From droughts to floods – analysing transitions under different hydro-climatic conditions
- P 13.6 Hanus S., Schuster L., Burek P., Maussion F., Seibert J., Marzeion B., Wada Y., Vivioli D.: Coupling a large-scale glacier and hydrological model – Towards a better representation of mountain water resources in global assessments
- P 13.7 Heinz M., Holzkämper A., Schäfli B., Raible C.: Agricultural adaptations to increasing drought extremes and their feedbacks on catchment hydrology
- P 13.8 Hirschberg J., Sadowski Y., Michel A., Mc Ardell B.W., Molnar P.: Climate change impacts on the debris-flow activity in a high-alpine catchment
- P 13.9 Kayitesi N. M., Mariethoz G.: Modeling River hydro-morphological responses to Land Use Land Cover Change in Tropical Regions: the case of Sebeya catchment, Rwanda.
- P 13.10 Kong X.-Z., Naets I., Ahkami M., Leard P., Schwendener D., Saar M.O.: What can pore-scale optical measurements do?
- P 13.11 Moeck C.: CH-GNet – Swiss Groundwater Network
- P 13.12 Moeck C., Berghuijs W.R., Luijendijk E., Gurdak J.: Global Potential Groundwater Recharge Response to Climate Variability
- P 13.13 Moraga J.S., Peleg N., Burlando P.: Preserving the temperature-scaling of high intensity precipitation for a more realistic projection of sub-daily extreme events
- P 13.14 Roy N., Traber D.: Results of hydrogeological investigations in the framework of Nagra's deep borehole program
- P 13.15 Schaller N., Vorlet S.L., Amini A., De Cesare G.: Morphological evolution of the Rhone River in the Martigny bend
- P 13.16 Scheidler S., Dresmann H., Epting J.: Regional-Scale Thermal Hydraulic Modeling for Preliminary Geothermal Potential Assessment – A Theoretical Approach using the example of Riehen
- P 13.17 Schoch J., Walther L., Nussbaum M., Carminati A., Lehmann P.: Pedotransfer functions for soil hydraulic properties of Swiss forest soils
- P 13.18 Tang Q., Delottier H., Schilling O.S., Kurtz W., Brunner P.: An ensemble based data assimilation framework for an integrated hydrological model: development and examples
- P 13.19 Traore Dosso A., Gillet H., Kouamé J.K., Dufour R.M., Chèvre N.: Impact of gold mining storage tailings on groundwaters and surface waters: the case of Hiré (southern Ivory coast)
- P 13.20 Wechsler T., Hug Peter D., Bätz N., Zappa M.: HYDROpot\_integgral: a tool to simultaneously assess hydropower potential and ecological potential
- P 13.21 Wiersma P., Zakeri F., Mariéthoz G.: Hydrological modeling with real and synthetic snow cover data assimilation
- P 13.22 Zou W., Hu G., Wiersma P., Mariethoz G., Peleg N.: Multiple-point Geostatistics-based spatial downscaling of heavy precipitation

## 13.1

### Mountain springs and climate change

Marie Arnoux<sup>1</sup>, Romain Sonney<sup>1</sup>, Alexandre Gillioz<sup>2</sup>

<sup>1</sup> Centre de recherche sur l'environnement Alpin (CREALP), CH-1950 Sion ([marie.arnoux@crealp.vs.ch](mailto:marie.arnoux@crealp.vs.ch))

<sup>2</sup> ALTIS, CH-1934 Le Châble

In Alpine valleys, drinking water comes mainly from mountain springs. Alpine regions are particularly sensitive to climate change, especially to decreasing snowfall and increasing periods of drought. Therefore, it is necessary to determine how these water resources will evolve in order to anticipate possible shortages. Thus, several springs located in the Val de Bagnes in Valais, for which flow rate data are available, have been selected. Two approaches were then combined: (1) the calculation of drought resistance indicators and (2) the hydrological modelling of spring flows with the latest climate projections for Switzerland. The water quality of the springs was also taken into account. The results show the differences in the sensitivity of the springs and allow the identification of the strategic groundwater resources, less sensitive to temporary drought events. This analysis also highlights the importance of developing a measurement network now, which is essential for future projections to anticipate and adapt drinking water management in Alpine regions.

## 13.2

### Novel approach for efficient injection of tracer gases into a flowing river

Théo Blanc<sup>1,2</sup>, Morgan Peel<sup>1</sup>, Matthias S. Brennwald<sup>2</sup>, Rolf Kipfer<sup>2</sup>, Philip Brunner<sup>1</sup>

<sup>1</sup> Centre for Hydrogeology and Geothermics of University of Neuchâtel (CHYN), Rue Emile-Argand 11, CH-2000 Neuchâtel (theo.blanc@unine.ch)

<sup>2</sup> Eawag, Swiss Federal Institute of Aquatic Science and Technology, Water Resources and Drinking Water, Ueberlandstrasse 113, CH-8600 Dübendorf

Bank filtration contributes with 40 % to the drinking water production of Switzerland. The quality of this water might get altered under changing conditions, such as land use, climate change, or river renaturation works. It is, therefore, crucial for drinking water management to understand river water - Groundwater interactions, and thus detect the associated dynamics.

Gas tracers have the potential to become informative tracers in this regard since they are invisible, non-toxic, and conservative. Furthermore, they are easy to handle and, since recent technology development of portable mass spectrometers, simple to measure directly and continuously on the field. They are therefore ideal tracers for groundwater, yet their application to surface water remains challenging, especially their injection into flowing river water. Such injection could be very interesting for gas tracer tests to study bank filtration. However, injecting gas into a river is inefficient and logically and financially prohibitive for long duration and high river discharge rates. Thus, it undermines the efficient application of gas tracers in this context.

In this study, we present an approach to resolve these challenges and efficiently inject a high amount of gas into a flowing river. We use diffusive injection as it provides very high injection efficiency and we selected cheap and accessible material for our setup. To demonstrate the robustness of our method, we applied it in the Emme (canton Bern, Switzerland). We were able to supersaturate the river water for 35 days by one order of magnitude in comparison to the natural dissolved gas concentration. We monitored the dissolved gas concentration both in the river and in a well located close by, therefore obtaining precious time series of both water bodies. This data provides quantitative information on the infiltration dynamics and proves the hydraulic connection between the river and the well. Furthermore, such long and continuous time series represent ideal input and output functions for physically based numerical models to quantify mixing ratios and transit time distribution.

### 13.3

## Extreme and moderate streamflow droughts are governed by different hydro-meteorological processes

Manuela I. Brunner<sup>1</sup>, Anne F. Van Loon<sup>2</sup>, and Kerstin Stahl<sup>1</sup>

<sup>1</sup> Institute of Earth and Environmental Sciences, University of Freiburg, Freiburg, Germany

(manuela.brunner@hydrology.uni-freiburg.de)

<sup>2</sup> Institute for Environmental Studies, Vrije Universiteit Amsterdam, Amsterdam, the Netherlands

Streamflow droughts are generated by a variety of processes including rainfall deficits, a lack of snow accumulation, or high evapotranspiration. The importance of different drought generation processes may vary with event severity but to date it remains unclear how. To study the link between event severity and the importance of different hydro-meteorological drivers, we propose a formal classification scheme for streamflow droughts and apply it to a large sample of catchments in Europe. The scheme assigns events to one of eight drought types using information about drought seasonality, precipitation deficits, and snow availability. Our findings show that drought driver importance varies regionally, seasonally, and by event severity. More specifically, we show that rainfall-deficit droughts are the dominant drought type in western Europe, while northern Europe is most often affected by cold-snow-season droughts. Second, we show that rainfall-deficit and cold-snow-season droughts are important from autumn to spring, while snowmelt and wet-to-dry-season droughts are important in summer. Last, we demonstrate that moderate droughts are mainly driven by rainfall deficits, while severe events are predominantly driven by snowmelt deficits in colder climate zones including the Alps and by streamflow deficits transitioning from the wet to the dry season in warmer climate zones. This high importance of evapotranspiration and a lack of snowmelt for the development of severe droughts suggests that these high-impact events might undergo the strongest changes in a warming climate because of their close relationship to temperature. As a consequence, the Alps are expected to be one of the regions in Europe most affected by future changes in drought generation processes and related magnitudes.

## 13.4

# Impacts of Climate Change on Swiss Alluvial Aquifers – Adaptation and Mitigation Measures using MAR and MSWR

Jannis Epting<sup>1</sup>, Love Råman Vinnå<sup>1</sup>, Annette Affolter<sup>1</sup>, Stefan Scheidler<sup>1</sup>

<sup>1</sup> Applied and Environmental Geology, Hydrogeology Research Group, Department of Environmental Sciences, University of Basel, Bernoullistrasse 32, CH-4056 Basel (jannis.epting@unibas.ch)

Artificial groundwater recharge and natural infiltration of surface waters are two factors determining water quantity and quality of alluvial aquifers. We evaluated a set of selected future climate scenarios to project future groundwater recharge and associated temperature imprint for three alluvial aquifers in the urban agglomeration of the city of Basel, Switzerland. 3D numerical groundwater flow and heat-transport modeling allowed quantifying and differentiating between natural and artificial groundwater recharge processes and thermal impacts. The influence of climate change on natural and artificial groundwater recharge processes could be distinguished. For aquifers where the infiltration of surface water is an important component in the groundwater balance, which is common to many alluvial aquifers, the effects of climate change will be influenced by changes in river flow and thermal regimes. As such, individual drinking water wells are exposed differently to the various components of groundwater recharge (Figure).

Our results show that seasonal shifts in natural groundwater recharge processes and adaptation strategies related to artificial groundwater recharge could be an important factor affecting groundwater resources in future. With increased groundwater recharge during high runoff periods in winter/spring, decreased groundwater temperatures can be expected (Epting et al. 2021). While increased artificial groundwater recharge in summer months, are likely to increase groundwater temperatures. In view of more frequent heatwaves and drought periods, our results highlight the importance of Managed Aquifer Recharge (MAR) and Managed Surface Water Recharge (MSWR) as useful tools for existing and future groundwater management.

## ACKNOWLEDGEMENTS

We acknowledge financial support of the Federal Office for the Environment (FOEN) within the scope of the research project “Energetic potentials - thermal use of surface water for artificial groundwater recharge” (EnerPot-MAR-MSWR).

## REFERENCES

Epting, J., Michel, A., Affolter, A., Huggenberger, P. (2021) Climate change effects on groundwater recharge and temperatures in Swiss alluvial aquifers. Journal of Hydrology, <https://doi.org/10.1016/j.jhydrol.2020.100071>

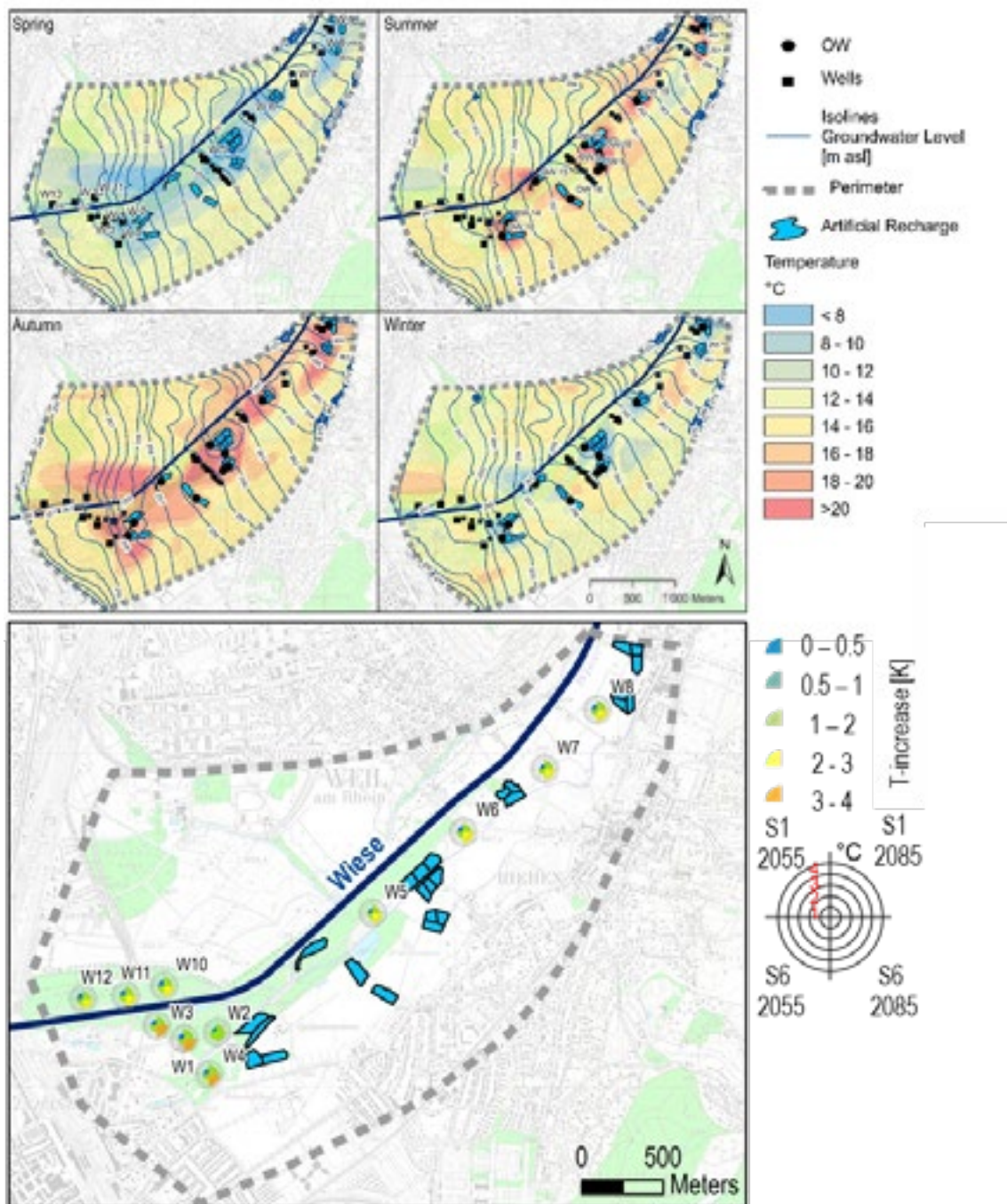


Figure: Above: Seasonal hydraulic and thermal groundwater regime 2018 for different seasons in the Lange Erlen case study area. Below: Temperature change for two climate scenarios (S1 and S6) for the years 2055 and 2085 compared to the reference state in 2000 of the drinking water wells in the Lange Erlen. Landeskarte<sup>©</sup> Bundesamt für Landestopografie.

## 13.5

### Hydrochemical evolution of geothermal waters in the Geneva Basin

Luca Guglielmetti<sup>1</sup>, Andrea Moscariello<sup>1</sup>

<sup>1</sup> Department of Earth Sciences, University of Geneva, Rue des Maraîchers 13, CH-1205 Geneva  
(luca.guglielmetti@unige.ch)

Groundwaters circulating in Upper Mesozoic carbonates are of great interest for geothermal heat production and storage applications in Switzerland. This study aims at providing new insights and improve interpretations about the mineral-water reactions and the fluid-flow paths mechanisms across the Geneva Basin (GB), which is the most active region in Switzerland in terms of geothermal exploration and implementation projects. Data from previous studies are combined by new one by new ones collected from cold and hot springs and geothermal exploration wells in 2018 and 2020 in the framework of the GEothermies ([www.geothermies.ch](http://www.geothermies.ch)) program and HEATSTORE project ([www.heatstore.eu](http://www.heatstore.eu)).

Major ions, trace elements, and the isotopes of Oxygen, Hydrogen, Sulfur, Strontium, and Carbon have been analysed constraining the meteoric origin, the circulation path, residence time revealing how Mesozoic carbonate aquifers act as preferential host rocks for geothermal waters. The Jura Mountains and the Saleve Ridge are the main catchment areas and an evolution from a pure Ca-HCO<sub>3</sub> footprint for the cold springs, to a Na > Ca-HCO<sub>3</sub> and a Na-Cl compositions, is observed from the NW to the SW sectors of the Geneva area. The residence time is in the order of a few years for the cold springs and reaches up to 15–20,000 years for the deep wells GEo-01 and Thonex-01.

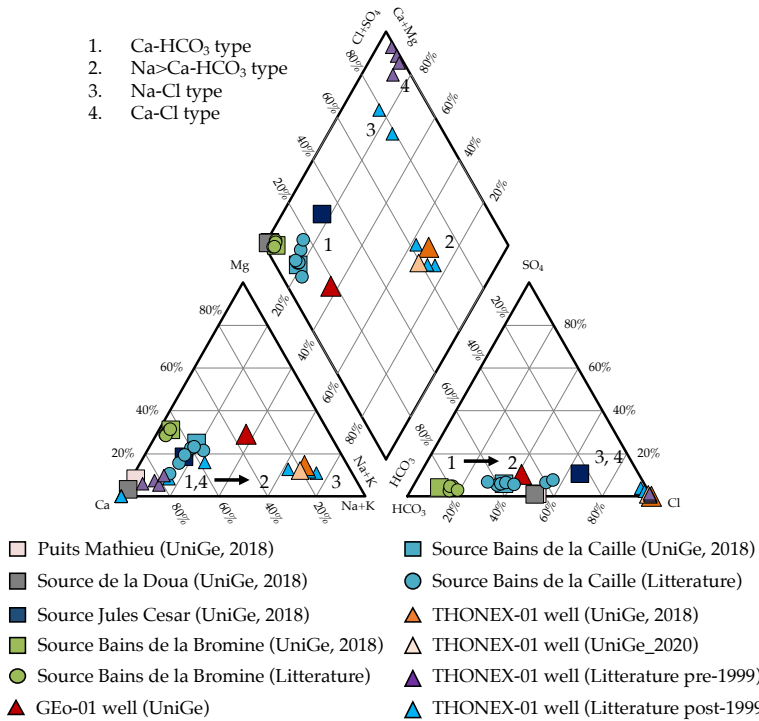


Figure 1. Piper diagram (Piper, 1944) for the groundwater types in the study area (modified from Guglielmetti et al., 2022).

Noble gases and hydrocarbons were also analysed. Noble gases reveal a meteoric origin without major inputs from deep sources. The Geo-01 hydrocarbon composition does not fall within the pure microbial nor thermogenic gas fields and rather shows a mix between microbial and thermogenic gas (Do Couto et al., 2021). The stable isotopic carbon and hydrogen composition of methane reveals that the thermogenic gas is most likely originating from an early mature source-rock. At Thonex-01 methane is close to the thermogenic with potential source rock from the Permo-Carboniferous.

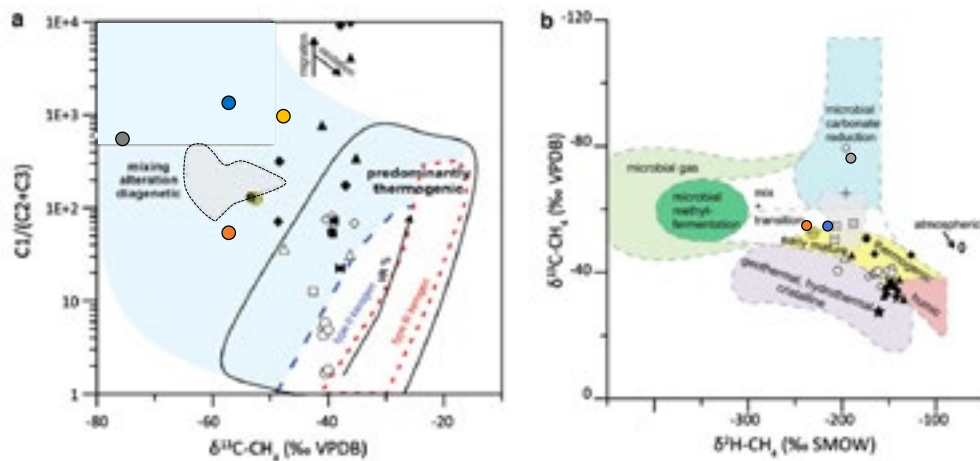


Figure 2. Modified “Bernard diagram” showing the methane carbon isotopic composition vs. dryness (modified after Bernard et al., 1976; Whiticar, 1999) showing the composite biogenic and thermogenic composition of the gas retrieved from Satigny (this study). b Interpretation of gas origin using stable carbon and hydrogen isotopic composition of methane according to Whiticar ( 1999). Data from this study combined to those retrieved from (Do Couto et al., 2021)

## REFERENCES

- Bernard, B. B., Brooks, J. M., & Sackett, W. M. (1976). Natural gas seepage in the Gulf of Mexico. *Earth and Planetary Science Letters*, 31(1), 48–54. [https://doi.org/10.1016/0012-821X\(76\)90095-9](https://doi.org/10.1016/0012-821X(76)90095-9)
- Do Couto, D., Garel, S., Moscariello, A., Bou Daher, S., Littke, R., & Weniger, P. (2021). Origins of hydrocarbons in the Geneva Basin: insights from oil, gas and source rock organic geochemistry. *Swiss Journal of Geosciences*, 114(1), 11. <https://doi.org/10.1186/s00015-021-00388-4>
- Guglielmetti, L., Heidinger, M., Eichinger, F., & Moscariello, A. (2022). Hydrochemical Characterization of Groundwaters' Fluid Flow through the Upper Mesozoic Carbonate Geothermal Reservoirs in the Geneva Basin: An Evolution more than 15,000 Years Long. *Energies*, 15(10), 3497. <https://doi.org/10.3390/en15103497>
- Piper, A. M. (1944). A graphic procedure in the geochemical interpretation of water-analyses. *Transactions, American Geophysical Union*, 25(6), 914. <https://doi.org/10.1029/TR025i006p00914>
- Whiticar, M. J. (1999). Carbon and hydrogen isotope systematics of bacterial formation and oxidation of methane. *Chemical Geology*, 161(1–3), 291–314. [https://doi.org/10.1016/S0009-2541\(99\)00092-3](https://doi.org/10.1016/S0009-2541(99)00092-3)

## 13.6

# Understanding the present and future state of groundwater in alpine headwater catchments using hydrogeophysics

Landon J.S. Halloran<sup>1,\*</sup>, Jeremy Millwater<sup>1</sup>, Marie Arnoux<sup>2</sup>, Daniel Hunkeler<sup>1</sup>

<sup>1</sup> Centre d'hydrogéologie et de géothermie, Université de Neuchâtel, Neuchâtel, Switzerland (\* landon.halloran@unine.ch)

<sup>2</sup> Centre de recherche sur l'environnement alpin, Sion, Switzerland.

In Switzerland and many other regions of the world, alpine groundwater plays a vital buffering role, ensuring perennial streamflow down-gradient. Globally, human reliance on alpine groundwater resources is expected to increase while the reliability of the resource is expected to be severely impacted by climate change. Given the increasing importance and uncertainty of the resource, there is a glaring lack of data on the mountain groundwater. In order to understand the future seasonal dynamics of water resources in alpine regions as snow- and ice-cover changes, it is vital to have quantitative, spatially-resolved hydrogeological information. Non-invasive geophysical methods such as time-lapse gravimetry (TLG) and electrical resistivity tomography (ERT) are uniquely adapted to fill this knowledge gap.

TLG involves measurements of acceleration due to gravity,  $g$ , at one or more locations at multiple points in time. Using absolute-referenced mobile relative gravimeters, single survey accuracy in the few parts-per-billion range is achievable. Under certain conditions, one can readily resolve changes in groundwater storage on the order of 10 cm equivalent water column. While TLG is ideal for providing spatially-resolved information on seasonal and annual variations in groundwater storage, accurate quantitative use requires a more advanced approach than the simple Bouguer plate approximation (BPA) fixed conversion factor. A first step in this direction is the integration of topographic or hydrostratigraphic data into the analysis (Halloran, 2022) which allows for more accurate estimates of groundwater storage changes using  $\Delta g$  data (Figure 1).

Studies in the alpine headwater catchment *Tsalet* (Vallon de Réchy, Valais; Figure 1) have employed TLG (Arnoux et al. 2020) and ERT (Millwater, in prep.) in order to characterise and delineate the complex moraine, talus and colluvium superficial aquifers. The ERT measurements have enabled three-dimensional characterisation of these units and their integration into a hydrogeological model. This geophysics-informed numerical model is used to evaluate hypotheses on the current groundwater dynamics as well as the response of the system to future climate-change impacts.

## REFERENCES

- Halloran, L. J. S. (2022). Improving groundwater storage change estimates using time-lapse gravimetry with Gravi4GW. *Environmental Modelling & Software*, 150, 105340.
- Arnoux, M., Halloran, L. J. S., Berdat, E., & Hunkeler, D. (2020). Characterizing seasonal groundwater storage in alpine catchments using time-lapse gravimetry, water stable isotopes and water balance methods. *Hydrological Processes*, 34(22), 4319–4333
- Millwater, J (in preparation). Aquifer mapping and modelling in a dynamic alpine headwater catchment. MSc thesis, Université de Neuchâtel.

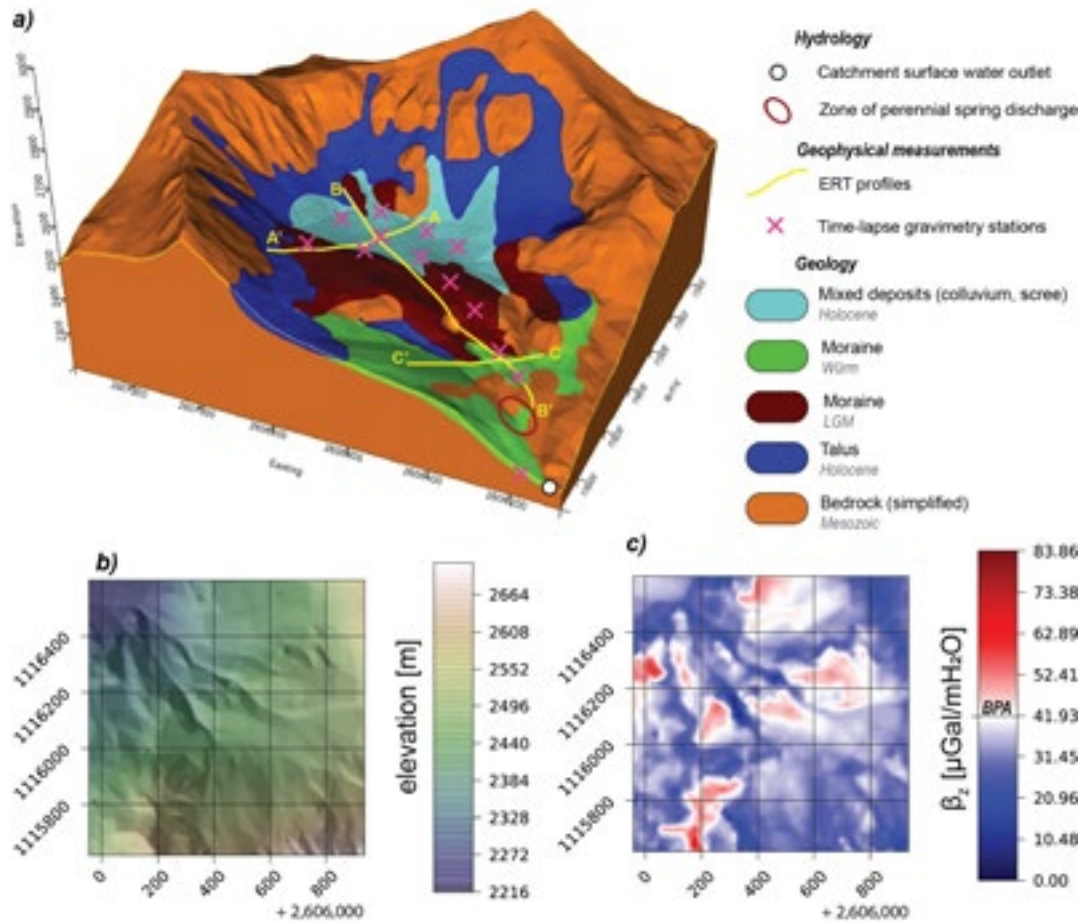


Figure 1. a) TLG and ERT survey locations in the *Tsalet* catchment (Vallon de Réchy) overlaid on a geological model. b) Topographic map of the lower catchment area. c) The corresponding topography-informed factor,  $\beta_z$  (Halloran, 2022), for conversion between changes in gravity and changes in groundwater storage. BPA = Bouguer plate approximation.

## 13.7

# Consequences of intermittent ventilation on the energy balance of a karst system

Claudio Pastore<sup>1</sup>, Marc Luetscher<sup>1</sup>, Frédéric Doumenç<sup>2,3</sup>, Amir Sedaghaktish<sup>1</sup>, Eric Weber<sup>1</sup>, Pierre-Yves Jeannin<sup>1</sup>

<sup>1</sup> Swiss Institute for Speleology and Karst Studies (SISKA), Rue de la Serre 68, 2300 La Chaux-de-Fonds, Switzerland, (claudio.pastore@isska.ch)

<sup>2</sup> Université Paris-Saclay, CNRS, FAST, 91405, Orsay, France

<sup>3</sup> Sorbonne Université, UFR 919, 4 place Jussieu, F-75252 Paris Cedex 05, France

A karst massif is crossed by a network of fractures and conduits driving water and air from the atmosphere deep into the massif. These fluids exchange heat at the boundaries between rock, air and water. The thermal characteristic of the medium together with thermal processes including convection, evapo-condensation, radiation and conduction, concur to settle the caves' temperature. The thermal length, the distance at which the external temperature fluctuations are dulled, and the energy balance of the cave system depend on its geometry and the fluxes therein. Understanding what modifies these thermal characteristics is of interest e.g. for paleoclimatic studies on speleothems or low-enthalpy geothermal exploitation. We equipped Longeague cave (Val-de-Travers, Jura mountains) with several sensors measuring airflow and temperatures along the main conduit network. The cave has a lower and upper entrance. It is mainly dry and is crossed by an intense airflow which complies with the chimney effect. The temperature oscillations observed throughout the cave are chiefly related to external temperature and airflow variations. Results from 8 monitoring stations reveal that more than 90% of the energy brought in by the air during ventilated periods is exchanged within the first tens of meters from the cave entrances. However, during periods of rainfall and snowmelt the cave can be flooded, interrupting temporarily this airflow several times per year. Our observations show that the transient nature of this airflow modifies the temperature signals in the cave. Here, we demonstrate that the intermittent aerialic regime affects the cave energy balance in a differentiated way according to seasonal hydrological conditions. In the light of climate change, we anticipate a progressive shift toward summer ventilation phases enhancing the warming of the system.

On longer time scales, comparable changes in the cave geometry may impact on the interpretation of speleothem temperature-sensitive proxy records.

## 13.8

# Predicting streamflow recession in alpine catchments: how does bedrock morphology control the dynamics?

Clément Roques<sup>1</sup>, David E. Rupp<sup>2</sup>, Jean-Raynald de Dreuz<sup>3</sup>, Ronan Abhervé<sup>3</sup>, Kerry Leith<sup>4</sup>, Sarah Leray<sup>5</sup>, Laurent Longuevergne<sup>2</sup>, James Thornton<sup>6</sup>, Philip Brunner<sup>1</sup>, Gordon Grant<sup>7</sup>, and John S. Selker<sup>8</sup>

<sup>1</sup> Centre for Hydrology and Geothermics (CHYN), Université de Neuchâtel, Neuchâtel, Switzerland.

<sup>2</sup> Oregon Climate Change Research Institute, College of Earth, Ocean, and Atmospheric Sciences, Oregon State University, Corvallis, OR, USA.

<sup>3</sup> Univ Rennes 1, CNRS, Géosciences Rennes - UMR 6118, F-35000 Rennes, France.

<sup>4</sup> Department of Earth Sciences, Institute of Geology, ETH Zürich, Zürich, Switzerland.

<sup>5</sup> Departamento de Ingeniería Hidráulica y Ambiental, Pontificia Universidad Católica de Chile, Santiago, RM, Chile

<sup>6</sup> Mountain Research Initiative, c/o University of Bern, Bern, Switzerland

<sup>7</sup> Pacific Northwest Research Station, Forest Service, U.S. Department of Agriculture, Corvallis, Oregon, USA.

<sup>8</sup> Department of Biological and Ecological Engineering, Oregon State University, Corvallis, Oregon, USA

Global-scale models project that by 2050 about 1.5 billion people worldwide will be directly dependent on streamflow contributions from mountains (Viviroli et al., 2020). However, due to the difficulties of gathering relevant data at high elevations and the lack of fundamental physically-based understanding on the processes involved, the representation of the groundwater flow in alpine catchment- to regional-scale hydrological models is currently overlooked. It is often limited to a simplified homogeneous and shallow layer with effective hydraulic properties. This raises questions regarding the validity of such models to quantify the potential impacts of climate change, where subsurface heterogeneity is expected to play a major role in their short- to long- term regulation (Hartmann et al. 2017).

Based on a comprehensive analysis of hydrological, climatic, geological and geomorphological databases available in the Alps, we provide evidence that such simplification lead to inaccurate estimates of groundwater and streamflow dynamics involved at baseflow (Roques et al., 2021). The analysis allows the identification of key features of the landscape which might control this deviation, with particular attention to slope, drainage density, depth to bedrock, and lithology as the main drivers. We use numerical modelling to validate the main hypothesis identified from the regional- scale data analysis. We specifically explore the role of vertical heterogeneity of hillslopes on groundwater flow and streamflow recession discharge (Roques et al., 2022). We found that when hydraulic properties are vertically compartmentalized (Figure 1), streamflow recession behaviour may indeed strongly deviate from what is predicted by homogeneous groundwater theory. We further identify the hillslope configurations for which the homogeneous theory derived from the Boussinesq solution approximately hold and conversely for which it fails. By comparing the modelled streamflow recession discharge and the groundwater table dynamics, we identify the critical hydrogeological conditions responsible for the emergence of strong deviations.

Our results confirm the critical importance of accounting for structural configuration and heterogeneity of the subsurface in catchment- to regional-scale hydrological models. We conclude by summarizing the current knowledge of physical mechanisms that could lead to complex hydrological behavior in Alpine contexts, and discuss implications in defining modeling strategies for the Critical Zone community.

## REFERENCES

- Hartmann, A., Gleeson, T., Wada, Y. and Wagener, T.: Enhanced groundwater recharge rates and altered recharge sensitivity to climate variability through subsurface heterogeneity, Proc. Natl. Acad. Sci. U. S. A., 114(11), 2842– 2847.
- Roques, C., Rupp, D. E., and Selker, J. S.: Improved streamflow recession parameter estimation with attention to calculation of  $-dQ/dt$ , Adv. Water Resour., 108, 29–43.
- Roques, C., Lacroix, S., Leith, K., Longuevergne, L., Leray, S., Jachens, E. R., Rupp, D. E., DeDreuz, J.-R., Cornette, N., de Palezieux, L. B., and et al.: Geomorphological and geological controls on storage-discharge functions of Alpine landscapes : evidence from streamflow analysis in the Swiss Alps and perspectives for the Critical Zone Community, Earth Sp. Sci. Open Arch., 39.
- Viviroli, D., Kummu, M., Meybeck, M., Kallio, M., & Wada, Y. (2020). Increasing dependence of lowland populations on mountain water resources. Nature Sustainability, 3(11), 917–928.

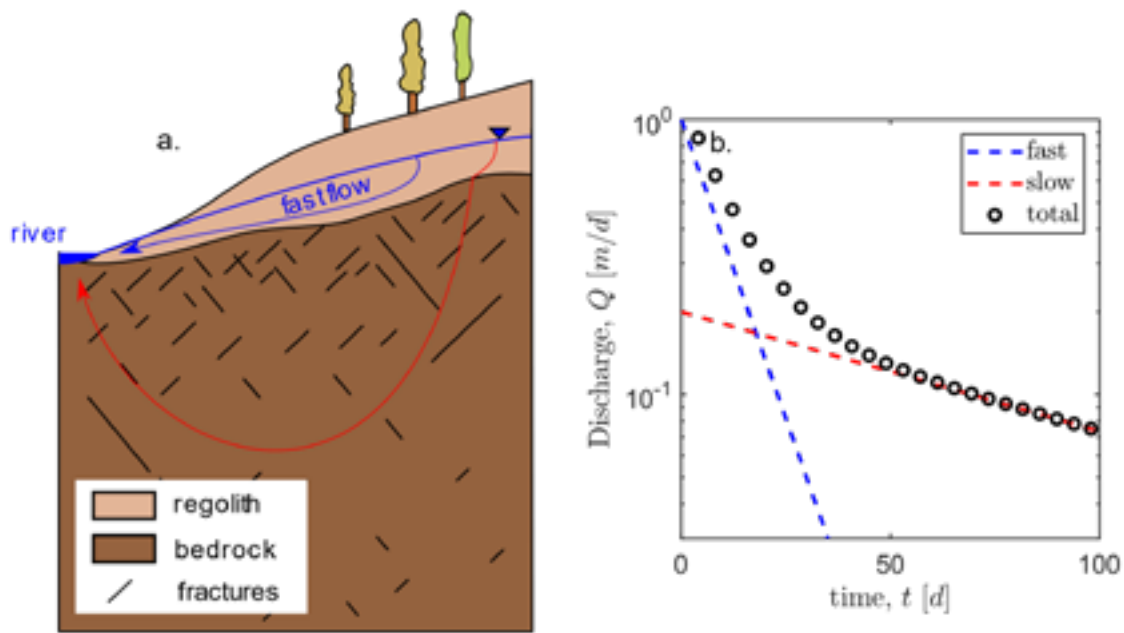


Figure 1. a. Conceptual model of a compartmentalized hillslope with groundwater flow distributed between fast flow within the shallow regolith/fractured aquifer and slow flow in the underlain bedrock; b. Theoretical streamflow behaviour considering two linear reservoirs ( $b=1$ ) in parallel with fast (blue line, ) and slow (red line, ) drainage timescales. From Roques et al. (2022).

## 13.9

# Buried paleo-channel detection with a groundwater model, tracer-based observations, and spatially varying, preferred anisotropy pilot point calibration

Oliver S. Schilling<sup>1,2</sup>, Daniel J. Partington<sup>3</sup>, John Doherty<sup>3,4</sup>, Rolf Kipfer<sup>2,5,6</sup>, Daniel Hunkeler<sup>7</sup>, Philip Brunner<sup>7</sup>

<sup>1</sup> Hydrogeologie, Departement Umweltwissenschaften, Universität Basel, 4056 Basel

<sup>2</sup> Abteilung Wasserressourcen und Trinkwasser, Eawag, 8600 Dübendorf

<sup>3</sup> National Centre for Groundwater Research and Training, Flinders University, Adelaide 5001, SA, Australia

<sup>4</sup> Watermark Numerical Computing, Corinda 4075, QLD, Australia

<sup>5</sup> Institut für Biogeochemie und Schadstoffdynamik, Departement Umweltsystemwissenschaften, ETH Zürich, 8092 Zürich

<sup>6</sup> Institut für Geochemie und Petrologie, Departement Erdwissenschaften, ETH Zürich, 8092 Zürich

<sup>7</sup> Centre d'Hydrogeologie et de Géothermie, Université de Neuchâtel, 2000 Neuchâtel

Buried paleo-channels in alluvial sand and gravel (ASG) aquifers are typically highly conductive for groundwater flow and responsible for preferential flow paths that are capable of transporting contaminants faster than the surrounding sediments. However, it is notoriously difficult to detect and delineate such buried structures of increased hydraulic conductivity in ASG aquifers with the commonly used geophysical and modelling techniques. Consequently, these anisotropic and connected structures are rarely considered in the delineation of groundwater protection zones or the models used for groundwater management. To bridge this gap, we developed a new framework based on a combination of hydraulic and tracer-based measurements and the calibration of a fully coupled surface water-groundwater model against these observations using a novel inversion approach (Schilling et al., 2022). Tracer-based observations consist of radioactive tracers (e.g., <sup>222</sup>Rn, <sup>37</sup>Ar, <sup>3</sup>H/<sup>4</sup>He), which allow characterization of groundwater residence times, and of atmospheric noble gases, which allow tracking recently infiltrated river water in ASG aquifers. Groundwater modelling is carried out with the integrated surface-subsurface hydrological simulator HydroGeoSphere. Calibration is based on an innovative pilot point inversion that considers the spatially-varying directionality of the alluvial sediments and facilitates the identification of buried and connected structures. The proposed approach is more efficient compared to other existing methods for paleo-channel detection, as the complex and often poorly constrained geostatistical simulations that are used in other approaches are not needed. The applicability of the framework is demonstrated on a real-world drinking water wellfield of an ASG aquifer in the Emmental, Switzerland.

## REFERENCES

- Schilling, O. S., et al. 2022: Buried paleo-channel detection with a groundwater model, tracer-based observations and spatially varying, preferred anisotropy pilot point calibration. *Geophys. Res. Lett.*, 49, e2022GL098944. <https://doi.org/10.1029/2022GL098944>

## 13.10

### GCOS project: Enhance snowfall estimates in existing Swiss precipitation products

Michael Schirmer<sup>1,2</sup>, Jan Magnusson<sup>1</sup>, Tobias Jonas<sup>1</sup>

<sup>1</sup> WSL Institute for Snow and Avalanche Research SLF, 7260 Davos, Switzerland ([michael.schirmer@wsl.ch](mailto:michael.schirmer@wsl.ch))

<sup>2</sup> Swiss Federal Institute for Forest, Snow and Landscape Research, 8903 Birmensdorf, Switzerland

Snow is an important component of the water cycle in Switzerland, contributing approximately 40% of the runoff in Swiss rivers. Yet, precipitation datasets are often associated with considerable uncertainties, in particular in mountainous terrain. In Switzerland, most precipitation gauges have no wind shields and are thus prone to undercatch of snowfall, which can be considerable (several 10%). Unlike other countries, Switzerland does not have monitoring networks to automatically measure snow water equivalent (SWE). However, there are hundreds of stations to measure snow depth, many of which are co-located with precipitation gauges. In the absence of sufficient SWE data, we used a combination of precipitation and snow depth data along with snow modelling and data assimilation methods to determine biases in existing precipitation products. These methods were applied at both the level of individual stations and of gridded products. For RhiresD, the daily precipitation product of MeteoSwiss, we found a bias for snowfall of several 10%, as expected, but with regional and seasonal variations. The optimised precipitation product was provided to an energy-balance snow model. This made it possible to compare modelled and observed snow depth and to quantify the quality of the correction using cross-validation.

For providing spatial averages of snow depth values, one of the challenges to overcome is so-called preferential deposition of snow. In mountainous terrain, preferential deposition causes snow measurements at flat observation site to (normally) overrepresent regional snowfall. Today, airborne LiDAR datasets can provide spatially extensive high-resolution datasets of snow depth. We leveraged this new data source to close the gap between snow data from typical observations sites and regionally representative snowfall. The combined gridded precipitation product acknowledges both precipitation gauge undercatch and snowfall over-representation at flat observation sites. This spatial product was tested in the context of hydrological modelling in two ways. First, it was tested if the water balance can be better described compared to uncorrected data for non-glaciated and relatively undisturbed catchments. Second, simple conceptual hydrological models (including GR4J and HBV) were calibrated and validated for these catchments using both original and corrected precipitation input.

## 13.11

### Changing patterns of heavy rainfall events across an urban area (Milan, Italy)

Herminia Torelló<sup>1</sup>, Francesco Marra<sup>2</sup>, Nadav Peleg<sup>1</sup>

<sup>1</sup> Institute of Earth Surface Dynamics (IDYST), University of Lausanne, Building Géopolis, CH-1015 Lausanne  
(herminia.torello@unil.ch)

<sup>2</sup> Institute of Atmospheric Sciences and Climate, National Research Council of Italy (CNR-ISAC), Bologna, Italy

Observations using remote sensing data reveal that urban areas affect the intensities and spatial structure of rainfall fields on small scales (i.e. at sub-hourly and sub-kilometer resolutions). However, since urban effects on rainfall have only been explored in a few cities and for a relatively short time, there is disagreement regarding the precise pattern of change (e.g. if cities act to enhance or reduce the area of storms) and the driving dynamic and thermodynamic forces behind it. As the hydrological response in urban areas is fast and highly sensitive to space-time rainfall variability, it is crucial to understand how urban areas change the spatial structure of rainfall to improve our abilities to nowcast rainfall and urban floods. We used weather radar data from MeteoSwiss (5 min and 1 km resolution) to analyze the spatial structure and intensity of heavy rainfall events that cross the city of Milan (Italy). We tracked these events over 7 years using a storm-tracking algorithm (from a Lagrangian perspective) and investigated the changes to the properties of the rainfall fields, such as their areal mean intensity, area, and areal rainfall, at varying distances relative to the city center. These radial distances were defined as either upwind or downwind using the storm's average direction of motion. We then evaluated composite storm properties at these different distances. Using an Eulerian perspective, we next explored how rainfall fields changed upwind and downwind of the city by considering fixed radar windows of 20 km by 20 km. At each window, we superimposed radar images that contained convective cells and centered them by their intensity peak. With the image composites, we examined changes in rainfall properties across windows. The results of the analysis from the two perspectives will be presented.

## 13.12

# Changes in rainwater productivity across the rainfed agricultural areas in Ethiopia

Mosisa Tujuba Wakjira<sup>1</sup>, Nadav Peleg<sup>2</sup>, Peter Molnar<sup>1</sup>

<sup>1</sup> Institute of Environmental Engineering, ETH Zurich, Stefano-Francini-Platz 5, CH-8093 Zurich (wakjira@ifu.baug.ethz.ch)

<sup>2</sup> Institute of Earth Surface Dynamics, University of Lausanne, 1015 Lausanne

Water scarcity is one of the major constraints on agricultural productivity, particularly in moisture-limited regions. The intensifying atmospheric evaporative demand and changes in precipitation under the future climate are likely to modify the moisture availability and productivity in agroecosystems. We examined the spatio-temporal changes in aridity and water productivity (WP) in various climatic zones, from arid to hyper humid, under the present and future climates across the rainfed agriculture (RFA) regions of Ethiopia.

To do this, we (i) downscaled the future precipitation, air temperature, and shortwave radiation to a 5 km grid resolution. We considered multiple GCM projections under three shared socioeconomic pathways (SSPs) namely, SSP1-2.6, SSP2-4.5, and SSP5-8.5 for three future periods: 2020-2049, 2045-2074, and 2070-2099. As a reference to the present climate (1981-2010), we used the CHIRPS rainfall, a bias-corrected ERA5-Land (BCE5) 2-m air temperature, and ERA5-Land shortwave radiation; (ii) computed the reference evapotranspiration using the FAO Penman-Monteith and derived the aridity index; (iii) simulated the actual evapotranspiration using a daily bucket soil water balance model considering the spatial heterogeneity of the soil properties; and (iv) determined the main growing season (May-September) Evaporative Stress Indexes (ESI) as a proxy for WP, assuming an average crop yield response factor of the main cereal crops grown in Ethiopia.

The results show that the dominant climatic zones (sub-humid and humid) of the RFA regions will likely experience a minor or no change in aridity while the semi-arid areas will become wetter, for example by up to 30% under SSP5-8.5 by the end of the century. Under the present climate, the median rainfall WP (percent of the potential WP) during the growing season is about 45% in semi-arid, 65% in dry sub-humid, 77% in sub-humid, and 90% in humid climates. The projected WP shows an increase in the sub-humid and humid zones (by up to 8%) as well as in the semi-arid zones (up to 16%) under the three SSPs already in the next few decades. However, in the mid of the century, WP is likely to decrease by up to 4% in major parts of the sub-humid and humid zones under the three SSPs, and this change tends to spatially expand by the end of the century. The observed changes are the combined effects of the nearly consistent (but at a spatially explicit rate) increase in precipitation (for example up to 30% under SSP5-8.5 in the 2080s) and rising temperature (up to 5°C under SSP5-8.5 in the 2080s) over the RFA region.

## 13.13

### Coupling a global glacier model to a global hydrological model prevents underestimation of glacier runoff

Pau Wiersma<sup>1,2</sup>, Jerom Aerts<sup>1</sup>, Harry Zekollari<sup>3,4,6</sup>, Markus Hrachowitz<sup>1</sup>, Niels Drost<sup>5</sup>, Matthias Huss<sup>6,7,8</sup>, Edwin H. Sutanudjaja<sup>9</sup>, and Rolf Hut<sup>1</sup>

<sup>1</sup>Department of Water Management, Faculty of Civil Engineering and Geosciences, Delft University of Technology, Delft, the Netherlands

<sup>2</sup>Institute of Earth Surface Dynamics, Faculty of Geosciences and Environment, University of Lausanne, Lausanne, Switzerland

<sup>3</sup>Department of Geoscience and Remote Sensing, Faculty of Civil Engineering and Geosciences, Delft University of Technology, Delft, the Netherlands

<sup>4</sup>Laboratoire de Glaciologie, Université Libre de Bruxelles, Brussels, Belgium

<sup>5</sup>Netherlands eScience Center, Amsterdam, the Netherlands

<sup>6</sup>Laboratory of Hydraulics, Hydrology and Glaciology (VAW), ETH Zürich, Zürich, Switzerland

<sup>7</sup>Swiss Federal Institute for Forest, Snow and Landscape Research (WSL), Birmensdorf, Switzerland

<sup>8</sup>Department of Geosciences, University of Fribourg, Fribourg, Switzerland

<sup>9</sup>Department of Physical Geography, Faculty of Geosciences, Utrecht University, Utrecht, the Netherlands

Global hydrological models have become an increasingly valuable tool in the quantification of changing hydrological processes and their impact on the environment and society globally. However, glacier parameterization is often simplistic or non-existent in global hydrological models. By contrast, global glacier models do represent complex glacier dynamics and glacier evolution, and as such hold the promise of better resolving glacier runoff estimates. In this study, we test the hypothesis that coupling a global glacier model with a global hydrological model leads to a more realistic glacier representation and consequently improved runoff predictions in the global hydrological model. To this end, the Global Glacier Evolution Model (GloGEM) is coupled with the global hydrological model PCR-GLOBWB 2 using the eWaterCycle platform. For the period 2001-2012, the coupled model is evaluated against the uncoupled PCR-GLOBWB 2 in 25 large-scale (>50.000 km<sup>2</sup>) glaciated basins. The coupled model produces higher runoff estimates across all basins and throughout the melt season. In summer, the runoff differences range from 0.07% for weakly glacier-influenced basins to 252% for strongly glacier-influenced basins. The difference can primarily be explained by PCR-GLOBWB 2 not accounting for glacier flow and glacier mass loss, thereby causing an underestimation of glacier runoff. The coupled model performs better in reproducing basin runoff observations mostly in strongly glacier-influenced basins, which is where the coupling has the most impact. This study underlines the importance of glacier representation in global hydrological models and demonstrates the potential of coupling a global hydrological model with a global glacier model for better glacier representation and runoff predictions in glaciated basins.

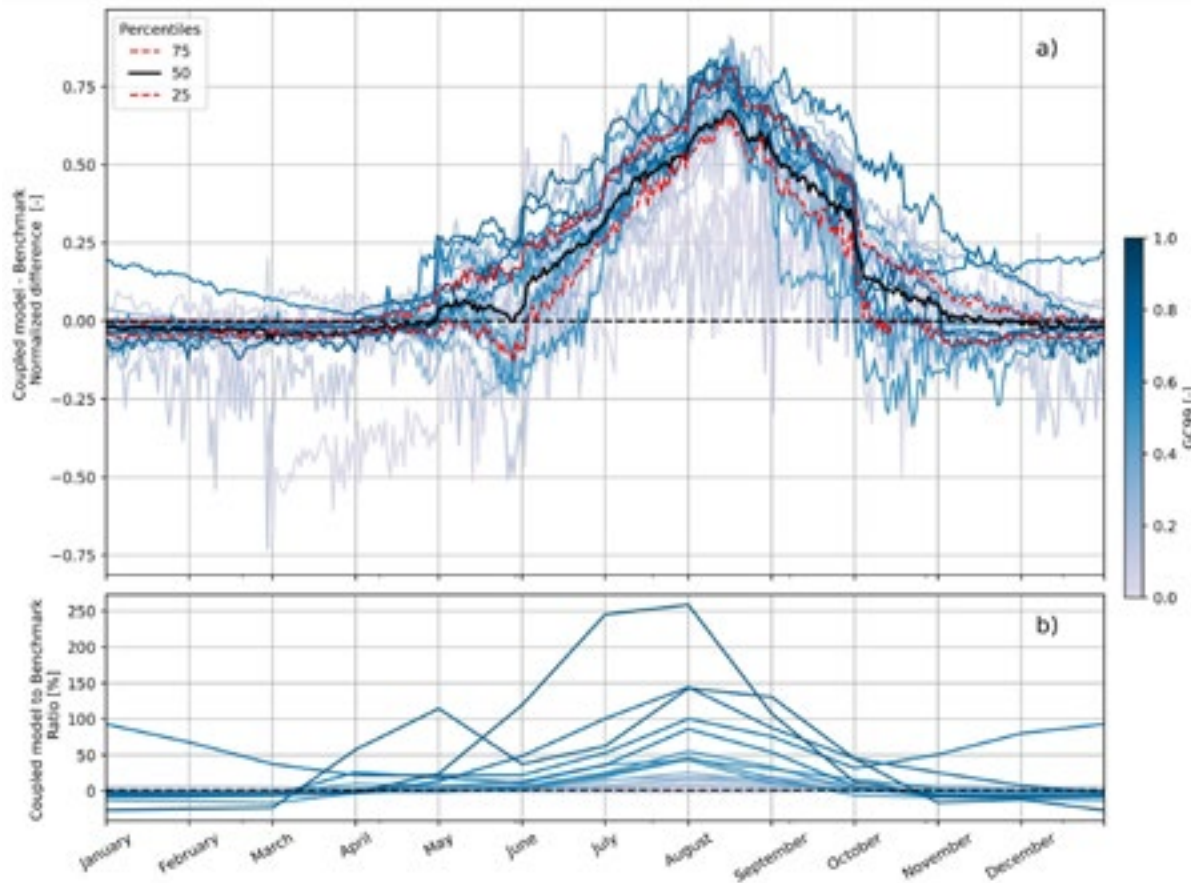


Figure 1. a) Mean normalized difference (ND) between the coupled model (PCR GLOWB 2 & GloGEM) and the benchmark (only PCR-GLOWB 2) for all 25 basins, showing that the coupled model produces higher runoff estimates throughout the melt season. The normalization is performed against the 99th percentile of the difference over the whole time range (2001-2012). The mean is computed for each calendar day over the same period. The solid black and dashed red lines represent the quartiles among the 25 basins. b) Ratio of the coupled model to the benchmark, averaged per month and over the period 2001-2012. The blue hue in both figures represents the 99th percentile of the routed GloGEM glacier runoff contribution to the coupled model runoff (GC99). The data of the three Southern Hemisphere basins are shifted six months forward in time to match the Northern Hemisphere months on the x-axis.

**P 13.1****Implementation of Sewer Network Structures into Numerical Heat Transport Models via an Adaptive Surrogate Approach**

Martin Binder<sup>1,2,3</sup>, Christian Engelmann<sup>2</sup>, Jannis Epting<sup>1</sup>

<sup>1</sup>Applied and Environmental Geology, Hydrogeology Research Group, Department of Environmental Sciences, University of Basel, Bernoullistrasse 32, CH-4056 Basel (martin.binder@unibas.ch)

<sup>2</sup>TU Bergakademie Freiberg, Chair of Hydrogeology and Hydrochemistry

<sup>3</sup>Helmholtz-Centre for Environmental Research, Department of Environmental Informatics

According to projections of the United Nations, more than two thirds of the world's population will live in urban regions by the mid of the current century. Rapid urbanization is associated with negative impacts on urban groundwater availability, with deteriorating factors for both quantity and quality. Adequate management strategies are required to increase the resilience of cities and their ecosystems. Sophisticated numerical models, designed for simulating the water flow as well as solute and heat transport processes in the subsurface, are powerful and established tools supporting decision making and planning and, hence, the sustainable use of subsurface resources.

Besides quantifying the water volumes available for abstraction, understanding the current thermal state of the subsurface and groundwater resources, as well as potential changes in the light of ongoing climate change and urbanization, is essential. Models designed for this very specific task should include at least all major objects (e.g., underground car parks, tunnels, sewer networks) which thermally contribute to groundwater heat regimes. For instance, heat exchange between the subsurface and sewer systems (the latter conducting comparably warm, untreated wastewaters from households and industry to treatment plants) may significantly contribute to the so-called subsurface urban heat island effect as especially observed in densely populated areas, and should, therefore, be addressed in groundwater management models.

However, fully 3-D implementations of all subsurface objects, especially of sewer networks with hundreds of kilometers of pipes, are typically out of question when applying such numerical models, since it would be associated with large computational demands (due to local refinements of model meshes) and, most likely, with increasing numerical instabilities of such simulations.

To overcome this limitation, the focus of our current research is to evaluate the suitability of an adaptive surrogate method as illustrated in Figure 1. Our method is based on quantitatively transferring the expected thermal exchange rates between, for instance, sewer pipes and their surrounding area in a simplified form to the elements of an existing model mesh. For this, the thermal interactions to be implemented are numerically investigated at multiple levels of complexity (e.g., multiple pipe sizes and shapes), and at multiple scales.

**FUNDING:** This work was supported by a postdoc fellowship of the German Academic Exchange Service (DAAD) granted to main author M.B. (project "DAAD.SewerHeat", PKZ 91724232). Further funding granted to co-author C.E. was contributed by the German Research Foundation (grant 499973567, project "ReCAp").

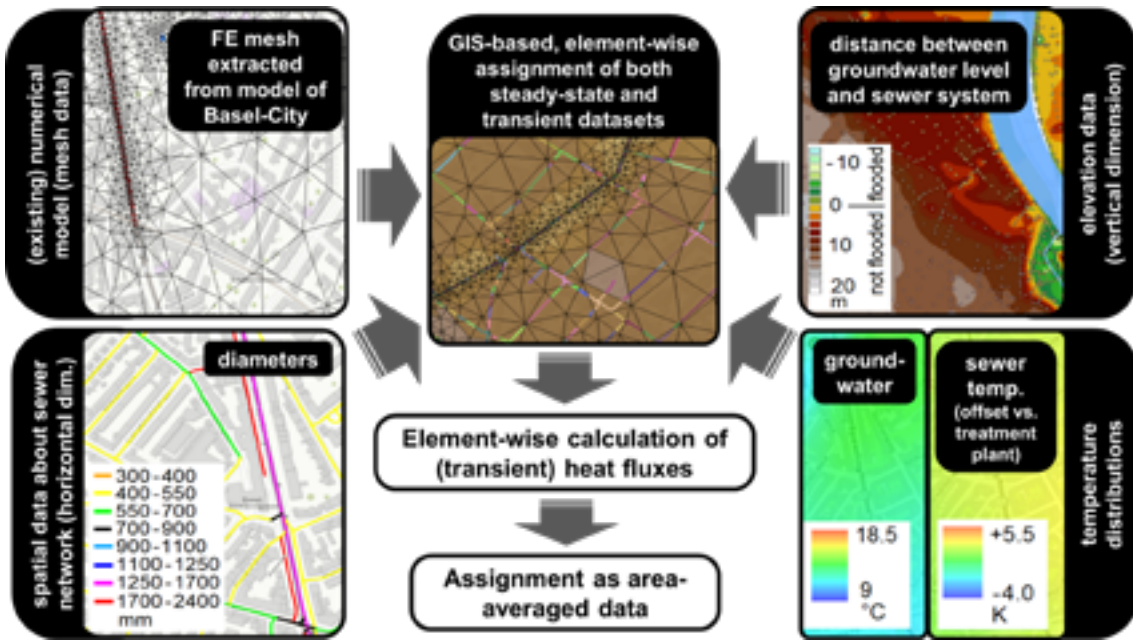


FIGURE 1: Concept of the adaptive surrogate approach (example: sewer networks) using both steady-state (e.g., pipe locations and shapes) and transient datasets (e.g., temperature distributions and distance to groundwater level).

## P 13.2

# Hybrid Forecasting of Sub-seasonal Streamflow and Lake Level in Switzerland

Annie Y.-Y. Chang<sup>1,2</sup>, Konrad Bogner<sup>1</sup>, Daniela I.V. Domeisen<sup>2,3</sup>, Massimiliano Zappa<sup>1</sup>

<sup>1</sup> WSL, Birmensdorf, Switzerland ([annie.chang@wsl.ch](mailto:annie.chang@wsl.ch))

<sup>2</sup> ETH Zürich, Zürich, Switzerland

<sup>3</sup> University of Lausanne, Lausanne, Switzerland

Hybrid forecasting – a system that combines a dynamical/conceptual model with a machine learning (ML) model. Such a setup is able to benefit from the statistical power of ML while maintaining the understanding of physical processes from the traditional model. As many sectors in Switzerland depend heavily on water resources, e.g., hydropower, navigation and transportation, agriculture, and tourism, the objective of this study is to investigate the potential of such a hybrid setup to predict streamflow and lake level at a monthly forecast horizon to provide decision-makers with early information on water availability for better management.

In this study, we set up a hybrid forecasting system combining the conceptual hydrological model PREVAH with the Gaussian Process. We are able to demonstrate that the deployed hybrid forecasting system is able to provide sub-seasonal forecasts of streamflow and lake level for Swiss basins with decent skill for up to 3 weeks. Uncertainty of the hydro-meteorological prediction chain is accounted for by using 51 hydrological ensemble members and the ML uncertainty is accounted for by performing numerous randomizations. We also investigate different predictability drivers by considering input features such as initial conditions, European weather regime forecasts, and a hydropower proxy. Informed ML models with additional input features achieve better performance than those obtained using hydrological model outputs only, but the selection of features plays a crucial role.

This study shines a light on the use of hybrid forecasting for sub-seasonal prediction to provide useful information for medium- to long-term planning from an integrated risk management perspective.

## P 13.3

# Analysis of the Swiss groundwater monitoring network using Pastas models and groundwater signatures

Raoul Collenteur<sup>1</sup>, Christian Moeck<sup>1,2</sup>, Steffen Birk<sup>3</sup>, Mario Schirmer<sup>1,4</sup>

<sup>1</sup> Eawag, Department Water Resources and Drinking Water (W+T), Ueberlandstr. 133, CH-8600 Dübendorf, Switzerland (Raoul.Collenteur@eawag.ch)

<sup>2</sup> Swiss Groundwater Network (CH-GNet), Ueberlandstr. 133, CH-8600 Dübendorf, Switzerland

<sup>3</sup> Institute of Earth Sciences, NAWI Graz Geocenter, University of Graz, Heinrichstr. 26, A-8010 Graz, Austria

<sup>4</sup> University of Neuchâtel, Centre of Hydrogeology and Geothermics (CHYN), Rue Emile-Argand 11, CH-2000 Neuchâtel, Switzerland

A good understanding of observed groundwater dynamics is of paramount importance for the sustainable use and management of groundwater resources. In this study, we analyzed groundwater level data from 29 boreholes in the Swiss groundwater monitoring network (NAQUA) operated by the FOEN (Collenteur et al., under review). To better understand the observed dynamics, the groundwater level time series were modelled using Pastas models (Collenteur et al., 2019), a lumped-parameter groundwater model with physically based impulse response functions. Additionally, the relationships between groundwater signatures, physiographic and climatic controls, and the calibrated model parameters were explored. The modeling results showed that most of the groundwater time series could be modelled with high accuracy using precipitation, potential evaporation, temperature, and often river stages as explanatory stresses. For some wells, there are indications that human interventions (e.g., pumping) may have influenced the groundwater levels. The influence of snow processes (snow storage and release as snowmelt) appears to impact only a few wells at higher altitudes, while most groundwater level data could be modelled well without taking snow processes into account. The resulting models can be used to select monitoring wells that are relatively free from anthropogenic influences and represent naturally occurring fluctuations. The analysis of the relationship between groundwater signatures, physiographic and climatic controls, and the calibrated model parameters revealed that strong correlations exist. We will argue that such relationships can be exploited to support the different phases of the modeling process, and provide examples of how this can be done.

## REFERENCES

- Collenteur, R. A., Bakker, M., Calié, R., Klop, S. A., & Schaars, F. 2019: Pastas: Open Source Software for the Analysis of Groundwater Time Series, *Groundwater*, 57, 877–885.  
Collenteur, R. A., Moeck, C., Schirmer, M., Birk, S. Under Review: Analysis of nationwide groundwater monitoring networks using lumped-parameter models and groundwater signatures.

## P 13.4

# Geothermal Modeling - Interrelated Evaluation of Measured Temperature Data from Borehole Heat Exchangers and Heat Transport in the Geological Subsurface

Elina Roth<sup>1</sup>, Horst Dresmann<sup>1</sup>, Andreas Ebert<sup>2</sup>, Stefan Scheidler<sup>1</sup>, Jannis Epting<sup>1</sup>

<sup>1</sup>Applied and Environmental Geology, Hydrogeology Research Group, Department of Environmental Sciences, University of Basel, Bernoullistrasse 32, CH-4056 Basel (elina.roth@stud.unibas.ch)

<sup>2</sup>Geo Explorers AG, Wasserturmstrasse 1, CH-4410 Liestal

Knowledge of the thermal properties of the geologic subsurface and heat transport processes is crucial for future geothermal well planning. We hypothesize great potential in the analysis of subsurface thermal anomalies, especially in connection with the consideration of geological structures derived from a 3D model of the Basel area (Dresmann et al., 2013) and the development of a thermal hydraulic model (THM) using FEFLOW®. In addition to the thermal properties of the various geologic units and the geothermal heat gradient, the THM also takes into account the regional topographic groundwater flow regime.

The pilot study area is located in Binningen, south of the city of Basel. The results of the THM are compared with high-resolution temperature measurements performed in 21 borehole heat exchangers (BHE) and discussed in relation to the lithological and heat properties as well as heat transport processes. Preliminary modeling results show that the thermal regime can be modeled accurately and that simulated and measured temperature data are in reasonable agreement. In a next step the developed methodology will be transferred to further regions in Northwestern Switzerland and additional BHE temperature profiles analyzed. The goal is to characterize thermal anomalies in relation to the groundwater flow and thermal regime, water occurrences and the specific geologic-stratigraphic settings.

*Acknowledgements: We thank the Office for Environmental Protection and Energy Basel-Landschaft AUE BL for providing the BHE temperature data in the context of the MSc thesis of Elina Roth.*

## REFERENCES

Dresmann Horst; Huggenberger Peter; Epting Jannis; Wiesmeier Stefan; Scheidler Stefan; GeORG - project team; (2013) A 3D spatial planning tool – application examples from the Basel region. Proceedings of the 33rd GOCAD Meeting, 17.-20. Sep. 2013, Nancy, France

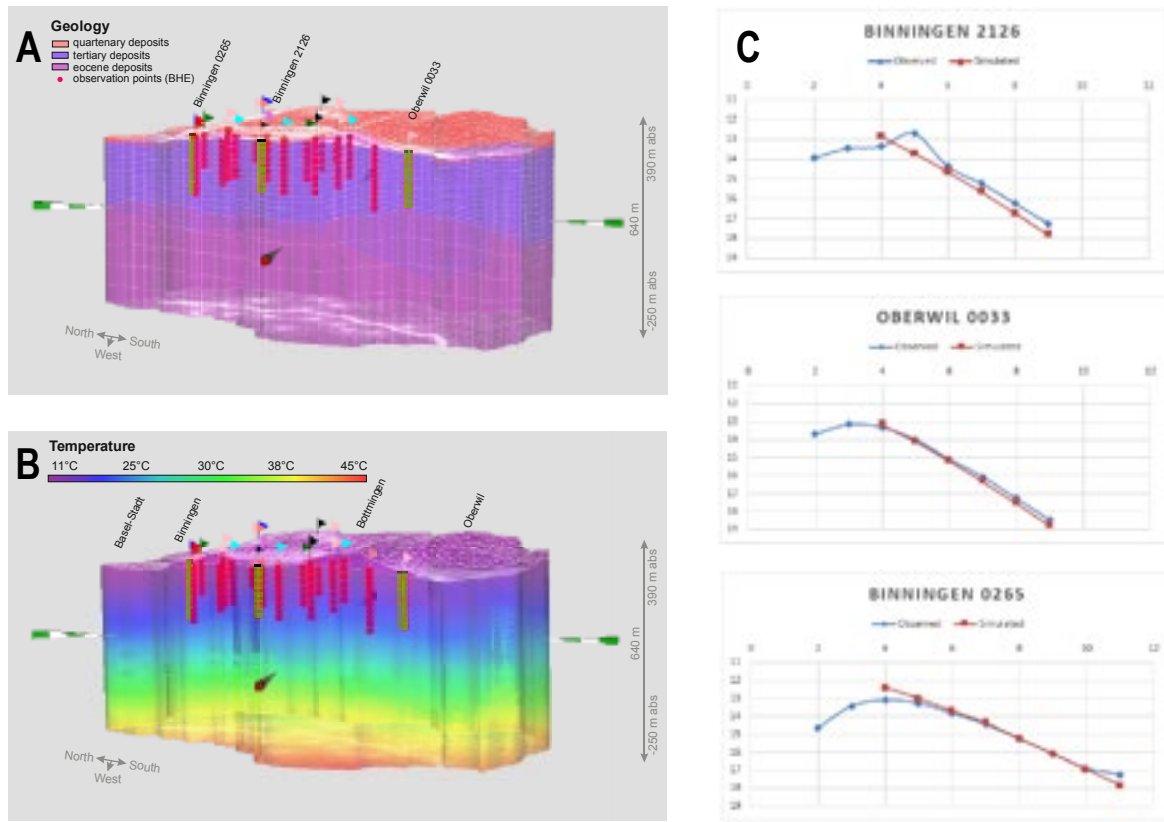


Figure: A – Geology; B – THM Model with simulated temperature distribution; C: Selection of measured and simulated BHE temperature data

## P 13.5

# From droughts to floods – analysing transitions under different hydro-climatic conditions

Jonas Götte<sup>1,2</sup>, Manuela I. Brunner<sup>1,2</sup>

<sup>1</sup> Institute of Earth and Environmental Sciences, University of Freiburg, Freiburg im Breisgau, Germany  
([jonas.goette@hydrology.uni-freiburg.de](mailto:jonas.goette@hydrology.uni-freiburg.de))

<sup>2</sup> from 1.11.2022: WSL Institute for Snow and Avalanche Research SLF, Davos, Switzerland

Drought-flood transitions greatly challenge water management and the development of adaption measures to extreme events. These transitions can occur rapidly but may also take many months or years and are often studied using climate instead of streamflow data – neglecting the role of surface processes. The time between one extreme event and the next one may depend on climate and catchment characteristics including topography, soil types and water use. However, it is yet unclear how drought-flood transition times vary regionally in dependence of climate characteristics, flow processes, and water storage.

In this study, we analyse how drought-flood transition times vary across different hydro-climates. Using the example of the contiguous United States, we investigate the relationship between the characteristics of droughts and subsequent floods. We analyse the durations of drought-to-flood transitions and the streamflow evolution during transition periods. Then, we link these properties to catchment and climate characteristics such as snow dominance and the degree of streamflow regulation. In doing so, we differentiate between different drought and transition seasonalities.

This analysis quantifies the time of occurrence and likelihood of (rapid) drought-flood transitions in different hydro-climatic regions. Such quantification is important because flood preparedness is often low during drought events, which potentially increases the severity of flood impacts.

## P 13.6

# Coupling a large-scale glacier and hydrological model – Towards a better representation of mountain water resources in global assessments

Sarah Hanus<sup>1</sup>, Lilian Schuster<sup>2</sup>, Peter Burek<sup>3</sup>, Fabien Maussion<sup>2</sup>, Jan Seibert<sup>1</sup>, Ben Marzeion<sup>4</sup>, Yoshihide Wada<sup>3</sup>, Daniel Viviroli<sup>1</sup>

<sup>1</sup> University of Zurich, Switzerland

<sup>2</sup> University of Innsbruck, Austria

<sup>3</sup> International Institute for Applied Systems Analysis, Austria

<sup>4</sup> University of Bremen, Germany

In high mountain areas, glaciers are an important part of the hydrological cycle and contribute significantly to runoff in the summer months. Due to climate change, the annual runoff volumes originating from glaciers are undergoing significant change, making it essential to consider glacial melt in hydrological models when we want to model future hydrological changes realistically, especially with regard to mountain water resources. On a catchment scale, routines are available for incorporating glaciers. On a global scale, however, glaciers have been largely neglected so far. This is an important limitation of large-scale hydrological models often used for global climate change impact studies.

We present a framework to couple the global glacier model OGGM (Open Global Glacier Model) and the hydrological model CWatM (Community Water Model) on 5arcmin resolution globally. For both models the source code is openly available. This framework facilitates an explicit inclusion of glacier runoff in large-scale hydrological modelling through dynamic modelling of glaciers and allows research into the hydrological importance of changing glaciers. Specifically, we evaluate how the inclusion of glaciers changes the amount and seasonality of simulated runoff in a large-scale hydrological model in the past and the future. Using selected major river basins in Europe and North America as study areas, benefits, challenges and limitations of the coupling are pointed out.

The large-scale glacio-hydrological modelling framework will be openly available to facilitate further research and the inclusion of glaciers in future large-scale hydrological studies. It can potentially also be used with other global hydrological models.

## P 13.7

# Agricultural adaptations to increasing drought extremes and their feedbacks on catchment hydrology

Malve Heinz<sup>1,2,3</sup>, Annelie Holzkämper<sup>1,3</sup>, Bettina Schäfli<sup>2,3</sup>, Christoph Raible<sup>3,4</sup>

<sup>1</sup> Agroscope Reckenholz, Air Pollution and Climate Group, Reckenholzstrasse 191, 8046 Zürich, Switzerland  
(malvemaria.heinz@agroscope.admin.ch)

<sup>2</sup> Institute of Geography, University of Bern, Bern, Switzerland

<sup>3</sup> Oeschger Centre for Climate Change Research, University of Bern, Bern, Switzerland

<sup>4</sup> Climate and Environmental Physics, Physics Institute, University of Bern, Bern, Switzerland

Climate is changing. In the future, summer and autumn streamflow is expected to decrease at low elevations in Switzerland and water availability is expected to play an increasingly critical role for agricultural production (BAFU 2021; Holzkämper 2020). To prevent drought-related yield losses, farmers may increase irrigation intensities and extend irrigated areas. Ongoing climatic changes and the anthropogenic responses to those changes may pose the risk of increasing water use conflicts (Klein et al. 2013; Zarrineh et al. 2020; Holzkämper et al. 2020). Solutions to stabilize agricultural production in the face of increasing drought frequencies, while minimizing the dependency on supplement irrigation will be crucial to reduce such risks. Possible solutions include planting deeper-rooted crops or varieties, mulching, or organic soil amendments to increase soil water retention. These measures also have direct impacts on key soil physical properties (i.e. hydraulic conductivity and thus infiltration capacity, and retention capacity) with consequences for runoff formation, evapotranspiration and groundwater recharge at the local scale. Because hydrologic responses at the catchment scale are highly dependent on such processes at the local scale, adjustments in agricultural management can have significant impacts on the hydrologic cycle and thus on the availability of water resources (and their quality). Depending on which adaptation measures farmers choose, hydrologic extremes (low and peak flows) may be exacerbated or, with the appropriate measures, mitigated. The potential benefits to be achieved through a large-scale implementation of measures to increase agricultural water use efficiency in Switzerland have not been quantified so far and may vary depending on climate projection and projection horizon.

We address this gap on the basis of a coupled modelling study exploring crucial interconnections between climate, soil hydrology, plant growth and catchment hydrology. The study will be conducted in the Broye catchment in the southwestern part of the Swiss Plateau (Figure 1). The study region is a focus area for agricultural production, has good coverage of hydrological data (Michel et al. 2020), and is known to be increasingly affected by water scarcity (Zarrineh et al. 2020). Water withdrawals for irrigation from the river have already been restricted or prohibited in past drought years and are likely to face increasing limitations in future drought years (Figure 1). Management adaptations increasing the water use efficiency are urgently needed to maintain agricultural productivity in the region. In this presentation, we present the conceptual framework of an integrated regional modelling study to address these issues. The approach builds on the agrohydrological model SWAP-WOFOST to determine current and future irrigation demands in the catchment depending on current and potentially adapted crop and soil management (e.g. adapted varieties and crops, mulching, cover-cropping or organic amendments). Different agricultural management scenarios will be evaluated in terms of achievable increases in agricultural water use efficiency. In addition to the benefits of mitigating drought-induced yield losses, we will also evaluate the hydrologic response to these measures at the catchment scale in terms of mitigating hydrologic extremes (low flows and peak flows) today and under future climate change. For this purpose, we will couple SWAP-WOFOST with the meso-scale hydrological model (mHM). By involving different research disciplines and actors (from agronomy, hydrology and climate modelling), we implement a holistic approach, which will allow to identify synergistic strategies for adaptation management in the region.

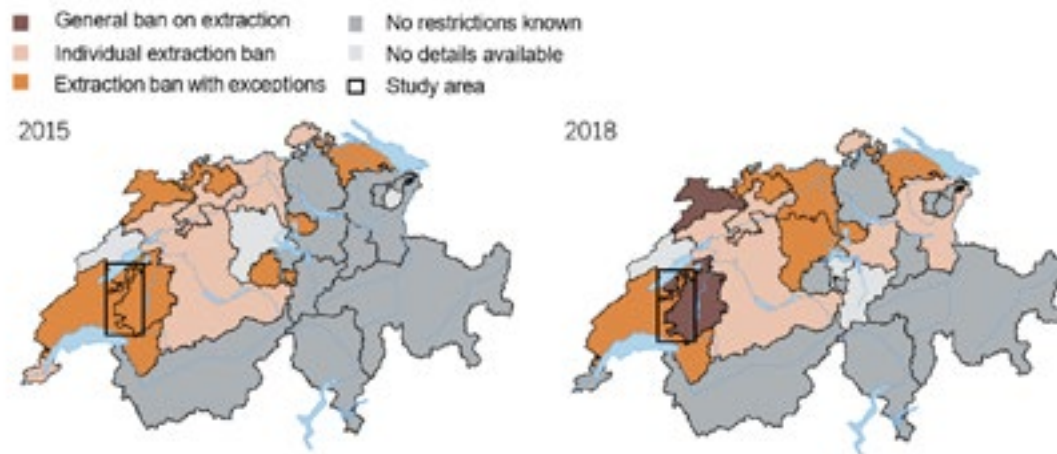


Figure 1. Restriction on water withdrawals for irrigation during the dry summers of 2015 and 2018 (adapted from BAFU 2021).

## REFERENCES

- BAFU, Bundesamt für Umwelt (2021). Auswirkungen des Klimawandels auf die Schweizer Gewässer. Hydrologie, Gewässerökologie und Wasserwirtschaft.
- Holzkämper, A., Cochand, F., Rössler, O., Brunner, P., & Hunkeler, D. (2020). AgriAdapt – Modellgestützte Untersuchung der Einflüsse von Klima- und Landnutzungsänderungen auf Grundwasserressourcen im Berner Seeland, im Auftrag des Bundesamts für Umwelt BAFU
- Michel, A., Brauchli, T., Lehning, M., Schaeffli, B., & Huwald, H. (2020). Stream temperature and discharge evolution in Switzerland over the last 50 years: annual and seasonal behaviour. *Hydrology and Earth System Sciences*, 24(1), 115-142. <https://doi.org/10.5194/hess-24-115-2020>
- Zarrineh, N., Abbaspour, K. C., & Holzkämper, A. (2020). Integrated assessment of climate change impacts on multiple ecosystem services in Western Switzerland. *Sci Total Environ*, 708, 135212. <https://doi.org/10.1016/j.scitotenv.2019.135212>

## P 13.8

# Climate change impacts on the debris-flow activity in a high-alpine catchment

Jacob Hirschberg<sup>1,2</sup>, Yoann Sadowski<sup>3</sup>, Adrien Michel<sup>3</sup>, Brian W. McArdell<sup>1</sup>, Peter Molnar<sup>2</sup>

<sup>1</sup> Swiss Federal Institute for Forest, Snow and Landscape Research WSL, Birmensdorf, Switzerland

(jacob.hirschberg@wsl.ch)

<sup>2</sup> Institute of Environmental Engineering, ETH Zürich, Zürich, Switzerland

<sup>3</sup> School of Architecture, Civil and Environmental Engineering, École Polytechnique Fédérale de Lausanne (EPFL), Lausanne, Switzerland

Debris flows are surging mixtures of water and sediments and can threaten humans and infrastructure. In alpine catchments, debris flows are often triggered by high runoff events as a response to intense rainfall, snowmelt, or a combination thereof. Therefore, debris-flow triggering is expected to be sensitive to predicted changes in temperature and precipitation in course of climate change. Quantifying these changes is, however, challenging. While changes in temperature are relatively certain, future precipitation characteristics have lower signal-to-noise ratios (e.g., Hirschberg et al., 2021). Furthermore, how such changes influence the seasonal snowpack is not trivial. For example, snowmelt is predicted to start earlier in the year, but at lower rates (Musselman et al., 2017). Quantifying changes in debris-flow triggering runoff events in high-alpine catchments therefore requires to study the complex interactions of changes in precipitation, temperature and the snowpack.

Our study focuses on the Grabengufer and the gully below (Fig. 1a). Grabengufer is a rock glacier above the municipality of Randa (Valais). The rock glacier front regularly delivers mobile sediments to the gully (1900 m a.s.l.), where debris flows are frequently triggered after rain and/or snowmelt. We use ALPINE3D, which is a spatially distributed version of the multi-layer snowmodel SNOWPACK (Lehning et al., 2002), to simulate the snowpack evolution and runoff in the Grabengufer basin. Due to the small size and the steepness of the basin, the discharge can be simplified as the snowmelt and liquid precipitation in each pixel and in each timestep (Fig. 1b). A debris-flow record consisting of 34 events between 1985 and 2016 allows for calibrating a debris-flow triggering discharge threshold. Meteorological data is available from MeteoSwiss and surrounding IMIS stations. Finally, we plan to use the AWE-GEN stochastic weather generator (Fatichi et al., 2011) and the CH2018 climate scenarios to study changes in debris-flow triggering discharge at hourly resolution. Although we cannot address the full complexity of such geomorphic systems leading to debris-flow triggering (e.g., rock-glacier dynamics), we study changes in extreme discharge, which is a key variable for future debris-flow hazards, by coupling state-of-the-art models. Furthermore, the studied basin is representative of high-alpine debris-flow torrents and the methods and results will be useful for researchers and authorities interested in climate change impacts on alpine mass movements.

## REFERENCES

- CH2018 Project Team 2018: CH2018 - Climate Scenarios for Switzerland. National Centre for Climate Services.
- Fatichi, S., Ivanov, V. Y., & Caporali, E. 2011: Simulation of future climate scenarios with a weather generator. *Advances in Water Resources*, 34(4), 448-467.
- Hirschberg, J., Fatichi, S., Bennett, G.L., McArdell, B.W., Peleg, N., Lane, S.N., Schlunegger, F., Molnar, P. 2021: Climate Change Impacts on Sediment Yield and Debris-Flow Activity in an Alpine Catchment. *J. Geophys. Res. Earth Surf.* 126.
- Lehning, M., Bartelt, P., Brown, B., and Fierz, C. 2002: A physical SNOWPACK model for the Swiss avalanche warning: Part III: meteorological forcing, thin layer formation and evaluation, *Cold Reg. Sci. Technol.*, 35, 169–184.
- Musselman, K. N., Clark, M. P., Liu, C., Ikeda, K., & Rasmussen, R. 2017: Slower snowmelt in a warmer world. *Nature Climate Change*, 7(3), 214-219.

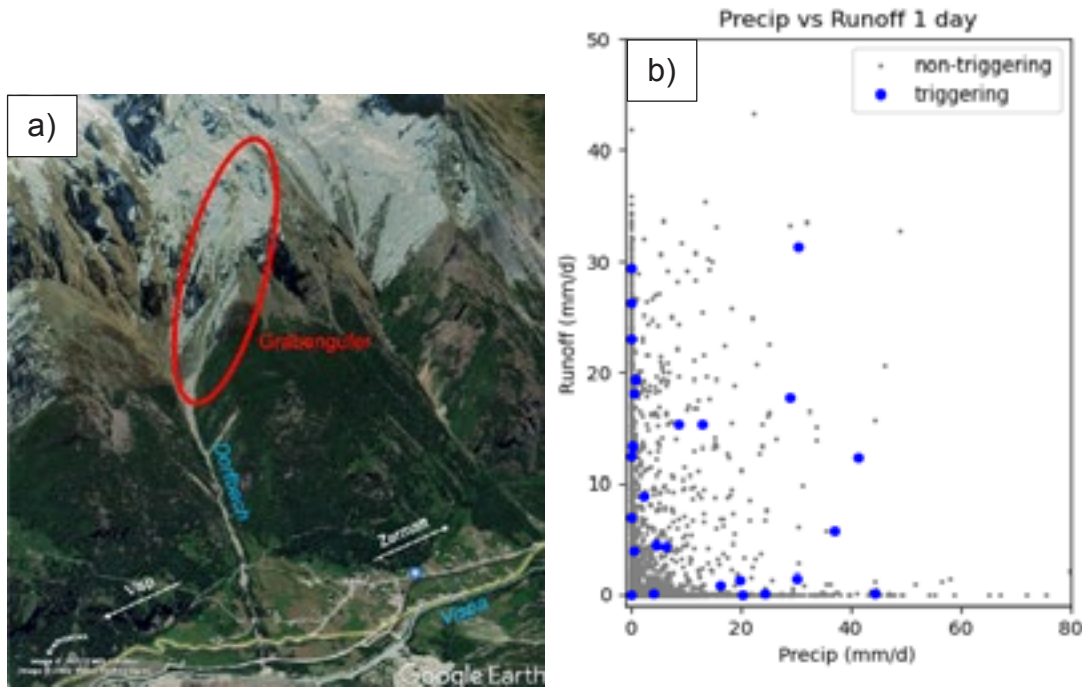


Figure 1. (a) Debris flows initiated at the bottom of the Grabenbachtal gully, flow into the Drotbach, and can potentially cause backwater effects in the Vispa. (b) Preliminary results from ALPINE3D showing that many debris flows are caused by intense rainfall, runoff from the snowpack, or both.

**P 13.9****Modeling River hydro-morphological responses to Land Use Land Cover Change in Tropical Regions: the case of Sebeya catchment, Rwanda.**

Naomie Kayitesi, Gregoire Mariethoz

*Institute of Earth Surface Dynamics, Université de Lausanne UNIL, 1015 Lausanne, Switzerland*

The tropics have experienced the fastest rate of Land Use Land Cover Change (LULCC) largely driven by demographic and socio-economic growth. Furthermore, climate change will likely intensify these changes due to global warming and increased frequency of extreme events. These changes have diverse effects on watershed and river hydro-morphological processes through alterations of the rainfall and runoff patterns, which translate into changes in the water balance components. Sebeya catchment in the domain of Western Province of Rwanda, is prone to flooding, associated with erosive processes, and mass movements. This is a result of the catchment geologic formation, steep topography, and the loss of forest cover on fragile soils, coupled with the increased prevalence of extreme rainfall events. This tropical catchment has a long history of deforestation, including the tremendous decline of Gishwati Forest, whose area decreased from 2,800 ha in 1980s to 600 ha in 2000s. The catchment forest cover has been converted to open land use for farming, pasture, and mining activities. These uncovered steep mountains with heavy rainfall, result in high water flow and flooding mainly at the downstream. Over the past thirty years, hundreds of people in the catchment have been displaced, while infrastructure and crops have been damaged yearly. Additionally, Sebeya River channels are subjected to morphological changes, due to high sedimentation which exacerbates during floods, as well as riverbank erosion.

Understanding the watershed hydro-morphological responses to the changes in climate and LULC –especially in tropical regions where rainy seasons are followed by dry seasons— is vital for effective land and water resources management, in the face of future changes. The objective of this study, therefore, is to quantify the catchment LULCC in the last three decades and predict future scenarios, using remote sensing data and LULC model. Furthermore, a hydrologic model is used to simulate and forecast the associated changes in hydro-morphological and flood frequency.

**P 13.10****What can pore-scale optical measurements do?**

Xiang-Zhao Kong<sup>1,+</sup>, Isamu Naets<sup>1</sup>, Mehrdad Ahkami<sup>1,2</sup>, Pierre Leard<sup>1</sup>, Dario Schwendener<sup>1</sup>, Martin O. Saar<sup>1,3</sup>

<sup>1</sup> Geothermal Energy and Geofluids (GEG) Group, Department of Earth Sciences, ETH Zurich, Sonneggstrasse 5, CH-8092 Zurich, Switzerland (+xkong@ethz.ch)

<sup>2</sup> Department of Engineering Geology and Hydrogeology, RWTH Aachen University, 52056, Aachen, Germany

<sup>3</sup> Department of Earth and Environmental Sciences, University of Minnesota, Minneapolis, USA

Despite progress in recent years, it is still a challenging task to understand the fundamental behaviour of fluid flow and transport at the pore scale, because pore-scale processes are often difficult to capture due to the opacity of porous media. In this presentation, we show our recent pore-scale optical measurements on fluid flow and solute/heat transport.

In a 3D-printed fractured porous medium, we measure pore-scale fluid velocities using both Magnetic Resonance Imaging (MRI) and Particle Image Velocimetry (PIV) techniques and analyse the stress jump and velocity slip coefficients at fracture-matrix interfaces. In addition to fluid flow quantifications, we use laser-induced fluorescence (LIF) techniques to quantify a pulse-like injection of fluorescent dye into the same fractured porous medium and to understand the role of permeability heterogeneity on solute transport. We also capture the development of the thermal plume and the corresponding fluid velocities using combined PIV and two-colour LIF methods when a heat flux is introduced into porous media.

We also use PIV-measured fluid velocities to characterize the evolution of fluid flow paths in a single, self-affine fracture with rough walls, as the fracture undergoes shear displacement. Moreover, we capture both drainage and imbibition processes when immiscible dual-phase flows are injected into the same fracture, which experienced shear displacements. These experiments enable us to delineate the effect of fracture aperture heterogeneity on fracture fluid flow, induced by shear displacement. We extend our measurements on fluid flow and solute transport to a bifurcating fracture to quantify the distribution of fluid and solute mass at fracture intersections.

**REFERENCES**

- Ahkami, M., Roesgen, T., Saar, M. O., Kong, X.-Z. 2019: High-Resolution Temporo-Ensemble PIV to Resolve Pore-Scale Flow in 3D-Printed Fractured Porous Media. *Transp. Porous Media*.
- Naets, I., Ahkami, M., Huang, P.-W., Saar, M. O., Kong, X.-Z. 2022: Shear induced fluid flow path evolution in rough-wall fractures: A particle image velocimetry examination. *Journal of Hydrology*.
- Kong, X.-Z., Ahkami, M., Naets, I., Saar, M. O., 2022: The role of high-permeability inclusion on solute transport in a 3D-printed fractured porous medium: An LIF-PIV integrated study. *Transp. Porous Media*.
- Schwendener, D. 2022: Velocity quantification of two-phase drainage and imbibition processes in rough wall fractures. MSc thesis.
- Ahkami, M. 2020: Experimental and numerical study of fluid flow, solute transport, and mineral precipitation in fractured porous media. PhD thesis.
- Naets, I. 2022: Fluid flow heterogeneity and solute transport in rough-walled fractures. PhD thesis.

## P 13.11

### CH-GNet – Swiss Groundwater Network

Christian Moeck<sup>1,2</sup>

<sup>1</sup> Swiss Groundwater Network (CH-GNet) ([Christian.moeck@eawag.ch](mailto:Christian.moeck@eawag.ch))

<sup>2</sup> Eawag, Swiss Federal Institute of Aquatic Science and Technology

There is a need for continuous competence building, expert support and a facilitated exchange between research and stakeholders in Switzerland to assess hydrogeological issues and challenges under the pressure of new developments. For this purpose, the CH-GNet was created.

The aims of the CH-GNet are to coordinate and promote practice-oriented research. Developed tools and gained information from the scientific community are to be made visible and transferred from science into practice. Scientific facts are to be compiled and strongly practice-oriented research is to be achieved by noticed groundwater-relevant problems as well as possible (voluntary) solutions. Together with the advisory board, the CH-GNet is setting concrete thematic priorities and is determining fundamental strategic directions.

Purely scientific facts are to be worked out for the respective topics and political statements are to be avoided. By bundling practice-relevant research results and making them visible, through organized workshops and the development of documents, help promoting continuous competence building, and a smooth exchange of information, the CH-GNet wants to support the cooperation of various interest groups and represent a source of information. In the present poster examples of the CH-GNet activities are shown



Figure 1. Swiss Groundwater Network. More Information can be found on our webpage <https://www.swissgroundwaternetwork.ch/>

## P 13.12

# Global Potential Groundwater Recharge Response to Climate Variability

Christian Moeck<sup>1</sup>, Wouter R. Berghuijs<sup>2</sup>, Elco Luijendijk<sup>3</sup>, Jason Gurdak<sup>4</sup>

<sup>1</sup> Eawag, Swiss Federal Institute of Aquatic Science and Technology, Switzerland ([Christian.moeck@eawag.ch](mailto:Christian.moeck@eawag.ch))

<sup>2</sup> Department of Earth Sciences, Free University Amsterdam, Netherlands

<sup>3</sup> Bundesgesellschaft für Endlagerung, Peine, Germany

<sup>4</sup> Valley Water, San Jose, USA

Periodic climate patterns such as climate teleconnections can have distinct effects on groundwater, and the ability to predict groundwater fluctuations in space and time is critically important for sustainable water resource management. However, the periodic controls on groundwater resources remain unconsidered in most studies. Teleconnections between global-scale climate oscillations and groundwater are poorly understood because the relationship between subsurface properties and surface infiltration can be highly nonlinear. Understanding of teleconnections is further hampered because many groundwater records are incomplete and groundwater levels are also anthropogenically influenced. Existing studies that have looked at how climate teleconnections control groundwater are based on a limited number of point measurements. Therefore, the spatial distribution of the teleconnections remains mostly unknown.

Here, based on an analytical solution derived from Richards' equation, we present a global assessment of when and where climate teleconnections are expected to propagate in groundwater levels. We model the response to idealized recharge oscillations below the root zone from five different global recharge model sources with periods that range from .monthly to decadal years. The largest periods are idealized representations of global-scale climate variability such as Pacific-North American Oscillation (PNA), North Atlantic Oscillation (NAO), El Niño/Southern Oscillation (ENSO), and Pacific Decadal Oscillation (PDO)

Our global-scale assessment reveals why in some regions periodic infiltration fluxes caused by climate variability remain absent in groundwater level fluctuations, whereas in other regions they result in more dynamic groundwater levels. We explore to what extent groundwater resources are sensitive to climate variability and may help forecast long-term groundwater levels.

**P 13.13****Preserving the temperature-scaling of high intensity precipitation for a more realistic projection of sub-daily extreme events**

Jorge Sebastián Moraga<sup>1</sup>, Nadav Peleg<sup>2</sup>, Paolo Burlando<sup>1</sup>

<sup>1</sup> Institute of Environmental Engineering, ETH Zürich, Zürich, Switzerland ([moraga@ifu.baug.ethz.ch](mailto:moraga@ifu.baug.ethz.ch))

<sup>2</sup> Institute of Earth Surface Dynamics, University of Lausanne, Lausanne, Switzerland. Innsbruck

According to the Clausius-Clapeyron (CC) relation, the water holding capacity of the atmosphere increases by about 7% for each °C of increase in air temperature. It has been widely observed at multiple regions and climates that there is a scaling of the most intense events on record with the near surface air temperature at rates that resemble that of the CC. Convection Permitting Models – dynamical models designed to model the very intense, short-duration convective rain cells that typically occur under warm conditions– have further confirmed this phenomenon and project it to intensify under future climate scenarios.

Stochastic weather generators (WG) are models typically parameterized based on observations and used to simulate large ensembles of plausible high-resolution time series that preserve the correlations and cross-correlations found in climate. This allows practitioners to carry out more robust extreme value analysis, to quantify the internal climate variability of variables of interest, and, when forced to follow the signals emanating from climate models, they provide unique insight into the impacts of warming climate at small scales. Combined with the outputs of dynamical climate models, it is possible to carry out these analyses under any assumed climate trajectory.

The two-dimensional Advanced Weather Generator AWE-GEN-2d (Peleg et al., 2017), as one of the few of its kind, is an ideal to generate the distributed and high resolution climate variables necessary to project the impacts over complex topography (Moraga et al., 2021). In this work, we further improve the model by incorporating an explicit dependency of storm properties with temperature, with the goal of simulating the CC scaling of intense events, while preserving all the other cross-correlations built into the model. In doing so, we find a balance between the expected intensification of extremes with rising temperatures and the overall precipitation trends projected by conventional climate models, thus generating a more realistic dataset that represents the changes to small-scale extreme events.

Using the example of a mountainous catchment in the Swiss Alps, we use the new AWE-GEN-2d-CC to generate large ensembles of present and end-of-century climate time series following the outputs of multiple climate models. These ensembles are consequently used as inputs to a physically-based hydrological model, Topkapi-ETH, that allows us to explore the effects of climate change on hydrometeorological extremes at the sub-kilometer and hourly scale .

The simulations show how incorporating the temperature dependence in the model reveal that extreme precipitation events will increase under future climate scenarios, especially for short durations and relatively small return periods, whereas the change is less noticeable for rarer events (e.g. T > 100 years). This has a clear impact on the hydrological response of small catchments, as the annual maximum hourly and daily flows are projected to increase rather than decrease or remain constant, as projected using the previous model version (Moraga et al., 2021). These results highlight the importance of accounting for the temperature-intensity relationship when analyzing the impacts of climate change on extreme events, particularly for small or highly heterogeneous catchments that are particularly sensitive to short and intense events.

**REFERENCES**

- Moraga, J.S., Peleg, N., Fatichi, S., Molnar, P., Burlando, P., 2021. Revealing the impacts of climate change on mountainous catchments through high-resolution modelling. *J. Hydrol.* 603, 126806. <https://doi.org/10.1016/j.jhydrol.2021.126806>
- Peleg, N., Fatichi, S., Paschalis, A., Molnar, P., Burlando, P., 2017. An advanced stochastic weather generator for simulating 2-D high-resolution climate variables. *J. Adv. Model. Earth Syst.* 9, 1595–1627. <https://doi.org/10.1002/2016MS000854>

## P 13.14

# Results of hydrogeological investigations in the framework of Nagra's deep borehole program

Nicolas Roy<sup>1</sup>, Daniel Traber<sup>1</sup>

<sup>1</sup> Nationale Genossenschaft für die Lagerung radioaktiver Abfälle, Hardstrasse 73, CH-5430 Wettingen  
(nicolas.roy@nagra.ch)

In the framework of the Swiss Sectoral Plan for Deep Geological Repositories, Nagra carried out a comprehensive exploration campaign to characterize the remaining three potential siting areas Jura Ost (JO), Nördlich Lägern (NL) and Zürich Nordost (ZNO) in northern Switzerland. Hydrogeological investigations at representative borehole locations contribute to the site comparison and to evaluate long-term safety of a repository for radioactive waste. The investigations focused on the host rock Opalinus Clay, its confining units and the regional aquifers above and below these low permeability units.

The hydrogeological survey comprised of in-situ tests as well as lab investigations of drill cores. In situ tests included fluid logging, hydraulic packer testing and groundwater sampling. Vertical hydraulic head distribution is also investigated in selected boreholes by means of long-term monitoring systems. Off-site lab investigations included measurement of matrix permeability and porewater investigations as evidence for transport processes.

The conducted investigations allowed to refine the knowledge from earlier investigations:

- In the siting areas NL and ZNO, the Malm aquifer is typically covered by several hundreds of meters of Molasse sediments. Fluid loggings conducted in the thick limestone unit of the «Felsenkalke» / «Massenkalk» and Villigen Fm. combined with FMI (Formation Micro Imager) of the boreholes provide an improved understanding of the nature and occurrence of water conducting features in this regional aquifer. In some areas, highly enriched stable isotope compositions and other isotope tracers in deep groundwaters evidence fossil components and low flow dynamics.
- The observed hydraulic properties of the Hauptrogenstein aquifer in the Bözberg area (JO) can be linked to the facies transition from the clay mineral-rich Klingnau Fm. in the east to the Hauptrogenstein carbonate platform in the west.
- Several local-scale aquifers were observed in the uppermost Keuper in association with different Members of the heterogeneous Klettgau Fm. The dolomitic Seebi Mb. in ZNO was found to constitute of an aquifer at least at the scale of the siting area. In NL, groundwater flow is locally occurring in association with fluvialite deposits within the Ergolz Mb. In JO, available data suggest that water is flowing in the porous and fractured dolostones of the Gansingen Mb. When present, the aquifers of the Klettgau Fm. represent the closest release pathway from the host rock.
- The investigations provide further evidence that the Muschelkalk is the dominant deep regional aquifer in Northern Switzerland. Comparably high hydraulic conductivities throughout the sites along with hydrochemical data support a well-connected regional flow system.
- Hydraulic packer tests in Opalinus Clay complement earlier datasets, notably from previous deep boreholes in Northern Switzerland and investigations in the Mont Terri Underground lab. Hydraulic conductivities are typically below  $1 \times 10^{-13}$  m/s and vary within a narrow range. Also, none of the test results suggests that fractures constitute discrete flow paths.
- Hydraulic packer tests in the confining units show generally low hydraulic conductivities typically varying between  $5 \times 10^{-12}$  and  $1 \times 10^{-14}$  m/s. Rare higher values are restricted to test intervals with fractures in thick sections with low clay mineral contents. Tests on drill-core samples allow to correlate matrix hydraulic properties with mineralogical composition and therewith to evaluate the role of individual lithofacies.

*Acknowledgements: We acknowledge numerous contributions to the investigations by Nagra staff as well as by third party companies.*

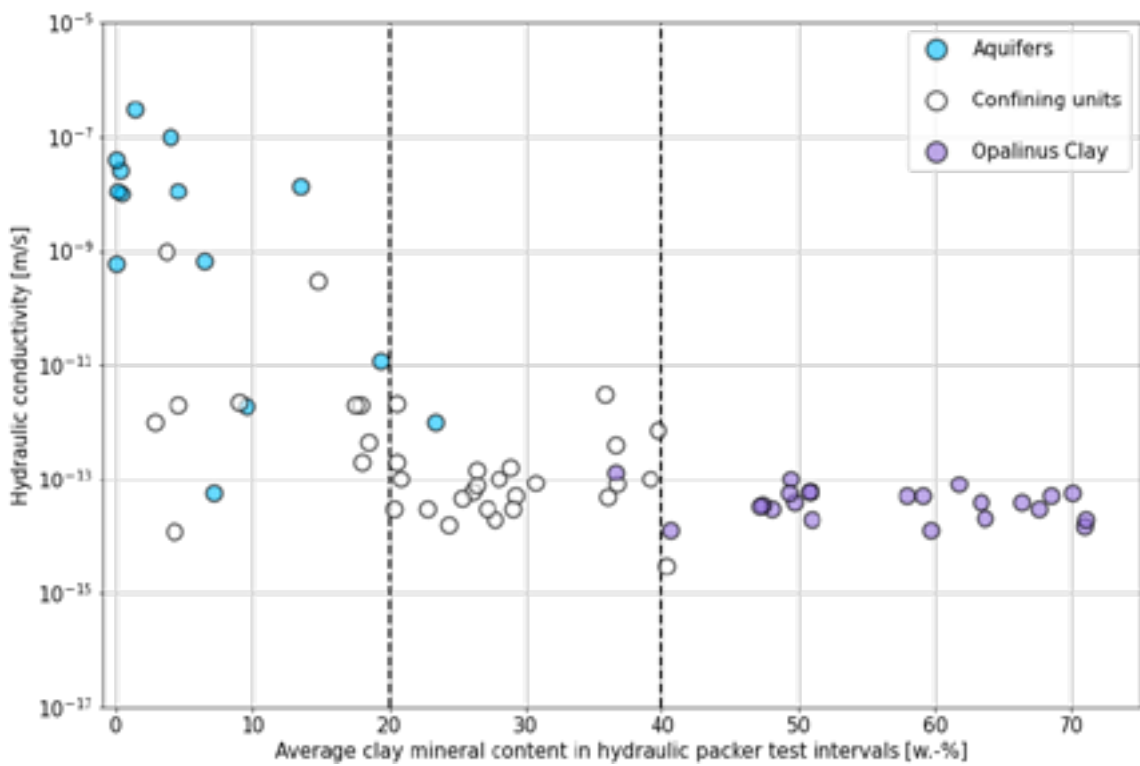


Figure 1. Hydraulic conductivities from hydraulic packer tests in function of the average clay content in test intervals (average clay content of the 5 m clay-poorest layer in test intervals considered).

## P 13.15

### Morphological evolution of the Rhone River in the Martigny bend

Najla Schaller<sup>1</sup>, Samuel Luke Vorlet<sup>1</sup>, Azin Amini<sup>1</sup>, Giovanni De Cesare<sup>1</sup>

<sup>1</sup> Platform of Hydraulic Constructions, Swiss Federal Institute of Technology in Lausanne, CH-1015 Lausanne (najla.schaller@epfl.ch)

#### INTRODUCTION

Extreme events and altered river discharges related to climate change are expected to become more frequent and more pronounced in the coming years, leading to new challenges for existing infrastructure (Berga, 2016). Sustainable water management is therefore a principal matter to ensure safety of waterways. In this framework, the correction of the Martigny bend is a priority measure of the 3rd Rhone River correction in Switzerland, which aims at increasing the flood protection in the region while ensuring sustainable conditions for the Rhone River (Arborino and Jordan, 2014). The project foresees widening the bed of the river to the regime width and lowering the bed in the bend. A numerical model is built to represent the priority measure, in order to evaluate the impact of the project on sediment transport capacity and the morphological evolution in the long term.

#### METHODOLOGY

Numerical simulations are run using BASEMENT v.2.8 software (Vetsch et al., 2020). The model represents a 4870 m long segment of the Rhone River, including the Martigny bend, and the confluence with the Dranse River and the Trient River. The analysis type is transient analysis (2D modeling) considering multiphase flow.

The model uses shallow water equations (SWE) and the Meyer-Peter & Müller formulation adapted for multiple grain size classes by Hunziker (MPM-H) to predict flow features sediment transport respectively.

A mesh sensitivity analysis is performed, and parameters, such as roughness, grain size distribution and critical shear stress are defined. The validity of the numerical model is assessed comparing the results with a physical model. The morpho-dynamic behavior is analyzed using a steady-flow simulation for a 10- years return period flood over a 15-days duration.

#### RESULTS

Figure 1 shows the evolution of the morphology at the upstream part of the model and indicates a deposition zone in the widening with an advancing sediment front close to the bend. The Dranse is bringing a greater concentration of sediments. These sediments are transported and deposited in the Rhone and create a second deposition zone with advancing front. At the upstream part of the Dranse River, a deposition and erosion dynamic leads to the formation of a preferential channel. The grain size evolution presented in Figure 2 indicates that there is a grain size sorting and that the deposits are composed of finer sediments than the bed bottom grain size, both in the widening and at the confluence of the Rhone. The areas with the highest  $d_{50}$  (200 mm) correspond to non-erodible zones.

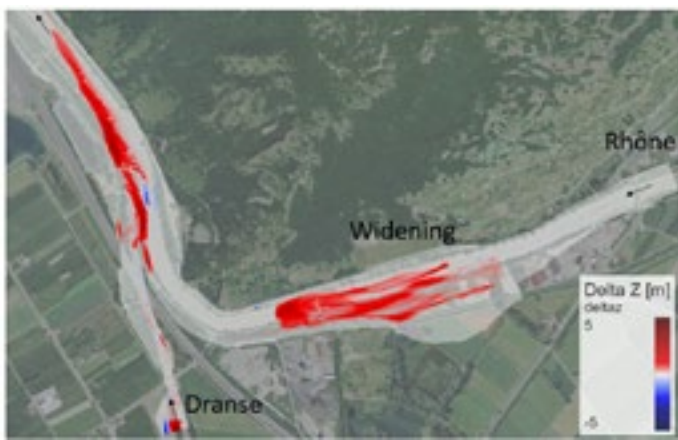


Figure 1 Bed variation of the Rhone River after 15 days



Figure 2 Diameter  $d_{50}$  of the Rhône River granulometry after 15 days

## CONCLUSION

A numerical model of the priority measure of the 3<sup>rd</sup> Rhône River correction is built to assess the impact of the project on the sediment transport capacity and the morphological evolution in long term. Results indicate that the river reach is dynamic. Erosion and deposition zones are identified and highlight that a preferential channel is established. In addition, sediment grain size sorting is observed on the river reach.

## REFERENCES

- Arborino, T., Jordan, J.-P., 2014. Flood protection along the Alpine Rhône river: Overall strategy and 3rd correction project, in: Swiss Competences in River Engineering and Restoration. CRC Press, pp. 49–59.
- Berga, L., 2016. The Role of Hydropower in Climate Change Mitigation and Adaptation: A Review. *Engineering* 2, 313–318. <https://doi.org/10.1016/J.ENG.2016.03.004>
- Vetsch, D., Bürgler, M., Gerke, E., Kammerer, S., Vanzo, D., Boes, R., 2020. BASEMENT – Softwareumgebung zur numerischen Modellierung der Hydro- und Morphodynamik in Fließgewässern. *Österr Wasser- und Abfallw* 72, 281–290. <https://doi.org/10.1007/s00506-020-00677-6>

## P 13.16

# Regional-Scale Thermal Hydraulic Modeling for Preliminary Geothermal Potential Assessment – A Theoretical Approach using the example of Riehen

Stefan Scheidler<sup>1</sup>, Horst Dresmann<sup>1</sup>, Jannis Epting<sup>1</sup>

<sup>1</sup> Applied and Environmental Geology, Hydrogeology Research Group, Department of Environmental Sciences, University of Basel, Bernoullistrasse 32, CH-4056 Basel (stefan.scheidler@unibas.ch)

Based on the approach of Tóth et al. (2020), we demonstrate how conceptual, generalized, and simplified Thermal Hydraulic Models (THM) can be used to simulate groundwater flow and heat transport and to support the identification of potential areas for the planned new medium-depth geothermal wells in the municipality of Riehen, Northwestern Switzerland. Regional-scale 2D THM were developed using COMSOL® based on geological section interpretations followed by an assessment of the influence of geological structures as well as the sensitivity of hydraulic and thermal parameters and boundary conditions. Preliminary modeling results show that the thermal regime can be modelled relatively accurately and reproduces measured temperature data (Figure). Furthermore, the most sensitive geologic units and parameters could be identified, which are faults (k-value and aperture) and aquitard (k-value, thermal conductivity) whereas the hydraulic parameters of aquifers have been recognized as not very sensitive.

The next step would be to use the gained experience and to update our existing high-resolution regional 3D geologic model, augment it with the recorded 3D seismic data, and develop a 3D THM. Information on 3D geothermal potential and groundwater flow regime would allow optimization of the location of production and injection wells for an efficient long-term use and to address groundwater protection issues already in the exploratory phase.

## REFERENCES

- Tóth, A., Gallo, A., Mádl-Szönyi, J. (2020) "Significance of basin asymmetry and regional groundwater flow conditions in preliminary geothermal potential assessment – Implications on extensional geothermal plays", Global and Planetary Change 195. DOI: doi.org/10.1016/j.gloplacha.2020.103344

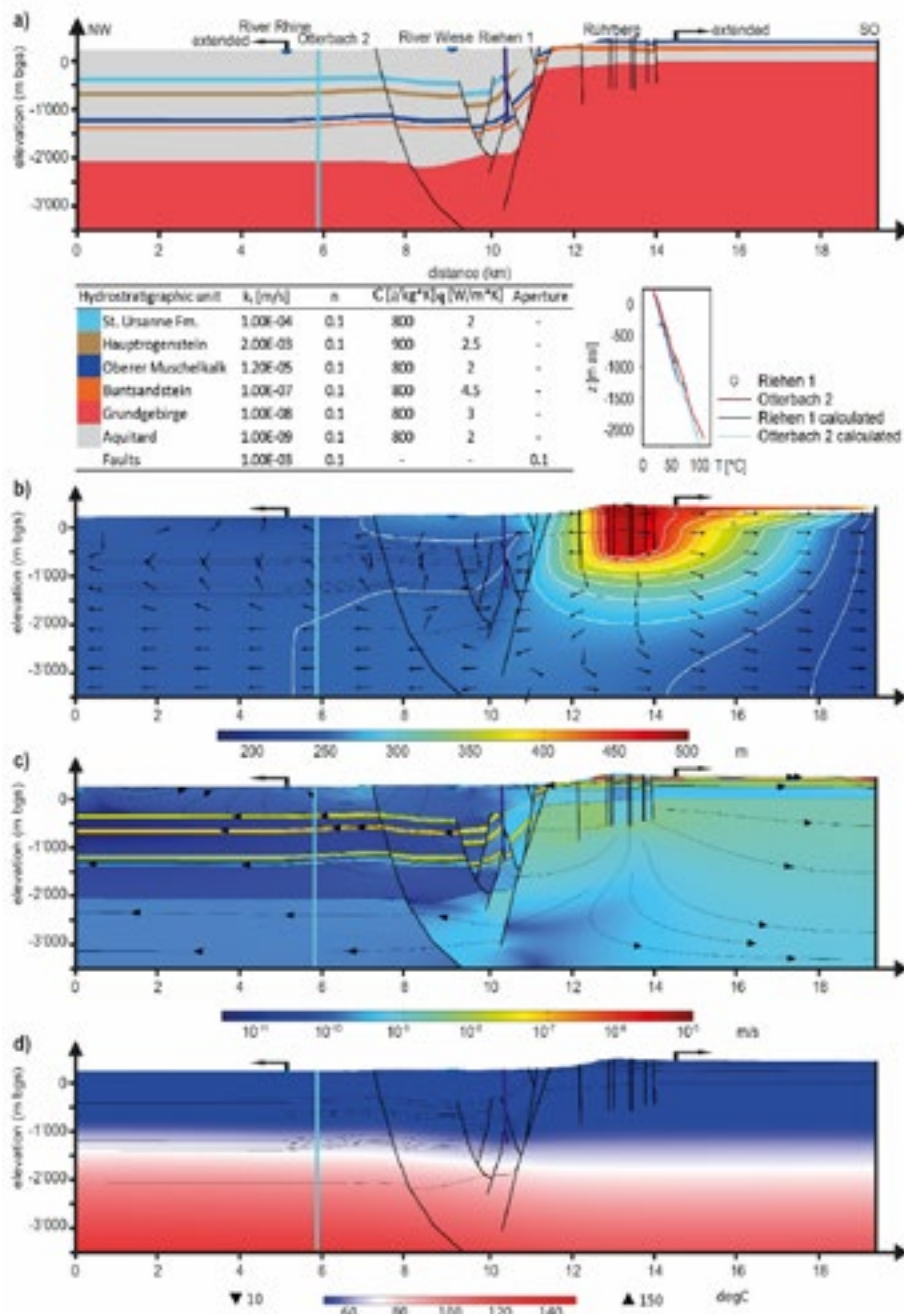


Figure: Regional-scale 2D THM: a) geologic profile extended on both sides to avoid boundary effects; b) simulated groundwater flow and thermal regime showing the hydraulic head and uniform Darcy velocity vector field; c) Darcy velocity magnitude with characteristic streamlines; d) simulated temperature field. The graph shows the measured and calculated vertical temperature profiles from the deep borehole Otterbach 2 in Basel and the existing geothermal well Riehen 1.

## P 13.17

# Pedotransfer functions for soil hydraulic properties of Swiss forest soils

Julian Schoch<sup>1</sup>, Lorenz Walther<sup>2</sup>, Madlene Nussbaum<sup>3</sup>, Andrea Carminati<sup>1</sup>, Peter Lehmann<sup>1</sup>

<sup>1</sup> Institute of Terrestrial Ecosystems, ETH Zürich, Universitätstrasse 16, CH-8092 Zürich

<sup>2</sup> Forest Soils and Biogeochemistry, WSL, Zürcherstrasse 111, CH-8903 Birmensdorf

<sup>3</sup> Forest and Food Sciences, BFH-HAFL, Länggasse 85, CH-3052 Zollikofen

Soil hydraulic properties (SHPs) are required to quantify water availability for water uptake by roots and to assess drought stress in forest trees from prolonged dry periods due to climate change. The measurement of SHPs is time consuming and requires complex instrumentation. An often-used alternative to measurements is the application of pedotransfer functions (PTFs) for estimating SHPs. PTFs are mathematical rules linking more easily obtainable soil information (e.g., soil texture, organic carbon content, pH, or cation-exchange capacity) with SHPs. Many of the available PTFs (for example, 'Rosetta', Schaap et al. 2001) were trained mainly on samples collected for arable land and therefore miss the effects of forest-specific soil formation processes (perennial vegetation, deep root systems, and high litter input alter the SHPs). These shortcomings can be avoided by building a PTF including soil samples from forests (Wessolek et al. 2009) or training it exclusively with forest soil samples as was done for southern Germany (Puhlmann and Wilpert 2011). However, as shown in Figure 1, none of the tested PTFs could successfully predict the water retention and hydraulic conductivity curve of Swiss forest soils that were described in Richard and Lüscher (1978, 1981, 1983, 1987). Consequently, we built a new PTF for Swiss forest soils using two statistical methods: linear regression and random forest. The new PTF was validated using soil samples collected from another study in Valais (Walther et al. 2021). The new PTF will be applied to estimate transpiration rates of forests in an ongoing research project.

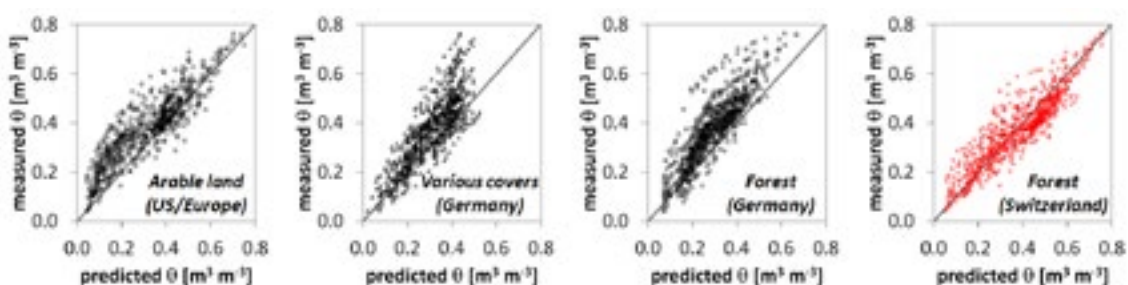


Figure 1. Comparison of water contents measured in Swiss forest soils (73 soil samples from 0 to 345 cm soil depth) with predictions using PTFs from the literature (black) and the new PTF (red). Each symbol denotes a water content measured at a specific matric potential. All previous PTFs underestimate the measured values (above 1:1 line).

## REFERENCES

- Puhlmann, H., & von Wilpert, K. 2011: Test und Entwicklung von Pedotransferfunktionen für Wasserretention und hydraulische Leitfähigkeit von Waldböden, Waldökologie, Landschaftsforschung und Naturschutz 12.
- Renger, M. et al. 2008: Ergebnisse und Vorschläge der DBG-Arbeitsgruppe „Kennwerte des Bodengefüges“ zur Schätzung bodenphysikalischer Kennwerte. Schriftenreihe „Bodenökologie und Bodengenese“, Heft 40.
- Richard, F. & P. Lüscher: Physikalische Eigenschaften von Böden der Schweiz. Vol. 1- 1978, 2-1981, 3-1983, 4-1987.
- Schaap, M. G. et al. 2001: Rosetta: a computer program for estimating soil hydraulic parameters with hierarchical pedotransfer functions. Journal of Hydrology 251.3, 163–176.
- Walther, L. et al. 2021: From the comfort zone to crown dieback: Sequence of physiological stress thresholds in mature European beech trees across progressive drought. Science of The Total Environment 753, 141792.

## P 13.18

### An ensemble based data assimilation framework for an integrated hydrological model: development and examples

Qi Tang<sup>1,2</sup>, Hugo Delottier<sup>1</sup>, Oliver S. Schilling<sup>1,2,3</sup>, Wolfgang Kurtz<sup>4</sup>, Philip Brunner<sup>1</sup>

<sup>1</sup> Centre for Hydrogeology and Geothermics (CHYN), University of Neuchâtel, 2000 Neuchâtel ([qi.tang@unine.ch](mailto:qi.tang@unine.ch))

<sup>2</sup> Hydrogeology, Department of Environmental Sciences, University of Basel, 4056 Basel

<sup>3</sup> Eawag, Swiss Federal Institute of Aquatic Science and Technology, 8600 Dübendorf

<sup>4</sup> Agrometeorology, Deutscher Wetterdienst, 63067 Offenbach, Germany

Ensemble-based data assimilation combines prior information from numerical model simulations with real-world observations to obtain the best estimates of model states (e.g. hydraulic heads) and even the parameters (e.g. hydraulic conductivity). In hydrological modeling, through assimilating tracers such as noble gases, the real-time operational simulation of water quantity, as well as quality, can be achieved. This can open, for instance, new windows for model-based operation of drinking water production. In this study, we developed a data assimilation framework for an integrated hydrological model. The Parallel Data Assimilation Framework (PDAF, <http://pdaf.awi.de>), which is a software environment for ensemble data assimilation has been coupled to the physically based hydrological model HydroGeoSphere for surface water – groundwater simulation. Multiple types of observations such as piezometric heads, streamflow, and tracer concentrations can be assimilated together. Both the model states and the parameters can be separately or jointly updated by the assimilation algorithm. Numerical experiments based on a Swiss drinking water wellfield are carried out for both the flow and transport simulations. One or multiple types of observations are assimilated. These observations include piezometric heads and noble gas concentrations such as <sup>222</sup>Rn, <sup>37</sup>Ar, and <sup>4</sup>He. The results are evaluated by comparing the estimated model variables with independent observation data between the assimilation runs and the free run where no data assimilation is conducted.

## P 13.19

# Impact of gold mining storage tailings on groundwaters and surface waters: the case of Hiré (southern Ivory coast)

Assiata Traore Dosso<sup>1</sup>, Hélène Gillet<sup>4</sup>, Jean Kan Kouamé<sup>3</sup>, Robin Marc Dufour<sup>1,2</sup>, Nathalie Chèvre<sup>1</sup>,

<sup>1</sup> IDYST, Faculty of Geosciences and Environment, University of Lausanne, Geopolis Building, CH-1015 Lausanne (assiata.traoredosso@unil.ch),

<sup>2</sup> VP DHI-Mining GBU-Senior Hydrogeologist, University of Neuchâtel, Rue Emile-Argand 11, CH 2000 Neuchâtel

<sup>3</sup> CURAT, University Centre for Research and Application in Teledection, University of Félix HOUPHOUËT-BOIGNY, Boulevard of University, 22 BP 801 Abidjan 22, Ivory Coast

<sup>4</sup> Hydrogeologist engineer and modeler, Ecole Nationale Supérieure de Géologie (Nancy) and Denis Diderot University – IPGP (Paris), France.

### Abstract

The development of the mining industry in Bonikro, started in 2007, was seen as an economic opportunity for the locality of Hiré. The expansion of artisanal gold mining led to the industrial mining event in the area. This so called “mining boom”, while generating huge amounts of capital, is putting an enormous pressure on both agricultural activities and the preservation of the environment, in particular water resources. In order to contribute to the safeguarding of water resources of this region, this research project was initiated.

It aims in modelling the impact of these mining activities on the water resources of the sites exploited in the Hiré region. As a first step, the description of the hydrogeological system of the area will be done. To achieve this, a conceptual model of the site was developed and used to identify the flows of water. Based on this description, a simplified model will be implemented under Feflow code to predict the flow direction of groundwater. Therefore, this modelling requires need accurate data such as topography, geology, rainfall, temperature, evaporation, water chemistry, boundary conditions, pumping rate, hydrological regime, faults, etc. However, for reasons of data confidentiality and difficulty of access to the industrial mining site, data acquisition for such a project is often difficult. Thus, hypotheses were formulated and data from the literature were used to overcome this difficulty. In addition, the results of a model require validation by field data. The first results of the modelling will be presented on the poster.

Key words: Bonikro, Hiré, gold mining activities, heavy metals pollution, ground and surface water quality

### General context

The locality of Hiré is located 45 km from Divo in the South Bandama region of Côte d'Ivoire. The mining activity, formerly practised by gold panners in alluvial and eluvial zones (Gaston, 1913; Chauveau, 1978), was taken over in 1920 in a semi-industrial manner by the colonists, thus putting an end to gold panning (Kouadio, 2008). From then on, the local population turned to the agricultural sector, which flourished before the cocoa crisis of the 1980s. This led to a shift in the economic model towards industrial mining in 2007, using a leaching process that produces a high recovery of gold (Haque, 1992), from the Bonikro gold deposits before spreading to the rest of the Hiré locality. Thus, mining generates large quantities of toxic waste, which must be properly managed to avoid impacting ecosystems ARIA, (2008) and AGC, (2015).

An analysis of investigations conducted (Bamba, 2012; Yapi et al., 2014; and ADHP, 2019) in surface and groundwater in Hiré ville and in the vicinity of the Bonikro mining site have shown the presence of cyanide, mercury, and TMEs at levels above the WHO limit values for drinking and irrigation water. In 2020, the Konan studies revealed the occurrence of new skin diseases in the Bonikro area. However, no study in Hiré has formally demonstrated a causal link between the presence of the mine and these new diseases.

As in Japan, causal links were established for Minamata disease (1950) due to mercury poisoning (Gillet, 2018). Moreover, Zhang et al, (2012), have shown that excess lead and cadmium can cause health effects (arthralgia, osteomalacia). It is therefore time to address the issues of the impact of mining on the environment and on the people living in the vicinity of the industrial mines in Hiré. To achieve this goal, it would be necessary to combine remote sensing and hydrogeological modelling to understand the hydrodynamic functioning of groundwater in the Hiré city in a context of environmental transformation.

### REFERENCES

AGC. (2015) : Artisanal Gold Council. L'orpaillage et la santé.

ARIA. (2008) : Pollution des eaux par des effluents cyanurés en Europe de l'Est Le 30 janvier 2000 Baia Mare Roumanie, article n°17265,

- Bamba, Y. (2012). Évaluation des impacts de l'exploitation de la mine d'or de Bonikro (côte d'ivoire) sur les ressources en eau. 55p
- Gillet. P (2018) : Histoire de l'écotoxicologie. Volume 1, N°1, pp : 01 - 04 (2018), ISSN : 2605-6208
- KONAN. K.H (2020) : Industrie minière et systèmes d'activités de ménages des populations rurales du secteur minier de Bonikro. La revue des Sciences Sociales « Kafoudal » N° Spécial Janvier 2020, 56p en ligne (Université Péléforo-Gbon-Coulibaly), Consulté le 01.12.2017 à 15h30
- Yapi et al. (2014). Evaluation de la pollution métallique d'un environnement minier aurifère : cas de la sous-préfecture de Hiré (Côte d'Ivoire), 118p.
- Zhang, X., Yang, L., Li, Y., Li, H., Wang, W., Ye B. (2012) : Impacts of lead/zinc mining and smelting on the environment and human health in China. Environ Monit Assess (2012) 184 :2261–2273

## P 13.20

# HYDROpot\_integreal: a tool to simultaneously assess hydropower potential and ecological potential

Wechsler Tobias<sup>1,2</sup>, Hug Peter Dorothea<sup>1</sup>, Bätz Nico<sup>3</sup>, Zappa Massimiliano<sup>1</sup>

<sup>1</sup> Swiss Federal Institute for Forest, Snow and Landscape Research WSL, Zürcherstrasse 111, 8903 Birmensdorf, Switzerland

<sup>2</sup> Institute of Geography (GIUB) and Oeschger Centre for Climate Change Research (OCCR) University of Bern, Hallerstrasse 12, 3012 Bern, Switzerland

<sup>3</sup> Swiss Federal Institute of Aquatic Science and Technology EAWAG, Seestrasse 79, 6047 Kastanienbaum, Switzerland

Low greenhouse gas emissions make hydropower a so-called climate-friendly electricity source. In Switzerland, hydropower is the most important electricity source, accounting for about 60% of total electricity production. However, the 1700 hydropower plants in Switzerland also alter river hydrology, habitats and connectivity, leading to biodiversity loss and ecosystem degradation. This leads to a conflict between the goals of the energy transition aiming for a climate-friendly energy production and the goal of natural conservation aiming for a reduction of negative impacts on freshwater ecosystems. A spatial explicit strategic assessment for hydropower localisation that compares environmental impact with hydropower production potential is crucial to reduce such conflicts. The tool HYDROpot\_integreal is based on 70 geospatial datasets that are used to quantify for each river segment both the hydropower potential and the ecosystem potential (respecting sustaining, cultural and providing ecosystem functions). HYDROpot\_integreal has been compiled for Switzerland and is freely accessible. In this study we show the potential of the tool and compare the current state with the potential impacts of a 20% increase of hydropower power production for the Kander catchment. The findings of the study contribute to address the challenges of the cumulative effects of hydropower and explore how to account for the longitudinal connectivity to better implement these effects in HYDROpot\_integreal.

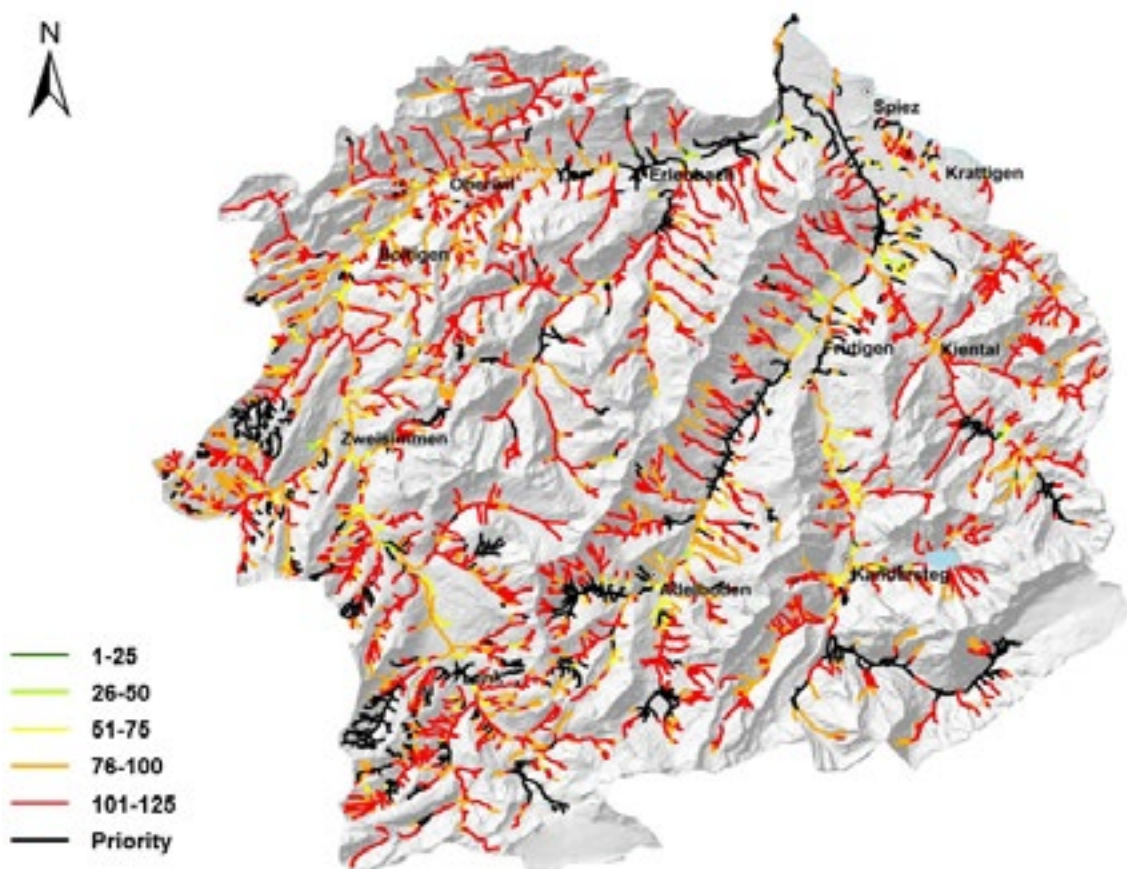


Figure 1. Quantification of sustaining, cultural and providing ecosystem functions in the Kander catchments (BE). Rank 1 is most suitable for hydropower production at minimum cost in terms of ecological and cultural ecosystem functions; rank 125 indicates the highest ecological and cultural ecosystem functions and the lowest economic functions and is therefore most suitable for protection; the Priority reaches (black) exclude use by law.

## REFERENCES

- Hemund, C. (2012): Methodik zur ganzheitlichen Beurteilung des Kleinwasserkraftpotentials in der Schweiz. Inauguraldissertation, Leiter: Prof. Dr. R. Weingartner. Universität Bern, Geographisches Institut.
- Hirschi, J., Wechsler, T., Rey, E., Weingartner, R. (2013): Ganzheitliche Beurteilung des Wasserkraftpotentials schweizerischer Fließgewässer – Handbuch zur GIS-gestützten Anwendung der Methode HYDROpot\_integral. Bericht im Auftrag des BfE. Publikation Gewässerkunde Nr. 608, Bern.
- Lange, K., Wehrli, B., Åberg, U., Bätz, N., Brodersen, J., Fischer, M., Hermoso, V., Liermann, C. R., Schmid, M., Wilmsmeier, L., Weber, C. (2019). Small hydropower goes unchecked. *Frontiers in Ecology and the Environment*, 17(5), 256–258.
- Laub, C., Wechsler, T., Hug Peter, D., Zappa, M., Weingartner, R. (2022). HYDROpot\_integral. EnviDat. doi:10.16904/envidat.325.

## P 13.21

# Hydrological modelling with real and synthetic snow cover data assimilation

Pau Wiersma<sup>1</sup>, Fatemeh Zakeri<sup>1</sup>, Grégoire Mariéthoz<sup>1</sup>

<sup>1</sup>*University of Lausanne, Faculty of Geosciences and Environment, Institute of Earth Surface Dynamics, Switzerland*

To study long-term changes in the hydrology of snow-fed catchments, there is a need for long-term time series of snow cover data. Satellite imagery and climate reanalysis can both be used to quantify past snow cover, but they lack in baseline period length and spatial resolution respectively. In this study we apply a similarity-based method to generate synthetic high-resolution daily snow cover maps, and consequently combine these maps with hydrological model outputs in a data assimilation framework. The results are benchmarked against a case without synthetic snow cover forcing and a case with only observed snow cover maps. The study is performed on the Thur-Jonschwil sub-catchment in Eastern Switzerland, a meso-scale catchment covering a wide elevation range and experiencing different degrees of snow intermittency. With the currently implemented Direct Insertion data assimilation, the streamflow simulation performance slightly deteriorates but the SWE estimates improve significantly. To further explore the robustness of the methodology and the validity of these findings we will consider other data assimilation algorithms and hydrological models in the near future.

## P 13.22

### Multiple-point Geostatistics-based spatial downscaling of heavy precipitation

Wenyue Zou, Guanghui Hu, Pau Wiersma, Grégoire Mariéthoz, Nadav Peleg

High-resolution precipitation data in space and time is critical for many hydrometeorological, ecological, and environmental applications. At regional scales, gridded precipitation data are often obtained through remote sensing. However, their spatial resolution is often too coarse (i.e.  $10^1$  km) and requires to be downscaled to a finer resolution (i.e.  $10^0$  km). We demonstrate how the Multiple-point Geostatistics (MPS) framework can be used to downscale the CMORPH precipitation product from 8 km to 1 km resolution. We take the city of Beijing as a case study, with a specific focus on extreme precipitation events during 1998 - 2009. The high-resolution CMAPS dataset (1 km, hourly), available for the period 2015 - 2020, is used as a source of training images in the MPS framework. Three ground stations with hourly rainfall observation from 1950 to 2012 were used for validation. The study shows that: (i) After quantile-correcting the CMORPH data based on the CMAPS data, its exceedance probabilities at the three stations are closer to that of upscaled CMAPS and observations, which helps improve the search for training images in the MPS model; (ii) Structural similarity indexes higher than 0.8 are found for 100% (summer), 94% (autumn), and 97% (spring) of the downscaled precipitation fields, meaning that the downscaled precipitation preserves the spatial structures well, especially for summer extreme precipitations; (iii) After an adjustment of the intensities of the downscaled precipitation field using a scaling law with a spatial coefficient of variation factor, the 25 - 75% quantile values (low-precipitation intensities) agree with that of ground station observations, while the 90 - 99% quantile values (high-precipitation intensities) agree with the expected intensification due to the changes in spatial scales expected from the theoretical rainfall areal reduction factor. The results indicate that the downscaled precipitation field obtained from the MPS model preserves the precipitation spatial structure well and adequately estimates the intensities, especially for heavy precipitation. The proposed downscaled approaches can be applied to other precipitation datasets and in other regions.



# 14 Limnology in Switzerland

Damien Bouffard, Michael Döring, Natacha Tofield-Pasche

*Swiss Society for Hydrology and Limnology SGHL*

## TALKS:

- 14.1 Bärenbold F., Herold T., Bouffard D., Schmid M.: Towards a Swiss lake temperature monitoring network
- 14.2 Einzmann T., Lehmann M., Zopfi J., Frey C.: Biogeochemical controls on nitrous oxide production and consumption in Lake Lugano, Switzerland
- 14.3 Ekoa Bessa A.Z., Ndjigui P.-D. , Adatte T.: Holocene lacustrine paleoenvironmental evolution, examples from Cameroon lakes (SW-Africa)
- 14.4 Escoffier N., Perolo P., Many G., Tofield Pasche N., Perga M-E.: Tracing calcite precipitation at fine scale in Lake Geneva
- 14.5 Forrest T., Cherubini T., Jeanneret S., Zdrachek E., Damala P., Bakker E.: Self-Contained Submersible Potentiometric Probe for Real-Time In Situ Carbonate and pH Concentration Measurements
- 14.6 Gressard T., Layglon N., Bakker E., Tercier-Waeber M.: In situ assessment of the behavior and fate of the dynamic fraction of inorganic arsenic species.
- 14.7 Gupana R., Damm A., Irani A., Minaudo C., Odermatt D.: Quantum yield and quenching: Investigating phytoplankton sun-induced fluorescence from in-situ hyperspectral measurements in Lake Geneva
- 14.8 Larivé O., Wynn HK., Kohn T.: Effect of lake exposure on a population of enteroviruses
- 14.9 Layglon N., Creffield S., Bakker E., Tercier-Waeber M-L.: Quantification of the nioxime-labile Ni and Co concentrations in Lake Geneva during a diurnal cycle
- 14.10 Many G., Escoffier N., Ferrari M., Jacquet P., Mariethoz G., Perolo P., Odermatt D., Perga M-E.: Long-term spatiotemporal variability of whiting in Lake Geneva from multispectral remote sensing and machine learning
- 14.11 Mettra F., Mattei F., Lemmin U., Barry D.A.: Effects of coastal upwelling and its relaxation along the northern shore of Lake Geneva
- 14.12 White M., Mittelbach B., Haghipour N., Blattmann T., Jacquin C., Dubois N., Eglinton T.: Radiocarbon and stable carbon isotope measurements of dissolved inorganic and organic carbon from the LéXPLORÉ platform on Lake Geneva

**POSTERS:**

P 14.1 Herr I., Perga M.E., Bouffard D.: Impact of inflow on mountain lake heat flux

P 14.2 Wegmann M., Tofield-Pasche N.: Two very different summers for Lake Geneva as observed by the LéXPLORÉ platform

## 14.1

### Towards a Swiss lake temperature monitoring network

Fabian Bärenbold<sup>1</sup>, Thilo Herold<sup>2</sup>, Damien Bouffard<sup>1</sup>, Martin Schmid<sup>1</sup>

<sup>1</sup> Dept. of Surface Waters – Research and Management, Eawag, Seestrasse 79, CH-6047 Kastanienbaum  
(fabian.baerenbold@eawag.ch)

<sup>2</sup> Hydrology Division, Federal Office for the Environment, Papiermühlestrasse 172, CH-3063 Ittigen

Lakes and reservoirs are experiencing major changes world-wide as a result of climate warming. For Swiss lakes, a reduction in ice cover, an increase of the duration of summer stratification and a shift of dimictic to monomictic mixing regime for mid-altitude lakes is expected (Vinnå et al., 2021). Such changes can have large impacts on lakes as ecosystems. The temperature of most larger lakes in Switzerland is already monitored by cantonal agencies. However, the time resolution of this monitoring is usually monthly to bi-monthly and therefore, long-lasting time series are needed to accurately detect and describe changes. (Bouffard et al., 2019).

The Swiss Federal Agency for the Environment (FOEN) has decided to establish its own monitoring network of lake and pond temperatures across Switzerland. It has mandated Eawag to deploy high-resolution pilot measurement stations in several lakes and ponds (see Figure 1) and to give recommendation on how to couple observations with numerical modelling.

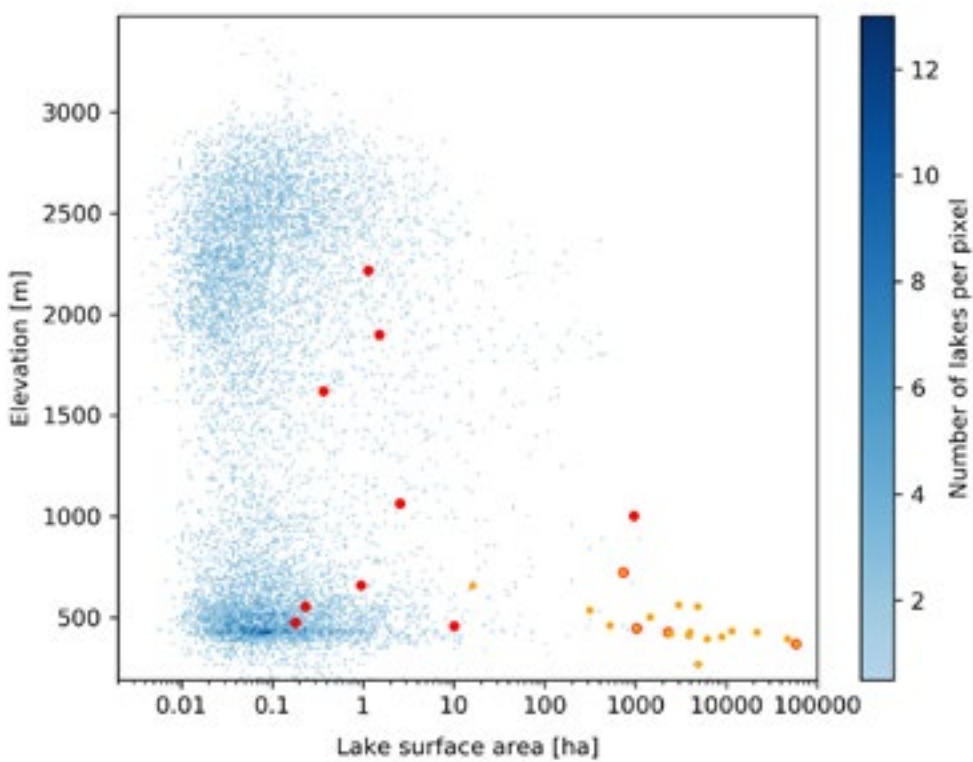


Figure 1. Distribution of the > 11'000 Swiss water bodies larger than 30 m<sup>2</sup> as a function of area and elevation (taken from the Swiss landscape model Vector25). Red dots indicate water bodies with pilot stations within this project; orange dots indicate lakes with at least 3 profiles per year by cantonal agencies.

Within this project we investigate the following research questions:

- How can small and remote water bodies be monitored in a cost and time effective way?
- Are low-cost temperature sensors accurate enough to document mixing dynamics in shallow ponds?
- Should temperature sensors be sheltered from sunlight and if yes, how?
- For larger lakes, is it more useful to have a temperature mooring (i.e. sensors at fixed depths) or a profiling system (i.e. one probe going up and down)?
- How, when and in which lakes should we monitor to achieve a representative monitoring system across Switzerland?
- How can numerical modelling be used to infer temperature dynamics of unobserved (i.e. without temperature measurements) lakes?

Here, we will present measurements from pilot monitoring stations along with learnings from the first 1.5 years of deployment. In addition, we show how water temperature sensors react to direct sunlight and discuss whether this is an issue for water temperature monitoring.

Because measurements are costly and time-consuming, we evaluate the use of the one-dimensional lake model Simstrat (Gaudard et al., 2019) as a complement to direct observations. The operational simulation platform <https://simstrat.eawag.ch> was extended to small lake and ponds and now simulates close to 100 Swiss lakes. These calibrated lakes can serve as a basis to infer model parameters of unobserved (and thus uncalibrated) lakes in the future.

## REFERENCES

- Bouffard, D., Dami, J., & Schmid, M. (2019). Swiss lake temperature monitoring program. Report Commissioned by the Federal Office for the Environment (FOEN).
- Gaudard, A., Råman Vinnå, L., Bärenbold, F., Schmid, M., & Bouffard, D. (2019). Toward an open access to high-frequency lake modeling and statistics data for scientists and practitioners—the case of Swiss lakes using Simstrat v2.1. *Geoscientific Model Development*, 12(9), 3955-3974.
- Vinnå, L. R., Medhaug, I., Schmid, M., & Bouffard, D. (2021). The vulnerability of lakes to climate change along an altitudinal gradient. *Communications Earth & Environment*, 2(1), 1-10.

## 14.2

# Biogeochemical controls on nitrous oxide production and consumption in Lake Lugano, Switzerland

Teresa Einzmann<sup>1</sup>, Moritz Lehmann<sup>1</sup>, Jakob Zopfi<sup>1</sup>, Claudia Frey<sup>1</sup>

<sup>1</sup> Department of Environmental Sciences, University of Basel, Bernoullistrasse 30, CH-4056 Basel  
(teresa.einzmann@unibas.ch)

Nitrous oxide ( $\text{N}_2\text{O}$ ) is a strong greenhouse gas and an ozone-destroying agent, the concentration of which in the atmosphere has been increasing significantly over the last few decades. The contribution of lacustrine systems to global  $\text{N}_2\text{O}$  emissions is uncertain because of a lack of understanding of the environmental controls on the production and consumption processes involved in  $\text{N}_2\text{O}$  cycling, and their spatial and temporal variability.

In this study, we investigate seasonal  $\text{N}_2\text{O}$  cycling in Lake Lugano, a eutrophic South alpine lake located at the Swiss-Italian border, which serves as an excellent model system for an anthropogenically impacted lake. The lake consists of two main basins with different mixing regimes. The North Basin is permanently stratified with an anoxic and sulfidic deep hypolimnion, whereas the South Basin shows seasonal stratification and bottom-water anoxia during summer and complete mixing in winter. These contrasting mixing dynamics can potentially lead to different seasonal  $\text{N}_2\text{O}$  emission patterns, which we investigate. While there is significant interannual and seasonal variability in  $\text{N}_2\text{O}$  concentrations particularly in the South Basin, the episodic occurrence of very high  $\text{N}_2\text{O}$  concentrations (up to 900 nmol/l) in both basins have been observed, which begs a more detailed investigation of processes that produce or consume  $\text{N}_2\text{O}$  in Lake Lugano.

$\text{N}_2\text{O}$  can be formed as a byproduct during nitrification in the oxic environment, i.e., the stepwise oxidation of ammonium to nitrate. Another important process contributing to  $\text{N}_2\text{O}$  production is nitrifier denitrification by ammonium-oxidizing bacteria at low oxygen levels, where nitrite is sequentially reduced to  $\text{N}_2\text{O}$ . Denitrification on the other hand is the main sink for  $\text{N}_2\text{O}$  via the reduction of nitrate over nitrite over  $\text{N}_2\text{O}$  to finally  $\text{N}_2$  under anaerobic conditions. However, incomplete denitrification can result in the accumulation of  $\text{N}_2\text{O}$  particularly at the suboxic-anoxic interface. Here, we study the isotopic composition of  $\text{N}_2\text{O}$  throughout the water column over one year in order to identify reductive versus oxidative  $\text{N}_2\text{O}$  production (the different  $\text{N}_2\text{O}$  production pathways are known to produce distinct  $\text{N}_2\text{O}$ -isotopic/isotopomeric signatures). Moreover, via tracer incubation experiments using  $^{15}\text{N}$  labeled nitrogen compounds ( $^{15}\text{NH}_4^+$ ,  $^{15}\text{NO}_2^-$ ,  $^{15}\text{NO}_3^-$ ,  $^{15}\text{N}_2\text{O}$ ), seasonal rate fluctuations of processes involved in  $\text{N}_2\text{O}$  cycling will be investigated throughout the water column of both basins. First results of  $^{15}\text{N}_2\text{O}$  incubation experiments show that in the permanently stratified North Basin, the last step in denitrification, i.e., the reduction of  $\text{N}_2\text{O}$  to  $\text{N}_2$ , only takes place in the presence of  $\text{H}_2\text{S}$ , highlighting sulfide-dependent chemolithotrophic denitrification as important control on the accumulation of  $\text{N}_2\text{O}$  in the water column. In contrast, in the South Basin, denitrification is not dependent on  $\text{H}_2\text{S}$  but was found to occur during the stratification period in the anoxic hypolimnion indicating heterotrophic denitrification. The ongoing work investigating the different processes producing and consuming  $\text{N}_2\text{O}$  in Lake Lugano will help to gain a better picture of  $\text{N}_2\text{O}$  cycling in this lake, and its role as a  $\text{N}_2\text{O}$  source or sink to the atmosphere throughout the year, with general implications for lacustrine  $\text{N}_2\text{O}$  emissions under different mixing regimes.

## 14.3

### Holocene lacustrine paleoenvironmental evolution, examples from Cameroon lakes (SW-Africa)

A. Z. Eko Bessa<sup>1</sup>, P-D Ndjigui<sup>2</sup>, T. Adatte<sup>1</sup>

<sup>1</sup>*University of Lausanne, Bâtiment Géopolis, UNIL-Mouline, CH-1015 Lausanne (armelekao@yahoo.fr)*

<sup>2</sup>*Faculty of science, University of Yaoundé 1 (CMR), PO BOX 812, Yaounde, Cameroun*

Lakes are the most attractive and expressive characteristics of a landscape. Lacustrine sediments provide a historical record of the conditions prevailing in the catchment environments. They are highly sensitive to paleoenvironmental change. The aim of this study is to reconstruct the paleoenvironment of 3 lakes located in Yaoundé, Dizangué and Ngaoundaba regions (Cameroon, SW-Africa) for the last 1000 years using a multiproxy approach including sedimentology, mineralogy, geochemistry, radiocarbon dating, diatoms and palynology.

Sediment samples were taken from a raft and polyvinyl chloride (PVC) pipes. They generally consist of sub-rounded and sometime rounded particles indicative of both aeolian and medium fluvial transport. Their physical and chemical features suggest both proximal and distal origins. The presence minerals such as quartz, kaolinite, smectite, hematite, goethite, feldspars, rutile and calcite with traces of illite, vivianite and ilmenite suggest high weathering under warm and humid conditions.

According to geochemistry, the sediments derived from felsic, intermediate and mafic rocks from nearby granitic, gneissic and basaltic rocks. Weathering indices indicate high intensity of alteration related to both active and passive margin tectonism. Element ratios indicate a low compositional maturity in oxic and low salinity paleoenvironment. These sediments were deposited in a shallow marine and fluvial depositional environments with an increase water depth environmental condition. According to radiocarbon dating, the studied sediments are Holocene in age. Palynological and diatom data reveal major hydrological changes, which occurred over the last 1000 years, mainly characterized by strong fluctuations in wet and dry conditions during the «Medieval Warm Period» (1100-800 yrs BP) and dry conditions during the «Little Ice Age» (500-300 yrs BP). These hydrological changes have controlled the dynamics of tropical rainforests in this part of Africa, resulting in their expansion during periods of heavy rainfall and contraction during periods of reduced rainfall.

Keywords: Sedimentology, geochemistry, diatoms, palynology, paleoenvironmental reconstruction, lacustrine sediments.

## 14.4

### Tracing calcite precipitation at fine scale in Lake Geneva

Nicolas Escoffier<sup>1</sup>, Pascal Perolo<sup>1</sup>, Gaël Many<sup>1</sup>, Natacha Tofield Pasche<sup>2</sup>, Marie-Elodie Perga<sup>1</sup>

<sup>1</sup> Institute of Earth Surface Dynamics, University of Lausanne, CH-1015 Lausanne ([nicolas.escoffier@unil.ch](mailto:nicolas.escoffier@unil.ch))

<sup>2</sup> Limnology Center, ENAC, Ecole Polytechnique Fédérale de Lausanne, CH-1015 Lausanne

In hardwater lakes, calcite precipitation is a pivotal yet understudied process of the lacustrine carbon cycle by which catchment-derived alkalinity (Alk) is transformed. While the thermodynamic conditions supporting the supersaturation of water with respect to calcite are theoretically well described, to date, the magnitude and conditions underlying calcite precipitation at fine temporal and spatial scales remain poorly constrained, especially in large and deep lakes. In this study, we used multi-sensor high frequency depth-resolved (0 – 30m) data collected over 18 months (June 2019 – November 2020) in the deeper basin of Lake Geneva to capture the dynamics of calcite precipitation fluxes at a fine temporal resolution (day to season) and to scale them to carbon fixation by primary production. Calcite precipitation occurred during the warm stratified seasons when surface water CO<sub>2</sub> concentrations were below atmospheric equilibrium. At the seasonal scale, the extent of Alk loss through calcite precipitation (i.e., [30 – 42] g C m<sup>-2</sup>) depended upon the level of Alk in surface waters. Moreover, interannual variability was related to the duration and depth of the stratification, conditioning the volume of the corresponding water layer susceptible to calcite precipitation. At finer timescales, calcite precipitation was characterized by a marked daily variability whose dynamics was strongly related to that of planktonic autotrophic metabolism. Increasing daily calcite precipitation rates (i.e., maximum values 9 mmol C m<sup>-3</sup> d<sup>-1</sup>) coincided with increasing net ecosystem production (NEP) during periods of enhanced water column stability. In these conditions, carbon-derived calcite precipitation and NEP rates eventually reached equimolar values. This study provides a refined mechanistic perspective on the conditions driving pelagic calcite precipitation, quantifying its essential role in the coupling of organic and inorganic processes within the lacustrine carbon cycle.

## 14.5

# Self-Contained Submersible Potentiometric Probe for Real-Time *In Situ* Carbonate and pH Concentration Measurements

Tara Forrest<sup>1</sup>, Thomas Cherubini<sup>1</sup>, Stéphane Jeanneret<sup>1</sup>, Elena Zdrachek<sup>1</sup>, Polyxeni Damala<sup>1</sup>, Eric Bakker<sup>1</sup>

<sup>1</sup> Department of Inorganic and Analytical Chemistry, University of Geneva, Quai Ernest-Ansermet 30, CH-1221 Genève (tara.forrest@unige.ch)

With an ever-growing concern about greenhouse gases being released into the atmosphere, being able to carefully monitor all species associated to the carbon cycle is of crucial importance. In freshwater systems, dissolved inorganic carbon is mainly found as carbonate and bicarbonate ions. They play a key role in many chemical processes, such as pH regulation. Increased carbon dioxide partitioning from the atmosphere may ultimately cascade into lake acidification or species extinction. Water quality is generally monitored at fixed sampling stations and only give intermittent indication on local concentrations. Due to the dynamic processes occurring between carbonate species and pH, *in situ* detection methods are greatly preferred over traditional sampling and remote analysis, which require rigorous and tedious procedures that are prone to errors.

Based on recent work (Forrest et al. *submitted*) we present here a new self contained submersible probe that can analyse carbonate and pH autonomously without an external power source or regular maintenance. The setup includes a raft equipped with solar pannels, a bluetooth antenna and a battery. It is estimated that just 2 h of sunlight are required daily to power the entire system. The excess can be stored in the backup battery and used to power the device during the night or in the absence of sunlight. When fully charged the battery can power the system for eight days. The probe is directly mounted to the raft and can be deployed at various depths, depending on the type of measurements that are required. The aquired data are stored internally on an SD card for backup but can be accessed remotely from any location thanks to the communication module implemented on the raft. Basic troubleshooting of the intrument can also be performed through this channel, reducing the need for on-site maintenance. Direct access to the concentration (not activity) of the analyte is made possible by a one-step calibration procedure that runs at predetermined time intervals. Improved signal stability and reduction of temperature dependence are achieved by using a new reference element based on the principle of electrochemical symmetry. This probe has been deployed in Lake Geneva during a field campaign performed at the LéXPLORÉ platform. Good crosscorrelation with reference methods and constant access to analyte concentration make this system a valuable tool for autonomous environmental analysis.

## REFERENCES

Forrest et al., 2022: Submersible Probe with In-line Calibration and Symmetrical Reference Element for Long-term Continuous Direct Nitrate Concentration Measurements [Manuscript submitted for publication]

## 14.6

### ***In situ assessment of the behavior and fate of the dynamic fraction of inorganic arsenic species.***

Tanguy Gressard<sup>1</sup>, Nicolas Laylon<sup>1</sup>, Eric Bakker<sup>1</sup>, Marylou Tercier-Waeber<sup>1</sup>

<sup>1</sup> Dept. of Inorganic and Analytical Chemistry, University of Geneva, 30 Quai E.-Ansermet, 1211 Geneva 4, Switzerland.

Arsenic, from natural and anthropogenic sources, is an ubiquitous metalloid of global concern. Arsenic is persistent, has carcinogen properties, tendency to bioaccumulate and bio-amplify through the food chain. Therefore, international provisional guidelines for water quality and water quality criteria have been established. However, all guidelines are based on the total dissolved As concentration, while it is well known that the toxicity and bioavailability of As is highly dependent on its chemical form and oxidation state [1]. Arsenic in the aquatic environment is mainly present under inorganic forms which are generally more toxic than the organic ones. Experiments performed in synthetic media, with higher As concentrations than the one encountered in natural media, shown that biotic parameters may regulate the inorganic arsenic speciation [1]. In natural waters, inorganic speciation evolve in time and space which highlight the need of in situ high resolution monitoring.

We report here, the determination of the dynamic inorganic As species on a nanofilament gold-plated microelectrode array (AuNF-GIME) covered with an antifouling gel incorporated in a submersible probe named TracMetal [2]. These fractions represent the fraction available for bio-uptake. The analytical method consists of a sequential detection of the dynamic inorganic As(III) followed by the total dynamic inorganic arsenic using Square Waves Anodic Stripping Voltammetry. The dynamic inorganic As(V) is then calculated by subtraction. The variation of the inorganic As speciation at hour time scale and space (in depth) during contrasting seasonal conditions will be presented. Preliminary hypothesis on the influence of biotic and abiotic processes on dynamic As species will be discussed by comparison of the in situ As and master bio-physicochemical parameters and complementary laboratory analyses in collected samples. This study is part of a LéXPLORÉ project (SyBAM: Synergic interaction between arsenic and microorganism).

#### REFERENCES

- [1] Barral-Fraga L, Barral MT, MacNeill KL, Martíñá-Prieto D, Morin S, Rodríguez-Castro MC, et al. 2020: Biotic and Abiotic Factors Influencing Arsenic Biogeochemistry and Toxicity in Fluvial Ecosystems: A Review, International journal of environmental research and public health, 17(7), 2331.
- [2] Tercier-Waeber M-L, Fighera M, Abdou M, Bakker E, van der Wal P. 2021: Newly designed gel-integrated nanostructured gold-based interconnected microelectrode arrays for continuous in situ arsenite monitoring in aquatic systems. Sensors and Actuators B: Chemical, 328, 128996.
- [3] Tercier-Waeber, M.-L., Confalonieri, F., Abdou, M., Dutruch, L., Bossy, C., Fighera, M., Bakker, E., Schäfer, J., 2021: Advanced multichannel submersible probe for autonomous high-resolution in situ monitoring of the cycling of the potentially bioavailable fraction of a range of trace metals, Chemosphere 282, <https://doi.org/10.1016/j.chemosphere.2021.131014>.

## 14.7

# Quantum yield and quenching: Investigating phytoplankton sun-induced fluorescence from in-situ hyperspectral measurements in Lake Geneva

Remika S. Gupana<sup>1,2</sup>, Alexander Damm<sup>1,2</sup>, Abolfazl Irani Rahaghi<sup>1</sup>, Camille Minaudo<sup>1,3</sup>, Daniel Odermatt<sup>1,2</sup>

<sup>1</sup> Eawag, Swiss Federal Institute of Aquatic Science & Technology, Surface Waters – Research and Management, Dübendorf, Switzerland ([remika.gupana@eawag.ch](mailto:remika.gupana@eawag.ch))

<sup>2</sup> Department of Geography, University of Zurich, Zurich, Switzerland

<sup>3</sup> Department of Ecology, University of Barcelona, Barcelona, Spain

Increasing capacity of satellite remote sensing for the measurement of sun-induced fluorescence (SIF) opens new pathways to advance estimates of chlorophyll-a concentration and primary productivity, which are key to determining the ecological status of aquatic ecosystems.

The complex energy partitioning of incoming solar light energy absorbed by phytoplankton in either 1) photosynthesis, 2) heat dissipation, or 3) fluorescence emission, complicates the interpretation of measured SIF. Photochemical Quenching (PQ) and Non-Photochemical Quenching (NPQ) of fluorescence is linked to photosynthesis and heat dissipation, respectively. Particularly problematic is to disentangle whether changes of SIF are related to a physiological regulation of PQ and NPQ by phytoplankton cells. In this context, the quantum yield of fluorescence ( $\phi_F$ ) (i.e. the ratio of photons emitted as fluorescence over the total irradiance absorbed) could be used to understand whether SIF is determined by PQ or NPQ occurrences.

Exploiting the capacity and defining strategies to utilize  $\phi_F$  for the interpretation of SIF requires detailed in-situ studies. The acquisition of SIF and  $\phi_F$  are, however, challenged by their high temporal and physiological variability. Furthermore, the need for combined measurements enclosing all relevant optical paths, particularly in inland waters, is scarce. In addition, information on diurnal and seasonal  $\phi_F$  in relation to PQ and NPQ are almost unknown.

In this contribution, we demonstrate how to estimate  $\phi_F$  using an ensemble of optical in-situ measurements, including hyperspectral downwelling irradiances and upwelling radiances, bulk absorption and scattering, and chlorophyll-a concentration acquired with an autonomous Thetis profiler in Lake Geneva. We use vertical and temporal changes in retrieved  $\phi_F$  to determine conditions at which NPQ dominates over PQ for the period between October 2018 and September 2021.

We observed NPQ in 36% of the total daytime profiles used in the  $\phi_F$  analysis. There was also a seasonal trend in PQ and NPQ occurrences observed with NPQ occurring in roughly half the cases in spring and summer while there was none in fall and winter. Available light (i.e. downwelling irradiance) is a main contributor to photosynthetic activity and whether saturation irradiance is reached. However, its role cannot be easily interpreted. Other factors such as phytoplankton photoregulation and seasonal succession of phytoplankton communities also likely play significant roles in determining the response to incident light and therefore, quenching mechanisms.

We conclude that an adapted approach exploiting in-situ data is suitable to determine diurnal NPQ occurrence and its seasonal patterns, and helps develop future remote sensing algorithms. We suggest to systematically exploit recent and future hyperspectral satellite missions (e.g. ESA's FLEX, ASI's PRISMA and NASA's PACE) and how they could facilitate the retrieval of aquatic SIF and  $\phi_F$  and related aquatic applications with their contiguous spectral coverage and high spectral resolution.

## 14.8

### Effect of lake exposure on a population of enteroviruses

Odile Larivé<sup>1</sup>, Htet Kyi Wynn<sup>1</sup>, Tamar Kohn<sup>1</sup>

<sup>1</sup> Laboratory of Environmental Chemistry, School of Architecture, Civil and Environmental Engineering, École Polytechnique Fédérale de Lausanne (EPFL), CH-1015 Lausanne, Switzerland

\* To whom correspondence should be addressed: e-mail: tamar.kohn@epfl.ch; phone: +41 21 69 30891

Enteroviruses are commonly circulating human viruses that are shed into the sewage by infected individuals. They are then discharged into the environment, where they can persist for long periods of time and can pose a threat of human health. The enterovirus genus displays diversity and not all enterovirus serotypes are equally affected by natural stressors. Their persistence in the environment will vary too, but the persistence in natural water of only few serotypes has been studied and most studies were performed in laboratory. The objective of this study was to evaluate the diversity in decay in Lake Geneva among a population of enteroviruses.

To measure the inactivation of enteroviruses *in-situ*, an environmental chamber was custom-designed to expose viruses safely to the lake environment, while being contained (Figure 1). The chambers were moored in the perimeter of the LéXPLORÉ platform. A population of eight enteroviruses was exposed to Lake Geneva in the environmental chamber for five days during winter and summer.

Our findings show that temperature is an important factor governing enteroviruses inactivation in the lake, inactivation being globally more important at higher temperatures. We observed a wide range of inactivation among serotypes during both seasons, but the relative sensitivity of the serotypes differed between seasons. As a result, enterovirus populations in the lake are expected to be dominated by different serotypes depending on season (though the final population composition will also be determined by serotype-specific shedding rates and removal efficiencies during wastewater treatment). Independent of season, the inactivation observed in the lake was found to be mainly microbial.

The project is subjected to the OFEV Permission number B21003.

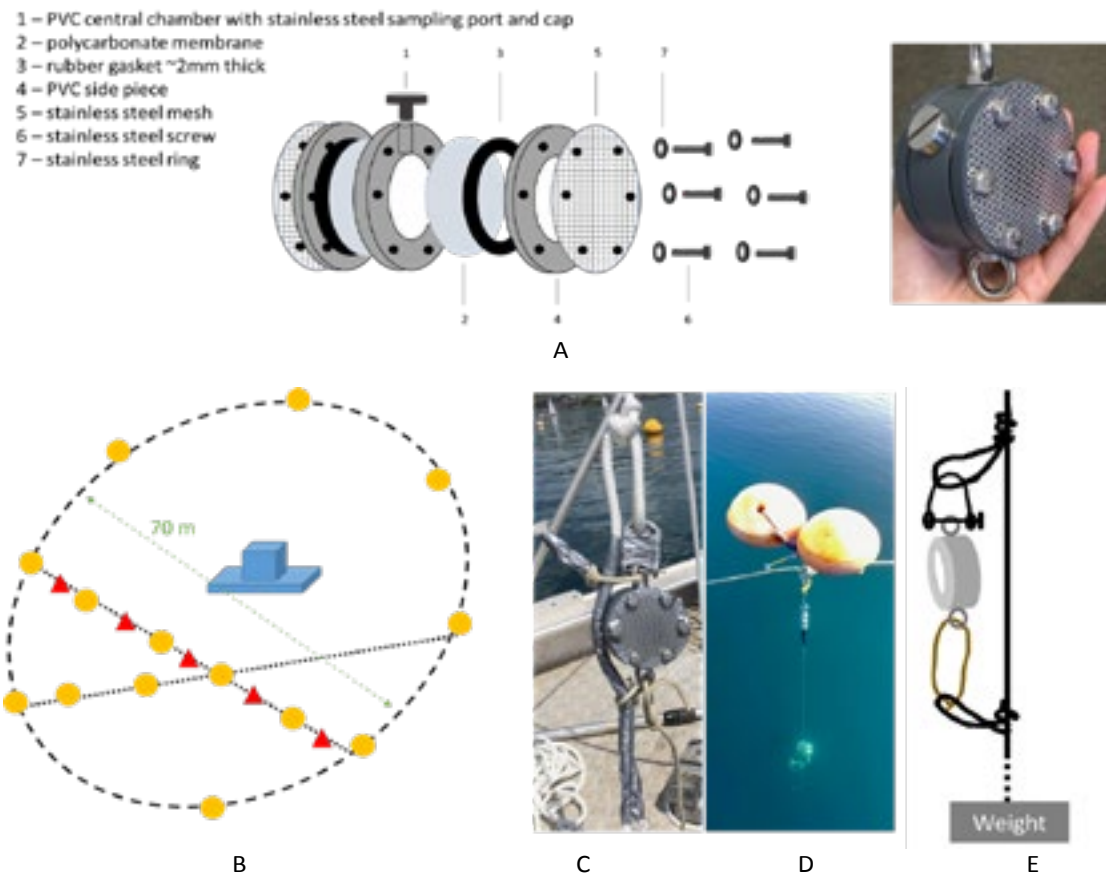


Figure 1. (A) Schematic of the environmental chamber constituents and picture of the environmental chamber. (B) Schematic of the mooring site of the chambers at the Lexplore platform, the yellow circles and red triangles representing the main and secondary buoys. (C) Protection of the chamber and of the rope to avoid deterioration by friction. (D) Picture of a test chamber deployed at 2 m depth. (E) Attachment of the chamber to the rope to avoid tension due to the weight.

## 14.9

# Quantification of the nioxime-labile Ni and Co concentrations in Lake Geneva during a diurnal cycle

Nicolas Layglon<sup>1</sup>, Sébastien Creffield<sup>1</sup>, Eric Bakker<sup>1</sup>, Mary-Lou Tercier-Waeber<sup>1</sup>

<sup>1</sup>University of Geneva, Sciences II, Quai E.-Ansermet 30, 1221 Geneva 4, Switzerland (Nicolas.layglon@unige.ch)

Assessing the impact of trace metals on aquatic ecosystems and ultimately human health is challenging. Trace metals are distributed in a variety of redox states and chemical species that may vary continuously in space and time [1,2]. Only some trace metal species are bioavailable. The development of robust and adaptive submersible sensitive trace metal bioavailability-assessment tools is therefore required to support the establishment of environmental quality standards and guidelines based on realistic risk assessment to protect aquatic life and biodiversity, and ultimately human health.

Toward this aim, we developed on-chip chemical sensors consisting of an array of interconnected iridium-based microdiscs that are electroplated with appropriate sensing elements and covered with a hydrogel as efficient antifouling membrane [2,3]. Incorporated in in-house submersible probes and interrogated by Square Wave Anodic Stripping Voltammetry (SWASV), these gel-integrated microelectrode arrays (GIME) allow for the direct *in situ* quantification of the dissolved metal species that are available for uptake by phytoplankton (first chain of the food-web) [2,3]. To date, only trace metals that can be electrochemically reduced and pre-concentrated at the surface of the electrode could be measured. A wider range of trace metals may become accessible by adsorptive cathodic stripping voltammetry (AdCSV). This technique has been mainly applied with renewable mercury or bismuth film electrodes which is difficult to adapt for *in situ* measurements.

We report here on the optimization and evaluation of AdCSV on GIME for the direct quantification of the sufficiently labile Co and Ni dissolved species in aquatic systems. The methodology was first characterized and validated in laboratory. The optimized protocol was then applied on a GIME incorporated in a submersible probe to *in situ* determine the sufficiently labile Co and Ni dissolved species in Lake Geneva (LeXPORE project). Samples were also collected to analyze the total acid-leachable, the total dissolved and the “truly” dissolved fractions. The combination of these four fractions allowed to better assess the Co and Ni speciation in the environment, something never achieved before.

## REFERENCES

- [1] Tercier Waeber, M.-L., Stoll, S., Slaveykova, V., Trace metal behavior in surface waters: emphasis on dynamic speciation, sorption processes and bioavailability. Arch. Sc. 2012, 65, 119–142.
- [2] Tercier-Waeber M-L, Hezard T, Masson M, Schäfer J., In Situ Monitoring of the Diurnal Cycling of Dynamic Metal Species in a Stream under Contrasting Photobenthic Biofilm Activity and Hydrological Conditions. Environ Sci Technol 2009, 43, 7237–7244.
- [3] Tercier-Waeber M-L, Confalonieri F, Abdou M, Dutruch L, Bossy C, Fighera M, Bakker E., Graziottin F., Van der Wal P., Schäfer J., Advanced multichannel submersible probe for autonomous high-resolution *in situ* monitoring of the cycling of the potentially bioavailable fraction of a range of trace metals. Chemosphere 2021, 282.

## 14.10

# Long-term spatiotemporal variability of whittings in Lake Geneva from multispectral remote sensing and machine Learning

Many, G.<sup>1</sup>, Escoffier, N.<sup>1</sup>, Ferrari, M.<sup>1</sup>, Jacquet, P.<sup>2</sup>, Mariethoz, G.<sup>1</sup>, Perolo, P.<sup>1</sup>, Odermatt, D.<sup>3</sup>, Perga, M-E<sup>1</sup>.

<sup>1</sup> Institute of Earth Surface Dynamics, University of Lausanne, Lausanne, Switzerland

<sup>2</sup> Scientific Computing and Research Support Unit, University of Lausanne, Lausanne, Switzerland

<sup>3</sup> Eawag, Swiss Federal Institute of Aquatic Science and Technology, Surface Waters, Research and Management, Dübendorf, Switzerland

**Abstract:** Whiting events are sudden and massive calcite precipitation events turning hardwater lake waters to a milky turquoise color. Changes in the timing and annual frequency of lakes' whittings have been speculated under global change. The transitory nature of whiting events and their variable spatial extent yet make them not well captured by traditional monitoring so that such a hypothesis remains mostly untestable due to a lack of adequate data. Herein, we use a multispectral remote sensing approach to reconstruct the occurrence and spatial extent of whiting events in Lake Geneva from 2013 to 2021. Landsat-8, Sentinel-2, and Sentinel-3 multispectral sensors are combined and intercalibrated to derive the AreaBGR index and identify whiting events over the studied period using appropriate filters. Results show that the combination of multi-spectral sensors is suitable for monitoring whiting events in Lake Geneva on large spatial and temporal scales. 95% of the detected whittings are located in the northeastern part of the lake, and occur in a highly reproducible environmental setting: a high Rhône River discharge ( $358.6 \pm 102.1 \text{ m}^3 \text{ s}^{-1}$ ), air and water temperatures of  $21.3 \pm 3.0 \text{ }^\circ\text{C}$  and  $18.0 \pm 1.9 \text{ }^\circ\text{C}$  respectively, and a deep thermocline in the lake during the stratified period (11.1  $\pm 0.6 \text{ m}$  depth). The full-time series of whittings is reconstructed from a random forest algorithm over the last 60 years and analysed through a Bayesian decomposition for annual and seasonal trends in the number of whiting days. Results show that the annual number of whiting days between 1958 and 2021 does not follow any particular monotonous trend. The inter-annual changes of whiting occurrences is significantly correlated to the Western Mediterranean Oscillation Index (WeMOI). Besides, spring whittings appear to increase since 1998 and significantly follow the variability of the Atlantic Multidecadal Oscillation index (AMO).

## 14.11

# Effects of coastal upwelling and its relaxation along the northern shore of Lake Geneva

François Mettra, Fedro Mattei, Ulrich Lemmin, David Andrew Barry

*Ecological Engineering Laboratory (ECOL), Institute of Environmental Engineering (IIE), Faculty of Architecture, Civil and Environmental Engineering (ENAC), Ecole Polytechnique Fédérale de Lausanne (EPFL), CH-1015 Lausanne  
(francois.mettra@epfl.ch)*

Human activities can have a considerable impact on lakes. Notably, contaminants coming from coastal areas via rivers, waste water treatment plant outflows or direct runoff can deposit in their nearshore zones. Most of the time, the nearshore zone is considered hydrodynamically independent of the pelagic zone, thus favoring the accumulation of contaminants in the nearshore region. In addition, the epilimnion, the surface layer above the strong thermocline that forms during the warm season, limits the exchange with deeper layers during that season. For that reason, water intakes, e.g., for drinking water, draw water from relatively deep layers and far from the shore. However, the offshore extent of the nearshore zone is poorly known in Lake Geneva. Furthermore, a strong tilt of the thermocline after wind events can lead to a brief, but relatively important deep vertical exchange.

Therefore, we designed a field study to better understand the hydrodynamics of the nearshore zone and observe how its extent evolves throughout the seasons and due to wind forcing. Moorings with Acoustic Doppler Current Profilers (ADCPs) and vertical thermistor lines were deployed on the northern shore of Lake Geneva near the village of Buchillon. A fiber optic cable, previously layed down along the sloping bed at the field site, provides bottom temperature on an 1800-m long cross-shore transect and provides a link to the pelagic zone. A turbulence platform was developed and installed to shed light on the effects of mixing in the nearshore zone on the littoral - deep interior exchange. Finally, a 3D hydrodynamic model of Lake Geneva allows interpreting the hydrodynamics on a larger scale.

In this study, we focus on *Vent* events (winds from the southwest) that induce coastal upwelling at the field site and on subsequent strong coastal fronts which form during the event relaxation and then travel along the coast in a Kelvin wavelike pattern. When these cyclonic (counterclockwise rotating) waves passed the field site, a strong downwelling was observed. Furthermore, this study showed that nearshore sediment was resuspended and potentially dispersed much deeper than the normal depth of the thermocline due to the downwelling. Surprisingly, hydrodynamic features evolving during the relaxation of the wind event seem to have a greater effect on the nearshore lakebed and the dispersal of contaminants than during the development period of the upwelling, i.e., during the wind event.

## 14.12

# Radiocarbon and stable carbon isotope measurements of dissolved inorganic and organic carbon from the LéXPLORÉ platform on Lake Geneva

Margot E. White<sup>1</sup>, Benedict V.A. Mittelbach<sup>1</sup>, Negar Haghipour<sup>1</sup>, Thomas Blattmann<sup>1</sup>, Céline Jacquin<sup>2</sup>, Nathalie Dubois<sup>1,3</sup>, and Timothy I. Eglinton<sup>1</sup>

<sup>1</sup> Department of Earth Sciences, ETH Zürich, Switzerland ([margot.white@erdw.ethz.ch](mailto:margot.white@erdw.ethz.ch))

<sup>2</sup> Department Process Engineering, EAWAG, Dübendorf, Switzerland

<sup>3</sup> Department Surface Waters Research & Management, EAWAG, Dübendorf, Switzerland

Radiocarbon Inventories of Switzerland (RICH) aims to construct the first national-scale census of carbon across aquatic, terrestrial, and atmospheric reservoirs. Within the Swiss carbon cycle, inland waters play a crucial role with lakes integrating carbon from various sources within their catchment in addition to that fixed by local primary productivity. Isotopic measurements of carbon pools can differentiate contributions from these various sources. Here we will present carbon isotope measurements of dissolved organic carbon (DOC) and dissolved inorganic carbon (DIC) from monthly water column samplings of Lake Geneva collected at 6 depths from the LéXPLORÉ platform beginning in April 2022. In addition to concentration and isotope measurements, we will use optical measurements (fluorescence and absorbance) of lake water to identify different organic matter contributions. Preliminary results show that the average radiocarbon signature of DIC in Lake Geneva is depleted relative to atmospheric CO<sub>2</sub>, indicating around 17% contribution from petrogenic (limestone-derived) carbon. The most depleted values of Δ<sup>14</sup>C (as low as -200 per mil) correspond with evidence of Rhone inflow reflected in profiles of turbidity and salinity. Consistent with increased primary productivity during the summer months, DOC concentrations increased compared to springtime observations.

## P 14.1

### Impact of inflow on mountain lake heat flux

Isabel Herr<sup>1</sup>, Marie-Elodie Perga<sup>1</sup>, Damien Bouffard<sup>2</sup>

<sup>1</sup> Institut des dynamiques de la surface terrestre, University of Lausanne, Bâtiment Geopolis, CH-1015 Lausanne  
(isabel.herr@unil.ch)

<sup>2</sup> Eawag, Seestrasse 79, CH-6047 Kastanienbaum

Mountain lakes are often described as sentinels for climate change as they react rapidly to the global and local climate. Due to their small size, small catchment areas, and steep surrounding slopes, mountain lakes also respond rapidly to changes in their catchment. Traditional one-dimensional models based solely on meteorologic conditions fail to represent their temperature cycles. In contrast to low altitude lakes, energy balances in mountain lakes are highly impacted by catchment properties such as snow cover and inflow rather than direct fluxes with the atmosphere. An additional practical challenge comes from the lack of accessibility and harsh field conditions of these lakes. The evolution of mountain lakes in a changing climate is thus still unknown.

This study quantifies the role of throughflow in the heat budget in various Alpine lakes in the French alps spanning from 2000 m to 3000 m a.s.l, in glacial and non-glacial watersheds using meteorological and water temperature data collected in the “Réseaux Sentinelles” Lakes in France. Our results highlight that these changes in the watershed must be included in the classical one-dimensional vertical description of the heat exchanges based on meteorological conditions to characterize the evolution of mountain lakes under climate changes.

All Codes are available at : <https://renkulab.io/gitlab/damien.bouffard/heat-flux-lac-sentinelles>

## P 14.2

### Two very different summers for Lake Geneva as observed by the LéXPLORÉ platform

Martin Wegmann<sup>1</sup>, Natacha Toefield-Pasche<sup>1</sup>

<sup>1</sup> Limnology Center, EPFL, Station 2, 1015 Lausanne (martin.wegmann@epfl.ch)

The floating platform LéXPLORÉ offers high-resolution observations for water properties of Lake Geneva (Wüest et al. 2021). With its permanently fixed location, it allows for pinpoint investigation of changes in the water column over time. Out of all the instruments connected with the platform, we use the Thetis profiler and meteo station to compare the summers 2021 and 2022. Defined by very different meteorological forcings, with low pressure conditions (warm and wet) in 2021 and high pressure conditions (hot and dry) 2022, we find strong differences in water temperature, salinity, dissolved oxygen and chlorophyll A properties in the water column below the platform. With reduced precipitation and runoff in spring and summer 2022, less nutrients were entering the surface layers of the lake. On top of that, invasive Quagga mussels probably consume large parts of the Lake's nutrients these days, but quantifying the impact of this consumptions is currently still extremely uncertain. Regardless, this years' atmospheric dynamics led to deeper maxima of chlorophyll A and oxygen production, even though temperatures and incoming solar radiation were much higher in 2022. Our findings highlight the complexity and counter-intuitive feedbacks of anthropogenic global warming with respect to algae dynamics in large oligotrophic lakes.

#### REFERENCES

- Wüest, A., Bouffard, D., Guillard, J., Ibelings, B. W., Lavanchy, S., Perga, M. E., & Pasche, N. 2021: LéXPLORÉ: A floating laboratory on Lake Geneva offering unique lake research opportunities. Wiley Interdisciplinary Reviews: Water, 8(5), e1544.

# 15 Cryospheric Sciences

Matthias Huss, Kathrin Naegeli, Nadine Salzmann, Theo Jenk, Andreas Vieli

*Swiss Snow, Ice and Permafrost Society*

## TALKS:

- 15.1 Amschwand D., Scherler M., Hoelzle M., Haberkorn A., Krummenacher B., Gubler H.: Energy fluxes in the coarse debris mantle of rock glacier Murtèl estimated from in-situ measurements
- 15.2 Echelard T., Delaloye R., Vivero S., Pellet C., Barboux C.: IPA Action Group – Towards standard guidelines for Rock Glaciers inventories (RoGI) : overview of the outcome documents, ongoing work and next steps.
- 15.3 Grazioli J., Ghiggi G., Billault-Roux A.-C., Berne A.: A database of images, descriptors and microphysical properties of individual snowflakes in free fall
- 15.4 Hunziker J., Slob E., Irving J.: Fast simulations of Ground Penetrating Radar data on glaciers
- 15.5 Iten Y., Steiner L., Grimm D.: Investigation of Long GNSS Refractometry Baselines for the Determination of the Water Equivalent of Snow Cover
- 15.6 Klahold J., Irving J., Schwarz B., Bauer A.: 3D diffraction imaging of alpine glacier GPR data
- 15.7 Kneib M., Fyffe C., Miles E.S., Lindemann S., Shaw T.E., Buri P., McCarthy M., Ouvry B., Sato Y., Kraaijenbrink P.D.A., Chuanxi Z., Molnar P., Vieli A., Yang W., Pellicciotti F.: Ice cliff formation, distribution and characteristics on debris-covered glaciers
- 15.8 Kneib-Walter A., Jouvet G., Lüthi M.P.: Ice stream flow dynamics of Jakobshavn Isbræ observed with detailed repeated UAV surveys
- 15.9 Moradi H., Furrer G., Margreth M., Wolpert L., Wanner Ch.: Massive mobilization of toxic elements from permafrost areas in the Eastern Alps: Insights on rock glacier melt dynamics
- 15.10 Ogier C., Hosli L., Huss M., Räss L., Bauder A., Farinotti D.: Characterization of a glacier collapse feature development at Rhonegletscher, Switzerland.
- 15.11 Pellet C., Barboux C., Echelard T., Vivero S., Delaloye R.: Rock Glacier Velocity as a new associated product to the ECV permafrost: basic concepts and exemplary results
- 15.12 Reinthaler J., Paul F.: Reconstructing the Little Ice Age glacier surface
- 15.13 Sedaghatkish A., Luetscher M.: Numerical simulation of ice column melting located in mountain permafrost due to global warming
- 15.14 Syed-Hammad A., Khushdar A., Tanzeel-Ur-Rehman., Nasir H., Mazhar A., Raza A., Impact assessment of Supraglacial debris thickness on the melting of glaciers in Karakoram based on In-Situ measurement
- 15.15 Van Tricht L., Huybrechts P.: Modelling the historical and future evolution of multiple glaciers in the Kyrgyz Tien Shan, Central Asia, using a 3D ice-flow model

**POSTERS:**

- P 15.1 Amschwand D., Tschan S., Scherler M., Aschwanden L., Hoelzle M.: Rock-glacier hydrology with the magnifying glass: Where do the solutes in the Murtèl outflow come from?
- P 15.2 Börsig S.: R-channel laboratory experiment: data evaluation and numerical simulations
- P 15.3 Gong Y., Rogohzhina I.: The importance of glacial headwater streams and their climate sensitivity in a glacierized river basin in western Norway
- P 15.4 Guidicelli M., Treichler D., Salzmann N.: Snow accumulation in observation-scarce high-mountain regions inferred from climate reanalyses, satellites and machine learning
- P 15.5 Hosli L., Ogier C., Huss M., Farinotti D.: Recent increase in collapse features on glacier snouts throughout the Swiss Alps
- P 15.6 Morard S., Westermann S., Wagner F., Mollaret C., Hauck C.: Application of the thermal model CryoGrid community model (version 1.0) in the Swiss Alps to assess permafrost degradation and to quantify volumetric ice content
- P 15.7 Naegeli K., Amschwand D., Hoelzle M.: Unlocking spatio-temporal variabilities of surface fluxes over rockglacier Murtèl with thermal infrared imaging
- P 15.8 Noetzli J., Pellet C. and the PERMOS Scientific Committee: How does the hot summer 2022 affect the permafrost in the Swiss Alps?
- P 15.9 Søndergaard A.S., Steineman O., Haghipour N., Wacker L., Ivy-Ochs S., Larsen N.K.: Developing an in-situ  $^{14}\text{C}$  chronology for North Greenland
- P 15.10 Robson B., Lambiel C., Ravanel L., Irving J., Baron L., Gentizon J.: Investigating hanging glacier geometries in the Mont-Blanc Massif (France) and Pennine Alpes (Switzerland) using ground penetrating RaDAR

## 15.1

# Energy fluxes in the coarse debris mantle of rock glacier Murtèl estimated from in-situ measurements

Dominik Amschwend<sup>1</sup>, Martin Scherler<sup>1†</sup>, Martin Hoelzle<sup>1</sup>, Anna Haberkorn<sup>2</sup>, Bernhard Krummenacher<sup>2</sup>, Hansueli Gubler<sup>3</sup>

<sup>1</sup> Department of Geosciences, University of Fribourg, Chemin du Musée 4, CH-1700 Fribourg ([dominik.amschwand@unifr.ch](mailto:dominik.amschwand@unifr.ch))

<sup>2</sup> GEOTEST AG, Bernstrasse 165, CH-3052 Zollikofen

<sup>3</sup> ALPUG GmbH, Richtstattweg 3, CH-7270 Davos-Platz

The debris mantle of ‘cold rocky landforms’ (Brighenti et al., 2021) like rock glaciers or undercooled talus slopes effectively decouples the underlying ice-rich permafrost from the atmosphere, preserving ground ice and rendering these landforms more resilient against climate change. The cooling effect of the openwork debris mantle is well known from field studies and several key processes have been successfully simulated separately, for example buoyancy-driven air circulation (e.g., Wicky & Hauck, 2020) or the interplay between sensible and latent heat storage (e.g., Renette et al., in review). However, heat transfer mechanisms across the debris mantle are complex and include conduction, convection by air and water, longwave radiation, and sensible and latent heat storage. Few microclimatological studies attempted to simultaneously parametrize all heat fluxes (Scherler et al., 2014), and few comprehensive subsurface hydro-thermal measurements beyond ground temperatures exist in blocky mountain permafrost (Rist & Phillips, 2005).

Here, we present our large sensor network that we installed in natural cavities within the debris mantle of rock glacier Murtèl (Upper Engadine) and show estimates of individual mass and heat flux components based on in-situ measurements for the two hydrological years 2020–2022. The ‘subsurface weathers station’ includes a variety of sensors such as thermistors, hygrometers, pyrgeometers, sonic anemometers, hot-wire anemometers, and heat flux plates. In addition, we complemented the ongoing PERMOS atmospheric measurements with eddy flux, precipitation, and snow temperature measurements. With this comprehensive data set, we quantify the volumetric energy budget of the debris mantle by accounting for heat storage and fluxes at the boundaries, in particular by a detailed surface energy balance, and also resolve fluxes within the debris mantle.

Our data-driven estimates of individual surface and subsurface energy fluxes in a coarse debris mantle will benefit the modelling of the ground thermal regime of cold rocky landforms. The gained quantitative process understanding eventually improves projections of the evolution of debris-mantled ice-rich permafrost landforms under climate change and of the generated runoff.

This work is part of the Innosuisse project ‘Permafrost Meltwater Assessment eXpert Tool’ (PERMA-XT) jointly run by the University of Fribourg (research partner) and GEOTEST (implementation partner and project management).

## REFERENCES

- Brighenti, S., Hotaling, S., Finn, D.S., Fountain, A.G., Hayashi, M., Herbst, D., Saros, J.E., Tronstad, L.M. and Millar, C.I. 2021: Rock glaciers and related cold rocky landforms: Overlooked climate refugia for mountain biodiversity, *Glob. Change Biol.*, 27, 1504–1517, <https://doi.org/10.1111/gcb.15510>.
- Renette, C., Aalstad, K., Aga, J., Zweigel, R. B., Etzelmüller, B., Lilleøren, K. S., Isaksen, K., and Westermann, S. in review: Simulating the effect of subsurface drainage on the thermal regime and ground ice in blocky terrain, Norway, *Earth Surf. Dynam. Discuss.* [preprint], <https://doi.org/10.5194/esurf-2022-39>.
- Rist, A., & Phillips M. 2005: First results of investigations on hydrothermal processes within the active layer above alpine permafrost in steep terrain, *Norsk Geografisk Tidsskrift - Norwegian Journal of Geography*, 59:2, 177–183, <https://doi.org/10.1080/00291950510020574>.
- Scherler, M., Schneider, S., Hoelzle, M., and Hauck, C. 2014: A two-sided approach to estimate heat transfer processes within the active layer of the Murtèl–Corvatsch rock glacier, *Earth Surf. Dynam.*, 2, 141–154, <https://doi.org/10.5194/esurf-2-141-2014>.
- Wicky, J., & Hauck C. 2020: Air convection in the active layer of rock glaciers. *Front. Earth Sci.*, 8:335, 1–17, <https://doi.org/10.3389/feart.2020.00335>.

## 15.2

# IPA Action Group - Towards standard guidelines for Rock Glaciers inventories (RoGI) : overview of the outcome documents, ongoing work and next steps.

Thomas Echelard<sup>1</sup>, Reynald Delaloye<sup>1</sup>, Sebastián Vivero<sup>1</sup>, Cécile Pellet<sup>1</sup>, Chloé Barboux<sup>1</sup>

<sup>1</sup> Department of Geosciences, University of Fribourg, CH-1700 Fribourg ([thomas.echelard@unifr.ch](mailto:thomas.echelard@unifr.ch))

Rock glaciers best express the creep of mountain permafrost and constitute an essential geomorphological heritage of the mountain periglacial landscape. Their dynamics largely depend on climatic factors and may locally affect human activities (e.g. debris flow initiated from a rock glacier snout). Observing changes in rock glacier kinematics provide clue information on the climatic impact and has the potential to become a key parameter of cryosphere monitoring in mountain regions.

In many high-altitude regions, initiatives have been developed for decades in order to inventory rock glaciers as a proxy for permafrost occurrence, but also in the perspective of ice (water) storage estimation, geohazards management, and climate reconstruction. However, these efforts often rely on different methodologies based on the unequal availability of source datasets, variable geomorphological skills and institutional support. In a context where open access to high-quality remotely sensed data is constantly increasing, there is a need for the scientific community to promote international cooperation and develop standard guidelines.

The International Permafrost Association (IPA) Action Group on Rock glacier inventories and kinematics (see Abstract Vivero et al.) has been running for four years since its initiation at the European Conference on Permafrost (EUCOP5 2018) in Chamonix. The Action Group activities have focused in particular on the definition of widely accepted guidelines for inventorying rock glaciers (RoGI) in mountain permafrost regions, including indications on the activity rate and the related operational development of a database/web platform.

The proposed presentation reports on the primary outcome documents, results and activities arising since 2018: edition of standard guidelines for inventorying rock glaciers (standardized definitions and terminology, activity class update, practical rules, etc.), database set-up (GIS tool for inventorying rock glaciers regarding the widely accepted standard guidelines, online platform, QA/QC, etc.), next steps and organization (scientific activity of the group, scientific and executive governance).

## 15.3

### A database of images, descriptors and microphysical properties of individual snowflakes in free fall

Jacopo Grazioli (1), Gionata Ghiggi, (1), Anne-Claire Billault-Roux (1) Alexis Berne (1)

(1) *Laboratoire de Télédétection Environnementale, EPFL, Lausanne, Switzerland*

Snowfall information at the scale of individual particles is rare, difficult to gather, but fundamental for a better understanding of solid precipitation microphysics.

We present a dataset, MASCDB, (and a dedicated python software) of in-situ measurements of snow particles in free fall collected by a multi-angle snowflake camera. The dataset, includes gray-scale (255 shades) images of snowflakes, co-located surface environmental measurements, a large number of geometrical and textural snowflake descriptors as well as the output of previously published retrieval algorithms. Noteworthy examples include: hydrometeor classification, riming degree estimation, identification of melting particles, discrimination of wind-blown snow, as well as estimates of snow particle mass and volume.

The measurements were collected in various locations of the Alps, Antarctica and Korea for a total of 2>555>091 snowflake images (or 851>697 image triplets).

MASCDB aims to accelerate reproducible research on precipitation microphysics and to address longstanding scientific challenges on snowflake research.

Given the large amount of snowflake images and associated descriptors, MASCDB can be exploited by the computer vision community for the training and benchmarking of image processing systems. MASCDB can be accessed on Zenodo (DOI: <https://doi.org/10.5281/zenodo.5578920>), while the pymascdb package at <https://github.com/ltelab/pymascdb>.

## 15.4

### Fast simulations of Ground Penetrating Radar data on glaciers

Jürg Hunziker<sup>1</sup>, Evert Slob<sup>2</sup>, James Irving<sup>1</sup>

<sup>1</sup> Applied and Environmental Geophysics Group, Institute of Earth Sciences, University of Lausanne, Lausanne, Switzerland  
(jurg.hunziker@unil.ch)

<sup>2</sup> Faculty of Civil Engineering and Geosciences, Delft University of Technology, Delft, The Netherlands

To simulate geophysical data, usually grid-based methods are chosen due to their flexibility in designing any arbitrary model geometry and their simplicity. However, when modeling Ground Penetrating Radar (GPR) data in a glacial environment, grid-based methods are computationally extremely expensive, because of the large domain size and the short wavelength.

Therefore, we propose another approach, which is based on the earlier work of Moran et al. (2003) and Shakas and Linde (2015). In this approach, a homogeneous background medium is assumed, in our case ice, in which the GPR pulses are propagated in a semi-analytical way. Only scatterers, such as inglacial and subglacial channels, and reflectors, such as the glacier bed, are discretized. The glacier surface is simulated by taking the far-field antenna radiation pattern (Engetha et al., 1982, Arcane, 1995) at the air-ice interface into account. By using a three-layer reflection coefficient (Bradford & Deeds, 2006), sediment layers and channels at the glacier bed can be simulated without the need of discretizing additional objects besides the glacier bed.

With this approach, realistic glacier models can be simulated with moderate runtime and memory use. As an example, we simulated a 3D survey on the tongue of the Otemma glacier (Valais, Switzerland) including a subglacial channel (Figure 1).

Our code is freely available on Github as a Matlab package (<https://github.com/jhunziker/FROGS>). A Python/C++ package is planned for the near future.

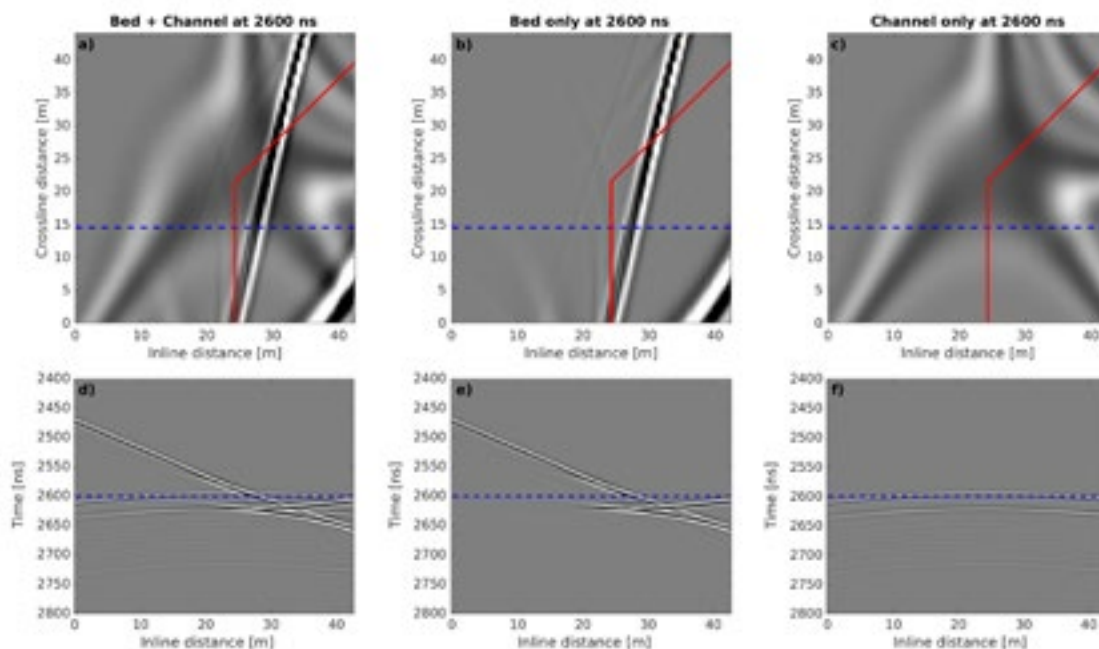


Figure 1. Simulated data on the tongue of the Otemma glacier. Subfigures a) to c) are time slices at 2600 ns and subfigures d) to f) are vertical cross-sections along the line measured at 14.5 m. a) and d) contain the reflections from the glacier bed as well as from the channel, b) and e) contain only the reflections from the glacier bed, and c) and f) only the reflections from the channel. The red lines show the position of the channel and the blue dashed lines show the position of the intersections between the time slices a) to c) and the vertical slices d) to f).

## REFERENCES

- Arcane, S.A. 1995: Numerical studies of the radiation patterns of resistively loaded dipoles, *Journal of Applied Geophysics*, 33, 39-52.  
 Bradford, J.H., & Deeds, J.C. 2006: Ground-penetrating radar theory and application of thin-bed offset-dependent reflectivity, *Geophysics*, 71, K47-K57.

- Engheta, N., Papas, C.H., & Elachi, C. 1982: Radiation patterns of interfacial dipole antennas, *Radio Science*, 17, 1557-1566.
- Moran, M.L., Greenfield, R.J., & Arcone, S.A. 2003: Modeling GPR radiation and reflection characteristics for a complex temperate glacier bed, *Geophysics*, 68, 559-565.
- Shakas, A., & Linde, N. 2015: Effective modeling of ground penetrating radar in fractured media using analytic solutions for propagation, thin-bed interaction and dipolar scattering, *Journal of Applied Geophysics*, 116, 206-214.

## 15.5

# Investigation of Long GNSS Refractometry Baselines for the Determination of the Water Equivalent of Snow Cover

Yanis Iten<sup>1</sup>, Ladina Steiner<sup>2</sup>, David Grimm<sup>1</sup>

<sup>1</sup> Institute of Geomatics, University of Sciences and Arts of Northwestern Switzerland (FHNW), Hofackerstrasse 30, 4132 Muttenz, Switzerland (david.grimm@fhnw.ch)

<sup>2</sup> Alfred Wegener Institute, Helmholtz Centre for Polar and Marine Research, Am Alten Hafen 26, 27568 Bremerhaven, Germany

GNSS refractometry can be used to determine the water equivalent of the snow cover at a given location. A GNSS receiver is placed on the ground and continuously covered by snow (rover). To precisely determine the position of the rover, a GNSS reference receiver is needed for differential GNSS processing. Up to now, only very short GNSS baselines (distance between the rover and base antenna reference points) are applied for SWE estimation with GNSS refractometry.

This feasibility study investigates the use of long GNSS baselines SWE estimation with GNSS refractometry. For short baselines up to 10 kilometers (km), GNSS path delays due to the atmosphere (troposphere and ionosphere), satellite orbits, and antenna phase center offset and variations are eliminated in differential GNSS processing due to their similarity for both stations. These effects are, however, relevant for longer baselines ( $> 10$  km) due to different path delays in the atmosphere and a changing observation geometry towards the tracked satellites. When using long baselines for precise GNSS positioning, these effects need to be addressed in the differential processing. The atmospheric path delays can either be modeled or estimated together with the SWE parameter. As the ionosphere is dispersive, a linear combination of dual-frequency signals can be used for its elimination. This, however, increases the noise by a factor of . Using precise post-processed instead of predicted transmitted GNSS ephemeris minimizes geometric distortions. The present study aims at answering the following research questions: a) Is it possible to estimate SWE using long GNSS refractometry baselines? b) Is it possible to separate the influence of atmospheric path delays from the path delay induced by the snow above the buried antenna? c) Which type of processing delivers best results (modeling or estimation of atmospheric path delays)? The accuracy of resulting SWE time series is assumed to decrease with longer baselines and higher elevation difference.

Available GNSS refractometry data from the test site Davos Laret of the Institute for Snow and Avalanche Research (WSL SLF) is therefore reprocessed for the season 2021/22 using the open-source GNSS post processing software RTKLIB. Selected reference stations with different baseline lengths and height differences are evaluated. Reference data is available from the Automated GNSS Network for Switzerland AGNES and the private reference network REFNET. Manual snow tube samples and snow scale observations from the same test site are provided by the WSL SLF for reference. Results differ strongly for our hypotheses and best results are achieved when not taking atmospheric delays into account (Figure 1). Neither the use of tropospheric or ionospheric models or the estimation of these delays together with the SWE provide sufficient results for baselines smaller than hundred km. The noise in the resulting SWE time series is significantly increased when taking care of the atmospheric biases. A reason could be the substantial decrease in the GNSS observations when forming a dual-frequency linear combination. The number of tracked satellites is thereby decreased to the minimum of four satellites for GNSS processing.

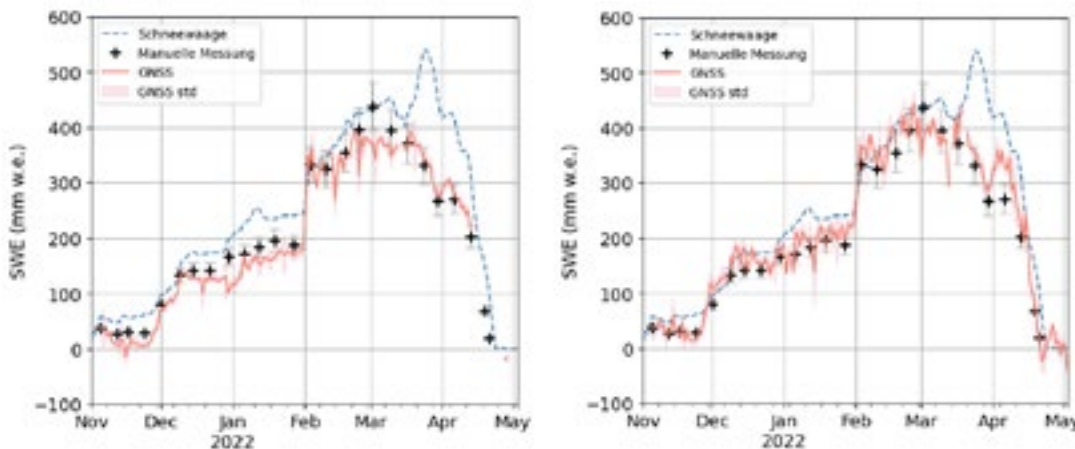


Figure 1. GNSS derived SWE estimates (red solid line), snow scale (dashed blue line), and manual observations (black crosses) for a very short (Davos Laret, a few meters, left) and a long baseline (AGNES SAM2, about 35 km, right).

## 15.6

### 3D diffraction imaging of alpine glacier GPR data

Johanna Klahold<sup>1</sup>, James Irving<sup>1</sup>, Benjamin Schwarz<sup>2</sup>, Alexander Bauer<sup>3</sup>

<sup>1</sup> Institute of Earth Sciences, University of Lausanne, Switzerland ([johanna.klahold@unil.ch](mailto:johanna.klahold@unil.ch))

<sup>2</sup> Fraunhofer Institute for Wind Energy Systems IWES, Bremen, Germany

<sup>3</sup> University of Hamburg, Institute of Geophysics, Hamburg, Germany

Ground-penetrating radar (GPR) is an established tool for glaciologists thanks to the excellent propagation characteristics of radar waves in snow and ice and the potential for high-resolution imaging. In this regard, 3D survey methods hold significant promise for studying the internal structure, properties, and dynamics of glaciers. Typically, 3D GPR data collected on alpine glaciers contain a vast amount of diffraction events, which are assumed to be caused by englacial and subglacial meltwater channels and voids. However, the diffracted wavefield typically has low amplitude and is often masked by more prominent arrivals. Standard processing schemes mostly ignore the diffracted energy and tend to focus on the more prominent bedrock reflection. In contrast, our approach specifically targets the diffraction events. By adapting state-of-the-art diffraction separation and imaging methods from the field of exploration seismology, we aim to obtain a comprehensive image of scatterer locations and investigate its correlation with the englacial and subglacial hydrological network.

Our processing workflow coherently approximates the dominant reflected wavefield in a fully data-driven fashion and subtracts it from the data. The remaining diffracted wavefield is then enhanced using local coherent stacking. Finally, the diffraction-only data are migrated to obtain an image of the distribution of subsurface scatterers.

The described workflow is applied to a 3D GPR data set acquired on the Haut Glacier d'Arolla (Valais, Switzerland). We find that our methodology is highly effective at isolating diffractions in glacier GPR data and provides resolved images of the diffracting features, which could be an indication of channel structures. We are currently exploring the application to more extensive 3D data sets that were acquired this summer with our newly developed drone-based GPR system.

## 15.7

# Ice cliff formation, distribution and characteristics on debris-covered glaciers

Marin Kneib<sup>1,2</sup>, Catriona Fyffe<sup>1,3</sup>, Evan S. Miles<sup>1</sup>, Shayna Lindemann<sup>1</sup>, Thomas E. Shaw<sup>1</sup>, Pascal Buri<sup>1</sup>, Michael McCarthy<sup>1</sup>, Boris Ouvry<sup>4</sup>, Yota Sato<sup>5</sup>, Philip D.A. Kraaijenbrink<sup>6</sup>, Zhao Chuanxi<sup>7,8</sup>, Peter Molnar<sup>2</sup>, Andreas Vieli<sup>4</sup>, Wei Yang<sup>8</sup>, Francesca Pellicciotti<sup>1,3</sup>

<sup>1</sup> High Mountain Glaciers and Hydrology Group, Swiss Federal Institute, WSL, Birmensdorf, Switzerland.  
(marin.kneib@wsl.ch)

<sup>2</sup> Institute of Environmental Engineering, ETH Zürich, Zürich, Switzerland

<sup>3</sup> Department of Geography and Environmental Sciences, Northumbria University, Newcastle upon Tyne, UK

<sup>4</sup> Department of Geography, University of Zurich, 8057 Zurich, Switzerland

<sup>5</sup> Graduate School of Environmental Studies, Nagoya University, Nagoya, Japan

<sup>6</sup> Utrecht University, Department of Physical Geography, PO Box 80115, 3508 TC, Utrecht, The Netherlands.

<sup>7</sup> College of Earth and Environmental Sciences, Lanzhou University, Lanzhou 730000, China

<sup>8</sup> State Key Laboratory of Tibetan Plateau Earth System, Environment and Resources (TPESER), Institute of Tibetan Plateau Research, Chinese Academy of Sciences, China

Ice cliffs are dynamic features of debris-covered glaciers that largely contribute to the glacier mass balance relative to debris-covered ice, despite their relatively small surface area. Their distribution across glaciers and its underlying controls are largely unknown, making it difficult to project their long-term evolution as well as their large-scale contribution to glacier melt. Here we assembled a unique dataset of 37537 ice cliffs and their surface characteristics across 86 debris-covered glaciers in High Mountain Asia (HMA), from high-resolution (2m) Pléiades satellite images. We combined this dataset with multi-temporal Unsupervised Aerial Vehicle (UAV) data of five HMA glaciers which we used to identify and characterize 202 ice cliff formation events. These observations show that the ice cliff formation and distribution are mainly controlled by the supraglacial hydrology in the form of pond and stream incision and undercutting. These pond- and stream-influenced cliffs represent 58.4% of the entire ice cliff population. Ice cliff density typically reduces exponentially with debris thickness, although ponds tend to maintain ice cliffs in areas of thick debris (>0.5 m). Where the debris is thinner and the glacier more active, water flow and accumulation at the surface is prevented by the presence of crevasses, which represent 19.7% of the ice cliffs at the surface of these debris-covered glaciers. The cliff slope, aspect, size and distribution density varies between these different categories, which bears implications for the local glacier surface mass balance. Therefore, the ice cliff distribution across debris-covered glaciers is symptomatic of their evolution stage, as it changes with thickening debris and the progressive stagnation of the glacier tongues. The quantification of the influence of these high order controls on the ice cliff distribution provides a framework to account for the variability in cliff density across glaciers and will allow modelling of their long-term evolution and therefore contribution to surface mass balance.

## 15.8

### Ice stream flow dynamics of Jakobshavn Isbræ observed with detailed repeated UAV surveys

Andrea Kneib-Walter<sup>1</sup>, Guillaume Jouvet<sup>1</sup>, Martin P. Lüthi<sup>1</sup>

<sup>1</sup> Department of Geography, University of Zurich, Winterthurerstr. 190, CH-8057 Zurich  
(andrea.walter@geo.uzh.ch)

Outlet glaciers and ice streams transport ice from the ice sheets to the ocean. Jakobshavn Isbræ (JI, Sermeq Kujalleq) is one of the largest and the most dynamic ice stream of the Greenland Ice Sheet with velocities up to 40 m/day. JI's ice stream is separated from the slower flowing ice sheet by a highly crevassed shear margin. Drone photogrammetrical surveys were conducted in July 2022 at JI within the framework of the COEBELI project along other field measurements including in-situ GPS, GPRI, seismometers and time-lapse imagery. This project aims at understanding the complex glacier flow and the processes occurring at the shear margin and the calving front of JI. Such processes are often neglected in numerical models inducing uncertainties in projections of the ice sheet evolution.

Despite challenging weather conditions and constraints due to flying restrictions, we acquired more than 10 repeated long-range flight surveys over the calving front of JI as well as along and perpendicular to the shear margins during about two weeks. As a result, we produced a large imagery data set, which was processed to infer high-resolution orthoimages and digital elevation models (DEM). These could be accurately geo-referenced due to differential GPS and PPK. Comparing the different products enables us to estimate changes in surface topography and ice dynamics by DEM differentiation and feature tracking.

In this work, we present the first outcomes of the drone observation within the 2022 fieldwork at JI. Especially, the repeated flights along the shear margins allow us to derive information on the complex ice dynamics of JI at high temporal and spatial resolution. With this we can capture short-term processes such as hydrological or tidal effects on the horizontal and vertical ice dynamics, speed-up events or the reaction of the glacier to large calving events. Several such large calving events occurred during the observation period enabling us to investigate the interaction between frontal processes and the ice flow dynamics of the ice stream. Having several ice stream profiles with increasing distance to the calving front allows us to further investigate how far upstream frontal processes can influence ice stream dynamics.

## 15.9

# Massive mobilization of toxic elements from permafrost areas in the Eastern Alps: Insights on rock glacier melt dynamics

Hoda Moradi<sup>1</sup>, Gerhard Furrer<sup>2</sup>, Michael Margreth<sup>3</sup>, Louisa Wolpert<sup>1</sup>, Christoph Wanner<sup>1</sup>

<sup>1</sup> Rock-Water Interaction Group, Institute for Geological Sciences, University of Bern, Baltzerstrasse 3, CH-3012 Bern (hoda.moradi@geo.unibe.ch)

<sup>2</sup> Institute of Biochemistry and Pollutant Dynamics (IDP), Department of Environmental Systems Science, ETH Zurich, CH-8092 Zurich

<sup>3</sup> Swiss Federal Institute for Forest, Snow and Landscape Research WSL, Mountain Hydrology and Mass Movements, Zürcherstrasse 111, CH-8903 Birmensdorf

In the Eastern Alps, an increasing number of high-altitude streams show distinctively white colored streambeds. The white color originates from the precipitation of nanocrystalline basaluminite  $[Al_4OH_{10}(SO_4) \cdot (H_2O)_5]$  sticking to the bed load of the streams (Bigham et al. 2000; Carrero et al. 2015). The phenomenon is triggered at the source of the streams where pyrite oxidation occurs in ice-rich permafrost bodies, i.e. in rock glaciers. This leads to the production of sulfuric acid and the subsequent dissolution of aluminum from the paragneiss host rocks. Owing to its pH-dependent solubility, basaluminite eventually precipitates when the acidic and aluminum-rich streams are neutralized along their flow paths (Wanner et al. 2018).

Acidic conditions in the affected streams are also accompanied by elevated concentrations of other toxic elements such as Ni, Mn, Zn and F mobilized from the host rock and strongly exceeding the drinking water limits. The ongoing retreat of permafrost in mountainous terrain might expose more fresh sulfide-rich bedrock to aerobic waters and will change the hydrogeological conditions. Therefore, the mobilization of toxic elements is expected to increase with ongoing climate change and to cause environmental problems on the regional scale (Todd et al. 2012; Wanner et al. 2018).

To assess the hazard of permafrost retreat in areas with pyrite-containing host rock for the regional water quality, in 2021 we have initiated a detailed monitoring of the Val Costainas catchment, Eastern Switzerland. The monitoring includes monthly sampling and discharge measurements at the rock glacier outlet to track element effluxes being mobilized from the permafrost area. In addition, we continuously track these fluxes about 5 km downstream, at the Präsüra gorge, using a combined pressure and conductivity probe. These data are used to apply the determined correlations between electric conductivity and element concentrations. In accordance with the same procedure, correlation between water table and discharge measurements is applied.

Our monitoring shows that the fluxes of toxic elements (Mn, Ni, Zn, F) at the two sampling locations are very similar, demonstrating that all elements are mobilized from the permafrost area. Considering that the mobilized elements are enriched in rock glacier ice (Krainer et al. 2015), this further suggests that the recorded fluxes can potentially be used to estimate ice melt production in rock glacier systems.

In 2021, our monitoring yielded surprisingly high annual fluxes between 1–10 t and a strong seasonal flux variation of the mobilized toxic elements (Mn, Ni, Zn, F). More than 60% of the annual element fluxes were mobilized during June, July and August. From January to July 2022, the fluxes and hence the ice melt production were about 20% lower than for the same period in 2021, although the spring and summer temperatures were mostly much higher. For both years, the peaks in element fluxes correlate with high discharges caused by snowmelt in May and June and heavy rainfall events in July and August. Moreover, in 2021 the total discharge between January to July was 80% higher than in 2022. These observations demonstrate that, unlike atmospheric temperature, the subsurface water flux in rock glacier systems (controlled by snowmelt and rainfall) has a strong control on ice melt production. The same applies for the toxic elements mobilized from the host rock because they are temporally stored in the permafrost ice before they are eventually exported during ice melt production in summer.

Monitoring in the upcoming years will track the evolution of annual toxic element fluxes and assess whether they will increase in the future in response to climate change. This may provide more insights into the coupled interaction between water percolation through the permafrost body, the host rock minerals and the rock glacier ice.

## REFERENCES

- Bigham, J.M., & Nordstrom, D.K. 2000: Iron and aluminum hydroxysulfates from acid sulfate waters, *Rev. Mineral. Geochem.*, 40, 351-403.
- Carrero, S., Pérez-Lopez, R., Fernandez-Martinez, A., Cruz-Hernandez, P., Ayora, C., & Poulain, A. 2015: The potential role of aluminium hydroxysulfates in the removal of contaminants in acid mine drainage, *Chem. Geol.*, 417, 414-423.
- Krainer, K., Bressan, D., Dietre, B., Haas, J.N., Hajdas, I., Lang, K., Mair, V., Nickus, U., Reidl, D., Thies, H., Tonidandel, D. 2015: A 10,300-year-old permafrost core from the active rock glacier Lazaun, southern Ötztal Alps (South Tyrol, northern Italy), *Quaternary Research*, 83, 324-335.
- Todd, A.S., Manning, A.H., Verplanck, P.L., Crouch, C., McKnight, D.M., & Dunham, R. 2012: Climate-change-driven deterioration of water quality in a mineralized watershed, *Environ. Sci. Technol.* 46, 9324-9332.
- Wanner, C., Pöthig, R., Carrero, S., Fernandez-Martinez, A., Jäger, C., & Furrer, G. 2018: Natural occurrence of nanocrystalline Al-hydroxysulfates: Insights on formation, Al solubility control and As retention, *GCA*, 238, 252-269.

## 15.10

# Characterization of a glacier collapse feature development at Rhonegletscher, Switzerland.

Christophe Ogier<sup>1,2</sup>, Leo Hösli<sup>1,2</sup>, Ludovic Räss<sup>1,2</sup>, Matthias Huss<sup>1,2,3</sup>, Andreas Bauder<sup>1,2</sup>, Daniel Farinotti<sup>1,2</sup>

<sup>1</sup> Laboratory of Hydraulics, Hydrology and Glaciology, ETH Zurich, Hönggerbergstrasse 26, CH-8049 Zurich (ogier@vaw.baug.ethz.ch).

<sup>2</sup> Swiss Federal Institute for Forest, Snow and Landscape Research (WSL), Zürcherstrasse 111, CH-8903 Birmensdorf.

<sup>3</sup> Department of Geosciences, University of Fribourg, Chem. du Musée 4, CH-1700 Fribourg.

A recent increase in collapse features of glacier snouts throughout the Swiss Alps has been reported in literature (Egli et al., 2021 ; Hösli et al., 2022). Collapse features have been associated with the development of a cavity over a subglacial channel at the glacier snout. Their development leads to the formation of circular crevasses at the surface due to ice creep and ice roof instability (Egli et al., 2021). These collapses can have important impacts on glacier length variation, subglacial hydrology and flood hazards (Dewald et al., 2021). In June 2022, early stage of circular crevasses at the tongue of Rhonegletscher (Switzerland) were observed (see Fig. 1a) and indicated the ongoing development of a collapse feature. We thus took the opportunity to extensively monitor its development to better understand the physical processes at play. Digital elevation model (DEM) comparison at the glacier tongue between August 2021 and October 2021 reveals first evidence indicating an additional subsidence -1.3 m (i.e. the surface elevation change corrected by the melt) in comparison to nearby elevation change, although the feature was not yet visually recognizable.

The monitoring program started in June 2022 and was constituted of mass balance measurements, repetitive topography measurements by uncrewed aerial vehicle (UAV), repetitive ground penetrating radar (GPR) to infer the cavity geometry and visual inspections through boreholes to constrain the geometry. The subsidence at the center of the collapse feature was 5.27 m between 20<sup>th</sup> June and 24<sup>th</sup> August (which is 8.5 cm d<sup>-1</sup> in average during the 62 days). The volume change inferred by GPR shows a significant increase in cavity height over the summer. We hypothesize, on the basis of visual observations, that the cavity volume change is most likely driven by mechanical failure (i.e. collapse of ice lamellas) rather than by subglacial melt owing to heat transfers. Numerical models accounting for visco-elasto-plastic ice rheology should support our findings. Interestingly, the development of the Rhonegletscher snout collapse appears to be significantly faster than the overall average of collapse development throughout Switzerland that is about five years (Hösli et al., 2022). The location of the subglacial-water pathway in the cavity vicinity indicates a meandering of the main subglacial channel that could have caused the cavity initiation, but more research is needed to fully resolve the initiation stages.

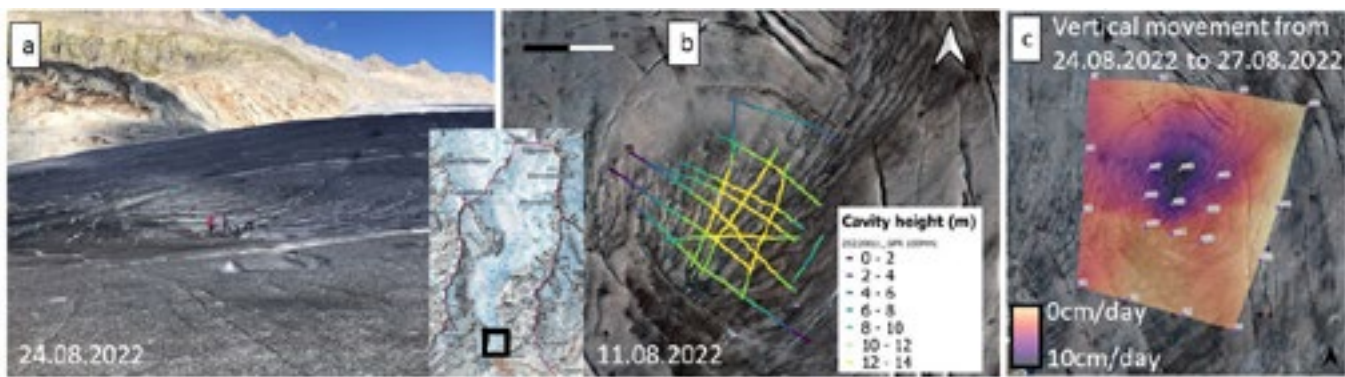


Figure 1. a) Circular crevasse development on Rhonegletscher in summer 2022, b) subglacial cavity height inferred from GPR measurements, and c) daily averages of vertical movement at the glacier surface over the subglacial cavity in August 2022.

## REFERENCES

- Egli, P. E., Belotti, B., Ouvry, B., Irving, J., & Lane, S. N. 2021: Subglacial channels, climate warming, and increasing frequency of Alpine glacier snout collapse. *Geophysical Research Letters*, Vol 48, n°21.
- Hösli, L., Ogier, C., Huss, M., Farinotti, D. 2022, Recent increase in collapse features on glacier snouts throughout the Swiss Alps, submitted to the Swiss Geosciences Meeting 2022, Lausanne.
- Dewald, N., Lewington, E. L., Livingstone, S. J., Clark, C. D., & Storrar, R. D. 2021: Distribution, characteristics and formation of esker enlargements. *Geomorphology*, Vol 392, p107919.

## 15.11

# Rock Glacier Velocity as a new associated product to the ECV permafrost: basic concepts and exemplary results

Cécile Pellet<sup>1</sup>, Chloé Barboux<sup>1</sup>, Thomas Echelard<sup>1</sup>, Sebastián Vivero<sup>1</sup>, Reynald Delaloye<sup>1</sup>

<sup>1</sup> Departement of Geoscience, University of Fribourg, Chemin du Musée 4, CH-1700 Fribourg ([cecile.pellet@unifr.ch](mailto:cecile.pellet@unifr.ch))

The response of mountain permafrost to ongoing climate change is hardly known in most mountainous regions worldwide due to a lack of observation data. On the global scale, the evolution of mountain permafrost is mainly assessed by temperature monitoring in boreholes, which is the only direct observation method. However, these observations are limited to single locations scarcely distributed around the world.

Rock glaciers are characteristic landforms associated with mountainous periglacial landscapes and have been widely exploited since the mid-20th century as visual indicators of mountain permafrost. Recently, studies have shown that the velocity of rock glaciers responds sensitively and almost similarly to inter-annual and decennial changes in ground temperatures and ground water content, thus providing proxy data on thermally-induced changes of permafrost conditions. For this reason, Rock Glacier Velocity (RGV) was adopted in 2021 as a new product to the Essential Climate Variable (ECV) Permafrost by the Global Climate Observing System (GCOS) and the Global Terrestrial Network for Permafrost (GTN-P, Streletschi et al. 2021). In order to consistently monitor this new parameter and to produce comparable long-term time series, basic concepts and practical guidelines need to be established. This is one of the main aim of the IPA-supported Action Group on Rock Glacier Inventories and Kinematics (RGIK), which was established in 2018 and now counts more than 190 members (see abstract from Vivero et al. and Echelard et al.).

In this contribution, we will present the content of the guidelines established within the framework of the RGIK action group, including the formal ECV requirements, and show exemplary results of standardized RGV time series.

## REFERENCES

Streletschi, D., Noetzli, J., Smith, S.L., Vieira, G., Schoeneich, P., Hrbacek, F., and Irrgang, A. M. 2021. Strategy and Implementation Plan for the Global Terrestrial Network for Permafrost (GTN-P) 2021-2024, doi:10.5281/ZENODO.6075468.

## 15.12

### Reconstructing the Little Ice Age glacier surface

Johannes Reinthaler<sup>1</sup> and Frank Paul<sup>1</sup>

<sup>1</sup> Department of Geography, University of Zurich, Winterthurerstr. 190, CH-8057 Zurich ([johannes.reinthaler@geo.uzh.ch](mailto:johannes.reinthaler@geo.uzh.ch))

Most glaciers in the world reached their Holocene maximum extent during the so-called Little Ice Age (LIA). To calculate glacier volume change since the LIA, information about glacier surface elevation is required. Glacier volume changes over the last 20 years are now globally available (Hugonnet et al. 2021), but information from before the satellite era is still sparse (but constantly improving). To reconstruct the glacier surface at the LIA maximum, recent studies interpolated the elevation from the values along the former outline, so that by now a range of surface reconstruction and interpolation methods have been developed and applied. However, no detailed comparison of the methods, their input data requirements or uncertainty analysis of the related surface reconstruction method has been presented so far.

In this study, we quantify the performance of different surface interpolation methods and what effect the different input datasets have when replicating modern glacier surfaces from a recent DEM. This was tested with the Arctic DEM for a sample of 85 glaciers in southern Novaya Zemlya, Russia with a total area of 644 km<sup>2</sup> during the LIA and 475 km<sup>2</sup> in 2016 (-26%). First results indicate, that the Natural neighbour as well as the Topo to Raster tool, are the most promising interpolation methods.

We also developed a method for LIA surface reconstruction, complementing outline elevation data with centre point elevations derived from elevation changes on the side of the glacier. This allowed us to generate a more realistic representation of the former glacier surface by accounting for concave or convex surfaces. A comparison of GIS based methods with modelled results (Jouvet 2022) indicates under/overestimates in the accumulation/ablation area.

The calculated volume change for the glacier sample in Novaya Zemlya is -14.8 km<sup>3</sup> or -0.14 m a<sup>-1</sup>. The change rates over the twentieth century are thus much smaller than the -0.8 ± m a<sup>-1</sup> derived for the same sample over the past two decades by Hugonnet et al. (2021).

#### REFERENCES:

- Hugonnet, R., McNabb R., Berthier E., Menounos B., Nuth C., Girod L., Farinotti D., Huss M., Dussaillant I., Brun F., & Kääb A. 2021: Accelerated Global Glacier Mass Loss in the Early Twenty-First Century. *Nature* 59, 2726–31. doi: [10.1038/s41586-021-03436-z](https://doi.org/10.1038/s41586-021-03436-z).
- Jouvet, G. 2022: Inversion of a Stokes Ice Flow Model Emulated by Deep Learning. *Journal of Glaciology* 1–14. doi: <https://doi.org/10.1017/jog.2022.41>.

## 15.13

### Numerical simulation of ice column melting located in mountain permafrost due to global warming

Amir Sedaghatkish<sup>1,2</sup>, Marc Luetscher<sup>1</sup>

<sup>1</sup> Swiss Institute for Speleology and Karstology (SISKA), CH-2300, La Chaux-de-Fonds, Switzerland

<sup>2</sup> Center for Hydrogeology and Geothermics (CHYN), University of Neuchâtel, 2000 Neuchâtel, Switzerland

Thawing mountain permafrost modifies inexorably the hydrological and ventilation regimes of Alpine karst systems. A two-dimensional numerical model has been developed to investigate the phase change behavior of an ice-filled shaft situated in mountain permafrost under the effect of deep geothermal heat flux and atmosphere temperature increase caused by global warming. We identify different heat transfer mechanisms controlling the melting rate and morphology of ice-water interface shape including heat conduction in water, ice and surrounding rock, the latent heat release due to phase change and the free convective heat flux of water flow coming from abnormal behavior of density inversion point between 0 and 4 °C which produces circulating water convection cells above the melting ice.

All the aforementioned mechanisms are coupled with each other to understand the playing role of each mechanism and parameters on the total heat transfer rate. The continuity, momentum equation with Boussinesq approximation and the energy equation using apparent heat capacity method are solved numerically. The results of this study illustrate the time required for the complete melting of any ice-filled with known diameter and length as well as the evolution of the ice-water interface at different times. Moreover, the computed velocity field and temperature distribution of water, ice and rock can provide useful information in glaciology and hydrogeology. We conclude that thermal breakthrough occurs within certain years, followed by rapid acceleration of heat transfers across the karst system.

## 15.14

### Impact assessment of Supra-glacial debris thickness on the melting of glaciers in Karakoram based on In-Situ measurement

Syed Hammad Ali<sup>1</sup>, Khushdar Ali<sup>1</sup>, Tanzeel Ur Rehman<sup>1</sup>, Nasir Hussain<sup>1</sup>, Mazhar Ali<sup>1</sup>, Raza Ali<sup>1</sup>

<sup>1</sup> Pakistan Water & Power Development Authority (WAPDA), Glacier Monitoring & Research Center (GMRC) (syedhammadali2001@yahoo.com)

Large numbers of glaciers in the HKKH region are covered with debris (boulders, rocks & sand) in the ablation zone, which are accessible in the lower elevations but are rarely observed in the field (Patel L.K., et. al 2021). The supra-glacial debris transported over the melting glacier surface acts as an insulating barrier between the ice and atmospheric conditions and has a strong influence on the spatial distribution of surface ice melt (Nicholson et al., 2018). We conducted in-situ measurements of point-wise ablation rate, supra-glacial debris thickness and its influence on ablation over two glaciers (Hispar and Yashkuk Yaz) in Hunza Basin of Karakoram during the ablation period (July - October 2021) and (May – September 2018). Hunza River basin with drainage area of 13,713 km<sup>2</sup> located in the high-altitude central Karakoram region, Pakistan. Total numbers of glaciers in Hunza basin are approximately 1,384 covering an area of 2,754 km<sup>2</sup> and about 15% of glacier area ranges from 2,409 – 5,297 m.a.s.l. are covered by debris with varying thicknesses. The stake wise debris thickness measured at Hispar glacier ranges from 5cm to 20cm, while 5cm to 80cm was measured at Yashkuk Yaz glacier. Surface velocities for both glaciers have also been calculated by using a distance-weighted average method. Our results demonstrate the importance of accounting for debris on glacier and measurements taken at the surface of glaciers shows strong relationship between the thickness of debris and the rate of ice melting which plays an important role in surface energy balance and the rate of glacier ablation. Emaciated debris cover enhances the melting of glacier ice while substantial layer of debris reduces the melt rate exponentially. This type of analysis is useful for the empirical parameterization of numerical models and understanding the relationships between surface debris and glacier melting for accurately predicting how debris-covered glaciers in Karakoram region will react to climate change, and whether changes in the patterns of ice melting will threaten communities living downstream (e.g. GLOFs & flooding).

## REFERENCES

- Patel LK, Sharma P, Singh A, Oulkar S, Pratap B and Thamban M (2021) Influence of Supraglacial Debris Thickness on Thermal Resistance of the Glaciers of Chandra Basin, Western Himalaya. *Front. Earth Sci.* 9:706312. doi: 10.3389/feart.2021.706312.
- Nicholson, L. I., McCarthy, M., Pritchard, H. D., and Willis, I. (2018). Supraglacial Debris Thickness Variability: Impact on Ablation and Relation to Terrain Properties. *The Cryosphere* 12 (12), 3719–3734. doi:10.5194/tc-12-3719-2018.

## 15.15

# Modelling the historical and future evolution of multiple glaciers in the Kyrgyz Tien Shan, Central Asia, using a 3D ice-flow model.

Lander Van Tricht<sup>1</sup>, Philippe Huybrechts<sup>1</sup>

<sup>1</sup>*Earth System Science and Department of Geography, Vrije Universiteit Brussel, Brussels, Belgium  
(lander.van.tricht@vub.be)*

High Mountain Asia (HMA) contains the largest concentration of glaciers outside the polar regions. These glaciers play an essential role in terms of water supply for the surrounding densely populated lowland areas of countries such as Kyrgyzstan, Kazakhstan and Uzbekistan. During summer months, the contribution of glacier meltwater to fresh water supply for households, agriculture and industry can increase to more than 50%. The retreat of these glaciers consequently can have a major impact on societies. However, few detailed modelling studies exist that examine in detail how individual ice bodies in the area are responding to climate change. Further, different climatic and topographic settings ensure a heterogenous impact on ice masses in the area. In this study, we focus on the western part of the Tien Shan mountain range in the northwest of HMA. During the Soviet era, various glaciological measurements were carried out in this region. After abandonment in the nineties, different measurement programs have reinitiated in the last decades. We use several recent measurements and reconstructions of the ice thickness, surface elevation, surface mass balance and ice temperature to study in detail six different ice masses in the Kyrgyz Tien Shan: 5 valley glaciers and 1 ice cap. The selected ice bodies are located in different sub-regions of the Tien Shan with different climate regimes, and they are all characterised by detailed recent glaciological measurements. A 3-dimensional higher-order model is calibrated and applied to simulate the evolution of the ice masses since the Little Ice Age and to make a prognosis of the future evolution up to 2100 under 4 different SSP climate scenarios.

## P 15.1

# Rock-glacier hydrology with the magnifying glass: Where do the solutes in the Murtèl outflow come from?

Dominik Amschwand<sup>1</sup>, Seraina Tschan<sup>1</sup>, Martin Scherler<sup>1†</sup>, Lukas Aschwanden<sup>2</sup>, Martin Hoelzle<sup>1</sup>

<sup>1</sup> Department of Geosciences, University of Fribourg, Chemin du Musée 4, CH-1700 Fribourg ([dominik.amschwand@unifr.ch](mailto:dominik.amschwand@unifr.ch))

<sup>2</sup> Institute of Geology, University of Bern, Baltzerstrasse 1+3, CH-3012 Bern

In rapidly deglacierizing mountains, streamflow contribution from degrading ice-rich permafrost might proportionally increase in late summer. Thereby released solute-rich meltwater attenuates seasonal water scarcity, but also impacts the downstream water quality. However, the ground ice itself is only rarely accessible for sampling and its chemical properties are often extrapolated from analyzed surface waters. Here, we present hydrological data from the outflow of rock glacier Murtèl (Upper Engadine). One of the few chemically analysed mountain permafrost cores was retrieved there in 1987 (Haeberli et al., 1990). Hence, we can directly compare the rock glacier outflow to the isotopic composition and major ion concentrations of the permafrost ice.

In summer 2021, discharge, stable water isotopes ( $\delta^{18}\text{O}/\delta\text{D}$ ), and electrical conductivity (EC) were measured as a proxy for water provenance and solute content of the rock glacier outflow. From July to September, discharge decreased (from ~50 to <3 L/sec),  $\delta^{18}\text{O}$  became enriched (from 16 to 10‰ VSMOW), and EC increased (from 40 to 120  $\mu\text{S}/\text{cm}$ ), indicating the shift from snowmelt-dominated to rainwater-dominated outflow (Fig. 1). The EC-discharge relationship changed during the summer, with increasing EC even for rainfall-driven high-outflow events with high dilution potential (event in late September, Fig. 1). Surprisingly, the permafrost ice of the drillcore has the properties of diluted groundwater (EC ~5–30  $\mu\text{S}/\text{cm}$ ) derived from winter precipitation ( $\delta^{18}\text{O}$  of 13 to 16‰; Haeberli et al., 1990). We suggest that during the summer increasing solute content of the Murtèl rock glacier outflow is the effect of decreasing discharge/dilution and rapid mineralisation in the progressively thickening active layer, rather than inherited from the melting permafrost ice.

Our measurements were continued in summer 2022 and contribute to the understanding of rock-glacier hydrology from the landform to the very small catchment scale.

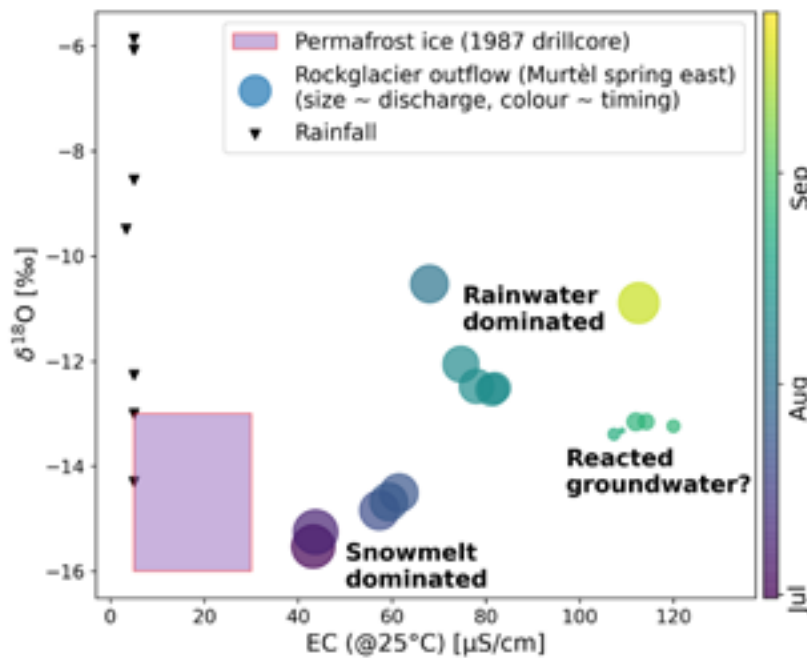


Figure 1. Characterisaton of the Murtèl rock-glacier outflow in terms of  $\delta^{18}\text{O}$ , electrical conductivity (EC), discharge and timing for summer 2021. The  $\delta^{18}\text{O}$ -EC of the permafrost ice (uppermost 28 m) is derived from Haeberli et al. (1990). The rainwater was sampled in the rock glacier forefield every 7–10 days in August and September.

## REFERENCES

- Haeberli, W. (ed.) 1990: Pilot analyses of permafrost cores from the active rock glacier Murtèl I, Piz Corvatsch, eastern Swiss Alps. A workshop report, VAW Arbeitsheft 9, 38 p (CRREL No. 44-004131).

## P 15.2

# R-channel laboratory experiment: data evaluation and numerical simulations

Stefanie Börsig<sup>1,2</sup>, Mauro A. Werder<sup>1,2</sup>, Alexander Jarosch<sup>3</sup>, Yuri Prohaska<sup>1,2</sup>, Daniel Farinotti<sup>1,2</sup>

<sup>1</sup> Laboratory of Hydraulics, Hydrology and Glaciology, ETH Zurich, Hönggerbergstrasse 26, CH-8049 Zürich ([sboersig@ethz.ch](mailto:sboersig@ethz.ch))

<sup>2</sup> Swiss Federal Institute for Forest Snow and Landscape Research WSL, Zürcherstrasse 111, CH-8903 Birmensdorf

<sup>3</sup> ThetaFrame Solutions, Hörfarterstrasse 14, A-6330 Kufstein ([info@thetaframe.com](mailto:info@thetaframe.com))

Englacial and subglacial drainage substantially controls glacier dynamics. However, the inside and bed of glaciers are not accessible for investigations and consequently few actual measurements exist. Therefore, the empirical relations in current models are either adopted from other research fields or based on theoretical arguments.

This study focuses on the channelized drainage system and determines the properties of R-channels. We evaluate a set of laboratory experiments and present numerical simulations that represent the flow properties of R-channels. These experiments were designed and conducted at VAW-ETHZ in 2016-2017. Channels with water flow in ice blocks represent pressurized, englacial R-channels. This work includes the evaluation of four experiments and complementary computational fluid dynamics simulations of their final geometries. We calculate the flow properties in two separate assessments to determine the measured and the simulated Darcy-Weisbach friction coefficients. Both from measurements and from simulations resulting friction coefficients are between 0.1 and 0.4 for three of the experiments and between 0.03 and 0.06 for an experiment with a wider initial channel. The agreement between the simulated and measured results and the comparison to recently published studies largely support the validity of the experimental set up and the numerical model. This suggests that both the laboratory experiment and the numerical simulation are good representations of the flow properties in R-channels. Finally, the Reynolds numbers of the experiments are between and , thus above the transition from laminar flow at around , and determine the flow in the ice channel as turbulent.

## P 15.3

# The importance of glacial headwater streams and their climate sensitivity in a glacierized river basin in western Norway

Yongmei Gong<sup>1</sup>, Irina Rogozhina<sup>1</sup>

<sup>1</sup> Department of Geography, Norwegian University of Science and Technology, NO-7491 Trondheim, Norway (yongmei.gong@ntnu.no)

Jostedøla river basin is amongst many highly glacierized drainage basins with complex terrain and local climate in Western Norway. Most headwater streams of the Jostedøla river and its tributaries are connected to the outlet glaciers of the largest icecap in mainland Europe - Jostedalsbreen icecap. These headwater streams contribute to hydropower production and support economically important fisheries.

In this study, we utilize a snow evolution mode coupled with a linear reservoir, water routine model with a daily temporal and 100m × 100m spatial resolution to investigate glaciers' contribution to streamflow and the climate elasticity of headwater streams in Jostedøla river basin in 2000-2014.

The results are analyzed at gauged and ungauged locations along the glacial headwater streams as well as the main river. The mean annual contribution of the water coming from the glacier-covered region ranges from 61.5% downstream the river to 100% at the glacier terminus. These waters are composed of mostly snow meltwater and glacier meltwater with rainwater being a minor contributor. The climate sensitivities of the headwater streams are also calculated. By comparing the annual and intra-annual variability of the discharge and climate sensitivities of the modeled results and the observation at the regulated reaches human influence of the stream flow is investigated.

**P 15.4****Snow accumulation in observation-scarce high-mountain regions inferred from climate reanalyses, satellites and machine learning**

Matteo Guidicelli<sup>1</sup>, Désirée Treichler<sup>2</sup> and Nadine Salzmann<sup>3,4</sup>

<sup>1</sup> Department of Geosciences, University of Fribourg, Fribourg, Switzerland

<sup>2</sup> Institute of Geosciences, University of Oslo, Oslo, Norway

<sup>3</sup> WSL Institute for Snow and Avalanche Research SLF, Davos, Switzerland

<sup>4</sup> Climate Change, Extremes and Natural Hazards in Alpine Regions Research Center CERC, Davos, Switzerland

Snow regimes in high-mountain regions are altering in response to climatic changes. However, the scarcity and limited accuracy of observations of snow and precipitation at high elevation reduce our understanding of cryosphere-climate linkage and the impacts to related components of the Earth System. Here, we compare the winter mass balance of 95 glaciers distributed over the Alps, Western Canada, Central Asia and Scandinavia, with the total precipitation as provided by the ERA-5 and the MERRA-2 reanalysis products during the snow accumulation seasons from 1981 until today. We propose a machine learning model to adjust the precipitation of reanalysis products to the elevation of the glaciers, in order to derive snow water equivalent (SWE) estimates over glaciers uncovered by ground observations and/or to fill observational gaps. We use a gradient boosting regressor (GBR), which combines several meteorological variables from the reanalyses (e.g. air temperature, relative humidity) with topographical parameters. These GBR-derived estimates are evaluated against the winter mass balance data of independent glaciers (site-independent GBR) or independent snow seasons (season-independent GBR). Both site-independent and season-independent GBRs allowed reducing (increasing) the bias (correlation) between the precipitation of the original reanalyses and the winter mass balance data of the glaciers. However, denser ground-based or improved remote sensing observations would enable to further evaluate and develop the presented methods and improving the quantification of high mountain snow accumulation. In current research, we thus aim at exploiting snow depth observations derived from the novel ICESat-2 satellite laser altimeter to improve the reliability of machine learning model-based snow estimates in high-mountain observation-scarce regions.

## P 15.5

# Recent increase in collapse features on glacier snouts throughout the Swiss Alps

Leo Hösl<sup>1,2</sup>, Christophe Ogier<sup>1,2</sup>, Matthias Huss<sup>1,2,3</sup>, Daniel Farinotti<sup>1,2</sup>

<sup>1</sup> Laboratory of Hydraulics, Hydrology and Glaciology, ETH Zurich, Hönggerbergstrasse 26, CH-8049 Zurich  
([hoesli@vaw.baug.ethz.ch](mailto:hoesli@vaw.baug.ethz.ch)).

<sup>2</sup> Swiss Federal Institute for Forest, Snow and Landscape Research (WSL), Zürcherstrasse 111, CH-8903 Birmensdorf.

<sup>3</sup> Department of Geosciences, University of Fribourg, Chem. du Musée 4, CH-1700 Fribourg.

When compared to surface mass balance, glacier snout collapses are considered to be less important for the retreat of alpine glaciers, but yet has important impacts on glaciers length variations, subglacial hydrology and natural hazards (Dewald et al., 2021). Egli et al. (2021) suggested that the occurrence of glacier snout collapse increased in the Western Swiss Alps from 1938 to present, due to increasing air temperatures and a decrease in longitudinal ice flux at the tongue. Observations also suggest that collapses are often preceded by the formation of concentric circular crevasses (Fig. 1).

In order to better understand the processes of collapse developments, we inventoried circular crevasses and snout collapse for all glaciers in Switzerland since 1970, thus extending the spatial scope of the work of Egli et al. (2021). For this purpose, we applied the geospatial intelligence software Picterra (<https://picterra.ch>) to aerial images of the Federal Office of Topography (swisstopo). As a first step, we manually delineated a set of circular crevasses to train the algorithm. In a second step, we ran the algorithm over all Swiss glaciers since 1970. Manual validation of the method was performed on several set of images and showed very good agreement: less than 10% of false positive were found, and were removed manually from the inventory. In total, 211 collapses were mapped over the period 1970-2021 (Fig. 2).

This new inventory of circular crevasses allows constraining the duration over which such features develop, can help in the prediction of future snout collapses, and confirms the general increase of glaciers snout collapses in Switzerland. Interestingly we observed a sharp increase in the development of circular crevasses since 2003, linked with strong air temperature increase for the same period. We suggest that snout collapses will become more common in the Alps in the coming decades, with strong implications on glacier retreat.



Figure 1. Circular crevasses and collapse feature on Mittelaletschgletscher, 2021 (image swisstopo).

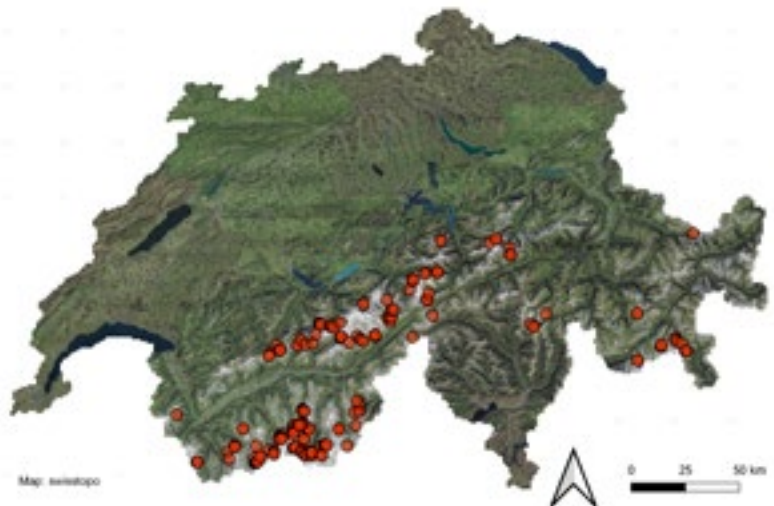


Figure 2. Glacier snout collapse events for all Swiss glaciers for the period 1970-2021 (211 events).

#### REFERENCES

- Egli, P. E., Belotti, B., Ouvry, B., Irving, J., & Lane, S. N. 2021: Subglacial channels, climate warming, and increasing frequency of Alpine glacier snout collapse. *Geophysical Research Letters*, Vol 48, n°21.
- Dewald, N., Lewington, E. L., Livingstone, S. J., Clark, C. D., & Storrar, R. D. 2021: Distribution, characteristics and formation of esker enlargements. *Geomorphology*, Vol 392, p107919.

## P 15.6

# Application of the thermal Model CryoGrid Community Model (Version 1.0) in the Swiss Alps to assess Permafrost Degradation and to quantify volumetric Ice Content

Sarah Morard<sup>1</sup>, Sebastian Westermann<sup>2</sup>, Florian Wagner<sup>3</sup>, Coline Mollaret<sup>1</sup>, Christian Hauck<sup>1</sup>

<sup>1</sup> Department of Geosciences, University of Fribourg, Fribourg, Switzerland ([sarah.morard@unifr.ch](mailto:sarah.morard@unifr.ch))

<sup>2</sup> Department of Geosciences, University of Oslo, Oslo, Norway

<sup>3</sup> Institute for Applied Geophysics and Geothermal Energy, RWTH Aachen University, Aachen, Germany

The CryoGrid community model is a thermal model built with modules through object-oriented programming. This model is used for simulating the ground thermal regime and quantifying ice and water content in permafrost or glacier contexts. CryoGrid includes different parametrizations and process representations as the subsurface heat transfer or the water balance. Moreover, it is an open-source model, that offers flexibility to adapt the model to specific case studies (Westermann et al., 2022). The model is based on meteorological input and some in-situ knowledge as for example the porosity, the mineral content of the ground. The presence of site-specific borehole information helps to validate the model results. CryoGrid was already tested for permafrost case studies to simulate the thermal regime and thaw processes by Westermann et al. (2016).

In this study, we combine the CryoGrid community model with a petrophysical joint-inversion (PJI) approach for geophysical data (Wagner et al., 2019 ; Mollaret et al., 2020) and used borehole data (PERMOS, 2022) for initialization and validation. The PJI provides information on the volumetric rock, water and ice content of the subsurface using electrical and seismic tomographic measurements. We applied the model to several permafrost sites of PERMOS / UNIFR where many ERT and RST measurements have been repeated in a monitoring context. This approach enables us to validate and compare the CryoGrid results with on-site geophysical measurements. Further, long-term meteorological and borehole (PERMOS, 2022) exist at these sites.

The PJI provides us only discrete insights into current ice and water content since we need a dataset of ERT and RST at the same date. In contrast, the CryoGrid community model provides a continuous time series into the past based on the weather station data and into the future using climate model simulations as forcing data. By this, it yields data on potential permafrost degradation. The final goal will be with CryoGrid the assessment of the future presence of taliks and the time-scales of permafrost degradation.

## REFERENCES

- Mollaret, C., Wagner, F. M., Hilbich, C., Scapozza, C., Hauck, C. (2020). Petrophysical Joint Inversion Applied to Alpine Permafrost Field Sites to Image Subsurface Ice, Water, Air and Rock contents. *Front. Earth Sci.* 8:75. doi: 10.3389/feart.2020.00085
- PERMOS (2022). <http://www.permos.ch/index.html> [Access on 27.08.2022]
- Wagner, F. M., Mollaret, C., Günther, T., Kemna, A., Hauck, C. (2019), Quantitative imaging of water, ice and air in permafrost systems through petrophysical joint inversion of seismic refraction and electrical resistivity, *J. Geophys. Int.*, 2019, 1866-1875, doi:10.1093/gji/ggz402
- Westermann, S., Langer, M., Boike, J., Heikenfeld, M., Peter, M., Etzelmüller, B., Krinner, G. (2016) : Simulating the thermal regime and thaw processes of ice-rich permafrost ground with the land-surface model CryoGrid3. *Geosci. Model Dev.*, 9, 523-546, doi:10.5194/gmd-9-523-2016
- Westermann, S., Ingeman-Nielsen, T., Scheer, J., Aalstad, K., Aga, J., Chaudhary, N., Etzelmüller, B., Filhol, S., Kääb, A., Renette, C., Steffensen Schmidt, L., Vikhamar Schuler, T., Zweigel, R. B., Martin, L., Morard, S., Ben-Asher, M., Angelopoulos, M., Boike, J., Groenke, B., Miesner, F., Nitzbon, J., Overduin, P., Stuenzi, S. M., Langer, M. (2022). The CryoGrid community model (version 1.0) – a multi-physics toolbox for climate-driven simulations in the terrestrial cryosphere. *Geoscientific Model Development*. <https://doi.org/10.5194/gmd-2022-127>.

## P 15.7

# Unlocking spatio-temporal variabilities of surface fluxes over rockglacier Murtèl with thermal infrared imaging

Kathrin Naegeli<sup>1</sup>, Dominik Amschwend<sup>2</sup>, Martin Hoelzle<sup>2</sup>

<sup>1</sup> Remote Sensing Laboratories, Department of Geography, University of Zurich, Winterthurerstr. 190, 8057 Zürich  
(kathrin.naegeli@geo.uzh.ch)

<sup>2</sup> Department of Geosciences, University of Fribourg, Chemin du Musée 4, 1700 Fribourg

Worldwide, the main alpine cryospheric components, such as snow, glaciers and permafrost, undergo drastic changes due to global climate change. The alpine cryosphere is particularly vulnerable and affected. The surface energy budget is out of balance and requires an improved monitoring, for rugged terrain in particular at the spatial length scale. It is crucial to be able to capture the individual heat fluxes and understand their spatial variability and interactions at the complex surface-atmosphere interface. Particularly key is an improved representation of all energy and mass fluxes that determine the ground thermal regime for high mountain permafrost in the first place. However, spatial monitoring of surface energy fluxes is challenging and requires imaging systems.

Here, we present a time series of terrestrial thermal infrared images and thus spatially distributed land surface temperature (LST) information of Murtèl rockglacier in the Engadin. We put a specific focus on the importance of individual processing steps, e.g. topographic and atmospheric correction, of such imagery and the use of point measurements (e.g. thermal infrared radiometers, short- and longwave radiation measurements) for calibration and validation.

Our study works towards an enhanced application of thermal infrared remote sensing techniques in rugged and complex terrain, but also fosters an advancement in energy budget assessments of cryospheric components at varying spatial length scales.

## P 15.8

# How does the hot summer 2022 affect the permafrost in the Swiss Alps?

Jeannette Nötzli<sup>1</sup>, Cécile Pellet<sup>2</sup>, and the PERMOS Scientific Committee

<sup>1</sup> WSL Institute for Snow and Avalanche Research SLF, Flüelastrasse 11, CH-7260 Davos Dorf ([jeannette.noetzli@slf.ch](mailto:jeannette.noetzli@slf.ch))

<sup>2</sup> Department of Geoscience, University of Fribourg, Chemin du Musée 4, CH-1700 Fribourg ([cecile.pellet@unifr.ch](mailto:cecile.pellet@unifr.ch))

Permafrost is classified as an Essential Climate Variable (ECV) by the Global Climate Observing System (GCOS) because of its sensitivity to changes in climatic conditions. The Swiss Permafrost Monitoring Network (PERMOS) is in charge of documenting the state and changes of permafrost in Switzerland. This is based on (1) ground temperatures measured in boreholes; (2) changes in ground ice content determined based on geophysical methods and (3) rock glacier velocities, which can be used as a proxy to assess the permafrost thermal regime.

In this contribution we will present a first assessment of the permafrost observations in the Swiss Alps during the hydrological year 2022. Following a warm winter and spring with below average snow heights (SLF 2022), summer 2022 was the second warmest on record with 2.3 °C above the average 1991–2020 (MeteoSwiss 2022a). End of July, for example, the highest temperature since the start of the measurements was recorded on Piz Corvatsch and the 0 °C isotherm reached a record altitude of 5184 m asl. (MeteoSwiss 2022b).

New record temperatures were also recorded in the uppermost metres in most of the permafrost boreholes in August 2022, where data can be accessed remotely. Also the 0°C isotherm was generally deeper than observed before at this time of the year. However, a large part of the PERMOS data are currently being collected in the field and first results will be available in autumn. We will present a preliminary evaluation of permafrost temperatures, changes in ground ice content and rock glacier velocity observed after the snow-poor winter and hot summer 2022, and put them in context with the long-term time series of the PERMOS network (PERMOS 2022). Due to the considerable time lag with which thermal conditions at the surface penetrate to depth, however, a full assessment of the effect of the summer 2022 heat wave on the permafrost in the Swiss Alps can only be done in the course of the year 2023.

## REFERENCES

- MeteoSchweiz 2022a. Hitzesommer, MeteoSchweiz Blog from the 25. August 2022, <https://www.meteoschweiz.admin.ch/home/aktuell/meteoschweiz-blog.subpage.html/de/data/blogs/2022/8/hitzesommer.htm>.
- MeteoSchweiz 2022b. Heisser und extrem sonniger Juli, MeteoSchweiz Blog from the 29. July 2022, <https://www.meteoschweiz.admin.ch/home/aktuell/meteoschweiz-blog/meteoschweiz-blog.subpage.html/de/data/blogs/2022/7/bilan-juillet-2022.html>.
- SLF 2022. Winterflash, Winterbericht 2021/2022, 11. April 2022, <https://www.slf.ch/de/lawinenbulletin-und-schneesituation/wochen-und-winterberichte/2021/22/winterbericht-2021/22.html>
- PERMOS 2022: Swiss Permafrost Bulletin 2021. Nötzli, J. and Pellet, C. (eds.) 22 pp, doi:10.13093/permos-bull-2022.

## P 15.9

### Developing an in-situ $^{14}\text{C}$ chronology for North Greenland

Anne Sofie Søndergaard<sup>1</sup>, Olivia Steineman<sup>1</sup>, Negar Haghipour<sup>1</sup>, Lukas Wacker<sup>1</sup>, Susan Ivy-Ochs<sup>1</sup>, Nicolaj Krog Larsen<sup>2</sup>

<sup>1</sup> Laboratory for Ion Beam Physics, ETH Zürich ([anneso@phys.ethz.ch](mailto:anneso@phys.ethz.ch))

<sup>2</sup> Centre for GeoGenetics, GLOBE Institute, University of Copenhagen

Determining the sensitivity of the Greenland Ice Sheet during the Holocene is a key prerequisite for understanding the future response of the ice sheet to global warming. It has proven difficult to constrain the glacial history of particularly North Greenland, an area predicted to be a key component in future mass loss from the ice sheet (Mouginot et al., 2019). To fill this gap, this project will be the first to use cosmogenic in-situ  $^{14}\text{C}$  exposure dating to constrain Holocene ice sheet fluctuations in North Greenland. Cosmogenic nuclides are produced in rocks when cosmic rays hit the surface of the Earth. The cosmogenic nuclide inventory of a rock surfaces is therefore a key tool for chronicling the waxing and waning of ice. The most commonly analysed nuclide is  $^{10}\text{Be}$ , which has a half-life of 1.4 Myr. However, a particular challenge arises in regions where the ice sheet base is cold and slow-moving. In these regions, erosion rates are low and  $^{10}\text{Be}$  inventories produced during earlier exposure periods accumulate instead of being removed, which result in exposure ages older than the last period of exposure (Heyman et al., 2011). To circumvent this problem, we use in-situ produced cosmogenic  $^{14}\text{C}$ . Due to the shorter half-life (5730 yr), in-situ  $^{14}\text{C}$  inventories will, contrary  $^{10}\text{Be}$ , decrease not only because of rock surface erosion but also due to shielding from ice cover. Measurements of in-situ  $^{14}\text{C}$ , carried out at the in-situ  $^{14}\text{C}$  line at Laboratory of Ion Beam Physics, ETH Zürich (Lupker et al., 2019), can therefore help to obtain more reliable ice reconstructions for North Greenland.

#### REFERENCES

- Heyman et al. 2011: Too young or too old: Evaluating cosmogenic exposure dating based on an analysis of compiled boulder exposure ages, *Earth and Planetary Science Letters*, 302, 71  
Lupker et al. 2019: In-situ cosmogenic  $^{14}\text{C}$  analysis at ETH Zürich: haracterization and performance of a new extraction system, *Nuclear Inst. and Methods in Physics Research B*, 457, 30  
Mouginot et al. 2019: Forty-six years of Greenland Ice Sheet mass Balance from 1972 to 2018, *PNAS*, 116, 9239

## P 15.10

# Investigating hanging glacier geometries in the Mont-Blanc Massif (France) and Pennine Alpes (Switzerland) using ground penetrating RaDAR

Ben Robson<sup>1</sup>, Christophe Lambiel<sup>2</sup>, Ludovic Ravanel<sup>3</sup>, James Irving<sup>4</sup>, Ludovic Baron<sup>4</sup>, Jérémie Gentizon<sup>1</sup>

<sup>1</sup> University of Lausanne, Mouline - Géopolis, CH - 1015 Lausanne ([ben.robson@unil.ch](mailto:ben.robson@unil.ch))

<sup>2</sup> Institut des dynamiques de la surface terrestre (IDYST), University of Lausanne, Mouline - Géopolis, CH - 1015 Lausanne

<sup>3</sup> Environnements, Dynamiques et Territoires de la Montagne (EDYTEM Lab.), Université de Savoie, CNRS, F-73376, Le Bourget-du-Lac, France

<sup>4</sup> Institut des sciences de la Terre (ISTE), University of Lausanne, Mouline - Géopolis, CH - 1015 Lausanne

Hanging glaciers (HGs) and ice aprons (IAs) are of significant interest to the scientific community. In the densely populated European Alps, the evolution and destabilisation of these steep ice bodies under a warming climate can have important consequences. Ice avalanches from HGs, for example, regularly threaten mountain infrastructure (Margreth et al., 2017), have caused human disasters (Pralong & Funk, 2006), and can be sufficiently large to threaten entire villages (Faillettaz et al., 2016). The current body of literature demonstrates that while many external parameters of both IAs and HGs are known, understanding of subglacial geometries is poor, which motivates this research.

The objectives of this project encompass:

- The determination of the subglacial geometry of selected HGs and the quantification of HG ice volumes using ground penetrating radar (GPR).
- The quantification of the summer melt response by drone-based photogrammetric surveys.
- Digital Elevation Model (DEM) production of a recently de-glaciated face and quantification of the historically lost ice volume. The study site is Aiguilles des Grands Charmoz, France, where an IA melted completely in 2017 (Guillet & Ravanel, 2020).

Data were acquired in mid-August 2022 at the Aiguille du Midi (Chamonix Mont-Blanc), at Jumeau Est (3600 m a.s.l.), Frendo Superior (3700 m) and Mallory (3800 m) HGs. At each site, a longitudinal GPR profile was made from the IA summit to the last major crevasse of the HG before the unstable ice lamella, with transect lengths of up to 280 m. At the end of single or double rope lengths, a controlled pendulum swing with the GPR instrument was made to acquire approximately horizontal profiles (Fig. 1). The precise locations of all GPR measurements were obtained via a differential Global Positioning System (dGPS) (Fig. 2).

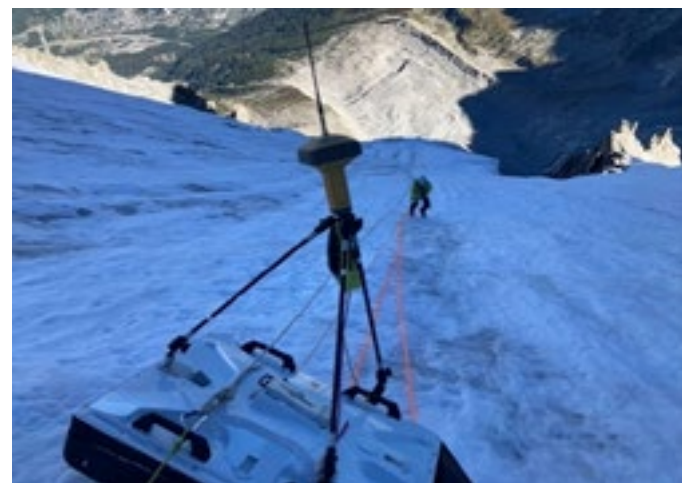
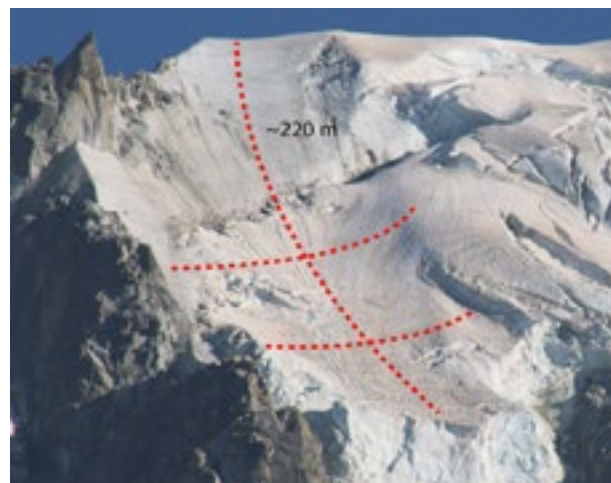


Figure 1 (left) : Conceptualised survey grid, HG Jumeau Est. Figure 2: Impulse Radar CO730 GPR and Topcon dGPS on HG Mallory

## REFERENCES

- Guillet, G., & Ravanel, L. (2020). Variations in surface area of six ice aprons in the Mont-Blanc massif since the Little Ice Age. *Journal of Glaciology*, 66(259), 777–789.
- Faillietaz, J., Funk, M., & Vagliasindi, M. (2016). Time forecast of a break-off event from a hanging glacier. *The Cryosphere*, 10(3), 1191–1200.
- Pralong, A., & Funk, M. (2006). On the instability of avalanching glaciers. *Journal of Glaciology*, 52(176), 31–48.
- Margreth, S., Funk, M., Tobler, D., Dalban, P., Meier, L., & Lauper, J. (2017). Analysis of the hazard caused by ice avalanches from the hanging glacier on the Eiger west face. *Cold Regions Science and Technology*, 144, 63–72.



## 16. Atmospheric Composition and Biosphere-Atmosphere Interactions +

## 17. Climatology +

## 18. Tackling the Climate Crisis: Interdisciplinary Perspectives on Climate Change Education and Communication

Convenors session 16: Martin Steinbacher, Christof Ammann, Stefan Brönnimann, Mana Gharun, Ulrich Krieger + Convenors session 17: Stefan Brönnimann, Daniela Domeisen, Jörg Franke, Sven Kotlarski, Martine Rebetez + Convenors session 18: Moritz Gubler, Petra Bättig-Frey, Christina Colberg, Andreas Linsbauer, Matthias Probst,

*Commission on Atmospheric Chemistry and Physics (ACP) + Swiss Commission for Phenology & Seasonality (CPS) + Verband Geographie Schweiz (ASG) + ProClim*

### TALKS:

- 16.1 Dorsch C.: Digitality for Future? – The potential of digital practices for climate education
- 16.2 Friedman A.R., Hand R., Samakinwa E., Brönnimann S.: Hydroclimate impacts of volcanic eruptions in the tropical Atlantic Basin during the late-19th and early-20th centuries
- 16.3 Gubler M., Probst M.: Integral models to assess the scope of action for a climate-friendly future
- 16.4 Hundt M., Aseev O.: MIRO Analytical's MGA10: A single device for greenhouse gas and air quality monitoring
- 16.5 Paul-Limoges E., Revill A., Maier R., Buchmann N., Damm A.: Partitioning Ecosystem Evaporation and Transpiration in Short-Statured Croplands
- 16.6 Rivoire P.: Assessing Drivers and Forecasts Across Timescales of Vegetation and Ecosystem Damage
- 16.7 Sabbatini D., Gubler M., Brügger A., Brönnimann S., Burger M.: Public perceptions of and behavioral responses to urban heat stress in Bern
- 16.8 Samakinwa E., Raible C., Brönnimann S.: On The Different Mechanisms Of Inter-annual AMOC Variability Under Stable Atmospheric CO<sub>2</sub> Forcing
- 16.9 Sasgen I., Salles A., Wegmann M., Wouters B., Fettweis X., Noël B.P., Beck C.: Arctic glaciers record wavier circumpolar winds
- 16.10 Schneider L., Comte V., Rebetez M.: Impacts of climate change on development season for polyvoltine pests in Switzerland
- 16.11 Schulz J., Brumann S.: Climate Change Education through Inquiry-based Learning – a suitable approach for action-oriented learning in upper-secondary school science propaedeutics?
- 16.12 Volery A., Weber H., Barandun M., Kronenberg M., Imanalieva I., Mathys T.: Empowering young women from Central Asia with a scientific communication program: "Adventure of Science: Women and Glaciers in Central Asia"

**POSTERS:**

- P 17.1 Blaser P., Lippold J., Jaccard S., Waelbroeck C., Pöppelmeier F., Kaboth-Bahr S., Repschläger J., Thornalley D.: Similar Atlantic Water Mass sourcing during the Last Glacial Maximum and Heinrich Stadial 1
- P 17.2 Comte V., Schneider L., Rebetez M.: Trends in spring frost risk and heat waves under future climatic scenarios in Neuchatel vineyards
- P 17.3 Eeckman J., Fallot J.: Interpolation of air temperature at Very High resolution in mountainous areas
- P 17.4 Hövel L., Hand R., Brönnimann S.: A Global Assessment of Heatwaves since 1850 in Different Datasets
- P 17.5 Imfeld N., Brönnimann S.: 250 years of impact-relevant weather indices for Switzerland
- P 17.6 Ragon C., Vérard C., Kasparian J., Brunetti M.: Three potential climates for the Permian-Triassic paleogeography
- P 17.7 Shastri R.P., Brönnimann S., Steinfeld D.: High-resolution modeling of historical forest fires in the Canton of Bern
- P 17.8 Wilhelm L., Martius O., Schroer K., Schwierz C.: Hail time series from radar proxies for decadal variability of hail in Switzerland
- P 17.9 Peyrotty G., Vimperg L., Farley N., Carraro D.: On the importance of video journalism in geosciences

## 16.1

# Digitality for Future? – The potential of digital practices for climate education

Christian Dorsch

<sup>1</sup> Institut für Humangeographie, Goethe-University Frankfurt, Theodor-W.-Adorno-Platz 6, D-60629 Frankfurt am Main  
(dorsch@geo.uni-frankfurt.de)

The «Fridays for Future» movement, campaigning for the expansion of measures to counter the climate crisis, brought the issue an enormous boost in public awareness and generated a great interest in climate-related topics among students. In addition to the strong physical presence in the form of demonstrations, one reason for this is the initiative's online presence, e.g. in social media. The particular way in which issues of climate protection or climate adaptation are negotiated in communities in social media ensures their appeal in this context. Followers use certain practices (e.g. in content creation, liking, and sharing), referred to by Stalder (2018) as practices of digitality, for mobilizing their followers but equally for their own forms of protest and dissemination of knowledge in the domain of climate and climate change.

Three questions arise from this for the paper: How do practices of digitality affect informal learning processes in the knowledge domain of climate & climate change? How can this informal learning be made fruitful for (formal) climate change education? Which meta-competencies also with regard to a maturity-oriented education (Dorsch 2022) are promoted? I explore this research perspective through a qualitative content analysis of selected posts that have been created in communities of the «Fridays for Future Germany» movement, as well as through interviews with community members. Initial results show that processes of identity formation and self-formation take place in the communities. If these knowledge practices are taken up and reflected upon in school, they can be transferred into formal educational processes. Therefore, the results also provide suggestions on how teachers can address the topic of the climate crisis in a motivating way in the classroom.

## REFERENCES

- Stalder, F. 2018. The digital condition. Hoboken.  
Dorsch, C. 2022. Mündigkeit und Digitalität: E-Portfolioarbeit in der geo-graphischen Lehrkräftebildung. Münster.

## 16.2

# Hydroclimate impacts of volcanic eruptions in the tropical Atlantic Basin during the late-19th and early-20th centuries

Andrew Ronald Friedman<sup>1</sup>, Ralf Hand<sup>1</sup>, Eric Samakinwa<sup>1</sup>, Stefan Brönnimann<sup>1</sup>

<sup>1</sup> Institute of Geography and Oeschger Centre for Climate Change Research, University of Bern, CH-3012 Bern (andrew.friedman@giub.unibe.ch)

The tropical Atlantic Basin is fundamental for the planetary biosphere and climate, with the surrounding continents holding the largest planetary rainforests, the largest rivers by discharge, and vital agricultural regions. Major volcanic eruptions are recognized as impacting tropical precipitation and river discharge around the Atlantic Basin, but comprehensive assessment of these impacts has been limited by their relative infrequency in the modern period. Here, we use recently updated early instrumental data back to the late-19th and early-20th centuries to revisit the hydroclimate impacts of large eruptions in the tropical Atlantic Ocean, Africa, and the Americas, focusing on the major eruptions of Krakatau (1883), Santa Maria (1902), and Katmai (1912). Understanding these eruption impacts allows us to contextualize the hydroclimate impacts of better-observed large eruptions since the second half of the 20th century and better anticipate the impacts of future large eruptions.

We examine the hydrological cycle impacts of these eruptions using long-term observational datasets including gridded and station precipitation, river discharge (Amazon, Congo, Paraná, Niger, and Senegal), and tropical Atlantic sea surface salinity, which provides insight into the marine freshwater balance. We also examine the mechanisms of hydroclimate impacts using latest-generation atmospheric reanalysis output and a medium-sized ensemble of prescribed volcanic-forcing experiments with the atmospheric general circulation model ECHAM6. We find that these volcanic eruptions caused detectable reductions in precipitation and discharge around the tropical Atlantic Basin. In particular, the high-latitude Katmai eruption induced northern hemisphere cooling, driving a southward displacement of the Atlantic intertropical convergence zone (ITCZ) and Hadley circulation, weakening the summer monsoon and causing extreme reductions in precipitation and discharge across West Africa and the greater tropical Atlantic region.

## 16.3

### Integral models to assess the scope of action for a climate-friendly future

Moritz Gubler<sup>1,2,3</sup> & Matthias Probst<sup>2,3,4</sup>

<sup>1</sup> Institut Sekundarstufe 1, Bern University of Teacher Education, Fabrikstrasse 8, CH-3012 Bern ([moritz.gubler@phbern.ch](mailto:moritz.gubler@phbern.ch))

<sup>2</sup> Geographisches Institut, University of Bern, Hallerstrasse 12, CH-3012 Bern

<sup>3</sup> Oeschger-Zentrum für Klimaforschung, University of Bern, Hochschulstrasse 4, CH-3012 Bern

<sup>4</sup> Institut Sekundarstufe 2, Bern University of Teacher Education, Fabrikstrasse 8, CH-3012 Bern

The topic of climate change is characterized by a high degree of complexity and controversy, not least due to the multifaceted nature of human-environment systems (e.g., complex cause-effect relationships, conflicting goals between ecological and socio-economic needs). Education about climate change is therefore facing the challenge of providing approaches to address complexity and controversy.

Especially when addressing the scope for action regarding a climate-friendly future, teachers and learners are equally challenged by different conceptions, processes that are not immediately visible, references between local and global phenomena, and a multitude of levels for implementation. For example, teaching materials on climate policy reveal a lack of scientifically grounded models and concepts that provide holistic and structured scopes of action for a climate-friendly future (Adamina et al., 2018).

Our theory- and practice-oriented presentation addresses the overarching question of the extent to which “integral models” can support the critical perception, analysis, and assessment of individual and collective scopes of action from a holistic perspective by students in the context of climate change education. By referring to the recently developed model “Integral Climate Risk Management” (Probst & Gubler, 2019), challenges and opportunities of integral and structuring models in climate change education will be illustrated and discussed.

#### REFERENCES

- Adamina, M., Hertig, P., Probst, M., Reinfried, S., Stucki, P., & Vogel, J. 2018: Klimabildung in allen Zyklen der Volksschule und in der Sekundarstufe II - Grundlagen und Erarbeitung eines Bildungskonzeptes. Schlussbericht Projektphase CCESO I 2016/2017 (vollständige Fassung). Bern: Globe Schweiz und Bundesamt für Umwelt.
- Probst, M., & Gubler, M. 2019: Klimawandel und Klimapolitik. Lernmedium für die Sekundarstufe II und Informationen für Lehrpersonen. Bern: Globe Schweiz und Bundesamt für Umwelt, <https://www.education21.ch/de/themendossier/klima#edu21-tab5> (access: 31.8.2022).

## 16.4

# MIRO Analytical's MGA<sup>10</sup>: A single device for greenhouse gas and air quality monitoring

Morten Hundt<sup>1</sup>, Oleg Aseev<sup>1</sup>

<sup>1</sup> MIRO Analytical AG, Widenholzstrasse 1, CH-8304 Wallisellen ([Morten.hundt@miro-analytical.com](mailto:Morten.hundt@miro-analytical.com))

Monitoring of air pollutants and greenhouse gases with high precision and selectivity is important to identify their sources and sinks, develop reliable models to predict air quality and ultimately to combat air pollution and climate change.

MIRO Analytical's new trace gas analyzers are capable of monitoring up to 10 gases simultaneously. These analyzers use direct laser absorption spectroscopy and combine several Quantum Cascade Lasers as light sources. The analyzers provide highest precision combined with best selectivity thanks to their operation in the mid-infrared spectral range. By monitoring green-house gases ( $\text{CH}_4$ ,  $\text{N}_2\text{O}$ ,  $\text{CO}_2$ ) and air pollutants ( $\text{NO}$ ,  $\text{NO}_2$ ,  $\text{CO}$ ,  $\text{NH}_3$ ,  $\text{SO}_2$ ,  $\text{O}_3$ ) our analyzers can serve as an all-in-one solution for ambient air monitoring.

Due to their compactness, high precision and stability our analyzers are well-suited for installation in monitoring stations as well as for mobile monitoring. The multi-compound ability opens new possibilities for emission source attribution and for studies of interactions of different trace gases. Furthermore, the analyzers operate at up to 10Hz measurement rate enabling eddy-flux monitoring of multiple gases simultaneously.

In this contribution we will shortly introduce the new MGA<sup>10</sup> multi-compound gas analyzer and will present examples of measurement campaigns that were recently performed by our customers.

## REFERENCES

- Tillmann, R. et al. 2022: Air quality observations onboard commercial and targeted Zeppelin flights in Germany – a platform for high-resolution trace-gas and aerosol measurements within the planetary boundary layer, AMT, 15, 3827-3842

## 16.5

# Partitioning Ecosystem Evaporation and Transpiration in Short-Statured Croplands

Eugenie Paul-Limoges<sup>1</sup>, Andrew Revill<sup>2</sup>, Regine Maier<sup>3</sup>, Nina Buchmann<sup>3</sup>, Alexander Damm<sup>1,4</sup>

<sup>1</sup> Department of Geography, University of Zurich, Winterthurerstrasse 190, 8057 Zurich, Switzerland

<sup>2</sup> School of Geosciences, University of Edinburgh, Crew Building, The Kings' Buildings, Edinburgh, EH9 3FF

<sup>3</sup> Institute of Agricultural Sciences, ETH Zurich, Universitaetstrasse 2, 8092 Zurich, Switzerland

<sup>4</sup> Eawag, Swiss Federal Institute of Aquatic Science and Technology, 8600 Dübendorf, Switzerland

Reducing water losses in agriculture needs a solid understanding of when evaporation (E) losses occur and how much water is used through crop transpiration (T). Partitioning ecosystem T is however challenging, and even more so when it comes to short-statured crops, where many standard methods lead to inaccurate measurements. In this study, we combined biometeorological measurements with a Soil-Plant-Atmosphere Crop (SPA-Crop) model to estimate T and E at a Swiss cropland over two crop seasons with winter cereals. We compared our results with two data-driven approaches: The Transpiration Estimation Algorithm (TEA) and the underlying Water Use Efficiency (uWUE).

Despite large differences in the productivity of both years, the T to evapotranspiration (ET) ratio had relatively similar seasonal and diurnal dynamics, and averaged to 0.72 and 0.73. Our measurements combined with a SPA-Crop model provided T estimates similar to the TEA method, while the uWUE method produced systematically lower T even when the soil and leaves were dry. T was strongly related to the leaf area index, but additionally varied due to climatic conditions. The most important climatic drivers controlling T were found to be the photosynthetic photon flux density ( $R^2 = 0.84$  and  $0.87$ ), and vapor pressure deficit ( $R^2 = 0.86$  and  $0.70$ ). Our results suggest that site-specific studies can help establish T/ET ratios, as well as identify dominant climatic drivers, which could then be used to partition T from reliable ET measurements. Moreover, our results suggest that the TEA method is a suitable tool for ET partitioning in short-statured croplands.

## REFERENCES

- Paul-Limoges E., Revill A., Maier R., Buchmann N., Damm A. (2022) Insights for the partitioning of ecosystem evaporation and transpiration in short-statured croplands. *Journal of Geophysical Research: Biogeosciences*, 127, e2021JG006760. <https://doi.org/10.1029/2021JG006760>

## 16.6

# Assessing Drivers and Forecasts Across Timescales of Vegetation and Ecosystem Damage

Pauline Rivoire<sup>1</sup>, Daniela Domeisen<sup>1</sup>, Antoine Guisan<sup>1</sup>, Pascal Vittoz<sup>1</sup>

<sup>1</sup> Institute of Earth Surface Dynamics, Faculty of Geosciences and Environment Géopolis Building, Lausanne, Switzerland  
([pauline.rivoire@unil.ch](mailto:pauline.rivoire@unil.ch))

Extreme meteorological events such as frost, heat, and drought can induce significant damage to vegetation and ecosystems. Furthermore, especially heat and drought events are projected to become more frequent under a changing climate. It is therefore crucial to predict the frequency (on climate timescales) and the occurrence (on timescales of weeks to months) of such extremes.

The subseasonal-to-seasonal (S2S) forecasting timescale refers to forecasting timescales from two weeks to a season. S2S prediction aim to fill the gap between weather forecasts and monthly or seasonal outlooks. Given the difficulty to provide skilful predictions on subseasonal or monthly timescales, this timescale was until recently a “predictability desert”, unlike short-range forecasts and seasonal outlooks that have already been operational for many years. However, skillful S2S forecasts of hydro-meteorological hazards can be of crucial importance to prevent large-scale vegetation damage. The utility of S2S forecasts for vegetation is very broad (agriculture, biodiversity and flora protection, wildfire risk management, forest management, etc.).

The goal of this research project is to bridge the research gap between the S2S forecast of atmospheric variables and the impact on the vegetation. The variables responsible for vegetation damage over Europe will be identified and the forecast skill of the identified variables will be assessed.

## 16.7

# Public perceptions and behavioral responses to urban heat stress in Bern

Doriana Sabbatini<sup>1,2</sup>, Moritz Gubler<sup>1,2,3</sup>, Adrian Brügger<sup>4</sup>, Stefan Brönnimann<sup>1,2</sup>, Moritz Burger<sup>1,2</sup>

<sup>1</sup> Oeschger-Zentrum für Klimaforschung, Universität Bern, Hochschulstrasse 4, CH-3012 Bern  
*(doriana.sabbatini@students.unibe.ch)*

<sup>2</sup> Geographisches Institut, Universität Bern, Hallerstrasse 12, CH-3012 Bern

<sup>3</sup> Institut für Forschung, Entwicklung und Evaluation, Pädagogische Hochschule Bern, Fabrikstrasse 8, CH-3012 Bern

<sup>4</sup> Institut für Marketing und Unternehmensführung, Universität Bern, Engehaldestrasse 4, CH-3012 Bern

Temperature extremes may severely affect human health (EEA 2017), especially in cities due to combined effects of anthropogenic climate change and urban heat islands. However, introducing heat warning systems can reduce the risk of death, as has been observed in recent years (Ragettli et al. 2017). In cities and cantons that do not yet have any or only a few such measures in place, it is important to establish and expand heat protection measures for the population (Ragettli & Röösli 2020). In order to develop targeted information campaigns, it is crucial to know about socio-demographic and socio-psychological factors influencing individual heat adaptation behavior. This master thesis aims at analyzing this relationship empirically among the general public in Bern, Switzerland.

In March and May 2022, written questionnaires were distributed to citizens in six different neighborhoods that are differently affected by urban heat stress. Based on regression analyses (N=228), our results indicate that psychological play a superimposed role in explaining adaptive behavior regarding heat stress when compared to housing and socio-demographic factors. Of the socio-psychological factors, perceived benefits and barriers to adaptive behaviors explain most of the variance in adaptive behaviors, whereas perceived vulnerability and severity are not found to be significant predictors. This is in line with the results of other studies as heat is often perceived as merely a nuisance rather than a serious threat (Heidenreich et al. 2020; Lefevre et al. 2015). Our recommendation for risk communication is thus to focus on reducing the barriers for adaptive behaviors and communicating the benefits of practicing such behaviors during periods of extreme heat.

## REFERENCES

- EEA (European Environment Agency) 2017: Climate change, impacts and vulnerability in Europe 2016. An indicator-based report. Luxembourg, 424pp.
- Heidenreich, A., Köhler, S., Seebauer, S., & Masson, T. 2020: Schutzhandeln bei Hochwasser, Hitze und Co. – Umweltpsychologische Theorien für die Naturrisikenforschung. *Umweltpsychologie*, 24(2), 92-109.
- Lefevre, C. E., Bruine de Bruin, W., Taylor, A. L., Dessai, S., Kovats, S., & Fischhoff, B. 2015: Heat protection behaviors and positive affect about heat during the 2013 heat wave in the United Kingdom. *Social Science & Medicine*, 128, 282–289.
- Ragettli, M.S., & Röösli, M. 2020: Gesundheitliche Auswirkungen von Hitze in der Schweiz und die Bedeutung von Präventionsmaßnahmen. Hitzebedingte Todesfälle im Hitzesommer 2019 – und ein Vergleich mit den Hitzesommer 2003, 2015 und 2018. SwissTPH, Basel.
- Ragettli, M.S., Vicedo-Cabrera, A.M., Schindler, C., & Röösli, M. 2017: Exploring the association between heat and mortality in Switzerland between 1995 and 2013. *Environmental Research*, 158, 703-709.

## 16.8

# On The Different Mechanisms Of Inter-annual AMOC Variability Under Stable Atmospheric CO<sub>2</sub> Forcing

Eric Samakinwa<sup>1,2</sup> Christoph Raible<sup>1,3</sup> & Stefan Brönnimann<sup>1,2</sup>

<sup>1</sup> Oeschger Center for Climate Change Research, University of Bern, Switzerland.

<sup>2</sup> Institute of Geography, University of Bern, Switzerland.

<sup>3</sup> Institute of Climate and Environmental Physics, University of Bern, Switzerland.

The Atlantic Meridional Overturning Circulation (AMOC) has profound impacts on the climate of the North Atlantic and the global climate at large. It plays a significant role in redistributing heat and freshwater around the globe. As such, it is a crucial tipping point in the climate system. Real-time AMOC measurement began in 2004, providing monthly observation of the stream function. Although this observation exhibits large intra-annual variability, the records are still too short for making a robust conclusion about intra-annual AMOC variability. Recent studies suggested the weakening of the AMOC in the 21<sup>st</sup> century due to increased and unstable radiative forcing through anthropogenic activities.

Here, we explore the capability of a stand-alone ocean model MPIOM in simulating a physically consistent AMOC state and analyze the possible atmospheric forcing of the strengthening and deepening of the AMOC under stable CO<sub>2</sub> forcing.

Simulated AMOC shows a reasonable agreement with proxy-based AMOC reconstructions and is physically consistent with GCM outputs. Our methodology defines high and low AMOC years based on a standardized AMOC index at 26.5°N. We use the Kolmogorov-Smirnov test to determine the threshold where the distributions differ significantly from the normal.

Composites of the atmospheric variables for the selected years show the dominant influence of the North Atlantic Oscillation on the deepening and strengthening of the AMOC, but with opposing signs. Furthermore, we found that the AMOC deepening is closely related to the eastward flow of weak North-Atlantic wind stress anomalies.

## 16.9

### Arctic glaciers record wavier circumpolar winds

Ingo Sasgen<sup>1</sup>, Annette Salles<sup>1,2</sup>, Martin Wegmann<sup>3,4</sup>, Bert Wouters<sup>5,6</sup>, Xavier Fettweis<sup>7</sup>, Brice Noël<sup>5</sup>, Christoph Beck<sup>8</sup>

<sup>1</sup> Division of Geosciences, Glaciology, Alfred-Wegener-Institut Helmholtz-Zentrum für Polar- und Meeresforschung, Am Handelshafen 12, 27570 Bremerhaven, Germany.

<sup>2</sup> School of Natural and Built Environment, Queen's University Belfast, Elmwood Avenue, Belfast, BT7 1NN, Northern Ireland, United Kingdom.

<sup>3</sup> Institute of Geography, University of Bern, Hallerstrasse 12, 3012 Bern, Switzerland.

<sup>4</sup> Limnology Center, EPFL, Station 2, 1015 Lausanne ([martin.wegmann@epfl.ch](mailto:martin.wegmann@epfl.ch))

<sup>5</sup> Institute for Marine and Atmospheric Research, Utrecht University, 279 Utrecht, Netherlands.

<sup>6</sup> Department of Geoscience & Remote Sensing, Delft University of Technology, 2600 AA Delft, Netherlands.

<sup>7</sup> Department of Geography, SPHERES research unit, University of Liège, 4000 Liège, Belgium.

<sup>8</sup> Institute of Geography, University of Augsburg, Alter Postweg 118, 86159 Augsburg, Germany.

Glaciers in the Arctic respond sensitively to climate change, recording the polar amplification of global warming with increasing mass loss. Here, we use glacier mass balances in Svalbard and northern Arctic Canada to categorize tropospheric variability and the associated summer circulation over the Arctic. We establish a link between annual glacier mass balances and their respective atmospheric forcings since 1950 using GRACE/GRACE-FO satellite data (2002–2021), as well as regional climate models and reanalysis data (1950–2019). We find that asynchronous behaviour of mass balance between the regions has become very likely since the early 2000s, exceeding the range of previous decadal variability. Related tropospheric circulation exhibits more meridional patterns, a greater influence of meridional heat advection and a wavier summer circulation. The traceable impact on glacier mass balances emphasizes the importance of dynamic next to thermodynamic climate changes for the future of glacier mass loss, Arctic ecology and societal impacts (Sasgen et al. 2022).

#### REFERENCES

- Sasgen, I., Salles, A., Wegmann, M., Wouters, B., Fettweis, X., Noël, B. P., & Beck, C. 2022: Arctic glaciers record wavier circumpolar winds. *Nature Climate Change*, 12(3), 249–255.

## 16.10

# Impacts of climate change on development season for polyvoltine pests in Switzerland

Léonard Schneider<sup>1,2</sup>, Valentin Comte<sup>1,2</sup>, Martine Rebetez<sup>1,2</sup>

<sup>1</sup> Institute of Geography, University of Neuchatel, Espace Tilo-Frey 1, CH-2000 Neuchatel (leonard.schneider@unine.ch)

<sup>2</sup> Swiss Federal Institute for Forest, Snow and Landscape Research (WSL), Zürcherstrasse 111, CH-8903 Birmensdorf

Climate change is predicted to have a major influence on the outbreaks of pest species during the next decades. As ectothermic organisms, insect demography is strongly sensitive to ambient temperature during development period. For instance, warmer temperatures during this period are likely to increase the number of annual generations for polyvoltine species (Altermatt, 2010) and to cause shifts in phenology, and therefore to lengthen the developmental season (Forrest, 2016). In Switzerland, these effects have already been observed since the 2000's on some species, such as the spruce bark beetle (*Ips typographus*, Jakoby, 2019). Other polyvoltine species may be concerned during the next decades, and we here focus on two crop pests, the grapevine moth (*Lobesia botrana*) and the marmorated stink bug (*Halyomorpha halys*), and on one forest pest, the box tree moth (*Cydalima perspectalis*). The extent of future damage that these pest species will cause is predicted to depend on the trajectory of temperature change.

In this study, we examine the trends for mean temperatures during the development season in Switzerland. We focus on the length of the development season and on the number of growing degree days (GDD) across different elevations and years. We first analyse how daily air temperatures have shifted between 1980 and 2021 using data from MeteoSwiss stations. Then, we use available data from CH2018 climatic scenarios to estimate possible trends along 21<sup>st</sup> century. Finally, we discuss the historic and projected impacts of climate change on the three polyvoltine pest species, depending on their thermal specific requirements.

## REFERENCES

- Altermatt, F. 2010: Climatic warming increases voltinism in European butterflies and moths, Proc. R. Soc. B.2771281–1287.  
Forrest, J. R. 2016: Complex responses of insect phenology to climate change. Current opinion in insect science, 17, 49-54.  
Jakoby, O., Lischke, H., & Wermelinger, B. 2019: Climate change alters elevational phenology patterns of the European spruce bark beetle (*Ips typographus*). Global change biology, 25(12), 4048-4063.

## 16.11

# Climate Change Education through Inquiry-based Learning - a suitable approach for action-oriented learning in upper-secondary school science propaedeutics?

Johannes Schulz<sup>1</sup>, Sebastian Brumann<sup>1</sup>

<sup>1</sup> Chair of Geography Education, Institute of Geography, University of Augsburg, Alter Postweg 118, D-86159 Augsburg, (johannes.schulz@geo.uni-augsburg.de)

One of the greatest challenges in the context of multiple crises is the current man-made climate change. Education aims to make a crucial contribution to mitigating and adapting to this symptom of the current Anthropocene. Nevertheless, educational approaches that address the issue of climate change are demanding. This is due to various factors like the high complexity of the topic (Meyer et al. 2018) and the persistent misconceptions that come along with it (Felzmann 2018). Further central difficulties consist in the spatio-temporal psychological distance to the topic of climate change which is perceived by many people (Gubler et al. 2019), and the often observed discrepancy between climate-relevant knowledge and action (Renn 2018). A promising approach to address these challenges is Inquiry-based Learning (IBL), as it integrates key elements and principles which are known to be supportive in successful climate change education (Brumann et al. 2022). Nevertheless, education formats with an explicit focus on fostering climate-related action are rare.

Consequently, as a first part of our presentation, we want to discuss, which central goals, conceptional approaches and challenges within Inquiry-based Climate Change Education can be identified to be particularly relevant for climate-related action in the context of the debate about Transformative Learning. For this purpose, we will present the results of a systematic literature review study, which we are currently conducting.

As a second step, we will outline an IBL climate change education conception for upper-secondary school students, which was developed at the University of Augsburg, together with its underlying key aspects. This conception initially pursued the goal of a regional, interest-based approach for Climate Change Education on the one hand, while on the other hand offering close-to-science propaedeutics through IBL. With regard to these objectives, the concept was successively improved based on an iterative design-based research (DBR) process and has so far been applied and evaluated in 62 schools with over 900 students.

In a third step, we want to reflect how this already established conception can also be enhanced with regard to climate-related action-oriented learning. For this purpose, we theoretically analyse the conception with reference to the results of the systematic literature review. In this regard, we want to identify strengths, weaknesses and, above all, potentials of the conception. Based on this analysis, potential future enhancements to complement IBL formats regarding climate-related action-oriented learning will be derived and discussed.

## REFERENCES

- Brumann, S.; Ohl, U.; Schulz, J. 2022: Inquiry-Based Learning on Climate Change in Upper Secondary Education: A Design-Based Approach. In *Sustainability* 14 (6), p. 3544. DOI: 10.3390/su14063544.
- Felzmann, D. 2018: Vorstellungen von Lernenden zu Ursachen und Folgen des Klimawandels und darauf aufbauende Unterrichtskonzepte. In Christiane Meyer, Andreas Eberth, Barbara Warner (Eds.): *Klimawandel im Unterricht. Bewusstseinsbildung für eine nachhaltige Entwicklung*. Braunschweig: Diercke, pp. 53–63.
- Gubler, M.; Brügger, A.; Eyer, M. 2019: Adolescents' Perceptions of the Psychological Distance to Climate Change, Its Relevance for Building Concern About It, and the Potential for Education. In Walter Leal Filho, Sarah L. Hemstock (Eds.): *Climate Change and the Role of Education*. Cham: Springer International Publishing (Climate Change Management), pp. 129–147.
- Meyer, C.; Eberth, A.; Warner, B. 2018: Einführung. In Christiane Meyer, Andreas Eberth, Barbara Warner (Eds.): *Klimawandel im Unterricht. Bewusstseinsbildung für eine nachhaltige Entwicklung*. Braunschweig: Diercke, pp. 4–5.
- Renn, O. 2018: Klimaveränderungen als systemisches Risiko erkennen – Wege zur Handlungsbereitschaft. In Christiane Meyer, Andreas Eberth, Barbara Warner (Eds.): *Klimawandel im Unterricht. Bewusstseinsbildung für eine nachhaltige Entwicklung*. Braunschweig: Diercke, pp. 77–85.

## 16.12

# Empowering young women from Central Asia with a scientific communication program: “Adventure of Science: Women and Glaciers in Central Asia”

Anouk Volery<sup>1</sup>, Helga Weber<sup>2</sup>, Martina Barandun<sup>3</sup>, Marlène Kronenberg<sup>1</sup>, Perizat Imanalieva<sup>4</sup>, Tamara Mathys<sup>1</sup>

<sup>1</sup> Department of Geosciences, University of Fribourg, Chemin du Musée 4, CH-1700 Fribourg  
(anouk.volery@unifr.ch ; centralasia@girlsonice.org)

<sup>2</sup> Oeschger Centre for Climate Change Research and Institute of Geography,

<sup>3</sup> University of Bern, CH-3012 Bern. Institute of Earth Observation, EURAC research, Bolzano, Italy.

<sup>4</sup> Central Asian Institute for Applied Geosciences, KG-720027 Bishkek.

“Adventure of Science: Women and Glaciers in Central Asia” offers scientific and glaciological expeditions to young women between 18-25 years old from Kazakhstan, Kyrgyzstan, Tajikistan, Turkmenistan, and Uzbekistan. The program is designed to empower young women from Central Asia with scientific and artistic outdoor exploration. It is inspired by “Girls on Ice”, a program organizing tuition-free glaciological expeditions for young girls across Europe, North America, and New Zealand. The program finds a unique echo in Central Asia because of structural barriers women face in the region and because of the region’s vulnerability to climate change.

Since the end of the Soviet era, inequalities towards women strengthened in many countries of Central Asia (Urbaeva, 2019). The increase of cultural patriarchal norms and attitudes regarding women’s status has generated economic, social, and political inequalities (Urbaeva, 2019 and Khitarishvili, 2016). While high disparities can be noted between women’s condition in the different countries of Central Asia, women tend to face pay gaps, low involvement in decision-making, gender-based violence, and low access to opportunities (UNDP, 2016). These barriers may prevent women to pursue academic and professional careers, even more so in male-dominated fields such as STEM fields. Moreover, Central Asia is particularly vulnerable to climate change due to increasing pressure on the water towers of the region, the mountainous, and cryospheric systems of the Tien Shan and Pamir (Xenarios et al, 2019; Barandun et al, 2020). The region faces many challenges in fields such as water management and disaster risk reduction and must develop innovative adaptation and mitigation strategies. In consequence, there is an urgent need of environmental researchers and environmentally informed citizens. Considering such a context, programs encouraging women empowerment and environmental interest are very valuable in Central Asia.

“Adventure of Science: Women and Glaciers in Central Asia” is organized around a ten-days excursion to the Golubin Glacier in Kyrgyzstan and includes hands-on training in geoscience topics and scientific methods. The age limit of 18-25 year old participants targets a critical age in the decision-making process in their education. The program creates a space free of gender roles, often dominant in Central Asian societies, with a team of women instructors and guide. The program provides a future network for participants interested in environmental science. The regional network and assistance is fostered by collaboration with local institutions and researchers, as well as through organized events and workshops on cryospheric topics. The involvement and engagement of local researchers, mentoring, and alumni network makes the program sustainable and will also lead to a self-management of the program by women of Central Asia in future.

“Adventure of Science: Women and Glaciers in Central Asia” is part of the project CROMO-ADAPT from the University of Fribourg and is financed by the Swiss Agency for Development and Cooperation in close collaboration with the UNESCO Office in Almaty. Such collaborations are essential for “Adventure of Science: Women and Glaciers in Central Asia” to achieve its aims, namely the creation of a transboundary and sustainable network for women in cryospheric and environmental fields in Central Asia.

## REFERENCES

- Barandun, M. et al. 2020: The state and future of the cryosphere in Central Asia. *Water Security* 11, 100072.
- Khitarishvili, T. 2016: Gender Dimensions of Inequality in the Countries of Central Asia, South Caucasus, and Western CIS. Levy Economics Institute 858.
- UNDP. 2016: Progress at Risk: Inequalities and Human Development in Eastern Europe, Turkey, and Central Asia. Regional Human Development Report 2016.
- Urbaeva, J. 2019: Opportunity, Social Mobility, and Women’s Views on Gender Roles in Central Asia. National Association of Social Workers 64(3), 207-215.
- Xenarios, S. et al. 2019: Climate change and adaptation of mountain societies in Central Asia: uncertainties, knowledge gaps, and data constraints. *Regional Environmental Change* 19, 1339-1352.

**P 17.1****Similar Atlantic Water Mass sourcing during the Last Glacial Maximum and Heinrich Stadial 1**

P. Blaser<sup>1</sup>, J. Lippold<sup>2</sup>, S. Jaccard<sup>1</sup>, C. Waelbroeck<sup>3</sup>, F. Pöppelmeier<sup>4</sup>, S. Kaboth-Bahr<sup>5</sup>, J. Repschläger<sup>6</sup>, D. Thornalley<sup>7</sup>

<sup>1</sup> University of Lausanne, Bâtiment Géopolis, UNIL-Mouline, CH-1015 Lausanne ([patrick.blaser@unil.ch](mailto:patrick.blaser@unil.ch))

<sup>2</sup> Heidelberg University (D)

<sup>3</sup> LOCEAN - IPSL (F)

<sup>4</sup> University of Bern (CH)

<sup>5</sup> University of Potsdam (D)

<sup>6</sup> Max Planck Institute for Chemistry (D)

<sup>7</sup> University College London (UK)

The oceans are a vital part of the climate system and played an integral role in modulating Quaternary glacial cycles. For an improved fundamental understanding of this role and of the ocean system it is important to get accurate information about the past sourcing of deep ocean water due to its profound impact on marine carbon storage, heat transport, and ventilation. Yet, to date deep Atlantic water mass sourcing during past glacials is still debated, and interpretations based on different proxies such as carbon and neodymium isotopes appear to be at odds.

Here, we present evidence for the existence of a Glacial North Atlantic Deep Water in the Subpolar North Atlantic. We then estimate Atlantic water mass sourcing by integrating data compilations of five different proxies (stable isotopes of carbon and oxygen, neodymium isotopes, carbonate ion concentration, and radiocarbon ventilation age) from the Last Glacial Maximum and Heinrich Stadial 1 with the help of a Bayesian mixing model.

We show that a moderate expansion of southern sourced waters in combination with widespread northern sourced deep water best explain proxy observations. Changes between LGM and HS1 were dominated by changes in water mass characteristics, rather than distribution, implying that deep water formation intensity may not have changed drastically. These analyses offer new detailed insights into glacial deep Atlantic water mass sourcing and reconcile findings from studies using individual proxies

## P 17.2

# Trends in spring frost risk and heat waves under future climatic scenarios in Neuchatel vineyards

Valentin Comte<sup>1,2</sup>, Léonard Schneider<sup>1,2</sup>, Martine Rebetez<sup>1,2</sup>

<sup>1</sup> Institute of Geography, University of Neuchâtel, espace Tilo-Frey 1, CH-2000 Neuchâtel (valentin.comte@unine.ch)

<sup>2</sup> Swiss Federal Institute for Forest, Snow and Landscape Research (WSL), Zürcherstrasse 111, CH-8903 Birmensdorf

Climate change has major impacts on vineyards, as they are highly sensitive to local climatic conditions (Jones and Davis 2000, van Leeuwen, Friant et al. 2004, Jones 2006). Warmer air temperature increases sugar concentration and potential alcohol content of wines and decreases total acidity of wines (Spayd, Tarara et al. 2002, Jones and Webb 2010). It also shifts phenological development stages of grape (Duchêne and Schneider 2005, Cuccia, Richard et al. 2010, Cook and Wolkovich 2016).

Climate change not only impacts mean temperature, but also extreme meteorological events which are crucial for wine production. For example, heat waves are expected to increase in both duration and frequency during the next decades, while trends remain unclear for spring frost. Late frost events can severely reduce yields, while temperatures above 35°C limit grapevine development (Kliewer 1977, Spayd, Tarara et al. 2002). In order to develop adaptation strategies for winegrowers, we therefore need to assess how heat waves and spring frost will impact vineyards under future climatic conditions.

In this study, we analysed trends in spring frost risk and in the number of very hot days ( $T_{max}>35^{\circ}\text{C}$ ) in the wine region of Neuchâtel for the period 1980-2099. We used two RCPs scenarios (RCP4.5 and RCP8.5) from CH2018 datasets (Croci-Maspoli, Schär et al. 2018). Spring frost risk was assessed using phenological models fitted on real observations across the last decades. The results should support winegrowers to develop their adaptation strategies to climate change.

## REFERENCES

- Cook, B. I. & Wolkovich, E. M. 2016: Climate change decouples drought from early wine grape harvests in France. *Nature Climate Change*, 6(7), 715-721.
- CH2018 2018: CH2018 - Climate Scenarios for Switzerland - Technical Report. Zurich, National Centre for Climate Services, Zurich, 1-271.
- Cuccia, C., Richard, Y., B. Bois, B., Castel, T. & Thevenin, D. 2010: Changement climatique : impacts sur la phénologie du Pinot Noir en Bourgogne. 23ème Colloque de l'Association Internationale de Climatologie, Rennes, France, Association Internationale de Climatologie, 143-148
- Duchêne, E. & Schneider, C. 2005: Grapevine and climatic changes: a glance at the situation in Alsace. *Agronomy for Sustainable Development*, 25(1), 93-99.
- Jones, G. V. 2006: Climate and terroir: impacts of climate variability and change on wine. *Fine Wine and Terroir: The Geoscience Perspective*, (9), 1-14.
- Jones, G. V. & Davis, R.E. 2000: Climate Influences on Grapevine Phenology, Grape Composition, and Wine Production and Quality for Bordeaux, France. *American Journal of Enology and Viticulture*, 51(3), 249-261.
- Jones, G. V. & L. B. Webb, L.B. 2010: Climate Change, Viticulture, and Wine: Challenges and Opportunities. *Journal of Wine Research*, 21(2-3), 103-106.
- Kliewer, W. M. 1977: Effect of High Temperatures during the Bloom-Set Period on Fruit-Set, Ovule Fertility, and Berry Growth of Several Grape Cultivars. *American Journal of Enology and Viticulture*, 28(4), 215-222.
- Spayd, S. E., Tarara, J.M., Mee, D.L. & Ferguson, J.C. 2002: Separation of sunlight and temperature effects on the composition of *Vitis vinifera* cv. Merlot berries. *American Journal of Enology and Viticulture*, 53(3), 171-182.
- van Leeuwen, C., Friant, P., Choné, X., Tregot, O., Koundouras, S. & Dubourdieu, D. 2004: Influence of climate, soil, and cultivar on Terroir. *American Journal of Enology and Viticulture*, 55, 207-217.

**P 17.3****Interpolation of air temperature at Very High resolution in mountainous areas****Judith EECKMAN<sup>1</sup>, Jean-Michel FALLOT<sup>1</sup>**

<sup>1</sup> Institut de géographie et durabilité, Université de Lausanne (Suisse), Géopolis, UNIL-Mouline, CH-1015 Lausanne, Suisse,  
[judith.eckman@unil.ch](mailto:judith.eckman@unil.ch), [jean-michel.fallot@unil.ch](mailto:jean-michel.fallot@unil.ch)

This work compares three methods to interpolate air temperature from in situ measurements at very high resolution in a small alpine valley (Vallon de Nant, Vaud canton, Switzerland): i) measured temperatures interpolated at the 25 m resolution, based on an inverse distance weighted method, coupled an altitudinal lapse rates; ii) temperatures are taken from the high resolution product CHCLIM25 product, based on a downscaling of MeteoSwiss kilometric data ; iii) temperatures are computed through the AWE-GEN-2d stochastic weather generator that integrates the local orography. This work shows that the interpolation of temperatures by weighted inverse distance, coupled with a vertical thermal gradient, makes it possible to model the annual dynamics of temperatures well, however the representation of the effects of local sites can be refined.

Keywords: spatial interpolation, air temperatures, climatology, Swiss Alps.

## P 17.4

# A Global Assessment of Heatwaves since 1850 in different Datasets

Laura Hövel, Ralf Hand, Stefan Brönnimann

*Institute of Geography and Oeschger Center for Climate Change Research, University of Bern, Switzerland*

Over the past century there was a significant increase in heatwaves in several regions around the globe. This increase is projected to continue with ongoing global warming and forms a serious risk for various ecosystems as well as human health. Changes in the occurrence and the characteristics of heatwaves since the middle of the 20th century are extensively studied in observational datasets and model simulations. However, there is a research gap concerning preindustrial (1850-1900) heatwaves and heatwaves in the early 20th century and their connections to forcings and large-scale variability modes.

In this study we analyse the occurrence of summer heatwaves and the spatial and temporal distribution of different heatwave characteristics using a 36-member ensemble of atmospheric model simulations with prescribed SSTs and observed volcanic forcings over the period 1409 -2009. In addition we use different observational datasets (20CRv3, ERA5, EUSTACE, station data) to compare to the model simulations. For the heatwave calculation we use a new approach, a 31-year running baseline climatology, which allows us to compare heatwave characteristics like heatwave days per season or cumulative intensity across different centuries. We further compare preindustrial heatwaves to recent heatwave events and analyse how global or local heatwave hotspots change over time.

Our analysis shows that the different observational datasets show a comparable distribution of heatwave characteristics. Furthermore, the ensemble spread of the atmospheric model simulations is able to capture the variability of the observational data (20CRv3) and can therefore be used to analyse preindustrial and early 20th century heatwaves. Additionally, the agreement with the observational datasets allows to use the simulations to analyse earlier preindustrial time periods that are not covered by observations. With our on-going analysis of preindustrial heatwaves, we consequently contribute to a better understanding of past climate extremes.

**P 17.5****250 years of impact-relevant weather indices for Switzerland**

Noemi Imfeld<sup>1,2</sup>, Stefan Brönnimann<sup>1,2</sup>

<sup>1</sup> Institute of Geography, University of Bern, Switzerland

<sup>2</sup> Oeschger Center for Climate Change Research, University of Bern, Switzerland

Meteorological events, such as late spring frost and prolonged dry periods can have significant adverse impacts on various sectors, for example, agriculture. Documentary data from the past reports on such events that led to significant yield losses or delayed harvests. So far, it has not been possible to study the related weather conditions, because on daily basis only very few single time series were available.

For Switzerland, now a new daily reconstruction of temperature and precipitation fields exists dating back to the year 1763. Based on this new reconstruction, we calculate impact-related weather indices for the past 250 years. These indices will include amongst others the ETCCDI indices, e.g. percentage of days with minimum temperature below the 10<sup>th</sup> percentile, the number of frost days, but also growing degree days that can be related to phenological stages of different species. These indices will be made available online for follow-up studies.

We compare the derived indices to phenological data available back to the mid-18<sup>th</sup> century, such as historical grape harvest dates that are available at various locations in Switzerland, the timing of the bud break of the horse chestnut in Geneva, and fruit tree bloom dates.

## P 17.6

### Three potential climates for the Permian-Triassic paleogeography

Charline Ragon<sup>1</sup>, Christian Vérard<sup>2</sup>, Jérôme Kasparian<sup>1</sup>, Maura Brunetti<sup>1</sup>

<sup>1</sup> Group of Applied Physics and Institute for Environmental Sciences, Bd Carl-Vogt 66, 1205 Geneva, University of Geneva, Switzerland (charline.ragon@unige.ch)

<sup>2</sup> Section of Earth and Environmental Sciences, University of Geneva, Rue des Maraîchers 13, CH-1205 Geneva, Switzerland

The climate is a complex non-equilibrium dynamical system that relaxes toward a steady state (attractor) under the continuous input of solar radiation and dissipative mechanisms. Multiple steady states are possible under the same forcing for different initial conditions. Up to now, such multistability has been observed in general circulation models with idealized ocean basin configurations (Rose 2015; Brunetti et al. 2019).

We use the MIT general circulation model (MITgcm) with a coupled atmosphere-ocean-sea ice-land configuration to perform simulations at the Permian-Triassic boundary (PTB, 250 Ma) with a paleogeographic reconstruction after PANALESI (Vérard 2018). Given an incoming solar radiation of  $334 \text{ W/m}^2$  and an atmospheric  $\text{CO}_2$  concentration fixed to 320 ppm, we find three climatic steady states with global mean temperatures of 31, 22, and 17 °C, respectively. By constructing the bifurcation diagram (Ragon et al. 2022), that shows how the global mean temperature changes as a function of the atmospheric  $\text{CO}_2$  content, we can evaluate the range of stability of each attractor, the position of tipping points and thus the required conditions for the system to shift from one climatic state to another.

As a first application, we have evaluated the vegetation cover in the three attractors. Through an offline coupling of the MITgcm with the vegetation model BIOME4 we have obtained the distribution of biomes for each attractor that we have compared with the ones inferred from macro fossils records of land plants before (Changhsingian) and after (Induan) the PTB (Nowak et al. 2020). The diversity of biomes reconstruction from the three climatic states shows good correlations, especially between the distribution of biomes in the cold climatic state and the fossil records before PTB.

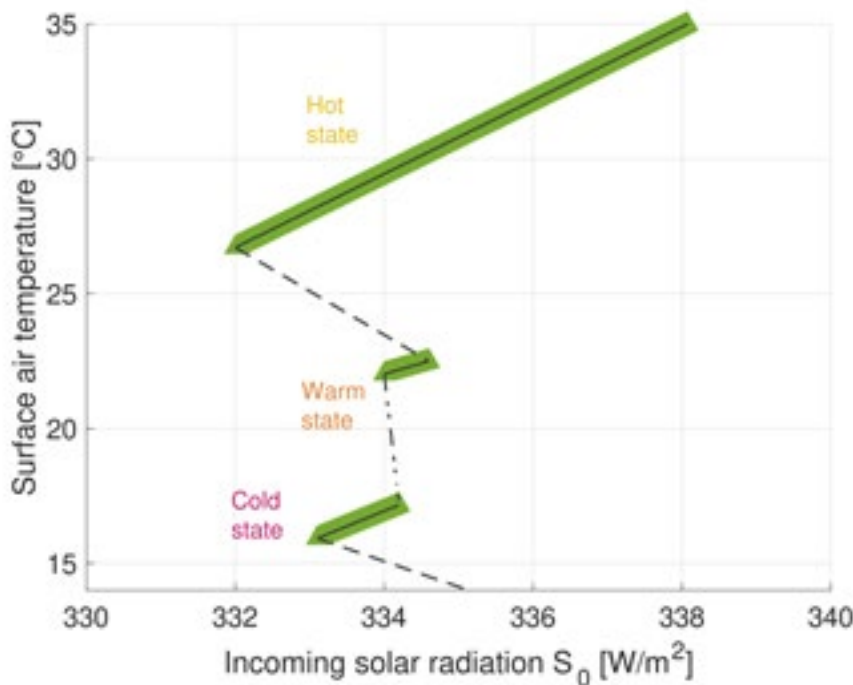


Figure 1. Preliminary bifurcation diagram of the three climatic states, described by their global mean surface air temperature as a function of the incoming solar radiation. Green lines represent the range of stability of each attractor, while dashed lines correspond to qualitative sketches of unstable branches.

## REFERENCES

- Brunetti, M., Kasparian, K., Vérard, C. 2019: Co-existing climate attractors in a coupled aquaplanet. *Clim. Dyn.* 53, 6293-6308.
- Nowak, H., Vérard, C., Kustatscher, E. 2020: Palaeophytogeographical patterns across the Permian-Triassic Boundary. *Front. Earth Sci.* 8, 613350.
- Ragon, C., Lembo, V., Lucarini, V., Vérard, C., Kasparian, J. & Brunetti, M. 2022: Robustness of competing climatic states. *Journal of Climate*, 35 (9), 2769-2784
- Rose, B. E. J. 2015: Stable 'WaterBelt' climates controlled by tropical ocean heat transport: a nonlinear coupled climate mechanism of relevance to Snowball Earth. *J Geophys. Res.: Atmos.* 120, 1404-1423.
- Vérard, C. 2018: PANALESIS : Towards global synthetic palaeogeographies using integration and coupling of manifold models. *Geological Magazine*, 156 (2), 320-330.

## P 17.7

# High-resolution modeling of historical forest fires in the Canton of Bern

Renuka P. Shastri<sup>1,2</sup>, Stefan Brönnimann<sup>1,2</sup>, Daniel Steinfeld<sup>1,2</sup>

<sup>1</sup> Institute of Geography, University of Bern, Hallerstrasse 12, CH-3012 Bern (renuka.shastri@giub.unibe.ch)

<sup>2</sup> Oeschger Centre for Climate Change Research, University of Bern, Switzerland

Forest fires are considered an important hazard in forested areas and a serious threat to forest ecosystems and buildings. The combination of drought, high temperatures, and wind, increases the risk of forest fires. To better understand the fundamental causes and consequences of fire, we need to study the historical fire regimes. In this study, the meteorological conditions were simulated with the WRF model (Weather Research and Forecasting; Skamarock et al. 2008) for three historical forest fires, in the Canton of Bern, Switzerland (La Neuveville, April 1893, Simmenflueh, August 1911, Kirchberg, April 1915). In terms of area, these are the largest fires in the canton of Bern in the Swiss fire database. The «Twentieth Century Reanalysis» version 3 (20CRv3, Slivinski et al. 2019) was used as a boundary condition. 20CRv3 has a spatial resolution of about 75 km and a temporal resolution of three hours. Using WRF version 4.1.2 20CRv3 has now been gradually downscaled to a resolution of 1x1 km<sup>2</sup>. Simulations suggest that the soil had dried out in the previous week and soil moisture had reached low values on the day the fire broke out. High-resolution fire weather indices are also calculated. A lack of precipitation and high temperatures led to high forest fire index values and a high to very high risk of forest fires.

## REFERENCES

- Slivinski, L. C. et al. (2019), Towards a more reliable historical reanalysis: Improvements to the Twentieth Century Reanalysis system. , Q. J. Roy. Meteorol. Soc. 145, 2876-2908.
- Pfister, L., S. Brönnimann, M. Schwander, FA Isotta, P. Horton, and C. Rohr, (2020) Statistical Reconstruction of Daily Precipitation and Temperature Fields in Switzerland back to 1864, Clim .past 16, 663-678.
- Skamarock, WC, et al. (2008) A Description of The Advanced Research WRF Version 3. NCAR Technical Note.
- Van Wagner, C.E. (1987): Development and Structure of the Canadian Forest Fire Weather Index System, Forestry Technical Report, Canadian Forestry Service Headquarters, Ottawa.

**P 17.8****Hail time series from radar proxies for decadal variability of hail in Switzerland**

Lena Wilhelm<sup>1</sup>, Olivie Martius<sup>1</sup>, Cornelia Schwierz<sup>2</sup>, Katharina Schröer<sup>3</sup>

<sup>1</sup> Oeschger Centre for Climate Change Research and Institute of Geography, University of Bern, Hallerstr. 12, CH-3012 Bern (lena.wilhelm@giub.unibe.ch)

<sup>2</sup> Institute of Environmental Social Sciences and Geography, University of Freiburg, Schreiberstr. 20, D-79098 Freiburg

<sup>3</sup> Federal Office of Meteorology and Climatology, MeteoSwiss, Operation Center 1, CH-8058 Zürich

In Switzerland hail regularly causes substantial damage to agriculture, cars, and infrastructure. However, addressing hail damage is challenging, as hail is related to severe thunderstorms, one of the most complex atmospheric phenomena due to its small spatial scale, vigorous development, and the intricate physical interactions. Especially in a changing climate, hail frequency and its patterns of occurrence are expected to change, which can lead to even larger agricultural hail impacts. The new Swiss hail climatologies (Barras et al. 2021, Madonna et al. 2018; Nisi et al. 2018; Nisi et al. 2020) revealed significant interannual hail variability that differs between the north and the south side of the Alps. Understanding the drivers of this variability is essential for possible adaptation strategies. In contrast to North America, where important drivers of interannual variability of severe convection are well studied (see Tippett et al. 2015 and Allen et al. 2020) a comprehensive analysis of the long-term variability of hail in Switzerland is still missing.

Therefore, in this study, a daily hail time series for Northern and Southern Switzerland from 1950 to today is produced from radar hail proxies and ERA-5 reanalysis data. Daily POH (Probability of Hail) data from MeteoSwiss is used to identify haildays in the region north and south of the Alps (plus 140km radar buffer) from 2002 to 2021 for the hail months April - September. The decision hailday yes/no is based on surpassing a POH  $\geq 80$  for a certain minimum footprint area of the domains (80<sup>th</sup> percentile). Next, one logistic regression model is built for each domain to predict the occurrence of a hailday depending on different environmental variables and indices. 70 different variables were tested. The predictors were chosen based on model performance, collinearity, and expert judgement. Seasonality, as well as long-term trends in the data, are addressed with a factor month and the absolute variable year. With the two best models, haildays will then be predicted back to 1950 to get the final timeseries for each region. The time series will then be used to study the local and remote drivers of interannual variability, e.g. central European weather types, cold fronts, large-scale variability patterns, etc., as well as to study past changes or shifts in hailstorm seasonality. With this knowledge, we could advance our understanding of the meteorological-climatological variability and change, as well as contribute to adaptation strategies to strengthen societal resilience against hail risk in Switzerland.

**REFERENCES**

- Allen, J. T. et al. 2020: Understanding Hail in the Earth System, *Reviews of Geophysics*, 58.
- Barras, H. et al. 2021: Multi-day hail clusters and isolated hail days in Switzerland – large-scale flowconditions and precursors, *Weather and Climate Dynamics*, 2, 1167.
- Madonna, E. et al. 2018: A Poisson regression approach to model monthly hail occurrence in Northern Switzerland using large-scale environmental variables, *Atmospheric Research* 203, 261.
- Nisi, L. et al. 2018: A 15 year hail streak climatology for the Alpine region, *Quarterly Journal of the Royal Meteorological Society* 144, 1429.
- Nisi, L. et al. 2020: Hailstorms in the Alpine region: Diurnal cycle, characteristics, and the nowcasting potential of lightning properties, *Quarterly Journal of the Royal Meteorological Society*, 146, 4170.
- Tippett, M. K. et al. 2015: Climate and Hazardous Convective Weather, *Current Climate Change Reports*, 1, 60.

## P 17.9

# On the importance of video journalism in geosciences

Peyrotty Giovan<sup>1</sup>, Vimpere Lucas<sup>1</sup>, Farley Nicholas<sup>1</sup>, Carraro Davide<sup>1</sup>

<sup>1</sup>SciencEscape Association – Scientific and educational video production, Geneva, Switzerland.

In recent decades, thanks to the continuous scientific progress and to the advent of new technologies, science has occupied a more central place in our society. This societal development has encountered two major obstacles: i) how to reinforce the link between science and the general public with respect to information, transparency, and education? and ii) how to assure the correct and adapted use of science and technology by every actor of the society, from citizens to their representatives?

Trust in research and researchers appears essential to meet these goals, which involves gaining the trust of the general public by delivering clear messages, fighting fake news to provide everyone with an understanding of new advances, and illustrate the risks associated with scientific research. This new reality, which puts science at the heart of our lives, must also be pushed forward and accompanied through vocations. It is therefore essential to inspire an interest in science among children, especially young adults, to ensure the scientific succession and the continuity of progress of our knowledge of the world. The higher the interest in scientific questions and appreciation of the importance of fundamental research, the greater the potential for funding. This naturally requires knowing how to be a force for persuasion, and finding the support of the public who does not always feel concerned by the question.

Scientific journalism is among the most engaging and efficient responses to these concerns. Unfortunately, some disciplines, such as geosciences, are rarely advertised. Despite their capital importance to meet current challenges, from climate change to the exploration of other planetary systems, the public is rarely aware of the important scientific questions geoscientists are trying to answer. However, a fantastic way to bring geoscience to the public's attention and communicate about our research is through videos. As geoscientists, we get to be witnesses of wonders of nature such as volcanoes, minerals, fossils, mountains, reefs, canyons, glaciers. Along with the adventure that represent each mission in the field, all of these beautiful features constitute a great material for the making of aesthetic and captivating videos for the general public.

Facing this challenge, the authors created a few years ago a non-profit association called 'SciencEscape' whose primary goal is the production of aesthetic and educational videos by geoscientists and professional video makers that focused mainly on geological high-impact topics for society. This association offers a media content to the general public (i.e., especially short documentaries) illustrating the adventures of scientists on the field. In the past three years, SciencEscape collaborated with many public institutes in Europe (i.e., universities, museums, natural parks, cantonal representatives) to produce content about volcanoes (e.g., Fagradalsfjall and Cumbre Vieja eruptions), geothermal energy, climate change (e.g., African humid period, decay of Swiss Glaciers), and paleontology. The feedback obtained from scientists and non-scientists on social media platforms are highly positive, which indicates a serious interest of the general public for geosciences as long as thematic are presented in an aesthetic and dynamic way matching the codes of current web media production. In order to produce an interesting scientific and journalistic content, it is thus essential to have a transmission axis that can touch as many people as possible. Filming and sharing researchers' field adventures and highlighting the scientific questions could be then one of the most effective ways to transmit scientific information.

# 19 Earth Observation and Remote Sensing

Alex Damm, Dominik Brunner, Othmar Frey, Claudia Röösli, Stefan Wunderle

*Swiss Commission on Remote Sensing*

TALKS:

- 19.1 Adams J., Damm A., Irani Rahaghi A., Odermatt D., Rietze N., Schaepman-Strub G., Schaepman M., Naegeli K.: Thermal Infrared (TIR) research in Switzerland: The TRISHNA T-SEC Project
- 19.2 Czyż E.A., Schmid B., Hueni A., Eppinga M.B., Schuman M.C., Schneider F.D., Guillén-Escribà C., Schaepman M.E.: Multitemporal airborne reflectance spectra constrained by intraspecific genetic diversity of temperate forest
- 19.3 Frey O., Werner C., Caduff R.: Mobile mapping of slope stability using a dual-frequency L-/Ku-band DInSAR system configuration
- 19.4 Gerber L., Randin C., Milano M., Reynard E., Mariéthoz G.: NDVI Explorer – A Google Earth Engine application to visualise and extract NDVI time-series
- 19.5 Graf L.V Perich G., Aasen H.: EOdal: A Unified Open-Source Framework for Earth Observation Data Analysis
- 19.6 Gupta S., Alewell C.: Mapping soil properties at high spatial resolution using remote sensing datasets and machine learning approaches
- 19.7 Kesselring J., Morsdorf F., Gastellu-Etchegorry J.-P., Damm A.: Comparing the variability of abiotic parameters in structurally different forests using 3D virtual scenes and radiative transfer modelling
- 19.8 Mhanna S., Brunner P., Halloran L., Zwahlen., Haj Asaad.: Remote sensing based assessment of the development of Syrian refugee camps in the Orontes basin
- 19.9 Perich G., Turkoglu M.O., Graf L.V., Wegner J.D., Aasen H., Walter A., Liebisch F.: Pixel-based yield mapping and prediction from Sentinel-2 using spectral indices and neural networks
- 19.10 Portenier C., Villiger L., Wunderle S.: A deep neural network to derive cloud base height from thermal camera images
- 19.11 Reinders K., Verhoeven G., Sartorelli L., Manconi A.: Detection Potential of Satellite Radar Interferometry (DInSAR) over Permafrost Areas in Switzerland
- 19.12 Rietze N., Assmann J., Naegeli K., Damm A., Schaepman-Strub G.: Effects of drought on land surface energy fluxes in the Siberian tundra
- 19.13 Routh D., Röösli C.: Global-Scale Mapping and Monitoring of Land Surface Phenology: an Essential Biodiversity Variable for Conservation
- 19.14 Russwurm M., Pasero L., Tuia D.: Marine debris detection with noisy annotations using Sentinel-2
- 19.15 Sauvageat E., Hou S., Maillard Barras E., Hocke K., Haefele A., Murk A.: Diurnal ozone variability in the middle atmosphere over Switzerland observed by two microwave radiometers
- 19.16 Schweiger A.K., Zehnder B. & Kneubühler M.: Tree species identification using Convolutional Neural Networks and AVIRIS-NG imaging spectroscopy data
- 19.17 Stefko M., Bernhard P., Frey O., Hajnsek I.: Multi-seasonal observations of Great Aletsch Glacier with a multi-modal ground-based radar
- 19.18 Sturm J.T., Humphrey V., Santos M.J., Damm A.: Assessing the 2018 drought response of Swiss forests and its dependence on different hydrological drivers

## POSTERS:

- P 19.1 Goudard B., Girona T., Lupi M., Caricchi L.: Earthquake-volcano interactions at oblique subduction margins; focus on Mount Sinabung volcano (Indonesia)
- P 19.2 Krochin W., Stober G., Murk A., Albers R., Plüss T.: A fully polarimetric 50 GHz temperature radiometer
- P 19.3 Shiyi L., Philipp B., Irena H.: Quantitative Characterization of Glacier Surging in Karakoram using Synthetic Aperture Radar Data
- P 19.4 Nguyen T.-A., Russwurm M., Kellenberger B., Tuia D.: Multi-temporal forest mapping at the Swiss alpine treeline
- P 19.5 Shi G., Krochin W., Murk A., Stober G.: Ozone and Water Vapor Variability in 2019/2020 Arctic Stratospheric Polar Vortex Compared to Climatology

## 19.1

# Thermal Infrared (TIR) research in Switzerland: The TRISHNA T-SEC Project

Jennifer Susan Adams<sup>1</sup>, Alexander Damm<sup>1,2</sup>, Abolfazl Irani Rahaghi<sup>2</sup>, Daniel Odermatt<sup>1,2</sup>, Nils Rietze<sup>1,3</sup>, Gabriela Schaepman-Strub<sup>3</sup>, Michael Schaepman<sup>1</sup>, Kathrin Naegeli<sup>1</sup>

<sup>1</sup> Department of Geography, University of Zurich, Winterthurerstrasse 190, 8057 Zurich, Switzerland  
(jennifer-susan.adams@geo.uzh.ch)

<sup>2</sup> Department Surface Waters – Research and Management, Eawag, Swiss Federal Institute of Aquatic Science and Technology, Ueberlandstrasse 133, 8600 Duebendorf, Switzerland

<sup>3</sup> Department of Evolutionary Biology and Environmental Studies, University of Zurich, Winterthurerstrasse 190, 8057 Zurich, Switzerland

The TRISHNA (Thermal infraRed Imaging Satellite for High-resolution Natural resource Assessment) mission is a high-resolution space-time thermal infrared (TIR) mission aimed to enhance our understanding of the water cycle and improve our management of the planet's water resources (Lagouarde *et al* 2018). TRISHNA is planned for launch in 2025, and will provide global high resolution (~60 m), high revisit (3 acquisitions over 8 days) thermal remote sensing measurements. The scientific objectives of the TRISHNA mission include monitoring of terrestrial ecosystems, of the urban environment, coastal and inland waters, the cryosphere, the atmosphere, and applications to the solid Earth.

Within the TRISHNA objectives, the Swiss TRISHNA – Science and Electronics Contribution (T-SEC) project funded by ESA Prodex is comprised of a commercial part led by Sydernal Swiss SA, and a scientific part led by the University of Zurich and Eawag. The scientific part of T-SEC aims to contribute towards the key TRISHNA scientific objectives, and focuses on using TIR remote sensing to understand and measure the water status and stress of continental ecosystems over mountainous and tundra regions.

This contribution aims to give an overview of the research themes addressed by T-SEC, including:

1. 3D modelling of directionality and energy balance over Swiss forests for ecosystem stress monitoring
2. Remote sensing of the surface energy budget of the alpine cryosphere
3. High resolution Lake Surface Water Temperature monitoring in Swiss perialpine and alpine lakes
4. Effect of ecosystem disturbances on land surface energy fluxes in the Siberian tundra

Priority sites in Switzerland have been identified for forests (Laegeren, Davos and Höllstein), alpine cryosphere (Murtèl/Corvatsch, Findelengletscher, Glacier de la Plaine Morte) and hydrosphere (Lake Geneva, Ägerisee, Lej da Vadret). At a tundra reference site in the northeast Siberian Arctic was selected to investigate the use of land surface temperature for land surface energy flux and permafrost thaw research.

The four sub-projects aim to collectively improve our understanding of thermal remote sensing data and its use for monitoring water resources and energy budgets in complex ecosystems. We particularly address energy budget modelling in mountainous and boreal/tundra environments using TRISHNA measurements; gain understanding and characterise the key challenges faced by thermal remote sensing observations (e.g. directionality effects, scaling); to contribute towards TIR calibration and validation activities over selected reference sites in Switzerland (forests, cryosphere and inland waters) and tundra regions; to conduct field campaigns and collect thermal in-situ data to help quantify uncertainties of TIR measurements and products; to set up state-of-the-art reconstructions of selected sites or “virtual laboratories” allowing modelling and better understanding of thermal measurements and products; and finally investigate multi-sensor approaches and synergies with thermal remote sensing data.

## REFERENCES

- J.-P. Lagouarde, B.K. Bhattacharya, P. Crébassol, P. Gamet, S.S. Babu, G. Boulet *et al.* (2018) “The Indian-French Trishna Mission: Earth Observation in the Thermal Infrared with High Spatio-Temporal Resolution”, *IGARSS 2018 - 2018 IEEE International Geoscience and Remote Sensing Symposium*

## 19.2

# Multitemporal airborne reflectance spectra constrained by intraspecific genetic diversity of temperate forest

Ewa A. Czyż<sup>1</sup>, Bernhard Schmid<sup>1</sup>, Andreas Hueni<sup>1</sup>, Maarten B. Eppinga<sup>1</sup>, Meredith C. Schuman<sup>1,2</sup>, Fabian D. Schneider<sup>3</sup>, Carla Guillén-Escribà<sup>1</sup>, Michael E. Schaepman<sup>1</sup>

<sup>1</sup> Department of Geography, University of Zurich, Winterthurerstrasse 190, CH-8057 Zurich, Switzerland

<sup>2</sup> Department of Chemistry, University of Zurich, Winterthurerstrasse 190, CH-8057 Zurich, Switzerland

<sup>3</sup> Jet Propulsion Laboratory, California Institute of Technology, 4800 Oak Grove Dr, Pasadena, CA 91109, USA  
(ewa.czyz@geo.uzh.ch)

Remote sensing has demonstrated its potential to monitor biodiversity. It overcomes the spatial limitations of ground-based measurements and allows acquiring high –spatial, -spectral and temporal resolution data. Temporal trajectories of plants reflectance spectra hold information about dynamic of plants physiological and morphological traits. These traits and their turnover are specific for different phylogenetic groups, but vary also between individuals depending on their environment and genetic background. Higher genetic variability of populations increases its resilience to diseases and widen its evolutionary potential. Therefore, maintaining genetically variable populations, understanding drivers of genetic diversity and monitoring current stage of genetic variation is important for preventing species loss under changing environmental conditions. We propose a multitemporal approach using remote sensing data to contribute to biodiversity monitoring at the level of genetic diversity within species.

We used the imaging spectrometer APEX (Airborne Prism Experiment) to obtain a data set consisting of 27 images from 2009 – 2019 acquired across the growing seasons for the study area (Laegern, 47°28'N, 8°21'E). We compared this data set with a genetic data set consisting of microsatellite data of 68 dominant *Fagus sylvatica* L. (common beech) individuals from the site. We constructed distance matrices between individuals based on spectral data and microsatellite data to derived spectra-genetic similarities per each time of acquisition and spectral region. Further, we tested the influence of environmental variables on spectral-genetic similarities. We found that genetically similar individuals expose spectrally similar responses under higher temperatures of the day of acquisition and towards end of growing season. Based on investigated data, we will present and discuss the potential of repeated-time airborne imaging spectroscopy to assess the genetic structure of tree species at the landscape level.

## 19.3

# Mobile mapping of slope stability using a dual-frequency L-/Ku-band DInSAR system configuration

Othmar Frey<sup>1,2</sup>, Charles Werner<sup>1</sup>, Rafael Caduff<sup>1</sup>

<sup>1</sup> Gamma Remote Sensing, Worbstrasse 225, CH-3073 Gümligen ([frey@gamma-rs.ch](mailto:frey@gamma-rs.ch))

<sup>2</sup> ETH Zurich, Earth Observation & Remote Sensing, Institute of Environmental Engineering, Leopold-Ruzicka-Weg 4, CH-8093 Zurich.

Recently, we have demonstrated mobile mapping of surface displacements using our in-house developed L-band interferometric synthetic aperture radar (SAR) system on a car and on a UAV (Frey et al. 2019 & 2021). Meanwhile we have consolidated our experience with repeat-pass SAR interferometry data acquisition, SAR imaging, and interferometric processing from such agile platforms and, in 2021/2022, we have started to deploy a second SAR system operating at Ku-band as part of our car-borne measurement configuration.

This new configuration permits acquiring simultaneously at L-band and at Ku-band. The Ku-band SAR system is essentially a Gamma Portable Radar Interferometer (GPRI) radar system (Werner et al. 2012, Caduff et al. 2015), yet using small horn antennas for the mobile mapping SAR mode instead of the 2m-long slotted waveguide antennas used in the regular stationary rotational real-aperture radar mode.

The dual-frequency setup is motivated by the following rationale: in steep slopes in alpine areas, which are typical objects of interest for displacement measurements and geohazard monitoring, the surface is often a mix of bare rock, debris, bare soil, and vegetation of different types and sizes. Interferometric radar measurements of these different types of land cover are variably affected by temporal decorrelation depending on the radar wavelength (see e.g. (Zebker & Villasenor 1992)). Also, different geological processes and terrain morphology leading to varying surface displacements velocities may play a role on the same mountain slope; a situation, which can be captured more accurately using different frequencies with different sensitivities towards the line-of-sight component of the displacements. In both cases frequency diversity is an advantage. Then, there are also technical aspects in the interferometric data processing, such as phase unwrapping, atmospheric path delay mitigation, and residual motion correction, for which the dual-frequency setup is beneficial.

In this work, we discuss mobile mapping of slope surface displacements from simultaneous L-band and K-band interferometric SAR measurements obtained around Innertkirchen and Guttannen, CH. We discuss the synergies of the dual-frequency measurement configuration in terms of the sensitivity to line-of-sight displacements and temporal decorrelation in a typical measurement scenario, and we highlight its potential to better separate nuisance parameters, such as residual positioning errors of the radar sensor trajectory.

## REFERENCES

- Caduff, R., Schlunegger, F., Kos, A., and Wiesmann, A., 2015: "A review of terrestrial radar interferometry for measuring surface change in the geosciences," *Earth Surface Processes and Landforms*, 40(2), 208–228.
- Frey, O., Werner, C.L. and Coscione, R., 2019: "Car-borne and UAV-borne mobile mapping of surface displacements with a compact repeat-pass interferometric SAR system at L-band," in *Proc. IEEE Int. Geosci. Remote Sens. Symp.*, 274–277
- Frey, O., Werner, C. L., Manconi, A., and Coscione, R., 2021: "Measurement of surface displacements with a UAV-borne/car-borne L-band DInSAR system: system performance and use cases," in *Proc. IEEE Int. Geosci. Remote Sens. Symp.*, 628–631.
- Werner, C. L., Wiesmann, A., Strozzi, T., Kos, A., Caduff, R., and Wegmüller, U., 2012: "The GPRI multi-mode differential interferometric radar for ground-based observations," in *Proc. EUSAR 2012*, 304–307.
- Zebker, H. and Villasenor, J., 1992: "Decorrelation in interferometric radar echoes," *IEEE Trans. Geosci. Remote Sens.*, 30(5), 950–959.

## 19.4

### ***NDVI Explorer – A Google Earth Engine application to visualise and extract NDVI time-series***

Loïc Gerber<sup>1</sup>, Christophe Randin<sup>2</sup>, Marianne Milano<sup>3</sup>, Emmanuel Reynard<sup>3</sup>, Grégoire Mariéthoz<sup>1</sup>

<sup>1</sup> Institute of Earth Surface Dynamics (IDYST), UNIL-Mouline, Geopolis, University of Lausanne, 1015 Lausanne, Switzerland  
(loic.gerber.2@unil.ch)

<sup>2</sup> Alpine Botanical Garden Flore-Alpe, 1938 Champex-lac, Switzerland

<sup>3</sup> Institute of geography and sustainability (IGD), UNIL-Mouline, Géopolis, University of Lausanne, 1015 Lausanne, Switzerland

Water shortages have become common in Valais (Switzerland) during dry summers due to climate change and the resulting modification of hydrological regimes. They are expected to become more frequent and severe in the near future. Shortages in irrigation water for crops and grasslands can have serious ecological, economic, and social consequences.

We focus on the analysis of NDVI time-series for several grassland plots around the Entremont valley (Valais, CH) to better understand the relationship between irrigation and vegetation growth and to minimise the volume of water used. The goal is to identify the effects of irrigation and mows on NDVI (Gao, 1996) time-series to help inform farmers and stakeholders. All calculations and analyses were performed in Google Earth Engine (GEE) using Sentinel-2 and Planet labs images. GEE is a free and powerful cloud-based geospatial analysis platform that enables users to visualise and analyse a vast catalogue of satellite images. The rather new possibility of creating web applications directly within GEE is used in this project to bring remote sensing research to stakeholders in a straightforward manner through *NDVI Explorer*, an application we created.

Our application is now available to researchers, stakeholders and farmers involved in the project. This valuable tool allows them to visualise the NDVI (amongst other indexes) of different plots over several years whenever a cloudless image is available for both Sentinel-2 and Planet labs imagery. It is also possible to manually draw an area to be analysed directly in the application. While Sentinel-2 imagery is free and readily available in GEE, Planet imagery is not openly accessible and needs to be imported on the platform. Furthermore, *NDVI Explorer* automatically extracts time-series of the median NDVI for a predefined or user-drawn geometry over the entirety of the available images time-series, as well as median and standard-deviation maps.

Overall, the possibility of creating applications in GEE using the same programming language as the one used for regular analyses is very interesting and can be especially useful in the transmission of knowledge to stakeholders that do not have the technical or programming expertise.

#### REFERENCES

- Gao, B. (1996). NDWI—A normalized difference water index for remote sensing of vegetation liquid water from space. *Remote Sensing of Environment*, 58(3), 257–266. [https://doi.org/10.1016/S0034-4257\(96\)00067-3](https://doi.org/10.1016/S0034-4257(96)00067-3).

## 19.5

# EOdal: A Unified Open-Source Framework for Earth Observation Data Analysis

Lukas Valentin Graf<sup>1,2</sup>, Gregor Perich<sup>1,2</sup>, Helge Aasen<sup>1,2</sup>

<sup>1</sup> Crop Science, Institute of Agricultural Science, ETH Zürich, Universitaetstrasse 2, CH-8092 Zürich  
(lukasvalentin.graf@usys.ethz.ch)

<sup>2</sup> Earth Observation and Analysis of Agroecosystems Team, Division Agroecology and Environment, Agroscope, Reckenholzstrasse 191, CH-8046 Zürich

The growing amount of Earth Observation (EO) data from satellites and in-situ measurements opens up unprecedented opportunities to study processes in the Earth system with high spatio-temporal resolution. However, to ensure that research in this area remains traceable and reproducible, a unified open-source framework for EO data management and analysis is required. Moreover, the framework should provide easy access to data and analysis for users without a background in geographic information science or remote sensing. For this reason, we developed the Earth Observation Data Analysis Library (EOdal). Eodal is entirely open-source (GPL v3.0 license) and written in Python3. This distinguishes Eodal from proprietary solutions such as the Google Earth Engine (GEE). GEE is user-friendly and a powerful tool, but the underlying backend is closed-source and the use of the platform implies a tight commitment to a single service provider. This can lead to disruptions, especially in the case of an adaptation of the usage agreements.

Eodal allows working on local premises, but also supports cloud environments such as the Microsoft Planetary Computer to enable rapid scaling of EO data workflows from local to global scale. Eodal takes over large parts of the data handling, so that users can fully concentrate on their actual research questions.

Application areas of Eodal are currently in agricultural and ecophysiological research: For instance, Eodal was used to propagate radiometric uncertainties in Sentinel-2 data into land surface phenological. Further areas of application are the estimation of crop yield on the pixel level using Sentinel-2 time series and the reconstruction of crop growth dynamics from Planet Scope imagery. However, the library is by no means limited to these application areas: Its modular structure with programming interfaces makes it almost infinitely extensible and customizable.

We will explain the main concepts beyond Eodal and show-cast its capabilities. Moreover, we will summarize lessons learned and present possible further developments and our vision about a future open-source (Swiss) Earth Observation ecosystem.

## 19.6

# Mapping soil properties at high spatial resolution using remote sensing datasets and machine learning approaches

Surya Gupta<sup>1</sup> and Christine Alewell<sup>1</sup>

<sup>1</sup> Department of Environmental Sciences, University of Basel, Bernoullistrasse 30, 4056 Basel, Switzerland

Spatial soil maps are essential for monitoring, management, and conservation. These maps are crucial to accessing the ecosystem services and helpful in guiding the farmers. Several global maps of soil properties are available, provided by SoilGrids (Poggio et al., 2021) and OpenLandMap (Hengl and Wheeler, 2018). However, the number of samples used and spatial resolution for these maps indicate a potentially high uncertainty and leave room for discussion. Moreover, these maps used very few samples to represent the soil properties of the whole of Switzerland. Therefore, the objective of this study was to produce soil property maps (soil organic carbon, soil texture, nitrogen, and phosphorus) for Switzerland using more data as compared to other studies (collected from the literature) with higher spatial resolution at different depths. We fitted the Quantile Random Forest (QRM) machine-learning model for spatial predictions. Each soil property was linked with environmental covariates such as topography, climate, and vegetation, which have an influence on soil properties. Each model was evaluated using five-fold spatial cross-validation. The results showed the concordance correlation coefficients (CCC) between 0.35–0.65 for predicted soil properties. To validate the resulting maps of soil properties and to compare the accuracy of the new maps with two global existing maps of soil properties such as SoilGrids and OpenLandMap, two independent datasets were used. The accuracy metrics for the new Swiss maps were considerably better than existing global maps.

## REFERENCES:

- Poggio, L., De Sousa, L. M., Batjes, N. H., Heuvelink, G., Kempen, B., Ribeiro, E., & Rossiter, D. (2021). SoilGrids 2.0: producing soil information for the globe with quantified spatial uncertainty. *Soil*, 7(1), 217–240.
- Tomislav Hengl, & Ichsan Wheeler. (2018). Soil organic carbon content in x 5 g / kg at 6 standard depths (0, 10, 30, 60, 100 and 200 cm) at 250 m resolution (v0.2) [Data set]. Zenodo. <https://doi.org/10.5281/zenodo.2525553>

**19.7****Comparing the variability of abiotic parameters in structurally different forests using 3D virtual scenes and radiative transfer modelling**

Jasmin Kesselring<sup>1</sup>, Felix Morsdorf<sup>1</sup>, Jean-Philippe Gastellu-Etchegorry<sup>2</sup>, Alexander Damm<sup>1,3</sup>

<sup>1</sup> Institute of Geography, University of Zurich, Winterthurerstrasse 190, CH-8057 Zürich ([jasmin.kesselring@geo.uzh.ch](mailto:jasmin.kesselring@geo.uzh.ch));

<sup>2</sup> Centre d'Etudes Spatiales de la Biosphère (CESBIO), Toulouse University (UPS, CNES, CNRS, IRD), 31401 Toulouse, France;

<sup>3</sup> Eawag, Swiss Federal Institute of Aquatic Science and Technology, 8600 Dübendorf

Vegetation releases water to the atmosphere due to transpiration, and CO<sub>2</sub> uptake is determined by the process of photosynthesis. The rate of this gas exchange depends on numerous biotic and abiotic variables specific to the underlying vegetation composition and ecosystem. Forest ecosystems are largely affected by water and carbon cycle dynamics, thus, studying forest gas exchange can help understanding and quantifying the consequences of climate change on these ecosystems. An established technique to estimate forest gas exchange is the use of eddy flux towers. With vertically distributed sensors, atmospheric variation of CO<sub>2</sub> and water vapor are measured as proxies for gas exchange on a local scale [Balocchi, 2003]. By combining multiple eddy covariance sites, connections between regions and different ecosystems can be made. However, scaling up these local observations to a larger scale, requires several assumptions on the spatial distribution of biotic and abiotic factors. An alternative approach is available via remote sensing (RS), especially from satellites. Satellite RS for environmental monitoring has the advantage of a high spatial coverage, being non-destructive and comparable for large regions. A notable disadvantage of RS is, however, its inherent top of canopy perspective that has limited sensitivity for the vertical heterogeneity of the canopy itself [Damm et al., 2020].

This study aims to understand how common RS estimates of abiotic and biotic factors and gas exchange are related to the real 3D variability of forest ecosystems. We construct 3D virtual scenes of two contrasting forests (i.e., the mixed deciduous forest Laegern, the coniferous forest Seehornwald in Davos) using LiDAR and optical RS data. The radiative transfer model DART (Discrete Anisotropic Radiative Transfer) [Gastellu-Etchegorry et al., 2015] was used in combination with these 3D virtual scenes to simulate the abiotic factors net radiation and temperature. We then quantify the 3D distribution of these factors between both forest types and evaluate differences between the RS and the real 3D perspective.

**REFERENCES**

- D. D. Baldocchi (2003): Assessing the eddy covariance technique for evaluating carbon dioxide exchange rates of ecosystems: Past, present and future. *Global Change Biology*, 9(4):479–492. A.
- Damm, E. Paul-Limoges, D. Kükenbrink, C. Bachofen, and F. Morsdorf (2020): Remote sensing of forest gas exchange: Considerations derived from a tomographic perspective. *Global Change Biology*, 26(4): 2717–2727.
- J. P. Gastellu-Etchegorry, T. Yin, N. Lauret, T. Cajgfinger, T. Gregoire, E. Grau, J. B. Feret, M. Lopes, J. Guilleux, G. Dedieu, Z. Malenovsk, B. D. Cook, D. Morton, J. Rubio, S. Durrieu, G. Cazanave, E. Martin, and T. Ristorcelli (2015): Discrete anisotropic radiative transfer (DART 5) for modeling airborne and satellite spectroradiometer and LIDAR acquisitions of natural and urban landscapes, *Remote Sensing*, 7(2):1667–1701.

## 19.8

# Remote sensing based assessment of the development of Syrian refugee camps in the Orontes basin

Saeed Mhanna<sup>1</sup>, Philip Brunner<sup>1</sup>, Landon Halloran<sup>1</sup>, Francois Zwahlen<sup>1</sup>, Ahmed Haj Asaad<sup>2</sup>

<sup>1</sup> Centre of Hydrogeology and Geothermics, University of Neuchâtel, Neuchâtel, Switzerland (saeed.mhanna@unine.ch)

<sup>2</sup> Geo Expertise, Geneva, Switzerland

Remote sensing is increasingly being used in the domain of humanitarian aid response, especially in areas with difficult access. Knowledge about the location and modes of expansion of refugee settlements is necessary for providing adequate aid. Because the development of these refugee settlements is often rapid and unorganized, humanitarian organizations often fall short in responding to the needs of their inhabitants. Moreover, uncontrolled expansions might place refugees at an elevated risk with respect to natural disasters (e.g., floods, storms and wildfires).

The ongoing armed conflict in Syria has so far resulted in 5.6 million refugees, mostly hosted in Turkey (65.1%) and Lebanon (14.8%) (UNHCR, 2022), as well as 6.7 million living in internal displacement (IDMC, 2021). In this study, we use satellite imagery and machine learning to produce yearly Landuse/Landcover (LU/LC) maps to track changes due to the conflict within the Orontes river basin, which extends across Lebanon, Syria and Turkey. Landsat 5, 7 and 8 datasets were selected spanning from 2004 to 2021 and processed using the cloud computing platform Google Earth Engine. Training/validation data points were collected from high resolution imagery and were used to train a Random Forest classifier to classify the yearly image composites. These maps allowed us to distinguish three different types of refugee camps/settlements. In Syria, Internally Displaced People (IDP) camps are characterized by a high degree of randomness and a significant sharp increase after 2019 (Figure 1). In Lebanon, refugees settled in the outskirts of major cities and peri-urban expansion commenced after the beginning of the war in 2011. Finally, highly organized camp sites were constructed in Turkey and informal settlements were restricted. The results of this study can be used to better manage the water resources for the refugees and IDPs within the Orontes river basin, in addition to monitoring and managing the expansion of these settlements.

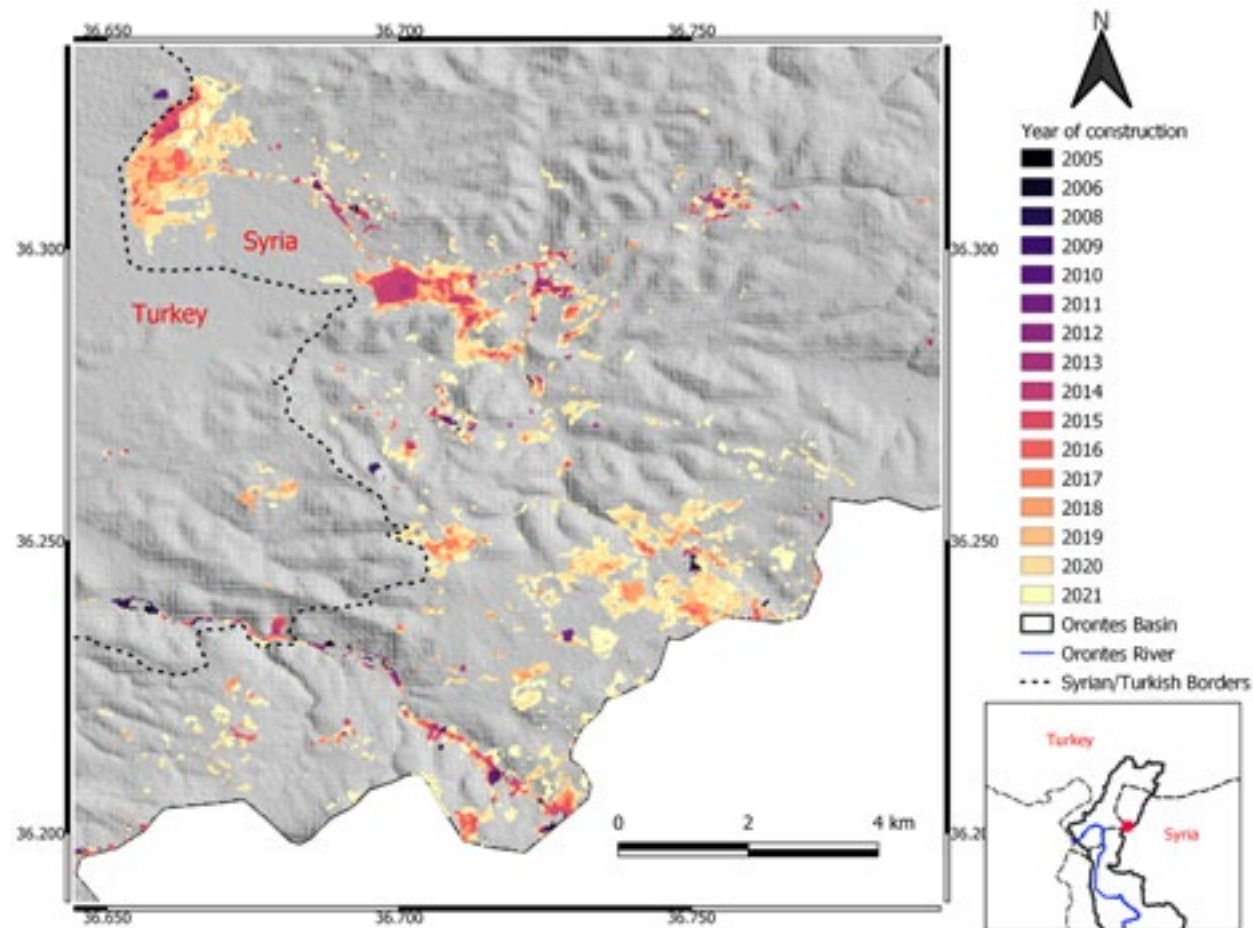


Figure 1. Yearly expansion of the IDP camps on the Syria/Turkish borders from 2005 to 2021.

**REFERENCES**

- IDMC. (2021, December). Total Number of IDPs. Retrieved from <https://www.internal-displacement.org/countries/syria>.  
UNHCR. (2022, July). Total Registered Syrian Refugees. Retrieved from [data.unhcr.org](http://data.unhcr.org).

## 19.9

# Pixel-based yield mapping and prediction from Sentinel-2 using spectral indices and neural networks

Gregor Perich<sup>1</sup>, Mehmet Ozgur Turkoglu<sup>2</sup>, Lukas Valentin Graf<sup>1,3</sup>, Jan Dirk Wegner<sup>2,4</sup>, Helge Aasen<sup>1,3</sup>, Achim Walter<sup>1</sup>, Frank Liebisch<sup>5</sup>

<sup>1</sup> Crop Science, ETH Zurich

<sup>2</sup> EcoVision Lab, Photogrammetry and Remote Sensing, ETH Zurich

<sup>3</sup> Remote Sensing Team, Agroecology and Environment, Agroscope

<sup>4</sup> Institute for Computational Science, University of Zurich

<sup>5</sup> Agroecology and Environment, Agroscope

Mapping and predicting crop yield on a large scale is increasingly important for use cases such as policy-making, risk insurance and precision agriculture applications at farm and field scale. These have the potential to better manage agro-ecosystems, therefore help reduce the environmental impact of agriculture. The higher spatial resolution of Sentinel-2 compared to Landsat allows for satellite-based crop yield mapping even in relatively small scaled agricultural settings such as found in Switzerland and other central European regions. In this study, five years (2017-2021) of cereal crop yield data from a combine harvester were used to model crop yield on a spatial scale corresponding to the Sentinel-2 pixel level. Three established methods from literature using i-ii) spectral indices and iii) raw satellite reflectance as well as iv) a recurrent neural network (RNN) were chosen for analysis. Although the RNN approach did not outperform the other methods, it was more efficient because of the comparatively simple end-to-end training of the model, resulting in much less time spent on data cleaning and feature extraction needed for spectral index time series analysis. The RNN was also able to discriminate cloudy data by itself, reaching similar performance levels as if using pre-processed, cloud-free data. Modelling was performed on individual years, all years combined and on unseen years using leave-one-year-out cross-validation. The models performed best when using data from all years ( $R^2$  up to 0.88, relative RMSE up to 10.49%) and showed poor performance when predicting on unseen data years, especially for years with previously unknown weather patterns. This highlights the importance of yearly model calibration and the need for continuous data collection enabling long time series for future crop yield models.

## 19.10

# A deep neural network to derive cloud base height from thermal camera images

Céline Portenier<sup>1</sup>, Leonie Villiger<sup>2</sup>, Stefan Wunderle<sup>1</sup>

<sup>1</sup> Oeschger Centre for Climate Change Research and Institute of Geography, University of Bern  
(celine.portenier@giub.unibe.ch)

<sup>2</sup> Institute for Atmospheric and Climate Science, ETH Zurich

Observing atmospheric conditions such as the height of a cloud ceiling is extremely important for air traffic management. Instruments to accurately measure the cloud's base height from the ground (so-called Ceilometers) are extremely expensive and are limited to point measurements vertically oriented to the atmosphere. An alternative solution are upward facing thermal cameras. The temperatures measured by such cameras decrease significantly if a cloud is present; the higher the cloud, the lower the measured temperature. However, the thermal camera does not correct for the atmospheric water vapour between the ground and the measured cloud. Thus, the relation between the measured temperature and the cloud base height is complex, but can be learned by a deep neural network (DNN). In our study, we propose to use parallel measurements of a Ceilometer, a thermal camera, and measurements of meteorological variables (surface pressure, relative humidity, and air temperature) as an input for a DNN to predict the cloud base height from temperatures measured by the thermal camera. We present different approaches using deep classification, deep regression, and a convolutional neural network and illustrate how the trained networks predict cloud base height compared to the nearby Ceilometer measurements. Finally, we use a hemispherical webcam to analyze different cloud types in relation to the predicted cloud base height information.

## 19.11

# Detection Potential of Satellite Radar Interferometry (DInSAR) over Permafrost Areas in Switzerland

Kristina Reinders<sup>1</sup>, Govert Verhoeven, Luca Sartorelli<sup>2</sup>, Andrea Manconi<sup>3</sup>

<sup>1</sup> Delft University of Technology, Stevinweg 1, NL-2628 CN Delft, The Netherlands ([k.j.reinders@tudelft.nl](mailto:k.j.reinders@tudelft.nl))

<sup>2</sup> SkyGeo, Oude Delft 175, NL-2611 HB Delft, The Netherlands

<sup>3</sup> WSL Institute for Snow and Avalanche Research SLF, Flüelastrasse 11, CH-7260 Davos

Glaciers and permafrost declined during the last decade and are expected to continue with this trend in almost all regions throughout the 21st century (Hock et al., 2019). This will increase the natural hazard potential in alpine regions (Hock et al., 2019; Gobiet et al., 2014; Probst et al., 2013). This year, glacier collapses in the Grand Combin and the Marmolada have already caused several fatalities (SRF, 2022).

Monitoring the alpine permafrost is therefore crucial to assess the vulnerability of structures in these areas and plan countermeasures. Currently, the most common method to monitor permafrost is with temperature and displacement measurements in boreholes. However drilling boreholes and monitoring temperature in high alpine environment is not trivial. In addition, the information is limited at few points and might be not representative of the spatial variabilities. For this reason, remote sensing can provide valuable solutions. For example, one method to monitor displacements over large areas is differential interferometry on spaceborne synthetic aperture radar (DInSAR) (Hanssen, 2001). However, this technique is still rarely used in common practice to monitor permafrost areas. This is due to several limitations in terms of spatial and temporal resolutions, as well as intrinsic limitations of DInSAR over high alpine areas. The advent of new modern satellite missions such as the ESA Copernicus Sentinel-1 provides new opportunities to perform systematic investigations and build monitoring programs at regional scales.

In this work, we explored the detection potential of permafrost areas in the Swiss Alps with DInSAR. We use Sentinel-1 data acquired over Switzerland spanning 5 orbits (descending tracks 136, 66, 168 and ascending tracks 88 and 15) the digital elevation model Copernicus 30 m, and the permafrost indication map provided by the Swiss Institute for Snow and Avalanche Research (SLF, 2019), to determine the theoretical detection potential and visibility of the areas of interest. We calculated the R-index, according to Notti et al. (2014) for entire Switzerland and then focused on only the permafrost areas. Fig. 1 shows an example of R-Index maps produced for the two ascending tracks. Secondly we analyzed the results of Persistent Scatterer Interferometry (PSI) obtained over the Canton Wallis to assess into details the real results over selected places of interest. Our results will help understand if displacements in permafrost areas can be detected efficiently and monitored, and if this approach can be used to optimise mitigation strategies in high alpine areas.

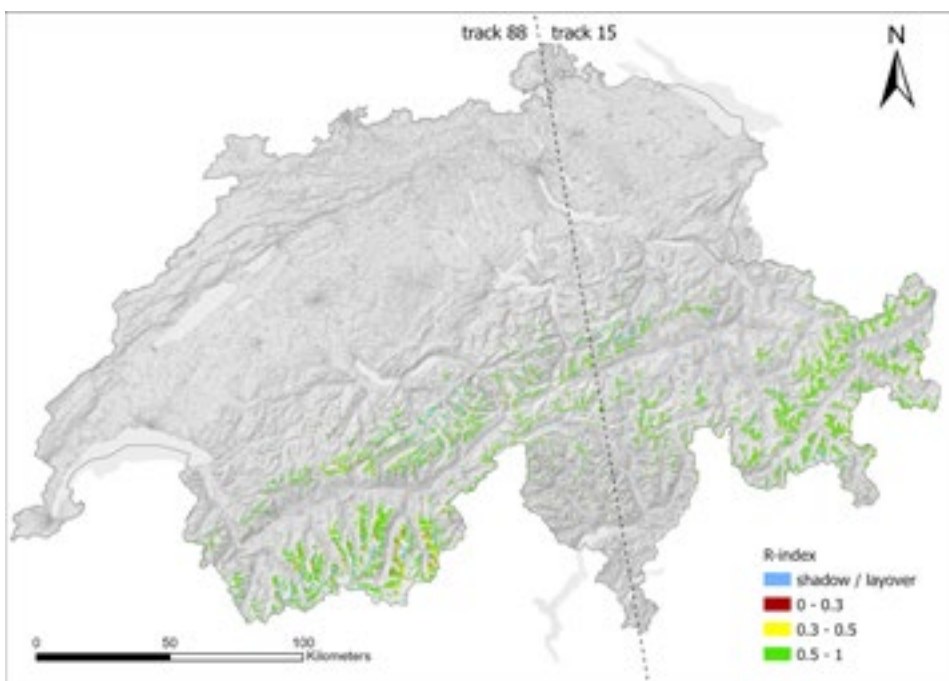


Figure 1. R-index for ascending tracks in permafrost areas, where red means the visibility of the area may not be good and green means that the area has a good visibility.

## REFERENCES

- Gobiet, A., Kotlarski, S., Beniston, M., Heinrich, G., Rajczak, J., and Stoffel, M. 2014: 21st century climate change in the European Alps—A review, *Science of The Total Environment*, 493, 1138–1151
- Hanssen, R. F. 2001: *Radar Interferometry: Data Interpretation and Error Analysis*, Kluwer Academic Publishers, Dordrecht
- Hock, R., Rasul, G., Adler, C., Cáceres, B., Gruber, S., Hirabayashi, Y., Jackson, M., Kääb, A., Kang, S., Kutuzov, S., et al. 2019: High Mountain areas
- Notti, D., Herrera, G., Bianchini, S., Meisina, C., García-Davalillo, J. C., and Zucca, F. 2014: A methodology for improving landslide PSI data analysis, *International Journal of Remote Sensing*, 35, 2186–2214
- Probst, T., Wicki, W., Zischg, A., and Pichler, A. 2013: Alpine strategy for adaptation to climate change in the field of natural hazards
- SRF, Zwei Tote nach Eissturz im Wallis, May 27, 2022, <https://www.srf.ch/news/schweiz/abgebrochene-eisbrocken-zwei-tote-nach-eissturz-im-wallis>
- SRF, gletscherabbruch-in-italien-fordert-tote, July 3, 2022, <https://www.srf.ch/play/tv/tagesschau/video/gletscherabbruch-in-italien-fordert-tote?urn=urn:srf:video:98cbc087-36ac-4637-a2d1-9dc8047a6a57>
- Swiss institute of snow and avalanche research, 2019: neue Permafrost- und Bodeneiskarte des SLF (PGIM), <https://www.slf.ch/pgim>

## 19.12

### Effects of drought on land surface energy fluxes in the Siberian tundra

Nils Rietze<sup>1</sup>, Jakob Assmann<sup>1</sup>, Kathrin Naegeli<sup>2</sup>, Alexander Damm<sup>2,3</sup>, Gabriela Schaepman-Strub<sup>1</sup>

<sup>1</sup> *Spatial Ecology and Remote Sensing, Department of Evolutionary Biology and Environmental Sciences, University of Zurich, Winterthurerstr. 190, CH-8057 Zürich (nils.rietze@uzh.ch)*

<sup>2</sup> *Remote Sensing Laboratories, Department of Geography, University of Zurich, Winterthurerstr. 190, CH-8057 Zürich*

<sup>3</sup> *Remote Sensing of Water Systems, Department of Geography, University of Zurich, Winterthurerstr. 190, CH-8057 Zürich*

The rapidly warming climate and associated changes, such as plant community shifts, droughts and wildfires, alter land surface energy fluxes in the Arctic tundra. Droughts and shifts in plant community composition might modify latent and sensible heat fluxes, resulting in altered land surface feedbacks to the regional climate.

Our study aims to analyse drivers of plant thermoregulation (the vegetation's ability to cool its canopy by evapotranspiration) combining remotely sensed estimates of heat fluxes and in situ data of microclimate. We collected drone-based optical and thermal imagery during peak growth season (July-August) of a very dry summer (2020) and a hydrologically average summer (2021) in the Kytalyk national reserve in north-eastern Siberia (70.83° N, 147.49° E).

Additionally, we measured biotic, soil and atmospheric variables, including species composition, soil temperature and moisture, precipitation, and air temperature. We first quantified the drivers of micro-scale thermoregulation across different plant communities, and then investigated the effects of summer drought on thermoregulation.

During both years, plant community types differed in their thermoregulation. Communities associated with moist soils had the strongest cooling of the canopy, whereas drier plant communities showed weaker thermoregulation or a complete lack thereof. Thermoregulation was weaker in the summer with drought (2020) across all vegetation types, indicating that the plants experience water limitation during drought conditions at the research site.

Overall, our study highlights the importance of considering plant community composition and drought conditions when estimating landscape energy fluxes in the Arctic tundra. Further work is needed to quantify the contributions of both factors to regional climate feedbacks across the Arctic tundra.

## 19.13

# Global-Scale Mapping and Monitoring of Land Surface Phenology: an Essential Biodiversity Variable for Conservation

Devin Routh<sup>1,2</sup>, Claudia Röösli<sup>2</sup>

<sup>1</sup> S<sup>3</sup>IT: Service and Support for Science IT; University of Zürich, Winterthurerstrasse 190, CH 8057 Zürich

<sup>2</sup> Remote Sensing Laboratories, Department of Geography; University of Zürich, Winterthurerstrasse 190, CH 8057 Zürich

**Keywords:** remote sensing, land surface phenology, conservation, monitoring, biodiversity, big data

Human society has placed enormous stress on ecosystems across the globe, with one of the many consequences being the loss of biodiversity (Johnson et al., 2017; Habibullah et al., 2022). Conservation efforts, however, can lessen these environmental stressors and mitigate some of the damage. As a direct response to initiatives aiming to reduce biodiversity loss, the Group on Earth Observations - Biodiversity Observation Network ([GEO BON](#)) has proposed a common framework of essential biodiversity variables (EBVs) to implement global-scale monitoring of several biodiversity metrics following the concept of the Essential Climate Variables (ECVs)(Bojinski et al., 2014). One contribution to the framework of these EBVs is Land Surface Phenology (LSP), which is the study of vegetation seasonal activity at the ecosystem scale (Schwartz, 2013). In response, our group has developed an algorithm to determine LSP metrics that uses remotely sensed satellite imagery to create global maps that will allow such ecosystem monitoring at a previously impractical scale. Using the Normalized Difference Vegetation Index (NDVI) time-series data from high resolution satellite imagery (i.e., based mainly on Sentinel-2 at 10m resolution), the algorithm harnesses state-of-the-art statistical methods to generate “seasonal curves” at every valid pixel location that will allow end-users and conservationists to study various plant growing season metrics such as start-of-season, end-of-season, length-of-season, etc. Because the algorithm is being implemented on Google Earth Engine, a planetary scale remote sensing and Geographic Information System (GIS) platform, it will be possible to generate these maps globally on both data from past years as well as on future data that is being continuously collected (Gorelick et al., 2017). Thus, generating new yearly maps will be both possible and efficiently achieved to support ongoing conservation monitoring efforts.

In this session we will present an overview of the methods that have been used in the project, the challenges that have been encountered, and an outlook of the upcoming work. As such, specific topics will include: (1) the statistical process used to create the “seasonal curves”, which is an algorithm called Differential Evolution Optimization that was chosen due to a variety of advantages including its functional flexibility and the straight-forward array mathematics used in its calculations (Mullen et al., 2011); (2) the application of the LSP algorithm at a global-scale involves deliberate planning and development on the Google Earth Engine platform to accommodate all ecosystem types (e.g., boreal forest, temperate forest, mediterranean scrubland, etc.) within a single framework; (3) the ultimate goal is the creation of a publicly available mapping portal that allows users to explore the outputs as they are available year-by-year.

## REFERENCES

- Bojinski, S., Verstraete, M., Peterson, T. C., Richter, C., Simmons, A., & Zemp, M. (2014). The Concept of Essential Climate Variables in Support of Climate Research, Applications, and Policy. *Bulletin of the American Meteorological Society*, 95(9), 1431–1443. <https://doi.org/doi:10.1175/BAMS-D-13-00047.1>
- Gorelick, N., Hancher, M., Dixon, M., Ilyushchenko, S., Thau, D., & Moore, R. (2017). Google Earth Engine: Planetary-scale geospatial analysis for everyone. *Remote sensing of Environment*, 202, 18-27. <https://doi.org/10.1016/j.rse.2017.06.031>
- Habibullah, .S., Din, B.H., Tan, SH. et al. Impact of climate change on biodiversity loss: global evidence. *Environ Sci Pollut Res* 29, 1073–1086 (2022). <https://doi.org/10.1007/s11356-021-15702-8>
- Johnson, C. N., Balmford, A., Brook, B. W., Buettel, J. C., Galetti, M., Guangchun, L., & Wilmshurst, J. M. (2017). Biodiversity losses and conservation responses in the Anthropocene. *Science*, 356(6335), 270 LP – 275. <https://doi.org/10.1126/science.aam9317>
- Mullen, K., Ardia, D., Gil, D., Windover, D., Cline, J. (2011). DEoptim: An R package for global optimization by Differential Evolution. *Journal of Statistical Software*, 40(6), 1-26. <https://doi.org/10.18637/jss.v040.i06>
- Schwartz, M. D. (2013). Phenology: An Integrative Environmental Science. In M. D. Schwartz (Ed.), *Phenology: An Integrative Environmental Science* (Vol. 9789400769). Springer Netherlands. <https://doi.org/10.1007/978-94-007-6925-0>

## 19.14

### Marine debris detection with noisy annotations using Sentinel-2

Marc Russwurm, Laura Pasero, Devis Tuia

*Environmental Computer Science and Earth Observation Laboratory (ECEO), École Polytechnique Fédérale de Lausanne, Rue de l'Industrie 17, CH-1950-Sion (marc.russwurm@epfl.ch)*

Marine Litter is a growing ecologic concern that needs to be addressed on a global scale. While satellite and meteorological data is abundant, few advances have been made toward continuously monitoring marine litter aggregated in floating patches on the oceans. As detecting individual objects is infeasible with current satellite resolutions, researchers resort to windrows as a proxy for marine litter (Arias et al., 2021). These windrows form lines of aggregated floating debris that often contain plastic litter at a sizeable fraction depending on the geographic region.

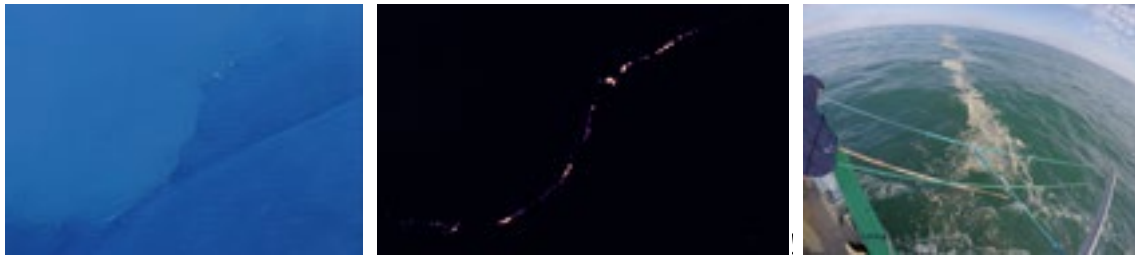


Figure 1. A Sentinel-2 image near Accra, Ghana, showing RGB representation of floating marine debris (left) alongside model predictions of Mifdal & Rußwurm (2021), which serves as a baseline for the detection module developed within ADOPT (center). The right image is by Ruiz et al. (2020), who studied the feasibility of collecting litter within these windrows on ship-based platforms at the Bay of Biscay, France.

In this work, we train a deep learning segmentation model (U-Net) to identify patches of floating marine debris that are detectable with Sentinel-2 resolution and serve as a proxy for marine litter. Figure 1 illustrates this problem with one example Sentinel-2 satellite image (left) and model predictions (Mifdal & Russwurm, 2021) (center). The shown line is a windrow similar to the image on the right of Ruiz et al., (2020), who proposed using these rows for efficient clean-up of marine litter that is often aggregated in windrows.

Label noise is a major challenge for this application. Marine debris is inherently difficult to annotate due to unclear boundaries and a permanent mixture with water. Additionally, labels are often coarse and simplified, as shown in Figure 2, where the original line-based hand annotations are displayed in the center column. These annotations roughly follow the shape of the marine debris but do not always capture the actual geometric shape. This leads to label noise in the available annotations, which provides a contradictory learning signal for the model. We address the noisy annotations by testing an automated refinement heuristic that clusters pixels in the local spatial neighborhood around an annotated debris into two classes: one for the debris itself and one for water as the background. The result of this heuristic is shown in the right column of Figure 2. We evaluated the approach experimentally in a hold-out region (near Lagos, Nigeria) and found that the model predictions improved substantially with our label refinement approach.

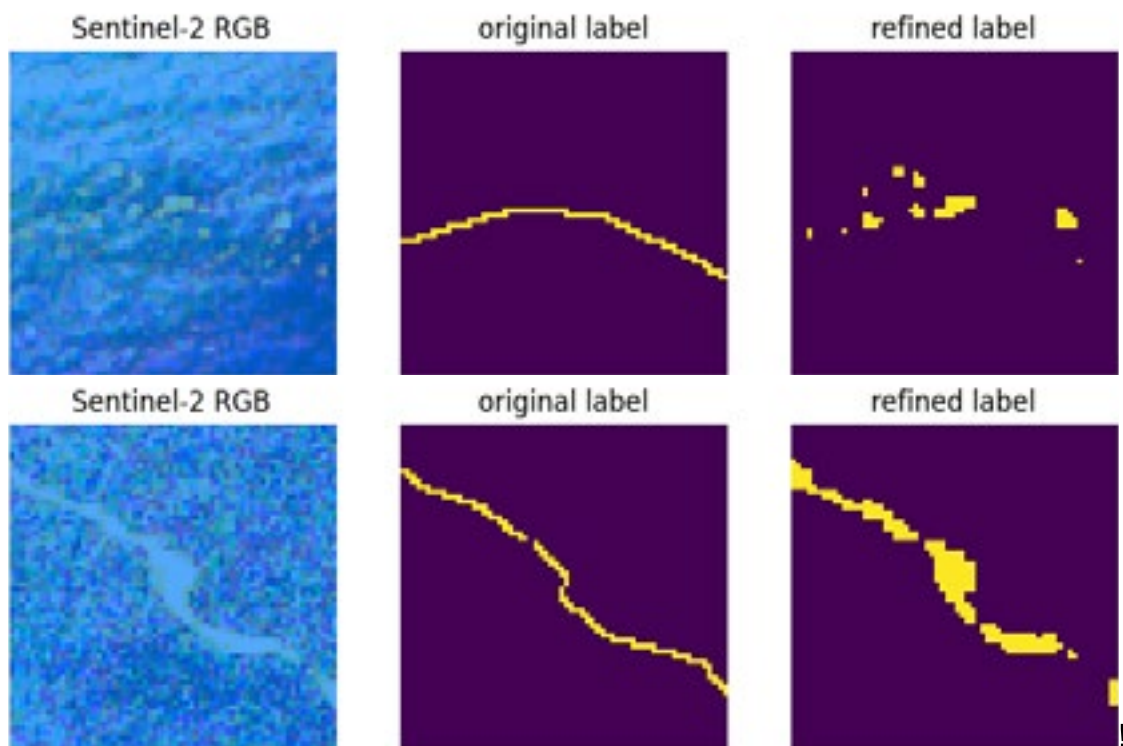


Figure 2. Two examples of the label refinement heuristic. In Mifdal & Russwurm (2021), rough annotations have been made by drawing lines. This does not always represent the true nature of objects shown in the images. The refinement algorithm clusters pixels by their similarity, leading to more realistic annotations (right).

## REFERENCES

- Arias, M., Sumerot, R., Delaney, J., Coulibaly, F., Cozar, A., Aliani, S., Suaria, G., Papadopoulou T., Corradi, P. & Corradi, P. (2021, July). Advances on Remote Sensing of Windrows as Proxies for Marine Litter Based on Sentinel-2/MSI Datasets. In 2021 IEEE International Geoscience and Remote Sensing Symposium IGARSS (pp. 1126-1129). IEEE.
- Mifdal, J., Longépé, N., and Rußwurm, M.: Towards detecting floating objects on a global scale with spatial features using Sentinel-2, ISPRS Ann. Photogramm. Remote Sens. Spatial Inf. Sci., V-3-2021, 285–293, <https://doi.org/10.5194/isprs-annals-V-3-2021-285-2021>, 2021.
- Ruiz, I., Basurko, O. C., Rubio, A., Delpey, M., Granado, I., Declerck, A., Mader, J. and Cózar-Cabañas, A. (2020). Litter windrows in the south-east coast of the Bay of Biscay: an ocean process enabling effective active fishing for litter. Frontiers in Marine Science. 7, 308.

## 19.15

# Diurnal ozone variability in the middle atmosphere over Switzerland observed by two microwave radiometers

Eric Sauvageat<sup>1,2</sup>, Shengyi Hou<sup>1</sup>, Eliane Maillard Barras<sup>3</sup>, Klemens Hocke<sup>1,2</sup>, Alexander Haefele<sup>3</sup>, Axel Murk<sup>1,2</sup>

<sup>1</sup> Institute of Applied Physics, University of Bern, Sidlerstrasse 5, CH-3012 Bern ([eric.sauvageat@unibe.ch](mailto:eric.sauvageat@unibe.ch))

<sup>2</sup> Oeschger Centre for Climate Change Research, University of Bern, Hochschulstrasse 4, CH-3012 Bern

<sup>3</sup> Office Fédéral de Météorologie et de Climatologie MétéoSuisse, Chemin de l'Aérologie 1, CH-1530 Payerne

Microwave radiometers can measure ozone profiles in the middle atmosphere (~20-75 km) over a large range of atmospheric conditions. Unlike many other remote sensing techniques, they are able to provide the high temporal resolution and continuous sampling required for a comprehensive study of ozone diurnal variability. In Switzerland, two ozone radiometers are operated in the vicinity of each other (40 km) since over 20 years in Payerne (MeteoSwiss) and in Bern (Institute of Applied Physics). Recently, their calibration and retrieval algorithms have been fully harmonized and updated time series are now available since 2010, showing significant improvements compared to the old time series (Sauvageat, 2022).

Using the harmonized ozone time series, we investigate the strato-mesospheric ozone diurnal cycle derived from these two instruments, in particular its seasonal and interannual variability over the last decade. We find a good agreement between the two radiometers and perform cross-validation study against various other datasets. First, we compare it with a climatology based on the Goddard Earth Observing System (GEOS-5) general circulation model. Second we use a set of free-running simulations from the Whole Atmosphere Community Climate Model (WACCM). Finally, we show first evidence of short-term diurnal cycle variability that can be detected in the radiometer time series.

## REFERENCES

Sauvageat, E., Maillard Barras, E., Hocke, K., Haefele, A., and Murk, A.: Harmonized retrieval of middle atmospheric ozone from two microwave radiometers in Switzerland, *Atmos. Meas. Tech. Discuss.* [preprint], <https://doi.org/10.5194/amt-2022-212>, in review, 2022.

## 19.16

# Tree species identification using Convolutional Neural Networks and AVIRIS-NG imaging spectroscopy data

Anna K. Schweiger<sup>1</sup>, Benjamin Zehnder<sup>1</sup>, Mathias Kneubühler<sup>1</sup>

<sup>1</sup> Remote Sensing Laboratories, Department of Geography, University of Zurich, Winterthurerstrasse 190, CH-8057 Zürich  
(anna.schweiger@geo.uzh.ch)

Tree species identification is important for biodiversity and ecosystem service assessments, carbon stock modeling and forest management. A Convolutional Neural Network (CNN) is a powerful type of Deep Learning that incorporates object context to identify objects within images. However, the general perception is that CNNs are relatively data-hungry, meaning that hundreds to thousands of training samples are needed to achieve reasonable predictive accuracy. Here we show that CNNs can be effectively trained for the identification of five common tree species based on only around 60 samples per species by using particularly information-rich remote sensing data, namely spectral imagery.

We conducted our study in Jurapark Aargau, a Swiss regional park of national importance. Our aim was to train a CNN for the identification of the five most common tree species in the area, which are beech (*Fagus sylvatica* L.), oak (*Quercus robur* L.), ash (*Fraxinus excelsior* L.), linden (*Tilia platyphyllos* Scop.) and red pine (*Pinus sylvestris* L.), based on AVIRIS-NG airborne imaging spectroscopy data. AVIRIS-NG collects spectral data in 431 bands covering the 380 nm to 2510 nm wavelength range with a mean spectral sampling interval of 5 nm and a spatial resolution of around 2 m on the ground. We collected tree identity and coordinate information of 331 trees in total. We matched tree positions to the airborne imagery using an individual tree crown delineation algorithm applied to the SwissSURFACE3D LiDAR (Light Detection and Ranging) product provided by Swisstopo. We reduced the AVIRIS-NG data to the main axes of spectral variation and augmented the tree crown images used for training the CNN by adding random noise, changing brightness and rotation. Our CNN correctly identified over 70% of all tree species and performed overall better than other classifiers, including Random Forest and Support-Vector Machine. Our study indicates that the high data demand of Deep Learning Algorithms may be counterbalanced by the information-richness of the data. We suggest further testing of this hypothesis through sensor integration, for example by including data collected by multispectral, LiDAR, thermal and SAR (Synthetic Aperture Radar) sensors.

## 19.17

# Multi-seasonal observations of Great Aletsch Glacier with a multi-modal ground-based radar

Marcel Stefko<sup>1</sup>, Philipp Bernhard<sup>1</sup>, Othmar Frey<sup>1</sup>, Irena Hajnsek<sup>1</sup>

<sup>1</sup> Chair of Earth Observation and Remote Sensing, ETH Zurich, Leopold-Ruzicka-Weg 4, CH-8093 Zurich  
 (stefko@ifu.baug.ethz.ch)

The Ku-band of the radio-frequency spectrum offers advantageous properties for observation of snow- and ice-covered areas with imaging radar (Ulaby et al. 1981, King et al. 2015). This can be attributed to a relatively short but non-zero penetration depth, which allows probing of physical characteristics of surface layers through polarimetry. Furthermore, the short wavelength of the Ku-band provides sensitivity to millimeter-scale displacements, which enables estimation and monitoring of glacier flow on short timescales through interferometry. However, most satellite radar sensors operate in other frequency bands, and thus comprehensive datasets observing snow and ice at Ku-band are still relatively rare. Furthermore, radar sensors usually operate in the so-called monostatic observation geometry, where the transmitter and the receiver are placed in the same location. Bistatic capabilities (i.e. placing the transmitter and the receiver in different locations) enable an extension of the observation space and can provide more information, but are not easily accessible.

In this submission we present preliminary results of a radar observation campaign in the Great Aletsch Glacier area. Using KAPRI, a ground-based real-aperture radar sensor with full-polarimetric, interferometric, and bistatic capabilities (Stefko et al., 2022), we monitored the Jungfraufirn area during two seasons (late summer 2021 and late winter 2022), acquiring a comprehensive dataset of monostatic and bistatic observations at Ku-band. The radar dataset is complemented with in-situ examinations of snow cover properties, as well as data from a local meteostation.



Figure 1: Primary KAPRI instrument observing the Jungfraufirn area from the terrace of High Altitude Research Station Jungfraujoch.

This dataset aims to provide insight into changes of the scattering properties of the snow cover over short timescales of the daily cycle, as well as longer, seasonal scales. Information about temporal decorrelation at Ku-band acquired in this campaign can be vital for planning and data evaluation of airborne or spaceborne interferometric radar campaigns with longer temporal baselines. Furthermore, the dataset also aims to serve as a testbed for development and validation of snow parameter inversion methods using bistatic Ku-band radar data.

Preliminary results show a major change in the polarimetric scattering properties of the snow cover between the summer and winter season (Figure 2), which can be linked to changes of the snow morphology. Furthermore, time-series observations show that while during winter the properties remain relatively constant over the course of the day, in summer the melt-freeze cycle causes rapid changes of the polarimetric properties over the course of hours.

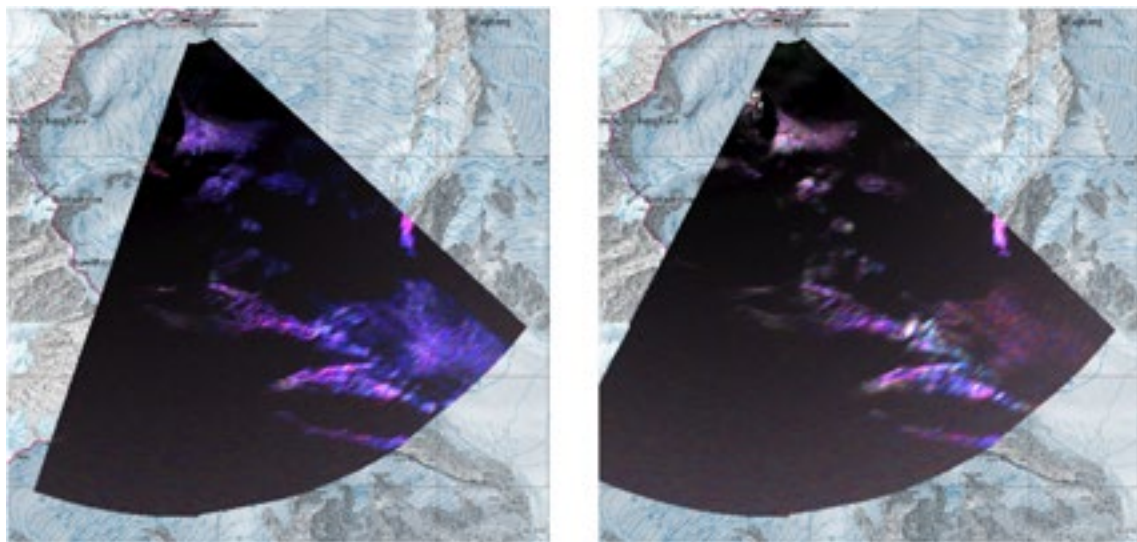


Figure 2. Bistatic polarimetric images of the snow cover acquired in summer (left) and winter (right), shown in the Pauli scattering basis (R: HH-VV, G: HV, B: HH+VV). In summer, dominant blue color indicates the prevalence of surface scattering, suggesting a low penetration depth and presence of melt-freeze crusts. In winter, a more diverse color mix indicates a more disordered medium and higher penetration, resulting in dominance of volume scattering processes.

## REFERENCES

- King, J., et al. 2015: Spatio-temporal influence of tundra snow properties on Ku-band (17.2 GHz) backscatter, *Journal of Glaciology*, 61(226), 267-279. doi:10.3189/2015JoG14J020
- Stefko, M., et al. 2022: Calibration and Operation of a Bistatic Real-Aperture Polarimetric-Interferometric Ku-Band Radar, *IEEE Transactions on Geoscience and Remote Sensing*, vol. 60, pp. 1-19, doi: 10.1109/TGRS.2021.3121466.
- Ulaby, F. T., et al. 1981: *Microwave remote sensing : active and passive*. Norwood (Mass.), Artech House.

## 19.18

# Assessing the 2018 drought response of Swiss forests and its dependence on different hydrological drivers

Joan Sturm<sup>1</sup>, Vincent Humphrey<sup>1,2</sup>, Maria J. Santos<sup>1</sup>, and Alexander Damm<sup>1,3</sup>

<sup>1</sup> Geographisches Institut, University of Zurich, Winterthurerstrasse 190, CH-8057 Zürich ([joantracy.sturm@geo.uzh.ch](mailto:joantracy.sturm@geo.uzh.ch))

<sup>2</sup> Institute for Atmospheric and Climate Science, ETH Zurich, Zürich, Switzerland

<sup>3</sup> Eawag, Swiss Federal Institute of Aquatic Science and Technology, Dübendorf, Switzerland

Consequences of current and projected climate change include the increasing frequency of extreme events. More and stronger drought events, for example, affect health and functioning of forest ecosystems, unsettle related ecosystem services with consequences for economy and human well-being. Thus, understanding the impact of droughts on forest ecosystems is crucial to optimize future forest management strategies.

Quantifying drought impacts on forests requires the understanding and decoupling underlying hydrological drivers. Precipitation is the largest driver of water availability, whereas temperature controls the atmospheric water demand. The combination of these push and pull processes control the water transport through the vegetation. Furthermore, tree height and location in forests determine the exposition of individual trees that additionally convolves the meteorological effects of precipitation and temperature. Current climate predictions suggest different trajectories and spatial pattern of precipitation and temperature, which challenges the assessment of drought impacts due to the high variability of the individual hydrological drivers in both space and time.

We present an approach to disentangle the partial impacts of these hydrological drivers, namely water availability, water demand, and exposure, on the response of Swiss forests to the extreme summer drought in 2018. Canopy water content was used as indicator of forest health and was approximated by the Normalised Difference Water Index (NDWI) derived from Sentinel-2 satellite imagery on 10x10 m pixel scale (Sturm et al. 2022). We calculated the potential water availability and combined it with the precipitation anomaly of 2018. The water demand was approximated by the water vapour pressure deficit. Tree exposure was derived from a digital vegetation height model. We then mapped the composition of partial impacts of water availability, demand, and exposure on forest drought responses across Switzerland to see which regions are dominated by one of these drivers. Furthermore, we analysed the strength, direction, and spatial consistency of the driver and impact relationships. Our results provide important insight about the spatial variability of hydrological drivers on forest drought responses and contribute advancing future forest management practices.

## REFERENCES

- Sturm, J., Santos, M. J., Schmid, B., & Damm, A. (2022). Satellite data reveal differential responses of Swiss forests to unprecedented 2018 drought. *Global Change Biology*, 28(9), 2956-2978.

## P 19.1

# Earthquake-volcano interactions at oblique subduction margins; focus on Mount Sinabung volcano (Indonesia)

Benoit Goudard<sup>1</sup>, Társilo Girona<sup>2</sup>, Luca Caricchi<sup>1</sup>, Matteo Lupi<sup>1</sup>

<sup>1</sup> Department of Earth Sciences, University of Geneva, Genève, Switzerland

<sup>2</sup> Geophysical Institute, University of Alaska Fairbanks, Fairbanks, AK, USA

In 2010 after four centuries of quiescence, Mount Sinabung (Northern Indonesia) erupted and released large amounts of ash and debris forcing thousands of residents to leave their villages. The system develops upon the Great Sumatran Fault, a major strike slip fault accommodating the oblique subduction of the Australian plate beneath the Sunda plate. Mount Sinabung began to inflate approximately 2 years after the occurrence of the Nias earthquake (8.7 Mw), 2005, that struck offshore Sumatra.

Several studies show causal relationships between earthquakes and volcanic eruptions, thus the Nias earthquake could have been responsible for the reawakening of Mount Sinabung in 2010. Here we determine through satellites-measurements the large-scale thermal unrest of Mount Sinabung from several years prior to 2010 until present-day. Radiance emitted by volcano surfaces and measured by MODIS instrument aboard Aqua and Terra satellites is a new method that can be used to analyse the temporal evolution of volcanic activity. We analyse the time evolution of radiance over an area of 20 km x 20 km around Mount Sinabung at 121 locations. We are testing if structural features control the different patterns we observe by correlating the location of major faults, the variations of radiance and the distribution of earthquakes following the Nias event. This new approach is promising as it may allow identifying volcanic unrest years before an eruption and in our case could serve to establish the causal relationships between the Nias earthquake and the 2010 Mount Sinabung eruption.

## P 19.2

# A fully polarimetric 50 GHz temperature radiometer

Witali Krochin<sup>1,2</sup>, Gunter Stober<sup>1,2</sup>, Axel Murk<sup>1,2</sup>, Roland Albers<sup>1</sup>, Tobias Plüss<sup>1</sup>

<sup>1</sup> Institute of Applied Physics, University of Bern, Sidlerstrasse 5, 3012 Bern ([witali.krochin@unibe.ch](mailto:witali.krochin@unibe.ch))

<sup>2</sup> Oeschger Centre for Climate Change Research, University of Bern, Hochschulstrasse 4, 3012 Bern

Continuous temperature measurements in the stratosphere (12-50 km) and the mesosphere (50-80 km) are crucial for the deeper understanding of the physical processes in the middle atmosphere and for the vertical coupling between the different atmospheric layers. Several studies have shown the importance of atmospheric waves such as planetary waves, tides, and gravity waves, their propagation and breaking at these altitudes, and its effect on the global circulation.

Investigating these effects requires long-term measurements with high temporal resolution and altitude coverage. Satellite data covers the required altitude range but provides limited temporal resolution due to its fixed orbital geometry. Active measurement techniques such as LIDAR are usually limited to nighttime and only a few instruments have daytime capability and therefore are unsuitable for continuous observations. Ground-based microwave radiometry provides a robust observational method that is independent of the daytime, almost independent of the weather conditions, and that permits to perform continuous soundings from 20-60 km altitude.

TEMPERA (TEMPErature RAdiometer) is a ground-based radiometer developed at the University of Bern in 2013 (Stähli 2013). It measures microwave radiation spectra from atmospheric oxygen in a range between 52 GHz and 53 GHz. Atmospheric temperature profiles can be retrieved from these spectra. In the last 9 years, the accuracy and performance of this instrument were continuously improved (Krochin 2022). The latest version of TEMPERA has a temporal resolution of one measurement per 30 min and temperature profiles can be retrieved up to an altitude of about 50 km.

The reason for the altitude limitation is the Zeeman effect, which occurs due to the interaction of the atmospheric oxygen with the Earth's magnetic field. The polarization of atmospheric radiation affected by the Zeeman effect depends on the orientation of the propagation direction to the magnetic field. Therefore, the altitude range for temperature retrievals could be further improved by decomposing the measured radiation in its polarization components. In addition, the inclusion of the Zeeman effect in the retrieval algorithm provides the ability to retrieve the Earth's magnetic field from measurements of atmospheric microwave emissions.

The microwave group from the Institute of Applied Physics of the University of Bern, is currently developing a temperature radiometer (TEMPERA-C), which is based on the former instrument (TEMPERA) but allows a fully polarimetric analysis of the atmospheric emission spectra (Krochin 2022). Here we present a simple calibration method and first measurements as well as simulations of atmospheric temperature and magnetic field retrievals from fully polarimetric microwave spectra.

## REFERENCES

- Krochin, W., & Navas-Guzmán, F., & Kuhl, D., & Murk, A., & Stober, G. 2022: Continuous temperature soundings at the stratosphere and lower mesosphere with a ground-based radiometer considering the zeeman effect, *Atmos. Meas. Tech.*, 15, 2231–2249
- Krochin, W., & Stober, G., & Murk, A. 2022: Development of a Polarimetric 50-GHz Spectrometer for Temperature Sounding in the Middle Atmosphere, *IEEE Journal of Selected Topics in Applied Earth Observations and Remote Sensing*, 15, 5644 – 5651
- Stähli, O., & Murk, A., & Kämpfer, N., & Mätzler, C., & Eriksson, P. 2013: Microwave radiometer to retrieve temperature profiles from the surface to the stratopause, *Atmos. Meas. Tech.*, 6, 9, 2477–2494

## P 19.3

# Quantitative Characterization of Glacier Surging in Karakoram using Synthetic Aperture Radar Data

Shiyi Li<sup>1</sup>, Philipp Bernhard<sup>1</sup>, Irena Hajnsek<sup>1,2</sup>

<sup>1</sup> Institute of Environmental Engineering, ETH Zurich, 8093 Zurich, Switzerland (shiyi.li@ifu.baug.ethz.ch)

<sup>2</sup> German Aerospace Center (DLR) e.V. Microwaves and Radar Institute, Wessling, Germany

The Karakoram range in High Mountain Asia (HMA) is well-known for the clustering of surge-type glaciers, which are distinguished by the quasiperiodic flow pattern including a long-lasting quiescent phase and a short-lived active phase. Investigating glacier surges helps to better understand local glacier evolution and to reduce glacier related risks such as glacier lake outburst flood (GLOF). However, the mechanisms of surging in the Karakoram Mountains are not yet fully understood due to the complexity of their dynamics.

In this work, we comprehensively characterized the recent surge of the South Rimo Glacier in Karakoram, which was observed between 2018 and 2020. The South Rimo Glacier represents one of the largest glaciers in the east range of Karakoram. The surge showed combined feature of both thermal and hydrological regulated processes, and thus is a very interesting example for studying surge mechanisms.

To depict the dynamics of the surge, we collected spaceborne Synthetic Aperture Radar (SAR) data from TanDEM-X and Sentinel-1. The main objective is to characterize the changes of the surface elevation, the flow velocity, and the surface thermal regime.

The TanDEM-X COSSC data were acquired between 2011 and 2019 and were used to derive Digital Elevation Models (DEMs). The obtained DEMs were differentiated to calculate the glacier surface elevation changes before and after the surge. The Sentinel-1 images were acquired between 2017-2020 in both ascending and descending orbits. They were adopted to map glacier flow velocities using the offset tracking method. To improve the robustness of offset tracking, we employed the stacked cross-correlation instead of the traditional pair-wise cross-correlation when estimating offsets.

The DEM differencing results showed that the surge front started building-up since 2013. Flow velocity was found gradually increasing starting from 2017, initiating the surge in summer 2018 and reaching the maximum in the mid of 2019. From the Sentinel-2 images, we identified that a supraglacial lake was formed in July 2019 when the surge velocity was maximized. The lake drained in September 2020, and meanwhile the velocity dropped to the pre-surge level.

In our work, inclusive datasets that depict the surge dynamics of the South Rimo Glacier, and quantitative investigation of the controlling mechanisms of the surge through simulations are presented. It is highlighted that the high spatial-temporal resolution SAR observations provided invaluable information in quantifying glacier dynamics.

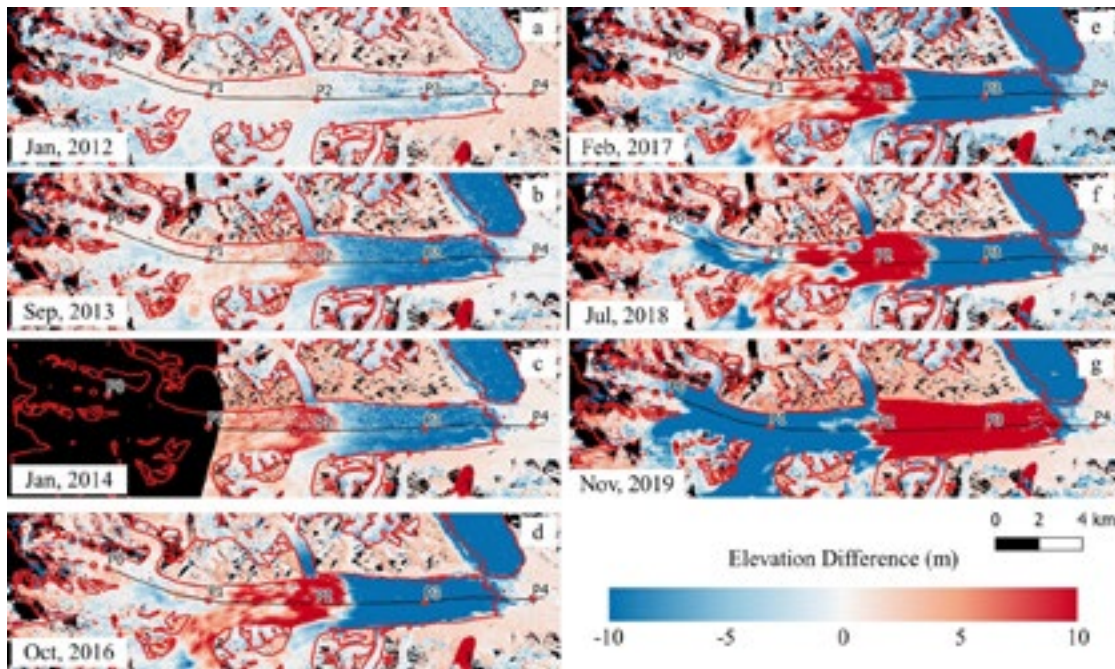


Figure 1. DEM difference maps with respect to 2011-07-15. Reference points P0–P4 roughly divides the manually drawn central flow line into five equal-length parts.

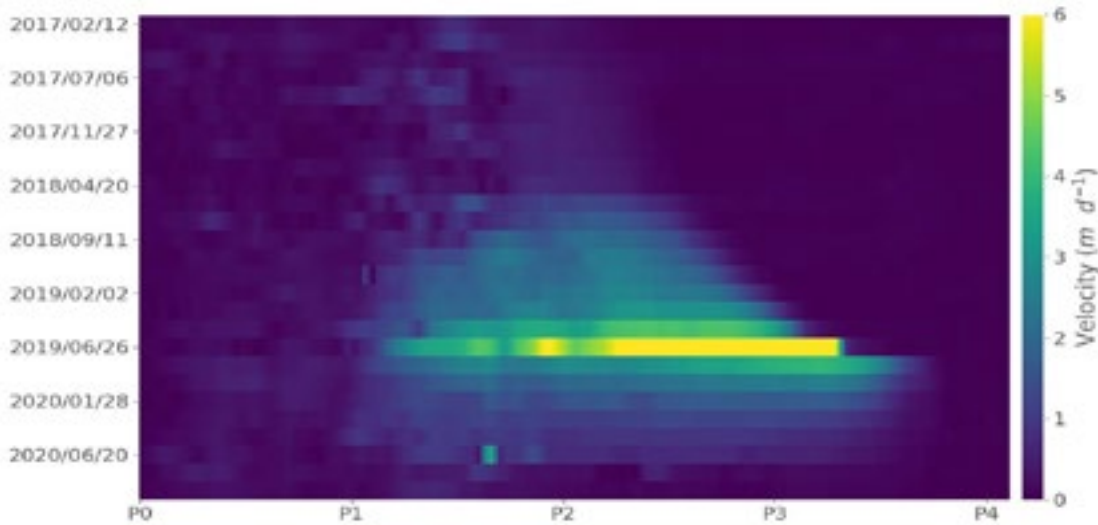


Figure 2. The surface flow velocity of the South Rimo Glacier.

## REFERENCES

- S. Li, S. Leinss and I. Hajnsek, „Cross-Correlation Stacking for Robust Offset Tracking Using SAR Image Time-Series,“ in IEEE Journal of Selected Topics in Applied Earth Observations and Remote Sensing, vol. 14, pp. 4765-4778, 2021, doi: 10.1109/JSTARS.2021.3072240.

## P 19.4

### Multi-temporal forest mapping at the Swiss alpine treeline

Thiên-Anh Nguyen<sup>1</sup>, Marc Russwurm<sup>1</sup>, Benjamin Kellenberger<sup>1,2</sup>, Devis Tuia<sup>1</sup>

<sup>1</sup> Environmental Computational science and Earth Observation laboratory, Ecole Polytechnique Fédérale de Lausanne, Rue de l'Industrie 17, CH-1950 Sion (thien-anh.nguyen@epfl.ch)

<sup>2</sup> Center for Biodiversity and Global Change and Department of Ecology and Evolutionary Biology, Yale University, New Haven, CT 06511, USA

The position of the upper alpine treeline is known to be highly sensitive to undergoing climate change. Rising temperatures and their impact on environmental conditions like snow cover shift the position of the treeline upwards in altitude. In the Swiss Alps, land use change (predominantly land abandonment caused by the decline of alpine farming) is also responsible for many of the forest cover changes observed at the treeline ecotone (Gehrig-Fasel et al. 2007). Measurements of treeline responses to such drivers have shown that treeline dynamics are slow and lagged in time. Such insights are traditionally derived from scarce and expensive field measurements, or comparison of coarse historical forest maps. This prevents the creation of multi-temporal and high spatial resolution forest maps spanning several decades, which are needed to better understand the drivers of treeline dynamics in space and across scales. We thus aim at providing high-resolution multi-temporal forest maps at the treeline ecotone over the Valais and Vaud Alps in Switzerland.

We use a collection of geo-referenced aerial images (SwissImage), captured between 1998 and 2017 in various lighting conditions and with various sensors, and downsampled to a common ground resolution of 50 cm. As forest reference and supervision source, we use a forest map derived from the Swiss Topographic Landscape Model (SwissTLM3D), corresponding to the state of the forest around 2017.

We develop a deep learning-based forest mapping method, which predicts a 1 m resolution forest map for each step of a time series of 5 to 9 aerial images. We adapt a mono-temporal forest mapping model (U-net, Ronneberger et al. 2015), pre-trained on the most recent images (2017), to obtain a multi-temporal model — we feed the time series sequentially, and for a given time step, reuse the model output corresponding to the previous time step as an additional input. We train this recurrent model to minimize both a forest segmentation loss applied to the last time step only and a temporal consistency loss, which encourages the output of the model to remain consistent over time.

Results obtained by applying our pre-trained mono-temporal model on the time series show that the pre-trained model can generalize to older images, for those images which are similar enough to the pre-training images (Figure 1). Using the fine-tuned, recurrent model helps aligning detection boundaries for sharp forest edges with no changes, but decreases the performance for the first time steps of the times series, due to the initialization of the recursion loop. This suggests the need for a model integrating more complex temporal components such as GRU (Cho et al. 2014) or LSTM (Hochreiter & Schmidhuber 1997) cells, enabling the model to make use of past predictions in a dynamical way. Future work will thus consist in incorporating such components in our model, while accounting for known forest dynamics at the treeline (slow forest gain, abrupt forest loss).

## REFERENCES

- Cho, K., Van Merriënboer, B., Gulcehre, C., Bahdanau, D., Bougares, F., Schwenk, H., & Bengio, Y. (2014). Learning phrase representations using RNN encoder-decoder for statistical machine translation. EMNLP 2014 - 2014 Conference on Empirical Methods in Natural Language Processing, Proceedings of the Conference, 1724–1734. <https://doi.org/10.3115/v1/d14-1179>
- Gehrig-Fasel, J., Guisan, A., & Zimmermann, N. E. (2007). Tree line shifts in the Swiss Alps: Climate change or land abandonment? *Journal of Vegetation Science*, 18(4), 571–582. <https://doi.org/10.1111/j.1654-1103.2007.tb02571.x>
- Hochreiter, S., & Schmidhuber, J. (1997). Long Short-Term Memory. *Neural Computation*, 9(8), 1735–1780. <https://doi.org/10.1162/neco.1997.9.8.1735>
- Ronneberger, O., Fischer, P., & Brox, T. (2015). U-net: Convolutional networks for biomedical image segmentation. Lecture Notes in Computer Science (Including Subseries Lecture Notes in Artificial Intelligence and Lecture Notes in Bioinformatics), 9351, 234–241. [https://doi.org/10.1007/978-3-319-24574-4\\_28](https://doi.org/10.1007/978-3-319-24574-4_28)

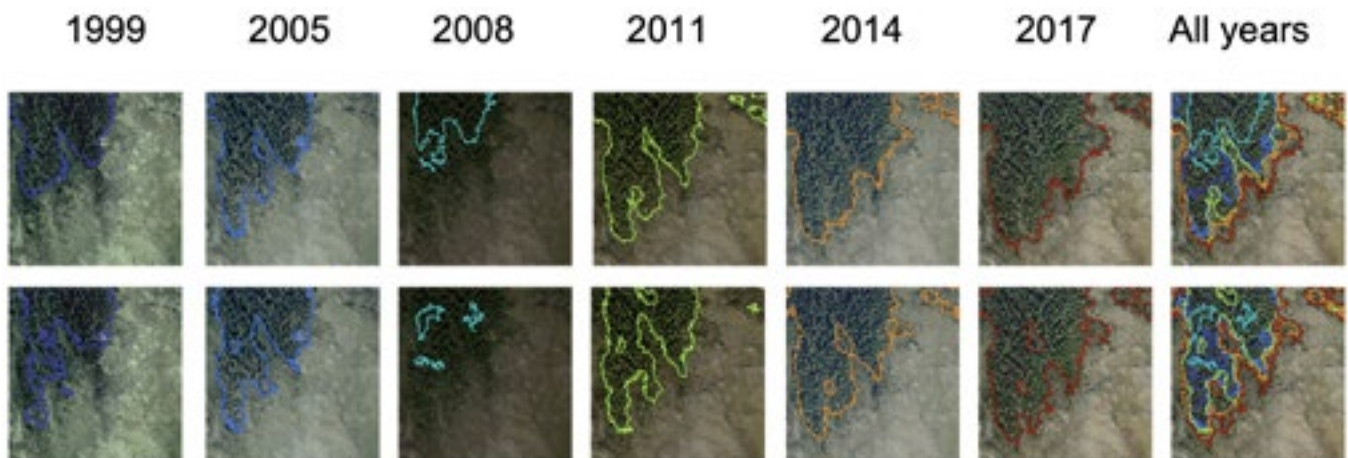


Figure 1. Segmentation boundaries in an alpine area undergoing a gradual treeline shift. Top row: mono-temporal pre-trained model, bottom: fine-tuned recurrent model.

**P 19.5****Ozone and Water Vapor Variability in 2019/2020 Arctic Stratospheric Polar Vortex Compared to Climatology**

Guochun Shi<sup>1,2</sup>, Witali Krochin<sup>1,2</sup>, Axel Murk<sup>1,2</sup>, Gunter Stober<sup>1,2</sup>

<sup>1</sup> Institute of Applied Physics, University of Bern, Sidlerstrasse 5, CH-3012 Bern (guochun.shi@unibe.ch)

<sup>2</sup> Oeschger Center for Climate Change Research, University of Bern, Hochschulstrasse 4, CH-3012 Bern

The stratospheric polar vortex in the 2019/2020 winter/spring was the long-lasting, strongest, and coldest on record in the Arctic. Using satellite observations, reanalysis data, and Microwave radiometer measurements we investigate the dynamic structure of the stratospheric polar vortex and relate them to the ozone and water vapor variability. Analyses of ozone and water vapor observations made over Ny-Ålesund indicate that stratospheric ozone was significantly below the climatological average, but mesospheric water vapor is above the climatological average during the stratospheric polar vortex. The polar vortex development to break up in 2019/2020 winter/spring caused unprecedented negative ozone anomalies throughout the winter and extremely high positive water vapor anomalies in mid-spring. High ozone anomalies concentrated along the vortex edge are due to both greater increases in diabatic descent along the vortex and chemical loss in the vortex interior. As a dynamical tracer, water vapor can separate air masses of different properties inside and outside the vortex. Water vapor anomalies across the polar vortex edge in the upper stratosphere and lower mesosphere are high because of the modulation of the polar vortex edge and the advection of extra-vortex air.



## 20 Geoscience and Geoinformation – From data acquisition to modelling and visualisation

Nils Oesterling, Massimiliano Cannata, Michael Sinreich, Elmar Brockmann

*Swiss Geological Survey  
Swiss Geodetic Commission  
Swiss Geophysical Commission  
Swiss Hydrogeological Society*

### TALKS:

- 20.1 Meles G.A., Linde N., Marelli S.: GPR Bayesian tomography with surrogate modeling
- 20.2 Melzner S.: Impact of quality of input data on 3D rockfall modelling
- 20.3 Morgenthaler J., Oesterling N., Heuberger S.: Revalue geoscientific archive data utilising machine learning
- 20.4 Mouzakidou, K., Cucci, D.A., Skaloud, J.: On the benefit of concurrent adjustment of active and passive optical sensors with GNSS & raw inertial data
- 20.5 Neven A., Schropp L., Renard P.: Stochastic Multiple Data Integration in consistent geological models
- 20.6 Schropp L., Straubhaar J., Neven A., Renard P.: Automated hierarchical 3D modeling of Quaternary aquifers – the ArchPy approach
- 20.7 Weidmann Y., Gabriel P., Arndt D., Filippioni M.: Inggeo-Tool, a web application for 3D-model based automated tunnel profile generation

**POSTERS:**

- P 20.1 Finch B., Ruiz-Villanueva V.: Insights from Graph Theory Application to Large Wood Supply and Transfer in River Networks
- P 20.2 Grove W., Lupi M., Villani F., Maraio S.: Evaluation of UAV weight drops as a viable source for active seismic surveys
- P 20.3 Mair D., Do Prado A., Garefalakis P., Schlunegger F.: Size of fluvial gravel measured by machine learning assisted image segmentation – a path forward with transfer learning?
- P 20.4 Stumpf D., Savard G., Barat C., Muñoz F., Lupi M.: Ambient noise tomography and automatic picking of dispersion curves with machine learning methods: case study at Vulcano-Lipari, Italy, with a nodal geophone array.
- P 20.5 Zede C.-N.: Geolocation of a panoramic camera by reference pairing
- P 20.6 Zhang C., Irving J., Gravey M., Mariethoz G.: Reconstruction of 3D high-resolution GPR data from 2D profiles: A multiple-point geostatistical approach
- P 20.7 Zwahlen J., Schenker P., Spataro A.: Spatial resolution of 3D maps of a heterogeneous ultramafic lense at the Cima di Gagnone, Cima Lunga unit

## 20.1

# GPR Bayesian tomography with surrogate modeling

Giovanni Angelo Meles<sup>1</sup>, Niklas Linde<sup>1</sup>, Stefano Marelli<sup>2</sup>

<sup>1</sup> Institute of Earth Sciences, University of Lausanne, Switzerland, CH 1015, Lausanne ([giovanni.meles@unil.ch](mailto:giovanni.meles@unil.ch))

<sup>2</sup> Department of Civil, Environmental and Geomatic Engineering, ETH Zurich, CH 8093, Zurich

Travel-time tomography refers to a large class of noninvasive imaging methods with applications comprising natural resource exploration, medical diagnosis and non-destructive testing. High-resolution travel-time tomography of the shallow subsurface can be performed using ground-penetrating radar (GPR). Deterministic GPR tomography can be carried out by considering the travel-time of the first-arrival signals, but even in ideal scenarios tends to be ill-posed, and regularization methods are often needed to stabilize the inversion. Probabilistic inversion approaches based on Bayesian statistics have been proposed as an alternative. A drawback of such global search methods is the high computational cost associated with the many (often hundreds of thousands) solutions of the forward problem required to locate and sample from the posterior distribution, which can be computationally prohibitive.

We present here a Bayesian tomography framework operating with prior-knowledge-based parametrization and accelerated by surrogate models. We rely on regression-based sparse polynomial chaos expansion (PCE) based on data-driven principal component modes associated with samples of a realistic generative model to approximate travel-times in a crosshole configuration, with a truncation determined by the performances of the standard solver on the full and reduced model domains (Meles et al., 2022). The proposed scheme is shown to approximate travel-times below commonly assumed noise level operating at a fraction of the cost of physics-based solvers. We then use the PCE model to perform Metropolis-Hastings Markov chain Monte Carlo, using the UQLab Matlab framework (Marelli et al., 2014). We show that a PCE trained with few hundreds design data sets is sufficient to provide reliable inversion outperforming schemes based on straight-line approximation. To provide an appropriate uncertainty quantification, we also show the effect of reintroducing the truncated higher-order principal components in the original model space after inversion.

## REFERENCES

- Marelli, S., & Sudret, B. *UQLab: A framework for uncertainty quantification in Matlab*. American Society of Civil Engineers, 2014.
- Meles, G. A., Linde, N., & Marelli, S. 2022: Bayesian tomography with prior-knowledge-based parametrization and surrogate modeling, *Geophysical Journal International*, 231, 673-691.

## 20.2

### Impact of quality of input data on 3D rockfall modelling

Sandra Melzner<sup>1</sup>

<sup>1</sup> GEOCHANGE Consulting e.U., Engineering Office for Technical Geology and Natural Hazards, Eppensteinerstraße 4/4, A-9020 Klagenfurt ([office@geochange-consulting.com](mailto:office@geochange-consulting.com))

Many areas in the Alps are recurrently affected by rockfall processes which pose a significant hazard to settlements and infrastructures. In times of decreasing financial resources, the demand for the investment in protection measures with a positive return on investment is of high importance. Hazard and risk assessments are essential tools in order to ensure an economically justifiable implementation of preventive measures.

This contribution summarizes existing challenges in the implementation of a standardised procedure for hazard zoning and risk analysis in the Alps. The discussion focuses on (i) the impact of data acquisition strategies on the quality of input data, (ii) the applicability of different 3D rock fall simulation models for hazard zoning in different topographic and geologic environments, (iii) definition of thresholds for hazard zoning (fig. 1) and the (iv) cartographic presentation of results.

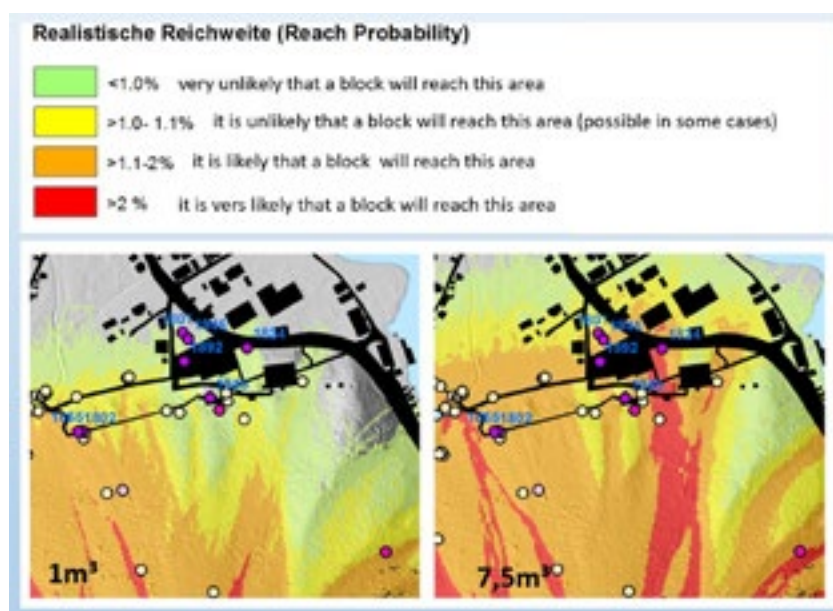


Figure 1. Definition of reach probability thresholds for hazard zoning for 1m<sup>3</sup> and 7,5 m<sup>3</sup> release scenario. Coloured dots = rockfall boulders of different sizes mapped in the field; dots with numbers= rockfall events only with qualitative size information from archive research (Melzner, S. 2017).

The evaluation of the applicability of model results is focused on the model sensitivity to the scale-dependent accuracy of input data and on the quality of the simulated travel distances (e.g., reach probabilities) and dynamics (e.g., energies, passing heights, velocities) (Melzner et al. 2011, Melzner and Preh 2012).

Depending on the source information and the method/technique used to collect the data, the content and detail of the collected rockfall data can vary significantly (Melzner and Guzzetti 2014, Melzner et al. 2020). For example, considering the forest in the 3D simulations is a great challenge: on the one hand LIDAR data acquisition is a time-consuming task; on the other hand, a near-time monitoring of changes in forest stand conditions greatly influence the quality of the model output (Melzner and Schiller 2022).

Calibration and validation of simulation results is usually performed with information about the geographic position of mapped rockfall boulders and/or rockfall event information from archives. For the latter, there is often no size specification available (Fig. 1). In order to define reproducible threshold values (i.e., reach probabilities) and to transfer them as a standard to other study areas, the model input data (e.g. roughness, damping) should be clearly indicated and published.

A further very important step is the joined cartographic presentation of the results of both, the simulations and the field mapping. Such combination of results issued from different approaches forms the basis for the final hazard zoning. ÖNORM rules should be supplemented with guidelines explaining in more detail different mapping strategies/techniques and model decisions to end users.

## REFERENCES

- Melzner, S. (2017): Challenges in rock fall hazard zoning in Austria, RocExs 2017, Barcelona, Spanien.
- Melzner, S., Moelk, M., Dorren, L., Reichenbach, P. & Guzzetti, F. (2011): Rock fall runout modelling for susceptibility evaluation: a multi-scale comparison at different sites, RocExs 2011 Igls, Austria.
- Melzner, S., Preh, A. (2012): Sturzmodelle und ihre Anwendbarkeit in der Praxis. Zeitschrift für Wildbach-, Lawinen-, Erosions- und Steinschlagschutz, Heft Nr. 169, 78-101.
- Melzner, S. & Guzzetti, F. (2014): Comparison of Rockfall Inventories in Austria and Italy- EGU General Assembly 2014, EGU2014-5072,02.05., Wien.
- Melzner, S., Rossi, M. & Guzzetti, F. (2020): Impact of mapping strategies on rockfall frequency-size distributions. Journal of Engineering Geology 272, 105639. <https://doi.org/10.1016/j.enggeo.2020.105639>.
- Melzner, S. & Schiller, G. (2022): Laserscanning und Photogrammetrie in der Geologie- Chancen und Herausforderungen, Wildbach- und Lawinenverbau- 76. Jahrgang, August 2022, Heft Nr. 189.

## 20.3

### Revalue geoscientific archive data utilising machine learning

Joël Morgenthaler<sup>1</sup>, Nils Oesterling<sup>2</sup>, Stefan Heuberger<sup>1</sup>

<sup>1</sup> Georesources Switzerland Group, Department of Earth Sciences, ETH Zürich, Sonneggstrasse 5, 8092 Zürich  
(joel.morgenthaler@erdw.ethz.ch)

<sup>2</sup> Swiss Geological Survey, Swiss Federal Office of Topography swisstopo, Seftigenstrasse 264, 3084 Wabern

Today, a huge amount of valuable geoscientific data is unused and mostly stored in analogue and poorly accessible archives. Within the framework of the Swiss federal strategy “Digitisation of the subsurface” (swisstopo 2021) we develop methods to reevaluate the already scanned national geoscientific archive of the Swiss Geological Survey. The archive is currently managed with a meta-database storing attributes like title, author, location, and data usage restrictions. Today, it is a time-consuming and inefficient task to find the most appropriate document for a given query as a content-related description as well as full-text search is missing.

Our project aims at building a new, semi-automated data management workflow, which accounts for the introduced digitisation mission. Hence, applications are sought for (a) easy exchange of freely accessible geological data between projects and other authorities or service companies, (b) filtering geological data with customised queries and full-text search and (c) providing detailed information on instances such as figures within geological reports.

In a first step, we use state-of-the-art Natural Language Processing (NLP) and Computer Vision (CV) methods to classify the documents to predefined geoscientific classes. Moreover, we detect objects like maps, profiles, well logs or graphics by employing an object detection model (Morgenthaler et al. 2022).

In a second step, we engineer a customised WebGIS application to combine all available metadata with the NLP and CV predictions with content-related and full-text search possibilities. Here we present the new data management workflow from unstructured to structured geological data and our current project standings as well as further developments.

#### REFERENCES

- Morgenthaler J., Frefel D., Meier J., Oesterling N., Perren G. & Heuberger S. (2022): Revalue Geoscientific Data Utilising Deep Learning, Swiss Bulletin of Applied Geology 27/1, 45-54.
- swisstopo (2021): Digitalisierung des geologischen Untergrunds - Umfeld, Herausforderungen und Massnahmen, Bericht an den Bundesrat, p. 38, <https://www.admin.ch/gov/de/start/dokumentation/medienmitteilungen.msg-id-83491.html>, Accessed 22 August 2022.

## 20.4

# Precise geo-referencing via a concurrent adjustment of aerial optical and navigation sensor datasets.

Kyriaki Mouzakidou<sup>1</sup>, Davide A. Cucci<sup>2</sup>, Jan Skaloud<sup>1</sup>

<sup>1</sup> Geodetic Engineering Laboratory (TOPO), Ecole Polytechnique Fédérale de Lausanne (EPFL), Switzerland,  
(kyriaki.mouzakidou, jan.skaloud@epfl.ch)

<sup>2</sup> Geneva School of Economics and Management, University of Geneva, Switzerland  
(davide.cucci@unige.ch)

Airborne laser scanning is one of the most powerful geo-spatial data acquisition technologies currently being employed to produce precise 3D geometric products. The high-frequency trajectory of the laser sensor is typically determined from inertial sensors and employed to directly geo-reference the acquired laser points. When low-cost MEMS inertial sensors are used, such as in lightweight drones, non-negligible errors in the estimated trajectory project to the final point-cloud, resulting in unsatisfactory accuracy on the ground. In this work, we present a synthesis of an alternative to the typical direct geo-referencing approach. Along with GNSS and raw inertial observations, we integrate optical observations, from both active and passive sensors, i.e. lidar and camera respectively. We fuse all the available information in a single step adjustment leveraging upon the dynamic networks, that were first introduced for photogrammetric applications by Colomina & Blazquez (2004) and constitute an extension of conventional geodetic networks. We extent the approaches put forward in Cucci et al. (2017) and Brun et al. (2022) and in a single adjustment we consider: [1] conventional tie-points, extracted from imagery acquired simultaneously with respect to the lidar points, with [2] 3D tie-points from overlapping parts of a coarsely geo-referenced point-cloud, [3] raw inertial and [4] GNSS observations. We study the effect of camera and lidar observations first separately and then jointly within a challenging corridor mapping scenario. The availability of a ground truth point-cloud with centimeter level accuracy allows us to precisely quantify the geo-referencing error in object space. We show that considering either 2D or 3D tie-points, along with inertial and GNSS observations results in a remarkably accurate point-cloud, even when low-cost inertial sensors are employed and even in presence of challenging surface textures, such as forest covered areas. Furthermore, since the distribution of the 2D and 3D tie-points is complementary, considering them together further increases the robustness of the adjustment due to higher redundancy. By employing the proposed approach, we were able to reduce the mean geo-referencing error on the point-cloud by a factor of 3 - 4, while the standard deviation (norm) is reduced by a factor of 2 - 3 in the studied challenging mapping scenario. In that way, 3D modelling moves a step forward to precisely rendering topography, when mapping and surveying challenging areas, e.g., closer to cliffs or in deep canyons where GNSS signal reception can be perturbed, and from higher altitudes, where errors in attitude become predominant. When properly combined in a geographic information system, the produced derived information, such as digital elevation model, can better meet the expectations in applications like agriculture, forestry, natural hazard management, and infrastructure monitoring.

## REFERENCES

- Brun, A., Cucci, D. A., Skaloud, J., 2022: LiDAR point-to-point correspondences for rigorous registration of kinematic scanning in dynamic networks, ISPRS Journal of Photogrammetry and Remote Sensing, 189, 185-200
- Colomina, I., Blazquez, M., 2004: A unified approach to static and dynamic modeling in photogrammetry and remote sensing, International Archives of Photogrammetry, Remote Sensing and Spatial Information Sciences, 35-B1, 178-183.
- Cucci, D. A., Rehak, M., Skaloud, J., 2017: Bundle adjustment with raw inertial observations in UAV applications, ISPRS Journal of Photogrammetry and Remote Sensing, 130, 1-12.

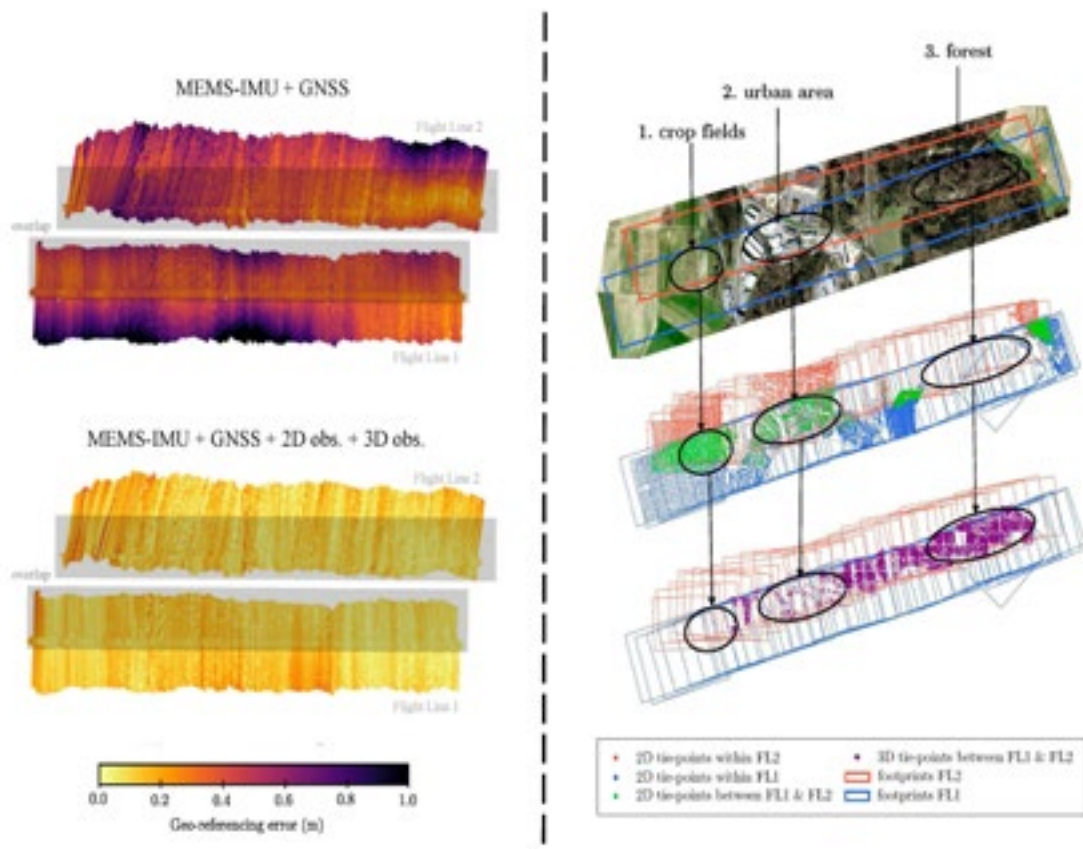


Figure 1. [Left] Geo-referencing error with typical direct geo-referencing as opposed to the one with the proposed approach, [Right] Distribution of 2D and 3D tie-points along the two flight lines and the mapping surface they correspond to.

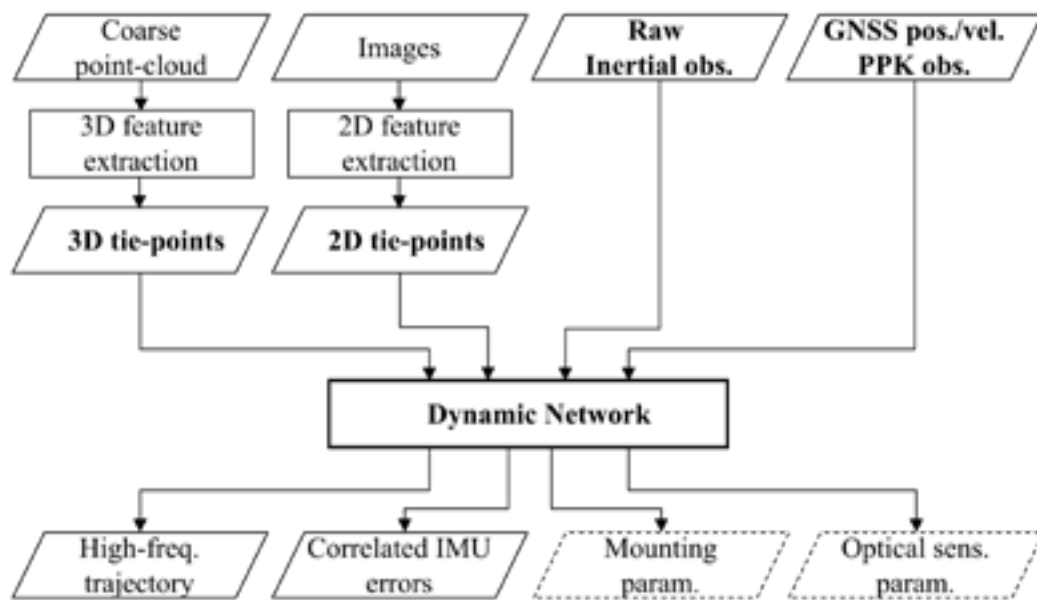


Figure 2. Integration of all the available sensor information in a single step.

## 20.5

### Stochastic Multiple Data Integration in consistent geological models

Alexis Neven<sup>1</sup>, Ludovic Schropp<sup>1</sup>, Philippe Renard<sup>1,2</sup>

<sup>1</sup> Centre of Hydrogeology and Geothermics, University of Neuchâtel, Neuchâtel, Switzerland ([alexis.neven@unine.ch](mailto:alexis.neven@unine.ch))

<sup>2</sup> Department of Geosciences, University of Oslo, Oslo, Norway

When approaching a geological or hydrogeological problem, the construction of an underground model is often required. Multiple data sources and types are frequently available on the same site, such as different geophysical data, regional conceptual knowledge, geological maps, lithologically described boreholes, or hydrogeological measurements. Combining them efficiently to ensure that the final model agrees with all of them and represents the uncertainty properly is difficult. Each measurement can be influenced by distinct underground parameters (e.g. permeability, resistivity, density, etc.) and processes occurring over different spatial resolutions and extent. Identifying them jointly through 3D stochastic inversion is time-consuming due to the high dimension of the direct problem. In this study, we propose to combine a stochastic geological model with a multidimensional stochastic inverse algorithm. The prior ensemble is generated with ArchPy, a tool ensuring that the geological models are both compatible with the boreholes, surface geological observations and the regional knowledge. Multiple field data are jointly inverted. The inversion proceeds by perturbing the 3D geological model, in order to minimize the misfit between the simulated and the measured data. Using such a workflow has the advantage of taking into account all the data available on site, while preserving geological principles in the models. In addition, processing is mainly automatic and models can easily be updated when new data becomes available. The quality of the final model and the quantification of its uncertainty is improved, within reasonable computing times.

## 20.6

# Automated hierarchical 3D modeling of Quaternary aquifers - the ArchPy approach

Ludovic Schorpp<sup>1</sup>, Julien Straubhaar<sup>1</sup>, Alexis Neven<sup>1</sup>, Philippe Renard<sup>1,2</sup>

<sup>1</sup> Center of Hydrogeology and geothermics of Neuchâtel, University of Neuchâtel, Switzerland ([ludovic.schorpp@unine.ch](mailto:ludovic.schorpp@unine.ch))

<sup>2</sup> Department of Geosciences, University of Oslo, Norway

When modeling groundwater systems in Quaternary formations, one of the first steps is to construct a geological and petrophysical model. This is often cumbersome because it requires multiple manual steps which include geophysical interpretation, construction of a structural model, identification of geostatistical model parameters, facies and property simulations. Those steps are often carried out in different softwares, which makes the automation intractable or very difficult. However, a non-automated approach is time consuming and makes the model updating difficult when new data are available or when some geological interpretations are modified. Furthermore, conducting a cross-validation procedure to assess the overall quality of the models and quantifying the joint structural and parametric uncertainty is tedious. To address these issues, we propose a new approach and a Python module, ArchPy, to automatically generate realistic geological and parameter models. One of its main features is that the modeling operates in a hierarchical manner. The input data consists of a set of borehole data and a stratigraphic pile. The stratigraphic pile describes formally and in a compact manner how the model should be constructed. It contains the list of the different stratigraphic units and their order in the pile, their conformability (eroded or onlap), the surface interpolation method (e.g. kriging, sequential Gaussian simulation (SGS), multiple-point statistics (MPS), etc.), the filling method for the lithologies (e.g. MPS, sequential indicator simulation (SIS), etc.) and the petrophysical properties (e.g. MPS, SGS, etc.). Then, the procedure is automatic. In a first step, the stratigraphic unit boundaries are simulated. Secondly, they are filled with lithologies and finally the petrophysical properties are simulated inside the lithologies. All these steps are straightforward and automated once the stratigraphic pile and its related parameters have been defined. Hence, this approach is extremely flexible. The use of ArchPy is easy and integrates many different utilities such as rasters and shapefiles handling, integration of geological maps, cross-validation, semi-automatic parameters inference, etc. The automation provides a framework to generate end-to-end stochastic models. Then, the proposed method allows for uncertainty quantification at any level and may be used for fully inversion. In this presentation, ArchPy is illustrated using data from an alpine Quaternary aquifer in the Upper Aare plain (south-east of Bern, Switzerland).

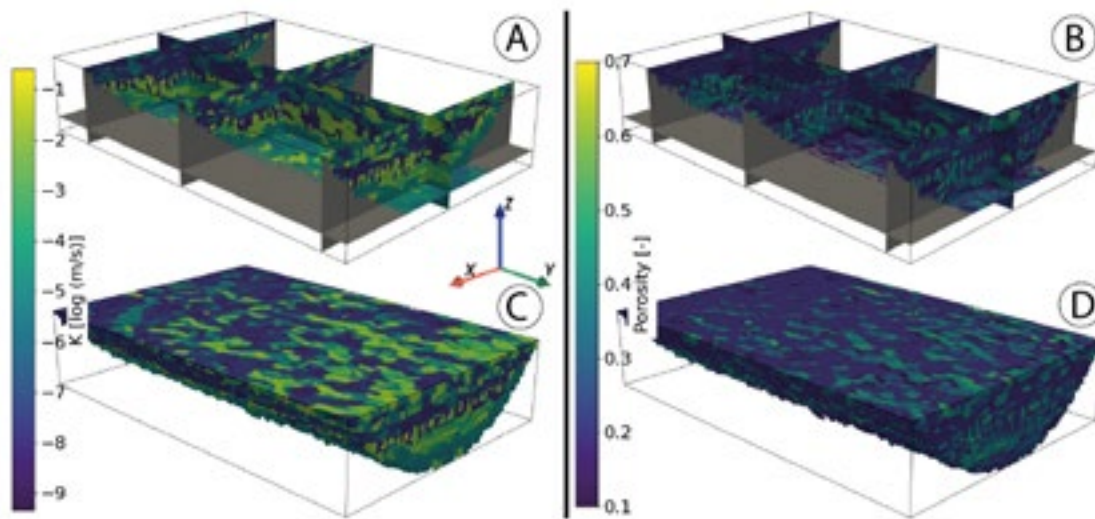


Figure 1 : 3D final property models using ArchPy. A, C : hydraulic conductivity model. B, D : Porosity model.

## 20.7

# Inggeo-Tool, a web application for 3D-model based automated tunnel profile generation

Yvo Weidmann<sup>1</sup>, Paul Gabriel<sup>2</sup>, Dirk Arndt<sup>3</sup>, Marco Filippini<sup>3</sup>

<sup>1</sup> GEOIDEE, Bellariastrasse 80, CH-8038 Zürich (yvo.weidmann@geoidee.ch)

<sup>2</sup> GiGa infosystems GmbH, Frauensteiner Strasse 59, D-09599 Freiberg (paul.gabriel@giga-infosystems.com)

<sup>3</sup> Nagra - Nationale Genossenschaft für die Lagerung radioaktiver Abfälle, Hardstrasse 73, CH-5430 Wettingen

Automated extraction of complex geological information is required to provide the basics for investigations of tunnel designs for deep geological repositories.

The Swiss National Cooperative for the Disposal of Radioactive Waste (Nagra) is responsible to identify the location for and construct a deep geological repository. Over the last years, Nagra has been conducting exploration campaigns with deep boreholes and 3D geophysical surveying to gather geological data for its planning purposes. The resulting information is compiled into 3D models.

The Engineering geological model consists of multiple units represented by tetrahedral objects and engineering geology key parameters. Both, geometry, and parameters are stored in a GST (Geosciences in Space and Time) database. Variant studies of tunnel axis for planning engineering work require the extraction of specific geological information from the 3D model. In Switzerland, SIA-199 standard regulates the basics describing geological, hydrogeological, and geotechnical situations regarding the planning, implementation, and use of underground constructions. The standard stipulates the terms and unifies the presentation and contents of technical drawings and reports.

The aim of this project was to develop an automated tool for generating tunnel profiles consistent with SIA-199 standard allowing for efficient scenario analysis of projected tunnels and shafts.



Figure 1. Subset of the automatically generated tunnel profile and extracted thematic attributes

The Inggeo-Tool is designed to retrieve information from the Engineering geological model for any user-defined tunnel axis from a provided file in ifc or GOCAD ASCII format. The tunnel designs may also include ramps and shafts. The tunnel axis is intersected with the model and the results unwrapped for graphical display. In the process of the intersection both the geological units as well as any number of attributes stored in the model will be retrieved. Model outputs include a datafile containing the entire dataset retrieved from the intersection process as well as a graphical presentation ready for print. Attributes are being extracted at a resolution corresponding to the resolution of the underlying 3D model.

The core of the Inggeo-Tool is facilitating machine-to-machine interaction. A set of rules has been elaborated for analysing and displaying any type of attributes stored in the 3D model. The Inggeo-Tool is set up as a webservice. A standard application of the Inggeo-Tool is available through a web interface. This one-click solution is ready for use after quality check by an engineering geologist. The Inggeo-Tool may also be used as a standalone webservice allowing individual script-based definition of data query and analysis. The advantage of a web based solution is simplicity of access to the Inggeo-Tool. No

installation is necessary, and the Inggeo-Tool is always available to its user in its most updated version.

The Inggeo-Tool outputs are the results of an interdisciplinary approach to report geological conditions in terms of geometry, content and representation as defined by the SIA-199 standard. The graphical presentation meets the requirements concerning intelligible visual display, as needed by a wider circle of users including designers, planners and construction companies. Its strength is facilitating fast production of basic information needed when investigating alternative tunnel designs in underground construction. Inggeo-Tool outputs are generic products and cannot provide for the details of manually elaborated tunnel profiles. However, they adhere fully to terms and definitions as described by SIA-199 standard and contribute highly to everyday workflows due to their high availability. Output formats include pdf and webfriendly svg graphics. Configuration of outputs using templates is not only flexibel but also straightforward.

It can be concluded that the Inggeo-Tool meets performance requirements when integrating construction designs for underground construction with complex geological 3D information. It is capable of displaying complex tunnel structures including combinations of ramps, shafts and tunnels. Additionally, the tool has been especially useful when running consistency checks of geological 3D models. The Inggeo-Tool is open to additional applications using the powerful 3D tetrahedral datastructure with any number of attributes which may be accessed using its interface. Thus, the tool is beeing used for data acquisition in the frame of the planning for a deep geological repository of radioactive waste, espeically in the current planning phase of the engeneering work.

## REFERENCES

SIA. (2015). SIA 199: Erfassen des Gebirges im Untertagbau

## P 20.1

# Insights from Graph Theory Application to Large Wood Supply and Transfer in River Networks

Bryce Finch<sup>1</sup>, Virginia Ruiz-Villanueva<sup>1</sup>

<sup>1</sup> Institute of Earth Surface Dynamics, University of Lausanne, Quartier Mouline, CH-1015 Lausanne (bryce.finck@unil.ch)

Large wood (LW) is a natural component of river ecosystems and provides ecological benefits as well as controls river morphodynamics and sediment dynamics. Contrarily, LW may be related to damages during flooding. LW is supplied to rivers through a variety of mechanisms including landslides, debris flows, bank erosion, and treefall. Modelling these processes is very challenging as they significantly vary in space and time. A key gap in the current research is a comprehensive model that incorporates all the different recruitment mechanisms into a singular model which demonstrates recruitable LW's spatial connections to river channels. The goal of this work is to advance the modelling of the wood supply by developing a network framework based on the graph theory (GT).

GT can simply be described as a set of objects, or nodes, connected by some relationship, or edge. The focus being to remove encumbering amounts of information and prioritize key properties of the objects and relationships at work. GT has already been practiced in fields such as sedimentology where insights were gained into the structural and spatial components involved in sediment transport (Heckmann & Schwanghart 2013). This was done by first modelling sediment transport and deposition processes within a geographic information system (GIS). Each cell, or node, representing sediment was tracked based on the process, or edge, that moved it until it was either deposited or reached the outlet. Similar workflow was potentially insightful for instream LW supply and transfer to river networks.

Instream LW is supplied and transferred to river networks via hillslope to channel and channel to channel processes. The recruitment mechanisms of bank erosion, landslides, debris flows, and treefall, were used to produce the lateral edge connections from hillslope to river network. The recruitment process prone areas were detected based on methodologies developed in the Fuzzy Logic Toolbox (FLT; Ruiz Villanueva and Stoffel 2018), which provided three scenarios based on their likely intensity or frequency (i.e., frequent, medium, and rare scenario). Some of the outputs from the FLT were then used as input data into our own model, from which we were able to realize our sources of LW as well as compare our results for wood volume computations. Within the river itself, fluvial forces related to LW transport vary based on channel dimensions and local substrate. These changes were identified during a field survey to establish unique channel segments/reaches, or nodes. Each channel node was connected to the downstream channel node to represent fluvial transfer of LW. In addition, the unique channel segments were used to produce subwatersheds based on flow direction. The subwatersheds were used to relate the recruitment processes to the channel. Furthermore, the heights of individual trees were extracted through the application of the FINT tool based on the normalized surface model (Find INdividual Trees; Dorren et al. 2017). The heights and locations of the trees were related to their respective distance to the channel segments to determine if a connection exists or not and its location.

Our current study site is the Vallon de Nant, Canton of Vaud, Switzerland. The catchment is relatively small, ~13.5 km<sup>2</sup>, and rests at an elevation from ~1,000 meters until approximately 3,000 m. The catchment is relatively protected with no infrastructure with the exception for a farmhouse, hiking paths, and seasonal grazing. The Avancon de Nant flows through the valley and is comprised of a high gradient channel.

During our work, we identified 38 unique channel reaches/segments. 18 of 38 channel nodes were predicted to recruit LW via the Rare Landslide scenario and 3 of 38 nodes for the Frequent Landslide scenario. For rare debris flows, 8 of 38 channel nodes were predicted to recruit LW. For rare and frequent bank erosion, 19 of 38 and 21 of 38 channel nodes had a LW connection. Lastly, 21 of 38 nodes were connected by natural treefall processes. Regarding wood budget computations, our GT-based network model predicted a volume of approximately 3,504 cubic meters of LW compared to the 4,081 cubic meters by the rare FLT scenario.

Insight on instream LW from this approach includes the identification of the active recruitment processes for LW at different segments along the river and the predicted volumes of LW. Thus, the work provides a means to evaluate local or regional hotspots of LW recruitment. The model's versatility already allows for the application of predicted or actual recruitment process prone areas determined by other modes than the FLT, which is a major advantage when working with different types of available data or when trying to predict or review an event. As we progress, we plan to have a functioning toolbox in ArcGIS or an external software that allows for easy application of this project's findings elsewhere.

## REFERENCES

- Dorren L., 2017. FINT – Find individual trees. User manual. ecorisQ paper ([www.ecorisq.org](http://www.ecorisq.org)): 5 p.
- Heckmann, T. & Schwanghart, W. 2013: Geomorphic coupling and sediment connectivity in an alpine catchment – Exploring sediment cascades using graph theory. *Geomorphology* 182, 89-103.
- Ruiz-Villanueva, V., Stoffel, M. 2018. Application of fuzzy logic to large organic matter recruitment in forested river basins. *Proceedings of the 5th IAHR Europe Congress New Challenges in Hydraulic Research and Engineering*, 467-468.

## P 20.2

# Evaluation of UAV weight drops as a viable source for active seismic surveys

William Grove<sup>1</sup>, Matteo Lupi<sup>1</sup>, Fabio Villani<sup>2</sup>, Stefano Maraio<sup>2</sup>

<sup>1</sup> Section des Sciences de la Terre et de l'Environnement, University of Geneva, Rue des Maraichers 13, CH-1205 Geneva ([william.grove@etu.unige.ch](mailto:wiliam.grove@etu.unige.ch) & [matteo.lupi@unige.ch](mailto:matteo.lupi@unige.ch))

<sup>2</sup> Istituto Nazionale di Geofisica e Vulcanologia, Via di Vigna Murata 605, IT-00143 Rome ([fabio.villani@ingv.it](mailto:fabio.villani@ingv.it) & [stefano.maraio@ingv.it](mailto:stefano.maraio@ingv.it))

Active seismic surveys are one of the most versatile geophysical methods for acquiring subsurface data both on land and at sea. However, this versatility often comes at a significant cost. In both cases, survey costs, which greatly depend on survey size and target depth, can quickly exceed millions of dollars, leading to such surveys being considered non-viable in less profitable industries.

In the case of onshore surveys, part of the cost constraint has been addressed through the development of various weight-drop techniques. However, current methods are limited by low transfers of elastic energy which significantly limits maximum penetration depths (e.g. hammer and plate) or their lack of mobility making them hard to deploy in complex topographic settings (e.g. accelerated weight drops). These constraints are negligible in their respective use cases; however, this has left a hole in the market for low-cost, mobile and high elastic energy transfer methodologies.

In the following project, a novel UAV weight drop methodology is proposed as a solution to this problem. In its current form, the methodology employs a UAV to drop 1-4kg steel cylinders from altitudes of 10-100m onto hard surfaces (e.g. roads). This combination allows for energy transfers ranging from 100J to 4000J. This range makes its uses cases on par with both low energy transfer hammer shots, and high energy transfer accelerated weight drop units currently on the market.

Furthermore, when coupled with wireless geophones, the methodology could be easily deployed in high-relief environments where current weight drop methods are near impossible to deploy.

Preliminary results from a high resolution and low penetration depth survey acquired in the Larderello geothermal field, (Italy), indicate that 3kg UAV weight drops at an altitude of 10m (estimated altitude) generate higher quality data than hammer and plate shots. When comparing waveforms, the UAV weight drop has higher power for frequencies around 80Hz and 110Hz whereas the hammer and plate shot has higher power at around 45Hz. These observations indicate that higher altitude UAV weight drop surveys will potentially generate data comparable to that of accelerated weight drop surveys.

**P 20.3****Size of fluvial gravel measured by machine learning assisted image segmentation – a path forward with transfer learning?**

David Mair<sup>1</sup>, Ariel Henrique Do Prado<sup>1</sup>, Philippos Garefalakis<sup>1</sup>, Fritz Schlunegger<sup>1</sup>

<sup>1</sup> Institute of Geological Sciences, University of Bern, Baltzerstrasse 1+3, 3012 Bern (david.mair@geo.unibe.ch)

In gravel-bed rivers, knowledge about the grain size is crucial for a quantitative understanding of such fluvial systems. This is the case because the particle size of sediment in the riverbed reflects the hydraulic conditions as well as the mechanisms of sediment entrainment and deposition. However, obtaining data on grain size traditionally involved time-consuming fieldwork, before image-based techniques has been developed over the last two decades. While reducing the effort for grain size measurements significantly, many of these methods still require experts to manually measure and correct the data, or the results suffer from a reduced accuracy or a systematic bias (e.g., Chardon et al., 2020; Mair et al., 2022). To mitigate these drawbacks, machine-learning approaches have recently been introduced to improve grain size measurements in images (e.g., Lang et al., 2021; Chen et al., 2022). These methods base on varying approaches, mostly based on convolutional neural networks, but all rely on dedicated training datasets and architecture to either predict grain size distributions directly or to delineate individual gravel instances and then to measure them. However, the complexity of natural fluvial setups, e.g., changing light conditions, varying vegetation cover, and differences in sediment composition and bedding, as well as different image acquisition platforms, pose limits on the general application potential of these models, despite large training datasets (e.g., >115'000 or >180'000 individually labelled grains for Lang et al., 2021; and Chen et al., 2022; respectively). Additionally, such large datasets are costly to produce and thereby impede the ability to retrain such models efficiently.

Here, we present a different approach, for which we use generalist models that were originally designed for segmentation in biomedical research. These models have been trained on large datasets (> 500 annotated images) of microscopy cell images and repeating objects, thus they learned to recognize cell-shaped objects in images. We exploit this potential for transfer learning by re-training these models to segment gravel grains on images that were taken from Swiss rivers. We achieve this by using a small data set (< 10'000 individual grains) of densely annotated images from gravel bars that we obtained with an UAV (uncrewed aerial vehicle). We test the accuracy of our models by comparing the model results with ground-truth grain size data collected in the field by hand. Based on these results, we explore the possibility of re-training our models with an even smaller data set of a few hundred grains, which will form the basis to further develop specialized models for specific tasks or datasets.

**REFERENCES**

- Chardon, V., Piasny, G., & Schmitt, L. 2020: Comparison of software accuracy to estimate the bed grain size distribution from digital images: A test performed along the Rhine River, *River Res. Appl.*, 1–10.
- Chen, X., Hassan, M. A., & Fu, X. 2022: Convolutional neural networks for image-based sediment detection applied to a large terrestrial and airborne dataset, *Earth Surf. Dyn.*, 10, 349–366.
- Lang, N., Irniger, A., Rozniak, A., Hunziker, R., Wegner, J. D., and Schindler, K. 2021: GRAINet: mapping grain size distributions in river beds from UAV images with convolutional neural networks, *Hydrol. Earth Syst. Sci.*, 25, 2567–2597.
- Mair, D., Do Prado, A. H., Garefalakis, P., Lechmann, A., Whittaker, A., & Schlunegger, F. 2022: Grain size of fluvial gravel bars from close-range UAV imagery—uncertainty in segmentation-based data, *Earth Surf. Dyn. Discuss.*, 1–33.

## P 20.4

# Ambient noise tomography and automatic picking of dispersion curves with machine learning methods: case study at Vulcano-Lipari, Italy, with a nodal geophone array.

Douglas Stumpf<sup>1</sup>, Geneviève Savard<sup>2</sup>, Célia Barat<sup>2</sup>, Francisco Muñoz<sup>2</sup>, Matteo Lupi<sup>2</sup>

<sup>1</sup> Institut des Sciences de la Terre, University of Lausanne, Quartier Mouline, CH-1015 Lausanne ([douglas.stumpf@unil.ch](mailto:douglas.stumpf@unil.ch))

<sup>2</sup> Section des Sciences de la Terre et de l'Environnement, University of Geneva, Rue des Maraîchers 13, CH-1205 Genève

The ambient noise tomography (ANT) method is widely adopted to reconstruct shear-wave velocity anomalies and image the crust and the upper-mantle with higher resolution. The key step of extracting surface-wave dispersion curves from cross-correlation functions of continuous ambient noise recordings is traditionally performed manually on the dispersion spectrograms through human-machine interfaces. Picking of dispersion curves is sometimes biased by human interpretation. Furthermore, it is a laborious and time-consuming task that needs to be resolved in an automated manner, especially when dealing with dense seismic arrays where the huge amount of generated data severely hinders manual picking approaches. In the last decade, machine learning methods have shown great performance in many seismological applications and is a promising approach to resolve this issue by considering the dispersion curve extraction as a visual recognition problem. Several previous studies successfully employed unsupervised (clustering) or deep (convolutional neural network) machine learning approaches that show great promise.

This study has the goal of reviewing and adapt these machine learning approaches to apply them on dispersion spectrograms performed with the usual frequency-time analysis (FTAN) processing on ambient noise cross-correlations. The data set consists of a dense local geophone array (150 short period stations sampling at 250 Hz) deployed for one month in October 2021 and of a sparser regional network composed of 18 permanent broadband stations (sampling at 100 Hz) maintained by the National Institute of Geophysics and Volcanology (INGV) in Italy. The performance of the dispersion curves extraction algorithm will then be evaluated and the automatically picked dispersion curves will be used to construct a shear-wave velocity model of the Vulcano-Lipari magmatic plumbing system and the surrounding area of the Aeolian archipelago.

## P 20.5

### Geolocation of a panoramic camera by reference pairing

Chahine-Nicolas Zede<sup>1</sup>, Adrien Gressin<sup>1</sup>

<sup>1</sup> University of Applied Sciences Western Switzerland (HES-SO / HEIG-VD), Insit Institute  
 (chahine-nicolas.zede, adrien.gressin)@heig-vd.ch

Knowledge of the territory plays a crucial role in the evolution of cities, subject to more demographic, logistical and climatic constraints. To help the decision-making in land use planning, the city of Geneva wants to update its cadastre of underground networks. Surveying each piece of pipe can be time consuming and repetitive. A solution proposed by previous works is to use a combination of photogrammetry and machine learning to automate the survey.

However, the use of GNSS (Global Navigation Satellite System) in a dense urban environment is affected by various phenomena (urban canyon, multi-path) which degrade the quality of positioning of the camera.

That is why this project aims to locate a panoramic camera in a dense urban environment, by extracting reference points from the view. The chosen camera is the GoPro MAX for its 360° video capture and its affordable price. The references are points with known coordinates, taken from the LiDAR and recognized in the fisheye image.

The strategy chosen is the pairing of a horizon line contour (HLC) in the image and in a 3D model. The image-HLC is formed with a sky extracting neural network and the LiDAR-HLC is created by keeping the highest point visible in each direction. Then, the Direct Time Warping (DTW) associates the indices of two temporal signals according to a distance costs matrix, matching points with similar properties. It can be used here to align the two HLC, thus creating ground control points (GCP) in our image, which allow an aero-triangulation calculation. A filtering step is added to keep only the horizon points on the sharp angle of the building. By knowing the geometry of the camera (the intrinsic parameters and the distortion coefficients), we can estimate the position of the camera thanks to the GCPs.

This study is initially limited to the localization of an image then extended to the SfM (Structure-from-Motion) to align all the views extracted from the video.

The use of multiple views with GCPs improves the orientation calculation.

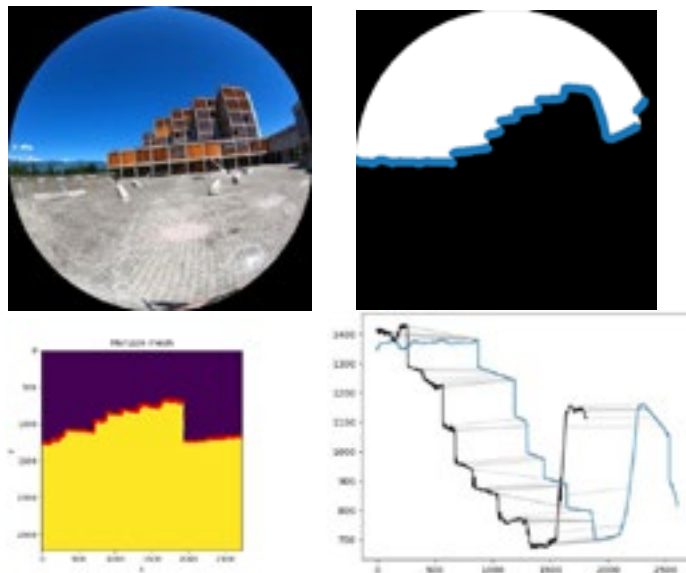


Figure 1: (top-left) Original fisheye view, (top-right). Sky detection in white and image-HLC in blue, (bottom- left) Sky dectection in from LiDAR data, and (bottom-right) result of the DTW pairing between the two HLC.

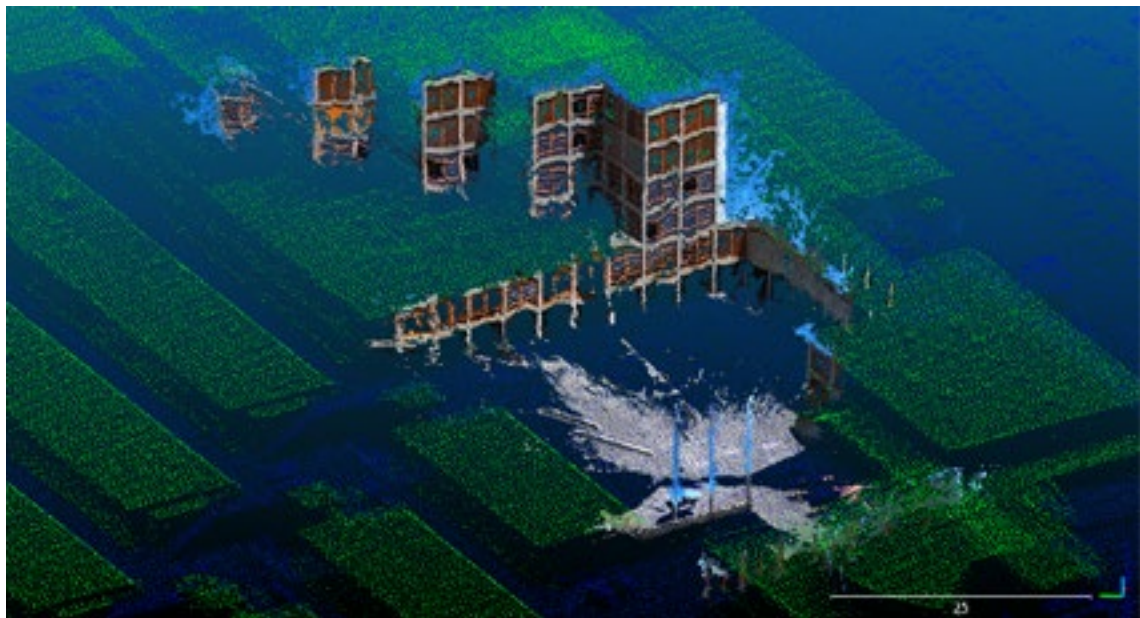


Figure 2: Result of a corrected georeferenced photogrammetric 3D point cloud (in real color) on the LiDAR point cloud (other colors).

## P 20.6

# Reconstruction of 3D high-resolution GPR data from 2D profiles: A multiple-point geostatistical approach

Chongmin Zhang<sup>1</sup>, James Irving<sup>1</sup>, Mathieu Gravé<sup>2,3</sup>, Grégoire Mariethoz<sup>2</sup>

<sup>1</sup> Institute of Earth Sciences, University of Lausanne, CH-1015, Lausanne, Switzerland ([chongmin.zhang@unil.ch](mailto:chongmin.zhang@unil.ch))

<sup>2</sup> Institute of Earth Surface Dynamics, University of Lausanne, CH-1015, Lausanne, Switzerland

<sup>3</sup> Department of Physical Geography, Utrecht University, Utrecht, Netherlands

Ground-penetrating radar (GPR) is a popular geophysical tool for high-resolution imaging of the shallow subsurface. In particular, 3D GPR data, where measurements are acquired along a series of parallel survey lines, offer great potential for gaining important information about complex subsurface environments. Such data are, however, extremely time consuming to collect, and a typical trade-off is that the measurement spacing along the survey lines is significantly denser than the line spacing. This introduces a strong resolution bias in the 3D dataset, and spatial aliasing is commonly present in the across-line direction. A common means of addressing this problem is to apply simple interpolation to fill the gaps between the existing lines (e.g., Luo et al., 2019). However, such an approach is only effective when the line spacing is already rather small and tend to lead to overly smoothed and unrealistic structures when the survey lines are spaced further apart.

In this research, we present another means of addressing this problem, which is via multiple-point geostatistics (MPS) simulation. To this end, considering that we only have a limited number of sparsely distributed 2D GPR profiles to begin with, we reconstruct the densely spaced 3D GPR data set using a series of separate 2D simulations in both the along-line and across-line directions. Training images, which are necessary for the application of MPS, come from the existing GPR profiles. To deal with the discontinuities in 3D spatial structures caused by performing independent 2D simulations, target profiles are selected randomly but simulations are performed alternately in both directions. We show the application of our approach to 100-MHz synthetic GPR data generated over a realistic sedimentary model (Koyan and Tronicke, 2020), where the effect of different line spacings of the original data is investigated. The test results show that our proposed methodology provides significantly better reconstructions than standard interpolation, in particular as the spacing between the GPR survey lines increases.

## REFERENCES

- Koyan, P., & Tronicke, J. 2020: 3D modeling of ground-penetrating radar data across a realistic sedimentary model, *Computers & Geosciences*, 137, 104422.  
Luo, T. X., Lai, W. W., Chang, R. K., & Goodman, D. 2019: GPR imaging criteria, *Journal of Applied Geophysics*, 165, 37–48.

## P 20.7

# Spatial resolution of 3D maps of a heterogeneous ultramafic lense at the Cima di Gagnone, Cima Lunga unit

Jodok Zwahlen<sup>1</sup>, Filippo Schenker<sup>1</sup>, Alessio Spataro<sup>1</sup>

<sup>1</sup> Dipartimento ambiente costruzione e design, SUPSI, via Flora Ruchat-Roncati 15, CH-6850 Mendrisio, (jodokz@gmx.ch)

Remote sensing helps to evaluate quantitatively geological processes by increasing the precision of 3D geological maps, especially in areas that are poorly accessible. In addition, mapping of a 3D model is a far more time-efficient process than field mapping. However, the spatial resolution of the 3D model might not allow for mapping of features with low color contrast. Therefore, the goal of this study is to investigate the feasibility and the maximum obtainable resolution of a digital geological map of a heterogeneous ultramafic body of 300 m length SSW of Cima di Gagnone.

We used a drone to take images at regular intervals and in different directions to generate a 3D model of the outcrop. The model was georeferenced using control points, whose exact coordinates were obtained with GNSS (model Geomax Zenith25 – rtk modality) in the field. In a first step, the ultramafic body was mapped using the 3D model and the information published about the occurring lithologies and their approximate locations.

In a second step, a detailed map of the ultramafic body was made directly in the field, using our high-precision 3D topographic model. In a last step, the produced maps were compared and discussed in terms of precision of limits, lithological content and of efficiency of methodology.



## 21 Spatial data science: extracting knowledge from geo-environmental data +

## 22 Virtual Representation of Forests: Methods and Applications

Convenors session 21: Marj Tonini (UNIL), Tom Beucler (UNIL), David Ginsbourger (UNIBE), Fabian Guignard (UNIBE), Amanda Burton (Agroscope), Cédric Métraux (swisstopo).  
Convenors session 22: Arnadi Murtiyoso, Amanda Mathys, Monika Niederhuber, Verena Griess

*Swiss Geocomputing Centre*

### TALKS:

- 21.1 Carreau A., Deillon Y., Gressin A.: Automatic determination of land objects – Use of oblique drone images
- 21.2 Fol C.R., Murtiyoso A., Griess V.C.: Inspection of Forest Point Cloud in Virtual Reality
- 21.3 Hari C., Davin E., Fischer M.: Combining future projections of land-use and climate change to assess their impact on biodiversity
- 21.4 Schmutz L., Thao S., Vrac M., Mariethoz G.: A multivariate approach to combine general circulation models using graph cuts
- 21.5 Tonini M., Trucchia A., Izadgoshasb H., Fiorucci P.: Comparison of the performance of machine learning models for wildfire susceptibility mapping
- 21.6 Weber M.S., Griess V.C.: Visualizing future forest changes in VR
- 21.7 Zermatten V., Santacroce N., Gros-Daillon J., Tuia D., Ackermann N.: Characterization of the Uncertainty in Land Cover Predictions near Train Tracks

## POSTERS:

- P 21.1 Amaya M., Linde N., Meles G.: Bayesian inversion using adaptive sequential Monte Carlo combined with surrogate modelling
- P 21.2 Eiholzer L., Tonini M., Losapio G.: Modelling the Impact of Glacier Retreat on Vegetation Dynamic
- P 21.3 Friedli L., Linde N., Ginsbourger D., Doucet A.: Sequential Monte Carlo for posterior risk assessment
- P 21.4 Jouvet G.: Generative adversarial network for paleo glacial landscape reconstruction
- P 21.5 Levy S., Laloy E., Linde N.: Combining inverse autoregressive flows with deep generative networks for improved efficiency and scalability of inverse problems
- P 21.6 Poloni A., Tonini M., Lambiel C.: Advanced spatial learning technique for automatic mapping of geomorphological features in alpine periglacial environment
- P 21.7 Jingjing Wang Gang Chen, Michel Jaboyedoff , Marc-Henri Derron: Mountain Landslide susceptibility assessment by Multi-sampling strategy combining optimization of BiLSTM algorithm

## 21.1

### Automatic determination of land objects - Use of oblique drone images

Antoine Carreauud<sup>1</sup>, Yves Deillion<sup>1</sup>, Adrien Gressin<sup>1</sup>

<sup>1</sup> University of Applied Sciences Western Switzerland (HES-SO / HEIG-VD), Insit Institute - (antoine.carreauud, yves.deillion, adrien.gressin)@heig-vd.ch

The determination of land objects and their updating for the different cadastre plans or BIM projects is still carried out with significant human resources: by field surveys and/or manual digitalization from orthoimages or laser surveys. Such operations are therefore expensive and time-consuming. In this context, we propose to study the possibilities of automating the recognition of land objects based on drone images using artificial intelligence (AI). Today, the use of orthoimages in AI is widely developed, however, it has limitations such as the determination of objects located in hidden areas (under the trees, at the foot of buildings...).

Futhermore, aerial oblique images are already widely used in areas like cities for complex 3D reconstruction and provide a large amount of information, which is no longer available in the orthoimage. Therefore, we propose to use such oblique images in a prototype project to automate the periodic updating of land cover objects in the Swiss official cadastral survey. This study was conducted in collaboration with the canton of Vaud (Switzerland).

For this study, we used 1700 nadir and oblique images, acquired with the fixed-wing drone Ebee, equipped with the SODA 3D sensor. Images have been acquired with an average resolution of 4 cm, over a 210 hectare area of the city of Lausanne. To automatically label the training images, the classes of the objects concerned (buildings, vegetation, hard surfaces, railway, water basins), from an existing cadastral plan, have been projected onto the oriented images (nadir and oblique). Then, the Deeplab v3+ convolution network has been trained to perform semantic segmentation on the drone images (Figure 1 shows an example of the inference result on an image from the validation set, and Figure 2 the resulting labelled 3D point cloud). Finally, we use the predictions in the form of masks to perform a 3D reconstruction by class on the validation areas of our dataset, using a Structure-From-Motion algorithm.

In these areas, we obtain a semantic accuracy of 94% with a recall rate of 91% on the 3D point cloud. Such precision is not yet sufficient to update the land cover objects of the Swiss official cadastral survey in a fully automatic way, but it allows us to imagine interesting perspectives such as detection of changes, semi-automatic updating methods, or land use statistics.



Figure 1. Inference on one validation image (batiment = building, dur = hard surface, vert = vegetation).

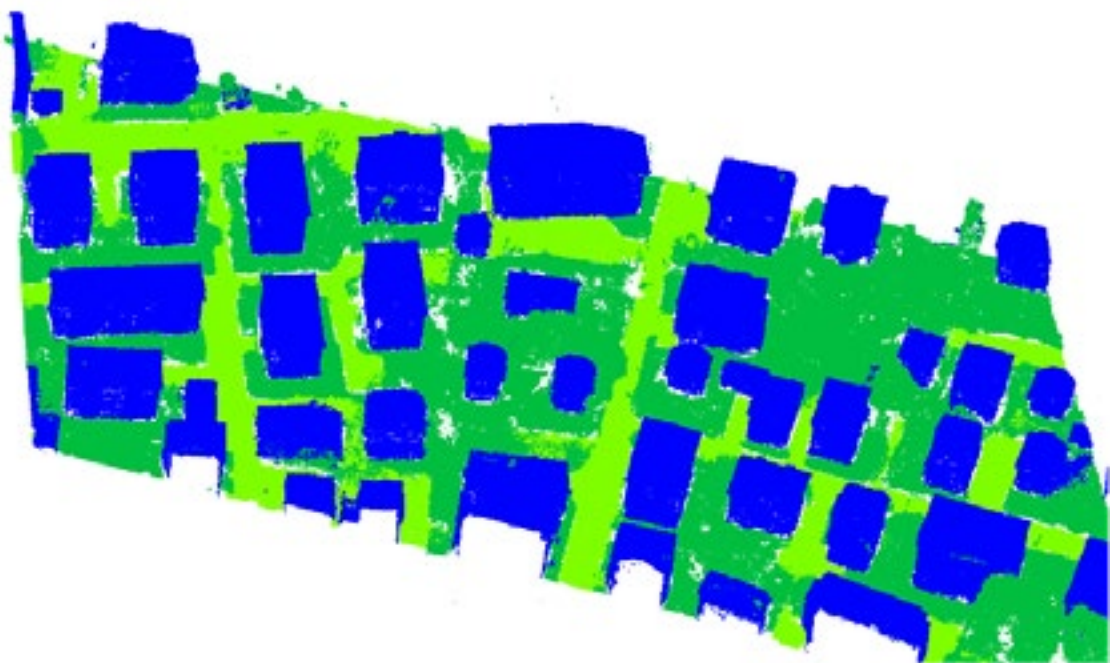


Figure 2. The resulting labelled 3D point cloud.

## 21.2

### Inspection of Forest Point Cloud in Virtual Reality

Cyprien R. Fol\*, Arnadi Murtiyoso, Verena C. Griess

*Forest Resources Management, Institute of Terrestrial Ecosystems, Department of Environmental Systems Science, ETH Zurich, Switzerland (cyprien.fol, arnadihestaratri.murtiyoso, verena.griess)@usys.ethz.ch*

#### 1) Introduction

Forest digitalisation opened up a completely new interpretation of forest ecology based on direct measurements in the 3D digital twin rather than using the classical DBH (diameter at breast height) centred approach that does not include any information on the forest architecture (Lines et al. 2022). Although the processing of 3D forest data has already allowed researchers to increase their understanding of different complex process such as radiative transfer modelling (Calders et al. 2018) and canopy microclimate (Zellweger et al. 2019), very little research has been done to enhance the visualisation and inspection of forests 3D data. In fact, the classical approach still involves computer software that display the 3D model on a 2D monitor which makes difficult the manipulation of large dataset. For this reason, VR (Virtual Reality) is a great alternative to facilitate the forest inspection by immersing the user inside the 3D model and allowing him to explore rapidly the virtual forest using the several VR motions options, i.e., walking and teleporting. In this research, a VR application was developed to turn the task of 3D forest data inspection into a more user-friendly and pleasant experiment.

#### 2) Methods

To begin with, the data type used in this study is point clouds because they represent most 3D data in the field of forestry. By reviewing the different state-of-the art solution for virtual forest visualisation, two projects stood out from the rest. First, Michael Hertz developed a GitHub repository called PointCloudXR, which is an open-source Unity3D application specifically designed for forest 3D data. In addition, the user can interact with the points, e.g., for distance measurements or removing noise. However, this application only handles point clouds with a maximum of 10 to 15 million points, which is adequate to work with single tree point clouds but far from sufficient for forest point clouds made of around 1 billion points. Nevertheless, a study from the cultural heritage field written by Kharroubi et al., 2019, achieved to visualise 2.3 billion points in real time and continuously in VR. These 2 projects share a common aspect: they both employ Unity and the GPU (Graphics Processing Unit) computing power to optimise the rendering process. Hence, we opted for a similar approach

#### 3) Results

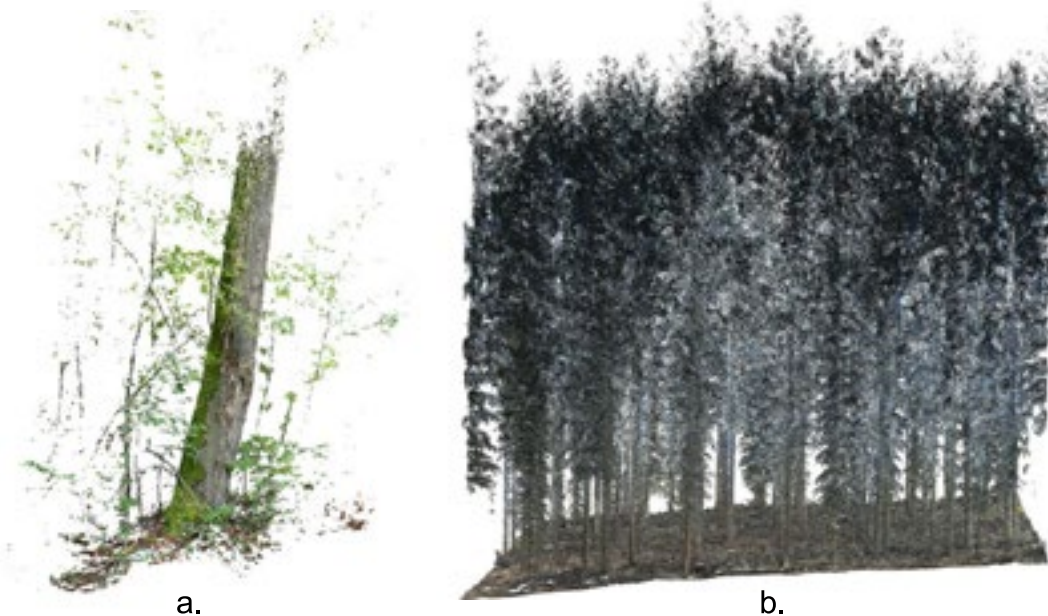


Figure 1: a) single tree point cloud of 27 314 314 points. b) forest point cloud of 28 000 000 points.

#### 4) Conclusion

In conclusion, VR gives users the opportunity to be immersed in the 3D model, allowing a more intuitive and thorough inspection of virtual forest. Furthermore, VR has the potential to be used for measuring directly forest parameters such as DBH (diameter at breast height) or total height of a tree (Mikael Hertz, accessed: 08-07-2022). The addition of this features will be considered for the further development of our application.

## REFERENCES

- Calders K, Origo N, Burt A, Disney M, Nightingale J, Raumonen P, Åkerblom M, Malhi Y, Lewis P. 2018. Realistic Forest Stand Reconstruction from Terrestrial LiDAR for Radiative Transfer Modelling, *Remote Sensing*; 10(6):933.
- Kharroubi, A., Hajji, R., Hajji, R., Billen, R., & Poux, F. 2019. Classification and integration of massive 3D points clouds in a virtual reality (VR) environment. *ISPRS - International Archives of the Photogrammetry, Remote Sensing and Spatial Information Sciences*. XLII-2/W17. 165-171
- Lines, E. R., Fischer, F. J., Owen, H. J. F., & Jucker, T. 2022. The shape of trees: Reimagining forest ecology in three dimensions with remote sensing. *Journal of Ecology*, 110, 1730– 1745.
- Mikael Hertz. GitHub Repository PointcloudXR. <https://github.com/mhzse/PointcloudXR>. Accessed: 08-07-2022.
- Zellweger, F., De Frenne, P., Lenoir, J., Rocchini, D., & Coomes, D. 2019. Advances in microclimate ecology arising from remote sensing. *Trends in Ecology & Evolution*, 34(4), 327–341.

## 21.3

# Combining future projections of land-use and climate change to assess their impact on biodiversity

Chantal Hari<sup>123</sup>, Édouard Davin<sup>123</sup>, Markus Fischer<sup>34</sup>

<sup>1</sup> Wyss Academy for Nature at the University of Bern, University of Bern, Kochergasse 4, CH-3011 Bern  
(chantal.hari@wyssacademy.org)

<sup>2</sup> Climate and Environmental Physics, Physics Institute, University of Bern, Sidlerstrasse 5, CH-3012 Bern

<sup>3</sup> Oeschger Centre for Climate Change Research, Hochschulstrasse 4, CH-3012 Bern

<sup>4</sup> Institute of Plant Sciences, Plant Ecology, Altenbergrain 21, CH-3013 Bern

Biodiversity loss, land degradation, and climate change are acknowledged environmental challenges faced by humanity (Newbold 2018; Rosenzweig et al. 2008). Climate change's impacts on biodiversity will likely intensify in the future (Pereira et al. 2020). Additionally, land use is a current key stressor of biodiversity (IPBES 2019). Generally, human activities including land-use changes are the cause of global change, thus, future projections of biodiversity impacts need to include both, climate change and land-use change. Here we aim to combine climate change and land-use change scenarios to assess their impacts on biodiversity.

Extensive research has been made on mapping and projecting the vulnerability of multiple species based on different climate mitigation scenarios or warming levels (e.g. Jenkins et al. 2021; Seddon et al. 2021; Strassburg et al. 2012; Thomas et al. 2004; Warren et al. 2013). What is lacking, is the inclusion of land-use trajectories in these projections (Cabral et al. preprint.). Hof et al., (2018) made a first step to overcome these deficiencies. They evaluated the potential future impacts of climate and land-use change on global species richness of terrestrial vertebrates. They used climate and land-use impact projections from the Inter-Sectoral Impact Model Intercomparison Project (ISIMIP) under a low-and high emission scenario. However, for both emission scenarios, they used the same land-use projections. This study aims to go further and combine future climate scenarios and a matrix of integrated assessment modeling (IAM) derived land-use projections to assess the impact on biodiversity through the application of species distribution modeling.

Species distribution data will be obtained for the world's amphibians, mammals, and reptiles from the IUCN Red List of Threatened Species as expert range maps (IUCN 2022). An ensemble model will be built to combine the information from individual models fitted with different modeling techniques at a 0.5° resolution. Namely, General Linear Models (GLM), General Additive Models (GAM), and the Random Forest (RF) algorithm will be used. For historical climate data, the W5E5 v.2.0 data will be used, which is a global dataset at 0.5° resolution covering the period 1979-2019, made available through ISIMIP (Lange et al. 2021). For future climate data, this study will use bias-corrected global scenarios produced by ISIMIP phase 3b (Lange & Büchner 2021). ISIMIP3b provides future scenarios for three Representative Concentration Pathways (RCPs) combined with Shared Socioeconomic Pathways (SSPs), SSP1-2.6, SSP3-7.0, SSP5-8.5, and five CMIP6 global climate models (GCMs), GFDL-ESM4, IPSL-CM6A-LR, MPI-ESM1-2-HR, MRI-ESM2-0, UKESM1-0-LL.

The Land Use Harmonization dataset v2 (LUH2; see Hurt et al. 2020) will be used to include future projections of land-use change. The probabilities of occurrence from the species distribution models will then be filtered by the land-use data to determine the implications for biodiversity among different scenarios. LUH2 reconstructs and projects changes in land use among 12 categories. To match the species' habitat preferences, data from IUCN Habitat and Classification Scheme for each species will be downloaded and then mapped onto the 12 land-use types represented in the LUH2 dataset according to the conversion table from Carlson et al. (2022). The land-use data is then used to refine the climatic envelope and filter out regions, where species cannot survive based on the land-use projections.

This approach then allows to quantify the uncertainties between different climate and land-use scenarios and combinations of both and provides quantitative information on the effects of also considering land-use change projections when running climate-driven species distribution models to determine the impact of future climate change on biodiversity.

## REFERENCES

- Carlson, C. J., Albery, G. F., Merow, C., Trisos, C. H., Zipfel, C. M., Eskew, E. A., Olival, K. J., Ross, N., & Bansal, S. 2022: Climate change increases cross-species viral transmission risk. *Nature* 2022 607:7919, 607(7919), 555–562.
- Hof, C., Voskamp, A., Biber, M. F., Böhning-Gaese, K., Engelhardt, E. K., Niamir, A., Willis, S. G., & Hickler, T. 2018: Bioenergy cropland expansion may offset positive effects of climate change mitigation for global vertebrate diversity. *Proceedings of the National Academy of Sciences of the United States of America*, 115(52), 13294–13299.
- Hurt, G. C., Chini, L., Sahajpal, R., Frolking, S., Bodirsky, B. L., Calvin, K., Doelman, J. C., Fisk, J., Fujimori, S., Klein Goldewijk, K., Hasegawa, T., Havlik, P., Heinemann, A., Humpenöder, F., Jungclaus, J., Kaplan, J. O., Kennedy, J., Krisztin, T., Lawrence, D., ... Zhang, X. 2020: Harmonization of global land use change and management for the period 850-2100 (LUH2) for CMIP6. *Geosci. Model Dev.*, 13, 5425–5464.
- Stefan Lange, Matthias Büchner (2021): ISIMIP3b bias-adjusted atmospheric climate input data (v1.1). ISIMIP Repository.

## 21.4

# A multivariate approach to combine general circulation models using graph cuts

Lucas Schmutz<sup>1</sup>, Soulivanh Thao<sup>2</sup>, Mathieu Vrac<sup>2</sup>, Grégoire Mariethoz<sup>1</sup>

<sup>1</sup> Institute of Earth Surface Dynamics (IDYST), UNIL-Mouline, Geopolis, University of Lausanne, 1015 Lausanne, Switzerland ([lucas.schmutz@unil.ch](mailto:lucas.schmutz@unil.ch))

<sup>2</sup> Laboratoire des Sciences du Climat et l'Environnement (LSCE-IPSL) CNRS/CEA/UVSQ, UMR8212, Université Paris-Saclay, Gif-sur-Yvette, France

General circulation models (GCMs) are of extreme importance to make future climate projections. Their predictions are used extensively by policymakers to manage their response to anthropogenic global warming and climate change.

To extract a robust global signal and evaluate uncertainties, individual models are often assembled in Multi-Model Ensembles (MMEs). Various approaches to combine individual models have been developed, such as the Multi-Model Mean (MMM) or its weighted variants.

Recently, Thao et al. (2022) developed a model comparison approach based on graph cuts. Graph cut optimization was developed in the field of computer vision to efficiently approximate a solution for low-level computer vision tasks such as image segmentation (Boykov et al., 2001). Applied to MMEs, it allows selecting for each pixel a set of best-performing models and produces a patchwork of models that maximizes performances while maintaining pixel-to-pixel continuity. It thus allows considering the local performance of ensemble members in contrast with approaches such as MMM or similar methods that use global weights.

Here we propose a new multivariate combination approach of MMEs based on graph cuts. Compared to the existing univariate graph cuts method, our approach ensures that the relationships between variables, that are present in ensemble members, are locally preserved while providing coherent spatial fields. Moreover, we exploit the design of the graph cut optimization to propose a stochastic version of model combinations that provides multiple similarly good solutions.

We demonstrate the efficiency of our approach by co-optimizing multi-decadal means of multiple variables. We compare the performance to univariate optimization and show that the loss of performance is small with a negligible increase in computational cost.

## REFERENCES

- Boykov, Y., Veksler, O., & Zabih, R. (2001). Fast approximate energy minimization via graph cuts. *IEEE Transactions on Pattern Analysis and Machine Intelligence*, 23(11), 1222–1239. <https://doi.org/10.1109/34.969114>
- Thao, S., Garvik, M., Mariethoz, G., & Vrac, M. (2022). Combining global climate models using graph cuts. *Climate Dynamics*, February. <https://doi.org/10.1007/s00382-022-06213-4>

## 21.5

# Comparison of the performance of machine learning models for wildfire susceptibility mapping

Marj Tonini<sup>1</sup>, Andrea Trucchia<sup>2</sup>, Hamed Izadgoshasb<sup>2</sup>, Paolo Fiorucci<sup>2</sup>

<sup>1</sup> Institute of Earth Surface Dynamics, Faculty of Geosciences and Environment, University of Lausanne, CH-1015 Lausanne, Switzerland ([marj.tonini@unil.ch](mailto:marj.tonini@unil.ch))

<sup>2</sup> International Center for Environmental Monitoring CIMA Research Foundation, 17100 Savona, Italy

Developing Wildfire Susceptibility Maps (WSM) and investigating the main driving factors for wildfire occurrence are fundamental to support forest protection and management plans. Namely, WSM indicate the likelihood for an area to be exposed to fire in the future based solely on the observed past events and on the local properties of a site (environmental and anthropogenic factors). Machine Learning (ML) based approaches are capable of learning from and make predictions on data by modelling the hidden/non-linear relationships between a set of input variables (i.e., the driving factors) and output observations; thus, they are particularly suited for WSM.

With the present study, Authors continue a research framework developed in a pioneeristic work at local scale for Liguria Region, and lately adapted to national scale (Italy). In these earlier investigations, a Random Forest-based modelling workflow was developed to assess the susceptibility to wildfires under the influence of several environmental driving factors (land cover, type of vegetation, altitude and its derivatives, nearby infrastructures). The main novelties and contributions of the present study are: (i) we compared three ML models, namely Random Forest, Multi-layer Perceptron, and Support Vector Machine, to assess their prediction capabilities and to estimate which model performs better; (ii) we used a more accurate vegetation map as input, allowing to evaluate the impact of different types of local and neighbouring vegetation on wildfires occurrence; (iii) we improved the selection of the testing dataset, in order to take into account both the spatial and the temporal variability of the burning seasons.

As main results, WSMs were elaborated based on the output probabilistic predicted values from the three ML models, and the spatial distribution of the more susceptible areas was discussed. The three ML models were compared by means of the AUC (Area Under the Curve) ROC (Receiver Operating Characteristics), evaluated over the testing dataset.

In addition, the variable importance ranking was estimated as by-product of Random Forest, which can handle both numerical variables (as for the percentage of neighbouring vegetation) and native categorical variables (as for the types of vegetation at pixel level). Vegetation resulted by far to be the most important driving factor; the marginal effect of each single type of vegetation was also evaluated and discussed.

## REFERENCES

- Tonini, M.; D'Andrea, M.; Biondi, G.; Degli Esposti, S.; Trucchia, A.; Fiorucci, P. (2000): A Machine Learning-Based Approach for Wildfire Susceptibility Mapping. The Case Study of the Liguria Region in Italy. *Geosciences*, 10, no. 3: 105. <https://doi.org/10.3390/geosciences10030105>.
- Trucchia, A.; Meschi, G.; Fiorucci, P.; Gollini, A.; Negro, D. (2022): Defining Wildfire Susceptibility Maps in Italy for Understanding Seasonal Wildfire Regimes at the National Level. *Fire*, 5,30. <https://doi.org/10.3390/fire5010030>.

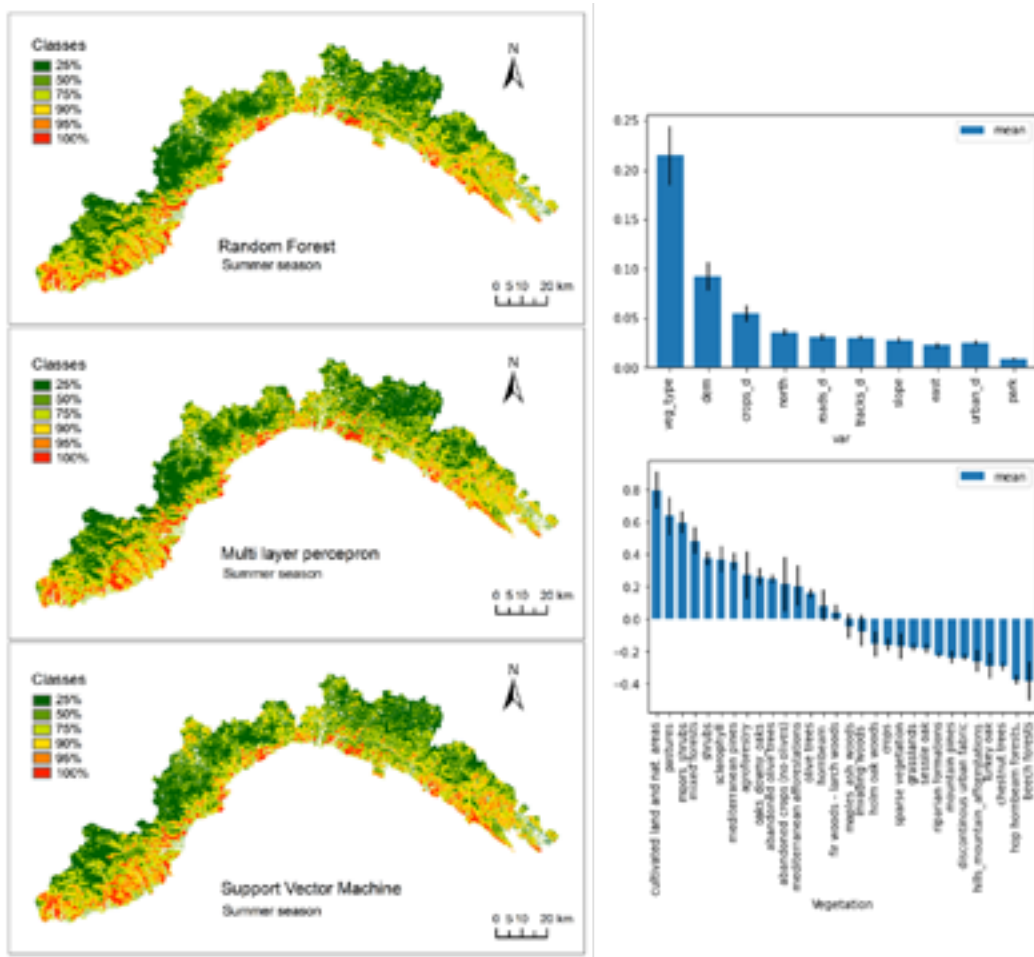


Figure 1. Wildfire Susceptibility Maps for Liguria region (Italy) (on the left). The variable importance ranking (top-right) and the partial plot of the types of vegetation (bottom-right).

## 21.6

### Visualizing future forest changes in VR

Michelle S. Weber\*, Verena C. Griess

*Forest Resources Management, Institute of Terrestrial Ecosystems, Department of Environmental Systems Science, ETH Zurich, Switzerland*

(michelle.weber, verena.griess)@usys.ethz.ch

This presentation shows the potential of the iVR (immersive Virtual Reality) technology for the visualization of research results on future climate-related scenarios. The project was developed at ZHdK, as part of a graduate project (BA Design, Scientific Visualization), in close collaboration with the FORM group at ETH Zürich.



Figure 1. Rendering of a sparse forest built in Unity.

Current predictive models have a great potential to help practitioners and forest owners foresee changes inside the forest. Based on their experience and the outcome of the predicted scenario, they can decide which forest intervention strategy to apply. However, most of today's forest interventions will have impacts that they will not experience in their entire lifetime. Therefore, iVR is particularly relevant to help them visualize the impact of their management strategy. Indeed, by immersing the user inside the future forest, this could greatly improve their understanding of forest development.

The VR-Experience prototype "*Here Comes the Sun*" showcases a common forest intervention - the thinning of the forest – and its potential influence on the forest. Visitors embark on a journey through time. They first explore a dense forest from the present, and then visit the same forest in 100 years' time. Several stations highlight different topics related to the forestry interventions, e.g., the use of wood as a resource. Users can teleport to each station, where a narrator provides further insight into the station's topic. This allows users to interactively learn about the advantages and disadvantages of thinning the forest.

In conclusion, this session will focus on the presentation of the VR-Experience prototype with an emphasis on the concept, the implementation and the potential of the project.

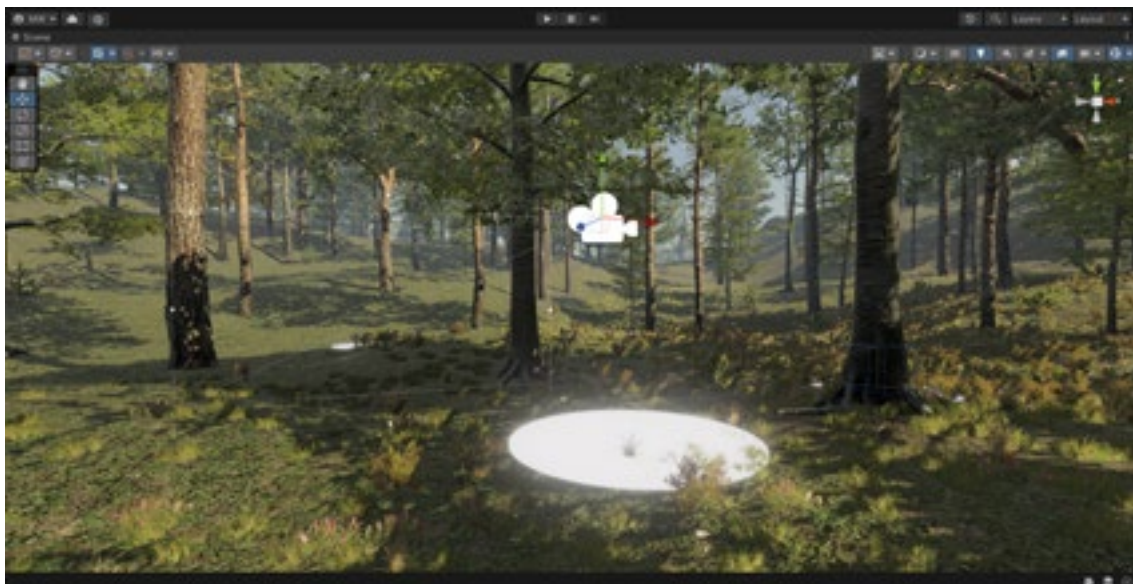


Figure 2. Setting up the forest environment with various information stations in Unity.



Figure 3. People testing the *VR-Experience* in the graduation exhibition.

## 21.7

# Characterization of the Uncertainty in Land Cover Predictions near Train Tracks

Valérie Zermatten<sup>1</sup>, Nicola Antonio Santacroce<sup>1,2,3</sup>, Jules Gros-Daillon<sup>1,2,3</sup>, Devis Tuia<sup>1</sup>, Nicolas Ackermann<sup>3</sup>

<sup>1</sup> Environmental Computational Science and Earth Observation Laboratory, EPFL, Ronquoz 35, 1950 Sion, (valerie.zermatten@epfl.ch)

<sup>2</sup> Environmental Sciences and Engineering, EPFL, Station 2, 1015 Lausanne

<sup>3</sup> Drone Development Department, SBB, Stöckackerstrasse 25, 3000 Berne

The Swiss Federal Railways (SBB) manage a rail network approximately 3,000 kilometres long. The maintenance of the vegetation in the surroundings areas is an important part of this work. A classification of the land cover in proximity of the train tracks is used to monitor the current state of vegetation and determine the location where fieldwork must be undertaken. This land cover map focuses especially on vegetation types and height and requires a high level of accuracy. Until now, the land cover maps were derived through a time consuming and costly process involving extended manual corrections.

The objective of this work is to benefit from the recent advances in computer vision to provide a land cover map in automated manner and reduce the need for manual corrections. Our work involved the setup of a semantic segmentation model to predict the land cover classification and a second module providing the uncertainty of the predictions.

Input data include orthoimages with RGB and infrared bands, digital surface model, a vegetation high model derived from lidar data and a partially complete building layer.

We use UNet (Ronneberger et al., 2015), a convolutional neural network to classify the land cover at every pixel location. To account for both model and data uncertainty, we used two approaches: test time augmentation (Gawlikowski et al., 2021) was used to observe the data uncertainty. Model uncertainty is predicted through a Bayesian network with a method called Monte Carlo Dropout (Gal and Ghahramani, 2016) that slightly modifies the neural network by randomly turning off some of the model connections at each forward pass. The resulting variations in the predictions are interpreted as the model uncertainty.

Our results showed that our baseline segmentation model reaches a high level of accuracy (>95%) for categories such as building, bare soil or wooded areas, but performs less well on vegetation classes with rule-based separation such as trees (>2m height) and bushes (<2m height), or classes defined by external information such as ruderal areas (see Figure 1). Uncertainty maps highlight the uncertainty in the prediction close to shadowed areas, class boundaries or unusual appearance of a class. Combining the uncertainty maps (see Figure 2) with the predictions accuracy make it possible to select areas where human verification is needed: some potential wrong predictions (low confidence, low accuracy), or mislabelled areas (high confidence, low accuracy).

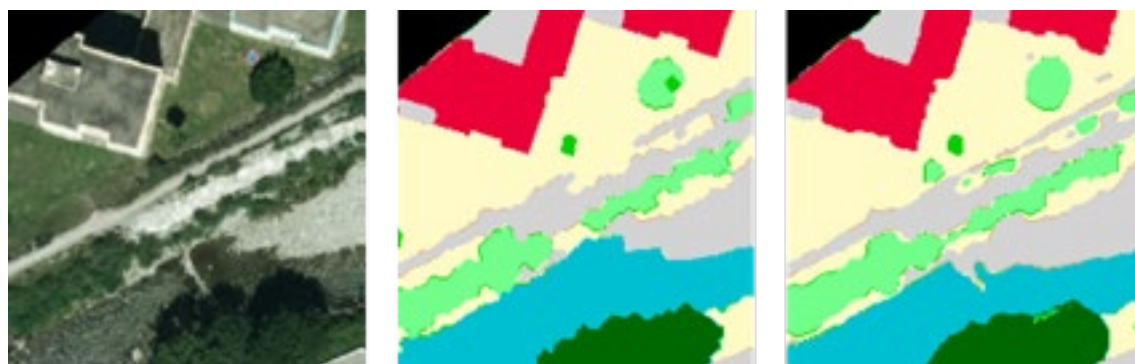


Figure 1: Left: an aerial image given as input; Center: the ground truth land cover labels; right: the classes predicted by our model.

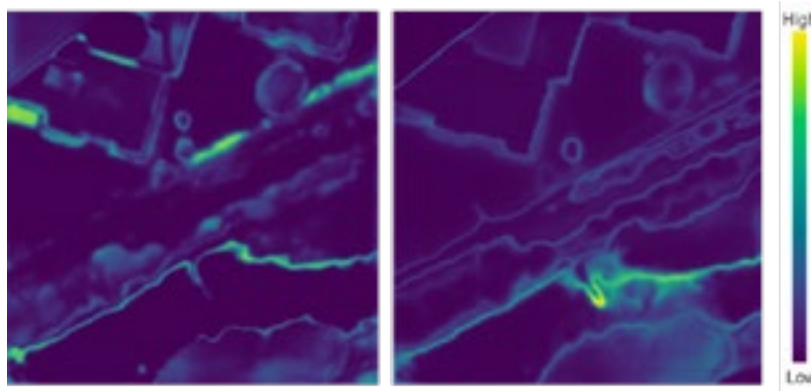


Figure 2: Left: Data uncertainty; Right: Model uncertainty for the example in Figure 1.

## REFERENCES

- Gal, Y., Ghahramani, Z., 2016. Dropout as a Bayesian Approximation: Representing Model Uncertainty in Deep Learning, in: Proceedings of The 33rd International Conference on Machine Learning. Presented at the International Conference on Machine Learning, PMLR, pp. 1050–1059.
- Gawlikowski, J., Tassi, C.R.N., Ali, M., Lee, J., Humt, M., Feng, J., Kruspe, A., Triebel, R., Jung, P., Roscher, R., Shahzad, M., Yang, W., Bamler, R., Zhu, X.X., 2021. A Survey of Uncertainty in Deep Neural Networks. arXiv.org.
- Ronneberger, O., Fischer, P., Brox, T., 2015. U-Net: Convolutional Networks for Biomedical Image Segmentation, in: Navab, N., Hornegger, J., Wells, W.M., Frangi, A.F. (Eds.), Medical Image Computing and Computer-Assisted Intervention – MICCAI 2015, Lecture Notes in Computer Science. Springer International Publishing, Cham, pp. 234–241. [https://doi.org/10.1007/978-3-319-24574-4\\_28](https://doi.org/10.1007/978-3-319-24574-4_28)

**P 21.1****Bayesian inversion using adaptive sequential Monte Carlo combined with surrogate modelling**

Macarena Amaya<sup>1</sup>, Niklas Linde<sup>1</sup>, Giovanni Meles<sup>1</sup>

<sup>1</sup> *Institute of Earth Sciences, University of Lausanne, Switzerland  
(macarena.amaya@unil.ch)*

In the context of Bayesian inversion, traditional Markov chain Monte Carlo (MCMC) methods are commonly used to estimate posterior probability density functions (PDFs). Their efficiency can be limited when the inverse problems is highly non-linear and high-dimensional, thereby, failing to properly explore and sample the posterior PDF given realistic computation budgets. One way to circumvent such issues is to rely on tempering, which gives less weight to the likelihood function and, therefore, enhances the freedom of exploration. In particular, Sequential Monte Carlo methods (SMC) are particle approaches that build a sequence of importance sampling steps between neighbouring tempered distributions called power posteriors, thereby, bridging the prior and the posterior PDF. To ensure high quality estimation, SMC methods perform resampling steps when the variance of the particle weights become too high. To optimize the tempering schedule, we rely herein in adaptive sequential Monte Carlo (ASMC), a method which tunes the reduction in temperature between neighbouring power posteriors that work well for many problem-settings where advanced state-of-the-art MCMC methods struggle or fail. Still, its computational cost is high as many expensive forward simulations are required. Surrogate modelling are used to emulate the behaviour of the expensive forward solvers at much faster computational times. In this study, we incorporate a polynomial chaos expansion (PCE) surrogate model to ASMC inversion and evaluate it for a cross-hole tomography problem. We compare our preliminary results with previously obtained results obtained with standard MCMC (with or without surrogate modelling) and explore the value of updating the surrogate model as the ASMC tempered sequence progresses.

**P 21.2****Modelling the Impact of Glacier Retreat on Vegetation Dynamic**

Luca Eiholzer<sup>1</sup>, Marj Tonini<sup>1</sup>, Gianalberto Losapio<sup>1</sup>

<sup>1</sup> Institute of Earth Surface Dynamics, University of Lausanne, Quartier UNIL-Mouline, Bâtiment Géopolis, CH-1015 Lausanne (luca.eiholzer@unil.ch)

The retreat of glaciers is one of the emblematic effects of global warming, especially in the Alps, which leave the mountain landscape progressively uncovered by ice (Joerin et al., 2006) and colonized by plants. However, plants that inhabit the areas in front of retreat glaciers are exposed to climate warming and glacier retreat, with extinction risk increasing for early colonizers and pioneers (Losapio, 2021). This master project aims at developing a spatio-temporal model to predict the vegetation dynamic following glacier retreat. Species distribution maps for plants most sensitive to glacier retreat and glacier disappearance will be developed. We aim to estimate the risk of extinction and biodiversity loss under different scenarios and factors. This interdisciplinary work, involving biology, botany, and geo-informatics, is important in the field of geo-environmental sciences and represents a promising application in conservation biology and ecosystem management. Indeed, political authorities are increasingly using ecological data modelling tools to establish protected areas.

The study area is located at Glacier du Mont Miné (Val d'Herens, Valais, Switzerland), where its foreland extend in the subalpine zone over 2 km from 1'900 m to 2'000 m asl. A second area in Anniviers Valley was chosen to evaluate the spatial generalization capability of the model, which is, if the model trained in Ferpecle Valley is able to make good prediction in another area holding similar characteristics. A vegetation survey with a stratified random sampling approach, was carried out in July and August 2022. First, by means of a GPS, we elaborated a spatial inventory of key plant species and plant functional types (herb, graminoid, shrub, tree seedling, tree sapling, and tree adult) in 120 plots of 1 x 1 m<sup>2</sup>. Tree diameter and height were measured too. We also developed environmental maps including different factors such as year of glacier retreat and geomorphology. The applied methodology is based on standard protocols for species distribution models ( Araújo et al., 2019; Zurell et al., 2020) involving model fitting (selection and complexity), assessment and predictions. The final goal is to reconstruct the colonization and local extinction of plant species and vegetation during the last 170 years and to forecast their distribution for the next 50 years. This work shall ultimately contribute to mitigate and anticipate the impact of glacier retreat on biodiversity and ecological systems.

**REFERENCES**

- Araújo, M. B., Anderson, R. P., Márcia Barbosa, A., Beale, C. M., Dormann, C. F., Early, R., Garcia, R. A., Guisan, A., Maiorano, L., Naimi, B., O'Hara, R. B., Zimmermann, N. E., & Rahbek, C. 2019: Standards for distribution models in biodiversity assessments. *Science Advances* 5(1), eaat4858. <https://doi.org/10.1126/sciadv.aat4858>
- Joerin, U. E., Stocker, T. F., & Schlüchter, C. 2006: Multicentury glacier fluctuations in the Swiss Alps during the Holocene. *The Holocene* 16(5), 697–704. <https://doi.org/10.1191/0959683606hl964rp>
- Losapio, G., Cerabolini, B. E. L., Maffioletti, C., Tampucci, D., Gobbi, M., & Caccianiga, M. 2021: The Consequences of Glacier Retreat Are Uneven Between Plant Species. *Frontiers in Ecology and Evolution* 8. <https://www.frontiersin.org/article/10.3389/fevo.2020.616562>
- Zurell, D., Franklin, J., König, C., Bouchet, P. J., Dormann, C. F., Elith, J., Fandos, G., Feng, X., Guillera-Arroita, G., Guisan, A., Lahoz-Monfort, J. J., Leitão, P. J., Park, D. S., Peterson, A. T., Rapacciulo, G., Schmatz, D. R., Schröder, B., Serra-Díaz, J. M., Thuiller, W., ... Merow, C. (2020). A standard protocol for reporting species distribution models. *Ecography* 43(9), 1261–1277. <https://doi.org/10.1111/ecog.04960>

**P 21.3****Sequential Monte Carlo for posterior risk assessment**

Lea Friedli<sup>1</sup>, Niklas Linde<sup>1</sup>, David Ginsbourger<sup>2</sup> and Arnaud Doucet<sup>3</sup>

<sup>1</sup> Institute of Earth Sciences, University of Lausanne, Switzerland;

<sup>2</sup> Institute of Mathematical Statistics and Actuarial Science and Oeschger Center for Climate Change Research, University of Bern, Switzerland;

<sup>3</sup> Department of Statistics, Oxford University, United Kingdom.

We consider non-linear Bayesian inversion problems in which we infer an unknown hydrogeological or geophysical property field by using hydrogeological or geophysical data. In practice, one is often not interested in the field itself, but in a quantity depending on the field through non-linear relationships, for instance, in the probability of this quantity exceeding a critical threshold. We estimate a hydraulic conductivity field using pumping tests and aim at predicting the probability of a contamination level exceeding a critical threshold at given time since the release of a pollutant. The classical approach to infer Bayesian posteriors is to apply a sampling method such as the Metropolis-Hastings (MH) algorithm or the Sequential Monte Carlo (SMC) method. A straightforward extension to risk estimation is then to perform forward modeling on the posterior samples in order to estimate the probability of exceeding the threshold of interest. However, since the rare events of interest are likely associated with the tails of the posterior, it is challenging to estimate their occurrence with such a brute force approach. Instead, we propose a sequential application of SMC algorithms. The first stage relies on a particle estimation of the posterior using a sequence of probability density functions giving increasing weights to the likelihood. To subsequently estimate the risk of the rare event, a second SMC is applied. Using an increasing sequence of thresholds, in each iteration the particles exceeding the threshold are selected and propagated. We compare the results of this Doubly Sequential Monte Carlo (DSMC) method with the brute force approach. Preliminary results show that the DSMC method requires significantly less samples to guarantee an accurate estimate of the risk.

## P 21.4

# Generative adversarial network for paleo glacial landscape reconstruction

Guillaume Jouvet<sup>1,2</sup>

<sup>1</sup> Institute of Earth Surface Dynamics, University of Lausanne, Lausanne, Switzerland ([guillaume.jouvet@unil.ch](mailto:guillaume.jouvet@unil.ch))

<sup>2</sup> Department of Geography, University of Zurich, Zurich, Switzerland

What would a satellite have seen if it had passed over the Alps during the last glacial maximum? To try to answer this question, we present a deep-learning generative model that predicts plausible glacial landscape texture from climate and glacier related variables. For that purpose, we use climate, topography and Sentinel 2 satellite imagery data of present-day glaciers worldwide to ``instruct'' a Generative Adversarial Network (GAN) how the texture of glaciers and their surroundings is explained from predictive variables. The GAN permits to re-interpret modeled glacier reconstructions into manufactured satellite-like images, which greatly improve the perception and visualization of the landscape. To illustrate the potential of the method, we reconstruct the texture of the Alpine landscape during the last glacial maximum, when most of it was cover by ice, from coupled climate-glacier model results presented in a companion SGM contribution (Jouvet and al., 2022).

## REFERENCES

- Jouvet G., D. Cohen, E. Russo, J. Buzan, Christoph C. Raible, U. H. Fischer, W. Haeberli, M. Imhof, J. K. Becker, A. Landgraf. Coupled climate-glacier modelling of the last glaciation in the Alps. 2022 SGM contribution in Symposia "10. Quaternary Environment".

**P 21.5****Combining inverse autoregressive flows with deep generative networks for improved efficiency and scalability of inverse problems**

Shiran Levy<sup>1</sup>, Eric Laloy<sup>2</sup>, Niklas Linde<sup>1</sup>

<sup>1</sup> Institute of Earth Sciences, University of Lausanne, Lausanne, Switzerland ([shiran.levy@unil.ch](mailto:shiran.levy@unil.ch))

<sup>2</sup> Institute for Environment, Health and Safety, Belgian Nuclear Research Centre, Mol, Belgium

We study the combination of two deep learning methods: normalizing flows and deep generative models, within the context of geophysical inverse problems as an efficient alternative to Markov chain Monte Carlo (MCMC) sampling. Normalizing flows is a series of transport maps transforming an initial density of random variables into a target density. Specifically, we use inverse autoregressive flows (IAF), in which transformation of one instance is conditioned on previous instances. In this context, the flows are blocks of autoregressive neural networks for which the outputs are scale and shift functions applied on the input variables. The target density resulting from the transformation is parameterized by the neural parameters, allowing for more expressive and complex distributions. The IAF transformation is trained by optimizing the neural parameters using variational inference (VI). The objective in VI is to approximate some target distribution parametrically for a given family of distributions. It provides a computationally-efficient approach that scales well to high-dimensional problems. In each training iteration of the IAF, samples from a normal distribution are pushed forward through the invertible, differentiable transformation onto a variational density approximating the posterior of interest. The parameters of the IAF are learned by maximizing the evidence lower bound which is essentially equivalent to minimizing the Kullback-Leibler divergence between the variational density and the target posterior distribution. In our study, we use two different deep generative models: a generative adversarial network (GAN) and a variational autoencoder (VAE), to encode the high-dimensional prior model into a low-dimensional, latent space of normally distributed variables. We compare the presented approach against popular methods for solving geophysical inverse problems such as deterministic gradient-based methods and MCMC sampling. Due to the nonlinearity of GANs, previous attempts incorporating GANs and deterministic gradient-based inversion failed. Nonetheless, when tested on channelized subsurface models given nonlinear physics the posterior approximation resulting from the IAF is in agreement with the true model for both types of generative models and provides a reliable uncertainty quantification when the VAE is used. Moreover, the training of the IAF is seven times faster than an equivalent MCMC inversion.

## P 21.6

# Advanced spatial learning technique for automatic mapping of geomorphological features in alpine periglacial environment

Alessio Poloni<sup>1</sup>, Dr. Marj Tonini<sup>1</sup>, Dr. Christophe Lambiel<sup>1</sup>

<sup>1</sup> Institut des Dynamiques de la Surface Terrestre (IDyST), University of Lausanne, Batiment Geopolis, CH-1015 Lausanne (alessio.poloni@unil.ch)

Permafrost corresponds to unconsolidated sediments or bedrock that remains frozen for at least two consecutive years (Rogger et al. 2017). This phenomenon is difficult to observe because it occurs in the sub-surface and is therefore invisible to the naked eye. Permafrost is an important component of high mountain regions, and its investigation is of current interest, especially with regard to its evolution in relation to ongoing climate changes. The main controlling factors are the mean annual air temperature, the solar radiation, the characteristics of the ground surface and of the active layer, and the snow duration and depth.

In mountainous regions such as the Alps, characterised by highly variable micro-climatic, topographical and terrain roughness conditions, the spatial distribution of permafrost is very heterogeneous. This complex pattern makes it difficult to map at the local scale. Several permafrost distribution models, based on physical, empirical or statistical approaches, have been developed, but these models tend to overestimate the actual extent of permafrost. In recent years, interest about prediction of the presence or absence of permafrost determined through the use of machine learning algorithms has grown.

Machine learning methods are increasingly applied in geo-environmental applications to predict the occurrence of a phenomenon based on the observations of its presence in a given area and on a set of predictive factors. The Machine learning domain includes algorithms capable of learning from data, by modelling the hidden relationships linking a set of input and output variables. For permafrost distribution, models based on Random Forest (RF) have proven to be efficient and accurate (Deluigi et al. 2017), but the algorithm is generally applied in a “non-spatially” way, and it cannot consider the spatial relationships between variables.

In this research, an advanced classification algorithm is developed with the aim of determining the occurrence of permafrost at the local scale with high accuracy. This algorithm is based on two methods derived from RF, which additionally allow a spatial analysis of the phenomenon: Geographical RF (Georganos et al. 2019) and Spatial RF (Benito 2021). The novelty of this approach consists also in the addition of new parameters related to the terrain roughness (Figure 1). The input dataset includes twelve control variables (air temperature, solar radiation, plan curvature, profile curvature, grain size, altitude, northness, eastness, slope degree, ndvi, poly and lithology). The final output will be a high-precision permafrost susceptibility map of the selected study area, which will also consider the spatial contiguity among the pixels.

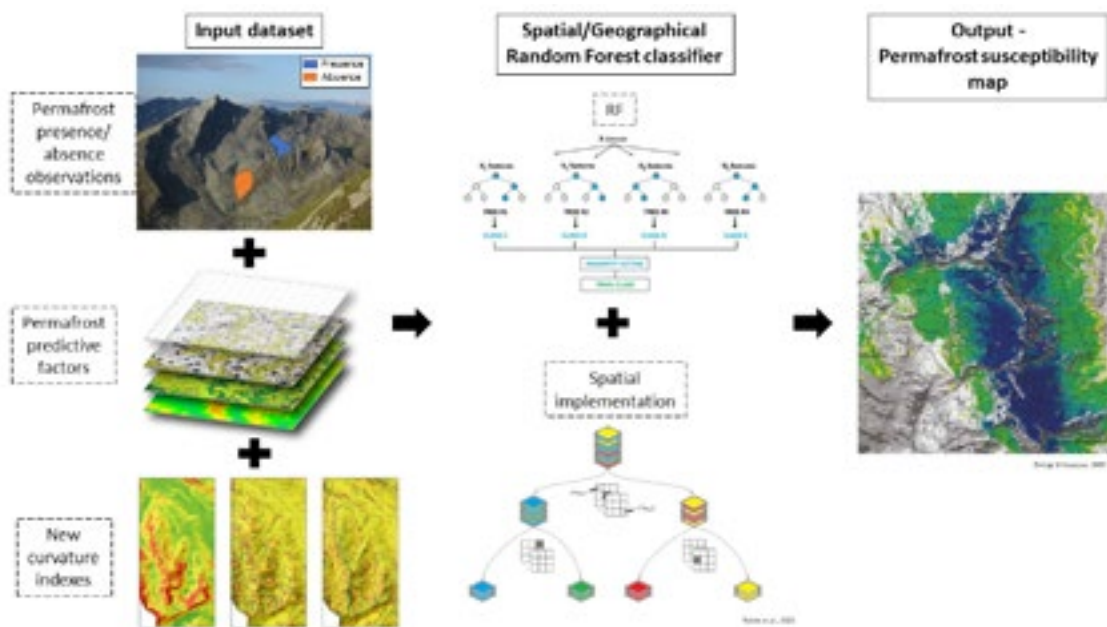


Figure 1. Methodology workflow diagram.

## REFERENCES

- Blas M. Benito. 2021. R package spatialRF: Easy Spatial Regression with Random Forest. doi: 10.5281/zenodo.4745208. <https://blasbenito.github.io/spatialRF/>
- Deluigi, N., Lambiel, C., & Kanevski, M. 2017. Data-driven mapping of the potential mountain permafrost distribution. *Science of The Total Environment*, 590-591, 370-380. <https://doi.org/10.1016/j.scitotenv.2017.02.041>
- Georganos, S., Grippa, T., Niang Gadiaga, A., Linard, C., Lennert, M., Vanhuysse, S., . . . Kalogirou, S. 2021. Geographical random forests: A spatial extension of the random forest algorithm to address spatial heterogeneity in remote sensing and population modelling. *Geocarto International*, 36(2), 121-136. <https://doi.org/10.1080/10106049.2019.1595177>
- Rogger, M., Chirico, G. B., Hausmann, H., Krainer, K., Brueckl, E., Stadler, P., & Bloeschl, G. 2017. Impact of mountain permafrost on flow path and runoff response in a high alpine catchment. *Water Resources Research*, 53(2), 1288-1308.

**P 21.7****Mountain Landslide susceptibility assessment by Multi-sampling strategy combining optimization of BiLSTM algorithm**

Jingjing Wang<sup>1,3</sup>, Gang Chen<sup>2</sup>, Michel Jaboyedoff<sup>3</sup>, Marc-Henri Derron<sup>3</sup>

<sup>1</sup>. Key Laboratory of Geological Survey and Evaluation of Ministry of Education, China University of Geosciences, Wuhan 430074, China (wangjingjing\_cug@163.com)

<sup>2</sup>. College of Marine Science and Technology, China University of Geosciences, Wuhan 430074, China

<sup>3</sup>. Institute of Earth Sciences, University of Lausanne, Lausanne 1015, Switzerland

Machine learning models have been widely used in landslide susceptibility assessment. However, landslide feature extraction, prediction quantification, and representation are still challenges. This paper proposes a multi-sampling strategy combining optimization of the BiLSTM (Bidirectional Long Short-Term Memory) algorithm to evaluate landslide susceptibility in mountainous areas. The proposed method mainly involves three steps: (1) The spatial correlations were analyzed between historical landslides and geographic environment factors, such as topography (DEM, slope, aspect, curvature, surface relief, faults, land subsidence, etc.), hydrogeology (terrain moisture index, rivers, etc.), vegetation cover, earthquake, and human activity (roads, land use) in Sichuan province. Then landslide Inducing factors were selected and expressed quantitatively. The landslide density within the statistical grid cell is used as a predictor to define the landslide probability. The landslide density statistical index refers to the ratio of the number of historical landslide points counted cell grid area. The index was used as the classification basis of susceptibility, which can better reflect the spatial clustering characteristics of landslides than traditional machine learning using a single landslide point as a classification. (2) Construction of multi-channel landslide feature engineering. With multi-band fusion technology, multi-band raster image files in datasets were read, processed, and visualized. The sample information was stored as an image with multiband information and then fed into the algorithm. The method can achieve pixel-by-pixel feature extraction of landslides from high-dimensional multi-source geographic data. Compared with the traditional pixel points represented by a set of matrices as input, it avoids the loss of landslide information because the landslide is a surface and not just a point. (3) The dataset is derived from the Qinba Mountains and the eastern Hengduan Mountains in Sichuan Province. The ratio of the number of samples in the training set, validation set, and test set is 6:2:2. The total number of examples in the data set varies, depending on different sampling strategies. Based on transfer learning, we use a realistic landslide distribution scenario simulation and Bayesian optimization variable strategy to analyze the influence of the proportion of positive and negative samples in the BiLSTM algorithm training process on the prediction results.

The consequence shows that the deep neural network model jointly optimized by multiple sampling strategies can effectively extract the spatial distribution of landslides in complex environments and accurately predict the spatial location of potential landslides.

**REFERENCES**

- Pham B T, Pradhan B, Bui D T, et al. J.2016; A comparative study of different machine learning methods for landslide susceptibility assessment: A case study of Uttarakhand area (India). Environmental Modelling & Software, 84: 240-250.
- Orhan O, Bilgilioglu S S, Kaya Z, et al. J.2022; Assessing and mapping landslide susceptibility using different machine learning methods. Geocarto International, 37(10): 2795-2820.

## 23 Alpine Hazards: Early Detection, Monitoring, Warning, Modelling, Mitigation

Andrea Manconi, Yves Bühler, Elisabeth Hafner, Cristina Pérez-Guillén, Antonio Abellán, Michel Jaboyedoff, Virginia Ruiz-Villanueva, Saskia Gindraux

### TALKS:

- 23.1 Aaron J., Spielmann R., McArdell B.W., Graf C.: In-Situ Measurements of Debris-Flow Surge Velocities and Feature Trajectories Derived from High-Frequency 3D LiDAR Scanners, Illgraben, Switzerland
- 23.2 Baracchini T., Brauchli T., Roquier B., Abellán A.: From observations to crisis management: developments of the MINERVE operational flood forecasting system for the canton of Wallis
- 23.3 Bickel V. T., Dasser G., Manconi A., Jacquemart M., Bühler Y., van Herwijnen A., Hendrick M.: Spatiotemporal Characterization of Snow Wetness Evolution with Sentinel-1
- 23.4 Choanji T., Fei Li., Wolff C., Sun C., Bourrier F., Gaucher R., Kouamé J.K., Derron M.H., Jaboyedoff M.: Monitoring rockfall stability along Massive external crystalline in Alps zone : Case of La Grave, France
- 23.5 Hafner E.D., Barton P., Daudt R.C., Wegner J.D., Schindler K., Bühler Y.: Deep learning approach to automatically identify avalanches in optical SPOT 6/7 imagery
- 23.6 Husmann L., Chmiel M., Walter F.: Seismic and infrasound monitoring at the active rock slope of Spitze Stei – Switzerland
- 23.7 Li F., Davide B., Tiggi C., Marc-Henri D., Michel J., Fabrizio T., Patrick T., Joëlle Hélène V., Charlotte W.: Analysis of slope failure activity on the Brenva rockslide scar based on a 5-year remote sensing survey under the ongoing climate change in the Alps (Mont Blanc massif, Aosta Valley, Italy)
- 23.8 Tessari G., Riccardi P., Cantone A., Defilippi M., Giardino A., Arrigo F., Zajc T., Pasquali P.: Land motion monitoring service over Switzerland through interferometric multi-temporal analyses of Sentinel-1 SAR data
- 23.9 Uhlmann D., Vicari J.H., Jaboyedoff M., Derron M-H., Wolff C., Gutiérrez A., Ravanel L., Fei L., Choanji T.: The Mont Blanc Massif high resolution topography project: a baseline for future rockfall and landslide events
- 23.10 Wolff C., Choanji T., Derron M.H., Fei L., Jaboyedoff M., Pedrazzini A., Rivolta C.: Combining remote sensing techniques for the study of active fractures in a challenging remote area: Case of Cima Del Simano rockslide

## POSTERS:

- P 23.1 Carrel M., Gassner J., Staehly S., Wahlen S.: Interferometric radar monitoring of the Spitze Stei landslide under challenging conditions
- P 23.2 Oppikofer T., Michoud C., Malet J.-P., Deprez A., Provost F., Foumelis M., Garcia Robles J., Pacini F.: Satellite Earth observation data for monitoring landslides in the Alps
- P 23.3 Oestreicher N., Manconi A., Roques C., Gualandi A., Loew S.: Postglacial Elastic Rebound and Pore Pressure Deformation from Satellite Radars
- P 23.4 Travaglini E., Roquier B., Brauchli T., Gimbert F., Moerschel J., Abellan A.: Bedload monitoring using seismic sensors
- P 23.5 Bula J., Guerin J., Baillifard F., Gressin A.: Low-cost terrestrial photogrammetry for rock cliff monitoring
- P 23.6 Dasser G., Manconi A., Buehler Y., Munch J., Bartelt P.: Identifying and classifying potential slope instabilities using space-borne radar interferometry in the Bhagirathi Valley, Uttarakhand, India
- P 23.7 Häusler M., Nicollier T., Fäh D.: Spektrum: implementing seismic techniques for landslide investigations in practice
- P 23.8 Biedermann B., Dubas O., Heller P., Le Doucen O., Lévy S.: Role of the forest and avalanche defensive structures on the torrential flooding of the Baye de Montreux
- P 23.9 Caduff R., Jones N., Strozzi T., Wegmüller U.: L-Band DInSAR Surface Motion Products in Alpine Regions with ALOS-2 PALSAR-2
- P 23.10 Walden J., Jacquemart M., Higman B., Farinotti D.: Paraglacial landslide response to glacier debuttressing in southern Alaska
- P 23.11 Schöttner J., Walet M.: Quantifying the role of microstructure to improve mechanical modeling of weak snow layers

## 23.1

# In-Situ Measurements of Debris-Flow Surge Velocities and Feature Trajectories Derived from High-Frequency 3D LiDAR Scanners, Illgraben, Switzerland

Jordan Aaron<sup>1</sup>, Raffaele Spielmann<sup>1,2</sup>, Brian W. McArdell<sup>1</sup>, Christoph Graf<sup>1</sup>

<sup>1</sup> Swiss Federal Institute for Forest, Snow and Landscape Research WSL, Zürcherstrasse 111, CH-8903 Birmensdorf (jordan.aaron@wsl.ch)

<sup>2</sup> Engineering Geology Group, Geological Institute, Department of Earth Sciences, ETH Zürich, Sonneggstrasse 5, CH-8092 Zürich

Debris flows are mixtures of coarse and fine grained particles, woody debris, and water that can travel for long distances at high velocities (Hung et al., 2014). They are an important hazard in mountainous areas, and an improved understanding of fundamental debris-flow mechanisms, such as longitudinal sorting and surging, requires detailed field observations of moving debris flows. In the present work, we detail the first results obtained from a new sensor system integrated into the WSL debris-flow monitoring station at Illgraben, Switzerland. The new system has collected data from four recent debris-flow events.

The newly installed sensor array includes multiple high-temporal resolution LiDAR scanners, and high-definition video cameras. It is comprised of three stations suspended over the channel at various positions on the fan. We process the data by fusing the LiDAR and video camera data, and by applying deep learning and machine vision algorithms (Figure 1), in order to derive dense surface velocity fields, flow depths, feature trajectories, and surge velocities.

We show that debris-flow behaviour is strongly influenced by the coarse fraction of the debris-flow mixture, and that the shape and velocity of debris flow surges strongly varies throughout the event. We further automatically derive the size and velocity of thousands of boulders present in one event (Figure 1), and show that the average size of large particles is at a maximum during the passage of the flow front, and steadily decreases thereafter. The new data collected provides a unique view into many aspects of debris-flow motion, and should provide the foundation for an improved understanding of this damaging natural hazard.

## REFERENCES

- Hung, O., Leroueil, S. & Picarelli, L. The Varnes classification of landslide types, an update. *Landslides* 11, 167–194 (2014). <https://doi.org/10.1007/s10346-013-0436-y>

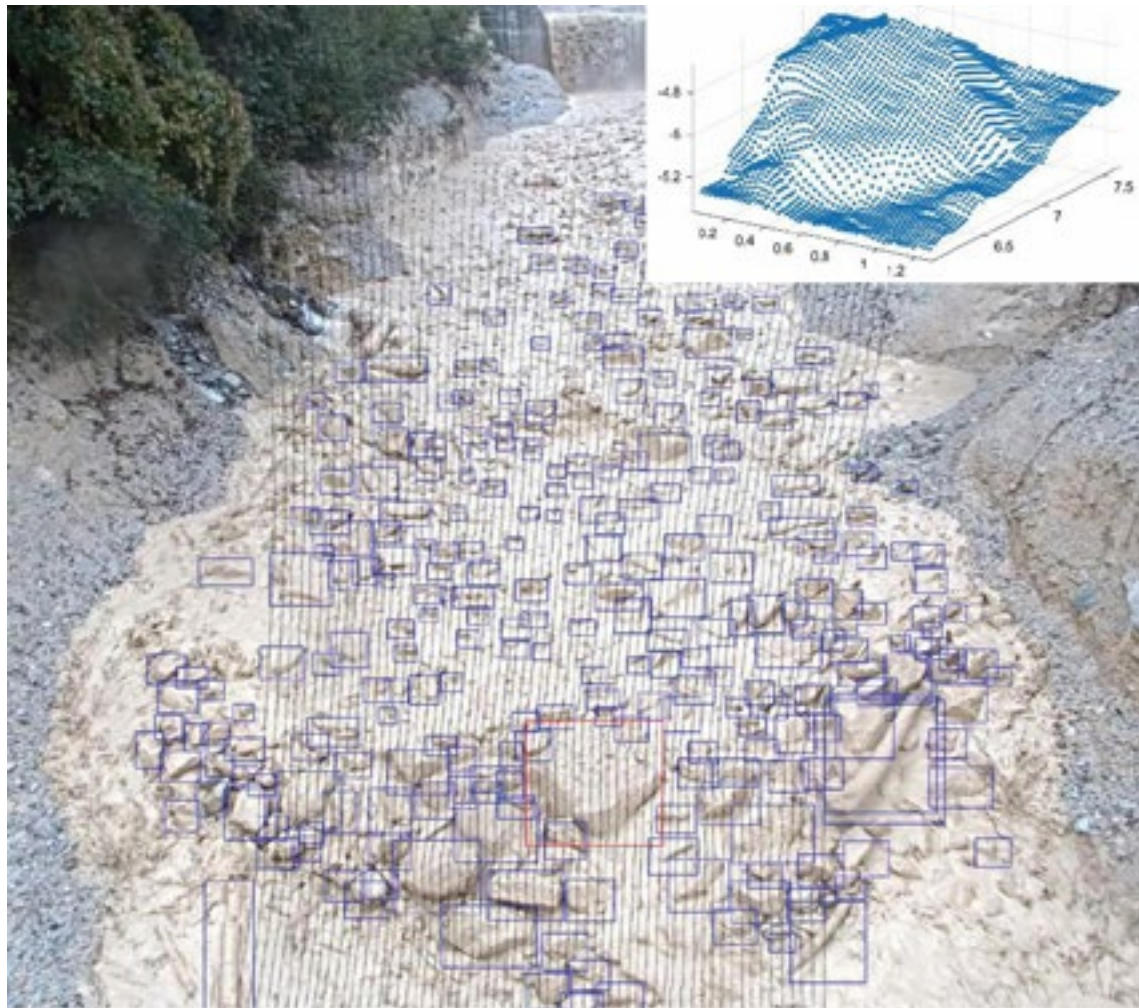


Figure 1: Example frame collected by the new monitoring system during an event. The blue boxes show features automatically detected with a convolutional neural network. The black dots show the LiDAR scan overlain on the image. The inset shows the point cloud associated with the detection in the red box, with axis labels in meters and referenced to a local coordinate system.

## 23.2

# From observations to crisis management: developments of the MINERVE operational flood forecasting system for the canton of Wallis

Theo Baracchini<sup>1</sup>, Tristan Brauchli<sup>1</sup>, Bastien Roquier<sup>1</sup>, Antonio Abellán<sup>1</sup>

<sup>1</sup> Centre de Recherche sur l'Environnement Alpin CREALP, Rue de l'industrie 45, 1950 Sion (theo.baracchini@crealp.vs.ch)

Alpine regions are particularly vulnerable to extreme precipitation and floods, yet due to their complex topography, capturing such dynamics is still among the major challenges of our time. Moreover, with climate evolving at a rapid pace and expected increases in extreme weather events (Witze 2018), understanding and forecasting changes in hydrological regime of alpine environments is now of paramount importance. In Switzerland, a number of recent flooding events has highlighted the need for more reliable forecasting systems to mitigate flood impacts (Liechti et al. 2022).

A complex hydrologic-hydraulic forecasting model for the entire Upper Rhone river basin funded by the canton of Wallis is continuously being operated since 2011 by CREALP (García Hernández et al. 2014). The MINERVE real-time flood forecasting system provides automated warnings to a crisis cell of the canton and is capable of providing guidance for preventive emptying operations of reservoirs to mitigate flood damage.

The system relies on 114 hydro-meteorological stations covering in real-time a domain split into 1440 hydrological models (altitude bands). It automatically collects meteorological forecasts from various providers and numerical atmospheric models, as well as numerous spatial observations (satellites, radars). A free in-house developed hydrological-hydraulic modelling software RS MINERVE (Foehn et al. 2020; García Hernández et al. 2020) performs the simulations, which are made available on an online platform called GUARDAVAL<sup>1</sup> (Figure 1). The MINERVE system is therefore a modern and advanced flood management system.

In this study, we present the functioning and latest developments of the MINERVE system. Emphasis is put on the hydrological model, which is based on a new variant of the well-established HBV model (Bergström 1995). Through the addition of non-linearities in the hydrological response, we are able to improve the performance of various watersheds models, particularly during flood events. Finally, we discuss the perspectives of such system by presenting on-going developments with new ensemble approaches and data assimilation.

Through this study, we provide a series of tools and frameworks for the implementation of operational hydrological forecasting systems, expandable to other regions of the world, capable of providing timely environmental information for evidence-based decision-making.

## REFERENCES

- Bergström S (1995) The HBV model. Computer models of watershed hydrology 443–476
- Foehn A, García Hernández J, Roquier B, Fluixá-Sanmartín J, Brauchli T, Paredes Arquiola J, De Cesare G (2020) RS MINERVE – User manual v2.15
- García Hernández J, Claude A, Paredes Arquiola J, Roquier B, Boillat J-L (eds) (2014) Integrated flood forecasting and management system in a complex catchment area in the Alps—implementation of the MINERVE project in the Canton of Valais. River Flow 2014, Special Session on Swiss Competences in River Engineering and Restoration. <https://doi.org/10.1201/b17134-12>
- García Hernández J, Foehn A, Fluixá-Sanmartín J, Roquier B, Brauchli T, Paredes Arquiola J, De Cesare G (2020) RS MINERVE – Technical manual v2.25
- Liechti K, Matter D, Lustenberger F, Badoux A (2022) Unwetterschäden in der Schweiz 2021. Hochwasser, Murgänge, Rutschungen und Sturzprozesse. Wasser, Energie, Luft 85–93
- Witze A (2018) Why extreme rains are gaining strength as the climate warms. Nature 563:458–460. <https://doi.org/10.1038/d41586-018-07447-1>

<sup>1</sup> See <https://crealp.ch/guardaval/> or [guardaval.vs.ch](http://guardaval.vs.ch)

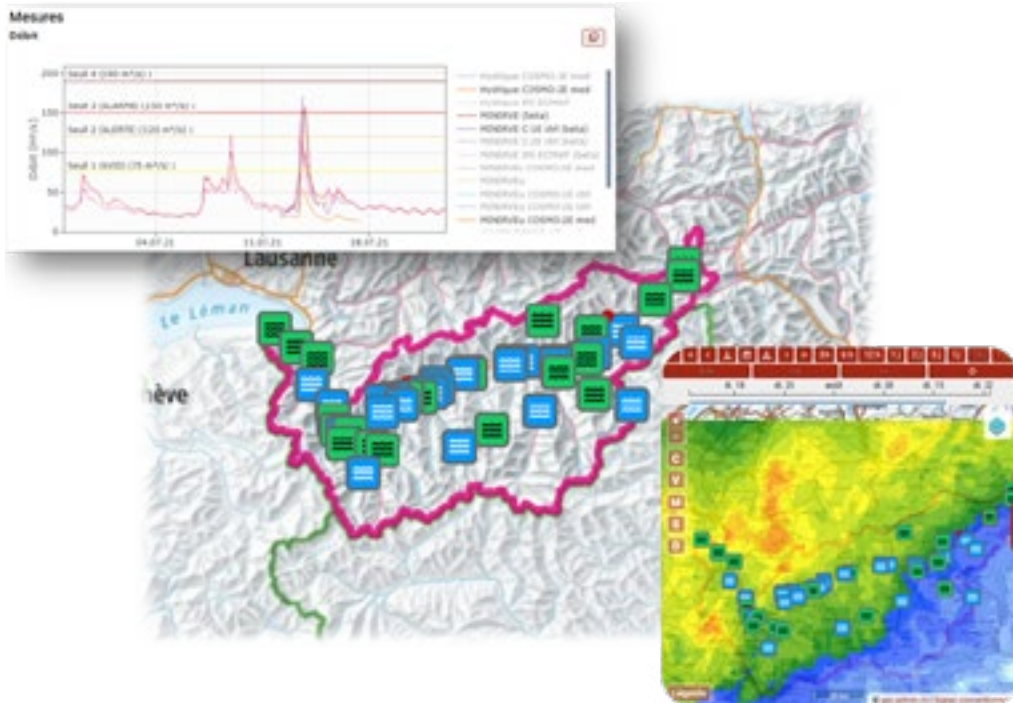


Figure 1. Web interface of the GUARDAVAL platform displaying the MINERVE flood forecasting output. Results of hydrological-hydraulic simulation (up), hydrological stations over the domain (center), spatial precipitation data (down).

## 23.3

### Spatiotemporal Characterization of Snow Wetness Evolution with Sentinel-1

Valentin T. Bickel<sup>1,2</sup>, Gwendolyn Dasser<sup>3,4</sup>, Andrea Manconi<sup>3,4</sup>, Mylène Jacquemart<sup>1,2</sup>, Yves Bühler<sup>3,4</sup>, Alec van Herwijnen<sup>3</sup>, Martin Hendrick<sup>3</sup>

<sup>1</sup> Laboratory of Hydraulics, Hydrology and Glaciology, ETH Zurich, Zurich, Switzerland ([bickel@vaw.baug.ethz.ch](mailto:bickel@vaw.baug.ethz.ch))

<sup>2</sup> Swiss Federal Institute for Forest, Snow and Landscape Research WSL, Birmensdorf, Switzerland

<sup>3</sup> WSL Institute for Snow and Avalanche Research SLF, Davos, Switzerland

<sup>4</sup> Climate Change, Extremes and Natural Hazards in Alpine Regions Research Center CERC, Davos, Switzerland

Wet snow avalanches pose a threat to human life and infrastructure in alpine environments. However, their detection and monitoring require continuous and high-resolution observations of wet snow evolution on large spatial scales and in complex terrain. Spaceborne SAR (Synthetic Aperture Radar) is able to meet those requirements by utilizing temporal changes in the backscattered radar signal. Currently available SAR-based and/or -derived products have several limitations, including limited spatial resolution, geometric artifacts, a dependency on a variety of data sources, and a lack of validation.

This work (1) addresses those limitations by optimizing existing Sentinel-1 (S1) data (pre-)processing routines; (2) demonstrates the potential of SAR data by deploying these routines on regional-scale, multi-year (2018-2021) Local Resolution Weighting (LRW) composites over Davos and Interlaken; and (3) validates the results with SLF weather station data, including observed and modelled parameters (SNOWPACK).

Outputs of this work include - among other things - large-scale, spatiotemporal maps and diagrams of wet snow distribution and evolution with a broad range of downstream applications.

## 23.4

### Monitoring rockfall stability along Massive external crystalline in Alps zone : Case of La Grave, France

Tiggi Choanji<sup>1,2</sup>, Li Fei <sup>1</sup>, Charlotte Wolff <sup>1</sup>, Chunwei Sun <sup>1</sup>, Frack Bourrier <sup>3</sup>, Romain Gaucher <sup>4</sup>, Kan Jean Kouamé <sup>5</sup>, Marc-Henri Derron<sup>1</sup>, Michel Jaboyedoff <sup>1</sup>

<sup>1</sup> Risk Group, ISTE, University of Lausanne, Geopolis – Quartier Mouline 1015 Lausanne (tiggi.choanji@unil.ch)

<sup>2</sup> Department of Geological Engineering, Islamic University of Riau, Pekanbaru Riau 28284, Indonesia

<sup>3</sup> Université Grenoble-Alpes, INRAE, ETNA, 38000 Grenoble, France

<sup>4</sup> Service Ingénierie, Département des Hautes-Alpes, Gap, Provence-Alpes-Côte d'Azur, France

<sup>5</sup> CURAT, Côte d'Ivoire, Bd. De l'Université, Université Félix HOUPHOUËT-BOIGNY d'Abidjan Cocody (Côte d'Ivoire)

Rockfall hazards have emerged as one of the most serious issues endangering highway safety in mountainous areas. The occurrence of rockfall hazards along the road will seriously affect the safety for the road users. As a result, monitoring of rockfall hazards along 17 km roads are required since number of event per year is affect the probabilities of realization to frequencies or return period which is useful for decision making. Historical data shows that from 1999 – 2020 resulting more than 15 events of rockfall along the road. So, by taking consideration of Massive external crystalline in study area which consist of metamorphic rocks (biotic gneiss, amphibolites, amphibolic gneiss) with highly fractured and jointed, annual measurement from LiDAR with point density (40-189 points/m<sup>3</sup>) and more than ± 10.000 of High resolution camera are used for detection and evaluation of rockfall. Based on comparison between two consecutive years (2020-2021), its been identified three blocks with total size  $0.2 \times 10^3$  m<sup>3</sup> falling from the hillslope. Although there are no update report detachment of rock and direct hit into the road, however this continuous monitoring using LiDAR could provide a helpful identification of potential rockfall in the future. Ongoing detailed work on characterization and classification the rock structure using Geological Strength Index (GSI) will be measured using combination of photo images and point cloud data as parameter for estimation rockfall vs block volume scenarios quantitatively.

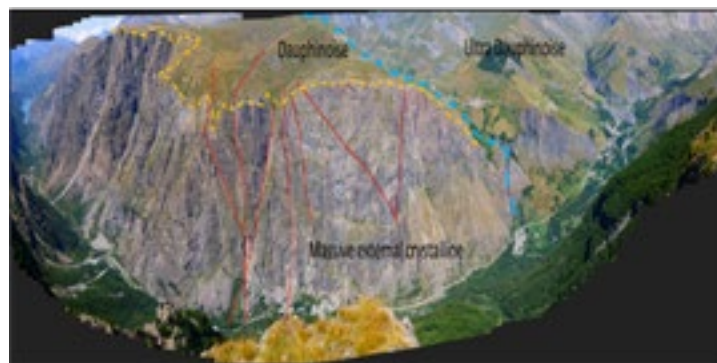


Figure 1. Panoramic view of study area which shows geological complex in Alps with Ultra Dauphinoise boundary with Dauphinoise zone that overlaying Massive External Crystalline in La Grave, France.

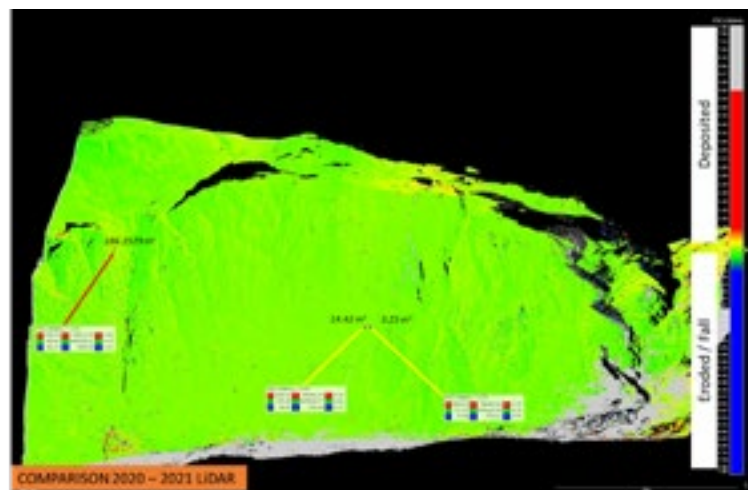


Figure 2. LiDAR Comparison of two consecutive years which showing detaching blocks from hillslope.

## REFERENCES

- Beach, A. 1981: Thrust structures in the eastern Dauphinois Zone (French Alps), north of the Pelvoux Massif, *Journal of Structural Geology*, 3(3), 299–308.
- Brevard, C., & Gidon, M. 1979: La structure du refers oriental du Massif du Hantz, D., Corominas, J., Crosta, G. B., & Jaboyedoff, M. 2021 : Definitions and Concepts for Quantitative Rockfall Hazard and Risk Analysis. *Geosciences*, 11(4), 158.
- Hantz, D., Colas, B., Dewez, T., Lévy, C., Rossetti, J.-P., Guerin, A., & Jaboyedoff, M. 2020: Caractérisation quantitative des aléas rocheux de départ diffus. *Revue Française de Géotechnique*, 163, 2.
- Pelvoux: observations et interprétations nouvelles, *Géologie Alpine*, 55, 23–33.
- Jaboyedoff, M., Oppikofer, T., Abellán, A., Derron, M. H., Loyer, A., Metzger, R., & Pedrazzini, A. 2012 : Use of LIDAR in landslide investigations: A review. *Natural Hazards*, 61(1), 5–28.
- Jaboyedoff, M., Choanji, T., Derron, M. H., Fei, L., Gutierrez, A., Loiotine, L., Noel, F., Sun, C., Wyser, E., & Wolff, C. 2021: Introducing uncertainty in risk calculation along roads using a simple stochastic approach. *Geosciences (Switzerland)*, 11(3), 1–8.
- Oppikofer, T., Jaboyedoff, M., Blikra, L., Derron, M. H., & Metzger, R. 2009: Characterization and monitoring of the Åknes rockslide using terrestrial laser scanning, *Natural Hazards and Earth System Science*, 9(3), 1003–1019.

## 23.5

# Deep learning approach to automatically identify avalanches in optical SPOT 6/7 imagery

Elisabeth D. Hafner<sup>1,2,3</sup>, Patrick Barton<sup>3</sup>, Rodrigo Caye Daudt<sup>3</sup>, Jan Dirk Wegner <sup>3,4</sup>, Konrad Schindler<sup>3</sup>, Yves Bühler<sup>1,2</sup>

<sup>1</sup> WSL Institute for Snow and Avalanche Research SLF, Davos Dorf, 7260, Switzerland ([elisabeth.hafner@slf.ch](mailto:elisabeth.hafner@slf.ch))

<sup>2</sup> Climate Change, Extremes, and Natural Hazards in Alpine Regions Research Center CERC, Davos Dorf, 7260, Switzerland

<sup>3</sup> EcoVision Lab, Photogrammetry and Remote Sensing, ETH Zurich, Zurich, 8092, Switzerland

<sup>4</sup> Institute for Computational Science, University of Zurich, Zurich, 8057, Switzerland

Spatially dense and continuous information on avalanche occurrences is crucial for numerous safety related applications such as avalanche warning, hazard zoning, hazard mitigation measures, forestry, risk management and numerical simulations. As such information is collected in a non-systematic way by observers in the field, there is, especially in situations with high avalanche danger, a strong bias towards avalanches in proximity to accessible infrastructure. In recent years research has shown that remote sensing is capable of mapping avalanches and complementing those existing databases over large areas (e.g. Bühler et al., 2019; Hafner et al., 2021).

After manually mapping avalanches in previous work, we have recently adapted a DeepLabV3+, a fully convolutional neural network (CNN), to automatically identify avalanches in optical SPOT 6/7 data. We used the 24'778 manually annotated avalanche polygons and split them into geographically disjoint regions for training, validating and testing. We achieved an average probability of detection (POD) of 0.610, positive predictive value (PPV) of 0.668 and an F1 score of 0.625 in our test areas (Hafner et al., 2022). In order to understand the current standard to which we could compare those results to, we conducted a reproducibility experiment where we asked experts to identify all visible avalanches in a test region. Our subsequent analysis showed that our model performance is in the same range as manual annotations from different experts.

The ability to automatically, and therefore in a timely manner, identify avalanches from optical satellite imagery is an important step forward in complementing existing databases and providing data for different applications. More complete and less biased avalanche datasets are an important preconditions to improve e.g. the avalanche warning, increasing the safety in Alpine Regions.

## REFERENCES

- Bühler, Y\*, Hafner, E. D\*, Zweifel, B., Zesiger, M., and Heisig, H. 2019: Where are the avalanches? Rapid SPOT6 satellite data acquisition to map an extreme avalanche period over the Swiss Alps, *The Cryosphere*, 13, 3225–3238, <https://doi.org/10.5194/tc-13-3225-2019>. (\* these authors contributed equally)
- Hafner, E. D., Techel, F., Leinss, S., and Bühler, Y. 2021: Mapping avalanches with satellites – evaluation of performance and completeness, *The Cryosphere*, 15, 983–1004, <https://doi.org/10.5194/tc-15-983-2021>.
- Hafner, E. D., Barton, P., Daudt, R. C., Wegner, J. D., Schindler, K., and Bühler, Y. 2022: Automated avalanche mapping from SPOT 6/7 satellite imagery: results, evaluation, potential and limitations, *The Cryosphere Discussions*, 2022, 1–20, <https://doi.org/10.5194/tc-2022-80>.

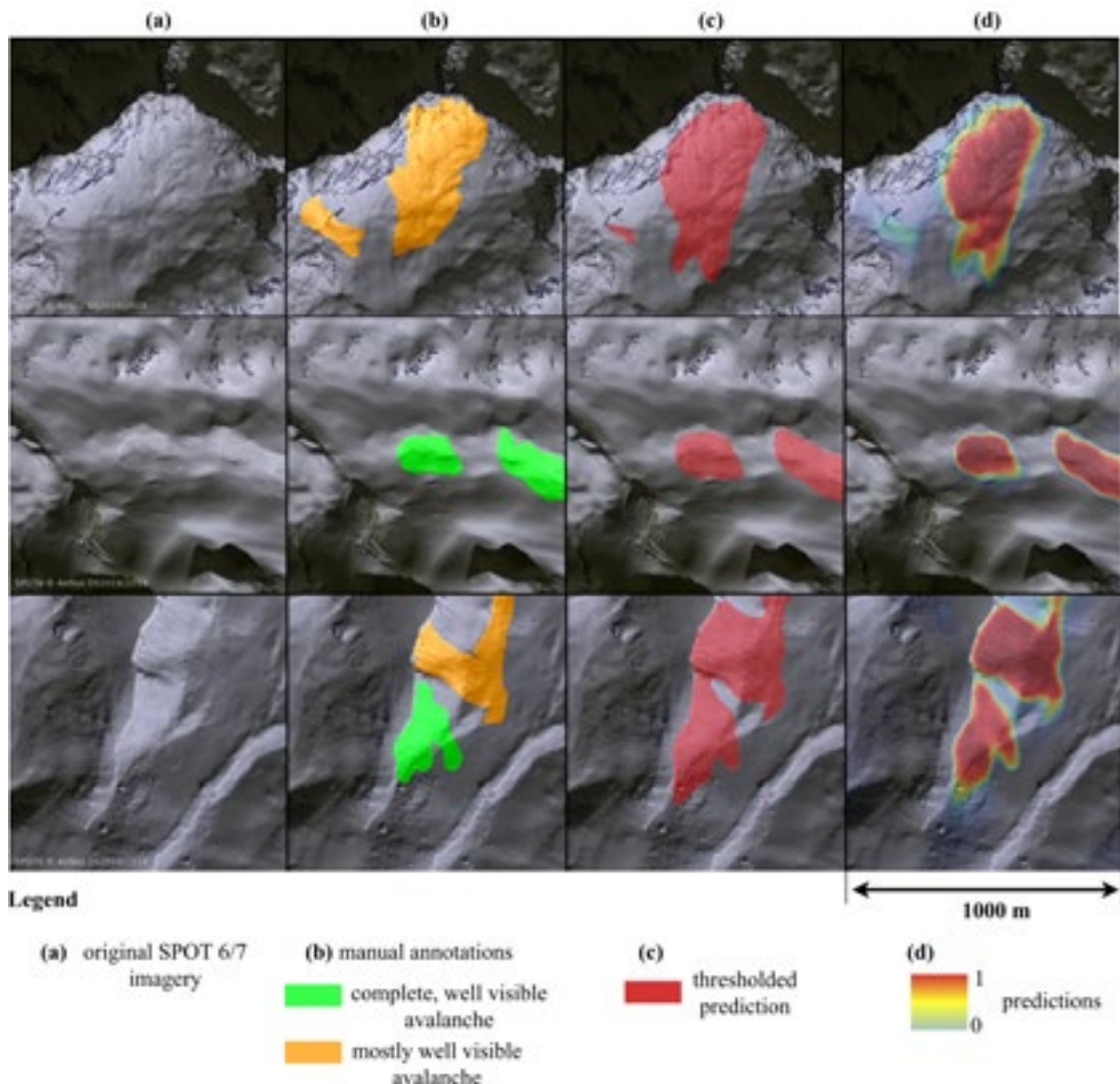


Figure 1. Comparison of results for three patches: (a) the original SPOT 6/7 image, (b) the manually mapped annotations used as reference, (c) the predictions thresholded at 0.5, and (d) the predicted avalanche probability (SPOT 6 data © Airbus DS 2018).

## 23.6

# Seismic and infrasound monitoring at the active rock slope of Spitze Stei - Switzerland

Lena Husmann<sup>1</sup>, Małgorzata Chmiel<sup>2</sup>, Fabian Walter<sup>2</sup>

<sup>1</sup> Institute of Geophysics, ETH Zürich, Sonneggstrasse 5, 8092 Zürich, (lhusmann@student.ethz.ch)

<sup>2</sup> Swiss Federal Institute for Forest, Snow and Landscape Research WSL, Zürcherstrasse 111, 8903 Birmensdorf

Alpine mass movements like landslides or rock falls occur regularly at the Spitze Stei slope, which is located next to the village of Kandersteg in the canton of Bern (Fig. 1). In recent years, activity has intensified, and with it the potential for a possible major event with secondary consequences such as debris flows and flooding (Geotest, 2021). Hence, since 2019, the unstable slope has been continuously monitored with velocity measurements (GPS, ground-based radar) to detect precursory creep acceleration before a major break-off event (Kienholz et al., 2021).

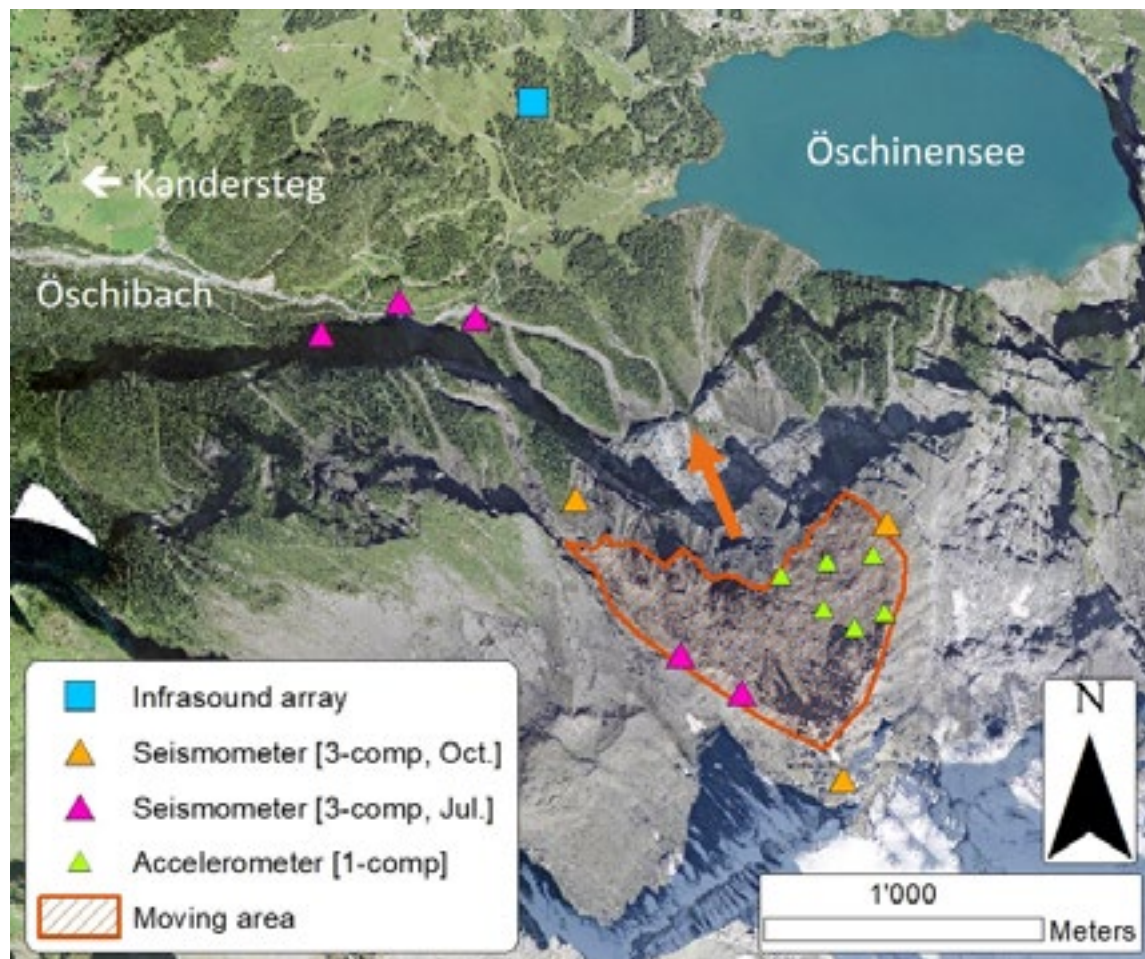


Figure 1. The map shows the area of the Spitze Stei and the unstable part with indicated moving direction (marked in orange). In addition, the installed instruments (seismometers, accelerometers and infrasound array) are marked.

Even though Spitze Stei is under close surveillance, seasonal variations of mass movement activity have not been quantified so far. We use seismic and infrasound measurements (Fig. 2) to investigate the temporal distribution of smaller slope failures producing rock falls and debris avalanches. Our aim is to identify triggers and cycles in slope dynamics by comparing time series of mass movement events to temperature or precipitation measurements, establishing a potential link to climatic factors.

Preliminary results show that a mass movement event can be detected in the seismometer and the infrasound records. We will compile a catalog of them to implement a machine learning algorithm following Chmiel et al., 2021, which allows us to analyze long time series at low costs.

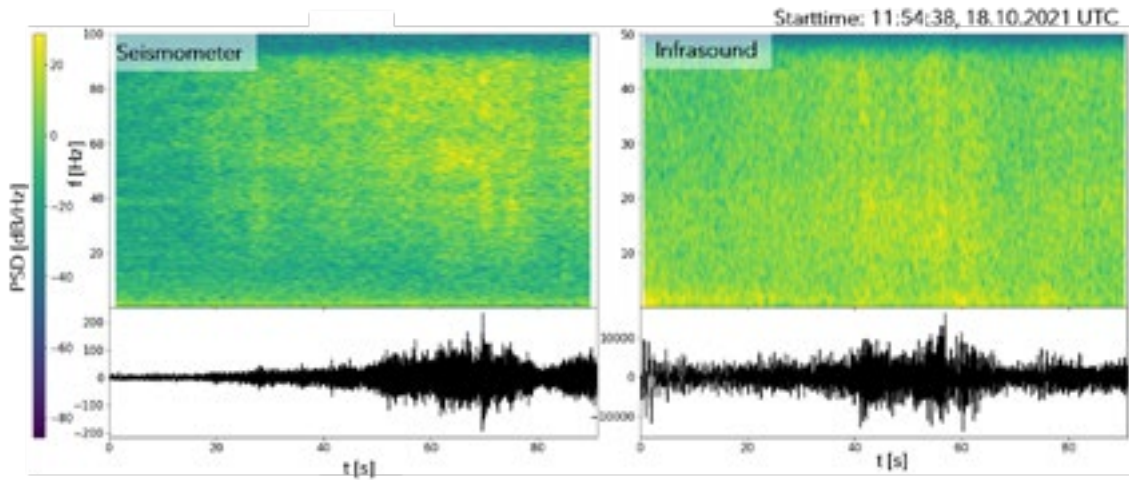


Figure 2. The seismic and infrasound signal of a mass movement event that was recorded by the station at the end of the eastern ridge and by one of the microphones (infrasound array) at Spitze Stei.

## REFERENCES

- M. Chmiel, M., F. Walter, M. Wenner, Z. Zhang, M.A. Brian, C.Hibert. Machine Learning improves debris flow warning, Geophysical Research Letters, 48, e2020GL090874, 2021  
Geotest. Kandersteg, Spitze Stei Sicherheitskonzept Gemeinde, Bericht Nr. 1418139.6a, 2021.  
C. Kienholz, R. Riner, K. Graf, D. Tobler, N. Hählen, and J. Häberle. Monitoring and Hazard Management at the Spitzestei Rockslide, Kandersteg. FAN Agenda, (1):54–62, 2021.

## 23.7

# Analysis of slope failure activity on the Brenva rockslide scar based on a 5-year remote sensing survey under the ongoing climate change in the Alps (Mont Blanc massif, Aosta Valley, Italy)

Li Fei<sup>1</sup>, Davide Bertolo<sup>2</sup>, Tiggi Choanji<sup>1</sup>, Marc-Henri Derron<sup>1</sup>, Michel Jaboyedoff<sup>1</sup>, Fabrizio Troilo<sup>3</sup>, Patrick Thuegaz<sup>2</sup>, Joëlle Hélène Vicari<sup>1</sup>, and Charlotte Wolff<sup>1</sup>

<sup>1</sup> Institute of Earth Sciences, University of Lausanne, Geopolis 3129, CH-1015 Lausanne, Switzerland ([li.fei@unil.ch](mailto:li.fei@unil.ch))

<sup>2</sup> Struttura Attività Geologiche, Regione Autonoma Valle d'Aosta, Italy

<sup>3</sup> Fondazione Montagna Sicura, Courmayeur, Aosta Valley, Italy

The Alps are characterized by the occurrence of rockfalls, rockslides, and rock avalanches that significantly alter the mountain topography and pose a high risk to residents and infrastructures below the failure source area or along the propagation path. Enhanced rock slope failure events in high mountain areas over the last 20 years have increased concern for alpine rock slope instability with climate warming (Gruber et al., 2004; Ravanel et al., 2017; Savi et al., 2021; Viani et al., 2020). The Brenva rockslide scar (Mont Blanc massif, Italy), formed by a large rock avalanche of  $2.0 \times 10^6 \text{ m}^3$  that happened in 1997, was reactivated in 2016 with a failure volume of  $3.5 \times 10^4 \text{ m}^3$ . Following this event, five years of annual Structure from Motion (SfM) photogrammetry survey was done to detect the rock failure activities and monitor the rock failure evolution. During the survey period from 2017 to 2021, 39 rockfall sources were detected with a total volume of  $2.2 \times 10^4 \text{ m}^3$  (Figure 1). The preliminary result shows that rockfall activity seems to have decreased in the recent two years. Still, it does not mean the scar will be stable from a long-term perspective, especially under global warming. The power law well fitted the rock failure magnitude-frequency relationship, and the predicted return period of seven potential rock failure scenarios defined by structural analysis and Slope Local Base Level (SLBL) method was analyzed in detail, which would benefit the risk management and mitigation design for such kinds of hazards. The undergoing survey using the LiDAR technique this summer will help to update the fitted power law and improve the risk estimation for the Brenva rockslide scar, especially after the Mont Blanc massif experienced another exceptional hot wave during the summer of 2022.

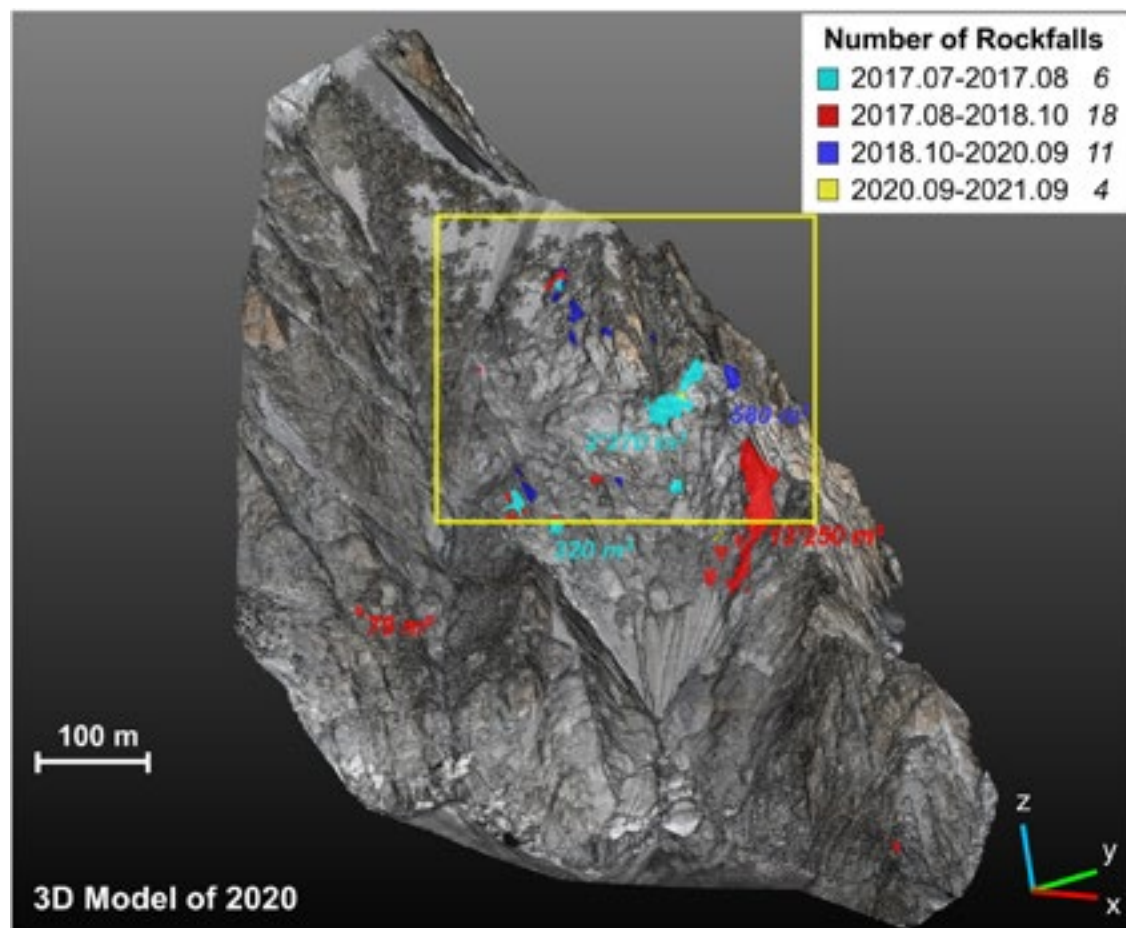


Figure 1. Rock failure activity highlighted for the Brenva rockslide scar employing SfM monitoring from July 2017 to September 2021.

## REFERENCES

- Gruber, S., Hoelzle, M., & Haeberli, W. 2004: Permafrost thaw and destabilization of Alpine rock walls in the hot summer of 2003. *Geophysical Research Letters*, 31(13). <https://doi.org/10.1029/2004GL020051>
- Ravanel, L., Magnin, F., & Deline, P. 2017: Impacts of the 2003 and 2015 summer heatwaves on permafrost-affected rock-walls in the Mont Blanc massif. *Science of the Total Environment*, 609, 132–143.
- Savi, S., Comiti, F., & Strecker, M. R. 2021: Pronounced increase in slope instability linked to global warming: A case study from the eastern European Alps. *Earth Surface Processes and Landforms*, 46(7), 1328–1347. <https://doi.org/10.1002/esp.5100>
- Viani, C., Chiarle, M., Paranunzio, R., Merlone, A., Musacchio, C., Coppa, G., & Nigrelli, G. 2020: An integrated approach to investigate climate-driven rockfall occurrence in high alpine slopes: the Bessanese glacial basin, Western Italian Alps. *Journal of Mountain Science*, 17(11), 2591–2610. <https://doi.org/10.1007/s11629-020-6216-y>

## 23.8

# Land motion monitoring service over Switzerland through interferometric multi-temporal analyses of Sentinel-1 SAR data

Giulia Tessari<sup>1</sup>, Paolo Riccardi<sup>1</sup>, Alessio Cantone<sup>1</sup>, Marco Defilippi<sup>1</sup>, Andrey Giardino<sup>1</sup>, Francesco Arrigo<sup>1</sup>, Tomas Zajc<sup>1</sup>, Paolo Pasquali<sup>1</sup>

<sup>1</sup> sarmap SA, via Stazione 52, CH-6987, Caslano, Switzerland ([gtessari@sarmap.ch](mailto:gtessari@sarmap.ch))

Protecting the population and their livelihood from natural hazards is one of the central tasks of Swiss state. Efficient prevention, preparation and intervention measures can be used to prevent or at least limit potential material damage and fatalities as a result of natural hazards. Warnings and alerts are particularly cost-effective instruments for reducing damage, as they allow emergency personnel and the population to take the prepared measures.

The Swiss Federal Office of Topography (swisstopo) therefore procures processed InSAR data to detect any changes in the terrain of the whole of Switzerland. The object of the service is the procurement of processed InSAR data for the entire surface of Switzerland. The data provided by the Sentinel-1 (S1) SAR satellite constellation, as part of the European Union's Copernicus Earth observation programme, are processed as the data basis for the Swiss-wide monitoring of surface motion. The service implementation includes the analysis of all the available historical (S1), from 2014 up to November 2020, followed by annual updates, at least up to 2023.

The area of interest is covering Switzerland and Liechtenstein, including a 5 km buffer, for a total surface of approximately 50'000 km<sup>2</sup>. This area is covered by five different S1 tracks, two ascending and three descending, from October 2014 up to now. The approximate number of acquisition per track is about 300, characterized by a 6-day revisiting time, which is showing a regular sampling with no data gaps starting from November 2015.

The end-to-end workflow of the production chain includes the S1 Data Ingestion, the core processing and a final quality control step.

Southern Switzerland is characterized by prominent topography, as it includes more than the 13% of the Alps, comprising several peaks higher than 4'000 m above sea level. In fact, the Alps cover 60% of Switzerland. Therefore, a preliminary analysis has been addressed on the creation of layover and shadow maps, for each S1 relative orbit, to identify the portions of the study area where the combination of topography and the satellite acquisition geometry do not allow getting information from InSAR techniques.

Additionally, the vast mountainous areas are often affected by seasonal snow cover, which, in turn, is affecting S1 interferometric coherence over long periods, resulting in loss of data for parts of the year. To handle the periodical data decorrelation or misinterpretation of the data phase information during the snow period, a specific strategy to correctly threat these circumstances has been designed.

The Core Processing is responsible for the generation of all required products, operating on S1 and ancillary data. The deformation products are obtained exploiting a hybrid algorithm, which is integrating of both Small Baseline subset (SBAS) and Persistent Scatterers Interferometry (PSI) methods, in order to estimate the temporal deformation at both DS and point-like PS. In the following, the terms low-pass (LP) and high-pass (HP) are used to name the low spatial resolution and residual high spatial frequency components of signals related to both deformation and topography.

The role of the SBAS technique is twofold: on the one hand, it provides the LP deformation time series in correspondence of DS points and the LP DEM-residual topography; on the other hand, the SBAS estimates the residual atmospheric phase delay still affecting the interferometric data after the preliminary correction carried out by leveraging GACOS products. The temporal displacement associated to PS points is obtained applying the PSI method to interferograms previously calibrated removing the LP topography, deformation and residual atmosphere estimated by the SBAS technique. This strategy connects the PSI and SBAS methods ensuring consistency of deformation results obtained at point-like and DS targets. A key aspect considered in the framework of the project implementation is related to the estimation and corrections of atmospheric effects affecting the area, generally more evident over the mountainous areas.

An initial correction is applied to each interferogram through the Generic Atmospheric Correction Online Service for InSAR (GACOS), which utilizes the Iterative Tropospheric Decomposition model to separate stratified and turbulent signals from tropospheric total delays, and generate high spatial resolution zenith total delay maps to be used for correcting InSAR measurements. This atmospheric calibration is later refined by the data-driven atmospheric delay estimation in order to obtain atmospheric delay maps at a much higher spatial resolution than that achievable by using external GACOS data.

GNSS data provided by swisstopo, consisting in more than 200 points over Switzerland, are used for the products calibration and later for the result validation during the quality control procedure.

The generated products consist of:

- Line-of-Sight (LOS) surface deformation time series for ascending and descending datasets in SAR geometry (Level 2a);
- Line-of-Sight (LOS) surface deformation time series for ascending and descending datasets in map geometry (Level 2b);
- Combination and projection of deformation results to calculate vertical and east-west deformations (Level 3).

The quality control (QC) procedures are divided into automatic QC and operator QC. The automatic QC include the analyses of point-wise indicators (coherence maps, precision maps, points density, deformation RMSE with respect to a smooth fitting model), quality indicators at sparse locations (comparison with GNSS data, consistency of stable targets) and other quality indicators (short-time interferogram variograms before and after atmospheric calibration, consistency of overlapping areas). The additional operator QC are focusing on a visual assessment of deformation maps reliability / realism leveraging also on a priori knowledge about the expected deformation behaviour.

The results of this service are delivered to swisstopo that manages the possibility of sharing the deformation maps through their national geo-portal.

## 23.9

# The Mont Blanc Massif high resolution topography project: a baseline for future rockfall and landslide events

Daniel Uhlmann<sup>1</sup>, Joëlle Hélène Vicari<sup>1</sup>, Michel Jaboyedoff<sup>1</sup>, Marc-Henri Derron<sup>1</sup>, Charlotte Wolff<sup>1</sup>, Amalia Gutiérrez<sup>1</sup>, Ludovic Ravanel<sup>2</sup>, Li Fei<sup>1</sup> and Tiggi Choanji<sup>1</sup>

<sup>1</sup> Risk-group, Institute of Earth Sciences, University of Lausanne; Geopolis 3793, CH-1015 Lausanne

<sup>2</sup> Université Savoie Mont-Blanc, CNRS EDYTEM

Alpine regions globally are subject to a multitude of natural hazards such as rock and icefall, and play a central role in downstream resource availability, particularly for water. Global warming has, in some cases, accelerated the rate and magnitude of topographic changes, and therefore could be contributing to an increase in relative hazards. Specifically in the European Alps, the winter of 2021/22 was one of the driest on record, followed by one of the hottest summers on record. Typically-permanent snow cover has been decimated, freezing levels have risen to unprecedented altitudes, and, generally speaking, the cryosphere has been degraded more than in recorded history. This has resulted in what is probably the most rapid period of topographic change since modern geologic records began. Anecdotally, mountain guides across Europe have ceased commercial activity in an unprecedented manner due to a heightened perception of risk in the Alpine zones, and what seems like a decade of topographic change has occurred within a few months.

The aim of the Mont Blanc Massif (MBM) high-resolution topography project is to create a precise 3D model of the MBM using ground-based and aerial Lidar, which will serve as a “time zero” baseline for future events. In the past, only events exceeding obvious size, and which were witnessed by the human eye were recorded. Modern remote sensing techniques, however, allow for a post-event identification by comparing subsequent 3D models. Gathered data will be used to estimate surficial changes, including snow, rock, and ice masses.

This project was initiated in 2021 and is ongoing, with approximately 60% of the MBM scanned as of August 2022. It was mainly carried out using a long-distance Terrestrial Laser Scanner (TLS) accompanied by high-resolution panoramic images. High-resolution point-clouds were obtained, ranging from 4-400 points/m<sup>2</sup> spacing, depending on the distance from which the rock walls were surveyed, and other factors. Data was obtained as far as 6 km from the scanning locations. The main limitations were related to instrument capabilities, atmospheric conditions (clouds, humidity), accessibility, and availability of safe zones which provide line-of-site visibility. The obtained point-clouds and high-resolution panoramas will be essential for periodic and continued monitoring of rockfall, ice loss, and other geomorphological change studies including glacier retreat, as well as the detection of evolving hazardous events.

Future phases of this project include the acquisition of complementary datasets using Airborne Laser Scanners (ALS), as well as drone-based Structure-for-Motion (SfM), in order to obtain the most complete 3D model possible. Due to the remoteness and inaccessibility of some parts of the MBM, these techniques would allow us to scan sectors of the alpine zone which are rarely seen, due to their distance, morphology and surroundings.

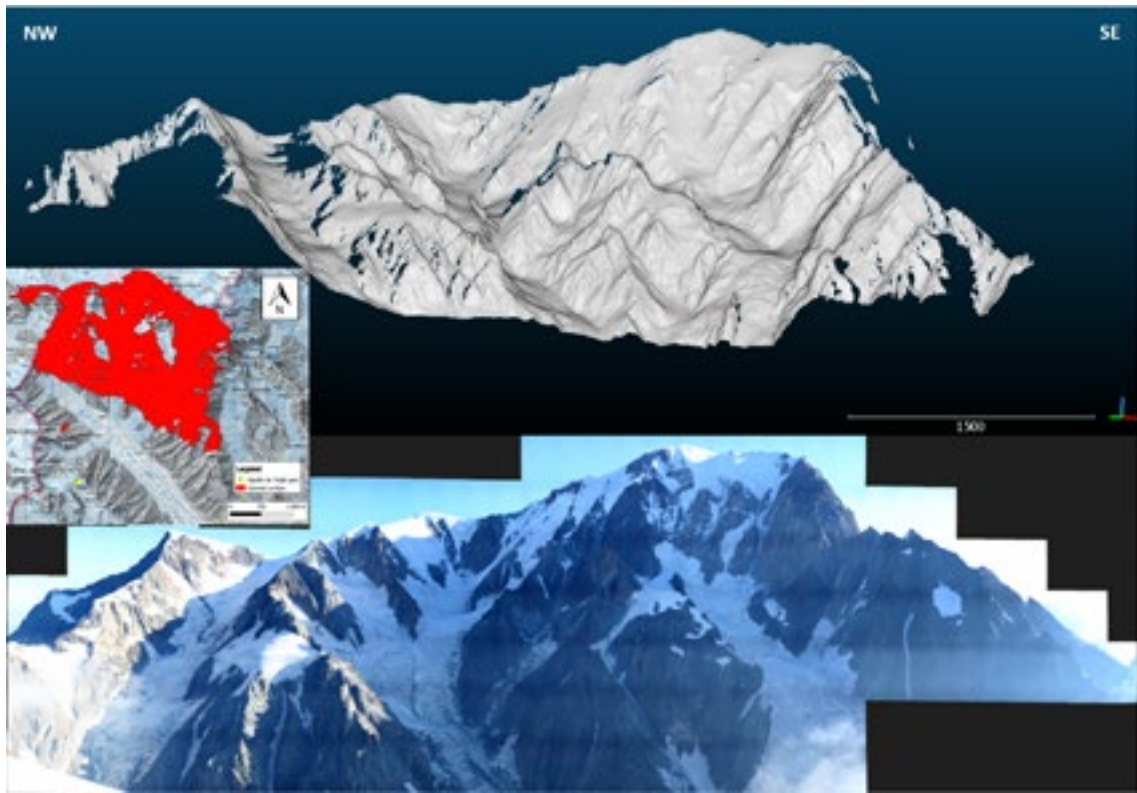


Figure 1: Hillshade (top) obtained from the scan of the Aiguille du Midi from the Plan de l'Aiguille, high-resolution panorama (bottom) of the same zone and location of the scan (middle left).

## 23.10

# Combining remote sensing techniques for the study of active fractures in a challenging remote area: Case of Cima Del Simano rockslide

Charlotte Wolff<sup>1</sup>, Tiggi Choanji<sup>1</sup>, Marc-Henri Derron<sup>1</sup>, Li Fei<sup>1</sup>, Michel Jaboyedoff<sup>1</sup>, Andrea Pedrazzini<sup>2</sup>, Carlo Rivolta<sup>3</sup>

<sup>1</sup> ISTE - University of Lausanne, Lausanne, Switzerland ([charlotte.wolff@unil.ch](mailto:charlotte.wolff@unil.ch))

<sup>2</sup> Sezione forestale- Repubblica e Cantone Ticino, Bellinzona, Switzerland

<sup>3</sup> Ellegi Srl - operational and administrative headquarters, Milano, Italy

The Ticino Canton in the Swiss Alps is characterized by very narrow valleys where multiple slope instabilities of various sizes have been mapped. One of those sites is located in the Valley di Blenio near the commune of Acquarossa. The Cima del Simano very fractured gneissic mountain presents one main 500 meters-long open fracture and several smaller fractures of various sizes closer to the crest. Some preliminary satellite InSAR results highlight small movements of the top. This instability is worthy to be studied and monitored since this hazard represents a risk for the main road passing at the bottom of the mountain and for the villages implanted on its slopes.

Nevertheless, this alpine mountain is very challenging to study because of (1) its bad accessibility: the top reaching an altitude of 2500m without any road to access and covered by snow half of the year and (2) the very strong atmospheric effects: the top of the mountain is very often hidden by clouds which makes difficult the accessibility by helicopter. For those reasons, the study is carried by combining several remote sensing techniques to acquire a maximal amount of information on the instability movements such as rockfalls, topplings of rock slabs and slow deep-seated landslides. Those techniques are extensometers, GPS, Lidar, satellite InSAR, Ground-Based InSAR (GB-InSAR) and drones Structure from Motion (SfM). They are aimed at confirming the failure scenarios that were predicted based on observations made in the field and by structural analyses.

With point clouds acquired with Lidar and SfM at different dates one is able to detect small (2-3m<sup>3</sup>) and fast-moving (cm/month) blocks and distinguish those that fell from those still in sliding or toppling. By means of GB-InSAR and satellite InSAR one can detect more long-term moving areas (few mm/year). We estimate the limits of those instabilities and their corresponding volume with structural analyses of the discontinuities with Coltop3D and by applying the Slope Local Base Level (SLBL) method.

For the main fracture, we also try to delimit the contours of the instability, but such an aperture and hypothetical instability edges are hardly explained by the actual topography. One explanation is that this fracture was inherited from an older important gravitational event, whose involved material collapsed and was washed out since the event occurred.

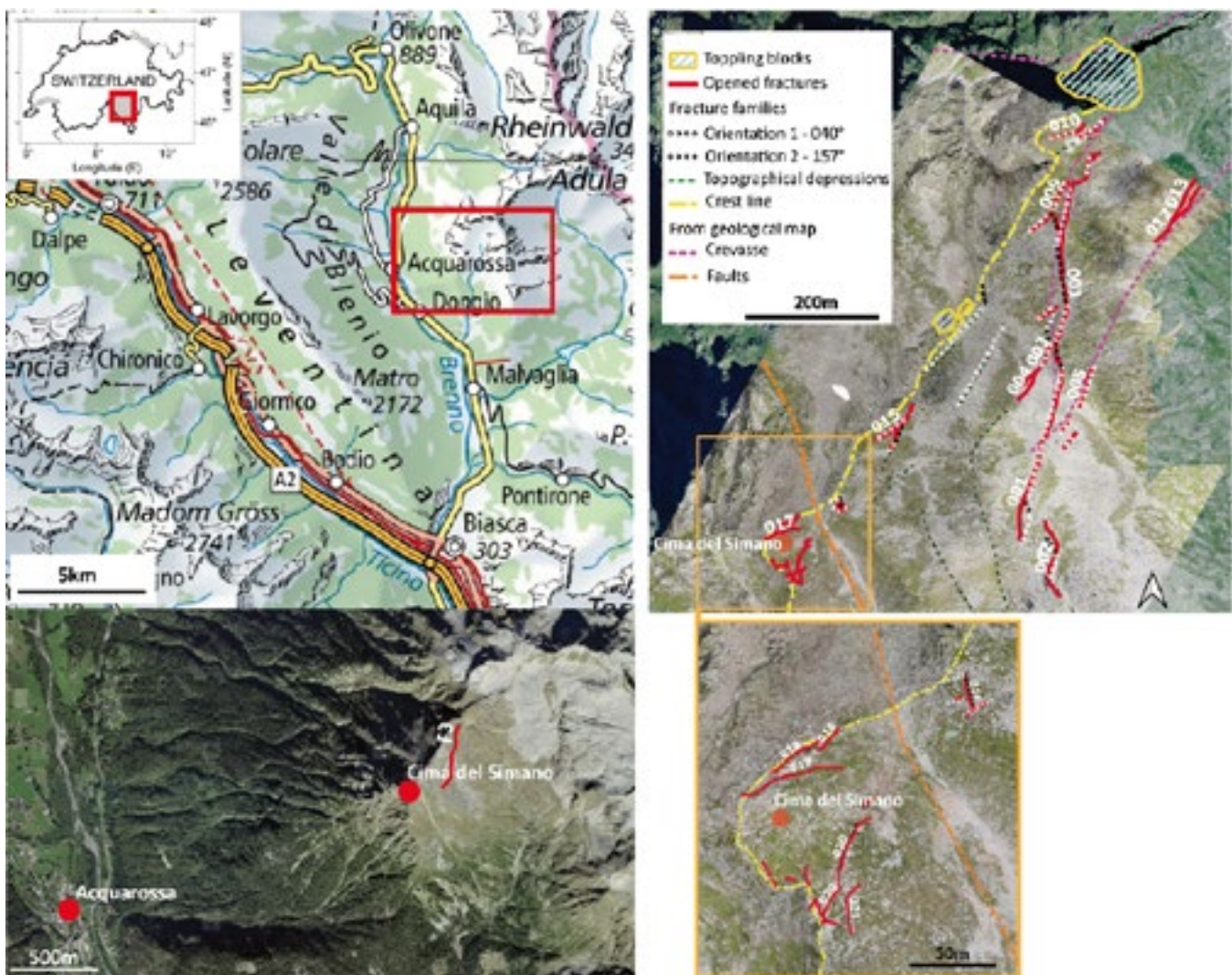


Figure 1. Left: Case study location: Cima del Simano in Ticino Canton (Switzerland). Right: Main fractures on top of the mountain. The fracture 001 corresponds to the largest opened fracture F3.

## REFERENCES

- Abellán, A., Derron, M.H. and Jaboyedoff, M. 2016. Use of 3D Point Clouds in Geohazards. Special Issue: Current Challenges and Future Trends. *Remote Sensing* 8, 2: 130.
- Abellán, A., Oppikofer, T. and Jaboyedoff, M. Rosser, N.J.; Lim, M. 2014 Terrestrial Laser Scanning of Rock Slope Instabilities. *Earth Surf. Process. Landf.*, 39, 80–97.
- Jaboyedoff, M. and Derron, M.H. 2005. A new method to estimate the infilling of alluvial sediment of glacial valleys using a sloping local base level, *Geogr. Fis. Dinam. Quat.* IT ISSN 1724-4757.
- Rouyet, L., Kristensen, L., Derron, M.H. Michoud C., Blikra L. H., Jaboyedoff, M and Lauknes, T. R., 2016, Evidence of rock slope breathing using Ground-Based InSAR, *Geomorphology*.
- Scapozza, C., Ambrosi, C., 2021, Landscapes and Landforms of Switzerland, Springer International Publishing, Cham, Switzerland.

## P 23.1

# Interferometric radar monitoring of the Spitze Stei landslide under challenging conditions

Maxence Carrel<sup>1</sup>, Johannes Gassner<sup>1</sup>, Severin Stähly<sup>1</sup>, Susanne Wahlen<sup>1</sup>

<sup>1</sup> Geopraevent AG, Räffelstrasse 28, 8045 Zürich ([susanne.wahlen@geopraevent.ch](mailto:susanne.wahlen@geopraevent.ch))

The Spitze Stei landslide has recently received a lot of media coverage in Switzerland. In summer 2018, it was observed that ca. 20 Mio cubic meters of rock material are unstable above Lake Oeschinen, one of the most iconic and touristic locations in the Bernese Alps. Subsequently, an extensive integrated monitoring campaign of the landslide has been implemented. Among others, GPS, tachymetric and interferometric radar data revealed an acceleration of the displacement velocity over recent years. Maximal displacement velocities as high as 10 cm / day for some locations of the landslide on some summer days in 2021 were measured. Different scenarios based on numerical modelling suggest that there is a low but realistic probability of important rockfall and mudflow events that could endanger the well frequented hiking paths to Lake Oeschinen and even some parts of the village of Kandersteg (Kienholz et al. 2021). Geopraevent AG is currently monitoring the landslide with an interferometric radar under challenging conditions.

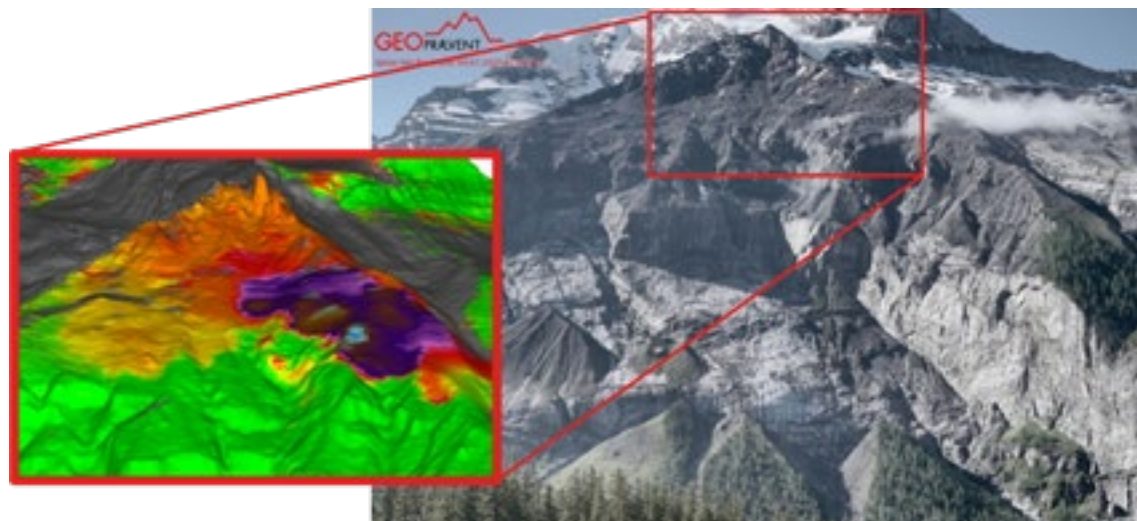


Figure 1. High resolution image of the landslide (right) and interferometric radar displacement measurements mapped on a digital terrain model (left).

Ground-based synthetic aperture radars (GB-SAR) allow to measure millimeter accurate displacements of landslides, rock or glacier instabilities over areas up to 5 km<sup>2</sup> at a distance up to 5 km in all weather and visibility conditions (Meier et al. 2018). For such measurements, a 1% air humidity rate variation induces a deformation of 1 mm at 1 km. In the present case, the maximal distance between the radar location and the upper part of the landslide is of ca. 3 km. Due to the proximity of the Lake Oeschinen, katabatic winds coming down from the Doldehorn glacier and thermal winds rising along the cliffs below the Spitze Stei area, substantial humidity rate variations were observed. This situation required the development of a new adaptive interferometric model. At this location, the radar records interferometers every 5 minutes. By comparing data in stable areas, the adaptive interferometric model selects data sets with similar atmospheric conditions, thus allowing an effective atmospheric correction (Gassner et al., 2022). An example of the results is displayed on Figure 2. In October 2020, a large pillar located at the top of the landslide collapsed, destroying a GPS system installed in the slope. The local acceleration of the landslide that led to the collapse is well visible on the measured interferometric radar data. Currently, this system is continuously used to monitor this landslide and provide data in order to understand the interplay of the processes at stake and to evaluate the evolution of the situation.

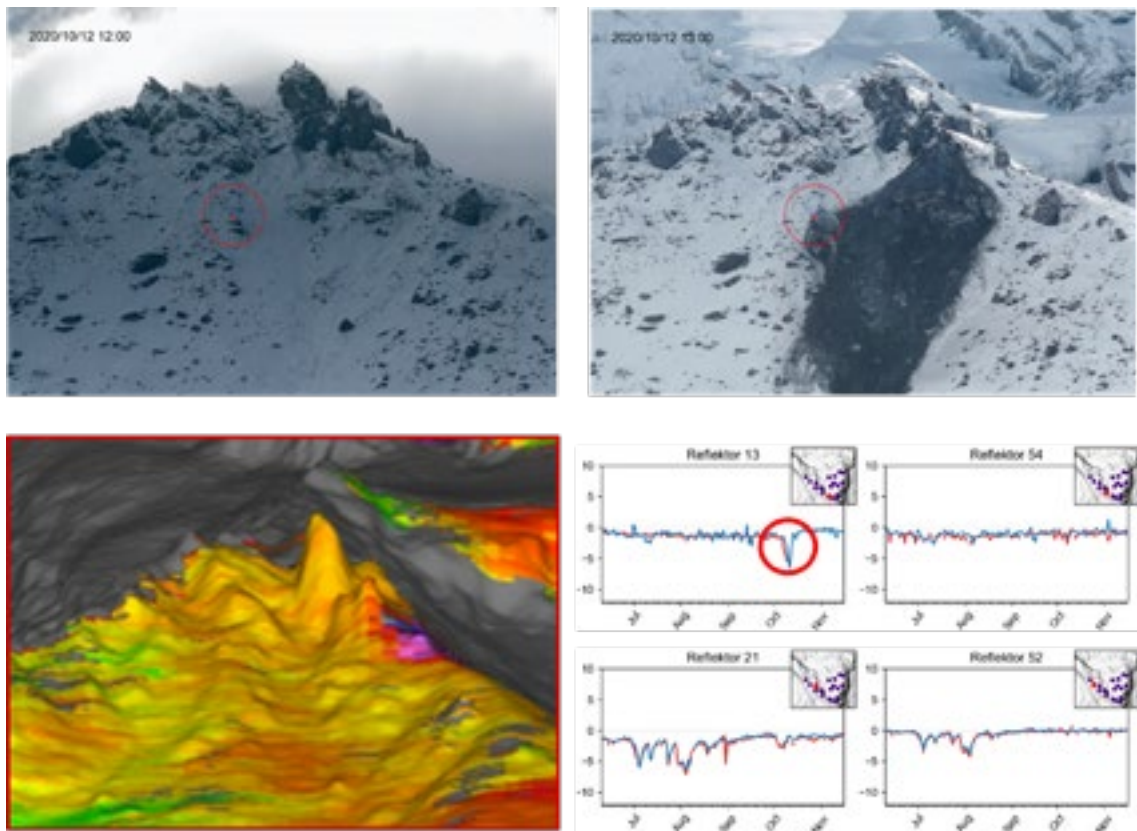


Figure 2. Two images of the upper part of the Spitze Stei landslide, before and after the collapse of a pillar (top, left and right, respectively). Interferometric data measured approximatively during the collapse (bottom left) and GPS (red) and interferometric radar data (blue) in cm / day for different regions of the landslide (bottom right). The red circle indicates the collapse of the pillar in October 2020.

## REFERENCES

- Gassner J., Wahlen S., Meier L. 2022, Radarüberwachung von Massenbewegungen, Schweizerische Zeitschrift für Forstwesen, 3:124-129.  
 Kienholz C., Tobler D., Riner R., Graf K., Haberkorn A. & Surdez M. 2021: Kandersteg «Spitze Stei» Gefahrenmanagement 2021, Geotest AG, 1-78.  
 Meier L., Jacquemart M., Steinacher R., Jäger D., Funk M. 2018, Monitoring of the Weissmies glacier before the failure event of September 10, 2017 with Radar Interferometry and high-resolution deformation camera, Proceedings of the International Snow Science Workshop, 661-664.

## P 23.2

# Satellite Earth observation data for monitoring landslides in the Alps

Thierry Oppikofer<sup>1</sup>, Clément Michoud<sup>1</sup>, Jean-Philippe Malet<sup>2</sup>, Aline Deprez<sup>2,3</sup>, Floriane Provost<sup>2</sup>, Michaelis Foumelis<sup>4</sup>, Javier Garcia Robles<sup>5</sup>, Fabrizio Pacini<sup>6</sup>

<sup>1</sup> Terranum Sàrl, Rue de l'Industrie 35b, CH-1030 Bussigny ([thierry.oppikofer@terranum.ch](mailto:thierry.oppikofer@terranum.ch))

<sup>2</sup> École et Observatoire des Sciences de la Terre (EOST), Université de Strasbourg, 5 rue Descartes, FR-67084 Strasbourg

<sup>3</sup> Applications for Satellite Survey (A2S), Université de Strasbourg, 5 rue Descartes, FR-67084 Strasbourg

<sup>4</sup> Aristotle University of Thessaloniki (AUTH), Thessaloniki, Greece

<sup>5</sup> TRE-Altamira, Barcelone, Espagne

<sup>6</sup> Terradue, Via Giovanni Amendola 46, IT-00185 Rome

The field of satellite-based Earth observation (EO) has experienced a great expansion in recent years, both for optical/multispectral and radar satellites. Among the many innovations and improvements are shorter repetition cycles in the order of 1 to 6 days (e.g. with the Copernicus Sentinel 1 & 2 or PlanetLabs satellites), better spatial resolution (e.g. Pleiades, WorldView-2, TerraSAR-X) and more sophisticated processing methods with computation on high-performance clusters or in the cloud.

In 2021, the European Space Agency (ESA) has launched the *eo4alps-landslides* project with the main objective of exploiting the potential of EO data for landslide hazards in the Alps. The *eo4alps-landslides* services are integrated in the online Geohazard Exploitation Platform (GEP, [geohazards-tep.eu](http://geohazards-tep.eu)), allowing direct access to EO data, particularly from Copernicus Sentinel missions, and to perform customized, on-demand processing of EO data.

Here, we present and compare various EO-based ground-motion maps generated by the *eo4alps-landslides* services for landslide detection and monitoring in the Alps:

- Interferometric Synthetic Aperture Radar (InSAR) ground-motion maps from radar satellite image series (Copernicus Sentinel 1 data) through several InSAR processing algorithms, either based on the Persistent Scatterer Interferometry (PSI) or (Small Baseline Subset) (SBAS) techniques: we compare the ground-motion maps from the SNAPPING (Foumelis et al. 2021), SNAPPING-HR and P-SBAS (De Luca et al. 2015) services with the commercial SqueezSAR® InSAR processor for different landslides in the Alps, such as the Embrun landslide (France), the Pointe des Savoleyres sackung (Vaud, Switzerland) or the Jegihorn landslide (Valais, Switzerland). InSAR ground-motion maps are suitable for regional-scale detection of landslides and other ground deformation (rock glaciers, subsidence), but also site-specific monitoring. InSAR techniques allow measuring slow displacement rates in the range of a few mm/yr to a few cm/yr, with full displacement time-series provided by PSI techniques. Common limitations of InSAR techniques are the measurements in the satellite line-of-sight and thus a poor sensitivity to displacements in N-S direction, and the requirement of good reflectors, such as buildings, large boulders, non-vegetated natural terrain.
- Offset tracking ground-motion maps using Multiple-Pairwise Image Correlation for OPTical image series (MPIC-OPT-SLIDE; Stumpf et al. 2017, Provost et al. 2022). This technique is suitable for local-scale studies of fast-moving landslides (from 1 cm/day to several meters per day), such as the La Clapière landslide in the French Alps or the Barmasse debris slide in the canton of Valais, Switzerland. The technique is however sensitive to snow, cloud cover, and shadows and cannot detect slow ground deformation.

At present, the *eo4alps-landslides* application on GEP is open for testing by selected stakeholders (national, regional and local authorities, private companies and research institutes from different alpine countries). In 2023, the application will be accessible for all interested stakeholders.

## REFERENCES

- De Luca, C., Cuccu, R., Elefante, S., Zinno, I., Manunta, M., Casola, V., Rivolta, G., Lanari, R. & Casu, F. 2015: An On-Demand Web Tool for the Unsupervised Retrieval of Earth's Surface Deformation from SAR Data: The P-SBAS Service within the ESA G-POD Environment, *Remote Sens.*, 7, 15630-15650, doi:10.3390/rs71115630
- Foumelis M., Delgado Blasco J.M., Brito F., Pacini F. & Pishehvar P. 2021: SNAPPING for Sentinel-1 mission on Geohazards Exploitation Platform: An online medium resolution surface motion mapping service, IEEE International Geoscience and Remote Sensing Symposium (IGARSS), Brussels, Belgium, 11-16 July 2021
- Provost, F., Michéa, D., Malet, J.-P. et al. 2022: Terrain deformation measurements from optical satellite imagery: the MPIC-OPT processing services for geohazards monitoring, *Remote Sens Environ.*, 274, 112949, doi:10.1016/j.rse.2022.112949
- Stumpf, A., Malet, J.-P. & Delacourt, C. 2017: Correlation of satellite image time-series for the detection and monitoring of slow-moving landslides, *Remote Sens Environ.*, 189, 40-55, doi:10.1016/j.rse.2016.11.007

## P 23.3

# Postglacial Elastic Rebound and Pore Pressure Deformation from Satellite Radars

Nicolas Oestreicher<sup>1</sup>, Andrea Manconi<sup>2</sup>, Clément Roques<sup>3</sup>, Adriano Gualandi<sup>4</sup>, Simon Loew<sup>1</sup>

<sup>1</sup> Department of Earth Sciences, ETH Zürich, Switzerland

<sup>2</sup> Climate Change, Extremes and Natural Hazards in Alpine Regions Research Center CERC, WSL Institute for Snow and Avalanche Research SLF, Davos, Switzerland

<sup>3</sup> Centre for Hydrogeology and Geothermics (CHYN), University of Neuchâtel, Switzerland

<sup>4</sup> Istituto Nazionale di Geofisica e Vulcanologia (INGV), Osservatorio Nazionale Terremoti (ONT), Roma, Italy

Surface deformation is a powerful tool to investigate processes occurring at and below the ground surface in remote alpine mountains. Interferometric Synthetic Aperture Radar (InSAR) is commonly used to get surface displacement, reflecting a mix of different physical processes, from the satellite. We show that using standard signal processing combined with a statistical source separation method makes it possible to differentiate sub-centimetric displacements close to the Great Aletsch Glacier, Valais. Our observations from the satellite are validated with an extensive in-situ ground monitoring network in our study area. The method can cope with large slope instabilities and the glacier in the middle of the study area, inducing decorrelation and substantial changes in surface elevation. Cyclic displacements are observed following groundwater recharge during infiltration from the snowmelt. Irreversible displacements in the direction of the valley center are also observed (Oestreicher et al. 2021). The driving factors of the long-term trends are mixed in the displacement signals. They may correspond to the postglacial elastic rebound induced by the current glacier unloading (~11 m in the vertical direction are lost each year on average, see GLAMOS, 2020), viscoelastic isostatic rebound from the past melting since the Last Glacial Maximum (LGM, around 18ky BP), and hydromechanical fatigue due to cyclic annual fluctuations of the groundwater table elevation. Based on our high-resolution surface displacement data, we find that the elastic rebound to the current glacier retreat, with an uplift in the vicinity of the glacier, is combined with hydromechanical fatigue, where the cyclic displacements are substantial. The approach could be generalized to other alpine areas with less extensive ground-truthing.

## REFERENCES

- GLAMOS (2020). Swiss glacier length change, release 2020, glacier monitoring Switzerland. <https://doi.org/10.18750/lengthchange.2020.r2020>
- Oestreicher, N., Loew, S., Roques, C., Aaron, J., Gualandi, A., Longuevergne, L., Limpach, P., & Hugentobler, M. (2021). Controls on spatial and temporal patterns of slope deformation in an Alpine Valley. *Journal of Geophysical Research: Earth Surface*, 126(12). <https://doi.org/10.1029/2021jf006353>

## P 23.4

### Bedload monitoring using seismic sensors

Eric Travaglini<sup>1</sup>, Bastien Roquier<sup>1</sup>, Tristan Brauchli<sup>1</sup>, Florent Gimbert<sup>2</sup>, Joseph Moerschel<sup>3</sup>, Antonio Abellan<sup>1</sup>

<sup>1</sup> Centre de Recherche sur l'Environnement ALPin, Rue de l'industrie 45, 1950 Sion ([crealp@crealp.vs.ch](mailto:crealp@crealp.vs.ch))

<sup>2</sup> Institut des Géosciences de l'Environnement UGA-IGE, CS 40700, 38058 Grenoble Cedex 9

<sup>3</sup> HES-SO Valais-Wallis, Rue de l'industrie 23, 1950 Sion

Sediment transport is the primary factor influencing the morphodynamics of mountain streams. It can also be the cause of destructive phenomena such as (flash) floods or debris flows and requires to be closely monitored. Estimation of sediment transport is usually performed using diverse equations based on laboratory experiments (Meyer-Peter 1948; Recking 2006; Rickenmann and Recking 2011; Schoklitsch 2013), and they normally assume a linear relationship between liquid and solid flows. Studies show, however, that the actual sediment transport is highly stochastic and greatly dependent on sediment availability and grain size distribution of both riverbed and external supply. Moreover, these data are generally uncertain or poorly estimated, resulting in the inability to correctly model bedload (Recking et al. 2012; Ancey 2020).

Direct measurement methods (such as Helley-Smith samplers) can be used as an ad hoc basis, but are often not suitable for continuous monitoring (Diplas et al. 2013). Indirect geophysical measurements can overcome these limitations, among them we can mention:

- Hydrophones recording river sounds with an underwater sensor, to isolate in this soundscape the noise generated by the sediments when they collide (Geay et al. 2017).
- Geophone Pipes which consist in putting a tube in the riverbed. The geophone records the vibrations emitted by the sediments in contact with the tube, thus allowing the estimation of the bedload (Mizuyama et al. 2010).
- Swiss Plate Geophones developed by Rickenmann et al. (2014), whose principle is to equip the bottom of the bed with metal plates coupled to geophones. The bedload is then deduced from the vibrations generated by the sediments during their impact on these plates.
- Seismic noise measurements on riverbanks. The estimation of solid transport is then carried out by inverting the seismic signal using the physical bedload model proposed by Bakker et al. (2020)»page»:»e2019JF005416»,»volume»:»125»,»issue»:»5»,»source»:»Wiley Online Library»,»abstract»:»Bedload transport drives morphological changes in gravel-bed streams and sediment transfer in catchments. The large impact forces associated with bedload motion and its highly dynamic spatiotemporal nature make it difficult to monitor bedload transport in the field. In this study, we revise a physically-based model of bedload-induced seismic ground motion proposed by Tsai et al. (2012).

Based on seismic measurements, CREALP developed the SismoRiv solution in partnership with the company Tétraèdre and the University of Applied Sciences HES-SO Valais-Wallis (Travaglini et al. 2016). This solution is currently deployed on the Navisence river in Zinal (VS), upstream of a calibrated Swiss Plate Geophones station (Nicollier et al. 2020). In order to evaluate the quality of the proposed solution, several indirect measurement systems were installed on the site:

- The Sismoriv solution that performs a batch acquisition with a 1D geophone at 300 Hz and offers wireless data transmission (3G).
- The Raspberry Shake® with an embedded 1D geophone and a continuous data acquisition at 100 Hz.
- The Digos DATA-CUBE allows a seismic measurement at a frequency of 100 Hz carried out with a 3D geophone.

These systems were tested against a well-established system for bedload transport monitoring (Swiss Plate Geophones). The results show a relatively good agreement between these systems, demonstrating the interest of the proposed cost-efficient solutions such as SismoRiv or Raspberry Shake®.

## REFERENCES

- Ancey C (2020) Bedload transport: a walk between randomness and determinism. Part 2. Challenges and prospects. *Journal of Hydraulic Research* 58:18–33. <https://doi.org/10.1080/00221686.2019.1702595>
- Bakker M, Gimbert F, Geay T, Misset C, Zanker S, Recking A (2020) Field Application and Validation of a Seismic Bedload Transport Model. *Journal of Geophysical Research: Earth Surface* 125:e2019JF005416. <https://doi.org/10.1029/2019JF005416>
- Diplas P, Kuhnle R, Gray J, Glysson D, Edwards T (2013) Sediment Transport Measurements. 307–353. <https://doi.org/10.1061/9780784408148.ch05>
- Meyer-Peter E (1948) Formulas for Bed-Load transport. IAHR, Stockholm
- Mizuyama T, Laronne J, Nonaka M, Sawada T, Satofuka Y, Matsuoka M, Yamashita S, Sako Y, Tamaki S, Watari M, Yamaguchi

- S, Tsuruta K (2010) Calibration of a Passive Acoustic Bedload Monitoring System in Japanese Mountain Rivers. U.S. Geological Survey
- Nicollier T, Rickenmann D, Boss S, Travaglini E, Hartlieb A (2020) Calibration of the Swiss plate geophone system at the Zinal field site with direct bedload samples and results from controlled flume experiments. pp 901–909
- Recking A (2006) Etude expérimentale de l'influence du tri granulométrique sur le transport solide par charriage. INSA de Lyon
- Recking A, Liébault F, Peteuil C, Jolimet T (2012) Testing bedload transport equations with consideration of time scales. *Earth Surface Processes and Landforms* 37:774–789. <https://doi.org/10.1002/esp.3213>
- Rickenmann D, Recking A (2011) Evaluation of flow resistance in gravel-bed rivers through a large field data set. *Water Resources Research* 47. <https://doi.org/10.1029/2010WR009793>
- Rickenmann D, Turowski JM, Fritschi B, Wyss C, Laronne J, Barzilai R, Reid I, Kreisler A, Aigner J, Seitz H, Habersack H (2014) Bedload transport measurements with impact plate geophones: comparison of sensor calibration in different gravel-bed streams. *Earth Surface Processes and Landforms* 39:928–942. <https://doi.org/10.1002/esp.3499>
- Schoklitsch A (2013) Handbuch des Wasserbaues: Zweiter Band. Springer-Verlag
- Travaglini E, Ornstein P, Moerschel J, Schneider T (2016) SismoRiv : Estimation du charriage en rivière à l'aide d'une mesure du bruit sismique présent dans les berges. [https://geoscience-meeting.ch/sgm2016/wp-content/uploads/abstracts/SismoRiv\\_SGM\\_09-01-16-06-36-57.pdf](https://geoscience-meeting.ch/sgm2016/wp-content/uploads/abstracts/SismoRiv_SGM_09-01-16-06-36-57.pdf). Accessed 2 Jun 2021

**P 23.5****Low-cost terrestrial photogrammetry for rock cliff monitoring**

Jason Bula<sup>1</sup>, Antoine Guerin<sup>2</sup>, François Joseph Baillifard<sup>2</sup>, Adrien Gressin<sup>1</sup>

<sup>1</sup> University of Applied Sciences Western Switzerland (HES-SO / HEIG-VD), Institute  
 (jason.bula, adrien.gressin)@heig-vd.ch

<sup>2</sup> Norbert SA, Géologie Technique et Hydrogéologie, Martigny, Switzerland  
 geol-my@norbert-sa.ch

The use of a single camera is a good low-cost alternative for rock wall survey and rockfall detection. Unlike laser scanners, the mono-photogrammetry (or monoplanning) only provides 2-D displacement measurements. However, 3-D change detection remains essential for the study of gravity movements and the understanding of their failure mechanisms. Modern Structure-from-Motion (SfM) photogrammetry techniques allow to generate at low-cost precise measures useful for remote instability detection.

In recent years, various photogrammetric rock cliffs monitoring systems have been published. They are based on systems installed close to the unstable area and make daily measurements. This kind of survey is very promising because it can in some cases avoid the installation of extensometers sometimes delicate to set up and expensive. However, if the objective is to avoid the use of high-cost cameras, the major drawback of this method is that the camera must be positioned close enough to the hazard area to obtain a sufficient image resolution to measure the movements accurately.

This project experiments the possibility of monitoring a rock cliff using two industrial cameras positioned at several hundred meters apart. To meet the challenge, we propose to use a super-resolution method and to take advantage of the stacking of images taken consecutively. This technique increases the resolution of the images in post-processing (Figure 1) in order to identify potential movements of the rock face while being positioned at a high distance from the hazard area. Image stacking would also allow to reduce atmospheric and scintillation effects.

To test our system, we focused on an unstable granitic flake located above the commune of Salvan (Canton of Valais, Switzerland). This rock sheet of about 30 m<sup>3</sup> has been monitored since June 2018 using periodic ground-based laser scans and then with two high-precision extensometers (Figure 2), starting in June 2020. In the context of this study, nine photogrammetric targets were implemented over stable and moving parts (Figure 2), as well as two measuring stations composed of cameras fixed at 650 m from the rock sheet. Those cameras film continuously and send their images to a server via the GSM network. The data then goes through the processing chain for super-resolution and calculate the targets displacements using SfM photogrammetry. Combined with targets, this new system would give the possibility to monitor in real time the movement of an unstable rock compartment.

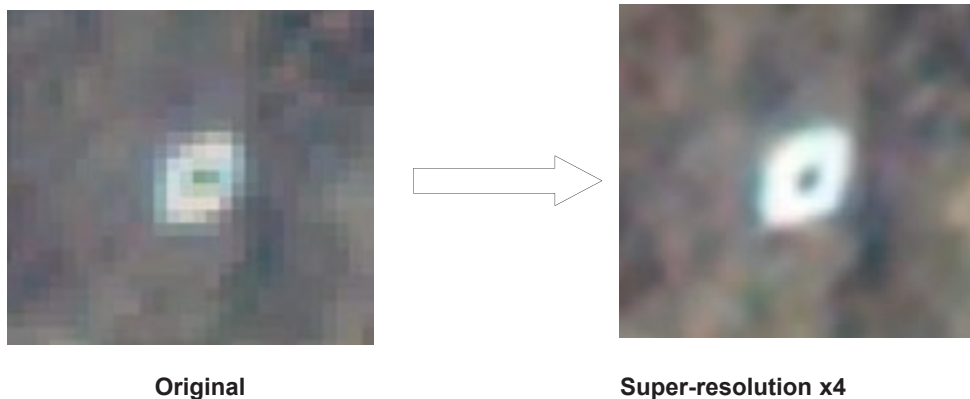


Figure 1. Result of the combined super-resolution and stacking of the images performed on a target fixed on an unstable rock sheet (see Fig. 2).

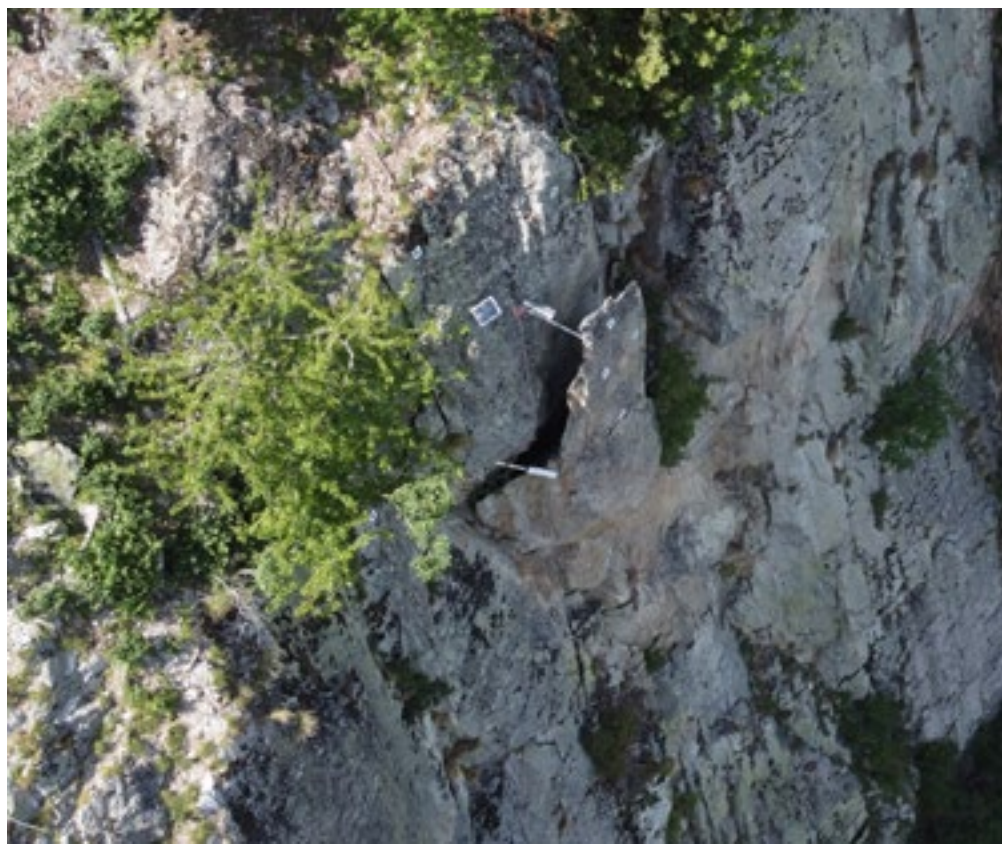


Figure 2. Overview of the monitored rock sheet (drone image). 9 targets (white squares) were installed on the moving (5) and stable (4) parts. The solar panel is used to power both extensometers (metal bars) visible along the back crack.

## P 23.6

# Identifying and classifying potential slope instabilities using space-borne radar interferometry in the Bhagirathi Valley, Uttarakhand, India

Gwendolyn Dasser<sup>1,2</sup>, Andrea Manconi<sup>1,2</sup>, Yves Buehler<sup>1,2</sup>, Jessica Munch<sup>1,2</sup>, Perry Bartelt<sup>1,2</sup>

<sup>1</sup> WSL Institute for Snow and Avalanche Research SLF, 7260 Davos Dorf, Switzerland ([gwendolyn.dasser@slf.ch](mailto:gwendolyn.dasser@slf.ch))

<sup>2</sup> Climate Change, Extremes and Natural Hazards in Alpine Regions Research Center CERC 7260 Davos Dorf, Switzerland

Systematic mapping and monitoring of existing slope instabilities as well as the investigation of past catastrophic slope failures are essential for an effective hazard assessment, risk management and disaster response (Zhou et al., 2022, Prakash et al., 2021). Accurate and timely observation of such mountain processes allows to detect indications and/or precursors of changes potentially impacting ecosystems across spatial scales. In geologically young mountain ranges the evolution of paraglacial and periglacial morphological processes are observable, i.e. all earth surface modifications that are directly conditioned by cyclic glaciation and deglaciation periods. Modifications of the mountain landscape due to large mass movements (i.e., glaciers, landslides of different size and typology and rock glaciers) are more and more observed due to current climatic changes and their impacts are expected to increase. In some cases, the rapid and potentially catastrophic evolution of such mass movements might directly affect anthropogenic infrastructure, economic activities, and also human lives (Liu et al., 2022).

In this contribution, we show the initial results obtained by processing and analyzing available satellite radar datasets acquired from the ESA Sentinel-1 mission in the period 2018-2021. We focused on the Bhagirathi Valley, Uttarakhand, India. This highly alpine area is more and more threatened by large and catastrophic slope collapses. Currently, different hydropower projects are under construction or in the planning phase within the region, increasing infrastructure at risk and the potential for cascading disasters such as the Chamoli rock/ice avalanche in 2021 (Pandey et al., 2022, Zhou et al., 2021).

We use standard radar interferometry to first identify and classify areas affected by potential instabilities. In addition, we focus on specific locations to determine the spatio-temporal evolution of surface displacements and to identify potential changes of trends associated to climatic variables – Figure 1 shows such a location with an active landslide. Preliminary results indicate a displacement velocity of more than 2 cm/year in line of sight (LOS). The result of this large scale and systematic investigation will be the base to test and calibrate numerical models of mass movements. With these models, the simulation of rock-, ice- and snow avalanches, as well as processes combining these input materials, enables the assessments of the hazard intensities and the generation of hazard indication maps for the region. These are essential tools for the planning of effective mitigation measures such as hazard zonation.

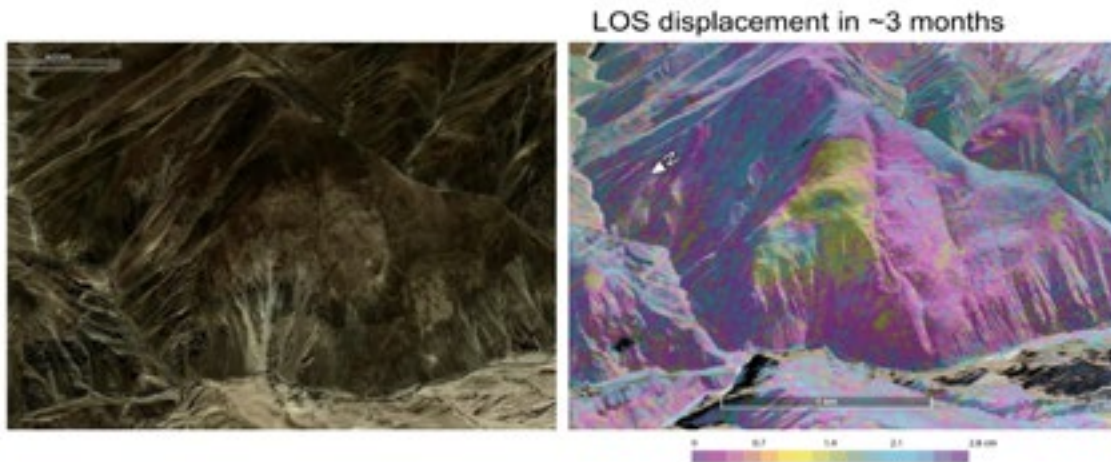


Figure 1: Comparison between optical imagery (left, Google Earth imagery) and displacement analysis based on InSAR (right, Sentinel-1 Track 063 Descending orbit, pair 2020-10-26 2021-01-18). The results indicate a large, deep seated landslide complex, with max velocity of > 2 cm/a.

## REFERENCES

- Liu, Z., Qiu, H., Zhu, Y., Liu, Y., Yang, D., Ma, S., Zhang, J., Wang, Y., Wang, L., & Tang, B. 2022: Efficient Identification and Monitoring of Landslides by Time-Series InSAR Combining Single-and Multi-Look Phases, *Remote Sensing*, 14(4).
- Pandey, V. K., Kumar, R., Singh, R., Kumar, R., Rai, S. C., Singh, R. P., Tripathi, A. K., Soni, V. K., Ali, S. N., Tamang, D., & Latief, S. U. 2022: Catastrophic ice-debris flow in the Rishiganga River, Chamoli, Uttarakhand (India), *Geomatics, Natural Hazards and Risk*, 13(1), 289–309.
- Prakash, N., Manconi, A., & Loew, S. 2021: A new strategy to map landslides with a generalized convolutional neural network, *Scientific Reports*, 11(1).
- Zhou, C., Cao, Y., Hu, X., Yin, K., Wang, Y., & Catani, F. 2022: Enhanced dynamic landslide hazard mapping using MT-InSAR method in the Three Gorges Reservoir Area. *Landslides*, 19(7), 1585–1597.
- Zhou, Y., Li, X., Zheng, D., Li, Z., An, B., Wang, Y., Jiang, D., Su, J., & Cao, B. 2021: The joint driving effects of climate and weather changes caused the Chamoli glacier-rock avalanche in the high altitudes of the India Himalaya. *Science China Earth Sciences*, 64(11), 1909–1921.

**P 23.7****Spektrum: implementing seismic techniques for landslide investigations in practice**

Mauro Häusler<sup>1</sup>, Tobias Nicollier<sup>2</sup>, Donat Fäh<sup>1</sup>

<sup>1</sup> Schweizerischer Erdbebendienst SED, Institut für Geophysik, ETH Zürich, Sonneggstrasse 5, CH-8092 Zürich

(mauro.haeusler@spektrum-geophysik.ch)

<sup>2</sup> Rovina & Partner AG, St. Martinistrasse 3, CH-3930 Visp

Geophysical techniques using ambient seismic vibrations proved to add valuable information to characterize and monitor rock slope instabilities. When propagating through slope instabilities, seismic waves are amplified and polarized perpendicular to dominating fracture systems. By mapping these properties, a slope instability can be detected and mapped independent of surface deformations and based on a few hours of data recordings only. This enables geologists to rapidly characterize the instability and optimize the resource usage for subsequent in-depth monitoring (e.g., by geodetic techniques). In addition, such passive seismic techniques can also be implemented to track structural changes, similar to structural health monitoring in civil engineering.

After more than a decade of academic research, the techniques are currently implemented in practice to support authorities and engineering companies to assess and mitigate landslide hazards. We provide an overview of the ongoing technology transfer project “SPEKTRUM” (2022) and show how the technology could be embedded in the current toolkit for landslide characterization and monitoring, including its key advantages as well as its limitations.

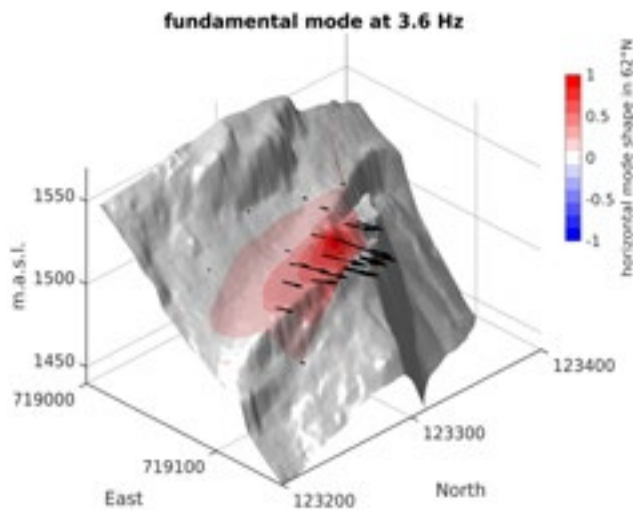


Figure 1. Normal mode behaviour with polarization vectors at the fundamental mode of 3.5 Hz at the slope instability of Preonzo, Ticino (Häusler et al., 2021).

**REFERENCES**

- Häusler, M., Michel, C., Burjánek, J., and Fäh, D. 2021. Monitoring the Preonzo rock slope instability using resonance mode analysis: Journal of Geophysical Research: Earth Surface, <https://doi.org/10.1029/2020JF005709>  
 SPEKTRUM, 2022: [www.spektrum-geophysik.ch](http://www.spektrum-geophysik.ch)

**P 23.8****Role of the forest and avalanche defensive structures on the torrential flooding of the Baye de Montreux**

Bernard Biedermann<sup>1</sup>, Olivier Dubas<sup>1</sup>, Philippe Heller<sup>2</sup>, Olivier Le Doucen<sup>2</sup>, Sébastien Lévy<sup>3</sup>,

<sup>1</sup> Nivalp SA, Rue des Grandschamps 18, CH-1971 Grimisuat ([bernard.biedermann@nivalp.ch](mailto:bernard.biedermann@nivalp.ch))

<sup>2</sup> Hydrique Ingénieurs, Chemin du Rionzi 54, CH-1052 Le Mont-sur-Lausanne

<sup>3</sup> Etat de Vaud, Direction générale de l'environnement, Avenue de Valmont 30b, CH-1014 Lausanne

On August 2, 1927, following a storm of tremendous intensity, a destructive torrential flood occurred in the Baye de Montreux (Canton de Vaud, Switzerland). The materials carried by the torrent overflowed in several places, causing numerous damages to the houses and infrastructures in the town of Montreux.

Following this event, the authorities considered that the best method to reduce the risk of such a disaster happening again was to proceed with a massive reforestation of the summit slopes of the catchment which were then completely bare.

This project started in 1930. Soon it became obvious that the success of the plantations could only be assured if they were protected from the avalanches that happened each winter on the steep slopes of the upper catchment. Hundreds of avalanche defensive structures were created, alongside of the plantation. The effort continued to the end of the 20th century and costed approx. CHF 50 millions.

In 2019, the authorities, wanting to planify the continuation of the project and the maintenance of the defensive structures have mandated specialists to review the condition of the entire protection system and to assess the need for action to ensure the protection of the town of Montreux.

The first part of the study details the historical causes of the project and the past assessments. Then the state of the protection system (forest and avalanche defensive structures) is analyzed in three steps: first, the current forest cover is computed and compared with the initial project goals. The condition of the avalanche defensive structures is then assessed with on-site surveys, highlighting the areas where they need to be repaired or replaced. In the third step, the effectiveness of the forest on erosive processes (landslides) and on avalanches is evaluated over the entire catchment, using the Swiss method PROTECT Bio. In the second part of the study, the sediment dynamics of the catchment are analyzed, first of all by identifying the different sources of sediment, and then on characterising the sediment transport process to Lake Leman. Finally, an action plan is proposed to ensure the operation of the protection system and to improve it when necessary, in a targeted and economically reasonable way.

**REFERENCES**

- Lugeon, J. 1928: Notice sur la trombe et la crue de la Baye de Montreux du 2 août 1927, Bulletin de la société vaudoise des sciences naturelles 56, 221 525-544.
- Niggli, R. 1949: Le reboisement du bassin de réception de la Baye de Montreux, Journal forestier suisse, 100, 283-296.
- Romang, H. 2008: PROTECT, Effet des mesures de protection, Plate-forme nationale "Dangers naturels" PLANAT, 289p.
- Wasser, B. & Perren, B. 2009 : PROTECT Bio, Méthode d'évaluation de l'effet des mesures de protection biologiques contre les dangers naturels comme base pour leur prise en compte dans l'analyse des risques, Impuls AG, 89p.

**P 23.9****L-Band DInSAR Surface Motion Products in Alpine Regions with ALOS-2 PALSAR-2**

Rafael Caduff<sup>1</sup>, Nina Jones<sup>1</sup>, Tazio Strozzi<sup>1</sup>, Urs Wegmüller<sup>1</sup>

<sup>1</sup> Gamma Remote Sensing, Worbstrasse 225, CH-3073 Gümligen ([strozzi@gamma-rs.ch](mailto:strozzi@gamma-rs.ch))

Ground surface deformation is an important indicator of spatial and temporal changes in landslide phenomena. A key technique for monitoring surface motion is space-based Differential Synthetic Aperture Radar Interferometry (DInSAR). Since 2014, the availability of ESA's Copernicus Sentinel-1 mission has enhanced the ability to detect and monitor surface displacements in Alpine regions and numerous authors have shown the potential for regional and country scale services (e.g. Crosetto et al., 2020). However, some intrinsic limitations of the Sentinel-1 sensors may affect the nominal performance of standard and advanced DInSAR techniques in Alpine environments, including (i) no information in areas affected by layover/shadow, (ii) reduced or complete loss of information in vegetated areas and during snow periods, (iii) reduction or loss of displacement information for relatively large motion rates (e.g., a few cm/year) and (iv) little or no ability to detect motion occurring along the approximate north-south direction. Given these limitations, L-Band satellites have the potential to complement the high frequency systems and, under certain conditions, provide information in vegetated areas and for comparatively large displacement rates (e.g. Strozzi et al., 2005).

The Advanced Land Observation Satellite 2 Phased Array L-band SAR 2 (ALOS-2 PALSAR-2) mission is operated by the Japan Aerospace Exploration Agency (JAXA), following a global acquisition plan (Suzuki et al., 2013). Over the Alpine regions, a few images in StripMap and ScanSAR mode were typically acquired every year since 2015 along descending and ascending tracks. ScanSAR data have a much wider swath width compared to StripMap data (i.e., 350 km vs. 70 km), but a lower nominal spatial resolution (i.e., about 40 m vs. 10 m). ALOS-2 PALSAR-2 ScanSAR and StripMap data acquired along the same orbit can be jointly exploited on interferometric point phases in order to enhance the temporal sampling and quality of the results (Strozzi et al., 2022). Analyses of ALOS-2 PALSAR-2 data over several regions of the Alps revealed widespread large-scale rock slope instabilities. In comparison with Sentinel-1, valid information is retrieved with L-Band particularly also over forests and for landslides moving at rates in the range of several cm/year, where only very limited information is available at C-Band (Figure 1). On the other hand, the accuracy of Sentinel-1 is higher than that of ALOS-2 PALSAR-2 for very slow-moving landslides, due to the larger number of available scenes and the higher frequency. Future satellite missions such as NISAR (<https://nisar.jpl.nasa.gov>), ALOS-4 PALSAR-3 (<https://global.jaxa.jp/projects/sat/atos4>) and ROSE-L ([https://www.esa.int/Our\\_Activities/Observing\\_the\\_Earth/Copernicus/Candidate\\_missions](https://www.esa.int/Our_Activities/Observing_the_Earth/Copernicus/Candidate_missions)) are planned to exploit L-Band and provide open data, thus our results are also important to evaluate the potential of such future L-band missions in Alpine landslide monitoring scenarios.

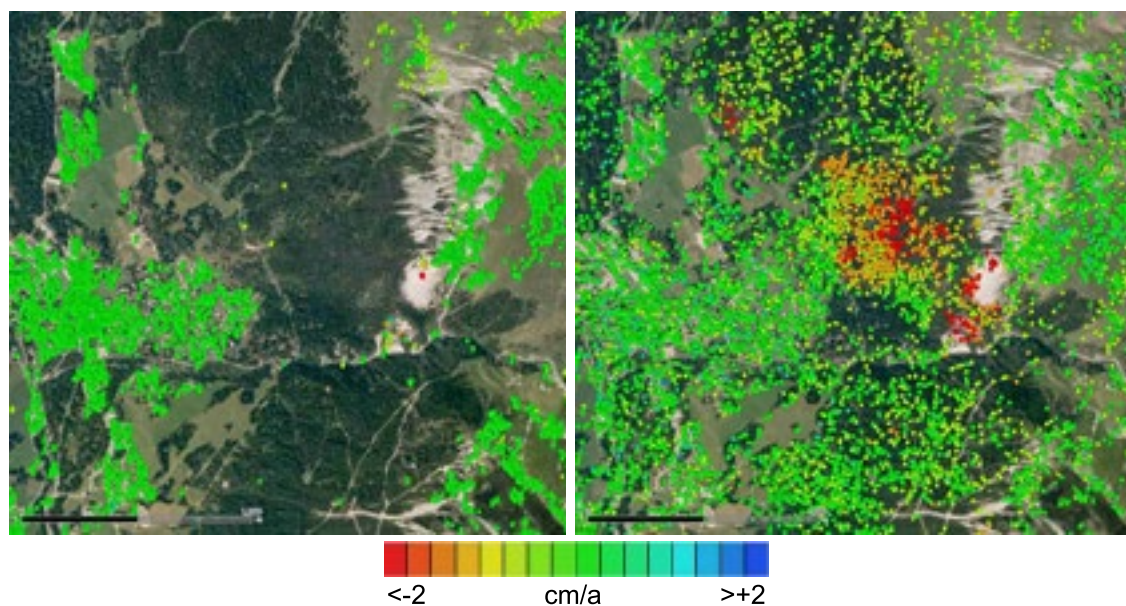


Figure 1. Lenzerheide (GR, Switzerland): line-of-sight displacement maps from Sentinel-1 (left) and ALOS-2 PALSAR-2 (right) of the descending orbit, where observations are made approximately from the east. Map data are from Google Earth.

## REFERENCES

- Crosetto, M., Solari, L., Mróz, M., Balasis-Levinsen, J., Casagli, N., Frei, M., Oyen, A., Moldestad, D.A., Bateson, L., Guerrieri, L., Comerci, V. & Andersen, H.S. 2020: The Evolution of Wide-Area DInSAR: From Regional and National Services to the European Ground Motion Service, *Remote Sens.* 2020, 12, 2043, doi: 10.3390/rs12122043.
- Strozzi, T., Farina, P., Corsini, A. Ambrosi, C., Thüring, M., Zilger, J., Wiesmann, A., Wegmüller, U. & Werner, C. 2005: Survey and monitoring of landslide displacements by means of L-band satellite SAR interferometry. *Landslides* 2, 193–201, doi: 10.1007/s10346-005-0003-2.
- Strozzi, T., Caduff, R., Jones, N. & Wegmüller, U. 2022: L-band Stripmap-Scansar Persistent Scatterer Interferometry in Alpine Environments with ALOS-2 PALSAR-2, *Proc. IGARSS'22*.
- Suzuki, S., Kankaku, Y. & Shimada, M. 2013: ALOS-2 acquisition strategy, *Proc. IGARSS'13*, pp. 2412-2415, doi: 10.1109/IGARSS.2013.6723306.

## P 23.10

# Paraglacial landslide response to glacier debuttressing in southern Alaska

Jane Walden<sup>1,2</sup>, Mylène Jacquemart<sup>1,2</sup>, Bretwood Higman<sup>3</sup>, Daniel Farinotti<sup>1,2</sup>

<sup>1</sup> Laboratory of Hydraulics, Hydrology and Glaciology, ETH Zürich, Hönggerbergstrasse 26, CH-8093 Zürich  
 (walden@vaw.baug.ethz.ch)

<sup>2</sup> Swiss Federal Institute for Forest, Snow and Landscape Research (WSL), Zürcherstrasse 111, CH-8903 Birmensdorf

<sup>3</sup> Ground Truth Trekking, PO Box 164, Seldovia, AK, USA, 99663

Glaciers worldwide are retreating at unprecedented rates as global temperatures rise due to anthropogenic climate change. The ice loss has far-reaching implications for the topography, climate, and hydrology of the regions in which glaciers exist. One consequence of the continued glacier retreat is the destabilization of paraglacial slopes as the buttressing force, or the support provided by the glacier, changes and eventually decreases to zero as glaciers dwindle. While the process of glacier buttressing was fundamentally questioned up until a few years ago (McColl et al., 2010), recent work shows clear correlations between glacier retreat and slope destabilization (e.g., Dai et al., 2020, LaCroix et al., 2022). However, the processes governing this buttressing, the amount of support glaciers can provide, and to what extent glacier retreat is responsible for landslide mobilization is poorly constrained, yet critical for understanding the hazard potential of paraglacial landslides.

Here, we investigate around ten large paraglacial landslides in southern Alaska (see Figure 1). This region is of particular interest because it is experiencing some of the fastest glacier retreat worldwide (Hugonnet et al., 2021). Additionally, many of the retreating glaciers are leaving behind deep ocean fjords, where landslides entering the water can lead to destructive and far-reaching tsunamis. We therefore compiled an inventory of landslides from which we selected ten that range in volume from 2 to 500 million m<sup>3</sup>. The selected landslides fall into three categories: (1) landslides that are in a pre-failure stage, where the landslide toe is in contact with the glacier and experiencing glacier thinning, showing only initial signs of destabilization, such as tension cracks, (anti-)scars, and actively forming talus slopes, (2) landslides that are undergoing active glacial debuttressing of the landslide toe, both through glacier thinning and retreat, and may be accelerating, and (3) landslides that have already experienced a catastrophic failure.

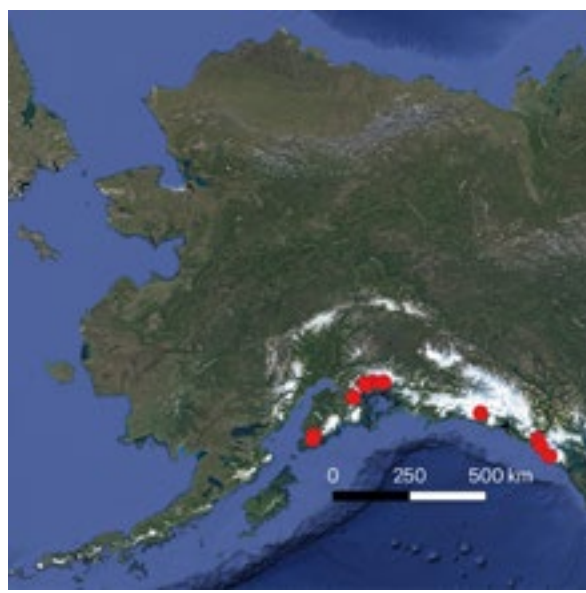


Figure 1. Locations of the selected landslides in southern Alaska (red points). Source of the background map is Google Maps.

We examine the similarities and differences between these sites using remote sensing data from the 1980s to present and generate a standardized dataset to allow for comparison. We reconstruct the deformation history using satellite and aerial images, determining when the landslides show signs of motion, as well as the displacement velocities. We compare the slope deformation rates to ice thinning rates, ice thickness changes, ice flow velocities, and the proximity of the landslide to the glacier terminus. Using these data, we better constrain the buttressing forces and the processes involved, as well as the preconditions that make certain sites prone to failure.

## REFERENCES

- Dai, C., Higman, B., Lynett, P., Jacquemart, M., Howat, I., Liljedahl, A., et al. 2020: Detection and assessment of a large and potentially tsunamigenic periglacial landslide in Barry Arm, Alaska, *Geophysical Research Letters*, 47, <https://doi.org/10.1029/2020GL089800>.
- Hugonnet, R., McNabb, R., Berthier, E. et al. 2021: Accelerated global glacier mass loss in the early twenty-first century, *Nature*, 592, 726–731. <https://doi.org/10.1038/s41586-021-03436-z>.
- Lacroix, P., Belart, J., Berthier, E., Sæmundsson, Þ., Jónsdóttir, K. 2022: Mechanisms of Landslide Destabilization Induced by Glacier-Retreat on Tungnakkíslarjökull Area, Iceland, *Geophysical Research Letters*, 49, <https://doi.org/10.1029/2022GL098302>.
- McColl, S., Davies, T., McSaveney, M. 2010: Glacier retreat and rock-slope stability: debunking debuttressing. Geologically active: delegate papers 11th Congress of the International Association for Engineering Geology and the Environment, Auckland, Aotearoa, 5-10 September 2010. Auckland, New Zealand; pp. 467-474.

## P 23.11

# Quantifying the role of microstructure to improve mechanical modeling of weak snow layers

Jakob Schöttner<sup>1</sup>, Melin Walet<sup>1</sup>, Alec van Herwijnen<sup>1</sup>, Jürg Schweizer<sup>1</sup>

<sup>1</sup> WSL Institute for Snow and Avalanche Research SLF, Flüelastrasse 11, CH-7270 Davos Platz, Switzerland  
(melin.walet@slf.ch)

Buried weak snowpack layers are a prerequisite of dry-snow slab avalanches, which are responsible for the majority of fatalities in winter sport activities. Understanding the failure behavior of weak snowpack layers is therefore important to improve the prediction of slab avalanche release. Weak layers in natural snowpacks exhibit a variety of different microstructures and densities and thus show different mechanical behavior. However, mechanical properties of snow are mainly evaluated based on bulk proxies such as snow density, while relevant microstructural characteristics are not accounted for.

To establish a link between the microstructure of weak layers and their mechanical properties in order to improve our understanding of snow mechanics and ultimately improve avalanche prediction, we perform experiments in the field on natural weak layers and in the cold laboratory with artificially grown weak layers.

In a first step, we performed a series of failure experiments using artificial samples with weak layers consisting of depth hoar grown in a controlled environment with variable conditions. To measure displacements and strains, we used Digital Image Correlation (DIC) and a mechanical testing machine to measure the peak force at the moment of weak layer failure. To facilitate the link between mechanical properties and microstructure, we use state-of-the-art snow characterization techniques such as a micro CT scanner, a Snow Micro Pen (SMP) and acoustic wave propagation setup. Based on these preliminary results we will design further experiments on weak snowpack layers with improved repeatability in the cold laboratories of SLF that will eventually be validated by experiments in the field in different snow conditions.

## 24 Human Geographies: Materials, Natures, Politics

Rony Emmenegger

*Swiss Association for Geography (ASG).*

### TALKS:

- 24.1 Bouzarovski S.: Energy geographies and the post-colonial condition: Eastern and Central Europe in crisis
- 24.2 Chalmandrier M., Salomon Cavin J.: "Get rid of them softly": experimenting ecologisation of urban pest control practices with invasive ants
- 24.3 Emmenegger R.: Unearthing the subterranean: On the political geology of nuclear waste disposal in Switzerland
- 24.4 Florentin D., Bognon S., Ramos A.: Cleaning, Regulating, Coexisting: strategies and practices of urban cleanliness management and the conflicts of environmental ethics
- 24.5 Fontcuberta A., Kaufmann A.: Zootopia: a multi-site participatory research about human-animal cohabitation
- 24.6 Glatron S., Franck-Neumann F., Philippot V.: The urban pedofauna, a forgotten part of nature in the city
- 24.7 Jokela-Pansini, M., Ippolito, Greenhough, B., Lora-Wainwright, A.: Mapping health inequalities and quality of life in high-risk environmental areas (Taranto, Italy)
- 24.8 Kullman K.: Landscape 'undesign' in a damaged World
- 24.9 Tschiderer L., Hartmann S., Thieme S.: Health commons: commoning work in healthcare
- 24.10 Tschumi P.: How does co-creation influence regulations? An analysis of co-creation in health care social innovations
- 24.11 Zumoberhaus J.: Phytosociologists vs. biocenologists: Epistemological duelling in Swiss geobotany 1940-1965

## 24.1

# Energy geographies and the post-colonial condition: Eastern and Central Europe in crisis

Bouzarovski Stefan<sup>1</sup>

<sup>1</sup> Department of Geography, University of Manchester, Manchester, UK (stefan.bouzarovski@manchester.ac.uk)

In this talk, I seek to shed a critical light on the overlapping post-colonial and geopolitical realities that shape Eastern and Central Europe's (ECE) contemporary energy geographies. I explore three contingencies that are at play in shaping ongoing state policies and responses to Russia's invasion of Ukraine: the infrastructural legacies of post-socialism and subsequent transformations, the region's positioning within Europe's imaginary and material geopolitical map, and contemporary socio-political relations within ECE itself. I interpret the region's inherited socio-technical systems through the lens of past visions, priorities and interests imposed by the Soviet power structure (Bouzarovski 2009). In post-socialism, however, many of ECE's infrastructural installations were subject to dynamics of privatisation and marginalisation from the 'collective West'. The path-dependencies that underpin the region's internally contradictory positioning within the European energy polity – characterized by conflicting security and climate objectives – are the product of these interconnected dynamics, and directly influence Europe's wider energy and climate development trajectories. They bring attention to the broader system of energy provision – from sites of production to practices of demand (Balmaceda 2021) – through emergent forms of everyday geopolitics. They also highlight the importance of articulating a global post-colonial lens to understand current and future energy crises.

## REFERENCES

- Balmaceda, M.M., 2021. *Russian Energy Chains. The Remaking of Technopolitics from Siberia to Ukraine to the European Union*. Columbia University Press.  
Bouzarovski, S., 2009. East-Central Europe's changing energy landscapes: a place for geography. *Area* 41(4):452-463

## 24.2

# “Get rid of them softly”: experimenting ecologisation of urban pest control practices with invasive ants

Maud Chalmandrier<sup>1</sup>, Joëlle Salomon Cavin<sup>1</sup>

<sup>1</sup> Institute of Geography and Sustainability, University of Lausanne, Quartier mouline, Bâtiment Geopolis, 1015 Lausanne (maud.chalmandrier@unil.ch)

Ecologisation of pest control can be defined as the use of alternative techniques that are less toxic for the environment and human health. Along with other lethal and nonlethal methods, one strategy is to act on the ecological niche of target species in order to make it less favorable for their settlement. To do so, professionals mobilize knowledge on the biology, behavior and ecology of species in their environment. Implying changing perceptions of animals, these management strategies are often framed as a shift from “control of” to “coexistence with” wildlife in urban environments (Hunold, 2020). With a slightly different perspective, we would like to explore how knowing, caring and killing non-humans articulate in ecologised pest control, by focusing on professionals’ practices and invertebrate species.

Our case study follows the discovery of ants *Tapinoma magnum*, considered as invasive, in the urban areas of Lausanne. We aim to explore how ecological experimental practices of pest control reconfigure relationships between ant biologists, pest controllers (called *désinfestateurs* in Romandie) and *Tapinoma magnum* ants. Our study is based on participant field observation, interviews and other written sources.

After a brief description of the late discovery of the species and of actors involved in the public mandate for invasive species management, the communication examines professionals’ attempts to control the size and expansion of ant populations, focusing on its experimental dimension. First, we will describe the active collaboration between practitioners and scientists: how they adapt their respective rationale and knowledge practices in order to find what they define as an efficient strategy. We follow the different approaches they have tested and their adjustments between field and lab conditions. Second, we will analyse the ethic associated with this pest control experimentation, that reject undifferentiated eradication in favour of a long-term liveable reduction of invasive ant populations. Both practitioners and scientists assume the “killing” aspects of their mission and justify it by *Tapinoma magnum* species behaviour in urban conditions, in particular the nuisances caused by their proximity with inhabitants and their hypothetical threat for local biodiversity. Nonetheless, they develop careful practices that combine repetitive field observation, a contextual and parsimonious use of insecticides, and methods with a low toxicity for environment.

Hence, this case study aims to provide a nuanced account of what ecologisation of pest control implies for relationships between professionals and animals, and to show the diversity of meanings and arbitrages that lethal management encompass in situation (see also Crowley et al., 2018).

## REFERENCES

- Hunold, C. & Mazuchowski, M. 2020: Human–Wildlife Coexistence in Urban Wildlife Management: Insights from Nonlethal Predator Management and Rodenticide Bans. *Animals* 10, 1983.
- Crowley, S. L., Hinchliffe, S. & McDonald, R. A. 2018: Killing squirrels: Exploring motivations and practices of lethal wildlife management. *Environment and Planning E: Nature and Space* 1, 120143.

## 24.3

### Science, Society and the Subterranean: On the Political Geology of Nuclear Waste Disposal in Switzerland.

Rony Emmenegger

*University of Basel (rony.emmenegger@unibas.ch)*

The deep geological underground has increasingly turned into a site for the projection of energy futures and pasts. This has included plans for dealing with the legacy waste of the nuclear era and for safely disposing nuclear waste in a deep geological repository for the next one million years. Despite an international agreement among experts and decision makers that deep geological disposal provides the safest option, site selection projects have failed worldwide due to local resistance at the surface. Addressing the according tensions between the state, science and society, social scientists have predominantly focused on risk perception, management, governance, ethics and politics in a social sphere. However, they have ignored society-subterranean relations emerging or shifting as disposal projects develop. Filling this gap, this paper studies the ongoing scientific exploration of the deep geological underground that has concretized the site selection process in Switzerland and culminated in a site selection in September 2022. Based on document analysis and ethnographic research, it scrutinizes how the underground is represented in geological maps and models, and how it is enacted in practices and performances of science communication directed towards the public. It demonstrates how the geological underground is brought into being as a stable stratigraphic layering in which techno-scientific interventions appear feasible and legitimate. In parallel, it reveals how human and geological agency can disrupt such political stabilizations in the course of the scientific underground exploration. On that basis, this paper highlights the inherent fragility of the geological underground as it comes to 'matter' in scientific and public controversies about nuclear waste disposal.

## 24.4

# Cleaning, Regulating, Coexisting: strategies and practices of urban cleanliness management and the conflicts of environmental ethics

Daniel Florentin<sup>1</sup>, Sabine Bognon<sup>2</sup>, Aurélien Ramos<sup>2</sup>

<sup>1</sup> Institut Supérieur d'Ingénierie et de Gestion de l'Environnement (ISIGE), associé au Centre de Sociologie de l'Innovation (CSI) Mines Paris PSL (daniel.florentin@minesparis.psl.eu)

<sup>2</sup> CESCO – Museum National d'Histoire Naturelle (sabine.bognon@mnhn.fr and aurelien.ramos@mnhn.fr)

This presentation questions the integration of non-human organisms and milieux in urban planning and public space management in the global North. It particularly focuses on the tension between processes of ecologisation of urban policies (Bognon and Thébault, 2020) and the persistence of an antagonist when not mortiferous relationship between city actors (elected people, urban technicians and city dwellers) and some urban animal species. Through an analysis of this tension in four French urban settings, we put at work the sociophilosophical project of Zoopolis developed by Jennifer Wolch. Through the lenses of urban animal management, and specifically those deemed undesirable, we discuss the Zoopolis framework and its material, professional and political implications.

We show how paradoxical and even divergent discourses and practices can coexist, reflecting frictions and hybridizations between different environmental ethics (Larrère, 2010) and a renewal of boundaries between acceptable and non-acceptable more-than-human agents, which can be characterised as new socio-politically constructed nature baselines (Ureta et al., 2020)

Despite growing discourse on the protection of biodiversity and their declensions in urban policies framework, some animal species continue to be envisioned and managed as “pests” (Crozes, 2018) and are not given room or even forms of agency in urban environments (Jerolmack, 2008). Specific animal species are thereby the object of progressive exclusion strategies in the city (Philo, Wilbert, 2000). Urban animals management falls into diverse city departments (urban cleanliness, hygiene, public health, environment); yet, a predominant trait remains a fight against the potential nuisance and damage (health, material, aesthetic) that they can cause in their cohabitation with city dwellers. This leaves little room for alternative and more ecological forms of coexistence, be they diplomatic (Morizot, 2016) or animist (Rose, 2013).

Based on a survey of urban services in charge of animal populations, we analyze three nodes of tension in the management practices and discourses of wild species in the city such as processionary caterpillars, rats, seagulls or corvids as well as feral species such as pigeons:

- ontological tension: how do certain animal species become the object of control, in spite of growingly a priori favorable to urban biodiversity regulations?
- practice-based tension: are undesired animals to be “managed” curatively, preventively, working on their ecosystem or directly on their corporeality
- organisational tension: who is in charge of this control and with what methods of evaluation?

By following the gestures, the strategies of public action and the speeches of those responsible for the management of animals in the city, we see the construction of new arbitrages, renegotiating the relations between humans and non-human animals, and which also reveals the influence of professional cultures and political choices that remain marked by a strong anthropocentrism.

## REFERENCES

- Bognon S. et Thébault E., 2020, « Ecologisation », in Bognon S., Magnan M. et Maulat J. (eds), *Urbanisme et Aménagement. Théories et débats*, Paris, Armand Colin, 41-62.
- Crozes A., 2018, « La place de l'anthropocentrisme dans la notion « d'espèce nuisible » : état des lieux et évolutions d'un statut fonctionnel », *Revue juridique de l'environnement*, 43(4), 693-718.
- Jerolmack C., 2008, « How Pigeons Became Rats: The Cultural-Spatial Logic of Problem Animals », *Social Problems*, 55(1), 72–94.
- Larrère C., 2010, « Les éthiques environnementales », *Nature Sciences Sociétés*, 18(4), 405-413.
- Morizot B., 2016, *Les diplomates : cohabiter avec les loups sur une autre carte du vivant*, Paris, Edition Wildproject, Domaine Sauvage
- Philo C., Wilbert C., 2000, *Animal Spaces, Beastly Places. New Geographies of human-animal relations*, London, Routledge.
- Rose D. B., 2013, « Val Plumwood's Philosophical Animism: Attentive Interactions in the Sentient World », *Environmental Humanities*, 3(1), 93–109.
- Ureta S, Lekan T & von Hardenberg WG, 2020, *Baselining nature: An introduction*. Environment and Planning E: Nature and Space, 3(1):3-19. doi:10.1177/2514848619898092
- Wolch J., 2012, « Zoopolis », in Hache E. (dir), *Écologie politique. Cosmos, communautés, milieux*, Paris, Editions Amsterdam, 381-404.

## 24.5

# Zootopia: a multi-site participatory research about human-animal cohabitation

Amaranta Fontcuberta<sup>1</sup>, Alain kaufmann<sup>1</sup>

<sup>1</sup>The ColLaboratory, Participatory and action-research unit, University of Lausanne, CH-1015 Lausanne  
(amaranta.fontcuberta@unil.ch; www.unil.ch/collaboratoire)

Non-human animals live among humans within our working and living environments. Together we compose hybrid communities (Lestel 2014), sharing spaces, but also resources, nesting sites, labor, customs and affects. Yet, animal presence and its effects on our daily and working lives are rarely part of public discussions and citizens' concerns. Bringing animality to the front of society's matters of concern is urgent given the current biodiversity crisis, in which -, among others, 41% of amphibians, 30 % of mammals and 13% of bird species, are at risk of extinction (IUCN 2022). Indeed, the ecological crisis is in a way a sensibility crisis (Morizot 2017), that calls for the need to rethink our ways of relating and paying attention to non-human beings.

Zootopia is a participatory action-research that aims to contribute to the reflection on modes of human-animal cohabitation, at the same time as experimenting with new ways of being aware and being together with non-human animals. The ambition is to co-construct with field actors participatory interventions tackling site-specific needs of knowledge production, renewed modes of attention to certain species, dialogue, and outreach. Through collaborative action and inquiry, we aim to explore and question contrasting modes of attention to animals, reflecting on the categories - either domestic, wild, or liminal (Donaldson and Kymlicka 2011)- and the physical and symbolical "right" place (Mauz 2002) attributed to specific animal populations.

We compare and intervene in three sites displaying contrasted human-animal relationships. The first one is the City of Lausanne, where the perception of "good" vs "bad" biodiversity as well as the status implicitly attributed to animals –either wild, if it is visiting the city, or liminal if it considered a resident– may affect both management strategies and citizen attitudes. The second is the University of Lausanne campus. An heterogenous territory composed of buildings, agricultural fields, and natural habitats. There, animals are viewed as study objects or research tools inside buildings, whereas outdoors animals live in wild populations or act as farming companions. The third site is the rural school/research-creation lab "Shanju" at the edge of the Vaud Jura Natural Park where humans and animals engage in intimate relationships and cooperation, that highlight individual animal biographies and explore emerging affects and abilities (<https://www.shanju.ch>).

Our research uses participant observation and exploratory interviews with key partners from each site, in order to identify specific settings of human-animal interactions, needs and concerns from each site. We then bring together representatives of every site for a concertation workshop to identify common interests. Together with key partners we co-design a pilot project in each site, which takes the form of participatory cartographies, multi-stakeholder dialogues and qualitative/ethnographic surveys.

## REFERENCES

- Donaldson, Sue, and Will Kymlicka. 2011. *Zoopolis: A Political Theory of Animal Rights*. Oxford, UK: Oxford University Press.
- IUCN. 2022. "The IUCN Red List of Threatened Species. Version 2022-1." 2022. <https://www.iucnredlist.org>.
- Lestel, Dominique. 2014. "Hybrid Communities." *Angelaki - Journal of the Theoretical Humanities* 19 (3): 61–73. <https://doi.org/10.1080/0969725X.2014.976049>.
- Mauz, Isabelle. 2002. "Les conceptions de la juste place des animaux dans les Alpes françaises." *Espaces et sociétés* 110–111 (3): 129–46. <https://doi.org/10.3917/esp.g2002.110-111.0129>.
- Morizot, Baptiste. 2017. *Manières d'être Vivant. Enquêtes Sur La Vie à Travers Nous*. Arles, France: Actes Sud

## 24.6

### The urban pedofauna, a forgottent part of nature in the city

Sandrine Glatron<sup>1,2</sup>, Florian Franck-Neumann<sup>1</sup>, Véronique Philippot<sup>1,2</sup>,

<sup>1</sup> Urban environmental workshop area, LTSER Strasbourg (Sandrine.glatron@misha.fr; veronique.philippot@unistra.fr)

<sup>2</sup> Interdisciplinary Laboratory in Cultural Studies (Lincs), UMR7369 - CNRS / University of Strasbourg, 5 allée Rouvillois, Fr-67000 Strasbourg

«Nature» in the city is generally associated with the presence of vegetation, particularly trees (and shrubs): this is evidenced, for example, by the terms used by the French to evoke nature, in a recent national survey, where «trees» and «forest» come out on top, and where «green» and «greenery» dominate (Ducarme & Pautard, 2021). The research world follows this same trend, sometimes even equating (without discussion) «nature» with vegetation (e.g. Bourdeau-Lepage, 2019). Interviewed in various surveys for more than 15 years (Blanc & al. 2012, Glatron & al. 2012), city dwellers quite rarely mention soil in all its dimensions and, even less, the organisms that populate it. Yet they are essential to life on earth. By contributing to the good health of the soil, the macrofauna in particular, essentially composed of invertebrates, participates in the proper functioning of all ecosystems, as emphasized by the FAO for example (FAO 2020). If they are relatively well known and well studied in the rural environment and for a large part considered undesirable (cf. all pesticide treatments), invertebrates are simply ignored in the city. When they encounter urban human societies, they generally provoke reactions of rejection or even disgust.

As part of the Solenville participatory research project, which focuses on knowledge of the macrofauna of the soils of the Strasbourg urban area (<https://zaeu-strasbourg.eu/presentation/projets/solenville/>), we surveyed the knowledge that city dwellers have of the «soil» compartment of urban «natural» environments. Their reactions to the role of the small animals that live there confirm their great ignorance of this compartment. However, the very fact that they were willing to take part in the interviews, conducted as part of our participatory research, aroused their curiosity and greatly reduced their initial repulsion. This reinforces our idea that companionship, «sensitization» and familiarity contribute to reducing fears and awakening curiosity, a «regime of attention» favorable to the preservation of insects and soils. Does this short-term observed evolution lead to lasting changes in perception, representations and even behavior with regard to this unloved world? Some of the reactions, captured in our interviews, would suggest this, but it has to be confirmed through medium- or long-term follow-up.

At the same time, whether it is a magnifying glass effect or a «real» broadening of concerns about urban biodiversity, we observe a greater place for invertebrates in the discourses and policies of «nature» in the city we are studying, Strasbourg. However, at no point did we find any occurrences of invertebrate conservation issues, even though numerous reports and articles highlight their alarming disappearance (Sánchez-Bao and Wyckhuys, 2019; Outhwaite & al. 2022) in rural areas and the effects on the entire food chain. Instead, official and managerial reports indicate that certain species are being controlled as undesirable or even dangerous, such as the tiger mosquito, which is closely monitored in urban parks and gardens.

## REFERENCES

- Blanc N., Glatron S., Schmitt G. 2012: Trames vertes urbaines : recherches en sciences humaines et sociales, Développement durable et territoire, Vol.3, 12, <http://developpementdurable.revues.org/9370> (6 p.)
- Bourdeau-Lepage L., 2019: De l'intérêt pour la nature en ville. Cadre de vie, santé et aménagement urbain, Revue d'économie régionale et urbaine, 2019/5, 893-911
- Ducarme F. et Pautard E., 2021: Une nature en quête de sens : état des lieux des représentations sociales de la nature dans la France contemporaine, In : Société, nature et biodiversité. Regards croisés sur les relations entre les Français et la nature, Thema Analyse Environnement, Ministère de la transition écologique, 10-24.
- FAO 2020. *State of knowledge of soil biodiversity. Status, challenges and potentialities. Summary for policy makers.* 40 p.
- Glatron S., Grésillon E., Blanc N., 2012: Les trames vertes pour les citadins : une appropriation contrastée à Marseille, Paris, Strasbourg, Développement durable et territoire, vol.3, n°12, juillet 2012, <http://developpementdurable.revues.org/9297> (15 p.).
- Outhwaite C., McCann P., Newbold T., 2022: Agriculture and climate change are reshaping insect biodiversity worldwide, Nature 605, 97-102.
- Sánchez-Bayo F. & Wyckhuys K.A.G., 2019: Worldwide decline of the entomofauna : A review of its drivers, Biological Conservation, 232, 8-27. <https://doi.org/10.1016/j.biocon.2019.01.020>

## 24.7

# Mapping health inequalities and quality of life in high-risk environmental areas (Taranto, Italy)

Jokela-Pansini, Maaret<sup>1</sup>, Ippolito, Raffaele<sup>2</sup>, Greenhough, Beth<sup>3</sup>, Lora-Wainwright, Anna<sup>4</sup>

*School of Geography and the Environment, University of Oxford*

*maaret.jokela-pansini@ouce.ox.ac.uk<sup>1</sup>, raffaele.ippolito@ouce.ox.ac.uk<sup>2</sup>, beth.greenhough@ouce.ox.ac.uk<sup>3</sup>, anna.lora-wainwright@ouce.ox.ac.uk<sup>4</sup>*

This study analyses how residents experience their health and quality of life in relation to environmental risks in Taranto, Southern Italy. Taranto is a high-risk environmental area because of its location next to one of the largest steel plants in Europe, as well as to an oil refinery, a concrete factory and illegal dumping sites. We combine ethnographic research with an online, participatory map-based survey and ask: how do residents in different neighbourhoods perceive their health in relation to environmental risks (spatially, materially and temporally), how do they mitigate such risks, and what kind of futures do they imagine?

The project relates to recent research in geography, anthropology and environmental studies exploring how residents in highly polluted areas experience environmental risks (Allen 2018; Cori et al. 2020; Davies 2018). Previous survey-based research has explored the extent to which residents perceive different sources of pollution as a risk or threat, how sensitive they are to sensorial impacts such as odours, and in what ways pollution influences (human and non-human) health and individuals' behaviour. In Italy, some comparative studies have investigated how residents in different locations experience pollution and how those experiences vary according to socio-demographic factors (Coi et al., 2014; Germani et al., 2018; Vigotti et al., 2011). Ethnographic research has also sought to understand differences in people's experiences according to gender, age, ethnicity, race or place (Davies 2018; Valdivia 2018; Vasudevan 2019). However, in Taranto and elsewhere, only a few qualitative studies have compared differences between residents' experiences across different neighbourhoods, with differing levels of exposure and proximity to environmental risks and differential access to health and other services.

Through a focus on health risks at the neighbourhood scale, this study contributes to debates on the inequalities arising from living in high-risk environmental areas, expanding our understanding of how human health and wellbeing are entangled with the material environment, and how this shapes bodily perceptions of and responses to environmental risks.

## REFERENCES

- Allen, B. 2018: Strongly Participatory Science and Knowledge Justice in an Environmentally Contested Region. *43(6): 947-971.*
- Cori, L., Donzelli G., Gorini F., Bianchi F., & Curzio O. 2020: Risk Perception of Air Pollution: A Systematic Review Focused on Particulate Matter Exposure. *International Journal of Environmental Research and Public Health 17(17): 6424.*
- Davies, T. 2018: Toxic Space and Time: Slow Violence, Necropolitics, and Petrochemical Pollution. *Annals of the Association of American Geographers 108(6): 1537–53.*
- Germani, A. R., Talamo, G., & Scaramozzino, P. 2018: Air Pollution and Migration in Italy: An Empirical Investigation at Provincial Level. *Energia, Ambiente e Innovazione, 1, 26–31.*
- Valdivia, G. 2018: "Wagering Life" in the Petro-City: Embodied Ecologies of Oil Flow, Capitalism, and Justice in Esmeraldas, Ecuador. *Annals of the American Association of Geographers 108(2): 549–57.*
- Vasudevan, P. 2019: An Intimate Inventory of Race and Waste. *Antipode 53(3): 770–90.*
- Vigotti, M. A., Scalamandrè, P., Dörbudak, Z., SimoneRusso, D., Candelli, F., Bruno, F., Loiacono, F., & Massimilla, P. 2011: An exploratory study of quality of life and perception of environmental pollution in Taranto, Italy, ISEE Conference Abstracts. <https://doi.org/10.1289/isee.2011.01531>

## 24.8

### Landscape ‘Undesign’ in a Damaged World

Kim Kullman<sup>1</sup>

<sup>1</sup> Department of Geography, The Open University, Walton Hall, Milton Keynes, MK7 6AA, The United Kingdom  
(kim.kullman@open.ac.uk)

Embedded within a fragile mountain ecology exposed by receding ice patches, the 1.1-kilometre walkway in Jotunheimen National Park, Norway appears unassuming. And yet the porous and provisional structure is a compelling instance of landscape ‘undesign,’ committed less to building new things than undoing human damage on the terrain by enacting a spatial and temporal interval between bodies and ground. The paper explores the distinctive features of this interval, demonstrating how it prevents erosion and provides latitude for the shifting polygon morphology and its microclimates, allowing lichens and plants to thrive. But above all, the walkway choreographs the mobility of visitors to evoke an environmental ethics of detachment and distance—one that cultivates gaps and pauses to facilitate, beyond the prevailing geographical language of entanglement, a tentative holding apart and foregrounding of the nonhuman particularities of the vulnerable site. Describing how users respond to this momentary state of separability, the paper delineates its implications for thinking through the contemporary terms of ecological entanglement.

## 24.9

### Health Commons - Commoning Work in Healthcare

Luca Tschiderer<sup>1</sup>, Sarah Hartmann<sup>1</sup>, Susan Thieme<sup>1</sup>

<sup>1</sup> *Geographisches Institut, University of Bern, Hallerstrasse 12, CH-3012 Bern (luca.tschiderer@giub.unibe.ch)*

In healthcare there is a tendency of the commodification of work, health and care-related knowledge and technologies. This raises questions about capacities and capabilities for social, economic, ecological innovation, emancipation, and justice in search for more sustainable ‘work’. Counter to that tendency, the Commons have gained increased attention in sustainability and social transformation debates at least since Elinor Ostrom’s “Governing of the Commons” (Ostrom 1990). However, until recently, most debates concerning the commons were focused on specific resources and their governance, so “resources held in common” (de Angelis 2017, p11) rather than on the social processes behind the Commons. We suggest thinking the Commons through the relational processes of social organization inherent in Commons, namely ‘commoning’ (de Angelis 2017, Caffentzis & Federici 2014, Helfrich & Bollier 2020) including material, social and political transformation of social organization (de Angelis 2017). In this sense, thinking through the Commons opens up opportunities to rethink central aspects of capitalist (re)production such as work, care and health: what kind of transformations, emancipations, enclosures, (re)appropriations – in short practices of collective self-governance – are opening up in everyday work that point towards the commoning of work and care?

We extend debates on transformative labour geographies (Grenzdörffer 2021) to highly institutionalised places of healthcare such as hospitals, care homes and in-house care. Based on very first empirical work in different healthcare settings we ask to what extent these hierarchical, but highly diverse settings offer spaces for commoning i.e., the practical decommodification of both, health and work?

#### REFERENCES

- De Angelis, Massimo. 2017. „Omnia Sunt Communia: On the Commons and the Transformation to Postcapitalism.“ Bloomsbury Academic.
- Caffentzis, G., Federici, S. 2014. „Commons against and beyond Capitalism.“ Community Development Journal, 49. <http://cdj.oxfordjournals.org/cgi/doi/10.1093/cdj/bsu006>
- Grenzdörffer, Sinje Marlene. 2021. “Transformative Perspectives on Labour Geographies – The Role of Labour Agency in Processes of Socioecological Transformations.” Geography Compass 15 (6). <https://doi.org/10.1111/gec3.12565>.
- Helfrich, Silke, and David Bollier. 2020. Frei, fair und lebendig - Die Macht der Commons. Bielefeld, Germany: Transcript Verlag.
- Ostrom, E. (1990). „Governing the Commons.“ Cambridge: Cambridge University Press.

## 24.10

# How does co-creation influence regulations? An analysis of co-creation in health care social innovations

Pascal Tschumi<sup>1</sup>

<sup>1</sup>*Institute of Geography & Center for Regional Economic Development, University of Bern, Hallerstrasse 12, CH-3012 Bern (pascal.tschumi@giub.unibe.ch)*

In recent years, social innovations are put forward as solutions to “grand challenges”, such as ensuring high quality health care provision (Farmer et al. 2018). Co-creation, i.e. the collaboration of actors who share their knowledge and skills, is one of the main features of social innovation and can thus be key to solve such challenges (Torfing et al. 2019; Kumari et al. 2020). At the same time, social innovations can have an impact on formal and informal institutions. However, research investigating how co-creation inside social innovation processes can influence formal institutions such as regulations is scarce. We address this gap by analysing how co-creation in social innovation can affect the ways social innovation actors can influence regulations in health care. We conduct three social innovation case studies in the Bernese Oberland, a Swiss mountain region facing the challenge of maintaining high quality health care provision.

From innovation biographies and semi-structured interviews, we found that two actor types, who were involved in co-creation, were also involved in influencing regulations. First, actors who are in a leading role in the social innovation. Second, actors who are part of the inner core of the social innovation and fulfil central tasks. They influenced regulations by inducing other actors to start the process of changing regulations, and by making propositions about changes. Co-creation helped these actors to influence regulations insofar as they learned knowledge and skills in co-creation, which helped them to perform these activities. However, the actors also had resources unrelated to co-creation, which helped them to influence regulations, such as an important actor network and skills in persuading others.

Co-creation can support social innovation actors in influencing formal institutions like regulations in highly regulated sectors, but by itself is not enough to influence regulations. Co-creation in social innovation processes can thus be seen as a way to support institutional change, but not as a guarantee for it.

## REFERENCES

- Farmer, J., Carlisle, K., Dickson-Swift, V., Teasdale, S., Kenny, A., Taylor, J., Croker, F., Marini, K., & Gussy, M. 2018: Applying Social Innovation Theory to Examine How Community Co-Designed Health Services Develop: Using a Case Study Approach and Mixed Methods. *BMC Health Services Research* 18 (1), 68–80.
- Kumari, R., Kwon, K., Lee, B., & Choi, K. 2020: Co-Creation for Social Innovation in the Ecosystem Context: The Role of Higher Educational Institutions. *Sustainability* 12 (1), 307.
- Torfing, J., Sørensen, E., & Roiseland, A. 2019: Transforming the Public Sector Into an Arena for Co-Creation: Barriers, Drivers, Benefits, and Ways Forward. *Administration & Society* 51 (5), 795–825.

## 24.11

# Phytosociologists vs. biocenologists: Epistemological duelling in Swiss geobotany 1940-1965

Jan Zumoberhaus<sup>1</sup>

<sup>1</sup> Department of Geosciences, University of Fribourg, CH-1700 Fribourg, Switzerland

As a subdiscipline of botany or plant ecology, geobotany describes and analyses the spatial occurrence of plant species and vegetation cover. Originating in Switzerland in the 1920s through the work of Josias Braun-Blanquet, phytosociology (also known as plant sociology) became the most important scientific approach within geobotany in Europe in the 20th century. This paper gives insights into the nonlinear, messy history of phytosociology. Based upon theoretical considerations on environmental history and the history of science, a corpus of historical data (field studies, scientific articles, textbooks, commission transcripts) from 1940 to 1965 is analysed using a historical discourse analysis.

In particular, it is shown that during this time span Swiss phytosociologists came under fierce attack from representatives of so-called biocenology. While phytosociologists based their approach in ecological holism, biocenologists pertained to reductionist ideas. However, and contrary to other interpretations of similar cases in the history of ecology, this paper argues that the debate between phytosociologists and biocenologists has not been primarily shaped by disputes over *-isms*, i.e. ideas about ecological nature itself. Rather, it is shown that the disputes in Swiss geobotany in the mid-20th century revolved around epistemological elements concerning the question of how scientists *know and should know* ecological nature. This analytic turn towards epistemology allows to draw the history of ecology back to its actual core: Geobotany, or ecological science in general, should not merely be historicised against an ideological background, but explicitly along its epistemological being a science, i.e. its production of knowledge about ecological nature.

## 25 Human Geographies: Bodies, Cultures, Societies

Nora Komposch, Devran Koray Öcal

*Swiss Association for Geography (ASG)*

### TALKS:

- 25.1 Bouzarovski S.: Energy geographies and the post-colonial condition: Eastern and Central Europe in crisis
- 25.2 Dijkema C.: War and peace as embodied and situated experiences
- 25.3 Fall J.J.: Territory, sovereignty and entitlement: thinking territory through the body
- 25.4 Komposch N., Escriva A., Akhatou I.: Access to reproductive health care in temporary liminal spaces: Insights into the geopolitics of im/mobility and population in Spain's strawberry industry
- 25.5 Schurr C., Perler L., Komposch N., Perez-Hernandez Y.: Towards a reproductive geopolitics

## 25.1

# Energy geographies and the post-colonial condition: Eastern and Central Europe in crisis

Bouzarovski Stefan<sup>1</sup>

<sup>1</sup> Department of Geography, University of Manchester, Manchester, UK (stefan.bouzarovski@manchester.ac.uk)

In this talk, I seek to shed a critical light on the overlapping post-colonial and geopolitical realities that shape Eastern and Central Europe's (ECE) contemporary energy geographies. I explore three contingencies that are at play in shaping ongoing state policies and responses to Russia's invasion of Ukraine: the infrastructural legacies of post-socialism and subsequent transformations, the region's positioning within Europe's imaginary and material geopolitical map, and contemporary socio-political relations within ECE itself. I interpret the region's inherited socio-technical systems through the lens of past visions, priorities and interests imposed by the Soviet power structure (Bouzarovski 2009). In post-socialism, however, many of ECE's infrastructural installations were subject to dynamics of privatisation and marginalisation from the 'collective West'. The path-dependencies that underpin the region's internally contradictory positioning within the European energy polity – characterized by conflicting security and climate objectives – are the product of these interconnected dynamics, and directly influence Europe's wider energy and climate development trajectories. They bring attention to the broader system of energy provision – from sites of production to practices of demand (Balmaceda 2021) – through emergent forms of everyday geopolitics. They also highlight the importance of articulating a global post-colonial lens to understand current and future energy crises.

## REFERENCES

- Balmaceda, M.M., 2021. *Russian Energy Chains. The Remaking of Technopolitics from Siberia to Ukraine to the European Union*. Columbia University Press.  
Bouzarovski, S., 2009. East-Central Europe's changing energy landscapes: a place for geography. *Area* 41(4):452-463

## 25.2

### War and peace as embodied and situated experiences

Claske Dijkema<sup>1</sup>

<sup>1</sup> swisspeace, University of Basel, Kasernenhof 8, 4058 Basel (claske.dijkema@unibas.ch)

Feminist approaches have made space for subaltern voices in geographies of peace by attributing importance to the body and to the everyday, revealing violence that is generally hidden from plain sight by cultural values. These approaches insist on the need to connect the levels of the everyday and the private, most generally not taken into account with a political science approach to Peace and Conflict Studies, with geopolitical developments. The contribution of these feminist approaches is important for understanding peace as a situated and embodied experience. If war can be analysed, as Sylvester suggests, as an experience which is partly physical in the sense of injuries to bodies, and partly affective and emotional, I consider that peace can also be understood as an experience. Experience is about living a reality, is situated in a position and a location, and depends on a certain continuity. I will empirically support this argument based on my field research in a marginalised social housing neighborhood that has become known nationwide for paroxysmal violence in 2010 and 2012. Based on my findings, I focus on four aspects of war as an experience: 1) the experience of the deployment of military material; 2) the destruction of bodies and personal relationships; 3) the fear for physical security; 4) and the withdrawal from public life into private spaces. The merit of widening the geographic scope of violently contested cities to non-war cities dealing with paroxysmal violence is that they open up a range of empirical sites that can be analysed with the feminist approaches to peace geographies.

## 25.3

### Territory, sovereignty and entitlement: thinking territory through the body

Juliet J. Fall

*Department of geography & environment, University of Geneva*

This paper builds upon feminist approaches within political science, international relations and geography that study how bodies haunt global politics, by exploring how entitlement to power connects through the scale of the body to that of the state. In a context of rising populism and war in Europe, and continued political bluster, there is a continued need to take seriously how discourses of statehood within security crises are gendered in specific ways. This paper argues that the concept of entitlement offers potential for geographic enquiry by opening up new perspectives on masculinist framings of territory and state in critical geopolitics and in critical international relations. It considers specifically how discourses ground and naturalize claims to territory by showing how states' entitlement to territory and masculinist forms of personal entitlement are connected. Methodologically, it mobilises the concept of entitlement to show how territorial claims are naturalized through rhetorical devices grounded in hegemonic forms of masculinity. It argues that a clearer understanding of the connections between discourses of personal entitlement and state territorial sovereignty can further our understanding of territory, and... perhaps... map new ways of moving towards an emancipatory, feminist security that do not seek to naturalise politics in reactionary ways.

## 25.4

# Access to reproductive health care in temporary liminal spaces: Insights into the geopolitics of im/mobility and population in Spain's strawberry industry

Nora Komposch<sup>1</sup>, Angels Escriva<sup>2</sup>, Ikram Akhatou<sup>2</sup>

<sup>1</sup> Institute of Geography, University of Bern, Hallerstrasse 12, CH-3012 Bern (nora.komposch@giub.unibe.ch)

<sup>2</sup> Department of Sociology, Social Work and Public Health, University of Huelva, Avda. de las Fuerzas Armadas s/n, 21007 Huelva (angeles.escriva@dstso.uhu.es, akhatou-ikram@hotmail.com)

Huelva is Europe's largest strawberry-producing region and every year tens of thousands of female migrant farmworkers from Morocco and Eastern European countries contribute with their labor to this export commodity. Most women who are being recruited have young children, which they leave behind in their home countries while working temporarily abroad. This guarantees the Spanish state that they will return home when their contract expires, and employers fear less resistance from workers due to their family dependencies. The farmworkers work long shifts, receive poor wages, live with several workers in small spaces, and are exposed to (reproductive) health risks such as pesticide use and sexual assault at work. Since most of the seasonal farmworkers live during their temporary work in Spain right on the farm, far from cities and health centers, accessing health care represents an additional challenge. In this study, we explore the questions of how female migrant farmworkers get access to health services, how they help each other out with feminist self-organization or political actions and the hurdles that remain to be overcome in this regard. Thereby we seek a better understanding of the entanglements between circular migration arrangements, the working conditions in Huelva's strawberry production and the female farmworkers' access to (reproductive) health.

## 25.5

### Towards a reproductive geopolitics

Carolin Schurr, Laura Perler, Nora Komposch and Yolinliztli Pérez-Hernandez

Only a few weeks after Swiss women organized the largest women strike in the country in June 2019, an asylum seeker lost her baby due to lacking access to prenatal care. Women in Mexico marched for their constitutional right to abortion as indigenous and rural women continued to be forced to take contraception in order not to lose social benefits. While Switzerland joined other countries in protecting homosexual people from public discrimination with its vote in February 2020, Swiss lesbian women still have to turn to international sperm banks to become pregnant. All these recent events are examples of what we call "reproductive geopolitics". Linking reproductive life to geopolitics, we start from the assumptions that reproductive technologies are caught up in geopolitics when individuals, states, international organizations, transnational corporations, and religious and nongovernmental organizations define whose reproduction counts as desirable and whose bodies are discarded as disposable. Access to reproductive technologies says much about whose lives count (Butler 2004; Fassin 2007, 2009) in any particular territory. While some have declared "the end of state biopolitics" (Rose 2001) and consider "population control history" (Connelly 2009), this talk takes the example of Mexico to show the disjunctions, continuities, and entanglements between traditional state biopolitics and new modes of reproductive geopolitics. While in Mexico in the past the territorial management of populations was explicitly framed as population politics, in the present the governance of reproduction takes place more implicitly through regimes of health care, migration, and sexual politics. Policies in these regimes continue to manage populations in a territorial fashion, but they do not officially pursue population control. The concept of reproductive geopolitics seeks to make these unperceived population politics explicit.

## 26 Human Geographies: Cities, Regions, Economies

Sven Daniel Wolfe, Julio Paulos

*Swiss Association for Geography (ASG)*

### TALKS:

- 26.1 Aelbrecht P., Stevens Q.: Researching the role of planning and urban design in promoting intercultural encounters and experiences of social cohesion
- 26.2 Albrecher R., Kaufmann V.: The bench: Service station for public space users
- 26.3 Bichsel C.: Infrastructure and decolonisation: the case of Central Asia
- 26.4 Bouzarovski S.: Energy geographies and the post-colonial condition: Eastern and Central Europe in crisis
- 26.5 Curnier S.: Children on Campus: a project to voice children's perspective in the pedestrianization of the EPFL campus
- 26.6 Günay M., Schöngart L.: Public spaces between resonance and affordance. Introducing a new perspective on experimental space production
- 26.7 Nikolotov A.: Appropriated Value: Social Economic Lives of Astronomical Infrastructures in Kazakhstan
- 26.8 Perekhoda H.: Where does Donbass belong? The role of economic path-dependency and imperial mental geographies in the Ukrainian state-building projects (1917-1920s)
- 26.9 Soroka Y., Males L., Podnos V.: The social infrastructure of toponym changes in independent Ukraine: war and post-colonial discourse.
- 26.10 Verheij J., Gerber J.-D., Nahrath S.: To whom does it belong? Changing property regimes of an urban green commons in a densifying neighbourhood in Bern, Switzerland
- 26.11 Widmer H.: Mixed neighbourhoods, mixed squares? Exploring social diversity in public space

## 26.1

# Researching the role of planning and urban design in promoting intercultural encounters and experiences of social cohesion

Patricia Aelbrecht<sup>1</sup> and Quentin Stevens<sup>2</sup>

<sup>1</sup> *Public Space Observatory Research Centre and Geography and Planning School, Cardiff University, UK  
(AelbrechtP@cardiff.ac.uk)*

<sup>2</sup> *School of Architecture and Urban Design, RMIT University, Melbourne, Australia*

This paper seeks to address long-standing questions in academia, practice, and policymaking regarding the role of urban planning and urban design in promoting crosscultural encounters and experiences of social cohesion in socially and culturally diverse urban contexts. It develops and tests an innovative theoretical and methodological framework which draws together key analyses of social cohesion by Jenson and Kearns and Forrest with recent urban design literature to hypothesize how four key social dimensions – ‘belonging and Identity’, ‘inclusion’, ‘participation’ and ‘recognition’ – that characterise the social experience of cohesion link to physical, management and use attributes of public space design. It builds on established theories and methods from experimental social psychology and urban design and integrates them with sociological and geographical theories and methods for studying social relationships. Its methodology consists of five different methods (design review, post-occupancy evaluation, non-verbal communication, ethnographic and biographical) that aim to collect five different types of data (design, spatial, behavioural, social, and cultural) for studying person-environment relationships. It tests its effectiveness to examine three London’s public spaces – Gillett Square, Windrush Square and Kings Crescent Estate public spaces – in areas that are similarly ethnically diverse and socio-economic deprived, but with distinctly different approaches to symbolic representation, spatial design, and programming.

The proposed theoretical and methodological framework develops a pathway for new knowledge. It addresses a gap between the built environment disciplines and social sciences in terms of methods for studying social encounters in public space by linking the spatiality and materiality of public spaces with the observed varieties of sociality underlying everyday’s intercultural encounters. It also provides a multi-dimensional analysis of how public spaces with different design approaches are connected to different experiences of social encounter and wider consequences for social cohesion.

## REFERENCES

- Aelbrecht, P., & Stevens, Q. (Eds.). (2019) Public space design and social cohesion: An international comparison. Routledge.
- Jenson, J. (1998) Mapping Social Cohesion: The State of Canadian Research (pp. 109-28). Ottawa: Canadian policy research networks.
- Kearns, A., and R. Forrest. (2000) “Social Cohesion and Multilevel Urban Governance.” *Urban Studies* 37 (5-6): 995–1017.
- Wood, P., and C. Landry. (2008) *The Intercultural City: Planning for Diversity Advantage*. London: Routledge.
- Peters, K., B. Elands, and A. Buijs. (2010) “Social Interactions in Urban Parks: Stimulating Social Cohesion?” *Urban Forestry & Urban Greening* 9: 93–100.

## 26.2

### The bench: Service station for public space users

Renate Albrecher<sup>1</sup>, Vincent Kaufmann<sup>1</sup>

<sup>1</sup>LaSUR Laboratory of urban sociology, EPFL, Station 16, 1015 Lausanne (renate.albrecher@epfl.ch)

We are all pedestrians in our daily lives, to varying degrees, and therefore all occasional users of benches in public space. In this paper we want to show that the bench is an essential ergonomic element to promote walking in everyday life.

The paper is based on work carried out within the framework of the LaSUR on the modal shift towards walking for several Swiss municipalities, as well as on investigations carried out within the framework of the European research programme EIT Urban Mobility. The results of this work show that immobility associated with public benches is a key component to promote active mobility. Benches invite to active and passive participation in social life, serve as placemaker but also represent potential physical and social obstacles. Benches are markers of an inhabited city and an explicit invitation to the appropriation of public space (Jolé 2003; Schenk 2014) it is commonplace for a motorist to sit in a car but it is more of a problem for a pedestrian. The presence of solid public seats in Paris at the end of the XIXth century, when most people tended to walk everywhere, has given way to mistrust of useful urban furniture for the poorest. Seats that were once large and intended for the general public have recently been required to conform to increasingly restrictive building standards and usages. However, the species does not seem to be an endangered one.”,”container-title”：“Les Annales de la recherche urbaine”,”DOI”：“10.3406/aru.2003.2515”,”ISSN”：“0180-930X”,”issue”：“1”,”journalAbbreviation”：“aru”,”language”：“fr”,”page”：“107-115”,”source”：“DOI.org (Crossref. Benches can request and demand particular lines of actions and encourage, discourage, refuse or allow uses - in varying ways for different users and circumstances (Davis 2020).

The representation of the use of benches differs from spontaneous practices, consisting in a broad variety of uses, of which even users are often not always aware of.

The variety of different user groups is characterised by a wide and often contradictory variety of needs, priorities, obstacles and criteria for the use – or non-use - of benches. Identified features concern their positioning and orientation, their equipment and microenvironment, but also their shapes, the material as well as the presence (or absence) of other users and uses of the public realm.

The design-process of public seating is value-laden and political, its stakeholders usually belong to a minority of bench-users equipped with highly normative power. Users with « other » needs and preferences are usually not represented in this decision-making processes.

The results of our research demonstrate the need for a higher number and more different and user-friendlier types of seating devices in a close-knit network of micro-places in order to serve as a service station to all types of pedestrians (“augmented pedestrian”) and their “multitasking walk” (Albrecher et al. 2022).

#### REFERENCES

- Albrecher, Renate, Garance Clément, Maya El Khawand, Kamil Hajji, and Vincent Kaufmann. 2022. ‘Mobilité piétonne : le rôle des bancs publics dans la promotion de la marche’. doi: 10.13140/RG.2.2.11704.42241.
- Davis, Jenny L. 2020. *How Artifacts Afford: The Power and Politics of Everyday Things*. The MIT Press.
- Jolé, Michèle. 2003. ‘Quand la ville invite à s’asseoir : Le banc public parisien et la tentation de la dépose’. *Les Annales de la recherche urbaine* 94(1):107–15. doi: 10.3406/aru.2003.2515.
- Schenk, Steffen. 2014. ‘Sitzen im öffentlichen Raum: Die soziologische Aneignung einer Haltung’. *Magisterarbeit, Albert-Ludwigs-Universität Freiburg im Breisgau* 102. doi: <https://nbn-resolving.org/urn:nbn:de:0168-ssoar-67228-7>.

## 26.3

### Infrastructure and decolonisation: the case of Central Asia

Christine Bichsel<sup>1</sup>

<sup>1</sup> Department of Geosciences, Geography Unit, University of Fribourg, Chemin du Musée 4, 1700 Fribourg  
(christine.bichsel@unifr.ch)

This paper will examine the relationship between infrastructure and decolonization. Its aims to explore this relationship conceptually, and to draw from own empirical research on multiple sites in Central Asia in order to elaborate and advance a framework for analysis.

Infrastructure is a key element of imperial policy and practice to the aim of establishing and perpetuating control over population and territory, creating desired political, economic and cultural orders, and performing and legitimising imperial forms of rule (van Laak 2004, Davies 2017, Cowen 2020). As a result, infrastructure is equally part of what Laura Ann Stoler (2008) terms “imperial debris” in the aftermath of empires, embodying their both tangible and invisible remains. Tentatively termed “post-imperial”, such infrastructures present a multi-faceted challenge to processes of decolonisation as they configure economic path-dependency, materialise ideological continuity and fix socio-spatial practices. At the same time, these infrastructures are often the focal point and linchpin for successor regimes’ reinterpretation of social orders, and may be assigned new ideas and values, repurposed, but also destroyed or left to decay.

This paper argues that to examine processes of decolonisation requires close attention to the trajectories and transformations of post-imperial infrastructure. While studies of decolonisation and decoloniality have addressed a range of themes such as knowledge, identity and spatiality (Radcliffe 2017, Radcliffe and Radhuber 2020), a conceptually informed engagement with infrastructure is to date missing.

To address this gap, the paper will draw on Stoler’s (2008, 2016) concept of “imperial formation” as relations of force that harbour political forms shaping objects, knowledge but also sentiments beyond their formal existence. It will bring it into conversation with literature on memory politics (Kohlstruck 2004), meanings and affects (Schwenkel 2020) and violence (Rodgers and O’Neill 2012) of infrastructure.

Empirically, the paper will focus on Central Asia as a case study to elaborate and further reflections on the relationship between infrastructure and decolonisation. The nature of coloniality of Soviet Central Asia has long been disputed in scientific debates (Kassymbekova and Chokobaeva 2021). The paper does not aim to engage with this debates, but follows Stoler (2008)’s wide definition of imperial formation as a sustained configuration of symbolic and material imperialities beyond conventional ideas of metropole, colony and periphery. It aims to pay attention to the decentred and multi-sited forms of power in Central Asia beyond often-held assumptions of Euro-American imperialism (Doyle 2014).

The paper will draw on previous empirical research from different sites based on the author’s long-term fieldwork in and on Central Asia during the past 20 years. These sites include small urban settlements, rocket debris and irrigation pump stations. Data stem from ethnographic and archival research as well as secondary literature.

#### REFERENCES

- Cowen, D. 2020: Following the infrastructures of empire: notes on cities, settler colonialism, and method, *Urban Geography* 41, 469-486.
- Davies, D. 2017: Imperial infrastructure and Spatial Resistance in Colonial Literature, 1880-1930. Oxford: Peter Lang.
- Doyle, L. 2014: Inter-Imperiality. Dialectic in a Postcolonial World History. *Interventions*, 16(2), 159-196.
- Kassymbekova, B. and A. Chokobaeva. 2021: On writing Soviet History of Central Asia: frameworks, challenges, prospects. *Central Asian Survey*, 40(4), 483-503.
- Kohlstruck, M. 2004. Erinnerungspolitik: Kollektive Identität, Neue Ordnung, Diskurshegemonie. In: B. Schwellung (ed.): *Politikwissenschaft als Kulturwissenschaft. Theorien, Methoden, Problemstellungen*. Wiesbaden, 173–193.
- Radcliffe, S.A. 2017: Decolonising geographical knowledges. *Transactions of the Institute of British Geographers*, 42, 329-333.
- Radcliffe, S.A. and I.M. Radhuber. 2020: The political geographies of D/decolonization: Variegation and decolonial challenges off/in geography. *Political Geography* 78: 102128.
- Rogers, D. and B. O’Neill. 2012: Infrastructural violence: Introduction to the special issue, *Ethnography* 13(4), 401-412.
- Schwenkel, C. 2020: Building Socialism: The Afterlife of East German Architecture in Urban Vietnam, Durham: Duke University Press.
- Stoler, A.L. 2008: Imperial Debris: Reflections on Ruin and Ruination, *Cultural Anthropology* 23(2), 191–219.
- Stoler, A.L. 2016: Duress: Imperial Durabilities in Our Times. Durham: Duke University Press.
- Van Laak, Dirk 2004: Imperiale Infrastrukturen. Deutsche Planung für eine Erschließung Afrikas 1880 bis 1960. Paderborn: Ferdinand Schöningh.

## 26.4

# Energy geographies and the post-colonial condition: Eastern and Central Europe in crisis

Bouzarovski Stefan<sup>1</sup>

<sup>1</sup> Department of Geography, University of Manchester, Manchester, UK (stefan.bouzarovski@manchester.ac.uk)

In this talk, I seek to shed a critical light on the overlapping post-colonial and geopolitical realities that shape Eastern and Central Europe's (ECE) contemporary energy geographies. I explore three contingencies that are at play in shaping ongoing state policies and responses to Russia's invasion of Ukraine: the infrastructural legacies of post-socialism and subsequent transformations, the region's positioning within Europe's imaginary and material geopolitical map, and contemporary socio-political relations within ECE itself. I interpret the region's inherited socio-technical systems through the lens of past visions, priorities and interests imposed by the Soviet power structure (Bouzarovski 2009). In post-socialism, however, many of ECE's infrastructural installations were subject to dynamics of privatisation and marginalisation from the 'collective West'. The path-dependencies that underpin the region's internally contradictory positioning within the European energy polity – characterized by conflicting security and climate objectives – are the product of these interconnected dynamics, and directly influence Europe's wider energy and climate development trajectories. They bring attention to the broader system of energy provision – from sites of production to practices of demand (Balmaceda 2021) – through emergent forms of everyday geopolitics. They also highlight the importance of articulating a global post-colonial lens to understand current and future energy crises.

## REFERENCES

- Balmaceda, M.M., 2021. *Russian Energy Chains. The Remaking of Technopolitics from Siberia to Ukraine to the European Union*. Columbia University Press.  
Bouzarovski, S., 2009. East-Central Europe's changing energy landscapes: a place for geography. *Area* 41(4):452-463

## 26.5

### Children on Campus: a project to voice children's perspective in the pedestrianization of the EPFL campus

Sonia Curnier<sup>1</sup>

<sup>1</sup> LaSUR Laboratory of urban sociology, EPFL, Station 16, 1015 Lausanne ([sonia.curnier@epfl.ch](mailto:sonia.curnier@epfl.ch))

Over the past two decades, the EPFL campus in Lausanne has developed into a mixed and lively urban environment, frequented by a broad variety of users. The outdoor spaces of the campus are currently in the process of being transformed into a “campus piéton”. If these spaces are to become genuine public spaces (diverse and inclusive) it is necessary to appreciate the plurality of their potential users, the diversity of their needs and aspirations.

The ongoing research project “Children on Campus” (2022-2023) part of the Habitat Research Center Living Lab initiative aims at reflecting specifically on the place given to (preschool) children on a university campus. With the increasing construction of EPFL/Unil’s care facilities, children represent a growing part of the campus’s users. They should therefore be considered in its transformation process, on equal terms as grown-ups.

Incorporating their perspective into the design of the campus piéton means envisioning outdoor spaces as places to be explored with their peers and their caregivers, as opportunities to develop motor and sensory skills and enjoy regular contact with nature, culture and the adult world. It also prompts to reflect on the surroundings of day-care facilities as places of encounter, for the children’s parents, the vast majority of whom are expatriates who suffer from a form of isolation in their parental status.

This case study provides an opportunity to explore age-appropriate tools and methods for incorporating the perspectives of preschoolers into a public space redesign process. It also allows for reflection on campuses as child-friendly environments if these are to be considered true urban and public places.

## 26.6

# Public spaces between resonance and affordance. Introducing a new perspective on experimental space production

Melis Günay<sup>1</sup>, Laura Schöngart<sup>2</sup>

<sup>1</sup> HafenCity University Hamburg

<sup>2</sup> Department of Open Space Planning, Hochschule Geisenheim University, Villa Monrepos, Rüdesheimer Str. 5, 65366 Geisenheim & HafenCity University Hamburg ([laura.schoengart@hs-gm.de](mailto:laura.schoengart@hs-gm.de))

As urban stages for public life and everyday practices, streets reflect on societies' socio-spatial conditions and relations. Studies of streets reveal power imbalances that have been inscribed and manifested in spatial forms and routinized practices over decades. Lately, these are being challenged by grassroot initiatives implementing temporal and low-budget interventions on site. Often referred to as Tactical Urbanism, these strategies clearly illustrate the fluid character of space and the therein laying potential: sustainable transition through a dynamic loop of (in)formal reproduction.

Literature exploring the bottom-up practices of 'making' suggests that their implementation promotes and builds on place-based attachments. This can lead to the adaptation of more sustainable behaviors and growing resilience. Furthermore, the experimental nature makes change tangible and allows for gradual transformation. Therefore, Tactical Urbanism strategies have long been 'formalized' by urban planning. Yet, implemented as means to political ends, they fail to promote the 'making'-practices key to fostering place attachments. The challenge for planning disciplines, to grasp and spatially implement these dynamics, remains.

We argue that Rosa's theory of resonance and Gibson's theory of affordance can be combined to outline the yet undefined 'zone' between formality and informality, framing and openness, offer and appropriation which enables 'making'-practices and place-based attachments. Understanding public spaces as processual entanglements between medium and agency, this contribution translates the two theories into an approach for studying experimental space production. The proposed theoretical framework ideally allows for conclusions on reflective planning and conceptualizations of spatial components of framing and openness.

## 26.7

### Appropriated Value: Social Economic Lives of Astronomical Infrastructures in Kazakhstan

Nikolotov Anton<sup>1</sup>

<sup>1</sup> Visiting Postdoctoral Fellow. Department of Geosciences, Geography Unit, University of Fribourg, Chemin du Musée 4, 1700 Fribourg (anton.nikolotov@unifr.ch).

I will examine how the local pastoralists and tourists appropriate the infrastructures belonging to the Fesenkov Institute of Astrophysics (FAI) located in the vicinity of the former capital Almaty. My aim here is to theorize the specific regime of values that emerge from the consumption of landscape and the multiple shared uses of the location, architecture, and the night sky. Founded by the group of astronomers from the European part of the USSR who were evacuated during the Second World War in 1941, FAI, today, is part of the Republic of Kazakhstan. After the collapse of the Soviet Union, most of the observatories have become parts of the national astrophysical and meteorological institutes. However, many others have turned into extraterritorial infrastructures on lease to the Russian academies of science, and are also sometimes located in the national border zones. Despite such complex entanglements of power relations, local entrepreneurship and inter-dependencies, there are currently no in-depth studies of the socialities of these spaces. This research aims to address this lacuna and contribute to a more nuanced understanding of economisation of infrastructure after post-Socialism.

## 26.8

# Where does Donbass belong? The role of economic path-dependency and imperial mental geographies in the Ukrainian state-building projects (1917-1920s)

Hanna Perekhoda<sup>1</sup>

<sup>1</sup> Institut des Etudes Politiques, Université de Lausanne, Quartier UNIL-Mouline, Bâtiment Géopolis, CH-1015 Lausanne (hanna.perekhoda@unil.ch)

As the revolution broke out in February 1917, the Russian Empire entered a phase of disintegration and numerous regions started to claim their political autonomy. Therefore, the definition of their territories became an important issue. One of the major controversies concerned the eastern part of Ukraine, a highly industrialized region commonly known as the Donbass. Drawing the state boundaries was indeed not a trivial matter, especially in a former continental empire which had several zones halfway between colonial periphery and metropolitan core and Eastern Ukraine was such a zone.

My research explores the cleavage within the Bolshevik Party opposing two groups: those who wanted the Donbass to be a part of Ukraine and those who perceived it as part of Russia. I will show how both economic and administrative path-dependencies and ideological continuities embodied in imperial infrastructures were determining political actors' "mental geographies", influencing their strategies, and guiding their political choices.

As the current war between Russia and Ukraine shows, the relationship between these two states is still bearing a heavy imprint of imperial legacies and Eastern Ukraine is a corner stone of both Russian and Ukrainian state and nation building concurring projects.

## 26.9

# The social infrastructure of toponym changes in independent Ukraine: war and post-colonial discourse.

Yuliia Soroka<sup>1</sup>, Lyudmyla Males<sup>2</sup>, Varvara Podnos<sup>3</sup>

<sup>1</sup> Human Geography unit, Fribourg university, Ch. du Musée 4, 1700 Fribourg (yuliia.soroka@unifr.ch); Department of sociology, N.V.Karazin Kharkiv national university, pl. Svobody, 4, 61022, Kharkiv, Ukraine.

<sup>2</sup> Faculty of Sociology, Taras Shevchenko National University of Kyiv, Volodymyrska Street, 60, 01033, City of Kyiv, Ukraine (lyudmylamales@gmail.com)

<sup>3</sup> Independent researcher, Dmytrivska st., 19, 61052, Kharkiv, Ukraine (varvara.podnos@gmail.com)

The initiatives to change the names of streets and other toponyms and the dismantling of monuments became the response of Ukrainian society to Russia's war in Ukraine beginning in February 2022. The Kharkiv city council has renamed Moscow Avenue, Belgorod highway, and two connecting toponyms<sup>1</sup>. The Kyiv city council has identified 279 names that must be renamed<sup>2</sup>. Monuments of Russian writer Alexander Pushkin were dismantled in Ternopil and Uzhhorod<sup>3</sup>. These and other actions continued the Ukrainian resistance to Russia's military aggression and moved it into a symbolic space of Ukrainian cities.

The media and public discourse quickly labeled these acts of symbolic struggle as anti-colonial or anti-imperial. It meant that Russia's unprovoked invasion of its sovereign neighbor, the country of Ukraine, manifested the Russian Federation as an empire trying to regain its colony. Russian and soviet symbols embodied in toponyms and monuments were designated as hostile and toxic, which denied the right of the Ukrainian nation to self-determination.

But using a critical and post-colonial methodology on the politics of toponyms brings us back to other questions.

Since the beginning of the 1990s, there have been several waves of renaming and struggle with monuments. The first connected with the struggle for Ukrainian independence, the next - with the adoption and implementation of the Decommunization law, and the current one is taking place in the war conditions. The state government, the public and civil organizations, political parties, the academic community, the particular institutions, and the local communities participated in the toponym changes process. The way of interaction, hierarchization, and cooperation of these diverse agents of toponym changes we call the social infrastructure of toponym changes.

We will compare the power structure implemented in volunteer movements, toponymic commissions, and civil hearings as social infrastructure-specific forms taking place during different waves of toponym changes in Ukrainian cities Kyiv and Kharkiv. We will try to understand, did the social infrastructure give a voice to city communities and other agents or not; what kind of participatory procedure toponym changes as a transformation process of symbolic spaces demands.

## REFERENCES

- In Kharkiv, the Moscow district, the avenue and two streets associated with the Russian Federation were renamed. *Suspilne novyny*. May 11, 2022
- Kyiv to change street names linked to Russia, Belarus. *The Kyiv Independant*, April 25, 2022.
- Monument to Russian writer Alexander Pushkin dismantled in Ternopil. *The Kyiv Independant*, April 9, 2022.

---

1 In Kharkiv, the Moscow district, the avenue and two streets associated with the Russian Federation were renamed. *Suspilne novyny*. May 11, 2022

2 Kyiv to change street names linked to Russia, Belarus. *The Kyiv Independant*, April 25, 2022.

3 Monument to Russian writer Alexander Pushkin dismantled in Ternopil. *The Kyiv Independant*, April 9, 2022.

## 26.10

# To whom does it belong? Changing property regimes of an urban green commons in a densifying neighbourhood in Bern, Switzerland

Jessica Verheij<sup>1\*</sup>, Jean-David Gerber<sup>1</sup>, Stéphane Nahrath<sup>2</sup>

<sup>1</sup> Institute of Geography & Center for Regional Economic Development (CRED), University of Bern. Hallerstrasse 12, 3012 Bern, Switzerland.

<sup>2</sup> Swiss Graduate School of Public Administration (IDHEAP), University of Lausanne, Switzerland

\* jessica.verheij@giub.unibe.ch

Urban green spaces can be conceptualized as common-pool resources, constituting resources that are shared among and used by a diverse set of users (Schlager and Ostrom 1992). Building on ‘the right to the city’ movement that developed on the work of Lefebvre (1991), scholars have conceptualized the idea of ‘urban commons’ not only as a collective resource that is shared among users, but also as a collective claim towards this resource: those involved in the use and co-production of the resource have a right to participate also in its management. Being, however, located in “spaces saturated with people, conflicting uses, and capitalist investments” (Huron 2015:977), maintaining the urban commons as a resource and form of management that is both collective and inclusive is challenging (Caffentzis and Federici 2014). In particular in contexts of densification, increased pressure on land within the existing (and often already congested) urban environment can lead to enclosure of the commons (Hodkinson 2012). In this regard, densification poses challenges to the production and maintenance of urban green spaces as urban commons. In this contribution, we aim to address this issue by focusing on the changing property regimes of urban green spaces, understanding property as a bundle of rights that goes beyond strictly public or private property (Blomley 2004b; Rose 1998; Schlager and Ostrom 1992). Given the many ownership claims that are enacted towards urban commons, the question “to whom does it belong” can have many different answers (Blomley 2004a; Krueckeberg 1995). In particular, densification leads to a redistribution of property rights of urban green commons among old and new users. Accordingly, we ask how densification, as spatial and political process that creates additional pressure and a multiplication of claims on urban land, affect the property regime of urban green commons, as collective resource that is co-produced and managed through everyday use by city dwellers and, as such, is subject to different ownership claims. We develop our theoretical argument based on empirical data collected through an in-depth case study of an urban green space located in an area undergoing densification for housing development in the city of Bern, Switzerland. Our research shows how, because of densification policies, ownership claims and feelings of belonging over the urban green commons change, and how, subsequently, property rights are redistributed - with implications for who is included/ excluded in having access to the resource.

## REFERENCES

- Blomley, Nicholas. 2004a. “Un-Real Estate: Proprietary Space and Public Gardening.” *Antipode* 614–41.
- Blomley, Nicholas. 2004b. *Unsettling the City - Urban Land and the Politics of Property*. New York: Routledge.
- Caffentzis, George and Silvia Federici. 2014. “Commons against and beyond Capitalism.” *Community Development Journal* 49(SI):92–105.
- Hodkinson, Stuart. 2012. “The New Urban Enclosures.” *City* 16(5):500–518.
- Huron, Amanda. 2015. “Working with Strangers in Saturated Space: Reclaiming and Maintaining the Urban Commons.” *Antipode* 47(4):963–79.
- Krueckeberg, Donald A. 1995. “The Difficult Character of Property: To Whom Do Things Belong?” *Journal of the American Planning Association* 61(3):301–9.
- Rose, Carol M. 1998. “The Several Futures of Property: Of Cyberspace and Folk Tales, Emission Trades and Ecosystems.” *Minnesota Law Review* 83(1):129–82.
- Schlager, Edella and Elinor Ostrom. 1992. “Property-Rights Regimes and Natural Resources: A Conceptual Analysis.” *Land Economics* 68(3):249–62.

## 26.11

# Mixed neighbourhoods, mixed squares? Exploring social diversity in public space

Hannah Widmer<sup>1</sup>

<sup>1</sup> Observatory for Cycling and Active Mobilities (OUVEMA) & Institute of Geography and Sustainability, University of Lausanne, Mouline – Géopolis, CH-1015 Lausanne (hannah.widmer@unil.ch)

As places where one can pass by or spend time alone or with others, public squares provide space for thin sociality (Bodnar 2015) between people from all walks of life. Even though most encounters between strangers are fleeting, they are a necessary condition for ‘thicker’ kinds of sociality (Middleton and Samanani 2022). It is not clear, however, to which extent squares function as social infrastructure for the co-presence of strangers (Latham and Layton 2019). Depending on the time of the day, their gender, age, class, family situation, etc., people use public squares differently and might never meet at all.

This paper examines three public squares in the city of Zurich (Switzerland), their accessibility and responsiveness to people’s needs, and the ensuing diversity of users. To explore the relationship between the squares and the neighbourhoods, I compare the users of the squares to the neighbourhood population and determine which groups are under- or overrepresented. Middle-class people, for example, are overrepresented in all three squares despite them being located in socioeconomically different neighbourhoods. Moreover, the analysis of survey and register data shows that the social diversity in the squares is lower than in the neighbourhood for many variables. This suggests that the squares do not cater to the needs of some parts of the population, thereby challenging its capacity as a social infrastructure. By turning to the squares’ materialities, affordances and atmospheres to account for the absence of certain groups, this paper contributes to debates on diversity and sociality in public space.

## REFERENCES

- Bodnar, J. (2015). Reclaiming public space. *Urban Studies*, 52(12), 2090–2104. <https://doi.org/10.1177/0042098015583626>
- Latham, A., & Layton, J. (2019). Social infrastructure and the public life of cities: Studying urban sociality and public spaces. *Geography Compass*, 13(7), e12444. <https://doi.org/10.1111/gec3.12444>
- Middleton, J., & Samanani, F. (2022). Whose city? Which sociality? *Urban Geography*, 43(5), 777–783. <https://doi.org/10.1080/02723638.2021.2007665>

## 27 Global change and sustainability issues in mountain areas

Carolina Adler, Jörg Balsiger, Raffaella Balzarini, Philippe Bourdeau, Mélanie Clivaz, Iago Otero, Emmanuel Reynard

### TALKS:

- 27.1 Cristofari H., Urbach D., Otero I., Reynard E., Guisan A., Randin C.: A conceptual model of mountain socio-ecological systems to support multi-stakeholder collaborations for the management and monitoring of mountain regions
- 27.2 Deléglise C., François H., Loucugaray G., Crouzat E.: Reducing vulnerability to drought of mountain livestock farming: identification of levers and barriers from pasture to territorial levels
- 27.3 Delves J.L., Schneiderbauer S.: Investigating the integration of social science concepts and methods in long-term monitoring in global mountains
- 27.4 Khardziani T., Maisuradze R.: Combining Land Use/Land Cover Change Detection & Participatory Mapping Techniques to Analyze Changes in the Mountain Landscapes of Georgia
- 27.5 Megerle H.E.: Agroforestry systems as a contribution to sustainable mountain development, Case study Burundi
- 27.6 Savoy A., Flaminio S., Nahrath S., Reynard E.: Multipurpose use of hydropower dam reservoirs: Exploring the governance regime to develop coherent management strategies
- 27.7 Schneiderbauer S., Fontanella-Pisa P., Szarzynski J., Delves J., Terzi S.: Safeguarding Mountain Social-Ecological Systems – a global summary of regional mountain challenges
- 27.8 Thornton J.M., Snethlage M.A., Sayre R., Urbach D.R., Vivioli D., Ehrlich D., Muccione V., Wester P., Insarov G., Adler C.: Human populations in the world's mountains: Spatio-temporal patterns and potential controls
- 27.9 Tiwari Prakash C.: Women's Innovative Land and Water Management Practices in Marginalized Mountains: A Learning Experience of Citizen Science in Climate Change Adaptation and Sustainable Development in Himalaya

**POSTERS:**

- P 27.1 Baud A.: Les stratotypes triasiques, géotopes encore mal connus du patrimoine géologique préalpin vaudois
- P 27.2 Khelidj N., Mottet L., Losapio G.: Glacier retreat shapes plant functional diversity
- P 27.3 Sati Vishwambhar Prasad: Sustainable eco-tourism development in the Uttarakhand Himalaya: a case study
- P 27.4 Shakas A., Hediger R., Pfister I., Meusburger K., de Pasquale G., Singha K., Wagner F., Maurer H.: Geophysical insights in a 20 year-long irrigation experiment of the Pfynwald forest (Valais)
- P 27.5 Thornton J.M Pepin N., Shahgedanova M., Adler C.: Coverage of In Situ Climatological Observations in the World's Mountains
- P 27.6 Tu B.N., Khelidj N., Losapio G.: Assessing the impact of glacier retreat on biodiversity and plant-insect interaction dynamics

## 27.1

# A conceptual model of mountain socio-ecological systems to support multi-stakeholder collaborations for the management and monitoring of mountain regions

Hélène Cristofari<sup>1</sup>, Davnah Urbach<sup>2</sup>, Iago Otero<sup>1</sup>, Emmanuel Reynard<sup>1</sup>, Antoine Guisan<sup>1</sup>, Christophe Randin<sup>1,3</sup>

<sup>1</sup> Centre interdisciplinaire de recherche sur la montagne, University of Lausanne, Chemin de l'Institut 18, CH - 1967 Brégis

<sup>2</sup> Global Mountain Biodiversity Assessment, Institute for Plant Sciences, University of Bern, Altenbergrain 21, CH – 3013 Bern

Mountain regions are facing growing challenges, ranging from climate change and associated risks and disasters to increasing pressure from tourism. These challenges have both ecological and social causes and consequences, which calls for interdisciplinary collaborations across scientific domains to understand and address them. Yet, research efforts are fruitful only if they are planned and carried out such as to enable action and support management strategies, which calls for the co-production of knowledge between scientists and politicians, practitioners, as well as other relevant stakeholders. Scientific interdisciplinarity and interprofessional collaboration and co-design both require a capacity to understand others' perspectives and constructively share different types of knowledge, different priorities, as well as different values. This in turn requires a shared understanding of the topic at hand and a shared language to discuss without recurrent misunderstandings. Our work aims at supporting mountain science and sustainable development by developing a conceptual model of mountain socio-ecological systems that can be used as a basis for dialogue consultations, and negotiations across discussion partners from within and outside of science.

This model for mountain socio-ecological systems (MtSES) is designed as a boundary object, i.e. a representation that both sums up commonalities and supports the expression of different perspectives. It results from (i) an assessment of the usability of the conceptual framework of the Intergovernmental Science-Policy Platform on Biodiversity and Ecosystem Services (IPBES) (Díaz et al. 2015) as well as Klein et al. (2019) work on the characteristics and challenges of mountain systems; (ii) 15 interviews with professionals from the sectors of tourism, agriculture, energy, and forestry, that were qualitatively analyzed; and (iii) a continuous bibliographical search. The interviews were performed within a study region comprising the Swiss cantons of Valais and Vaud and followed a method based on the description and categorization of pictures.

The model is constructed around the distinction, which pervaded the interviews, between nature and humans. We thus give an equal representation to both, with a Natural Mountain System and a Human Mountain System. This equal representation represents a major difference between our suggested model and existing ones. Additionally, the model distinguishes between direct and indirect human drivers of change of the natural system as well as direct and co-produced nature's contributions to people. The latter require joint natural and human inputs, as is the case for agricultural production for instance. Human direct drivers of change of the human system in turn include events such as global social change or conflicts and wars which directly affect mountain populations, without transforming first the natural system. Similarly, natural direct drivers of change of the natural system include events such as global tectonic movements which may directly affect the natural system through earthquakes for instance.

We view this model as a tool to support the expression of different perspectives and facilitate scientific interdisciplinarity and multi-actor collaboration. The next steps will be to test the usability of this model for identifying interdisciplinary research questions and in the context of transdisciplinary workshops. Supporting tools such as game materials (e.g. cards) might be developed in the future to facilitate the uptake and use of this model in different contexts.

## REFERENCES

- Díaz, S., Demissew, S., Carabias, J., Joly, C., Lonsdale, M., Ash, N., et al. (2015). The IPBES Conceptual Framework—connecting nature and people. *Current opinion in environmental sustainability*, 14, 1-16.
- Klein, J. A., Tucker, C. M., Nolin, A. W., Hopping, K. A., Reid, R. S., Steger, C., et al. (2019). Catalyzing transformations to sustainability in the world's mountains. *Earth's Future*, 7(5), 547-557.

## 27.2

# Reducing vulnerability to drought of mountain livestock farming: identification of levers and barriers from pasture to territorial levels

Claire Deléglise<sup>1</sup>, Hugues François<sup>1</sup>, Grégory Loucoguaray<sup>1</sup>, Emilie Crouzat<sup>1</sup>

<sup>1</sup> Univ. Grenoble Alpes, INRAE, LESSEM, 2 rue de la Papeterie, BP 76, F-38402 St-Martin-d'Hères, France  
 (claire.deleglise@inrae.fr)

Extensive livestock farming is a central activity in mountain areas. It contributes significantly to their economy and plays a central role in their attractiveness (landscapes, bio-cultural diversity...). As the functioning of mountain livestock farms largely relies on rain-fed grasslands and rangelands, these systems are highly impacted by climate change, and in particular very sensitive to droughts.

To anticipate the consequences and adapt to the increased frequency and intensity of droughts, increased knowledge on mountain livestock farms' vulnerability to drought is urgently needed. Vulnerability diagnoses are particularly suited to investigate the interlinkages between human activities and their socio-ecological surroundings and therefore appear an ideal tool to tackle the issues of adaptation to climate change in agriculture (Fellman 2012). By identifying the levers and barriers to adaptation, they can assist stakeholders in selecting their paths of action. Therefore our study holds operational dimensions for stakeholders of the case-study area, while also contributing to scientific advances by developing a methodological sequence on how to inform the vulnerability framework in the specific context of extensive mountain livestock systems.

We conducted this work in the Vercors Regional Park (French Prealps), as a case study for the Interreg Alpine Drought Observatory project. Droughts are becoming a concern in this region which is characterized by a transitional climate between the Southern Alps (Mediterranean influences) and the Northern Alps (more oceanic and/or continental influences), superficial soils and a draining subsoil typical of a limestone karstic massif. Sensitivity to droughts is particularly notable for extensive livestock farming systems (cattle, sheep and goat breeding for milk and/or meat, often recognized with quality certifications) that directly depend on natural resources (forage, water). This set of characteristics makes the Vercors Regional Park a preferential field of investigation to develop operational tools supporting the adaptation to climate change for key mountain socio-economic sectors such as agriculture. Using the IPCC analytical framework of vulnerability, we analysed the vulnerability of a diversified sample of mountain livestock farms through a three-step diagnosis:

- i) agroclimatic characterisation of the exposure of farms to drought,
- ii) analysis of the sensitivity of farms (i.e. degree of drought impacts),
- iii) identification of adaptive capacities (i.e. how farmers react at short-term and adapt at mid to long term).

According to this framework, a livestock farm is vulnerable to droughts when it is exposed and sensitive to droughts and when it has low adaptive capacities.

In the first step of our analysis, we characterized the temporal and spatial variability of droughts in the study area (frequency, magnitude and duration of drought events) using climatic re-analysis data over the last 60 years period.

- ➔ We showed that although droughts are not getting more intense or longer in average over the last decades, they are significantly more frequent and tend to occur earlier in the season. We also highlight the spatial heterogeneity of drought exposure within the study area, with the southern and western parts of the massif being prone to the most noticeable increase in the drought frequency.

To carry out the next steps of the vulnerability diagnosis, we conducted semi-structured interviews with 20 farmers spread over the study area and whose farm's size, production orientation and functioning were representative of the local livestock farming systems. We assessed how mountain livestock farmers perceive being impacted by droughts as well as how they respond to these extreme events.

- ➔ We found that the sensitivity of farms to drought is mainly determined by the sensitivity of agro-pastoral resources (grass- and rangelands, fodder crops...) while drought impacts on water and herds appear to be less important so far. In each farm, sensitivity is therefore closely related to the pedo-climatic and agro-ecologic conditions of parcels in combination with farmer's management at the parcel level.
- ➔ Adaptive capacities of farms depended both on internal factors, especially for reactive short-term adjustments, and on external (off-farm) factors, especially for longer-term adaptations. Internal factors encompass, for instance, the type and spatial arrangement of farm's parcels, the herd size, the type of production system (e.g., dairy or suckling), the income level (allowing external hay purchases or not) or the know-how of farmers. External factors relate for instance to the possibility to access to supplementary agricultural land, to set up water storage infrastructures or to modify collective rules on summer pastures. At the different levels, from the plot to the territory, we identified both barriers (e.g., natural harsh climate and topography, land pressure, wolf predation risk) and levers to adaptation (e.g., collective dynamics for the dissemination of agronomic levers, opportunities for direct selling and diversification in relation to tourism).

Our study identifies the factors at play in farms' vulnerability to droughts, and highlights the different biophysical and socio-economic barriers and levers to adaptation, from pasture to territory levels. This diagnosis has locally been shared with stakeholders related to mountain livestock farming in the Vercors Regional Park (farmers, agricultural organizations, local or regional authorities...) in order to support their adaptation needs. The challenge ahead lies in enhancing the transformation of mountain livestock farms towards more climate-resilient systems in a way that also preserve their current agro-ecological functioning and positive externalities.

## REFERENCES

- Fellmann, T. 2012: The assessment of climate change related vulnerability in the agricultural sector: Reviewing conceptual frameworks. In: Building resilience for adaptation to climate change in the agriculture sector (Ed. by Meybeck, A., Lankoski, J., Redfern, S., Azzu, N. & Gitz, V.). Rome, Italy: Food and Agriculture Organization (FAO), pp 37–61.

## 27.3

# Investigating the integration of social science concepts and methods in long-term monitoring in global mountains

Jess L Delves<sup>1,2</sup>, Stefan Schneiderbauer<sup>1,2,3</sup>

<sup>1</sup> United Nations University, Institute for Environment and Human Security, 53113 Bonn, Germany

<sup>2</sup> Centre for Global Mountain Safeguard Research, Eurac Research, 39100 Bozen/Bolzano, Italy ([jdelves@eurac.edu](mailto:jdelves@eurac.edu))

<sup>3</sup> Department of Geography, Qwaqwa Campus, University of the Free State, 9301 Bloemfontein, South Africa

Healthy mountain social-ecological systems not only support local societies but also provide myriad ecosystem services to lowlands (e.g. biodiversity, climate regulation, water cycle, provisioning of recreation, cultural or spiritual values etc.). Interventions aimed at balancing sustainable management of mountain ecosystems and human well-being need a sound scientific basis; this is the rationale behind the long-term monitoring of climatic and ecological change. But in the Anthropocene - or rather, the Capitalocene - physicochemical and biophysical changes of the earth's systems cannot be studied as independent from human systems, so influential are they on one another.

A growing recognition of the human dimensions of ecological change has been reflected in the increased representation of social science concepts and methods in long-term monitoring, notably with the addition of the 'socio' in Long-Term Socio-Ecological Research (LTSER) in the mid-2000s. There are approximately 80 LTSER platforms globally which host place-based socio-ecological research and monitoring. LTSER platforms are included – along with approximately 700 Long Term Ecological Monitoring sites - in the International Long Term Ecological Research (ILTER) network, which supports these sites with network infrastructure and services.

The value of multi-, inter- and transdisciplinarity has been expounded for decades: citizen participation in site-specific monitoring has been shown to increase environmental literacy and public support of conservation, to promote knowledge exchange, to increase social capital and ultimately to benefit the ecosystems being monitored (Conrad & Hilchey, 2011). However, several studies have highlighted conceptual and tangible barriers to inter- and transdisciplinary integration in site-specific long-term monitoring (see Orenstein et al., 2019).

The here-presented research investigates the challenges and opportunities in inter- and transdisciplinarity in long-term monitoring in global mountainous regions across two scales, site-specific and global. At the site-specific resolution, I conducted seven semi-structured interviews with site managers (from mountain sites in Austria, Israel, Italy, southern Africa and UK) to understand the extent to which the human dimension is, has been, or has tried to be incorporated into environmental monitoring activities, and what barriers have been encountered in inter- and transdisciplinary processes.

Some of these barriers exist not only in site-specific monitoring in mountains but also in global monitoring. In order to understand how global processes shape mountain social-ecological systems, monitoring is also needed at global scales. The socioeconomic, sociocultural and sociopolitical conditions of human populations can be monitored by way of data on demographics, education, housing, living standards, values and traditions, migration, perceptions and much more. Currently much of this information, particularly pertaining to intangible elements of society, is either unavailable, disproportionately available and/or unstandardised across time and space. In light of this information gap, in early 2022 the Task Group 2.3 (TG2.3) was established by the Group on Earth Observations (GEO) Global Network for Observations and Information in Mountain Environments (GEO Mountains), an initiative of GEO which aims to fill data gaps pertaining to global change drivers, condition and trends through earth observation and in-situ data (Adler et al., 2018). The objective of TG2.3 is to produce a set of essential socioeconomic variables to be monitored in global mountains and define their associated characteristics, following on from the identification of Essential Mountain Climate Variables (Thornton et al., 2021).

I therefore draw on my experience as co-lead of the GEO Mountains TG2.3, and a literature review carried out in the context of this project, to investigate interdisciplinarity in global-scale mountain monitoring. The preliminary results show that, at global resolution, the meaningful integration of societal and biophysical data appears to remain a methodological impasse due to differences in data collection methods, while the challenges to overcome in the creation of a harmonised global dataset of socioeconomic variables include, among others: differences in data definitions, collection and analysis methods, and data availability and quality. In addition, at site-specific resolution, challenges in inter- and transdisciplinarity identified in previous studies in the lowlands may be more prominent in mountains, and different challenges exist that relate to mountain specificities (e.g. remoteness, heterogeneity in ethnic and linguistic groups, frequent natural hazards). The results provide the basis for reflections and recommendations for a more meaningful integration of social science concepts and methods in long term monitoring research design across both site-specific and global scales.

## REFERENCES

- Adler, C., Palazzi, E., Kulonen, A., Balsiger, J., Colangeli, G., Cripe, D., Forsythe, N., Goss-Durant, G., Guigoz, Y., Krauer, J., Payne, D., Pepin, N., Peralvo, M., Romero, J., Sayre, R., Shahgedanova, M., Weingartner, R., & Zebisch, M. (2018). Monitoring mountains in a changing world: New horizons for the global network for observations and information on mountain environments (GEO-GNAME). *Mountain Research and Development*, 38(3), 265–269. Scopus. <https://doi.org/10.1659/MRD-JOURNAL-D-8-00065.1>
- Orenstein, D. E., Angelstam, P., Dick, J., Holzer, J., & Sijtsma, F. (2019). Long-term socio-ecological research platforms: A best practices guide book.
- Thornton, J. M., Palazzi, E., Pepin, N. C., Cristofanelli, P., Essery, R., Kotlarski, S., Giuliani, G., Guigoz, Y., Kulonen, A., Pritchard, D., Li, X., Fowler, H. J., Randin, C. F., Shahgedanova, M., Steinbacher, M., Zebisch, M., & Adler, C. (2021). Toward a definition of Essential Mountain Climate Variables. *One Earth*, 4(6), 805–827. <https://doi.org/10.1016/j.oneear.2021.05.005>

## 27.4

# Combining Land Use/Land Cover Change Detection & Participatory Mapping Techniques to Analyze Changes in the Mountain Landscapes of Georgia

Tamar Khardziani<sup>1,2</sup>, Roman Maisuradze<sup>3</sup>

<sup>1</sup> Institute of geography, Tbilisi State University, Tamarashvili st. 6, 0177 Tbilisi, Georgia (tamar.khardziani@tsu.ge)

<sup>2</sup> Institute of geography, Heidelberg University, Im Neuenheimer Feld 348, 69120 Heidelberg, Germany (tamar.khardziani@uni-heidelberg.de)

<sup>3</sup> Independent researcher, Moscow ave. 19, 0137 Tbilisi, Georgia

Land use/land cover (LULC) change detection and the inclusion of local knowledge became essential techniques in landscape mapping and analysis. Human activities change the landscape structure, land-use types, natural ecosystems, and “the capacity of landscapes to deliver desired ecosystem services” (Turner & Gardner, 2015). Around the globe, apart from climate, land-use change is also the primary driver of environmental degradation and the subsequent loss of ecosystems and biodiversity. “A major challenge today and into the future is to maintain or enhance beneficial contributions of nature to a good quality of life for all people” (Díaz et al. 2018). Remote Sensing (RS) Data-based analysis of land use/land cover change is a widely recognized instrument in the study of land conservation, resource management, sustainable development and landscape research. However, the inclusion of local people’s perceptions in landscape valuation is still under discussion. The importance of local knowledge emerged in response to the question about who’s voices matter in the valuation of the landscape. The local knowledge system, popularly known as local cultural wisdom, involves elements of values and practice. Local case studies are essential for understanding complex human-nature systems (O’Rourke, 2005). The public participation GIS (PPGIS) approach (Schroeder, 1996) is considered, by many researchers, as a way of local community participation in the landscape valuation process. PGIS is seen as a tool for democratizing GIS-based decision-making processes, empowering local stakeholders in spatial decisions to make planning more inclusive and avoid anticipated conflict among stakeholders (Elwood, 2006; Dunn, 2007; Brown & Kyttä, 2014; Duží et al. 2019). Geoparticipation is also discussed under the concept of citizen science, which supports “the empowerment of relationships between science and society” (Duží et al. 2019). It is considered “a more socially aware type of GIS which gives greater privilege and legitimacy to local or indigenous spatial knowledge” (Dunn, 2007). Our case study is based on a catchment area in the Caucasus mountain of Georgia, namely the Mestiachala and Mulkhura river basins. The primary goal of the research was to analyze changes in the mountain landscapes of Georgia by using land use/land cover change detection and participatory mapping techniques. The research question was, did land use and the land cover change affect the landscape values assigned by local people? Moreover, if so, which LULC classes and attached values were affected the most? In addition, what were the main factors and drivers of such changes? We used the land use/land cover change detection technique in the QGIS environment to answer these questions based on the Copernicus CORINE Land Cover dataset from 2015 (Buchborn et al. 2020a) and 2019 (Buchborn et al. 2020b). LULC data study implied verification stage with field data. For the valuation of the landscape by using local knowledge, we collected point geodata from the study area residents in three thematic categories: biodiversity, water resources and tourist attractions.

Because the questions were constructed around the benefits people obtain from ecosystems, they can be interpreted within the frame of the ecosystem services (ES) (World Resources Institute, 2005). Finally, we analyzed the correlation between locally perceived biodiversity, water resources and tourist attraction hotspots and changed LULC locations.

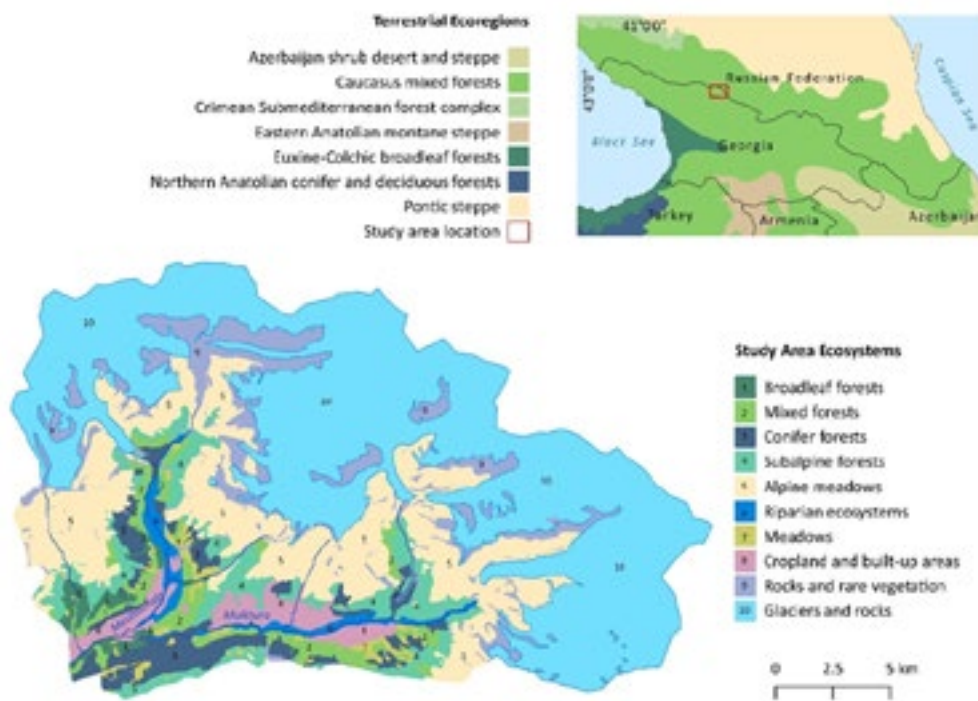


Figure 1. Study area location and its ecosystems. (source: author's map).

## REFERENCES

- Turner, M. G., & Gardner, R. H. 2015: Landscape Ecology in Theory and Practice: Pattern and Process. Springer, 365-381.
- Díaz, S., Pascual, U., Stenseke, M., Martín-López, B., Watson, R. T., Molnár, Z., ... Shirayama, Y. 2018: Assessing nature's contributions to people, *Science*, 359(6373), 270-272.
- O'Rourke, E. 2005: Landscape planning and community participation: local lessons from mullaghmore, the burren NationalPark, Ireland, *Landscape Research*, 30(4), 483-500.
- Schroeder, P. 1996: Report on public participation GIS workshop, *GIS and society: The social implications of how people, space and environment are represented in GIS*, NCGIA Technical Report, 96-97.
- Elwood, S. 2006: Critical issues in participatory GIS: Deconstructions, reconstructions, and new research directions, *Transactions in GIS*, 10(5), 693-708.
- Dunn, C. E. 2007: Participatory GIS-a people's GIS?, *Progress in human geography*, 31(5), 616-637.
- Brown, G., & Kyttä, M. 2014: Key issues and research priorities for public participation GIS (PPGIS): A synthesis based on empirical research, *Applied Geography*, 46, 122-136.
- Duží, B., Osman, R., Lehejček, J., Nováková, E., Taraba, P., & Trojan, J. 2019: Exploring citizen science in post-socialist space: Uncovering its hidden character in the Czech Republic, *Moravian Geographical Reports*, 27(4), 241-253.
- Buchborn, M., Smets, B., Bertels, L., De Roo, B., Levis, M., Tsendlbazar, N. E., Herold, M., & Fritz, S. 2020a: Copernicus Global Land Service, Land Cover 100 m, collection 3, epoch 2015, *Globe* (V3.0.1) [Data set].
- Buchborn, M., Smets, B., Bertels, L., De Roo, B., Levis, M., Tsendlbazar, N. E., Herold, M., & Fritz, S. 2020b: Copernicus Global Land Service, Land Cover 100 m, collection 3, epoch 2019, *Globe* (V3.0.1) [Data set].
- World Resources Institute. 2005): *Ecosystems and Human Well-Being: Synthesis, A Report of the Millennium Ecosystem Assessment*.

## 27.5

# Agroforestry systems as a contribution to sustainable mountain development, Case study Burundi

Heidi Elisabeth Megerle

*Hochschule für Forstwirtschaft Rottenburg, Schadenweilerhof, D-72108 Rottenburg am Neckar, megerle@rottenburg.de*

The topography of the central African country Burundi is characterized by mountain ranges and plateaus with altitudes of up to 2,670m (Mount Heha). As a least developed country, Burundi is still very much defined by agriculture and has a primary sector rate of 91%, which is predominantly small-scale subsistence agriculture (UNCTAD 2013, 54). The high population growth has resulted in the decline of usable land to 0.12 ha per person (Megerle and Niragira 2020). Even with the intensification of cultivation and the abandonment of what are otherwise much needed fallow periods, there is an increasing encroachment into protected forest reserves, such as Kibira National Park, as these very small areas are no longer sufficient for food security.

Due to the limited availability of land, the high importance of wood as virtually the only source of energy, and the urgent need for domestic food production, forms of multiple-purpose use must be developed with which these demands on the limited resource of space can be combined. So-called agroforestry systems lend themselves to this objective. Agroforestry systems can make significant contributions to the protection of resources (soil, water, plant raw materials) and to the promotion of biodiversity. The CO<sub>2</sub> sequestration of the trees contributes to active climate protection and to the provision of energy through the use of wood. Furthermore, agroforestry systems can significantly improve the livelihood of small farmers.

18 coffee cooperatives with a total of 10,000 smallholder families (approx. 70,000 people in total) are involved in the agroforestry project supported by the partner state of Baden-Württemberg. The accompanying research by the Rottenburg University of Applied Sciences together with the Université Burundi integrates both natural and social science aspects. Since the positive ecological effects of agroforestry systems (erosion, water and soil protection, biodiversity, microclimate, etc.) have been proven in principle in numerous studies, the natural science studies in Burundi concentrate on the most suitable shade tree species.

The social and economic effects of agroforestry systems, on the other hand, have received far less attention to date despite playing an equally important role. Initial surveys on the acceptance of agroforestry systems by smallholders showed that economic aspects are of crucial significance (Ndihokubwayo et al 2021; Windbühler 2021). In-depth studies on the necessary Living Income, a currently intensively discussed approach, are thus being carried out in the context of the agroforestry project as a pilot project. Based on a basic data research among smallholder families integrated in the Burundian cooperative association COCOCA and in the agroforestry project, the actual and the required family income will be calculated, factors that positively or negatively influence the achieved income will be identified, and measures will be developed to reduce challenges and risks (e.g. processing, logistics, supply chains) where possible. This is supplemented by a comparison with conventional cultivation.

First results of this socio-scientific research on agroforestry systems in mountain areas and their contribution to sustainable development will be presented.

## REFERENCES

- Megerle, H., & Niragira, S. 2020: The Challenge of Food security and the Water – Food – Energy – Nexus: Case Study Burundi. In: Biesalski HK (Hrsg.): Hidden Hunger and the Transformation of Food Systems. How to Combat the Double Burden of Malnutrition? World Rev Nutr Diet. Basel, Karger, 2020, 121, 183-192 (DOI:10.1159/000507488)
- Megerle, H., & Nkurunziza, P., & Rau, F. 2017: Wasserstress trotz Wasserreichtum – Ökonomisch bedingte Wasserknappheit am Beispiel Burundis, Geo-Öko, XXXVII, 5-30
- Ndihokubwayo, S.; Havyarimana, T.; Windbühler, S.; Niragira; S.; Habonimana, B.; Kaboneka, S.; Megerle, H. 2021: Farmers' Perception of Coffee Agroforestry Systems in an Area Targeted for Organic Certification in Burundi. East African Journal of Forestry and Agroforestry, 3 (1), 40-53; DOI: <https://doi.org/10.37284/eadfa.3.1.352>
- UNCTAD 2013: The least developed countries report. New York.
- Windbühler, S. 2021: Acceptance of Agroforestry Systems in Coffee Cultivation by Smallholders in Burundi. Abschlussarbeit. Hochschul

## 27.6

# Multipurpose use of hydropower dam reservoirs: Exploring the governance regime to develop coherent management strategies

Andréa Savoy<sup>1,2,3</sup>, Silvia Flaminio<sup>2,3</sup>, Stéphane Nahrath<sup>1,3</sup>, Emmanuel Reynard<sup>2,3</sup>

<sup>1</sup> University of Lausanne, Swiss Graduate School of Public Administration (IDHEAP), 1015 Lausanne ([andrea.savoy@unil.ch](mailto:andrea.savoy@unil.ch))

<sup>2</sup> University of Lausanne, Institute of Geography and Sustainability (IGD), 1015 Lausanne

<sup>3</sup> University of Lausanne, Interdisciplinary Centre for Mountain Research (CIRM), 1967 Bramois

Dam reservoirs have been built since the end of the 19<sup>th</sup> century in the Swiss Alps to produce indigenous energy and respond to the growing demand for electricity from industry (Zurbriggen 1952). The water right concessions granted hydroelectric companies an exclusive right to use the hydraulic power of surface waters within the licenced perimeter for a maximum of 99 years, and 80 years since the adoption of the *Federal Act on the Use of Hydraulic Power* in 1916 (Fournier 2002). Over time, however, the uses of water stored in alpine reservoirs have become more diverse: some hydropower reservoirs supply for example drinking water to the surrounding *communes* (municipalities), are used for artificial snow production or their pumped storage function allows them to stabilise the electricity network as a complement to intermittent energy sources. At the same time, the Swiss water public policy has addressed the issue of environmental degradation and moved towards more sustainable river management (Reynard et al. 2001) – the most obvious example being residual flows – and discussions have recently been initiated on the (re)operation of hydroelectric dams to face some effects of climate change such as droughts (Kellner 2019). These various changes have led to an increase in the number of actors involved in the direct or indirect use of dams and water since the concessions were granted. How are their new uses regulated in public and/or private law? To what extent is the current regulatory regime well adapted and capable of managing these new, essentially non-hydroelectric uses? In other words, does the existing governance system provide a sustainable and coherent management model for the more and more diversified and heterogeneous uses of dams and their waters?

In this paper, we investigate the way multipurpose use of hydropower plants is regulated in Switzerland in general and in the mountainous Valais Canton in particular. This study proposes a policy-oriented approach to analyse the regulation of the uses of the resources “dam” and “water” through the Institutional Resource Regime approach (IRR) (Knoepfel et al. 2001; Gerber et al. 2009). Such a framework enables in this case the identification of current and future challenges in dam operation by allowing to underline the effects of four different types of regimes (*non-existent, simple, complex, integrated*) on the sustainability of the two resources mentioned above. This approach also reveals the action tools available to the different stakeholders to defend their interests. Our analysis of the body of legislation relating to dams and water under public and private law at different institutional levels (*communes, cantons, Confederation*), completed by interviews with water and energy stakeholders, has provided us with a global understanding of the current situation of the multifunctionality of dams at the Swiss and Valais levels.

The past decade has been characterised by the beginning of the renewal of multi-decennial hydropower concessions in the Valais Canton. Such a renewal is both a moment of great stakes and an opportunity to redefine the rules for the eventual integration of other stakeholders and/or a new regulation of uses. In this context, the IRR approach allowed us to identify the grey areas in the current governance regime, especially the tension between the rights initially granted to concession holders and new uses, as well as environmental obligations related to environmental residual flows. We finally discuss how the IRR approach allows formulating concrete and sustainable proposals to address upcoming challenges in the field of water governance and hydropower production in mountain areas.

## REFERENCES

- Fournier, J. 2002: Vers un nouveau droit des concessions hydroélectriques: ouverture, marchés publics, protection de l'environnement, Editions Universitaires de Fribourg, Fribourg, 442 pp.
- Gerber, J.-D., Knoepfel, P., Nahrath, S. & Varone F. 2009: Institutional Resource Regimes: Towards sustainability through the combination of property-rights theory and policy analysis, Ecological Economics, 798-809.
- Kellner, E. 2019: Multi-purpose reservoirs for alleviating water shortages: Opportunities and challenges in the governance processes to coordinate competing resource uses under climate change, Inaugural dissertation of the Faculty of Science (University of Bern), Bern, 205 pp.
- Knoepfel, P., Kissling-Näf, I. & Varone, F. 2001: Institutionelle Ressourcenregime. In: Knoepfel, P., Kissling-Näf, I. & Varone, F. (Eds.) 2001: Institutionelle Regime für natürliche Ressourcen: Boden, Wasser und Wald im Vergleich - Régimes institutionnels de ressources naturelles: analyse comparée du sol, de l'eau et de la forêt, Helbing & Lichtenhahn, Basel, 11-48.
- Reynard, E., Thorens, A. & Mauch C. 2001: Développement historique des régimes institutionnels de l'eau en Suisse entre 1870 et 2000. In: Knoepfel, P., Kissling-Näf, I. & Varone, F. (Eds.) 2001: Régimes institutionnels de ressources naturelles: analyse comparée du sol, de l'eau et de la forêt, Helbing & Lichtenhahn, Basel, 101-139.
- Zurbriggen, M. 1952: Le développement de l'industrie électrique en Valais, Imprimerie Schmid, Sion, 178 pp.

## 27.7

# Safeguarding Mountain Social-Ecological Systems – a global summary of regional mountain challenges

Stefan Schneiderbauer<sup>1,2,3</sup>, Paola Fontanella-Pisa<sup>1,2</sup>, Jörg Szarzynski<sup>1,2,4,5</sup>, Jess Delves<sup>1,2</sup>, Stefano Terzi<sup>1,2</sup>

<sup>1</sup> United Nations University, Institute for Environment and Human Security, 53113 Bonn, Germany  
 (schneiderbauer@ehs.unu.edu)

<sup>2</sup> Centre for Global Mountain Safeguard Research, Eurac Research, 39100 Bozen/Bolzano, Italy

<sup>3</sup> Department of Geography, Qwaqwa Campus, University of the Free State, 9301 Bloemfontein, South Africa

<sup>4</sup> Disaster Management Training and Education Centre for Africa (DiMTEC), University of the Free State, PO Box 339, Bloemfontein 9300, South Africa

<sup>5</sup> International Research Institute of Disaster Science (IRIDeS), Tohoku University, Aoba 468-1, Aramaki, Aoba-ku, Sendai, Miyagi 980-8572, Japan

Half of all global land relies on mountain ecosystem services. At the same time, mountain social-ecological systems – particularly due to their rugged terrain and remoteness - face particular mountain-specific challenges linked to the adverse effects of climate and other global change processes (e.g., demography, migration and urbanization). Mountains provide key ecosystem services (e.g., water, biodiversity, recreation areas) that support the economic development of lowland areas, but nevertheless mountain issues are under-represented in international frameworks when compared to, for example, coastal areas or mega-cities. The heterogeneity of mountains – of their biophysical, social-cultural and economic characteristics – makes it difficult to communicate the global significance of healthy mountain social-ecological systems for wider society. Therefore, supporting the sustainable development of mountain regions comprises both the engagement in context-specific research and targeted action at local and mountain range level as well as encouraging lobbying and interventions at global level with global actors.

The United Nations University's (UNU) efforts to promote sustainable mountain development began in the late 1970s with the 'Highland-Lowland Interactive Systems project' (later renamed Mountain Ecology and Sustainable Development). This international project produced remarkable scientific results, triggered many subsequent mountain research activities and led to the inclusion of a mountain-specific article in the Agenda 21 of 1992 (Rio Declaration, UNDSD, 1992). The results are summarized in the book 'Mountains of the World: A Global Priority' (Messerli & Ives, 1997).

In 2020 the newly established UNU programme 'GLOMOS' (Global Mountain Safeguard Research) launched a follow-up book project to gather together examples of the many and varied activities supporting sustainable development across all major global mountain areas, with a focus on safeguarding mountain social-ecological systems. The upcoming book covers both global perspectives as well as taking a region-specific lens and includes research from more than 200 authors from a large variety of scientific disciplines and working in different domains such as academia, multi-lateral governmental and non-governmental initiatives. The book counts over 70 articles providing a unique and broad spectrum of perspectives on mountain regions and approaches to support them. These papers highlight key challenges for mountain social-ecological systems at multiple scales and for all major highlands including those less known such as the mountains of African Islands. The book's publication is foreseen for the end of 2022 / beginning 2023.

This contribution will provide first insights into the identified gaps in research and practice that need to be addressed to sustainably develop and safeguard global mountain ranges in the context of the challenges posed by global change. It brings to light the contradictions in the treatment of mountains in different scientific fields, some of which conceive mountains as being highly vulnerable to global change while others claim that mountain societies are inherently highly resilient. The contribution also underlines the importance of building upon the intrinsic capacities and experiences of mountain populations whilst emphasising the need to consider global processes of mobility and trade when discussing possible measures to safeguard mountain regions. Finally, this paper links the activities that support sustainable development of mountains with the various UN frameworks, notably the United Nations Sustainable Development Goals (SDGs, UNGA, 2015).

## REFERENCES

- Messerli B, Ives JD, editors. 1997. Mountains of the World: A Global Priority. New York, NY, and Carnforth, UK: Parthenon Publishing Group. Google Scholar
- UNDSD [United Nations Division for Sustainable Development]. 1992. United Nations Conference on Environment and Development. Rio de Janeiro, Brazil, 3 to 14 June 1992. Agenda 21. New York, NY: UNCD [United Nations Conference on Environment and Development]. <https://sustainabledevelopment.un.org/content/documents/Agenda21.pdf>; accessed on 17 September 2020. Google Scholar
- UNGA [United Nations General Assembly]. 2015. Transforming Our World: The 2030 Agenda for Sustainable Development. A/RES/70/1. New York, NY: UNGA. [https://www.un.org/ga/search/view\\_doc.asp?symbol=A/RES/70/1&Lang=E](https://www.un.org/ga/search/view_doc.asp?symbol=A/RES/70/1&Lang=E); accessed on 17 September 2020. Google Scholar

## 27.8

# Human populations in the world's mountains: Spatio-temporal patterns and potential controls

James M. Thornton<sup>1</sup>, Mark A. Snethlage<sup>2</sup>, Roger Sayre<sup>3</sup>, Davnah R. Urbach<sup>2</sup>, Daniel Vivioli<sup>4</sup>, Daniele Ehrlich<sup>5</sup>, Veruska Muccione<sup>4</sup>, Philippus Wester<sup>6</sup>, Gregory Insarov<sup>7</sup> and Carolina Adler<sup>1</sup>

<sup>1</sup> Mountain Research Initiative, University of Bern, Bern, Switzerland ([james.thornton@unibe.ch](mailto:james.thornton@unibe.ch))

<sup>2</sup> Global Mountain Biodiversity Assessment, University of Bern, Bern, Switzerland

<sup>3</sup> U.S. Geological Survey, Reston, VA, United States of America

<sup>4</sup> Department of Geography, University of Zurich, Zurich, Switzerland

<sup>5</sup> Joint Research Center, European Commission, Ispra, Italy

<sup>6</sup> International Centre for Integrated Mountain Development (ICIMOD), Kathmandu, Nepal

<sup>7</sup> Institute of Geography, Russian Academy of Sciences, Moscow, Russia

Changing climate and human demographics in the world's mountains will have increasingly profound environmental and societal consequences across all elevations. Quantifying current human populations in and near mountains is crucial to ensure that any interventions in these complex social-ecological systems are appropriately resourced, and that valuable ecosystems are effectively protected. However, comprehensive and reproducible analyses on this subject are lacking. Here, we develop and implement an open workflow to quantify the sensitivity of mountain population estimates over recent decades, both globally and for several sets of relevant reporting regions, to alternative input dataset combinations.

Relationships between mean population density and several potential environmental covariates are also explored across elevational bands within individual mountain regions (i.e. "sub-mountain range scale"). Globally, mountain population estimates vary greatly—from 0.344 billion (<5% of the corresponding global total) to 2.289 billion (>31%) in 2015. A more detailed analysis using one of the population datasets (GHS-POP) revealed that in ~35% of mountain sub-regions, population increased at least twofold over the 40-year period 1975–2015. The urban proportion of the total mountain population in 2015 ranged from 6% to 39%, depending on the combination of population and urban extent datasets used. At sub-mountain range scale, population density was found to be more strongly associated with climatic than with topographic and protected-area variables, and these relationships appear to have strengthened slightly over time. Such insights may contribute to improved predictions of future mountain population distributions under scenarios of future climatic and demographic change. Overall, our work emphasizes that irrespective of data choices, substantial human populations are likely to be directly affected by—and themselves affect—mountainous environmental and ecological change. It thereby further underlines the urgency with which the multitudinous challenges concerning the interactions between mountain climate and human societies under change must be tackled.

## REFERENCE

- Thornton JM, Snethlage MA, Sayre R, Urbach DR, Vivioli D, Ehrlich D, et al. (2022) Human populations in the world's mountains: Spatio-temporal patterns and potential controls. PLoS ONE 17(7): 10.1371/journal.pone.0271466

## 27.9

# Women's Innovative Land and Water Management Practices in Marginalized Mountains: A Learning Experience of Citizen Science in Climate Change Adaptation and Sustainable Development in Himalaya

Prakash C. Tiwari

*Professor of Geography, Kumaun University, Nainital 263001, Uttarakhand, India*

In Himalaya, due to geo-environmental limitations, subsistence farming constitutes the main source of community food and livelihood. The constraints of the subsistence economy compel a large proportion of the youth-male population to out-migrate the region in search of livelihood leading to the feminization of farming and the natural resource management system (Grainger et al., 2021). Hence, women are considered primary resource developers and important agents of sustainable mountain development. Climate change has stressed the Himalayan farming system through higher temperatures, altered precipitation patterns and more frequent and severe extreme weather events (Heath et al., 2020).

Women experience these changes acutely and disproportionately due to prevailing gender differentiating cultural and social norms and institutions, skewed gender division of labour, multiple roles and responsibilities, and their exclusion from decision and policy-making processes (International Water Management Institute, 2020). These social norms limit women's access to education, restrict ownership of natural resources, and fade the process of their educational, economic and political mainstreaming (Joshi, 2018). Hence, women are often in the frontline regarding the impacts of a changing climate. However, women have developed critical knowledge to perceive the impacts of and respond to rapidly changing climatic conditions and cope with natural risks through adaptive management of land, water, forests, pastures and biodiversity resources within and across diverse environments (International Centre for Integrated Mountain Development, 2021). The study aims to analyze innovative adaptation practices and coping mechanisms the mountain women have evolved and are practicing to adapt to changing climatic conditions and evaluate their contribution towards climate change adaptation and sustainable mountain development with an empirical study of Kumaon Himalaya, India.

The methodology included documentation and mapping of women's innovative adaptation mechanism and adaptive natural resource management practices through empirical studies, ground observations and a comprehensive socio-economic survey. Results indicated: (i) women in 27% of villages replenished water sources by employing traditional water conservation practices; (ii) 19% of women changed cropping patterns, (iii) women in 25% of villages developed indigenous rainwater harvesting systems; (iv) 21% women adjusted crop-rotation; and (v) 27% women relocated agriculture; (vi) 55% women taking all decisions related with the management of land and water resources; and (vii) 37% women are now solely responsible for utilization, processing, and marketing of their agricultural products. It was observed that women's innovative adaptation measures are not only building climate change resilience in the subsistence mountain farming system but reducing the gender gap by providing women with the opportunity to come closer to the mainstream of sustainable development through improved participation and decision-making. These adaptation practices are helping mountain women to come closer to the mainstream of sustainable development with economic growth, improved infrastructure and growing linkages with local, national and international markets for their farm-products. It is expected that traditional adaptation mechanisms developed by women would play a crucial role in building climate change resilience and should therefore form an important component of the overall climate change adaptation strategy across the Himalaya and in other mountain regions of developing world.

**Keywords:** Subsistence farming, feminization of agriculture, gender differentiating norms, empirical studies, reducing gender gap, Kumaon Himalaya

## REFERENCES

- Grainger, C. Tiwari, Prakash C., Joshi, Bhagwati, Reba, Meredith, and Seto, Karen (2021). Who Is Vulnerable and Where Do They Live? Case Study of Three Districts in the Uttarakhand Region of India Himalaya, Mountain Research and Development, International Mountain Society 41(2), URL: <https://doi.org/10.1659/MRD-JOURNAL-D-19-00041.1>
- Heath, Lance C.; Tiwari, P. C.; Sadhukhan, B.; Tiwari, S.; Chapagain, P.; Xu, T.; Li, G.; Ailikum; Joshi, B. and Yan, Z. (2020). Building Climate Change Resilience by Using A Versatile Toolkit for Local Governments and Communities in Rural Himalaya, Environmental Research, <https://doi.org/10.1016/j.envres.2020.109636>
- International Centre for Integrated Mountain Development (2021). Gender Audit - Final Report, ICIMOD, Kathmandu, Nepal
- International Water Management Institute (2020). IWMI Gender and Inclusion Strategy 2020-2023: New landscapes of water equality and inclusion. Colombo, Sri Lanka: International Water Management Institute (IWMI). 16p. doi: <https://doi.org/10.5337/2020.205>
- Joshi, B. (2018). Recent Trends of Rural Out-migration and its Socio-economic and Environmental Impacts in Uttarakhand Himalaya, Journal of Urban and Regional Studies on Contemporary India 4(2): 1-14

**P 27.1****Les stratotypes triasiques, géotopes encore mal connus du patrimoine géologique préalpin vaudois**Aymon Baud<sup>1</sup><sup>1</sup>*Institut des sciences de la Terre, Université de Lausanne, Geopolis, CH-1015 Lausanne ( aymon.baud@unil.ch)*

Le stratotype est un affleurement type qui avec son nom géographique, sert de référence à la désignation d'une succession de couches sédimentaires déposées à une époque donnée, telle une Formation ou un Membre, utilisés aussi bien dans les descriptions de l'histoire de la Terre que dans la cartographie géologique. Géopatrimoine souvent ignoré, il est d'une valeur scientifique importante comme référence, car agréé par une autorité scientifique (comité de stratigraphie) ; mais il va au-delà par son aspect pédagogique, car il contribue au développement culturel et à la compréhension de la biodiversité, du climat et des changements globaux dans les époques reculées de l'histoire de la Terre et peut servir de leçon pour la compréhension de la géohistoire actuelle. Il existe trois régions des Préalpes vaudoises qui ont le privilège de montrer les stratotypes d'unités sédimentaires triasiques agréées par le Comité suisse à la suite de travaux scientifiques reconnus pour être directement utilisés en cartographie géologique (géocartes des Préalpes vaudoises, bernoises et des terrains triasiques du pennique valaisan). De plus, ces stratotypes vaudois permettent des corrélations précises sur de vastes distances, à l'intérieur du bassin briançonnais qui s'étend de la Suisse centrale et occidentale jusqu'aux Alpes maritimes franco-italiennes. Ces trois régions comprennent:

- 1 Les collines de Saint-Triphon dans la vallée du Rhône.
- 2 Le cirque ou combe du Pralet dans les Rochers de Château-d'Oex qui jouxte la réserve naturelle de la Pierreuse et possible futur géoparc.
- 3 Le cirque ou combe de Luan au-dessus de Corbeyrier, au cœur du massif des Tours d'Aï.

L'histoire de la géologie vaudoise est marquée d'abord par la première découverte du Trias dans les Alpes, ceci déjà en 1822 dans les collines de Saint-Triphon par Mousson, alors professeur à Zürich « Ich habe Muschelkalk bei St-Triphon gefunden », puis par Renevier qui en 1864 propose l'usage du terme « Rhétien » comme étage qui marque la fin de l'époque triasique, ceci après l'étude dans la Combe de Luan des couches de Plan Falcon. Puis ce sont Jaccard (1907), et Jeannet (1912-13) qui poursuivent les travaux de Renevier et détaillent les successions lithologiques et leur contenu fossile triasique, aussi bien dans les Rochers de Château-d'Oex qu'à Saint-Triphon et à Plan Falcon. Lors de la cartographie géologique, les stratotypes seront proposés par A. Baud (1987) pour la Formation de Saint-Triphon d'âge Anisien inférieur et moyen. Pour donner suite à la révision des âges attribués aux couches du Trias moyen Briançonnais par Baud et al., (2016), la Formation du Pralet est proposée comme nouveau stratotype des couches du Ladinien des Préalpes. Quant à la Formation de Plan Falcon c'est M. Mettraux (1983-1989) qui en a défini le stratotype pour les couches du Rhétien préalpin.

Voici quelques détails sur chaque région :

1- Les collines de Saint-Triphon qui abritent le stratotype de la Formation montrent quelques uns des plus fascinants affleurements du Briançonnais dans les Alpes occidentales, tout d'abord en termes d'histoire des sciences géologiques, mais aussi d'histoire des géoressources vaudoises avec l'exploitation d'anciennes carrières décrites et illustrées par Pradervant et Baud, (2007). On y trouve aussi des affleurements uniques et pédagogiques pour l'enseignement des sciences de la terre et l'éducation permanente. A ce sujet, un grand panneau d'explications géologiques figure dans la carrière des Fontenailles à l'instigation de la Fondation Nicole Debarges (Baud et al., 2012).

2- Une coupe complète des calcaires et dolomies du Trias moyen des Préalpes médianes rigides se trouve dans un des profils de référence qui suit la crête du Rocher Plat dans les Rochers de Château-d'Oex ; le stratotype de la Formation du Pralet est l'un des rares endroit qui permet de faire le lien complet et régulier (Baud et al., 2016, fig. h) entre des ensembles lithologiques qui sont séparés tectoniquement dans les Préalpes internes. Ce stratotype mérite à l'avenir le statut de géotope et un panneau explicatif serait utile à la Pierreuse et dans la partie supérieure du sentier qui descend de la Vidmanette à Rougemont.

3- C'est dans la partie interne des Préalpes médianes plastiques, la combe de Luan au cœur de l'anticlinal des Tours d'Aï, que se trouve le stratotype de la Formation de Plan Falcon décrit en détail par M. Mettraux en 1983 et proposé comme stratotype dans sa thèse en 1989. En 1985, elle invite le Musée cantonal de Géologie à Lausanne à effectuer des fouilles paléontologiques et celles-ci vont dégager une plaque couverte de vertèbres et côtes d'ichtyosaure ainsi qu'une dent de dinosaure qui seront vedettes dans l'exposition « Archives de la Vie » inaugurée en 1993 au Palais de Rumine. Là aussi, le statut de géotope et un panneau explicatif sur la route des Agites seraient à étudier.

## BIBLIOGRAPHIE

- Baud, A. 1987: Stratigraphie et sédimentologie des calcaires de Saint-Triphon (Trias, Préalpes, Suisse et France). Mémoires de Géologie, Lausanne, 1, 1-322.
- Baud, A., Escher, A., Epard, J.-L., Jaboyedoff, M. & Masson, H. 2012: La géologie des collines de Saint-Triphon. Poster-panneau réalisé pour le site d'escalade de la carrière des Fontenailles à Saint-Triphon et financé par la Fondation Nicole Debarge.
- Baud, A., Plasencia, P., Hirsch, F., & Richoz, S. 2016: Revised middle Triassic stratigraphy of the Swiss Prealps based on conodonts and correlation to the Briançonnais (Western Alps). Swiss Journal of Geosciences, 109, 365-377.
- Jaccard, F., 1907: La région Rüбли-Gummifluh (Préalpes médianes, Suisse). Bulletin de la Société Vaudoise des Sciences Naturelles, 43, 407-548.
- Jeannet, A., 1912–1913: Monographie géologique des Tours d'Aï et des régions avoisinantes. Matériaux pour la Carte géologique de la Suisse (NS), 34, 1–701
- Mettraux, M., 1983 : Etude géologique des Préalpes médianes dans la région des Tours d'Aï. Travail de diplôme, Université de Fribourg, 1-152.
- Mettraux, M., 1989 : Sédimentologie, paléotectonique et paléocéanographie des Préalpes médianes. (Suisse Romande) du Rhétien au Toarcien. Travail de Thèse, Université de Fribourg, 1-126.
- Pradervand, B. & Baud, A., 2007 : Les collines de Saint-Triphon, un géotope unique. In Guignard, H.L. et Pradervand, B., éditeurs : Ollon Villars. Association de l'Académie du Chablais, 98-107.

## P 27.2

### Glacier retreat shapes plant functional diversity

Nora Khelidj<sup>1</sup>, Lucia Mottet<sup>1</sup>, Gianalberto Losapio<sup>1,2</sup>

<sup>1</sup> Institut of Earth Surface Dynamics, University of Lausanne, CH-1015 Lausanne, Switzerland ([nora.khelidj@unil.ch](mailto:nora.khelidj@unil.ch))

<sup>2</sup> Department of Biosciences, University of Milan, 20133 Milan, Italy

Glacier retreat is a striking example of global warming. All over the world, glaciers are retreating and exposing new areas (glacier foreland) for potential colonisation by living organisms, including plants. However, we are lacking knowledge on the impact of glacier retreat on plant functional diversity, despite its importance for shaping ecosystem processes. Here, we assessed how plant functional diversity responds to glacier retreat. Along a glacier foreland (Mont Miné, Val d'Hérens, Switzerland), we surveyed plant communities along four deglaciation stages that ranges from the Little Ice Age (year 1864) until recent years. Using a plant trait database (TRY database) and our own measures, we associated plant species with morphological and functional traits including Leaf Dry Matter Content, Specific Leaf Area, Leaf Carbon Content, and Leaf Nitrogen Content. We predict differences in the diversity and similarity of plants and traits, as well as a shift in dominant traits along the glacier foreland. We expect a high taxonomic and functional diversity, heterogeneity of traits and specialised species in recent deglaciation areas. Whereas we expect a decrease of diversity with the stabilisation of the ecosystem with one century after glacier retreat. Understanding the relationships among plants, traits and deglaciation is necessary to conserve and restore glacier ecosystems, which are particularly vulnerable to climate change.

## P 27.3

# Sustainable eco-tourism development in the Uttarakhand Himalaya: a case study

Vishwambhar Prasad Sati

*Department of Geography and Resource Management, Mizoram University, Aizawl – 796004, India (vpsati@mzu.edu.in)*

The concept of 'Eco-tourism' was postulated in the 1980s. It aimed to promote sustainable tourism in natural, forest, and cultural areas. Eco-tourism is related to recreation in the wilderness – mainly in forest areas. In the recent past, eco-tourism is practiced in national parks, wildlife sanctuaries, and conservation reserves. Wall (1994) observed that eco-tourism is a new name for tourism, which was practiced in natural locales in the past. Eco-tourism is also termed 'Responsible Tourism' because it has multifaceted nature – examining the impact of tourism on the environment, community participation in eco-tourism development, and conservation of nature (Black, 1996; Bansal and Kumar, 2011). The Uttarakhand Himalaya has a diversified climate that varies along the altitudes from the river valleys to mid-altitudes and highlands. Accordingly, the faunal, floral, and avifaunal resources vary. Tourism is one of the important service sectors in Uttarakhand. It ranks 12<sup>th</sup> in the global tourism ranking (Sati, 2018) and shares a total of 52% of Gross State Development Product (SGDP). In the Uttarakhand Himalaya, the practices of tourism vary from pilgrimage tourism to nature and adventure tourism – mountaineering, river rafting, and trekking. Pilgrimage tourism is practiced largely, followed by nature tourism, and then adventure tourism. Eco-tourism, one of the major forms of tourism, has a high potential for the development of the Uttarakhand Himalaya. It obtains spectacular forest landscapes and a feasible climate. However, eco-tourism is in its initial stage and has yet to be developed.

This paper examines sustainable eco-tourism development in the Uttarakhand Himalaya by analyzing both the potential of eco-tourism development and eco-tourism resource base. Data were gathered from the Uttarakhand Forest Statistical Diary 2017-18 and the Uttarakhand Eco-Tourism Corporation, Dehradun, respectively. The trends of eco-tourists inflow in NPs and WLSSs and revenue earned from it were examined. The key results from the data analyses depict that the Uttarakhand Himalaya has plenty of eco-tourism resource bases – six national parks ( $5006.76 \text{ km}^2$ ), seven wildlife sanctuaries ( $2683.73 \text{ km}^2$ ), and four conservation reserves ( $212.54 \text{ km}^2$ ) along with rich faunal, floral, and avifaunal diversity. These resource bases have significant potential for eco-tourism development. The trends of eco-tourist inflow in the NPs and WLSSs are increasing, mainly domestic tourists ( $r^2= 0.941$ ). However, in comparison to natural and pilgrimage tourism, eco-tourists inflow is low. In terms of the annual growth rate of eco-tourist inflow, it has been decreasing ( $r^2=0.168$ ). The main reasons for decreasing growth rate of eco-tourist inflow were remoteness, fragile landscape, rugged terrain, frequent geo-hydrological hazards, and lacking infrastructural facilities – transportation, accommodation, and institutional support in eco-tourism destinations. This study suggests policy measures for eco-tourism development in the Uttarakhand Himalaya through the creation of eco-tourism circles, development of eco-tourism parks, and providing adequate infrastructural facilities – transportation, accommodation, institutions, and communication.

**Keywords:** Eco-tourism, national parks, wildlife sanctuaries, trends, eco-tourist inflow, Uttarakhand Himalaya.

## REFERENCES

- Black, R. (1996). Eco-tourism. What does it really mean? Range 34: 4–7.
- Bansal, S.P. and Kumar, J. (2011). Eco-tourism for Community Development: A Stakeholder's Perspective in Great Himalayan National Park. International Journal of Social Ecology and Sustainable Development, 2(2), 31-40.
- Sati, V.P. (2018). Carrying Capacity Analysis and Destination Development: A Case Study of Gangotri Tourists/Pilgrims' Circuit in the Himalaya, Asia Pacific Journal of Tourism Research Vol. 23 (3): 312-322, DOI: 10.1080/10941665.2018.1433220.
- Wall, G. (1994). Eco-tourism: Old wine in new bottles? Trends 31(2): 4-9.

## P 27.4

# Geophysical insights from a 20 year-long irrigation experiment in the Pfynwald forest (Valais)

Alexis Shakas<sup>1</sup>, Roman Hediger<sup>1</sup>, Isabelle Pfister Hediger<sup>1</sup>, Katrin Di Bella Meusburger<sup>2</sup>, Giulia de Pasquale<sup>3</sup>, Kamini Singha<sup>4</sup>, Florian Wagner<sup>5</sup>, Hansruedi Maurer<sup>1</sup>

<sup>1</sup> Department of Earth Sciences at ETH, Sonneggstrasse 5, CH-8092 Zürich ([alexis.shakas@erdw.ethz.ch](mailto:alexis.shakas@erdw.ethz.ch))

<sup>2</sup> Swiss Federal Institute for Forest, Snow and Landscape Research (WSL), Birmensdorf, Switzerland

<sup>3</sup> CEAZA, Campus Andrés Bello Universidad de La Serena, La Serena, Región de Coquimbo, Chile

<sup>4</sup> Hydrologic Science and Engineering Program, Colorado School of Mines, Golden, CO, 80401, USA

<sup>5</sup> Institute for Applied Geophysics and Geothermal Energy, RWTH Aachen University, Mathieustraße 30, 52074 Aachen, Germany

Adverse effects of climate change on Alpine forests have been observed more than half a century ago. To monitor these effect on Pine trees, the Swiss Federal Institute for Forest, Snow and Landscape Research (WSL) initiated a controlled irrigation experiment in the protected Pfynwald Forest in Valais. During the last year we conducted a series of geophysical measurements in Pfynwald to better understand the interplay between subsurface processes, such as water redistribution in the soil, to what is observed on the surface and inside trees. Our analyses combine results from electrical resistivity imaging below ground and on tree trunks, as well as other independent measurements such as drone imaging of drought stress indices. We present a novel approach of effectively monitoring sap flow in tree trunks by combining (non-destructive) ground penetrating radar imaging to electrical resistivity measurements. Moreover, our time-lapse resistivity measurements of the soil between irrigated and control plots reveal that trees in the irrigated plots seem to create drier conditions than the control plots prior to irrigation. This pattern reverses some months after the irrigation phase.

## REFERENCES:

- Hediger, Roman. 2022: Investigating soil water redistribution during an irrigation experiment: Implications on tree mortality, ETH Zurich M.Sc. Thesis, ETH Research Collection.
- Pfister, Isabelle. 2022: Investigating soil water redistribution during an irrigation experiment: Implications on tree mortality, ETH Zurich M.Sc. Thesis, ETH Research Collection.

## P 27.5

# Coverage of In Situ Climatological Observations in the World's Mountains

James M. Thornton<sup>1</sup>, Nicholas Pepin<sup>2</sup>, Maria Shahgedanova<sup>3</sup>, and Carolina Adler<sup>1</sup>

<sup>1</sup> Mountain Research Initiative, University of Bern, Bern, Switzerland ([james.thornton@unibe.ch](mailto:james.thornton@unibe.ch))

<sup>2</sup> School of the Environment, Geography and Geosciences, University of Portsmouth, Portsmouth, United Kingdom

<sup>3</sup> Department of Geography and Environmental Science, University of Reading, Reading, United Kingdom

Many mountainous environments and ecosystems around the world are responding rapidly to ongoing climate change. Long-term climatological time-series from such regions are crucial for developing improving understanding of the mechanisms driving such changes and ultimately delivering more reliable future impact projections to environmental managers and other decision makers. Whilst it is already established that high elevation regions tend to be comparatively under-sampled, detailed spatial and other patterns in the coverage of mountain climatological data have not yet been comprehensively assessed on a global basis. To begin to address this deficiency, we analyse the coverage of mountainous records from the Global Historical Climatological Network-Daily (GHCNd) inventory with respect to space, time, and elevation. Three key climate-related variables—air temperature, precipitation, and snow depth—are considered across 292 named mountain ranges. Several additional datasets are also introduced to characterize data coverage relative to topographic, hydrological, and socio-economic factors. Spatial mountain data coverage is found to be highly uneven, with station densities in several “Water Tower Units” that were previously identified as having great hydrological importance to society being especially low. Several mountainous regions whose elevational distribution is severely undersampled by GHCNd stations are identified, and mountain station density is shown to be only weakly related to the human population or economic output of the corresponding downstream catchments. Finally, we demonstrate the capabilities of a script to produce detailed assessments of individual records’ temporal coverage and measurement quality information. Overall, our contribution should help international authorities and regional stakeholders identify areas, variables, and other monitoring-related considerations that should be prioritized for infrastructure and capacity investment. Finally, the transparent and reproducible approach taken will enable the analysis to be rapidly repeated for subsequent versions of GHCNd, and could act as a basis for similar analyses using other spatial reporting boundaries and/or environmental monitoring station networks.

## REFERENCE

- Thornton J.M., Pepin N., Shahgedanova M. & Adler C. 2022. Coverage of In Situ Climatological Observations in the World's Mountains, *Frontiers in Climate* 4. 10.3389/fclim.2022.814181

**P 27.6****Assessing the impact of glacier retreat on biodiversity and plant–insect interaction dynamics**

Ngan Bao Tu<sup>1,2,3</sup>, Nora Khelidj<sup>1</sup>, Gianalberto Losapio<sup>1,2</sup>

<sup>1</sup> Institut of Earth Surface Dynamics, University of Lausanne, CH-1015 Lausanne, Switzerland ([baongan.tu@unil.ch](mailto:baongan.tu@unil.ch))

<sup>2</sup> Department of Biosciences, University of Milan, 20133 Milan, Italy

<sup>3</sup> Department of Chemistry and Biology, University Grenoble Alpes, 38400 Grenoble, France

The retreat and extinction of glaciers worldwide is followed by the loss of plant and insect species from ecological networks and local communities. Furthermore, due to glacier retreat, new plant and insect species are moving up to higher altitude, causing changes in species diversity, species composition and also in plant-insect interactions. An integrative understanding of network dynamics and ecosystem functions following glacier retreat is therefore of major importance to biodiversity maintenance and environmental health. At Mont Miné glacier, Swiss Alps, we reconstructed the retreat of glacier during the last two centuries using geochronology and addressed four main stages of deglaciation ranging from recently ice-free terrains to late stages of development since the end of the Little Ice Age (c 1864). Following this glacier retreat gradient, we surveyed plants and pollinator insects to investigate the structure and dynamic of pollination networks and unveil their assembly by means of network analysis. We observed sharp changes in biodiversity of both plants and pollinators following glacier retreat. Communities close to the glacier are characterized by pioneer plant species characteristic of glacier environments but pollinator species from lowland. We found an increase in the abundance and richness of interactions shortly after glacier retreat. Yet, the complexity of pollination network decreased in late stages a century after the retreat of glacier. These results indicate that, in the long-term, glacier retreat can decrease the diversity and stability of ecological networks.

